

# AGARD

ADVISORY GROUP FOR AEROSPACE RESEARCH & DEVELOPMENT

7 RUE ANCELLE 92200 NEUILLY SUR SEINE FRANCE

AGARD CONFERENCE PROCEEDINGS No. 159

on

## Electromagnetic Noise Interference and Compatibility

NORTH ATLANTIC TREATY ORGANIZATION



REPRODUCED BY  
NATIONAL TECHNICAL  
INFORMATION SERVICE  
U. S. DEPARTMENT OF COMMERCE  
SPRINGFIELD, VA. 22161

# **N O T I C E**

**THIS DOCUMENT HAS BEEN REPRODUCED FROM THE  
BEST COPY FURNISHED US BY THE SPONSORING  
AGENCY. ALTHOUGH IT IS RECOGNIZED THAT CER-  
TAIN PORTIONS ARE ILLEGIBLE, IT IS BEING RE-  
LEASED IN THE INTEREST OF MAKING AVAILABLE  
AS MUCH INFORMATION AS POSSIBLE.**

REPORT DOCUMENTATION PAGE			
1. Recipient's Reference	2. Originator's Reference AGARD-CP-159	3. Further Reference	4. Security Classification of Document UNCLASSIFIED
5. Originator Advisory Group for Aerospace Research and Development North Atlantic Treaty Organization 7 rue Ancelle, 92200 Neuilly sur Seine, France			
6. Title Electromagnetic Noise Interference and Compatibility			
7. Presented at the Joint Avionics/Electromagnetic Wave Propagation Panels Symposium held in Paris, France, 21-25 October 1974.			
8. Author(s) Various			9. Date November 1975.
10. Author's Address Various			11. Pages
12. Distribution Statement This document is distributed in accordance with AGARD policies and regulations, which are outlined on the Outside Back Covers of all AGARD publications.			
13. Keywords/Descriptors Avionics Electromagnetic interference Compatibility Aircraft		Spread spectrum Integrated circuits Antennas Multiplexing	14. UDC 629.73.054:621.317.7
15. Abstract  The recent past has seen a great proliferation of avionics equipment and subsystems to meet new and expanded mission requirements resulting in very large systems.  Not only are the actual numbers increasing, but also they are now appearing in all parts of the frequency spectrum, many of them simultaneously.  The application of these systems in aircraft and the resulting mobility of the ground forces results in a very dynamic ever-changing highly interactive environment.  New levels of interference are being encountered as a result of a greater number and closer spacing of channels and the utilization of new energy levels, and at the same time a desire to go further into the noise to receive desired signals.  This meeting examined this area and provided a reassessment as to how new systems can be provided to meet operational requirements on a cost-effective basis.			

**NORTH ATLANTIC TREATY ORGANIZATION**  
**ADVISORY GROUP FOR AEROSPACE RESEARCH AND DEVELOPMENT**  
**(ORGANISATION DU TRAITE DE L'ATLANTIQUE NORD)**

**AGARD Conference Proceedings No.159**  
**ELECTROMAGNETIC NOISE INTERFERENCE AND COMPATIBILITY**

14  
Copies of papers presented at the Joint Avionics/Electromagnetic Wave  
Propagation Panels Symposium held in Paris, France, 21-25 October 1974.



## THE MISSION OF AGARD

The mission of AGARD is to bring together the leading personalities of the NATO nations in the fields of science and technology relating to aerospace for the following purposes:

- Exchanging of scientific and technical information;
- Continuously stimulating advances in the aerospace sciences relevant to strengthening the common defence posture;
- Improving the co-operation among member nations in aerospace research and development;
- Providing scientific and technical advice and assistance to the North Atlantic Military Committee in the field of aerospace research and development;
- Rendering scientific and technical assistance, as requested, to other NATO bodies and to member nations in connection with research and development problems in the aerospace field;
- Providing assistance to member nations for the purpose of increasing their scientific and technical potential;
- Recommending effective ways for the member nations to use their research and development capabilities for the common benefit of the NATO community.

The highest authority within AGARD is the National Delegates Board consisting of officially appointed senior representatives from each member nation. The mission of AGARD is carried out through the Panels which are composed of experts appointed by the National Delegates, the Consultant and Exchange Program and the Aerospace Applications Studies Program. The results of AGARD work are reported to the member nations and the NATO Authorities through the AGARD series of publications of which this is one.

Participation in AGARD activities is by invitation only and is normally limited to citizens of the NATO nations.

The content of this publication has been reproduced  
directly from material supplied by AGARD or the author.

Published November 1975

Copyright © AGARD 1975

629.73.054:621.317.7



LL

*Printed by Technical Editing and Reproduction Ltd  
Harford House, 7-9 Charlotte St. London W1P 1HD*

## THEME

The recent past has seen a great proliferation of avionics equipment and subsystems to meet new and expanded mission requirements resulting in very large systems.

Not only are the actual numbers increasing, but also they are now appearing in all parts of the frequency spectrum, many of them simultaneously.

The application of these systems in aircraft and the resulting mobility of the ground forces results in a very dynamic ever-changing highly interactive environment.

Within the equipment and the subsystems themselves we have witnessed a dramatic change in the technology used. The use of spread spectrum, new synthesizer techniques, large scale integrated circuits, multiplexing of antennas, new power generation and switching techniques are but a few. New levels of interference are being encountered as a result of a greater number and closer spacing of channels and the utilization of new energy levels, and at the same time a desire to go further into the noise to receive desired signals.

Therefore, it would seem appropriate to re-examine this area and provide a reassessment of how we can provide new systems to meet an operational requirement on a cost-effective basis.

## PROGRAM AND MEETING OFFICIALS

**PROGRAM CHAIRMEN:** Mr T.J.Sueta (Avionics Panel)  
Deputy Director  
Avionics Laboratory  
U.S. Army Electronics Command  
Fort Monmouth, N.J.07703  
U.S.A.

Capitaine de Fregate P.Halley  
(Electromagnetic Wave Propagation Panel)  
Ingenieur en Chef au C.N.E.T.  
38-40, rue du General Leclerc  
92131, Issy-les-Moulineaux  
France

## PROGRAM COMMITTEE

Ing. Gen. Bertrais  
F.N.I.E.  
Paris,  
France.

Prof. P.Gudmandsen  
Technical University,  
Lyngby,  
Denmark

Mr F.Harrison  
RRE, Malvern,  
UK

Dr T.R.Hartz  
CRC, Ottawa,  
Canada

Prof. M.F.Horner  
Radio and Space Research Station  
Slough,  
U.K.

Dr T.L.Maxwell  
Colorado State University  
Fort Collins  
U.S.A.

Ir. H.A.Timmers  
NLR Amsterdam,  
Netherlands

Mr S.Zacchari  
Griffiss AFB, N.Y.  
U.S.A.

## PANEL OFFICERS

### Avionics Panel

Chairman: Mr K.Voles, EMI, Hayes, UK  
Deputy Chairman: Mr J.N.Bloom, CRC, Ottawa, Canada

### Electromagnetic Wave Propagation Panel

Chairman: Prof. I.Ranzi  
Istituto Superiore P.T.Roma, Italy  
Deputy Chairman: Capt. de Fregate P.Halley  
C.N.E.T., Paris, France

## EXECUTIVE

Dr N.R.Ogg  
AGARD

12

## CONTENTS

	Page
THEME	iii
PROGRAM AND MEETING OFFICIALS	iv
	Reference
 <u>SESSION I - INVITED PAPERS ON THE FUNDAMENTALS OF EM NOISE AND EMC</u>	
DEFINITIONS AND FUNDAMENTALS OF ELECTROMAGNETIC NOISE, INTERFERENCE AND COMPATIBILITY by G.H.Hagn	1
ATMOSPHERIC DISCHARGES AND NOISE (AND COMMUNICATIONS SYSTEMS INTERFERENCE REDUCTION) by M.M.Newman and J.D.Robb	2
MAN-MADE ELECTROMAGNETIC NOISE FROM UNINTENTIONAL RADIATORS: A SUMMARY by G.H.Hagn and R.A.Shepherd	3
LES BRUITS COSMIQUES par A.Boischot	4
LAND AND SEA AND ATMOSPHERIC THERMAL NOISE by P.G.Davies	5
IONOSPHERIC AND TROPOSPHERIC SCINTILLATION AS A FORM OF NOISE by E.J.Fremouw and C.L.Rino	6
 <u>SESSION II - CONTRIBUTED PAPERS ON EM NOISE</u>	
THE INFLUENCE OF PARTICULAR WEATHER CONDITIONS ON RADIO INTERFERENCE by C.Fengler	7
LES CHARGES ELECTROSTATIQUES ET LES PERTURBATIONS QU'ELLES ENTRAINENT DANS LES LIAISONS RADIOELECTRIQUES par C.Févré	8
POLARIZED NOISE IN THE ATMOSPHERE DUE TO RAIN by A.Mawira and J.Dijk	9
DEPOLARISATION AND NOISE PROPERTIES OF WET ANTENNA RADOMES by J.Dijk and A.C.A. van der Vorst	10
ANTENNA RESPONSE TO RANDOM ELECTRIC FIELDS DUE TO THERMODYNAMIC DENSITY FLUCTUATIONS IN PLASMAS by R.Grahowski	11
THE INFLUENCE OF FREQUENCY AND RECEIVER APERTURE ON THE SCINTILLATION NOISE POWER by M.J.M. van Weert	12
 <u>SESSION III - EMC SPECIFICATIONS</u>	
DOD ELECTROMAGNETIC COMPATIBILITY PROGRAM - AN OVERVIEW by J.J.O'Neil	13
GENERAL EMC SPECIFICATION OR SYSTEMS ORIENTED EMC SPECIFICATIONS by D.Jaeger	14

	Reference
<b>SPECIFICATIONS EMC</b> by J.C.Delpech	15
<b>A STATUS REPORT OF THE IEEE/ECAC ELECTROMAGNETIC COMPATIBILITY FIGURE OF MERIT COMMITTEE</b> by G.H.Hagn and M.N.Lustgarten	16
<b><u>SESSION IV - EMC AND PFI DESIGN AND MANAGEMENT TECHNIQUES</u></b>	
<b>ELECTROMAGNETIC COMPATIBILITY IN MILITARY AIRCRAFT</b> by D.H.Hight and W.A.Kelly	17
<b>ELECTROMAGNETIC COMPATIBILITY CONTROL PLANS</b> by P.D.Campbell	18
<b>MANAGEMENT OF AN EMC ENGINEERING DESIGN PLAN*</b> by J.E.R.Fogg and M.T. Le Grys	19
<b>A CASE FOR AN EVALUATION AND ADVISORY SERVICE</b> by E.M.Frost	20
<b>INTERFERENCES DANS LES SYSTEMES A MODULATION DE FREQUENCES</b> par G.Crocombette	21
<b>RADAR INTERFERENCE REDUCTION TECHNIQUES</b> by W.Fishbein, R.Olesch and O.Rittenbach	22
<b><u>SESSION V - COMPUTER MODELLING, SIMULATION AND ANALYSIS APPLIED TO EMC</u></b>	
<b>APPLICATION OF PROGRAMMABLE CALCULATORS TO EMC ANALYSIS</b> by J.P.Georgi and P.D.Newhouse	23
<b>APPLICATION OF MARKOV CHAIN THEORY TO THE MODELLING OF IFF/SRR SYSTEMS</b> by S.J.Sutton and C.Wayne Ehler	24
<b>COMPUTER GENERATION OF AMBIGUITY SURFACES FOR RADAR WAVEFORM SYNTHESIS</b> by R.J.Morrow and G.Wyman	25
<b>ANTENNA-TO-ANTENNA ELECTROMAGNETIC COMPATIBILITY ANALYSIS OF COMPLEX AIRBORNE COMMUNICATION SYSTEMS</b> by W.L.Dillion	26
<b>ANALYSE DU BRUIT ET DE SON INFLUENCE SUR LES SYSTEMES DE COMMUNICATION</b> par R.Gouillou	27
<b>COMPUTER MODELING OF COMMUNICATIONS RECEIVERS FOR DISTORTION ANALYSIS</b> by J.F.Spina and D.D.Weiner	28
<b>COMPARATIVE ANALYSIS OF MICROWAVE LANDING SYSTEMS WITH REGARD TO THEIR SENSITIVITY TO COHERENT INTERFERENCE</b> by B.Forsell	29
<b>THE CROSSED-DIPOLE STRUCTURE OF AIRCRAFT IN AN ELECTROMAGNETIC PULSE ENVIRONMENT</b> by R.W.Burton	30
<b><u>SESSION VI - INSTALLATION AND INTERFACE PROBLEMS</u></b>	
<b>PROBLEMES POSES PAR LA TRANSMISSION DANS UN SYSTEME INTEGRE AEROPORTE</b> par C.David et M.Vannetzel	31

---

\* Not available at time of printing

**DIGITAL DATA TRANSMISSION IN AIRCRAFT: EMC-PROBLEMS AND POSSIBLE SOLUTIONS**

by R.Rode

32

**GENERATIONS ET EFFETS DES TENSIONS PARASITES DE CONDUCTION ET DE RAYONNEMENT ENTRE ENSEMBLES D'UN MEME SYSTEME**

par A.Quidet

33

**THE REDUCTION OF EMC DUE TO NON LINEAR ELEMENTS AND UNINTENDED RANDOM CONTACTING IN THE PROXIMITY OF ANTENNAS OF HIGH POWER RF TRANSMITTERS**

by K.Landt

34

**IMPROVED DESIGN OF INTERFERENCE SUPPRESSORS AND MEASUREMENT OF ATTENUATION CHARACTERISTICS**

by M.L.Jarvis and J.D.Hawkett

35

**SESSION VII - EMC TESTING, TECHNIQUES AND EQUIPMENT****MISSILE INTERSYSTEM EMC TESTING**

by C.D.Ponds

36

**MEASUREMENT OF INTERWIRING COUPLED NOISE**

by B.Audone and L.Bolla

37

**ON THE EVALUATION OF MAN-MADE ELECTROMAGNETIC NOISE INTERFERING WITH COMMUNICATIONS IN THE E.L.F. RANGE**

by G.Tacconi

38

**AUTOMATIC TESTING OF AVIONICS SYSTEMS FOR ELECTROMAGNETIC COMPATIBILITY**

by E.T.Tognola and J.Rubin

39

**DESIGN OF A COMMUNICATION TEST (TEMPEST) RECEIVER FOR MAXIMUM BROAD BAND DYNAMIC RANGE**

by J.B.Hager, J.C.Jones and J.R.VanCleave

40

**A STRAIGHT FORWARD COMPUTER ROUTINE FOR SYSTEM CABLE EMI ANALYSIS**

by M.Russo and O.Hartal

41

**A UNIVERSAL ELECTROMAGNETIC COMPATIBILITY (EMC) ANALYZER UTILIZING BASIC CIRCUIT MODULES**

by K.E.Wieler and W.A.Kesselman

42

VII

1-1

DEFINITIONS AND FUNDAMENTALS OF ELECTROMAGNETIC  
NOISE, INTERFERENCE, AND COMPATIBILITY

G. H. Hagn  
Stanford Research Institute  
1811 North Kent Street  
Arlington, Virginia 22209  
USA

SUMMARY

The terms electromagnetic noise, interference, and compatibility are defined, and some of the different definitions for these terms in current usage are discussed with emphasis on international definitions. For this paper, noise is defined as all electromagnetic energy except that associated with the desired signal for a specific system of interest. Categories of noise are specified according to source: undesired signals from intentional radiators, noise from intentional radiators other than the desired signal from that radiator, and the noise that is generated by unintentional radiators. Interference is considered to be an undesirable effect of electromagnetic noise upon a system or subsystem (i.e., the degradation produced) rather than as a cause or source of noise. Electromagnetic compatibility is the condition that prevails when telecommunications equipment is collectively performing its individually assigned functions in a common electromagnetic environment without causing or suffering unacceptable interference. Selected aspects of the fundamentals of noise, interference, and compatibility are discussed, and suggested definitions for these terms are offered for the purpose of this meeting.

1. INTRODUCTION

The radio frequency spectrum is a reusable quantity having the dimensions of frequency, time, and space; and our telecommunications\* systems are users of this "invisible resource," as LEVIN (1971) has called it. The multidimensional spectrum is occupied primarily by electromagnetic noise from natural and man-made sources; desired signals for any given system account for only a small part of it (Fig. 1). To get our telecommunications systems to operate effectively together while sharing this resource we must employ the tools of modern spectrum engineering and management: analyses, measurements, data bases, and coordination processes (JTAC, 1988). In peacetime we must accomplish this within the framework of the international regulatory process (ITU, 1968, 1971, 1973), and during wartime we must accomplish this through coordination among allies.

The topic of this meeting is electromagnetic noise (EMN), interference (EMI), and compatibility (EMC); and the subject of this paper is definitions and fundamentals. For a given system, electromagnetic noise is all the electromagnetic energy in the environment of that system exclusive of that forming the desired signal. EMN exists as a fact of life (Fig. 1). Electromagnetic interference is considered here only as an undesirable effect, namely the effect of degradation of the operational performance of a telecommunications system or systems by EMN. The important topic of electronic warfare (EW) is not within the scope of this paper. Electromagnetic compatibility is many things to many people. It can be viewed as a goal that is achieved when systems or subsystems are able to function adequately in their operational environment without experiencing or causing unacceptable interference. EMC also can be considered to be the condition of having reached the goal. This latter interpretation is most consistent with common (nontechnical) usage of the term compatibility. A useful distinction exists between design EMC and operational EMC. In many cases it is better to obtain the "solution" during the design of a system without waiting for the "problem" to occur during actual operations. The relationship between EMN, EMI, EMC, and spectrum engineering is illustrated in Fig. 2. Definitions of these terms that are in common usage are discussed in Sec. 2, and definitions suggested for use during this meeting are presented in Sec. 4.2.

It is difficult to say much that is new regarding the most basic fundamentals of electromagnetic noise, interference, and compatibility. Textbooks already exist (e.g., COOK, A. H., 1971; FICCHI, R. F., 1971; TAYLOR, R. E., 1971; WHITE, D.R.J., 1971a, 1971b, 1973; DUFF, W. G. and WHITE, D.R.J., 1972; EVERETT, W. W. Jr., 1972), and they are being improved. It is useful to categorize the noise sources that contribute to the composite electromagnetic noise environment according to their origin (natural or man-made) and, for the man-made sources, according to whether the source of the radiation (or induction or conduction) is an intentional radiator or not (Fig. 3). Additional subcategories are mentioned in Sec. 3.1. The papers in the remainder of this session will presumably address most of these subcategories, discuss their technical characteristics and comment on their contribution to the composite

\* Telecommunications, as used here, is broadly defined to mean any transmission, emission or reception of signs, signals, writing, images, and sounds or information of any nature by wire, radio, visual or other electromagnetic systems.

electromagnetic noise environment. The units in which the noise (from all the sources) is measured are fundamental; the present situation is confused because of lack of standardization (see Appendix). Some of the fundamentals of the equally important topics of the effects of noise on specific systems of interest (i.e., description of the interference it causes to these systems) and mitigation of the negative aspects of the effects by spectrum engineering to produce EMC are discussed briefly.

## 2. DEFINITIONS

### 2.1. Scope of Definition Discussion

The term spectrum engineering was coined long ago and was used as part of the title for the Joint Technical Advisory Committee (JTAC) [of the Institute of Electrical and Electronics Engineers (IEEE) and the U.S. Electronics Industries Association (EIA)] report on the topics of noise, interference, compatibility, and related matters (JTAC, 1968): "Spectrum Engineering--The Key to Progress." Agreement on basic definitions is a requisite for progress in all disciplines including spectrum engineering.

Standardization of the definitions of general engineering terms, as well as the special terms used in spectrum engineering and management is necessary not only from the standpoint of technical needs but also from the standpoint of regulatory (legal), economic and even social and political needs. Occasionally conflicts arise among these needs that impact directly on the definitions. Within the North Atlantic Treaty Organization (NATO) community, standard definitions for the principal electromagnetic symbols have been most recently summarized by HALLEY (1974). These symbols represent some of the basic building blocks for sound spectrum engineering; standardization of the units for these symbols is important. Even acronyms and abbreviations are among the useful tools (e.g., WHITE, D.R.J., 1971c), and unnecessary confusion results when the same acronym is used for different things.

Certain terms are required specifically for working in the area of spectrum engineering and management. At the international regulatory level, the International Telecommunication Union (ITU) is the recognized authority. The ITU obtains its primary technical input from the International Radio Consultative Committee (CCIR) which itself draws on support from other groups. Some of these special terms have been defined and agreed upon within nonregulatory international groups, such as the International Electrotechnical Commission (IEC) which is affiliated with the International Organization for Standardization. Other terms enjoy national definitions (e.g., the American National Standards Institute, ANSI, and equivalent organizations in other countries), and still other terms are defined to facilitate the work of specific groups some of which, such as the IEEE, have international memberships. The IEEE defers to the IEC whenever possible (IEEE, 1972). NATO has generated some definitions (e.g., NATO, 1972). The Advisory Group for Aerospace Research and Development (AGARD) functionally supplements NATO in a manner somewhat analogous to that in which the CCIR supplements the ITU. LEIVE (1970) and BURTON (1972, 1973) discuss some of the organizational and functional relationships of some of these international bodies; but the exact details of these relationships, as they pertain to the definitions of technical terms, are difficult to construct in a simplified format. It may be observed that there is some considerable variation among definitions of even the most basic terms within the standard references of these groups. In addition to the terms in these "standard" references, there are certain terms of controversy that have not yet achieved even the level of agreement and consistency as those in the references (e.g., some of the terms used by national groups or subgroups). Still other terms remain as yet undefined and in need of definition. The terms that form the title of this meeting, electromagnetic noise, interference, and compatibility, will each be addressed in greater detail and a few other terms will be mentioned to represent examples of the terms of controversy and terms still requiring some definition. Some comments are also made on the standard definitions for general engineering practice and the modifications or additions to them that are necessary when they are applied to spectrum engineering.

### 2.2 International Regulatory Definitions of Noise, Interference and Compatibility

#### 2.2.1. Background

There are no regulatory (legal) definitions of either electromagnetic noise or electromagnetic compatibility at the international level, although the CCIR works on noise and compatibility problems (e.g., CCIR, 1964, 1974); however, there are regulatory definitions of interference (ITU, 1968, 1973). International activities can and do provide useful inputs to the regulatory processes of individual countries even when no international regulations apply. For example, some of the recommendations of the International Special Committee on Radio Interference (CISPR, see STUMPERS, F. L., 1970, 1971, 1973) have been incorporated into the regulatory processes of several countries regarding limits of emissions from specific types of devices. The CISPR also makes inputs to the CCIR, as do other international groups, e.g., the International Union of Radio Science (URSI).



## 2.2.2. Interference

1-3

The international regulatory (legal) definitions of interference are generated by the ITU. The term harmful interference has been in use for a long time. It is defined in Article 1, No. 93 of the ITU Radio Regulations (ITU, 1968):

"Harmful Interference: Any emission, radiation or induction which endangers the functioning of a radionavigation service or of other safety services or seriously degrades, obstructs or repeatedly interrupts a radiocommunication service."

At its most recent Plenipotentiary Conference in Torremolinos, Spain, in 1973, the ITU reaffirmed in Article 4, Purposes of the Union, that the Union shall in particular:

- a) effect allocation of the radio frequency spectrum and registration of radio frequency assignments in order to avoid harmful interference between radio stations of different countries;
- b) coordinate efforts to eliminate harmful interference between radio stations of different countries and to improve the use made of the radio frequency spectrum." (Italics added by author.)

Prior to the World Administrative Radio Conference on Space Telecommunications (ITU, WARC-ST) in 1971, harmful interference was the only term with an international regulatory meaning. In the United States this term has been part of national regulatory process for many years (OTF, 1974; FCC, 1974), and we believe that this is the case in other countries. At the ITU WARC-ST in 1971, the concept of planned interference was introduced, and the terms "acceptable (or unacceptable)" and "permissible" interference were used. Definitions of these terms were not included in the Final Acts of the WARC-ST (ITU, WARC-ST, 1971). However, Recommendation SpA 2-15, Para. 2.12, requested the CCIR to study the terms "acceptable (or unacceptable) and harmful interference" with a view toward formulating clear definitions. In Para. 2.5. of this same recommendation, the CCIR was asked to study the criteria of permissible interference for the various space and terrestrial radio communication services sharing the frequency bands allocated by the WARC-ST. Study Group 1 (Spectrum Utilization and Monitoring)\* of the CCIR addressed the matter of definitions of interference in Geneva in February and March of this year and again in July (CCIR, 1974) and agreed to retain the definition of harmful interference stated above with the replacement of "Any emission, radiation or induction which endangers ..." by "Any interference which endangers ...." The CCIR Study Group 1 made the following observations: "To avoid ambiguities, it is desirable to define the term 'interference' itself before defining qualifications or gradations of it. Since the sole purpose of a receiving system is to extract information from a wanted emission, it appears reasonable to judge unwanted energy by its effect on such wanted information, and to define that effect as interference." (Italics added.)

Several definitions were put forward. The definition preferred by Study Group 1 was: "Interference. The effect of one or a combination of emissions, radiations, or inductions upon reception in a radiocommunication system, manifested by any degradation, misrepresentation, or loss of information which could be extracted in the absence of such unwanted energy."

An alternative suggestion was: "Interference. The effect of unwanted energy represented by one or a combination of emissions, radiations, or inductions, upon reception in a radiocommunication system, manifested by any degradation, misrepresentation or loss of information."

A simpler definition has also been suggested: "Interference. The effect of unwanted energy comprised of one or a combination of emissions, radiations, or inductions, upon reception in a radiocommunication system."

The CCIR Study Group 1 also observed that in connection with Radio Regulations (ITU, 1968, 1973), there is need for a term for a signal determined to be a cause of interference:

"Interfering signal. An emission, radiation, or induction originating in a radiocommunication system, which is determined to be the cause of interference."

An undesired signal has the potential to cause interference, but it does not become an interfering signal until it has caused degradation.

No formal CCIR Recommendation was forthcoming, even after considerable effort was made to reach agreement on the definition of this most basic term, interference. This observation is not made as a criticism. On the contrary, the CCIR Study Group 1 is to be commended for its efforts. The report (CCIR, 1974) was accepted by the XIIIth Plenary Assembly of the CCIR in Geneva in July. This example

\* An ad hoc working group on definitions, chaired by Mr. R. C. Kirby (USA, currently Director, CCIR, Geneva), provided a focal point for generating much of the information contained in the remainder of Sec. 2.2.2.

illustrates that considerable effort will be required to obtain international regulatory definitions of EMI, RFI, EMC, and related terms.

1-4 The term "unacceptable interference" was used in the Final Acts, WARC-ST in Sec. IX, Space Radio Telecommunication Services, 470VA, Spa 2, Para. 25, regarding protection for geostationary satellites from nongeostationary space stations in the fixed-satellite service (and their associated earth stations), and footnote 470VA.1, Spa 2 added that "The level of unacceptable interference shall be fixed by agreement between the administrations concerned, using relevant CCIR Recommendations as a guide." This same footnote is repeated as 470VE.1 in Para. 26, regarding satellite networks. These terms were used without precise definition in the Final Acts of the WARC-ST (1971) and became part of the ITU Radio Regulations on 1 January 1972. When the CCIR Study Group 1 addressed defining acceptable (or unacceptable) interference at its February-March 1974 meeting in Geneva, other terms (e.g., permissible interference) also were discussed:

"There may be associated with the planning or operation of any service, or with any frequency-sharing situation, a low degree of interference, or a sharing criterion, which if complied with, is intended to assure satisfactory performance. This degree of interference is variously referred to as negligible, tolerable, permissible, etc. System planning and coordination must be conducted on such a basis, relying on quantitative predictive tools which allow predicted interference to be bounded by suitable quantitative criteria. Such criteria may be agreed internationally in the C.C.I.R. or adopted as a matter of Radio Regulation. A definition is proposed which emphasizes the authoritative nature of the international agreements required for quantitative criteria for such permissible interference:

"Permissible interference. Observed or predicted interference which complies with quantitative interference and sharing criteria contained in the Radio Regulations or in Recommendations of the C.C.I.R. or in regional agreements as provided for in the Radio Regulations."

"In certain services, interference not complying with the criteria for permissible interference, may be regarded immediately as harmful. In other services, there may exist a range of interference between permissible interference and harmful interference, in which the interference may be accepted by agreement between the administrations concerned or may be regarded as unacceptable. Views representing various services are contained in the documents of several Study Groups."

There was general agreement that as one escalated from no interference toward harmful interference one would next have permissible interference. Figure 4 gives a general interpretation and references to CCIR documents used as working papers at the meeting. Two basic questions were involved: (1) Should there be a range of severity of interference between harmful (as historically defined) and permissible (as defined above) for the various types of service, and (2) if such a grey area or "margin" were to be defined what should it be called? Representatives of most of the types of service (except broadcasting and radio astronomy) concluded that there should be such a grey area, but no real consensus emerged about what to call it.

Some delegates expressed the view that definitions of the concept of acceptable or unacceptable interference attempt to define the obvious. Instead of definitions, the following explanatory text was suggested:

"Permissible interference and harmful interference could have in some radiocommunication services different quantitative values so that there exists between these two values a margin in which a given interference exceeding the permissible interference is accepted mutually by agreement between the administrations concerned. The 'acceptable interference' and 'unacceptable interference' referred to in the Radio Regulations are situated in this margin."

Nevertheless, a number of delegations felt that a definition should be considered, and the following definition was discussed:

"Acceptable (or Accepted) interference. Interference which does not, or does not appear to, comply with quantitative criteria for permissible interference, but is nevertheless by agreement between the administrations concerned, considered to be acceptable for an existing or planned system, without prejudice to services of other administrations."

The conclusion reached by the CCIR in Geneva read as follows:

"Tentative, and in some cases alternative, definitions have been suggested for interference, interfering signal, harmful interference, permissible interference and acceptable (or unacceptable) interference."

"Further study of these terms, and efforts to apply their definitions in practical planning and operational situations", may be expected to lead to their improvement or replacement by the time of the XIVth Plenary Assembly in advance of the planned 1979 Administrative Radio

Conference. In particular, service-oriented Study Groups are urged to consider the quantitative interference and sharing criteria which will be essential to meaningful use of the qualitative definitions." 1-5

The author believes that a margin or grey area should be defined between permissible and harmful interference for use by certain types of service. The author prefers a scale of severity of interference: none → permissible → negotiable → harmful. The term none would equate to the condition of no degradation. Permissible would correspond to the amount of degradation permitted under the ITU Rules and Regulations. Negotiable would correspond to more degradation than that permitted by the ITU Rules and Regulations but less than any of the interested parties would finally agree was truly harmful (as defined in the ITU Rules and Regulations). Such a negotiated level of interference would, after negotiation, be "acceptable" to the negotiating parties but it would not apply to others. Various proposed levels in this grey area upon which agreement has not been reached might be termed "unacceptable" prior to agreement on a final "acceptable" level. These terms are qualitative; the boundaries between the categories still require analysis and technical quantification. After this quantification has been accomplished for each type of service the boundaries could be plotted on an absolute scale analogous to the relative scale used in Fig. 4. When this is done, the boundaries probably will not be aligned evenly as they are in the conceptual representation of Fig. 4. The boundary between none and permissible could correspond to the minimum interference threshold (MIT, e.g., KRAVITZ, F., 1973), and the boundary between permissible and negotiable could be quantified by the CCIR for the various types of service. There may be utility to a firm boundary between permissible and negotiable, while it may be useful to leave the boundary between negotiable and harmful subject to interpretation on a case-by-case basis.

### 2.3. International Technical Definitions of Electromagnetic Noise, Interference, and Compatibility

#### 2.3.1. Electromagnetic Noise

There are no NATO or Allied Communication Publication (ACP) definitions of electromagnetic noise (JCS, 1971/1973). The definitions of electromagnetic noise available from several other sources are observed to be different, and the terms noise and disturbance are sometimes used interchangeably (Table 1).

TABLE 1 DEFINITIONS OF ELECTROMAGNETIC NOISE AND ELECTROMAGNETIC DISTURBANCE

Term	IEEE Dictionary, 1972	IEC International Electrotechnical Vocabulary (IEV), 1973
Electromagnetic noise	An electromagnetic disturbance that is not of a sinusoidal character.	An electromagnetic phenomenon that does not correspond with any signal and that is usually impulsive and random but may be of a periodic nature.  Note: In some countries, periodic phenomena are not encompassed by the term "noise."
Electromagnetic disturbance	An electromagnetic phenomenon that may be superimposed on a wanted signal.	Electromagnetic noise which is liable to be superimposed on a wanted signal.  Note: The two terms above have very similar meanings and in some countries the definitions may be the reverse of those given above.

Some of the terms in the IEEE Dictionary (1972) were submitted to the IEC in the preparation of the International Electrotechnical Vocabulary (IEV; IEC, 1973) by the IEEE Group-27 on EMC. It is interesting to note that the IEEE Dictionary attributes at least part of its source for the definition of electromagnetic noise to CISPR, which prepared Chapter 902 of the IEV. The point of all this is not to find fault with either the IEC or the IEEE\* but to note that there are still inconsistencies among their documents regarding the definition of electromagnetic noise. These inconsistencies are most difficult for the neophyte who attempts to use "standard" terminology when writing a paper or report or attempts to read one.

The author's personal preference is to consider all electromagnetic energy but that conveying the intelligence in a desired (wanted) signal (or energy required to extract the intelligence such as reference tone) as electromagnetic noise.

#### 2.3.2. Interference

This topic was discussed in the international regulatory sense in Sec. 2.2. Here the discussion focuses on additional technical aspects. There are two basic causes of confusion regarding the term interference: (1) The term is commonly used to describe both a cause (i.e., source, e.g., JCS 1971/1973;

\* The IEEE Dictionary states that the IEEE Technical Committees have been instructed to give preference to IEC Recommendations, and obviously the IEC has benefitted from many IEEE suggestions.

1-6  
NATC, 1972) and an effect on a victim system (e.g., IEC, 1973). Webster's New Collegiate Dictionary (1974) defines interference as "confusion of received radio signals due to strays or undesired signals," and also as "something that produces such confusion"; and the IEEE Dictionary recognizes the fact that both uses of the term are common (IEEE, 1972). The IEEE definition applies to signal transmission systems. Table 2 summarizes these definitions. (2) The terms noise and interference are commonly used

TABLE 2 COMPARISON OF DEFINITIONS OF INTERFERENCE

Source	Term and Definition
IEC, IEV 1973	Electromagnetic interference: Impairment of the reception of a wanted electromagnetic signal caused by an unwanted electromagnetic signal, or by an electromagnetic disturbance.
JCS 1971/ 1973	Interference: Any electrical disturbance which causes undesirable responses in electronic equipment.
NATO 1972	Interference: Interference is defined as any electrical or electromagnetic disturbance, phenomenon, signal or emission, manmade or natural, which causes or can cause undesired response, malfunctioning or degradation of performance of electrical and electronic equipment, or premature and undesired location, detection or discovery by enemy forces, except deliberately generated interference (electronic countermeasures).
IEEE 1972	Interference: Either extraneous power, that tends to interfere with the reception of the desired signals, or the disturbance of signals that results. Note: Interference can be produced by both natural and manmade sources either external or internal to the signal transmission system.

interchangeably. The author's preference is to consider noise as a cause and the interference that may result as an effect. The JCS (1971/1973) definition of harmful interference is identical to that given by ITU (1968) except that it adds "operating in accordance with international regulations" to the end of the ITU definition.

#### 2.3.3. Electromagnetic Compatibility

The term electromagnetic compatibility was coined to give a positive focus to the field of endeavor that had previously been called radio frequency interference (RFI) and prior to 1964 the IEEE Transactions on Electromagnetic Compatibility were called IEEE Transactions on Radio Frequency Interference. As stated in Sec. 1, EMC is many things to many people. To some it is a goal toward which to strive in designing and planning for the deployment of systems. To others it is an operational state in which harmful interference does not exist. There is no definition of EMC in ACP 167(C), as promulgated by the JCS (1971/1973). To the IEEE (1972), IEC (1973), and NATO (1973), it is a capability of electronic equipment or systems as described in Table 3. All three of these definitions are similar to the U.S. Department of Defense definition (DOD, 1967/1972), which has been added to Table 3 for comparison.

TABLE 3 DEFINITIONS OF ELECTROMAGNETIC COMPATIBILITY

Source	Definition
IEEE, 1972	The capability of electronic equipments or systems to be operated in the intended operational electromagnetic environment at designed levels of efficiency.
IEC, 1973	The ability of signals and interference to coexist without loss of the information contained in the wanted signal.
NATO, 1973	The capability of aircraft electrical and electronic systems, subsystems, assemblies and equipment to operate, as installed on an aircraft, without experiencing degradation of performance beyond specification limits due to mutual interference.
DOD 1967/ 1972	Electromagnetic compatibility (EMC) is the condition which prevails when telecommunications equipment is collectively performing its individually designed functions in a common electromagnetic environment without causing or suffering unacceptable degradation due to unintentional electromagnetic interference to or from other equipment system in the same environment.

The NATO (1973) definition is limited to aircraft applications; and, appropriately, there has been a major emphasis on intrasystem EMC. A discussion of the analysis of intrasystem EMC in large ground and aerospace systems has been given by HIEBERT and SCHARFF (1974) and a discussion of intersystem EMC was given by DUFF (1973). DUFF (1973) also discussed the advantages and disadvantages of both measurements and analysis for this class of EMC problems.

The author prefers the NATO, DOD, and IEEE definitions to the IEC definition because the latter does not allow for planned interference (see Sec. 2.2.2.) which, while causing some loss of information, is not "harmful." A good case can be made for considering EMC to be a condition as well as the capability to achieve a condition (e.g., as pertinent to operational and design EMC, respectively).

## 2.4. National Administration and Group Definitions

Many of the international definitions discussed in the preceding paragraphs are adopted by national administrations and groups and these groups suggest definitions to the international organizations. It is beyond the scope of this paper to do more than acknowledge that numerous definitions of noise, interference, and compatibility exist at this level. It might be noted in passing that the U.S. DOD (1967/1972) found it convenient to distinguish between design and operational compatibility:

"Design compatibility is EMC achieved by incorporation of engineering characteristics or features in all electromagnetic radiating and receiving equipments (including antennas) in order to eliminate or reject undesired signals, either self generated or external, and enhance operating capabilities in the presence of natural or man-made electromagnetic noise.

Operational compatibility is EMC achieved by the application of C-E equipment flexibility to ensure interference-free operation in homogeneous or heterogeneous environments of C-E equipments. It involves the application of sound frequency management and clear concepts and doctrines to maximize operational effectiveness. It relies heavily on initial achievement of design compatibility."

## 2.5. Terms of Controversy

It may appear that at the international regulatory level all definitions involve terms of controversy except, perhaps, harmful interference, which is usefully vague and which has been employed for a long time. A number of differences still remain to be worked out at the international technical level between the definitions put forth by the IEC, IEEE, etc. Controversy still exists, for example, over the various definitions of system and subsystem. The IEEE (1972) defines system as "an integrated whole even though composed of diverse, interacting, specialized structure and subjunctions," and subsystem as "a division of a system that in itself has the characteristics of a system." SACHS (1974) has taken the opposite approach and defined a system as "a combination of sub-systems that performs a specified operational function," and a subsystem as "any combination of circuit components that performs a specified technical function." These definitions seem reasonable enough until one attempts to apply them to a spectrum engineering problem. Just as one man's signal is another man's noise, so one man's system is another man's subsystem. If a system is composed of subsystems it may be necessary to define interfaces between the subsystems for the purpose of specifying EMC performance. The hierarchy of component, equipment, subsystem, and system can be useful for some applications, but it is beyond the scope of this paper to pursue this topic further.

## 2.6. Concepts and Their Related Terms Requiring Definition

Many concepts related to spectrum engineering and management, when better formulated, will generate terms requiring definition. One such concept for which a definition has recently been put forth is that of an EMC figure of merit for a system (or subsystem) based upon the concept of channel denial (HAGN, G. H. and LUSTGARTEN, M. N., 1974). This concept pertains to the capacity for compatibility of specific equipment as deduced from measurements one can make in a laboratory as differentiated from their actual operational performance in any given situation. Extensions of this concept (and definition) may be required.

Another important concept that requires definition is spectrum saturation. This topic was addressed by JTAC (1968), but specific criteria were not developed. Channel occupancy has been defined by DAYHARSH et al. (1969), HAGN et al. (1971, 1973a) and others (e.g., BARGHAUSEN, A. F. and HAILEY, L. G., 1974). It is possible to develop algorithms relating waiting time to access a channel to channel occupancy. One could then observe occupancy, estimate waiting time, and define saturation of a given channel to occur when the mean waiting time (or some other statistic) exceeded a given value (chosen to be germane to the mission) for a given percentage of the time. Other definitions of saturation in a given region should be explored for channels, bands of channels, etc.

Spectrum pollution by unintentional radiators was addressed by PETERSON (1974), in a session at the International Conference on Communications titled "The Radio Spectrum--Polluted Pond or Flowing River?" which reviewed the activities of the JTAC. Peterson notes: "The performance of many radio systems is limited by man-made radio noise, but relatively few definitive data are available regarding the sources, characteristics, or effects of the noise. Even less is available concerning the impact of man-made noise on spectrum utilization and its economic significance. Discussion of noise characteristics and changes with time have been made difficult in the past by the lack of consistent, widely accepted definitions and units along with reliable standardized measurements, procedures and equipments."

Having considered the definitions of noise, interference, and compatibility, let us now consider a few selected fundamentals that pertain.

## 3. FUNDAMENTALS

Since it is not possible to discuss all the fundamental aspects of electromagnetic noise, interference, and compatibility in this paper, we will select several of the more important aspects of each of these topics.

### 3.1. Noise

1-8 The sources that contribute to the composite electromagnetic noise (EMN) environment can be categorized as natural and man-made (e.g., Fig. 3) and each of these categories can be further subdivided in a variety of ways (e.g., Fig. 5).

#### 3.1.1. Noise--A Random Process

It is most fundamental that noise be considered as a random process. BENDAT and PIERSON (1971) have defined four main types of statistical functions used to describe the basic properties of random data: (a) mean-square values, (b) amplitude probability density functions, (c) autocorrelation functions, and (d) power spectral density functions. The mean-square value, which is simply the average of the squared values of the time history, furnishes a rudimentary description of the intensity of any random data. The amplitude probability density function furnishes information on the properties of the data in the amplitude domain, namely, the probability that the amplitude will fall within some defined range at any instant of time.\* The autocorrelation function and the power spectral density function furnish similar information in the time domain and frequency domain, respectively. For stationary data (in the strict sense) the power spectral density function technically supplies no new information over the autocorrelation function since the two are Fourier transform pairs.

The noise process of interest is the one that is seen by the part of our receiving system where we are attempting to extract information from the desired signal. We need to describe this process in order to evaluate the performance of a particular system, and we also need it to design future systems that are more nearly optimum for operation in specific types of noise environments. The same statistical tools of the technical trade are required for both analysis and synthesis. We are almost always interested in a narrow-band noise process that is capable of being characterized by an envelope and phase. This condition exists when we employ systems where the bandwidth of a bandpass filter is a small fraction of the center frequency,  $f_c$ , to which the filter is tuned. The instantaneous value of the noise process at the output of a narrow-band filter can be represented as

$$n(t) = v(t) \cos [2\pi f_c t + \phi(t)] ,$$

where  $v(t)$  is the envelope process and  $\phi(t)$  is the phase process. We would like to know the statistics of  $n(t)$  at the output of the various stages of a proposed receiver to facilitate receiver synthesis, but it is especially important to know it at the output of the predetection filter to facilitate performance analysis. When we can assume  $\phi(t)$  is uniformly distributed (as we frequently can in the absence of undesired signals), we can focus on the envelope statistics that would be observed at the output of a linear detector.

The average noise power (the mean-square value of the envelope voltage appropriately normalized by multiplication by the real part of the admittance across which the voltage is developed) is the most fundamental measure of the noise envelope in the random-process context. The basic unit used to describe the average noise power is watts (or dBW). For white noise (i.e., noise with an autocorrelation of zero except at zero lag), it is possible to divide the average noise power by an effective noise power bandwidth to obtain the noise power spectral density (PSD) in W/Hz. The contribution to PSD from the external environment can be expressed in terms of an effective antenna noise factor,  $F_a$  (CCIR, 1964). For non-stationary data, the PSD function over a given sample interval still has some utility, provided the process, while not stationary in the strict sense, can still be considered "stationary enough." The definition of  $F_a$  is

$$F_a = 10 \log_{10} f_a , \quad \text{in decibels} , \quad (1)$$

where

$$f_a = \frac{P_n}{k T_o b} ; \quad (2)$$

$P_n$  is the external noise power (in watts) available from an equivalent lossless antenna in bandwidth  $b$ ;  $k$  is Boltzmann's constant =  $1.38 \times 10^{-23}$  J/K;  $T_o$  is the reference temperature, 288K; and  $b$  is the noise power bandwidth (in hertz). Note that  $f_a$  is a dimensionless quantity, however, it gives (numerically) the available noise PSD in terms of  $k T_o$  and the available noise power in terms of  $k T_o b$ . For this reason, one commonly sees  $F_a$  with units attached (e.g., dB >  $k T_o b$ ).

Equation (2) can be given as

$$P_n = F_a + B - 204 \text{ dBW} , \quad (3)$$

where  $P_n = 10 \log_{10} P_n$ ,  $B = 10 \log_{10} b$ , and  $-204 = 10 \log_{10} k T_o$ .

\*The integral of the amplitude probability density function from minus infinity to some value of interest is the amplitude probability distribution (APD) function.

The relationship between  $f_a$  and the noise power in terms of an effective antenna noise temperature is given by

$$f_a = T_a / T_0 \quad (4)$$

where  $T_a$  is the effective antenna noise temperature (in K).

Since the noise level with which a desired signal must compete may result from a combination of noise generated internal to the receiving system and external noise from the antenna, it is convenient to express the resulting noise by means of NORTON'S (1953) generalization of FRIIS' (1944) definition of the noise figure of a radio receiver. The system noise factor,  $f_s$ , can be defined in terms of the losses and actual temperatures of the various parts of the system. Loss in the circuit is taken here to be the ratio of available input power to available output power and will differ from the loss in delivered power unless a matched load is used.

If all temperatures are equal to  $T_0$ , the system noise factor is given by

$$f_s = f_a - 1 + f_c f_r \quad (5)$$

where  $f_c$  is the noise factor of the antenna circuit,  $f_t$  is the receiving antenna transmission line noise factor, and  $f_r$  is the receiver noise factor (SPAULDING, D. A., and DISNEY, R. T., 1974). Equation 5 is presented to emphasize that it is fundamentally improper simply to take the sum of the antenna noise factor and the receiver noise factor to obtain the system noise factor. Note that what has been termed processing noise in Fig. 5 is a man-made source in one sense but must be reduced to an equivalent  $f_r$  value for use in Eq. (5), while the other man-made sources contribute to  $f_a$ .

### 3.1.2. Noise Spectra

It is useful to study the average noise power that each of the sources in Fig. 5 contributes (or can contribute) to the composite electromagnetic environment as a function of frequency. Figures 6 and 7 show such data, excluding intentional radiators and quantizing noise and natural sources such as scintillation (which can be viewed as distortion of the desired signal rather than natural noise in the same sense as the other sources). Man-made noise from unintentional radiators is highly dependent on proximity to the radiator. The empirical model of SPAULDING and DISNEY (1974) gives average man-made noise power levels for business, residential, rural, and quiet rural areas. For comparison, atmospheric noise data for Washington, D.C. in summer are plotted for day and night (CCIR, 1964). Note that, for the vicinity of Washington, D.C. in summer, atmospheric noise from lightning tends to be important below about 10 MHz at night (Fig. 6); and man-made noise tends to become increasingly important when atmospheric noise drops off with increasing frequency above about 20 MHz. During daytime, atmospheric noise is relatively unimportant above 0.1 to 1 MHz for the same location and season. For this example, galactic noise is important only in quiet rural areas for frequencies above about 20 MHz. Figure 6 is applicable for omnidirectional vertically polarized antennas such as a short grounded monopole.

Solar noise and thermal terrestrial noise tend to be important at the higher frequencies (see Fig. 7). When the sun is in the beam of a high-gain antenna, it can be a very important noise source for frequencies well down into the VHF range. Figure 7 is applicable for vertically polarized antennas. Note that Figure 7 also gives receiver noise figures,  $F_r = 10 \log_{10} f$  (See also Eq. 5.)

### 3.1.3. Noise Parameters

Many parameters besides  $F_a$  have been used to report the data from noise measurements. For example, the APD of the envelope process, the average crossing rate (ACR) for positive crossings of a given threshold by  $v(t)$ , etc., have been found useful by various workers (see HAGN, G. H., 1973b).

Parameters in common usage for measures of the envelope voltage-time waveform  $v(t)$ , include the following (GESELOWITZ, D.B., 1961):

- The peak voltage for the time period (T),  $V_p$ , which can be defined as the maximum value of  $v(t)$  observed during T, although no satisfactory definition for this parameter has yet been standardized (see MATHESON, R. J., 1970; SHEPHERD, R. A. et al., 1974).
- Quasi-peak voltage,  $V_{qp}$ , the voltage of the quasi-peak circuit output waveform (averaged over time T) that results when the noise envelope is passed through a circuit with a very short charging time and a relatively long discharging time. Since the quasi-peak voltage depends on both the amplitude and the time behavior of the interfering noise, it has been found useful in subjectively determining system performance (BURRILL, C. M., 1942), but it cannot be related to other statistical measures of  $v(t)$  analytically, except for special waveforms (e.g., a CW signal or a deterministic radar signal).
- The rms voltage,  $V_{rms}$ , is the root-mean-square (rms) value of the envelope voltage,  $v(t)$ , computed over time interval T.

- The average voltage,  $V_{avg}$ , is the average of the detected envelope voltage,  $v(t)$  for the time interval  $T$ .

These parameters are listed in order of their magnitude for a given input waveform (i.e.,  $V_p > V_{qp} > V_{rms} > V_{avg}$ ). The origins of the parameters  $V_{rms}$  (used to compute  $F_n$ ) and  $V_{avg}$  lie in statistical communication theory, whereas  $V_p$  and  $V_{qp}$  probably evolved from a desire to observe an upper bound (worst case) of  $v(t)$  and correlate it empirically with degradation. Frequently,  $V_{avg}$  is given in terms of  $V_{rms}$ :  $V_d = 20 \log_{10} (V_{rms}/V_{avg})$ , in decibels. Data on  $V_d$  for atmospheric noise from lightning were presented by the CCIR (1964), and data on  $V_d$  for man-made noise were presented by SPAULDING and DISNEY (1974).

For impulsive noise consisting of nonoverlapping impulses, it is useful to define the impulse spectral intensity (ARTHUR, M. G., 1974)\* to describe the strength of the impulse. The maximum value of  $v(t)$  for any given impulse,  $V_m$ , can be related to the impulse spectral intensity ( $S_1$ ) by the impulse bandwidth ( $b_1$ ) of the receiver:

$$V_m = 2 S_1 b_1$$

where  $S_1$  is in volt-seconds (or V/Hz) and  $b_1$  is in Hz. For the concept of impulse bandwidth to be useful and the above equation to apply, the amplitude-time waveform of  $v(t)$  must be narrow enough at the input for the response at the output to be dominated by the impulse response of the filter. When the impulses are overlapping, it is unclear whether the concept of impulse bandwidth is useful.

The time history of these impulses is also important. The rate at which the impulses occur represents one measure in the time domain. Other useful parameters include the impulse spacing statistics.

The units used to report the results of noise measurements are not standardized; this has led to great confusion, waste of considerable technical manpower, and significant errors in analyses. The appendix discusses some of these problems.

### 3.2 Interference (EMI)

We have observed in Section 2.3.2. that the term interference is commonly used to describe both a cause of operational degradation and the effect of such degradation. Since we have defined the composite electromagnetic noise (EMN) environment to be a cause, it seems appropriate to comment here on how the effect of interference (EMI) can be quantified, prior to proceeding to a discussion of the fundamentals of electromagnetic compatibility (EMC).

It is fundamental that the effect of EMN upon any given system be defined in terms that are meaningful to the operational users of that system. The degradation produced, as observed at the system output, must be relatable to some operational scenario (see Fig. 8). Frequently there is a requirement to define a linkage between the description of the performance of the system being degraded as observed by the system and some analytical measure that can be calculated by an interference analyst (e.g., KRAVITZ, F., 1973). For example, the degradation to a voice communication system might be specified in terms of the reduction in an articulation score (AS, the percentage of the words understood correctly in a system experiencing interference) as generated by a listener panel. The analyst might be able to compute a signal-to-noise ratio (SNR) at the system output, and he would then require the relationship between the SNR and AS for the system of interest. If the system involves nonlinearities, he might also need the relationship between the carrier-to-noise ratio (CNR) at the system input to the SNR at the system output.

Among the user-oriented descriptions of performance that might be useful for voice systems are the articulation score, articulation index (e.g., KRAVITZ, F., 1973), and perhaps the ratio of the time required to transmit a complete error-free message (with the verification) to the time required to read the message once. With digital communication systems, the user is frequently interested in throughput,<sup>†</sup> whereas the system analyst can more readily compute binary error rate (ber). The relationship between

\* ARTHUR (1974) pointed out that numerous terms for impulse spectral intensity have been used in the literature (e.g., spectral intensity, spectral density, voltage spectrum, impulse strength and interference intensity), and that none of these terms seem adequate. He also points out the IEEE Dictionary (1972) definition for spectrum amplitude, ( $1/\pi$  times the magnitude of the Fourier transform of a time-domain signal function) is in error;  $1/\pi$  should be replaced by the numeric 2. A proposed IEEE standard for impulse strength and impulse bandwidth (IEEE, 1973) clarifies and corrects this error.

<sup>†</sup> Throughput was defined by LECN and EVANOWSKY (1971) as the ratio of the number of good blocks of data received to the total number of blocks of data transmitted, expressed in percent. A good block of data is a block that has no bit in error whereas a bad block has one or more bits in error.



ber and throughput usually depends on the protection scheme (e.g., coding) used, and frequently it is not possible to have a purely analytical relationship between ber and throughput, except on the average over a long period. For radar systems, the operator may be interested in such descriptors as tracking error, radar range reduction, and false alarm rate. /-//

For all the above cases, there is a need to specify system inputs in terms of descriptions of the desired signal, the total noise environment, and the outputs, in user-oriented terms. There is also a need to specify the performance level below which further degradation will be unacceptable. Some of the fundamentals of system performance analyses are discussed in the following section.

### 3.3. Compatibility (EMC)

The fundamentals of EMC have been much discussed. This section will concentrate on a few main points. The essence of a classical EMC analysis problem is illustrated in Fig. 9. The composite EMN environment couples into some system of interest and competes with that system's desired signal. The coupling mechanisms of the signal and the EMN may be similar or different. The essence of the problem is to determine the effect of the undesired EMN in terms of some measure of the performance of the system that is meaningful in an operational context, as discussed in Section 3.2, and to devise a remedy if the degradation is unacceptable. A first step is usually to obtain a rough estimate of the performance of the system of interest in the absence of the EMN (but including system processing noise). If the system operates adequately for this case, the computation can be repeated in the presence of the EMN. If the system performance is clearly adequate for this case, the analysis is complete. If it is not, steps must be taken to increase the level of the desired signal by increasing the signal power at the source or increasing the coupling to the signal, to decrease the sources of the noise contributing to the EMN, or to reduce the coupling of the EMN into the system. For example, DELISLE and CUMMINS (1973) considered mutual coupling effects in optimizing antenna arrays for SNR. Frequently it is not possible to do more than attempt to reduce the coupling of the EMN into the system. This can be accomplished in various ways. For example, one can increase the distance between the dominant sources of EMN and the victim system, or one can change the frequency of operation of the system; a combination of these remedies may be applied. Alternatively, filters or shielding and bonding techniques can be employed to reduce the coupling, or different antennas can be employed. Recently, adaptive antennas have been developed to increase SNR. These actions may be costly, and it may be necessary to perform more refined analyses.

EMC analyses are appropriate at various stages in the life cycle of a system (DOEPFNER, T. W., 1972; JANOSKI, J. R., 1972, 1973a,b; HIEBERT, A. L., and SHARFF, S. A., 1974). At each phase (e.g., concept validation, full-scale development, production, and deployment), it is appropriate to assess the cost-benefit aspects of recommendations for system modification derived from EMC analyses.

Finally, it should be mentioned that many of the tools of spectrum engineering, as applied to EMC problems, are the same tools required for working on problems in electronic warfare (EW) and in electromagnetic hazards and effects (EHE) due to nonionizing radiation (see CORY, W. E., and FREDERICK, C. L., 1974). It would be useful for these technical communities to share their analytical tools, to the extent practicable.

## 4. CONCLUSIONS AND RECOMMENDATIONS

### 4.1. Conclusions

The standardized definitions of EMN, EMI, and EMC are likely to change slowly with time (e.g., a 5- to 10-year time constant). The international definitions are tending to converge (the 1979 World Administrative Radio Conference provides incentive), but complete convergence may be more of a goal than a fact in 1984. Continuing effort is needed within NATO/AGARD and the rest of the world community, to overcome the various difficulties (including simple language difficulties) and to work toward the goal of standardized definitions. The "fundamentals" probably will not change much in the next 10 years, but the tools (e.g., analytical models, desk-top calculators, data base, and measurement instrumentation and techniques) and knowledge of how to use them should continue to proliferate. The lack of standardization of the parameters and units used to report noise data has generated much confusion and wasted numerous man-years of technical effort.

### 4.2. Recommendations

The AGARD list of standard symbols (HALLEY, P., 1974) should be expanded to include terms such as noise power bandwidth and others germane to the study of noise, interference, and compatibility. It is recommended that the term electromagnetic noise, as broadly defined in this paper, be used to describe the source of the electromagnetic environment and that the term interference be reserved for the effect of the environment on a system or subsystem. EMC should be considered as a condition. The following definitions are suggested for use during this meeting:

- Electromagnetic noise (EMN) is all electromagnetic energy from both intentional and unintentional radiators (except the desired signal for a specific system of interest).

- 1-12
- Electromagnetic interference (EMI) is the impairment of the extraction of information from a desired electromagnetic signal caused by electromagnetic noise.
  - Electromagnetic compatibility (EMC) is the condition that prevails when telecommunications equipment is collectively performing its individually assigned function(s) in a common electromagnetic environment without causing or suffering unacceptable electromagnetic interference--or the capability of achieving that condition.

The parameters and units used to report noise data should be standardized, and a mechanism should be established within AGARD to accomplish this for NATO.

#### APPENDIX: Units of Noise Measurement

##### A.1. INTRODUCTION

This Appendix describes some of the units used to report the results of noise measurements. The relationships (or their lack) between the different units are discussed, and some of the problems in attempting to compare noise data taken with different instrumentation are examined. Preferred units are recommended.

##### A.2. DISCUSSION OF FACTORS AFFECTING THE UNITS USED FOR REPORTING THE RESULTS OF NOISE MEASUREMENTS

As observed by WALKER (1972), "a bewildering array of different units have been used by different researchers to report on measurement of even the simplest of the noise parameters." He mentioned 19 examples of units for reporting on noise measurements (see Table A-1); it should be noted that Table A-1 is far from complete.

TABLE A-1 EXAMPLES OF UNITS USED TO REPORT THE RESULTS OF NOISE MEASUREMENTS

dB above $kT_0 B$	$\text{dBn/kHz}$
dB above $1 \mu\text{V/MHz}$	$\text{dBn/m}^2$
dB above $1 \mu\text{V/m/kHz}$	$\mu\text{W/Hz}$
$\text{dB}\mu\text{V/m/MHz}$	$\mu\text{V/m/kHz}$
$\text{dB}\mu\text{A/m/MHz}$ (conducted)	$\text{W/m}^2$
$\text{dBm(RMS)/MHz}$	$\text{W/cm}^2$
$\text{dBm(peak)/MHz}$	$\text{nW/cm}^2$
$\text{dBm/MHz}^2$	Joules (conducted)
$\text{dBm/kHz/m}^2$	Tesla (magnetic)
$\text{dBm/(kHz)}^n$ $1 \leq n \leq 2$	

To try to clarify some of the confusion generated by this proliferation of units, let us first consider the elements of a basic noise meter. The noise meters in use today employ four basic elements: antenna, receiver (through the IF), detector, and metering and/or data-processing device (see Fig. A-1). The antenna and receiver select the data spatially and spectrally, respectively. In the case of a very narrowband antenna and a wideband receiver, the antenna may also contribute to the spectral filtering process. The units used to describe the results of a given measurement are determined primarily by the calibrator, detector, and meter, but the antenna and receiver characteristics are often used to normalize the data in a way that directly affects the units used to report the results. Let us first consider these normalizations.

The antenna normalization separates the units that pertain to electromagnetic field quantities from those that pertain to circuit quantities. The antenna normalization involves converting a known (measured) circuit quantity (e.g., voltage or power) to a field quantity (e.g., field strength or power flux density) by normalizing by a known antenna effective length or effective area. Hence, a standard (or calibrated) antenna must be used, and the appropriate circuit equation must be solved. For example, a measured input voltage is related through a circuit equation to a Thevenin equivalent voltage source defined as the dot product of the incident electric field strength in  $\text{V/m}$  and the vector effective length of the antenna in meters. This is one of the procedures used to calibrate field-strength meters (TAGGART, H. E. and WORKMAN, J. L., 1969). After this normalization, the received voltage in volts is given as an incident electric field in  $\text{V/m}$ . Had the antenna effective area been used to normalize a received power, the units would have been  $\text{W/m}^2$ .

The receiver normalization involves the effective bandwidth. The measured noise voltage or power is observed in some bandwidth. Many workers normalize their results in terms of some unit bandwidth (1 Hz, 1 kHz, or 1 MHz). This is useful, but it can lead to problems when the effective bandwidth used for the measurement is not identical to the unit bandwidth being used in the normalization. Care must be taken to select the appropriate bandwidth for normalization. For example, effective noise power bandwidth as defined in Sec. 3.1.1. is germane for white noise and average noise power measured with an rms voltage

detector calibrated with a Gaussian noise source. The impulse bandwidth as defined by the IEEE (1973) is germane for impulsive noise consisting of individual (nonoverlapping) impulses and for peak voltage as measured with a peak detector calibrated with an impulse generator. 1-13

The detector in Fig. A-1 was designed to produce the desired statistic of the noise envelope to be measured. This statistic gives rise to the basic parameter to be metered, as discussed in Sec. 3.1.3. The units in which the statistic are measured depend on the calibration source, the detector, and the meter (and/or data processor). To avoid confusion it is useful to specify the type of detector as part of the description of the parameter being measured and also to state the method of calibration used.

It would be useful to consolidate into the units the information on the type of detector as well as the type of calibrator used. One method for doing this would be to put the type of detector in parentheses after the electrical unit and to use a subscript to indicate the type of calibrator. For example, field strength for noise might be expressed:

$$\text{dB} > 1\mu\text{V}(X)_Y/\text{m}, \text{ or } \text{dB} > 1\mu\text{V}(X)_Y/\text{m/kHz} ,$$

where

$X$  = type of detector (peak, qp, rms, or avg) and

$Y$  = type of calibrator (i for impulse generator, s for sine-wave generator, and g for Gaussian noise source).

Here it is assumed that the impulse generator is calibrated in terms of the rms value of a sine wave, as has become standard practice. MAGRAB and BLOMQUIST (1971) summarized the error produced for several selected waveforms when peak and average detectors were calibrated with a CW signal generator and used to measure other waveforms.

Finally, the meter (or data processing) can influence the units.

#### A.3. RELATIONSHIPS BETWEEN UNITS FOR DIFFERENT PARAMETERS AND PROBLEMS IN COMPARING NOISE DATA OBTAINED WITH DIFFERENT EQUIPMENT AND BY DIFFERENT INVESTIGATORS

Workers have tried, due to the general paucity of man-made noise data, to convert noise data taken with systems using detectors other than rms voltage detectors into average power or power spectral density. This has been done in order to compare data taken by different workers and to try to determine the frequency dependence of composite environmental noise. An additional motivation for combining data samples has been to try to determine the variation of noise level with distance from a metropolitan center (e.g., SKOMAL, E. N., 1965). Of course, these conversions of peak, quasi-peak, and average voltage noise data to equivalent rms voltage cannot be done rigorously for the case of composite EMN. Such conversions should not be attempted without making some approximations or assumptions based on empirical data for a given type of noise environment and instrumentation.

For example, the reading of a peak detector of the type used by the SAE in the USA and a quasi-peak detector of the type used by the CISPR in Europe (and elsewhere) for noise from the ignition system of a single automobile running at 1500 rpm is said to have been determined empirically to be about 20 dB (SAE, 1974; BALL, A. A., and NETHERCOT, W., 1961). This conversion factor has been adopted by the CISPR and SAE, but SHEPHERD et al. (1974) contended that this conversion may be very approximate.\* The difference between the readings of an rms detector and those of a quasi-peak detector has been measured for several types of noise, but the relationship varies significantly as the input waveform or filter characteristics vary. One observation (by MATHESON, R. J., 1970) indicated that one type of quasi-peak detector read about 10 dB higher for one type of man-made noise in an effective noise bandwidth of 10 kHz. As more data have become available, it has become possible to report separately the frequency and distance dependencies inferred from data obtained with different detectors (e.g., SKOMAL, E. N., 1973).

MAGRAB and BLOMQUIST (1971) noted the errors that can occur when various detectors are calibrated with a sine wave, using a CW signal generator, and used to measure other waveforms. This error can be compounded by taking the data from a peak, quasi-peak, or average voltage detector in  $\text{dB} > 1\mu\text{V}$ , converting to volts, squaring, dividing by 50, calling the result the average power in watts, and subsequently converting to dBW, dBm,  $\text{mW}/\text{cm}^2$  (e.g., SMITH, S. W., and BROWN, D. G., 1973). It cannot be emphasized too strongly that this is not a correct procedure. If one is going to attempt to convert to average power, even to get crude estimates, one must make some estimate of the conversion factor from the kind of microvolts ( $\mu\text{V}$ ) measured to  $\mu\text{V}$  (rms) before squaring the voltage and multiplying by the real part of the admittance to get power. The error due to variation of the true input impedance from its nominal value is usually small relative to the error due to uncertainty in the correct (for the input time waveform measured) conversion factor from whatever type of voltage was measured to rms voltage. The uncertainty in such a conversion is generally unknown, indeed unknowable, for most man-made noise waveforms.

\* While the 20-dB empirical relationship between the readings of peak and quasi-peak detectors may be especially useful (and sufficiently accurate) for facilitating international trade, it should not be taken as a deterministic constant.

1-14 A second type of problem relates to the bandwidth normalization. Here, several types of mistake are common: (1) normalizing by the wrong bandwidth (i.e., using 3-dB bandwidth when noise power bandwidth should have been used), (2) using the wrong normalization rule, (3) operating improperly on a normalized voltage per unit bandwidth quantity to compute power spectral density, (4) normalizing from a bandwidth that did not contain a uniform spectrum, and (5) combinations of these mistakes.

It is common practice to use voltage per unit bandwidth to report the peak value of impulsive noise data. This is because an impulse can be described in terms of volt-seconds (the area under the input voltage-time curve), and the response of a receiver to a very sharp impulse (i.e., delta function) is indeed the "impulse-response" of the receiver which depends only on the volt-seconds of the source and the filter characteristic of the receiver (e.g., ARTHUR, M. G., 1974). This gives rise to the concept of the impulse bandwidth of the receiver, the correct bandwidth to use for normalization of peak voltage readings. When an impulse generator is used for calibration, the units might well be  $\text{dB} > 1 \mu\text{V}/\text{MHz}$ . If this quantity is converted to power by squaring volts/MHz and normalizing by impedance, the units become  $\text{watts}/(\text{MHz})^2$ , and this is not the power spectral density (PSD). Also, the volts that were squared were peak volts not rms volts. If one sees  $\text{dBm}/\text{MHz}$ , it is important to know whether the power was computed first and then normalized by the effective noise power bandwidth,  $b$ , to yield power spectral density or whether some operation has been done on the voltage-per-unit-bandwidth quantity and some assumption made about the relationship between the peak and rms voltages. This problem has given rise to the units  $\text{dB} > 1 \mu\text{V}/(\text{MHz})^{1/2}$  used (sometimes incorrectly) by some workers attempting to compute PSD. Still another bandwidth-related problem has to do with normalizing to a unit bandwidth (e.g., 1 Hz, 1 kHz) when the data were taken in a larger bandwidth (e.g., 10 MHz). Here the problem is that the assumption is made that the PSD is constant across the total bandwidth(s) of interest, when this might not be the case.

As previously mentioned, some authors prefer to report average noise power measurements in terms of the parameter  $F_a$  (a circuit quantity), and others prefer to use an rms field strength in bandwidth (b),  $E_n$ , in  $\text{dB} > 1 \mu\text{V}/\text{m}$  (a field quantity). One can relate these two parameters for data taken with a short, grounded vertical monopole antenna (CCIR, 1964):

$$E_n = F_a + 20 \log_{10} f_{\text{MHz}} + 10 \log_{10} b - 95.5 \quad \text{dB} > 1 \mu\text{V}(\text{rms})/\text{m}$$

This equation can be erroneously used in two ways: It can be used to calculate  $F_a$  from  $E_n$ , where the measure of  $E_n$  was something other than rms voltage (usually average voltage),\* and it can be used for antennas other than short, grounded vertical monopole antennas, where it does not necessarily apply.

Some confusion also exists when data are reported in units of  $\text{dB} > 1 \mu\text{V}(\text{rms})/\text{m}/\text{kHz}$  because of uncertainty as to whether the (rms) means that an rms detector was used or that a peak detector was used but calibrated with a CW signal generator reading the rms value of a sine wave. This particular confusion can be resolved by using the nomenclature suggested in this appendix.

While not comprehensive, this discussion of problems at least illustrates some of the difficulties regarding units and conversion between units that arise in measuring and comparing noise data.

#### A.4. PREFERRED UNITS

Of the units discussed above, there are some preferences that will help avoid some of the problems described in the preceding section. These preferences can be related both to the types of detectors used and the types of noise sources observed, as well as the use to be made of the data. For noise data obtained on a specific noise source, it is important to specify the distance from the source and the polarization of the observing antenna. For this case it is preferable to normalize out the antenna effective length (or area) and report the results in terms of field strength (or power flux density). In some cases, an additional normalization by bandwidth is desirable, whereas in other cases (e.g., CW noise) it is not. For noise data obtained in specific types of environment (e.g., business, or residential), it is preferable to express the noise data in terms of  $F_a$  and to state the noise power bandwidth and antenna polarization, directional characteristics and type, and height above ground.

For CW noise, watts are preferred for circuit quantities. Volts can be used if the impedance across which they are measured is specified. When a calibrated field strength meter is used, then  $\text{V}/\text{m}$  (or  $\text{W}/\text{m}^2$ ) are appropriate for field quantities. Units involving bandwidth normalization (e.g.,  $\text{V}/\text{kHz}$ ) should be avoided for specifying the results of CW (or narrowband) noise measurements. The dB equivalents of these units are equally acceptable when the reference is adequately specified (e.g., dBW).

For white noise it is useful to relate the EMV power available from the antenna to that available from a resistor at room temperature; hence,  $F_a$  is a preferred parameter.  $F_a$  can be expressed as the noise power

\* Still another problem arises from the current method of constructing RFI meters. These meters claim to measure average voltage, whereas log amplifiers are used prior to the averaging, and what is really measured is the average of the log of the received voltage. The parameter  $V(\text{avg})$  can be estimated for man-made noise, from such data, by using an empirical relationship given by SPAULDING and DISNEY (1974).

spectral density in  $\text{dB} > \text{KT}$ ; or, alternatively, as a noise power in  $\text{dB} > \text{KT}$  b. The preferred detector type is the rms voltage detector. An average voltage detector can also be used: It will read 1.049 dB lower than an rms detector for the same white Gaussian noise at the input. 1-15

An rms detector is useful for giving the average power of high-duty-cycle repetitive impulse waveforms; the preferred unit is the watt. A peak detector is useful for giving the peak of low-duty-cycle repetitive impulse waveforms, in units of  $\text{V(peak)}/\text{Hz}$  where the impulse bandwidth is used for normalization. It is also important to specify the pulse repetition frequency (PRF) in pulses per second (pps).

An rms detector is useful for giving the average power of random impulsive noise waveforms; the preferred unit is watts. Frequently, though, the APD and other parameters are required to describe this type of noise adequately. The APD can be given in decibels relative to a known average power value. The average numbers of positive level-crossings or of pulses per second exceeding a given threshold are also useful, and the period over which the average was computed should be specified. The type of calibrator used to establish the thresholds should also be stated. When the ratio of  $V_{\text{rms}}$  to  $V_{\text{avg}}$  is large (i.e., large  $V_d$ ), it is sometimes necessary to use a peak detector to observe the noise at all. For this case, it is desirable to calibrate with an impulse generator and use  $\text{V}/\text{Hz}$  as the units. This measurement procedure is applicable only to relatively large, nonoverlapping impulses.

These preferred units are the author's; clearly additional discussion of this topic is required.

#### REFERENCES

- ANTHUR, M. G., 1974, "Impulse Spectral Intensity--What Is It?," Report NBSIR 74-365, U.S. National Bureau of Standards, Boulder, Colo. (May).
- BALL, A. A., and NETHERCOT, W., 1961, "Radio Interference from Ignition Systems--Comparison of American, German and British Measuring Equipment, Techniques and Limits," Proc. IEE (London), Vol. 108, Part B, No. 39.
- BARGHAUSEN, A. F., and HAILEY, L. G., 1974, "Radio Spectrum Measurement System--Current Applications, Experience, Results," IEEE Electromagnetic Compatibility Symposium Record, IEEE 74CH0803-7 EMC, San Francisco, Calif., pp. 140-145 (July).
- BENDAT, J. S., and PIERSON, A. G., 1971, Random Data: Analysis and Measurement Procedures, Wiley-Interscience, New York, N.Y.
- BURRILL, C. M., 1942, "An Evaluation of Radio Noise Meter Performance in Terms of Listening Experience," Proc. IRE, Vol. 30, pp. 473-478.
- BURTON, J. B., 1972, "Spectrum Management and EMC," NAVAIR EMC Seminar, Avionics Division, Naval Air Systems Command, Washington, D.C., pp. 2-1 to 2-8.
- BURTON, J. B., 1973, "Spectrum Management and EMC," Proceedings, Seminar on Electromagnetic Compatibility, Society of Automotive Engineers, SAE AE-4, Washington, D.C., 11 May, pp. 1-1 to 1-8.  
Note: This is a slightly modified version of BURTON, J. B., 1972.
- CCIR, 1964, "World Distribution and Characteristics of Atmospheric Radio Noise," Report 322, International Radio Consultative Committee, International Telecommunication Union, Geneva.
- CCIR, 1974, "Definitions of Interference," Study Group 1 Report on Question 45/1, Document 1/1048-E, XIIIth Plenary Assembly, International Radio Consultative Committee, Geneva.
- COOK, A. H., 1971, Interference of Electromagnetic Waves, Clarendon Press, London.
- CORY, W. E., and FREDERICK, C. L., 1974, "Effects of Electromagnetic Energy on the Environment--A Summary Report," IEEE Trans. Aerospace Electronics and Systems, Vol. AES-10, No. 5, pp. 738-742 (September).
- DAYHARSH, T. I., YUNG, T. J., and VINCENT, W. R., 1969, "A Study of Land Mobile Spectrum Utilization; Part A: Acquisition, Analysis, and Application of Spectrum Occupancy Data," Final Report, SRI Project 7379, Stanford Research Institute, Menlo Park, Calif. (July).
- DELISLE, G. Y., and CUMMINS, J. A., 1973, "Mutual Coupling in the Signal-to-Noise Ratio Optimization of Antenna Arrays," IEEE Trans. Electromagnetic Compatibility, Vol. EMC-15, No. 2, pp. 38-44 (May).
- DOD, 1967/1972, "Department of Defense Electromagnetic Compatibility Program," U.S. Dept. of Defense Directive No. 3222.3, DDM&E, Washington, D.C. (revised 27 September 1972).
- DOEPPNER, T. W., 1972, private communication.
- DUFF, W. G., and WHITE, D.R.J., 1972, "EMI Prediction and Analysis Techniques," A Handbook Series on Electromagnetic Interference and Compatibility, Vol. 5, Don White Consultants, Germantown, Md.

DUFF, W. G., 1973, "Intersite EMI Prediction and Analysis," IEEE Electromagnetic Compatibility Symposium Record, IEEE 73CHO781-S EMC, New York, N.Y., pp. 177-181.

EVERETT, W. W., Jr., 1972, Topics in Intersystem Electromagnetic Compatibility, Molt, Reinhart, and Winston, Inc., New York, N.Y.

FCC, 1974, Rules and Regulations, Federal Communications Commission, Washington, D.C.

FICCHI, R. F., 1971, Practical Design for Electromagnetic Compatibility, Hayden Book Co., New York, N.Y.

FRIIS, H. T., 1944, "Noise Figure of Radio Receivers," Proc. IRE, Vol. 32, p. 419.

GESELOWITZ, D. B., 1961, "Response of Ideal Radio Noise Meter to Continuous Sine Wave, Recurrent Impulses, and Random Noise," IRE Trans. Radio Frequency Interference, pp. 210 (May).

HAGN, G. H., FRALICK, S. C., SHAVER, H. N., and BARKER, G. E., 1971, "A Spectrum Measurement/Monitoring Capability for the Federal Government," Final Report, SRI Project 8410, Contract OEP-SE-70-102, Stanford Research Institute, Menlo Park, Calif.

HAGN, G. H., and DAYHARSH, T. I., 1973a, "Technical Assistance for the FCC National and Regional Spectrum Management Program," Final Report, SRI Project 8652-1, Stanford Research Institute, Menlo Park, Calif. (January).

HAGN, G. H., 1973b, "Commission 8: Radio Noise of Terrestrial Origin; 8.4 Man-Made Noise Environment," Radio Science, Vol. 8, No. 6, pp. 613-621 (June).

HAGN, G. H., and LUSTGARTEN, M. N., 1974, "A Status Report of the IEEE/ECAC Electromagnetic Compatibility Figure of Merit Committee," Paper No. 16, NATO/AGARD Meeting on Electromagnetic Noise, Interference and Compatibility, Paris (21-25 October).

HALLEY, P., 1974, "Standardisation of the Principal Electromagnetic Symbols," AGARD Report No. 576, Revision No. 1, North Atlantic Treaty Organisation, Advisory Group for Aerospace Research and Development, 7 Rue Ancelle, 92200 Neuilly sur Seine, France.

HIEBERT, A. L., and SCHARFF, S. A., 1974, "An Electromagnetic Compatibility Program for the 1970s," Report R-1114/1-PR, The RAND Corp., Santa Monica, Calif. (August).

IEC, 1972, "Advanced Edition of International Electrotechnical Vocabulary, Chapter 902: Radio Interference," Bureau Central de la Commission Electrotechnique Internationale, Geneva.

IEEE, 1972, IEEE Standard Dictionary of Electrical and Electronics Terms, IEEE Std. 100-1972, Wiley-Interscience, New York, N.Y.

IEEE, 1973, "Proposed Standard for the Measurement of Impulse Strength and Impulse Bandwidth," draft, IEEE, New York, N.Y. (revised February).

ITU, 1968, Radio Regulations, International Telecommunication Union, Geneva.

ITU, 1971, Final Acts, World Administrative Radio Conference on Space Telecommunications, International Telecommunication Union, Geneva.

ITU, 1973, International Telecommunication Convention Final Protocol, Additions, Provisions, Resolutions, Recommendations and Opinions, Malaga-Torremolinos, Spain, International Telecommunication Union, Geneva.

JANOSKI, J. R., 1972, "Review and Summary," in NAVAIR EMC Seminar, Avionics Division, Naval Air Systems Command, Washington, D.C., pp. 11-1 to 11-10.

JANOSKI, J. R., 1973a, "Review and Summary," Proceedings, Seminar on Electromagnetic Compatibility, Society of Automotive Engineers, SAE AE-4, Washington, D. C., 11 May, SAE-AE-4, pp. 8-1 to 8-10. (See also JANOSKI, J., 1972.)

JANOSKI, J. R., 1973b, "Electromagnetic Environment Considerations in the Conceptual Phase of C-E Development," 2nd Biennial Allied Radio Frequency Agency (ARFA) Symposium, NATO Headquarters, Brussels, 26-28 November.

JCS, 1971/1973, "Glossary of Communications-Electronics Terms," APC 167(C), U.S. Joint Chiefs of Staff, U.S. Government Printing Office, 1971-431-271/5, Washington, D.C. (revised February 1973).

JTAC, 1968, "Spectrum Engineering--The Key to Progress," Joint Technical Advisory Committee, IEEE, New York (March).

KRAVITZ, F., 1973, "Communications/Electronics Receiver Performance Degradation Handbook," Technical Report No. ESD-TR-73-014, Dept. of Defense, Electromagnetic Compatibility Analysis Center, Annapolis, Md. (June).

LEIVE, D., 1970, International Telecommunications and International Law: The Regulation of the Radio Spectrum, Sijthoff/Leyden, New York, N.Y.

LEMON, J. R., and EVANOWSKY, J. B., 1971, "The Meaning and Measurement of Throughput," Rome Air Development Center, Technical Report RADC-TR-71-279 (November).

LEVIN, H., 1971, The Invisible Resource: Use and Regulation of the Radio Spectrum, The Johns Hopkins Press, Baltimore and London.

MAGRAB, E. B., and BLOMQUIST, D. S., 1971, The Measurement of Time Varying Phenomena, Wiley-Interscience, New York, N.Y. [See also: DAVIDSON, J. J., 1961, "Average vs. RMS Meters for Measuring Noise," IRE Trans. Audio, pp. 108-111 (July-August).]

MATHESON, R. J., 1970, "Instrumentation Problems Encountered Making Man-Made Electromagnetic Noise Measurements for Predicting Communication System Performance," IEEE Trans. Electromagnetic Compatibility, EMC-12, No. 4, pp. 151-158 (November).

NATO, 1972, "STANAG 3516 AE (and Draft--Edition No. 2)--Electromagnetic Compatibility Test Methods for Aircraft Electrical and Electronic Equipment," MAS(AIR) (72)299, Military Agency for Standardization, North Atlantic Treaty Organization, Brussels (21 December).

NATO, 1973, "2nd Draft STANAG 3614 AE--Electromagnetic Compatibility (EMC) of Aircraft Systems," Annex A, MAS(AIR) (73)3, Military Agency for Standardization, North Atlantic Treaty Organization, Brussels (17 January).

NORTON, K. A., 1953, "Transmission Loss in Radio Propagation," Proc. IRE, Vol. 41, p. 146.

OTP, 1974, "Manual of Regulations and Procedures for Radio Frequency Management," Office of Telecommunications Policy, Washington, D.C. (revised 1 September).

PETERSON, A. M., 1974, "Noise Pollution of the Radio Spectrum," Conference Record, IEEE International Conference on Communications, Minneapolis, Minn., pp. 19E-1 to 19E-4 (June).

SACHS, H. M., 1974, private communication.

SAE, 1974, "Measurement of Electromagnetic Radiation from Motor Vehicle or Other Internal Combustion Powered Device (Excluding Aircraft) (20-1000 MHz)," SAE J551c, Society of Automotive Engineers, New York, N.Y.

SHEPHERD, R. A., GADDIE, J. D., and NIELSON, D. L., 1974, "Variability in Measurement Procedures for Ignition Noise," Final Report, SRI Project 3253, Stanford Research Institute, Menlo Park, Calif.

SKOMAL, E. N., 1965, "Distribution and Frequency Dependence of Unintentionally Generated Man-Made VHF/UHF Noise in Metropolitan Areas," IEEE Trans. Electromagnetic Compatibility, Vol. EMC-7, pp. 263-278 (September).

SKOMAL, E. N., 1973, "An Analysis of Metropolitan Incidental Radio Noise Data," IEEE Trans. Electromagnetic Compatibility, Vol. EMC-15, No. 2, pp. 45-57 (May).

SMITH, S. W., and BROWN, D. C., 1973, "Nonionizing Radiation Levels in the Washington, D.C., Area," IEEE Trans. on Electromagnetic Compatibility, Vol. EMC-15, No. 1, pp. 2-6 (February).

SPAULDING, A. D., and DISNEY, R. T., 1974, "Man-Made Radio Noise, Part I: Estimates for Business, Residential, and Rural Areas," OT Report 74-38, Office of Telecommunications, U.S. Dept. of Commerce, Boulder, Colo.

STUMPERS, F.L.H.M., 1970, "Progress in the Work of CISPR," IEEE Trans. Electromagnetic Compatibility, Vol. EMC-12, pp. 29-32 (May).

STUMPERS, F.L.H.M., 1971, "Interference to Communications and the Work of CISPR," Conference Record, International Conference on Communications, Montreal, pp. 37-14, 37-19.

STUMPERS, F.L.H.M., 1973, "The Activities of CISPR During Recent Years and Their Impact on Society," International Electromagnetic Compatibility Symposium Record, IEEE, New York, 73CH0751-8 EMC pp. V-X.

TAGGART, H. E. and WORKMAN, J. L., 1969, "Calibration Principles and Procedures for Field Strength Meters (30 Hz to 1 GHz)," Technical Note 370, U.S. National Bureau of Standards, Boulder, Colo. (March).

TAYLOR, R. E., 1971, "Radio Frequency Interference Handbook," NASA SP-3067, National Aeronautics and Space Administration, Goddard Space Flight Center, Greenbelt, Md.

VINCENT, W. R. and DAYHARSH, T. I., 1968, "A Study of Land Mobile Spectrum Utilization, Part B: Analysis of the Spectrum Management Problem," Final Report, Contract RC-10056, SRI Project 7379, Stanford Research Institute, Menlo Park, Calif. (July).

WALKER, P. M., 1972, private communication (15 June).

Webster's New Collegiate Dictionary, 1974, G. & C. Merriam Co., Springfield, Mass., p. 602.

WHITE, D.R.J., 1971a, "Electrical Noise and Interference Specification," Vol. 1, A Handbook Series on Electromagnetic Interference and Compatibility, Don White Consultants, Germantown, Md.

WHITE, D.R.J., 1971b, "EMI Test Instrumentation and Systems," Vol. 4, A Handbook Series on Electromagnetic Interference and Compatibility, Don White Consultants, Germantown, Md.

WHITE, D.R.J., 1971c, A Glossary of Acronyms, Abbreviations, and Symbols, Don White Consultants, Germantown, Md.

WHITE, D.R.J., 1973, "EMI Control Methods and Techniques," Vol. 3, A Handbook Series of Electromagnetic Interference and Compatibility, Don White Consultants, Germantown, Md.

ZIMBALATTI, A. G., 1972, "Contractor Implementation of Aircraft Electromagnetic Compatibility Programs," NAVAIR EMC Seminar, Avionics Division, Naval Air Systems Command, Washington, D.C., pp. 7-1 to 7-8.

#### ACKNOWLEDGMENTS

The author gratefully acknowledges useful comments on an early draft of this paper, by T. W. Doeppner, J. R. Janoski, and D. M. Jansky. Discussions with these individuals, as well as with M. G. Arthur, W. G. Duff, M. N. Lustgarten, H. M. Sachs, R. M. Showers, and A. D. Spaulding, were most helpful in clarifying certain points. The appendix on units for noise measurements relies heavily on materials the author prepared for JTAC Committee 71.1 (chaired by A. M. Peterson) and had the benefit of comments from members of that committee.

The author appreciates the permission of the International Telecommunication Union, the Institute of Electrical and Electronics Engineers, the Bureau Central de la Commission Electrotechnique Internationale, and G. and C. Merriam Company to quote selected definitions.

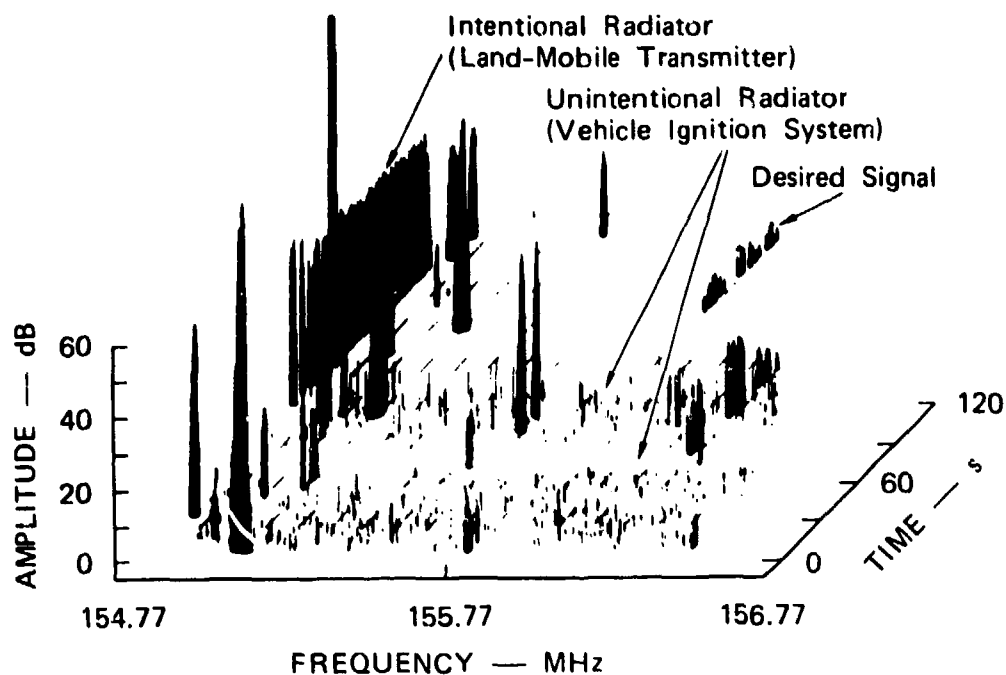
It is a pleasure to acknowledge the support of Stanford Research Institute during the preparation of this paper. The views expressed are, however, those of the author alone, and he is solely responsible for any errors.

Note Added in Proof: The author learned of a very relevant reference after this paper was prepared:

STUMPERS, F.L.H.M., 1974, "Electromagnetic Compatibility," Bulletin des Schweizerischen Elektrotechnischen Vereins de l'Association Suisse des Electriciens; des Verbandes Schweizerischer Elektrizitätswerke de l'Union des Centrales Suisses d'électricité, Bull. ASE/USC Vol. 65, No. 16, pp. 1216-1221 (10 August).

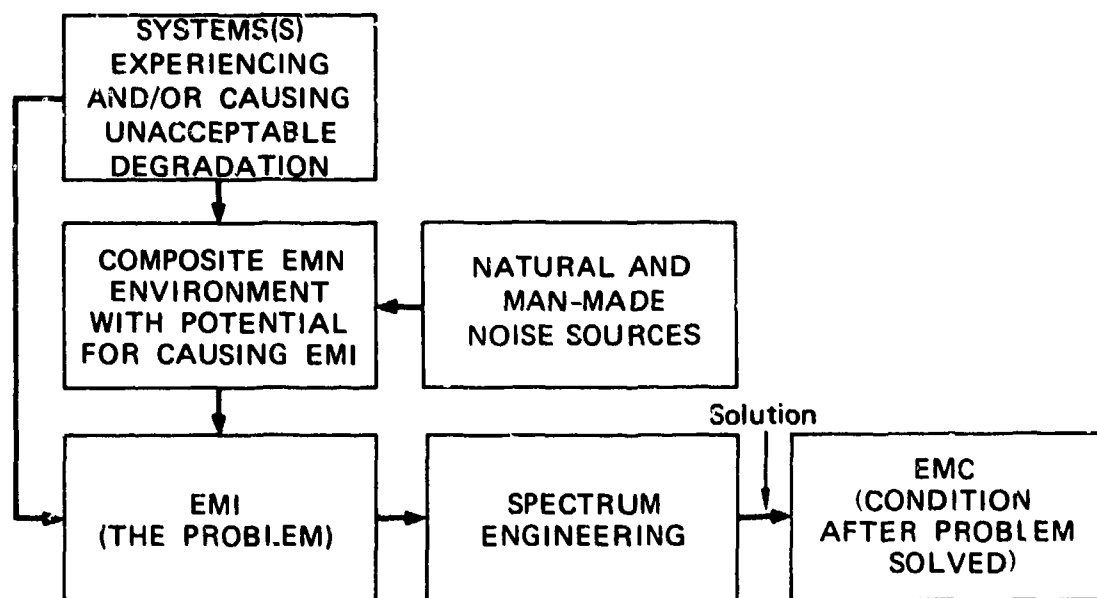
This English-text paper defines EMC very broadly and, in addition to telecommunications systems discusses electromagnetic pulses from nuclear explosions, electromagnetic hazards and biological effects, and other topics.





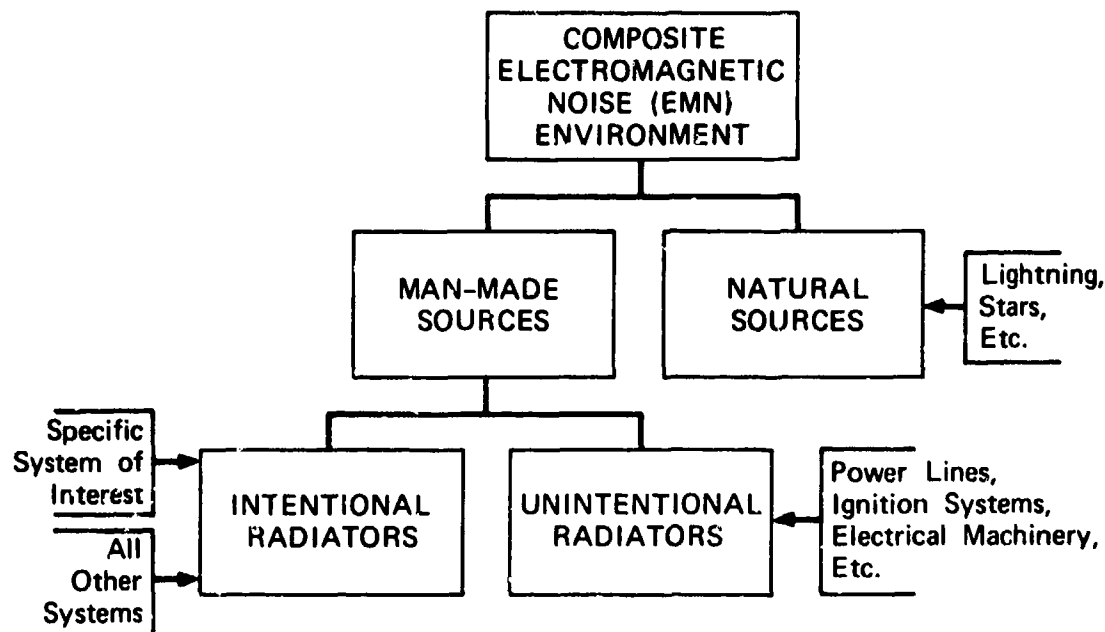
TA-913522-22

**FIGURE 1** EXAMPLES OF CONTRIBUTIONS TO THE COMPOSITE ELECTROMAGNETIC ENVIRONMENT BY INTENTIONAL AND UNINTENTIONAL RADIATORS-- AS OBSERVED WITH A SCANNING RECEIVER (AFTER VINCENT, W. R., AND DAYHARSH, T. I., 1969)



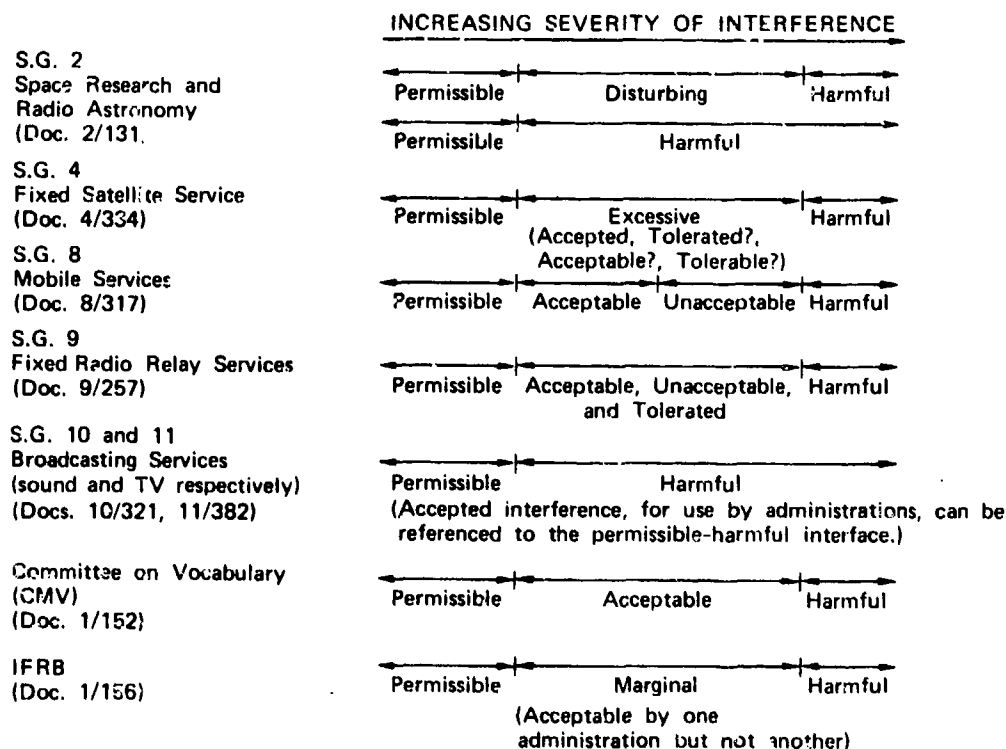
TA-913522-23R

**FIGURE 2** RELATIONSHIP BETWEEN ELECTROMAGNETIC NOISE (EMN), INTERFERENCE (EMI), COMPATIBILITY (EMC), AND SPECTRUM ENGINEERING



TA-913522-30

**FIGURE 3 CATEGORIES OF SOURCES CONTRIBUTING TO THE COMPOSITE ELECTROMAGNETIC NOISE ENVIRONMENT**



TA-913522-25R

**FIGURE 4 THE SPECTRUM OF SEVERITY FOR INTERFERENCE TERMINOLOGY FOR SELECTED SERVICES AS DISCUSSED BY CCIR, GENEVA, 1974**

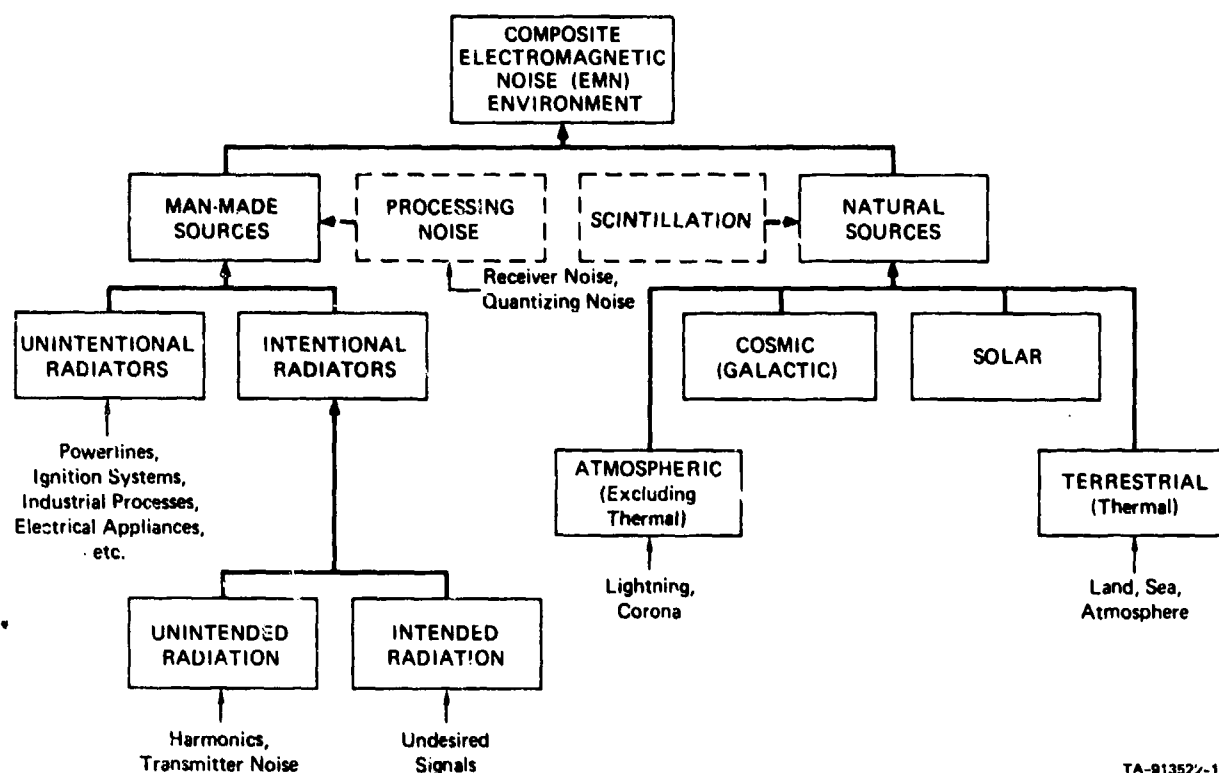


FIGURE 5 SOURCES OF THE COMPOSITE ELECTROMAGNETIC NOISE (EMN) ENVIRONMENT

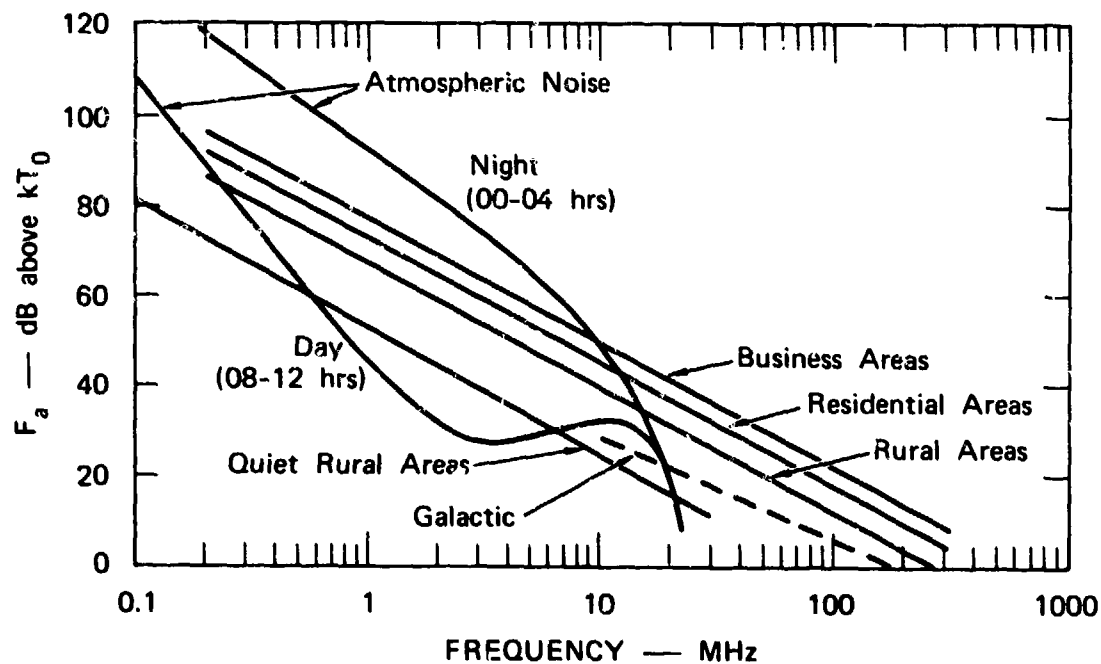


FIGURE 6 ESTIMATES OF MEDIAN VALUES OF MAN-MADE, ATMOSPHERIC, AND GALACTIC NOISE EXPECTED NEAR WASHINGTON, D.C. DURING SUMMER (AFTER SPAULDING AND DISNEY, 1974, AND CCIR, 1964)

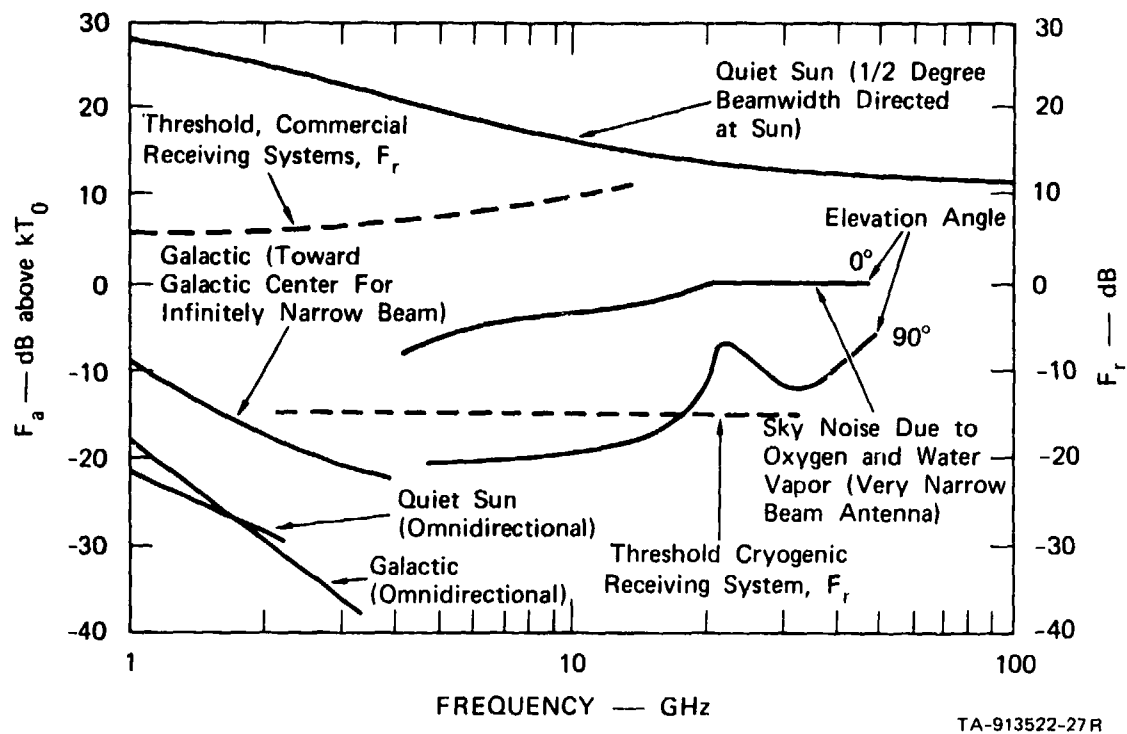


FIGURE 7 TYPICAL RECEIVER NOISE FIGURES AND EXTERNAL NOISE FACTORS FOR VARIOUS RADIO NOISE SOURCES (PRIVATE COMMUNICATION, A. D. SPAULDING, 1974)

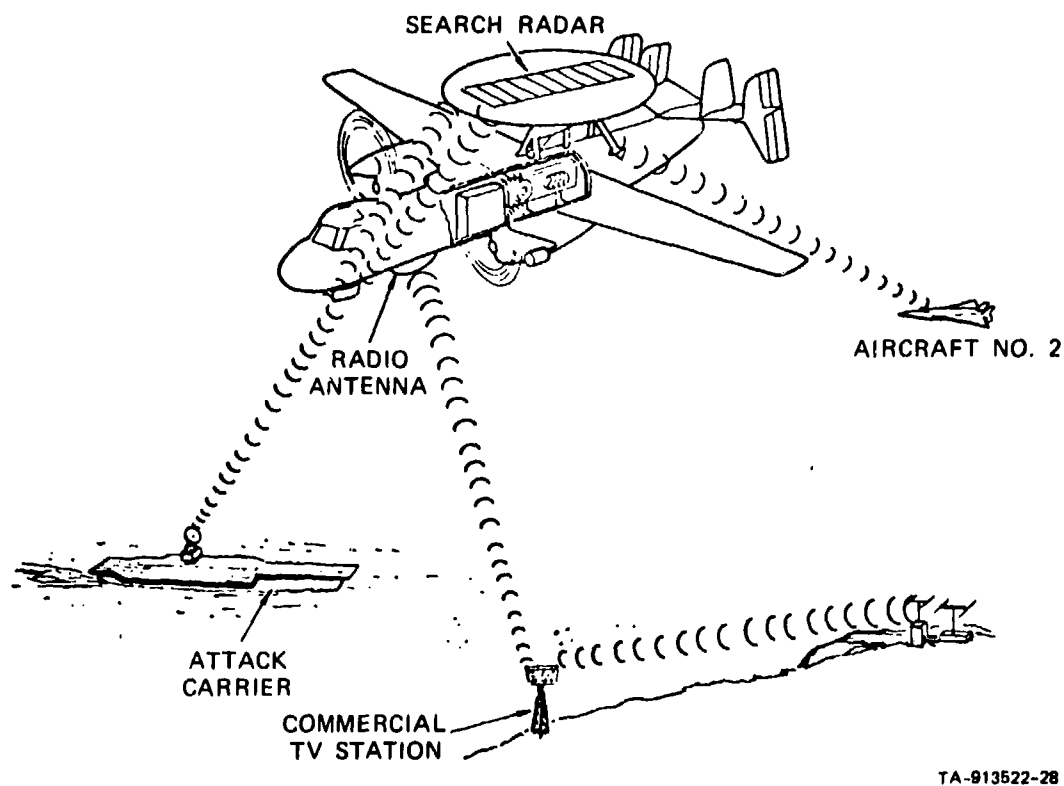
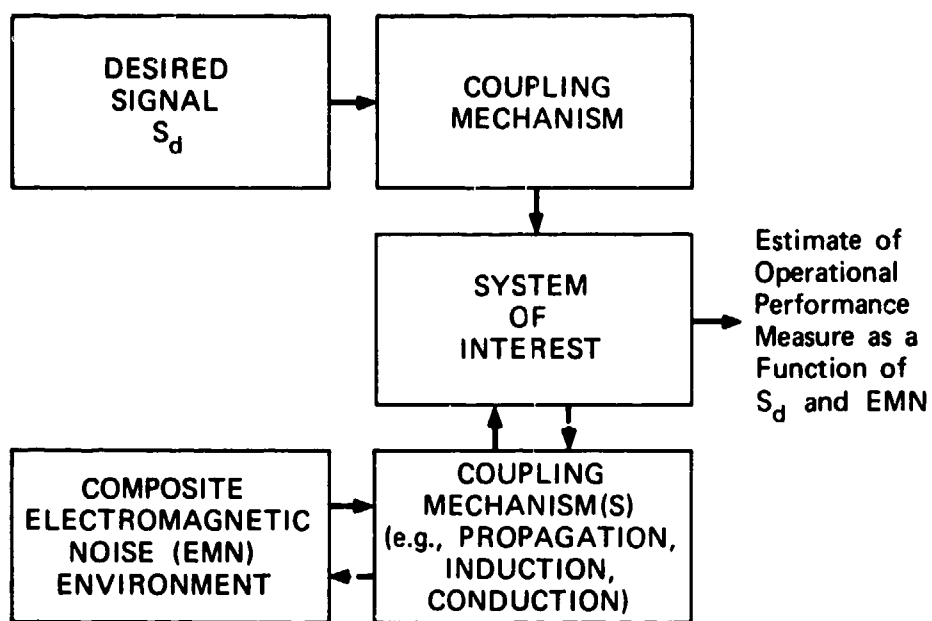
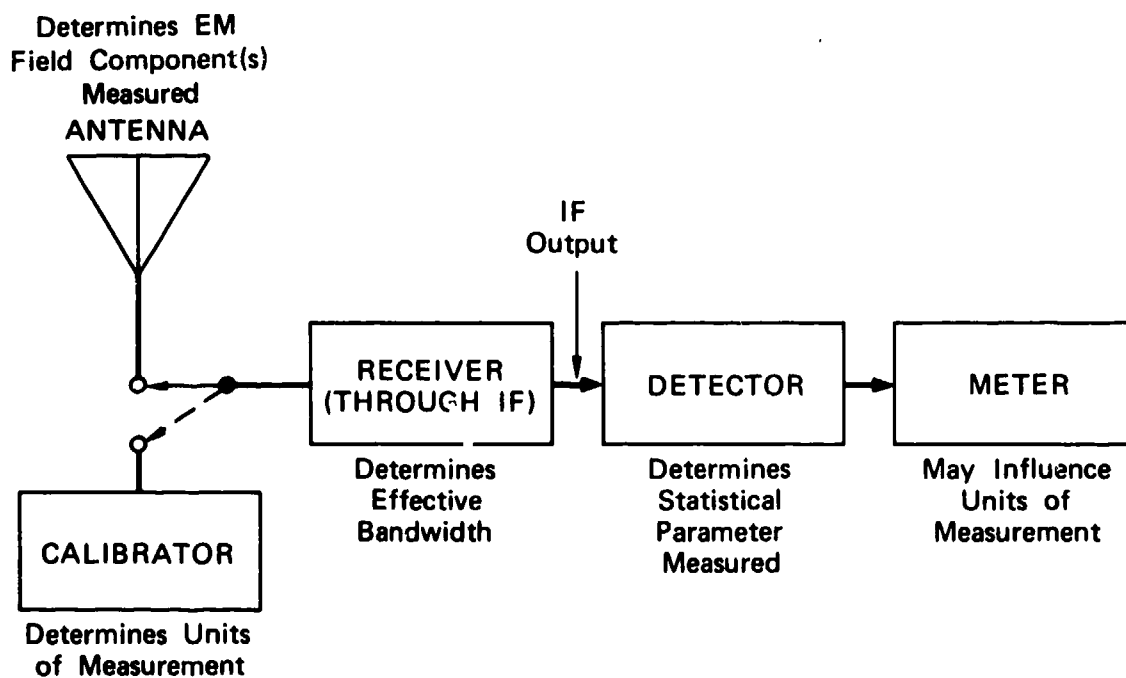


FIGURE 8 EXAMPLE OF OPERATIONAL SCENARIO (AFTER ZIMBALATTI, A. G., 1972)



TA-913522-29

FIGURE 9 EXAMPLE OF A CLASSICAL EMC ANALYSIS SITUATION



TA-913522-30

FIGURE A-1 NOISE MEASUREMENT SYSTEM FUNCTIONAL BLOCK DIAGRAM

## DISCUSSION

1-24 F. J. CHESTERMAN: Qualitative definitions are relatively easy, but quantitative definitions are extremely difficult if not impossible.

G. H. HAGN: Qualitative definitions are not exactly easy, but quantitative definitions are orders of magnitude more difficult. Nevertheless good progress was made by the CCIR this year on qualitative definitions of categories of interference of increasing severity. Hopefully quantitative definitions of permissible interference, etc. will be put forward for each type of service and agreement can be reached on both qualitative and quantitative definitions of several gradations of interference severity prior to the World Administrative Radio Conference in 1979.

G. TACCONI: I ask whether in the <<Spectrum Engineering>> definition namely the word "Spectrum" has to be interpreted in strict sense or broad sense.

G. H. HAGN: The word spectrum is used in the broad sense. Spectrum engineering and management involves the use of analyses, measurements, data bases and coordination processes to achieve EMC.

M. THUÉ: The negotiable noise level cannot be set quantitatively; the acceptable noise level depends on local environment conditions and should be agreed on by the organizations responsible for the various systems considered.

On the other hand, the permissible noise level (which can always be accepted) and the harmful noise level (which can never be accepted) have already been decided upon by a number of Committees of CCIR for some systems (fixed source by Hertzian beam or by satellite, broadcasting, television) and within some bandwidths.

G. H. HAGN: I agree. It is against the very principle of negotiation to do more before a specific situation arises than define where the negotiation must begin (e.g., in this case the boundary between permissible and negotiable). The true definition of permissible really lies in the quantification of the boundary (i.e., the level of severity of interference above which one must negotiate).

S. C. KLEINE: What makes officials hesitate to agree upon qualitative and quantitative definitions, bad or useful at least provisionally, just for the sake of having a common definition?

G. H. HAGN: There are many reasons why it is difficult to obtain agreement on basic definitions, and the process by which internationally accepted definitions evolve is a topic worthy of study in its own right. Regarding definitions of electromagnetic noise, interference and compatibility I can mention a few reasons. Agreement on qualitative definitions is hampered by many factors including:

1. Differences in current usage (e.g., the dual usage of the term interference to describe both the source of degradation and the degradation produced).

Differences in the languages into which the definitions must be translated.

Differences in the level of detail required by different groups.

And Human factors such as pride of authorship (e.g., the "not-invented-here" phenomenon). Agreement on quantitative definitions is somewhat less hampered by the items discussed above. The true vested interests of the types of services as well as those of the national administrations are even more strongly impacted on by the method used to quantify a qualitative term (e.g., permissible interference) and the actual level chosen for a given type of service. There may be differences in tolerance to interference by users of the same type of service in different countries. The definitions, once accepted, may be difficult to modify (even when modifications become desirable due to advances in technology). The economic implications as well as other nontechnical implications may be very large.

CPT P. HAILLEY: In Figure 5 of your paper, you have indicated designations which are either verbal descriptors or literal expressions of the disturbing effects of interferences. It would be advisable to devise a more accurate description, with references to a conventional code from 0 to 5, like that of QSA. I would suggest the following table:

QSA	Interference	Signal
5	None	Pure
4	Permissible	$S \gg I$
3	Disturbing	$S > I$
2	Harmful	$S < I$
1	---	$S \ll I$
0	Pure	None

G. H. HAGN: I believe such a code may be useful in its own right as well as being an intermediate step in the development of definitions of these terms from the qualitative to the quantitative. Perhaps it would not be necessary to have the six levels you define; rather, it should be sufficient to employ only as many levels as there are qualitative terms (e.g., none, permissible, negotiable and harmful). Regarding nomenclature, I believe it would be better to avoid the use of the symbol "I" as you have used it since this would tend to encourage the use of the term interference to describe the source. If we define  $S_d$  as the average power for the desired signal and  $N_t$  as the total average electromagnetic noise (EMN) power in the bandwidth of interest, then one could attempt to quantify  $S_d \gg N_t$  as it relates to grade of service for the different types of service. For some types of service this may be sufficient for quantifying what is meant by permissible; but for others it may be necessary to give more information (e.g., the percent of locations that a given grade of service will be exceeded for a given percentage of the time, as has been discussed by K. A. Norton, P. L. Rice, and others). It is important that the quantitative definition finally worked out be capable of verification by measurements for existing systems and be capable of estimation by analytical models for systems which are being planned.

Atmospheric Discharges and Noise  
( And Communications Systems Interference Reduction )

M. M. Newman\* and J. D. Robb

Lightning and Transients Research Institute

2-1

SUMMARY

Most studies of atmospheric in the past have dealt with the subject on the basis of the frequency domain as a linear phenomenon. From the special point of view of working to improve communications systems performance, there are advantages to be derived in viewing the problem in the time domain. This permits the application of nonlinear techniques, for example, by circuitry gating at the input before the noise pulses shock excite resonant circuits. This paper deals with wide band measurements, up to 200 megahertz of the "fine-structure" of radiation from individual discharges, as well as longer consecutive records of the character and spacing of pulse components of branching streamers and repeated discharges, which have hitherto been unavailable.

Direct lightning interception studies both by us in the U.S.A. and recently in France, are discussed in relation to discharge noise characteristics. Also our research on artificial lightning discharge 'noise' propagation and reception at various distances, are presented as a unique tool for atmospheric propagation studies.

1.0 INTRODUCTION

In attempting to improve communication systems performance in the presence of atmospheric noise, there are advantages to be derived from viewing the problem both in the frequency and time domain. Consideration of atmospheric generation from numerical calculations of the channel current during the formative stages along with laboratory reproductions and time resolved panoramic measurements of natural atmospheric suggest some approaches to improved signal detection in the presence of atmospheric.

2.0 LIGHTNING STROKE DISCHARGE MECHANISMS AND NOISE

The complexity of atmospheric wave shapes and corresponding radio interference are influenced strongly by the ionized streamer propagation mechanism of the lightning discharge. When spark breakdown of a stressed region occurs, the rate of current transfer is influenced by the rate of transfer of charge in the cloud mass itself and by the characteristics of the ionized path of breakdown. Photographs taken by Schonland, with a rotating Boys camera, illustrated the formative stages of the lightning stroke and showed that the development of the breakdown is a progressive process, the leader stroke proceeding by a series of steps, such as illustrated in Figure 1a.

As a group of branch streamers develops, electrical charges are transferred from the cloud to the newly ionized streamer channels which act as charge storage (capacitive) element. The corresponding charging time through the nonlinear resistance of the feeding channel, which is high initially and drops in value as a function of the charge transfer through it, causes a time delay of potential propagation along the streamer as new streamer channels are charged. These in turn will then be raised sufficiently high in potential at their tips to form new branching streamers, and so the process is continued. This results in a step process with corresponding multiple current peaks during the lightning channel propagation period.

An equivalent circuit for the stepped leader stroke is assumed to be that shown in Figure 1b. The resistance in a part of the channel through which current is passing is assumed to vary with the time according to the formula  $r = k/q$ , where  $k$  is a constant and  $q(t) = \int i dt$  is the charge which has passed through that part of the channel. A formula of this form has been found by M. Toepfer to be valid for the resistance per unit length of short sparks. The capacitance  $C$  represents the large storage capacitance of multiple charge tapping streamers within the cloud. The capacitances  $C_2, C_3, \dots$  are estimated from the empirical photographic data on the lengths of the steps of the leader stroke.

Owing to the presence of the nonlinear resistances in the equivalent circuit, calculations were made by numerical step-by-step methods, using reasonable circuit parameters based on observed leader dimensions. The calculated form of the discharge current at the cloud is shown in Figure 1c.

The resultant current flow shown in Figure 1c is seen to be in a series of pulses with an increasing spacing corresponding to audio frequency pulse train decreasing from about 12 kc, which is of some interest as it would account for some short whistling notes observed in low frequency sferic measurements. It also follows from a study of the course of the step-by-step calculations, that as the channel approaches the earth plane or an oppositely charged cloud area, the gradient would increase for successive steps which would result in an ascending frequency note. Thus this mechanism could conceivably account for some short observed "whistlers" or "tweaks" of both ascending and descending frequency. This suggestion is not proposed as a substitute for the ionosphere propagation theory proposed originally by Eckersley, and more recently by Storey, for the

---

\* Presently Research Professor, Florida Institute of Technology and Research Director of Lightning and Oceanics Research Institute.

long-delayed whistlers and whistler trains, but rather to possibly account for a number of short audio pulse trains like tweeks, tweets, etc. somewhat similar to "whistlers" which may need to be accounted for separately from the whistlers explainable by ionospheric propagation theory.

The calculated stepped pulse spacing of Figure 1c turned out to be in surprisingly close agreement with corresponding spacing of light intensifications of Dr. Schonland's stepped leader photographic records. Thus the proposed channel mechanism electrical circuit equivalent seems a fairly accurate and useful representation from which various characteristics of radiated interference may be readily deduced and checked with corresponding laboratory experiments.

### 3.0 LABORATORY REPRODUCTION OF THE LIGHTNING CHANNEL BRANCHING EFFECTS

Little is known from direct measurements of the manner in which the propagating discharge channel taps charges within the cloud. It is reasonable to expect that channel streamers will also propagate inwardly into the cloud mass, a process which besides commencing simultaneously in multiple paths into the cloud could be expected to speed up after the 'reflected' current wave in a stroke to ground lowers the cloud potential at the origin of the groundward channel.

The channel propagation mechanism equivalent circuit of Figure 1b was reproduced experimentally, as shown in Figure 2a.

The system of vertical lines seen in the photograph are rubber hoses with slightly conductive water inside coupled to a parallel grounded feed system overhead. Conductivities of the branch paths are readily varied to correspond to lightning branch streamers. In the above experiment the branch channel, at A, formed a main discharge to ground, while the guided discharge seen faintly from A to B with no ground return stroke represented the equivalent of a cloud to cloud discharge.

An important conclusion from the artificial channel experiments, in relation to theory of cloud charges, is that the progressive charging of new areas by the advancing streamer of a lightning discharge, as illustrated in Figure 2a, requires relatively low cloud potentials. This is further shown in the illustrated demonstration setup of Figure 3(a) where a 20,000 volt charged condenser produces a two foot long spark which is about 50 times as long as a single spark unaided by the step-by-step branch streamer equivalent mechanism shown schematically in Figure 3(b).

### 4.0 INFLUENCE OF THE DISCHARGE MECHANISM ON THE RESULTANT CHANNEL CURRENT AND RADIATED SPHERICS WAVE SHAPES

The discharge channel characteristic pulses shown in Figure 1c are considered a very important factor in determining the nature of atmospherics. Consequently the artificial lightning generator and propagation mechanism setup of Figure 2 is being expanded to provide discharge channels over 50 meters in length so that measurements of channel resistivities, surge impedances, and propagation velocities can be studied on a scale comparable to natural lightning phenomena.

In the preliminary investigations with the small model channel, illustrated in Figure 3(a), oscillographic records were made of the current variations across the shunts as shown in Figure 3(b); the shunt locations left and right correspond to the top and bottom of the channel. Though equivalent branching streamer capacitances and jumping distances are on a much smaller scale than actual lightning discharges, the oscillograms obtained, as shown in Figure 4(a,b,c), show characteristic pulses of the lightning channel discharge current propagation process which are similar to the current oscillogram shown in Figure 4(d) obtained in an airplane which intercepted a natural lightning discharge considered to have taken place between clouds.

Considering the many separate pulses contributed by the main channel streamers, illustrated in calculated curves and oscillograms, and also similar processes in tapping different cloud charge centers, we obviously obtain in the radiated 'spherics' complex wave forms sometimes difficult to distinguish from multiple reflected simpler discharges. Propagating streamers such as have been observed to progress for tens of kilometers for as long as a second could thus produce almost continuous interference ranging from short audio frequency pulse trains to components of several hundred megacycles. Figure 5 shows some oscillograms of induced lightning wave forms in the four meter single turn shielded aperiodic loops located, as shown in Figure 2a, on top of the laboratory.

Aside from lightning atmospherics, other transient disturbances may be induced on an antenna under thunderstorm conditions. Figure 6 illustrates possible transients from corona, adjacent insulator surface streamering, and from charged rain drops. While these transients should not be aircraft communications and probably account for much of the radio interference encountered under thunderstorm conditions. In making measurements of spherics it is therefore important to reduce possible interference from associated corona streamer and rain drop effects by properly shielding the antenna systems.

After making sure by proper antenna shielding and checking tests that the interference wave forms were related directly to lightning discharges, we resolved typical atmospherics into harmonic components both analytically and by direct measurement of excitation effect on different frequency range communication receivers.

### 5.0 RESOLUTION OF ATMOSPHERICS BY HARMONIC ANALYSIS

Mathematical representation of atmospherics involves difficulties which arise from the fact that atmospherics are stochastic. In simple (but not completely accurate) language, this means



that a given atmospheric noise train is only one member of an infinite sample space of possible noise trains and that the situation is best described by the probability distribution over this sample space of noise trains.

2-3

If one wishes to avoid a treatment of atmospheric noise which is based on the above considerations, one might treat each observed atmospheric by means of harmonic analysis. It is to be hoped, for example, that a survey of the harmonic analyses of many atmospheric noise trains would permit one to draw conclusions concerning the relative statistical frequencies with which certain parts of the radio spectrum appear among the components. The mechanical procedures for such harmonic analyses are simple though tedious; several lightning wave forms of the type shown in Figure 5 were analyzed. Figure 7b compares the original wave segment of 7a with a recombination of the harmonic components illustrating accuracy for the interval resolved. Since the transient is nonrepetitive, there is no longer a fit outside the interval chosen, therefore such decomposition can be considered only an approximation.

#### 6.0 RESOLUTION OF ATMOSPHERICS USING PANORAMIC ANALYZER EQUIPMENT

The L & T Laboratory had earlier developed a panoramic interference analyzer covering the frequency range of 100 kHz to 1000 MHz. For purposes of this investigation a simplified system was built up using five calibrated receivers tuned respectively to 15 kHz, 190 kHz, 1 MHz, 9 MHz and 150 MHz, whose audio envelopes were applied to a five beam cathode-ray tube indicator unit built up with simple positioning controls. Figure 8 illustrates the equipment used in the atmospheric studies and Figure 9 presents a corresponding schematic diagram.

The panoramic section with the five receivers and a five beam cathode-ray tube is shown to the right in Figures 8 and 9. The center section has a dual beam cathode-ray unit which records the stroke direction and the antenna voltages directly with a resolution equivalent to the receiver responses. The center section also contains standard precision crystal controlled oscillator providing a time standard controlled clock which is required for synchronization of data with other cooperating observatories. To the left is shown a wide band oscillograph for recording fine structure radiation with greater resolution corresponding to higher frequency stroke components.

Sample records of respective receiver responses to the atmospheric are shown in Figure 10a. A sample replot from an enlarged projection of these records is presented in Figure 10b. The amplitudes shown are to a scale corresponding to the adjusted receiver sensitivity and were selected by adjusting sensitivities to values sufficient to give measurable deflection during periods of atmospheric activity.

Additional replots of the film data on a condensed scale as given in Figures 11 and 12 present extended indications of receiver susceptibility for different frequencies and also an indication of relative location and lengths of spaces free from noise. Figure 11a shows electric field variations over a 15 minute period during a summer thunderstorm illustrating the frequency of major charge redistributions in the vicinity. Figures 11b, 11c, and 11d, present graphs of the communication time available for receiving input signal levels of the order of 500 microvolts over typical local lightning periods of three seconds and 60 seconds respectively.

The graphs indicate that for moderate strength signals, considerable amount of "clear" space exists which might permit continued communications if the disturbing effect of the more severe interference peaks could be removed. Some possible circuitry methods of selectively rejecting such interference are briefly discussed in the next section on atmospheric interference with communications and possible reduction methods.

#### 7.0 MEASUREMENTS OF TRIGGERED NATURAL LIGHTNING DISCHARGE CHANNEL CURRENTS

Direct lightning channel current measurements have been made at the base of a triggered lightning channel. This is defined as one triggered by a rocket born fine wire carried to heights of 300 to 900 feet at a time when the electric field indicates that a lightning discharge is probable. This is a technique which has been pioneered by LTRI as a technique for studying both the channels and the radiated signals. These measurements have shown the highly random nature of the current variation and the periods of lower intensity, as shown in Figure 12, and as observed in the radiated field measurements shown in Figures 10 through 11.

#### 8.0 GENERATION OF ARTIFICIAL ATMOSPHERICS FOR PROPAGATION STUDIES

A useful tool in the study of atmospheric propagation has been developed in which pulses of one to nine million volts are fed into the base of a five kilometer vertical antenna which is supported by a small helicopter. This technique permits the study of ground and skywaves separately at distances of several kilometers away and can be detected at distances of thousands of kilometers. The signal is received most conveniently by use of a clock synchronized oscilloscope at the receiving station. Using this technique simulated atmospheric waveforms as determined in the measurements program could be applied to the antenna for the generation of representative interference and simulation of even nearby effects on communications systems.

#### 9.0 ATMOSPHERICS INTERFERENCE WITH COMMUNICATIONS AND REDUCTION METHODS

The preceding illustrations of recorded atmospheric wave shapes and their effect in shock excitation of the different frequency range receivers, composing the panoramic interference analyzer, indicated time variation effects of local thunderstorms and effects which disturbed communications from lowest frequencies to over 150 MHz.

2-4  
J. R. Carson has pointed out in some of his early work\* that narrowing the bandwidth by increasing selectivity of the receiver circuits still leaves an irreducible minimum of interference which might still block communications if the original interference were great enough. Carson's theoretical work and consequent pessimistic view of ultimate limited possibilities of improvement of signal to impulsive-noise ratio was based on the study of linear circuits; considerable improvements are possible by the introduction of non-linear elements to eliminate the high-level interfering impulses.

The complexity contributed by radiation from the branching formation process of the lightning discharge, as discussed earlier, introduces at variable times very high pulse repeat rates. The high pulse rates introduce overlapping shock excitation envelopes within the receiver that would completely swamp signals; and if the interference amplitudes were limited by conventional limiters or clippers inside the receiver the audio output may be quieted but will have caused loss of signal modulation and hence intelligibility.

Earlier reported work\*\* of the L & T laboratory has brought out both desirability and feasibility of removing the interference before it reaches the receiver so that a very much smaller portion of the signal carrier is lost and a very much greater number of disturbances can be tolerated than with any scheme of limiting within the receiver. This basic approach of interference reduction ahead of the receiver has resulted in improvement ratios of the order of 50 db applied under thunderstorm precipitation static conditions inducing corona pulses, of the type shown in Figure 6, with repeat rates of the order of 100,000. Although atmospherics present much more severe problems, the records from this investigation do indicate some possibilities of reducing their interfering effects as will be developed in the following discussion.

The original form of the interference rejection scheme which has proved effective for corona interference induced in both thunderstorm and precipitation-static conditions is illustrated by the block diagram, reproduced from the earlier referenced paper, in Figure 13.

The "demon" block section of Figure 13, in a similar manner to Maxwell's famous postulated "demon" sorting particles by their speed, serves to detect the arrival of interfering impulses by their characteristic transient features of high voltage rates of rise and amplitudes, and thereupon operates the "gating" section.

In the case of distinct corona impulses it is possible to close off the "gate" or effectively "blank" for such short intervals that the total percentage of blanking may be less than 20% even with 100,000 pulse repeat rates. The 'flywheel' action of the following receiver narrow-band tuned circuits fills in the blank time gaps, and loss of signal time of 20% of a time interval short relative to modulation amplitude changes would introduce a 20% reduction in signal modulation amplitude for the same interval; and actually 50% blanking times were encountered and found satisfactory in precipitation-static corona interference reduction. Theoretically, on a sampling basis, higher blanking space ratios than 50% are usable so long as the average 'gating' rate remained steady at rates over 10,000 (in order to reproduce up to 5000 cycle signal components), and the related blank space to signal space ratio remained fairly constant, thus effectively providing a signal sampling system which when triggered by an approximately recurrent interference such as with some corona discharges would correspond to sampling systems used in some time sharing modulation systems.

However the atmospherics records presented earlier show that wide variations occur in pulse rates and duration cycles; hence a space factor first 20%, then 80%, then perhaps 0 in adjacent intervals would obviously introduce corresponding severe signal cross modulation from the interference, and therefore relatively simple blanking would be ineffective for the widely varying space factor spheres.

Since actually there are frequently recurring intervals relatively free of atmospheric interference we might arbitrarily ahead of time consider reducing the average gated signal-passing time to a sort of lowest common denominator selected time interval segment, and thus remove the cross modulation from gating time variations. Ideally we could go one step further and postulate a completely effective interference reduction system for atmospherics having some relatively interference free space available for sampling at rates of at least twice the maximum desired signal intelligence frequency. If we assumed 5 kc as maximum desired signal modulation frequency to be passed, we would need to divide the sampling time into intervals repeated at at least 10 kc, or less than 100 microsecond lengths. Actually because of possible misses or bunching effects we might choose shorter intervals. Let us consider a time graph of signal carrier and superposed atmospherics sectioned into 20 microsecond intervals as illustrated in Figure 14 and let us choose a gate interval of 10% of the sampling space interval, or 2 microsecond width.

Ideally we would like to explore the entire segmented interval and choose the best 10% section; practically we could do it in a fashion of checking each step and move along time-wise in this way and open the gate for the first interval in which the interference is below a preset level. It is conceivable some intervals may not have any such favorable interval in which case it might be desirable to increase time of pass in a succeeding interval to compensate for lost intervals. The 10% pass factor is chosen on the assumption that on the average that percentage space might be relatively free of interference. It might be desirable, and preferably automatically, to have the gate pass duration variable so that in case of less severe average interference a larger pass space factor could be used; and when the interference is infrequent the periodic gating scheme will revert to the simple triggered blanking basis. Actually the addition of the above functions is relatively simple compared with the primary requisites for the original blanking scheme discriminator which detects and examines the interference and acts to operate the gate. Thus, in Figure 13 the main schematic corresponds to one of the forms of the original simple blanking function scheme, on

which a patent was issued, and the inserted four tube circuit converts it to a selective gating system basically capable of handling more complex atmospherics, as outlined above.

Because of the long periods between peaks in atmospheric noise, a major problem in developing the above approaches has been that of obtaining delay lines with sufficient time delay. The development of acoustic surface wave delay lines with much longer delay times than earlier transmission line types appears to be ideally suited for this application.

#### 10.0 SUMMARY REVIEW OF OUR PAST AND PLANNED FUTURE ATMOSPHERICS RESEARCHES.

Under early Navy Bureau of Aeronautics and Air Force programs, the concern was primarily to improve aircraft communications in thunderstorms and thus our researches have had a main goal of measurement and recording of incident atmospherics to determine possibilities of selecting signal intervals in between peak atmospheric activity with electronic circuitry rejecting the most severe interference ahead of the receiver shock excitable tuning networks.

From an early review, we had made of the literature on atmospherics, it was clear that other studies fell into two main categories, first relatively low band width measurements, mostly below 300 kilohertz, of individual spheric wave shapes with components reflected from the various heaviside layers and, second, long time integrated variations of spheric activity systematically measured at different locations in terms of receiver audio output. The available data and earlier programs were valuable in relation to determining power levels that would be needed in respect to different communication systems in different frequency ranges, but from our point of view of working to reduce interference by circuitry gating at the input of the receiver earlier available data was considered insufficient. Therefore we devoted our efforts to wide band measurements, up to 200 megahertz of the "fine-structure" of radiation from individual discharges as well as longer consecutive records of the character and spacing of pulse components of branching streamers and repeated discharges which had hitherto been unavailable.

In addition to research and related instrumentation development work summarized in this report and the development of interference reduction we had worked out a laboratory atmospherics generator prototype design along the lines of a high power pulse generator developed by us under another program with different wave shape component pulses controlled and modulated by a high speed magnetic tape or oscillographic film scanning system, in which different types of atmospheric recordings can be readily reproduced.

A companion instrument to the atmospherics generator had been devised to provide a direct intelligibility record using either natural interference or the atmospherics generator. The instrument design provides a rather versatile "intelligibility" meter, in terms of percent error count based on a gating comparator of original coded message elements and their resultant after being mixed with interference and passed through the receiver. This approach permits evaluation of improvement ratios with rejection circuitry far better than by conventional noise meter comparisons or listening tests.

Another technique considered and begun in the atmospherics program is the classification of atmospherics components by an adaptation of a "counter-type analyzer" developed under another program. The results have been encouraging to date and accordingly we expect and plan for continuation along the above lines of research and related instrumentation development.

There are several phases of our originally planned program in which our rate of progress to date has disappointed us but which we consider important and hope to continue. One of our plans had been to generate artificial spherics using our nine million crest voltage impulse generator with the artificially propagated long spark discharges simulating branch streamers. Calculations have shown that we could have peak radiated components of the order of megawatts in the 100 kilohertz region which with the advantages of being producible at specific times, we had planned to record in our mobile laboratory at different distances and also at different times to study ionospheric effect variations. The other part of our original plans which also was disappointingly delayed was our program of simultaneous coordinated measurements by us and several other cooperating laboratories. Our atmospherics work discussed in this report is just a portion of combined programs on reducing thunderstorm hazards to aircraft, with the effects on communications originally considered of secondary importance, consequently at later stages of the work emphasis on lightning protection aspects diverted both time and funds and slowed down instrumentation for the triangulation measurements. Continuation with such coordinated measurements is also certainly worthwhile, and we have applied to this phase some of our own laboratory's industry granted research funds.

It should be noted that our wide band approaches are difficult and expensive for general observations. It is preferable (and in case of our own researches on circuitry methods of atmospherics rejection we, of course consider it essential) to record atmospherics wave shapes and spacing characteristics as they would appear at the receiver input rather than at the output where the wave shapes are essentially converted to be characteristic of the receiver tuned circuits.

As a final comment, we might refer again to the practical value of the "fine-structure" and essentially wide band type of atmospherics studies that we have been carrying on and hope to continue. Using the proposed scheme and some other modifications, it should be possible to design a plug in replacement unit for several tubes in conventional (100 kilohertz - 2 megahertz range) radio direction finders and greatly reduce their vulnerability to both precipitation-static and atmospherics under thunderstorm conditions. The reduction of aircraft hazards by more dependable communication in severe thunderstorm conditions which is materializing from progress in these atmospherics research programs certainly justifies continued support of

most of these outlined researches; and though, from time to time, supporting budget variation may reduce the more fundamental phases of longer range importance at a slower pace, we hope to continue the various atmospheric study phases we have discussed in this report.

#### 11.0 REFERENCES AND BIBLIOGRAPHY

1. J.R. Carson, "Selective Circuits and Static Interference", Bell System Tech. Jour., vol. 4, pp. 265-279, April, 1925
2. M.M. Newman, "Corona Interference with Radio Reception in Aircraft", Proc. NEC., vol. 4, pp 91-95; November 1948
3. M.M. Newman, "Impulsive Radio Interference and Reduction Methods", Proc N.E.C., vol. 6, pp. 238-242; September, 1950
4. M. M. Newman, " Bibliography Relating to Lightning Atmospheric Location", L&T Report No. 181, Final Report U.S. Office of Naval Research Contract N6, ONR-230-II
5. M.M. Newman and J.D. Robb, "Precipitation-Static and Atmospheric Interference Reduction," Final Report - U.S. Navy Bureau of Aeronautics Contract NOa(s)-12017
6. J.R. Stahmann, "Broad-Band High Voltage Type Impulse Noise Generator, Interim Report No. 1, Contract AF 33(616)-410., L&T Report No. 266
7. M.M. Newman, J.R. Stahmann, and R.C. Schwantes, "Counter Type Interference Analyzer ", Final Report - U.S. Air Force Contract No AF33(038)-17144.
8. M.M. Newman, " Research Information Available and/or Lacking on Atmospheric in Relation to Working Out Circuitry Methods for Sferic Interference Reduction," L&T Report No. 316
9. M.M. Newman, J.R. Stahmann and J. D. Robb, "Experimental Study of Triggered Natural Lightning Discharges", Final Report under U.S. Federal Aviation Agency Contract No. FA66NF-156

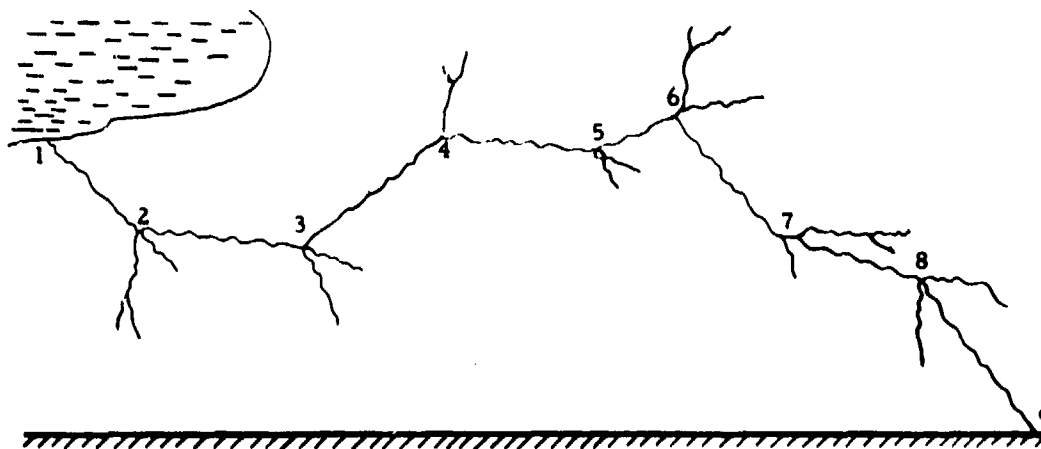


Fig.1(a) Progressive branching of lightning discharge channel

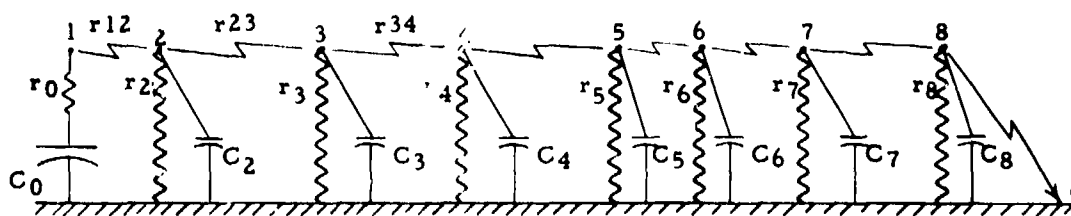


Fig.1(b) Equivalent electrical circuit during initial propagation stages

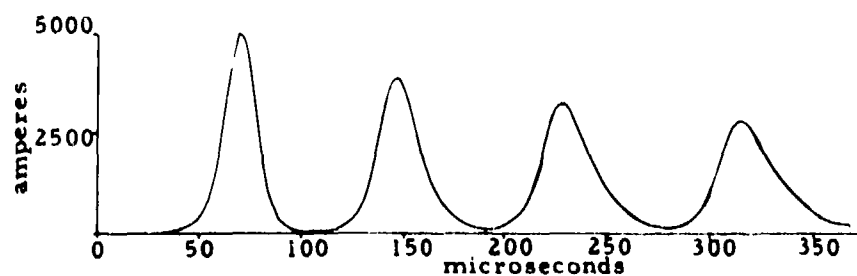


Fig.1(c) Calculated current variation at cloud end of discharge channel assuming  $r_{12}, r_{23}$ , etc. to vary inversely as total charge passing

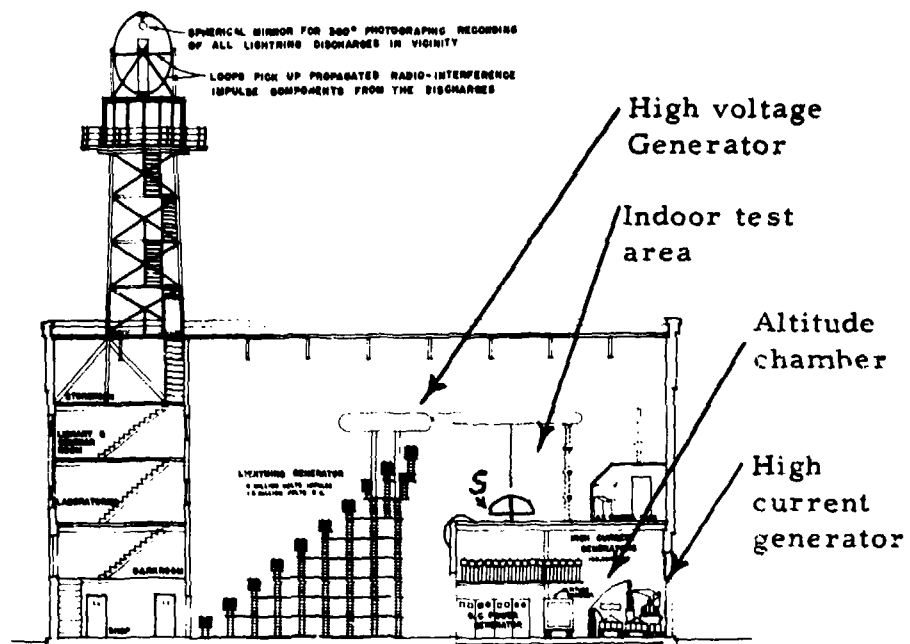


Fig.2(a) Cross section view of laboratory test arrangement with high voltage DC generator depositing charge on hemi-spherical plexiglas surface, S

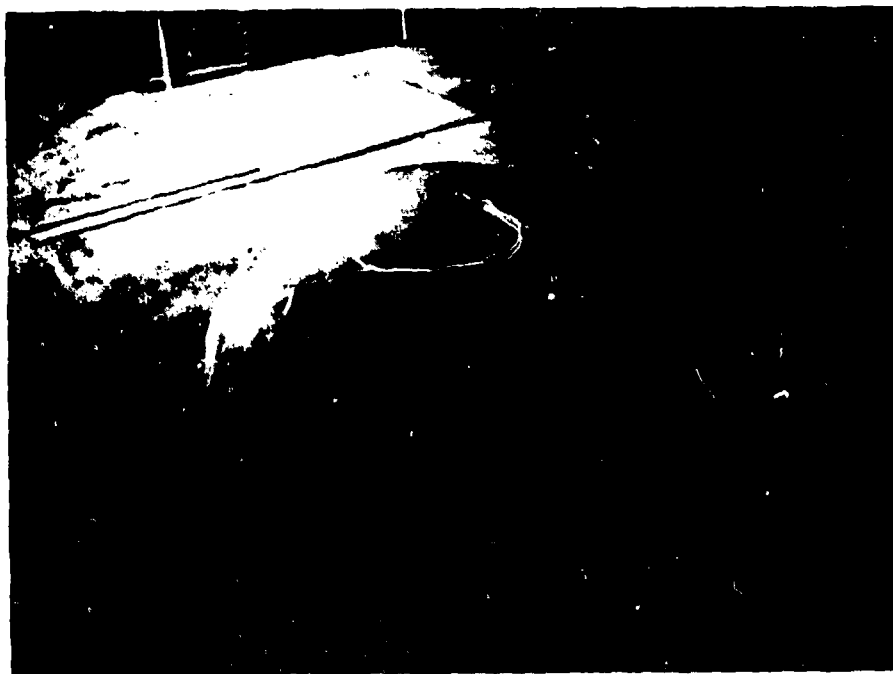
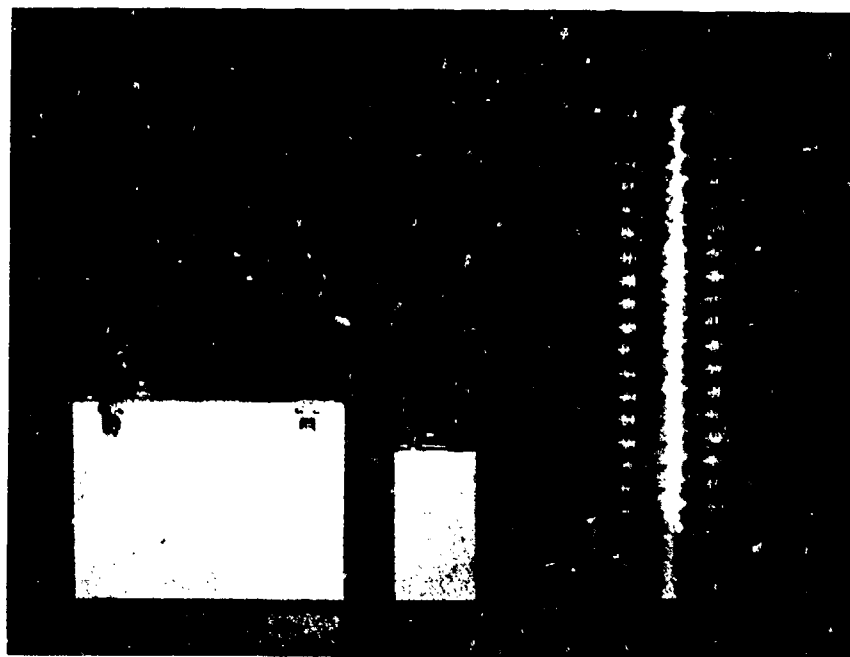


Fig.2(b) Photograph of discharge streamer tapping charged areas on the surface of a plexiglas hemi-sphere, analogous to charged cloud streamers



Fig.2(c) Laboratory lightning branching discharges of fifty foot lengths from a two million volt impulse, illustrating the streamer mechanism permitting propagation of very long discharges from relatively low cloud potentials

(a)



(b)

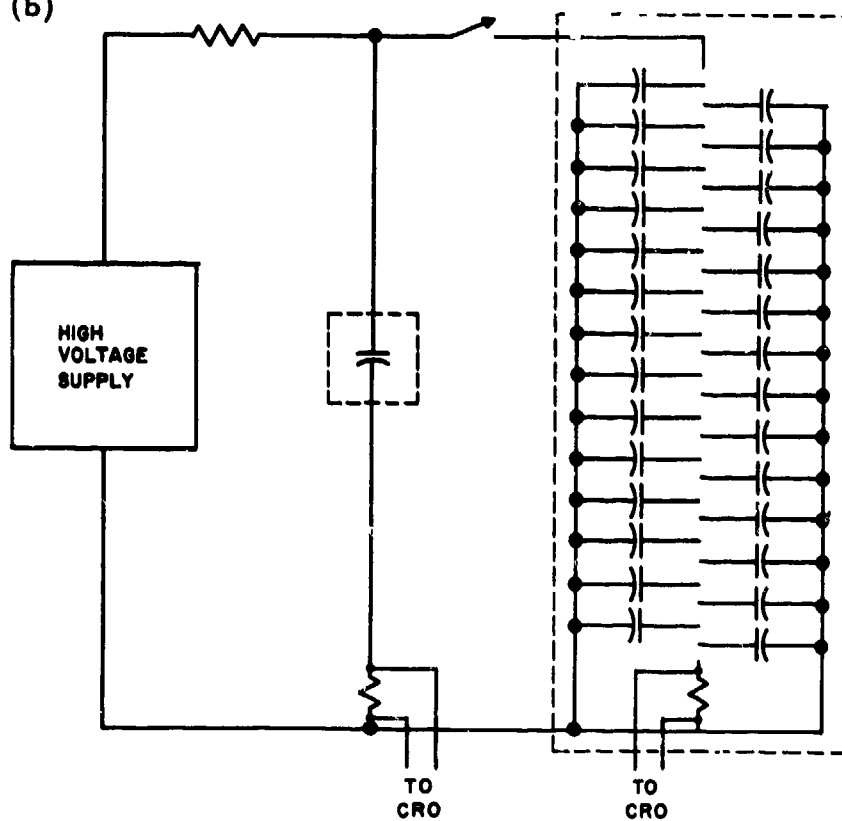


Fig.3 Photograph (a) and schematic diagram (b) of model of lightning discharge channel



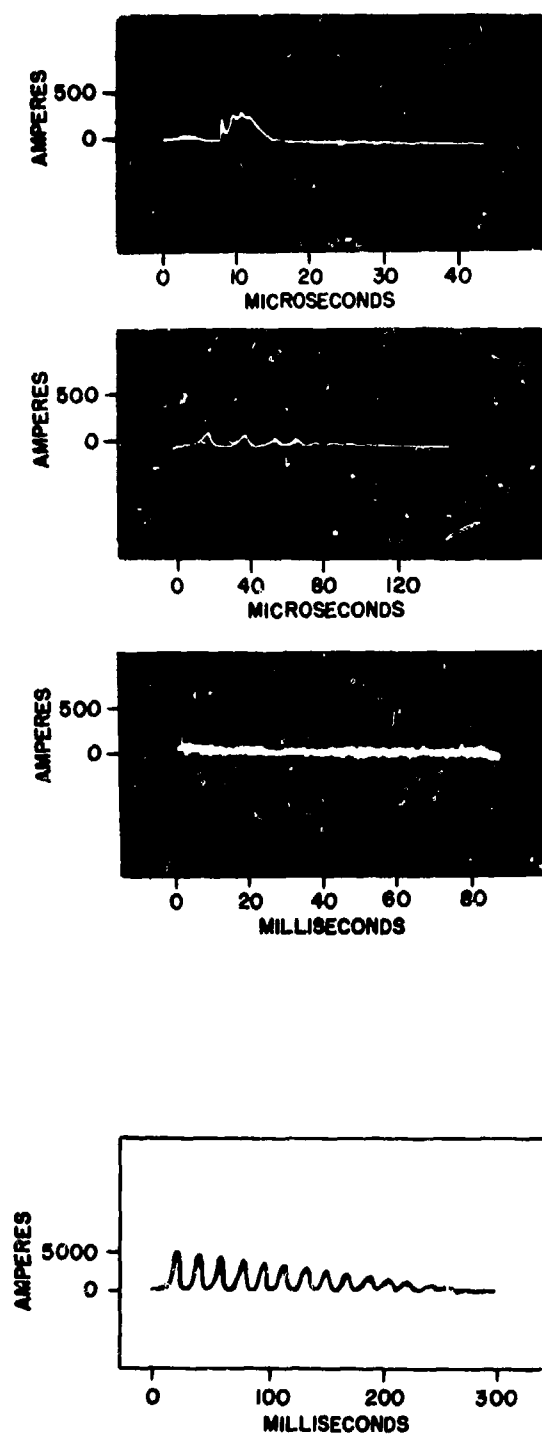


Fig.4 Top three current oscillograms obtained with model channel circuit of preceding Figure 3(b) showing similar characteristics as bottom oscillogram, recorded in flight investigations, of a lightning discharge through an airplane

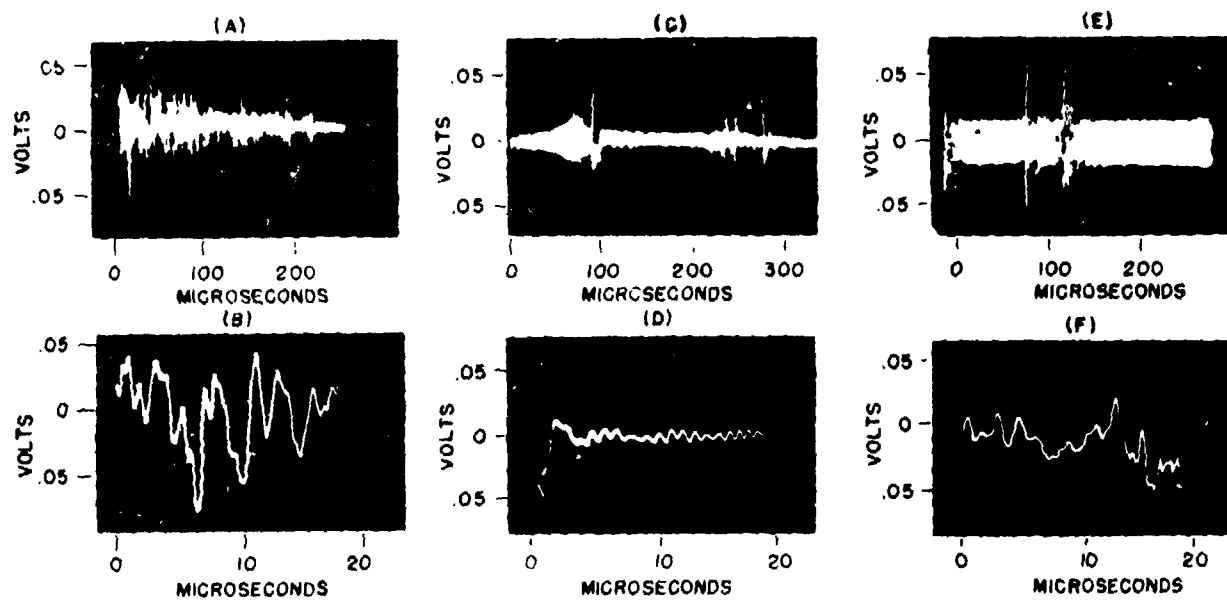


Fig.5 Typical oscillograms of induced potential wave forms, in an aperiodically terminated single turn 4 meter loop, about 3--5 miles from lightning area

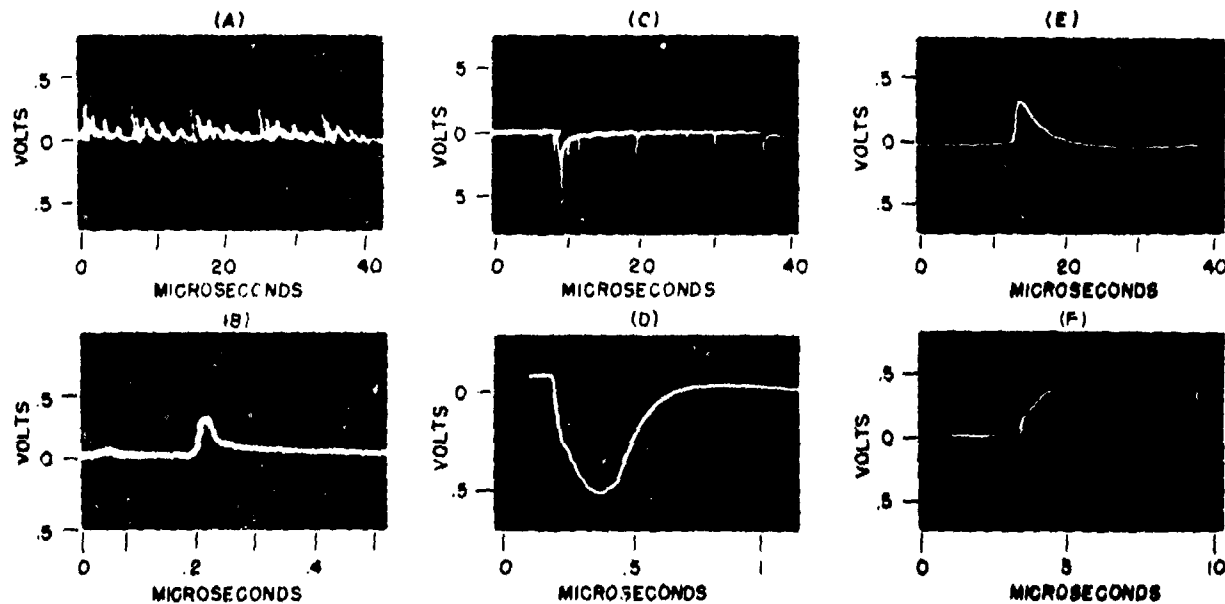
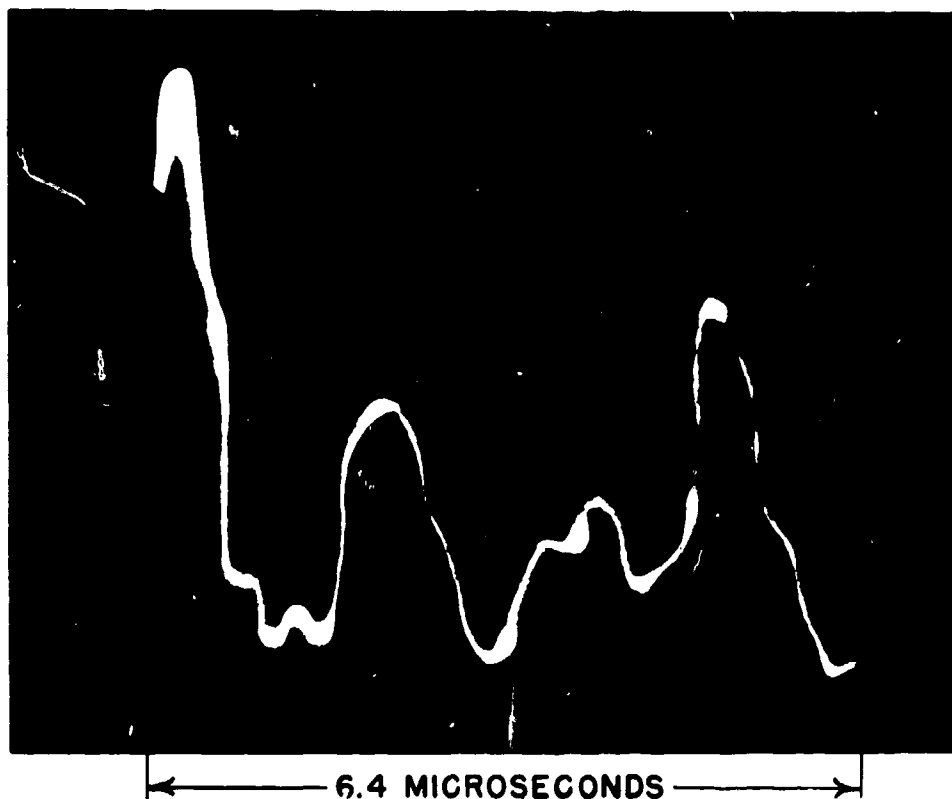


Fig.6 Laboratory oscillograms of interference transients to be expected on an antenna, other than lightning atmospherics, under thunderstorm conditions A and B, corona on bare wire antenna; C and D, from adjacent insulating surface streamering; E and F, from charged rain drops hitting the antenna

(A)



2-13

(B)

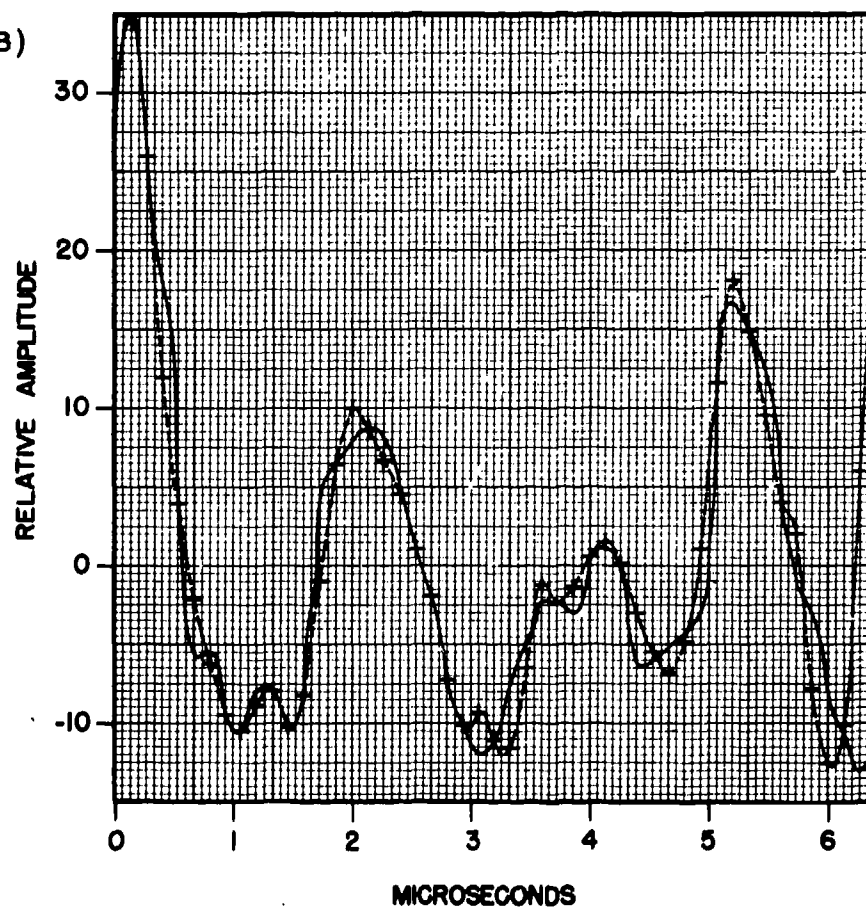


Fig.7 A (above) Oscillogram #1 resolved into harmonics  
B (below) Comparison of original wave and reconstruction of harmonics

2-14



Fig.8 Atmospherics measurement, equipment including: 150 mc broad band oscillograph, direction finding and crystal controlled oscillator timing equipment, and the panoramic interference analyzer

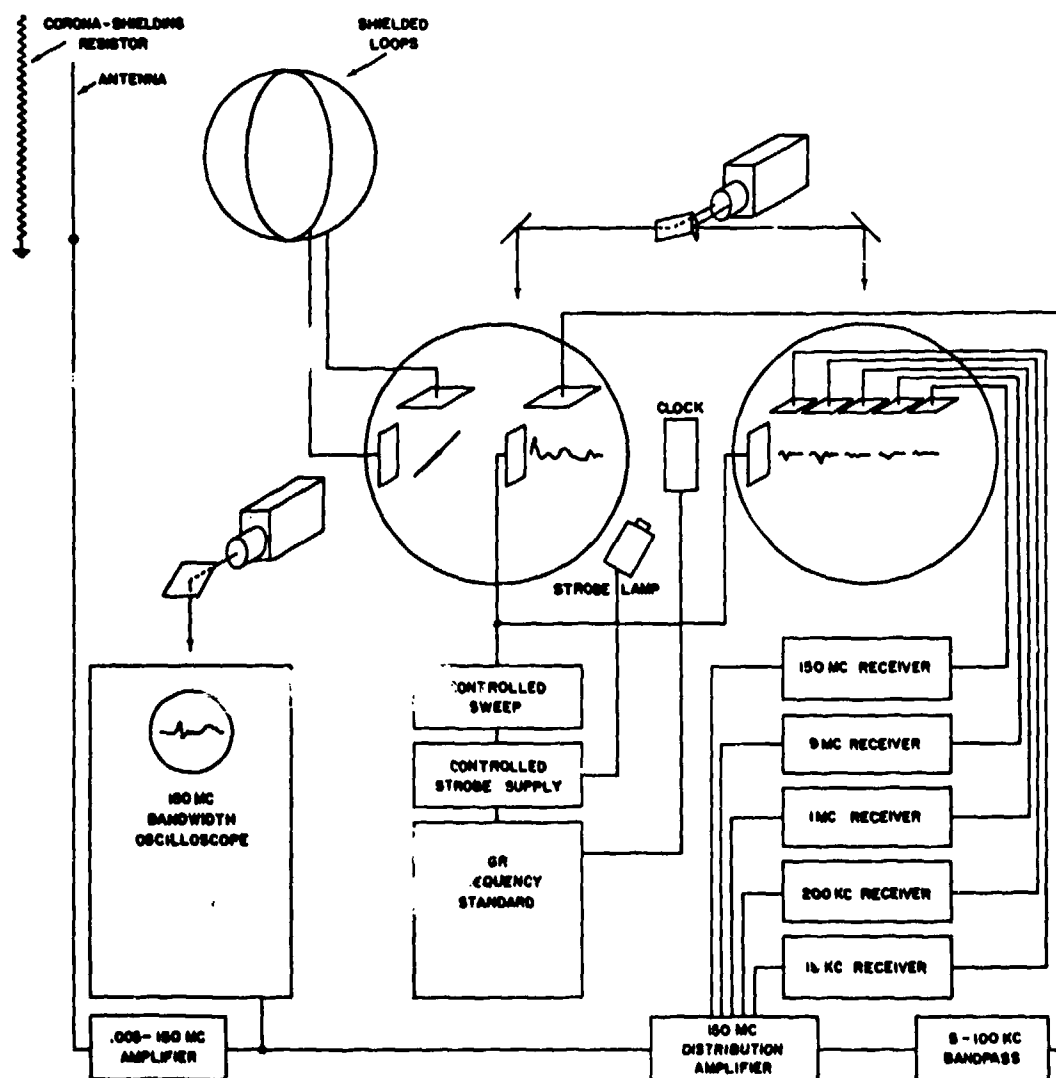


Fig.9 Block diagram of the atmospheric recording equipment

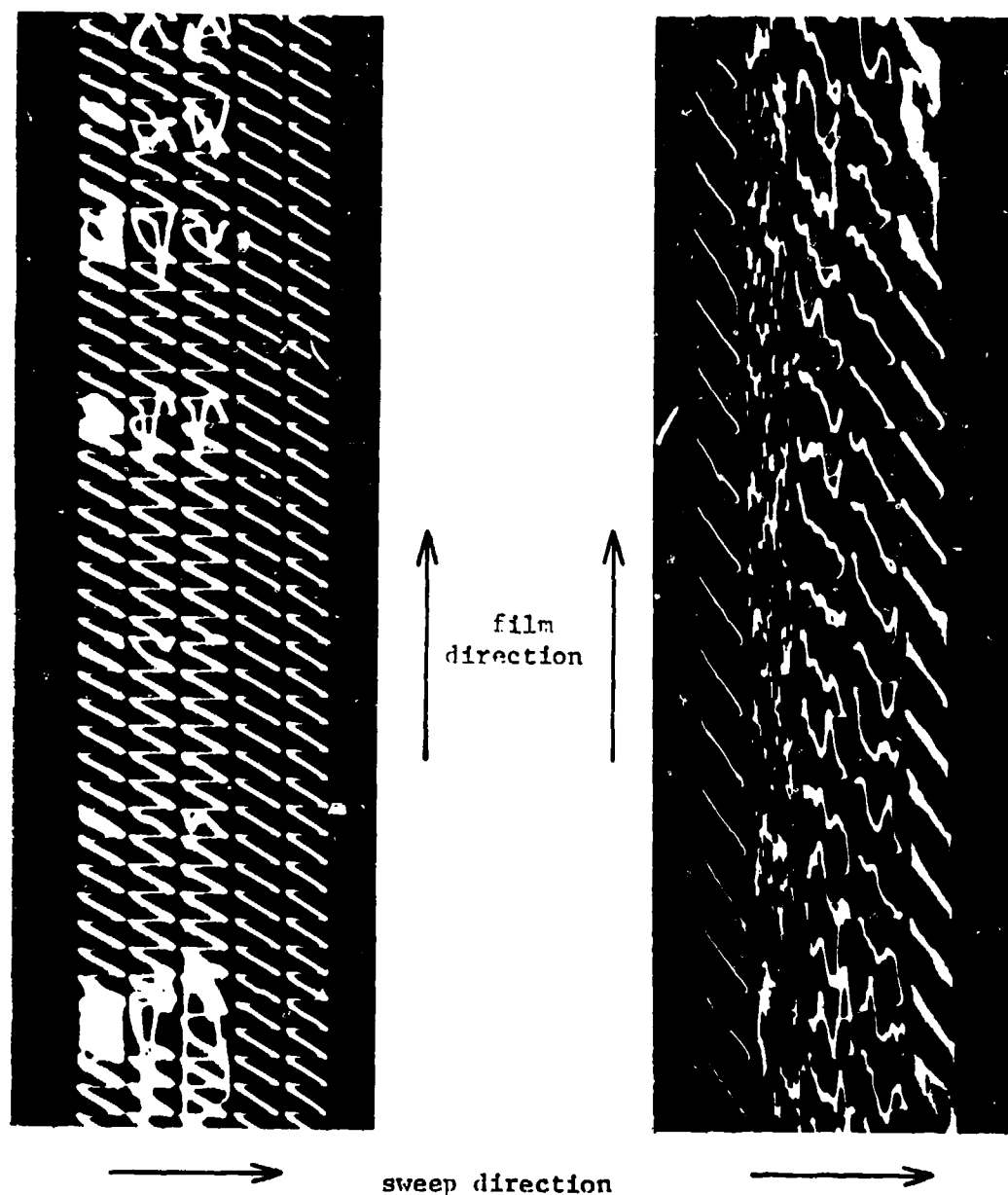


Fig.10(a) Five beam oscillograms showing simultaneous atmospheric induced shock excitations of five radio receivers, each tuned to a separate frequency. From left to right, beam 1 -- 15 kc, beam 2 -- 190 kc, beam 3 -- 1 mc, beam 4 -- 9 mc, beam 5 -- 150 mc. Sweep duration is 1.8 millisecond

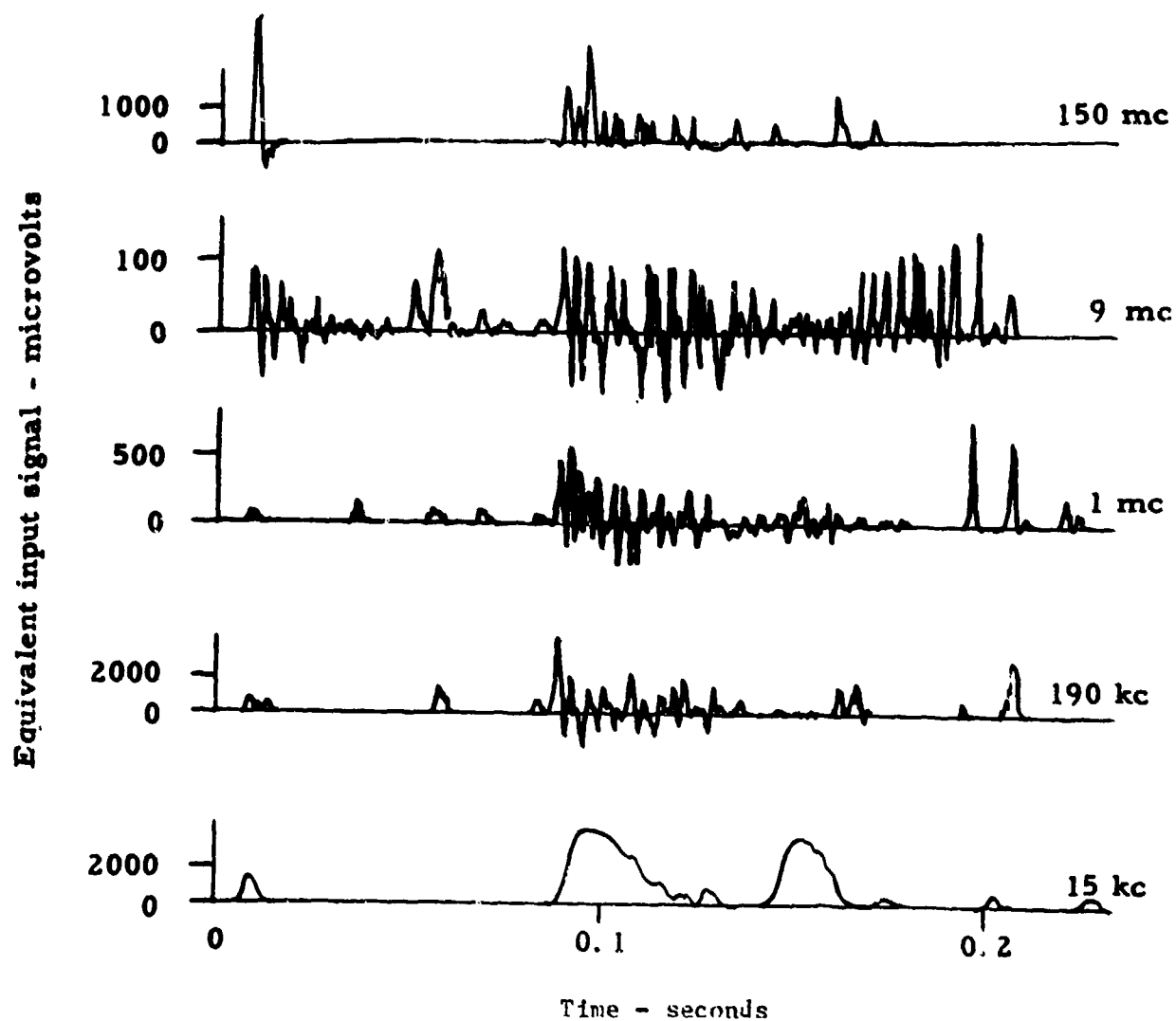


Fig.10(b) Replot of sawtooth sweep recorded panoramic receiver responses of Figure 10(a) to a calibrated linear time scale, showing relative interference levels and space factors

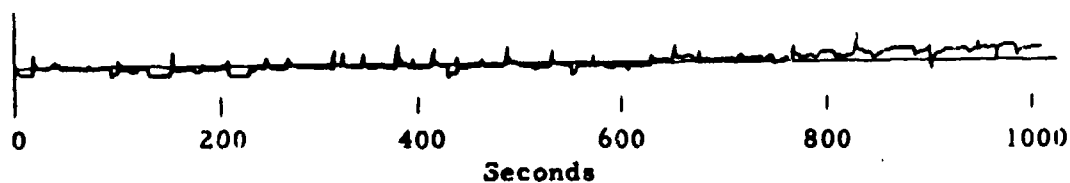


Fig. 11(a) Gradient record showing distribution of bursts of lightning activity over 1000-second interval

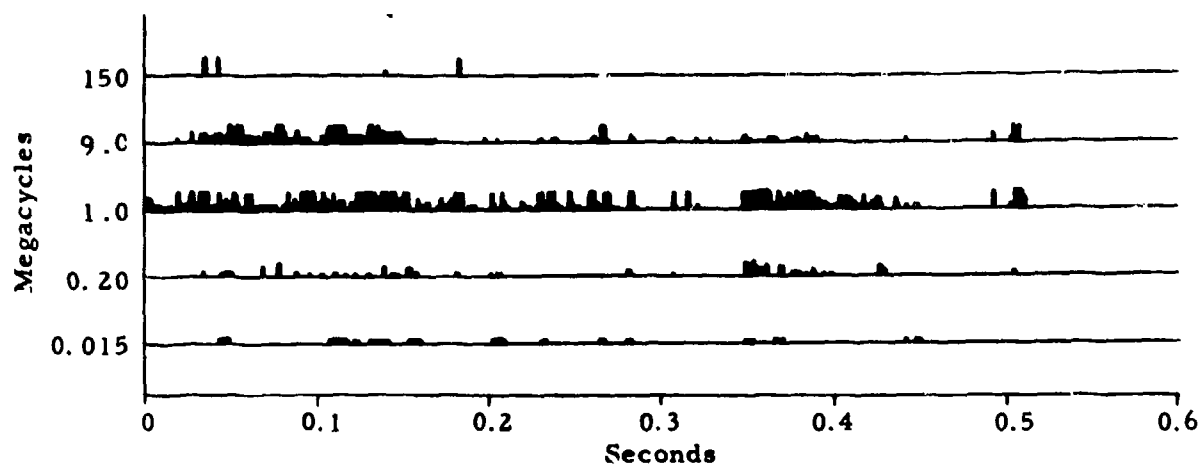


Fig. 11(b) Frequency distribution of receiver disturbances over 0.6-second period of lightning activity

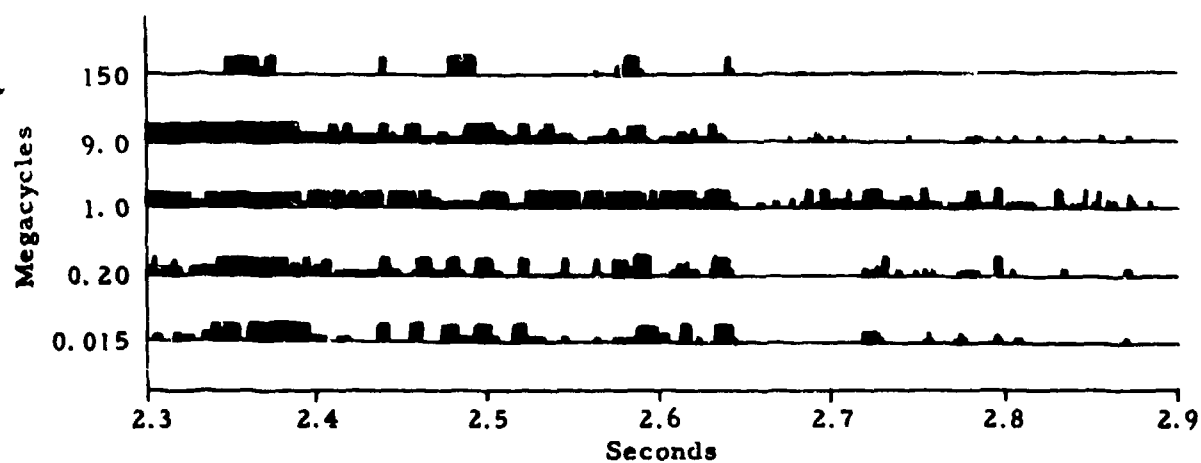


Fig. 11(c) Frequency distribution of receiver disturbances over next 0.6-second period of lightning activity

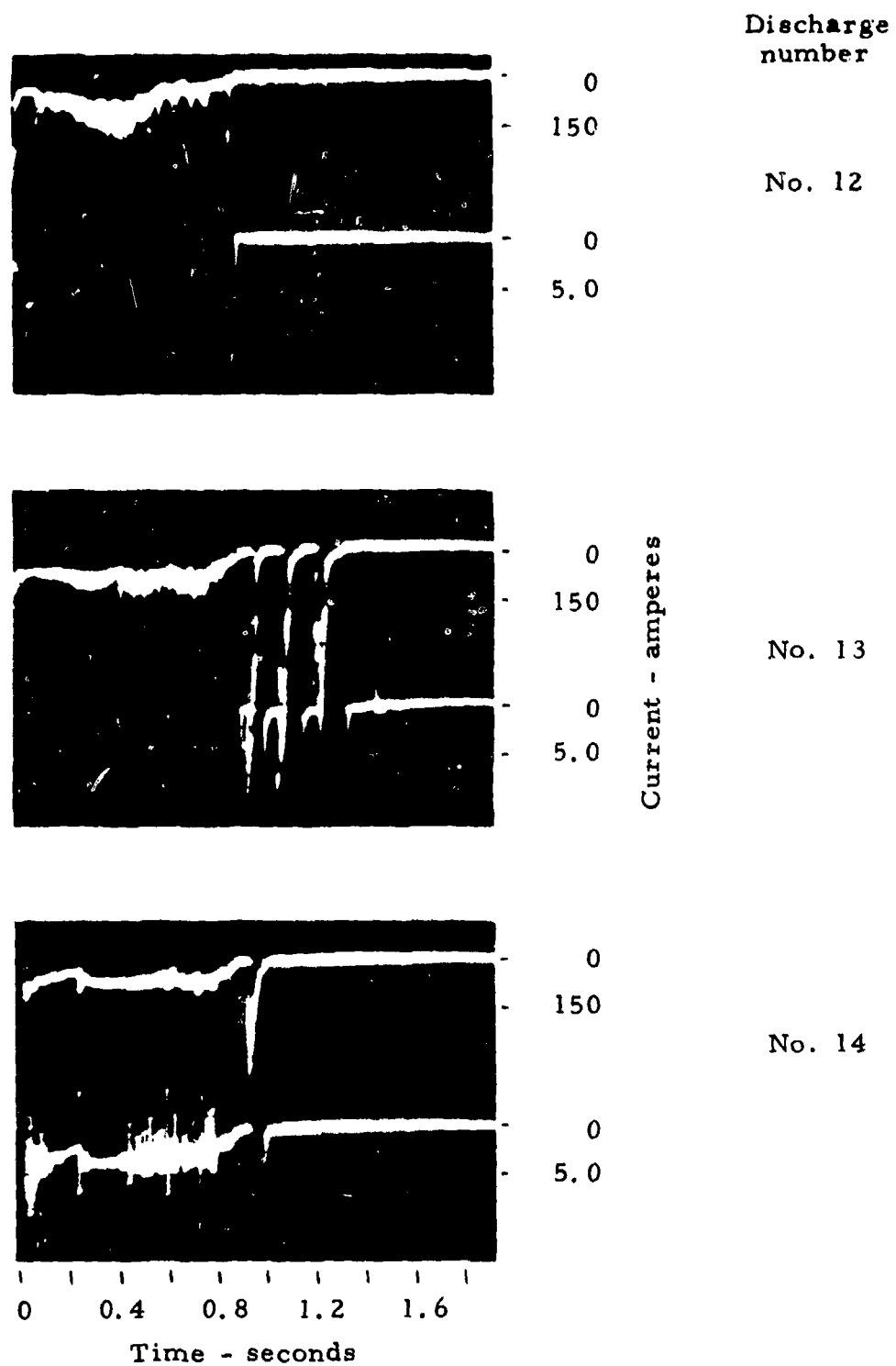


Fig.12(a) Slow oscillograms showing overall time current history of lightning discharges



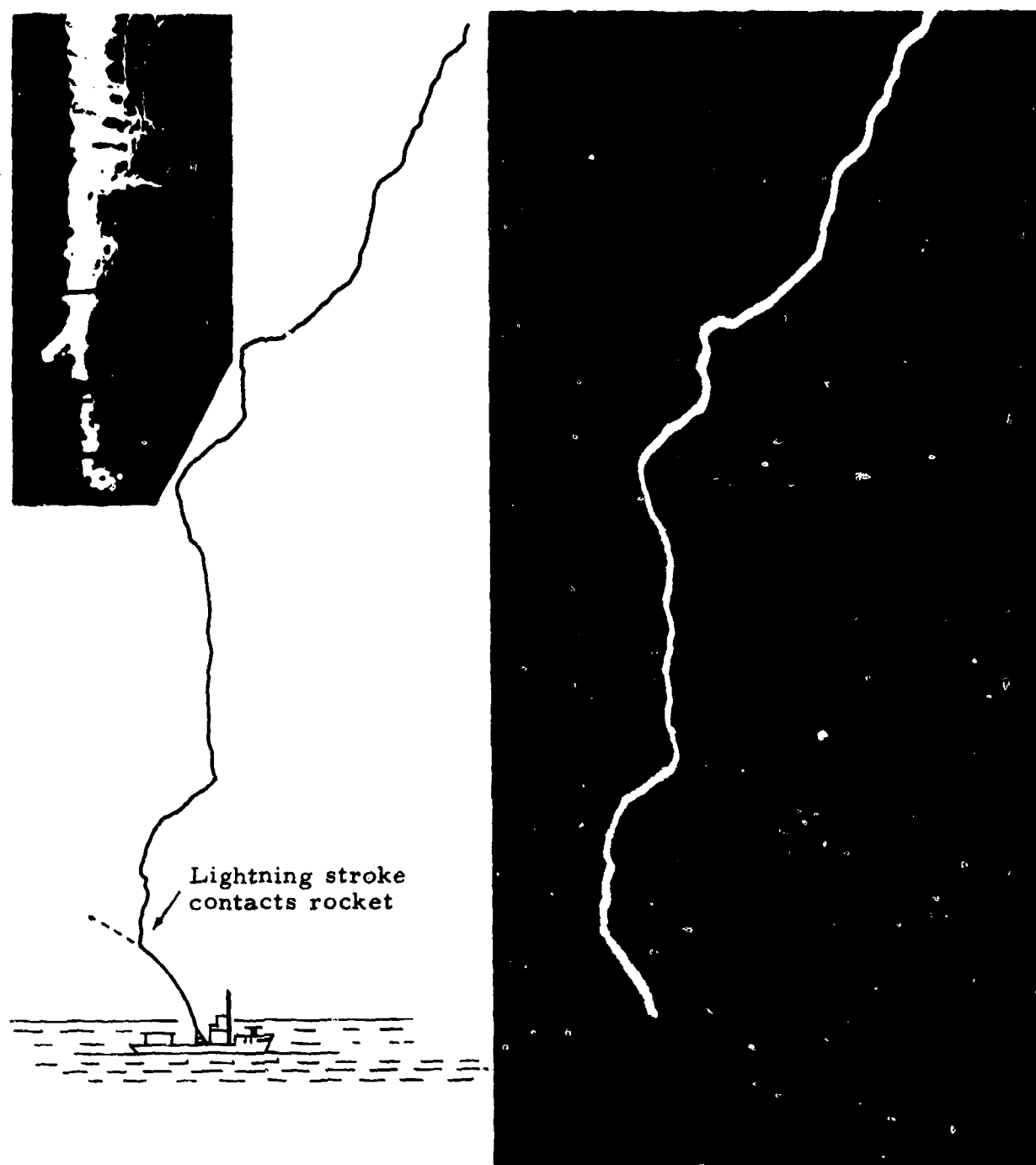


Fig.12(b) Photograph and diagram of triggered natural lightning discharge used to study natural lightning discharge channel currents. Insert shows close up photograph of channel and restrikes

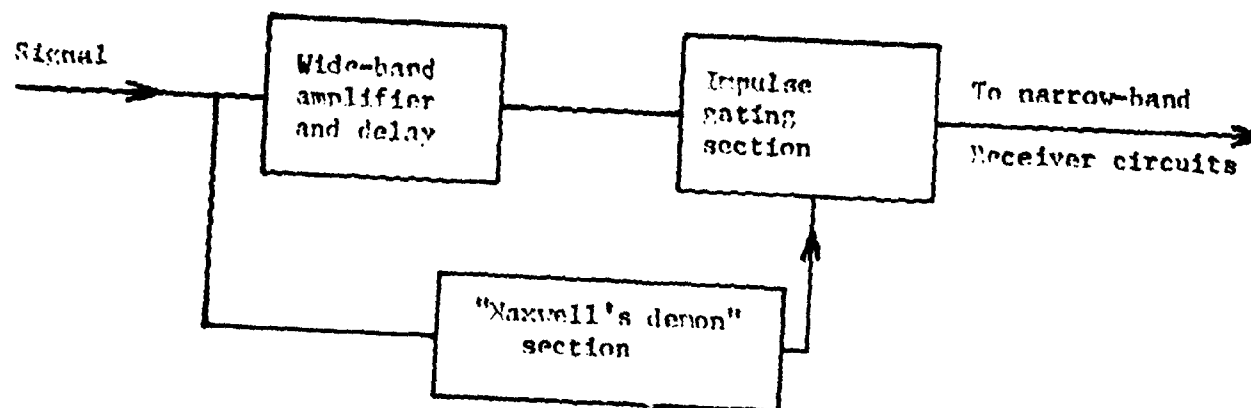


Fig.13 Interference reduction ahead of receiver circuits

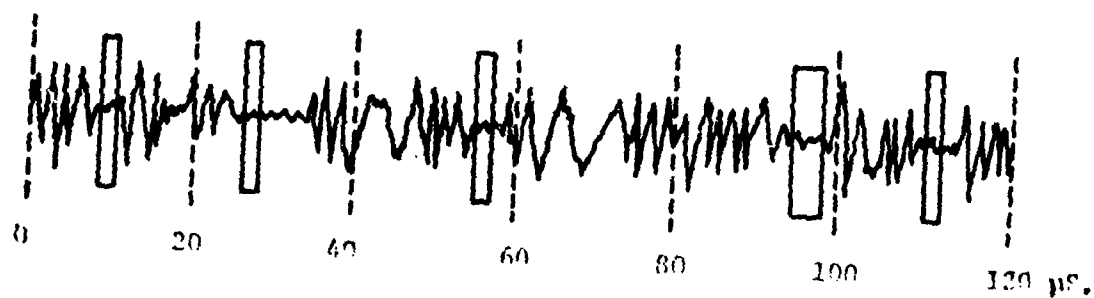


Fig.14 Selective sampling at times of low interference

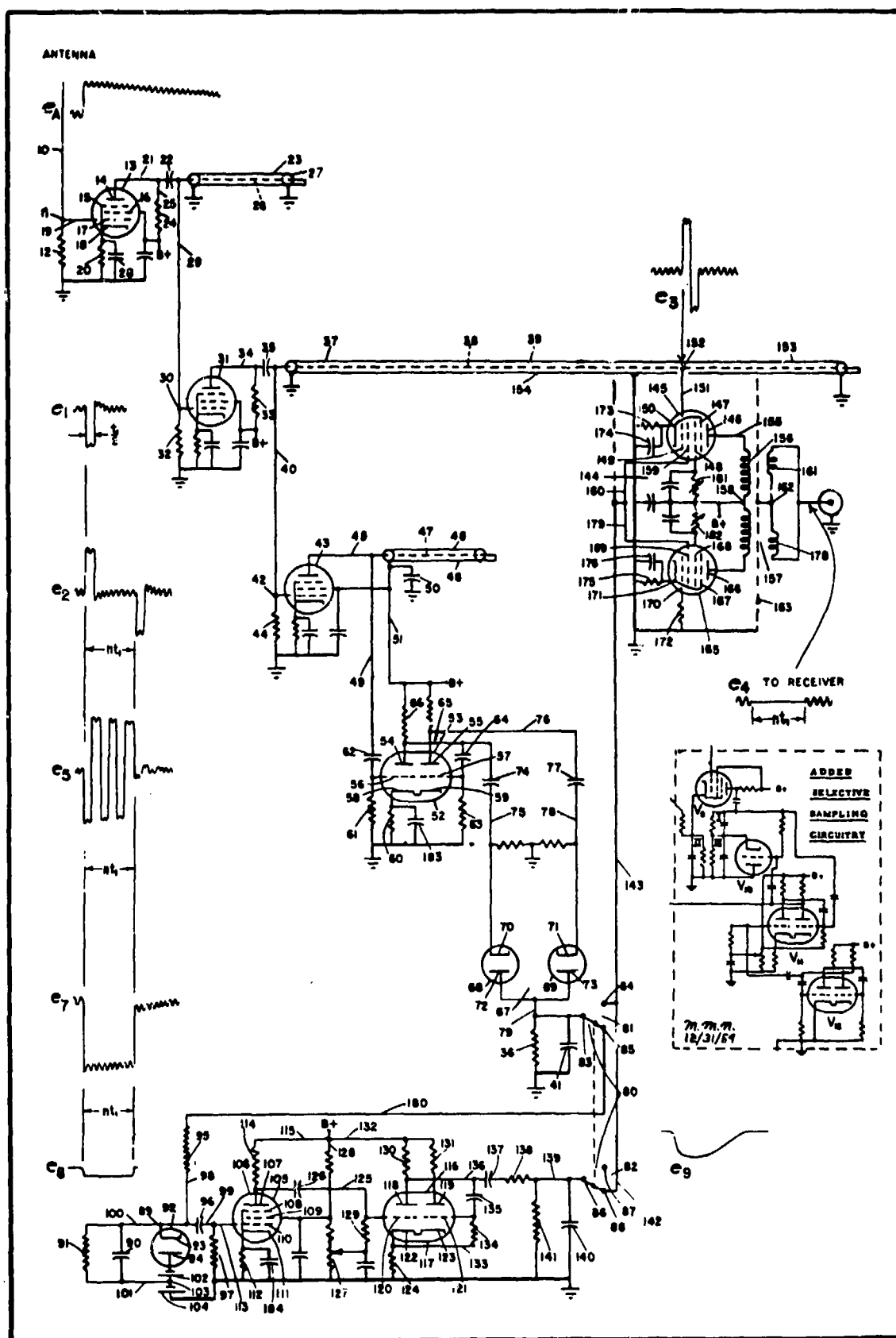


Fig.15 Selective sampling in between interference, by means of the new circuitry involving tubes  $V_9-V_{12}$  superposed in the lower right of the above photostated original patent schematic drawing

## DISCUSSION

D. J. HARRIS: The Figure 10b suggests that the VHF noise signal can be very large. This is surprising. The NBS atmospheric noise measurements suggest that the noise level is very low at 20MHz, but the authors show that the level is high at 150MHz. Could this be discussed?, and could the authors indicate the source of the noise. How is it generated?

J. D. ROBB: The NBS data is based on average power which is very low for the VHF components even though the peaks may be quite high. Two reasons are suggested.

1. The VHF components are observed only at line of sight distances, characteristic of propagation at these frequencies and thus fall well below the lower frequencies which propagate for much greater distances.

2. As may be noticed in Figure 11b, the VHF components are quite sparse which again results in a low average power.

This illustrates one of the basic points which we have attempted to make; the importance of examining communications systems in the time domain of peak amplitudes and frequencies of occurrence as well as in the frequency domain of average power density.

We believe that the VHF components are generated primarily in the formative stages of the discharge with a relatively short duration of milliseconds as compared with the average duration of the total lightning flash of about one half second.

G. H. HAGN: Comment on a question to J. D. Robb. The rms voltage at VHF may be extremely small (e.g., the CCIR Report 322 indicates that  $F_a$  for atmospheric noise from lightning is negligible at VHF and above) even though the maximum value of the instantaneous voltage can be quite large for brief intervals. Some designers of digital data systems which are intended to operate within line of sight of storms producing lightning have been led astray by their interpretation of the CCIR Report 322 curves. The parameter  $F_a$  (which is based on rms voltage) is not useful for frequencies where the contribution to the system noise factor is not dominated by the external noise power from the antenna. At VHF and above, it is useful to know the statistics of the impulse spectral intensity (i.e., strength of the equivalent delta function corresponding to each impulse from lightning in volt-seconds at the receiver input) and the time of arrival statistics of these impulses. These data would be a useful supplement to the information given in CCIR Report 322.

J. D. ROBB: I agree.

F. D. GREEN: One item I would hope to be covered in conjunction with studies of lightning flashes is the development of devices to protect solid state devices from these natural EM pulses. Our Department of Transport has quite a problem in protecting solid state beacons and communication receivers from lightning discharges which arrive on the antenna systems.

I would also like to say that there has been some success at CRC in measuring auto ignition at frequencies about 7GHz. It seems that it will certainly be necessary to protect or shield space link receiver antennas from auto ignition and similar short pulses, especially if they must be located near an autoroute.

J. D. ROBB: No answer.

CPT P. HALLEY: CCIR has published a report on atmospheric noise which makes it possible to predict noise in a given location on the earth, at a given hour of a given season as a function of the frequency for a unit (?) passband.

Is there a world network of atmospheric noise measurement stations? Are the measurements collected in international data centres? Is it contemplated to have the CCIR document revised and brought up-to-date in view of these new data as well as of older data?

J. D. ROBB: No answer.

# MAN-MADE ELECTROMAGNETIC NOISE FROM UNINTENTIONAL RADIATORS: A SUMMARY

G. H. Hagn  
Stanford Research Institute  
1611 N. Kent Street  
Arlington, Virginia 22209  
USA

and R. A. Shepherd  
Stanford Research Institute  
333 Ravenswood Avenue  
Menlo Park, California 94025  
USA

3-1

## SUMMARY

Electromagnetic energy from man-made devices contributes to the composite electromagnetic noise environment in which telecommunications-electronics systems must operate. For a given system, all energy except that of the signal desired for the system can be considered noise, and the portion of noise attributable to man-made devices is termed man-made noise. This paper considers the noise from electrical and electromechanical devices that are not designed as intentional radiators but that produce electromagnetic energy as a by-product. A complete discussion of undesired signals, as well as the other undesired energy produced by transmitters or receivers (e.g., harmonics, transmitter noise, and local oscillator radiation) is beyond the scope of this paper. The emphasis here is on description of the noise from electrical power transmission and distribution lines and from vehicle ignition systems; these two sources are known to be important below and above 20 MHz, respectively. Other sources are mentioned, and prediction of the composite environment due to unintentional radiators is considered. Finally, voids in our knowledge of man-made radio noise are noted.

### 1. SCOPE

The composite electromagnetic noise environment is generated by many natural and man-made sources (Figure 1). This paper concentrates on the unintentional man-made radiators, describes selected major sources (e.g., power lines and vehicles) in technical terms, and assesses their relative contribution to the composite electromagnetic noise environment exclusive of the signal environment. Figure 2 gives an example of a brief observation of the composite electromagnetic environment in the VHF land mobile band in the United States: amplitude versus frequency and time, as observed by a scanning receiver and processed by a computer. The portion of the composite electromagnetic noise environment produced by unintentional radiators is described in terms that permit its prediction. However, the actual assessment of the effects of man-made noise on the operational performance of systems and the subject of noise suppression and control, while extremely important, are beyond the scope of this paper.

### 2. INTRODUCTION

Numerous unintentional radiators have been identified over the years. PETERSON (1974) mentioned that noise voltages induced in the receiving antennas of communications systems in use around 1900 were said to have "fritted" the "coherers" of these systems, and DINGER (1962) noted that perhaps the first known case of man-made interference to radio signals occurred in 1902, when Dr. A. H. Taylor heard ignition noise from a two-cylinder automobile. HERMAN (1970) summarized some of the work on man-made noise prior to 1970, and HAGN (1973) updated this summary.

Primary types of unintentional radiators are listed in Table 1.

TABLE 1 CATEGORIES OF UNINTENTIONAL RADIATORS

Overhead power transmission and distribution lines.
Ignition systems (e.g., automotive, aircraft, small engines, etc.).
Industrial fabrication and processing equipment (including arc welders).
Electric motors and generators.
Electric busses and trains (excluding their power lines).
Contact devices (e.g., thermostats, bells, and buzzers).
Electrical control, switchings, and converting equipment (e.g., SCRs, and ac/dc converters).
Medical and scientific apparatus.
Lamps (e.g., gaseous discharge devices and neon signs).
Various electrical consumer products.

The relative importance of these sources as potential causes of interference depends on their number and distribution (e.g., their proximity to the susceptible equipment), their output characteristics in frequency and in time, and the type of victim service being considered. For example, noise from automobile ignition systems (Figure 2) is an important source of interference to mobile receivers in the VHF land mobile radio service (DEITZ, J., et al., 1973), while it is relatively insignificant for the LF navigation

32 service, where atmospheric noise is often dominant (SHOWERS, R. M., 1974). However, in the vicinity of cities, man-made noise sometimes limits the use of LF and VLF navigation systems by aircraft. Many LF/VLF aircraft navigation system applications are not feasible because of man-made noise limitations in and around urban areas (VINCENT, W. R., 1974). System checks and Omega coordinate setting before take-off may be hampered or rendered impossible by the man-made noise. One way (by no means flawless) to assess the importance of noise sources relative to various types of services is to record complaints of interference when investigations have shown the complaints to be valid and when positive identification of the sources has been made. This is done on a nationwide scale by some countries in Europe (McLACHLAN, A. S., 1973) and elsewhere (ROBERTSON, E., 1971). Many of these complaints are summarized in a standard format for the International Special Committee on Radio Interference (CISPR). Another way to assess the relative importance of sources is to observe the correlation of some measure of a suspected source with the composite background noise level (SPAULDING, A. D., and DISNEY, R. T., 1974).

Let us consider the correlation of the composite man-made noise level with population density before addressing its measured correlation with specific electromagnetic sources. Because of the attenuation of noise field strength with distance from the source, it seems reasonable that man-made noise levels should correlate, at least broadly, with population in urban areas. ALLEN (1960) presented data relating quasi-peak field strength values measured at street level to urban population. He computed the probability of various levels being exceeded at 1 MHz as a percentage of locations in an urban area. This was done over a population range from  $10^3$  to  $10^6$  persons. Although Allen reported a gross correlation between population and noise levels, attempts to correlate average noise power levels with population density, as measured on a finer scale, in U.S. Census Bureau standard location areas (SLAs)--of 1 to 5 square miles--have not been successful (SPAULDING, A. D., et al., 1971). SPAULDING (1972) investigated the relationship between population density and average noise power spectral density,  $F_n$ , in decibels above  $kT_0$ , in signal-free channels in the band 250 kHz to 48 MHz. In the population density range of 1,000 to 25,000 per square mile, in San Antonio, Texas, he found no significant correlation between the average population density of an SLA and the average values of noise level taken at several locations within the SLA. Correlation on a finer scale (down to an individual city block) has not been attempted.

SPAULDING et al. (1971), DISNEY (1972), SPAULDING (1972), and SPAULDING and DISNEY (1974) did find significant correlation between vehicular traffic density and average noise power spectral density (Figure 3), especially for frequencies above 20 MHz (Figure 4). Data taken later than those in Figure 4 indicate that the correlation remains high between 50 and 250 MHz. Therefore, it seems reasonable to conclude that vehicle ignition systems will be potentially important sources of interference to radio systems operating above 20 MHz, especially near roads. In rural areas remote from power lines and other sources, automobiles may be the dominant noise sources below 20 MHz.

Overhead power lines are known to be an important source of man-made noise below 15 to 20 MHz. SPAULDING and DISNEY (1974) reported relatively good correlation between electrical power consumption in an area and the root mean square (rms) value of the noise envelope voltage below 20 MHz. They noted, however, that information on local power consumption in the United States is difficult to obtain. Overhead lines can be important above 15 MHz (WARBURTON, F. W., et al., 1969), and the interference to television from power lines has recently been discussed (e.g., LOFTNESS, M. O., 1970; JUETTE, G. W., 1972; CORTINA, R., et al., 1973). We have observed that nearby power lines sometimes establish the baseline noise level at MF and HF. This has been documented by power-on/power-off tests with omnidirectional antennas and by use of directional antennas in areas where the location of power lines is known.

### 3. POWER LINES

#### 3.1 General Comments

Power lines operating on ac can be categorized by their function (power transmission or distribution), which determines their operating voltage and, thereby the mechanisms by which they produce radio noise under normal operating conditions. In general, the lower-voltage distribution and transmission lines (below about 70 kV) produce noise from various types of discharges in gaps, while the higher-voltage transmission lines (110 kV and higher) generate noise by various kinds of corona (PAKALA, W. E. et al., 1968). The high rate of current rise transforms to a broader spectrum for gap noise than for corona noise, as observed with a peak detector (PAKALA, W. E., and CHARTIER, V. L., 1971). The low-voltage lines may also radiate noise resulting from switching transients and other effects from devices connected to the lines as sources of power.

High-voltage dc transmission lines are coming into use (KAUFERLE, 1972), but there is not yet much information about the noise from such lines. ANNESTRAND (1972) points out that noise is generated at the converter stations, which then propagates on the lines. Shielding and filtering at the converter stations can reduce the noise significantly.

Most of the measurements of power-line noise reported in the literature have been made by using quasi-peak detectors, although some data on power-line noise measured with peak and average detectors are available (THOMPSON, W. I., III, 1971). Measurements made with an rms detector are not generally available in the literature (DISNEY, R. T., et al., 1974), but some data of this type are given in this paper and were given by DISNEY and LONGLEY (1973) and SPAULDING and DISNEY (1974). From the standpoint of potential for causing interference, the frequency ranges of interest include the audio spectrum (60 Hz to 5 kHz) for

telephone use, the line carrier spectrum (5-150 kHz), and the radio-frequency spectrum above 150 kHz. This paper is primarily concerned with the radio spectrum.

### 3.2 Gap Noise

Gap noise is that noise resulting from a complete discharge between two metal objects (sparks) or between a metal object and an electrically charged surface (microsparks) (WARBURTON, F. W., et al., 1969). The sources of gap noise include air gaps in insulators, at tie wires, and between hardware parts; excessive electrical stress across wood, at corroded joints, between neutral wires and ground wires and, in electrical apparatus that is defective, damaged, improperly designed, or badly installed. Gap noise is the predominant source of power-line noise for frequencies above 15 MHz.

### 3.3 Corona Noise

The primary noise source on power lines above about 110 kV is corona. Although gap noise can and does occur on high-voltage transmission lines (greater than 110 kV), the gaps can usually be found and eliminated. Several types of corona discharge contribute to the radio noise from high-voltage transmission lines (positive streamers, negative glow, negative streamers, and so on). The noise from corona begins to decrease above about 1 MHz. The spectrum from negative corona (glow as well as negative streamers) decreases at the rate of 20 to 25 dB per frequency decade, while that from positive streamers falls off at 35 to 40 dB per decade, according to JUETTE (1972) (Figure 5).

### 3.4 Fair-Weather Average Noise Power

Fair-weather noise levels measured by using peak and quasi-peak detectors have been reported in the literature. Figure 6 presents median values of average noise power spectral density data obtained by several investigators at MF, HF, and VHF with rms detectors. Vertical monopole antennas were used; the antennas were positioned directly under the line, with the exception of the 15-kV/16.67-Hz line. One of the most interesting observations is that the 115-kV lines were noisier than the lines with higher or lower operating voltage. At any given frequency, the difference between measured medians for the noisiest and the quietest line was about 30 dB.

### 3.5 The Spatial Variables

Three spatial variations are of interest: the variation of noise level with height directly under the line, that of the noise level along the line, and that with distance laterally away from the line. Examples of these variations are discussed below.

The variation with antenna height beneath a 15-kV power line operating at 16-2/3 Hz in Germany was measured at 2.5 MHz with a 1-m vertical rod antenna and a receiver with an rms detector. The conductor was approximately 8 m above ground. The average noise power was observed to increase as the Stoddart NM-25T, modified to measure  $F_a$  (see MATHESON, R. J. and BEASLEY, K. R., 1972), was raised from the ground: +7 dB at 1.2 m, +12 dB at 1.8 m, and +15 dB at 1.9 m.

Longitudinal variations as great as 15 dB were observed from place to place under the same line over a distance of about 1 km, but the typical variation between towers was 2 to 5 dB, with an increase often noted at the tower. The relative profile laterally from this line, measured at midspan at 2.5 MHz with a short vertical monopole antenna, was: 0 dB under the line, -10 dB at 21 m, -15.5 dB at 43 m, -19.5 dB at 61 m, and -19.0 dB at 76 m.

In the presence of rain, an  $F_a$  value of 104 dB above  $kT_0$  was observed directly beneath the line. More typically, values of 80 dB above  $kT_0$  were observed there.

### 3.6 Seasonal Variation of Fair-Weather Radio Interference (RI) Levels

The seasonal variation of fair-weather radio noise was investigated by LaFOREST (1968) by studying one year of data on a 500-kV line in the northeastern United States. He noted the effects of relative air density, relative humidity, and wind speed, as well as seasonal variations, and he deduced correction terms for fair-weather RI levels (field strengths measured with a quasi-peak detector). He noted that summer readings were higher than winter readings by about 12 dB. Various others have recorded the increase in RI during rain or other bad weather.

### 3.7 Variations Due to Foul Weather

YAKALA and CHARTIER (1971) stated that noise increases of 17 dB were likely during rain. The IEEE (1965) indicated increases of 15 to 25 dB during foul weather and also (1971) indicated increases of 20 dB during bad weather. Data on RI levels taken on a Bonneville Power Administration 345-kV line between May 1965 and May 1966 (Figure 7) show an average RI level during rain of approximately 20 dB above that shown during clear weather, while during snow the average level was nearly 26 dB higher than the clear-weather level (BAILEY, B. M., and BELSHER, M. W., 1968). FORREST (1969) pointed out that "defect" noise on lower-voltage (11- to 66-kV) lines, caused by sparks and microsparks, tended to determine the fair-weather RI

levels above 10 MHz. He noted that wet weather could cause RI increases of 5 to 15 dB in the band 100 kHz to 10 MHz, due to corona, while causing RI levels above 10 MHz to decrease, due to the shorting out of arcing gaps.

### 3.8 Effects of Insect and Other Particles

The effects of the presence of particles on or near EHV conductors were studied by NEWELL et al. (1968). Observations of the variation in RI levels over a one-year period on a 230-kV tower line showed that water particles caused the highest RI levels. However, insect and vegetable particles caused high RI levels approximately 80 percent of the time.

### 3.9 Polarization Effects

PAKALA and CHARTIER (1971) observed that, in 60 percent of their measurements, those made with horizontally polarized dipoles produced greater noise than those made with vertically polarized dipoles. The differences ranged from 0 to 10 dB over the frequency band 15 kHz to 10 GHz.

### 3.10 Concluding Comments

Our knowledge of the noise from power lines is far from complete. Little of the noise measurements to date have been with rms meters, and even fewer data on the amplitude probability distribution of the noise exist. The main characteristics of noise from both low-voltage distribution and high-voltage transmission lines have been discussed. It is not possible to construct totally noise-free lines. However, good engineering practices in line design and good maintenance practice for operational lines can greatly reduce the contributions of the noise from power lines to the composite man-made radio noise environment.

## 4. IGNITION SYSTEMS

### 4.1 Introductory Comment

Ignition noise is generally found wherever automobiles or other vehicles using spark-initiated power systems (e.g., trucks, boats, aircraft, and snowmobiles) are used. This noise is highly impulsive and spreads over much of the frequency spectrum. At the low end of the spectrum (below about 20 MHz), ignition noise is generally believed to be exceeded by power-line noise when both sources are present, as discussed in Section 2 (see also JTAC, 1968). The actual lower limit will, of course, be determined by specific situations, including the density of automobile traffic and the proximity of power lines. The high-frequency limit to the automobile ignition noise spectrum has not been as well studied. Generally, instrumentation capability or investigator interest tapers off before the establishment of a clear upper limit. SRI made a brief investigation this year in a suburban area in California, using a spectrum analyzer with a noise figure of about 30 dB.\* This investigation indicated that ignition noise is still an important noise component in the range from 1 to 3 GHz. Although much of the time only receiver noise was found, increased traffic intensity associated with the rush hour commonly produced noise spikes 30 to 40 dB above the receiver noise in a 100-kHz bandwidth at 1.2 and 2.9 GHz.

### 4.2 Details of the Source

Ignition noise has three principal sources. In their order of occurrence during the ignition cycle they are: (1) the impulsive release of stored charge in the ignition system secondary wiring when the air gap within the distributor breaks down, (2) the similar impulsive current flow in the spark-plug wire about 10 to 20  $\mu$ s later when the spark-plug gap breaks down, and (3) the abrupt commencement of current flow in the breaker-point-to-coil wire when the breaker points are closed to restart the cycle anew. This last source should not be a problem in the newer automobiles with electronic ignition systems. In measurements of the radiation from a particular vehicle, it is not generally recognized that the first two sources given above are separate entities, because of their close spacing in time. However, special measurements (such as those using wideband current probes) can be made that clearly show the two sources. Noise from the third source occurs about 1 or 2 ms after the first two and is easily distinguishable. Let us next consider the radiating system in which these impulsive currents flow.

Modern resistive ignition secondary wiring forms a very lossy antenna, with attenuation of about 0.4 dB/cm at 10 MHz, 1.4 dB/cm at 100 MHz, and 3.1 dB/cm at 500 MHz. The high loss means that the two ends of the "wire" from the distributor to the spark plug are isolated from each other at RF and that probably for only the first few inches at each end is the wire an effective radiator. Impulses at either end of the wire couple energy to the adjacent wiring and metal parts, so the ignition wire becomes the driven element in a highly irregular antenna system. Therefore, within an N-cylinder automobile having the standard inductive-discharge ignition system with breaker points, each of the N spark-plug wires is pulsed at each end, and the single breaker point wire is pulsed for each plug, so that there are  $2N + 1$  individual little radiating antenna systems under the hood (bonnet). If the automobile engine is operating at R rpm,

\* For explanations of noise figure and other concepts, see MUMFORD and SCHEIBE (1968), and ARTHUR (1974).



there are N · R/120 spark-plug firings per second, each with three impulses (caused by the two gap breakdowns and the breaker point closure) into the radiating systems. The first two impulses often cannot be resolved with narrow-band detectors. NIELSON (1974) noted that a receiver with 16-MHz bandwidth still seems to be band-limited when looking at ignition noise at 1.37 GHz. The rise time of the ignition noise pulse is of the order of 1 ns, and it depends on the suppression techniques used (BURGETT, R. R., et al., 1974), so one might expect significant radiation to at least 1 GHz. 3-5

The frequency characteristic of the automobile as a radiating system driven by all these sources is highly irregular. Measurements made at 10 m using a frequency-scanning peak detector are shown in Figure 8. Since the automobile system is excited with brief impulses, the determining element in the frequency response is the automobile's radiating efficiency. The response shows broad peaks where some portion of the vehicle's structure is radiating effectively and wide nulls where no such resonances exist. An examination of the automobile's radiated field with regard to frequency shows a complex structure varying with the angle from which the vehicle is viewed. Additional variations in the observed spectrum can be introduced by the propagation or coupling mechanisms and by the receiving system.

As an additional complexity, successive pulses from an automobile are not of the same amplitude; they vary by 20 or 30 dB (STORWICK, R. M., et al., 1973; HSU, H. P., et al., 1973, 1974) and even with successive pulses from the same cylinder (MAXAM, G. L., et al., 1973a, b). The studies just referenced were all pulse-height measurements, although the term amplitude distribution (easily confused with amplitude probability distribution, APD) was used to describe the presentation by HSU et al. (1973, 1974) and STORWICK et al. (1973). MAXAM et al. (1973a, b) called the same distributions pulse-height distributions.

Part of the pulse-to-pulse variation is probably attributable to the differences in breakdown potential that result from inhomogeneities in the air-fuel mixture and possibly from air turbulence within the distributor cap. Gap breakdown characteristics may also be influenced by microchanges in the electrodes. There are also longer-term (several-second to several-minute) trends in the field. Automatic plotting of a peak detector's output (SHEPHERD, R. A., et al., 1974b) sometimes shows sudden 10- to 20-dB changes in the noise output and often shows slower changes of the same magnitude over a minute or less. Although the reason for this is not clear, it is certain that a quick look at the noise from the automobile will provide only a small sample of a possibly nonstationary random process. It is evident that this contributes to the problem of obtaining consistent or repeatable measurements of ignition noise from vehicles.

#### 4.3 Measurement Techniques and Descriptive Parameters

Various techniques and parameters have been used to measure the noise from automobiles. For uniform test procedures, both the IEEE (1966) and the SAE (1974) standards require peak field-strength measurements. However, neither standard furnishes a working definition of, or guidance about, what is meant exactly by peak field strength. Without this guidance, different results can be obtained from the same source since the automobile is a source of highly random impulsive noise (SHEPHERD, R. A., et al., 1974a). In Europe a quasi-peak detector is favored by CISPR (1971) over the peak detector used in the United States for the same sort of measurements (see also STUMPERS, F. L., 1971; BAUER, F., 1973). Although suggestions can be found that at 1500 rpm the peak field strength is 20 dB greater than the quasi-peak field strength (e.g., BAUER, F., 1973; and SAE, 1974), this does not appear to be consistently the case. Measurements made in Anderson, Indiana, in 1959 by BALL and NETHERCOT (1961), using several vehicles and several measurement systems, resulted in an empirically determined peak-to-quasi-peak ratio of about 21 dB. Quasi-peak detectors with charge time constants of 1 ms and discharge time constants of 500 and 600 ms were used. These measurements were made between about 30 and 200 MHz, with engine speeds generally about 1000 rpm (for 4-cylinder to 8-cylinder vehicles). The average of a number of peak-to-quasi-peak comparisons was about 21 dB, but under various measurement situations the ratio ranged from about 26 dB to about 13 dB. More recently, comparative measurements of a number of individual vehicles with V-8 engines were made in San Antonio by SCHULZ et al. (1973). The engines were operated at 1500 rpm; the antenna height was 3 m and the spacing was 10 m, as required by SAE J551 (SAE, 1974). The measurements were made at seven fixed frequencies between 36 and 1000 MHz, using an Electrometrics EMC-25 having both peak and quasi-peak detector functions. The quasi-peak detector had charge and discharge time constants of 1 ms and 600 ms, respectively. These measurements indicated an even greater variability of the peak-to-quasi-peak ratio. While the 20-dB empirical relationship between the readings of peak and quasi-peak detectors may be a useful (and sufficiently accurate) approximation for facilitating international trade, it should not be taken as a deterministic constant.

Root-mean-square (rms) field strength measurements have been made at fixed frequencies by a number of experimenters, but no frequency-scanning measurements with an rms detector have been noted in the literature (according to DISNEY, R. T., et al., 1974). SRI researchers have observed that the average noise power as measured from the front of a single vehicle can exhibit variability with frequency in the range of 15 to 30 MHz (Figure 9) and have also noted a significant increase in noise level from the same vehicle after "routine" maintenance, during which new plugs, breaker points, condenser, and resistive wiring harness were installed. A model was developed by SPAULDING et al. (1971) (see also SPAULDING, A. D., 1972) to estimate the noise power spectral density,  $F_a$  (watts/hertz), from distributions of vehicles as a function of road geometry and radio frequency.

#### 4.4 Recent Amplitude Probability Distribution (APD) Measurements of Automobile Ignition Noise

36 The APD is the cumulative distribution of a receiver's envelope amplitude. Only a few measurements of the APD of ignition noise from single vehicles are known to have been made (and none from aircraft); these were made by using two different techniques, over a wide frequency range. The measurement system used by SCHULZ and SOUTHWICK (1974) had an adjustable threshold and a timer system, so that the percentage of time that the threshold was exceeded could be measured. Since this system examined only one threshold level at a time (for 1 second), any changes in the behavior of the automobile as a noise source between the measurement at one level and that at the next level could be a source of difficulty. These APDs were made at a number of frequencies between 36 and 1000 MHz and at several bandwidths between 3 and 300 kHz. Figure 10 shows APDs for a single vehicle, synthesized by averaging the results for four vehicles. SCHULZ and SOUTHWICK (1974) noted the repeatability of the data, especially when three or more vehicles were observed simultaneously on several days or when the results of several vehicles were averaged. These APDs exhibited much the same structure as the upper (impulsive) portion of the APD measurements on automobiles made at HF by SHEPHERD et al. (1973) using a different technique (see also SHEPHERD, R. A., 1974).

SHEPHERD et al. (1973) sampled a detector output at 200 times per second for about 10 minutes and converted the data to digital form for computer processing to provide the APDs over a 54-dB dynamic range. Simultaneously, the rms level and the parameter  $V_d$ , the ratio in decibels of the rms to the average envelope voltage, were computed. Figure 11 shows a set of these APDs for two vehicles with V-8 engines (a 1962 Chevrolet pickup truck and a 1967 Mercury Cougar) and one vehicle with a 4-cylinder engine (a 1962 Volkswagen). The Chevrolet pickup used for these APDs had been deliberately made noisy by replacing its resistive secondary cabling with metal wiring, but the other two vehicles had not been modified. When the engines were idling, the pickup's maximum levels and the average power were about 15 dB above those for the other two vehicles. When the engines were racing, the maximum values for both the pickup and the Mercury decreased, while their noise power increased, although by only 0.5 dB for the Mercury. The Volkswagen's maximum remained about the same, but its power increased by about 8 dB. At 4000 rpm it had the same pulse rate as an 8-cylinder car at 2000 rpm. These APDs demonstrate that vehicles behave differently in terms of their average power and their maximum observed levels. (We refer to maximum levels on the APDs instead of to peak levels to avoid confusion with the peak parameter measured with a peak detector.)

Although the APDs for different vehicles may vary widely (SHEPHERD, R. A., 1974; SCHULZ, R. B., and SOUTHWICK, R. A., 1974), the APDs are not greatly different for changes in traffic intensity on a rural freeway, because they "average together" the wide variety of noise-producing vehicles that pass. This averaging effect was noted within an urban area by SPAULDING et al. (1971) as "an encouraging find," since the APD is sometimes sufficient for system performance analysis and for system design. Figure 12 demonstrates the striking similarity in APDs made over 10-minute periods on three days, at the same location, for traffic intensities with a three-to-one range.

A very general model for estimating the APDs from a group of cars was developed by COHEN (1972), and the modeled APDs were compared with the measurements of SHEPHERD et al. (1973) by GILLILLAND and BREWER (1974). Most of the predicted APD values differed from the measured values by only 1 or 2 db across the intended range of model applicability (i.e., APD values of 2 percent and lower, corresponding to frequency-shift-key (FSK) bit error probabilities in the range  $10^{-2}$  and lower).

#### 4.5 Variability from One Automobile to Another

The rms measurements have been used to note the great variability in noise from one automobile to another. Measurements made in Spain by ENGLES (1974) and on Guam by SRI, using modified NM-25T and NM-26T receivers with 38-cm loop antennas, show quite clearly the wide range of noise production observed with even a small sample of vehicles in service (Figure 13). About 2 percent of the cars were found to be 30 to 35 dB noisier than the median vehicle. The measurements were made while the vehicles moved slowly past the antenna, one at a time. Similar measurements made in Scotland by ENGLES (1974) indicated (again from only a small sample of vehicles) that an even smaller percentage of vehicles in Scotland are extremely noisy (the 2-percent level was above the median by only about 15 dB, and the median vehicle seems to have been about 3 dB quieter than the medians for the measurements in Spain and Guam). This trend of proportionally fewer noisy vehicles appears in measurements made by SRI in Germany in 1971 with the same type of receiver but with a 3-m whip antenna and also in measurements made in the United States (SPAULDING, A. D., 1972). The U.S., Scottish, and German distributions all have the same general slope (although we cannot understand why the U.S. measurements are so far above the others), indicating that there appear to be proportionally fewer very noisy vehicles in those countries than in Spain or Guam. It is not clear why this should be so, but experiments designed to identify and classify the particularly noisy vehicles would help in determining whether some vehicle types are inherently noisy or whether this characteristic is acquired with age or as a result of some modification (such as replacing resistive ignition wiring with solid copper wiring).

The effects of the small proportion of noisy vehicles are much greater than those of the majority of the vehicles on the streets. In observations of the effects on land mobile communications, DEITZ et al. (1973) referred to the existence of these "super-noisy" vehicles and showed that a group of vehicles containing some that are super-noisy can degrade narrow-band FM voice communications by about 10 dB more than a similar group of vehicles not containing the super-noisy ones. In their tests, degradation was defined as the increase in signal power required to reestablish the quality of reception obtained without the ignition noise.

Figure 14 is an example of automobile ignition noise as it appeared near a freeway. This measurement was made by recording the rms meter voltage of a modified NM-25T receiver while the antenna was about 16 m from the nearest lane of a freeway (SHEPHERD, R. A., et al., 1973). During the measurement period, traffic was passing at a rate of about 24 cars per minute.\* The flat portions of the chart record represent the periods when only quiet vehicles were passing. The noisy vehicles were sometimes 40 dB above the quiet vehicles. Considering the traffic speeds involved (about 100 km/hr) and the fact that the noisy vehicles can be observed for a period of 30 seconds or so, it follows that the noise from the noisy vehicles at about 400 m exceeds that from the quiet vehicles passing as close as 16 m. 3-7

#### 4.6 Concluding Comments

Ignition systems are highly variable sources of man-made radio noise, which contribute to the composite electromagnetic noise environment even up into the microwave region. While data have been taken on individual vehicles, relatively little is known about the causes of the variability and even less is known about the range of variability of the noise of automobiles in service. The relatively few analytical models for the noise from vehicles have yet to be adequately checked against experimental data.

#### 5. OTHER SOURCES OF MAN-MADE NOISE

Power lines and automobile ignition systems are not the only sources of broad-band electromagnetic noise. Numerous other sources exist within the categories listed in Table 1, and it appears that no portion of the spectrum and few areas of the world are unpolluted. As a low point within the electromagnetic spectrum, as well as with respect to the earth's surface, BENSEMA et al. (1974) and KANDA (1974) reported spectrum measurements of man-made noise from 1 to 100 kHz arising from the operation of dc machinery in a coal mine. As an example of remoteness (although the source in question was power-line noise), STUART and SITES (1973) noted that "from a communicator's and experimenter's point of view, man-made noise is a definite problem in Antarctica," and they found it necessary in that part of the world to go several kilometers from the centers of activity before natural noise became the limiting source.

Since the automobile has sources of noise other than its ignition system, these additional sources will have the potential of causing disruption whenever the automobile is used. Considering the lower-frequency observations first, BOLTON (1972) reported that the high-level noise at 76 kHz in a public parking lot in Denver was due to noise generated by automobile starters. Fortunately, this noise generally lasts for only a few seconds per vehicle.

Another source of noise within the automobile is the alarm buzzer intended to alert the driver that he is opening the door with the key still in the ignition lock. (Presumably, the other alarm buzzers that alert one of unfastened seat belts and so on also make noise.) Comparisons of the rms voltage of the noise from the door-alarm buzzer with that of the ignition noise were made by SHEPHERD et al. (1973) and by LAUBER (1974) at 20, 25, and 30 MHz. These fixed-frequency measurements indicated that a car's door buzzer noise might exceed its ignition noise in the upper part of the HF band by up to 25 dB.

SRI made frequency-scanning measurements on a vehicle, using a peak detector at a distance of 10 m, in accordance with SAE J551c (SAE, 1974) standard. These measurements indicated that buzzer noise is comparable to ignition noise up through 1000 MHz. Figure 15 shows some comparative measurements up through 500 MHz, made without moving the vehicle or the antenna. Fortunately, buzzer noise is usually intermittent relative to ignition noise.

An automobile's horn is used only seldom, which is fortunate from the standpoint of audio-frequency and radio-frequency noise. During a brief measurement session SRI observed that the major noise source at 413 MHz in a narrow street in San Francisco was a back-up signal horn on a truck about 50 m away. It exceeded the truck's ignition noise by at least 15 dB.

Some other transportation systems are also generators of man-made radio noise. VINCENT and ELLISON (1974) made measurements alongside the tracks of the new Bay Area Rapid Transit (BART) system in the San Francisco area. These measurements show that, although the general background noise level between 4 and 8 MHz in the urban area was already quite high, impulsive noise from the trains (powered by a 1000-V dc third rail) exceeded the background by 20 to 30 dB. Strong radio noise bursts associated with bright arcing in the wheel area of trains approaching a station were noted. This noise was not observed to be associated with departing trains. The departing trains produced impulses at about 220 pulses per second, "probably associated with the drive motor control circuitry." This impulse noise was noted to disappear for about 2 seconds as the propulsion system power was reduced, and it then resumed with a slightly different structure as power was reapplied.

In Germany SRI researchers noted noise over the HF band from the electric trains and their 15-kV, 16.67-Hz power line. (Diesel-electric engines on the same track were not observed to generate significant noise above ambient.) The power line was a major source of noise, with large groups of impulses occurring at 33.33 Hz, signifying a number of gap breakdowns at one or more places on the line for each voltage maximum.

\* The record was made at the same time and on the same antenna at one of the APDs of Figure 12.

38 The measuring system used by Vincent and Ellison has also been used to observe noise from silicon-controlled rectifiers (SCRs) and from industrial heating devices such as those used for plastic welding. At HF this noise may propagate for thousands of miles by ionospheric reflection, it is becoming more and more a problem as large SCRs are increasingly used in industrial and manufacturing processes (VINCENT, W. R., 1974). Figure 16 shows three views of a 3-second period of the noise from a desk-top electromechanical calculator in the 30- to 50-MHz region. FORD (1972) observed that modern pocket-sized calculators are also potentially significant noise sources.

City noise consists of the accumulation of all the high-level, short-duration pulses from switching, operation of machinery, and so on that take place in a city. Automobile ignition noise (and other automobile noise) and power-line noise certainly contribute to city noise. Other noise sources are arc welders, superregenerative receivers, and household appliances (MARTIN, H., and TABOR, F., 1972; MILLS, A. H., 1971). The sources for this noise are so numerous that the pulses generally overlap in a receiver, and the resolution of individual sources is not possible. LYNN (1972) referred to this noise as "electromagnetic smog." He described a number of electromagnetic compatibility problems (not all from broad-band noise) to show the "generally insidious and sometimes ridiculous" nature and effects of man-made noise.

City noise was measured from aircraft over Seattle at HF and below by BUEHLER and LUNDEN (1966), over Florida at VHF by FLOUSSIOS (1968), and over Illinois at frequencies up to 440 MHz by SWENSON and COCHRAN (1973). In the Seattle area, Buehler and Lunden concluded that at otherwise quiet times city noise may control reception at 1 MHz about 65 km from the city center over land and out to about 160 km from the city over salt water. While flying at about 3 km over highly populated areas in Northern California, ROTH (1958) observed increases of about 12 dB above the ambient galactic noise at 40.38 MHz.

The Swenson and Cochran measurements were made from an aircraft altitude of approximately 700 m over about 20 cities and towns ranging in population from 200 to 90,000. At 222 MHz, all (except possibly one) produced discernible noise. Similar flights over a large coal-fired power-generating plant and over power-switching yards did not provide noticeable noise. One village (population about 500) was found to have an unusually large amount of noise. A ground search turned up a superregenerative receiver on an automatic garage door opener, radiating continuously over a wide frequency band.

There are various sources of radiation in aircraft (e.g., ignition and electrical systems including inverters and alternators) in addition to the transmitters they carry. The noise levels to which an airplane is subject are the composite of those produced by the on-board equipment and those produced by sources on the ground (e.g., the noise discussed above). Swenson and Cochran found it necessary to equip their receiving system with a noise-blanker to keep their small plane's shielded ignition system from interfering with the measurements.

Man-made radio noise can be found even in remote rural areas, although whether it is a problem there is not certain. CONE (1972) made measurements at 137 MHz to determine the suitability of a remote rural area in South Dakota for a satellite tracking station. He found that galactic noise generally predominated but that man-made noise was sometimes the limiting noise. Automobiles were particularly noticeable when they were in "close proximity," which in this survey was within 0.8 km of the measurement location. An electric fence about 3.2 km from the site established the noise threshold for many hours.

This discussion of miscellaneous sources of man-made electromagnetic noise is far from complete and is intended primarily to illustrate by example the diversity among some recognized sources.

## 6. MAN-MADE RADIO NOISE PREDICTIONS

SPAULDING and DISNEY (1974) discussed two methods of predicting man-made radio noise. One method is based directly on past measurements; the other depends on the correlation of past noise measurements with some predictable parameter(s) of the environment.

The first prediction method assumes that the behavior patterns noted at "typical" locations will be the same at similar locations in the future. Analysis of the available data base for each category of location will then provide the estimates of the man-made radio noise conditions to be found in future locations in the same category. Spaulding and Disney defined three basic location categories: business, residential, and rural. Figure 17 shows median power spectral density values for the band 250 kHz to 250 MHz for these categories. This is an updated version of a similar plot for urban, suburban, and rural areas given by JTAC (1968). The user of the data base must determine the category that best describes the location for which he desires to predict the parameter.

The data base consists of about 300 hours of data collected simultaneously on eight frequencies<sup>\*</sup> in six states and in Washington, D.C., at various times between 1966 and 1971. The measurements were made in 103 different areas, generally in the morning hours so that atmospheric noise would be at a low enough level that the man-made noise would predominate. The standard deviation of all the medians for the measurements in the 23 business areas about the values given in Figure 17 was approximately 7 dB. For the 38

<sup>\*</sup> Some data were taken at 1 and 10 MHz, in addition to the standard measurement frequencies listed in Table 2.

residential and 31 rural areas, the corresponding standard deviations were approximately 5 and 6.5 dB, respectively. The expected variation of man-made noise levels about the median  $\bar{F}_L$  value observed within a given hour are summarized in Table 2 for each basic category.

TABLE 2 EXPECTED VARIATION, WITHIN AN HOUR, IN MAN-MADE RADIO NOISE LEVELS ABOUT THE MEDIAN VALUES\*

Frequency (MHz)	Business Area		Residential Area		Rural Area	
	$D_u$ (dB) <sup>†</sup>	$D_L$ (dB) <sup>‡</sup>	$D_u$ (dB)	$D_L$ (dB)	$D_u$ (dB)	$D_L$ (dB)
0.25	8.1	6.1	9.3	5.0	10.6	2.8
0.5	12.6	8.0	12.3	4.9	12.5	4.0
1.0	9.8	4.0	10.0	4.4	9.2	6.6
2.5	11.9	9.5	10.1	6.2	10.1	5.1
5	11.0	6.2	10.0	5.7	5.9	7.5
10	10.9	4.2	8.4	5.0	9.0	4.0
20	10.5	7.6	10.6	6.5	7.8	5.5
48	13.1	8.1	12.3	7.1	5.3	1.8
102	11.9	5.7	12.5	4.8	10.5	3.1
250	6.7	3.2	6.9	1.8	3.5	0.8

\* See Figure 17 for median values.

<sup>†</sup>  $D_u$  = ratio of upper decile to median, in decibels.

<sup>‡</sup>  $D_L$  = ratio of median to lower decile, in decibels.

Eleven areas did not fall neatly into any one of the three standard location categories. The data from interstate highways outside of main towns or cities and those from fairly large parks and university campuses within cities were treated separately.

The second major type of estimation method involves the correlation of the received noise with various predictable parameters of the environment. The most successful "predictor" found to date for frequencies above about 20 MHz is traffic density. This, combined with traffic engineering estimates of future highway usage, may provide the best estimate of future radio noise levels at many locations. Use of the model developed by SPAULDING and DISNEY (1974) for vertical-monopole antennas requires the following information: (1) the mean and the variance of the power spectral density (in decibels) radiated from individual vehicles at some particular measurement distance of interest, (2) the traffic density in vehicles per hour, and (3) the average speed of the vehicles. For antennas other than the vertical monopole, the model requires a modification in the antenna gain pattern.

The predictions described above pertain to the ground environment. It would be useful to have models for the noise levels from unintentional radiators to be encountered by aircraft and possibly even by some satellites. Although some attempts at such models have been made (e.g., SKOMAL, E. N., 1970; BUEHLER, W. F., and LUNDEN, C. D., 1966), this work is far less advanced than the work on models for the ground environment.

#### 7. VOIDS IN KNOWLEDGE ABOUT MAN-MADE RADIO NOISE

One would like to know whether man-made noise levels are increasing, decreasing, or staying about the same, but currently there is only a sketchy answer to this question. Increases in the number of noise sources (e.g., the number of power-line miles, and the number of registered automobiles) or in the parameters probably related to man-made noise (e.g., power consumption) have been noted in the United States (JTAC, 1968). The data on the proliferation of silicon-controlled rectifiers and other more recently developed noise sources may be useful. As discussed by SPAULDING and DISNEY (1974), these data indicate that the noise levels in the United States are probably increasing, but they are not useful for estimating the electromagnetic environment at any given location. LYNN (1972) looked at equipment densities on a regional basis, but even this is too coarse for predicting levels as a function of the local environment. Identification of trends (if any) in the average noise power levels over a period of years can only be made by measurements.

Long-term measurements of man-made radio noise at the same location are relatively scarce (ENGLES, J. W., and HAGN, G. H., 1973), making it difficult to identify trends in noise levels. Some limited data for Washington, D.C., for 1960 and 1966, suggest that the levels are staying about the same in highly developed urban areas where vehicle traffic density is already very large (SPAULDING, A. D., and DISNEY, R. J., 1974).

3-10  
Spaulding and Disney's data base on man-made radio noise in business, residential, and rural areas in the USA for the frequency range 250 kHz through 250 MHz is probably the best information available on average noise power spectral density. It can be used for predicting changes in noise levels as an area is developed from rural to either residential or urban. The time rate of change of noise levels would be related to the development time scale. The information given in Figure 17 has been adopted internationally (CCIR, 1974), but it has not yet been extensively checked outside the USA. Few data on average noise power or power spectral density are available for frequencies above about 250 MHz. SKOMAL (1973) has summarized some results extending to 1 GHz.

Few data have been taken simultaneously in different bandwidths with the same type of detector. Therefore, rules for extrapolating data from one bandwidth to another are not well worked out for man-made radio noise. A method has been developed for this type of extrapolation for atmospheric radio noise (SPAULDING, A. D., et al., 1962), but this method has not been adequately verified experimentally except over a very limited bandwidth range (SPAULDING, 1974).

Still another category of void in our knowledge pertains to the lack of standardization of nomenclature and measurement techniques. The CISPR requires a quasi-peak meter whose time constants are chosen to correlate with an annoyance factor for AM broadcasting. Attempts have been made to correlate the readings from CISPR quasi-peak meters with degradation to other types of service, such as television (e.g., STUMPERS, F. L., 1970, 1971, 1973; BAUER, F., 1973; CORTINA, R., et al., 1973).

Unfortunately, when dealing with random processes it is not possible to relate analytically the response of a quasi-peak detector to that of an rms detector, which measures the average noise power as used to calculate signal-to-noise ratio in statistical communications theory (GESELOWITZ, D. B., 1961; MATHESON, R. J., 1970). MAGRAB and BLOMQUIST (1971) discussed the problem of measuring transients and low-duty-cycle waveforms.

Another variety of void pertains to our knowledge of how best to sample the more general classes of nonstationary random processes. BENDAT and PIERSOL (1971), MAGRAB and BLOMQUIST (1971), COX and LEWIS (1966), and others, have addressed the problems associated with the measurement and analysis procedures for random data. MIDDLETON (1972) discussed the concept of macrostationarity. He defined a macrostationary process as one that is not truly stationary in the analytical sense but that can be treated as such for periods during which the changes in the source conditions are small. In any given case, it is usually the sample data themselves that reveal the degree of nonstationarity. Even if the changes in source conditions are large, the data can be treated in a meaningful way if the sources have operated long enough to have been in most of their possible states during the observation interval. KANDA (1974) successfully used the variance analysis of ALLAN (1966) to determine the minimum length of time required for observing the electromagnetic noise in mines. Other distribution-free techniques are also potentially useful (e.g., WALSH, J., 1962, 1965, 1968).

The final category of void concerns our ability to relate the effects of additive non-Gaussian noise, as measured in the environment, to the performance of specific systems. Many of the electromagnetic environmental data available are not directly applicable to the analysis of the performance of particular communication systems. There are several reasons for this. The most direct approach to the analysis of communication systems is to develop an analytical model for the performance of the particular system, requiring, as inputs to the model, information about the desired signal and the noise; to gain confidence in the model by simultaneously measuring the performance of the system and parameters necessary for the model's use; and to compare the modeled performance with the observed performance. It is then possible to acquire the appropriate noise environmental data base by measuring the noise parameters required by the model and, perhaps further, to model the noise in a way that will facilitate estimating the required parameter for situations for which measurements are impractical. If this were done for a variety of systems it would probably be noted that certain noise parameters are frequently required. It follows that those common parameters should be measured whenever practical, in order to fill in some of the current voids in our present knowledge of man-made noise.

Statistical communication theory gives general guidelines for analysis and design of systems intended for operation in impulsive noise environments. The power spectral density of the noise and the amplitude probability distribution function of the instantaneous amplitude at the output of the predetection filter of the communications receiver are frequently necessary but not always sufficient to analyze the performance of digital modems.

Commonly measured parameters, such as the peak and quasi-peak voltage have been correlated with the performance of analog voice and television systems (BURRILL, C. M., 1942; JUETTE, G. W., 1972; CORTINA, R., et al., 1973). While considerable data on these parameters exist they are not particularly useful for analyzing digital systems.

#### ACKNOWLEDGMENT

Examples of noise data have been selected from the literature referenced as well as from the authors' own work. The authors would like to acknowledge support for their past and current work by the U.S. Navy, the Federal Communications Commission, the Motor Vehicle Manufacturers Association, and Stanford Research Institute.

The authors are pleased to mention that they received numerous useful suggestions and comments on a draft of this paper from E. T. Pierce, E. M. Skomal, A. D. Spaulding, and W. R. Vincent (who also provided Figure 16). The power line noise data in Figure 6 from Scotland and Virginia were provided by L. J. Crippen, and J. W. Engles provided data on noise from vehicles used in Figure 13. 3-11

The authors are solely responsible for this paper, and any errors which may have inadvertently been incorporated.

#### REFERENCES

- ALLAN, D. W., 1966, "Statistics of Atomic Frequency Standards," Proc. IEEE, Vol. 54, No. 2, pp. 221-230.
- ALLEN, E. W., 1960, "Man-Made Radio Noise," in The Radio Noise Spectrum, ed. D. H. MENZEL, Harvard University Press, pp. 1-6.
- ANNESRAND, S. A., 1972, "Radio Interference from HVDC Converter Stations," IEEE Trans. Power Apparatus and Systems, Vol. PAS-91, No. 3.
- ARTHUR, M. G., 1974, "The Measurement of Noise Performance Factors: A Metrology Guide," NBS Monograph 142, U.S. Government Printing Office, Washington, D.C., S. D. Catalog Number C 13.44:142 (June).
- BAILEY, B. M., and BELSHER, M. W., 1968, "Discussion on Newell, H. H., et al.," IEEE Trans. Power Apparatus and Systems, Vol. PAS-87, No. 4.
- BALL, A. A., and NETHERCOT, W., 1961, "Radio Interference from Ignition Systems--Comparison of American, German and British Measuring Equipment, Techniques and Limits," Proc. IEEE (London), Vol. 108, Part B, No. 39.
- BAUER, F., 1973, "Efforts of SAE, IEEE, and CISPR to Control Radio Spectrum Pollution from Motor Vehicles," International Electromagnetic Compatibility Symposium Record, IEEE 73 CHO 751-8 EMC.
- BENDAT, J. S., and PIERSON, A. G., 1971, Random Data: Analysis and Measurement Procedures, Wiley, Interscience, New York, N.Y.
- BENSENA, W. D., KANDA, M., and ADAMS, J. W., 1974, "Electromagnetic Noise in Robens No. 4 Coal Mine," NBS Technical Note 654, U.S. Department of Commerce, Boulder, Colo.
- BOLTON, E. C., 1972, "Simulating LF Atmospheric Radio Noise and Comparative Characteristics of Man-Made Noise and Atmospheric Radio Noise at 60, 76, and 200 kHz," OT TM-97, Institute for Telecommunication Sciences, Boulder, Colo.
- BUEHLER, W. E., and LUNDEN, C. D., 1966, "Signature of Man-Made High-Frequency Radio Noise," IEEE Trans. Electromagnetic Compatibility, Vol. EMC-8, No. 3 (September).
- BURGETT, R. R., MASSOLL, R. E., and VAN UUM, D. R., 1974, "Relationship Between Spark Plugs and Engine Radiated Electromagnetic Interference," IEEE Trans., Vol. EMC-16, No. 3, pp. 160-172.
- BURRILL, C. M., 1942, "An Evaluation of Radio Noise Meter Performance in Terms of Listening Experience," Proc. IRE, Vol. 30, pp. 473-478.
- CCIR, 1974, "Man-Made Radio Noise," Report 258-1 (Revised), International Radio Consultative Committee, Geneva.
- CISPR, 1971, "Organization, Rules and Procedures of the C.I.S.P.R.," Publication 10, International Electrotechnical Commission, Geneva.
- COHEN, D. J., 1972, "A Statistical Ignition Noise Model," ECAC-PR-72-041, Electromagnetic Compatibility Analysis Center, Annapolis, Md.
- CONE, V. D., 1972, "Summary of Radio-Frequency Environmental Measurements at Sioux Falls, South Dakota," Final Report, SRI Project 8713, Stanford Research Institute, Menlo Park, Calif.
- CORTINA, R., SFORZINI, M., DEMICHELIS, F., and SERRAVALLI, W., 1973, "Experimental Research on the Most Suitable Instrumentation for Measuring Television Interference from Electric Line and Substation Elements," presented at 1973 IEEE International Symposium on EMC, New York, N.Y.
- COX, D. R., and LEWIS, F.A.W., 1966, The Statistical Analysis of Series of Events, Methuen and Co., Ltd., London.
- DEITZ, J., LUCIA, F., and LIENHAR, M., 1973, "Degradation of Mobile Radio Reception at UHF and VHF," Report No. R-7302, Federal Communications Commission.
- DINGER, H. E., 1962, "Radio Frequency Interference Measurements and Standards," Proc. IRE (May).

3-12  
DISNEY, R. T., 1972, "Estimates of Man-Made Radio Noise Levels Based on the Office of Telecommunications, ITS Data Base," Conference Record, IEEE International Conference on Communications, Philadelphia, 72 CHO6224-COM, pp. 20-13 to 20-19.

DISNEY, R. T., and LONGLEY, A. G., 1973, "Preliminary Telemetry Link Performance Estimate for Department of Transportation High-Speed Test Track," OTM 73-130, Institute for Telecommunications Sciences, Boulder, Colo.

DISNEY, R. T., SPAULDING, A. D., and HUBBARD, A. G., 1974, "Man-Made Radio Noise; Part II: Bibliography of Measurement Data, Applications, and Measurement Methods," OT Report 74-38, Office of Telecommunications, U.S. Dept. of Commerce (in preparation).

ENGLES, J. W., 1974, private communication.

ENGLES, J. W., and HAGN, G. H., 1973, "MF and HF Man-Made Radio Noise Measurements," Program and Abstracts, 1973 USNC-URSI Meeting held 24 August in Boulder, Colo. National Academy of Sciences, Washington, D.C., pp. 107-108 (abstract only).

FORD, R. R., 1972, "Electronic Calculators," IEEE EMC Newsletter, Pacific Area Committee, GEMC 7, p. 3 (December).

FORREST, J. S., 1969, discussion of paper by Warburton, F. W., et al. (1969) IEEE Trans. Power Apparatus and Systems, Vol. PAS-88, No. 10, p. 1498 (October).

GESELOWITZ, D. B., 1961, "Response of Ideal Radio Noise Meter to Continuous Sine Wave, Recurrent Impulses, and Random Noise," IRE Trans. Radio Frequency Interference, pp. 2-10.

GILLILLAND, K. E., and BREWER, T. A., 1974, "Experimental Verification of Ignition Noise APD Model and Digital-Receiver Bit-Error Probability Model," Technical Report ESD-TR-73-036, Electromagnetic Compatibility Analysis Center, Annapolis, Md.

HAGN, G. H., 1973, "Commission 8: Radio Noise of Terrestrial Origin; 8.4 Man-Made Noise Environment," Radio Science, Vol. 8, No. 6, pp. 613-621.

HERMAN, J. R., 1970, "Survey of Man-Made Radio Noise," in Progress in Radio Science, 1966-1969, Vol. 1, ed. by G. M. Brown, N. D. Clarence, and M. J. Rycroft, URSI, Brussels, pp. 315-348.

HSU, H. P., STORWICK, R. M., SCHLICK, D. C., and MAXAM, G. L., 1973 "Measured Amplitude Distribution of Automotive Ignition Noise," 1973 IEEE International Electromagnetic Compatibility Symposium Record, IEEE 73 CHO 751-8 EMC (June).

HSU, H. P., STORWICK, R. M., SCHLICK, D. C., and MAXAM, G. L., 1974, "Measured Amplitude Distribution of Automotive Ignition Noise," IEEE Trans. Electromagnetic Compatibility, Vol. EMC-16, No. 2 (May).

IEEE Radio Noise Subcommittee of the IEEE Transmission and Distribution Committee, 1965, "Transmission System Radio Influence," IEEE Trans. Apparatus and Systems, Vol. PAS-84, No. 8 (August).

IEEE, 1966, "Measurement of Radio Noise Generated by Motor Vehicles and Affecting Mobile Communications Receivers in the Frequency Range 25 to 1000 Mc/s," IEEE Standard 263, IEEE Trans., Vehicular Communications, Vol. VC-15.

IEEE Radio Noise Subcommittee--Working Group No. 3, 1971, "Radio Noise Design Guide for High-Voltage Transmission Lines," IEEE Trans. Power Apparatus and Systems, Vol. PAS-90, No. 2 (March/April).

JTAC, 1968, "Spectrum Engineering--The Key to Progress," Joint Technical Advisory Committee, IEEE, New York.

JUETTE, G. W., 1972, "Evaluation of Television Interference from High Voltage Transmission Lines," IEEE Trans. Power Apparatus and Systems, Vol. PAS-91, No. 3.

KANDA, M., 1974, "Time and Amplitude Statistics for Electromagnetic Noise in Mines," NBSIR 74-378, National Bureau of Standards, Boulder, Colo.

KÄUFERLE, J., 1972, "Using DC Links to Enhance AC System Performance," IEEE Spectrum, Vol. 9, No. 6, pp. 31-37 (June).

LAFOREST, J. J., 1968, "Seasonal Variation of Fair-Weather Radio Noise," IEEE Trans. Power Apparatus and Systems, Vol. PAS-87, No. 4.

LAUBER, W. R., 1974, private communication.

LOFTNESS, M. O., 1970, "The Location of Power Line TVI: Some Reduction Considerations," IEEE Trans. Power Apparatus and Systems (May-June).



LYNN, J. F., 1972, "Man-Made Electromagnetic Noise in Southern California and Nevada," IEEE Trans. Electro-  
magnetic Compatibility, Vol. EMC-14, No. 3, pp. 92-96.

MAGNAB, E. B., and BLONQUIST, D. S., 1971, The Measurement of Time Varying Phenomena, Wiley, Interscience,  
New York, N.Y. See also J. J. Davidson, 1961, "Average vs. RMS Meters for Measuring Noise," IRE Trans.  
Audio, pp. 108-111 (July-August).

MARTIN, H., and TABOR, F., 1972, "The Electromagnetic Compatibility of Aeronautical Communication and  
Navigation Systems with Radio Frequency Dielectric Heaters and Superregenerative Receivers," Final Report,  
Contract DOT-FA70WAI-175 Task 10, Report FAA-RD-72-80, 11, Electromagnetic Compatibility Analysis Center,  
Annapolis, Md.

MATHESON, R. J., 1970, "Instrumentation Problems Encountered Making Man-Made Electromagnetic Noise Measure-  
ments for Predicting Communication System Performance," IEEE Trans. Electromagnetic Compatibility,  
Vol. EMC-12, No. 4 (November).

MATHESON, R. J., and BRASLEY, K. R., 1972, "Field Intensity Meter Modified to Measure RMS and Average  
Noise Envelope Voltage," Technical Memorandum OT TM-119, Institute for Telecommunication Sciences,  
Boulder, Colo.

MAXAM, G. L., HSU, H. F., SCHLICK, D. C., and STORWICK, R. M., 1973a, "Measured Pulse Height Distributions  
of Industrial Engine Cylinder Ignition Noise," Research Publication GMR-1727, General Motors, Warren, Mich.

MAXAM, G. L., HSU, H. F., SCHLICK, D. D., and STORWICK, R. M., 1973b, "Measured Pulse Height Distributions  
of Industrial Engine Cylinder Ignition Noise," presented URSI Commission VIII, Boulder, Colorado, Abstracts,  
USNC-URSI, National Academy of Sciences, Washington, D.C., p. 104.

McLACHLAN, A. S., 1973, "Radio Interference Complaints for the Year 1972," RTD Technical Memorandum No. I-12,  
Directorate of Radio Technology, Ministry of Posts and Telecommunications, United Kingdom.

MIDDLETON, D., 1972, "Statistical-Physical Models of Urban Radio-Noise Environments--Part I: Foundation,"  
IEEE Trans. Electromagnetic Compatibility, Vol. EMC-14, No. 2, pp. 28-36 (May).

MILLS, A. H., 1971, "Measurement of Radio Frequency Noise in Urban, Suburban, and Rural Areas," Final  
Report, Contract NAS3-11531, Convair Division, General Dynamics, San Diego, Calif. (December).

MUMFORD, W. W., and SCHIKER, E. H., 1968, Noise Performance Factors in Communications Systems, Horizon  
House.

NEWELL, H. H., LIAO, T. W., and WARBURTON, F. W., 1968, "Corona and RI Caused by Particles on or near EMV  
Conductors: II Foul Weather," IEEE Trans. Power Apparatus and Systems, Vol. PAS-87, No. 4 (April).

NIELSON, D. L., 1974, "Impulsive Ignition Noise at 1370 MHz," Abstracts, International Union of Radio Science,  
Annual USNC-URSI meeting, Boulder, Colo., 14-17 October, National Academy of Sciences, 2101 Constitution  
Avenue N.W., Washington, D.C. 20418.

PARALA, W. E., et al., 1968, "Radio Noise Measurements on High Voltage Lines from 2.4 to 345 kV," 1968  
IEEE Electromagnetic Compatibility Symposium Record, IEEE 68C12-EMC.

PARALA, W. E., and CHARTER, V. L., 1971, "Radio Noise Measurements on Overhead Power Lines from 2.4 to  
800 kV," IEEE Trans. Power Apparatus and Systems, Vol. PAS-90, No. 3, pp. 1155-1165.

PETERSON, A. M., 1974, "Noise Pollution of the Radio Spectrum," Conference Record, IEEE International  
Conference on Communications, June 1974, Minneapolis, Minn., pp. 19K-1 to 19K-4.

PLOUSSIOS, G., 1968, "City Noise and Its Effects upon Airborne Antenna Noise Temperatures at VHF,"  
IEEE Trans. on Electronics and Aerospace Systems, Vol. AES-4, No. 1.

ROBERTSON, K., 1971, "Some Examples of Powerline Interference and Suggested Remedial Measures," Proc. IEEE  
(Australia), pp. 396-404 (November).

ROTH, I., 1958, "Airborne Tests of Meteor Burst Communications," Scientific Report 7, SRI Project 1422,  
Stanford Research Institute, Menlo Park, Calif.

SAE, 1974, "Measurement of Electromagnetic Radiation from a Motor Vehicle or Other Internal Combustion  
Powered Device (Excluding Aircraft) (20-1000 MHz)," SAE J551c, Society of Automotive Engineers, New York,  
N.Y.

SCHULZ, R. B., and SOUTHWICK, R. A., 1974, "APD Measurements of V-R Ignition Emissions," IEEE Electro-  
magnetic Compatibility Symposium Record, IEEE, 74 CH003-7EMC, pp. 50-57.

SCHULZ, R., SOUTHWICK, R., and SMITHFETER, C., 1973, "Measurement of Electromagnetic Emissions Generated  
by Vehicle Ignition Systems," report prepared for Motor Vehicle Manufacturers Association under NVMA  
Agreement SW 7303-C339 by Southwest Research Institute, San Antonio, Texas.

3-14 SHEPHERD, R. A., 1974, "Measurements of Amplitude Probability Distributions and Power of Automobile Ignition Noise at HF," IEEE Trans. Vehicular Technology, Vol. VT-24, No. 3.

SHEPHERD, R. A., GADDIE, J. C., HATFIELD, V. E., and HAGN, G. H., 1973, "Measurements of Automobile Ignition Noise at High Frequency," Final Report, Contract N00-39-71-A-0223, Stanford Research Institute, Menlo Park, California.

SHEPHERD, R. A., GADDIE, J. D., and NIELSON, D. L., 1974a, "Variability in Measurement Procedures for Ignition Noise," Final Report to Motor Vehicle Manufacturers Assoc., SRI Project 3253, Stanford Research Institute, Menlo Park, Calif.

SHEPHERD, R. A., GADDIE, J. C., and NIELSON, D. L., 1974b, "Improved Suppression of Radiation from Automobiles used by the General Public," Final Report to Federal Communications Commission, Contract FCC-0072, Stanford Research Institute, Menlo Park, California (in preparation).

SHOWERS, R. M., 1974, private communication.

SKOMAL, E. N., 1970, "The Range and Frequency Dependence of VHF-UHF Man-Made Radio Noise in and Above Metropolitan Areas," IEEE Trans. Vehicular Technology, Vol. VT-19, No. 2 (May).

SKOMAL, E. N., 1973, "An Analysis of Metropolitan Incidental Radio Noise Data," IEEE Trans. Electromagnetic Compatibility, Vol. EMC-15, pp. 45-57 (May).

SPAULDING, A. D., 1972, "The Determination of Received Noise Levels from Vehicular Traffic Statistics," IEEE 1972 NTC Record, 72 CHO601-5-NTC.

SPAULDING, A. D., 1974, private communication.

SPAULDING, A. D., AHLBECK, W. H., and ESPELAND, R. R., 1971, "Urban Residential Man-Made Radio Analysis and Predictions," OT/ITS Telecommunications Research and Engineering Report 14, Office of Telecommunications, U.S. Dept. of Commerce, Boulder, Colo.

SPAULDING, A. D., and DISNEY, R. T., 1974, "Man-Made Radio Noise, Part I: Estimates for Business, Residential, and Rural Areas," OT Report 74-38, Office of Telecommunications, U.S. Dept. of Commerce, Boulder, Colo.

SPAULDING, A. D., ROBIQUE, J. J., and CHRICHLOW, W. Q., 1962, "Conversion of the Amplitude-Probability Distribution Function for Man-Made Radio Noise From One Bandwidth to Another," J. Res. Nat'l Bur. St., Vol. 66D, No. 6, pp. 711-720 (November-December).

STORWICK, R. M., SCHLICK, D. C., and HSU, H. P., 1973, "Measured Statistical Characteristics of Automotive Ignition Noise," SAE Paper 730133, International Automotive Engineering Congress.

STUART, G. F., and SITES, M. J., 1973, "Man-Made Radio Noise at 150 kHz to 32 MHz near a large Antarctic Base," IEEE Trans. Electromagnetic Compatibility, Vol. EMC-15, No. 3 (August).

STUMPERS, F.L.H.M., 1970, "Progress in the Work of CISPR," IEEE Trans. Electromagnetic Compatibility, Vol. EMC-12, pp. 29-32 (May).

STUMPERS, F.L.H.M., 1971, "Interference to Communications and the Work of CISPR," Conference Record, International Conference on Communications, Montreal, IEEE, pp. 37-14, 37-19.

STUMPERS, F.L.H.M., 1973, "The Activities of CISPR During Recent Years and Their Impact on Society," International Electromagnetic Compatibility Symposium Record, IEEE, 73 CH0751-8 EMC pp. V-X.

SWENSON, Jr., G. W., and COCHRAN, W. W., 1973, "Radio Noise from Towns: Measured from an Airplane," Science, Vol. 181, No. 4099 (August).

THOMPSON, W. I. III, 1971, "Bibliography on Ground Vehicle Communications and Control: A KWIC INDEX," Report No. DOT-TSC-UMTA-71-3, Urban Mass Transportation Administration, U.S. Dept. of Transportation, Cambridge, Mass., Vol. II (July).

VINCENT, W. R., 1974, private communication.

VINCENT, W. R., and DAYHARSH, T. I., 1969, "A Study of Land Mobile Spectrum Utilization, Part B: Analysis of the Spectrum Management Problem," Final Report, Contract N00-39-71-A-0056, Stanford Research Institute, Menlo Park, Calif.

VINCENT, W. R., and ELLISON, R. W., 1974, "RF Noise Radiated by a Rapid Transit System," IEEE Electromagnetic Compatibility Symposium Record, 74CH0803-7 EMC.

WALSH, J. E., (1962, 1965, 1968) Handbook of Non-Parametric Statistics, 3 Vols., Van Nostrand, New York, N.Y.

WARBURTON, F. W., et. al., 1969, "Power Line Radiations and Interference above 15 MHz," IEEE Trans. Power Apparatus and Systems, Vol. PAS-88, No. 10 (October).

315

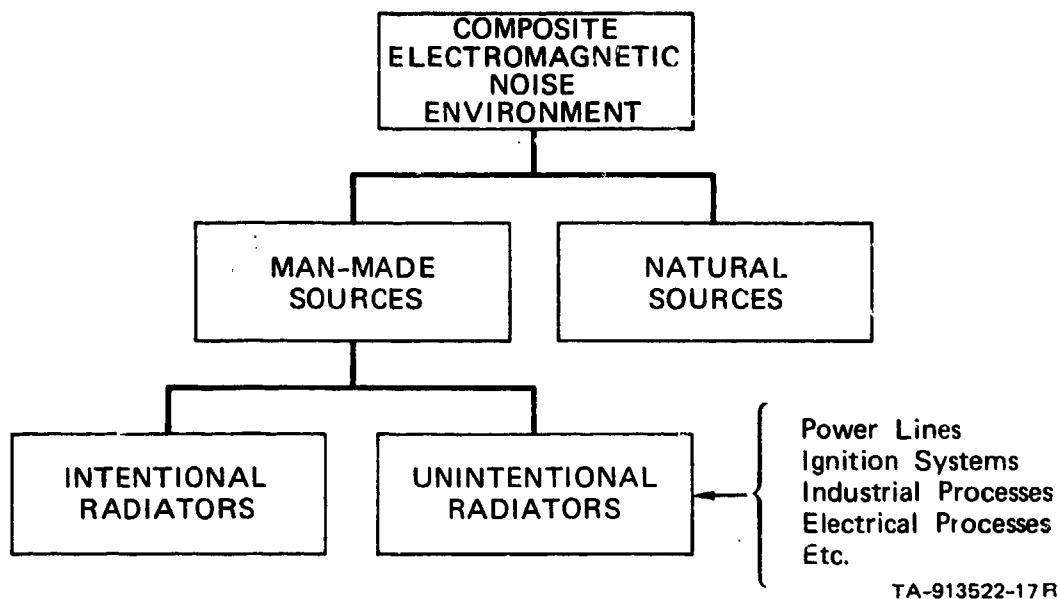
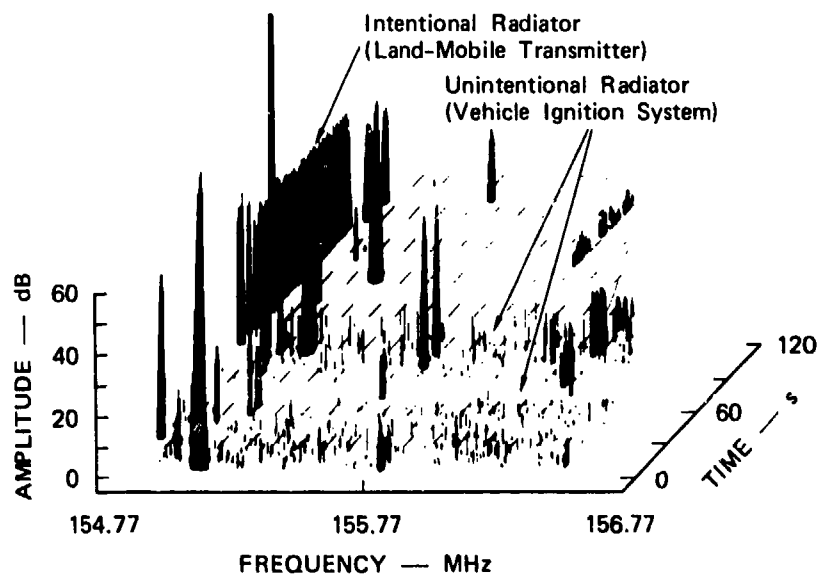
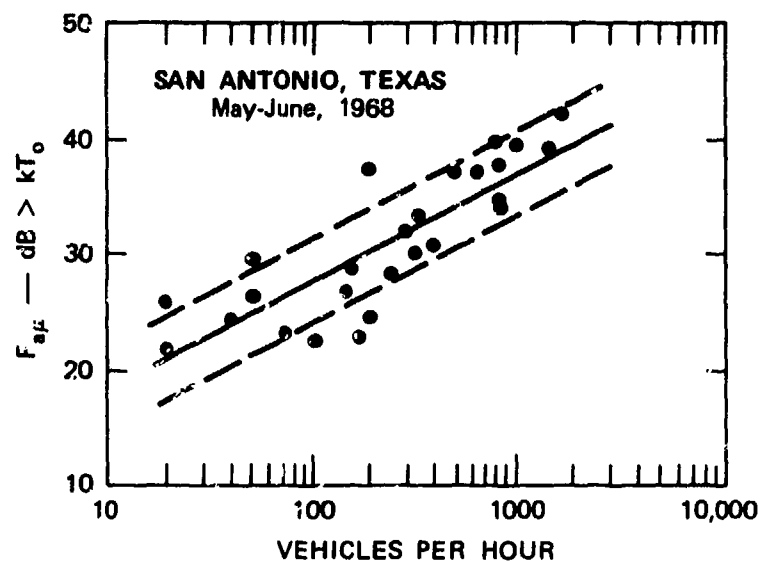


FIGURE 1 CATEGORIES OF SOURCES CONTRIBUTING TO THE COMPOSITE ELECTROMAGNETIC NOISE ENVIRONMENT



D-7379-130

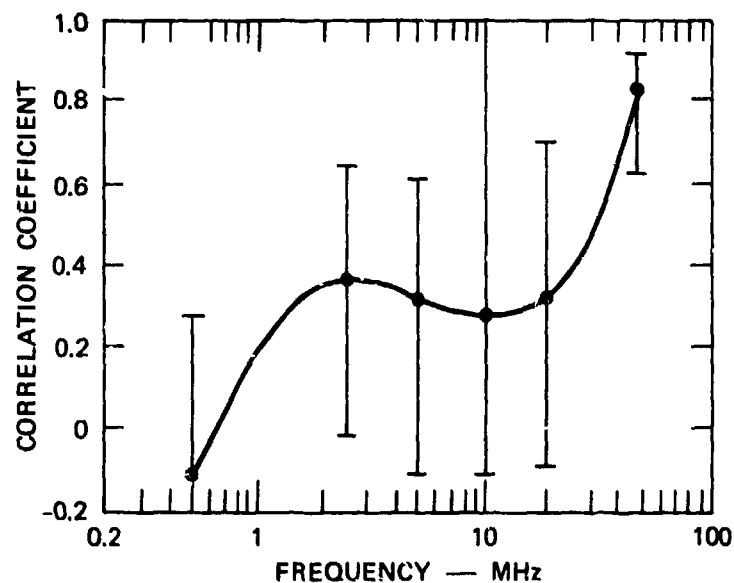
FIGURE 2 EXAMPLES OF CONTRIBUTIONS TO THE COMPOSITE ELECTROMAGNETIC NOISE ENVIRONMENT BY INTENTIONAL AND UNINTENTIONAL RADIATORS-- AS OBSERVED WITH A SCANNING RECEIVER (AFTER VINCENT, W. R., AND DAYHARSH, T. I., 1969)



SOURCE: Spaulding, A. D., 1972.

TA-913522-8R

FIGURE 3 LINEAR REGRESSION OF THE MEAN OF 48 MHz  $F_a$  VALUES ALONG A THOROUGHFARE ( $F_{aμ}$ ) VERSUS LOG HOURLY TRAFFIC COUNT ALONG THE THOROUGHFARE (26 THOROUGHFARES)



SOURCE: Spaulding, A. D., 1972.

TA-913522-9

FIGURE 4 CORRELATION COEFFICIENTS ALONG WITH THE 95-PERCENT CONFIDENCE LIMITS FOR EACH OF THE MEASUREMENT FREQUENCIES,  $F_{aμ}$  VERSUS LOG HOURLY TRAFFIC COUNT

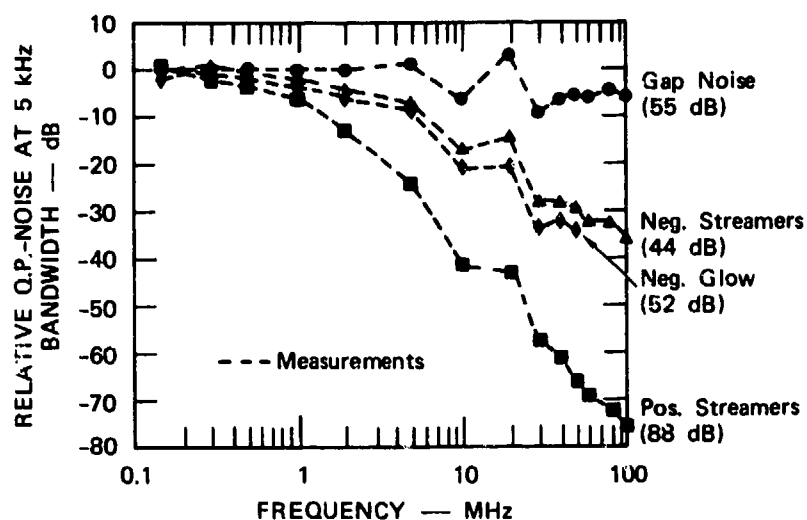


FIGURE 5 RELATIVE FREQUENCY SPECTRA FOR DIFFERENT TYPES OF NOISE FROM POWER LINES (THE NUMBERS IN PARENTHESES ARE THE ABSOLUTE VALUES MEASURED AT 0.150 MHz, AFTER JUETTE, G. W., 1972)

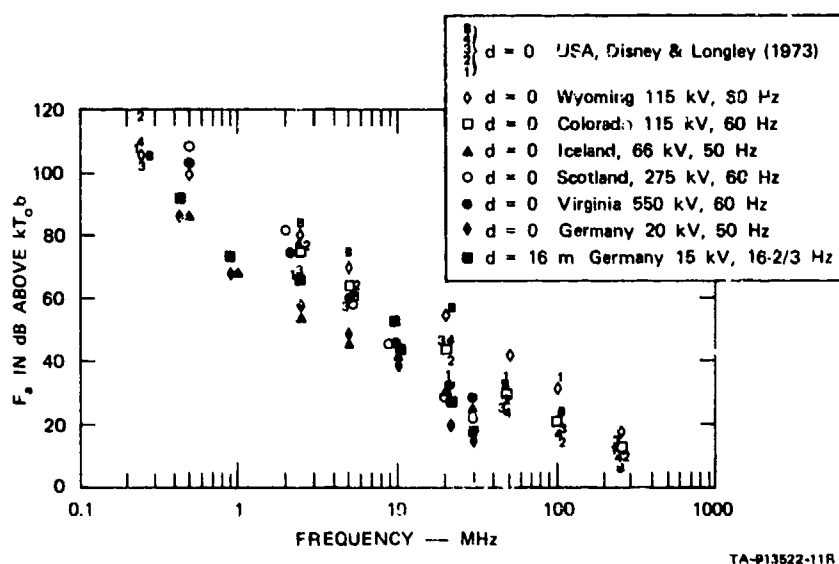
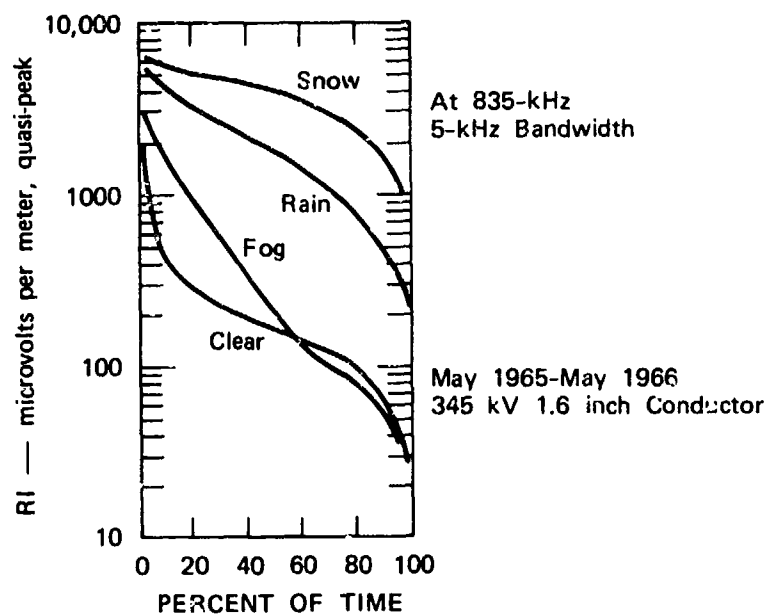


FIGURE 6 MEDIAN VALUES OF AVERAGE NOISE POWER SPECTRAL DENSITIES APPROXIMATELY UNDERNEATH SELECTED POWER LINES



SOURCE: Bailey, B. M. and Belsher, M. W., 1968.

TA-913522-12

FIGURE 7 RI DISTRIBUTION, PERCENT OF TIME RI LEVEL  
EQUALS OR EXCEEDS ORDINATE

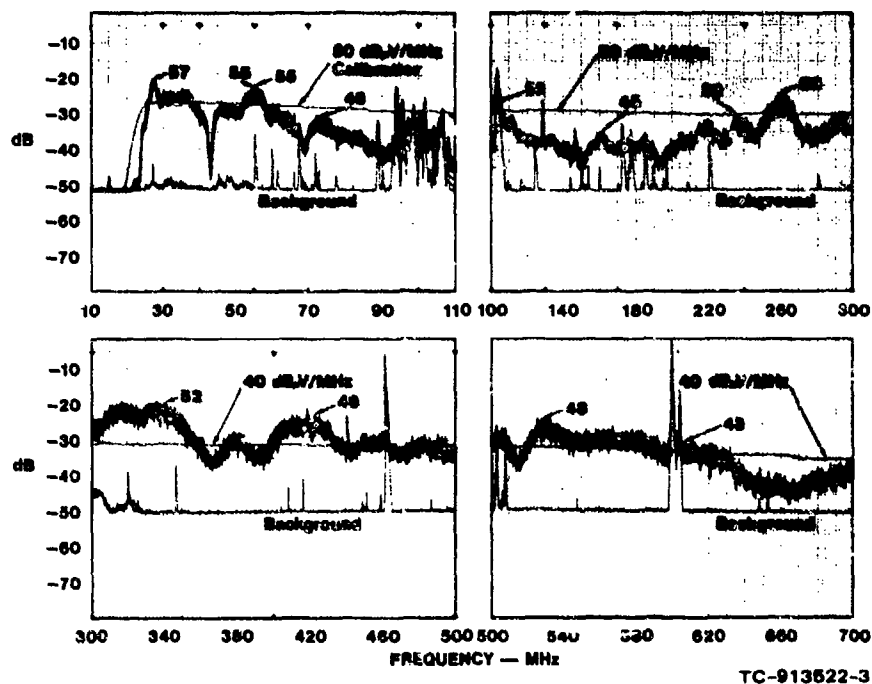
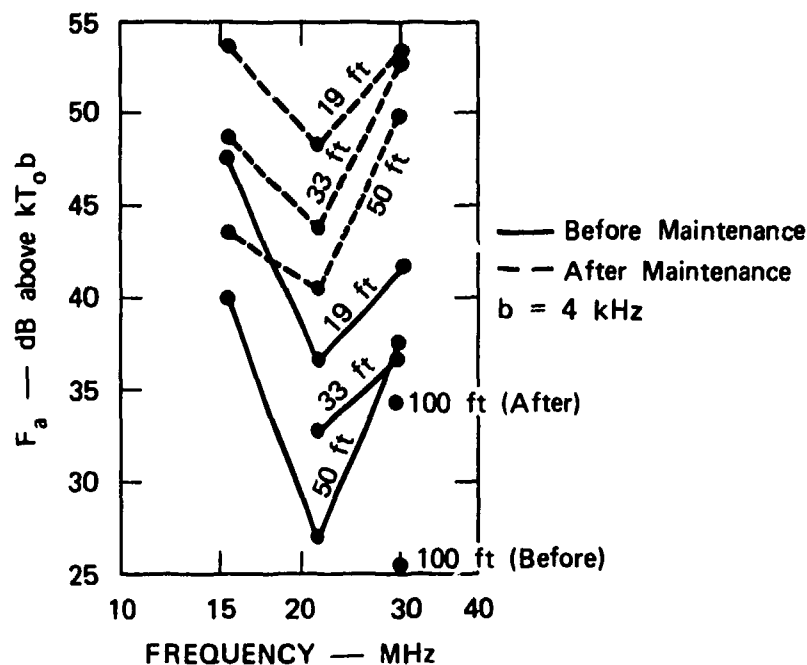
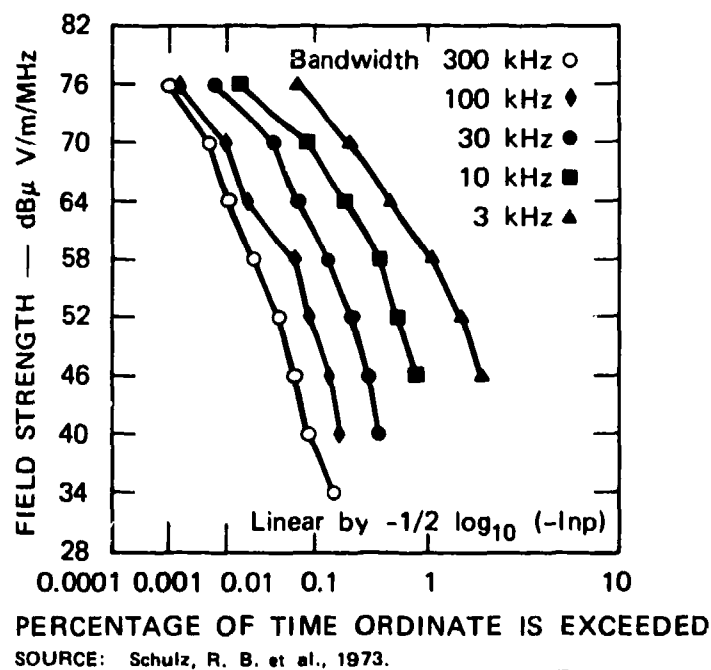


FIGURE 8 IGNITION NOISE--LEFT SIDE 1972 BUICK LE SABRE, VERTICAL  
POLARIZATION, 10 m



SA-1022-4R

FIGURE 9 VEHICLE IGNITION NOISE, 1963 FORD PANEL TRUCK (SIX CYLINDER, 4 x 2), VERTICAL POLARIZATION



TA-913422-13R

FIGURE 10 SINGLE-VEHICLE APD DATA (AVERAGE OF FOUR VEHICLES)

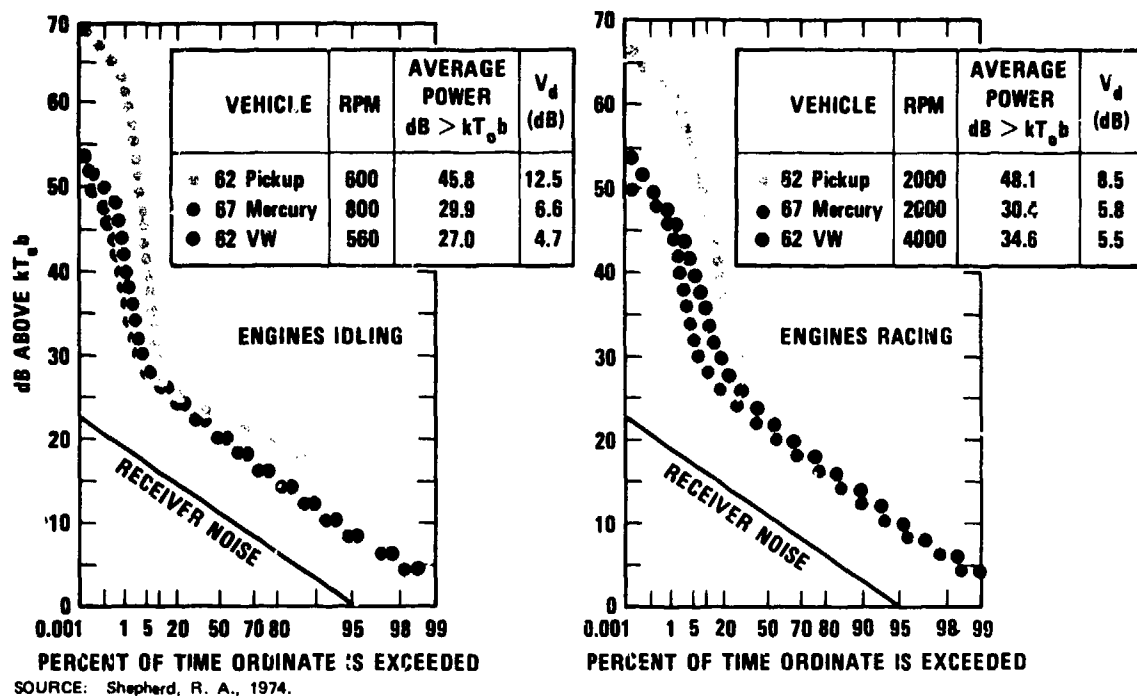


FIGURE 11 APDs OF THREE VEHICLES, RIGHT SIDE AT 10 m, 24.11 MHz, 8 kHz NOISE BANDWIDTH

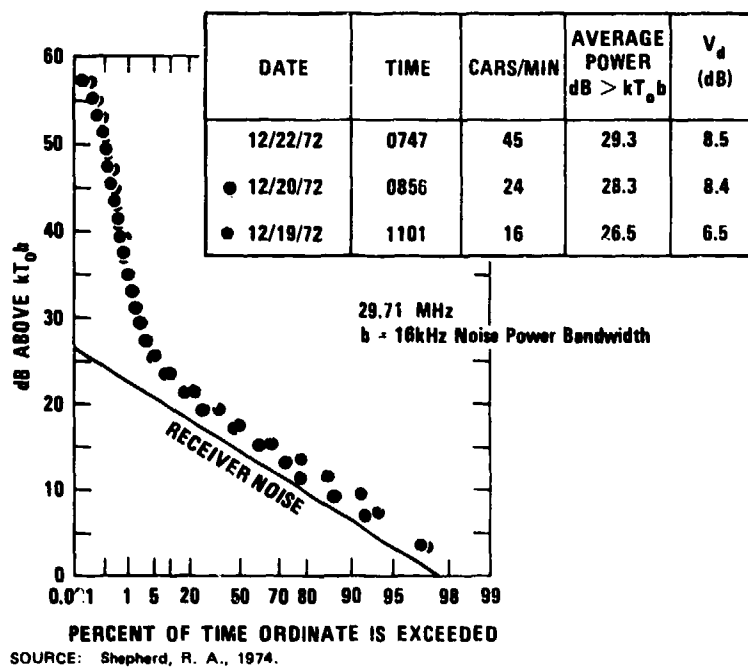


FIGURE 12 APDs SHOWING LIGHT, MODERATE AND HEAVY TRAFFIC



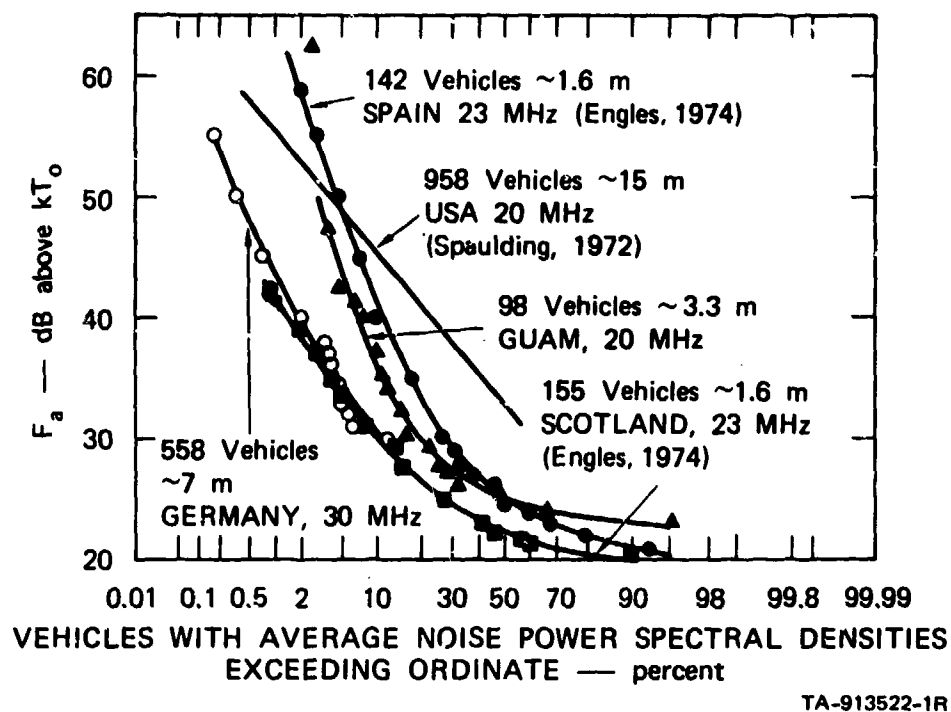
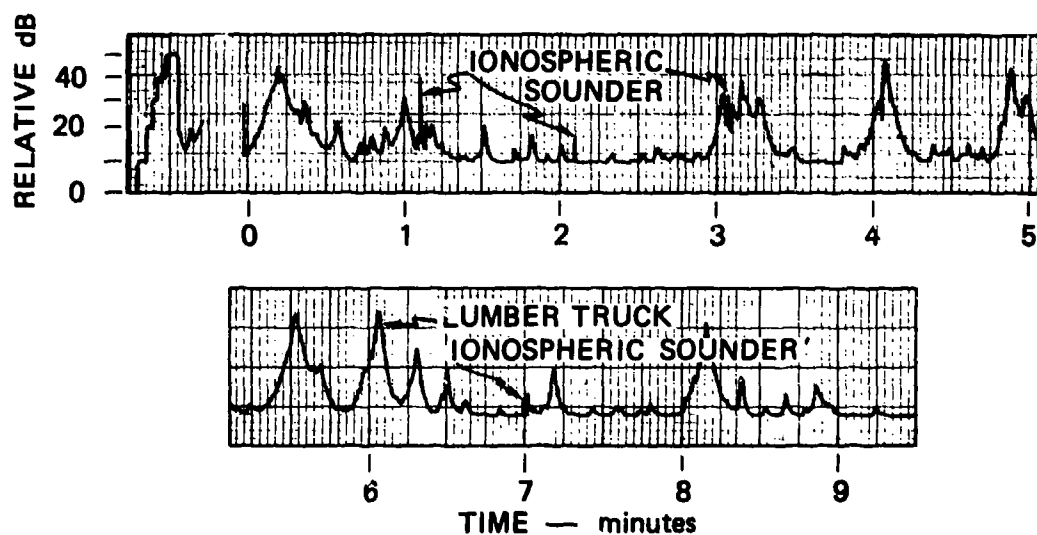


FIGURE 13 DISTRIBUTIONS OF IGNITION NOISE POWER SPECTRAL DENSITIES MEASURED AT SEVERAL LOCATIONS (MOVING VEHICLES)



SOURCE: Shepherd, R. A. et al., 1973.

SA-2061-30

FIGURE 14 CHART RECORD OF IGNITION NOISE POWER AT 29.71 MHz NEAR THE FREEWAY

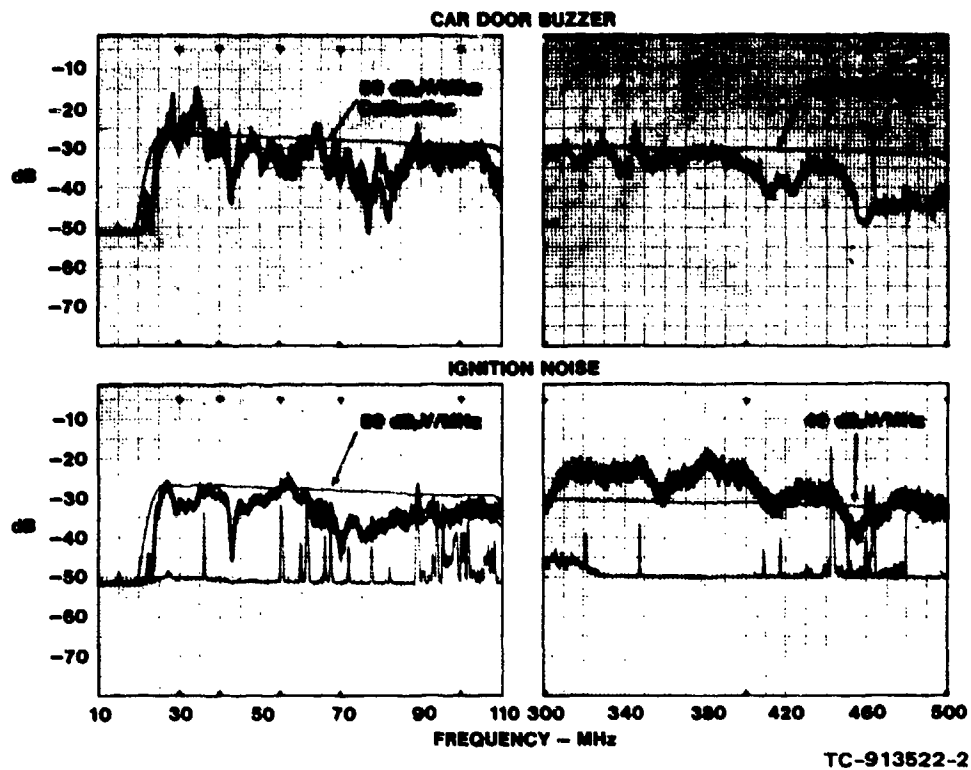


FIGURE 15 COMPARISON OF IGNITION NOISE AND BUZZER NOISE--1972 BUICK LE SABRE, HORIZONTAL POLARIZATION, 10 m



323



IF Bandwidth 30 kHz  
Sweep Time 50 ms/Scan  
Sweep Rate 20 Scans/s  
Amplitude Log  
Time Axis 3 s

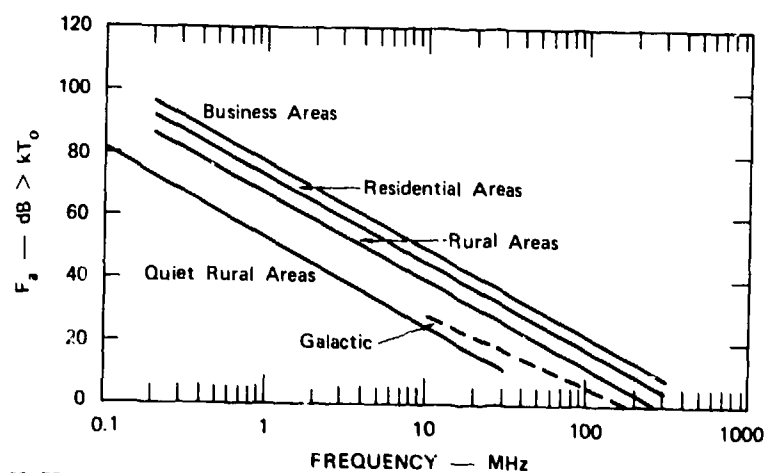
30 40 50

FREQUENCY — MHz

SOURCE: Vincent, W. R., 1974.

TA-913522-5

FIGURE 16 CALCULATOR NOISE



SOURCE: Spaulding, A. D. and Dinzy, R. T., 1974

TA-913522-14R

FIGURE 17 ESTIMATES OF MEDIAN VALUES OF MAN-MADE AND GALACTIC NOISE POWER SPECTRAL DENSITIES EXPECTED AT TYPICAL LOCATIONS ON A LOSSLESS SHORT GROUNDED VERTICAL MONOPOLE

## DISCUSSION

F. D. GREEN: One reason why there have not been many measurements of man-made noise at VHF (in land mobile band) is because there have not been many complaints of noise at VHF in urban areas. My experience has been not to be able to obtain support for measurements in this range because complaints are few. This is undoubtedly because sufficient power is permitted to cover the urban area on each assignment. Nonetheless, it seems important to make noise measurements in the VHF range, otherwise, like the "horsepower" race in automobiles, we will arrive at a stage where the noise, like the danger, may be intolerable.

R. A. SHEPHERD: What can I do but agree? We should also note that the degradation caused by the noise may not be noticeable to the user of the land mobile system. It may operate against the AGC circuit to decrease the sensitivity of the receiver, an effect that may not be noticeable to the user.

G. H. HAGN: Complaints are a useful input to the identification of potential problems, but they are neither necessary nor sufficient when it comes to assessing where additional work is required. Mr. J. Deitz of the US Federal Communications Commission has recently quantified how much additional transmitter power (effective radiated power) is required for the VHF land mobile radio systems to override the noise for a given grade of service. Also, one might expect that in areas of "fringe coverage" the FM and TV broadcast listeners might suffer interference and some of them might even complain if they thought they could get a remedy.

D. BOSMAN: In the noise data on power lines a dependence on weather conditions is quite clear. Can you tell us which antenna types were used in the experiments, and whether the antennas were shielded from or exposed to the parameter in question, i.e., rain or snow? (Background of the question: What was mainly measured; power of the noise source, variation in transmission and/or effects on the antenna characteristics?)

R. A. SHEPHERD: The power line data shown as a function of weather condition was all abstracted from material in the open literature and I do not recall the situations of the antennas' possible exposure. The noise increases, however, are real; they have also been observed when short sections of test lines are subjected to sprinkling of water, etc. We would not expect rain or snow in the air to appreciably affect the path between the source and the receiver at the frequencies (LF and HF) used.

G. H. HAGN: The precipitating particles impacting on an unprotected antenna have the potential to cause noise which can be observed at the receiver output, usually due to corona from the antenna itself. It is important to be able to sort out noise from this source and the noise from the power-line under observation. For the data (described in the last paragraph of Section 3.5) taken during rain I used a 1-m vertical rod antenna which was completely exposed. I assured myself that the observed noise came from the power line by moving the antenna around and correlating changes in level of several dB with proximity to the power line towers.

F. S. STRINGER: Is it practicable to identify the direction along which a high power line lies and the direction of the nearest point to the observer by DF techniques? If so, what practical maximum range is likely to be obtainable?

R. A. SHEPHERD: It is possible to locate the sources of gap type noise but this is generally done in ad hoc manner in order to tighten the hardware or to otherwise suppress the sources. A system to identify the direction to and the direction of power lines that are radiating corona noise has not been, so far as I know, attempted. The range limitations would depend upon the other sources of noise in the area and the system's ability to discriminate between the noise from the power line and that from other sources.

G. H. HAGN: It should be possible in some cases to use direction finding techniques to locate power lines which are acting as distributed sources of noise from corona as well as for locating the noise from specific gaps. Both airborne and ground-based techniques can be applied to this problem. The success in general, should be highly variable, and any given case will probably depend on the exact details of the system used, the geometry of the line, the weather, and the composite electromagnetic noise environment at the location of the receiving antenna.

## LES BRUITS COSMIQUES

A. Boischot

Observatoire de Paris  
92190 - Meudon, France

4-1

### Sommaire

On fait l'inventaire des sources de bruit naturelles dans tout le domaine radioélectrique, en précisant la nature de ces bruits. Certaines émissions sont continues et à spectre très large (émission galactique, radiosources) d'autres sporadiques et à spectre irrégulier (sursauts du Soleil et de Jupiter, Pulsars).

On donne leurs caractéristiques moyennes dans les diverses parties du spectre, en précisant leur effet "parasite" sur les télécommunications terrestres.

### I - Introduction

Du point de vue de l'Astronome, les émissions radioélectriques des astres ont une importance considérable. Elles nous renseignent sur de très nombreux problèmes d'astrophysique, depuis la structure de la magnétosphère de Jupiter jusqu'à l'évolution même de l'Univers.

Du point de vue des radiocommunications terrestres par contre, ces "bruits cosmiques" constituent une nuisance, car ils vont, dans de nombreux cas, limiter la sensibilité des instruments, et pourront parfois être confondus avec les signaux "utiles" que l'on cherche à détecter.

Il est donc important de faire l'inventaire de ces bruits cosmiques, en regardant leur intensité, leur distribution sur le ciel, et leur spectre dynamique, c'est-à-dire, dans le cas des sources très variables, les variations de leur intensité en fonction de la fréquence et du temps.

L'usage, en radioastronomie, est d'exprimer l'intensité d'une émission, quand la source est beaucoup plus petite que le lobe de l'antenne, par sa densité de flux exprimée en watt par mètre carré de surface réceptrice sur la Terre et par Hertz de bande passante. L'unité habituelle est de  $10^{-26} \text{ W.m}^{-2} \text{ Hz}^{-1}$ , et les sources connues s'étagent entre  $10^{-16} \text{ W.m}^{-2} \text{ Hz}^{-1}$  et  $10^{-29} \text{ W.m}^{-2} \text{ Hz}^{-1}$ .

Quand les sources sont très étendues, on définit plutôt la "brillance"  $B$  qui est égale au flux reçu, en watt, par mètre carré de surface réceptrice au sol, par Hertz de bande passante et dans un angle solide de 1 stéradian vu de la Terre.

Ceci nous conduit à définir la Température de brillance,  $T_b$  qui, pour les sources de dimension apparente sensible est égale à la température que devrait avoir un corps noir de même dimension que la source pour rayonner l'intensité observée. On montre facilement que l'on a les relations

$$S = \frac{2k T_b}{\lambda^2} \Omega \quad (1)$$

$$b = \frac{2k T_b}{\lambda^2} \quad (2)$$

Ceci n'est autre que l'approximation dans le domaine radio de la loi de rayonnement du Corps noir de Planck. ( $k$  = constante de Boltzman,  $\Omega$  = angle solide sous-tendu par la source,  $\lambda$  = longueur d'onde)

Il faut insister sur le fait que la Température de brillance ne représente généralement pas la Température réelle de la source. Ceci n'est vrai que dans le cas d'un astre solide, comme la lune ou les planètes, aux fréquences où leur coefficient de réflexion est nul, et des nuages gazeux dont l'émission est dite "thermique" et l'épaisseur optique très grande. Mais dans la majorité des cas, la Température de brillance fait intervenir l'épaisseur optique du gaz émissif et surtout le mécanisme d'émission lui-même. On peut ainsi avoir des températures de brillance comprises, suivant les astres 0°K (ou 3°K pour le fond continu "cosmologique" sur ondes millimétriques) et 1022°K pour certains pulsars.

Nous dirons pour terminer cette étude quelques mots sur les techniques de détection des bruits cosmiques. Mais pour compléter les définitions, il faut définir la "Température d'antenne" plus souvent utilisée en radioastronomie qu'en télécommunication.

La Température d'antenne est la température que devrait avoir une résistance adaptée mise à la place de l'antenne pour envoyer au récepteur une tension de bruit égale à celle envoyée par l'antenne.

La puissance reçue par l'antenne est ainsi, pour une bande passante  $B$

$$P = k T_a B \quad (3)$$

elle est égale à la puissance envoyée au récepteur, donc

$$P = \frac{E^2}{R}$$

(4)

La théorie thermodynamique des antennes montre que, dans le cas d'une source de température de brillance  $T_b$  entourant entièrement l'antenne, ou de dimension supérieure à son diagramme de réception on a

$$T_a = T_b$$

Enfin, on peut relier l'unité radioastronomique d'intensité, la densité de flux  $S$ , à l'unité habituelle des radioélectriciens, l'amplitude  $E$  en volt par mètre. Dans une bande de fréquence de largeur  $B$  nous aurons

$$E = (Z_0 SB)^{1/2} \quad (5)$$

où  $Z_0$  est l'impédance du vide (377  $\Omega$ ).

## II - Les bruits cosmiques

### II-1 Nature des sources de bruit

Tous les astres et les gaz diffus qui constituent l'Univers sont sources d'une émission radioélectrique, mais avec des intensités très différentes. Certains d'entre-eux, comme la grande majorité des étoiles, sont trop faibles pour être détectés sur Terre avec les instruments dont nous disposons actuellement. Par contre, certains autres donnent sur Terre, un flux d'un ordre de grandeur égal ou même supérieur à ceux utilisés dans les différentes techniques de radiocommunications.

Du point de vue de leur nuisance, on peut classer les sources de bruits cosmiques en trois grandes catégories :

- Les sources à distribution quasi continue sur le ciel, qui seront reçues par les antennes quelle que soit leur direction de visée. Ces sources auront pour effet d'ajouter un bruit continu à l'entrée des récepteurs, et donc de diminuer la sensibilité des systèmes de réception.
- Les radiosources de petites dimensions apparentes qui ont une émission stable dans le temps. Ces sources ne seront généralement pas trop gênantes, sauf pendant les courtes périodes où l'une d'elle passe, par suite du mouvement diurne, dans le lobe de l'antenne. Par contre, ces radiosources pourront être très utiles pour la détermination des caractéristiques des antennes (Guidice et Castelli, 1970).
- Les sources variables, qui sont essentiellement le Soleil, la Terre et Jupiter. Ces sources sont extrêmement intenses dans certains domaines de fréquences et leur émission peut avoir pour effet de brouiller les radio communications terrestres moins intenses, ou éventuellement être confondues avec elles.

### II - 2 L'émission du "fond du Ciel"

C'est une émission distribuée à peu près uniformément sur toute la voûte céleste. En réalité elle a trois origines différentes, les émissions correspondantes ayant des spectres différents. Le résultat est que chacune d'elle prédomine dans une gamme d'ondes déterminée. Deux de ces émissions proviennent du gaz interstellaire de notre Galaxie, l'autre a une origine plus curieuse.

#### Le rayonnement thermique de la Galaxie

Un gaz ionisé, de température  $T$  rayonne un rayonnement analogue à celui du corps noir, dû au mouvement des électrons libres dans le champ des protons (émission free-free). Cette émission est dite thermique, car l'énergie qui est convertie en rayonnement est empruntée à l'énergie d'agitation thermique des électrons du gaz. Par conséquent, l'énergie émise sera fonction de la température du gaz. Il s'agit en réalité de la queue dans le domaine radioélectrique de la loi de Planck bien connue dans les domaines visible et infrarouge.

La température de brillance sera fonction de la température électronique du gaz et de son épaisseur optique  $\tau$

$$T_b = T_e (1 - e^{-\tau}) \quad (6)$$

$$\text{avec} \quad \tau = \int_{\text{rayon}} K \frac{N_e^2}{r^2 T_e^{3/2}} dr \quad (K \text{ étant constante}) \quad (7)$$

$T_b$  sera donc toujours inférieure à  $T_e$ . Autrement dit, l'émission ne sera jamais très intense.

En pratique, les gaz sont plus denses dans le plan de notre galaxie que dans les régions de latitude galactique élevée. Il s'ensuit que l'émission ne sera pas uniformément distribuée sur la sphère céleste, mais sera plus intense au voisinage du plan galactique, c'est-à-dire, vu de la Terre, le long de la Voie Lactée, et particulièrement dans la direction du centre galactique. La figure 1 donne en exemple la carte des isophotes de  $T_b$  à la fréquence de 400.

- Le rayonnement non thermique qui correspond à l'émission synchrotron de la composante électronique des rayons cosmiques. Cette émission est particulièrement intense sur longueur d'onde métrique et décimétrique.

L'énergie nécessaire à ce rayonnement est fournie par les électrons relativistes du rayonnement cosmique, et n'est donc pas limitée par la formule (6). Les températures de brillance correspondantes peuvent donc être beaucoup plus élevées. Elles atteignent  $10^6$  K sur 10 MHz.

L'intensité du champ magnétique galactique, et probablement la densité des rayons cosmiques étant plus grande aux basses latitudes galactiques, les émissions seront comme pour le rayonnement ther-

mique plus intenses au voisinage de la Voie Lactée.

La figure 2 donne le spectre de ces émissions, qui suit approximativement une loi de puissance de la forme  $T_b = r^{-0,8}$ . Le tableau 1 donne également un certain nombre de valeurs de  $T_b$  qui peuvent être utilisées pour calculer la sensibilité d'un système de réception. Il est évident que la température à utiliser sera généralement intermédiaire entre  $T_{min}$  et  $T_{max}$ . Elle variera suivant la direction de visée, c'est-à-dire suivant l'heure pour une antenne fixe, et dépendra des dimensions du lobe d'antenne.

TABLEAU 1  
EMISSION CONTINUE DE LA GALAXIE

Fréquence (MHz)	$\lambda$	$T_b$ Plan Galactique	$T_b$ Pôle Galactique
10	30 m	$10^6$	$2 \times 10^5$
20	15	$2 \times 10^5$	$4 \times 10^4$
50	6	$9 \times 10^4$	$4 \times 10^3$
100	3	$1 \times 10^4$	$6 \times 10^2$
200	1,50	$2 \times 10^3$	$1 \times 10^2$
500	60 cm	$2 \times 10^2$	10
1 000	30	40	5
2 000	15	10	5
3 000	6	5	3
10 000	3	3	3
37 000	8 mm	3	3

Si on extrapole dans le domaine des microondes le spectre des émissions thermiques et non thermiques précédentes, on devrait observer une température de brillance très voisine de zéro. Or, des mesures particulièrement soignées ont montré que, dans ce domaine, le spectre remontait vers les hautes fréquences.

La pente de ce spectre, et son intensité correspond à celles d'un corps noir dont la température serait de 3,5°K.

Ceci n'est probablement pas très important pour les problèmes de communications, bien qu'il faille en tenir compte si l'on veut faire des déterminations très précises de la température de système d'un ensemble récepteur.

Du point de vue Astrophysique par contre, ce rayonnement est extrêmement intéressant. On l'interprète à l'heure actuelle comme dû à la température résiduelle du gaz intergalactique. A l'origine de l'Univers, ce gaz aurait été très concentré, et à très haute température. Mais par suite de l'expansion de l'Univers, déduite du phénomène de récession des galaxies, depuis environ 10 milliards d'années, la température aurait décroché, pour devenir égale, actuellement, à 3,5°K.

## II - 3 Les radiosources

On regroupe généralement sous ce nom tous les objets de petites dimensions apparentes qui sont source d'une émission radio détectable. Cette émission a toujours un spectre très étendu et, si la sensibilité des instruments est suffisante, on les observe depuis les ondes millimétriques jusqu'aux ondes les plus longues détectables sur la Terre, entre 30 et 50 m.

En réalité ces radiosources correspondent à des objets très différents dans le ciel : nuages gazeux galactiques, restes de supernovae, galaxies, quasars, etc... On peut cependant classer leur spectre en deux grandes catégories.

a) Les spectres thermiques qui sont ceux des radiosources ayant un rayonnement thermique, essentiellement certaines étoiles et les grands nuages de gaz (région HII) qui parsèment la Galaxie. Ces radiosources sont surtout intenses sur ondes courtes, ondes millimétriques et centimétriques. Leur densité de flux est approximativement constante dans ce domaine, dans lequel la source est optiquement épaisse. Pour les longueurs d'onde plus grandes, la source devient plus transparente, et par suite moins émissive, et la densité de flux décroît comme l'inverse du carré de la fréquence.

Certaines radiosources thermiques sont, sur microondes, parmi les plus intenses du ciel. citons par exemple la nébuleuse d'Orion, les nébuleuses de la Rosette et Omega. Dans certains cas, on a pu les utiliser pour mesurer le diagramme des antennes à grand gain et étalonner les systèmes de réception. Mais souvent leurs dimensions apparentes sont trop grandes (Plusieurs minutes d'arc) pour ce faire.

b) La majorité des radiosources a cependant un spectre non thermique qui, à l'inverse du précédent, décroît généralement des basses vers les hautes fréquences. Ces sources émettent par effet Synchrotron : rayonnement d'électrons relativistes dans un champ magnétique.

De nombreux objets cosmiques finissent un rayonnement synchrotron. Comme celui-ci nécessite la présence d'électrons de très grande énergie, on peut prévoir a priori que ces objets seront instables,

ou bien posséderont une région dans laquelle une activité non négligeable sera capable d'accélérer les électrons.

En pratique, on peut classer les radiosources non thermiques en trois catégories : Les restes de supernovae, les "radiogalaxies" et les quasars.

Les supernovae sont des étoiles instables qui explosent et émettent pendant quelques semaines ou quelques mois un rayonnement dans le visible extrêmement intense : leur intensité après l'explosion peut atteindre  $10^8$  à  $10^{10}$  fois l'intensité d'une étoile normale. Lors de ces explosions des électrons sont certainement accélérés, et l'étoile éjecte une enveloppe gazeuse qui peut encore être observée, des centaines ou des milliers d'années après l'explosion, comme de fins filaments formant une enveloppe quasi circulaire autour de l'étoile.

La radiosource la plus intense du ciel, Cassiopée A, est le reste d'une supernova explosée en 1750. D'autres exemples sont données dans le tableau 2.

Les radiogalaxies sont des nébuleuses extragalactiques (galaxies) : ensembles de milliards d'étoiles distribuées plus ou moins régulièrement (galaxies spirales, elliptiques, ou irrégulières). La majorité des galaxies ont un rayonnement radio peu intense mais certaines, les radiogalaxies sont des émetteurs très puissants. Il est très probable que cette émission est la conséquence d'explosions répétées dans les régions centrales de la galaxie, explosions qui provoqueraient l'accélération d'une très grande quantité d'électrons. La radiosource du Cygne qui fut la première à être détectée est le meilleur exemple de radiogalaxie. Sa structure, comme celle de la plupart des radiogalaxies, est complexe, l'émission provenant de deux ou plusieurs sources éloignées, situées de part et d'autre de la galaxie visible.

Les quasars sont des cas particuliers des radiogalaxies qui ont entre autre, une émission optique beaucoup plus intense que les galaxies normales. Ceci permet de les détecter dans le domaine visible à des distances beaucoup plus grandes ; d'où l'intérêt des quasars pour l'étude de l'évolution de l'Univers. Vu leur éloignement, les quasars sont généralement des radiosources de très petites dimensions apparentes. La technique de l'interférométrie intercontinentale a permis de montrer que certains d'entre-eux avaient des dimensions angulaires inférieures au millième de seconde d'arc.

Les radiosources non thermiques ont en général des émissions radio constantes dans le temps dans le domaine des ondes décimétriques et métriques. Une des seules exceptions est Cassiopée A, la plus intense du ciel. C'est, comme nous l'avons dit, le reste d'une supernova explosée il y a moins de 250 ans. Son enveloppe est donc encore en expansion rapide, et il s'ensuit une diminution lente de l'intensité de son émission radio, de l'ordre de 1 % par an.

D'autre part, on a découvert depuis quelques années qu'un grand nombre de radiosources, quasars pour la plupart, avaient une intensité variable en ondes centimétriques. Ces variations sont généralement irrégulières et correspondent probablement à des explosions localisées dans la source.

Le spectre des quatre radiosources les plus intenses est donné sur la figure 3.

TABLEAU 2

POSITIONS DE QUELQUES RADIOSOURCES

Objet	Nature	Ascension droite			Déclinaison	
		h	m	s	°	'
M 31 . . . . .	Galaxie normale	0	40	0	+ 40	0
S.N. Tycho-Brahé . . . . .	Supernova	1	22	28	+ 63	52
3 C 47 . . . . .	Quasar	1	33	40	+ 20	42
3 C 48 . . . . .	Quasar	1	34	49	+ 32	53
M 77 . . . . .	Galaxie Seyfert	2	40	12	- 0	13
Perseus A. NGC . . . . .	Radiogalaxie	3	16	27	+ 41	21
CTA 21 . . . . .	Quasar	3	16	22	+ 16	19
Fornax NGC 1316 . . . . .	Radiogalaxie	3	20	25	- 37	22
Auriga A . . . . .	Supernova	4	57		+ 46	30
Taurus A (Nébuleuse du Crabe) . . . . .	Supernova	5	31	30	+ 21	58
Orion A (M 42) . . . . .	Région H II	5	32	48	- 5	27
3 C 147 . . . . .	Quasar	5	38	43	+ 49	50
IC 443 . . . . .	Supernova	6	14	36	+ 22	43
Nébuleuse Rosette . . . . .	Région H II	6	29	18	+ 4	57
Puppis A . . . . .	Supernova	8	20	18	- 42	48
Hydre A . . . . .	Radiogalaxie	9	15	43	- 11	52



M 82 . . . . .	Radiogalaxie	9 51 28	+ 69 56
3 C 273 . . . . .	Quasar	12 26 33	+ 2 20
Virgo A . . . . .	Radiogalaxie	12 28 18	+ 12 40
Centaure A. NGC 5128 . . .	Radiogalaxie	13 22 28	- 42 46
M 101 . . . . .	Galaxie normale	14 1 24	+ 54 36
3 C 295 . . . . .	Radiogalaxie	14 9 34	+ 52 26
Hercule A . . . . .	Radiogalaxie	16 48 43	+ 5 6
S N Kepler . . . . .	Supernova	17 27 43	- 21 28
Sagittaire A . . . . .	Centre Galactique	17 42 30	- 28 55
Nébuleuse Omega . . . . .	Région H II	18 17 48	- 16 9
Cygnus A . . . . .	Radiogalaxie	19 57 45	+ 40 36
Bouche du Cygne . . . . .	Supernova	20 49 30	+ 29 50
C T A 102 . . . . .	Quasar	22 29 53	+ 11 28
Cassiopee A . . . . .	Supernova	23 21 11	+ 58 33

45

Citons pour terminer une classe tout à fait particulière de radiosources, les Pulsars, bien que ceux-ci puissent difficilement constituer une gêne pour les radiocommunications terrestre. Mais leur présence dans le champ de visée d'une antenne pourrait intriguer certains.

En réalité, on ne peut plus guère parler d'un "bruit" cosmique. Il s'agit au contraire d'une émission très organisée et à spectre étroit qui se présente comme un train d'impulsions très brèves (quelques millisecondes) parfaitement périodique. Les périodes observées s'étagent entre 0,03 sec et 4 secondes suivant les pulsars (Tableau 3).

Ces impulsions dérivent rapidement en fréquences des hautes vers les basses fréquences ; mais ceci n'est pas dû à l'émission du pulsar lui-même. C'est un effet de la propagation des ondes dans le gaz ionisé interstellaire. Ce gaz n'est pas un vide parfait, et il a donc un indice de réfraction différent de l'unité et, qui plus est, qui dépend de la fréquence. Une impulsion, émise simultanément sur toutes les fréquences par le pulsar mettra plus de temps à nous parvenir sur basses fréquences que sur haute fréquences. C'est l'origine de la dérive en fréquence des émissions des pulsars. Cette dérive dépend de la quantité totale de gaz traversé :

et sa mesure permet de déterminer la densité <sup>Pulsar</sup> du gaz interstellaire.

Le spectre des pulsars décroît vers les hautes fréquences et leur détection est le plus facile dans la gamme des ondes métriques. Le tableau 3 donne la position et la période des pulsars les plus intenses.

TABLEAU 3

PERIODE ET POSITION DE QUELQUES PULSARS

Pulsar	$\alpha$ (1950,0)	$\delta$ (1950,0)	Période (seconde)
CP 0328 . . . . .	3 <sup>m</sup> 28 <sup>h</sup> 52 <sup>a</sup>	+ 54° 23'	0,714 518 563
CP 0527 . . . . .	5 25 45	+ 22 0	3,745 391
CP 0532 . . . . .	5 31 26	+ 22 1	0,033 091 12
CP 0808 . . . . .	8 8 50	+ 74 42	1,292 241 26
CP 0834 . . . . .	8 34 22	+ 6 7	1,273 764 2
CP 0950 . . . . .	9 50 29	+ 8 11	0,253 065 038
CP 1133 . . . . .	11 33 36	+ 16 8	1,187 911 019
HP 1506 . . . . .	15 7 50	+ 55 41	0,739 677 626
CP 1919 . . . . .	19 19 37	+ 21 47	1,337 301 133
PSR 2045 . . . . .	20 45 48	- 16 28	1,961 663 3

## II - 4 La lune et les planètes

La lune et les planètes, corps solides chauffés par le rayonnement du soleil, émettent un rayonnement radio qui est fonction de leur température superficielle. Cette émission est surtout intense en microondes où la planète Jupiter et la lune sont parmi les astres les plus brillants du ciel.

En ondes décimétriques - centimétriques la lune a une température de brillance uniforme de 250°K, tandis que sur ondes millimétriques apparaissent des différences de température entre les mers lunaires et le reste de la surface. Il faut en tenir compte quand on utilise la lune pour étalonner les antennes à grand gain dans cette gamme de longueurs d'onde.

La densité de flux des planètes dépendra évidemment de leur température superficielle, qui est fonction de leur distance au soleil, et de leur diamètre apparent, qui est variable au cours de l'année. Le tableau 4 donne les températures de brillance mesurées.

TABLEAU 4

TEMPERATURE DE BRILLANCE DES PLANETES

Planète	$\lambda$ (cm)	$T_b$ (°K)	T infrarouge
Mercure . . . . .	1 - 10	145 - 280	150 - 375
Vénus . . . . .	0,33	290	370 face éclairée. 250 face obscure.
	0,4	360	
	0,8	400	
	3,2	580	
	10,0	600	
	21,0	600	
Mars . . . . .		211	215
Jupiter . . . . .	0,34	145	140
	0,8	140	
	3,2	180	
	10,0	700	
	22,0	3 000	
	31,0	5 500	
	68,0	50 000	
Saturne . . . . .		160	92
Uranus . . . . .		180	68
Neptune . . . . .	1,9	125	55

Jupiter est une planète particulièrement intéressante en radioastronomie. En plus de l'émission thermique précédente, elle rayonne par deux mécanismes non thermiques :

En ondes décimétriques, un rayonnement synchrotron par des électrons relativistes piégés dans le champ magnétique de la planète pour former des "zones de Van Allen" analogues à celles qui existent autour de la Terre. Ce rayonnement correspond à une densité de flux sensiblement constante des ondes centimétriques aux ondes métriques, égal à  $4 \cdot 10^{-26} \text{ W. m}^{-2} \text{ Hz}^{-1}$  (rapportée à une distance de 4,04 unités astronomiques). Ceci n'est certainement pas suffisant pour gêner les communications terrestres.

Par contre sur ondes décamétriques, plus précisément sur les fréquences inférieures à 40 MHz, Jupiter est source d'une émission extrêmement puissante, pouvant surpasser celle du soleil et atteindre  $10^{-18} \text{ W. m}^{-2} \text{ Hz}^{-1}$ . Elle peut alors être détectée avec un simple dipôle. Il s'agit d'une émission très irrégulière dont l'origine est encore mal comprise. Elle se présente sous forme d'orages formés de sursauts très brefs (de quelques millisecondes à plusieurs secondes) de structure très complexe, et pouvant durer quelques dizaines de minutes à plusieurs heures.

Cette émission provient de trois sources localisées sur la surface de la planète. Les émissions seront donc récurrentes, avec la période de rotation de la planète qui est de  $9^{\text{h}}55^{\text{m}}29^{\text{s}}$ . Mais ces sources ne sont pas actives en permanence. Il faut en plus que l'un des satellites de la planète, Io, soit dans une position favorable de son orbite pour qu'une émission soit observée. On peut ainsi, en combinant le mouvement de la planète et celui de Io prévoir dans une certaine mesure les émissions décamétriques de Jupiter.

La figure 4 donne un exemple d'orage Jovien observé sur deux fréquences différentes.

Signalons pour être complet qu'un rayonnement semblable à celui de Jupiter a été très récemment découvert en provenance de la Terre.

Ce rayonnement, également sous forme d'orages, est particulièrement intense au dessus des zones des aurores polaires. Mais il n'existe que sur très basses fréquences, inférieures à quelques mégahertz. Il s'ensuit qu'il ne peut être détecté au niveau du sol, à cause du blindage dû à l'ionosphère. Par contre il constitue une source extrêmement intense pour les satellites artificiels et les sondes spatiales qui ont des récepteurs dans cette gamme de fréquences.

## II - 5 Le Soleil

Comme dans le domaine visible, le soleil est la radiosource la plus intense du ciel. C'est une source complexe, qui émet plusieurs types de rayonnement de caractéristiques très différentes. Certains sont stables dans le temps ou très lentement variables. D'autres, qui peuvent atteindre des intensités bien plus considérables, sont sporadiques, et correspondent à des phénomènes d'activité solaire sur le

soleil. Ils durent d'une fraction de seconde à plusieurs heures, suivant les cas, et ont généralement des spectres très complexes, souvent à bande étroite.

Ces émissions sporadiques sont désignées sous le nom de sursauts solaires. Ce sont les sursauts qui dans certains cas peuvent perturber les instruments terrestres. Les intensités correspondantes sont données sur la figure 5.

L'atmosphère solaire est formée d'un gaz ionisé (plasma) et possède donc la propriété de ne pouvoir propager toutes les ondes radio. Seules peuvent se propager les ondes de fréquences supérieures à la "fréquence critique" du plasma au point considéré, fréquence qui ne dépend que de la densité électronique :

$$f = 9 \sqrt{N_e} \quad (\text{Système MKS})$$

La densité électronique  $N_e$  décroissant avec l'altitude dans l'atmosphère solaire, à chaque fréquence correspondra une altitude (altitude critique) au dessous de laquelle l'onde ne pourra se propager. Autrement dit, cette onde ne pourra parvenir à la Terre que si elle est émise à une altitude supérieure à l'altitude critique, qui sera d'autant plus élevée que la fréquence de l'onde sera plus basse.

Pour les ondes millimétriques et centimétriques les altitudes critiques sont de l'ordre de 1.000 à 20.000 km (c'est-à-dire dans la photosphère et la chromosphère), pour les ondes décimétriques dans la basse couronne ; ensuite l'altitude devient de plus en plus élevée quand la fréquence décroît, atteignant par exemple 1,5 millions de kilomètres (2 Rayons solaires) sur 25 MHz. Les ondes encore plus longues, qui ne peuvent d'ailleurs pas atteindre la surface de la Terre par suite du blindage dû à l'ionosphère, sont émises dans le milieu interplanétaire. Par exemple près de l'orbite terrestre, la densité électronique est d'environ  $10 \text{ el/cm}^3$ , soit une fréquence critique de 30 KHz.

#### II - 5 - 1 Emission thermique du "soleil calme"

L'atmosphère solaire est un gaz chaud et va donc émettre un rayonnement thermique dont l'intensité est fonction de sa température d'une part, et de son épaisseur optique d'autre part, cette dernière étant elle-même fonction de la température et de la densité électronique.

Pour les ondes inférieures à 1 m environ, on peut considérer que l'épaisseur optique est élevée. La température de brillance croît donc de  $6\,000^\circ\text{K}$  aux ondes millimétriques (température de la couronne). Simultanément le diamètre apparent du soleil augmente, puisque les régions émissives sont à des altitudes croissantes.

Pour les ondes plus longues, la couronne devient transparente et la température de brillance ainsi que l'intensité émise décroît. En dessous de 80 MHz, il faut utiliser des antennes de très grand gain pour détecter l'émission du soleil calme.

Le tableau 5 donne les valeurs des densités de flux du soleil calme pour diverses longueurs d'onde.

#### II - 5 - 2 Composante lentement variable

Sur ondes centimétriques et décimétriques il s'ajoute à l'émission précédente celles de régions localisées dans la couronne où la densité et la température sont plus élevées qu'en moyenne. Ces "condensations coronales" sont généralement situées au dessus des centres d'activité visibles (taches solaires, facules, etc ...) et ont une durée de vie de quelques mois.

Par suite de la rotation du soleil sur lui-même en 27 jours, ce rayonnement formera une composante lentement variable du rayonnement solaire, dans laquelle on retrouve une quasi période de 27 jours. A l'aide d'un instrument dont le pouvoir séparateur est de quelques minutes d'arc au plus, il est facile de localiser ces émissions à la surface du soleil.

L'intensité de la composante lentement variable dépend de la fréquence. Elle peut atteindre 2 à 3 fois celle du soleil calme (Tableau 5).

TABLEAU 5

INTENSITE DE L'EMISSION RADIO DU SOLEIL  
(Soleil calme + condensations)

$\lambda$ (cm)	f (MHz)	$T_b$ (°K)		$S \times 10^{22}$ (W. m <sup>-2</sup> . Hz <sup>-1</sup> )	
		Maximum	Minimum	Maximum	Minimum
0,33	91 000	$6,4 \times 10^3$		1 100	
0,4	75 000	$7,5 \times 10^3$		880	
0,8	37 500	$8,0 \times 10^3$		235	
3	10 000	$17,5 \times 10^3$	$15 \times 10^3$	32	27
10	3 000	$80 \times 10^3$	$40 \times 10^3$	13	6,5

... / ...

(Tableau 5 - suite)

48

25	1 200	$2 \times 10^5$	$1 \times 10^5$	7	3,5
50	600	$6 \times 10^5$	$3 \times 10^5$	5	2,5
75	400	8 x '05			2,7
150	200	1 x 10 <sup>6</sup>			0,83
300	100	$1,5 \times 10^6$			0,3
1 000	30	$2 \times 10^6$			0,035

## II - 5 - 3 Les sursauts solaires

Plusieurs types d'émissions accompagnent généralement les phénomènes sporadiques visibles à la surface du soleil, en particulier les éruptions chromosphériques. Ce sont les émissions les plus intenses qui parviennent à la Terre.

Suivant leur spectre dynamique (leur spectre et ses variations dans le temps) on en a distingué plusieurs types différents, dont les plus fréquents sont les sursauts de type I, II, III et IV.

- Type I : Ce sont des émissions très brèves (quelques dixièmes de seconde) et de faible largeur de bande (quelques megahertz) qui se superposent à une émission continue pour former les "Orages de bruit". Ces orages peuvent être très intenses; et sont les émissions les plus fréquemment observées sur le soleil. Ils accompagnent le passage des centres actifs visibles les plus importants, et peuvent durer plusieurs jours de suite.

- Type II : Ce sont des émissions relativement rares observées au début des grandes éruptions chromosphériques. Ils sont connus également sous le nom de sursauts à dérive lente, l'émission apparaissant d'abord sur les fréquences élevées, et dérivant lentement vers les fréquences plus basses. Leur durée est de l'ordre d'une dizaine de minutes.

- Type III : Ce sont des sursauts très brefs (inférieurs à 1 s) qui dérivent également des hautes vers les basses fréquences mais beaucoup plus rapidement : 10 à 20 MHz/s. Les types III sont des émissions très fréquentes, apparaissant soit au moment des éruptions chromosphériques, soit, en ondes décamétriques seulement, sous forme d'orages pouvant durer plusieurs jours.

Les sursauts de type II et III sont dus à des oscillations du plasma coronal, excitées par une perturbation qui monte dans la couronne, pour les premiers une onde de choc, pour les seconds, un jet de particules. Ils sont surtout intenses en ondes métriques et décamétriques, mais il faut noter que les types III sont également observés à des fréquences beaucoup plus basses. A l'aide de satellites artificiels on a pu en détecter jusqu'à 30 KHz. Ils correspondent sur cette fréquence à l'arrivée du jet d'électrons au voisinage de l'orbite terrestre.

Les sursauts de type IV s'observent par contre dans une gamme beaucoup plus large, à partir des ondes millimétriques. Ce sont les émissions solaires les plus intenses, mais ne sont observées qu'au moment des éruptions les plus importantes. Quand le soleil est très actif on peut en recevoir une moyenne de un par jour.

Le sursaut de type IV est une émission complexe qui correspond certainement à plusieurs mécanismes d'émission : effet synchrotron d'électrons relativistes, oscillations du plasma et effet Cerenkov. La source de l'émission est soit fixe dans la basse couronne, soit éjectée par l'éruption : on peut alors la suivre jusqu'à plusieurs millions de kilomètres de la surface solaire.

## II - 5 - 4 Prévision de l'activité solaire

Un problème important qui se pose à propos du rayonnement solaire est celui de sa prévision, non seulement parce que celui-ci peut être directement nuisible pour les communications terrestres, mais surtout parce qu'il accompagne d'autres émissions solaires, en particulier rayons X, ultraviolets et particules qui vont venir perturber l'ionosphère terrestre et par suite la propagation des ondes radio utilisées pour les communications.

Depuis quelques années, la prévision de l'activité solaire a fait de grands progrès. Il existe dans le monde plusieurs centres de prévisions qui utilisent les observations optiques, rayons X, radio, etc ... faites à partir du sol ou de satellites artificiels pour prévoir l'apparition des éruptions importantes. Mais il ne s'agit là que de donner une probabilité pour ces éruptions. L'origine même de l'activité solaire n'étant pas encore comprise, il n'est pas possible pour l'instant de prévoir avec précision l'heure et la position sur le soleil de cette activité.

## III - Conclusion

En résumé, on peut dire que les bruits cosmiques peuvent constituer une nuisance pour les communications terrestres, mais que celle-ci dépend beaucoup de la sensibilité des instruments, et du type de signal transmis.

Sur ondes longues, c'est d'abord le fond galactique qui limitera la sensibilité des systèmes de réception, en ajoutant sur l'antenne un niveau de bruit continu et à très large bande, généralement supérieur au bruit des récepteurs eux-mêmes. En particulier, le problème des récepteurs à très faible bruit : masers, paramétriques, etc ... ne se pose pas dans cette gamme d'onde.

Sur ondes longues également, le soleil et parfois jupiter peuvent être source d'émissions sporadiques extrêmement intenses qui peuvent brouiller certaines liaisons radio pendant quelques minutes à quelques heures.

Sur ondes courtes, centimétriques et millimétriques, il est peu probable que les bruits cosmiques puissent gêner beaucoup les radiocommunications terrestres bien qu'il faille parfois en tenir compte pour la détermination de la sensibilité des systèmes de réception.

Par contre, dans les deux gammes de fréquence, les radiosources seront particulièrement utiles pour la détermination des diagrammes de rayonnement et l'étalonnage des antennes à très grand gain.

#### Bibliographie

- Boischot, A. 1973, Annuaire du Bureau des Longitudes, ch. 8, La Radioastronomie, p. 535.  
 Boischot, A. 1972, La radioastronomie des planètes. Industries Atomiques et Spatiales, n° 5, p. 65.  
 Howard, W.E., Maran, S.P. 1965, General Catalogue of Discrete Radiosources, Astrophys. J. Suppl., vol 10, p. 1.  
 Kraus, J.D. 1966, Radio Astronomy, Mc Graw Hill Book Co. New-York.  
 Kundu, M.P. 1965, Solar Radio Astronomy, Interscience Publishers (New-York, London).  
 Proceedings of the I.E.E.E., Special issue on Radio Astronomy. Septembre 1973.

4-10

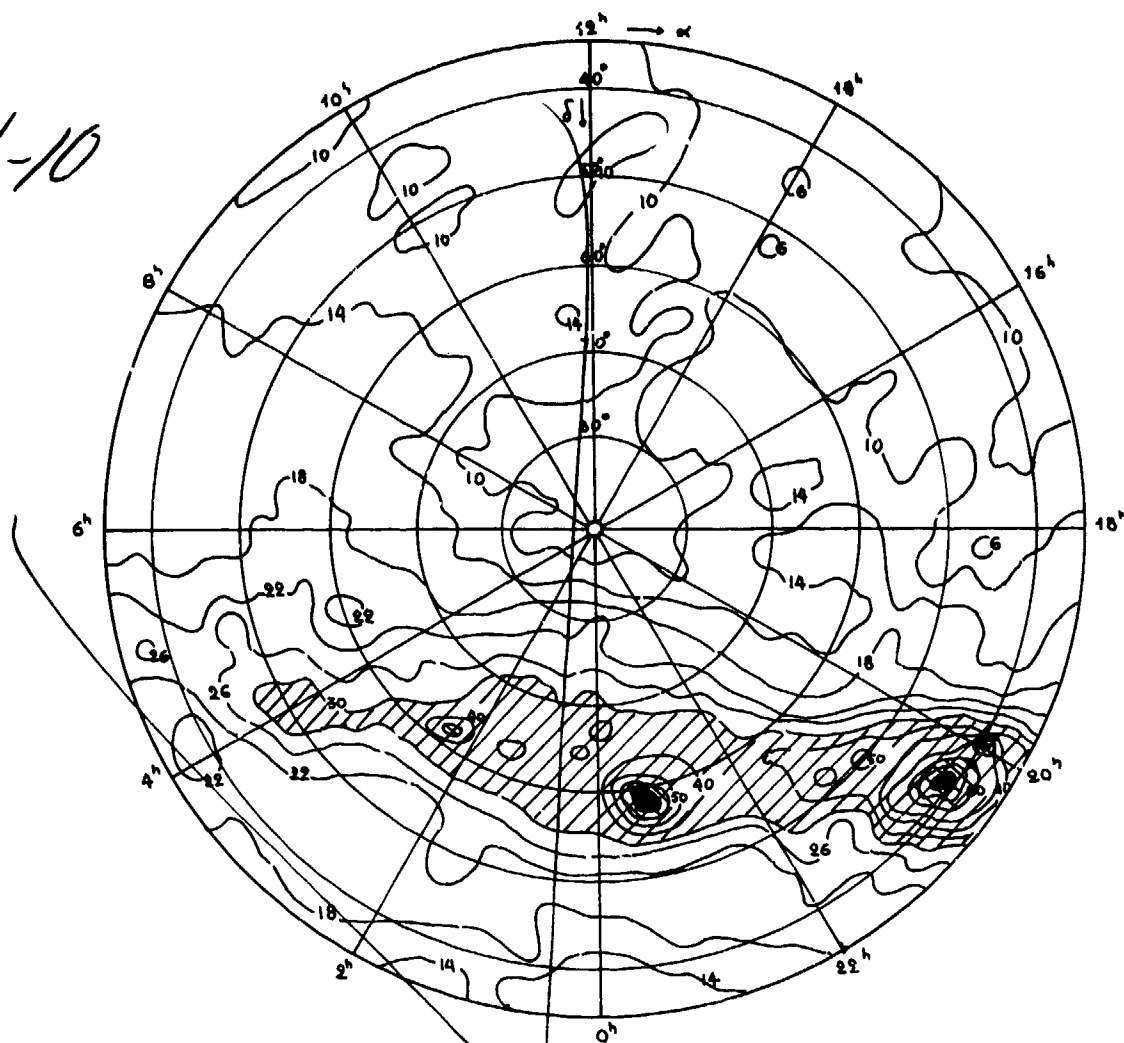


Figure 1 : Carte du bruit galactique sur 400 MHz dans les régions de déclinaisons supérieures à 35°.

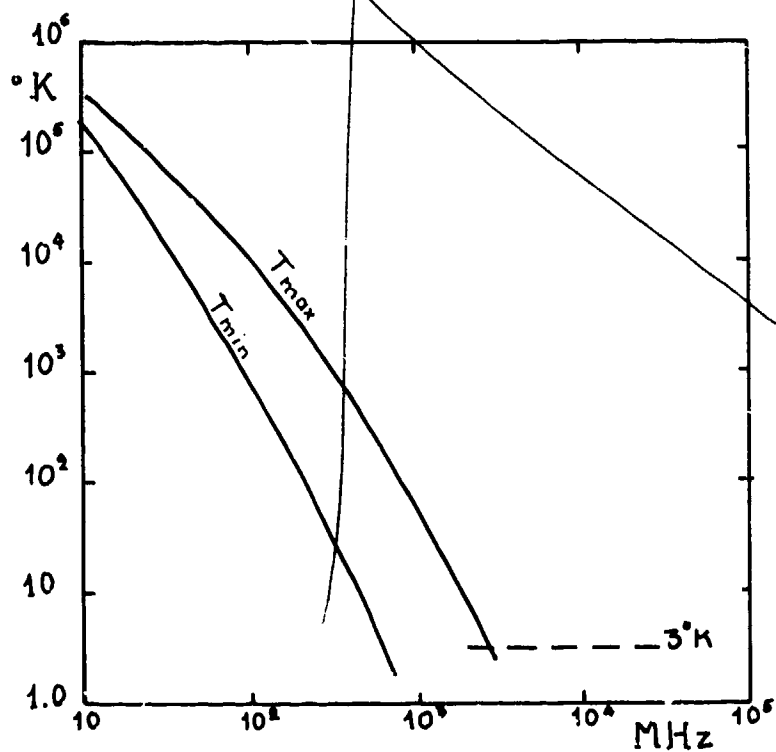


Figure 2 : Spectre de la Température de brillance du fond du ciel.  $T_{\max}$  : le long du plan galactique.  $T_{\min}$  : à hautes latitudes galactiques.

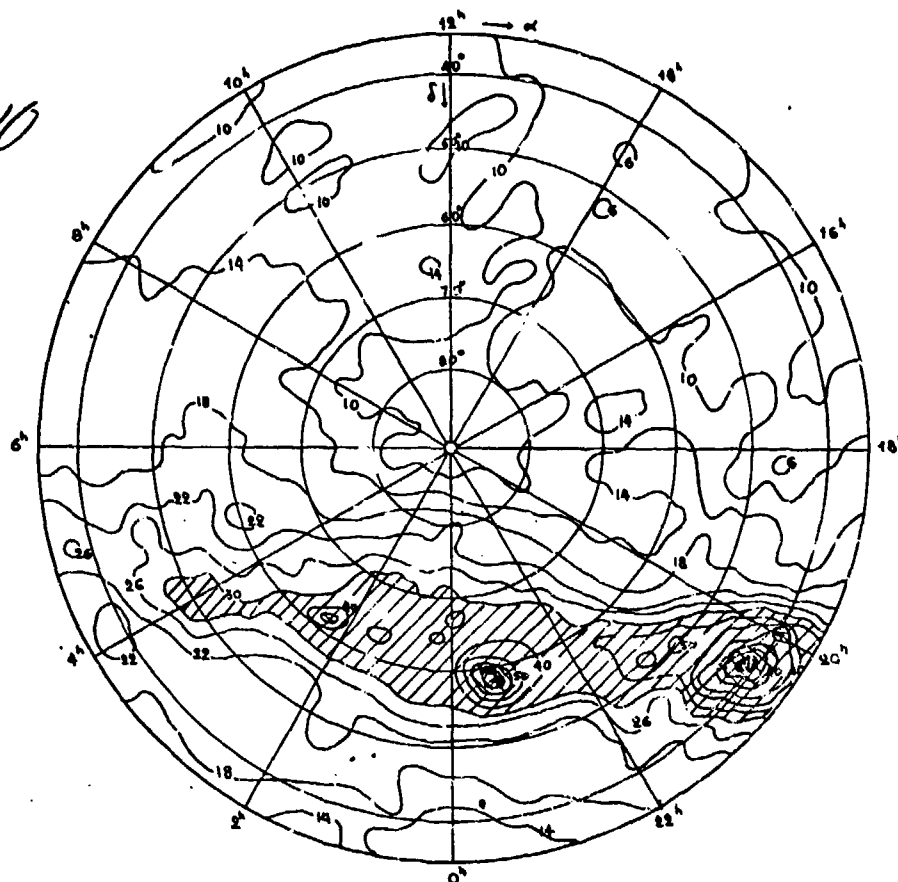


Figure 1 : Carte du bruit galactique sur 400 MHz dans les régions de déclinaisons supérieures à 35°.

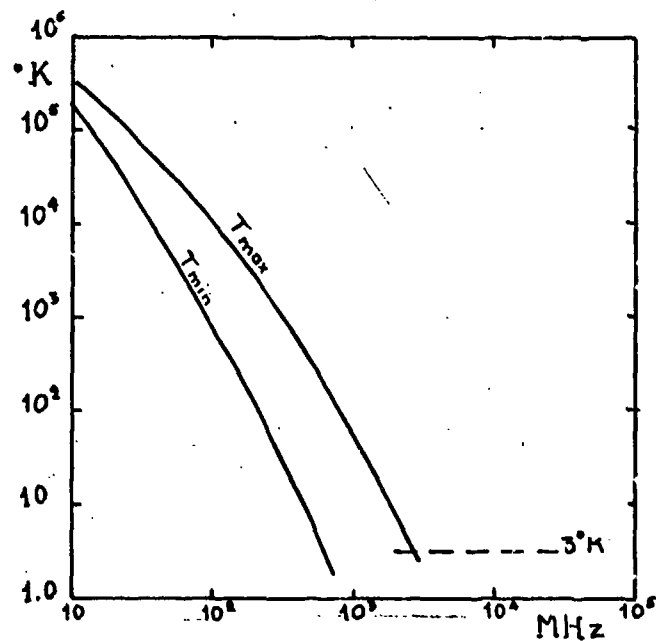


Figure 2 : Spectre de la Température de brillance du fond du ciel.  $T_{\max}$  : le long du plan galactique.  $T_{\min}$  : à hautes latitudes galactiques.

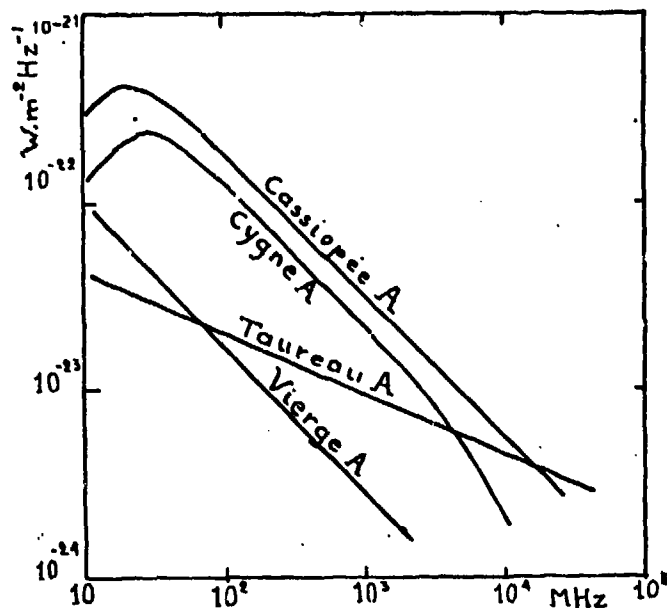


Figure 3 : Spectre des quatre radiosources les plus intenses sur ondes métriques. La densité de flux de Cassiopee A décroît d'environ 1% par an.

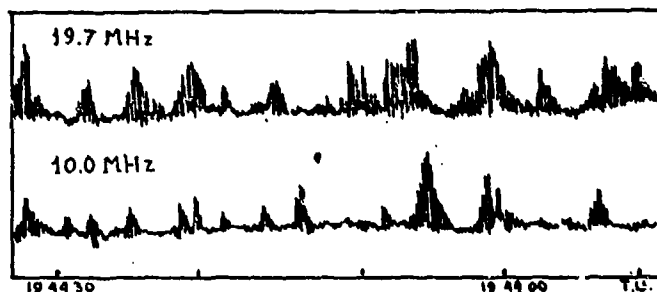


Figure 4 : Emissions décamétriques de Jupiter observées sur deux fréquences voisines.

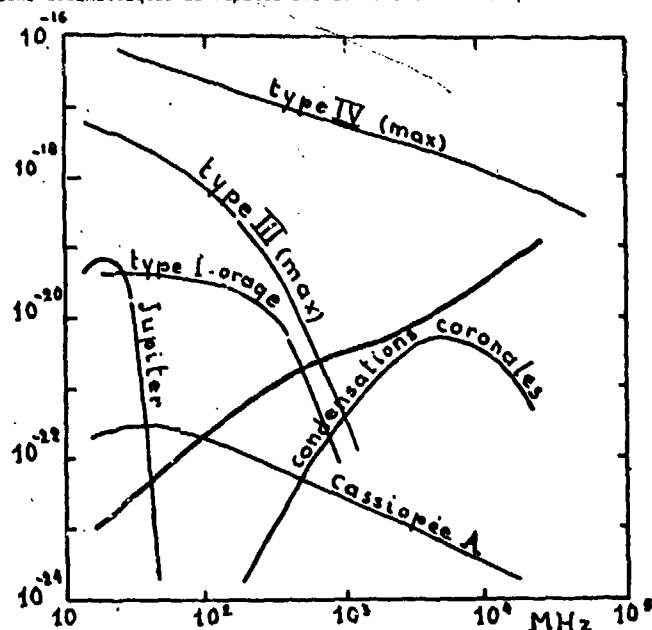


Figure 5 : Spectre des émissions solaires. On a indiqué, pour comparaison les spectres des sursauts décamétriques de Jupiter, et de la radiosource Cassiopee A.



## DISCUSSION

E. J. FREMOUW: 1) What is the mechanism by which the Jovian decametric radio bursts vary in frequency? 2) On what antenna was the observation of the moving solar-flare plasma made?

M. A. BOISCHOT: 1) The burst mechanism is not well known. It is believed to involve electrons moving along magnetic field lines, producing a plasma instability. 2) An 18-MHz ring array in Australia.

P. HALLEY: The satellite "IO" (Jupiter's natural moon Iovienne) seems to cause electromagnetic emissions from Jupiter. Could this celestial body, for example, have ferromagnetic characteristics which would explain its action (this phenomenon)?

M. A. BOISCHOT: This is very probable. IO has an ionosphere (discovered by Pioneer 10), and is therefore partly conducting. One thinks that, by cutting Jupiter's magnetic lines of force, it frees a part of the electrons which are trapped there. These electrons will fall into the Iovian ionosphere and will create plasma instabilities, which are sources of radio emissions.

P. HALLEY: You have mentioned radioelectrical emissions on the earth, connected to the aurora and observed by satellites. Professor Harang of Norway observed from ground stations radio emissions of the aurora. Do you know whether these two emissions are connected and whether they concern the same auroral phenomenon?

M. A. BOISCHOT: The two phenomena are certainly connected. Earth emissions in the kilometer-wave range are perfectly correlated with the presence of great auroral arcs, but the kilometer waves are observed above the ionosphere while the waves observed by Harang originate in the auroral arcs themselves. The sources are therefore probably different.

J. AARONS: Solar noise lasting for many minutes to hours can affect systems and appear as jamming. Briefing of personnel on solar-burst characteristics is therefore of importance.

I would like to point out that solar emission (the slowly varying component) is measured from 245MHz to 35 GHz routinely by the USAF and is reported through NOAA. These values allow solar noise to be used positively, i.e., to be used to calibrate antenna and receiving systems routinely by measurements of 5-10% accuracy.

M. A. BOISCHOT: This is true.

P. G. Davies  
SCIENCE RESEARCH COUNCIL  
Appleton Laboratory  
Ditton Park  
Slough Berks. SL3 9JX England

5-1

SUMMARY

This paper reviews thermal emission from the natural environment within the microwave, far infra-red and medium infra-red bands of the E-M spectrum down to a wavelength of about  $3\mu$  where reflection of solar radiation begins to predominate. In recent years much information has been acquired in this portion of the spectrum as a result of remote-sensing programmes using aircraft and satellite platforms and ground-based radiometers. In this review, the emphasis is primarily on the fundamental aspects of the emissive properties of the atmosphere and various surfaces and the relationship of this thermal emission to the thermal, absorptive and scattering properties of the atmosphere in slant path propagation. A nomogram technique for determining the noise signal at a point in the atmosphere is considered and a bibliography of recent work on thermal emission is included.

1. INTRODUCTION

Thermal emission and radiation reflected at the Earth's surface over the frequency range  $10^9$  to  $10^{14}$  Hz (1 GHz to 100 THz) corresponding to the wavelength range 30 cm to 3 micron ( $\mu$ ) are considered in this paper. Figure 1 gives the relationships between frequency and the various wavelength scales used. Apart from military applications, this portion of the E-M spectrum has been the subject of much attention recently as a result of the passive and active remote sensing programmes of the U.S.A., U.S.S.R. and ESRO involving theoretical studies, reviews and experimental measurements with ground-based and airborne radiometers and from satellites (e.g. Explorer VII and the TIROS, ESSA, NIMBUS and COSMOS series). Most of the satellites have carried infra-red equipment for studies of the weather and atmosphere, and some of the later NIMBUS satellites have microwave radiometers notably at frequencies of about 19, 22, 31, 37 and 53-58 GHz. The Earth Resource Technology Satellite ERTS1 is concerned only with measurements in the visible and near infra-red bands.

In this short contribution, it will be possible to give only a very general review. However much additional information can be obtained from the bibliographies given by Shifrin (1969); Kondrat'yev et al. (1971); Adey (1972); Derr (1972) and other papers from the Conference of reference 13.

The magnitude of the thermally-emitted noise or interference signal received by a downward-pointing airborne aerial depends particularly upon the frequency, altitude, nadir angle, prevailing atmospheric conditions and upon the nature and temperature of the underlying terrain. This review considers these aspects with reference to the atmosphere and terrain separately and also in a combined situation.

2. GENERAL PRINCIPLES

2.1. Black-Body Radiation Laws and Definition of Radiometric Quantities

The starting point for any discussion on land, sea and atmospheric thermal emission must inevitably be a reference to Planck's equation for black-body radiation, either in its full form or as a derivative. A confused situation in the scientific literature exists concerning the application of Planck's equation to radiometric probing, and is further complicated by the fact that there is no internationally agreed system of radiometric units.

In this paper the definition of radiometric quantities, but not the symbols used to denote them, confirms with those given by Bell (1959), except that radiance refers to unit projected area of the source, i.e. unit area normal to the direction of the emission. This definition of radiance gives a useful measure of the radiant emission from rough surfaces and from the atmosphere. Also, for surfaces obeying Lambert's law, which states that the emission in a direction at an angle  $\theta$  to the normal of an emitting surface element is proportional to  $\cos \theta$ , the radiance is constant, independent of direction. The unit of length used here for quantities other than wavelength is the metre (m) rather than the centimetre. An additional quantity not defined by Bell is brightness. The brightness of a source or surface element observed from some remote place is the power (flux) received per unit projected area at the receiver per unit solid angle subtended by the source. Hence the brightness  $B$  and the radiance  $N$  of a source are numerically equal and  $B_\lambda = N_\lambda$  where the suffix  $\lambda$  indicates that the quantities refer to unit wavelength interval.

The basic equations for black-body radiation are summarised below.

$$U_\lambda = \frac{8\pi ch}{\lambda^5 (e^{hc/\lambda kT} - 1)} \quad (\text{Planck's equation}) \quad (1)$$

$$U_\lambda d\lambda = - U_\nu d\nu, \quad d\nu = - cd\lambda/\lambda^2 \quad (2)$$

$$E_\lambda = cU_\lambda/4 \quad (3)$$

For surfaces which obey Lambert's law the spectral emittance  $E_\lambda$  into a hemisphere can also be expressed as a function of the spectral radiance  $N_\lambda$ . Thus

5-2

$$E_{\lambda} = \pi N_{\lambda}$$

(4)

In the above,  $c$  is the velocity of light

$h$  is Planck's constant ( $6.624 \times 10^{-34}$  Joule.sec)

$k$  is Boltzmann's constant ( $1.38 \times 10^{-23}$  Joule. $^{\circ}\text{K}^{-1}$ )

$\lambda$  is the wavelength, expressed here in micron ( $\mu$ )

$\nu$  is the frequency in Hz

$T$  is the temperature in  $^{\circ}\text{K}$ , and other terms are as defined in Table 1.

For long wavelengths, the Rayleigh-Jeans approximation  $\lambda kT \gg hc$  applies and hence

$$(e^{hc/\lambda kT} - 1) = 1 + \frac{hc}{\lambda kT} + \frac{1}{2!} \left( \frac{hc}{\lambda kT} \right)^2 + \dots - 1 \approx \frac{hc}{\lambda kT} \quad (5)$$

Table 1 summarises some of the forms of Planck's law and associated constants useful in thermal emission work, and Figure 1 gives plots of the spectral distribution  $E_{\lambda}$  for various temperatures. The total emittance or emissive power  $E$  is given by

$$E = \pi N = \int_0^{\infty} E_{\lambda} d\lambda = \frac{2\pi^5 k^4 T^4}{15h^3 c^2} = \sigma T^4 \quad (6)$$

where  $\sigma$ , the Stefan-Boltzmann constant has the value  $5.668 \times 10^{-8}$  watt. $\text{m}^{-2}$ . $^{\circ}\text{K}^{-4}$ . It will be noted that at  $300^{\circ}\text{K}$ , most of the emission occurs at wavelengths  $\sim 10\mu$  where  $E_{\lambda} \approx 31$  watts. $\text{m}^{-2}$ . $\mu^{-1}$ ,  $E_{\nu} \approx 1.05 \times 10^{-11}$  watts. $\text{m}^{-2}$ . $\text{Hz}^{-1}$  at  $3 \times 10^{13}$  Hz and  $E \approx 460$  watts. $\text{m}^{-2}$ .

## 2.2. Application of Planck's law to Non-Black Bodies

Electromagnetic radiation incident upon a black-body is completely absorbed, and the body radiates according to Planck's law. For non-black-bodies the radiation incident on a surface may be either reflected at the surface or transmitted through the surface. The transmitted component may be completely absorbed or some radiation may pass through the material and escape. For a thick or highly absorbing medium with no transmitted component, the sum of the reflectance  $\rho$  and the absorptance  $a$  is unity, where  $\rho$  and  $a$  are the ratios of the radiant energy reflected or absorbed to that incident on the body. Also, the emissivity  $\epsilon$  defined as the ratio of the rate of radiant energy emission from a body to that from a black-body at the same temperature, will be less than unity.

Kirchhoff's law states that if a body has reached an equilibrium temperature, it is emitting the same amount of radiant power as it absorbs and emissivity equals absorptance. Hence

$$\rho + a = 1, \quad a = \epsilon, \quad \epsilon = 1 - \rho \quad (7)$$

For most surfaces the monochromatic or spectral emissivity is a function of wavelength and to a lesser extent of the temperature of the body.

A surface for which the monochromatic emissivity is less than unity and does not vary rapidly with wavelength is called grey-body. The spectral distribution of energy will be very similar to that for a black-body.

The emission characteristics of non-black-bodies can be described using the concept of brightness temperature, defined as the temperature a black-body would have to give the same spectral brightness at the same frequency. For long wavelengths, when the Rayleigh-Jeans approximation is valid, there is a linear relationship between the radiant power emitted from a surface and its temperature. The emissivity is then given by

$$\epsilon = \left( \frac{2\pi ck T_{br}}{\lambda^4} \right) / \left( \frac{2\pi ck T}{\lambda^4} \right) = \frac{T_{br}}{T} \quad (8)$$

where  $T_{br}$  is the brightness temperature. Equation (8) is particularly useful at microwave wavelengths and forms the basis of passive remote probing in this band.

## 2.3. Smooth and Rough Surfaces : Polarisation Effects

Apart from a wavelength and temperature dependence, the spectral emissivity will, in general, also depend upon the observation angle, surface roughness and composition (e.g. water content), and upon the polarisation of the emission being monitored. For a smooth dielectric surface the reflection coefficients  $\rho_v$  and  $\rho_h$  for the electric vector in the plane of incidence and perpendicular to the plane of incidence respectively are given by the well-known Fresnel formulae (e.g. Stratton 1941). These show that  $\rho_v = \rho_h$  for normal incidence, but  $\rho_v$  experiences a minimum at the Brewster angle. Hence by equation (7), the emissivity for the vertically polarised electric vector has a maximum at the Brewster angle. The difference between the brightness temperature at this angle for these two orthogonal polarisations can amount to  $100^{\circ}\text{K}$  and greater. However, this difference is considerably reduced for emission from rough surfaces (Hagfors and Moriello 1965).

For very rough surfaces the brightness temperature is virtually constant, independent of observation angle, but surfaces of limited roughness will appear to become increasingly smooth as the nadir angle is increased. In such cases the brightness temperature decreases with increasing nadir angle.

### 3. ATMOSPHERIC ABSORPTION AND EMISSION (NOISE) 53

#### 3.1. The Clear Atmosphere

An extensive bibliography and general review of the transmission in the atmosphere has been given by Thompson (1971). The main features of the transmission and absorption characteristics of the entire clear atmosphere at zenith in the waveband 30 cm to  $4\mu$  ( $10^9$  to  $3 \times 10^{14}$  Hz) is shown in Figure 2. The molecules primarily responsible for the atmospheric absorption in the microwave region are  $H_2O$  vapour and  $O_2$ , and in the infra-red region, the absorption is chiefly due to  $H_2O$  vapour,  $CO_2$  and stratospheric  $O_3$  (which gives a strong absorption at about  $9.6\mu$ ), although the minor constituents such as  $CO$ ,  $CH_4$ ,  $N_2O$  and  $HDO$  (Howard et al - see Valley 1965) also have absorption bands in the infra-red. Several thousand individual lines occur, but at low resolution are often merged into bands. Absorption takes place with molecules possessing a magnetic dipole moment (e.g.  $O_2$ ) or an electric dipole moment (e.g.  $H_2O$ ). The electromagnetic field then excites molecular resonances between the fine structure rotational (microwave) and the vibrational (infra-red) energy states. In the infra-red region additional attenuation in the 'clear' atmosphere will occur through scattering by aerosols such as smoke, fog and haze particles (Valley 1965).

Studies of transmission measurements in the clear atmosphere in the far infra-red and in the frequency range 1 to 1000 GHz (Lukes - see Thompson 1971) have shown that many regions of strong absorption separated by window regions occur. However, in the far infra-red the attenuation between the various absorption lines of water vapour depends strongly upon the water vapour content i.e. depends upon the location and altitude of the ground site and upon the temperature and season (Gaitskell et al. 1969). In general, the attenuation at wavelengths shorter than  $860\mu$  exceeds 10 dB at zenith, and, for any considerable path length, the atmosphere can be considered to radiate as a black-body. In the microwave region, an absorption band at 60 GHz, studied in detail by Liebe and Welch (1973), and an absorption line at 119 GHz are due to oxygen, while other absorption lines at 22.2, 183.3 and 323 GHz are due to water vapour. In the lower atmosphere, pressure and doppler broadening extends the lines into absorption bands. Since the wings of these water vapour bands cross window regions and since water vapour is subject to diurnal, seasonal and temporal changes, the window regions are not precisely defined, particularly the one centred at 95 GHz which has been studied in some detail (Thompson 1971, Gibbins et al. 1973). It is also speculated that water complexes, e.g. dimers, can increase the attenuation in the windows over and above that due to water vapour in its monomeric form.

The principal regions of transparency of the atmosphere, called windows, in the medium and far infra-red are approximately in the ranges 3.0 to  $4.2\mu$ , 8 to  $12\mu$  and with less transparent regions about  $4.6$  to  $4.9\mu$  and  $18\mu$ . For large altitudes or long path lengths at frequencies outside these windows where the transmission through the atmosphere is small and ground emission is cut off, the atmosphere will radiate as a black-body with a temperature equal to its effective kinetic temperature, which can be considerably lower than  $300^\circ K$  (Jamieson et al. 1963). For lower altitudes and shorter paths, as the atmospheric transparency increases, the contribution from the ground can become increasingly important, and for surfaces with an emissivity  $\sim 1$ , the overall resulting emission will depend upon ground temperature.

Few measured data are available for infra-red transmission along slant paths from various altitudes and estimates are therefore normally obtained from theoretical considerations. However, the procedure is complex (Jamieson et al. 1963, Plass and Yates - see Wolfe 1965) since the half-width of the various spectral lines contributing to the absorption vary with pressure and both the half-width and intensity vary with temperature. Also, the concentration of the absorbing gas will usually not be constant along the slant path. In the microwave region of the spectrum, the characteristics of the clear atmosphere at zenith and along slant paths, where a secant law is applicable for zenith angles less than about  $85^\circ$ , are fairly well-known. (CCIR ref. 31).

Within most spectral windows, emission from the ground will dominate the noise signal existing at all altitudes at nadir but for long paths at low angles of elevation the noise emission from the atmosphere can predominate. Most of the measurements and calculations associated with the weather satellite and earth resource survey programmes have been made at frequencies within the atmospheric windows.

#### 3.2. Effect of Hydrometeors within the Atmospheric Windows

Hydrometeors in the form of rain, cloud, fog, etc. attenuate electromagnetic radiation either directly as absorption or indirectly as scattering, and, in accordance with Kirchhoff's law, will re-radiate depending upon the magnitude of the absorptance (emissivity) and the effective temperature of the atmosphere down to ground level. In the presence of intervening hydrometeors, emission from the ground will become increasingly masked as the cloud/rain absorption increases and be replaced by radiation characteristic of the absorption and temperature of the cloud/rain. The effect will be most severe within the window region of the spectrum, but may be of some consequence outside the windows for low flying aircraft.

In the infra-red region at wavelengths of  $5\mu$  and greater, clouds can be strongly absorbing and although some scattering occurs it can generally be neglected. Rayleigh scattering by cloud and the clear atmosphere is far more important in the near infra-red and visible portions of the spectrum and considerably complicates any analysis of path transmission. An aircraft flying just above an opaque cloud would monitor radiation in the medium and far infra-red windows corresponding to the cloud temperature which could be several tens of degrees lower than that of the underlying ground emission.

The most transparent portion of the spectrum in the range considered here extends from 1 to about 20 GHz. It is sometimes referred to as an all-weather spectral region and has received much attention in recent years for use in studies on microwave passive remote sensing of the environment and Earth-satellite

5-4 communication systems. However, it is not in fact unaffected by changing meteorological conditions since heavy rain can cause considerable attenuation at frequencies above 10 GHz, but it is very much less affected by cloud than in the infra-red regions. Naturally occurring radiation within the band 1 to 10 GHz has been discussed by Groom (1964) and is the region least affected by the weather.

The other window regions of the clear atmosphere in the micro-wave spectrum are approximately 20 to 48 GHz (zenith attenuation < 1 dB), 67 to 108 GHz (zenith attenuation > 1 dB, < 5 dB) and 200 to 300 GHz (zenith attenuation > 5 dB, < 10 dB). The spectrum up to 140 GHz has been studied extensively (Thompson 1971) whereas only a few measurements such as those of Ulabiy and Straiton (1969) have been made in the 200 to 300 GHz window. Within the frequency bands given above, cloud and rain, particularly heavy rain, produce significant absorption and thermal noise. Attenuation by rain increases with rainfall rate and frequency for frequencies less than 100 GHz (CCIR ref. 31). Scattering of electromagnetic radiation by rain drops as described by Mie (see Medhurst 1965) also occurs and becomes increasingly important at frequencies above 20 GHz as the wavelength decreases towards the size of the rain drops, and will therefore depend on the drop size distribution. The effect of scattering is to increase the value of attenuation obtained by direct measurement along a path, without producing a corresponding increase in thermal noise (Zavody 1974).

In the last few years measurements of atmospheric attenuation of cloud and rain along slant paths at frequencies above 10 GHz have been carried out at various locations throughout the world to provide statistics for the planning and operation of Earth-space communication links. Direct measurement of the transmission from the satellite ATS-5 (Ippolito 1972) and radiometer measurements of the thermal noise from the sun or atmosphere have been made. If the atmosphere has fractional absorption or absorptance  $a$  and effective kinetic temperature  $T_{AT}$  along a Sun-Earth path of the radiometer measurement, the brightness temperature of the atmosphere along the path is  $aT_{AT}$  and the brightness temperature (antenna temperature)  $T_{SUN}$  for the received signal is

$$T_{SUN} = (1 - a)T_E + T_{SKY} \quad (9)$$

where  $T_{SKY} = aT_{AT} \quad (10)$

and  $T_E$  is the effective brightness temperature of the sun for the particular antenna used and for zero atmospheric attenuation.

$T_{SKY}$  is obtained by pointing the radiometer along a path adjacent to the sun. The brightness temperature corresponding to the attenuated solar signal is  $T_{SUN} - T_{SKY}$  and must be compared with  $T_E$  to derive a value for the attenuation in dB. It is well known that for an antenna temperature  $T$  and within the frequency passband  $\Delta\nu$ , the corresponding noise power  $P$  available is given by  $P = kT\Delta\nu$ . Hence

$$\text{Attenuation (dB)} = 10 \log_{10} \frac{T_E}{(1 - a)T_E} = 10 \log_{10} \left\{ \frac{1}{1 - a} \right\} \quad (11)$$

Equations (10) and (11) give the relationship between attenuation and brightness temperature in the micro-wave region and is illustrated in Figure 3 for various values of  $T_{AT}$ .

In practice,  $T_E$  cannot be measured from the ground and the values of attenuation are often computed with respect to the signal which would be received by the radiometer on a clear day. If values for the total attenuation are required, the contribution from the clear atmosphere must be added on. If the fractional absorptions of the clear atmosphere and of the cloud/rain at the same temperature are  $a_1$  and  $a_2$ , then the total effective absorptance is  $a_1 + a_2 - a_1a_2$ .

Results from measurements in the U.K. within band 12 to 37 GHz, together with references and a comparison with similar data obtained in other parts of the world have been described by Davies (1972). Other measurements at 110 GHz have been described by Gibbins et al. (1973). Typical values of the atmospheric brightness temperatures derived from these measurements for an effective kinetic temperature of 273°K are shown as a function of location and percentage of time in Table 2. The effect of scattering on the sun-tracking measurements has been neglected in computing these values which should therefore be higher than the actual emission temperatures. Although the measured data refer to paths through the total atmosphere, they will also be applicable for aircraft flying above the weather. A procedure for the prediction of the attenuation at a location where there are no measured data, but where the rainfall characteristics are known has been described by the CCIR (ref. 31).

#### 4. LAND EMISSION AND REFLECTION

The noise signal from the ground is the resultant of the natural emission from the surface, radiated in the manner described in section 2, and reflected radiation from the sun and atmosphere. Daytime measurements show a minimum in the spectral radiance of most surfaces at a wavelength of about  $3\mu$  (Kuth - see Wolfe 1965) where the intensity of the reflected solar radiation begins to exceed that of the thermal emission from bodies at ambient temperature. At wavelengths  $\sim 10\mu$  the reflected radiation from an overcast sky can be equivalent to a rise in surface temperature of several °K. At microwave frequencies, the brightness temperature of solar radiation isotropically scattered at the Earth's surface is small and is given by

$$\frac{T_s \Omega_s}{2\pi} \approx 0.06^\circ\text{K for total reflection,}$$

where  $T_s \sim 6000^\circ\text{K}$  at  $\lambda = 1 \text{ cm}$  and  $\Omega_s \sim 7 \times 10^{-5}$  steradian.

Most surfaces have a specular emissivity peculiar to that particular surface and to the particular conditions prevailing at the time of the measurement. Such a radiation is termed a signature. The acquisition and interpretation of signatures as a function of time and location form the basis of the environmental remote sensing programmes. For rough surfaces obeying Lambert's law, even if the emissivity is independent of temperature, the brightness temperature of the ground will experience temporal, diurnal and seasonal changes arising from changes in surface temperature. Also, in areas of vegetation and in areas where freezing occurs, the surface emissivity will undergo seasonal changes. 5-5

In order to interpret the various signatures, laboratory and field studies are now in progress to determine the spectral radiance and surface emissivity of naturally occurring materials. Also, measurements from aircraft and satellites are being analysed in conjunction with ground truth data. Most of the work is at frequencies within the atmosphere windows.

In the infra-red region Buettner and Kern (1965) have made laboratory measurements of the emissivity of many mineral materials at wavelengths between 8 and  $12\mu$ . Most of the values of emissivity in the normal or near normal direction are greater than 0.9 and do not exhibit a strong temperature dependence. The emissivity for various types of sand, wet and dry, lies within the range 0.914 to 0.936. In directions away from the vertical, the emissivity decreases. At  $12\mu$ , the emissivity of water at  $80^\circ$  from the normal is only about 60% of its value at  $0^\circ$ . Buettner and Kern also quote some values of emissivity measured by other workers. Melting snow seems to have a very large emissivity  $\sim 0.99$ . Ice gives a low reflectance (large emissivity) in the range 6 to  $10\mu$  and experiences a maximum in the reflectance at  $13\mu$ .

A survey of the literature and knowledge of land and sea microwave emission to the end of 1970 and with particular reference to hydrology and oceanography was prepared by Falkenmark and Karstrom (1972) as part of a series of ERO Reports. A summary of the various land values of emissivity found in this survey is given in the first part of Table 3. In general, the values of emissivity for land surfaces are high, and, away from the normal, rough surfaces are brighter than smooth surfaces. However, the emissivity for water (see Table 4) is much lower  $\sim 0.4$ . Hence dry soils emit radiation more strongly than wet soils as can be seen from Figure 4 of reference 9. It is also to be expected that the emissivity of land surfaces will be lower during and immediately after a rainfall than for dry conditions. The emissivity tends to decrease with increasing wavelength for vegetation and to increase with decreasing wavelength for water. The differences in brightness temperature across land at a constant temperature are expected to fall generally within the range 10 to  $30^\circ\text{K}$ . However, large differences in brightness temperature up to about  $150^\circ\text{K}$  can occur across land/water boundaries.

Recent measurements from aircraft of the emission from bare soils at wavelengths of 21 cm, 1.55 cm and 0.8 cm have been reported by Schmugge et al. (1974) who correlated brightness temperature with soil moisture content. At 0.8 cm, the emission is sensitive to surface moisture while emission at 21 cm responds to moisture in a layer 3 to 4 cm thick. Straiton et al. (1958) measured the brightness temperatures of lake water, asphalt, grass with weeds, and gravel at 4.3 mm wavelength as a function of polarisation and angle of emission. Reflected sky radiation is included in these values of brightness temperature quoted by Straiton et al.

## 5. EMISSION AND REFLECTION FROM WATER

The application of remote sensing techniques for studies of properties such as surface temperature, sea state, salinity, ice cover and oil pollution has long been realised and has received much attention, particularly since the sea is fairly uniform over large areas and can be probed with sensors of comparatively low angular resolution. However, most of the published work refers to measurements and calculations at cm and mm wavelengths.

At infra-red wavelengths the measurements of Buettner and Kern gave a value of 0.993 for the emissivity of pure water in the range 8 to  $12\mu$ , with smaller values at longer wavelengths. Water contaminated with oil has values less than that for pure water. From the values of reflectance quoted by Clark (1967), the emissivity of the sea is 0.98 at normal, 0.96 at  $45^\circ$ , 0.94 at  $60^\circ$  and considerably less at large nadir angles.

At cm and mm wavelengths, the emissivity of water is comparatively small as shown in Table 4. Perfectly flat water behaves as a Fresnel reflecting surface and in directions other than the normal exhibits strong polarisation effects (e.g. Figure 2 of ref. 9). Calm water has an emissivity of about 0.4, but the emissivity from a rough sea can be very much larger, giving an increase in brightness temperature up to  $100^\circ\text{K}$  (Nordberg et al. 1971), depending upon the wave structure and particularly upon the foam coverage. A detailed theoretical treatment by Stogryn (1972) illustrates the complexity of the problem. In Stogryn's analysis, the foam coverage is related to the wind velocity (0 to 30 m/sec) and the results obtained for the overall emission from the sea as a function of angle for both polarisations compare reasonably well with the experimental data of Hollinger (1971) at 1.41, 8.36 and 19.34 GHz and Nordberg et al. (1971) at 19.4 GHz. Computations of the emission from foam itself at 13.4, 19.4 and 37 GHz from an analysis of radiometric data are also given by Stogryn as a function of nadir angle for both polarisations.

Ice and sea ice have values of emissivity much larger than water. Consequently, sharp changes in brightness temperature  $\sim 150^\circ\text{K}$  can occur across an ice/water interface. At low frequencies  $\sim 2\text{ GHz}$  and less, ice does not attenuate strongly, and if the ice is less than about 3 m thick, attenuated radiation from the water below is also emitted. Since the emissivity of water is considerably less than for ice, the overall brightness temperature is less than for ice alone and gives a method for estimating ice thickness (Adey 1972).

The discussion above has been concerned solely with the emission of radiation at the surface. However, since the emissivity of water is about 0.4, the reflectance for sky radiation will be about 0.6 at normal incidence.

## 6. COMBINED EFFECTS OF LAND, SEA AND ATMOSPHERIC THERMAL EMISSION

56 It is the purpose of this section to present general equations and techniques for estimating the radiance and brightness temperature for a downward-pointing sensor at a point in the atmosphere, taking into account the thermal emission from a land/sea surface, reflection of downcoming radiation by the surface, the attenuation of both of these radiations by the atmosphere and the emission from the atmosphere itself along the slant path of interest. Weger (1960) has computed brightness temperatures for a receiver at an altitude of 10 km for wavelengths from 0.43 to 3 cm for three types of weather condition.

Consider the situation illustrated in Figure 4. The radiance at the aircraft in the frequency range  $\nu$  to  $\nu + d\nu$  resulting from emission from the ground, atmosphere and background will be designated  $N_m(\nu, T_m)d\nu$  and is given by

$$N_m(\nu, T_m)d\nu = t(\nu)\epsilon(\nu)N_b(\nu, T_g)d\nu + t(\nu)(1 - \epsilon(\nu))N_a(\nu, T_a)d\nu + N_{ap}(\nu, T_{ap})d\nu \quad (12)$$

$$\text{or} \quad N_m = t\epsilon N_b + t\rho N_a + N_{ap} \quad (13)$$

where  $N_b(\nu, T_g)$ ,  $N_a(\nu, T_a)$  and  $N_{ap}(\nu, T_{ap})$  are the spectral radiances at the frequency  $\nu$  of a black-body at ground temperature  $T_g$ , the atmosphere and background at ground level with effective temperature  $T_a$ , and the atmospheric path between ground and aircraft with effective temperature  $T_{ap}$ .  $\epsilon(\nu)$  is the ground emissivity,  $\rho(\nu)$  is the reflectance and  $t(\nu)$  is the transmittance of the atmosphere between ground and aircraft.  $N_b(\nu, T_g)$  is the Planck spectral radiance or brightness function  $(2h\nu^3/c^2)/(e^{h\nu/kT} - 1)$  where  $T$  has the constant value  $T_g$ . If the ground emits as a grey-body,  $\epsilon(\nu)$  will be constant.  $N_a(\nu, T_a)$  and  $N_{ap}(\nu, T_{ap})$  are also Planck functions to give the equivalent radiation from a black-body at the frequency  $\nu$ , but in general, the values of  $T_a$  and  $T_{ap}$  will vary with frequency.

Equation (12) is very difficult to handle and requires numerical integration. However, it is often used in the following simplified integrated form (Clark 1967, Blampitt 1970).

$$N_m = t_b\epsilon_b N_b + t_a(1 - \epsilon_a)N_a + N_{ap} \quad (14)$$

where  $N_m$ ,  $N_b$ ,  $N_a$  and  $N_{ap}$  are radiances of the form  $\int N d\nu$ , and  $t_a$ ,  $\epsilon_a$  and  $t_b$ ,  $\epsilon_b$  are the effective values of transmittance and emissivity over the distributions  $N_a$  and  $N_b$ .

At microwave frequencies, since the spectral radiance is  $2\nu^2 kT/c^2$ , equation (12) reduces to

$$T_m = t\epsilon T_g + t(1 - \epsilon)T_a + T_{ap} \quad (15)$$

and can be further simplified for particular cases. In the absence of scattering, the term  $T_{ap}$  can be related to the path transmittance  $t$  or to the absorptance equal to  $1 - t$ . If, also, the brightness temperature  $T_a$  is separated into components  $aT_{AT}$  and  $(1 - a)T_x$  from the atmosphere and from external radiation, equation (15) gives the measured brightness temperature as

$$T_m = (1 - a_p) \left\{ \epsilon T_g + \rho[aT_{AT} + (1 - a)T_x] \right\} + a_p T_p \quad (16)$$

where  $a$ ,  $T_{AT}$  and  $T_x$  are the total atmospheric absorptance, effective atmospheric and effective external temperature averaged over a hemisphere and appropriate to diffuse reflection with coefficient  $\rho$  at the ground. For specular reflection,  $\rho = 1 - \epsilon$  and  $a$ ,  $T_{AT}$  and  $T_x$  are the values along the specular path.  $T_p$  is the effective temperature along the ground-to-aircraft path and  $a_p$  is the associated absorptance.

Based on special cases of equation (14), Blampitt has described a nomogram technique for determining the ground temperature if the other quantities are known or have been estimated. The same technique can be used in particular cases to obtain the radiance or brightness temperature at an aircraft if the land/sea and atmospheric emission parameters are known.

## 7. SUMMARY AND CONCLUSIONS

A maximum emission of about  $31 \text{ watt.m}^{-2}.\mu^{-1}$  from a black-body at  $300^\circ\text{K}$  occurs at a wavelength of about  $10\mu$ . The values of emissivity of many types of land surface are between 0.9 and 1 at infra-red and microwave frequencies. Hence, within the most transparent atmospheric window regions, the radiation received by an airborne nadir-pointing radiometer on a clear day will be virtually identical with that from a black-body at the ambient surface temperature. Within the opaque far infra-red and submillimetre regions and within the infra-red windows in the presence of heavy cloud, ground emission can be cut off and replaced by emission from the atmosphere at temperatures as low as  $250^\circ\text{K}$ . In the microwave region, cloud attenuation and emission are considerably smaller than in the infra-red region, but emission, absorption and scattering by rain become increasingly important at frequencies above 10 GHz, depending upon the rainfall rate or percentage of the observation time.

Water behaves almost as a black-body at infra-red frequencies, but at microwave frequencies can act more like a mirror or Fresnel surface with strong reflection and polarisation effects. In particular, solar radiation can be strongly reflected by calm water and produce a large effective noise temperature at angles near the specular direction, producing a glitter effect. Also, reflected cloud/rain radiation can add

considerably to the surface emission. However, a rough foam covered sea is more radiant than a calm sea.

From considerations of interference due to terrestrial thermal noise, airborne equipment operating within the band  $10^{10}$  to  $10^{14}$  Hz should be designed to cope with a background emission from a black-body at the highest kinetic temperature likely to be encountered along a viewing path. In most cases, however, the radiation received will correspond to a lower brightness temperature. This paper discusses the fundamental aspects and gives methods and references for estimating the true path brightness temperature or radiance if other parameters are known.

#### REFERENCES

1. ADEY, A. W., 1972, "Microwave Radiometry for Surveillance from Spacecraft and Aircraft", Communications Research Centre Report 1231, Ottawa
2. BEIL, E. E., 1959, "Radiometric Quantities, Symbols and Units", Proc. IRE., 47, 1432
3. BLIAMPTIS, E. E., 1970, "Nomogram relating True and Apparent Radiometric Temperatures of Grey-bodies in the Presence of an Atmosphere", Remote Sensing of Environment, 1, 93
4. BUETTNER, K. J. K., and KERN, C. D., 1965, "The Determination of Infra-red Emissivities of Terrestrial Surfaces", J.G.R., 70, 1329
5. CLARK, H. L., 1967, "Some Problems Associated with Airborne Radiometry of the Sea", Appl. Opt., 6, 2151
6. CROON, D. L., 1964, "Naturally Occurring Radiation in the Range 1-10 Gc/s", Proc. IEE, 111, 967
7. DAVIES, P. G., 1972, "Slant Path Attenuation at Frequencies above 10 GHz", AGARD-CP-107. Conf. on Telecommunications Aspects on Frequencies between 10 and 100 GHz
8. DERR, V. E., 1972, "Remote Sensing of the Troposphere", U.S. Government Printing Office, Washington, D.C. 20402
9. FALKENMARK, M., and KARSTROM, U., 1972, "Identification, Description and Justification of Passive Microwave Applications to the Fields of Hydrology and Oceanography", ESRO CR-75
10. GAITSKELL, J. N., NEWSTEAD, R. A., and BASTIN, J. A., 1969, "Submillimetre Solar Radiation at Sea Level", Phil. Trans. Series A, 264, 125
11. GIBBINS, C. J., GORDON-SMITH, A. G., and CROON, D. L., 1973, "Atmospheric Emission and Attenuation in the Region 85 to 118 GHz", IEE Conf. Publ. No. 98 on Propagation of Radio Waves at Frequencies above 10 GHz
12. HAGFORS, T., and MORIELLO, J., 1965, "The Effect of Surface Roughness on the Polarization of Thermal Emission from a Surface", Radio. Sci. 69D, 1614
13. HOLLINGER, J. P., 1971, "Remote Passive Microwave Measurements of the Sea Surface", AGARD-CP-90-71. Conf. on Propagation Limitations in Remote Sensing
14. IPPOLITO, L. J., 1972, "Earth-Satellite Propagation above 10 GHz", GSFC Report X-751-72-208, Greenbelt, Maryland, U.S.A.
15. JAMIESON, J. A., McFEE, R. H., PLASS, G. N., GRUBE, R. H., and RICHARDS, R. G., 1963, "Infra-red Physics and Engineering", McGraw Hill Book Co.
16. KONDRAT'YEV, K. Ya., and TIMOFEEV, Yu. M., 1971, "Thermal Sensing of the Atmosphere from Satellites", NASA Translation TT F-626
17. LIEBE, H. J., and WELCH, W. M., 1973, "Molecular Attenuation and Phase Dispersion between 40 and 140 GHz for Path Models from Different Altitudes", U.S. Office of Telecommunications Report 73-10
18. MEDHUPST, R. G., 1965, "Rainfall Attenuation of Centimetre Waves : Comparison of Theory and Measurement", IEEE, Trans. AP., 13, 550
19. NORDBERG, W., CONWAY, J., ROSS, D. B., and WILHEIT, T., 1971, "Measurements of Microwave Emission from a Foam-covered, Wind-driven Sea", J. Atmos. Sci., 28, 429
20. SCHMUGGE, T., GLOERSEN, P., WILHEIT, T., and GEIGER, F., 1974, "Remote Sensing of Soil Moisture with Microwave Radiometers", J.G.R., 79, 317
21. SHIFRIN, K. S., 1969, "Transfer of Microwave Radiation in the Atmosphere", NASA Translation TT F-590
22. STOGRYN, A., 1972, "A Study of Radiometric Emission from a Rough Sea Surface", NASA Report CR-2088
23. STRAITON, A. W., TOLBERT, C. W., and BRITT, C. O., 1958, "Apparent Temperatures of Some Terrestrial Materials and the Sun at 4.3 millimetre Wavelengths", J. Appl. Phys., 29, 776
24. STRATTON, J. A., 1941, "Electromagnetic Theory", McGraw Hill Book Co.
25. THOMPSON, W. I., 1971, "Atmospheric Transmission Handbook", NASA Report DOT-TSC-NASA-71-6

5-7



26. ULABY, F. T., and STRAITON, A. W., 1969, "Atmospheric Attenuation Studies in the 183-325 GHz Region", IEEE Trans. AP., 17, 337
27. VALLEY, S. L., 1965, "Handbook of Geophysics and Space Environments", Air Force Cambridge Research Laboratories, U.S.A.F.
28. WEGER, E., 1960, "Apparent Thermal Noise Temperatures in the Microwave Region", IEEE Trans. AP., 8, 213
29. WOLFE, W. L., 1965, "Handbook of Military Infra-red Technology", Office of Naval Research, U.S. Government Printing Office, Washington D.C. 20402
30. ZAVODY, A. M., 1974, "Effect of Scattering by Rain on Radiometer Measurements at Millimetre Wavelengths", Proc. IEE., 121, 257
31. CCIR : 1974, Documents of the XIIIth Plenary Assembly, I.T.U., Geneva

#### ACKNOWLEDGEMENT

This review was carried out at the Appleton Laboratory and is published with permission of the Director.

Table 1 Quantities Associated with Planck's Law : Units and Dimensions

Symbol and Quantity	Planck form	Constant and Values	Rayleigh Jeans form	Constant and Values
$U_\lambda$ : Energy density per unit wavelength interval	$\frac{8\pi ch}{\lambda^5 \left( e^{\frac{hc}{\lambda kT}} - 1 \right)}$	$8\pi ch = 4.99$ (Joules $\mu^4 m^{-3}$ )  $\frac{hc}{k} = 1.439 \times 10^4$ ( $\mu^0 K$ )	$\frac{8\pi kT}{\lambda^4}$	$8\pi k = 3.468 \times 10^{-4}$ (J. $\mu^3 \text{ } ^\circ K^{-1} m^{-3}$ )
$U_\nu$ : Energy density per unit frequency interval	$\frac{8\pi h \nu^3}{c^3 \left( e^{\frac{h\nu}{kT}} - 1 \right)}$	$\frac{8\pi h}{c^3} = 6.166 \times 10^{-58}$ (J. Hz $^{-4} m^{-3}$ )  $\frac{h}{k} = 4.796 \times 10^{-11}$ (Hz $^{-1} \text{ } ^\circ K$ )	$\frac{8\pi k \nu^2 T}{c^3}$	$\frac{8\pi k}{c^3} = 1.285 \times 10^{-47}$ (J. Hz $^{-3} \text{ } ^\circ K^{-1} m^{-3}$ )
$E_\lambda$ : Spectral emittance :- Power radiated per unit surface area per unit wavelength interval	$\frac{2\pi c^2 h}{\lambda^5 \left( e^{\frac{hc}{\lambda kT}} - 1 \right)}$	$2\pi c^2 h = 3.742 \times 10^8$ (watts $\mu^4 m^{-2}$ )	$\frac{2\pi ckT}{\lambda^4}$	$2\pi ck = 2.601 \times 10^4$ (watts $\mu^3 \text{ } ^\circ K^{-1} m^{-2}$ )
$E_\nu$ : Spectral emittance :- Power radiated per unit surface area per unit frequency interval	$\frac{2\pi h \nu^3}{c^2 \left( e^{\frac{h\nu}{kT}} - 1 \right)}$	$\frac{2\pi h}{c^2} = 4.624 \times 10^{-50}$ (watts Hz $^{-4} m^{-2}$ )	$\frac{2\pi k T \nu^2}{c^2}$  $= \frac{2\pi k T}{\lambda^2}$	$\frac{2\pi k}{c^2} = 9.634 \times 10^{-40}$ (watts Hz $^{-3} \text{ } ^\circ K^{-1} m^{-2}$ )  $2\pi k = 8.671 \times 10^{-11}$ (watts $\mu^2 \text{ } ^\circ K^{-1} m^{-2} \text{ Hz}^{-1}$ )
$B_\lambda$ : Spectral brightness :- Brightness per unit wavelength interval	$\frac{2c^2 h}{\lambda^5 \left( e^{\frac{hc}{\lambda kT}} - 1 \right)}$	$2c^2 h = 1.192 \times 10^2$ (watts $\mu^4 m^{-2} sr^{-1}$ )	$\frac{2ckT}{\lambda^4}$	$2ck = 8.280 \times 10^3$ (watts $\mu^3 \text{ } ^\circ K^{-1} m^{-2} sr^{-1}$ )
$B_\nu$ : Spectral brightness :- Brightness per unit frequency interval	$\frac{2h \nu^3}{c^2 \left( e^{\frac{h\nu}{kT}} - 1 \right)}$  $= \frac{2hc}{\lambda^3 \left( e^{\frac{h\nu}{kT}} - 1 \right)}$	$\frac{2h}{c^2} = 1.472 \times 10^{-50}$ (watts Hz $^{-4} m^{-2} sr^{-1}$ )  $2hc = 3.934 \times 10^{-7}$ (watts $\mu^2 \text{ Hz}^{-1} m^{-2} sr^{-1}$ )	$\frac{2\nu^2 kT}{c^2}$  $\frac{2kT}{\lambda^2}$	$\frac{2k}{c^2} = 3.067 \times 10^{-40}$ (watts Hz $^{-3} \text{ } ^\circ K^{-1} m^{-2} sr^{-1}$ )  $2k = 2.76 \times 10^{-11}$ (watts $\mu^2 \text{ Hz}^{-1} \text{ } ^\circ K^{-1} m^{-2} sr^{-1}$ )

Table 2 Values of Brightness Temperature Exceeded for the specified Percentage Times for an Atmosphere at 273°K

New Jersey U.S.A. 30 GHz		New Jersey U.S.A. 16 GHz		Washington U.S.A. 15.3 GHz		Tokyo Japan 16 GHz		Hitaka Japan 17 GHz		Toyokawa Japan 9.4 GHz		Setagaya Japan 11.8 GHz		Malaysia 11.8 GHz	
$T_b$ (°K)	Time (%)	$T_b$ (°K)	Time (%)	$T_b$ (°K)	Time (%)	$T_b$ (°K)	Time (%)	$T_b$ (°K)	Time (%)	$T_b$ (°K)	Time (%)	$T_b$ (°K)	Time (%)	$T_b$ (°K)	Time (%)
161	2	83	1.5	75	1	118	1	84	0.2	63	0.5	100	0.1	56	1
188	1	92	1	120	0.5	105	0.5	135	0.1	100	0.1	125	0.05	102	0.5
248	0.5	123	0.5	206	0.1	240	0.1	187	0.05	118	0.05	218	0.01	238	0.1
273	0.1	243	0.1	248	0.05	260	0.05	262	0.01	177	0.01	248	0.006	256	0.05
		266	0.05			273	0.01	268	0.005	200	0.005			263	0.03
		273	0.01					273	0.001	237	0.001			265	0.02

**Data from Slough U.K.**

12 GHz		19 GHz		37 GHz		110 GHz	
$T_b$ (°K)	Time (%)	$T_b$ (°K)	Time (%)	$T_b$ (°K)	Time (%)	$T_b$ (°K)	Time (%)
70	1	75	5	86	5	176	5
92	0.5	122	1	178	1	230	1
105	0.1	152	0.5	201	0.5	249	0.5
136	0.05	197	0.1	244	0.3	273	0.1
173	0.01	207	0.05				
184	0.005	246	0.03				
205	0.001						

Table 3 Emissivity of Terrain at cm and mm Wavelengths

Substance	Emissivity at Normal Incidence	Frequency GHz	Wavelength cm	Reference No.	Comments
Grass	~ 1				Grass behaves as a rough surface with virtually no polarisation or angular effects
Sand	~ 1				
Concrete	~ 1				
Dry natural surfaces	0.8 to 0.95		cm	9	Depends upon vegetation cover
Vegetation	~ 1				
Rough dry soils	~ 1				
Dry specular soils	0.7 to 0.9				Polarisation and angular effects
Moist specular soils	lower than dry soils	13.4			Depends upon polarisation and nadir angle - see figure 4 of ref. 9
Average for land areas	0.85		1.35 to 1.9		
Snow					Emissivity can approach unity but depends on moisture content
Soil (varying moisture)	0.94 to 0.75		21		Emissivity values for 0-30% weight of water
	0.94 to 0.73		1.55	20	Emissivity values for 0-35% weight of water
	0.98 to 0.85		0.8		Emissivity values for 0-30% weight of water

Table 4 Emissivity of Water, Ice and Foam at cm and mm Wavelengths

Substance	Emissivity at Normal Incidence	Frequency GHz	Wavelength cm	Reference No.	Comments
Calm water	0.4		3		
Calm water	0.33		3.3		
Calm water with 100% foam	0.8			9	Laboratory study
Ice	~ 1				
Sea ice	0.93				
Sea water	0.43	19.4		19	Wind speed 6 m/sec
Sea water	0.54	19.4			Wind speed 25 m/sec
Sea water	0.45	19.4			Wind speed 6 m/sec
Sea water	0.55	19.4			Wind speed 25 m/sec
Sea water	0.63	19.4			Wind speed 30 m/sec
Sea water	0.51	37			Wind speed 10 m/sec
Sea water	0.69	37		22	Wind speed 30 m/sec
Sea water	0.41	13.4			Wind speed 10 m/sec
Sea water	0.58	13.4			Wind speed 30 m/sec
Sea foam	0.78	13.4			
Sea foam	0.91	19.4			
Sea foam	0.89	37			
Lake water			0.43	23	Brightness temp. 220°K includes reflected sky radiation

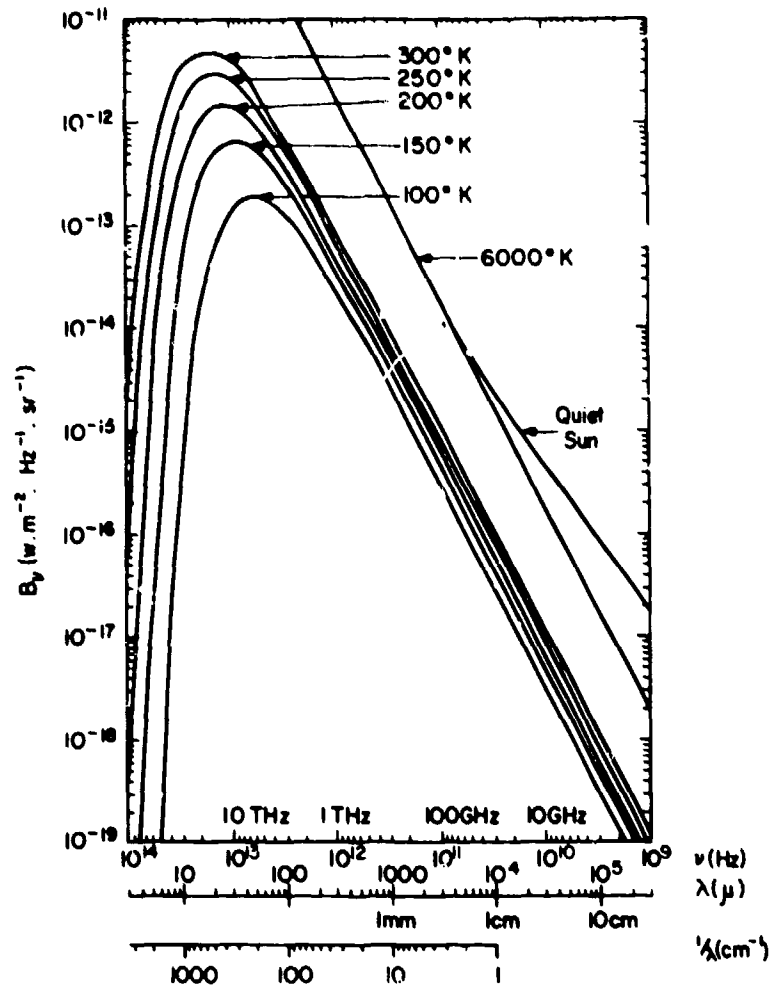


Fig. 1 Planck's black-body spectral brightness function  $B_\nu$  for various temperatures plotted against Frequency (Hz), Wavelength ( $\mu$ ) and Wavenumber ( $\text{cm}^{-1}$ ).  
 N.B. Solid angle of sun at  $\lambda < 1 \text{ cm} \approx 6.8 \times 10^{-5} \text{ sr}$   
 $\lambda > 1 \text{ cm} > 6.8 \times 10^{-5} \text{ sr}$

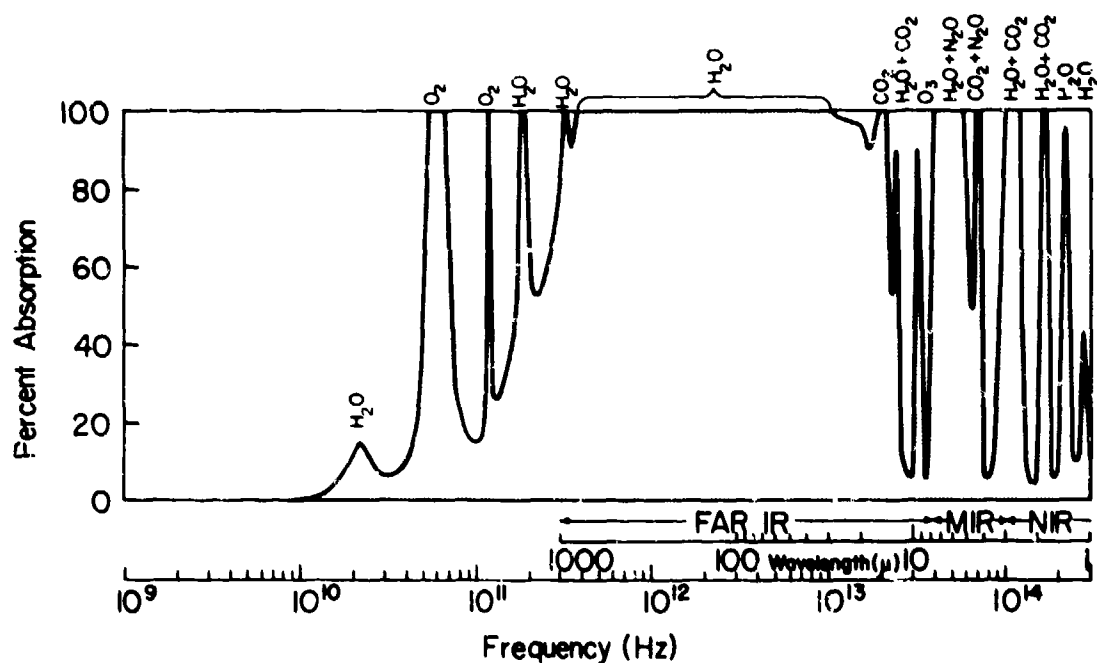


Fig. 2 Transmission and absorption in the clear atmosphere at zenith

5.14

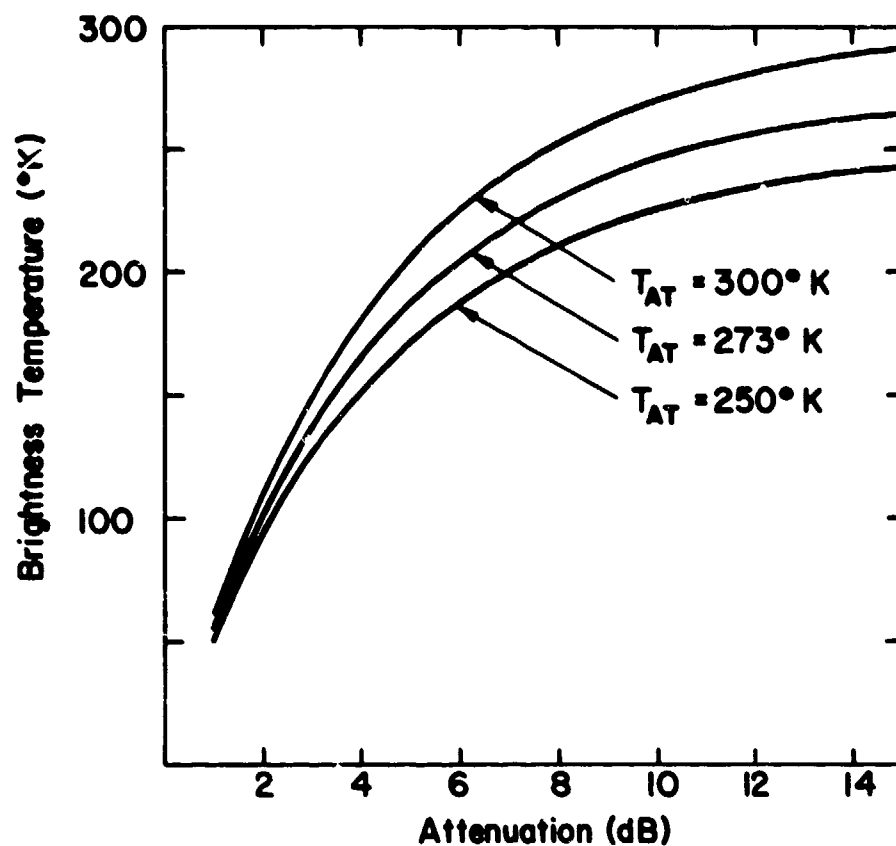


Fig. 3 Brightness temperature vs attenuation (dB) for various values of effective kinetic temperature of absorbing medium

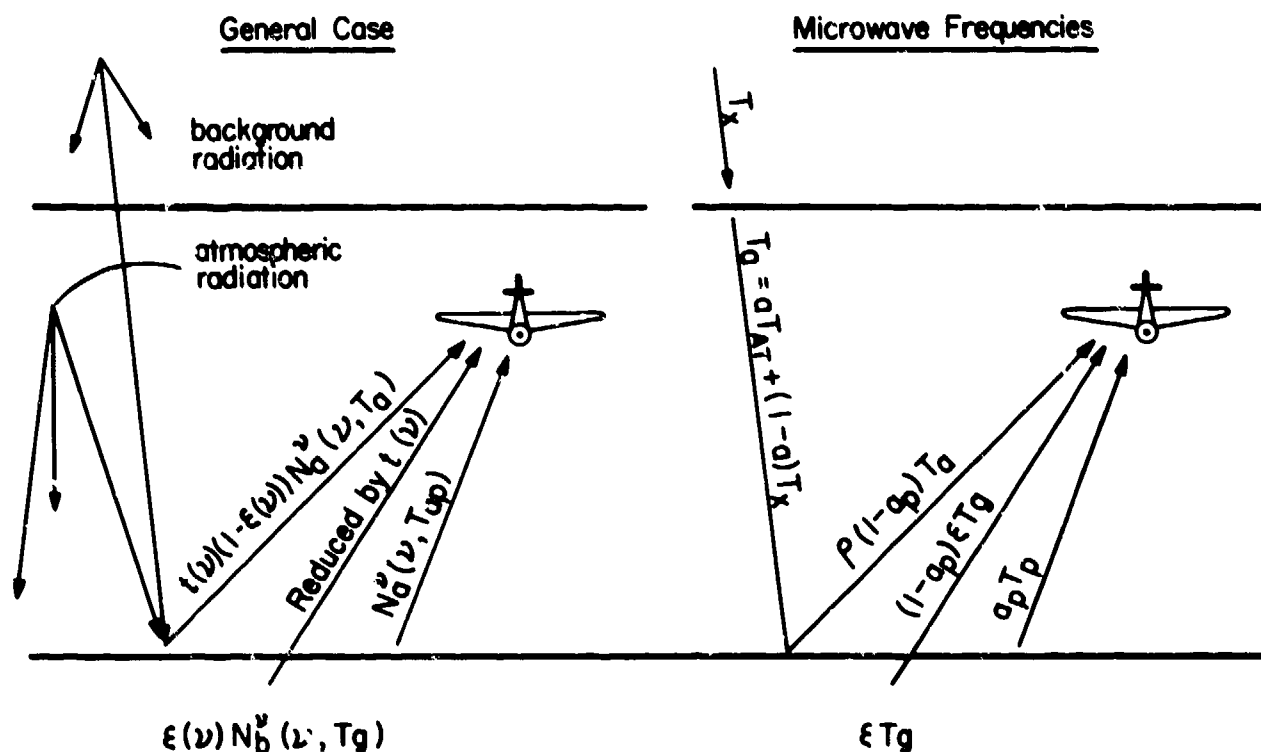


Fig. 4 Schematic diagram illustrating the component radiation received at a point in the atmosphere

## DISCUSSION

H. J. ALBRECHT: This is a supplementary comment to the excellent review just presented on the subject of land, sea, and atmospheric thermal noise. Referring to the apparent dependence of brightness temperature of the ground upon moisture and temperature of the ground, world maps of brightness temperature based on satellite measurements were shown during the URSI (Union Radio Scientific International) Specialists' Meeting on the subject of remote sensing held in Berne, Switzerland in September 1974. It is interesting to note that, on an as yet qualitative basis, these maps agree very well with world maps of electrical ground conductivity first presented during an EPP (then EPC) Meeting in 1967 (H. J. A.: On the geographical distribution of electrical ground parameters and its possible effects on navigational systems; in Agardograph No. CP 33, "Phase and Frequency Instabilities in Electromagnetic Wave Propagation," Technivision 1970). Although the latter map was also based on moisture and temperature of the ground, as well as on its type, the agreement is remarkable because, other than in the case of ground conductivity for lower frequencies, the brightness temperature is only affected by the upper surface layer of a thickness of a few centimeters.



# IONOSPHERIC AND TROPOSPHERIC SCINTILLATION AS A FORM OF NOISE

by  
E. J. Fremouw  
C. L. Rino  
Radio Physics Laboratory  
Stanford Research Institute  
Menlo Park, CA 94025 USA

6-1

## ABSTRACT

Scintillation has many of the detrimental effects of noise, in that it produces random fluctuation of the complex envelope of a modulated signal. A useful way to characterize scintillation effects is to describe the signal statistics that result when a CW wave is transmitted through a random medium that imposes complex modulation during propagation to the receiver. Many theoretical treatments, based essentially on the first Born approximation, describe the signal statistics in a manner identical with the noise theory of Rice. Other treatments, following the Rytov expansion, suppose the phase and the log of amplitude to be Gaussian random variates. Most data tests have favored the latter, "log-normal," statistics. The Born-based theory predicts Rice statistics only at very great distance from the perturbing medium, however, and it has been suspected that generalization to permit the quadrature components of the scattered signal to be partially correlated Gaussian variates of unequal variance might better match the observed signal statistics. Recent tests of signals observed through the ionosphere, the solar wind, and a laboratory plasma have consistently confirmed this speculation and have revealed a surprising consistency in parameters describing the first-order statistics of a signal caused to scintillate by a randomly structured plasma. This paper describes a means for exploiting these new findings in a transionospheric communication channel model; a similar effort for nondispersive media such as the troposphere might also be profitable.

## 1. INTRODUCTION

When a radio wave is scattered in a medium with random refractive-index structure, the resulting electromagnetic wave-field becomes a spatially random variable. When there is relative motion between the medium and the radio line of sight, the voltage delivered by an antenna to a receiver takes on many of the attributes of a signal buried in noise. In particular, its amplitude and phase--or, alternatively, its quadrature components--display random variations that we call "scintillation." In describing scintillation for application to communication system design and operation, we are concerned with the resulting signal statistics. If we obtain the statistics for a CW incident wave, the results can be generalized to modulated signals by Fourier techniques.

## 2. FIRST-ORDER STATISTICS

### 2.1 Evidence for Gaussian Signal Statistics

We begin by considering the simple phasor diagram shown in Figure 1, where  $E$  represents the instantaneous complex amplitude of the received quasi-CW signal (CW except for the random modulation imposed by scintillation). The scattered component of the signal is represented by the randomly varying phasor,  $E_s$ , and the nonscattered component by  $\langle E \rangle$ , the mean value of  $E$ . Thus we have chosen to reference all phases to the phase that the received signal would have in the absence of scintillation.

Our interest is in relating the signal statistics to properties of the medium, which requires that the scattering problem be treated by some approximate solution of Maxwell's equations. There are several approaches, but two--the Rytov method of smooth perturbations and the application of the first Born approximation--exemplify the differing signal-statistical results obtained. The differences arise essentially from the quantities chosen to represent the scattered wave in a perturbation calculation: phase and the logarithm of amplitude in the Rytov approach, replaced by quadrature components in the alternative approach. A loose application of the Central Limit Theorem to the chosen quantities results in a hypothesis on which the signal statistics can be formulated.

In the Rytov approach, it is natural to postulate that phase and the log of amplitude are jointly Gaussian variates leading to so-called log-normal statistics for amplitude. This postulate may also be appealing to those familiar with the phase-screen approach to calculating scintillation effects, as developed, for instance, by Bramley (1955). For those familiar with the scattering theory of Booker and Gordon (1950), on the other hand, it is equally natural to postulate that the quadrature components of the scattered signal  $E_s$  are jointly Gaussian variates, yielding so-called Gaussian signal statistics.

62. If the quadrature components were uncorrelated and had equal variances, the statistics of the complex voltage  $E_s$  would be identical to those of noise, and the statistics of the resultant signal  $E$  would be those described by Rice (1945) for a CW signal with band-limited white noise added. Since the scattering is described by a field component added in phase quadrature to the incident wave at the scattering location, however, there is no a priori reason for making the equal-variance assumption at an observing point. Moreover, calculation of the resultant signal expected at an observing point attributes the real (relative to  $\langle E \rangle$ ) component of  $E_s$  to diffractive phase rotation of the initially imaginary scattered wave. Thus no valid basis exists for assuming the real and imaginary parts of  $E_s$  to be uncorrelated either.

It is well known (Beckman and Spizzichino, 1963) that, for generalized Gaussian statistics, a contour of equal probability for the complex value of  $E_s$ , and therefore of  $E$ , is an ellipse such as the one shown in Figure 1. In the special case of Rice statistics, the ellipse reduces to a circle. To describe the first-order statistics of  $E$ , we are interested in the characteristics of the ellipse: its size, eccentricity, and orientation angle.

Let us define the quadrature components of  $E_s$  and their variances and covariance as follows:

$$E_s = X + iY \quad (1)$$

$$\sigma_x^2 \triangleq \langle (X - \langle X \rangle)^2 \rangle = \langle X^2 \rangle - \langle X \rangle^2 \quad (2)$$

$$\sigma_y^2 \triangleq \langle (Y - \langle Y \rangle)^2 \rangle = \langle Y^2 \rangle \quad (3)$$

$$\sigma_{xy}^2 \triangleq \langle (X - \langle X \rangle)(Y - \langle Y \rangle) \rangle = \langle XY \rangle \quad (4)$$

Now suppose for the moment that  $X$  and  $Y$  are uncorrelated ( $\sigma_{xy} = 0$ ). Then, clearly, the ellipse is aligned along one of the axes of the complex plane ( $\delta = 0$ , say). In this special case, the axial ratio of the ellipse obviously is equal to the ratio  $\sigma_y/\sigma_x$ . Furthermore, the size of the ellipse depends on  $\sigma_x^2 + \sigma_y^2$ .

It can be shown (Bello, 1971) that the characteristics of the ellipse are dictated by one real and one complex quantity:

$$R_0 = \langle E E^* \rangle \quad (5)$$

and

$$B_0 = \langle E E \rangle \quad (6)$$

The importance of  $R_0$  and  $B_0$  for describing the correlation ellipse comes from the fact that they completely dictate the variances and covariance of  $X$  and  $Y$ , as follows:

$$\sigma_x^2 = \frac{1}{2} (R_0 + \text{Re} \{B_0\}) \quad (7)$$

$$\sigma_y^2 = \frac{1}{2} (R_0 - \text{Re} \{B_0\}) \quad (8)$$

$$\sigma_{xy}^2 = \frac{1}{2} \text{Im} \{B_0\} \quad (9)$$

From the above relations it can be shown that the eccentricity of the correlation ellipse, in general, is related to  $|B_0|/R_0$  and that its orientation angle is given by  $\tan(2\delta) = \text{Im} \{B_0\}/\text{Re} \{B_0\}$ . Clearly, its size depends on  $\sigma_x^2 + \sigma_y^2 = R_0$ , which represents the scattering coefficient of the medium.

Although for application to communication systems, we are interested in the complex-signal statistics, most scintillation observations have been of real amplitude,  $|E|$ , only. Furthermore, most observations have been reported in terms of some scintillation index related to the variance of either  $|E|$  or  $|E|^2$ . A useful index is the normalized second moment,  $S_4$ , or received signal intensity, defined by Briggs and Parkin (1963) as

$$S_4^2 = \frac{\langle |E|^2 \rangle^2 - \langle |E| \rangle^2}{\langle |E| \rangle^2} \quad (10)$$

If the underlying signal statistics were log-normal, there would be a unique probability density function (pdf) for  $|E|$  or for  $|E|^2$  for a given value of  $S_4$ . On the other hand, for Gaussian statistics, a family of amplitude or intensity pdf's exists for a given  $S_4$ , depending on the scattering coefficient  $h_0$  and the remaining two ellipse parameters,  $|B_0|/R_0$  and  $\delta$ . We shall see shortly that the latter two parameters can be reduced to a single variable,  $Z$ , for a particular representation of the scattering medium.

Figure 2 shows two members of the family of pdf's for the signal intensity derived from the Gaussian signal-statistics hypothesis, for  $S_4 = 0.5$ , compared with the unique intensity pdf derived from log-normal

statistics for the same  $S_4$ . As the values of  $Z$  vary from very small to very large, the Gaussian-based pdf's range from a highly peaked function to the limiting curve predicted by Rice statistics. 6-3

Various scintillation researchers have compared intensity histograms with the intensity pdf's based on log-normal and on Rice statistics and have found a closer fit to the former (e.g., Cohen et al., 1967). It is incorrect to conclude from such tests that the Rytov approach to scattering calculations is superior to that based on the first Born approximation, however, because Rice statistics represent only a limiting form of the first-Born statistical results.

More recent tests have included a procedure for searching the Gaussian-based family of pdf's for the best fit to the data (Rino and Fremouw, 1973a; Rino, Livingston, and Whitney, 1974). The results, an example of which is shown in Figure 3, consistently show that a better fit is obtained to Gaussian than to log-normal statistics and that the best-fit Gaussian-based pdf is more peaked than the log-normal pdf, implying small values of  $Z$ . The significance of this latter fact will be explored shortly.

The histogram in Figure 3 is from observations of the 137.5-MHz beacon on ATS-5 made from Sagamore Hill, Massachusetts, by the AFCRL group. Similar tests have been made with simultaneously collected 412-MHz data, with data obtained by observing radio-star scintillation produced by the solar wind, and with microwave-scatter data from a laboratory plasma. The fits, measured by the chi-squared ( $\chi^2$ ) or mean-square ( $\langle \Delta^2 \rangle$ ) error, have been consistently better for Gaussian than for log-normal statistics, as shown in Table 1.

Table 1 Summary of Data Fits to Gaussian and Log-Normal Statistics

Scattering Medium	Frequency (MHz)	Error Parameter	
		Gaussian	Log-Normal
Laboratory Plasma	31,000	$\chi^2 = 429$	$\chi^2 = 624$
Laboratory Plasma	31,000	$\chi^2 = 7038$	$\chi^2 = 1365$
Solar Wind	75	$\langle \Delta^2 \rangle = 36$	$\langle \Delta^2 \rangle = 99$
Solar Wind	75	$\langle \Delta^2 \rangle = 70$	$\langle \Delta^2 \rangle = 75$
Solar Wind	75	$\langle \Delta^2 \rangle = 80$	$\langle \Delta^2 \rangle = 88$
Ionosphere	138	$\chi^2 = 689$	$\chi^2 = 1062$
Ionosphere	138	$\chi^2 = 1156$	$\chi^2 = 1638$
Ionosphere	138	$\chi^2 = 308$	$\chi^2 = 502$
Ionosphere	138	$\chi^2 = 433$	$\chi^2 = 949$
Ionosphere (Fig. 3)	138	$\chi^2 = 200$	$\chi^2 = 1496$
Ionosphere	412	$\chi^2 = 433$	$\chi^2 = 611$
Ionosphere	412	$\chi^2 = 277$	$\chi^2 = 519$
Ionosphere	412	$\chi^2 = 171$	$\chi^2 = 272$
Ionosphere	412	$\chi^2 = 205$	$\chi^2 = 323$
Ionosphere	412	$\chi^2 = 150$	$\chi^2 = 386$
Computer (Fig. 4)	---	$\chi^2 = 468$	$\chi^2 = 390$

The above results seem to imply a superiority of Born-based scattering theories over those based on the Rytov expansion. One might, however, suspect that the results arise because of the extra parameter available in searching the Gaussian family for a best fit to a finite-sample histogram. To test this possibility empirically, a simulated data set was drawn from a computer-generated random-number table forced to obey log-normal statistics. The computer-generated data set was then submitted to the curve-fitting process used for the real data.

The result, shown in Figure 4, was that the process did properly find the computer-generated data set to be better described by log-normal statistics than by the best-fit Gaussian statistics. The chi-squared errors for the simulated data are given in the last row of Table 1. We conclude that the consistently better fit of real scintillation data to Gaussian-based statistics than to log-normal statistics is a valid result and not an artifact of the analysis technique.

Not only have the data tests consistently favored Gaussian over log-normal statistics, they have also consistently yielded small values of  $Z$  for the best-fit pdf's. We shall soon see that this means rather eccentric correlation ellipses ( $|B_0|/R_0 \approx 1$ ) oriented quite vertically on the complex plane ( $\delta \ll 45^\circ$ ). One ramification of this fact is that the corresponding pdf's for phase can depart considerably from the

simple Gaussian shape predicted by both Rice and log-normal statistics. Some examples are shown in Figure 5, for ellipse-parameter values corresponding to small to moderate  $Z$ . Note the asymmetry of the curves for  $\delta > 0$ . Similar curves generated for larger values of  $S_4$  (Rino and Hatfield, 1974) show a double-peaked structure.

## 2.2 Relation to Scattering Medium

The relation of the ellipse parameters to  $Z$ --in fact the precise definition of  $Z$ --depends upon the spatial spectrum of the refractive-index irregularities in the medium. In general,  $Z$  is a measure of the relative size of the radio Fresnel zone at the distance of the scattering region and of the scatterers producing the scintillation. For a power-law spectrum of the form

$$\eta(\kappa) = [1 + (\alpha\kappa)^2]^{-(\nu + \frac{1}{2})} \quad (11)$$

it can be shown (Rino and Fremouw, 1973b) that

$$Z = \frac{\lambda_z}{2\pi\alpha^2} \quad (12)$$

where  $\sqrt{\lambda_z}$  is the Fresnel-zone radius and  $\alpha$  is an irregularity scale-size parameter.

For scattering in a layer of plasma-density irregularities having a spatial spectrum similar to Eq. (11) but allowing for elongation along one axis (the geomagnetic field in the ionospheric case), the ellipse parameters can be shown (Rino and Fremouw, 1973b) to be:

$$R_o = 2\sqrt{\pi} r_e^2 \lambda^2 L \sec^2 \theta \frac{\Gamma(\nu - \frac{1}{2})}{\Gamma(\nu - 1)} \frac{a}{\beta} \alpha \sigma_n^2 \quad (13)$$

where

- $r_e$  = classical electron radius
- $\lambda$  = radio wavelength
- $L$  = scattering-layer thickness
- $\theta$  = incidence angle on the layer
- $\nu$  = spectral index in Eq. (11)
- $a$  = axial ratio of irregularity scale size along the magnetic field to across it
- $\beta^2 = a^2 \cos^2 \psi + \sin^2 \psi$ , where  $\psi$  = magnetic dip angle
- $\alpha$  = scale parameter in Eq. (11)
- $\sigma_n^2$  = variance of electron density in the layer

$$\frac{|B_o|}{R_o} = \frac{\beta}{\pi} (\nu - \frac{1}{2}) |\mathcal{J}(Z, \mathcal{E})| \quad (14)$$

and

$$\delta = \frac{1}{2} \tan^{-1} \frac{\text{Im} \{ \mathcal{J}(Z, \mathcal{E}) \}}{\text{Re} \{ \mathcal{J}(Z, \mathcal{E}) \}} \quad (15)$$

where  $\mathcal{J}$  is an integral over spatial wavelength,  $\kappa$ , depending upon  $Z$  and a function of  $\mathcal{E}$  determined by the thickness and shape of the layer.

The main point to be noted in Eqs. (14) and (15) is that the eccentricity and orientation angle of the correlation ellipse are not independent. Rather, they are functionally related through the integral  $\mathcal{J}$ , which in general requires numerical evaluation. They vary systematically in post-scattering propagation as  $Z$  increases because of its dependence on Fresnel-zone size.

In Figure 6 we show several numerically evaluated points on a plane of  $\delta$  vs.  $|B_o|/R_o$ , for a power-law spectrum with index  $\nu = 4/3$ . For comparison, we have also plotted a solid curve for a Gaussian spectrum, for which the integral can be evaluated analytically. For both spectra, the calculations shown are for the case of normal incidence on a layer containing isotropic irregularities. Similar curves are obtainable for different geometries.

What Figure 6 shows is that as the scattered wave propagates from  $Z = 0$  to  $Z \gg 1$ , the correlation ellipse rotates from being aligned along the imaginary axis in Figure 1 to being at an angle approaching  $45^\circ$ , simultaneously circularizing ( $|B_0|/R_0 \rightarrow 0$ ). The rate at which this approach to Rice statistics takes place as the propagation distance,  $z$ , increases depends on the scale parameter  $\alpha$ .

The fact that ionospheric scintillation data display best fits to amplitude pdf's consistent with small  $Z$  and varying little with  $\lambda$  implies very large values of  $\alpha$ . These results are consistent with both in situ (Dyson, McClure, and Hanson, 1974) and remote-sensing (Rufenach, 1972) estimates of the outer scale of ionospheric irregularities, which indicate values exceeding several tens of kilometers. 6-5

The same in-situ and remote-sensing measurements indicate that the spatial spectrum of ionospheric irregularities is, under most conditions, well approximated by a power law with index  $\nu \approx 4/3$  and not by a Gaussian law as has often been assumed for mathematical tractability. This in itself is unfortunate for quantitative modeling of ionospheric scintillation for systems application, because the integral that dictates  $|B_0|/R_0$  and  $\delta$  must then be solved numerically. In Figure 6, the structure in the dashed curve for values of  $Z$  greater than about unity is an artifact of numerical integration over finite limits. It is not efficient to extend the limits, because the integration is very time-consuming even on large machines. The integration proceeds more rapidly for small values of  $Z$ , however. Thus the observation that small values of  $Z$  prevail for situations of applications interest and that they vary only weakly with observing frequency is fortuitous for modeling.

An example of our interest in evaluating the probability-ellipse parameters is given in Figure 7, which shows how the scintillation index  $S_4$  varies with the ionospheric scattering coefficient  $R_0$  and the eccentricity and orientation angle of the ellipse, for Gaussian statistics. Solely on the basis of Gaussian-statistics hypothesis, one obtains the following relation:

$$S_4^2 = 2R_0 (1 - R_0) \left( 1 - \frac{|B_0|}{R_0} \cos 2\delta \right) + R_0^2 \left( 1 + \frac{|B_0|^2}{R_0^2} \right), \quad (16)$$

which is plotted in Figure 7 for scattering coefficients of 4, 16, 36, and 64 percent.

The dominant factor in dictating the scintillation index is the scattering coefficient, but the experimental evidence indicates that transionospheric communication systems operate in the regime where the ellipse eccentricity and orientation are also significant. They become increasingly important as one desires increasing signal-statistical generality for modeling (i.e., parameters beyond simply scintillation index), especially for complex-signal statistics.

To date, however, the only quantitative modeling of ionospheric scintillation that has been performed has been for scintillation index (Aarons, Whitney, and Allen, 1971; Fremouw and Rino, 1973). Furthermore, this modeling has been based on very approximate theory and, in some instances, on data reported in terms of quasi-subjective indices only crudely related to a theoretically calculable index such as  $S_4$ .

Recently, however, Whitney (1974) performed careful calibration of the ad hoc index, SI, devised at AFCL and widely used for manual scaling of amplitude scintillation records. This permitted accurate comparison of VHF observations performed by the AFCL group (Aarons, Mullen, and Basu, 1964) with calculations of  $S_4$  based on the empirical model of Fremouw and Rino (1973) for scintillation-producing ionospheric irregularities. The comparison, shown in Figure 8, revealed a closer correspondence than was believed to hold when the model was published (prior to accurate calibration of SI in terms of  $S_4$ ).

Although the existing model appears to provide a good basis for calculating the VHF scintillation index for a considerable range of observing conditions (latitude, time of day, season, and sunspot number), it is seriously deficient at the higher frequencies, as shown in Figure 9. The reason probably lies in the approximate nature of the theory on which the modeling was based. The model was developed by calculating  $S_4$  according to the weak-scatter theory of Briggs and Parkin (1963), comparing results with published values of scintillation index (obtained mainly at VHF), and adjusting the ionospheric parameters (mainly the variance of electron density) until agreement had been obtained with a wide variety of observations. The resulting model for ionospheric irregularity strength is thus subject to errors induced by assumptions in the scattering theory, which included approximation of Eq. (16) and use of a Gaussian spatial spectrum for calculating  $R_0$ ,  $|B_0|/R_0$ , and  $\delta$ .

Possibly important for modeling is the limitation imposed by assumption of weak, single scatter. This assumption has also been made in more recent theoretical developments, such as that leading to Eqs. (13), (14), and (15) for the ellipse parameters. Unfortunately, this assumption often breaks down at VHF. The result is that a model based on VHF observations and weak-scatter theory results in underestimation of the strength of ionospheric irregularities. Then, when the model is applied to higher frequencies, where the weak, single-scatter assumption may in fact be valid, scintillation is underestimated.

At present, no completely general scattering theory exists for calculating parameters of the probability ellipse when multiple scatter occurs. However, one important multiple-scatter effect that influences the frequency dependence of scintillation can be accounted for: extinction of the nonscattered signal component

as it propagates through multiple scattering layers. From the work of Fejer (1953) and of Bramley (1955), it follows that extinction can be accounted for by replacing the single-scattering coefficient  $R_0$  by a multiple-scattering coefficient  $\sigma_m^2$ , defined by

$$\sigma_m^2 = 1 - e^{-R_0} \quad (17)$$

which clearly reduces to  $R_0$  when the scattering coefficient is small. Since  $R_0$  is proportional to  $\lambda^2$ , as can be seen from Eq. (13), use of  $\sigma_m^2$  in modeling would significantly decrease the dependence of scintillation on frequency. In a current modeling effort, it is intended to account for extinction in this way, which should result in a model valid for UHF as well as for VHF scintillation.

### 3. SECOND-ORDER SIGNAL STATISTICS

In all the above, we have been concerned with the first-order statistics of the complex voltage  $E$ . Also important for communication channel modeling are second-order statistics in the temporal, spatial, and spectral domains. For instance, to apply the CW signal-statistical results to broadband systems, one must be concerned with the joint probability of  $E(f)$  and  $E(f + \delta f)$ , where  $\delta f$  represents a frequency increment within the system's passband. Similarly, for space-diversity systems one is concerned with the joint probability of  $E$  at different receiving antennas.

For second-order temporal statistics, one is concerned, in general, with the joint statistics of  $E(t)$  and  $E(t + \delta t)$ . With the fact established that the underlying signal statistics are Gaussian, the second-order signal statistics are fully described by autocorrelation functions in the various domains. Alternatively, they can be presented in terms of Fourier transforms of the autocorrelation functions. For temporal statistics, the fluctuation spectrum of  $E$  is clearly of interest.

Most scintillation observations are of real amplitude  $|E|$  only. Fluctuation spectra of real amplitude, or of intensity  $|E|^2$ , have been recorded in recent years by various workers. Figure 10 is an example recorded by Rufenach (1972), showing the power-law form imposed by the spatial spectrum of ionospheric irregularities and a low-frequency flattening resulting from diffraction effects. It is hoped that such spectra will soon be available for the quadrature components of  $E$ , from observations of a multifrequency beacon (DNA-002) to be launched about the end of this year (Fremouw, 1972). Such observations, when interpreted by the emerging theory of second-order signal statistics (Fremouw and Rino, 1974), should provide a firm basis for definitive signal-statistical modeling of ionospheric scintillation.

Presumably, the same procedures could be applied to modeling of tropospheric scintillation. Prior to such remodeling, however, data tests should be performed to establish whether the underlying signal statistics are Gaussian or log-normal. The tests summarized in this paper have all been of data resulting from scattering by a structured plasma and collected outside the scattering medium. Similar tests of data for scattering by a structured nondispersive medium collected within the medium (as would be the case for tropospheric radio scintillation) should shed considerable light on the relative merits of Born-based and Rytov-based scattering theories for application to communication-channel modeling in general.

### 4. CONCLUSION

In summary, we point out that rather general models of time-varying communication channels can be devised for use in system planning and operation, when the underlying signal statistics resulting from radio-wave scattering are known. It has been established that the amplitude of CW signals scattered by three different structured plasmas obeys the statistics expected when the signals' quadrature components are jointly Gaussian variates of unequal variance and finite covariance (i.e., Gaussian statistics). The result is a probability density function (pdf) for received signal intensity that is more peaked than the pdf resulting from either Rice statistics or log-normal statistics. The corresponding pdf for phase is somewhat asymmetrical and is broader than that resulting from Rice or log-normal statistics for the same scattering coefficient.

Scattering theories based on the first Born approximation lead to the observed first-order signal statistics of amplitude, while those based on the Rytov expansion do not. It remains to be seen whether the generalized Gaussian statistics observed for weak and moderate scintillation endure for strong scintillation, especially in the presence of multiple scatter. Meanwhile efforts are under way to apply the above signal-statistical results to mathematical modeling of the transionospheric radio communication channel. Similar data tests and theoretical developments could probably be used to model tropospheric channels for microwave and laser communication systems.

### 5. ACKNOWLEDGEMENT

This paper is largely a review of work published in the references cited. The authors gratefully acknowledge support of their past scintillation research by NASA under Contracts NAS5-21551 and NAS5-21891 and by the Defense Nuclear Agency (DNA) under Contract DASA01-68-C-0104, and support of their current work under Contract DNA001-74-C-0255 and by ARPA and Rome Air Development Center under Contract F30602-74-C-0279.

## REFERENCES

- Aarons, J., Mullen, J. P., and Basu, S., 1964, "The Statistics of Satellite Scintillations at a Subauroral Latitude," J. Geophys. Res., Vol. 69, No. 9.
- Aarons, J., Whitney, H. E., and Allen, R. S., 1971, "Global Morphology of Ionospheric Scintillations," Proc. IEEE, Vol. 59, No. 2, pp. 159-172.
- Beckman, P., and Spizzichino, A., 1963, The Scattering of Electromagnetic Waves from Rough Surfaces, Pergamon Press, pp. 119-136.
- Bello, P. A., 1971, "A Study of the Relationship Between Multipath Distortion and Wavenumber Spectrum of Refractive Index in Radio Links," Proc. IEEE, Vol. 59, No. 1, pp. 47-75.
- Booker, H. G., and Gordon, W. E., 1950, "A Theory of Radio Scattering in the Troposphere," Proc. IRE, Vol. 38, No. 4, pp. 401-412.
- Bramley, E. N., 1955, "Some Aspects of the Rapid Directional Fluctuations of Short Radio Waves Reflected at the Ionosphere," Proc. IEE, Vol. 102, No. 4, pp. 533-540.
- Briggs, B. H., and Parkin, J. A., 1963, "On the Variation of Radio Star and Satellite Scintillations with Zenith Angle," J. Atmos. Terrest. Phys., Vol. 25, pp. 339-365.
- Cohen, J. H., Gundermann, E. J., Hardebeck, H. E., and Sharp, L. E., 1967, "Interplanetary Scintillations, Observations," Astrophys. J., Vol. 147, pp. 449-466.
- Dyson, P. L., McClure, J. P., and Hanson, W. B., 1974, "In Situ Measurements of the Spectral Characteristics of F-Region Ionospheric Irregularities," J. Geophys. Res., Vol. 79, No. 10, pp. 1497-1502.
- Evans, J. V. (editor), 1973, "Millstone Hill Radar Propagation Study: Scientific Results--Part II," Technical Report 509, Joint Radar Propagation Study, Lincoln Laboratory, Massachusetts Institute of Technology, Lexington, Massachusetts.
- Fejer, J. A., 1953, "The Diffraction of Waves in Passing Through an Irregular Refracting Medium," Proc. Roy. Soc. A., Vol. 220, pp. 455-471.
- Fremouw, E. J., 1972, "A Planned Polar-Orbiting Wideband Beacon," paper presented at the Symposium on the Future Application of Satellite Beacon Measurements in Graz, Austria.
- Fremouw, E. J., and Rino, C. L., 1974, "Modeling of Transionospheric Radio Propagation," Quarterly Technical Report for Period 15 May - 15 August 1974, Contract F30602-74-C-0279, Stanford Research Institute, Menlo Park, California.
- Fremouw, E. J., and Rino, C. L., 1973, "An Empirical Model for Average F-Layer Scintillation at VHF/UHF," Radio Science, Vol. 8, No. 3, pp. 213-222.
- Rice, S. O., 1945, "Mathematical Analysis of Random Noise," Part III, Bell Sys. Tech. J., Vol. 24, No. 1, pp. 47-159.
- Rino, C. L., and Fremouw, E. J., 1973a, "Statistics for Ionospherically Diffracted VHF/UHF Signals," Radio Science, Vol. 8, No. 3, pp. 223-233.
- Rino, C. L. and Fremouw, E. J., 1973b, "Ionospheric Scintillation Studies," Final Report, Contract NAS5-21891, Stanford Research Institute, Menlo Park, California.
- Rino, C. L., and Hatfield, E., 1974, "Analysis of Scintillation Effects on Communication and Radar Systems," Bimonthly Progress Report 1, Contract DNA001-74-C-0255, Stanford Research Institute, Menlo Park, California.
- Rino, C. L., Livingston, R. C., and Whitney, H. E., 1974, "Some New Results on the Statistics of Radio Wave Scintillation. A. Empirical Evidence for Gaussian Statistics," submitted for publication in J. Geophys. Res.
- Rufenach, C. L., 1972, "Power-Law Wavenumber Spectrum Deduced from Ionospheric Scintillation Observations," J. Geophys. Res., Vol. 77, No. 25, pp. 4761-4772.
- Whitney, H. E., 1974, "Notes on the Relationship of Scintillation Index to Probability Distributions and Their Uses for System Design," Environmental Research Papers No. 461, Report No. AFCRL-TR-74-0004, Ionospheric Physics Laboratory, Air Force Cambridge Research Laboratories, L. G. Hanscom Field, Bedford, Massachusetts.

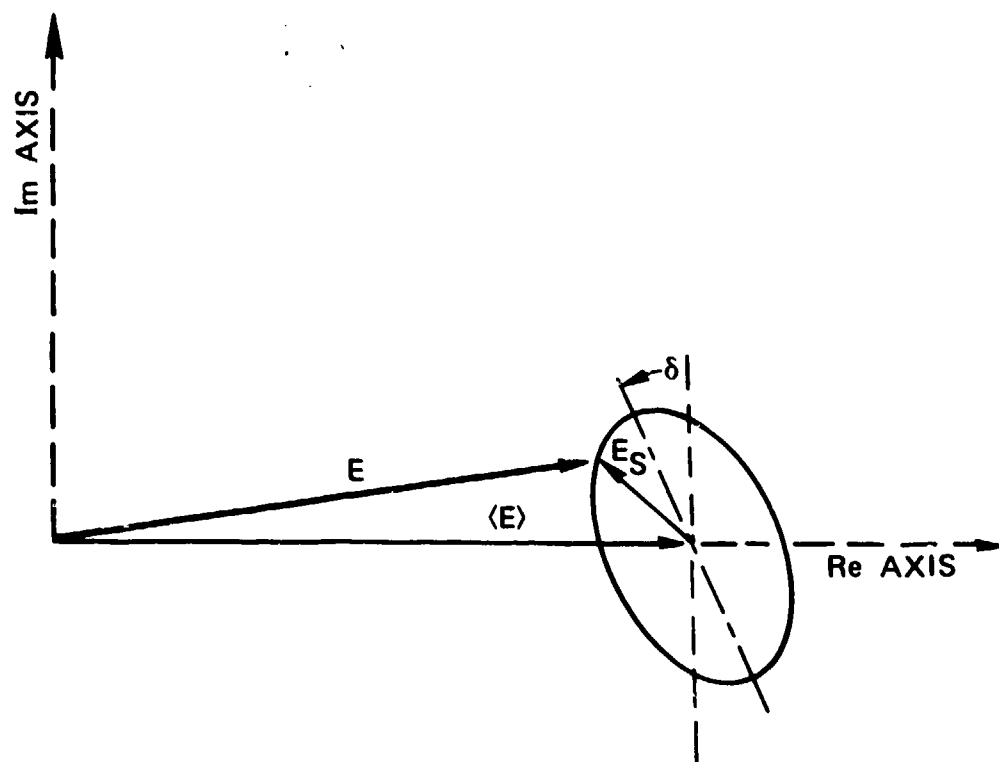


Fig. 1 Phasor diagram illustrating a contour of equal probability for the complex-amplitude of a scintillating CW signal.

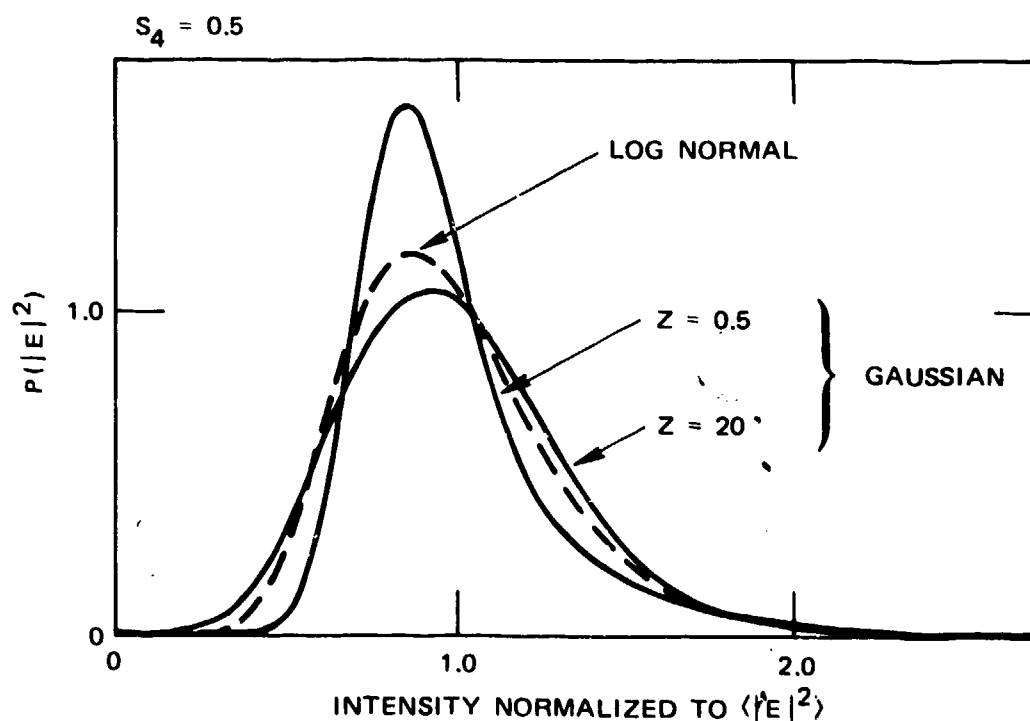


Fig. 2 Probability density functions (pdf's) for received signal intensity, comparing log-normal with Gaussian statistics.



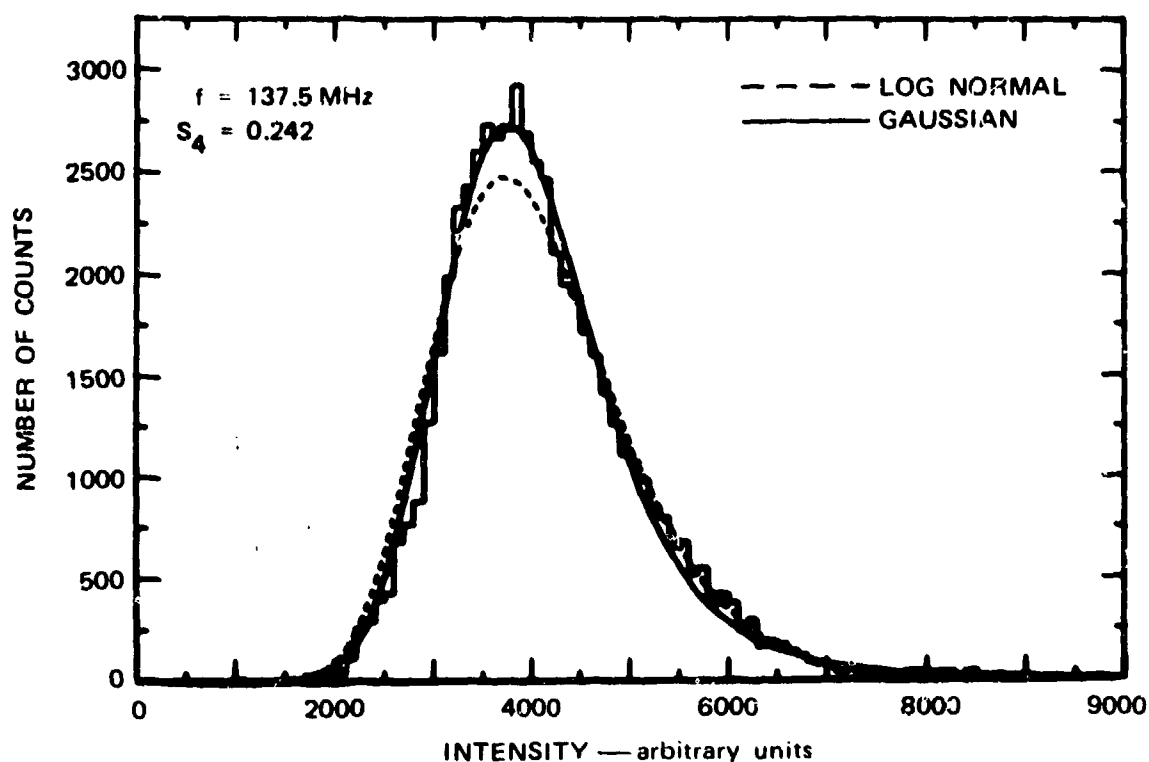


Fig. 3 Data histogram for signal intensity received at Sagamore Hill, Massachusetts, from a synchronous satellite compared with Gaussian and log-normal pdf's.

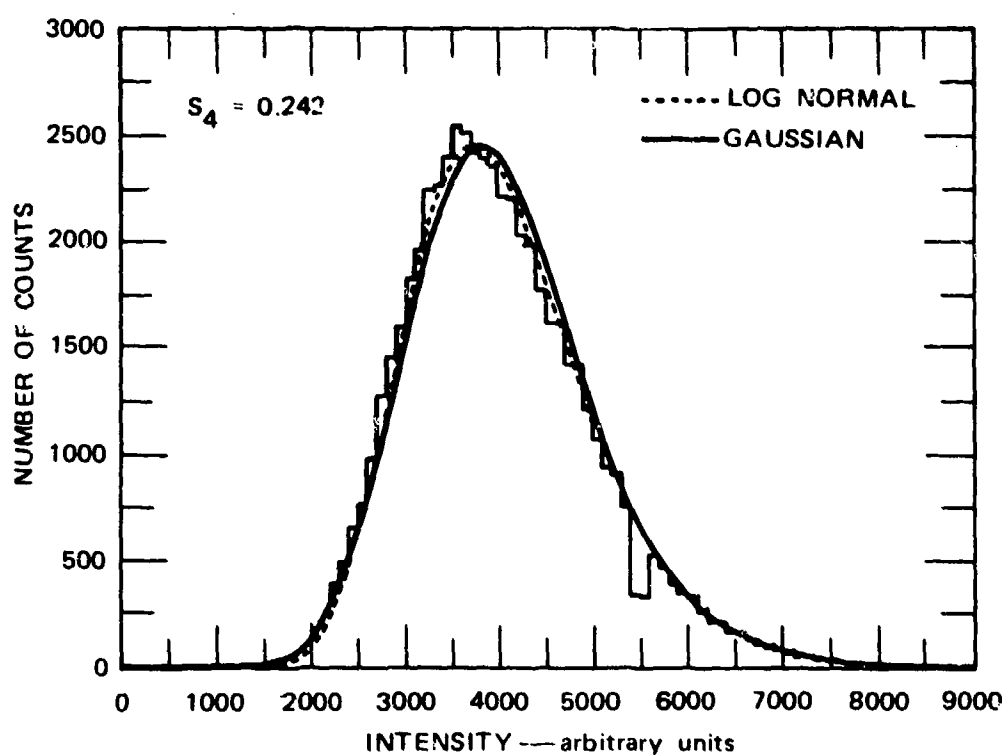


Fig. 4 Histogram of computer-generated intensity data compared with log-normal and best-fit Gaussian pdf's.

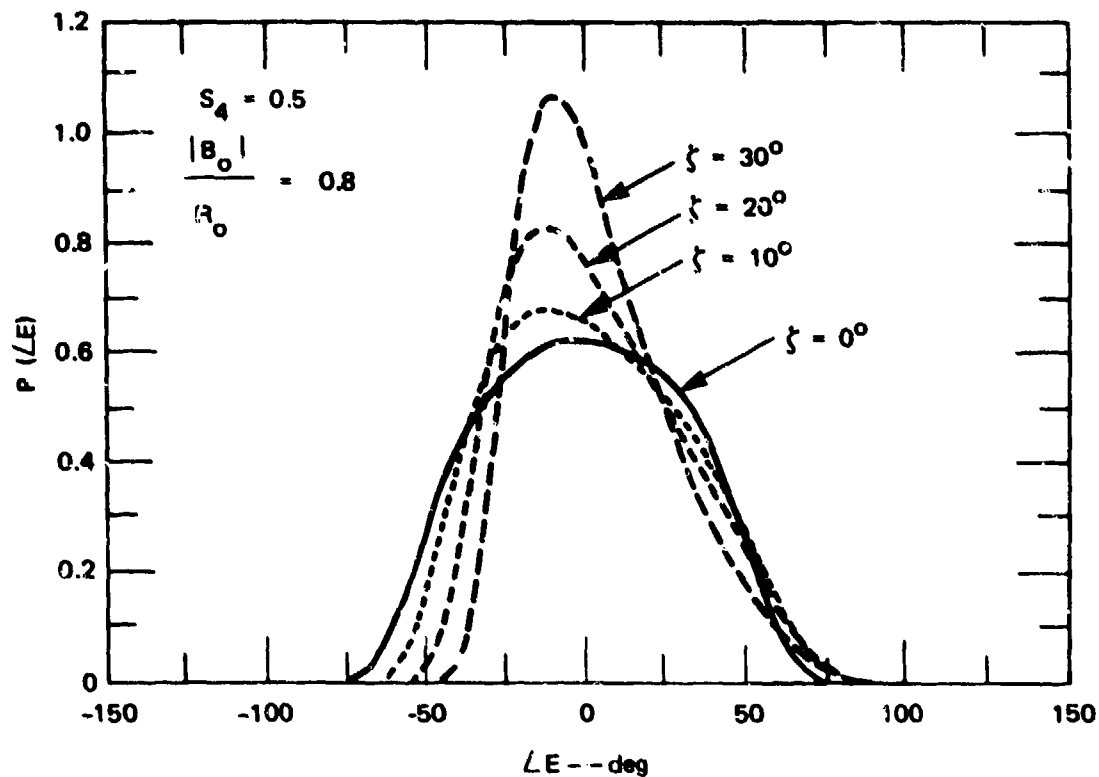


Fig. 5 Calculated pdf's for phase of the received signal.

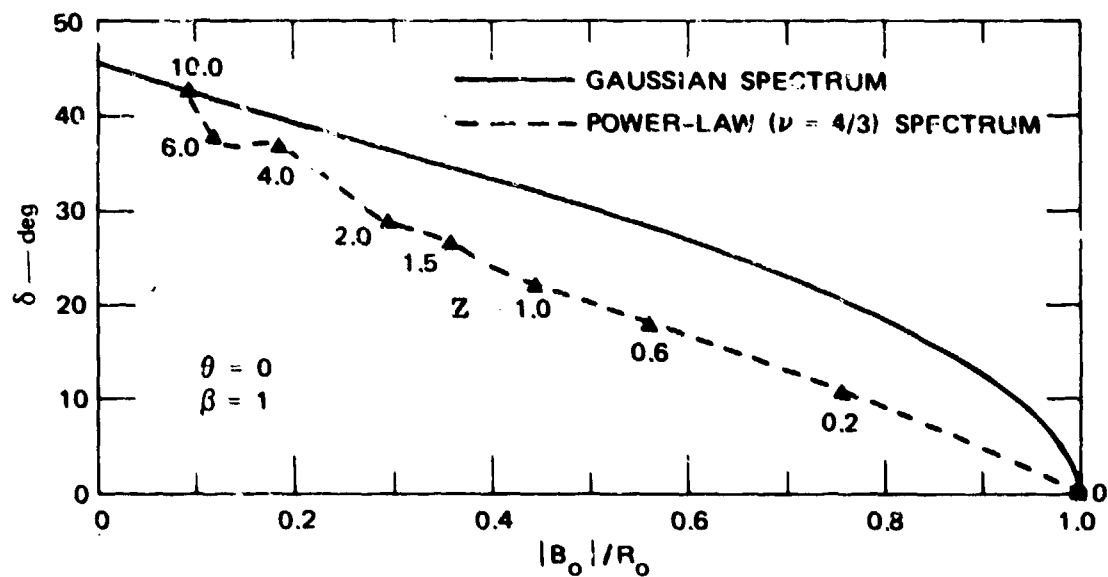


Fig. 6 Variation of ellipse eccentricity and orientation angle during post-scattering propagation.

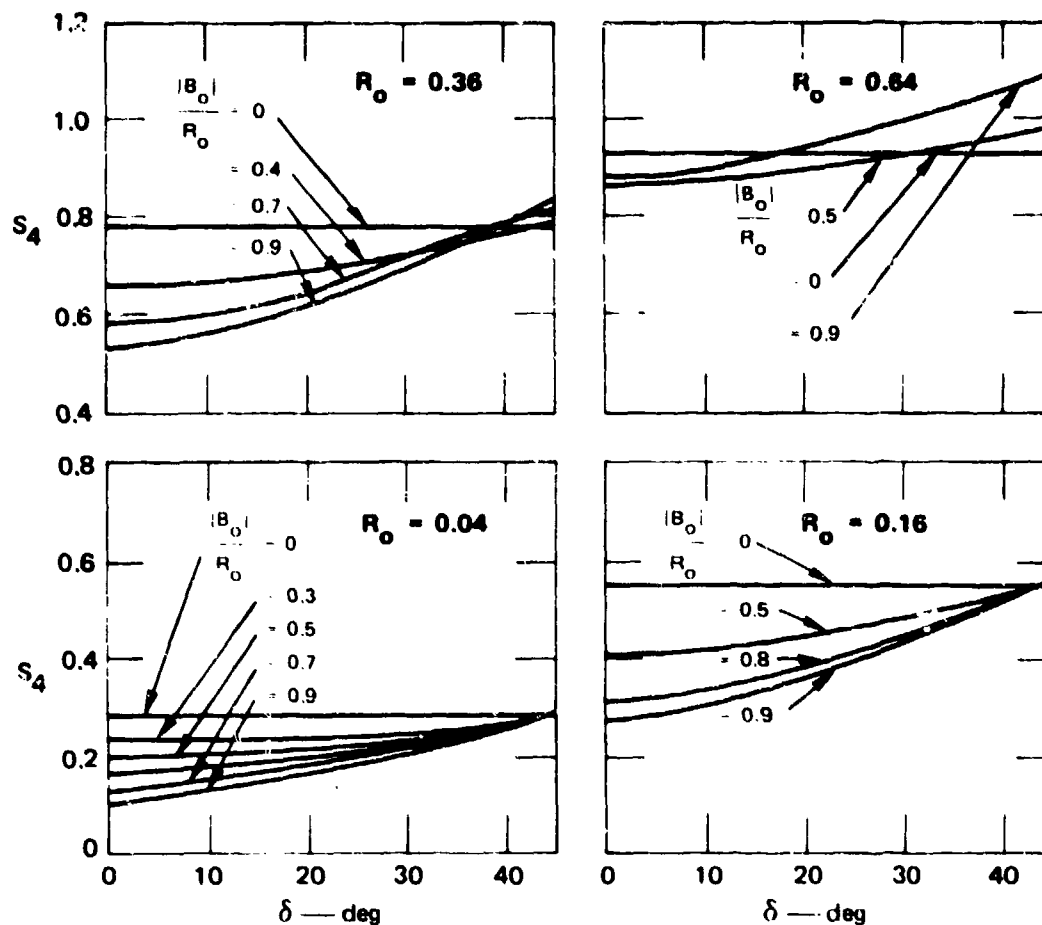


Fig. 7 Variation of scintillation index  $S_4$  with ellipse eccentricity and orientation for four different scattering coefficients.

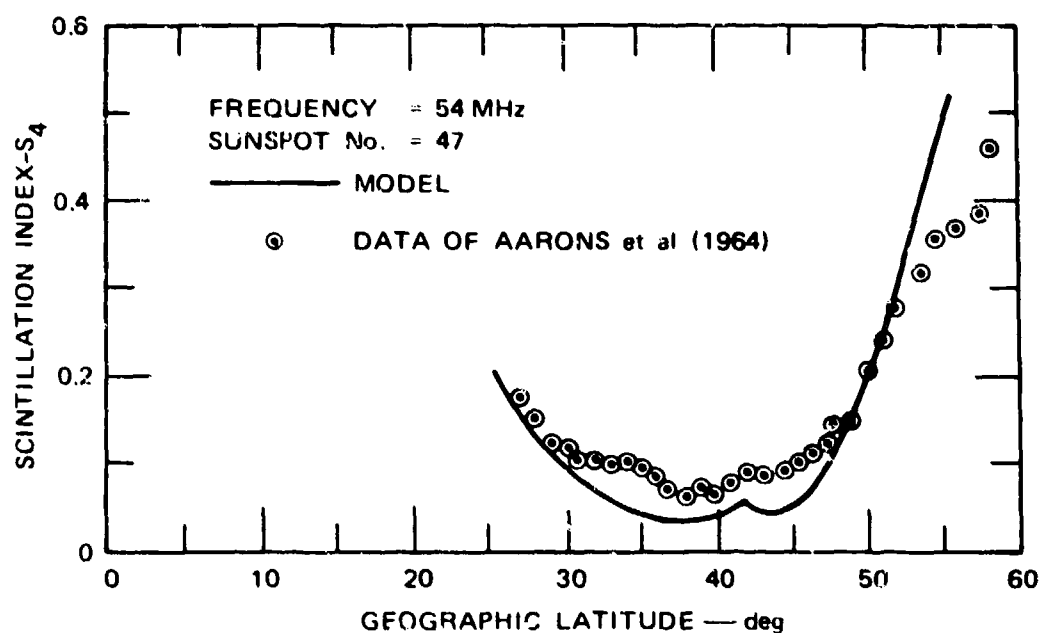
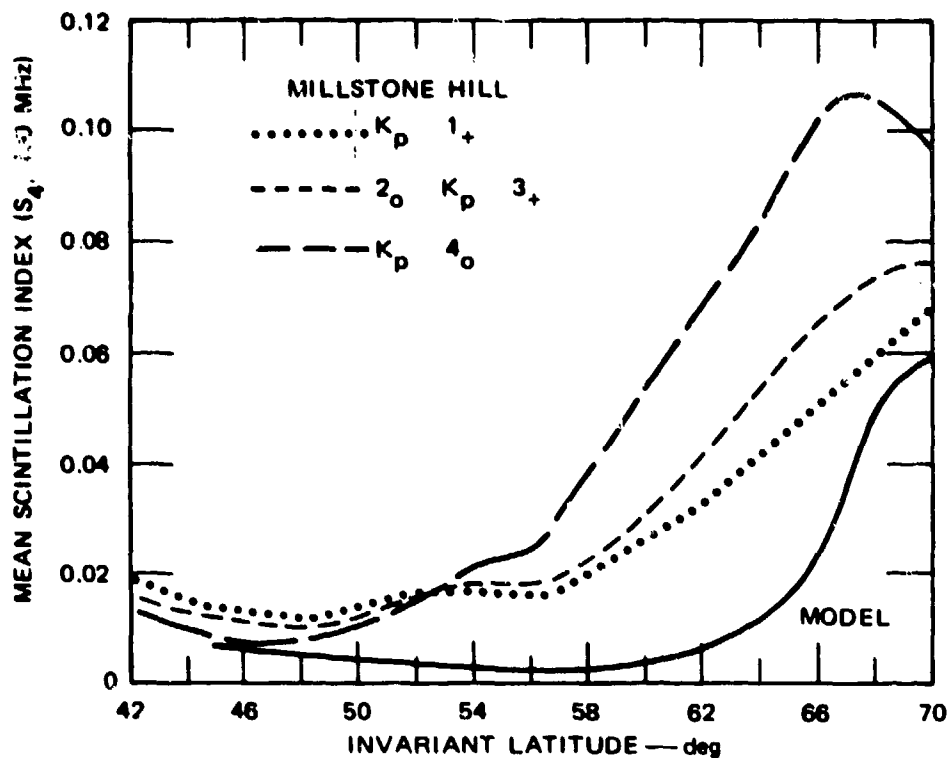


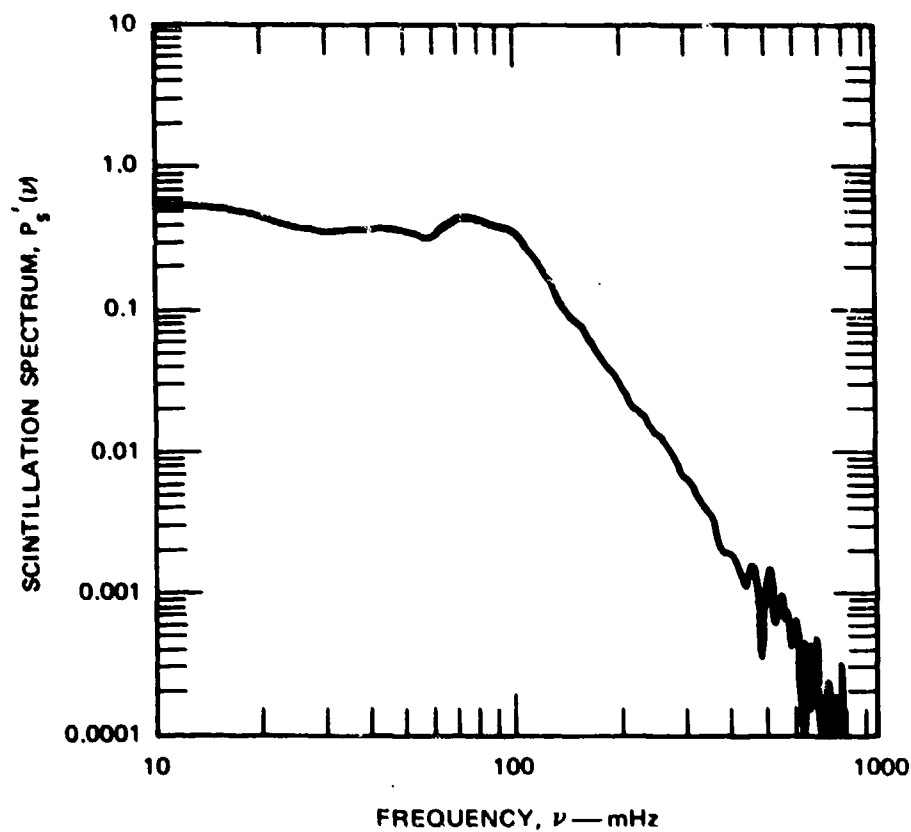
Fig. 8 Comparison of Fremouw and Rino (1973) model with VHF scintillation-index observations performed in the northeast United States.

6-12



SOURCE: Evans (1973)

Fig. 9 Comparison of model with UHF scintillation-index observations performed in the northeast United States.



SOURCE: Rufenach (1972)

Fig. 10 An example of second-order signal statistics: fluctuation spectrum of the received intensity of a scintillating 26-MHz, radio-star signal.

## DISCUSSION

P. HALLEY: In the statistical studies that you have conducted concerning scintillation at the reception of the field emitted by a satellite and having crossed the ionosphere, you have determined the characteristics of the transfer function. What was the measurement time interval used for this purpose? 6-13

In links established by ionospheric reflection between two points on the ground, we noted at CNET that the deterministic as well as the random part of the transfer function presented approximately the same characteristics for three minutes only.

E. J. FREMOUN: The data were grouped in blocks of 1024 samples, and I don't remember the basic sample rate. In the analysis, which was performed by my colleague, Dr. Rino, the mean and standard deviation were calculated for each data block. If either of these moments changed significantly, the data were declared nonstationary. Stationary sets of data were analysed together to reduce statistical variation in the results. Acceptable stationarity usually existed for several minutes in the case of synchronous satellite observations. I think the largest such period was about 45 minutes, but this was unusual. It is certainly true that there are nonstationarities in the signal statistics, arising from nonhomogeneity of the ionosphere's spatial statistics. The nonhomogeneity can have more fundamental influence on the signal characteristics, via the scattering process. Dr. Rino is currently exploring the theoretical aspects of locally (as opposed to strictly) homogeneous statistics, and I'll have to account for the effects in future modeling.

Quasi-deterministic trends arise in scintillation as well as in ionospheric (a form of nonstationarity) reflection.

E. M. FROST: The paper is concerned with the case where the signal is large compared with received background.

In satellite measurements the signal to noise ratio is poor. A problem is to separate the added noise (thermal noise, etc.) from the multiplying noise (scintillation). One clue is that with thermal noise the power output is proportional to pre-detector bandwidth, while this not necessarily so with multiplying noise.

Has the author any advice?

E. J. FREMOUN: Further clues: 1) Two receivers will produce noise that is uncorrelated, while scintillations will be correlated on signals from two receivers--even with antennas separated by many 10's or even hundreds of meters; 2) The fluctuation spectra of the two are different. Bandlimited white noise will, of course, have a spectrum dictated by the receiver. The fluctuation spectrum of scintillation often has a characteristic power-law shape.

F. J. CHESTERMAN: Is the Rice distribution in your slide a Rayleigh or Square Gaussian distribution? Is it the integral of the Gaussian PDF? Considering the vector components there are a family of Rice curves and the Rayleigh is one special case.

E. J. FREMOUN: It is not the integral of the Gaussian PDF.

F. J. CHESTERMAN: Do you find in practice higher order amplitudes in the tail of the distribution than theory predicts? Some departure from theory in practice inevitable.

E. J. FREMOUN: This was not my point. My point was that there are more large-amplitude samples than predicted by log-normal statistics, and that this fact is consistent with Gaussian statistics, which result in a longer "tail" in the amplitude PDF than is the case for log-normal.

H. J. ALBRECHT: Referring to the suitability of scintillation models to describe the enhancement in the equatorial region, it would be interesting to learn whether the model here mentioned could be adapted to this purpose, with particular regard to the ionospheric scintillations recorded on SHF-frequencies as, for instance, in the INTELSAT-net.

E. J. FREMOUN: The same scattering theory should be applicable. However, there are in-situ satellite data showing a structured spatial spectrum in the equatorial ionosphere--i.e., there are "bumps" in the spectrum at preferred spatial frequencies. I suspect that these structured spectra are responsible for the SHF scintillation. It remains to be seen whether the integrals arising in the scattering theory in the presence of such spectra can be solved analytically. If not, then one could evaluate them numerically. In either case, it will be important to know how the spectrum varies with geophysical conditions. When this is established, then it should be quite possible to adapt the model to SHF scintillation, and we hope to do so.

H. J. ALBRECHT: With the theoretical difficulties you just mentioned or with the "bumps" in the spectrum of those scintillations, are you actually referring to properties related to the oscillatory nature of the auto-correlation function?

E. J. FREMOUN: Yes.

J. AARONS: Equatorial scintillations (recently) have been found to have "bumps" or enhancement of particular frequencies.

E. J. FREMOUN:

J. AARONS: Didn't the solar wind analysis show log-normal statistics?

E. J. FREMOUN: They showed that log-normal is more accurate than the amplitude probability density function arising from the special case of Rice statistics. Our results showed that a non-Rician member of the generalized Gaussian statistical family is still more accurate.

# THE INFLUENCE OF PARTICULAR WEATHER CONDITIONS ON RADIO INTERFERENCE

C. Fongler

SIGMA Association  
Alsterkrugchaussee 429  
D-2 Hamburg 63, Germany

## SUMMARY

The various propagation properties of the atmosphere are associated to the variation of the refractive index. A stratified atmosphere shows due to the meteorological parameters a strong change which corresponds for example to variations of parameters as k-factor or radio horizon and noise temperature. The case of an atmosphere with embedded discontinuities is illustrated by experimental results, which were obtained on line-of-sight ground links, links with a distance near the radio horizon, transhorizon links as well as earth-space links. It concludes that most radio interference is to be expected during days with strong radiation and the influence of cold fronts.

## 1. INDEX OF REFRACTION

The propagation properties of the atmosphere for electromagnetic waves are characterized by the dielectric constant  $\epsilon$  and the index of refraction  $n$ , respectively. In the troposphere both depend on the local temperature  $T$  [°K], the pressure  $p$  [mb], and the water vapour  $e$  [mb] according to the relation (valid for frequencies up to about 3 GHz)

$$\sqrt{\epsilon} = n = 1 + \frac{77.6 \cdot 10^{-6}}{T} \left( p + \frac{4.81 \cdot 10^3}{T} e \right).$$

In the general form the dielectric constant is complex, i.e.  $\epsilon = \epsilon_1 + i \epsilon_2$ . For frequencies higher than 3 GHz the imaginary part  $\epsilon_2$  is dominating and herewith absorption due to the presence of water vapour and oxygen as well as precipitation.

This investigation only concerns situations associated with reflection, refraction, scattering, and ducting which result from the local variation of the dielectric constant. These effects dominate at frequencies smaller than 3 GHz and they are active besides the absorption at frequencies higher than 3 GHz which is not treated here.

The difference between the index of refraction of vacuum ( $n = 1$ ) and the actual one at the earth's surface has the amount of some  $10^{-3}$ . It is convenient to introduce the refractivity  $N$

$$N = (n - 1) \cdot 10^6.$$

Figure 1 shows the dependence of the refractivity  $N$  on the temperature  $T$  and the relative humidity  $RH$  at a pressure of  $p = 1000$  mb. The value of  $N = 320$  corresponds for instance to  $t = 20$  °C and  $RH = 50$  %.

If we consider the boundary of two air masses 1 and 2 we get a discontinuity in refractivity  $\Delta N = N_1 - N_2$ . For air masses with the same temperature ( $t = 10$  °C) and pressure ( $p = 1000$  mb) but a different relative humidity  $RH_1 = 100$  % and  $RH_2 = 50$  %  $\Delta N$  amounts  $\Delta N = 30$ .

Concerning ionospheric propagation the index of refraction is characterized by the density of free electrons  $N_e$  [cm<sup>-3</sup>] and the frequency of the incoming wave. Here the value  $\Delta N = 30$  against vacuum is reached for instance if we assume an electron density of  $8 \cdot 10^3$  cm<sup>-3</sup> at 100 MHz and  $8 \cdot 10^5$  cm<sup>-3</sup> at 1 GHz, respectively (Figure 2).

## 2. ATMOSPHERIC STRUCTURE

If the index of refraction is not equal one but constant no influence on the straight-line propagation will occur. Only the variability of temperature, humidity, and pressure in time and space due to the present structure of the atmosphere induces a variability of refractivity and effects the electromagnetic wave propagation.

## 2.1 THE NORMAL HORIZONTAL STRATIFICATION

Due to the force of gravity of the earth the density of the air decreases exponentially with height; therefore the air is horizontally stratified around the earth's surface. The corresponding refractivity decreases like the density of the air exponentially with the height  $h$  to

$$N(h) = N_s \exp\left(-\frac{h}{H}\right) \quad (1)$$

where  $N_s$  is the value of  $N$  at the height zero (assumed to be the height of the surface) and  $H$  is the scale height. This profile is introduced as standard atmosphere. The relation (1) can be linearly approximated by

$$N(h) = N_s \left(1 + \frac{1}{N_s} \frac{\partial N}{\partial h} h\right) \quad (2)$$

where  $\frac{\partial N}{\partial h}$  is assumed to be constant. Introducing  $\Delta N(h) = N_s - N(h)$  and choosing  $h = 1$  km, we get for  $\frac{\partial N}{\partial h} \sim \frac{\Delta N}{h} = N_s - N_{1\text{km}}$ . The value  $N_s - N_{1\text{km}}$  as well as  $N_s$  are averaged and world-wide known (Bean, B.R. et al 1960).

In the assumed profile of the atmosphere the rays are bended. Considering the ray equation for a concentrically stratified medium together with (2) the rays can be considered as straight lines if a new, effective earth's radius  $R_{\text{eff}}$  is introduced by the relation

$$R_{\text{eff}} = k R_0 \quad \text{with} \quad k = \frac{1}{1 + R_0 \frac{dn}{dh}} \quad (3)$$

with  $R_0 = 6375$  km.

The standard atmosphere can be approximated by  $k = 4/3$ . But in the real case  $k$  depends on the present structure of the troposphere and the values of  $k$  vary between 1 and 3 (temperate climate). The case  $k = 1$  corresponds to  $\frac{dn}{dh} = 0$  and the case  $k = 3$  to  $\frac{dn}{dh} = 104.5 \cdot 10^{-6} \text{ km}^{-1}$ . The derived value of the radio horizon  $d$  (Figure 3)

$$d = 3.57 \cdot \sqrt{k} \cdot \sqrt{h} \quad (4)$$

with  $h$  = height of the transmitter antenna yields for the assumed values of  $k$  the distribution of Figure 4. Concerning  $h = 400$  m the radio horizon varies between 71 and 124 km corresponding to  $k = 1$  and  $k = 3$ .

The E-field inside the line-of-sight area is evaluated by the superposition of the direct and the indirect rays. Near the radio horizon this interference field passes over to the diffraction field characterized by a rapid field strength decrease with distance from the transmitter for the here treated wave lengths of the UHF range as well as shorter waves. The location of this transition zone varies due to the value of  $k$ . If the location of the radio horizon is moved to greater distances from the transmitter the level of field strength increases considerably beyond the horizon previously defined by the standard atmosphere.

## 2.2 THE ATMOSPHERE WITH EMBEDDED DISCONTINUITIES

With regard to reality there are more or less wide-spread discontinuities embedded in the normal stratified atmosphere. These discontinuities result from air masses which differ in temperature and humidity from the surroundings. These different air masses correspond to dynamic processes in the atmosphere like radiation, advection, subsidence, and turbulence. Areas of different air masses correspond to areas of different refractivity. For mathematical treatments it is assumed that they are separated by a boundary. By these boundaries effects like reflection, refraction, and ducting are stimulated as well as focussing and defocussing which are present if the waves are not only considered as rays but also as beams. Enhancement as well as diminishing of field strength follow compared with the field strength associated with a standard atmosphere. These effects cannot be neglected if the incidence at the boundary occurs with small grazing angle. Phase effects will appear at every direction of incidence.

A similar situation arises in the ionosphere if there are embedded areas of different concentration of free electrons compared with the surroundings. It can be shown that this kind of ionospheric areas will be active up to 100 GHz if the thick-

ness is sufficient (Fengler, G. 1972).

## 2.3 NOISE

The sky noise depends on frequency. Up to 1 or 3 GHz the cosmic noise is dominating; it is a function of geographical location, season, and daytime. At higher frequencies the main contribution of noise originates from water vapour and atmospheric gases. The influence of precipitation is not considered here. At these frequencies the noise therefore depends on air masses along the path and herewith on the direction of the antenna. If in the considered direction only dry air masses are present, the noise temperature is smaller than in the case of wet air masses. In order to come to an estimation of the influence of different air masses, the sky noise for dry air (relative humidity 50 %) and for very wet air (relative humidity 100 %) at a temperature of 23 °C and elevation angles of 90° and 30° was derived from calculations (Hogg, D.C. and Semplak, R.A. 1961) and is represented by Figure 5. Table 1 shows the sky noise temperature for 10 GHz and 6 GHz. Concerning the differences of sky noise temperature between relative humidities of 50 % and 100 % follow some degrees Kelvin for high elevation angles (90°) and about 10 degrees Kelvin for smaller elevation angles (30°).

Table 1 Sky noise temperature in dependence on relative humidity RH. & elevation angle

RH		10 GHz		6 GHz	
		50 %	100 %	50 %	100 %
$\vartheta = 90^\circ$	sky noise	3.8	9	3.0	4.2
$\vartheta = 30^\circ$	tempera- ture	7.0	18	8	16

## 3. EXPERIMENTAL RESULTS

The influence of particular weather conditions on various kinds of radio services is studied with experimental links. i.e. line-of-sight ground links, links with path lengths near the value of the radio horizon, transhorizon links, and space-earth links.

### 3.1 LINE-OF-SIGHT GROUND LINKS

From line-of-sight links, i.e. links with the distance transmitter - receiver within the radio horizon, numerous measurements are known which show the influence of the troposphere. Such links are characterized by small variations of the average field-strength level. However, during the morning and the early night of calm days with strong radiation fadings can be observed with depths up to 50 dB (Großkopf, J. 1970), in particular if running over moist ground. These deep fades are in accordance with the conception of the formation and deformation of ground-based discontinuities.

### 3.2 FIELD STRENGTH NEAR THE RADIO HORIZON

Comparing the diurnal variation of the mean field strengths at the receiver of a path with a length of about the distance of the radio horizon ( $k = 4/3$ ) with line-of-sight links as well as transhorizon links of sufficient path length we get a large diurnal variation of the field in the area near the radio horizon. This is due to the diurnal variation of the factor  $k$  (Figure 4). In Figure 6 the mean diurnal field-strength variations of paths of 115 km, 200 km, and 320 km at 0.5 GHz are plotted for days with strong radiation. The variations result from radiation processes in the lower troposphere (Fengler, G. 1964). In opposition to links over land, which are treated here, links over sea show no pronounced diurnal variation because of the heat retaining capability of water.

### 3.3 TRANSHORIZON LINKS

If only the presence of the standard atmosphere is presumed transhorizon links should have field strengths nearly constant with time due to scattering as the predominating propagation mechanism. In reality these links show field-strength variations according to the influence of embedded discontinuities in the troposphere (Figure 6). An example of this influence gives a detailed analysis of field strengths observed on paths of 115 km, 200 km, 270 km and 320 km lengths at a frequency of 0.5 GHz over three days (Figure 7, Fengler, G. 1964). A pronounced dependence on the



height of the layer over the paths can be clearly seen from this example. This correlation was confirmed by the statistical evaluation of a great number of field strength recordings with respect to the presence of the height of the simultaneously observed discontinuity.

Other observations show the influence of a front passage on the field strength. Due to the variation of the turbulence properties in the area of a front the scatter field diminishes (Albrecht, H.J. 1968).

### 3.4 EARTH - SPACE LINKS

Due to the ray bending in the standard atmosphere the rise time of an orbiting satellite in a height of 750 km has an anticipation of about 4 sec. in opposition to the geometrical path (without atmosphere). The set time has a corresponding delay of 4 sec. However, the analysis of a great number of observations of rise time at 0.136 GHz show in about 50 % of all cases deviations from the calculated value of 4 sec. and in about 15 % considerable deviations which are due to particular weather conditions (Table 2; Fengler G. 1971).

**Table 2** Satellite rise time (by radio measurement) and corresponding meteorological conditions

Radio effect (136 MHz)	Meteorological Condition
anticipation > 30 sec	cold front in direction of satellite
delay 0 to 60 sec	thrust of wet warm air in direction of satellite
delay > 60 sec.	strong discontinuities in strong high pressure system

It follows that very strong discontinuities during days with strong radiation in the central area of an extensive high pressure system and embedded warm and wet air masses cause a delay of rise time. This result can be interpreted in terms of ray deflection or defocussing at boundaries in suitable position. Otherwise an anticipation of rise time is observed if the observations of the satellite signals occur at the periphery of a high pressure system and when in particular the influence of a cold front is effective. The interpretation of the anticipation of rise time due to the meteorological conditions follows in terms of ducting processes at the boundary between warm and cold air and the ground. Disturbances due to these meteorological conditions are confirmed by other observations.

### 4. CONCLUSIONS REGARDING TO RADIO INTERFERENCE

Considering radio interference the preceding results according to field strength enhancements compared with field strength corresponding to the standard atmosphere are of particular interest. It was found that field strength enhancements can be explained by an increase of the k-factor and herewith by an increase of the radio horizon, by reflection and ducting processes due to the presence of ground-based and free discontinuities in suitable position and intensity as well as by the influence of cold fronts. The common weather conditions belonging to the described effects are the presence of a pronounced high pressure system where radiation causes the formation of discontinuities or where boundaries arise by advection in face of cold air masses. The more these weather situations are pronounced the stronger should be the effect, i.e. the enhancement of field strength. Enhancement of field strength means enlargement of the range of the considered service, that often means interference with other services operating on the same frequency. Of same interest is of course the case of diminishing of field strength which promotes interference, too, if it becomes necessary to increase the sensibility of the receiver. It was outlined that this will occur with satellite paths in the centre of strong high pressure systems as well as in connection with a thrust of warm and wet air followed by a cold front.

The importance of a high pressure system for the occurrence of extended radio ranges results also from investigations done by Fehlhaber and Großkopf (1968).

Although most of the observations are concerned with the VHF- and UHF-ranges it has to be expected that outlined weather conditions will effect other frequencies too; but not in such a severe form like precipitation is doing.

## REFERENCES

1. Albrecht, H.J., 1968, "Theoretical analysis of medium-dependent fluctuations with tropospheric scatter links and comparison with new experimental data including side-scatter characteristics". AGARD CP No.37, Pos. 16
2. Bean, B.R. et al, 1960, "Climatic charts and data of the radio refractive index for the United States and the world", NBS Monograph 22
3. Fehlhaber, L. and Grosskopf, J., 1968, "Häufigkeit und Ursachen von troposphärisch bedingten Überreichweiten", FTZ A 455 TBr 4
4. Fengler, G., 1972, "The phase of a plane electromagnetic wave transmitting a wide-spread atmospheric discontinuity". AGARD-CP-107, Pos. 3
5. Fengler, G., 1964, "The influence of inversions on UHF-propagation over land". Proc. 1964 World Conf. on Radio Meteorology, Boulder, Col., pp.80-83
6. - , 1971, "Tropospheric effects on the propagation of VHF-satellite signals", Kleinheubacher Berichte, Vol. 14, p.59.
7. Grosskopf, J., 1970, "Wellenausbreitung I", BI-Hochschultaschenbücher 141
8. Hogg, D.C. and Semplak, R.A., 1961, "The effect of rain and water vapor on sky noise at centimeter wavelengths", The Bell System J., Vol. 40, 1331

7-6

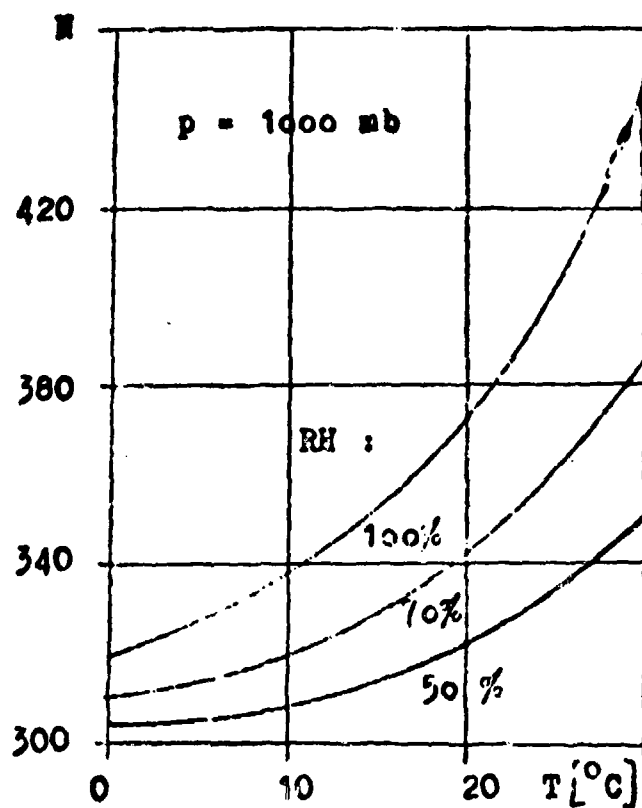


Figure 1 Refractivity  $N$  in dependence on temperature  $T$  and relative humidity  $RH$

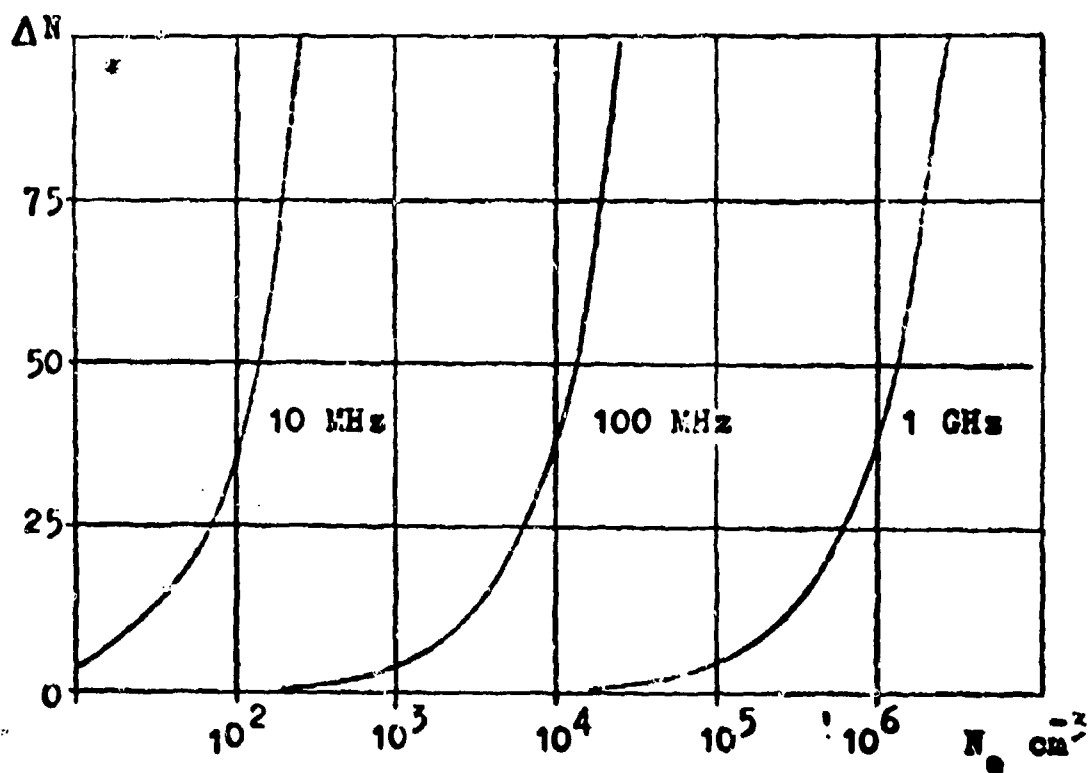
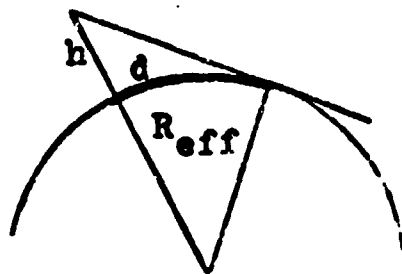


Figure 2 Difference between actual refractivity and vacuum in dependence on concentration of free electrons and frequency



7-7

Figure 3 Geometry of radio horizon

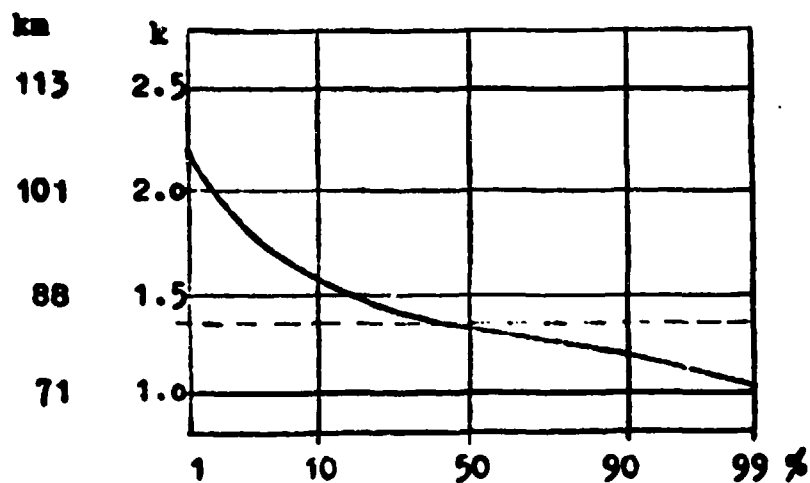


Figure 4 Statistical distribution of k-factor /7/

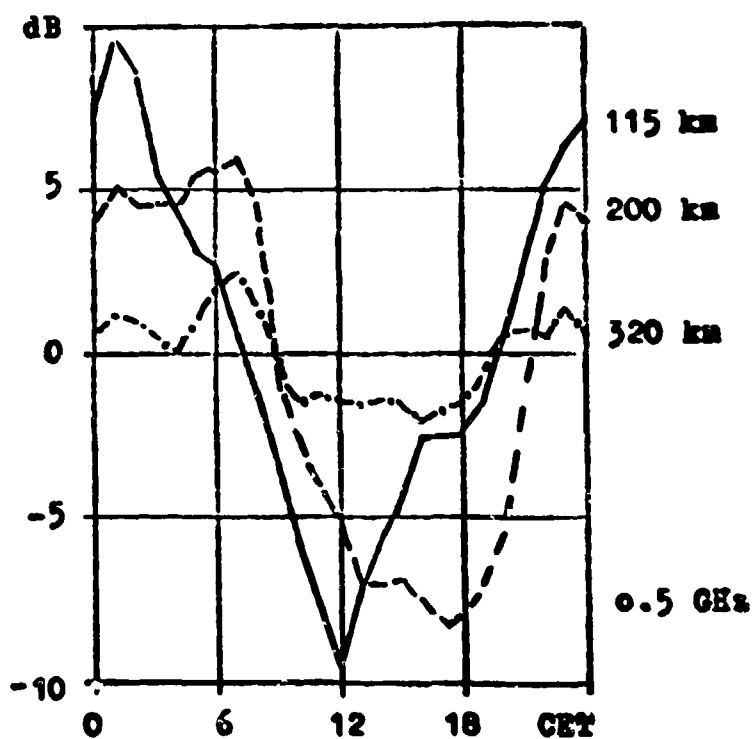


Figure 6 Diurnal variation of field strength (0.5 GHz) on days with strong radiation in dependence on path length. — 115 km, ---- 200 km, -.-.- 320 km

7-8

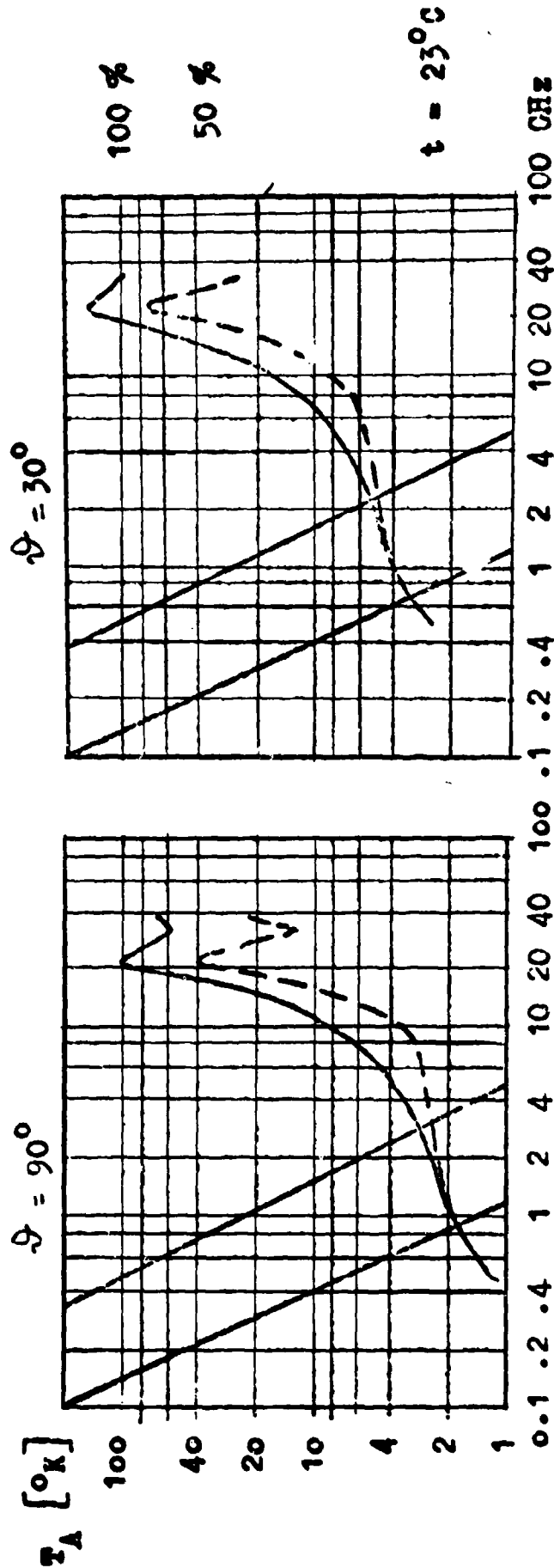


Figure 5 Sky noise temperature in dependence on frequency and relative humidity (RH) for  $t = 23^{\circ}C$  and elevation angle a)  $\vartheta = 90^{\circ}$ , b)  $\vartheta = 30^{\circ}$ .  
 ----- RH = 50 %, ——— RH = 100 %, within straight lines: range of cosmic noise

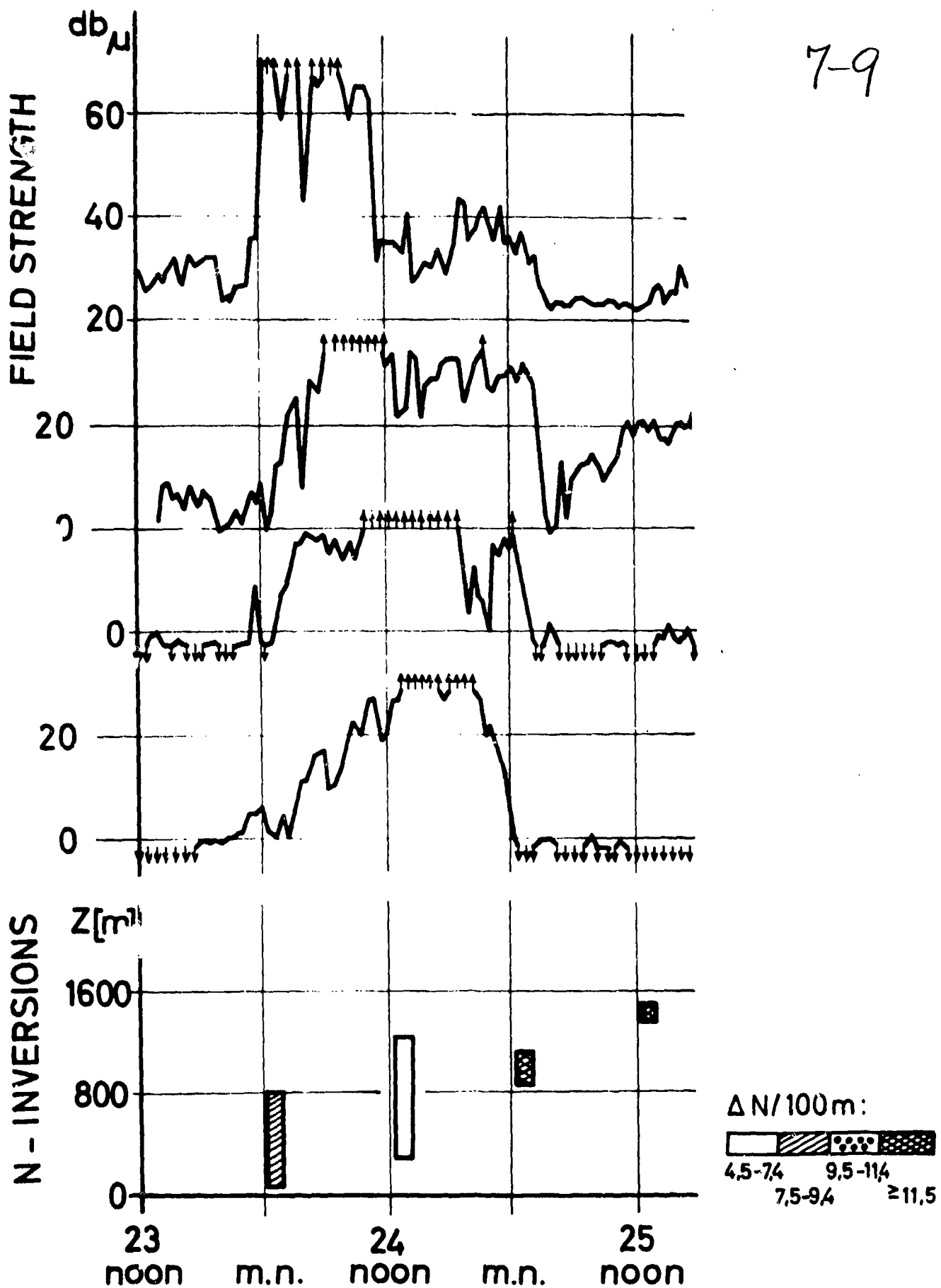


Figure 7 Variation of field strength associated with the variation of the altitude of a discontinuity /5/

## DISCUSSION

E. CHIARUCCI: Data on the minimum value of the tropospheric index  $k$  as a function of distance are known and have been published (for a given climate). These data are currently used to determine the minimum distance to the radio horizon and path clearance for line-of-sight communication systems; however, from the standpoint of interference, what one would like to know is something about the maximum values of  $k$  which are not exceeded for a given percentage of the time, say 99.9%. Does the speaker know of any published experimental data in this sense?

C. FENGLER: I do not know of any published data for this part of the distribution of  $k$  values.

## LES CHARGES ELECTROSTATIQUES ET LES PERTURBATIONS QU'ELLES ENTRAINENT DANS LES LIAISONS RADIOELECTRIQUES

C. Pévrot, SEPTIM, 19, rue Lagrange, 75005 Paris, France

### Introduction

Les charges électrostatiques qui se créent dans l'atmosphère peuvent générer des décharges atmosphériques susceptibles de détruire, tout ou partie, d'un aéronef ou d'un engin et en tous cas de perturber fortement le fonctionnement des liaisons radio, des calculateurs, etc ...

L'exposé présent ne traitera pas de cet aspect très important du problème. D'autres types de charges perturbent, par différents mécanismes, les télécommunications. Ce sont celles qui se déposent, se créent, s'évacuent ou se recombinaient à la surface de l'aéronef.

### I.1. L'équipotentialité de la surface des aéronefs :

Les charges électrostatiques qui se créent à la surface des aéronefs auront une action très différente suivant que la surface de l'aéronef est isolante ou conductrice.

Or, il est évident que la surface d'un aéronef ne peut être intégralement conductrice, ne serait-ce que par la nécessité de recevoir, sur les antennes, les champs électromagnétiques extérieurs.

a) les charges qui se répartissent sur une surface métallique, en raison de la bonne conductibilité d'une telle surface et de la faible valeur des charges, on pourra considérer cette surface comme parfaitement équipotentielle. Mais, et c'est là où réside le phénomène important, la différence de potentiel entre la surface et l'air ambiant peut être très importante.

b) les charges qui se créent, séjournent et se recombinaient sur les surfaces isolantes, là également les différences de potentiel peuvent être élevées entre ces surfaces et l'air ambiant, mais également entre deux points de la surface même très proches.

### I.2. La création et l'évacuation des charges électrostatiques :

Le tableau ci-dessous que nous commenterons en II. schématise l'origine des charges électrostatiques :

	influence des champs électriques extérieurs
Création et évacuation par un phénomène lié au milieu ambiant	frottement sur les particules neutres et triboélectricité
	collecte de charges préexistantes.
Création et évacuation par un phénomène lié à l'aéronef	évacuation par les déperditeurs de potentiel - involontaires - volontaires
	évacuation par les gaz ionisés des moteurs.

Nous n'incorporons pas, dans ce tableau, les créations ou évacuations de charges dans des circonstances particulières :

- freinage au sol sur une piste sèche,
- séparation des étages d'une fusée,
- ravitaillement en vol,
- etc ...

### I.3. L'influence des charges électrostatiques sur l'environnement et les communications radioélectriques

Sur le plan purement radioélectrique, la présence des charges électrostatiques se traduit par :

- a) lorsqu'elles sont relativement peu nombreuses, l'augmentation du bruit de fond (bruit blanc ou peu différent du bruit blanc)
- b) lorsqu'elles sont importantes, par des décharges se traduisant par un brouillage intense.

Création des charges : le rôle joué par la météorologie

### II.1. Influence des champs électriques extérieurs

Dans une atmosphère non chargée, mais où règne un champ électrique, il y a fatalement une différence de potentiel entre la structure conductrice et l'atmosphère. Or, de tels champs existent au voisinage du sol ou d'un cumulo-nimbus, par exemple.

### II.2. Frottement et triboélectricité

C'est la source de charges électriques la plus fréquente. Un nuage de cristaux de glace, de poussières industrielles, de sable, etc ... est constitué d'un très grand nombre de microparticules. Entraînées par le vent, ces particules frottent notamment sur les bords d'attaque et dans certains cas sont rompues par lui. Or, ces phénomènes s'accompagnent de la création de charges électriques.

.../...



Il est évident que l'étude de ces phénomènes n'est pas simple car :

8-2

1. Il n'existe pas de moyen au sol permettant d'étudier de tels phénomènes dans les conditions réelles. Une soufflerie restituant l'ambiance en régime supersonique à haute altitude, à échelle 1, est, pour le moment du moins, du domaine de l'utopie.
2. L'étude en modèle réduit n'est pas envisageable car la dimension et la forme des cristaux jouent sûrement un grand rôle et il paraît difficile de réaliser des cristaux de la dimension voulue ayant une réelle homothétie.
3. L'étude directe en vol est possible, mais comme les charges dépendent beaucoup des conditions météorologiques, il est indispensable d'effectuer beaucoup d'heures de vol pour retrouver les mêmes conditions d'ambiance.

Cette dernière méthode a déjà fourni cependant un certain nombre de lois que nous résumons ci-dessous :

- a) la charge de l'aéronef par frottement ou par triboélectricité rend toujours l'aéronef négatif par rapport à l'air ambiant,
  - b) le champ électrique autour de l'aéronef résulte de la combinaison du champ dû aux charges abandonnées sur l'avion avec le champ dû aux charges spatiales qui, créées après la percussion du cristal, sont entraînées par celui-ci,
  - c) les cristaux de glace sont, à densité égale, infiniment plus actifs que les gouttes d'eau des nuages bas.
4. Les charges créées augmentent, toutes choses égales par ailleurs, avec la vitesse, la section droite, etc ...

### II.3. La captation des charges électriques prééxistantes

Il existe, le phénomène est connu depuis longtemps, des nuages constitués de particules de glace ou d'eau chargées positivement ou négativement.

Dans un cumulo-nimbus l'aéronef peut traverser, suivant son altitude et sa position par rapport à l'axe (si l'on ose s'exprimer ainsi), des zones de charges positives, négatives ou des zones de charges alternativement positives et négatives et réciproquement.

Or, ces charges sont extrêmement importantes et peuvent être transportées en quasi-totalité sur l'aéronef. Ce phénomène de "captation" peut masquer totalement l'effet de frottement et l'effet de triboélectricité.

L'aéronef pourra être donc positif ou négatif, par rapport à l'air ambiant et ce avec des tensions extrêmement élevées.

### II.4. L'évacuation des charges électriques par les déperditeurs de potentiel, volontaires ou non, ou l'évacuation des charges électriques par les pointes :

Il est notoire que lorsqu'un conducteur électrique est chargé, au voisinage des pointes, les charges statiques ont tendance à s'évacuer. Le phénomène connu depuis longtemps s'applique heureusement et malheureusement au cas qui nous occupe. En effet, on place, depuis de nombreuses années, sur des aéronefs, des déperditeurs de potentiel qui sont tous basés sur la propriété des pointes. Mais il existe également des déperditeurs involontaires : ce sont les angles vifs de certaines pièces, ce sont les antennes lorsqu'elles ne sont pas encastrées. En résumé, tout ce qui possède une courbure plus ou moins accentuée est susceptible d'évacuer des charges électrostatiques.

Ce phénomène se produit avec un seuil. Malheureusement, les bruits de fond auxquels nous avons fait allusion dans les généralités se produisent bien avant que ces évacuations commencent. D'autre part, il n'est pas possible de faire évacuer par une pointe un courant extrêmement intense en raison de la création des charges spatiales qui freinent le phénomène.

L'étude même de la décharge des pointes dans des conditions d'ambiance d'un aéronef est assez mal connue.

Nous reviendrons plus loin sur l'aspect de la décharge par les pointes en parlant des perturbations qui peuvent se produire sur les antennes lorsque le potentiel de l'aéronef dépasse une valeur exagérée.

### II.5. Evacuation des charges électriques par les gaz ionisés chauds

Tous les aéronefs possèdent des moteurs assurant la propulsion de ceux-ci. Nous donnons au mot "moteur" un sens extrêmement général. Si on regarde, sur le plan global, ceci veut dire qu'en utilisant souvent le comburant de l'air, parfois un comburant propre à l'engin, on expulse des gaz plus ou moins chauds vers l'extérieur. Or, ces gaz ont une ionisation spontanée du fait de la température élevée. Si l'ionisation est négligeable, dans beaucoup de cas, il n'en est pas de même pour les moteurs à réaction à haute température et encore moins pour les tuyères des engins, les gaz expulsés sont extrêmement chauds ; 1500° ne sont pas rares.

Puisque les gaz sont ionisés, ils possèdent des charges plus et des charges moins. Si les charges étaient expulsées en quantités identiques, il est évident que la charge de l'avion n'en serait pas affectée mais il n'en est pas ainsi, d'abord parce que les vitesses propres des ions ne sont pas identiques suivant leurs signes, mais également parce que lorsque l'aéronef est chargé le champ électrique créé modifie la répartition de ces charges.

.../...

En tout cas, un fait expérimental très net est le parallélisme entre la charge électrostatique d'un avion rapide et la position des manettes des gaz ainsi que la suppression totale de toute charge électrostatique en post-combustion.

### Les brouillages

Nous avons dit plus haut que les charges électrostatiques brouillent les télécommunications et ce par divers mécanismes.

#### III.1. Augmentation du bruit de fond dans les récepteurs au sens général du mot

Nous avons dit que les charges électrostatiques étaient générées notamment par triboélectricité, frottement ou captation. Dans tous les cas, ceci veut dire que, lorsqu'une charge arrive le potentiel de l'avion monte d'une façon discontinue. Or, ces charges sont loin d'être unitaires, c'est à dire que la captation d'une goutte d'eau chargée dans un cumulo-nimbus correspond non pas à un électron mais à plusieurs centaines et même plusieurs milliers d'électrons et ce d'une façon quasi-instantanée. Ces marches d'escaliers dans le potentiel de l'avion se traduisent on le sait par l'augmentation du bruit de fond.

Il en est de même pour les déperditeurs de potentiel, lorsqu'un électron quitte la pointe, volontaire ou non, d'un déperditeur de potentiel, il s'accompagne, par avalanche, d'un nombre relativement élevé de descendantes. Enfin, le phénomène principal concerne les antennes encastrées et les surfaces isolantes où il peut se créer des charges à la fois positives et négatives qui vont se recombiner au fur et à mesure de leur augmentation, ces recombinaisons amenant la disparition des charges certes mais aux dépens de la création fugitive d'un courant électrique. Toutes ces causes multiples font que le bruit de fond augmente en fonction des charges. D'ailleurs, l'expérience a été faite maintes fois : plus la charge électrostatique est élevée, plus le bruit de fond est important.

Des mesures, qui ne sont pas très précises, confirment que les bruits de fond sont pratiquement des bruits blancs. Ils sont d'autant plus "bruits blancs" que la dimension des particules génératrices de charges électrostatiques est petite. Ainsi, lorsqu'un aéronef est chargé, par suite de frottement des cristaux de glace, de cirrus légers, autant que les mesures permettent de l'affirmer, on obtient, sur les antennes, un bruit blanc intégral. Par contre, lorsqu'il s'agit de traverser des couches de nuages où la densité des charges est très élevée, le bruit est loin d'être blanc, les composantes basse fréquence prenant le pas sur les composantes H.F. dans les parasites de bruit de fond recueillis.

#### III.2. Les parasites par amorçage des décharges

Si le potentiel de l'aéronef continue de monter, il va se superposer au phénomène de bruit que nous venons d'évoquer, le phénomène de décharge électrique qui sera cause de parasites infiniment plus intenses.

Lorsque le potentiel augmente, les électrons qui sont issus de la pointe vont créer une filiation de plus en plus nombreuse et de cette filiation elle-même va arriver à se créer une autre filiation. On a amorcé une décharge en avalanche. Cette décharge en avalanche s'accompagne en général d'émission de lumière, mais elle s'accompagne surtout de courants relativement intenses et de parasites extrêmement importants.

Le phénomène s'accroît encore lorsque la décharge peut s'amorcer sur une antenne proprement dite. Ainsi une antenne encastrée peut être perturbée par des décharges qui s'amorcent à la surface même de l'isolant mais également une antenne type "fouet" peut très bien, à un moment donné, jouer le rôle de déperditeur de potentiel involontaire et on conçoit aisément que l'amorçage d'une étincelle sur une antenne proprement dite perturbe le fonctionnement des appareils radioélectriques qui sont liés à cette antenne.

#### Généralités sur la métallisation des aéronefs

La métallisation des aéronefs devrait, sur le plan des charges électrostatiques, être totale, c'est à dire que l'enveloppe extérieure de l'aéronef devrait être constituée d'un corps conducteur. Certes, cette conductibilité superficielle n'a pas besoin d'être excellente comme dans le cas d'un foudroiement mais elle a besoin d'être impeccablement continue.

#### IV.1. Les imperfections de la métallisation superficielle

Cette métallisation superficielle ne peut pas être parfaite pour des raisons extrêmement variées.

Passons en revue ces différentes raisons :

- a) des raisons purement chimiques,
- b) l'utilisation de peintures à des fins d'identification,
- c) l'existence des antennes encastrées,
- d) l'existence des pièces transparentes,
- e) enfin, pour des raisons purement mécaniques, on s'oriente de plus en plus vers l'utilisation de matériaux plastiques, plus légères à résistance égale.

#### IV.2. Protection par des couches superficielles

Il n'est pas indispensable d'avoir une conductibilité parfaite pourvu que celle-ci soit continue. En effet, les courants de véhicule sont toujours très faibles et même si la résistance superficielle n'est pas nulle ou négligeable, les différences de potentiel entre deux points de l'aéronef seront, en tout état de cause, très faibles.

Le problème se scinde en deux :

1. peut-on trouver une peinture transparente dont la conductibilité soit indifférente ?  
On souhaiterait même qu'elle soit excellente,

2. et des peintures dont la résistivité peut être relativement élevée amenant ainsi à chercher un compromis entre le désir de supprimer les charges électrostatiques donc à diminuer le bruit dans le récepteur et le désir de ne pas stopper le passage des ondes radioélectriques, c'est à dire de laisser le signal atteindre l'antenne.

Malheureusement il faut chercher des peintures, en accordant à ce mot un sens très général, qui possèdent des qualités difficiles à trouver. Ces "peintures" doivent être solides mécaniquement, résister à l'abrasion, résister aux agents chimiques, résister aux fortes doses d'ozone que l'on trouve dans la haute atmosphère, résister aux grands froids ainsi qu'à la grande chaleur, résister à la dépression, aux passages dans l'eau, bref on demande à ces peintures des qualités assez exceptionnellement rassemblées et dans ce sens des travaux nombreux ont été entrepris déjà et le sont encore.

On ne peut dire si ces travaux donneront satisfaction totalement, ensuite il ne faut pas oublier que les questions de prix sont tout de même à considérer.

#### Conclusions

Les charges électrostatiques ont une influence néfaste sur les télécommunications, ceci est bien connu, mais il faut reconnaître que l'on s'est habitué à cet inconvénient, dans l'impossibilité de lutter contre.

A l'heure actuelle où le problème des communications devient de plus en plus important, où les erreurs de transmission qu'elles soient analogiques ou logiques dans des calculs où l'intelligence humaine n'intervient plus, la présence de renseignements erronés ou brouillés peut entraîner des catastrophes extrêmement graves.

Charles FEVROT, Ingénieur ENSPCI, 1974, "Les charges électrostatiques et les perturbations qu'elles entraînent dans les liaisons radioélectriques"

#### DISCUSSION

F. D. GREEN: Since papers 9 and 10 were not presented, and Dr. Fevrot did not mention it, I feel that some mention should be made of precipitation static for the ground environment. I know that this exists at HF, and is relevant to air-ground communications, particularly with long-range patrol aircraft.

At CRC we have noted severe rain and snow static on HF log periodic directional antenna, and that an inverted HF discone antenna is much less affected. I would be interested to know if anyone here has had or knows of precipitation static on air-ground links at VHF and/or UHF. I realize that data can be obtained only when a storm provides the opportunity.

G. H. HAGN: No one in the audience seems to have experienced this problem at frequencies above HF. Perhaps, because the frequency spectrum of the corona causing this interference is falling off with increasing frequency, the noise from this source can be smaller than the noise from other sources at VHF and above.

DR. HARTH: Permit me to show a slide which indicates the direction and approach of a storm centre over the Bay of Biscay. This slide was obtained from a direction-finding system operating at VLF. It could be possible, under certain conditions, to anticipate when precipitation static might occur, and hence plan an experiment to look for this effect at VHF and UHF.

A. Mawira and J. Dijk

Eindhoven University of Technology  
Eindhoven, Netherlands.Summary

Equations describing the propagation of plane waves through a medium containing axisymmetric rain drops are presented. They lead to a general expression for the cross polarization parameter. A transfer equation involving the Stokes spectral parameters associated with the electromagnetic field in this medium, is also given. The solution of this equation shows that a polarization of the thermal emission in the atmosphere can be caused by rain. The evaluation of the cross polarization parameter from the emission measurements is also discussed.

1. Introduction

Microwaves with wavelengths in the centimeter and millimeter ranges are strongly affected by the presence of rain. The individual raindrops absorb and scatter the incident wave, the absorption being dominant at frequencies below 15 GHz [16]. The combined effects of these mechanisms causes, amongst others, the attenuation of the traversing wave. The non spherical shape of raindrops with an axial symmetry, combined with a non random distribution of the orientations of their axes, generally lead to a depolarization of the propagating wave. Consequently, serious performance degradation, due to rain, might be expected for frequency reuse systems.

The application of a frequency reuse system to satellite-to-ground telecommunication has stimulated some relevant investigations on this matter [1]-[6]. In this paper we shall deal with some further theoretical investigations concerning the propagation of electromagnetic waves through rain. Some aspects of the associated thermal emission will also be presented. We have assumed, that multiple scattering effects are negligible.

2. Mathematical model

The basic assumptions underlying this article, which concerns the propagation of radio waves through a rain filled medium, are the following:

A. Composition of the rain drop.

The rain medium is composed of axisymmetric raindrops, i.e. each raindrop has an axis of rotational symmetry. These raindrops may be of different types (for instance spheres, oblate spheroids, prolate spheroids, etc.) and of different sizes, an effective radius  $r$  being a measure for the latter. The orientation of each raindrop is fixed by the unit vector  $\hat{n}(\phi, \theta)$  (Fig.1) along its axis of symmetry, where  $\phi$  and  $\theta$  are called the canting and incident angle respectively; in the orthogonal  $xyz$  coordinate (Fig.2) the  $z$  axis is taken along the propagation direction of the incident wave, while the  $y$  axis, perpendicular to it, should be in a horizontal direction.

The composition of the rain medium is characterized by the distributions density  $f_i(x, r, \phi, \theta)$  for raindrops of a certain type, labelled  $i$ , where

$$dN_i(x) = N_i(x) f_i(x, r, \phi, \theta) dr d\phi d\theta \quad (2.1.1)$$

represents the number of this type per  $m^3$  that have their effective radii  $r$ , their canting angle  $\phi$  and their angles of incidence  $\theta$  (Fig. 2) situated in an infinitesimal interval

B. Statistically-independent single scattering.

This assumption implies that the relevant electromagnetic properties of the raindrops are sufficiently described by the forward-scatter complex amplitude functions for each of those raindrops. For an axisymmetric raindrop these functions, viz.  $S_{//}^\omega(r, \theta, \omega)$  and  $S_{\perp}^\omega(r, \theta, \omega)$  for a special drop type labelled  $i$ , occur in the relation (Fig.3)

$$\begin{pmatrix} E_{//}^{out} \\ E_{\perp}^{out} \end{pmatrix} = \frac{k^2 e^{-jkR}}{2\pi R} \begin{pmatrix} S_{//}^\omega & 0 \\ 0 & S_{\perp}^\omega \end{pmatrix} \begin{pmatrix} E_{//}^{in} \\ E_{\perp}^{in} \end{pmatrix} \quad (2.1.2)$$

9-2 where  $//$  and  $\perp$  refer, respectively, to the component of the electric field in the "plane of incidence" (containing the propagation direction and the symmetry axis), and the component perpendicular to it; both these components are parallel to the  $xy$  plane in view of the TE character of the wave. The relation (2.1.2) determines the forward-scattered field at a distance  $R$  versus the incident field [4];  $\omega$  represents the angular frequency of the harmonic time dependence.

The diagonal character of the matrix in Eq. 2.1.2 is a consequence of the assumed symmetry property of the raindrops.

The relation between the  $x$  and  $y$  components of the incident and the scattered field may now be obtained, for an arbitrary orientation of the raindrop by applying suitable rotational transformation to 2.1.2 (Fig.4). This results in

$$\begin{pmatrix} E_x^{scat} \\ E_y^{scat} \end{pmatrix} = k_0^2 \frac{e^{-jkR}}{2\pi R} \begin{pmatrix} \cos\phi & -\sin\phi \\ \sin\phi & \cos\phi \end{pmatrix} \begin{pmatrix} S_{//}^{\omega} & 0 \\ 0 & S_{\perp}^{\omega} \end{pmatrix} \begin{pmatrix} \cos\phi & \sin\phi \\ -\sin\phi & \cos\phi \end{pmatrix} \begin{pmatrix} E_x^{inc} \\ E_y^{inc} \end{pmatrix}, \quad (2.1.3)$$

or, worked out, in

$$\begin{pmatrix} E_x^{scat} \\ E_y^{scat} \end{pmatrix} = k_0^2 \frac{e^{-jkR}}{2\pi R} \begin{pmatrix} S_{//}^{\omega} \cos^2\phi + S_{\perp}^{\omega} \sin^2\phi & (S_{//}^{\omega} - S_{\perp}^{\omega}) \sin 2\phi \\ (S_{//}^{\omega} - S_{\perp}^{\omega}) \frac{\sin 2\phi}{2} & S_{//}^{\omega} \sin^2\phi + S_{\perp}^{\omega} \cos^2\phi \end{pmatrix} \begin{pmatrix} E_x^{inc} \\ E_y^{inc} \end{pmatrix}. \quad (2.1.4)$$

#### C. Pure absorption.

The single scattering albedo  $\omega_s$ , defined as the ratio of energy scattered to energy lost through both scattering and absorption (cf [13],[16]), is taken to be zero.

#### D. Local thermodynamic equilibrium of the rain medium.

### 3. Propagation of a plane wave through the rain medium

#### 3.1. The differential equation

According to our model the complex monochromatic TE wave travels through the rain medium in the  $z$  direction. Its electric field  $\vec{E}(z)$  has the form<sup>†</sup>

$$\vec{E}(z) = E_x(z) \hat{u}_x + E_y(z) \hat{u}_y, \quad (3.1.1)$$

where  $E_x$  and  $E_y$  are complex functions of  $z$ , while  $\hat{u}_x$  and  $\hat{u}_y$  are the unit vectors in the  $x$  and  $y$  directions respectively. The above assumption of statistically-independent single scattering leads to a differential equation of the type (cf [4])

$$-\frac{d\vec{E}(z)}{dz} = \bar{\Gamma}(z, \omega) \vec{E}(z), \quad (3.1.2)$$

with the  $2 \times 2$  transmission coefficient matrix  $\bar{\Gamma}$ . This matrix has the following form with respect to the bases  $\hat{u}_x, \hat{u}_y$

$$\bar{\Gamma} \cong \begin{pmatrix} \Gamma_{xx} & \Gamma_{xy} \\ \Gamma_{yx} & \Gamma_{yy} \end{pmatrix}, \quad (3.1.3)$$

<sup>†</sup> the  $z$  dependence has been omitted.

the elements of which are obtained by a summation of the elements in Eq. 2.1.4 over the individual drops of various types contained in an infinitesimal slab perpendicular to the  $z$  axis. The resulting expressions read:

$$\begin{aligned} \bar{\Gamma}_{xx}(z, \omega) &= jk \left( 1 + \sum_i N_i \int \int f_i(z, \theta, \phi) \{ S_{xx}^{\omega}(r, \theta, \omega) \sin^2 \theta + S_{zz}^{\omega}(r, \theta, \omega) \cos^2 \theta \} d\theta d\phi \right), \\ \bar{\Gamma}_{yy}(z, \omega) &= \bar{\Gamma}_{zz}(z, \omega) = jk \sum_i N_i \int \int f_i(z, \theta, \phi) \{ S_{yy}^{\omega}(r, \theta, \omega) - S_{zz}^{\omega}(r, \theta, \omega) \} d\theta d\phi \end{aligned} \quad (3.1.5)$$

In general  $\bar{\Gamma}_{xy}$  differs from zero. However,  $\bar{\Gamma}$  has a diagonal representation with respect to its own eigenvectors as bases; the eigenvalues then constitute the diagonal elements. The normalized eigenvectors,  $\hat{A}_A$  and  $\hat{A}_B$  say, and their corresponding eigenvalues  $\bar{\Gamma}_A$ ,  $\bar{\Gamma}_B$ , can be derived by solving the equations

$$\begin{aligned} \bar{\Gamma} \hat{A}_A &= \bar{\Gamma}_A \hat{A}_A, & \hat{A}_A^* \cdot \hat{A}_A &= 1, \\ \bar{\Gamma} \hat{A}_B &= \bar{\Gamma}_B \hat{A}_B, & \hat{A}_B^* \cdot \hat{A}_B &= 1, \end{aligned} \quad (3.1.5)$$

e.g. with respect to the bases  $\hat{u}_x$  and  $\hat{u}_y$ . The solution is represented by

$$\begin{pmatrix} \hat{A}_A \\ \hat{A}_B \end{pmatrix} = \{ \cosh 2\phi_1 \}^{\pm \frac{1}{2}} \begin{pmatrix} \cosh \phi_1 & j \sinh \phi_1 \\ -j \sinh \phi_1 & \cosh \phi_1 \end{pmatrix} \begin{pmatrix} \cos \phi_2 & \sin \phi_2 \\ -\sin \phi_2 & \cos \phi_2 \end{pmatrix} \begin{pmatrix} \hat{u}_x \\ \hat{u}_y \end{pmatrix}, \quad (3.1.6)$$

$$\bar{\Gamma}_A(z, \omega) = jk \left( 1 + \sum_i N_i \int \int f_i(z, \theta, \phi) \{ S_{xx}^{\omega}(r, \theta, \omega) \cos^2(\phi - \phi_2) + S_{zz}^{\omega}(r, \theta, \omega) \sin^2(\phi - \phi_2) \} d\theta d\phi \right),$$

where  $\phi_1$  and  $\phi_2$  are the real and imaginary parts of the "effective average complex canting angle"  $\phi$ , which in turn is to be determined from the relation

$$\tan(2\phi_2) = \frac{\sum_i N_i \int \int f_i(z, \theta, \phi) \{ S_{xx}^{\omega}(r, \theta, \omega) - S_{zz}^{\omega}(r, \theta, \omega) \} \sin(2\phi) d\theta d\phi}{\sum_i N_i \int \int f_i(z, \theta, \phi) \{ S_{xx}^{\omega}(r, \theta, \omega) - S_{zz}^{\omega}(r, \theta, \omega) \} \cos(2\phi) d\theta d\phi} \quad (3.1.7)$$

Eq. 3.1.8 shows that  $\phi$  is independent of  $z$  provided that the distribution densities  $f_i$  and  $N_i$  do have this property. The medium then admits two non-interfering channels, i.e. the elliptically polarized electric field components  $E_A \hat{A}_A$  and  $E_B \hat{A}_B$ , directed along the complex directions  $\hat{A}_A$  and  $\hat{A}_B$ , propagate through a medium without interfering with each other. These two elliptical polarizations reduce to two orthogonal linear polarizations in the case of a real  $\phi$ .

As an illustrative example we shall consider the case of a rain medium composed of raindrops of a single type only, and for which the relation

$$S_{xx}^{\omega}(r, \theta, \omega) - S_{zz}^{\omega}(r, \theta, \omega) = \Delta S^{\omega}(r, \omega) \sin^2 \theta, \quad (3.1.8)$$

with

$$\Delta S^{\omega}(r, \omega) = S_{xx}^{\omega}(r, \pi, \omega) - S_{zz}^{\omega}(r, \pi, \omega), \quad (3.1.9)$$

holds. This situation corresponds to dipole approximations of the raindrop scattering mechanism (cf [13]). In this approximation each raindrop is characterized by three planes of symmetry with the property that an electric field vector parallel to any of the three associated principle axes induces dipole moments proportional to this field vector. The scattered field can then be derived from the values of these dipole moments. In this situation Eq. 3.1.7 reduces to

9-4

$$\tan(2\phi) = \frac{\iint f(r, \phi, \theta) \Delta S(r, \omega) \sin(2\phi) \sin^2 \theta \, dr \, d\phi \, d\theta}{\iint f(r, \phi, \theta) \Delta S(r, \omega) \cos(2\phi) \sin^2 \theta \, dr \, d\phi \, d\theta} \quad (3.1.10)$$

If next, moreover, the distribution of the orientations of the raindrops happens to be independent of their sizes, i.e. if  $f(r, \phi, \theta) = g(r)h(\phi, \theta)$  then  $\tan(2\phi)$  will become real  $\phi_0 = 0$  according to the relation

$$\tan(2\phi) = \frac{\iint h(\phi, \theta) \sin(2\phi) \sin^2 \theta \, d\phi \, d\theta}{\iint h(\phi, \theta) \cos(2\phi) \sin^2 \theta \, d\phi \, d\theta} \quad (3.1.11)$$

The two eigenvectors then represents two orthogonal linear polarizations; in the case of a homogeneous medium these polarizations do not interfere throughout. From this special example it may be inferred that the possible dependence of the raindrop orientations on their sizes, and on the differences on their shapes may lead to a complex value of  $\phi$ .

### 3.2. Solution of the differential equation; the cross-polarization parameter

The evolution of the TE wave, as it propagated from  $z_0$  to  $z$  through the rain medium, can be described by the solution of Eq. 3.1.2. This solution may be represented by

$$\bar{E}(z) = \bar{F}(z, z_0; \omega) \bar{E}(z_0), \quad (3.2.1)$$

where the evolution matrix  $\bar{F}(z, z_0; \omega)$  results from

$$\bar{F}(z, z_0; \omega) = \left\{ \sum_{n=0}^{\infty} \bar{F}_n(z, z_0; \omega) \right\} e^{-\int_{z_0}^z \Gamma(z'; \omega) dz'}, \quad (3.2.2)$$

here  $\bar{F}_0 = \bar{I}$ , with  $\bar{I}$  being the unit matrix operator in the  $xy$  space; the other  $\bar{F}_n$ 's are to be determined from the recurrence relation

$$\bar{F}_n(z, z_0; \omega) = -\frac{1}{2} \int_{z_0}^z \bar{Q}(z'; \omega) \bar{U}(z'; \omega) \bar{F}_{n-1}(z, z'; \omega) dz'; \quad (3.2.3)$$

the other relevant quantities are defined by:

$$\Gamma_0 = \frac{1}{2} \{ \Gamma_A + \Gamma_B \}, \quad \bar{Q}_0 = \Gamma_A - \Gamma_B, \quad (3.2.4)$$

and by the following matrix referring to the bases  $\hat{M}_A, \hat{M}_B$

$$\bar{U} \triangleq \begin{pmatrix} 1 & 0 \\ 0 & -1 \end{pmatrix}; \quad (3.2.5)$$

in the representation with respect to  $x$  and  $y$  we should have

$$\bar{U} \triangleq \begin{pmatrix} \cos(2\phi_0) & \sin(2\phi_0) \\ -\sin(2\phi_0) & \cos(2\phi_0) \end{pmatrix}. \quad (3.2.6)$$

The cross-polarization parameter  $XPL$ , a measure for the depolarization, is defined by (cf [5])

$$XPL(z_0, z) = \left| \frac{E_x(z)}{E_y(z)} \right|^2,$$

provided that  $E_y(z_0) = 0$ .

Applying Eq. 3.2.1 to this definition gives

$$XPL(z, z) = \left| \frac{\overline{T}_{xx}(z, z)}{\overline{T}_{yy}(z, z)} \right|^2, \quad (3.2.8)$$

which is in general an inconvenient expression for calculations. However, if the rain path  $[z, z]$  causes only weak depolarization effects, i.e. if

$$|(z - z_0) \delta_p| \ll 1, \quad (3.2.9)$$

the series in Eq. 3.2.2 will converge rapidly. In this case only the matrix  $\overline{T}_i$  is wanted for an approximate analysis. A first-order approximation of the cross-polarization parameter is then given by

$$XPL = \frac{1}{4} \left| \int_0^z \delta_p^*(z') \sin\{2\phi(z')\} dz' \right|^2. \quad (3.2.10)$$

The integrand here occurring can be represented as follows

$$\delta_p^* \sin(2\phi) = \left\{ \delta_R^* + j \delta_I^* \right\} \left\{ \sin(2\phi_R) \cosh(2\phi_I) + j \cos(2\phi_R) \sinh(2\phi_I) \right\}, \quad (3.2.11)$$

where

$$\delta_R^* = \text{Re } \delta_p^*, \quad \delta_I^* = \text{Im } \delta_p^*. \quad (3.2.12)$$

This formula shows that the value of  $XPL$  may increase if the effective average canting angle  $\phi$  is complex instead of real. Fig. 5 shows  $|\sin(2\phi)/\sin(2\phi_R)|^2$  and  $|\sin(2\phi)|^2$  as functions of  $\phi_R$  and  $\phi_I$ . This quantity indicates the increase of  $XPL$  due to the imaginary part of  $\phi$ , when the rain medium is homogeneous.

### 3.3. The electromagnetic parameters of rain

The electromagnetic properties of a rain medium which agree with the given model, are completely determined by the functions  $N_i(u)$  and  $h_i(u, r, \phi, \theta)$ . Macroscopically these functions only appear in the three independent parameters  $\phi(z)$ ,  $\rho(z)$ ,  $\delta_p^*(z)$ . Therefore, these three parameters may be used to characterize the rain medium; this characterization will be useful in particular if the parameters in question can be related to the rain intensity.

## 4. Thermal emission

### 4.1. The transfer equation

It is known that in general any absorbing medium emits noise like electromagnetic energy, known as the thermal emission. The power spectrum of this emission is related to that of a blackbody (cf [9]), at least if the medium is in a state of local thermodynamic equilibrium.

Let us consider a plane wave propagating in the direction of the  $z$  axis. The complex analytic electric vector of such a wave may be given by

$$\vec{E}(z, t) = E_p(z, t) \hat{u}_p + E_z(z, t) \hat{u}_z, \quad (4.1.1)$$

where  $E_p(z, t)$  and  $E_z(z, t)$  are complex analytic functions (cf [10], [11]), while  $\hat{u}_p$  and  $\hat{u}_z$  are two independent unit complex vectors in the  $xy$  plane. Since the field due to thermal emission is of a stochastic nature it is often convenient to describe it by a set of suitably defined correlation parameters. The Stokes correlation parameters, which may be combined in a single correlation vector

$$\vec{C} \equiv \{C_p, C_z, C^{(p)}, C^{(z)}\}, \quad (4.1.2)$$



are given by

9-6

$$\begin{aligned} C_p(z, \tau) &= \alpha \langle E_p(z, t+\tau) E_p^*(z, t) \rangle, \quad C_z(z, \tau) = \alpha \langle E_z(z, t+\tau) E_z^*(z, t) \rangle, \\ C^{(p)}(z, \tau) &= \alpha \{ \langle E_p(z, t+\tau) E_z^*(z, t) \rangle + \langle E_p^*(z, t) E_z(z, t+\tau) \rangle \}, \\ C^{(z)}(z, \tau) &= \alpha \{ \langle E_p(z, t+\tau) E_z^*(z, t) \rangle - \langle E_p^*(z, t) E_z(z, t+\tau) \rangle \}. \end{aligned} \quad (4.1.3)$$

The ensemble average will be assumed to be identical with the time averages, i.e. the field is ergodic [12]. We then have for all relevant averages

$$\langle \dots \rangle = \lim_{T \rightarrow \infty} \frac{1}{2T} \int_{-T}^T \dots dt. \quad (4.1.4)$$

$\alpha$  is a constant of such magnitude and dimension that  $C_x(z, 0)$  and  $C_y(z, 0)$  may be interpreted as the power flux density per radians<sup>2</sup>, at  $z$ , flowing in the  $z$  direction. The normalization of power per radians<sup>2</sup> in place of the more usual power per meter<sup>2</sup> is due to the fact that the thermal emission field must be regarded as being made up of infinitesimal plane waves summed up over all directions. The Stokes spectral vector  $\vec{J}(z, \omega)$  will now be introduced as the Fourier transform of the Stokes correlation vector, so as to have

$$\vec{J}(z, \omega) = \int_{-\infty}^{\infty} \vec{C}(z, \tau) e^{-j\omega\tau} d\tau. \quad (4.1.5)$$

From these definitions we infer that all Stokes spectral parameters are real functions of  $z$  and  $\omega$ . The propagation of an electromagnetic field, characterized by its Stokes spectral vector  $\vec{J}$ , is governed by the extinction and emission mechanisms in this medium. In fact, by considering the variation of the Stokes spectral vector after propagation through a slab of thickness  $dz$ , a radiative transfer equation of the following form can be derived

$$-dz \vec{J}(z, \omega) = \vec{K}(z, \omega) \{ \vec{J}(z, \omega) - \vec{S}(z, \omega) \}. \quad (4.1.6)$$

Our rain medium model explains the first term of the right-hand-side. If  $p$  and  $q$  refer to the components of  $\vec{E}$  with respect to the normalized eigenvectors  $\vec{A}_A$  and  $\vec{A}_B$  the explicit form of  $\vec{K}$  then results from the application of Eq. 3.1.2 when differentiating Eq. 4.1.5, remembering Eq. 3.1.5. We thus find

$$\vec{K} \triangleq \begin{pmatrix} \kappa_{AA} & 0 & 0 & 0 \\ 0 & \kappa_{BB} & 0 & 0 \\ 0 & 0 & \kappa^{AA} & \kappa^{AB} \\ 0 & 0 & \kappa^{BA} & \kappa^{BB} \end{pmatrix}, \quad (4.1.7)$$

where the elements are given by

$$\begin{aligned} \kappa_{AA} &= 2 \operatorname{Re} \{ \Gamma_A \}, \quad \kappa_{BB} = 2 \operatorname{Re} \{ \Gamma_B \}, \quad \kappa^{AA} = \kappa^{BB} = \operatorname{Re} \{ \Gamma_A + \Gamma_B \}, \\ \kappa^{AB} &= -\kappa^{BA} = -\operatorname{Im} \{ \Gamma_A + \Gamma_B^* \}. \end{aligned} \quad (4.1.8)$$

As to the second contribution in Eq. 4.1.6, we there have to do with the source function vector representing the thermal emission. The explicit form of this source function may be obtained by considering a homogeneous rain medium, of temperature  $T$ , that is in a state of thermodynamic equilibrium with an enclosing blackbody radiator of the same temperature. The second law of thermodynamics supplemented by the well known expression of the power spectrum for blackbody relations leads to the following form of  $\vec{S}$  referring to the bases  $\vec{u}_x, \vec{u}_y$

$$\vec{S} \triangleq [1, 1, 0, 0] \frac{B_\nu(T)}{2}, \quad (4.1.9)$$

$B_\nu(T)$  being Planck's function for blackbody relation;  $T$  is the temperature of the medium at  $z$ ;  $\nu$  is the frequency in Hz i.e.  $\nu = \omega/2\pi$ .

Eq. 4.1.6 is a generalization of the classical transfer equation for non-scattering media. It reduces to this classical form (cf [13]) when the medium is isotropic so that  $\vec{\Gamma}_A$  equals  $\vec{\Gamma}_B$ .

4.2. Solution of the transfer equation

The general solution of the radiative transfer equation can formally be represented by an analysis analogous to that given in section 3.2 for Eq. 3.1.2 without an emission term. We find

$$\bar{I}(z; \omega) = \bar{H}(z, z_0; \omega) \bar{I}(z_0; \omega) + \int_{z_0}^z \bar{H}(z, z'; \omega) \bar{H}(z', \omega) \bar{S}(z', \omega) dz', \quad (4.2.1)$$

where the  $4 \times 4$  evolution-matrix operator  $\bar{H}$  is given by

$$\bar{H}(z, z_0; \omega) = \left[ \sum_{n=0}^{\infty} \bar{H}_n(z, z_0; \omega) \right] e^{-\beta(z, z_0; \omega)}; \quad (4.2.2)$$

here  $\bar{H}_0 = \bar{I}$ , while the other  $\bar{H}_n$ 's result from the recurrence relation

$$\bar{H}(z, z_0; \omega) = - \int_{z_0}^z \left\{ \delta \Gamma_R(z', \omega) \bar{D}_R(z', \omega) + \delta \Gamma_J(z', \omega) \bar{D}_J(z', \omega) \right\} \bar{H}(z, z'; \omega) dz'; \quad (4.2.3)$$

$\beta(z, z_0, \omega)$  is here defined as

$$\beta(z, z_0, \omega) = \int_{z_0}^z \kappa_0(z', \omega) dz', \quad (4.2.4)$$

where the average extinction coefficient  $\kappa_0(z, \omega)$  is given by

$$\kappa_0 = \kappa^{AA} = \kappa^{BB} = \frac{1}{2}(\kappa_{AA} + \kappa_{BB}) = \text{Re}(\Gamma_A + \Gamma_B); \quad (4.2.5)$$

the  $4 \times 4$  matrix operators  $\bar{D}_R$  and  $\bar{D}_J$  are defined by the following representations referring to the bases  $\hat{u}_R$  and  $\hat{u}_J$ .

$$\bar{D}_R \cong \begin{pmatrix} \text{ch } \zeta & 0 & \frac{1}{2} \text{ch } \zeta & \frac{1}{2} \text{sh } \zeta \\ 0 & -\text{ch } \zeta & \frac{1}{2} \text{ch } \zeta & -\frac{1}{2} \text{sh } \zeta \\ \text{ch } \zeta & \text{ch } \zeta & 0 & -\text{sh } \zeta \\ -\text{sh } \zeta & \text{sh } \zeta & -\text{sh } \zeta & 0 \end{pmatrix}, \quad \bar{D}_J \cong \begin{pmatrix} \text{sh } \zeta & 0 & -\frac{1}{2} \text{sh } \zeta & \frac{1}{2} \text{ch } \zeta \\ 0 & -\text{sh } \zeta & -\frac{1}{2} \text{sh } \zeta & -\frac{1}{2} \text{ch } \zeta \\ -\text{sh } \zeta & -\text{sh } \zeta & 0 & -\text{ch } \zeta \\ \text{ch } \zeta & -\text{ch } \zeta & \text{ch } \zeta & 0 \end{pmatrix}, \quad (4.2.6)$$

where the following abbreviations have been used

$$\text{si} = \sin(2\phi_R), \quad \text{co} = \cos(2\phi_R), \quad \text{sh} = \sinh(2\phi_J), \quad \text{ch} = \cosh(2\phi_J). \quad (4.2.7)$$

The solution of Eq. 4.2.1 is as follows if  $\bar{S}$  is assumed constant throughout the integration path

$$\bar{I}(z, \omega) = \bar{H}(z, z_0; \omega) \bar{I}(z_0, \omega) + \{ \bar{I} - \bar{H}(z, z_0; \omega) \} \bar{S}(\omega). \quad (4.2.8)$$

The independence of  $\bar{S}$  on  $z$  means that the temperature throughout the "rain-path" should also be independent of  $z$ .

A first order approximation of  $\bar{H}(z, z_0; \omega)$  may be justified when  $\phi_R$  and  $\phi_J$  are sufficiently small. By substituting this approximation in Eq. 4.2.8 and by using the Rayleigh-Jeans approximation for  $B_\nu$ , an expression is obtained for the difference between the emission temperatures

$$T_x(z) = 2\pi \lambda^2 k_B^{-1} J_x(z) \quad (4.2.9)$$

for  $\hat{u}_R$  polarization, and

$$T_y(z) = 2\pi \lambda^2 k_B^{-1} J_y(z) \quad (4.2.10)$$

for  $\hat{u}_J$  polarization. We find

9-8

$$T_x(z) - T_y(z) = 2 e^{-\beta(z, z)} (T - T_{inc}) \int_{z_0}^z \{ \epsilon_{Rr}^2 \cos \chi + \epsilon_{Ri}^2 \sin \chi \} dz' \quad (4.2.11)$$

In the derivation the incident radiation at  $z_0$  has been assumed to be the completely unpolarized sky-emission radiation so that

$$\begin{aligned} I_x(z_0) &= I_y(z_0) = \frac{1}{2\pi} k_B \lambda^{-2} T_{inc}, \\ I_x^{(v)}(z_0) &= I_y^{(v)}(z_0) = 0, \end{aligned} \quad (4.2.12)$$

$k_B$  being the well known Boltzmann constant.

Eq. 4.2.11 shows that the thermal emission in the atmosphere due to rain may be a little polarized. Figures 6 and 7 show  $\Delta T = T_x - T_y$  as functions of different rain-path-lengths  $L = z - z_0$  and rain intensities  $p$  for a frequency of 11 GHz. It has been assumed there that the raindrops are of the oblate spheroidal type and that all of them are oriented according to  $\phi = 15^\circ$ ,  $\theta = 90^\circ$ ; the values used for the extinction coefficients are those given by [14] where Laws and Parsons raindrop-size distribution has been assumed. These figures show that the above mentioned polarization of thermal emission due to rain is quite small,  $|\Delta T|$  being always smaller than 9 K in the range considered.

The polarization of thermal emission, as derived above, is due solely to the anisotropy of the medium. It is possible to show (cf Appendix) that multiple scattering effects, which is only operative if  $\alpha$  does not vanish, may also cause some polarization of the thermal emission.

Nevertheless, if the frequency considered is not too large,  $\alpha$  will have a small value. Consequently, in this case, the anisotropy of the medium will still be the main source of polarization (Appendix).

#### 5. The relation between emission temperatures and the cross polarization parameter

The above consideration on thermal emission phenomena suggest the possibility to use thermal emission measurements to calculate the parameter  $XPL$ . Also of interest is the number of rain parameters, such as  $\phi, \epsilon_{Rr}, \epsilon_{Ri}, p, L$ , that may be determined from such measurements. The usefulness of this method will depend, first of all, on whether the model used to derive the relationships between the relevant parameters is reliable, since this model must sufficiently describe the processes that takes place in the physical situation.

The most general model introduced above does not seem to yield simple relationships between thermal emission strengths and  $XPL$ . We may compare, for instance, Eq. 4.2.11 together with

$$T^{(v)}(z) = 2T \int_{z_0}^z \{ \epsilon_{Rr}^2 \cos \chi - \epsilon_{Ri}^2 \sin \chi \} dz' e^{-\beta(z, z)} \quad (5.1)$$

With the equation for the cross polarization parameter  $XPL$  as given by Eqs 3.2.10 and 3.2.11. However, the factor  $\beta(z, z)$  can be determined, as shown by several authors [7], [8], from measurements of  $\frac{1}{2}(T_x + T_y)$  or  $T_x$  when use is made of estimates for  $T$  and  $T_{inc}$ . In order to be able to relate the cross polarization parameter  $XPL$  to the temperatures  $T_x, \Delta T, T^{(v)}$  more information concerning the rain structure should be available. This information, together with the possible existing relationships between, for instance,  $\epsilon_{Rr}, \epsilon_{Ri}$  and  $\bar{\mu}_R = \frac{1}{2}\mu_0$  may then deliver useful equations. Figures 8 and 9 show  $\epsilon_{Rr} = \epsilon_{Rr}/\mu_R$  and  $\epsilon_{Ri} = \epsilon_{Ri}/\mu_R$  respectively as functions of the rain intensity  $p$ ; it has been assumed here that all the raindrops are of the oblate spheroidal type, and that all the raindrops are equally oriented with  $\theta = \frac{\pi}{2}$ ; the size distributions are those of Laws and Parsons, while the frequency is 11 GHz. Table 1 indicates the parameter that may be estimated when some information on the rain medium is given together with some measured values of the thermal emission temperatures.

The following example serves to illustrate the principles presented above.

Consider a rain medium with the following properties

- (i) the distribution density  $f_r(z, \mu, \theta, N, \mu)$  and the shapes of the occurring raindrops are such that the average effective canting angle  $\chi(z)$  is real.
- (ii) the incident radiation at the boundary of the rain medium is the totally unpolarized sky emission radiation so that  $T^{(v)}$  and  $T^{(h)}$  vanish at that boundary while  $T_{inc}$  is 26 K.
- (iii) the temperature of the medium is constant throughout the rain path with a value of 290 K.

In this medium the following values are supposed to have been measured, at 11 GHz,

$$\begin{aligned}\frac{1}{2}(T_A + T_B) &= 100 \text{ K}, \\ \Delta T &= 5 \text{ K}, \\ \frac{\Delta T}{T^{(u)}} &= 7.6\%, \\ T^{(u)} &= 0 \text{ K}.\end{aligned}$$

9-9  
(5.2)

The vanished  $T^{(u)}$  is a consequence of the fact that the incident radiation at the boundary is totally unpolarized, as can be seen from Eqs. 4.2.6, 4.2.7 and 4.2.8. Next, since  $\phi$  vanishes, the following expressions hold

$$\frac{1}{2}(T_A + T_B) \approx e^{-\beta(z, z_0)} T_{inc} + (1 - e^{-\beta(z, z_0)}) T, \quad (5.3)$$

$$T^{(u)} = 2 e^{-\beta(z, z_0)} T \int_{z_0}^z \sigma_R(z') \sin\{2\phi_R(z')\} dz', \quad (5.4)$$

$$\Delta T = 2 e^{-\beta(z, z_0)} (T - T_{inc}) \int_{z_0}^z \sigma_R(z') \cos\{2\phi_R(z')\} dz', \quad (5.5)$$

$$XPL \approx \frac{1}{4} |1 + jc|^2 \left| \int_{z_0}^z \sigma_R(z') \sin\{2\phi_R(z')\} dz' \right|^2; \quad (5.6)$$

$c$  in (5.6) is to be estimated from the slowly varying curve given by Fig. 6, e.g.  $c = 5$ .

An expression for  $XPL$  can be derived by substituting Eqs. 5.3 and 5.4 into Eq. 5.6,

$$XPL \approx \frac{1}{4} \left| \frac{T^{(u)}(T - T_{inc})(1 + jc)}{2T \left\{ T - \frac{1}{2}(T_A + T_B) \right\}} \right|^2. \quad (5.7)$$

Substituting the given values of  $T^{(u)}$ ,  $\frac{1}{2}(T_A + T_B)$ ,  $c$ ,  $T$  and  $T_{inc}$  in the above equation, we find

$$XPL \approx 0.21 \cdot 10^{-2}. \quad (5.8)$$

Moreover, if  $\phi_R$  is a constant, this parameter proves to be related to  $T^{(u)}$ ,  $T$ ,  $T_{inc}$ , as shown by the relation

$$\tan(2\phi_R) = \left\{ 1 - \frac{T_{inc}}{T} \right\} \frac{T^{(u)}}{T}. \quad (5.9)$$

For temperature mentioned above  $\phi_R$  is approximately  $15^\circ$ .

## 6. Conclusions

The average effective canting angle  $\phi$ , introduced in this paper, proves to be an important quantity in the depolarization theory of rain. A dependence of raindrop orientations on their sizes leads generally to a complex value of the quantity  $\phi$ . Moreover, the occurrence of raindrops of different shapes may also produce this effect.

The determination of the average effective canting angle  $\phi$  is useful since the cross polarization parameter  $XPL$  depend on it.

However, because of the lack of information on the statistics of raindrop orientations it is not yet possible to get a reliable value of the quantity  $\phi$ . The statistics of  $\phi$  along the rain path are needed as well, for instance if  $\phi$  is real and alternates randomly between equal positive and negative values, while  $\sigma_R$  is constant, then Eq. 3.2.10 shows that the  $XPL$  will vanish, at least to a first order approximation.

We wish here to point out that a model concerning the canting of the individual raindrop has recently been put forward by Brussaard [15]. In this model the laminar flow of air directly above the earth's surface has been shown to be an important factor in the effectuation of the said canting of the raindrops.

The effect of thermal emission has been described by the Stokes spectral parameters and it has been shown that the propagation of these parameters through the rain is governed by an equation that is a slight generalization of the classical transfer equation for non-scattering media.

The solution of this equation shows that thermal emission in the atmosphere due to rain may be a little

polarized. Further, it seems that under certain circumstances measurements of thermal emissions may be used to calculate values of the cross polarization parameter.

Finally, we mention here that measurements of thermal emission temperatures, using a double Dicke radio-meter Fig. 11, are now being carried out. The results of these measurements will be published in the near future.

#### 7. Acknowledgement

The authors wish to thank prof. dr. H. Bremmer for his valuable help in the preparation of this paper.

#### References

1. Watson, P.A., Arbabi, M.: "Rainfall cross polarization at Microwave frequencies", Proc. IEE, 1973, 120, (4), pp. 413-418.
2. Thomas, D.T.: "Cross polarization distortion in microwave radio transmission due to rain", Radio Science, 1971, 6, (10), pp. 833-839.
3. Taur, R.R.: "Rain depolarization: theory and experiment", Comsat Technical Review, 1974, 4, (1), pp. 187-190.
4. Capsoni, C., Paraboni, A.: "Depolarization of an electromagnetic wave travelling through a stratified aerosol of non-spherical scatterers", 18th AGARD Technical Meeting on "Telecommunication Aspects on Frequencies between 10 and 100 GHz", 1972.
5. Evans, B.G., Troughton, J.: "Calculation of cross polarization due to precipitation", IEE Conference Publ, 1973, 98; "Propagation of radiowaves at frequencies above 10 GHz".
6. Oguchi, T.: "Attenuation of electromagnetic waves due to rain with distorted raindrops" (part II), "Journal of the radio research laboratories", 1964, 11, (53), pp. 19-44.
7. Wulfsberg, K.N., Altschuler, E.E.: "Rain attenuation at 15 and 35 GHz", IEEE Trans., 1972, AP-20, (2), pp. 181-187.
8. Ippolito, L.Y.: "Effects of Precipitation on 15.3 and 31.65 GHz Earth Space Transmissions with the ATS-V Satellite", Proc. IEEE, 1971, 59, (2), pp. 189-205.
9. Oliver, B.M.: "Thermal and Quantum noise", Proc. IEEE, 1965, May, pp. 436-454.
10. Born, M., Wolf, E.: "Principles of Optics", (Pergamon Press, 1964), Chap. 10, pp. 494-504.
11. Papoulis, A.: "Probability Random Variables and Stochastic Processes", (McGraw-Hill, 1965), Chap. 10, pp. 356-357.
12. Perina, J.: "Coherence of Light", (van Nostrand, Reinhold, London, 1972), Chap. 6, pp. 16, 77-79.
13. Chandrasekhar, S.: "Radiative Transfer", (Dover, New York, 1960), Chap. 6, 18, pp. 9, 45-46.
14. Glimmerveen, L.J., Koppers, M.F.M.: "Het Meten van Depolarisatieruis bij 11 GHz", Master thesis, Eindhoven University of Technology, Netherlands, 1974.
15. Brussaard, G.: "Rain induced cross polarization and raindrop canting", Electronic Letters, 1974, 10, (20), pp. 411-412.
16. Crane, R.K.: "Propagation Phenomenon Affecting Satellite Communication Systems Operating in the Centimeter and Millimeter Wavelength Bands", Proc. IEEE, 1971, 59, (2), pp. 173-188.

# Appendix

Let us consider a rain medium for which the following transfer equation holds

$$-(\hat{p} \cdot \text{grad}) \bar{I}(\vec{r}, \hat{p}) = \bar{K}(\vec{r}, \hat{p}) \left\{ \bar{I}(\vec{r}, \hat{p}) - (1 - \omega_s) \bar{S}(\vec{r}) - \frac{1}{4\pi} \int \bar{P}(\vec{r}, \hat{p}, \hat{p}') \bar{I}(\vec{r}, \hat{p}') d\Omega_{\hat{p}'} \right\}, \quad (A1)$$

where

$\hat{p}$  - direction vector

$\vec{r}$  - space coordinates

$\bar{I}(\vec{r}, \hat{p})$  - the Stokes spectral vector, at  $\vec{r}$ , representing the power flow in direction  $\hat{p}$

$\bar{K}(\vec{r}, \hat{p})$  - the 4 x 4 extinction matrix, at  $\vec{r}$

$\omega_s$  - albedo for single scattering, the ratio of energy scattered to energy lost through both scattering and absorption

$\bar{P}(\vec{r}, \hat{p}, \hat{p}')$  - the phase matrix, that gives the fraction of the power flow in  $\hat{p}'$  direction that is scattered in the  $\hat{p}$  direction

$d\Omega_{\hat{p}'}$  - an element of solid angle in the direction  $\hat{p}'$ .

Eq. A1 is a generalization of the classical transfer equation for a scattering and absorbing medium [13], [16]. The generalization being apparent from the tensor form of the extinction coefficient  $\bar{K}$ .

The third term in Eq. A1 represents the contribution of scattering to the total variation of  $\bar{I}$  in the  $\hat{p}$  direction.

In this article it is assumed that  $\omega_s$  is zero. In reality it is not zero. However, for a certain frequency and rain intensity range  $\omega_s$  has a small value.

In this case a Born series representation of  $\bar{I}$  may be used to solve Eq. A1

$$\bar{I}(\vec{r}, \hat{p}) = \sum_{n=0}^{\infty} \omega_s^n \omega^n \bar{I}(\vec{r}, \hat{p}). \quad (A2)$$

By substituting Eq. A2 in Eq. A1, and then arranging and grouping the elements in the equation to equal powers of  $\omega_s$ , the following equations can be obtained

$$\omega_s^0: -(\hat{p} \cdot \text{grad}) \omega^0 \bar{I}(\vec{r}, \hat{p}) = \bar{K}(\vec{r}, \hat{p}) \left\{ \omega^0 \bar{I}(\vec{r}, \hat{p}) - \bar{S}(\vec{r}) \right\}, \quad (A3)$$

$$\omega_s^1: -(\hat{p} \cdot \text{grad}) \omega^1 \bar{I}(\vec{r}, \hat{p}) = \bar{K}(\vec{r}, \hat{p}) \left\{ \omega^1 \bar{I}(\vec{r}, \hat{p}) + \bar{S}(\vec{r}) - \frac{1}{4\pi} \int \bar{P}(\vec{r}, \hat{p}, \hat{p}') \omega^0 \bar{I}(\vec{r}, \hat{p}') d\Omega_{\hat{p}'} \right\}, \quad (A4)$$

$$\omega_s^2: -(\hat{p} \cdot \text{grad}) \omega^2 \bar{I}(\vec{r}, \hat{p}) = \bar{K}(\vec{r}, \hat{p}) \left\{ \omega^2 \bar{I}(\vec{r}, \hat{p}) - \frac{1}{4\pi} \int \bar{P}(\vec{r}, \hat{p}, \hat{p}') \omega^1 \bar{I}(\vec{r}, \hat{p}') d\Omega_{\hat{p}'} \right\}. \quad (A5)$$

Eq. A3 has the same form as a transfer equation for a non-scattering medium, in fact by choosing  $\hat{p} = \hat{e}_z$  we can see that it is the same equation as Eq. 4.1.6. The term  $\bar{K}_1 = \sum_{n=1}^{\infty} \omega_s^n \omega^n \bar{K}(\vec{r}, \hat{p})$  gives the error obtained when we use Eq. 4.1.6 in place of the rigorous form of Eq. A1.

To acquire some idea concerning the magnitude of this correction, we shall estimate  $\bar{K}_1$  for the following situation, conforming to the illustration given in Fig. 9.:

1. the rain medium extends indefinitely in the horizontal plane and is enclosed below and above by a non-scattering ground and a cloud, resp., the  $\hat{z}$  direction is taken to lie in the  $\hat{x}\hat{y}$  plane.
2. the rain medium is homogeneous and isotropic, i.e.  $\bar{K} = K_0 \bar{I}$  with  $K_0$  being independent of  $\vec{r}$
3. the temperature  $T$  of the rain medium is constant and is equal to the ground temperature.
4. the ground is considered to be a blackbody radiator.
5. the cloud is assumed to be non-reflecting, the emission there being the totally unpolarized sky emission.
6. the phase function is Rayleigh phase function [13], and is given by the following representation referring to a local spherical coordinate system:

$$\bar{P} \cong \frac{1}{2} \begin{pmatrix} 2 \sin^2 \theta \sin^2 \phi + \cos^2 \theta \cos^2 \phi & \cos^2 \theta \\ \cos^2 \theta & 1 \end{pmatrix}. \quad (A6)$$

9-12 In view of the assumed homogeneity of the medium only the first two components of the Stokes spectral vector is of interest, this explains the  $2 \times 2$  dimension of  $A_6$ ;  $(\psi, \theta)$  and  $(\psi', \theta')$  indicating the  $\hat{p}$  and  $\hat{p}'$  directions respectively; the orthogonal linear polarizations have been taken along the meridian and longitudinal directions respectively.

The solution of Eq. A3 is now given by

$$\omega(\vec{r}, \hat{p}) = \omega(\vec{r}_0, \hat{p}) e^{-\kappa_0 \hat{p} \cdot (\vec{r} - \vec{r}_0)} + (1 - e^{-\kappa_0 \hat{p} \cdot (\vec{r} - \vec{r}_0)}) \bar{S} \quad (A7)$$

This formula substituted in Eq. A4 delivers the expression

$$-(\hat{p}, \text{ground}) \omega(\vec{r}, \hat{p}) = \kappa_0 \left\{ \omega(\vec{r}, \hat{p}) - \frac{1}{4\pi} \iint \bar{P}(\vec{r}; \hat{p}, \hat{p}') [\omega(\vec{r}_0, \hat{p}') - \bar{S}] e^{-\kappa_0 \hat{p}' \cdot (\vec{r} - \vec{r}_0)} d\Omega_{\hat{p}'} \right\}, \quad (A8)$$

where use has been made of the relation

$$\iint \bar{P}(\vec{r}; \hat{p}, \hat{p}') \bar{S} d\Omega_{\hat{p}'} = \iint \bar{P}(\vec{r}; \hat{p}, \hat{p}') d\Omega_{\hat{p}'} \bar{S} = 4\pi \bar{S} \quad (A9)$$

which is here valid since  $\bar{S}$  is independent of the direction  $\hat{p}$ .

In Eq. A8 we may choose the boundary points  $\vec{r}_0$  in such a way that the integral on the right hand side may be split in two terms

$$\iint \dots \frac{d\Omega_{\hat{p}'}}{4\pi} = \frac{1}{4\pi} \iint_{\text{ground}} \dots d\Omega_{\hat{p}'} + \frac{1}{4\pi} \iint_{\text{cloud}} \dots d\Omega_{\hat{p}'}, \quad (A10)$$

the first refers to all boundary points on the ground and is zero in view of the assumed blackbody character to the ground, i.e.  $\omega(\vec{r}_0, \hat{p}) = \bar{S}$ , while the second refers to the boundary points of the clouds and may be approximated by

$$-\frac{1}{4\pi} \iint \bar{P}(\hat{p}, \hat{p}') e^{-\kappa_0 \hat{p}' \cdot (\vec{r} - \vec{r}_0)} d\Omega_{\hat{p}'}, \quad (A11)$$

since the cloud intensity of sky emission is usually much smaller than  $\bar{S}$ . Now, by choosing  $\hat{p} = \hat{u}_z$  and  $\omega(\vec{r}_0, \hat{p})|_{\text{cloud}} = \bar{0}$  we obtain for the solution of Eq. A 8 the following expression

$$\begin{pmatrix} \omega_x(L) \\ \omega_y(L) \end{pmatrix} = \int_0^L dz' e^{-\kappa_0(L-z')} \frac{3}{2} \kappa_0 \int_0^1 \begin{pmatrix} 2(1-\mu^2)(1-\mu'^2) + \mu^2 \mu'^2 & \mu^2 \\ \mu'^2 & 1 \end{pmatrix} e^{-\kappa_0 \frac{L}{2} \frac{z'}{L}} \begin{pmatrix} \frac{1}{2} B_1 \\ \frac{1}{2} B_2 \end{pmatrix} dz' \quad (A12)$$

where  $\mu = \cos \psi$   $\mu' = \cos \psi'$ .

We are in the first place interested in the polarization of  $\omega$  i.e. in the term  $\Delta \omega = \omega_x - \omega_y$

$$\Delta \omega = \frac{3}{2} (1-\mu^2) B_2(T) z' e^{-\kappa_0 L} \varphi, \quad (A13)$$

with

$$\varphi = \int_0^1 d\mu' \int_0^L dz' \kappa_0 e^{\kappa_0 z'} e^{-\kappa_0 \frac{L}{2} \frac{z'}{L}} (1-3\mu'^2). \quad (A14)$$

By splitting  $\varphi$  in a positive and negative part we can give the following estimation for  $|\varphi|$

$$|\varphi| < \left( \frac{1}{\sqrt{3}} - \frac{1}{3} \right) \max \left\{ \frac{|e^{\kappa_0(L-H)}|}{|1 - \frac{H}{L}|}, \frac{|e^{\kappa_0(L-\sqrt{3}H)}|}{|1 - \sqrt{3} \frac{H}{L}|} \right\} = \varphi_m. \quad (A15)$$

With the aid of this expression we obtain the following estimation of  $|\omega_x - \omega_y|$ :

$$|\omega_x - \omega_y| < \frac{3}{2} (1-\mu^2) \left( \frac{1}{\sqrt{3}} - \frac{1}{3} \right) B_2(T) e^{-\kappa_0 L} \varphi_m, \quad (A16)$$

or, using emission temperature concepts (cf Eq. 4.2.9)

$$|\Delta T| < \frac{1}{2} (1 - \kappa^2) \left( \frac{1}{T_1} - \frac{1}{T_2} \right) T e^{-\kappa_0 L} D_M . \quad (A17)$$

We can compare this formula with the expression delivered by Eq. 4.2.11

$$|\Delta T| = \epsilon T L |S \kappa_0 \cos(2\phi_R)| e^{-\kappa_0 L} , \quad (A18)$$

where  $\phi_R$  is assumed real, while all the variables are taken to be independent of  $\phi$ . The polarization of thermal emission temperatures caused by anisotropy is larger than that caused by scattering if

$$\omega < V_M = \frac{1}{2} \left( \frac{1}{T_1} - \frac{1}{T_2} \right)^{-1} D_M^{-1} \left| \frac{S \kappa_0 \cos(2\phi_R)}{1 - \kappa^2} \right| ; \quad (A19)$$

we also have the following estimation

$$\left| \frac{\Delta T}{\Delta T} \right| < \omega V_M^{-1} . \quad (A20)$$

Table 2 shows  $V_M$ ,  $\omega$  and  $\omega V_M^{-1}$  for different rain intensities  $p$ , at 11 GHz when  $L = 4 \text{ km}$ ,  $H = 2 \text{ km}$ ,  $\phi_R = 15^\circ$ ,  $\nu = 30^\circ$ ; the values used for  $S \kappa_0$  and  $\kappa_0$  have been taken from [14], where Laws and Parsons distribution has been assumed; while  $\omega$  has been interpolated from a figure given by [16]. This table shows that, at 11 GHz, polarization of sky temperatures is mainly due to the anisotropy of the rain medium.



Relevant parameters :

9-14  $\phi_0 = \phi_R + j\phi_I, \Gamma_R, \delta\Gamma_R, \delta\Gamma_I, L, XPL, \beta = \int \Gamma(z) dz, \delta\beta = \int \delta\Gamma_R(z) dz,$   
 $\delta\beta = \int \delta\Gamma_I(z) dz.$

Theoretical relationships :

TR1:  $\delta\Gamma_I = c\delta\Gamma_R,$

TR2:  $\delta\Gamma_R = q\Gamma_R.$

Information  
available.

Parameters that may be derived from measurements of:

	$T_x$	$T_x, T_y$ or $T_x, \Delta T$	$T_x, T^{(x)}$	$T_x, \Delta T, T^{(x)}$
None	$\beta$	$\beta$	$\beta$	$\beta$
$\phi_I = 0.$	$\beta$	$\beta$	$\beta$	$\beta$
$\phi_I = 0,$ TR1 .	$\beta$	$\beta$	$\beta, XPL$	$\beta, XPL$
$\phi_0$ is a con- stant.	$\beta$	$\beta$	$\beta$	$\beta$
$\phi_0$ is a cons- tant, TR1, TR2.	$\beta$	$\beta$	$\beta$	$\beta, \delta\beta_R, \delta\beta_I,$ $\phi_R, \phi_I.$
$\phi_0 =$ a given constant	$\beta$	$\beta$	$\beta$	$\beta, \delta\beta_R, \delta\beta_I$ ( if $\phi_I = 0$ ), XPL.
$\phi_0 =$ a given constant, TR1, TR2.	$\beta$	$\beta, \delta\beta_R, \delta\beta_I,$ XPL, possibility of testing the given value of $\phi_0.$	$\beta, \delta\beta_R, \delta\beta_I,$ XPL, possibi- lity of tes- ting the gi- ven value of $\phi_0.$	$\beta, \delta\beta_R, \delta\beta_I,$ XPL, possibility of testing the given value of $\phi_0.$

Table 1. Emission temperatures and their  
related rain parameters.

$p$ mm/hour	$v_M$	$\omega_0$	$\omega_0/v_M$
25	1.36	0.10	0.07
50	0.73	0.11	0.15
100	0.39	0.13	0.33
150	0.20	0.15	0.75

Table 2. The albedo  ~~$\omega_0$~~  and the quantity  $\omega_0/v_M$   
for different rain intensities  $p$   
at 11 GHz.

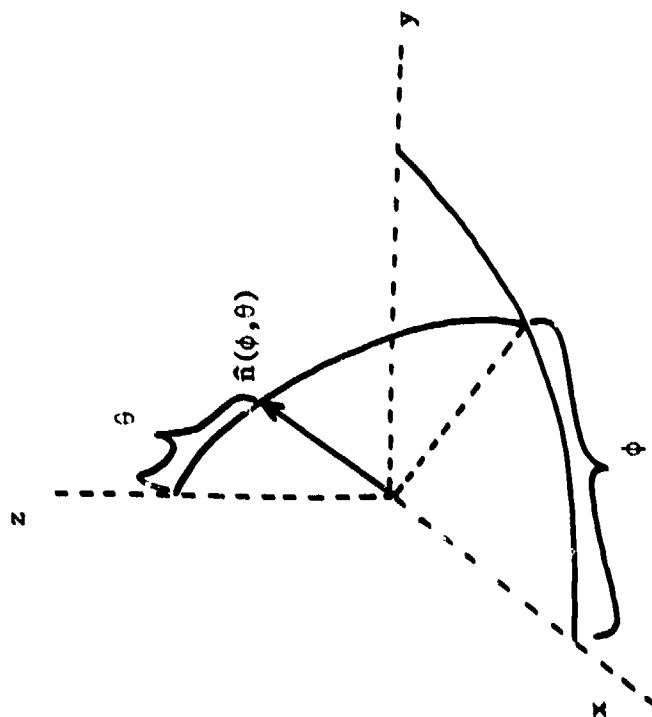


Fig.1 An axisymmetric raindrop, with the unit vector  $\hat{n}$

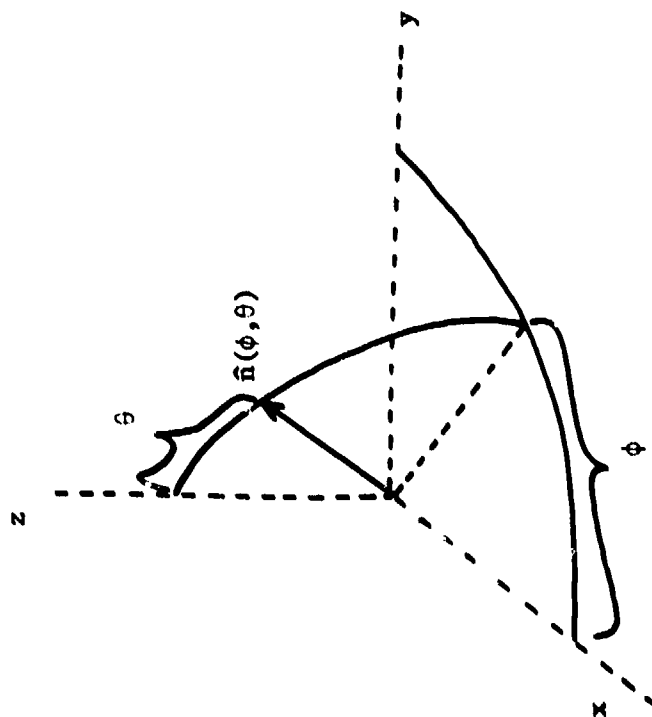


Fig.2 The orthogonal  $xyz$  coordinate system showing the canting angle  $\phi$  and the incident angle  $\theta$ .

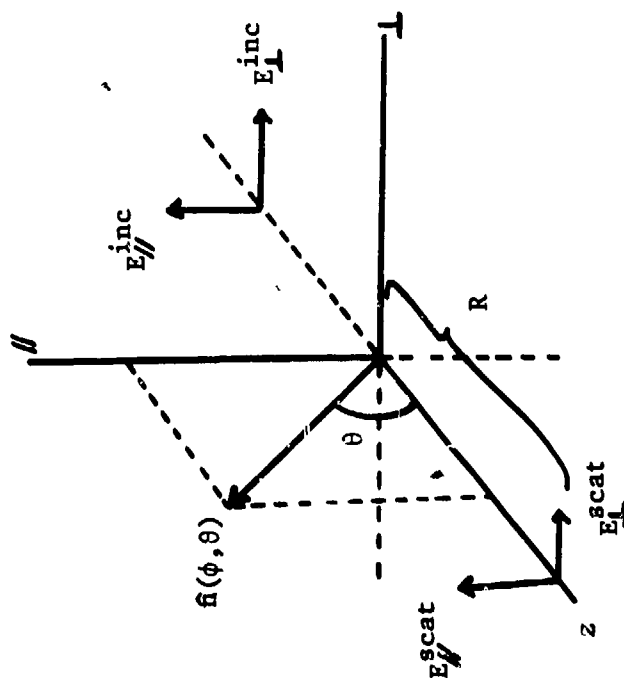


Fig.3 The incident versus the scattered field in the  $L//z$  coordinate system.

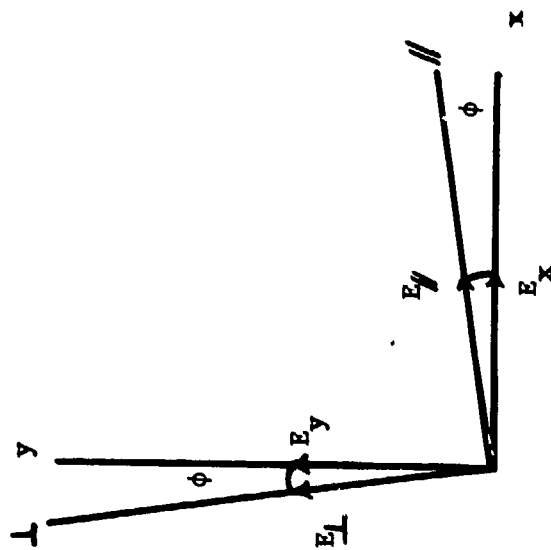


Fig.4 A coordinate transform in the  $xy$  plane.

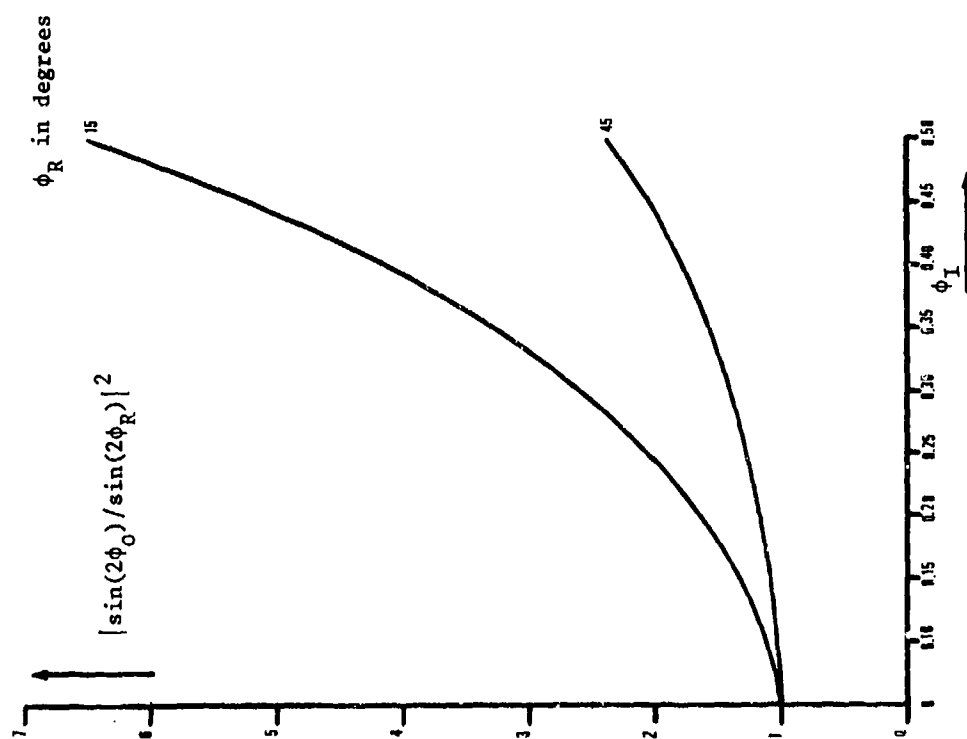
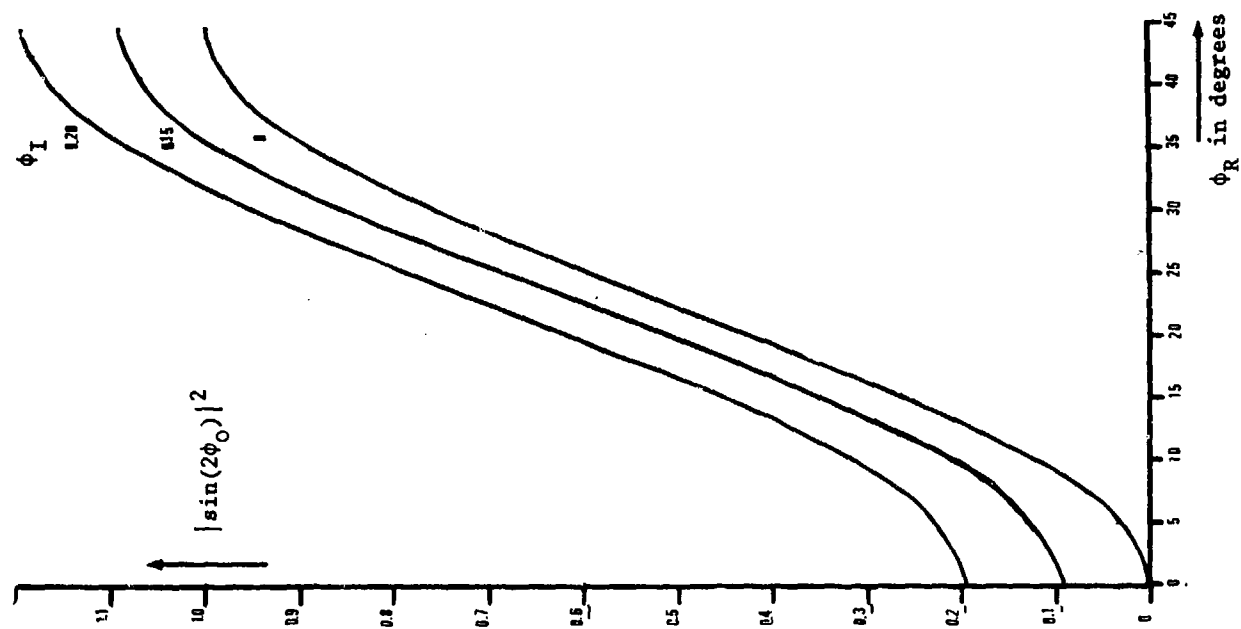


Fig. 5  $|\sin(2\phi_0)/\sin(2\phi_R)|^2$  and  $|\sin(2\phi_0)|^2$  as functions of  $\phi_R$  and  $\phi_I$ .

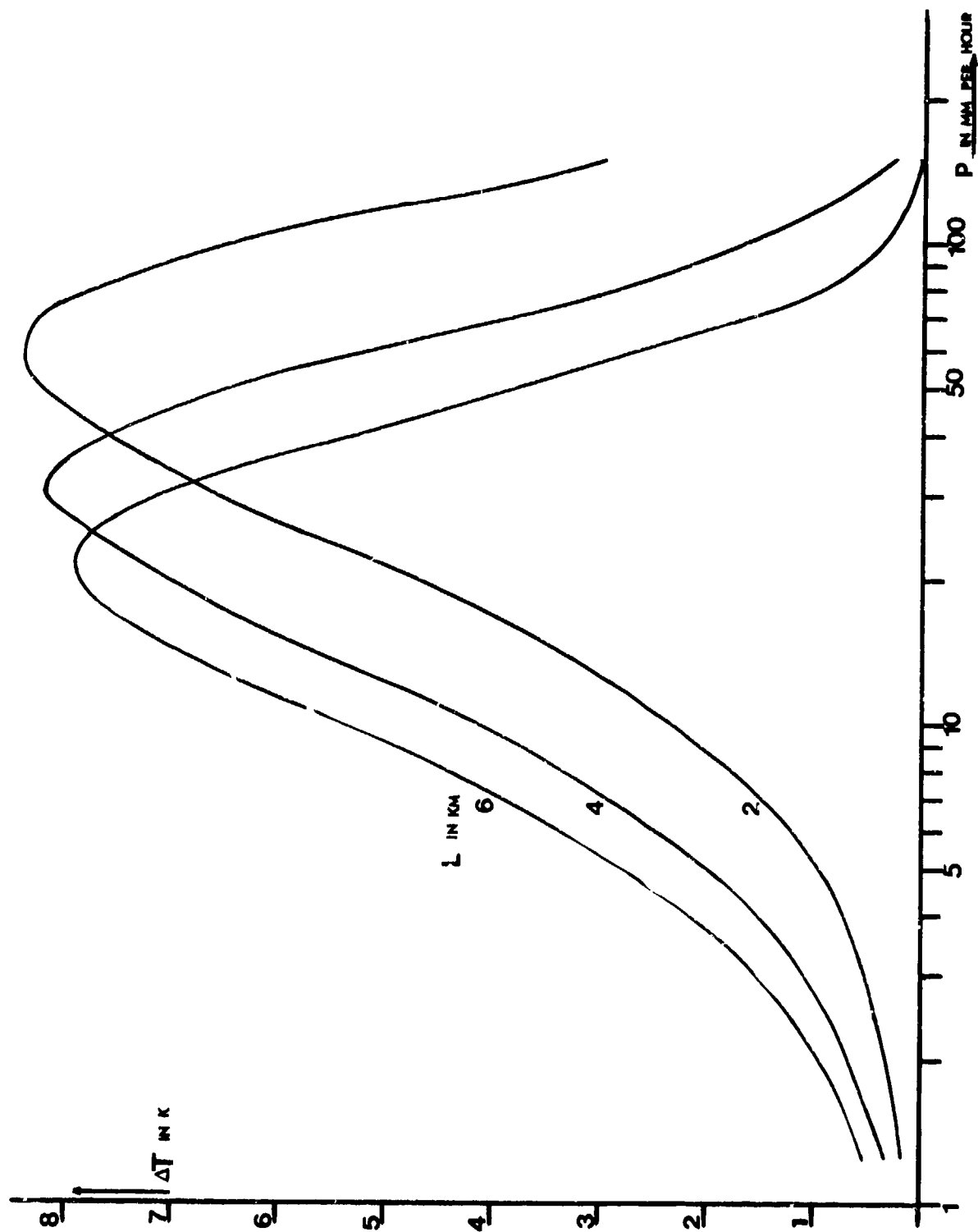


Fig. 6  $\Delta T$  as function of the rain intensity  $p$ ,  
with the rain path length  $L$  as parameter ( at 11 GHz ).

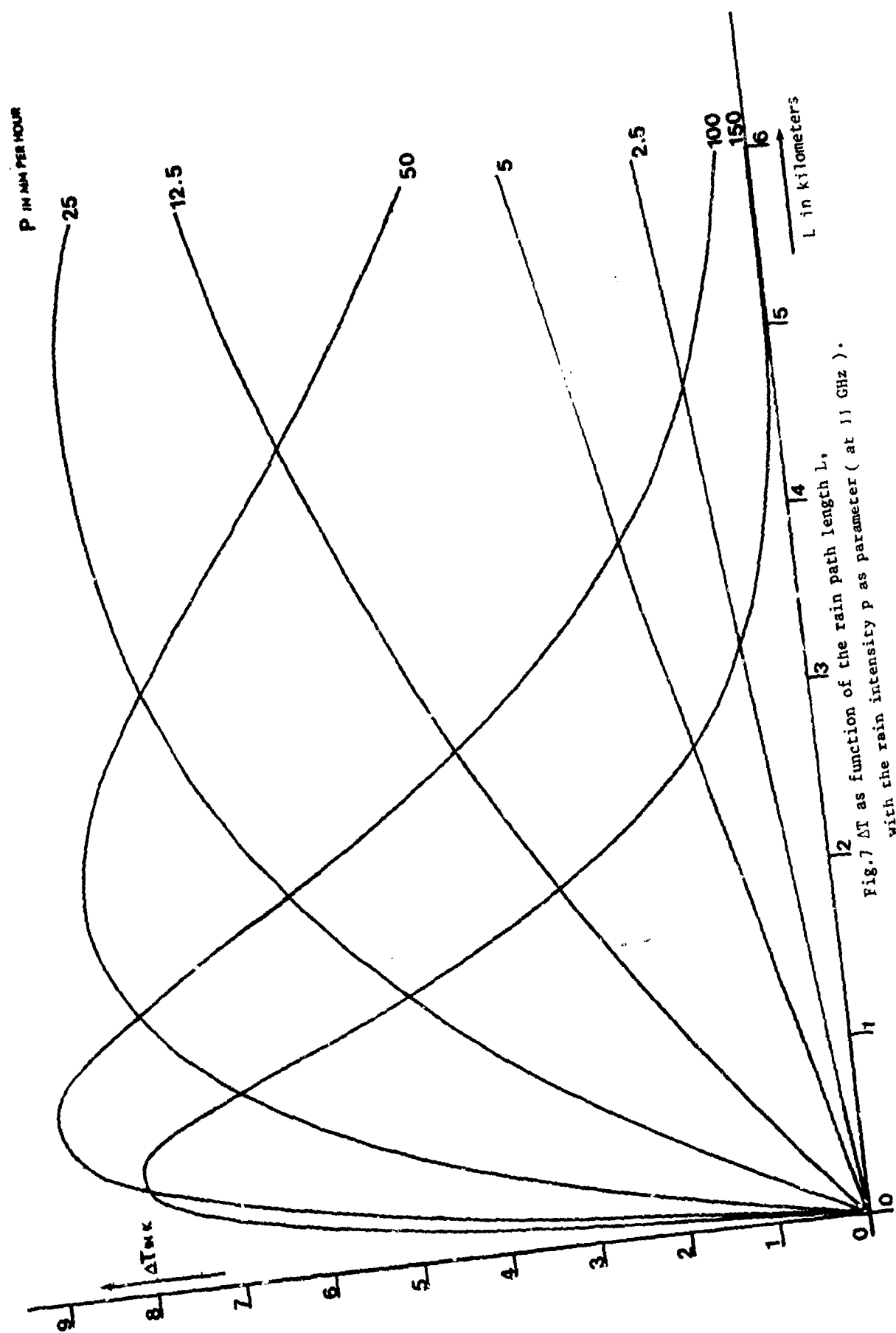


Fig. 7  $\Delta T$  as function of the rain path length  $L$ ,  
with the rain intensity  $p$  as parameter ( at 11 GHz ).

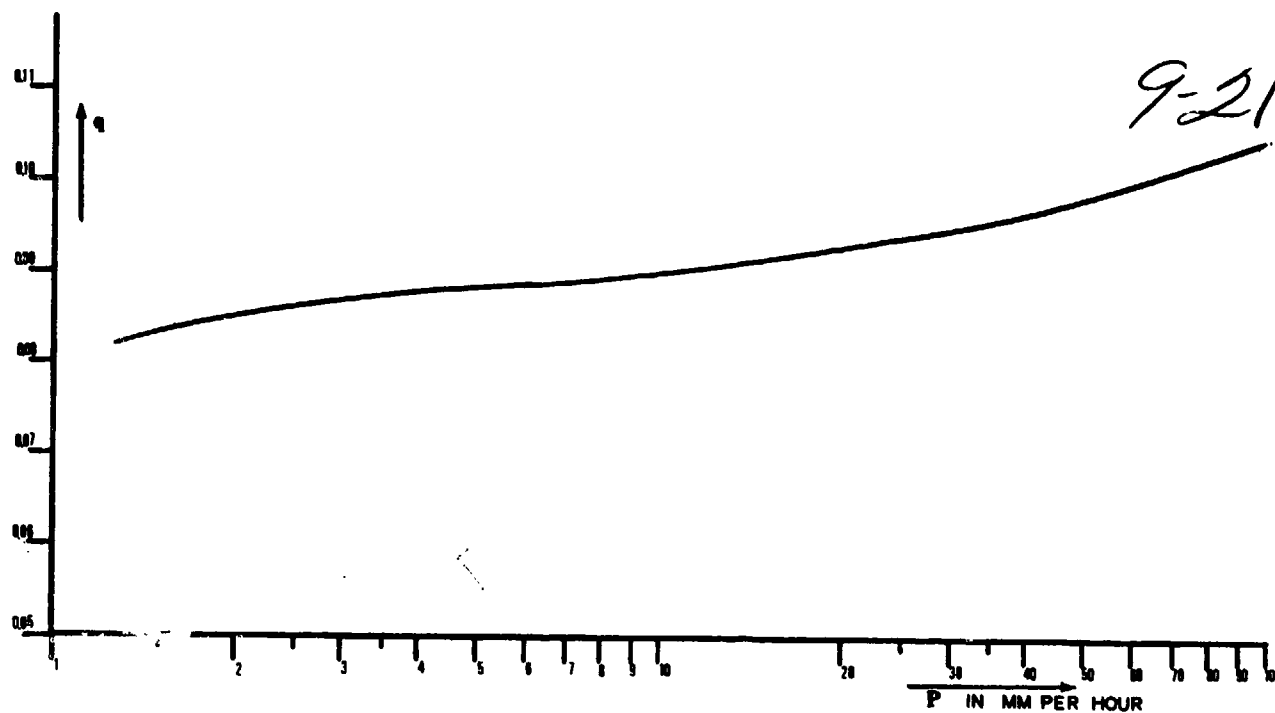


Fig.8  $q = \Delta\Gamma_R / \Gamma_R$  as function of the rain intensity  $p$  ( at 11 GHz ).

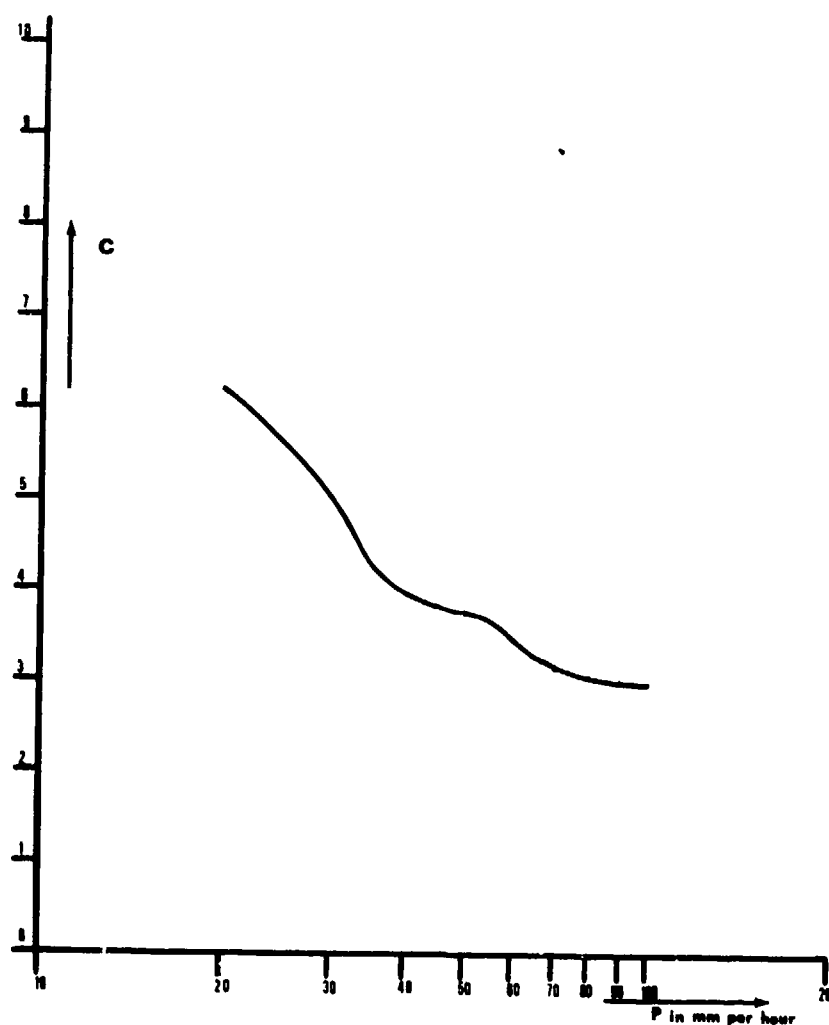


Fig.9  $c = \Delta\Gamma_I / \Delta\Gamma_R$  as function of the rain intensity  $p$   
( at 11 GHz ).



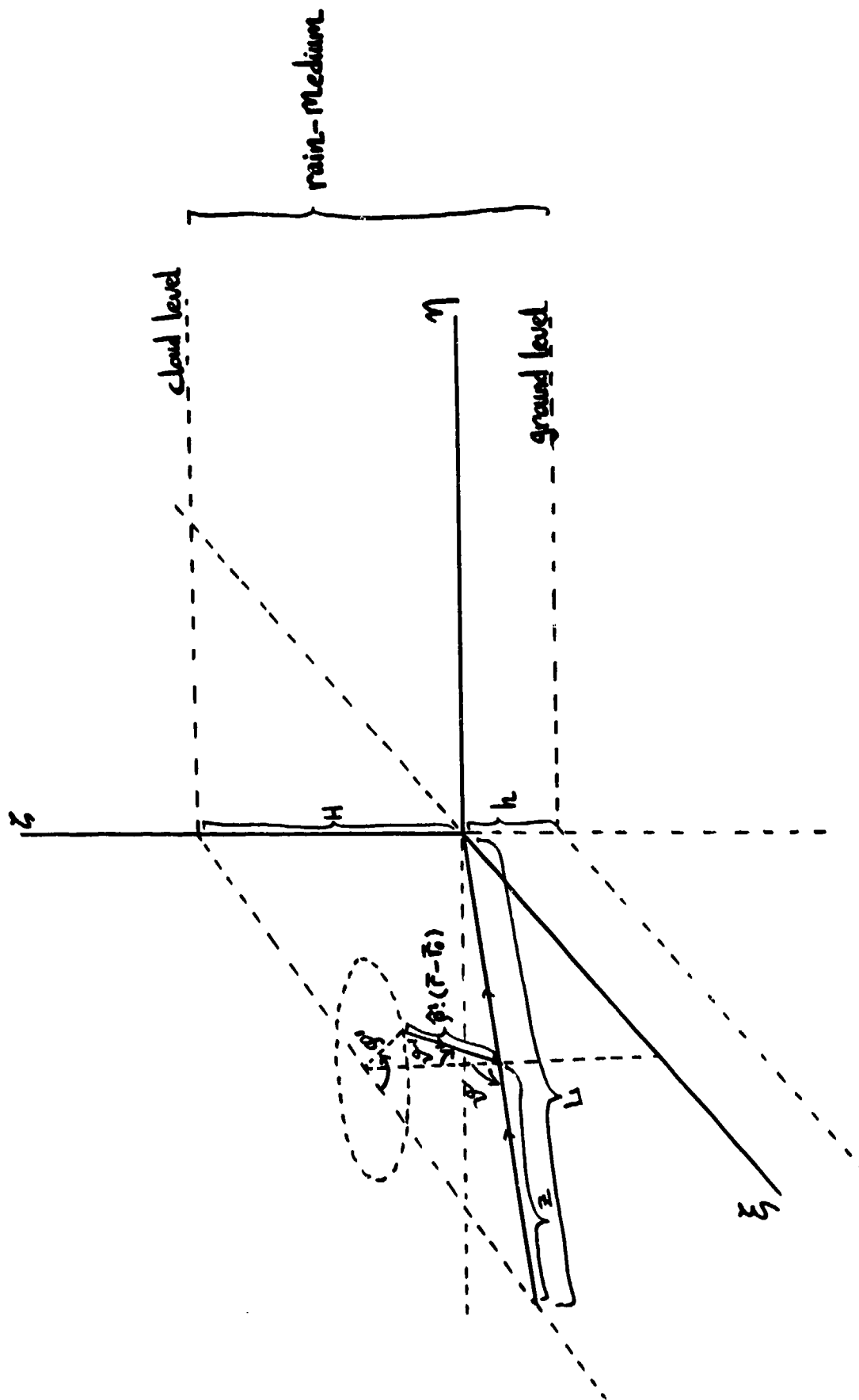


Fig.10 The rain medium extending indefinitely in the horizontal plane, between cloud and horizon.

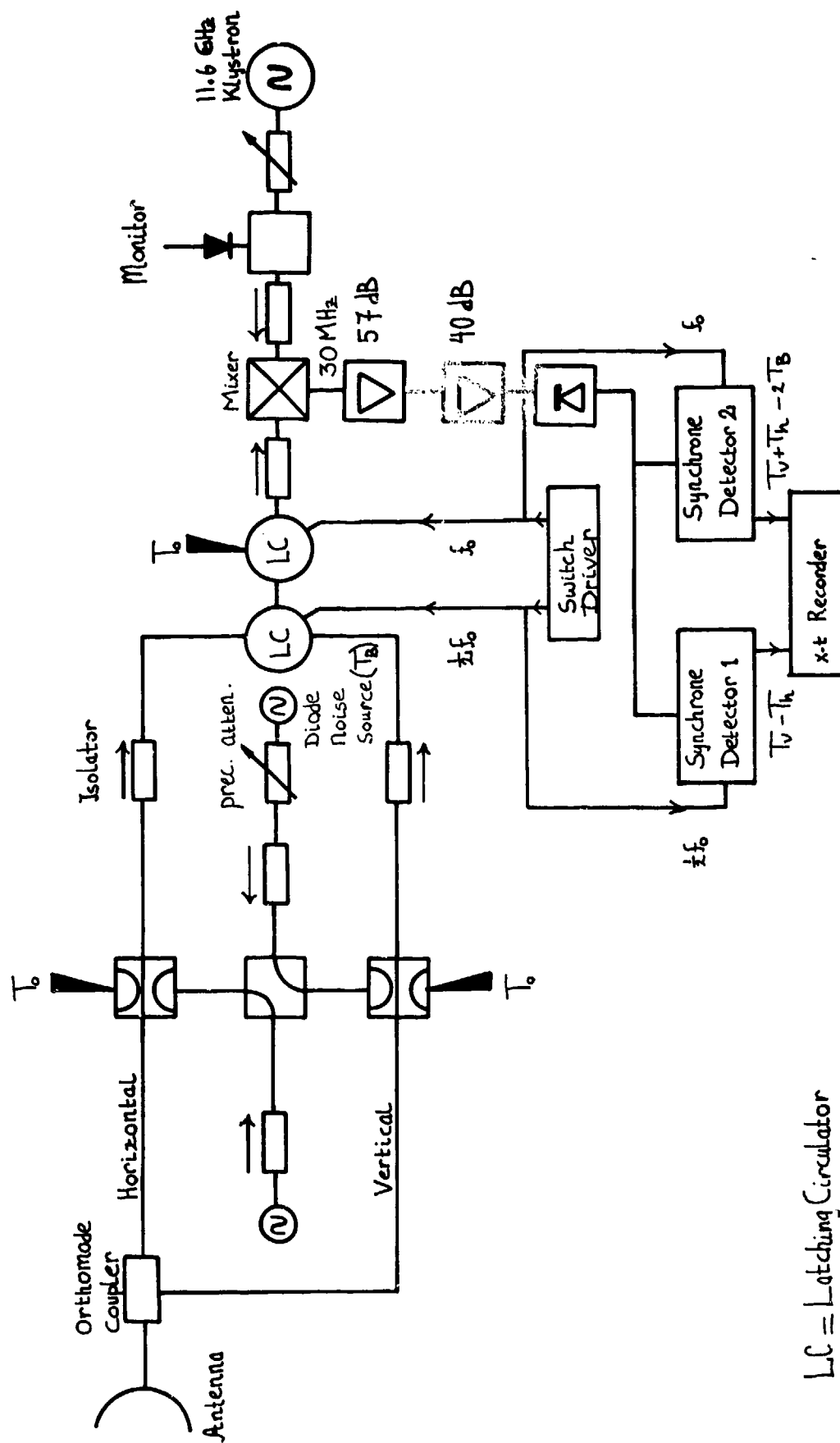


Figure 11. The double Dicke radiometer.

by J. Dijk and A.C.A. van der Vorst.  
Eindhoven University of Technology, Netherlands

10-1

### Summary

This paper deals with the measurements of the influence of artificially wetted radome panels of different materials (Tedlar, Mylar, Teflon) on the performance of antenna systems covered with radomes.

Noise, transmission and depolarization measurements have been carried out and when possible compared with the theory. The complete research programme is explained.

### 1. Introduction

For large antennas such as used in satellite communications the presence of radomes [1] has the advantage that the antenna structure is less influenced by rain and wind, but the disadvantage that the electrical performance of the antenna is affected. Owing to scattering and absorption the transmission properties will decrease and the system noise temperature [2] increase, although above 10 GHz noise is no longer the limiting factor, so that the use of radomes may have advantages. In the past, several authors [3, 4, 5, 6] have discussed the decrease in the gain to noise temperature ratio of reflector antennas surrounded by a radome. Owing to rain, the antenna system performance could even be more affected. Calculations predicting the influence of rain were based on the assumption that a uniform water film is created at the radome's surface after rain [3]. Most of the polyester coating materials used for radomes, such as Tedlar, justify this approach. However, new materials having a different behaviour, are now becoming available. They are often coated with a layer of Teflon, a material having a strong water repellent character. These remarks apply to some extent also to radome protected feeds and line of sight antennas. It is the purpose of this paper to describe the behaviour of these materials with respect to rain and to compare them with the more common materials such as Tedlar. For this purpose a method has been developed to measure the noise temperature increase, transmission and depolarization properties of these materials under several conditions of rain. The entire radome is not measured but only parts of it erected parallel to the aperture plane of a rectangular horn antenna. These panels are wetted by an installation producing artificial rain with a variable rain rate up to 30 mm/h. A second horn antenna close to the first one serves as a reference. The measurement employs a Dicke radiometer and the frequency is 8.75 GHz. In general, the intention of this research programme is the following:

- to develop a rapid testing method of new radome materials which needs only small parts of them. The measuring results are only qualitative and are not dependent on the measuring arrangement and the environment;
- to develop a theoretical model to investigate the various noise contributions of an antenna with radome;
- to determine reflection, absorption and transmission coefficients of a wet panel from measurements; the scattering parameters  $S$  may then be determined;
- to determine transmission, polarization and group delay;
- to estimate the performance of any other system enclosed with the measured radome material from the scattering parameters  $S$ .

From comparative measurements between various radome materials the following new results are reported:

- great advantages obtained if the radome panels are coated with a thin layer of Teflon because the water distribution on a Teflon surface results in a much lower noise temperature increase;
- Teflon panels show an antenna noise temperature increase depending on the horizontal or vertical polarization of the antenna;
- The measuring method is very suitable for testing new radome materials simply and rapidly.

Radome protected antennas will no longer be built in the 4 - 6 GHz range but radome protected antennas may become important to satellite communications above 10 GHz and are in use for military satellite communication systems.

## 2. Measuring procedure

### 2.1. Introduction

A method has been developed for measuring the noise temperature increase in different radome materials under varying conditions of rain. The entire radome is not measured but only parts of it having an area of about  $0.5 \text{ m}^2$ . The radome panels are positioned under an elevation angle of  $45^\circ$  (Fig. 1) illuminated by a pyramidal horn antenna with aperture dimensions  $40 \times 30 \text{ cm}$  in such a way that the panels are parallel to the aperture plane. When carrying out transmission and depolarization measurements, a transmitting antenna, mostly a horn type, was located at the other side of the panel. The panel could be removed quickly from its position to make comparison possible between measurements with and without a radome panel. The panels were wetted by an artificial rain simulating system. In this system the water was supplied to the top of the panel by a system of sprinklers. By applying compressed air to one sprinkler and water to a second sprinkler, the water was applied well atomized to the top of the radome panel. The photographs Figs. 2 and 3 give a more detailed picture of the location of the panel with respect to the rain installation and the horn antenna. For the measurement of the noise temperature two pyramidal horn antennas were used connected to a Dicke radiometer (Fig. 1) operating at a frequency of  $8.75 \text{ GHz}$ . For the calculation of the noise transmission in the system we introduced scattering parameters  $S$  and the reflection coefficients  $\Gamma$ . It has been proved [8] that the output noise temperature  $T_{\text{out}}$  of a passive linear four-port network corresponding with the available noise power  $kT_{\text{out}}B$ , ( $k$  is the Boltzmann constant,  $B$  the noise bandwidth) and the network on a physical temperature  $T_0$  is:

$$T_{\text{out}} = T_1\tau_{14} + T_2\tau_{24} + T_3\tau_{34} + (1 - \tau_{14} - \tau_{24} - \tau_{34})T_0 \quad (2.1.a)$$

or

$$T_{\text{out}} = T_0 + (T_1 - T_0)\tau_{14} + (T_2 - T_0)\tau_{24} + (T_3 - T_0)\tau_{34} \quad (2.1.b)$$

where  $kT_iB$ , ( $i = 1, 2, 3$ ) is the available generator power at input port  $i$  and  $\tau_{i4}$  ( $i = 1, 2, 3$ ) the available transmission factor between port  $i$  and  $4$ .

Eq. 2.1.a has the advantage that the calculation of the noise output is more straightforward since beside the term  $T_0$  only the transmission of noise from the input to output port has to be taken into account.

### 2.2. Detailed description of noise transfer in the microwave part

In Fig. 2.1.b the most important components for the noise transfer in the microwave part of the radiometer are shown. In general this part can be described as a four-port noisy linear passive network with available transmission factors  $\tau_{14}$ ,  $\tau_{24}$ ,  $\tau_{34}$ .

Port 1 is terminated by a measuring antenna A. The noise temperature of antenna A is characterized by  $T_A(r, t)$  because this temperature is a function of the artificial rain rate  $r$  and also of the time  $t$  owing to the fact that the atmospheric noise may change as a function of time.  $\Gamma_A(r)$  is the reflection coefficient depending on the artificial rain rate  $r$ .

Port 2 is terminated by the reference antenna R. The noise temperature of antenna R is described by  $T_R(t)$ . In the case that there is no radome panel under test in front of the measuring antenna, the relation  $T_A(t) = T_R(t)$  holds owing to the fact that the antennas are identical and in the same surrounding.

Port 3 is terminated by a solid state noise source B with noise temperature  $T_B$ .

Port 4 is the four-port output port with output noise temperature  $T_S^1$  or  $T_S^0$  depending whether the microwave switchable three-port circulator S can be in "position 1" or position 0".

Within the four-port we distinguish the following components which are at physical temperature  $T_0$ :

- isolator I with available transmission factor  $\tau_I(r)$  as a function of the artificial rain rate  $r$  owing to the fact that  $\tau_I(r)$  comprises the factor  $\Gamma_A(r)$  (the reflection coefficient of antenna A);
- attenuators E and V described by  $\tau_E$  and  $\tau_V$ ; these are used for balancing purposes;
- directional coupler D with transmission factors  $\tau_{D13}$  and  $\tau_{D23}$ ;
- precision attenuator P with transmission factor  $\tau_P$ ;
- switchable circulator S which can be switched in "position 0" or "position 1".

10-3

The corresponding transmission coefficients are

$$\text{for "position 1" : } \tau_{S13}^1 \ll \tau_{S23}^1$$

$$\text{for "position 0" : } \tau_{S13}^0 \gg \tau_{S23}^0$$

It is now possible to calculate a general expression for  $T_A(r, t)$  as a function of the parameters mentioned above. For  $T_S^1$  and  $T_S^0$  we find

$$T_S^1 = T_0 + \{T_A(r, t) - T_0\}\tau_{14}^1 + \{T_R(t) - T_0\}\tau_{24}^1 + (T_B - T_0)\tau_{34}^1 \quad (2.2.a)$$

and

$$T_S^0 = T_0 + \{T_A(r, t) - T_0\}\tau_{14}^0 + \{T_R(t) - T_0\}\tau_{24}^0 + (T_B - T_0)\tau_{34}^0 \quad (2.2.b)$$

#### Bridge balancing

In general the microwave bridge will be balanced with attenuators E and V and this means that  $T_S^1 = T_S^0$ . Subtracting Eq. 2.2.a from Eq. 2.2.b yields:

$$\{T_A(r, t) - T_0\}(\tau_{14}^1 - \tau_{14}^0) + \{T_R(t) - T_0\}(\tau_{24}^1 - \tau_{24}^0) + (T_B - T_0)(\tau_{34}^1 - \tau_{34}^0) = 0. \quad (2.3)$$

From Fig. 2.1.b the general transmission factors  $\tau_{14}$ ,  $\tau_{24}$  and  $\tau_{34}$  can be deduced with the switch in the two positions. Therefore, the following relations apply

$$\tau_{14}^1 - \tau_{14}^0 = \tau_I(r)\tau_E(\tau_{S13}^1 - \tau_{S13}^0) = \tau_I(r)\tau_E\tau_{S13} \quad (2.4)$$

$$\text{with } \tau_{S13} = \tau_{S13}^1 - \tau_{S13}^0$$

$$\tau_{24}^1 - \tau_{24}^0 = \tau_V\tau_{D13}(\tau_{S23}^1 - \tau_{S23}^0) = \tau_V\tau_{D13}\tau_{S23} \quad (2.5)$$

$$\text{with } \tau_{S23} = \tau_{S23}^1 - \tau_{S23}^0$$

$$\tau_{34}^1 - \tau_{34}^0 = \tau_P\tau_{D23}\tau_{S23}. \quad (2.6)$$

Substituting Eqs. 2.4, 2.5 and 2.6 in Eq. 2.3 results in:

$$0 = \{T_A(r, t) - T_0\}\tau_I(r)\tau_E\tau_{S13} + \{T_R(t) - T_0\}\tau_V\tau_{D13}\tau_{S23} + (T_B - T_0)\tau_P\tau_{D23}\tau_{S23} \quad (2.7)$$

Without radome panels, the antenna temperatures  $T_A(t)$  and  $T_R(t)$  are equal; therefore, it is possible to adjust the transmission factor  $\tau_E$  and  $\tau_V$  in such a way that  $T_S^1 = T_S^0$ . It is thereby necessary to switch off  $T_B$  so that  $T_B = T_0$ . Eq. 2.7 may now be rewritten for  $T_B = T_0$  giving

$$\{T_A(t) - T_0\}\tau_I(0)\tau_E\tau_{S13} + \{T_R(t) - T_0\}\tau_V\tau_{D13}\tau_{S23} = 0 \quad (2.8)$$

Since  $T_A(t) = T_R(t)$  (antenna without radome) it follows that

$$\tau_I(0)\tau_E\tau_{S13} = -\tau_V\tau_{D13}\tau_{S23} \quad (2.9)$$

with  $\tau_I(0)$  the isolator transmission factor without radome. Eq. 2.9 may now be substituted in Eq. 2.7 as an edge condition and after some calculations the latter becomes:

$$T_A(r,t) = (\tau_I(0))/(\tau_I(r))\{T_R(t) + (T_B - T_0)(\tau_p \tau_{D2})/(\tau_V \tau_{D1})\} + (1 - (\tau_I(0))/(\tau_I(r)))T_0 \quad (2.10)$$

In this equation  $T_A(r,t)$  does not depend on  $\tau_I(r)$ , i.e. the reflection coefficient of antenna A with radome to a great extent.

### 2.3. Calculation of $T_B$

The noise temperature  $T_B$  may be calculated by a substitution method using the radiometer under consideration.

The noise temperatures at the output of the waveguide switch connecting either the load on a stable reference temperature of 100° C or the diode noise source B via the precision attenuator P should be equal. We now have the following relation

$$\tau_p T_B + (1 - \tau_p)T_0 = T_{100} = 373 \text{ K}$$

Therefore,

$$T_B = (T_{100} - (1 - \tau_p)T_0) / \tau_p \quad (2.11)$$

$T_B$  is estimated to be approx 68000 K.  $\pm 2\%$

The noise source diode current  $I_d$  is set to the point  $(dI_d)/(dT_B) = 0$  at a current of 16 mA.

The sensitivity of the radiometer

$$\sqrt{\Delta T^2} = 0.2 \text{ K}$$

The accuracy of the measurements is  $\pm 5\%$ .

### 2.4. Relevance of the use of a reference antenna instead of a matched load on $T_0$

Let the noise temperature of antenna A without radome be  $T_A(t) = T_A(t_0) + \Delta T$  and the available transmission factor of the radome  $\tau_R$ . The antenna A temperature  $T_A(r,t)$  is then

$$T_A(r,t) = \{T_A(t_0) + \Delta T\} \tau_R + (1 - \tau_R)T_0 \quad (2.12)$$

The difference in temperature with respect to  $T_R(t)$  is

$$T_A(r,t) - T_R(t) = -\{T_A(t_0) + \Delta T\}(1 - \tau_R) + (1 - \tau_R)T_0$$

because  $T_A(t) = T_R(t)$  and  $(1 - \tau_R)T_0$  is the panel contribution.

The measuring error due to a change  $\Delta T$  in the antenna noise temperature

$$T_A(t_0) = -\Delta T(1 - \tau_R) \quad (2.13)$$

For  $\tau_R \approx 1$  there is a good compensation owing to the reference antenna R.

It is now possible to replace the reference antenna R by a matched load at temperature  $T_0$ . The antenna A temperature is given by Eq. 2.12. It is compared with  $T_A(t_0)$  as this is the measurement reference. The difference temperature with respect to  $T_A(t_0)$  is

$$T_A(r,t) - T_A(t_0) = \{T_A(t_0) + \Delta T\} \tau_R - T_A(t_0) + (1 - \tau_R)T_0 = -\{T_A(t_0)(1 - \tau_R) + \Delta T \tau_R\} + (1 - \tau_R)T_0$$

The measuring error due to a change  $\Delta T$  in the atmospheric noise temperature  $T_A(t_0)$  is  $\Delta T \tau_R$ . This error reaches its maximum at  $\tau_R \approx 1$ . Comparing this error with the error  $-\Delta T(1 - \tau_R)$  of the two-antenna method described above, it is clear that for  $\tau_R \approx 1$  the method with reference antenna is preferred and for  $\tau_R \approx 0$  the method with a matched load is preferred. The crossover point is reached at  $\tau_R = 0.5$  with the

criterion that the measuring error of both methods must be equal.

### 3. Radome panels and rain

10-5

#### 3.1. The definition of the rain intensity in relation to the measuring system

If the rain falls perpendicularly on the radome [Fig. 4], which is considered to be spherical, the amount of rain coming down is confined to an area of  $\frac{1}{4}\pi D^2$ , where D is the diameter of the radome. If it rains h mm/hour, the radome subtends

$$\frac{1}{4}\pi D^2 h \cdot 10^{-3} / 60 \text{ m}^3/\text{minute}.$$

The water streams downwards and falls off at the equator of the radome. Here, the water collected per running metre is

$$\frac{\frac{1}{4}\pi D^2 h \cdot 10^{-3} / 60}{\pi D} = 4.17 h D \text{ cm}^3/\text{min.}/\text{metre}.$$

If the rain installation has a measuring length of P cm and a quantity of Q cm<sup>3</sup>/min. water comes down from the radome, the following relationship applies:

$$h = \frac{100 Q}{4.17 P D} \text{ mm/hour} \quad (3.1)$$

In Fig. 4 Eq. 3.1 has been plotted for P = 40 cm. With a given quantity of water Q cm<sup>3</sup>/min., the rain intensity is inversely proportional to the radome diameter D.

#### 3.2. Calculation of the (effective) water layer thickness

Assuming a uniform water layer over the radome with diameter D, the thickness  $d_w$  of the water layer can be calculated according to [9]

$$d_w = 0.0045 \left( \frac{1}{4} D h \right)^{7/12} (\sin \theta)^{1/4} \quad (3.2)$$

where  $\theta$  is defined in accordance with Fig. 4.

Since this equation depends only little on  $\theta$  for  $10^\circ < \theta < 90^\circ$ , a more or less uniform water layer with the same thickness exist over the radome. In the case that D = 38 m we find for  $d_w$

$$d_w = h^{7/12} \text{ mm.} \quad (3.3)$$

Assuming that the theory of Mei [9] may also be applied to radome parts and substituting Eq. 3.1 in Eq. 3.2, the following relation is found

$$d_w = 0.0045 \left( \frac{100 Q}{4.17 \cdot 2 \cdot P} \right)^{7/12} (\sin \theta)^{1/4} \quad (3.4)$$

This relation is plotted in Fig. 5 and is independent of the diameter D of the radome. It shows the thickness of the uniform water layer over a panel for different elevation angles as a function of the collected water Q cm<sup>3</sup>/min. The measuring length P over which the water is collected is 40 cm. A uniform water layer only appears on Tedlar panels. With Teflon panels drops and spirts are formed on the surface (Fig. 7). The water distribution on Mylar panels lies between those on Tedlar and Teflon panels (Fig. 8). For Tedlar and Mylar it is not possible to assume a uniform water layer but an effective uniform water layer may be defined. This may be calculated with Eq. 3.4 measuring a water flow of Q cm<sup>3</sup>/min.

### 4. Noise measurements

The difference of the antenna noise temperature between the antennas A and R has been measured using the

materials Tedlar, Mylar and Teflon with the water flow as a parameter. The thickness of the material is only of importance to the noise increase due to the dry radome. With respect to Secs. 2 and 3 the difference in noise temperature becomes

$$\Delta T = T_A(r, t_0) - T_R(t_0) \quad (4.1)$$

and is plotted against the panel water flow (normalized for 1 m measuring length)  $Q$  cm<sup>3</sup>/min/metre. For each material the measurements have been carried out for horizontal and vertical polarization. By means of Fig. 5, it is possible to relate the water flow  $Q$  to the (effective) water layer thickness, and when the diameter  $D$  is introduced, the measurements can be related to the rain intensity  $h$  mm/hour using Fig. 4. The measuring results are plotted in Fig. 8 for Tedlar and in Fig. 9.a and b for Teflon and Mylar. On Tedlar, a uniform water layer exists and this explains the fact that the noise temperature increase is high and independent of the polarization. On Teflon, drops and vertical spirts are formed and this explains the fact that the vertical polarization noise increase is higher than the horizontal. The results obtained with Mylar lie between those of Teflon and Mylar. Radome materials covered with a layer of Teflon are more in favour than Tedlar with respect to the noise performance. However, coating of radomes with a layer of Teflon is still a serious technological problem.

##### 5. Calculation of the antenna noise temperature increase due to a wetted radome panel

We shall assume that a transmission line model from the atmosphere is a matched generator and that the radome panel is a lossy two-port at temperature  $T_0$  with an available transmission factor  $T_R$  consisting of the scattering parameters  $S_{11}$ ,  $S_{21}$ ,  $S_{12}$ ,  $S_{22}$  (Fig. 10). It may be shown from [10] that the panel noise contribution  $\Delta T_1$  is

$$\Delta T_1 = \{1 - |S_{22}|^2 - |S_{21}|^2\} T_0$$

if the panel is covered with a uniform water layer. The calculated noise contribution due to the panel is plotted in Fig. 10. The panel thickness is 1 mm,  $\epsilon_r = 4$  and  $\tan \delta = 0.02$ .

This calculated value are in accordance with the CCIR curves for noise contributions from uniform water layers [7]. When the calculated values are compared with the measured values for Tedlar panels (Figs. 8 and 10) it appears that the accordance is not good. It can be shown [11] that due to multiple reflections the noise temperature increase  $\Delta T_2$  of a small antenna within a complete radome becomes

$$\Delta T_2 = \frac{\{1 - |S_{22}|^2 - |S_{21}|^2\} T_0}{1 - |S_{22}|^2} = \frac{\Delta T_1}{1 - |S_{22}|^2}$$

This calculated noise temperature increase with multiple reflections is plotted in Fig. 10.

Comparing the measured values for Tedlar panels with the calculated values with multiple reflections it appears that multiple reflections have to be taken into consideration.

##### 6. Transmission measurements

Transmission measurements with wetted panels are carried out at the same frequency as used for the noise measurements. At a distance of 12 metres a horn antenna is located on top of a tower 12 metres high. The incident field is sufficiently uniform in phase and amplitude. The measurements have been carried out with an H.P. network analyzer. The measured results are plotted in Fig. 11 for horizontal polarization and in Fig. 12 for vertical polarization. Fig. 10 shows the theoretical transmission factor  $|S_{21}|^2$  for a panel with uniform water layer. The correspondence with Tedlar panels is quite good. More work is required to obtain theoretical values for panels with drops and spirts.

##### 7. Conclusions and remarks

Some preliminary conclusions may be found in Sec. 4. The theoretical model is not in accordance with the practical situation for Tedlar panels with uniform water layers. The observed values for Teflon should be compensated for noise which is scattered in the measuring system due to drops and spirts. The noise



measurement of one panel offers the possibility of estimating the noise temperature of a complete radome. However, a number of factors should be taken into consideration.

- The radome panels are mostly mounted in a metal space frame radome causing a transmission loss for which the temperature has to be corrected.
- The antenna may produce circular polarization.
- If the rain falls perpendicularly only the top half of the radome is wetted decreasing the noise values.
- Multiple reflections within the radome result in higher temperatures.
- If it rains,  $T_A$  will be higher since the sky noise temperature increases also.

The relationship of the noise temperature of a complete radome and only one panel is still the object of further study.

#### Acknowledgement

We acknowledge Messrs. A.C.M. Schepens, R.D. van der Does, L. Wijdemann and A. Maartens for their valuable technical and scientific support.

#### References

1. IEEE Standard Definitions of Terms for Antennas, IEEE Std 149 - 1971, 2 August 1971.
2. J. Dijk, M.K.J. Jenken and K.J. Maander: "Antenna noise temperature", Proc. IEE Vol. 115, pp. 1401-1410, Oct. 1968.
3. R.C. Blevins: "Losses due to rain on radomes and antenna reflecting surfaces", IEEE Trans. Antenna and Prop., pp. 175-176, Jan. 1965.
4. J. Rume: "More on wet radomes", IEEE Trans. Antennas and Prop., 823-824, Nov. 1965.
5. R.C. Blevins: "Rain effects on radomes and antenna reflection", Conference on Large Steerable Antennas, London 1966.
6. K.P. Romeiser: "Beeinflussung von Güte, Gewinn und Rauschtemperatur der 25 Meter Antenne Raketendurch künstliche Beregnung des Radoms", NIN-URSI Tagung Antennen, Darmstadt, Oct. 1967.
7. CCIR: "Effects on earth station performance due to water on radomes" Rep. 192-1, CCIR New Delhi 1970.
8. T.Y. Otonari: "The effects of mismatched components on microwave noise temperature calibrations", IEEE Trans. Microwave Theory and Techn., pp. 678-687, Sept. 1968.
9. C.C. Mei: "Rainfall effects on rigid radomes", M.S.D. Lincoln Laboratory consulting service contract no. 2940 as part of the CAMROX study.
10. J. Dijk, A.C.M. Schepens, A.C.A. van der Vorst: "Noise properties of wet antenna radomes", Seminar über Antennen Technik, Internationales Elektronik Zentrum, München 22-23 Nov. 1971.
11. W. Keizer: "On the carrier to noise ratio with antennas for satellite communications surrounded by a radome", Master thesis Sept. 1970, Eindhoven University of Technology, Electr. depart., Eindhoven Netherlands.

10-8

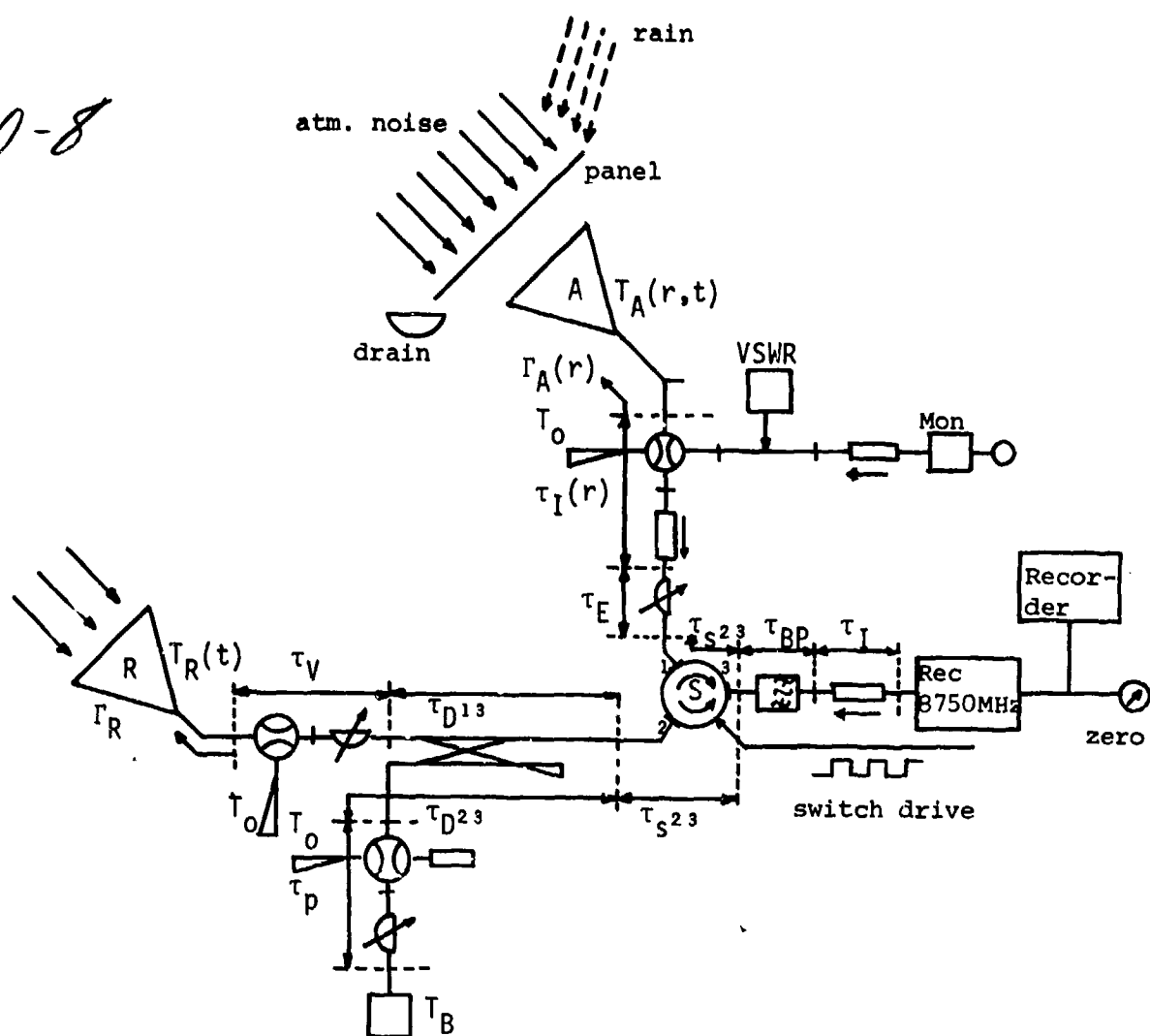


Fig. 1 a: Schematic diagram of the measuring arrangement.

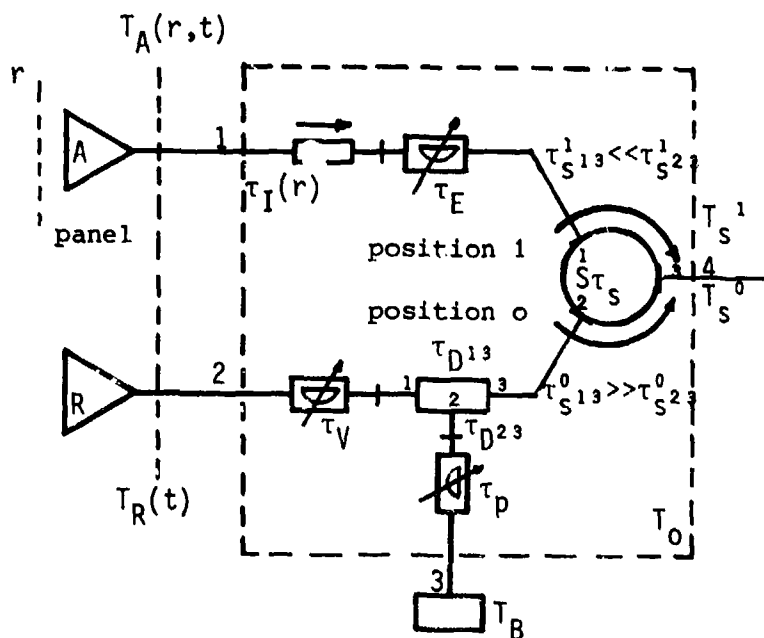


Fig. 1 b: Microwave part of the radiometer.



Fig. 2: General view of the measuring set up.

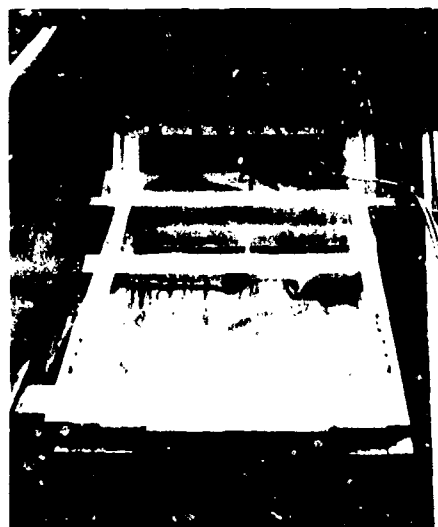


Fig. 3: Artificial rain installation with sprinklers.

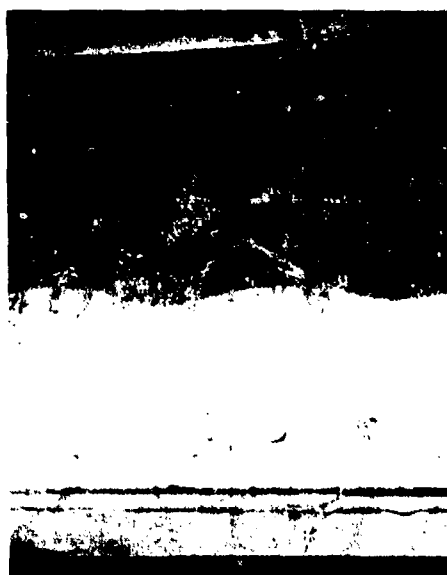


Fig. 6: Water distribution on Mylar panels.



Fig. 7: Water distribution on Teflon panels.

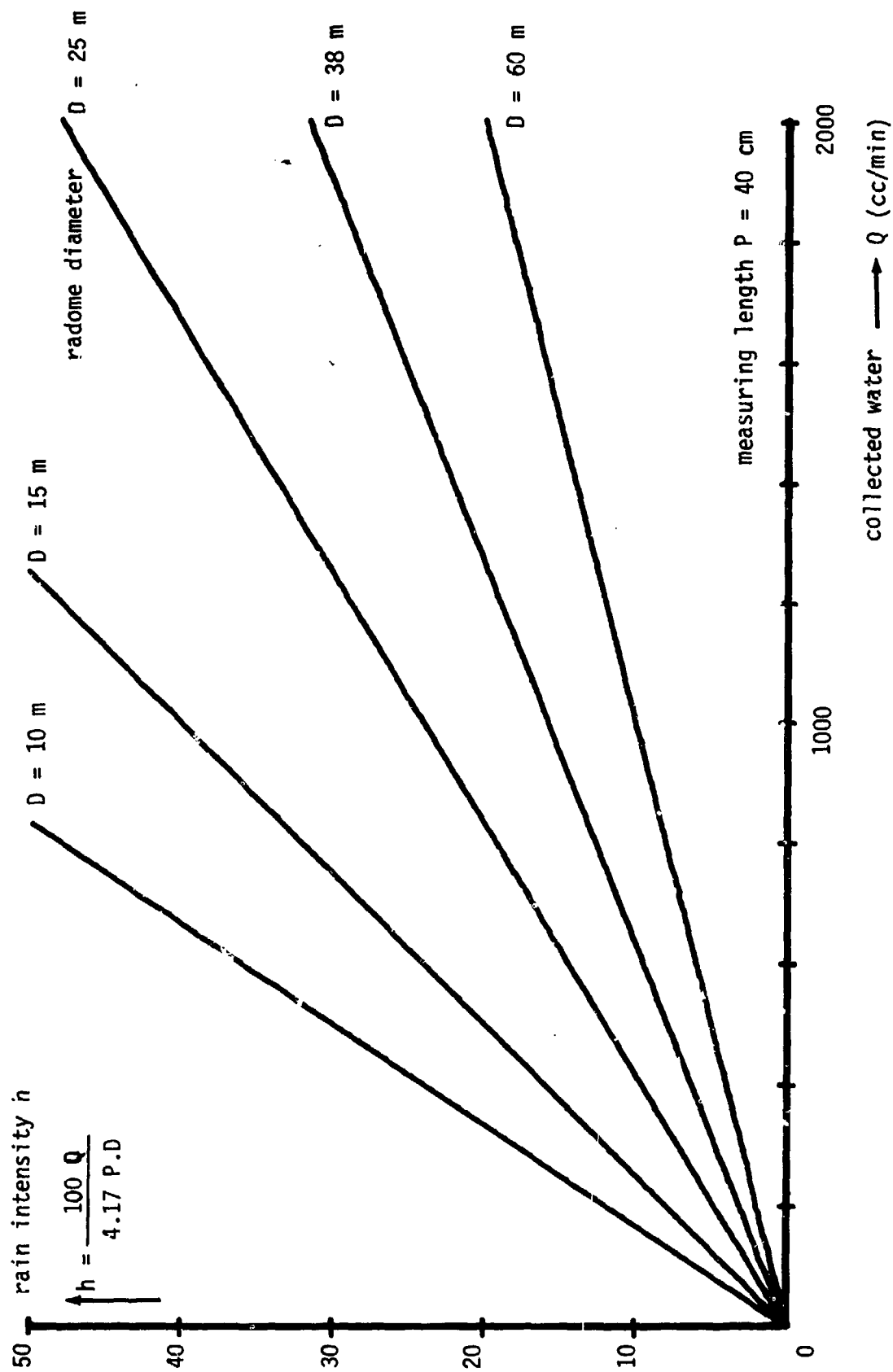


Fig. 4: Collected water  $Q \text{ cm}^3/\text{min}$  as a function of rain rate  $h \text{ mm/hour}$  with the measuring length  $P = 40 \text{ cm}$ , the diameter  $D$  of the real radome being a parameter.

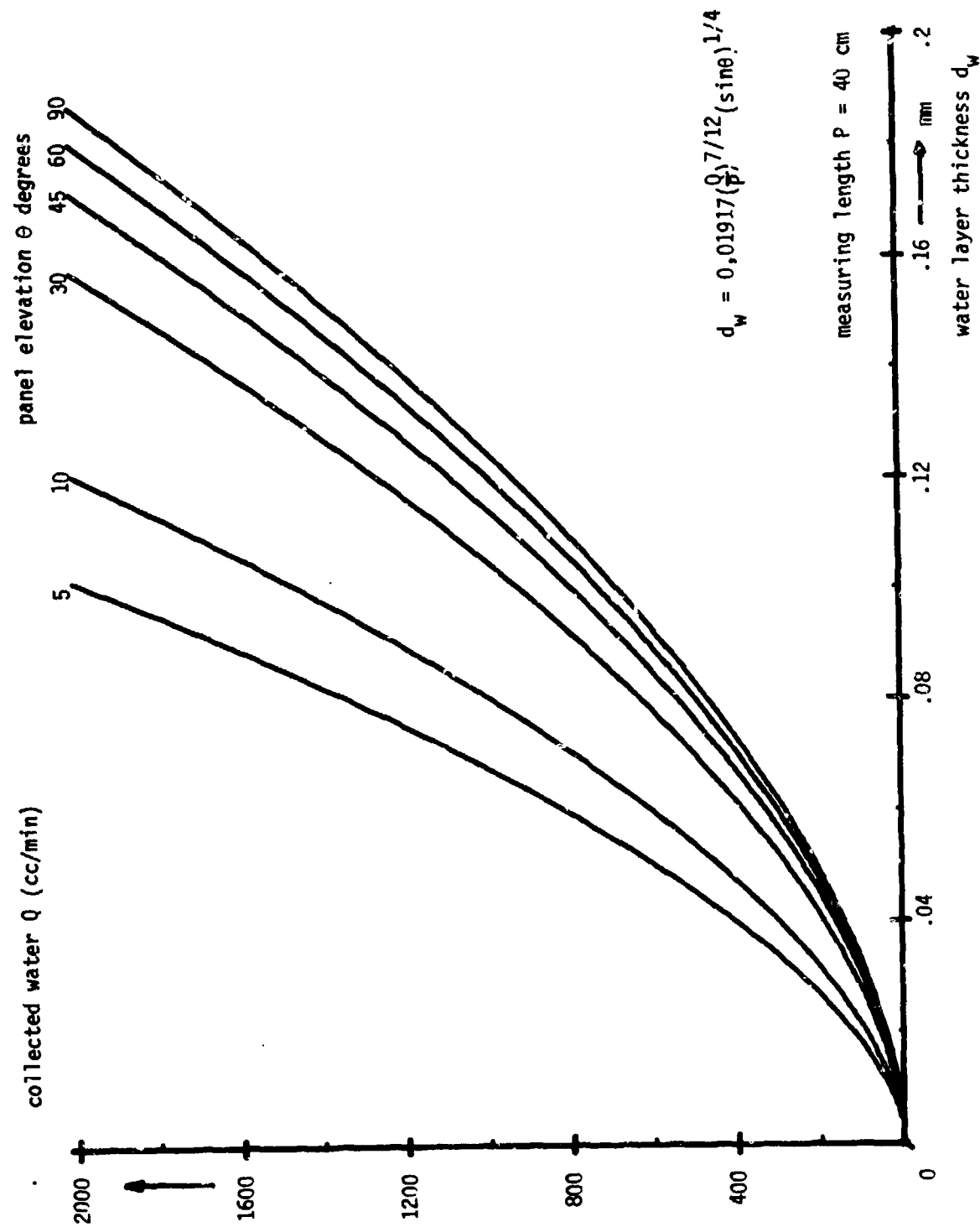


Fig. 5: Water layer thickness in mm of the collected water  $Q$  cm<sup>3</sup>/min with the panel elevation as a parameter.

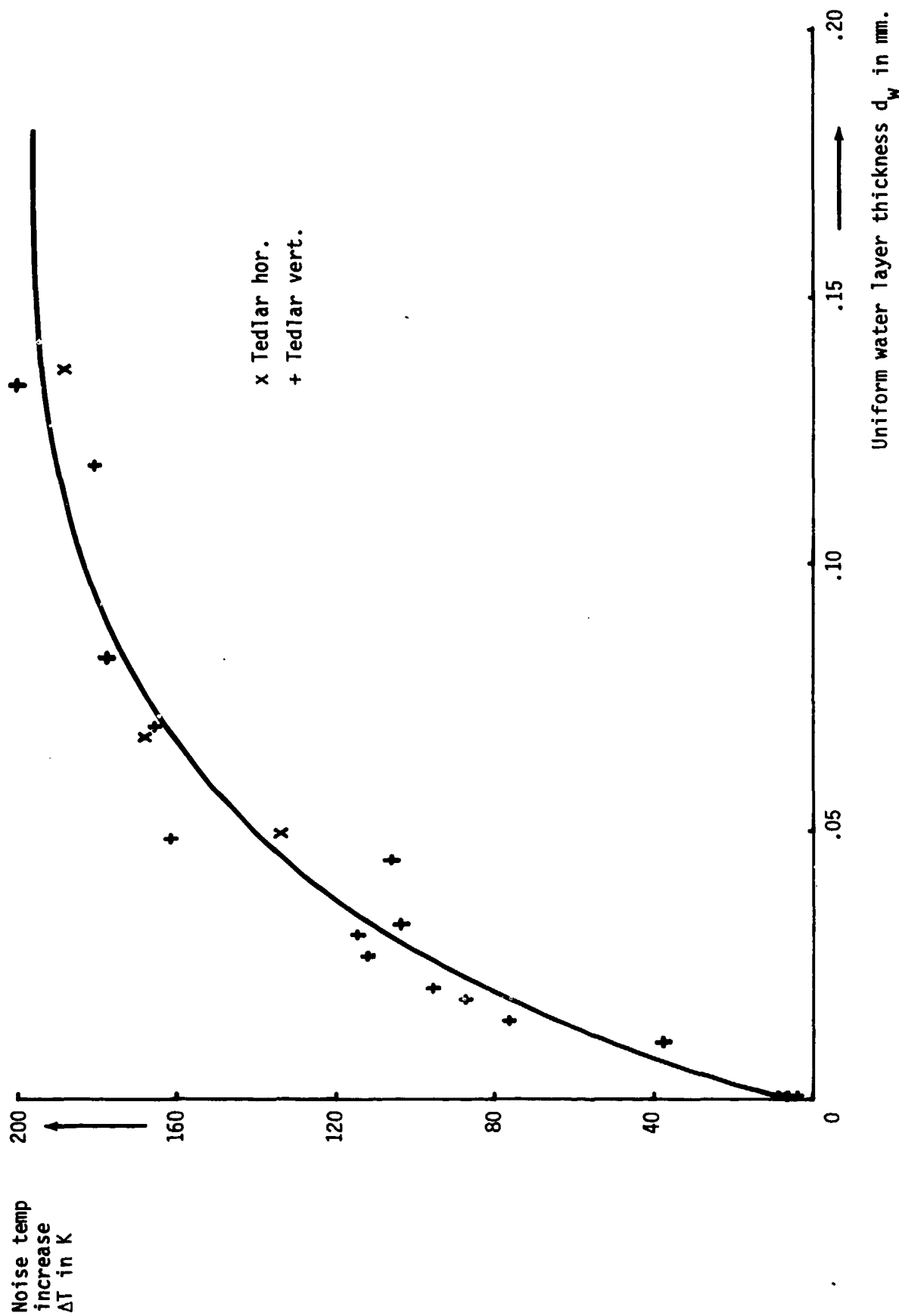


Fig. 8: Measured noise temperature increase for Tedlar panels.

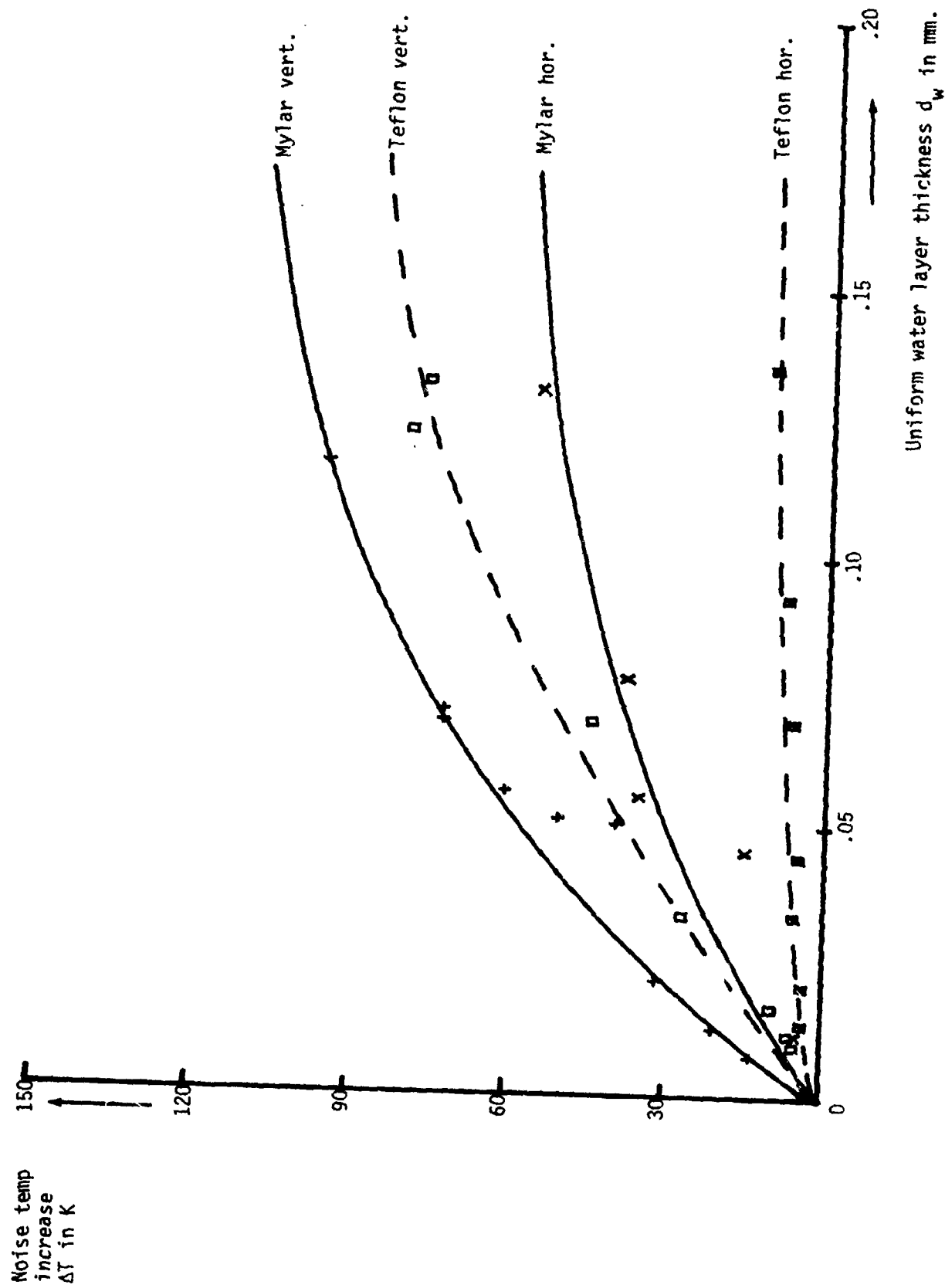


Fig. 9: Measured noise temperature increase for Mylar and Teflon panels.

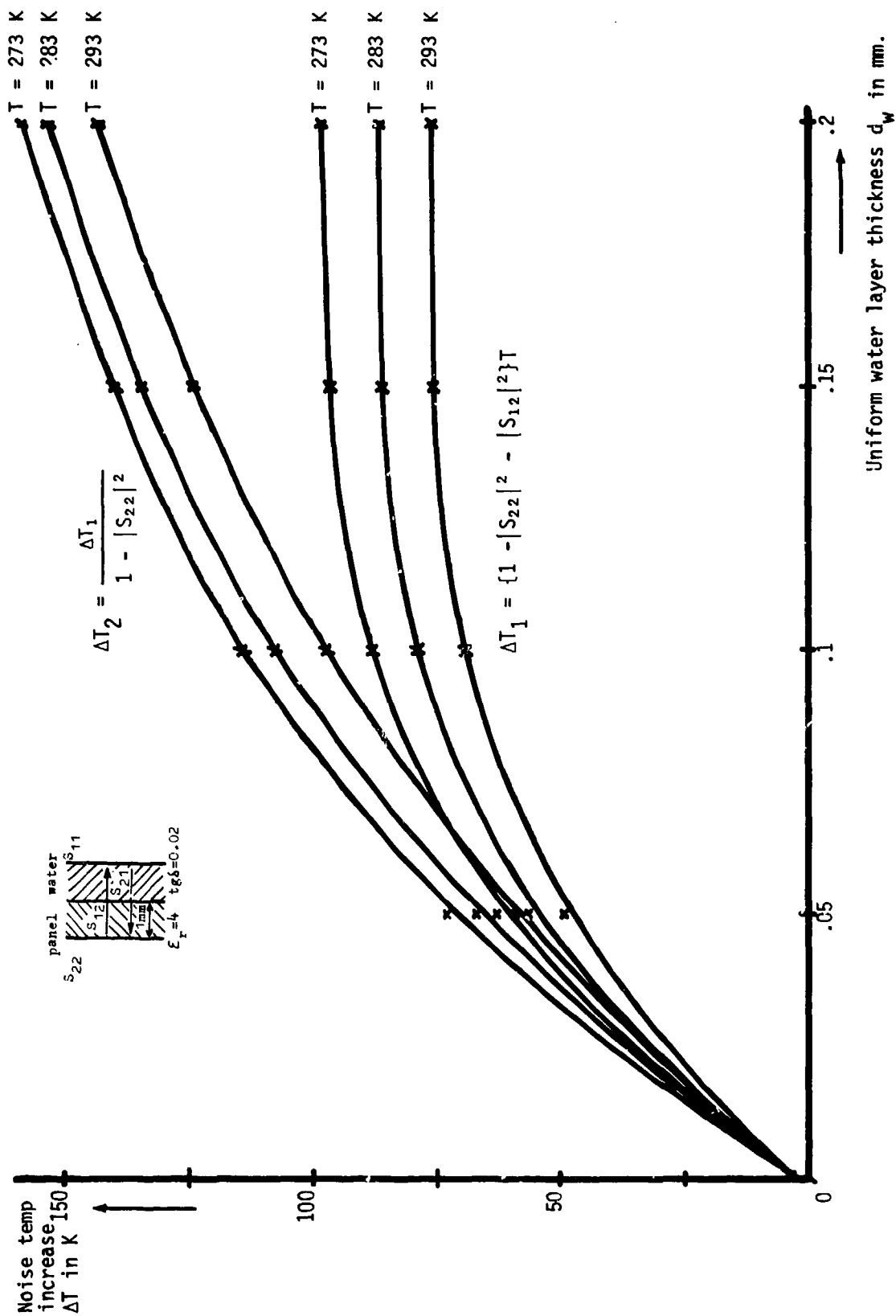


Fig. 10: S parameter representation of a panel with uniform water layer.  
 Calculated antenna noise temperature increase  $\Delta T_1$  without multiple scattering. Calculated antenna noise temperature increase  $\Delta T_2$  with multiple scattering in a full radome.



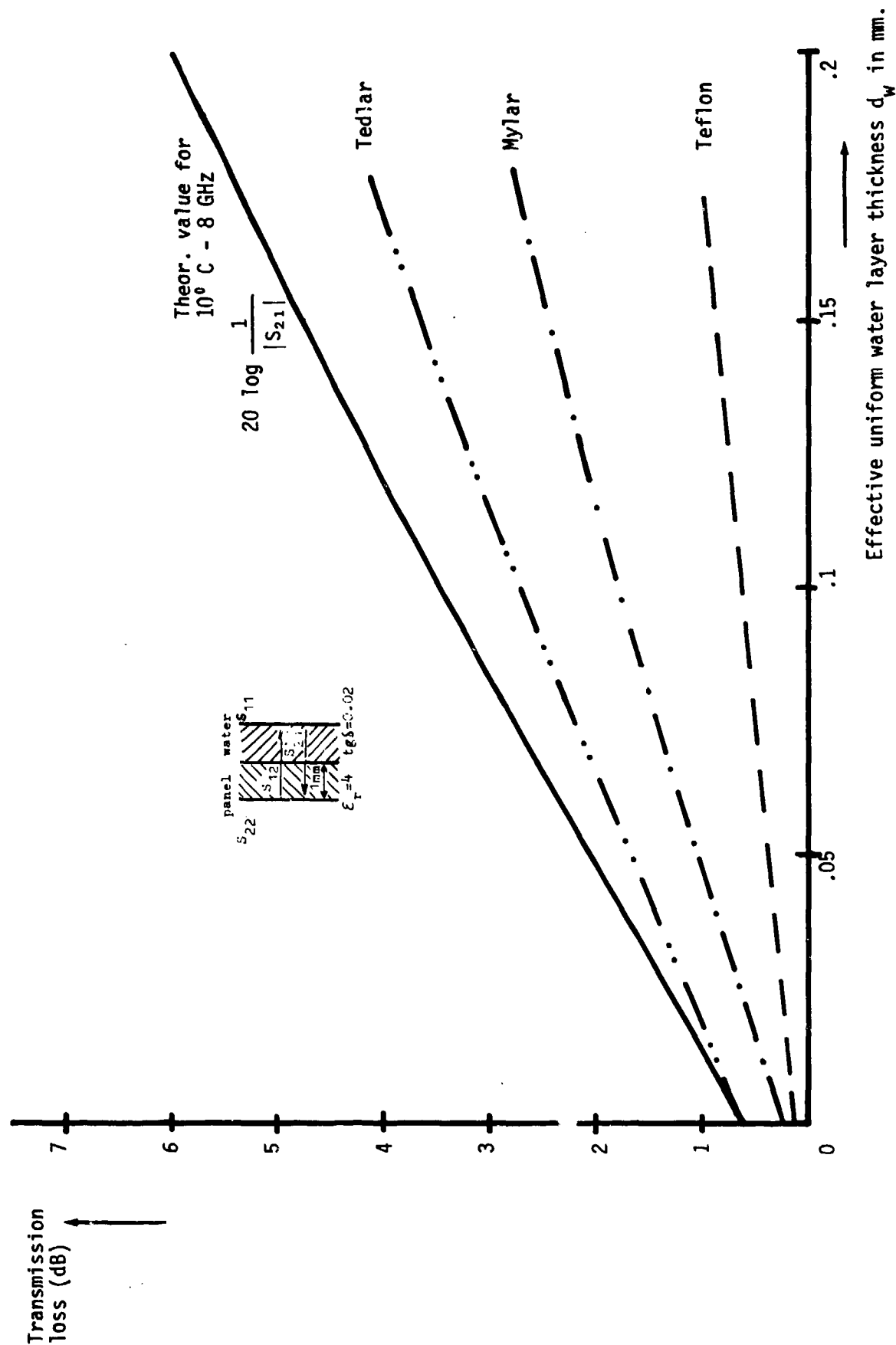


Fig. 11: Measured transmission loss through Tedlar, Mylar and Teflon panels for horizontal polarization.

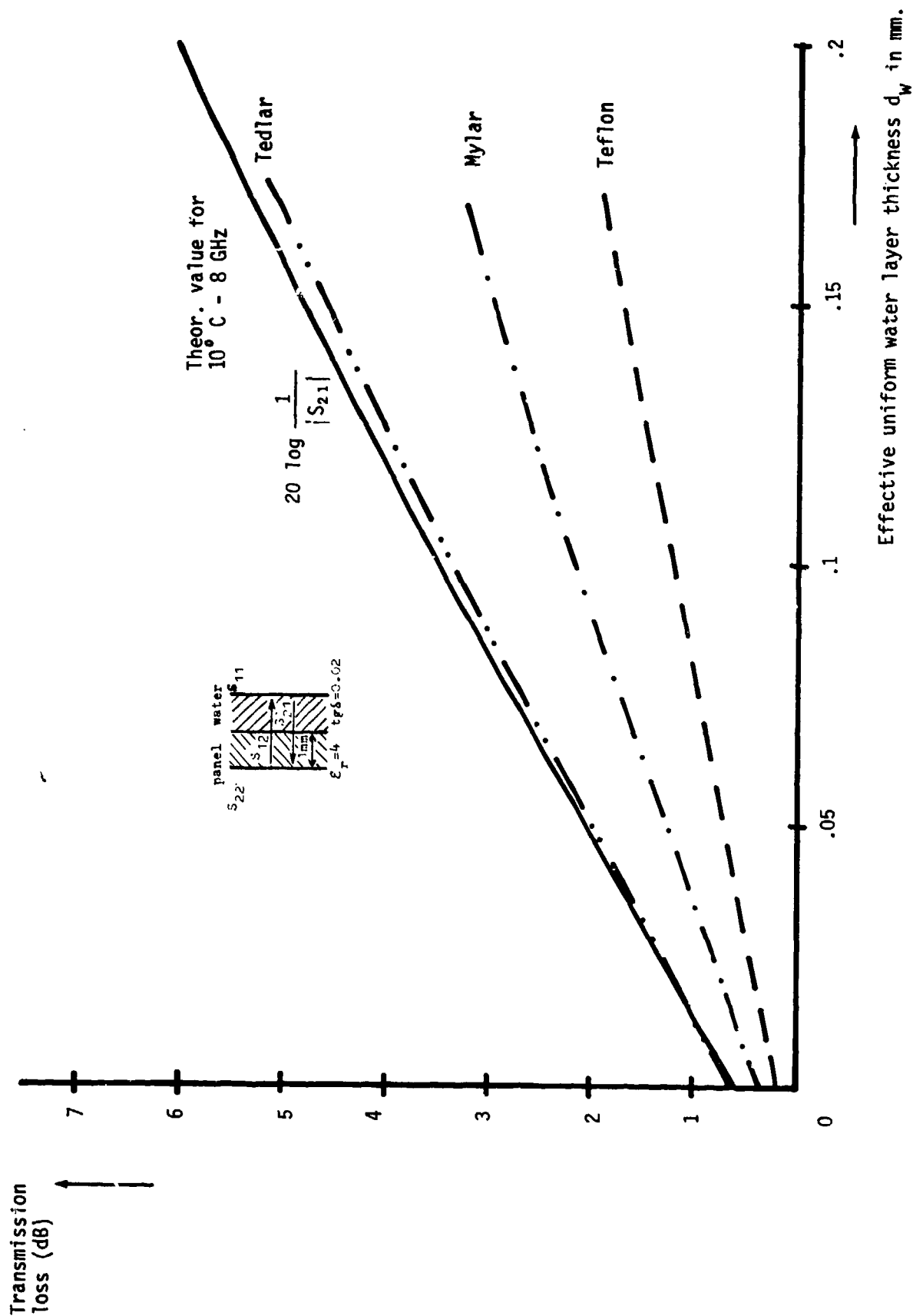


Fig. 12: Measured transmission loss through Tedlar, Mylar and Teflon panels for vertical polarization.

11-1

ANTENNA RESPONSE TO RANDOM ELECTRIC  
FIELDS DUE TO THERMODYNAMIC DENSITY  
FLUCTUATIONS IN PLASMAS

R. Grabowski  
Institut für physikalische Weltraumforschung  
der Fraunhofer-Gesellschaft  
78 Freiburg  
Germany

SUMMARY

Thermodynamic density fluctuations of positively and negatively charged components in a plasma are responsible for the occurrence of random electric fields. The antenna response to these fields may be characterized by the quadratic or power spectrum of the voltage fluctuations in a measuring device connected with the antenna. The response is dependent upon the antenna configuration and is described as a filtering effect in wave vector space. - Theoretical quadratic spectra are presented for equilibrium plasmas streaming parallel to the antenna axis. The bulk velocity has a strong influence upon the shape of the spectra, especially as it is the cause for a periodic fine structure.

1. INTRODUCTION

Thermodynamical fluctuation phenomena in plasmas differ from the corresponding phenomena in neutral gases by the fact that they include fluctuations of the electric field. The reason is that differences in the local fluctuating densities of the positively and negatively charged components occur, representing a fluctuating charge separation. In collisionless plasma these fluctuations may be seen as the result of two counteracting effects, the random initiation and growth of instabilities and the collisionless damping mechanisms. Both, instabilities and damping, are the consequence of a particle-wave-interaction typical for collisionless plasmas and often called phase resonance. As this type of interaction is one of the most exciting properties of plasmas, fluctuation phenomena have drawn the attention of scientists (ROSTOKER, 1960; MONTGOMERY & TIDMAN, 1964).

But in general the question remained unsolved how these fluctuations could be measured, especially the fluctuating electric field, and what would be the response of an antenna imbedded in the plasma. One expects that a certain kind of external noise will appear within the antenna system. A first investigation has been made by the author (GRABOWSKI, 1972). Without performing extensive numerical calculations it was possible only to consider the limiting case of zero frequency.

The present investigation is more comprehensive, but due to very hard mathematical difficulties we had to restrain our considerations to a non-magnetic plasma. As any measurement of the fluctuating field in an extraterrestrial plasma will be feasible only on board of a spacecraft we did consider not only a plasma at rest but also a streaming plasma.

2. QUADRATIC SPECTRUM OF FIELD FLUCTUATIONS

The random fluctuating electrostatic field vector can be interpreted as a stochastic process depending upon four parameters. The parameters are time and three space coordinates. Usually a stochastic process is described by its correlation properties, that is by the measure to which extent the value of the stochastic variable at a first point in parameter space determines the value at a second point. A measure for this kind of correlation is the autocorrelation function. As in our case the stochastic variable is a vector quantity,

$$E_i(t, x_1, x_2, x_3), \quad (i = 1, 2, 3),$$

the autocorrelation function will be a matrix,

$$C_{ij}(t-t', x_h-x_h') \equiv \langle E_i(t, x_h) E_j(t', x_h') \rangle.$$

It has been assumed that the process is stationary. Thus, the autocorrelation matrix depends on the differences of the parameters only. In nearly all practical cases not the autocorrelation function itself but its Fourier transform, the quadratic or power

spectrum, is of interest:

$$11-2 \quad s_{ij}(\omega, k_n) = \int_{-\infty}^{\infty} d\tau dr_1 dr_2 dr_3 c_{ij}(\tau, r_n) \exp(i\omega\tau + ik_n r_n) .$$

An expression for the matrix  $s_{ij}$  has already been derived, based upon statistical mechanics (ROSTOKER, 1960; MONTGOMERY & TIDMAN, 1964). To be more flexible in view of possible applications and of numerical handling this expression is given here in dimensionless quantities:

$$S_{ij}(\Omega, K_n) = 2 \frac{K_i K_j}{K^4} \frac{\sum_{\alpha} j_{\alpha} T_{\alpha}}{|D|^2} , \quad (1)$$

$$T_{\alpha} \equiv \int_{-\infty}^{\infty} dV_1 dV_2 dV_3 \frac{F_{\alpha}(V_i)}{\Omega + K_j V_j} ,$$

$$D = 1 - \sum_{\alpha} \frac{1}{\mu_{\alpha} K^2} \int_{-\infty}^{\infty} dV_1 dV_2 dV_3 \frac{K_i \frac{\partial F_{\alpha}(V_i)}{\partial V_i}}{\Omega + K_j V_j} .$$

The Greek indices mark the contributions of different plasma components, the Latin indices are used to describe vector coordinates in an orthogonal system. The dimensionless quantities have been defined with the help of the following constants:

Reduced particle mass  $\bar{m}$ ,

$$\frac{1}{\bar{m}} = \sum_{\alpha} \frac{1}{m_{\alpha}} ;$$

Reduced temperature in units of energy  $\bar{\theta}$ ,

$$\frac{1}{\bar{\theta}} = \sum_{\alpha} \frac{1}{\theta_{\alpha}} ;$$

Angular plasma frequency  $\bar{\omega}_p$ ,

$$\bar{\omega}_p^2 = \sum_{\alpha} \frac{q^2 N}{\epsilon_0 m_{\alpha}} = \frac{q^2 N}{\epsilon_0 \bar{m}} ;$$

Debye length  $\bar{r}_D$ ,

$$\frac{1}{\bar{r}_D^2} = \sum_{\alpha} \frac{q^2 N}{\epsilon_0 \theta_{\alpha}} = \frac{q^2 N}{\epsilon_0 \bar{\theta}} .$$

The dimensionless constants and variables occurring in (1) are the following, given in relation to their corresponding dimensioned quantities:

Particle mass of the plasma component  $\alpha$

$$\mu_{\alpha} = m_{\alpha} / \bar{m} ,$$

Temperature of the plasma component  $\alpha$

$$\tau_{\alpha} = \theta_{\alpha} / \bar{\theta} ,$$

Angular frequency

$$\Omega = \omega / \bar{\omega}_p ,$$

Wave vector

$$K_i = k_i \bar{r}_D ,$$

Velocity coordinates in phase space

$$V_i = v_i (\bar{m} / \bar{\theta})^{1/2} ,$$

Bulk velocity of the plasma

$$W_i = w_i (\bar{m} / \bar{\theta})^{1/2} ,$$

Distribution function of the plasma component  $\alpha$

$$F_{\alpha} = f_{\alpha} (\bar{\theta}/\bar{m})^{3/2},$$

Quadratic spectrum of the field fluctuations

$$S_{ij} = s_{ij} \epsilon_0 \bar{\omega}_p / \bar{\theta}.$$

11-3

As distribution function we have assumed the equilibrium distribution in a streaming plasma:

$$F_{\alpha}(V_i) = \left( \frac{m_{\alpha}}{2\pi \bar{m}} \right)^{3/2} \exp \left( - \frac{m_{\alpha}}{2\bar{m}} |V_i - W_i|^2 \right).$$

It may be interesting to point out that in the derivation of expression (1) the same joint probability function is involved as used in the treatment of the incoherent backscattering of radio waves due to density fluctuations (MONTGOMERY & TIDMAN, 1964).

### 3. ANTENNA RESPONSE

The antenna response to a fluctuating electrostatic field will be associated with a filter effect because the antenna will not react on different spectral components  $E_i(\Omega, K_j)$  to the same extent. Thus, e.g. the field components perpendicular to a thin straight antenna will give no contribution at all. Therefore, the filter characteristic of the antenna has to be evaluated as a function of frequency  $\Omega$  as well as of wave vector  $K_i$ , if the observed external noise voltage impressed into the antenna is to be explained.

In the following we assume that the impressed antenna voltage  $U(t)$ , the quantity directly observed in the antenna system, is related to the electric field by the line integral

$$U(t) = \int_0^l E_i(t, x_i) dx_i. \quad (2)$$

The integration path is assumed to be a straight line with length  $l$  which may be identified as the effective antenna length. If  $E_i$  is a stochastic variable then this is true also for the antenna voltage  $U(t)$ . The relation between the autocorrelation function

$$c(t-t') \equiv \langle U(t) U(t') \rangle$$

of the voltage and the autocorrelation matrix of the field has already been derived (GRABOWSKI, 1972). This has been done via the corresponding quadratic spectra

$$S(\Omega) \text{ and } S_{ij}(\Omega, K_h)$$

respectively.

Perhaps it is worth mentioning that the quadratic spectrum  $S(\Omega)$  has the advantage of yielding directly the mean square voltage  $\langle U(t)^2 \rangle$  according to

$$\langle U(t)^2 \rangle = \int_{-\infty}^{\infty} \frac{d\omega}{2\pi} S(\omega),$$

a quantity which often is the main interesting feature of the external noise.

Here again  $S(\Omega)$  is a dimensionless quantity related to its corresponding dimensioned quantity by

$$S(\Omega) = s(\omega) \epsilon_0 \bar{\omega}_p \bar{r}_D / \bar{\theta}.$$

Using a coordinate system of which the  $x_3$ -axis is parallel to the line AB, where A and B are the points defining the effective antenna length, the quadratic spectrum of the external noise voltage is given by

$$S(\Omega) = 2 \int_0^{2\pi} \frac{d\varphi}{2\pi} \int_{-\pi/2}^{\pi/2} \frac{d\vartheta}{2\pi} \int_0^{\infty} \frac{dK}{2\pi} \frac{\cos \vartheta}{\sin^2 \vartheta} (1 - \cos(KL \sin \vartheta)) S_{33}(\Omega, K, \vartheta, \varphi). \quad (3)$$

In this expression the cartesian coordinates  $K_i$  have been replaced by spherical ones according to

$$K_1 = K \cos \vartheta \cos \varphi,$$

$$K_2 = K \cos \vartheta \sin \varphi,$$

$$K_3 = K \sin \vartheta,$$

and

$$L = \ell / \bar{v}_D$$

is the dimensionless antenna length. In expression (3) the factor

$$(1 - \cos(KL \sin \vartheta))$$

is a filter function already known from many other problems.

The filtering may be described qualitatively as following. The fluctuating field can be seen as composed of plane waves with a wave length  $2\pi/K$  and direction  $(\vartheta, \varphi)$ . The antenna responds to the projection of these plane waves on the antenna axis AB. These projections have virtual wavelength  $2\pi/(K \sin \vartheta)$ . If the projection is an integer multiple of the antenna length  $L$ ,

$$L = n 2\pi / (K \sin \vartheta), \quad (n = 1, 2, \dots),$$

then positive and negative contributions to the line integral (2) compensate to zero, they do not contribute to the impressed voltage  $U(t)$ . Integrating the contributions of all plane waves results in expression (3).

When introducing (from (1)) the explicit representation of  $S_{33}(\Omega, K_i)$  into expression (3), the spectrum of the impressed voltage is given by the following explicit formula for a plasma streaming parallel to the antenna axis:

$$S(\Omega) = 4 \int_0^{2\pi} \int_{-\pi/2}^{\pi/2} \int_0^\infty \frac{d\varphi}{2\pi} \frac{d\vartheta}{2\pi} \frac{dK}{2\pi} \frac{\cos \vartheta}{K^2} (1 - \cos(KL \sin \vartheta)) \frac{\sum_{\alpha} \text{Im } T_{\alpha}}{|\Omega|^2}, \quad (4)$$

$$T_{\alpha} = \left( \frac{a_{\alpha}^2}{\pi} \right)^{3/2} \int_{-\infty}^{\infty} dV_{\parallel} \int_0^{\infty} dV_{\perp} \int_0^{2\pi} d\chi \frac{\exp(-a_{\alpha}^2 V_{\perp}^2) \exp(-a_{\alpha}^2 |V_{\parallel} - W|^2) V_{\perp}}{\Omega + K_{\parallel} V_{\parallel} + K_{\perp} V_{\perp} (\cos \vartheta \cos \chi + \sin \vartheta \sin \chi)},$$

$$D = 1 + \frac{1}{K^2} - \frac{1}{K^2} \sum_{\alpha} \frac{1}{\tau_{\alpha}} (\Omega + K_{\parallel} W) T_{\alpha},$$

$$a_{\alpha} = \left( \frac{\mu_{\alpha}}{2 \tau_{\alpha}} \right)^{1/2}.$$

The integration with respect to the velocity coordinates will be performed in cylindrical coordinates defined by

$$V_1 = V_{\perp} \cos \chi,$$

$$V_2 = V_{\perp} \sin \chi,$$

$$V_3 = V_{\parallel}.$$

It is clear that expression (4) is useful only to the extent to which the integrations involved can really be performed, analytically or numerically.

#### 4. INTEGRATION

The integrations involved in the term  $T_{\alpha}(V_{\alpha}, V_{\alpha}, \chi)$  of expression (4) can be done analytically, if we range

$$\phi(x) = \int_0^x \exp(y^2) dy$$

11-5

among the elementary functions.

If as the first step we integrate with respect to  $\chi$  then a common substitution leads to the sum of two integrals of the form

$$I(z) = \int_{-\infty}^{\infty} \frac{dt}{t-z} - \int_{-\infty}^{\infty} \frac{dt}{t-z^*}$$

which requires special consideration because the integration path may cross a singularity. Depending on which of the two relations

$$\frac{K_{\alpha} V_{\alpha}}{\Omega + K_{\alpha} V_{\alpha}} \geq 1$$

$$\frac{K_{\alpha} V_{\alpha}}{\Omega + K_{\alpha} V_{\alpha}} < 1$$

is valid the quantity  $z$  (and its complex conjugate  $z^*$ ) will be either real or complex. The value of  $I(z)$  can be found by application of Cauchy's Integral Theorem. In the case of a complex  $z$ , clearly one obtains

$$I(z) = i2\pi$$

Things are less simple in the case of a real  $z$ , i.e. when a singularity is found on the real axis. In this case we follow a general convention (MORSE & FESHBACH, 53). As result we take the mean value of two limiting integration paths surrounding the singularity, the first one excluding it, the other including it. Then in the limit  $\text{Im}(z) \rightarrow 0$  we get the result

$$I(z) = i\pi - (-i\pi) = i2\pi$$

i.e. the same as in the case before. This kind of singularity is a typical feature of Kinetic Plasma Theory and has been treated in more detail elsewhere (MONTGOMERY & TIDMAN, 1964; VAN KAMPEN & FELDERHOF, 1967).

The further treatment of the term  $T_{\alpha}$  brings up an integral of the form

$$J(a, b) = \int_{-\infty}^{\infty} dy \phi(ay+b) \exp(-y^2)$$

$$\phi(x) = \int_0^x dt \exp(t^2)$$

This integral can be evaluated by writing it as

$$J(a, b) = J(a, 0) + \int_0^b \frac{\partial J(a, b')}{\partial b'} db'$$

and by observing that the integrand of  $J(a, b)$  is an odd function of  $y^+$

Finally the term  $T_{\alpha}$  takes the form given in Equation (5). As the term  $T_{\alpha}$  is not dependent on  $\mathcal{V}$ , and as this is true also for the term  $\phi$ , we can integrate analytically also with respect to  $\mathcal{V}$ . The remaining integrations with respect to  $\mathcal{V}$  and  $K$  can be treated only numerically. Thus the numerical evaluation of the following double integral remains:

+) We thank Dr. J. SLAVIK for communicating that this integral can be handled analytically in this way.

$$S(\Omega) = \frac{1}{\pi^2} \int_{-\pi/2}^{\pi/2} \int_0^{\infty} aK \frac{\cos \vartheta}{K^2} (1 - \cos(KL \sin \vartheta)) \frac{\sum_{\alpha} \text{Im} T_{\alpha}}{|D|^2} d\vartheta dK \quad (5)$$

$$\text{Re} T_{\alpha} = 2a_{\alpha} \frac{1}{K} \exp\left(-a_{\alpha}^2 \frac{(\Omega + \Delta\Omega)^2}{K^2}\right) \phi\left(a_{\alpha} \frac{\Omega + \Delta\Omega}{K}\right),$$

$$\text{Im} T_{\alpha} = \pi^{1/2} a_{\alpha} \frac{1}{K} \exp\left(-a_{\alpha}^2 \frac{(\Omega + \Delta\Omega)^2}{K^2}\right),$$

$$|D|^2 = \left(1 + \frac{1}{K^2}\right)^2 - \left(1 + \frac{1}{K^2}\right) \frac{\Omega + \Delta\Omega}{K^2} \sum_{\alpha} \frac{\text{Re} T_{\alpha}}{v_{\alpha}} + \frac{(\Omega + \Delta\Omega)^2}{K^4} \left[ \left(\sum_{\alpha} \frac{\text{Re} T_{\alpha}}{v_{\alpha}}\right)^2 + \left(\sum_{\alpha} \frac{\text{Im} T_{\alpha}}{v_{\alpha}}\right)^2 \right],$$

$$\phi(x) = \int_0^x dy \exp(y^2),$$

$$\Delta\Omega = WK \sin \vartheta,$$

$$a_{\alpha} = \left(\frac{m_{\alpha}}{2v_{\alpha}}\right)^{1/2}.$$

## 5. RESULTS

Before presenting the numerically determined results we give an additional interpretation of the dimensionless quadratic spectrum  $S(\Omega)$ . It is related to the dimensionless real spectrum by

$$s(\omega) = \frac{i}{\epsilon_0 \omega_p^2} \bar{\theta} S(\Omega).$$

The factor  $1/(\epsilon_0 \omega_p^2)$  has the dimension of a resistance. Thus the relation has the form of the well known Nyquist formula for the noise of resistors. Therefore the dimensionless spectrum may be interpreted as modulating the Nyquist formula for "white" noise reflecting typical properties of the plasma.

The following results refer to a plasma consisting of electrons and protons only, both having the same temperature. The antenna has been chosen as to be hundred times as long as the Debye length. The bulk velocity is directed parallel to the antenna axis.

Fig. 1 reveals the calculated spectrum for a plasma at rest. The value obtained for zero frequency is identical with that obtained analytically for great  $L$  in a less comprehensive investigation already mentioned (GRABOWSKI, 1972), i.e.

$$S(\Omega) = \pi^{-3/2} \sum_{\alpha} \left(\frac{m_{\alpha}}{2v_{\alpha}}\right)^{1/2}.$$

The results show that to use the value for zero frequency as an approximation for other frequencies is possible only for a very small frequency domain. The spectrum for higher frequencies is found in Fig. 5. The shape of the spectrum cannot be described generally by a simple arithmetic expression.

In Fig. 2 one finds the spectrum for a streaming plasma. The existence of the bulk velocity (parallel to the antenna axis) manifests itself in the appearance of a periodic structure. More strongly marked periodic structures of this kind are seen for higher bulk velocities in Figs. 3 and 4. The following relations between velocity  $W$



and period  $\Omega_0$  of this structure can be derived:

$$\Omega_0 = 2\pi W/L.$$

The numerical results confirm this relation.

Comparing the trend of the spectra (see Fig. 5) we find that by increasing the bulk velocity the spectra will get lower values for low frequencies, but higher values in the domain of higher frequencies. We further find that the spectra decrease more slowly with increasing frequency in the case of higher bulk velocity.

The results presented first provide information upon the noise level to be expected in an antenna immersed in a plasma. A second-surprising - result is the appearance of a periodic structure in the case of a streaming plasma (parallel to the antenna). As the periodicity sharply depends upon the magnitude of the bulk velocity the observation of the fine structure of the quadratic spectra seems to be a suitable means for the determination of this velocity.

#### REFERENCES

- GRABOWSKI, R., 1972, "Influence of field fluctuations upon the measurement of slowly varying electric fields in the outer ionosphere and in the magnetosphere", Planet. Space Sci. 20, 571-579.
- MONTGOMERY, D.C., TIDMAN, D.A., 1964, "Plasma Kinetic Theory", § 5.3, § 8, § 14.2.
- MORSE, P.M., FESHBACH, H., 1953, "Methods of Theoretical Physics", I, § 4.2.
- ROSTOKER, N., 1960, "Fluctuations of a plasma (I)", Nuclear Fusion 1, 101-120.
- VAN KAMPEN, N.G., FELDERHOF, B.U., 1967, "Theoretical Methods in Plasma Physics", § 12.1.

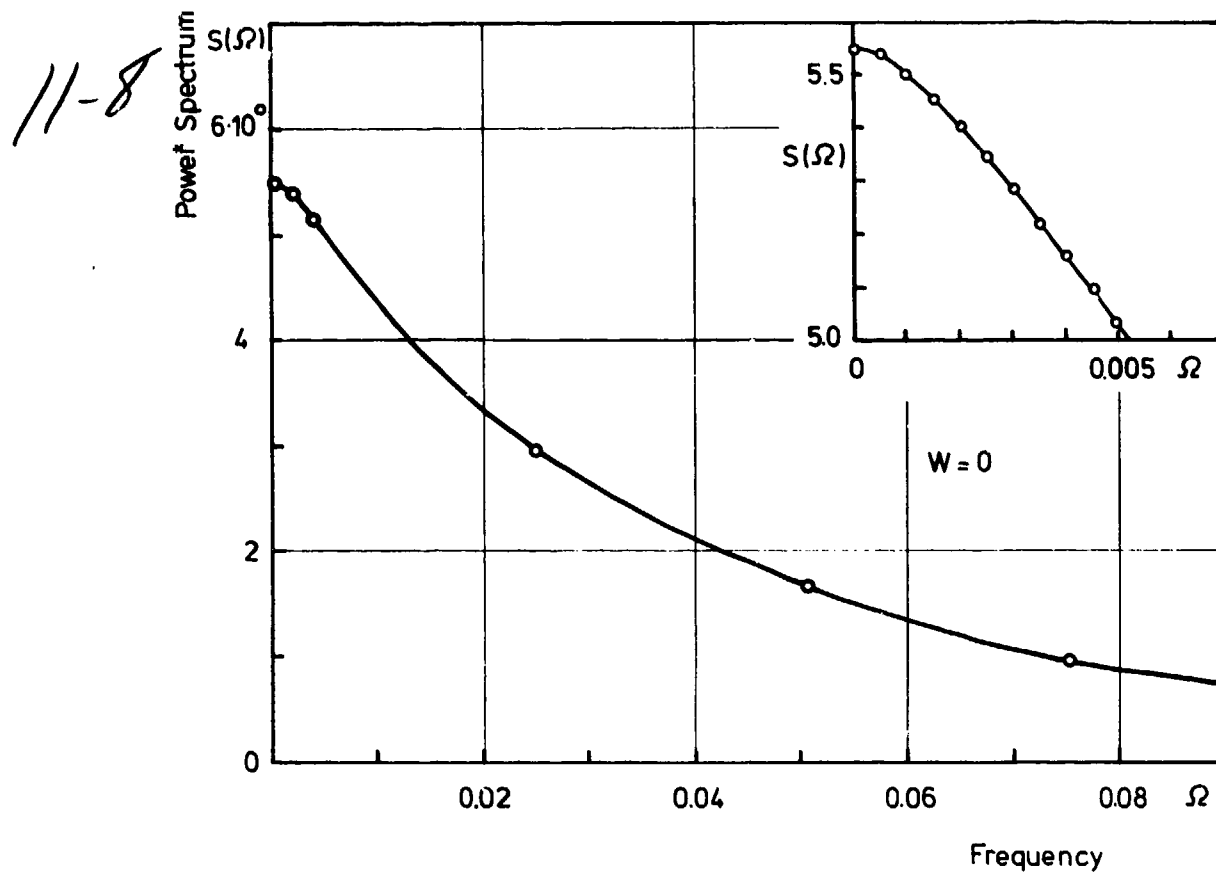


Fig.1 Power spectrum  $S(\Omega)$  for an antenna with effective length  $L = 100$  in an electron-proton plasma. Temperatures  $\tau_{(+)} = \tau_{(-)} = 1$ . Bulk velocity (parallel to the antenna)  $W = 0$

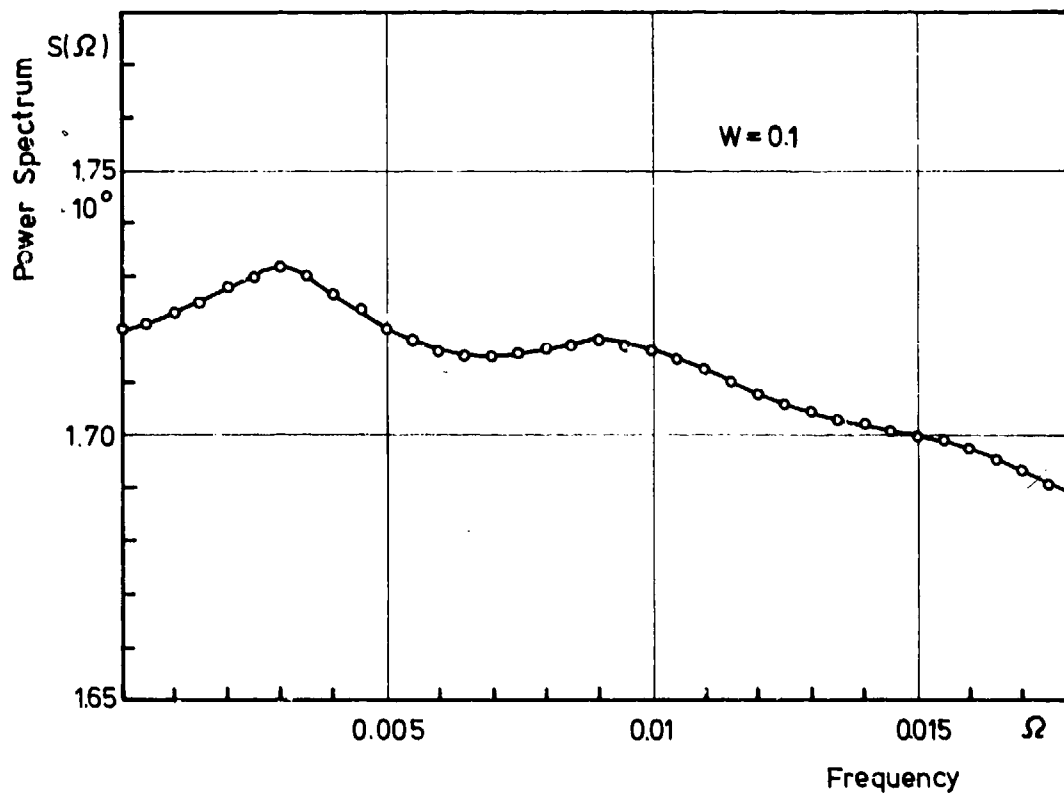


Fig.2 Power spectrum  $S(\Omega)$  as in Figure 1, but with bulk velocity  $W = 1$

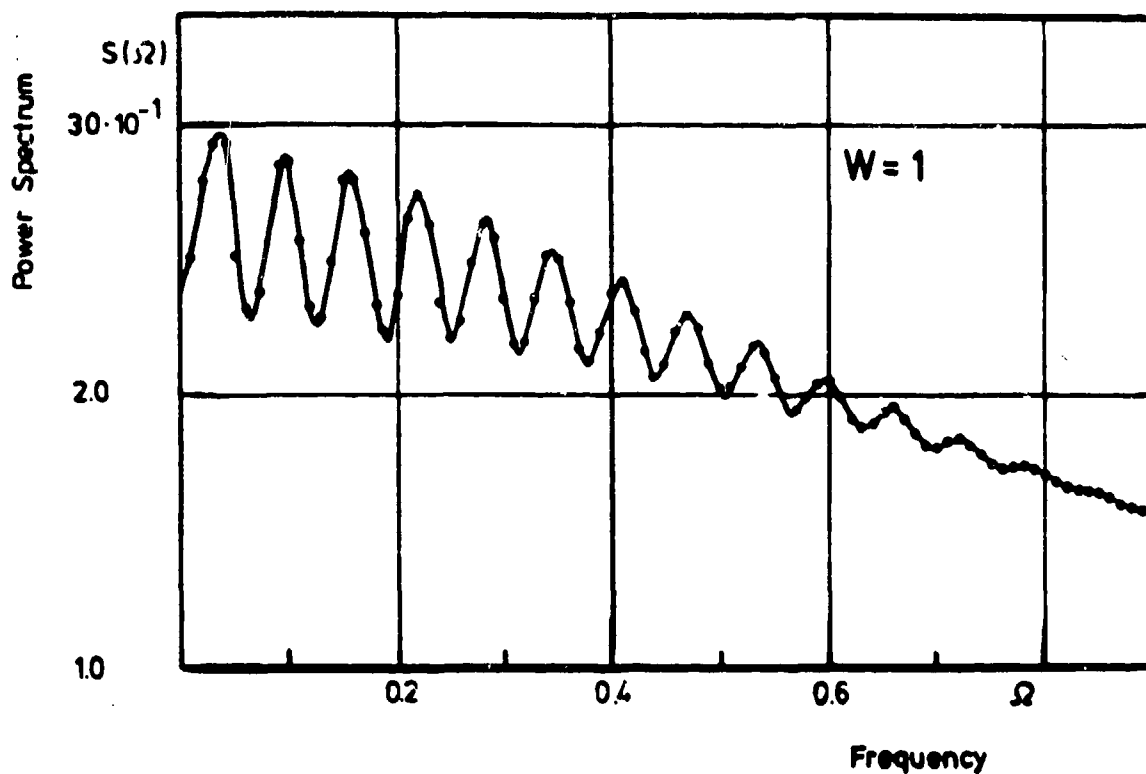


Fig.3 Power spectrum  $S(\Omega)$  as in Figure 1, but with bulk velocity  $W = 8$

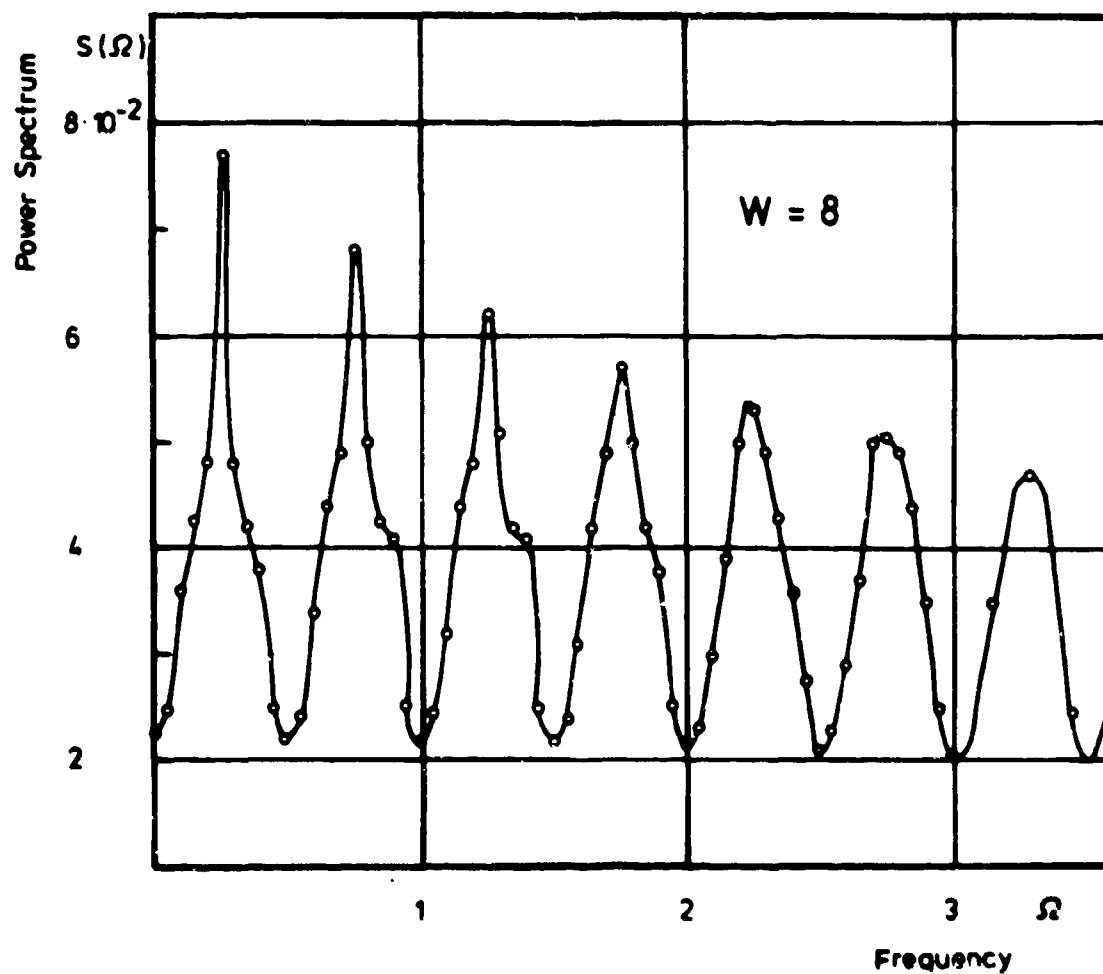


Fig.4 Power spectra as in Figure 1 for bulk velocities  $W = 0$ ,  $W = 1$  and  $W = 8$

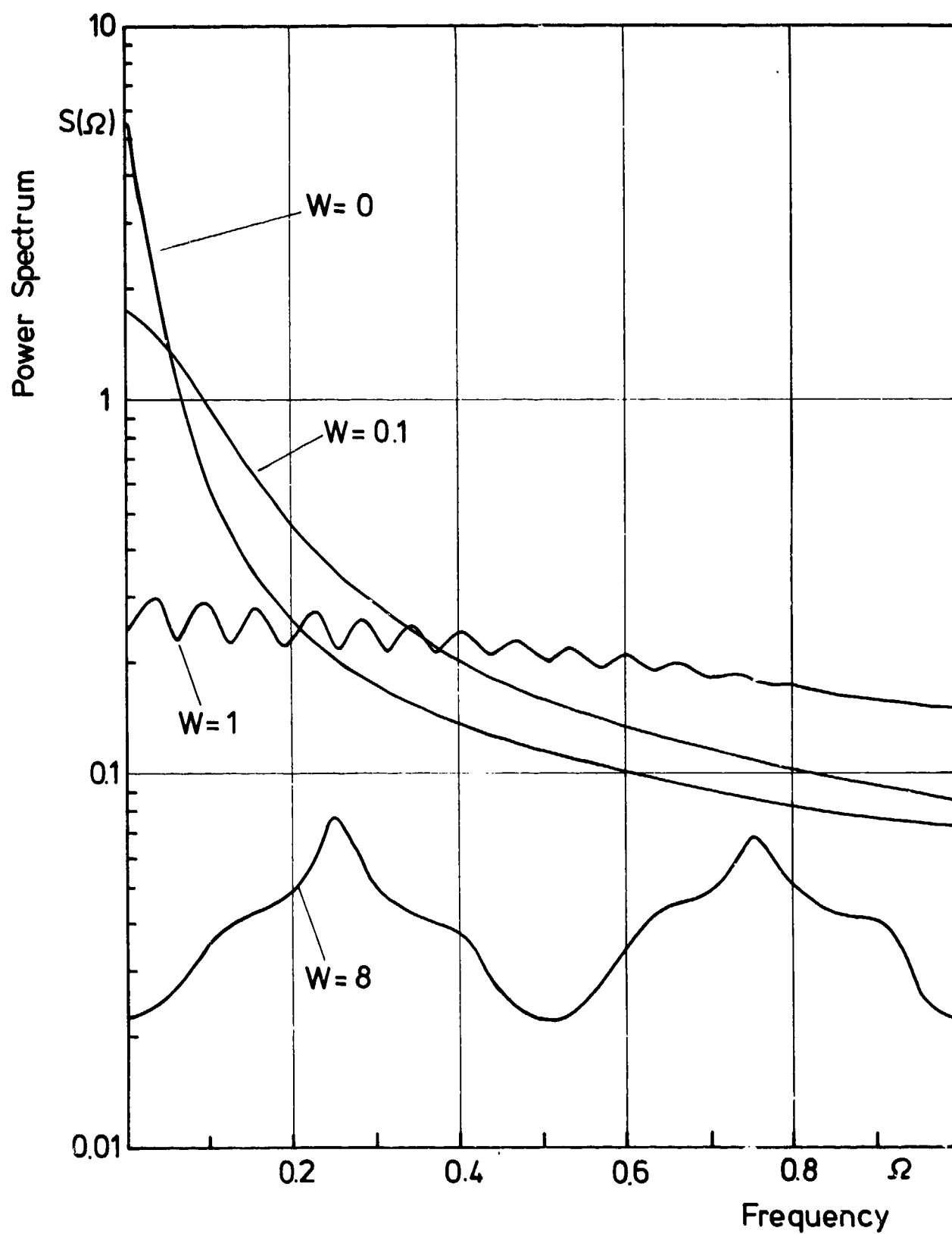


Figure 5

## DISCUSSION

E. J. FREMOUW: 1) Incoherent scatter observations of the ionosphere show two components of the temporal spectrum--one dominated by positive ion motions and one dominated by electron motions (the plasma lines). Are there corresponding effects in the spectrum of fields detected by an antenna in a plasma? 2) Could you test your theoretical results in the ionosphere by means of Spacelab?

R. GRABOWSKI: 1) Though the fluctuations of both plasma components, the ions and the electrons, have been included in our calculations, no feature in the shape of the spectra attributable to one or the other component can be seen in the results; but the absolute value of the spectra depends upon the (theoretical) condition, that the ions participate in the fluctuations or not. This can be seen in the paper of R. Grabowski (1972), cited in the Conference Proceedings. 2) A test seems to be possible, if a device is used with sufficiently high sensitivity, i.e., a sensitivity of  $10^{-12}$  to  $10^{-16}$  V<sup>2</sup>/Hz, depending on the ionospheric height range.

G. N. TAYLOR: I notice you have assumed equal positive ion and electron temperatures for your calculated curves. What would be the effect of making these temperatures unequal?

R. GRABOWSKI: At present, calculations with different temperatures have not been performed; therefore, nothing can be said about the effect, but some modification is expected due to different temperatures as well as to a magnetic field.

12-1

M.J.M. van Weert  
Eindhoven University of Technology  
Eindhoven - the Netherlands

### Summary

In the present paper we will discuss some properties of the scintillation noise power. The used model is essential the same as used by Lee and Harp. Some calculations of different statistical properties of the scintillation noise will be shown. Special attention will be paid to the influence of receiver aperture and frequency on the scintillation noise power. It will be shown that both parameters have a significant influence on the amplitude scintillation, but hardly on the phase scintillation. This behaviour will be explained. To decide whether scintillation does have a significant influence on the performance of a communication link, the total scintillation noise power will be compared with the thermal noise power on an earth to satellite path.

### 1. Introduction

For several years the interest in the propagation of microwaves of frequencies above 10 GHz through a turbulent atmosphere has been increasing considerably. In such an atmosphere slight variations of pressure, temperature and humidity cause slight variations of the refractive index. The latter cause small variations in the amplitude and phase of the received signal, generally known as scintillation. Since these variations are of a stochastic nature, it is appropriate to consider scintillation as a form of noise. The additional noise will have some influence on the reliability of a communication system, so that an increase in transmitter power will be necessary to guarantee a required performance of the total link (C. Tsao-1973, M. Nisenberg-1967). In the present paper calculations will be given for the scintillation noise power. The theoretical derivation is based on a method described earlier in the literature (Lee and Harp-1969), but with an extensive use of the plane wave spectrum representation of the electromagnetic fields (Clemmow). The use of this representation offers the possibility of readily substituting practical transmitting and receiving apertures. Some calculations of the scintillation noise to signal ratio for different receiving apertures will be shown. A comparison between scintillation noise and thermal noise on an earth to satellite path will also be made. Although the effect of scintillation noise on a modulated carrier will be entirely different, this comparison may give some information on the relative importance of scintillation noise.

### 2. Scintillation noise

The model used to calculate the scintillation noise is a very simple one. A plane wave, polarised in the x direction and propagating in the positive z direction of a Cartesian coordinate system, is incident at  $z = 0$  upon the random medium (fig.1). We divide the region  $z > 0$  into thin slabs of thickness  $dz$  perpendicular to the z direction. Consider the slab at  $z = z_0$ . The refractive index in such a slab can be written as

$$n(x, y, z_0) = 1 + n_1(x, y, z_0) \quad (2-1)$$

where  $n_1$  is a stochastic function of place, for which we assume

$$n_1 \ll 1 \quad ; \quad \langle n_1 \rangle = 0$$

Here  $\langle \cdot \rangle$  denotes an ensemble average. We will assume that the influence of one slab on the incoming wave can be taken into account by an additional phase delay

$$\varphi(x, y) = k n_1(x, y, z_0) dz \quad (2-2)$$

where  $k = \frac{\omega}{c}$  is the wavenumber and  $dz$  represents the thickness of one slab. If the incoming wave can be written as

$$E(x, y, z_0) = e^{jkz_0}$$

then the wave leaving the slab at  $z = z_0 + dz$ , can be written as:

$$E(x, y, z_0 + dz) = e^{jk(z_0 + dz)} e^{j\varphi(x, y)}$$

Since both  $n_1$  and  $dz$  are very small, we find:

$$E(x, y, z_0) = e^{jkz_0} \{ 1 + jk n_1(x, y, z_0) dz \} \quad (2-3)$$

Since  $n_1$  and hence  $E(x, y, z)$  are stochastic functions of  $x$  and  $y$ , we use the two-dimensional Fourier-Stieltjes representation of the field, e.g.:

$$E(x, y, z_0) = \frac{1}{4\pi^2} \iint_{-\infty}^{\infty} e^{j(k_x x + k_y y)} d\zeta(k_x, k_y, z_0) \quad (2.4)$$

where

$$d\zeta(k_x, k_y, z_0) = e^{jkz_0} \{ 4\pi^2 \delta(k_x) \delta(k_y) dk_x dk_y + jk dz d\eta(k_x, k_y, z_0) \} \quad (2.5)$$

Here,  $d\eta$  represents the Fourier-Stieltjes transform of  $n(x, y, z)$ . If one neglects multiple scattering, the field of (2-3) will propagate undisturbedly to the receiver plane  $z = L$ . Hence,

$$\begin{aligned} d\zeta(k_x, k_y, L) &= e^{jk_z(L-z_0)} d\zeta(k_x, k_y, z_0) \\ &= 4\pi^2 e^{jk_z L} \delta(k_x) \delta(k_y) dk_x dk_y + jk_z e^{jk_z(L-z_0)} e^{jk_z z_0} dz d\eta(k_x, k_y, z_0) \end{aligned}$$

where  $k_z = \sqrt{k^2 - k_x^2 - k_y^2}$

The total field is given by a summation of the contribution of all slabs between  $z = 0$  and  $z = L$ .

$$\begin{aligned} d\zeta(k_x, k_y, L) &= 4\pi^2 e^{jk_z L} \delta(k_x) \delta(k_y) dk_x dk_y \\ &\quad + jk_z \int_0^L dz e^{jk_z(L-z)} e^{jk_z z} d\eta(k_x, k_y, z) \end{aligned} \quad (2-6)$$

If the electromagnetic wave is received with the aid of a parabolic antenna, the averaging of the fluctuations over the aperture will occur. The focal point of the antenna is the point  $(x_0, y_0)$ . The amplitude gain function will be denoted by  $g_a(k_x, k_y)$ . The received field will then be given by:

$$\begin{aligned} E(x_0, y_0, L) &= \frac{1}{4\pi^2} \iint g_a(-k_x, -k_y) d\zeta(k_x, k_y, L) \\ &= g_a(0, 0) e^{jk_z L} + \frac{jk_z}{4\pi^2} \int_0^L dz e^{jk_z(L-z)} \iint e^{jk_z z} g_a(-k_x, -k_y) d\eta(k_x, k_y, z) \end{aligned} \quad (2-7)$$

, where the usual exponential factor  $\exp. j(k_x x_0 + k_y y_0)$  is a part of the antenna gain function.

Write  $E(x_0, y_0, L) = C + n_{sc}$

where  $C = g_a(0, 0) e^{jk_z L}$  is the wanted carrier

and

$$n_{sc} = \frac{jk_z}{4\pi^2} \int_0^L dz e^{jk_z z} \iint e^{jk_z(L-z)} g_a(-k_x, -k_y) d\eta(k_x, k_y, z)$$

is the scintillation noise due to the turbulent atmosphere. In Appendix I it will be shown that the covariance function of the scintillation noise may be written as:

$$\frac{1}{|C|^2} C_n(\rho) = \frac{k^2}{2\pi} \int_0^L ds \int_0^\infty x dx \Phi_n(x) \left| \frac{g_a(x)}{g_a(0)} \right|^2 J_0(x\rho) \quad (2-8)$$

Here  $\Phi_n$  is the three-dimensional spatial power spectrum of the refractive index fluctuations,  $J_0$  is the zero-order Bessel function, and  $s$  the distance of the receiver plane to a plane in the turbulent atmosphere.

Since the strength of the turbulence is a decreasing function of the height above the earth, we write:

$$\Phi_n(x) = \exp\left(-\frac{s \sin \theta}{h_0}\right) \Phi_{n0}(x) = \exp\left(-\frac{s}{s_0}\right) \Phi_{n0}(x)$$

where  $\Phi_{n0}$  is the power spectrum just above the ground,  $\theta$  is the elevation angle and  $h$  is of the order of a few kilometers (Lane-1968, Brookner-1970). Therefore, on earth to satellite paths the covariance function is

$$\frac{1}{|C|^2} C_n(\rho) = \frac{k^2}{2\pi} s_0 (1 - e^{-L/s_0}) \int_0^\infty x dx \Phi_{n0}(x) \left| \frac{g_a(x)}{g_a(0)} \right|^2 J_0(x\rho) \quad (2-9)$$

In the literature one usually defines both amplitude and phase scintillation. In Appendix II we will show that the covariance function of the amplitude scintillation is equal to

$$\frac{1}{|C|^2} C_n(\rho) = \frac{k^2}{4\pi} \int_0^\infty x dx \Phi_{n0}(x) \left| \frac{g_a(x)}{g_a(0)} \right|^2 J_0(x\rho) \int_0^L ds e^{-s/s_0} \left\{ 1 - \cos \frac{x^2 s}{k} \right\} \quad (2-10)$$

Since  $C_n(\rho) = C_a(\rho) + C_\varphi(\rho)$  (see Appendix II), the covariance function of the phase noise is given by

$$\frac{1}{|C|^2} C_\varphi(\rho) = \frac{k^2}{4\pi} \int_0^\infty x dx \Phi_{n0}(x) \left| \frac{g_a(x)}{g_a(0)} \right|^2 J_0(x\rho) \int_0^L ds e^{-s/s_0} \left\{ 1 + \cos \frac{x^2 s}{k} \right\} \quad (2-11)$$

### 3. Temporal power spectrum of the scintillation noise

To calculate the power spectrum from expression 2-9, we have to use Taylor's "frozen-in" hypothesis to transform the spatial functions to temporal ones. (Taylor-1938). It is assumed that the turbulent airmass is moved with the wind velocity  $\bar{v}$  perpendicular to the propagation direction. It is further assumed that the statistics of the turbulence does not change very rapidly. In this case the covariance function between two antennas a distance  $\rho$  apart is equal to the temporal covariance function of the received signal with time-lag  $\tau = \rho/\bar{v}$ , that is

$$\frac{1}{|C|^2} R_n(\tau) = \frac{1}{|C|^2} C_n(\rho = \bar{v}\tau)$$

The temporal power spectrum will then be given by

$$\begin{aligned} W_n(\omega) &= \frac{1}{|C|^2} \int_{-\infty}^{\infty} R_n(\tau) e^{-j\omega\tau} d\tau \\ &= \frac{k^2}{2\pi} S_0 (1 - e^{-L/L_0}) \int_0^{\infty} x dx \frac{\Phi_{n_0}(x)}{\bar{v} \sqrt{x^2 - \frac{\omega^2}{\bar{v}^2}}} \left| \frac{q_n(x)}{q_n(0)} \right|^2 \int_{-\infty}^{\infty} \delta(\bar{v}\tau x) e^{-j\omega\tau} d\tau \end{aligned} \quad (3-1)$$

The integral over  $\tau$  is the so-called Weber-Schafheitlin integral and is found in different handbooks (Abramowitz). The expression then becomes:

$$W_n(\omega) = \frac{k^2}{\pi} S_0 (1 - e^{-L/L_0}) \int_0^{\infty} x dx \frac{\Phi_{n_0}(x)}{\bar{v} \sqrt{x^2 - \frac{\omega^2}{\bar{v}^2}}} \left| \frac{q_n(x)}{q_n(0)} \right|^2$$

Substitution of  $\Omega = \frac{\omega}{\bar{v}}$  gives

$$\bar{v} \cdot W_n(\Omega) = \frac{k^2}{\pi} S_0 (1 - e^{-L/L_0}) \int_0^{\infty} x dx \frac{\Phi_{n_0}(x)}{\sqrt{x^2 - \Omega^2}} \left| \frac{q_n(x)}{q_n(0)} \right|^2 \quad (3-2)$$

The above expression gives the power spectrum as a function of different parameters such as the frequency, antenna gain function, etc. For numerical calculations we have to substitute known functions for  $\Phi_{n_0}$  and  $|q_n(x)/q_n(0)|^2$ .

For  $\Phi_{n_0}$  we will use the von Kármán representation of the Kolmogorov spectrum (Tartaski-1961, Strohbehn-1968), so

$$\Phi_{n_0}(x) = C_{n_0}^2 (x^2 + \frac{1}{L_0^2})^{-11/6} \quad (3-3)$$

Here,  $C_{n_0}^2$  is the structure constant, and it is related to the strength of the atmospheric turbulence.

$L_0$  is the outer scale of turbulence, that is,  $L_0$  is the largest inhomogeneity for which the atmosphere can be considered as isotropic. In normal circumstances the value of  $L_0$  lies between 1 and 100 metres. A typical value for  $L_0$  is 10 metres (Brookner-1970), and this value will be used throughout this paper. We will choose a Gaussian aperture illumination for the receiver antenna, so

$$\left| \frac{q_n(x)}{q_n(0)} \right|^2 = e^{-x^2 \sigma_r^2} \quad (3-4)$$

The standard deviation  $\sigma_r$  is a measure of the physical dimensions of the antenna. If we compare this antenna with one having a radius  $R$  and a uniform illumination, then both antennas will have the same gain for  $R = 2\sigma_r$ .

Substitution of both  $\Phi_{n_0}$  and  $|q_n(x)/q_n(0)|^2$  leads to

$$\bar{v} \cdot W_n(\Omega) = \frac{k^2}{\pi} C_{n_0}^2 S_0 (1 - e^{-L/L_0}) \int_0^{\infty} x dx \frac{(x^2 + \frac{1}{L_0^2})^{-11/6}}{\sqrt{x^2 - \Omega^2}} e^{-x^2 \sigma_r^2} \quad (3-5)$$

The power spectrum of the amplitude scintillation noise can be found in the same way, and is given by:

$$\bar{v} \cdot W_a(\Omega) = \frac{k^2}{2\pi} C_{n_0}^2 \int_0^{\infty} x dx \frac{(x^2 + \frac{1}{L_0^2})^{-11/6}}{\sqrt{x^2 - \Omega^2}} e^{-x^2 \sigma_r^2} \int_0^L ds e^{-s/L_0} \left\{ 1 - \cos \frac{k^2 s}{k} \right\} \quad (3-6)$$

Fig. 2 shows a graph of both power spectra for several values of the effective aperture radius  $\sigma_r$ . From these plots it is clear that the shape of the spectra for higher frequencies depends on  $\sigma_r$ . The shape for  $\sigma_r = 0$  is simply  $\omega^{-8/3}$ , and is in accordance with other results found in the literature (Ishimaru-1972). However, the shape of the spectra for values of  $\sigma_r$  greater than zero are strongly influenced by the effective aperture radius.



#### 4. Calculation of the scintillation noise to carrier ratio

Substituting  $\rho = 0$  in the expression (2-9) we obtain the scintillation noise to carrier ratio,

$$12-4 \quad \frac{\sigma_a^2}{|C|^2} = \frac{k^2}{4\pi} s_0 (1 - e^{-1/s_0}) C_{n0}^2 \int_0^\infty x dx (x^2 + 1/4)^{-11/6} e^{-x^2 \sigma_r^2} \quad (4-1)$$

Here we have substituted the expressions (3-3) and (3-4) for  $\phi_{n0}$  and  $|g_n(\omega)/g_n(0)|^2$  respectively. This practice will be continued in the rest of this paper without notice. Since the integral in the above expression is independent of the wavenumber  $k$ , the scintillation noise to carrier ratio is proportional to  $f^2$ , where  $f$  is the frequency. The corresponding expression for the amplitude scintillation is:

$$\frac{\sigma_a^2}{|C|^2} = \frac{k^2}{4\pi} C_{n0}^2 \int_0^\infty x dx (x^2 + 1/4)^{-11/6} e^{-x^2 \sigma_r^2} \int_0^L ds e^{-s/s_0} \{1 - \cos \frac{x^2 s}{k}\} \quad (4-2)$$

and now the integral over  $x$  is dependent on  $k$ . Fig. 3 shows a plot of  $\sigma_a^2/|C|^2$  versus frequency for different aperture sizes. From these plots it is clear that  $\sigma_a^2/|C|^2$  will increase for increasing frequencies, although this increase may be very small for large aperture sizes. Since the increase in  $\sigma_a^2/|C|^2$  is always less than 6 dB per octave (the increase in  $\sigma_n^2/|C|^2$ ), and since  $\sigma_n^2 = \sigma_a^2 + \sigma_\phi^2$ , we may conclude that for higher frequencies phase scintillation becomes relatively more important than amplitude scintillation. Therefore, for very high frequencies scintillation consists almost entirely of phase scintillation.

Fig. 4 shows a graph of both  $\sigma_n^2/|C|^2$  and  $\sigma_a^2/|C|^2$  versus the effective aperture radius  $\sigma_r$ . Since the frequency dependence of  $\sigma_n^2/|C|^2$  is again simply  $f^2$ , we have plotted this figure for only one frequency. For the amplitude scintillation case we have plotted two lines for 10 and 90 GHz respectively. All lines show a decrease with increasing aperture size, although for  $\sigma_n^2$  this decrease is not very strong. The decrease for  $\sigma_a^2$  shows that for relatively large apertures scintillation noise consists almost entirely of phase noise, and this effect is more pronounced for higher frequencies. Besides these effects, the plot of  $\sigma_n^2$  at 90 GHz clearly shows a saturation effect, i.e. the decay of  $\sigma_a^2/|C|^2$  as a result of an increasing aperture size is less pronounced for relatively large aperture sizes.

The foregoing behaviour of the amplitude noise to carrier ratio for various frequencies and receiver aperture sizes can be explained simply. As stated earlier, the turbulent atmosphere causes a plane dependent phase-distortion of the incident plane wave. Owing to this distortion the wave will split into several plane waves, all propagating in various directions (fig.1). Amplitude scintillation is the result of destructive interference of all these plane waves in the aperture plane. To reduce amplitude scintillation, one could use some form of spatial filtering, viz. a highly directive antenna, which suppresses plane waves having an angle of incidence greater than the beam-width of the antenna, and which prevents the waves from contributing to the amplitude scintillation noise any longer. An increase in frequency will then result in a decrease in the antenna beamwidth; hence a given aperture size will be a more effective spatial filter for higher frequencies, as can be clearly seen from the plots in fig.3.

#### 5. Scintillation noise versus thermal noise

In a satellite communication system operating above 10 GHz one has to deal with thermal noise in addition to scintillation noise. To decide which of these noises will play a dominant part in the overall performance of the communication system, one has to know the influence of scintillation noise on the bit error rate of a digitally modulated carrier. This influence depends on the type of modulation, and therefore falls outside the scope of this paper. We shall deal here only with the scintillation to thermal noise power ratio, since it depends mainly on this ratio whether scintillation noise will play an important part in the overall performance. The carrier to thermal noise ratio may be written as:

$$\frac{|C|^2}{N_{th}} = \frac{P_r}{k T_s B} \quad (5-1)$$

, where  $k$  is the Boltzmann constant,  $T_s$  the system noise temperature, and  $B$  the bandwidth.  $P_r$  is the received power, that is

$$P_r = \frac{P_t G_t}{4\pi r^2} |g_n(0,0)|^2 \quad (5-2)$$

Here,  $P_t G_t$  is the satellite E.I.R.P. and in the currently used systems it is about 27 dBW. The factor  $r$  is the distance from the satellite to the receiver point on earth and is about  $4 \cdot 10^7$  metres. We again choose a Gaussian function for the receiver aperture, so  $g_n(0,0) = 2\sigma_r/\pi$ . Substitution in the above carrier to noise ratio gives

$$\frac{|C|^2}{N_{th}} = \frac{\alpha}{k T_s B} 4\pi \sigma_r^2 \quad (5-3)$$

where

$$\alpha = \frac{P_t G_t}{4\pi r^2} \approx -135 \text{ dBW/m}^2$$

Using the expression (4-1), the scintillation to thermal noise power ratio is given by:

$$\frac{\sigma_a^2}{N_{th}} = \frac{\alpha 4\pi \sigma_r^2}{k T_s B} \frac{k^2}{4\pi} s_0 (1 - e^{-1/s_0}) C_{n0}^2 \int_0^\infty x dx (x^2 + 1/4)^{-11/6} e^{-x^2 \sigma_r^2} \quad (5-4)$$

Fig. 5 shows a plot of  $\sigma_n^2/N_{th}$  as a function of the effective antenna radius  $\sigma_r$  for 10 GHz. We have used the following constants:

$$\alpha = -135 \text{ dBW/m}^2$$

$$T_s = 30^\circ \text{K}$$

$$C_{no}^2 = 5 \cdot 10^{-12} \text{ m}^{-2/3} \quad (\text{strong turbulence}) \quad B = 3 \cdot 10^3 \text{ Hz}$$

A plot of  $\sigma_n^2/N_{th}$  versus  $\sigma_r$  at 10 and 90 GHz is also shown in the figure. It is clear from this plot that for strong turbulence scintillation noise is much larger than thermal noise. The same statement holds for the amplitude scintillation, although there is a maximum value for this ratio. However, the fact that scintillation noise is larger than thermal noise does not say that the influence of scintillation on the performance of the system will be more important. Since scintillation noise has a very narrow power spectrum, its influence on a modulated carrier can not directly be compared with that of white thermal noise.

## 6. Conclusion

We have given a theoretical derivation for several statistical properties of the scintillation noise. Although the model used is a very simple one, the results are in agreement with others found in the literature (Tatarski-1961; Lee and Harp-1969). Some calculations of the scintillation noise to signal ratio are shown. From these it is clear that the higher the frequency the more important becomes phase scintillation relative to amplitude scintillation. From the practical point of view this is a drawback, since the measurement of phase scintillation is much more difficult than that of amplitude scintillation. In addition it seems reasonable to assume that phase scintillation will have a greater influence on a digital phase-modulated carrier, which is the modulation method generally accepted for frequencies above 10 GHz.

In the latter part of this paper we have seen that the scintillation noise power is at least comparable with the thermal noise power. So it seems reasonable to assume that scintillation noise will have an influence on the reliability of satellite communication systems working in the frequency band above 10 GHz. But so far, no exact calculation of this influence has been published. This should be the subject of further study.

## Appendix I : Calculation of the covariance function

In section 2 we found for the received field

$$E(x_0, y_0, L) = C + n_{sc}$$

where

$$C = g_s(0,0)e^{jkL}$$

and

$$n_{sc} = \frac{jk}{4\pi^2} \int_0^L dz \int_{-\infty}^{\infty} \int_{-\infty}^{\infty} e^{jkz} e^{j\mathbf{k}_s(L-z)} g_s(-k_x, -k_y) d\eta(k_x, k_y, z)$$

The normalised covariance function is given by

$$\begin{aligned} \frac{1}{|C|^2} C_n(x,y) &= \frac{1}{|C|^2} \langle n_{sc}(x_0, y_0) n_{sc}^*(x_0+x, y_0+y) \rangle \\ &= \frac{1}{|C|^2} \frac{k^2}{4\pi^2} \int_0^L dz_1 \int_0^L dz_2 \int_{-\infty}^{\infty} \int_{-\infty}^{\infty} e^{jk(z_1-z_2)} e^{j\mathbf{k}_s(L-z_1)} e^{-j\mathbf{k}_s(L-z_2)} \times \\ &\quad \times g_{s1}(-k_{x1}, -k_{y1}) g_{s2}^*(-k_{x2}, -k_{y2}) \langle d\eta(k_{x1}, k_{y1}, z_1) d\eta^*(k_{x2}, k_{y2}, z_2) \rangle \end{aligned} \quad (A1-1)$$

Since

$$\langle d\eta(k_{x1}, k_{y1}, z_1) d\eta^*(k_{x2}, k_{y2}, z_2) \rangle = 4\pi^2 \delta(k_{x1} - k_{x2}) \delta(k_{y1} - k_{y2}) F_n(k_{x1}, k_{y1}, z_1 - z_2) dk_{x1} dk_{y1} dk_{x2} dk_{y2} \quad (\text{Tatarski-1961})$$

and

$$g_{s2}(k_{x2}, k_{y2}) = g_{s1}(k_{x2}, k_{y2}) e^{j(k_{x2}x + k_{y2}y)}$$

we find

$$\begin{aligned} \frac{1}{|C|^2} C_n(x,y) &= \frac{k^2}{4\pi^2} \int_0^L dz_1 \int_0^L dz_2 \int_{-\infty}^{\infty} \int_{-\infty}^{\infty} dk_{x1} dk_{y1} e^{jk(z_1-z_2)} e^{j\mathbf{k}_s(L-z_1)} \left| \frac{g_s(-k_{x1}, -k_{y1})}{g_s(0,0)} \right|^2 \times \\ &\quad \times F_n(k_{x1}, k_{y1}, z_1 - z_2) e^{j(k_{x1}x + k_{y1}y)} \end{aligned} \quad (A1-2)$$

Here  $F_n$  denotes the two-dimensional power spectrum of the refractive index fluctuations.

Rearrangement of the terms in the above expression gives:

$$\frac{1}{|C|^2} C_n(x, y) = \frac{k^2}{4\pi^2} \iint_{-\infty}^{\infty} dk_x dk_y e^{j(k_x x + k_y y)} \left| \frac{g_n(k_x, -k_y)}{g_n(0, 0)} \right|^2 \int_0^L dz_1 dz_2 e^{j(k-k_2)(z_1-z_2)} F_n(k_x, k_y, z_1, z_2) \quad (A1-3)$$

Substitution of  $\xi = z_1 - z_2$  and  $s = \frac{1}{2}(z_1 + z_2)$  in the last integral gives

$$\text{Integral I} = \iint_D d\xi ds e^{j(k-k_2)\xi} F_n(k_x, k_y, \xi)$$

where the area D is a rhomb. A similar integral has been evaluated earlier in the literature (Tatarski-1961) and this will not be repeated here. We only state that under the assumption  $F_n(\xi) \rightarrow 0$  for  $\xi > L_0$  (the outer scale of turbulence) and  $L_0 \ll L$  the integral is approximately equal to:

$$I \approx \int_0^L ds \Phi_n(k_x, k_y, k-k_2)$$

where  $\Phi_n$  is the threedimensional power spectrum of the refractive index fluctuations. In an isotropic stochastic field  $\Phi_n$  is only a function of  $\kappa = \sqrt{k_x^2 + k_y^2}$ . In addition,  $\Phi_n$  will only have a non-zero value for  $\kappa$ -values much smaller than  $k$ . But since  $k_x \approx \sqrt{k^2 - \kappa^2}$  we can write

$$k - k_2 \approx k - (k - \frac{\kappa^2}{2k}) \approx \frac{\kappa^2}{2k} \rightarrow 0 \quad \text{for } \kappa \ll k$$

In this case

$$I \approx \int_0^L ds \Phi_n(k_x, k_y) = \int_0^L ds \Phi_n(\kappa) \quad (A1-4)$$

Substitute

$$\begin{aligned} x &= \rho \cos \psi & \text{and} & & k_x &= \kappa \cos \theta \\ y &= \rho \sin \psi & & & k_y &= \kappa \sin \theta \end{aligned}$$

then

$$\begin{aligned} \frac{1}{|C|^2} C_n(\rho, \psi) &= \frac{k^2}{4\pi^2} \int_0^L ds \int_0^{2\pi} d\theta \int_0^\infty \kappa d\kappa \Phi_n(\kappa) \left| \frac{g_n(\kappa)}{g_n(0)} \right|^2 e^{j\kappa \rho \cos(\theta - \psi)} \\ &= \frac{k^2}{2\pi} \int_0^L ds \int_0^\infty \kappa d\kappa \Phi_n(\kappa) \left| \frac{g_n(\kappa)}{g_n(0)} \right|^2 J_0(\kappa \rho) \end{aligned} \quad (A1-5)$$

We have assumed implicitly that the antenna gain function has rotational symmetry round its main axis, which in practice is a fairly good approximation.

## Appendix II: Covariance function for amplitude and phase scintillation

The amplitude fluctuations of the received field are given by:

$$\delta_a = \left| 1 + \frac{n_{sa}}{C} \right| - 1 \quad (A2-1)$$

Since in section 2 we assumed  $n_{sc} \ll 1$  and since  $|C| \approx 1$ , we can write (Lee and Harp-1969):

$$\delta_a = \left\{ (1 + \operatorname{Re} \frac{n_{sa}}{C})^2 + (\operatorname{Im} \frac{n_{sa}}{C})^2 \right\}^{1/2} - 1 \approx 1 + \operatorname{Re} \frac{n_{sa}}{C} - 1 = \operatorname{Re} \frac{n_{sa}}{C}$$

Therefore

$$\begin{aligned} \delta_a &= \frac{1}{2} \left\{ \frac{n_{sa}}{C} + \left( \frac{n_{sa}}{C} \right)^* \right\} = \\ &= \frac{k^2}{4\pi^2} \int_0^L dz \iint_{-\infty}^{\infty} \frac{g_n(k_x, -k_y)}{g_n(0, 0)} \sin(k-k_2)(L-z) d\eta(k_x, k_y, z) \end{aligned} \quad (A2-2)$$

where we have used the relations  $g_n^*(k_x, k_y) = g_n(-k_x, -k_y)$  and  $\sin^*(-k_x, -k_y, z) = \sin(k_x, k_y, z)$ , both functions being the Fourier-transforms of real spatial functions. The amplitude covariance function is given by:

$$\begin{aligned} \frac{1}{|C|^2} C_a(x, y) &= \langle \delta_a(x, y) \delta_a^*(x_0 + x, y_0 + y) \rangle = \\ &= \frac{k^2}{8\pi^4} \int_0^L dz_1 dz_2 \iiint_{-\infty}^{\infty} \sin(k-k_2)(L-z_1) \cdot \sin(k-k_2)(L-z_2) \times \\ &\quad \times g_{a1}(-k_{x1}, -k_{y1}) g_{a2}^*(-k_{x2}, -k_{y2}) \langle d\eta(k_{x1}, k_{y1}, z_1) d\eta^*(k_{x2}, k_{y2}, z_2) \rangle \end{aligned} \quad (A2-3)$$

The evaluation of this expression is similar to that in Appendix I. We find

$$\frac{1}{|C|^2} C_n(\rho) = \frac{k^2}{4\pi} \int_0^L ds (1 - \cos \frac{k^2 s}{k}) \int_{-\infty}^{\infty} x dx \Phi_n(x) \left| \frac{q_n(x)}{q_n(0)} \right|^2 J_0(k\rho) \quad (A2-4)$$

The phase fluctuations are given by the expression

$$\delta\varphi = \arg\left(\frac{n_{sc}}{C}\right) \approx \lambda_n\left(\frac{n_{sc}}{C}\right) \quad (A2-5)$$

Now the covariance of  $n_{sc}$  can be written as:

$$\begin{aligned} \frac{1}{|C|^2} C_n(x, y) &= \frac{1}{|C|^2} \langle n_{sc}(x_0, y_0) n_{sc}^*(x_0 + x, y_0 + y) \rangle \\ &= \langle \left( \frac{n_{sc}(x_0, y_0)}{C} \right) \left( \frac{n_{sc}(x_0 + x, y_0 + y)}{C} \right)^* \rangle \\ &= \left\langle \left[ R_e \frac{n_{sc}(x_0, y_0)}{C} R_e \frac{n_{sc}(x_0 + x, y_0 + y)}{C} + \lambda_n \frac{n_{sc}(x_0, y_0)}{C} \lambda_n \frac{n_{sc}(x_0 + x, y_0 + y)}{C} \right] \right\rangle \\ &= \frac{1}{|C|^2} C_n(x, y) + \frac{1}{|C|^2} C_\varphi(x, y) \end{aligned}$$

Hence,

$$\frac{1}{|C|^2} C_n(x, y) = \frac{1}{|C|^2} C_n(x, y) + \frac{1}{|C|^2} C_\varphi(x, y) \quad (A2-6)$$

Therefore, the phase covariance is given by

$$\frac{1}{|C|^2} C_\varphi(\rho) = \frac{k^2}{4\pi} \int_0^L ds (1 + \cos \frac{k^2 s}{k}) \int_{-\infty}^{\infty} x dx \Phi_n(x) \left| \frac{q_n(x)}{q_n(0)} \right|^2 J_0(k\rho) \quad (A2-7)$$

## References

- Abramowitz, M., Stegun, I.A., "Handbook of Mathematical Functions", Dover Publications Inc.
- Brookner, E., 1970, "Atmosphere Propagation and Communication Channel Model for Laser Wavelengths", IEEE Trans., Vol. Com-18, No. 4.
- Clemmow, P.C., 1966, "The Plane Wave Spectrum Representation of Electromagnetic Fields", Pergamon Press.
- Ishimaru, A., "Temporal Frequency Spectra of Multifrequency Waves in Turbulent Atmosphere", IEEE Trans., Vol. AP-20, No. 1.
- Lane, J.A., 1968, "Scintillation and Absorption Fading on Line-of-Sight Links at 35 and 100 GHz", Conf. on Tropospheric Wave Propagation, Conf. Publ. 48, Oct. 1968.
- Lee, R.W., Harp, J.C., 1969, "Weak Scattering in Random Media, with Applications to Remote Probing", Proc. IEEE, Vol. 57, No. 4.
- Nisenberg, M., 1967, "Error Probability for Multipath Fading", IEEE Trans., Vol. Comm. -15, No. 6.
- Strohbehn, J.W., 1968, "Line-of-sight Wave Propagation through the Turbulent Atmosphere", Proc. IEEE, Vol. 56, p. 1301.
- Tatarski, V.I., 1961, "Wave Propagation in a Turbulent Medium", Dover Publications Inc.
- Taylor, G.I., 1938, "The Spectrum of Turbulence". Proc. Roy. Soc. (Ondon), Vol. A 164, p. 476.
- Tsao, C.K.H., Roche, J.F., de Bettencourt, J.T., Worthington, D.T., 1973, "EHF Radio Waves For High Speed Data Communications", IEE Conf. Publ. 98, Propagation of Radiowaves at Frequencies above 10 GHz.

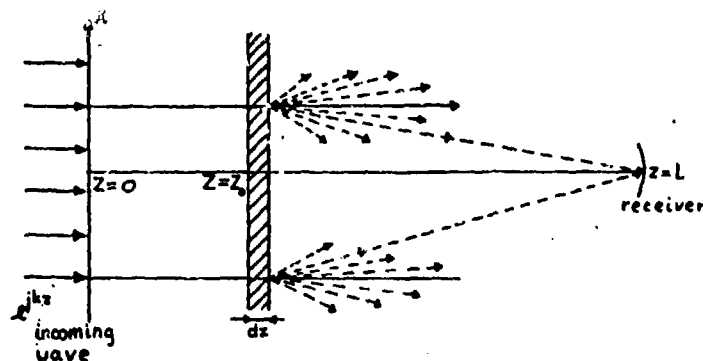


Fig. 1 The used propagation model.

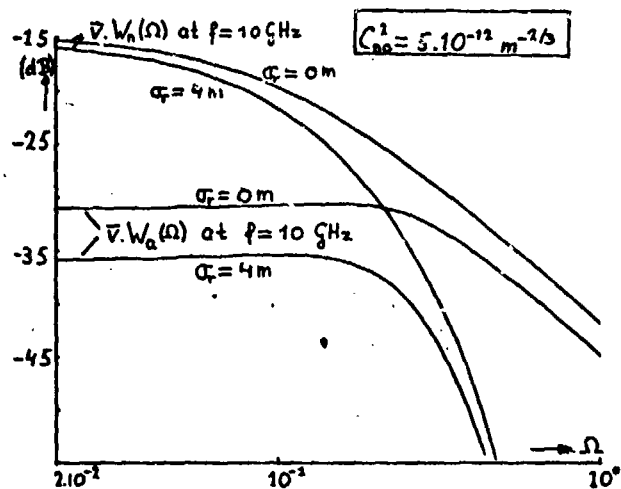


Fig. 2 Calculated power spectra of the scintillation noise.

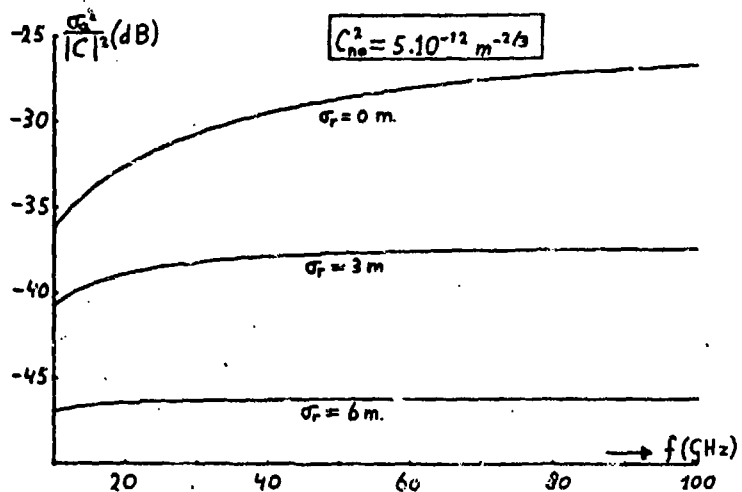


Fig. 3 Amplitude scintillation to carrier ratio versus frequency.

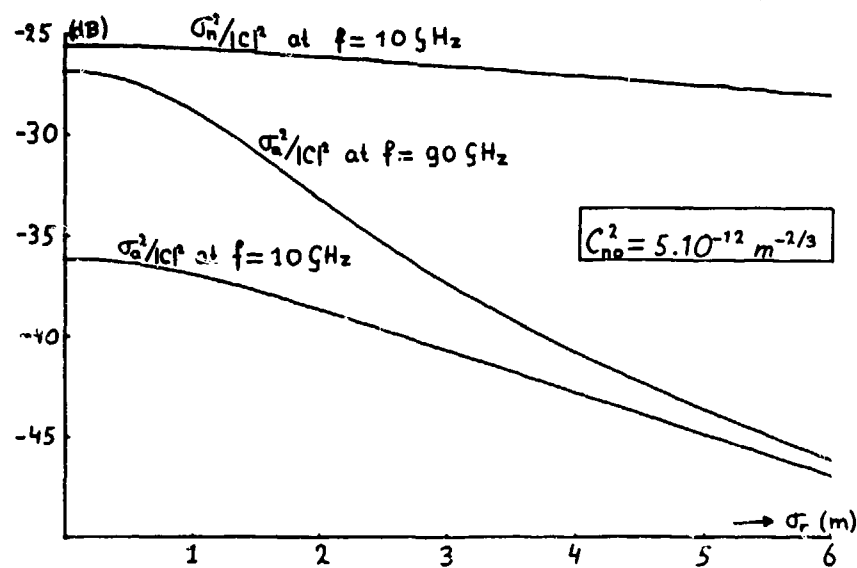


Fig. 4 Scintillation noise to carrier ratio versus the effective aperture radius.

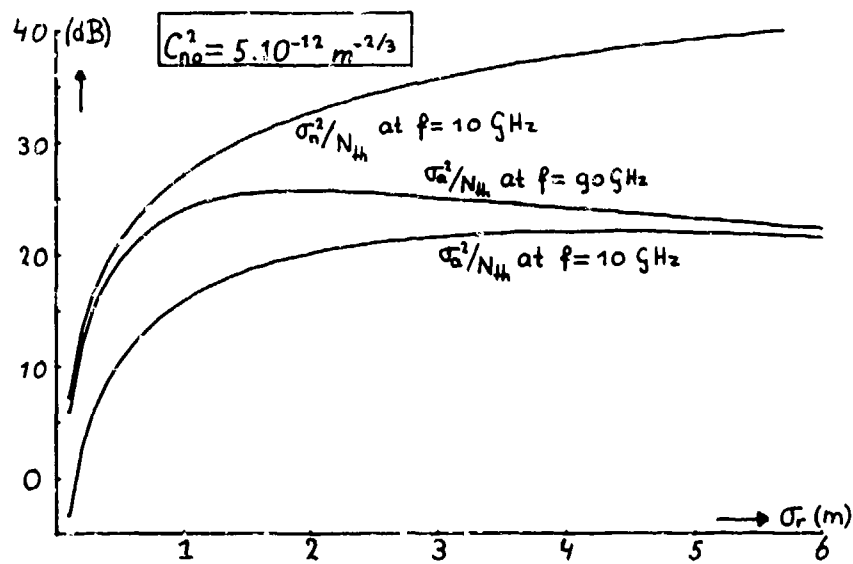


Fig. 5 Scintillation noise to thermal noise ratio.

## DISCUSSION

E. J. FREMOUW: 1) Paper is fine example of systematic application of scientific results to an engineering question. 2) I think you are dealing more directly with quadrature components of the complex signal than with amplitude and phase. Terminology may be important to engineers trying to apply results. 3) Do you have any data or plan any experiments to examine the first-order statistics of a tropospherically scintillating CW signal on the complex plane?

M. J. M. VAN WEERT: This comment of Mr. Fremouw is in essence correct, since in Appendix II of my paper, amplitude and phase of the received wave are given as the real and imaginary part of the complex wave; but in the case when the scintillation is very small, as I have assumed here, the difference between amplitude and phase and the quadrature components will be negligible. 3) In 1975, we have planned an experiment on a horizontal link, where we will measure amplitude and phase scintillations. We will also examine the first-order statistics.

## DOD ELECTROMAGNETIC COMPATIBILITY PROGRAM - AN OVERVIEW

John J. O'Neil  
Communications/AEP Laboratory,  
U.S. Army Electronics Command  
Fort Monmouth, New Jersey  
United States of America

13-1

### SUMMARY

An overview of the Department of Defense Electromagnetic Compatibility Program is presented. This integrated program intended to ensure the electromagnetic compatibility of all electrical and electronic equipments, subsystems and systems produced and operated by components of the Defense Department in any electromagnetic environment, resulted in the establishment of eight major program areas. The status of each of these areas is examined with particular emphasis on the areas of EMC Standards and Specifications and Measurement Techniques and Instrumentation. Plans of the Department of Army to solve operational problems are also reviewed.

#### 1. INTRODUCTION

The Department of Defense in 1960 issued a Memorandum to the Secretaries of the Army, Navy and Air Force defining policy and objectives and establishing a comprehensive program in major areas of what was then termed Radio Frequency Compatibility. Although each Service had in being at that time, and for many years previously, a program to cope with their interference problems this memorandum cited specific actions to be initiated and established relatively short target dates for their accomplishment. The most immediate response to this memorandum was the establishment of the Electromagnetic Compatibility Analysis Center (ECAC) which will be discussed later.

The initial results of this action to the Tri-Service Secretaries was most encouraging, however, the Directive did not assign detailed responsibilities nor assure an integrated DoD program. Thus, in 1967 DoD issued Directive No. 3222.3 entitled, "Department of Defense Electromagnetic Compatibility Program". This Directive assigned specific or joint responsibilities to DoD components for leadership in eight program areas. These areas were Standards and Specifications which was assigned to the Navy Dept; Measurement Techniques and Instrumentation to the Army; Data Base and Analysis to the Air Force; Test and Validation to the Army. Education for EMC and EMC Design Techniques were assigned to all DoD components and Concepts and Doctrine and Operational Problems to the Joint Chiefs of Staff. The Directive was broad in scope as its cited purpose was to ensure Electromagnetic Compatibility of all Military communications-electronics equipments, subsystems and systems during conceptual, design, acquisition and operational phases. Its objective was three-fold -

- a. Achievement of Electromagnetic Compatibility of all electronic and electrical equipments, subsystems and systems produced and operated by components of the Department of Defense, in any electromagnetic environment.
- b. Attainment of built-in design compatibility rather than use of after-the-fact remedial measures.
- c. Fostering of common DoD-wide philosophies, approaches and techniques in the design, production, test and operation of C-E equipments.

Further, the Directive incorporated the following definition of EMC which has become the accepted standard; "Electromagnetic Compatibility is the ability of communications-electronics (C-E) equipment, subsystems and systems to operate in their intended operational environments without suffering or causing unacceptable degradation because of unintentional electromagnetic radiation or response". The Directive also required that whenever possible all capabilities attained under this program be made available to other Government agencies and the civilian community and that a close relationship be maintained with Electronic Countermeasures (ECM), Electromagnetic Pulse (EMP) and the Radiation Hazards (RAD HAZ) Programs.

It should be noted that the Directive has been updated several times since its original issuance but the changes have been relatively minor.

Subsequent to the issuance of this Directive each Service issued their own regulation implementing the DoD Directive. AR 11-13 was issued by the Army, the Secretary of the Navy issued SECNAVINST 2410.1B and the Air Force, AFR 80-23. Thus, for the first time the problem of achieving electromagnetic compatibility was fully recognized at the highest levels and a comprehensive integrated Program delineated for all major areas.

#### 2. GENERAL INFORMATION

##### 2.1. Standards and Specifications.

Prior to the establishment of the DoD Electromagnetic Compatibility Program considerable confusion existed in requirements for the electromagnetic compatibility of equipments and systems as each Service had their own specifications. Consequently, there were instances wherein identical materiel used jointly by two or more Services were frequently required to meet widely differing requirements. This, of course,



was confusing to the manufacturers and certainly not cost effective. In addition, there were numerous other documents which were directly allied to the electromagnetic compatibility program which required review and updating.

Upon issuance of the DoD Directive the Office of the Assistant Secretary of Defense requested that immediate action be initiated to correct the problem of overlapping EMC requirements for equipments and after numerous Tri-Service meetings MIL-STD 461, entitled: "Electromagnetic Interference Characteristics Requirements For Equipment", MIL-STD 462, entitled: "Electromagnetic Interference Characteristics, Measurement Of", and MIL-STD 463, entitled: "Definitions and Systems of Units, Electromagnetic Interference Technology" were issued. These documents superseded numerous single service specifications and have been updated several times since their original publication. The latest draft revision of MIL-STD's 461 and 462 were circulated for review in late 1970 and 1971. Evaluations of the comments on each are almost complete. Prior to issuance, the tri-service working group will fulfill its commitment to meet with representatives from the Aerospace Industries Association, Electronic Industries Association and the Society of Automotive Engineers EMC committees to indicate the disposition of the Industry comments.

The revisions, which will be published as "B" issues of each standard will incorporate the requirements now published in the various notices of MIL-STD 461A. The requirements and limits established in the standard will be based upon the mission, type, characteristics, function and intended installation of the specific equipment and will be applicable to the extent specified in the individual equipment specification, contract or order. Specific requirements that must be met are to be based on those in the standard and defined in the procurement documentation. At least two sets of requirements tables will be included. One set will define the emission and susceptibility requirements for categories of equipments (i.e. communications, surveillance, navigation, etc.) and specific types of equipments within that category (i.e. receivers, transmitters, amplifiers, etc.) The second set of tables will define emission and susceptibility requirements for equipments intended for installation in the categories defined in the standard (i.e. aircraft, spacecraft, missiles, shipboard, submarine, shore stations, etc.) Each emission and susceptibility requirement will have a limit which may be invoked regardless of the intended installation of the equipment and each will have modified limits based on the intended installation. Specific requirements which would be applicable for a given procurement must be specified by the procuring activity in accordance with its departmental regulations and procedures. Additional tailoring may be recommended in response to the request-for-proposal (RFP) for approval by the procuring activity; however, justifications for the recommendations must also be submitted.

It is recognized that some confusion may exist when the revisions are issued. Accordingly, an appendix will be included in MIL-STD 461B providing guidance for its use and procedures for determining and specifying the applicable requirements.

MIL-STD 463 was also recently updated and is currently being circulated to all DoD elements for review and comment.

In addition to these three basic standards there are other standards which are presently undergoing revisions and updating. At present the EMC Standardization Program consists of the following tri-service and single service documents:

#### A. Tri-Service Documents.

1. MIL-STD 220, entitled: "Method of Insertion Loss Measurement". This standard is being revised to include several test procedures for determining the filter insertion loss in other than a 50-ohm system. A draft is expected in the second quarter of FY-75.

2. MIL-STD 285, entitled: "Attenuation Measurements for Enclosures, Electromagnetic Shielding for Electronic Test Purposes, Method Of". This standard is scheduled for revision to update the testing requirements and procedures for determining the attenuation of shielded enclosures including shielded buildings. No firm completion schedule has been established.

3. MIL-STD 449, entitled: "Radio Frequency Spectrum Characteristics, Measurement Of". The "D" revision of this document was issued 22 Feb 1973. The Navy is considering replacing this Standard with an Equipment Signature Handbook which will provide greater flexibility as well as a standardized computer format.

4. MIL-STD 469, entitled: "Radar Engineering Design Requirements for EMC". A revision of this Standard is required to reflect the Radar Spectrum Engineering Criteria issued by the Office of Telecommunications Policy (OTP) in its Manual of Regulations and Procedures for Radio Frequency Management. However, the Interdepartment Radio Advisory Committee of OTP is planning to recommend revisions to the criteria. Accordingly, the MIL-STD 469 revision is being held in abeyance until OTP has determined what changes are deemed necessary. In the interim, DoD activities will be invoking MIL-STD 469 and/or the requirements of the criteria in radar design specifications. It is envisioned that the revised MIL-STD 469 will invoke the criteria as a minimum and also include additional requirements deemed necessary by the military departments to ensure EMC. The present schedule calls for a revision in the fourth quarter of FY75; however, the pending OTP action will probably delay preparation of a draft revision for at least 6 months.

5. MIL-B-5087, entitled: "Bonding, Electrical, and Lightning Protection for Aerospace Systems". There is no formal project for the revision of this document. However, the Air Force study project on lightning simulation as well as related efforts by the Society of Automotive Engineers AE-4 Committee on EMC may lead to the development of a revision of this document.

6. MIL-E-6051, entitled: "EMC Requirements for Systems (Aerospace)". This specification is applicable to aerospace and weapons systems. Both Navy and Army activities are in need of a system EMC document and therefore either a revision to MIL-E-6051 or a new system standard may be prepared in the next year or eighteen months.

7. MIL-HDBK-237, entitled: "Electromagnetic Compatibility/Interference Program Requirements". This handbook presents guidelines to military activities and industry for establishing an EMC program for a particular project and outlines the role of each of the EMC standards which may be applicable to the project. The document was issued in April 1973 and was the first attempt to develop an overall EMC program standard formerly numbered MIL-STD 460. While it failed in that regard, the Navy as preparing activity is working towards improvements.

8. ANSI C95.2-1966, entitled: "Radio Frequency Radiation Hazard Warning Symbol", and ANSI C95.3-1972, entitled: "Techniques & Instrumentation for the Measurement of Potentially Hazardous Electromagnetic Radiation at Microwave Frequencies". These documents are concerned with the area of radiation hazards. The Naval Electronic Systems Command was co-sponsor with the IEEE and the American National Standards C93 Committee on Radio Frequency Radiation Hazards on the preparation of these documents, which were coordinated with, and approved for use by DoD.

#### D. Single Service Documents.

1. MIL-R-9673 (USAF), entitled: "Radiation Limits Microwave and X-Radiation Generated by Ground Electronic Equipment (as Related to Personnel Safety)". This Air Force document concerns radiation hazards to personnel. A draft revision was circulated about 12-18 months ago and comments were such that the revision project was cancelled.

2. MIL-STD-1541 (USAF), entitled: "EMC Requirements for Space Systems" and 1542 (USAF), entitled: "EMC Requirements for Space System Ground Facilities". These standards were issued in October 1973 to cover EMC requirements for space systems and associated ground facilities.

3. MIL-STD-1310 (Navy), entitled: "Shipboard Bonding and Grounding Methods for EMC and Safety". The "C" revision of this standard was issued in November 1973 and covers shipboard grounding and bonding methods for EMC and safety.

4. MIL-STD-1385 (Navy), entitled: "Preclusion of Ordnance Hazards in Electromagnetic Fields: General Requirements For". This document covers the Navy's requirements to preclude hazards from electromagnetic radiation. It was issued in April 1972.

5. MIL-STD-1605 (Ships), entitled: "Procedures for Conducting A Shipboard EMC Survey (Surface Ships)". This standard was issued in April 1973 by the Naval Ship Engineering Center and defines the procedures for conducting shipboard EMC surveys.

6. MIL-HDBK-238 (Navy), entitled: "Electromagnetic Radiation Hazards". This document was issued in August 1973 as a compilation of the Navy's radiation hazard criteria and procedures for precluding such hazards.

7. MIL-HDBK-235 (Navy), entitled: "Electromagnetic (Radiated) Environment Considerations for Design and Procurement of Electrical and Electronic Equipment". This document was issued in June 1972 by the Naval Electronic Systems Command. It is intended to provide guidance and establish a uniform approach for the protection of Navy electronics from the adverse effects of the electromagnetic environment. Examples of systems, subsystems and equipments to which the handbook may be applicable are: (1) aerospace and weapons systems; (2) ordnance; (3) support and checkout equipment and instruments; and (4) any other electronic equipment or system which may be exposed to a high intensity electromagnetic environment during its life cycle. The handbook may also be used to tailor the radiated susceptibility limit of MIL-STD 461 and the requirements of MIL-E-6051. The handbook is issued in three parts with Part 1 providing general information on the use of the handbook and Parts 2 and 3 describing the electromagnetic levels which may be encountered by the Navy's systems. Recently, action was taken to update the handbook as well as expand its coverage to aircraft and shore station environments. In addition, other DoD agencies were requested to furnish data on environments to which their equipments may be exposed so that all electromagnetic environment data can be contained in one document. A draft revision is expected in third quarter of FY-75.

#### 2.1.1 Waivers of Standard Requirements.

The efforts devoted to the preparation of standards are wasted if, when cited in a contract, the requirements are subsequently waived. The DoD Directive took cognizance of this fact and required that authority for waiver control be established at a level determined by the Secretary of the Military Department. In the instance of the Department of Army this authority originally was vested in the Office of Assistant Chief of Staff for Communications-Electronics. However, since the reorganization of the Army Staff the U. S. Army Communications Command is the responsible organization. In practice when a contractor requests a waiver, the government project engineer with the assistance of his EMC specialist can generally recommend a solution to the problem. If a solution is not readily forthcoming, the matter is referred through channels to HQ, AMC who then may elect to call on EMC specialists in another command. Rarely do requests for waivers reach the higher echelons and rarely are they approved.

## 2.2 Measurement Techniques and Instrumentation.

134  
As mentioned above the coordination responsibility for EMC Measurement Techniques and Instrumentation was assigned to the Department of Army and subsequently to the Electronics Command. The most visible output of this assignment is the issuance of an annual plan which provides a comprehensive listing of the efforts of the three Services and their needs in this area. The plan is forwarded thru channels to the Joint Chief of Staff and serves as a ready reference for many other offices. Each Service has its own program to satisfy their particular needs.

The Army's program is based on the general philosophy that the profit motive and competition at this time are such that industry is willing to expend its own resources for general type of instruments. Therefore, the Army concentrates on the development of advanced instrumentation concepts, design of improved instrumentation circuitry, design of special application instruments, development of improved measurement techniques and calibration standards. Following are typical examples of recent Army tasks:

- a. Established measurement techniques and permissible levels of interference for digital receivers and transmitters.
- b. Completed the design of a modularized measuring instrument covering the frequency range of 30 Hz to 40 GHz. This instrument was designed so that only the modules required for a specific task are used. Thus, the system can vary from a fully automatic computer controlled system for laboratory type measurements to a small portable ruggedized unit suitable for field surveys.
- c. Developed calibration techniques for impulse generators.
- d. Initiated the investigation of the EMC characteristics of MM Wave equipments.
- e. Continued the investigation of improved measurement techniques in shielded enclosures including the development of a set of new antennas.

## 2.3 Data Base and Analysis.

The responsibility for the Data Base and Analysis Program was assigned to the Air Force who established the Electromagnetic Compatibility Analysis Center (ECAC). ECAC provides analysis support for EMC problems in Joint interservice and civilian-military electromagnetic environments. They specialize in site-oriented or fixed location type analysis and have expertise in the analysis of large radar systems. The Center has a very extensive data base which can be categorized as follows:

- a. Environmental data
  - b. Equipment technical characteristics data
  - c. Topographic data
  - d. Spectrum allocations and usage data
  - e. Organizational platforms and allowances data.
- (1) Environmental data indicates the disposition and use of C-E equipment in various regions of the world. The data is contained in an Environment File, a Frequency Allocation Application File, a Tactical File, a Future File and a Frequency Records File.
  - (2) Equipment characteristics data identify the technical characteristics of C-E equipment both military and civilian. These data are contained in the Nominal Characteristics File; there are additional data in the Library of Spectrum Signatures for more detailed analysis involving selected equipments.
  - (3) Topographic data are stored in computer form to support propagation calculations and site analyses.
  - (4) Spectrum allocations and usage data identify rules and regulations promulgated by U.S. and foreign national, and international agencies governing use of the electromagnetic spectrum.
  - (5) Organizational platforms and allowances data identify communications-electronics emitters and receivers contained in various configurations, systems and organizations, including tactical units, ships and other marine vessels, aircraft, satellites, missile systems and major communications-electronics systems of all military departments and the Department of Defense. A limited number of other government and non-government systems are also included.

The Army also uses the EMC data base maintained by the U. S. Army Management System Support Agency. This data base has three types of EMC files:

- a. Tactical Deployments File. This file contains large scale C-E deployments developed and maintained to satisfy the analysis of EMC problems related to defined force structures, including C-E equipments for both friendly and opposing forces. The deployments are centered around major Army studies and provide the basic tool for analyzing the EMC implications of new equipments, organization and concepts.
- b. Tactical Fixed Files. These files are used to create deployments. They consist of the Equipment Authorization File, which contains a summary of the emitting and receiving equipment in all Tables of Organization and Equipment, Tables of Authorization, and Aircraft Configurations; The Equipment Characteristics File; The Antenna File; The Equipment Application File; The Net File; and the Code File.

c. Technical Files. These files contain the essential information from all DoD Frequency Allocation (Frequency Allocation to Equipment File) and Cost and Quantity Information plus some limited Logistical Information on all Army Equipment covered by an Allocation (Army Equipment Records File). They are used to generate the Army portion of the Military Reliance Report, to provide special retrievals, and the Frequency Allocation to Equipment File is provided annually to specific DoD offices.

The ECAC and USARESA data bases are continuously updated as new equipments are developed, procured or authorized. These data files are continuously queried for information to support EMC analyses and evaluations.

In the Analysis Area, ECAC performs analysis involving equipment, site selections and EMC evaluations, co-site analyses of co-located equipments, inter- and intra-system environmental EMC analyses as related to facilities operating in both COMUS and foreign environments. The analyses determine the impact of proposed C-2 system on the environment and vice-versa. Frequency assignment guidelines and degradation to system performance are typical ECAC outputs as result of analyses. Also included are radar coverage diagrams, line-of-sight profiles and power density plots which are all terrain dependent.

## 2.4 Test and Validation.

The Test and Validation program was also assigned to the Department of Army and subsequently to the Test and Evaluation Command. The DoD Directive established this program area to establish confidence in EMC standards and analysis and prediction efforts and to ensure service test and operational evaluations of equipments and systems in typical electromagnetic environments. The Electromagnetic Environmental Test Facility (EMETF) located at Fort Huachuca, Arizona is the largest tri-service facility of this type. All Army materiel which depend on, or respond to, electromagnetic phenomena must demonstrate that it is compatible with its electromagnetic environment and thus equipments at various stages of its life cycle are subjected to examination at Fort Huachuca. The facility, which is contractor operated, uses seven interrelated capabilities to accomplish its tasks: an Instrumented Work Shop, a Weapon System Simulator, a Scoring Facility, a Digital Scoring System, a Spectrum Signature Facility, a Field Facility and an Interference Prediction Model.

An example of EMC testing of equipment early in the life cycle is found in the current testing of a complex, highly automated developmental air defense system comprising a number of advanced subsystems. The design includes multiple-function capability and incorporates fire control and communications relay elements requiring considerable electromagnetic activity.

The planned immersion of this system in the electromagnetic environment of the Army necessitated that a complete EMC analysis be conducted, to include the effect of the environment on the system as well as the effect of the system on the environment. Compatibility with other friendly systems and vulnerability to enemy countermeasures were examined for missile, communications, and radar components. A digital communications system was involved, requiring the assessment of the effect of the electromagnetic environment on the bit error rates of messages either sent or received. Although the missile components were not yet available for measurement, the analysis was accomplished on the basis of specifications, design data, and the results of preliminary hardware tests.

A 'test bed' was selected which contained all deployed friendly and enemy equipment in the time frame (period of calendar time pertinent to the analysis) of interest as a basis from which to determine the effect on and from the system under test. Based on such considerations as frequency assignments, characteristics of transmissions, and location of equipment in the test bed, potential EMC problems were ranked in accordance with relative effect and possibility of occurrence.

## 2.5 Education.

Each Service is responsible for providing EMC instructional material to their design, maintenance and operational people. Consequently, each Service has issued manuals, pamphlets, etc., describing EMC techniques. The Army has a two volume design guide which is currently being updated; the Navy also has a two volume guide. The Air Force has a single volume which is constantly updated and an Interference Notebook detailing design practices. Further, the Services have prepared training films, the most recent being a set of ten prepared by the Navy. The inputs for this material are obtained either as a result of specific design efforts or from techniques evolved during the design of an equipment or system.

## 2.6 Operational Problems.

Each Service is also responsible for solving their problems of reported interference in the field.

The Communications Command has this responsibility in the Army. This command is also responsible for the conduct of field surveys in connection with the Radiation Hazard problem and gathering propagation data. At the present time that command is publishing an Operational Concept Plan which will outline procedures for responding to complaints in the field and to MIJT reports (Mishearing, Intrusion, Jamming and Interference). In addition, Transportable Automatic EMC Measurement System Vans are being procured and will be deployed at strategic sites throughout the world. Thus, the Army will have for the first time a capability to promptly investigate and remedy complaints received from the field. The results of these efforts will also serve as excellent inputs to the other EMC program areas.

## 3. CONCLUSION

The Department of Defense Electromagnetic Compatibility Program has assured that each Service has a viable program in the area of EMC, that close coordination among the Services is maintained and that careful consideration is given to the EMC problem throughout the life cycle of its electronic materiel.

## DISCUSSION

F. J. CHESTERMAN: Paragraph 2.1.1 Waiver of Standard Requirements: "Government Project Engineer and EMC Specialist can be overruled on a contractor's request for a 'Waiver' by HQ--this rarely happens."

UK philosophy is that the Project Manager has the complete executive responsibility for the Project and cannot be overruled by an "advisory EMC" specialist--but the final accountable responsibility rests on the Project Manager, even though EMC specifications are mandatory.

J. J. O'NEIL: The Department of the Army has regulation AR 11-13 which establishes procedures for waiver control. The final authority for granting waivers originally was vested in the Office of the Assistant Chief of Staff for Communications-Electronics. Since the recent reorganization of the Army Staff, the authority rests with the U. S. Army Communications Command. The channels for a waiver request is from the contractor - to the procuring organization - to his headquarters - and finally to the Communications Command, with review by EMC specialists at each echelon. In only very rare cases of very high priority items are waivers granted.

E. M. FROST: In your paper you have not made a reference to information cooperation, particularly the Quadripartite Standardization Agreement ABCA QWG/ES SWP/EMC. Table B now in active being. Where does this under standardization fit into your organization?

J. J. O'NEIL: The EMC Standardization Program discussed in the paper is a formally established Department of Defense program, coordinated by the Department of Navy with participants from the Departments of Army and Air Force, and is concerned only with Department of Defense standards and specifications as related to EMC. The ABCA Standardization Agreement is an entirely different, although equally important program and was not discussed in the paper as it is not considered a part of the DOD EMC Standardization Program.

14-1

D. Jaeger  
Messerschmitt-Bölkow-Blohm GmbH  
Ottobrunn/Munich  
Germany

### SUMMARY

To ensure electromagnetic compatibility in systems, EMC equipment specifications are required to limit for each unit the interferences emitted and specify a certain degree of unsusceptibility to interference signals. An examination is made as to whether it is more favourable to use a general EMC specification or system-oriented specifications for this purpose. The following solution is obtained: The test methods and the test philosophy should be uniform for all systems. MIL-STD 462 (+ 463) could represent a good basis. However, updating and expansion in various respects seem desirable. As far as the limit values are concerned, it becomes evident that the characteristics of the systems themselves, their environment, and the systems in conjunction with which they must possibly function differ too greatly. Uniform limit values either solve the compatibility problems with an insufficient degree of probability or with too high expenditure. Establishing system-related limit values is considered the optimum solution; fixing limit values for certain system classes (e.g. satellites, ships, etc.) is regarded as a good practical solution.

#### 1. INTRODUCTION

Advanced systems in the fields of aerospace and defense technology incorporate a large number of electronic items concentrated in a very small space. These items, on the one hand, are used to convert extremely high electrical powers with all secondary effects into any possible frequencies and levels and, on the other, must be capable of receiving and processing lowest electrical signals satisfactorily.

In order to ensure the electromagnetic compatibility (EMC), it is therefore absolutely necessary for each electrical item within the system to limit the interference emitted to the environment as well as to be insusceptible to a certain extent to external interferences.

The US were the first to face this problem. The US Army, Air Force and Navy as well as the space industry established various EMC specifications which several years ago were compiled to form a single three-part specification known as the MIL-STD 461/462/463. This specification is continually supplemented by notices. It is also widely used in Germany for a great variety of systems. This report will investigate whether a single specification to be applied to all systems is really expedient, whether the above-mentioned MIL-STD is suited for this purpose and which improvements could be made. Generally, an EMC equipment specification may be divided into two sections, namely into the test methods, including the definitions, and the limit values. When investigating the question as to whether a general specification for all systems is expedient, differentiation between these two sections should be made.

#### 2. DISCUSSION OF TEST METHODS

The test methods shall be used to determine and characterize the interferences emitted by a unit during all operational statuses to the environment as well as any possible susceptibilities to interference signals from the environment. The measurements may be limited to the frequency range which is of technical interest resp. expedient.

The test methods should approximate those in practice and supply clear and reproducible results. If possible, quantities should be measured which are independent of certain measuring instruments. In addition, the test operations should not be very complicated. Furthermore, it is expedient to bear in mind when performing the EMC equipment measurements that the equipment compatibility within the overall system must be demonstrated subsequently. Thus, it should be possible to use the results of the equipment measurements as far as practicable for this purpose.

The problems inherent in the acquisition and evaluation of the emitted interferences and the EMI susceptibilities are essentially identical for most of the electrical systems. It is irrelevant whether an aircraft, a satellite, a missile, a ship or even a factory hall with electronically controlled machine tools is concerned. Any differences which may exist can be eliminated in the most cases by fixing the limit values. It is therefore considered expedient to have a general EMC specification including test methods. In the following a survey is given as to the test methods which should be included in such a specification. Subsequently, a comparison is made with the only existing specification of this kind, i.e. MIL-STD 462.

Fig. 1 shows an electrical unit with antenna, e.g. a receiver or transmitter. It is coupled with its environment in the following ways:

- (a) Conductive coupling: i.e., through the power supply and signal lines.
- (b) Inductive coupling: i.e., through magnetic fields across the cable harness and the equipment.
- (c) Capacitive coupling: i.e. through electrical fields across the cable harness and the equipment.
- (d) Electromagnetic coupling (RF): differentiation can be made between the antenna and the unit with its cable harness.

On these links the unit can emit interferences as well as pick up interferences from the environment, i.e. be susceptible to interference. Thus, to start with, test methods must be available which consider all these possibilities.

The individual units, in part, emit rather differing interference signals and respond differently to them. It is therefore recommended that not only the spectrum be recorded but also more detailed differentiation be made. Theoretically an infinite number of signal shapes would have to be considered. However, practical experience has shown that it suffices for EMC to characterize any possible signal shapes through the following (fig. 2):

- (A) Short-duration signals (repetition frequency < approx. 10 Hz), switching operations when switching on, off or over produce.
- (B) Continuous signals.  
The following can be distinguished:
  - a) narrowband signals
  - b) wideband signals
    - (i) pulse spectrum (repetition frequency > approx. 10 Hz) e.g., voltage converter,
    - (ii) Random signals e.g., collector motor.

When combining the possible coupling links and the signal shapes proved significant by experience, a survey is obtained of the overall measurements which would be required to ensure the compatibility of a unit with a system. The survey is shown in Fig. 3. On the left-hand side those interferences which can be emitted are shown and on the right side those which can be picked up from the environment.

The ideal EMC specification would include test methods for all links and signal types shown. It would then be possible to describe the EMC characteristics of an unit almost completely.

Let us briefly examine to which extent the presently applicable sole EMC specification containing test methods for equipment, namely MIL-STD 462, meets this ideal concept. Notice 2 is usually applied in Germany to aeronautical equipment. The results are illustrated in Fig. 4. The results for the more recent notice 4 are shown in Fig. 5. It can be seen that in either case a large number of measurements is covered, however, in part, using not entirely perfect test methods or frequency limits. Nevertheless, this MIL-STD can be regarded as a good basis for any conceivable system in the fields of aerospace, maritime and military technology. It might even be easily used in the civil sector for the solution of the EMC problems where to date no comparable specifications have yet been established. However, before long such a specification will certainly be required there as well since the concentration of electrical and electronic equipment is increasing in that field, too. In this connection it should be pointed out that the test methods delineated in MIL-STD 462 have been applied successfully by MBB since several years so as to make process computing facilities electromagnetically compatible in factory halls.

Thus, MIL-STD 462 constitutes a sound basis for the acquisition and evaluation of interferences emitted as well as for the susceptibilities to interference. In spite of this, some improvements should still be made in certain directions. They are mentioned briefly in the following together with some examples:

- (a) Revising existing test methods. Some methods have not been defined to a sufficiently accurate extent, i.e. definition of quantities which exert great influence on the test results (e.g., the internal resistance of the power source in test CE01).
- (b) Modifying the frequency limits and the types of interference signals.  
Most of the high-frequency tests, such as intermodulation, cross modulation, etc. have an upper frequency limit of 12.4 GHz. Thus, the X band is only just covered. No consideration has been given to the fact that recently radar equipment, transmission lines, etc., are increasingly operating on the Ku-band. It seems absolutely necessary to extend the frequency range for the above mentioned tests to 18 GHz.

In other cases, however, the frequency limits are too high. Mention should be made here of the conducted susceptibility test CS 02, where measurements up to 400 MHz are to be made. At most 100 MHz are technically practicable.

The susceptibility to spikes is tested exclusively by using a 10  $\mu$ sec spike. Practice has shown that this is too slow for advanced digital electronics. Some cases

were observed in which digital equipment was insusceptible to the MIL spike but showed high susceptibility to spikes of shorter duration.

- (c) Introducing new test methods. As illustrated in Figs. 4 and 5, only a part of the test methods is covered by MIL-STD 462. It would be necessary to supplement the test methods.

In practice not all of the tests listed are equivalent. Some are used very frequently, others only in special cases. Still others are covered by different ones already existing. Thus, it does not seem necessary to complete them now or in the near future. Nevertheless some indications as to potential expansion may be of interest.

Since several years MBB has been using a test which has proved to be quite successful. Apart from feed-in of spikes and sinusoidal interference signals on the power lines, wideband interference signals are impressed during an additional measurement. Noise in defined frequency bands is used, e.g. 20 Hz to 100 kHz or 100 kHz to some MHz. The test set-up is similar to that in tests CS 01/CS 02. The test rapidly detects weak points and, in addition, is required to demonstrate general system compatibility. Not only a sole interference frequency but a mixture of a great number of frequencies is generally available on the power supply lines of a unit in a system.

Checking the units and their leads respect to short-time electrical fields has proved very expedient at MBB. Computers are frequently proved to be susceptible. A similar test set-up was selected as in RS 04 of notice 2.

When summarizing the results laid down in this section, it becomes evident that with regard to the test methods a sole EMC specification is expedient for all electrical and electronic systems; this is not only practicable but even desirable since this section includes the major part of the EMC philosophy. MIL-STD 462 may be applied as the basis for this specification. Some updating and extension would, however, be required.

### 3. DISCUSSION OF LIMITS

The second important part of an EMC equipment specification are the limit values. This is a somewhat different case from that of the test methods.

To achieve electromagnetic compatibility within a system, the interferences emitted must be limited for each unit on the one hand, and a certain insusceptibility to external interference signals must be ensured, on the other.

What are the levels at which these limits are reasonably set? The problems shall briefly be explained as follows:

A significant aspect is the safety margin. A system is considered electromagnetically compatible if the available interference signals in every important system circuit during any possible operational status and any possible environmental influence fall below the EMI threshold level by a certain factor. The latter is called the safety margin. It must be ensured with regard to any type of interference signal which occurs.

Fig. 6 shows an example. Curve A depicts the interferences available on the power supply lines of a unit as a function of the frequency, whereas curve B illustrates the threshold level. The safety margin is then C. The system is certainly disturbed in its function if C is smaller than 0. Its operation is unstable if C is equal to or only slightly greater than 0. Its operation is stable if C is substantially greater than C.

The safety margin depends on the type of system, the significance of the circuit concerned with regard to the system, and the accuracy at which the safety margin can be proved. In simple cases 6 dB are sufficient (in minor circuits and low-frequency interferences); in complicated cases at least 20 dB should be used (in extremely critical circuits and RF interferences, e.g. induction of electromagnetic fields in firing circuits).

The safety margin is a merely relative quantity. It solely indicates the ratio of the threshold level to the actually available interferences. However, it does not give any indication as to the limits to be set for the interferences emitted and the level of unsusceptibility required.

Theoretically, a system could be made compatible if the interferences emitted would be completely suppressed for all units. The susceptibility to interference signals could then have any low value. However, the expenditure for interference suppressed devices would then be very high. The same applies to the other extreme case. Compatibility can also be achieved by calling for complete insusceptibility to all interference signals. The interferences emitted may then have any high value. Between these extreme cases there is generally a point or range at which optimum electromagnetic compatibility can be attained. Fig. 7 gives an approximate idea of the entire curve. Said optimization can be made for all types of interference signals, considering the limitations described below. The system would then be optimally compatible.

As far as respective optimum is concerned, the requirements according to which optimization is to be made are decisive. Optimization can, for example, be performed from the aspects concerning the weight of the overall system, the space requirement, the costs or reliability. The technologies and interference suppression possibilities which can be applied in the system depend on the respective requirement. Only in very rare cases is the same optimum achieved with the differing requirements. Generally, it will be similar to that illustrated in Fig. 8. i.e., the permissible levels of emitted



Interference and necessary unsusceptibilities depend on the system requirements.

14-4 The aspects playing a role in the design of a system, however, differ basically. Whereas, for example, with ships the weight is almost of no significance, it may be of utmost importance with aircraft and especially satellites. As far as large-scale quantity production of missiles or automobiles is concerned, financial reasons will be of major importance. The limitation of the interferences emitted and the EMI susceptibility thus depends on the system requirements in a certain way.

In some instances optimization is not yet possible for certain types of interference signals. This, for example, is the case if the system incorporates receivers or transmitters in certain frequency ranges. They are inherent susceptibilities or interference sources for which no interference suppression can be effected and to which the overall system must be tailored. Through the antenna and the airframe they are decoupled from the other electronic units only by a certain value which cannot be exceeded. Optimization is no longer possible in such a case. The practical conditions must be used as the starting point (Fig. 9).

The unavoidable interference sources and susceptibilities existing in the individual systems as well as their decoupling from the overall system generally differ greatly from one another. Whereas a satellite, for example, features only a transmitting power of some 10 W, a transmitting power of some 100 kW may be available in advanced ships and aircraft. The latter usually exhibit a great amount of unavoidable susceptibility as well, namely the RF receivers. The amount of decoupling of the RF equipment from the other electronic units differs likewise. Whereas this value may be nearly 0 dB for a helicopter, for example, it amounts to at least 20 - 30 dB in a tank. Some systems, e.g., wire-guided missiles or torpedos, incorporate neither on-board RF receivers nor RF transmitters. All in all the differences between the individual systems are extremely great, as far as certain limit values are concerned. This statement relates above all to the field strength measurements (radiated emission and radiated susceptibility).

With regard to electromagnetic compatibility the environment in which the system must function is of great importance. Only a very few systems can operate in an environment that is electromagnetically clean or can be subjected to any degree of contamination. This applies approximately to torpedos and possibly only just to satellites. In most of the cases the system must be compatible with the environment, i.e., it may emit only certain levels to the environment and must be capable of withstanding a certain amount of interference. Let us look at the KORMORAN missile as an example (Fig. 10). It is carried by an aircraft up to a distance of some 10 km from a ship target and fired thereon. Its approach flight is radar-controlled and proper functioning of the missile must be ensured up to some 100 m from the ship. The compatibility problems are illustrated in Fig. 11. The missile must be internally compatible. It must likewise be compatible when operating in conjunction with the carrier aircraft equipment, i.e., on the links through which it is coupled with the aircraft. Essentially, this is the power supply (at the beginning effected from the aircraft) and the RF link (avoiding disturbance of the aircraft receivers as well as disturbance of the missile due to the aircraft transmitters). In addition, the missile must be compatible with the RF equipment of the ship target. Due to the high field strengths of radar equipment, this task could be jeopardized unintentionally, in principle. The EMC equipments for the KORMORAN system result from the consideration of the internal system compatibility, the compatibility with the other system and the compatibility with the targets.

The requirements resulting from the environment may vary greatly. In the case of KORMORAN they were decisive, for example, for the radiation susceptibility. In other cases, such as the torpedo, they are almost irrelevant. As far as an automobile without own equipment is concerned, the radiated emission must solely be limited to the extent that any radio receiver in its vicinity is not disturbed. The requirements set by the environment with regard to the different systems, thus, vary for the interferences emitted and the EMI susceptibility.

Specifying uniform limit values for all systems with regard to interferences emitted and EMI susceptibility, MIL-STD 461 tries to solve all the problems set forth above, such as optimization of the limit values by weight, costs, etc., consideration of the inherent system interference sources and EMI susceptibility as well as the various electromagnetic environment conditions. It can easily be understood that in many cases the limit values do not suffice to ensure compatibility; in some other cases the limit values are by far too rigid. This means that some requirements are too rigid, whereas others are too relaxed.

Some relevant examples are indicated below:

- (a) For the ROLAND missile, a low-level anti-aircraft missile, the susceptibility to voltage peaks on the power supply lines could be limited to  $\pm 1.5$  V (MIL-STD 461 calls for  $\pm 56$  V).
- (b) For the HOT weapon system, an anti-tank missile, the limit curves for the interferences emitted via the power supply lines could be increased in part by 40 dB. No disturbances occurred.
- (c) As far as the BO 105 helicopter is concerned, the application of the limit curves for the radiated emission resulted in a disturbance of the radio compass. The limit values had to be lowered in part by about 25 dB.
- (d) For the KORMORAN missile, an anti-ship missile, the values for the radiation susceptibility, rejection of undesired signals at antenna terminal, etc., of the seeker head had to be increased substantially, as compared with the MIL-STD. Otherwise, interferences (in principle, unwanted) from the targets would have been unavoidable.

These few examples already show that it is rather critical to use uniform limit values for all systems.

Some uncertainty with regard to the limit exists in MIL-STD 461 A too, changing the limit values from notice to notice. The radiation susceptibility values, for example, were, in part, increased by 20 dB from notice 1/2 to notice 3. As far as the radiated emission is concerned, the limit values were decreased by up to 30 dB. The limits for the conducted emission via the power supply lines were, in part, increased by 10 dB (in notice 3) and then decreased again by 10 dB (in notice 4).

Which solutions exist to cope with these difficulties? The optimum approach to ensure the electromagnetic compatibility within a system is to establish system-related limit values. On the basis of the sources and susceptibilities existing in the system, the limit values could be fixed, taking the environmental stresses and the special requirements into consideration. It would even be possible to split up the limit values for the various units. Such an action would in all probability make the system optimally compatible from the technical and economic points of view. To accomplish this, detailed knowledge of the new system and its environment as well as a great amount of experience with similar systems would, however, be required. The most unfavourable solution is to use uniform limit values for all systems. On the one hand, the electromagnetic compatibility is ensured only with a certain degree of probability and, on the other, the expenditure specified for interference suppression is frequently too high. However, scarcely and knowledge of the new system to be developed nor any experience in the EMC field is required. It would be a good compromise to classify the systems in question by system characteristics, the requirements for interference suppression and the environment to which they are exposed (interferences emitted and susceptibilities). Separate limit values could then be established for each class. This method would entail the advantage that compatibility would be ensured with an extremely high degree of probability, that the expenditure would not be too high from the technical and economic aspects and, in addition, that it would be possible to solve the compatibility problems satisfactorily even without wide EMC experience.

Which system classes are now conceivable? It would be somewhat premature to define them accurately as early as now. A great number of experience and a large amount of knowledge must be used as the basis and, if required, extensive investigations must be made. However, the following classification would be conceivable:

- (a) satellites
- (b) launch vehicles
- (c) aircrafts (possibly with the sub-class of helicopters)
- (d) ships (subdivided into submarine and surface ships)
- (e) surface vehicles (armoured and not armoured)
- (f) missiles (subdivided by type)
- (g) ground stations.

This list could also be extended by incorporating special limit values for equipment in computing centers, hospitals, and factories, for example.

#### 4. CONCLUSION

An examination was made as to whether it is more favourable to use a general EMC specification or system-oriented specifications for this purpose. The following solution is obtained: The test methods and the test philosophy should be uniform for all systems. MIL-STD 462 (+ 463) could represent a good basis. However, updating and expansion in various respects seem desirable. As far as the limit values are concerned, it becomes evident that the characteristics of the system themselves, their environment, and the systems in conjunction with which they must possibly function differ too greatly. Uniform limit values either solve the compatibility problems with an insufficient degree of probability or with too high expenditure. Establishing system-related limit values is considered the optimum solution; fixing limit values for certain system classes (e.g. satellites, ships, etc.) is regarded as a good practical solution.

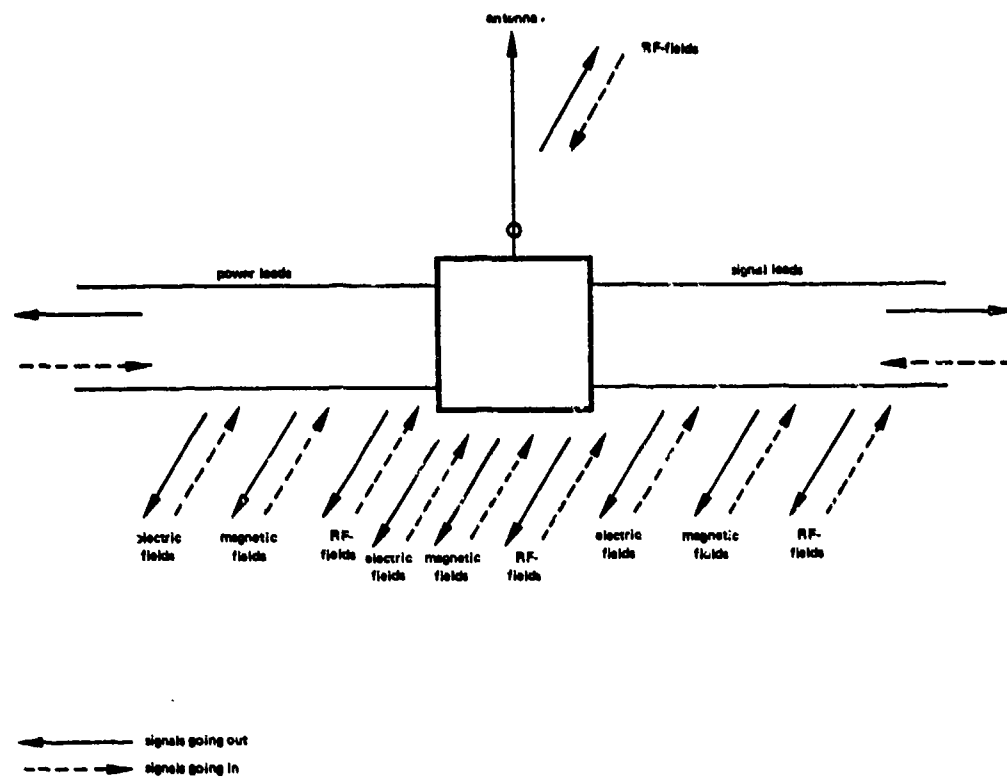


Fig. 1 Interference signal coupling

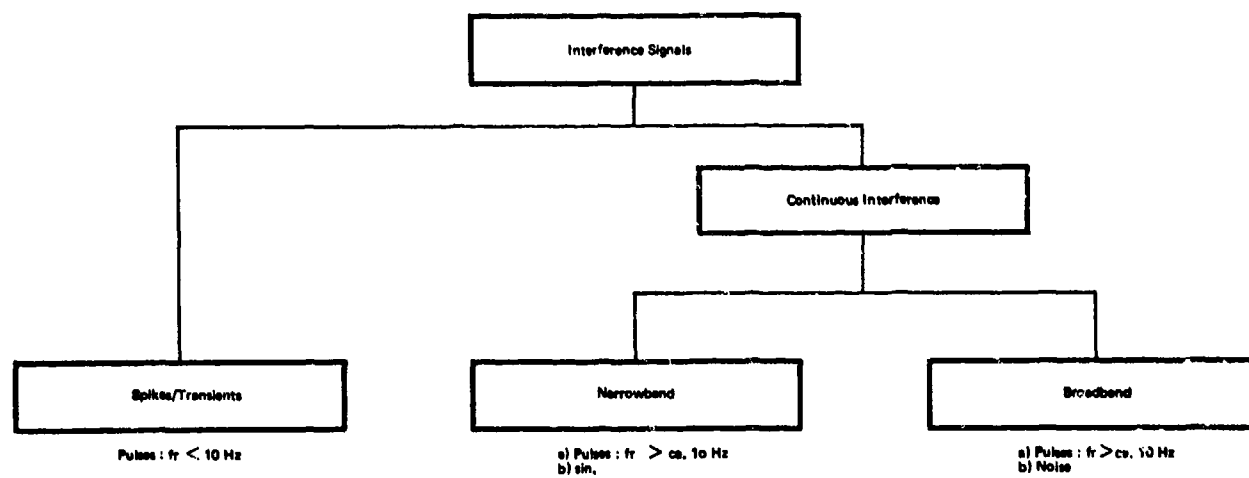


Fig. 2 Kinds of interference signals

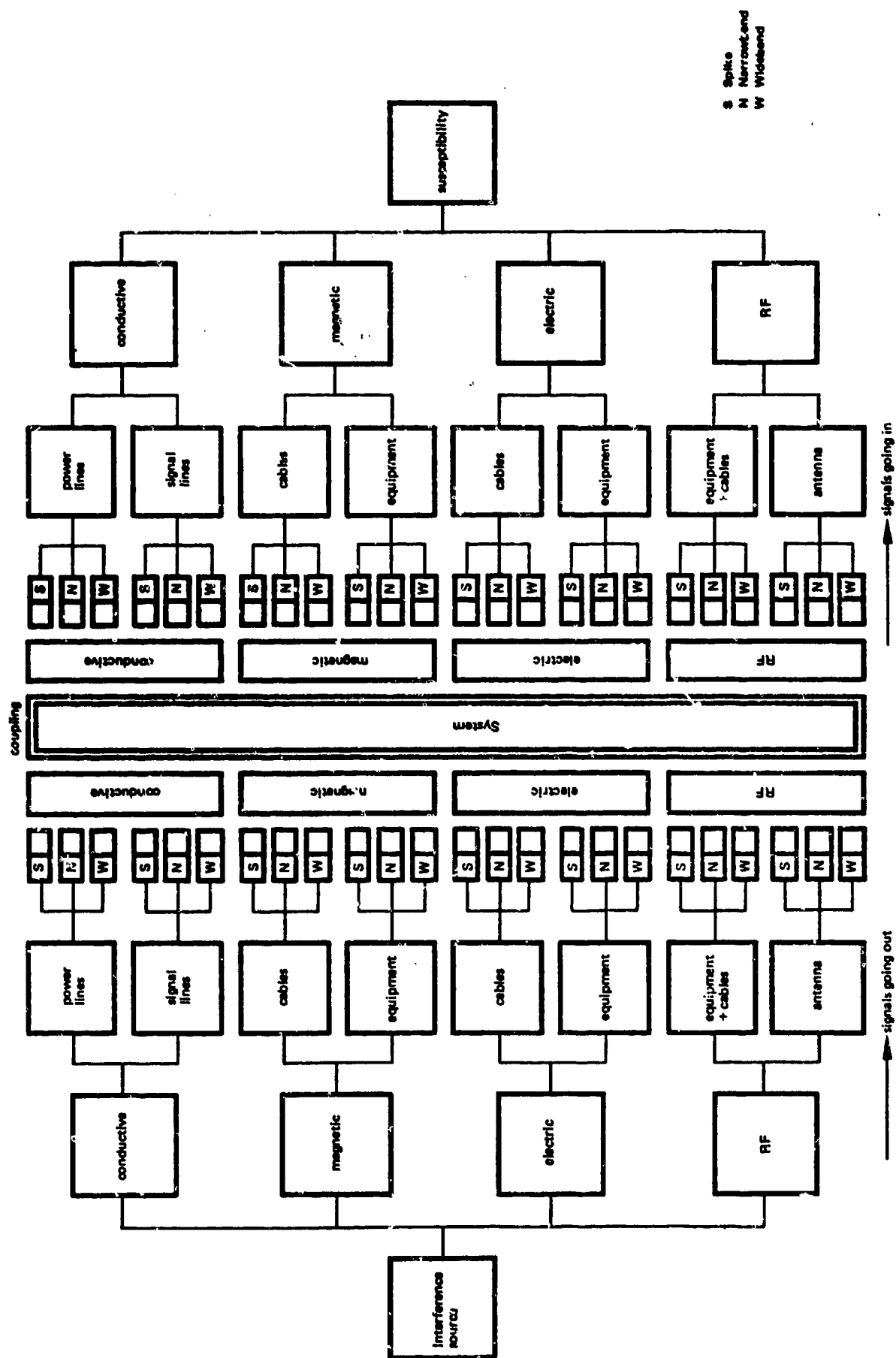


Fig. 3 Measurements to check EMC-characteristics

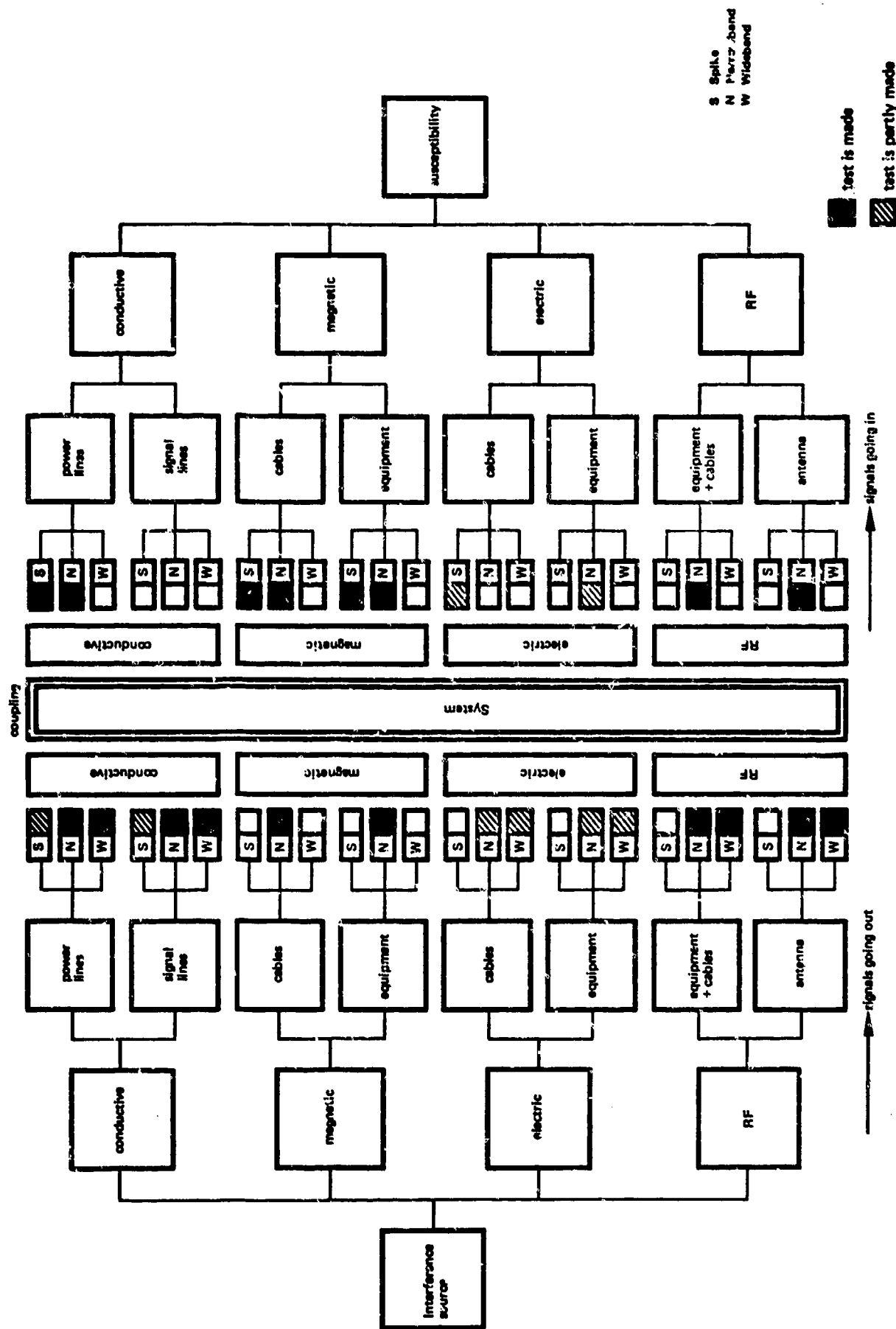


Fig. 4 EMC measurements of MIL-STD 462, Notice 2

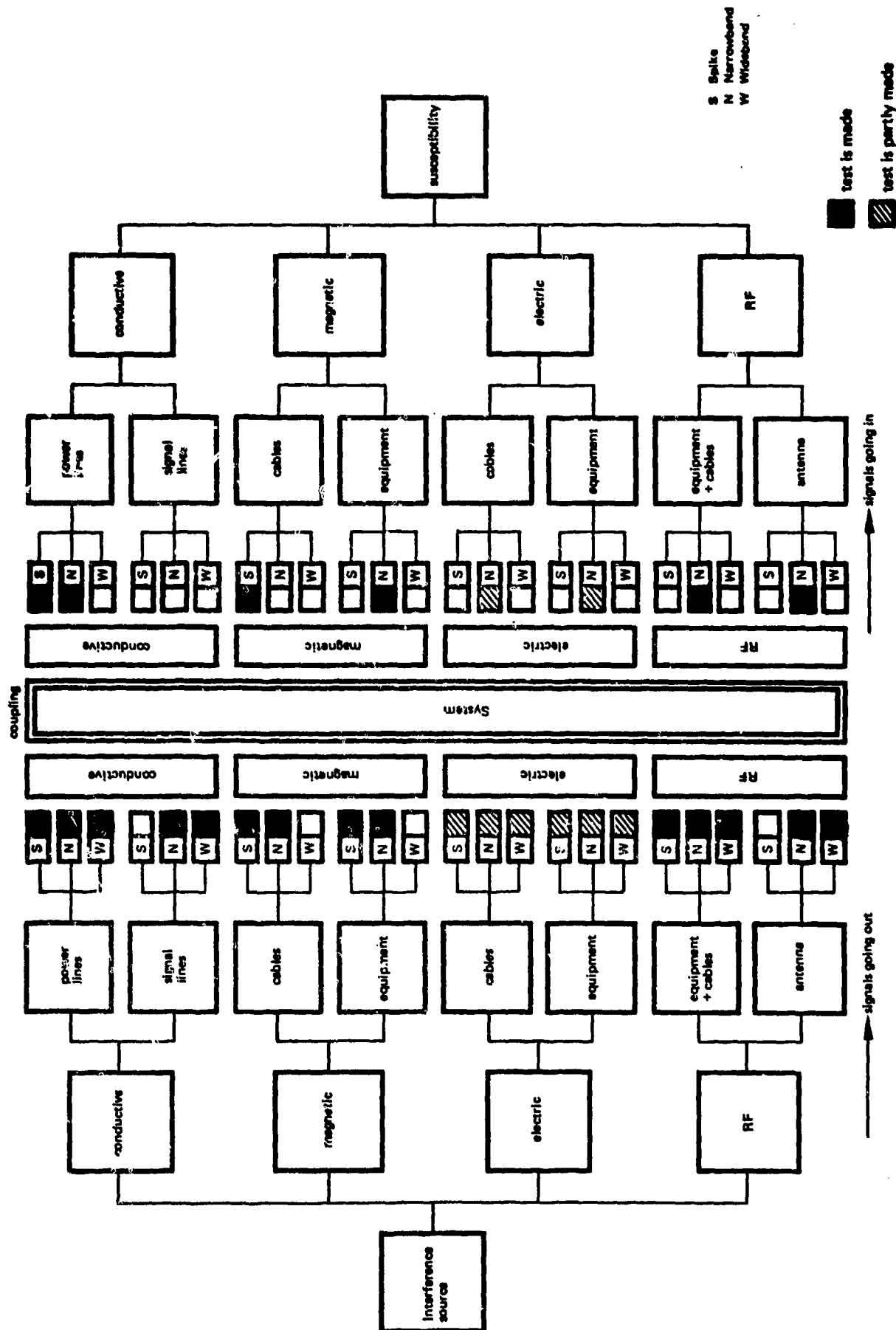


Fig. 5 EMC tests of MIL-STD 362, Notice 3

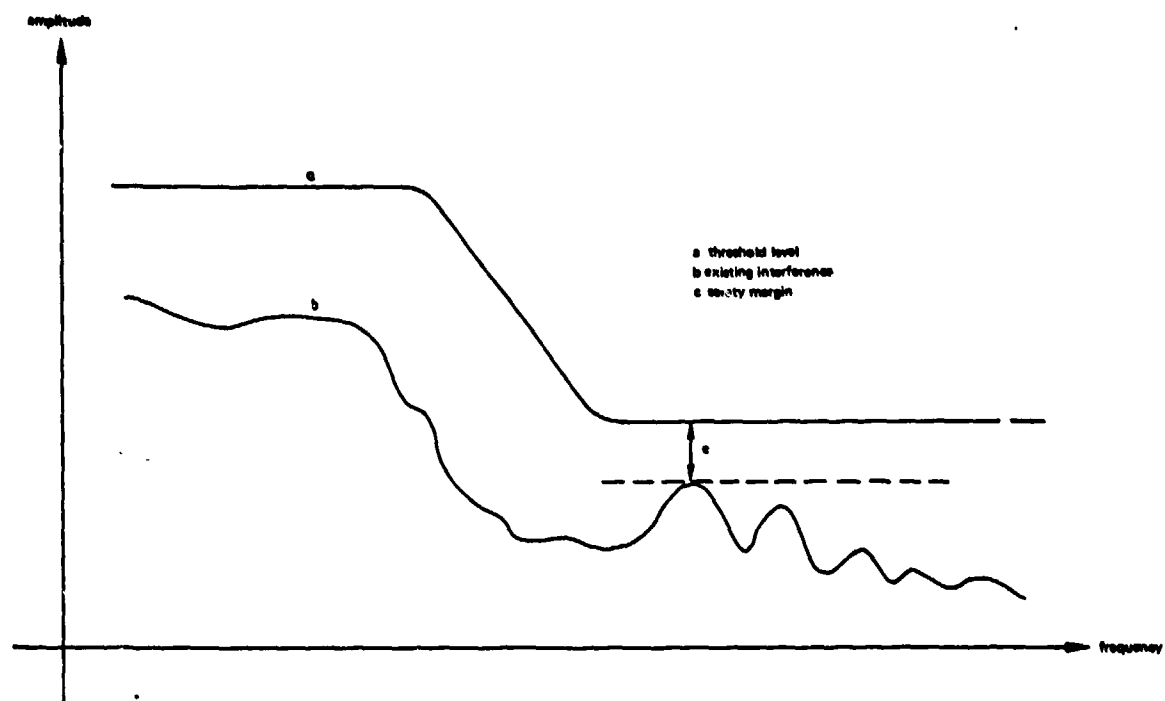


Fig. 6 Description of the safety margin

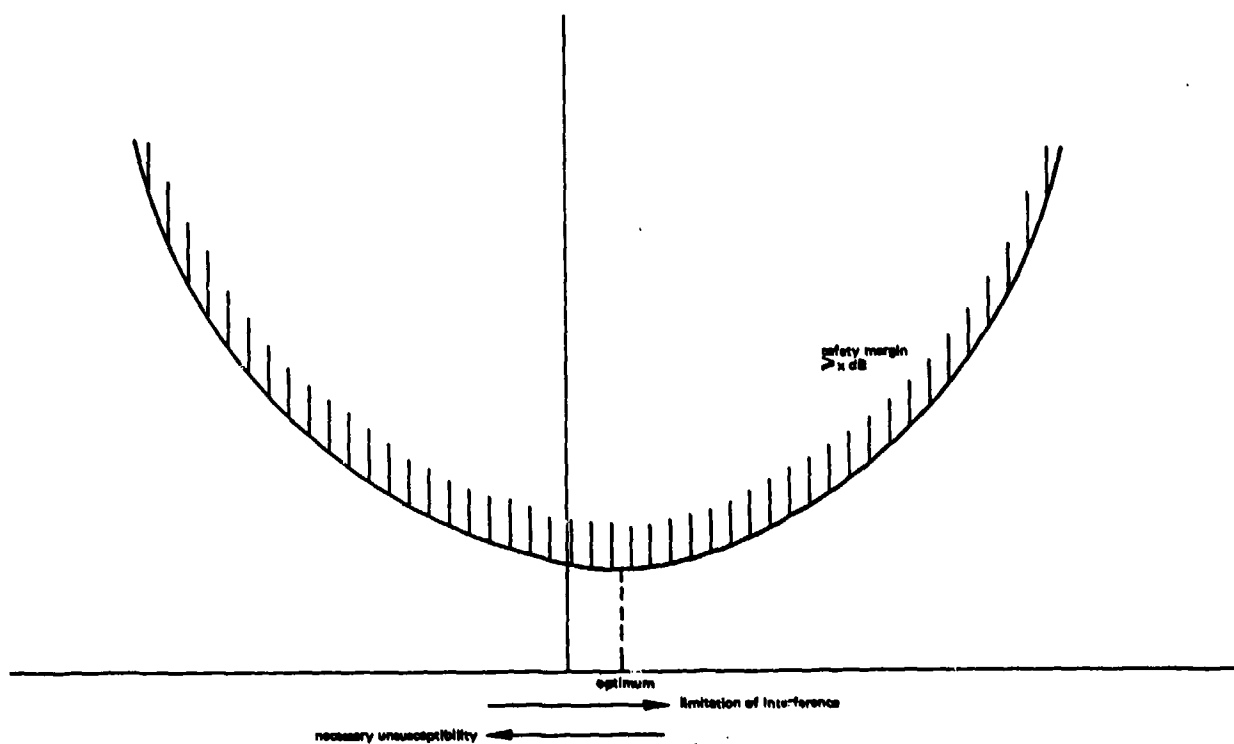


Fig. 7 Optimization of EMC-limits

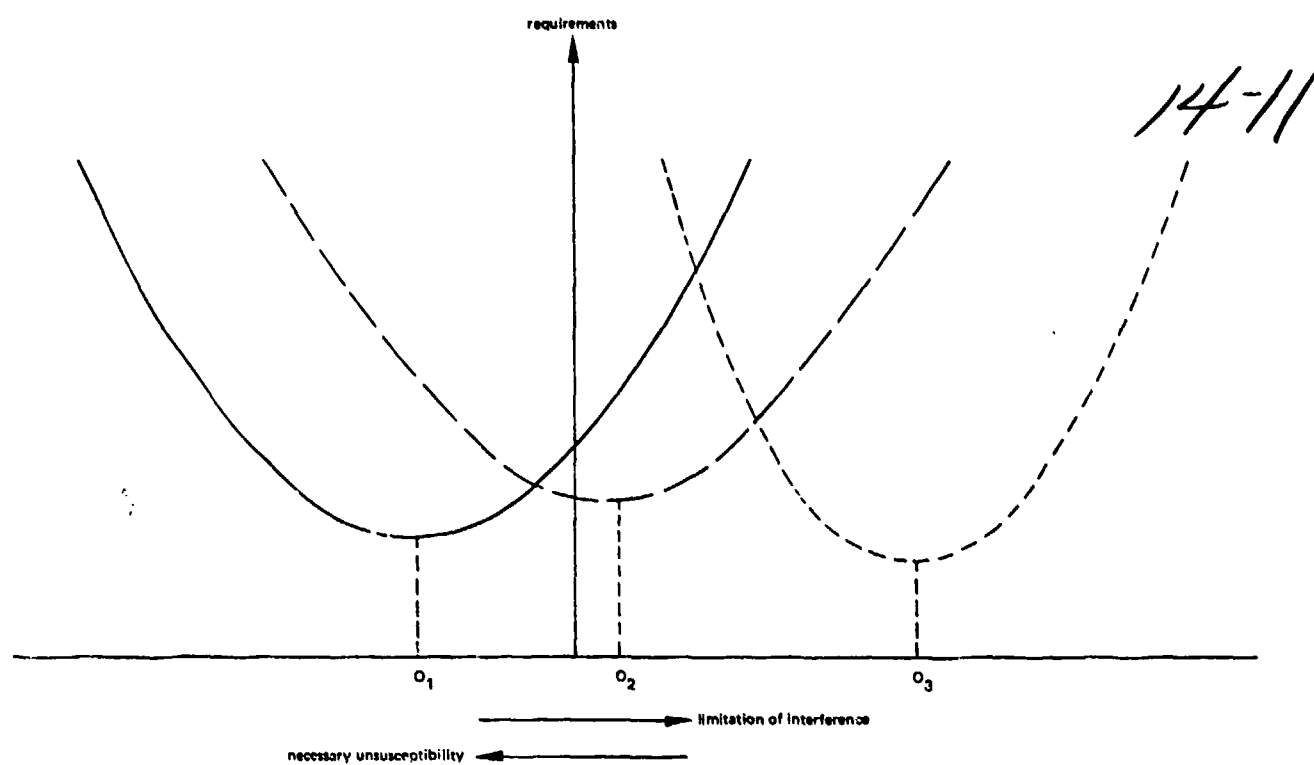


Fig. 8 Optimization of EMC-limits for different requirements

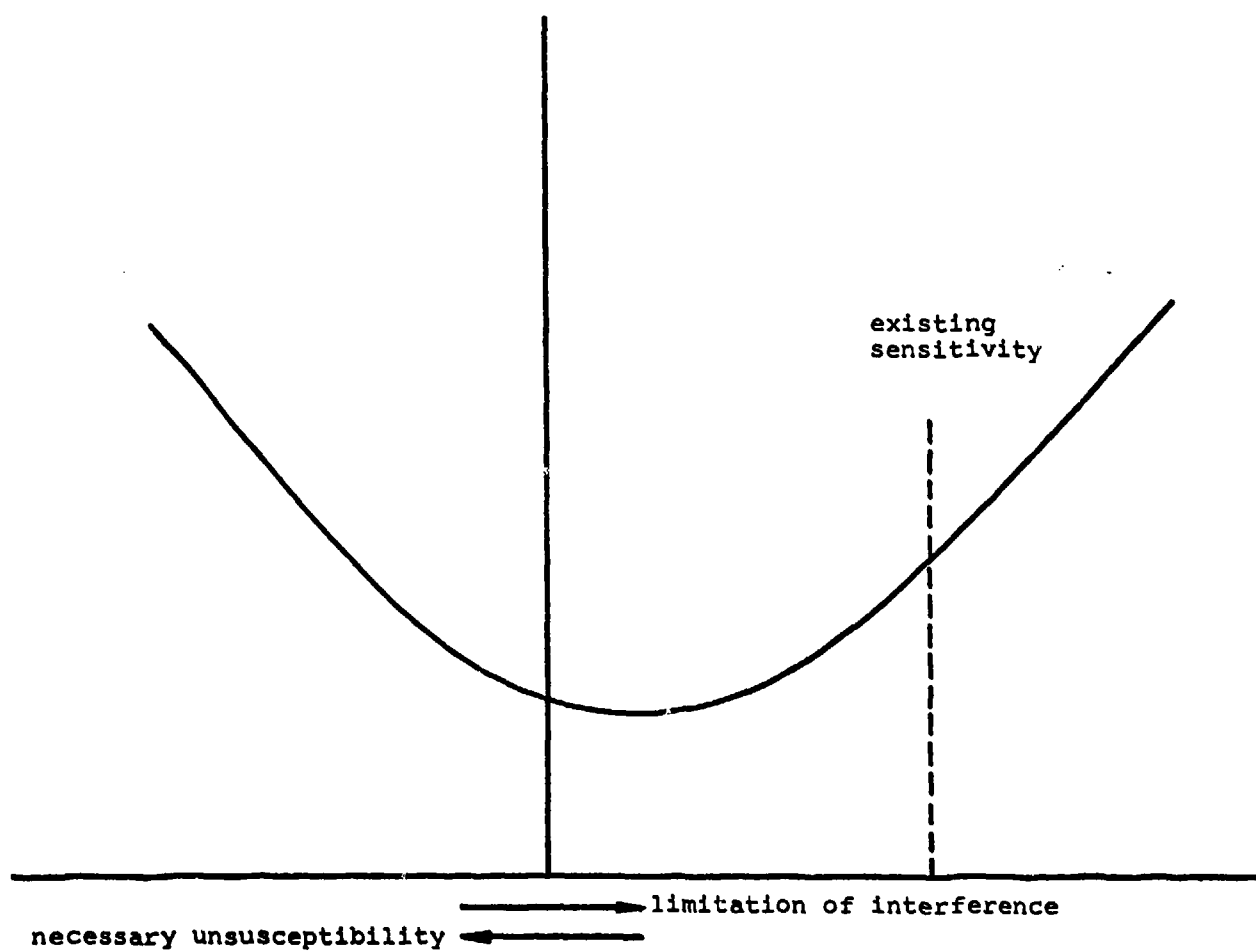


Fig. 9 Definition of limits in function of existing sensitivities or (interference) sources



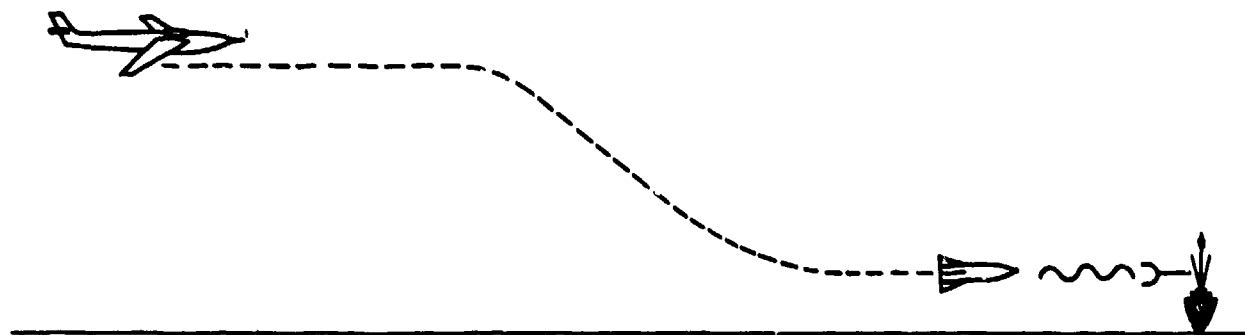


Fig. 10 Weapon system KORMORAN

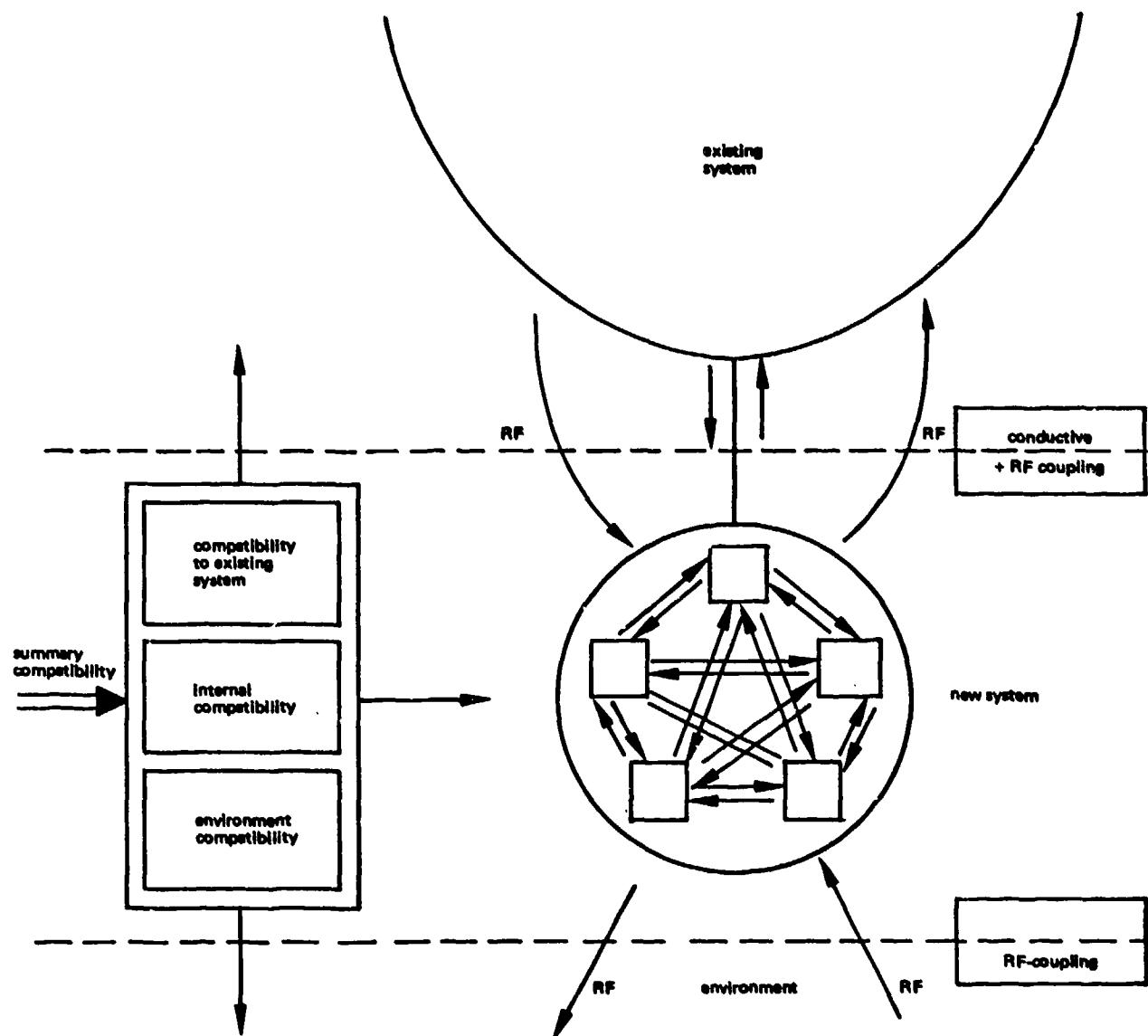


Fig. 11 Kinds of compatibility

## SPECIFICATIONS EMC

J. C. DELPECH

SNIAS- LABORATOIRE 621

31700 BLAGNAC - FRANCE

151

### I - SOMMAIRE

Il s'agit de comparer les différentes normes et spécifications EMC les plus connues à l'heure actuelle et particulièrement adaptées aux équipements avionables. La comparaison fera apparaître les points communs et les différences essentielles entre ces normes concernant les types d'essai envisagés, les bandes de fréquences, la sévérité, le mode opératoire et le matériel préconisé. On attirera également l'attention sur :

- 1°/ L'insuffisance des essais demandés par certaines normes lorsqu'il s'agit par exemple d'évaluer la susceptibilité des équipements numériques.
- 2°/ Les essais nouveaux demandés dans les normes les plus récentes.
- 3°/ Le manque de définition, les mauvais recoupements entre certaines limites qui ont été observés expérimentalement.
- 4°/ La supériorité de certaines normes quant au principe de la mesure et aux accessoires utilisés.

### II - NORMES et SPECIFICATIONS COMPAREES

- Norme américaine MIL-STD-461A/462 notices 3 et 4 du 9/2/71
- Recommandations américaines RTCA-DO-138 chapitres 10 à 13 et appendix A du 27/6/68.
- Norme française AIR-510-C du 15/2/63
- Norme anglaise 3G 100 documents 70/30510 et 70/30511 d'Octobre 1970.
- Projet italien UNAVIA-ISO/TC20/SC-1-82 de Mars 1973
- Spécifications avionneurs :
  - LOCKHEED - document n° 422.966 du 10/2/72
  - BOEING - document n° D6.16050 du 8/9/68
  - DOUGLAS - document E4I/WZZ 7000 du 9/2/68
  - AEROSPATIALE/AIRBUS - document n° 449.836/68- chapitres 19-22-23 de Mai à Juin 1971.

La spécification GENERAL ELECTRIC département réacteurs code n° 07482 du 26/8/69 est absolument identique à la spécification DOUGLAS. En ce qui concerne les essais aux transitoires de courte durée nous nous référons à la norme française AIR 2021/D. Aucun essai de susceptibilité aux parasites n'est prévu dans la norme AIR-510-C.

### III - BUT et CLASSIFICATION DES ESSAIS EMC

Le but de cet essai est de mesurer aussi bien le niveau de parasites émis par un équipement ou un système afin de s'assurer qu'il ne dépasse pas certaines limites, que de soumettre cet équipement à un niveau perturbateur donné afin de contrôler dans quelle mesure il est susceptible. Les parasites émis ou reçus par un système sont classés en deux grandes catégories : de conduction sur les câbles et de rayonnement.

### IV - ETUDE COMPARATIVE DES NORMES EMC

#### 1 - PARASITES EMIS PAR CONDUCTION

##### 1.1 - Sur les conducteurs de puissance

Par conducteurs de puissance on entend :

- les conducteurs d'alimentation (conducteurs d'entrée).
  - les conducteurs à la sortie des sources de puissance telles que : génératrices, alternateurs, convertisseurs, etc.
- Cette définition clairement donnée par BOEING et DOUGLAS est malheureusement omise dans les autres normes.

Le mode opératoire est donné planche 15 A essai 1-2-3 et les niveaux limites planches 15B-C-D

Il n'est pas conseillé d'utiliser le LISN habituellement recommandé par les normes, en dessous de 150 KHz, car la tension mesurée à sa sortie dépend de l'impédance de la source d'alimentation à la fréquence considérée. (voir planche 15Q). La norme MIL dans son essai CEO2 débutant à 10 KHz préconise un LISN particulier calculé pour des fréquences plus basses. A 0 Hz le transformateur de l'essai CEO1 de la norme MIL (essai 2) est en général plus sensible que la pince de la spécification UNAVIA (essai 3). Pour une source 115V/400Hz d'impédance interne 0,2 Ohm prévue pour débiter 50A, le condensateur de 10µF des essais 2 et 3 commence à jouer son rôle de filtrage en dessus de 80 KHz. Or dans les essais MIL et UNAVIA la fréquence la plus basse est de 30 Hz. Pour des fréquences comprises entre 30 Hz et 80 KHz il faut que la source soit absolument pure; s'il est possible d'obtenir une telle source en continu (MIL), le problème est beaucoup plus ardu en alternatif (UNAVIA). Le DO138 et les spécifications qui s'en inspirent (AEROSPATIALE-LOCKHEED) permettent d'utiliser la sortie du LISN entre 90 KHz et 30 MHz et la pince entre 15 KHz et 90 KHz, cette dernière bande de fréquences étant réservée aux équipements classés dans la catégorie la plus sévère (cat.Z). On constate par le calcul, à partir de l'impédance de transfert du LISN, et c'est confirmé par l'expérience, que le recoupement entre les limites avec pince et avec LISN est très mauvais. La courbe de variation de l'impédance de transfert du LISN en fonction

154 de la fréquence est donnée planche 15Q. En bande étroite à 90 KHz, un équipement tangent à la limite avec LISN est avec la pince hors norme de + 7 à + 13 dB.u.a suivant l'impédance de la source d'alimentation. En bande large à 90 KHz un équipement tangent à la limite LISN est nettement dans la norme de -12 à -18 dB.u.a avec la pince. De telles contradictions rendent parfois difficile la certification d'un équipement en catégorie 2.

#### 1.2 - Sur les conducteurs dans les câbles d'interconnexion

Par câbles d'interconnexion on entend tous les câbles autres que les câbles d'alimentation ou de génération de puissance, interconnectant entre eux des équipements ou des sous-systèmes. Se référer à la planche 15.A essai 4 et aux courbes planches 15 C et 15 D. Le capteur de mesure utilisé est toujours la pince ampèremétrique ; seule la norme 3G 100 permet d'utiliser également un LISN si ce dernier ne crée aucun trouble de fonctionnement dans les circuits d'interconnexion. Nous allons donner une interprétation résumée du mode opératoire préconisé par le document MIL 462 en nota au paragraphe 4 des essais CEO3 et CEO5 :

--- la sonde de courant ne doit contenir qu'un groupe de fils "aller" ou un groupe de fils "retour" dans la mesure évidemment où les retours ne se font pas directement par le plan de masse. Si le niveau mesuré est hors norme, il faut séparer le ou les fils fautifs et les sonder séparément. Pour cela il est nécessaire de prévoir une extension du toron d'interconnexion où chacun des conducteurs pourra être entouré par la pince y compris ceux des câbles torsadés et où le blindage, le cas échéant, aura été enlevé.

Les spécifications DOUGLAS et UNAVIA précisent bien que les conducteurs "aller" et "retour" ne doivent pas être sondés ensemble mais elles font une exception non justifiée pour les câbles torsadés. A partir du moment où on prévoit une "extension" il n'est plus question de déplacer la sonde pour rechercher le maximum dû à l'apparition d'ondes stationnaires. Le câble d'interconnexion doit avoir la longueur prévue sur avion et l'extension doit être placée du côté de l'équipement pouvant être perturbé, c'est-à-dire du côté opposé à l'équipement perturbateur essayé.

Le document D0138, les spécifications AEROSPATIALE et LOCKHEED qui s'en inspirent, la norme 3G 100 et la spécification BOEING ne sont pas suffisamment explicites sur le mode opératoire. Sur le schéma de montage du D0138 on représente une pince entourant la totalité du câble d'interconnexion. L'expérimentateur non averti va croire que la pince doit entourer aussi bien les conducteurs "aller" que les conducteurs "retour" ; il va mesurer ainsi le champ magnétique au voisinage du toron, ce dernier dépendant de la somme vectorielle des courants "aller" et "retour", de l'efficacité du torsadage, du blindage magnétique, etc.. Or le but de la manipulation est primo d'isoler les fils d'interconnexion de l'équipement essayé pouvant véhiculer des courants parasites élevés susceptibles de perturber l'équipement connecté et secondo de mesurer les courants dans chacun de ces fils.

D'autre part, la norme MIL précise que si les deux équipements interconnectés sont fournis par le même constructeur comme faisant partie d'un même système l'essai est inutile. En effet on suppose que l'essai de bon fonctionnement du système a été effectué chez le fournisseur ou à la réception chez le client et qu'il s'est avéré positif. Si les équipements interconnectés appartiennent à des constructeurs différents, la mesure des courants parasites sur les câbles d'interconnexion est recommandée, surtout si l'essai de bon fonctionnement du système complet est prévu postérieurement. Dans ce cas l'équipement est livré seul et essayé seul, les ordres sur ces entrées et les charges sur ces sorties étant simulés. Aucune autre norme que la MIL ne fait intervenir cette notion, l'essai étant obligatoire ou seulement lié à une catégorie d'équipements.

#### 2 - PARASITES EMIS PAR RAYONNEMENT

Se référer à la planche 15E pour le mode opératoire et aux planches 15F et 15G si on veut comparer les niveaux limites du champ électrique.

##### 2.1 - Composante continue du champ magnétique - essai 1

Le champ magnétique continu peut perturber les vannes de flux ou le compas de secours d'un avion. Cet essai ne figure pas toujours dans les documents EMC (MIL 461-3G 100- AIR 510/C-BOEING) ce qui ne veut pas dire nécessairement qu'on omet de le faire ; on peut le trouver dans un chapitre ou dans un document séparé intitulé par exemple "essai d'interférence magnétique".

##### 2.2 - Champ magnétique audio et radio-fréquences - essai 2

Les gammes de fréquences, les distances, la boucle ou la bobine de mesure étant différentes on ne peut comparer l'essai RE01-MIL et celui du D0138.

##### 2.3 - Champ électrique radio-fréquences - essai 3

###### 2.3.1 - Essai du type RE02 de la norme MIL 461/462

Les limites étant exprimées en unité de champ électrique, les antennes ne sont pas à priori imposées mais plutôt conseillées. Si les gammes de fréquences de deux antennes différentes se recouvrent on peut aussi bien utiliser l'une que l'autre dans la bande de recouvrement.

Dans la gamme 30 MHz à 2000 MHz on conseille l'emploi d'antennes biconiques (20 à 200 MHz), coniques-log-spirales (200 à 1000 MHz) ou cornets à double arête (200 à 2000 MHz). Ce sont des antennes large bande modernes qui ne demandent aucune intervention manuelle d'adaptation et qui facilitent de ce fait les enregistrements automatiques de niveau. L'antenne biconique a une longueur de l'ordre de 1,4 m rendant son utilisation commode dans une cage de Faraday.

#### 2.3.2 - Essai préconisé par la norme AIR 510C

La limite de large bande est donnée planche 15F. La limite en bande étroite est curieusement exprimée en  $\mu V/m/KHz$ , il s'agit certainement d'une erreur.

#### 2.3.3 - Essai du type préconisé par le DO138

Les limites étant exprimées en tension aux bornes de l'antenne à vide (antenne induite) le type d'antenne suivant la gamme de fréquences est imposé. Pour des fréquences comprises entre 25 MHz et 1000 MHz l'antenne est un dipôle accordé sur 35 MHz entre 25 et 35 MHz et résonnant en demi-onde aux fréquences supérieures. Le dipôle est d'un emploi mal commode ; il demande en effet de nombreuses interventions manuelles d'accord au cours d'un balayage en fréquence et sa longueur est importante dans la partie inférieure de sa gamme d'utilisation. A 35 MHz on doit pouvoir disposer d'une cage de FARADAY de 5,5 m de longueur.

### 3 - TOLERANCES COMPLEMENTAIRES A L'EMISSION DE PARASITES

Se référer à la planche 15 H.

Ces tolérances concernent l'émission de parasites lors de la manipulation d'un interrupteur. Les documents MIL et UNAVIA ne considèrent que le cas où la perturbation est émise par conduction. DOUGLAS et LOCKHEED n'admettent pas de tolérance ; pourtant on a constaté expérimentalement qu'une tolérance complémentaire de 20 dB au dessus des limites normales était souvent insuffisante même pour un appareil satisfaisant largement aux exigences de ces limites.

#### 4 - SUSCEPTIBILITE AUX PARASITES DE CONDUCTION

##### 4.1 - Signaux injectés dans les câbles de puissance

###### 4.1.1 - Signaux sinusoïdaux dans la gamme 30 Hz à 150 KHz - planche 15 I

Les niveaux les plus sévères sont 3 V eff sur le 28 V.DC et 5 % de la tension nominale à 400 Hz aux bornes de l'équipement. Les documents MIL et UNAVIA limitent la puissance injectée à 50 W sous une impédance de 50  $\Omega$  pour les équipements consommant fortement.

###### 4.1.2 - Porteuse sinusoïdale modulée ou non dans la gamme 15 KHz à 400 MHz - planche 15 J

Ces essais, très divers sont difficilement comparables. Les caractéristiques de la modulation sont importantes ; à ce sujet la norme MIL est la plus complète et la plus explicite. Pour les équipements numériques très sensibles aux perturbations à front raide il est conseillé de moduler la porteuse en impulsions ou en signaux carrés dont la largeur et la fréquence de répétition sont égales à celles des signaux logiques qu'ils génèrent. La modulation d'amplitude du DO138 est à ce sujet insuffisante.

###### 4.1.3 - Subtransitoires - planche 15 K

L'essai aux transitoires de courte durée ( $t < 500 \mu s$ ) sur les câbles de puissance ne fait pas toujours partie des documents EMC. Il est souvent classé dans un chapitre à part concernant les essais à tous les types de transitoires que l'on peut trouver sur le réseau de bord ; c'est le cas du DO138, de la 3G 100 et des spécifications AIRBUS et CONCORDE de l'AEROSPATIALE. La norme française AIR 2021/D concernant les caractéristiques générales du réseau électrique de bord donne les limites en tension d'un transitoire rectangulaire fictif en fonction de sa durée. La méthode de conversion d'un transitoire réel en transitoire rectangulaire équivalent est également explicitée. A partir de ces indications la norme laisse le soin aux spécifications particulières de préciser les conditions d'application, notamment la durée et la forme du transitoire. La valeur crête du subtransitoire de la norme MIL est limité en tension mais pas en puissance crête. Dans la spécification AEROSPATIALE cette puissance est limitée du fait que la tension est réglée à vide sur un générateur d'impédance interne 50  $\Omega$  ; plus l'équipement consomme de la puissance, plus la tension crête du subtransitoire à ses bornes est faible, ce qui paraît tout à fait logique. Les auteurs de la spécification UNAVIA qui s'inspirent de la norme MIL ont bien compris qu'il fallait limiter la puissance du générateur.

##### 4.2 - Signaux injectés dans les câbles d'interconnexion - planche 15 L

Le mode opératoire préconisé par le DO 138 n'est pas suffisamment explicite et le schéma de montage représente une pince entourant la totalité d'un toron d'interconnexion. Cette méthode ne serait valable que si le toron était constitué seulement de conducteurs "aller", les "retours" se faisant directement par le plan de masse. Si on entoure à la fois un fil "aller" et un fil "retour" d'un même circuit, le champ magnétique produit par la pince ne traverse pas la boucle constituée par les deux fils et leurs impédances terminales ; on n'induit aucun courant si la boucle est bien isolée du plan de masse. Il serait donc nécessaire de préciser que la pince ne doit entourer qu'un groupe de fils "aller" ou un groupe de fils "retour" des différents circuits ;

si on constate que l'équipement est susceptible on doit isoler le ou les fils fautifs et les sonder séparément.

Comme on l'a déjà dit au paragraphe 1.2, ce type d'essai est inutile si les deux équipements interconnectés sont fournis par le même constructeur comme faisant partie d'un même système.

Aucune norme ne spécifie qu'il faut envoyer des subtransitoires sur les câbles d'interconnexion. Or toutes les sorties d'un équipement connectées à des charges selfiques (bobines de contacteurs, de relais, d'électrovanne, etc...) peuvent être soumises à des subtransitoires aussi importants que ceux qu'on peut trouver sur le réseau. En général ces subtransitoires ne sont pas étouffés à la source sauf dans les rares cas où leur valeur crête peut dépasser les limites imposées par la spécification sur la génération électrique de bord ; auquel cas on se contente de limiter cette valeur crête par des diodes fonctionnant en Zener ou des "Transsorb". Les sorties d'équipements commutant statiquement des charges selfiques à partir de semi-conducteurs ou de transistors et non pas à partir de contacts mécaniques reliés au réseau de bord devraient être classés dans une catégorie à part et soumis aux essais de subtransitoires.

## 5 - SUSCEPTIBILITE AUX CHAMPS RAYONNES

### 5.1 - Susceptibilité du boîtier de l'équipement à un champ magnétique - planche 15 M

Seules les spécifications DOUGLAS et UNAVIA soumettent le boîtier de l'équipement à un champ magnétique impulsionnel. Ce type d'essai devrait être envisagé systématiquement pour les équipements numériques.

### 5.2 - Susceptibilité du boîtier de l'équipement et de tous ses câbles à un champ électrique radio-fréquences planche 15 N

#### 5.2.1 - Essais du type préconisé par la norme MIL 461/462.

Les niveaux sont exprimés en unité de champ électrique soit en V/m. Peu importe le type d'antenne utilisé pourvu que l'équipement soit placé dans une zone où on a préalablement mesuré et ajusté le champ à la valeur demandée. De ce fait on peut utiliser des antennes ou des lignes ayant un très bon coefficient de transmission (TAF) compris entre + 12 dB et 0 dB, à des distances de l'ordre de quelques dizaines de centimètres à 1 mètre. Ces antennes du type: ligne à bande large, cornet à arête longitudinale, ligne à plaques parallèles, filaire dans une cage de Faraday (hauteur inférieure à 2,3 m) permettent d'obtenir un champ relativement élevé de 10 V/m à partir d'un générateur de signaux de puissance inférieure à 2 W. Les niveaux "Sheltered" de la norme MIL sont encore plus élevés que les niveaux non "sheltered" figurant sur la planche 15 N et peuvent atteindre 50 V/m entre 30 MHz et 2000 MHz.

#### 5.2.2 - Essais du type préconisé par le DO138

Les niveaux sont exprimés en tension aux bornes du générateur soit à vide, soit aux bornes de l'antenne, soit aux bornes d'une résistance de 50Ω. Le type d'antenne et sa distance par rapport à l'équipement sont imposés. Entre 35 MHz et 1000 MHz on doit utiliser une antenne dipole accordable très peu commode (se référer au paragraphe 2.3.3). Si on compare les limites de LOCKHEED et celles de BOEING converties en dB.μV aux bornes d'un dipole résonnant d'impédance 73Ω on constate qu'elles sont sensiblement identiques dans la plage 35 MHz à 1000 MHz ; elles sont nettement plus élevées que celles du DO138 et de la 3G 100 surtout entre 100 et 150 MHz. Par exemple à 130 MHz le niveau limite du DO 138 est de 46 dB inférieur à celui de LOCKHEED ce qui est conséquent.

Le TAF d'un dipole résonnant en demi-onde est de l'ordre de + 8 dB à un pied à une fréquence supérieure à 185 MHz où on considère que l'antenne est à une distance de champ lointain. Entre 185 MHz et 1000 MHz la spécification LOCKHEED prescrit un niveau de 114 dB.μV soit un champ de  $114+8 = 122 \text{ dB.}\mu\text{V/m} = 1,35 \text{ V/m}$ . Dans cette gamme la norme MIL prescrit un champ minimum de 10 V/m (non sheltered) et le DO 138 un champ calculé maximum de 0,1 V/m aux alentours de 1000 MHz.

Pour les équipements numériques, une modulation en impulsions ou en signaux carrés s'impose alors que dans les spécifications qui s'inspirent du DO138, seule une modulation en amplitude est prévue.

### 5.3 - Susceptibilité des câbles d'interconnexion aux effets de couplage - planches 15.O et 15P

Un fil inducteur parcouru par un signal perturbateur longe le toron d'interconnexion on l'entoure avec un pas donné sur une longueur minimum imposée. Il est préférable d'enrouler le fil inducteur sur le toron si son diamètre est assez important car tous les conducteurs intérieurs seront également influencés par le champ. Le pas d'une spire doit être grand devant le diamètre du toron si on veut un couplage inductif voisin du couplage maximum. A la limite, si le fil inducteur était enroulé à spires jointives, le champ magnétique serait parallèle aux conducteurs du toron et le couplage serait nul. Considérons les trois types de signaux envoyés sur le fil conducteur :

#### 1°/Subtransitoires normalisés

La spécification DOUGLAS est la plus sévère. La tension crête étant réglée à 200 V pratiquement à vide, le subtransitoire est envoyé sur le fil inducteur sans résistance limitatrice. L'impédance interne du générateur

étant très faible, le courant est limité essentiellement par la réactance du fil inducteur pour la fréquence fondamentale du subtransitoire. La norme MIL limite la variation du front de courant à 10 A en 0,5µs, le DO 138 à 5 A en 1µs, l'AEROSPATIALE à 12 A en 0,5µs pour une longueur de couplage de 10 m (au lieu de 1,2 à 1,8 m pour les autres normes).

### 2°/ Signaux sinusoïdaux 400 Hz

A 400 Hz le produit du courant par la longueur de couplage est de 200 Axm (650 Ax Ft) pour l'AEROSPATIALE, de 200 A xFt pour BOEING, de 100 A xFt pour LOCKHEED, de 66 A xFt pour UNAVIA (à 5cm) et de 60 A xFt pour DOUGLAS.

Le produit de la tension appliquée au fil inducteur à vide ( $I=0$ ) par la longueur de couplage est de 12000 V eff x Ft pour BOEING et 6000 V eff xFt pour LOCKHEED.

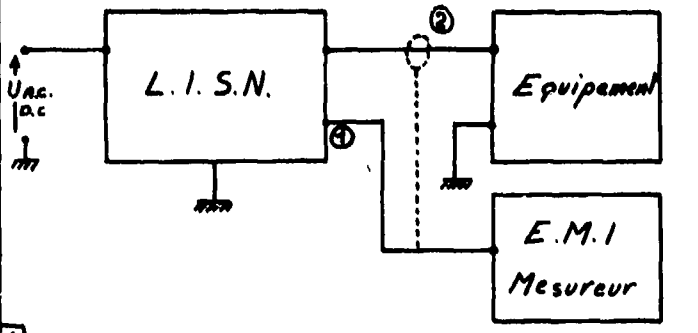
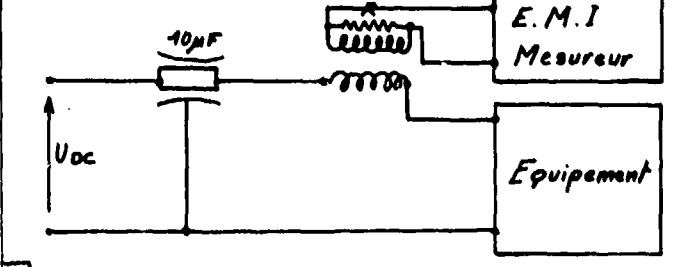
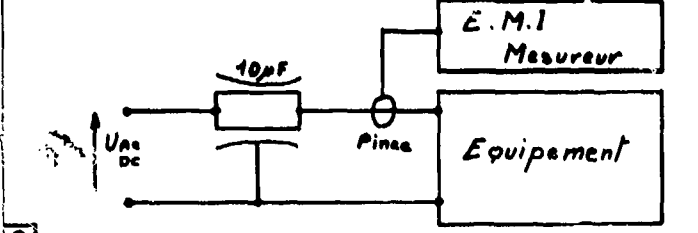
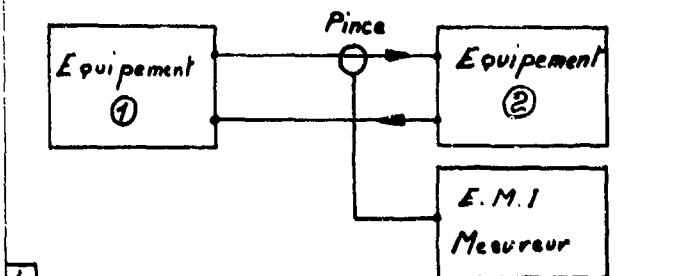
Si l'équipement est alimenté en 400 Hz il est recommandé de provoquer un phénomène de battement entre cette fréquence d'alimentation et la fréquence du signal qui parcourt le fil inducteur, ce qui est proposé par BOEING et LOCKHEED. Cette dernière spécification a également choisi comme fréquence d'essai les harmoniques du 400 Hz de rang 3, 6 et 12.

### 3°/ Extra courant de rupt. d'une bobine de relais

Seuls BOEING et LOCKHEED prescrivent systématiquement cet essai. On doit utiliser le relais et l'interrupteur définis par leur numéro de code au standard militaire américain, ou leurs équivalents. Pour les deux spécifications considérées, cette forme de subtransitoire remplace le subtransitoire normalisé vu au 1°/.

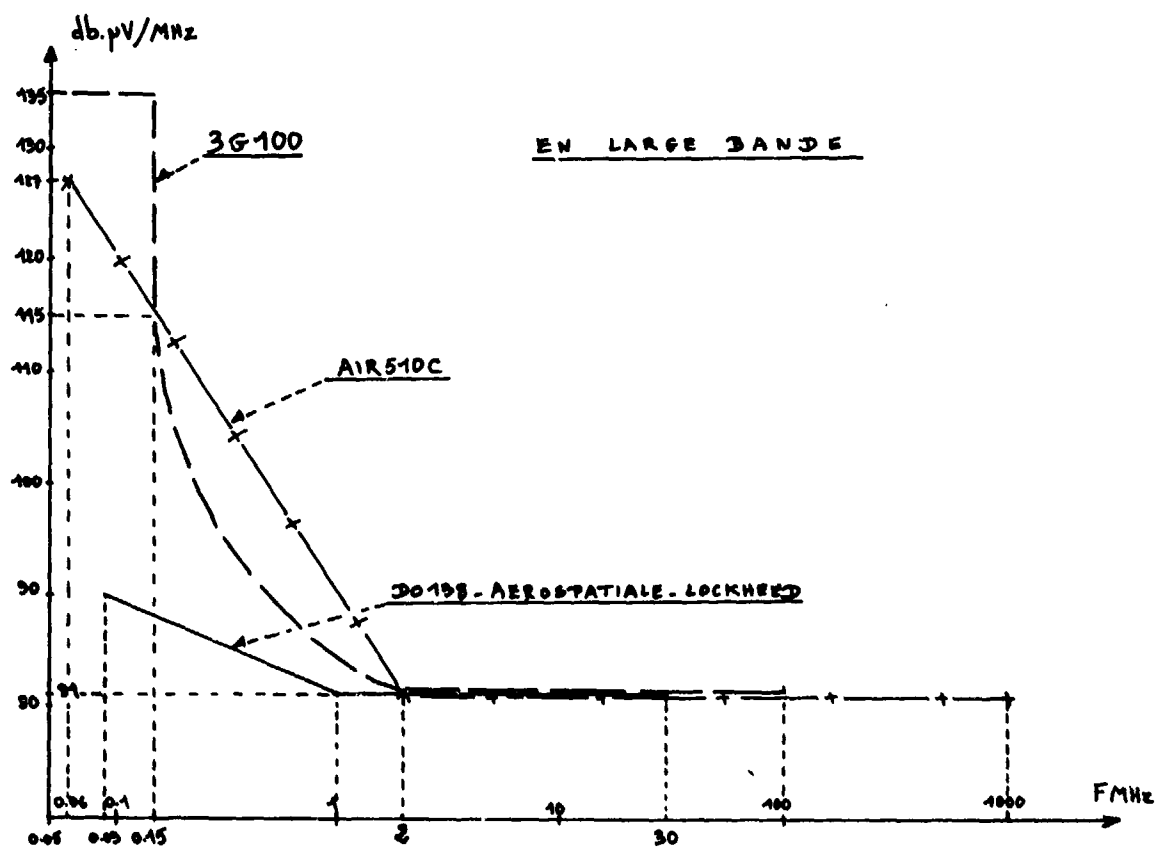
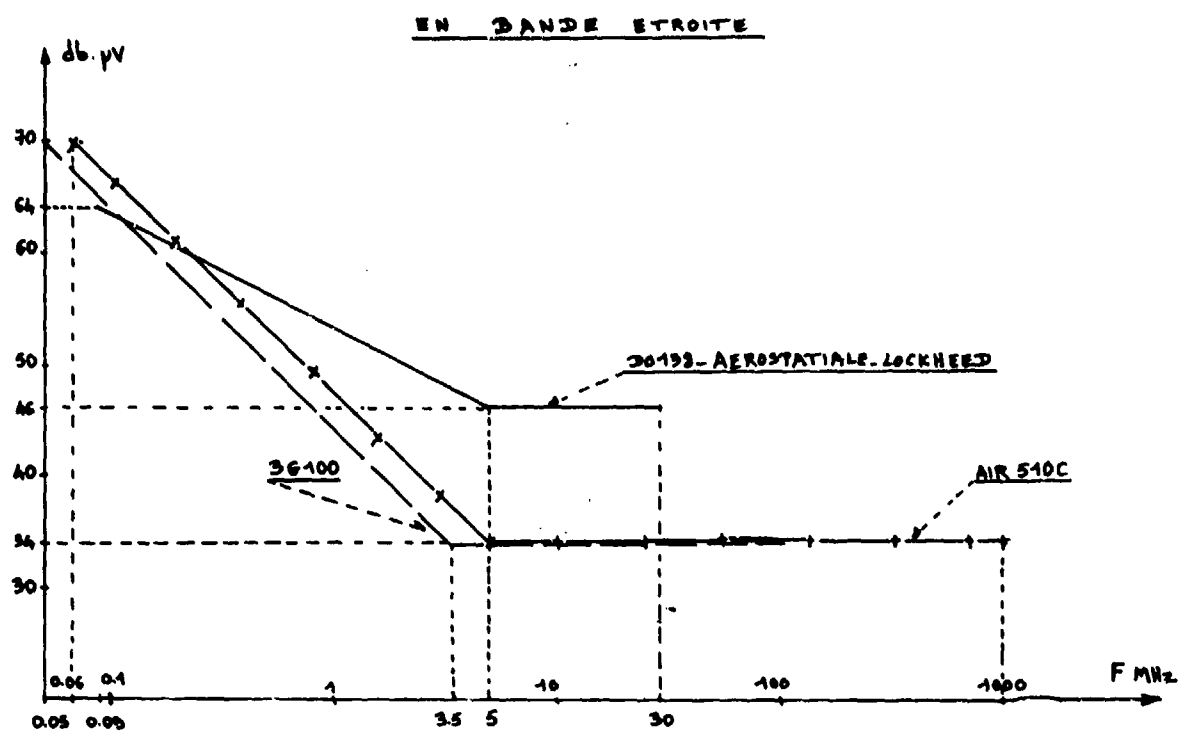
A l'AEROSPATIALE ce type de perturbation tend également à remplacer le subtransitoire de l'essai de la planche 15.0. Elle est produite par la bobine d'un contacteur triphasé de 200 A alimentée en 28 V ; son amplitude est de 400 V CC pendant 600µs et elle se termine par une onde inverse de -700 V C de largeur 15 µs à la base.

Cet essai est réaliste et devrait être fait plus systématiquement car le toron d'interconnexion d'un équipement peut côtoyer sur plusieurs mètres le câble d'alimentation de la bobine d'un relais ou d'un contacteur. Un tel extra-courant de rupture est beaucoup plus énergétique que le subtransitoire normalisé et son spectre s'étend plus haut en fréquences. Au début du train d'oscillations la fréquence peut atteindre quelques MHz ce qui correspond à des fronts de montée de plusieurs centaines de volts en moins de 200 ns. Il est particulièrement recommandé de faire cet essai sur les lignes de transmission de données des équipements numériques. Toutefois il est difficile de reproduire de manière identique de tels trains d'oscillations dans différents Laboratoires d'essais SMC même si on utilise des relais et des interrupteurs normalisés. La durée et la valeur crête à crête de la perturbation telles qu'elles sont données dans les spécifications BOEING et LOCKHEED ne suffisent pas à la caractériser. En général la fréquence des oscillations de forme sensiblement triangulaire diminue avec le temps et leur amplitude augmente. Il faudrait définir un train d'oscillations standard qu'on essaierait de reproduire avec un générateur.

Câbles	Mode opératoire	Référence Norme
de puissance	 <p>1</p>	<p>3G 100-AIR 510/C-sortie LIGN seulement en (1).  MIL 461 : CE 02 sur AC de 10KHz à 50 KHz et CE 04 sur AC/DC de 50 KHz à 50 MHz- Pince en (2) seulement.</p> <p>DO 138 -AEROSPATIALE et LOCKHEED : Sortie LIGN en (1) si <math>f \geq 90</math> KHz et pince en (2) si <math>f &lt; 90</math> KHz.</p>
	 <p>2</p>	<p>MIL 461/462 -CE 01 de 30 Hz à 50 KHz sur DC seulement</p>
	 <p>3</p>	<p>UNAVIA - (30 Hz ou 20 KHz à 100 MHz)  DOUGLAS (15 KHz à 400 MHz)  BOEING (50 KHz ou 150 KHz à 25 MHz)  (1)</p>
d'inter-connexion	 <p>4</p>	<p>Toutes les normes et spécifications (CE 03 et CE 05 de MIL 461 notamment) excepté AIR 510 C</p>

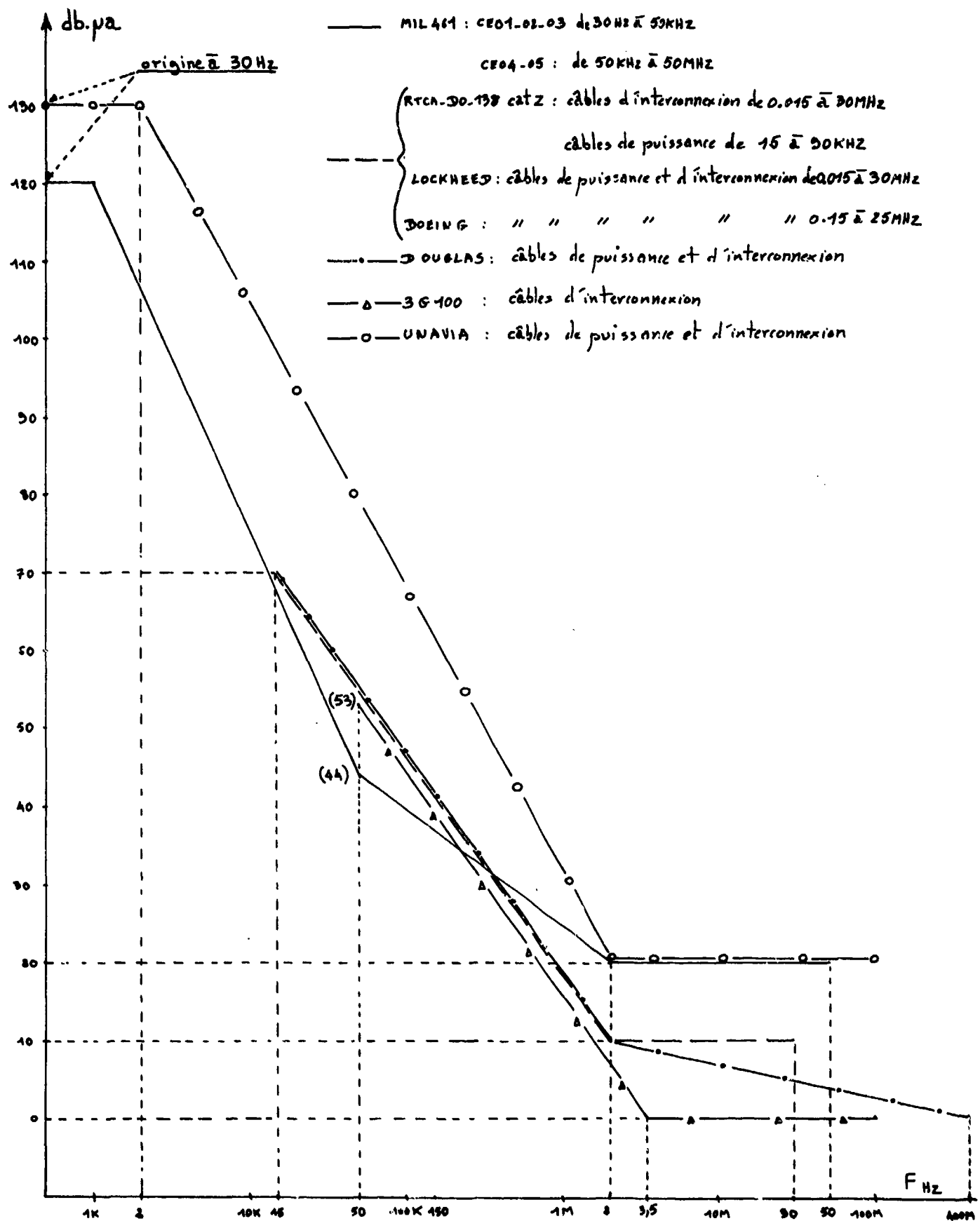
(1) en Bande large on ne descend jamais en dessous de 15 KHz.

Pl.15 A Mode opératoire pour les mesures de parasites émis par conduction

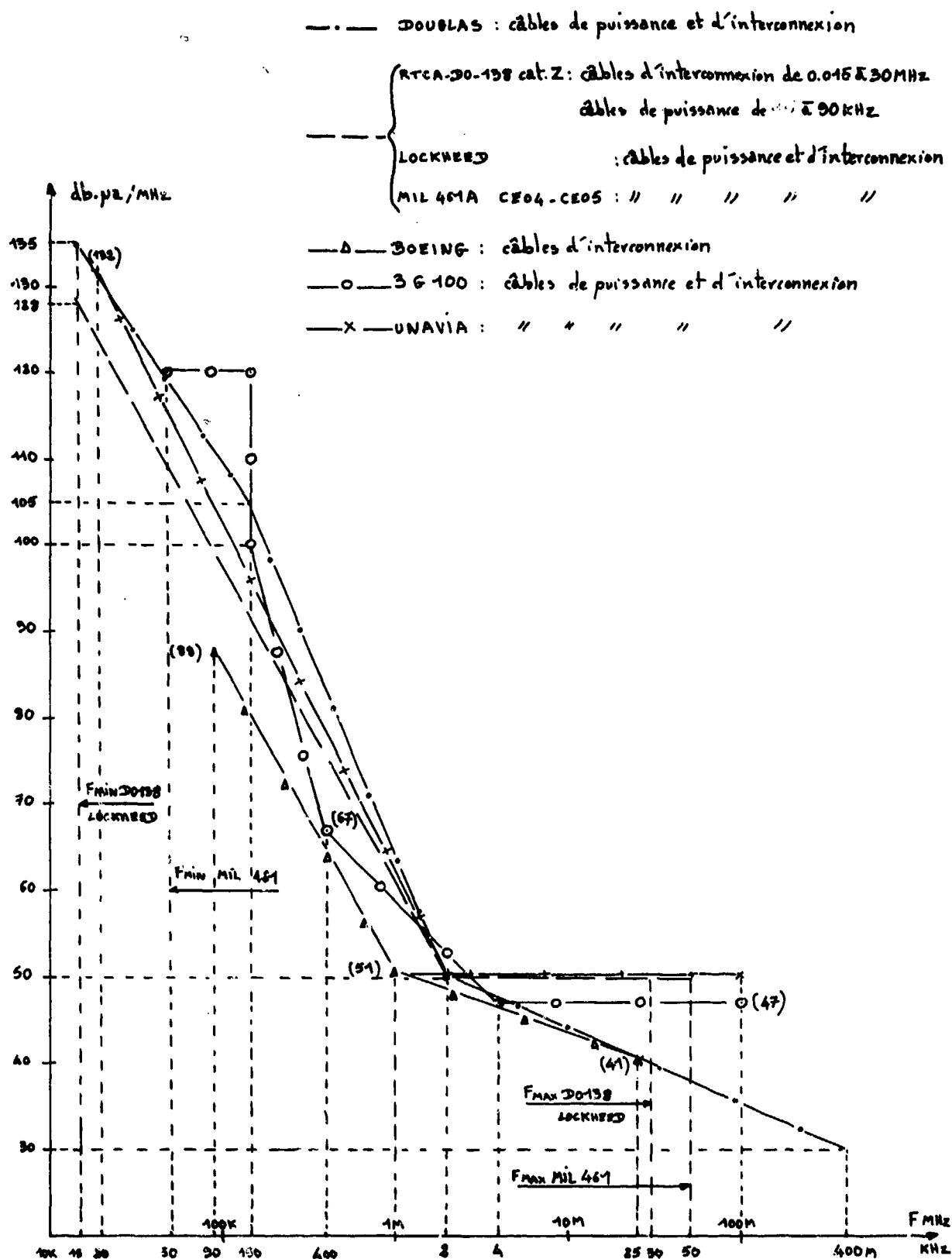


Pl.15 B Niveaux limites de parasites émis par conduction avec LISN

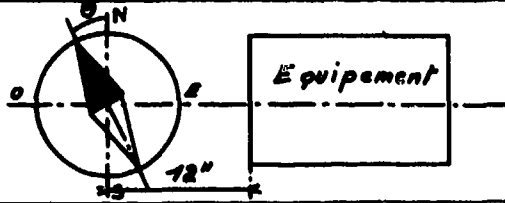
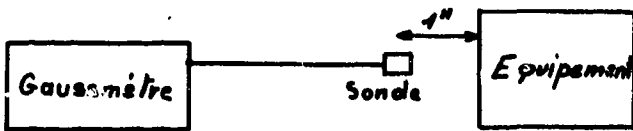
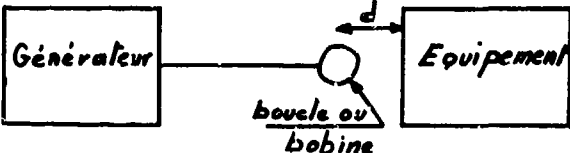
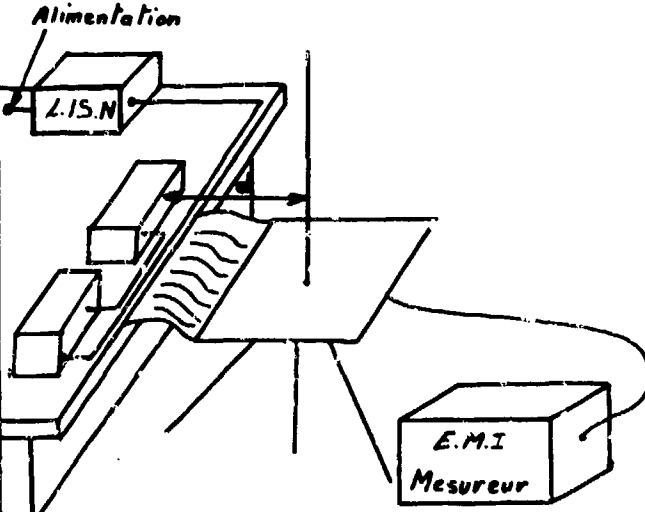




Pl.15 C Niveaux limites de parasites émis par conduction en bande étroite avec pince



Pl.15 D Niveaux limites de parasites émis par conduction en bande large avec pince

Champ	Mode Opérateur	Référence, norme
magnétique continue		DO 138 - LOCKHEED : $\theta_{MAX} = 5^\circ$ AEROSPATIALE-UNAVIA $\theta_{MAX} = 1^\circ$
		MIL 461-3 G 100 - AIR 510 C BOEING : non prévu ou non classé comme essai EMC  DOUGLAS : 1 gauss maximum à 1 pouce
magnétique AF et RF (3) (4)	 <p>Boucle déplacée autour de l'équipement et orientée de manière à obtenir le maximum de signal</p>	RE 01 de MIL 461 - d = 7 cm - 30 Hz à 30 KHz  DO 138 - AEROSPATIALE-BOEING-LOCKHEED : essais identiques avec d = 12" de 150 KHz à 25 MHz  3G 100 - AIR 510 C - DOUGLAS - UNAVIA : pas d'essai de ce type de prévu
Electrique RF (4)	 <p>Cas particulier de l'antenne tige : 14 KHz <math>\leq</math> F <math>\leq</math> 25/30 MHz</p>	RE02 de MIL 461-UNAVIA DOUGLAS Limites en unité de champ électrique. d = 1 m, 14 KHz à 10 GHz NB (1) 14 KHz à 1 GHz BB (2)  antennes <u>conseillées</u> : tige-bico- nique - conique log. spirale - cornet à double arête  AIR 510 C - Limites en unité de champ électrique 50 KHz à 1 GHz - aucune indica- tion sur le type d'antenne. d = 0,5 m pour un matériel sur avion  DO 138-AEROSPATIAL-LOCKHEED- BOEING-3 G 100 : limites en ten- sion aux bornes de l'antenne à vide. d = 12", F MIN = 90 KHz à 150 KHz F MAX = 1 à 1,215 MHz sauf BOEING : 10 GHz  antennes <u>imposées</u> : tige-dipole accordé - cornet

(1) NB (narrowband) : bande étroite

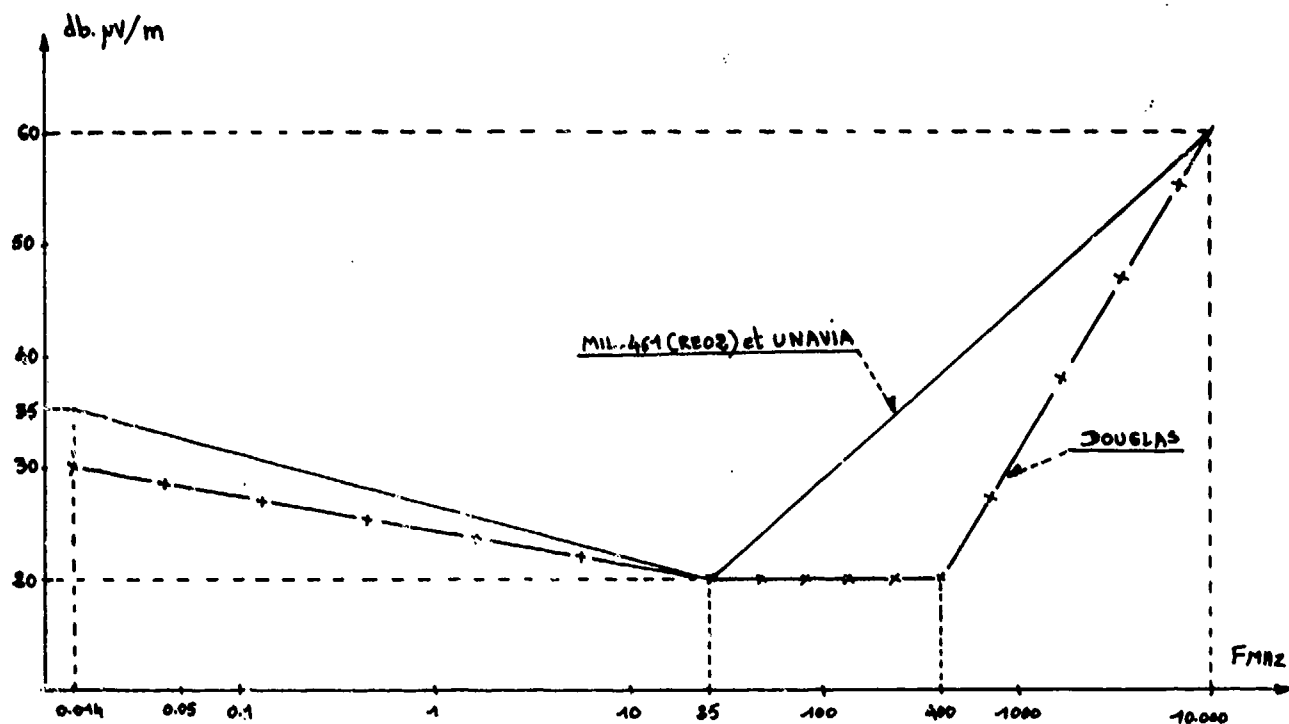
(2) BB (broadband) : bande large

(3) AF audio-fréquences

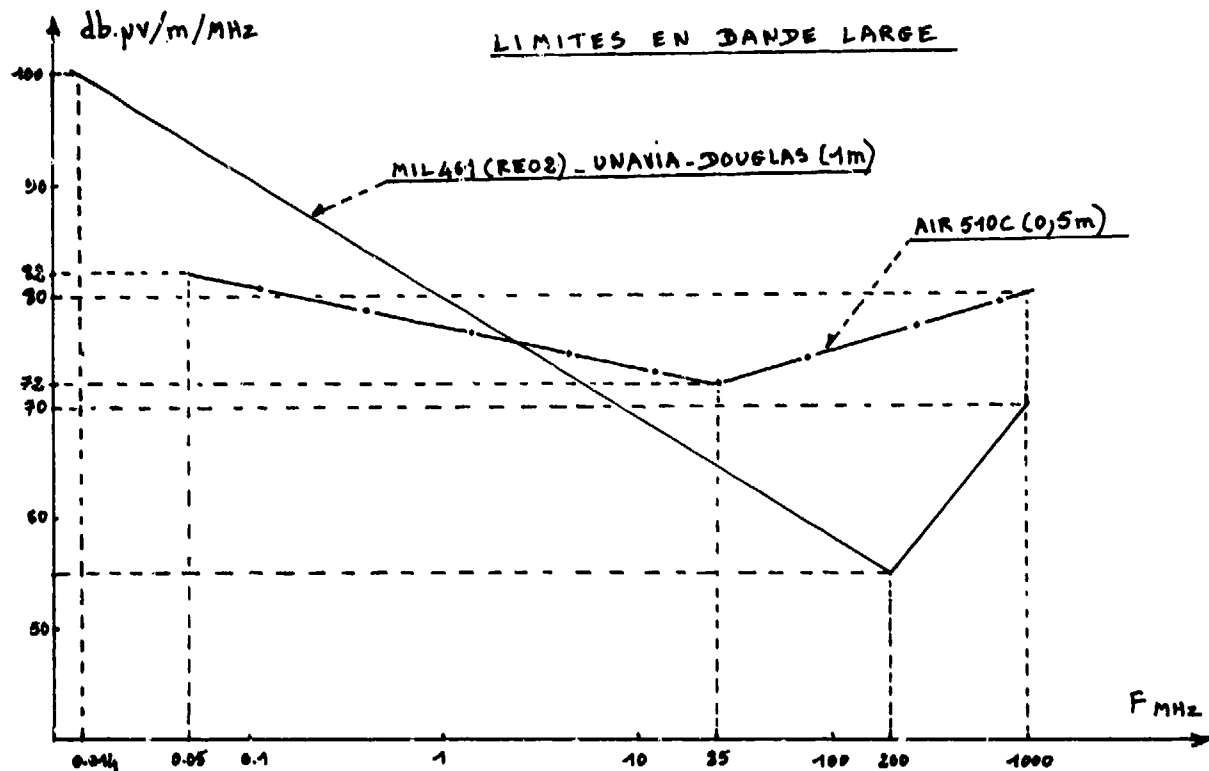
(4) RF : radio-fréquences

Pl.15 E Parasites émis par rayonnement - mode opératoire

# LIMITES EN BANDE ETROITE

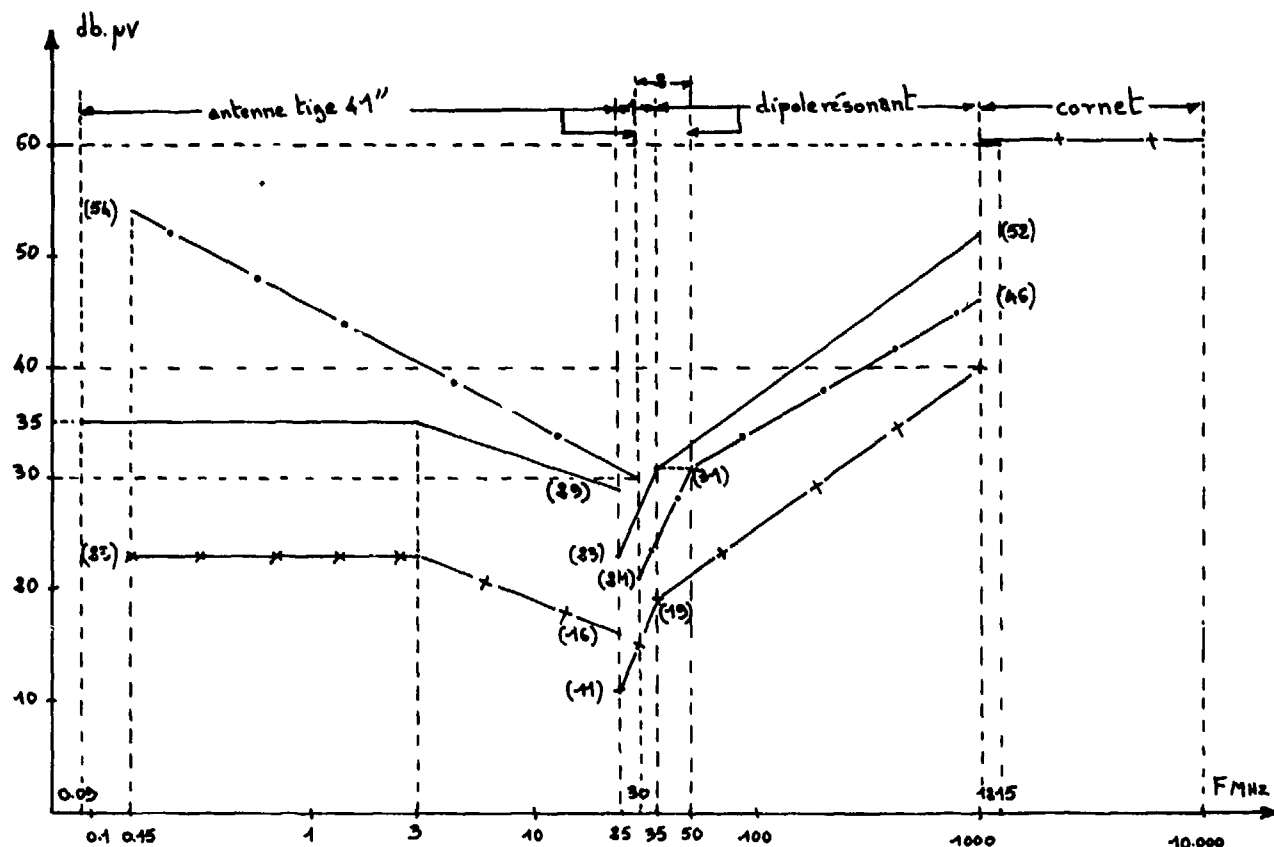


# LIMITES EN BANDE LARGE

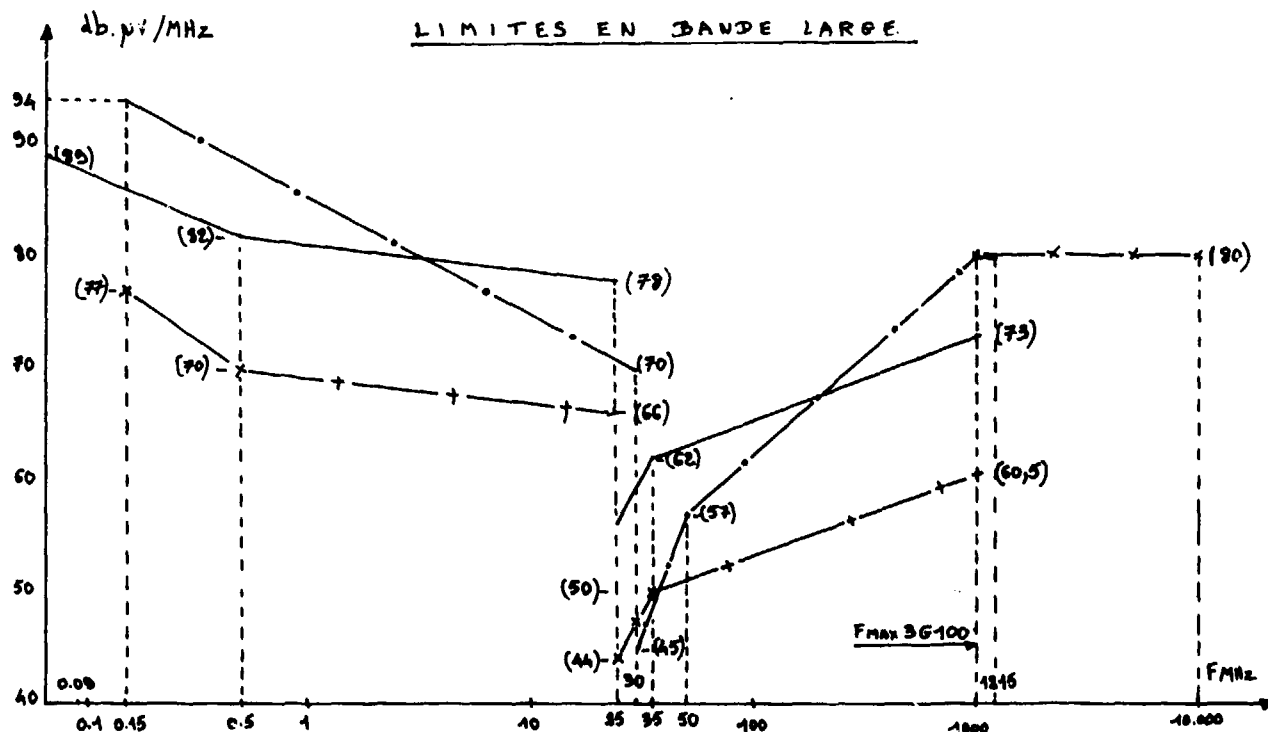


Pl.15 F Niveaux limites en unité de champ, du champ électrique émis

## LIMITES EN BANDE ETROITE



## LIMITES EN BANDE LARGE



DO 133 - AEROSTATIALE (1)

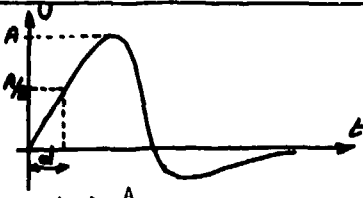
X - BOEING - LOCKHEED (1)

—•— 36-100 (2)

(1) : dipole accordé sur 35 MHz

(2) : dipole accordé sur 50 MHz

Pl.15 G Niveaux limites du champ électrique émis aux bornes de l'antenne a vide (antenne induite)

Norme spécification	Perturbation émise par conduction	Perturbation émise par rayonnement
MIL 461/462	 <p> <math>2 A d \leq 10 U_n</math>  <math>A</math> : tension max de la perturbation en volts.  <math>d</math> : durée à <math>\frac{A}{2}</math> en <math>\mu s</math>  <math>U_n</math> : tension nominale de la ligne en volts.            Aucune tolérance pour les boutons poussoirs de transmission de parole d'émetteurs.         </p>	Néant
DO 138 AEROSPATIALE	Néant	20 dB au dessus du niveau normal imposé si l'émission dure moins de une seconde.
BOEING	40 dB en dessus du niveau normal imposé pourvu que le temps s'écoulant entre deux manoeuvres successives soit inférieur à 1 minute.	
UNAVIA	Comme la MIL 461, l'interrupteur étant actionné 10 fois et l'impédance de la source d'alimentation étant inférieure à $0,5 \Omega$ . Les interrupteurs de puissance actionnés manuellement avant et après le vol ne sont pas soumis à cette exigence.	Néant
AIR 510 C	20 dB au dessus de la limite normale si la perturbation dure moins de 1 seconde et se répète moins de 1 fois toutes les 3 minutes. Sans limitation si la perturbation dure moins de 3 s et se répète 2 fois par période d'utilisation normale.	
DOUG LOCKHEED	Aucune tolérance pour les perturbations de courte durée (on ne parle pas de manoeuvre d'interrupteur).	
3 G 100	Rien à ce sujet	

Pl.15 H Tolérance complémentaire aux niveaux limites de perturbations émises lors du fonctionnement d'un interrupteur actionné manuellement, abstraction faite des opérations électriques et mécaniques qui en découlent

Norme ou Spécification	Niveau eff. sur DC (1)	Niveau eff. sur AC (2)	Gamme sur câbles DC (1)	Gamme sur câbles AC (2)
DO 138 AEROPATIALE	aux bornes de l'équipement $F < 1 \text{ KHz} : 2\% U_N$ $F \geq 1 \text{ KHz} : 5\% U_N$	$5\% U_N (3)$	200Hz - 15KHz	750Hz - 15KHz
LOCKHEED	aux bornes de l'équipement $6\% U_N (3)$	$5\% U_N (3)$	200 Hz - 15 KHz	
BOEING	$5\% U_N$ aux bornes d'un générateur à vide d'impédance interne $Z_i \leq 0,6 \Omega$		20 Hz - 15 KHz	
DOUGLAS UNAVIA	3 V.eff aux bornes de l'équipement		30 Hz - 150 KHz	
3 G 100	Pas d'essai avec transformateur en dessous de 15 KHz			
CS 01 de MIL 461/462		Néant sur AC	30 Hz à	50 KHz
<p>Mode Opérateur</p> <p>K fermé si DC K ouvert si AC <math>Z_i \leq 0,5 \Omega</math></p>				

(1) DC : courant continu

(2) AC : courant alternatif

(3)  $U_N$  : tension nominale sur le câble de puissance.


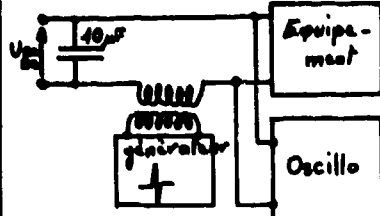
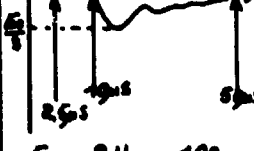
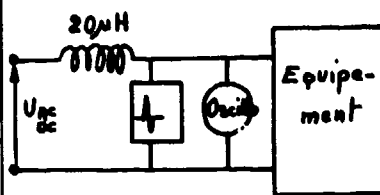

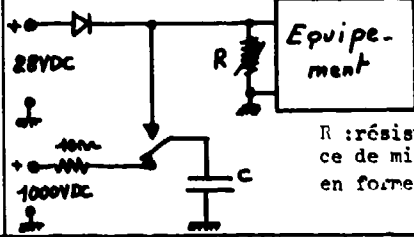
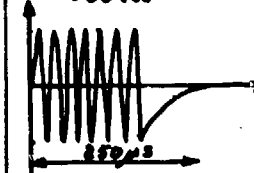
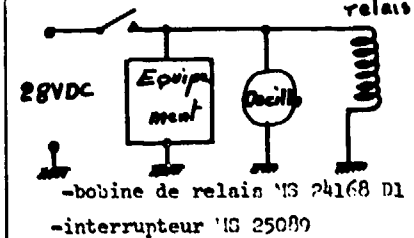
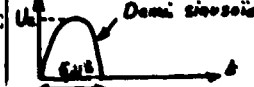
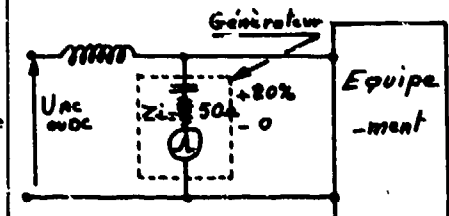
Pl.15 I Signaux sinusoïdaux injectés sur les câbles de puissance dans la gamme 30 Hz à 150 KHz – susceptibilité de conduction

Norme ou spécification	Gamme	Modulation	Niveaux	Mode opératoire
CS 02 de MIL 461/462	50 KHz à 50 MHz	AM-50% - 1000Hz A <sub>0</sub> (1) F' - ΔF=10KHz-1000Hz A <sub>0</sub> (1) Pas de modulation (1) impulsions (1)	$\Delta S \text{ db. } V_A A = 10 \log_{10} U_A \times I$ 	
DO 138 AEROSPATIALE	15KHz ou 90 KHz à 30 MHz	AM 30 % à 400 ou 1000 Hz	$V_A \text{ db. } \mu V, \text{ K ouvert}$ 	
LOCKHEED	15 KHz à 30 MHz	comme BOEING	Comme catégorie Z du DO 138	
3 G 100	15KHz/400MHz pour la catégorie A.	Comme prescrite dans spécification individuelle.	Cat. A pour avions militaires et civils complexes : $U_G = 120 \text{ dB. } \mu V$ K ouvert	Pour CS 02 de MIL 461 : I et mesuré avec la pince et $U_e$ au voltmètre RF
BOEING	90 KHz à 30 MHz	Type de modulation et fréquence donnant le maximum de susceptibilité. Si AM : taux de 80%	$V = 10 \text{ mV eff. constant}$ aux bornes du voltmètre	
DOUGLAS	150KHz à 400MHz	taux 75%	$V_A, K \text{ ouvert :}$ 2 V de 0,15 à 50MHz 1,5V de 50 à 400MHz	
UNAVIA	50 KHz à 100 MHz	non précisé	Générateur chargé par 50 Ω à part : $V_P = 7 \text{ V eff constant}$	

- (1) Modulation CS 02 MIL : a) récepteurs AM et équipements non accordés - b) récepteurs F' c) récepteurs SS B - d) équipements numériques ou avec canaux vidéo autres que récepteurs. Pour équipements numériques choisir la durée de l'impulsion et la fréquence de répétition égales à celles utilisées dans l'équipement.

Pl.15 J Signaux à porteuse sinusoïdale injectés dans les câbles de puissance dans la gamme 15 KHz à 400 MHz - susceptibilité de conduction



Norme spécification	Forme de l'impulsion et niveau	Modalités d'essais	Mode opératoire						
CS 06 de MIL 461 DOUGLAS	Câbles AC ou DC 	Taux de répétition : 3 à 10PPS Durée d'application : 10' Sur DC : autant d'impulsions + que - Sur AC: déphasage continu de l'impulsion de 0 à 360°	Injection série 						
UNAVIA	 $E_a = 2 U_n \approx 100v$	Comme CS06 mais durée: 30' Si équipement trop puissant, on cale le générateur à 20H sur R = 0,5A et on commute sa sortie sur l'équipement.	Injection parallèle 						
DO 138	Sur câbles AC : comme CS 06 de MIL 461  Sur câbles 28V DC	2 PPS- déphasage aléatoire et durée non fixée  Autant d'impulsions + que - avec une durée d'application non fixée	Injection série ou parallèle au choix  Impulsion positive sur DC  R : résistance de mise en forme						
LOCKHEED	comme DO 138	Comme DO 138 sur AC et DC mais durée d'application fixée à 60 s							
BOEING	sur câbles 28 V.DC 500 Vcc 	10 ON.OFF pendant 5 minutes.	 -bobine de relais 'IS 24168 D1 -interrupteur 'IS 25089						
AEROSPATIALE	 <table data-bbox="353 1474 604 1647"><tr><td>U<sub>AC</sub></td><td>200/115/167</td><td>V</td></tr><tr><td>U<sub>C</sub></td><td>1200/1000/250</td><td>600V</td></tr></table>	U <sub>AC</sub>	200/115/167	V	U <sub>C</sub>	1200/1000/250	600V	Tension crête réglée à vide monophasée { 5 imp à 90° 5 imp à 270° triphasée { 2 imp à 90° par phase 2 imp à 270° phase DC : 10 impulsions	
U <sub>AC</sub>	200/115/167	V							
U <sub>C</sub>	1200/1000/250	600V							


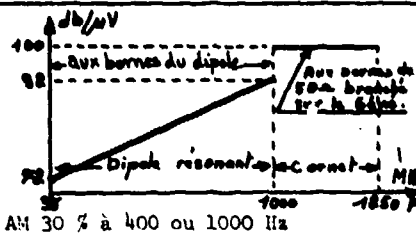
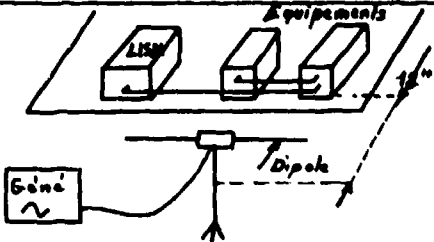
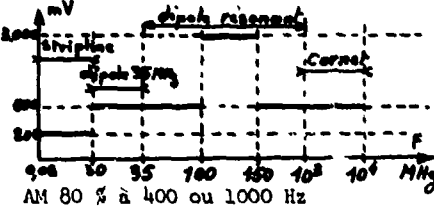
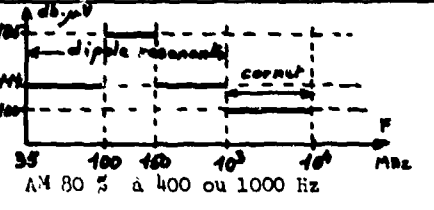
Pl.15 K Subtransitoires injectés dans les câbles de puissance - susceptibilité de conduction

Norme Spécification	Gamme	Modulation	Niveau	Mode opératoire
DO 138 AEROSPATIALE	15 KHz à 30 MHz	AM 30 % à 400 ou 1000 Hz	10 mV aux bornes de la spire quelle que soit la fré- quence.	<p>15</p>
BOEING	90 KHz à 30 MHz	modulation et fréquence donnant le maximum de susceptibilité. AM: Taux de 80 %		
DOUGLAS 3G 100	Comme sur les câbles de puissance (voir planche 15 J) et G 100 : essai à faire seulement si la spécification individuelle de l'équipement le demande.			
MIL 461 UNAVIA LOCKHEED	rien de prévu			

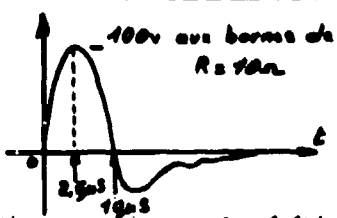
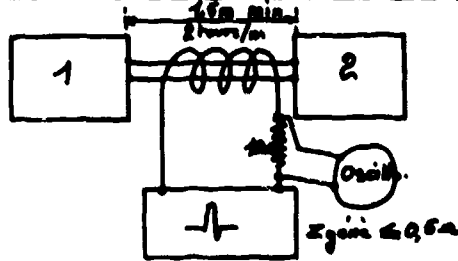
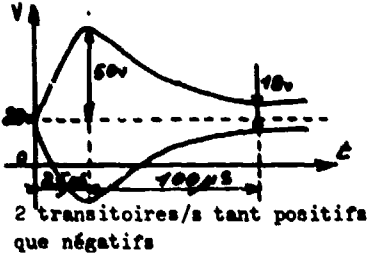
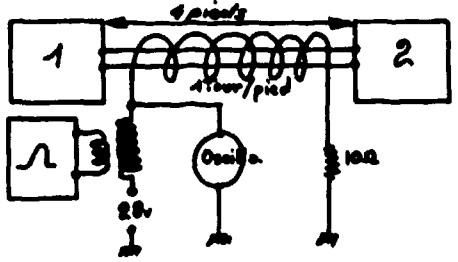
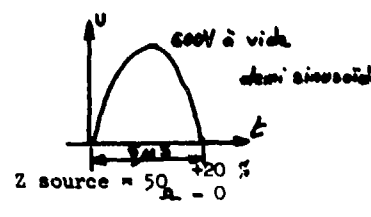
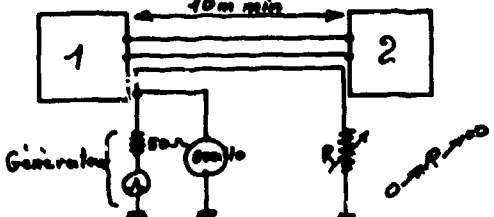

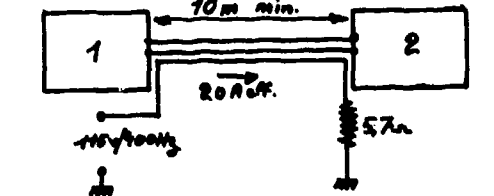
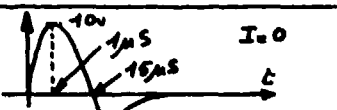
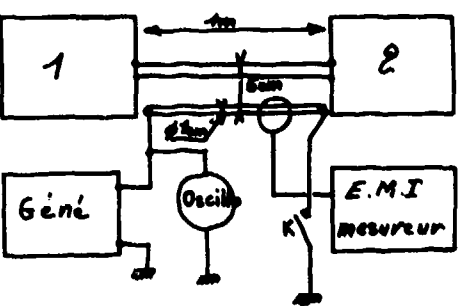

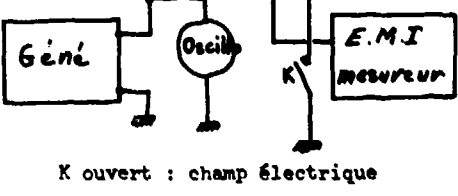
Pl.15 L Signaux a porteuse sinusoïdale injectes dans les câbles d'interconnexion susceptibilité de conduction

Norme Spécification	Gamme	Forme niveau	Mode Opératoire
MIL 461 Essai RS 01	30 KHz à 30 KHz		
DO 138 AEROSPATIALE LOCKHEED	400 Hz	DO 138 : Cat A I = 20 A eff Cat B I = 2 A eff Cat C : pas d'essai AEROSPATIALE-LOCKHEED: 20 A eff	
	15 KHz à 30 MHz	10 mV aux bornes de la boucle- eff AM 30 % à 400 ou 1000 Hz sauf LOCKHEED ou AM 80 %	
BOEING	400 Hz	Comme DO 138 - catégorie A seulement	
3 G 100	400 Hz	Comme DO 138 - catégories A., B, C	
DOUGLAS	400 Hz	10 A eff	
	Subtran- sitoire		
UNAVIA	400 Hz	I = 20 A eff	
	Subtran- sitoire	même forme que DOUGLAS avec U <sub>C</sub> = 50 V dans 50 Ω	

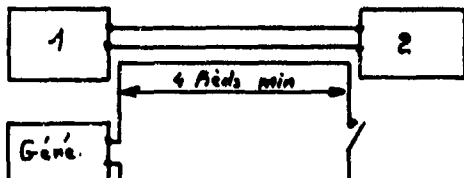
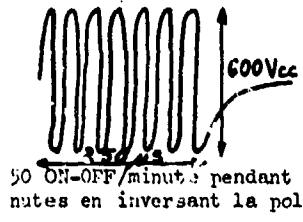
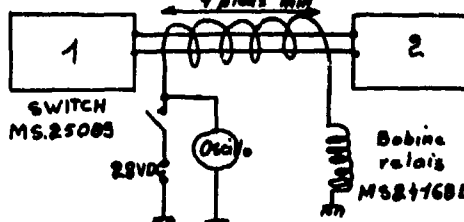
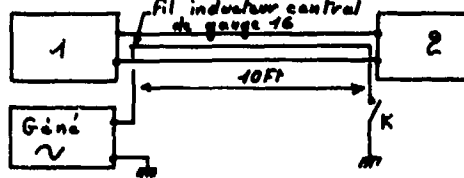
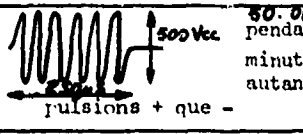
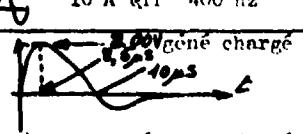
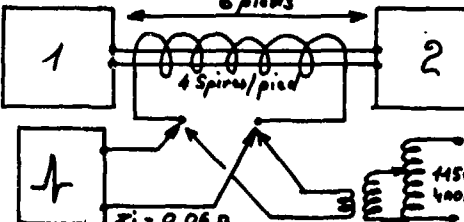
Pl.15 M Susceptibilité du boîtier de l'équipement au champ magnétique

Norme Spécification	Gamme	Niveaux, type de modulation	Mode opératoire
MIL 461/462 Essais : RS 03.0 RS 03.1 RS 03.2	14 KHz à 400 MHz pour RS 03.0 et à 10 GHz pour RS 03.1 et 2	RS 03.0 niveaux "non sheltered" 10 KHz $\leq f \leq 2$ MHz : 1 V/m 2 MHz $\leq f \leq 30$ MHz : 5 V/m 30 MHz $\leq f \leq 400$ MHz : 10 V/m Même règles de modulation que pour l'essai C S 02 (voir planche 15 J)	A priori le type d'antenne émettrice n'est pas imposé mais seulement conseillé. On fait une mesure préliminaire du champ à l'emplacement où sera posé l'équipement. La distance entre l'antenne et l'équipement n'est pas également imposée pourvu que ce dernier soit dans le faisceau à 3 dB du diagramme de l'antenne.
UNAVIA	14 KHz à 10 GHz	14 KHz à 35 MHz : 5 V/m 35 MHz à 10 GHz : 2 V/m Modulation comme CS 02 Norme MIL 461 (voir planche 15 J)	
DOUGLAS	14 KHz à 10 GHz	2 V/m dans toute la gamme modulation  75 %	
DO 138 AEROSPATIALE	35 MHz à 1215 MHz	 AM 30 % à 400 ou 1000 Hz	
BOEING	90 KHz à 10 GHz	 AM 80 % à 400 ou 1000 Hz	Même disposition que DO 138 au dessus de 30 MHz, la tension étant mesurée aux bornes du géné à vide. En dessous de 30 MHz la tension est mesurée à l'extrémité de la ligne à bandes.
LOCKHEED	35 MHz à 10 GHz	 AM 80 % à 400 ou 1000 Hz	Même disposition que DO 138. La tension est mesurée aux bornes du dipole résonant ou aux bornes de 50 Ω si on utilise le cornet.
3 G 100	15 KHz à 400 MHz	Niveau "a": 100 dB/μV aux bornes de l'antenne sur avions militaires ou civils complexes. Pas de modulation.	-Pour $F \geq 30$ MHz : dipole et même disposition que DO 138 -Antenne tige pour $F < 30$ MHz

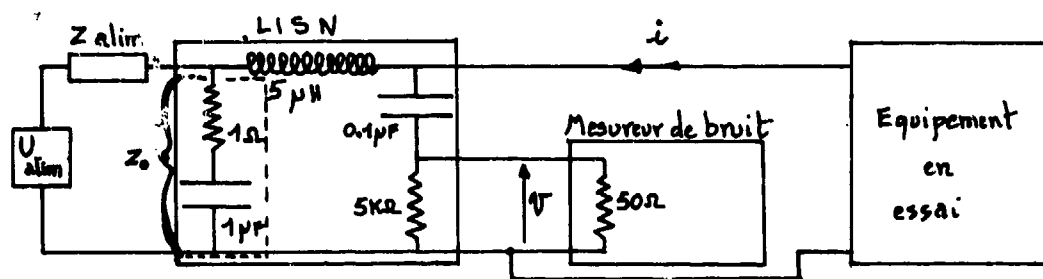
Pl.15 N Susceptibilité du boîtier de l'équipement et de ses câbles à un champ électrique à portuse sinusoïdale

Norme spécification	Couplage	Forme-niveau-gamme	Mode opératoire
MIL 461 essai RS 02	Magnétique	 <p>100v aux bornes de <math>R = 10\Omega</math></p> <p>Rien sur fréquence de répétition et durée.</p>	
DO 138	Magnétique	 <p>50V</p> <p>2 transitoires/s tant positifs que négatifs</p>	
AEROSPATIALE (1)	Magnétique et électrique	 <p>600V à vide</p> <p>Z source = <math>50\Omega</math></p>	
	Magnétique	<p>20 A/400 Hz</p> 	
UNAVIA	Electrique	<p><math>V = 10 \text{ V eff}, I = 0</math></p> <p>20 Hz à 150 KHz</p>  <p>10V</p> <p>1μs</p> <p>15μs</p> <p><math>I = 0</math></p>	
	Magnétique	<p>1 A eff 20 Hz- 150 KHz</p> <p>20A eff 400 Hz</p> <p>20Hz - 15 KHz</p>  <p>1A</p>	 <p>K ouvert : champ électrique</p>
3 G 100		rien de prévu	

(1) L'AEROSPATIALE n'applique pas ces essais sur tous les équipements mais seulement sur ceux qu'elle estime pouvoir être perturbé de cette manière

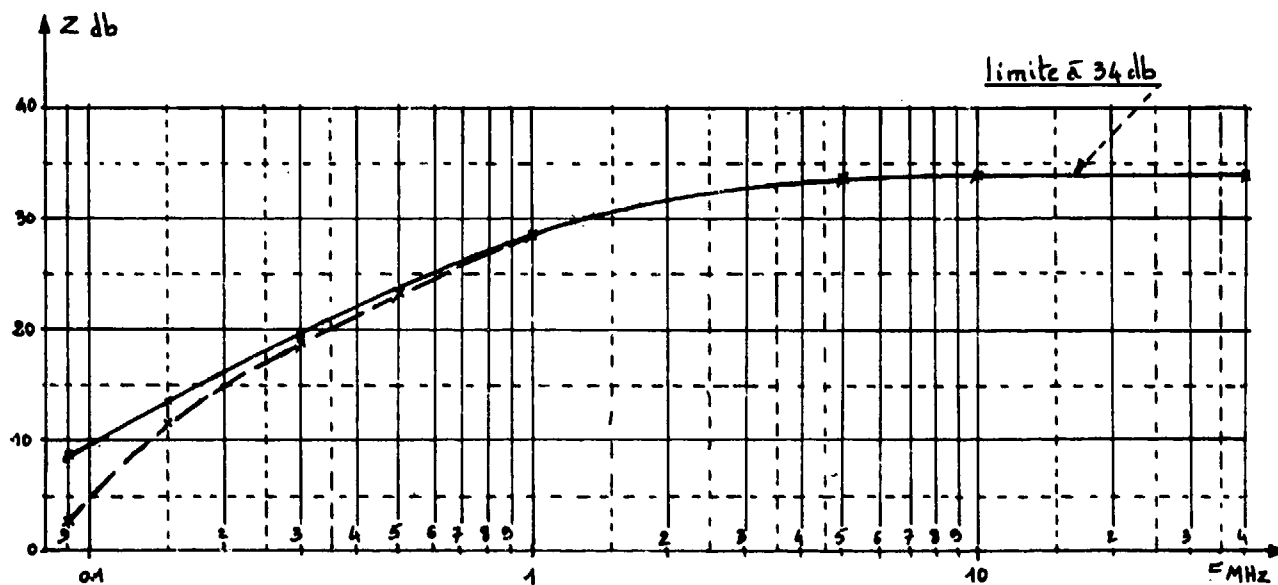
Norme spécification	Couplage	Forme-niveau-gamme	Mode opératoire
LOCKHEED	Magnétique	400 Hz: 100 A x pied eff $\infty$ 1200 Hz: 50 A x pied eff 2400 Hz: 30 A x pied eff 4800 Hz: 20 A x pied eff	
	électrique	$\infty$ 6000 V x pied eff de 390 Hz à 410 Hz (battement)	
	magnétique		
BOEING	magnétique	$\infty$ 20 A eff de 390 à 410 Hz	
	électrique	$\infty$ 1200 V eff I = 0 de 390 à 410 Hz	
	magnétique		comme LOCKHEED mais avec fil inducteur central de gauge 16
DOUGLAS	magnétique	$\infty$ 10 A eff 400 Hz 	

Pl.15 P Susceptibilité des câbles d'interconnexion aux effets de couplage (2ème partie)



Impédance de transfert du LISN :  $Z = \frac{V}{i}$  soit  $Z_{db} = V_{db.pV} - i_{db.pA}$

F MHz	Z db pour $Z_{alim} \ll Z_0$	Z db pour $Z_{alim} \gg Z_0$	$Z_0 (\Omega)$
0.090	8,5	2,6	8,0
0.150	13,4	11,4	1,5
0.300	19,5	18,8	1,1
0.500	23,6	23,3	1
1	28,6	28,4	1
5	33,6	33,6	1
>5	34	34	1



Pl.15 Q Fonction de transfert du LISN

# A STATUS REPORT OF THE IEEE/ECAC ELECTROMAGNETIC

## COMPATIBILITY FIGURE OF MERIT COMMITTEE

G. H. Hahn  
Stanford Research Institute  
1611 N. Kent Street  
Arlington, Virginia 22209  
USA

and M. N. Lustgarten  
IIT Research Institute, ECAC  
North Severn  
Annapolis, Maryland 21402  
USA

16-1

### SUMMARY

The Institute of Electrical and Electronics Engineers (IEEE) Electromagnetic Compatibility Professional Group and the Electromagnetic Compatibility Analysis Center (ECAC) have jointly sponsored an ad hoc committee to devise a practical technical procedure for specifying an electromagnetic compatibility (EMC) Figure of Merit (FOM) for various electronic devices and systems. This paper summarizes the status of the committee's work.

An EMC FOM for single-channel voice communication systems, based on the channel-denial concept, was developed by using a building-block approach. The building-block approach involves the use of relatively simple scoring formulas for selected EMC parameters, which are then linearly combined, with appropriate weighting factors, to calculate FOMs for transmitters, receivers, and systems (i.e., transmitter-receiver pairs). A co-site environment is assumed, and measured (or calculated) equipment data are required. The parameters chosen for transmitters include spurious emissions, noise near the carrier (i.e., broadband emissions outside the band containing desired modulation components), and intermodulation products. Those chosen for receivers were spurious responses, adjacent-signal interactions, and intermodulation products. A channel was considered denied if  $(S + I + N)/(I + N) > 10$  dB in a moderately dense co-site environment. The parameter scoring equations were developed to reflect the frequency spectrum denied by each parameter. The weighting factors for the building-block approach were determined by running a computer program that kept track of the number of channels denied by each parameter. Example calculations for HF, VHF, and UHF systems are given, and the interpretation of the scores is discussed.

The procedure developed enables quantification of EMC characteristics of transmitting and receiving equipment. The EMC FOM provides system planners, as well as design engineers and management, with a technical tool to facilitate making objective, consistent decisions (e.g., it can be used to quantify the benefit side of an EMC cost-benefit analysis. It also has potential value for those concerned with EMC specifications and standards. The EMC FOM does not, however, indicate the absolute probability that compatibility will be obtained; rather, it gives information about the relative chance of obtaining compatibility. Therefore, experience in using the FOM (and user feedback) will be needed in order to help determine the minimum FOM score required for a specific type of equipment or system in a given type of application.

### 1. COMMITTEE CHARTER

The purpose of the committee is to generate a general technical procedure for calculating an EMC Figure of Merit (FOM) for a selected group of electronic system components. The procedure will use a minimum number of significant parameters to define the "goodness" of components. Emphasis will be placed on determining EMC FOMs for transmitters and receivers of a specified class: single-channel voice communications.\* Some effort will also be devoted to developing a generalized expression for "system" effectiveness, which will include the "goodness" measures of the transmitters and receivers.

The transmitter and receiver FOMs will be derivable from measured data obtained by using specified procedures. The FOMs will also be derivable by analytical means, if suitable analytical models are used.

The EMC FOM will be useful to equipment design engineers, system planners, regulatory personnel, and managers in related areas. In effect, the FOM will represent numerical measures of spectrum utilization (primarily transmitters) and RF environmental susceptibility (primarily receivers). The measures will be so designed that they are readily understandable to management as well as the technical community. Interim and final reports will be issued, describing the procedure, providing numerical examples relative to several different devices, and suggesting approaches that can be used to address other classes of equipment and systems. Specific recommendations will be made regarding the application of the EMC FOM to individual transmitters and receivers and to other electronic components and systems.

\* This class was chosen because: (1) It contains literally millions of equipment; (2) considerable amounts of measured data are available for nonmilitary and military equipment; and (3) the committee manpower and time available necessitated some restrictions.

## 2. COMMITTEE MEMBERSHIP AND ACTIVITIES

The committee consists of the following members:

16-2

W. G. Duff	Atlantic Research Corp. 5390 Cherokee Avenue Alexandria, Virginia 22314
G. H. Hagn	Stanford Research Institute 1611 N. Kent Street Arlington, Virginia 22209
J. S. Hill	RCA Service Company 5260 Port Royal Road Springfield, Virginia 22151
M. N. Lustgarten (Chairman and ECAC Representative)	IITRI, ECAC North Severn Annapolis, Maryland 21402
R. J. Mohr	AIL Division of Cutler Hammer Deer Park Long Island, New York 11729
R. B. Schulz (IEEE Representative)	Southwest Research Institute 8500 Culebra Road San Antonio, Texas 78284
N. H. Shepherd	General Electric Company Mountain View Road Lynchburg, Virginia 24502

The committee has met approximately 20 times over the two-year period beginning September 1972. A significant amount of the initial effort was devoted to reviewing the literature (JTAC, 1968; DUFF, W. G., 1969; VERSAR, 1971; BERRY, L. A. and EWING, D. R., 1972; SCHULZ, R. B., 1973, 1974a). A much larger list of references could have been compiled if other fields that use the FOM concept (e.g., reliability) had been included. The committee attempted to use the best aspects of the reported techniques. An interim report has been issued (IEEE/ECAC, 1973), and a final report has been drafted (IEEE/ECAC, 1974). A symposium was conducted in November 1973 to obtain comments from the U.S. EMC community. An overview paper was presented at the 1974 IEEE International Conference on Communications in Minneapolis (LUSTGARTEN, M. N., 1974a), and a session on the EMC FOM was held at the IEEE International EMC Symposium in San Francisco (LUSTGARTEN, M. N., 1974b; DUFF, W. G., 1974; MOHR, R. J., 1974; SCHULZ, R. B., 1974b; HAGN, G. H., 1974).

## 3. GENERAL COMMENTS ON THE EMC PROBLEM

### 3.1. Introductory Remarks

Before the work of the committee is directly addressed, several comments seem appropriate. Electro-magnetic compatibility is a complex multifaceted problem, which is not discussed in detail here. Its goals are closely related to those of "spectrum management." DAVIE (1959) said that the goals of spectrum management are "to allocate the radio-frequency spectrum among competing needs, to integrate its uses so that interference is prevented, and to conserve the spectrum, recognizing the limitations of the resource." It is apparent that the spectrum management/EMC problem is analogous to the various ecological problems (e.g., air and water pollution), as well as to the various resource allocation problems facing individuals, nations, and the international community.

It should be recognized that even the best equipment can cause or experience interference, and, conversely, even the poorest equipment may operate quite satisfactorily in a relatively sparse electro-magnetic environment. However, if a user has equipment that is "good" from an EMC standpoint, the likelihood is much greater that it can be accommodated in any environment (i.e., that interference will not be caused or experienced), and greater flexibility in spectrum management will be achievable.

Apart from the issue of which competing user group should be favored over another (a subject not amenable to technical analysis), a number of related factors can be considered in an objective, technical manner: cost, the state of the art, equipment/system performance, and standards.

### 3.2. Cost

Better EMC frequently implies higher initial cost. However, if improved EMC is incorporated in the original design specifications, total (life-cycle) costs may be considerably lower than if no attention is paid to EMC during the design stage and "fixes" are required after the equipment has been manufactured and placed in operation. An EMC FOM can, when related to requirements for a given application, provide the EMC benefit portion of a cost-benefit analysis performed to determine whether higher initial cost is worth the investment.



### 3.3. State of the Art

The state of the art in EMC, or in most related fields, cannot always be defined precisely. Many advanced techniques are described in the literature, and many advanced devices exist as prototype models or laboratory "lash-ups." However, given actual operational hardware, standard measurements can be performed to determine whether one equipment has better EMC characteristics than another. The equipment that represents the state of the EMC art will, by definition, be given the highest EMC FOM score. Hence, the FOM will provide a ruler for measuring any specific equipment or system relative to the EMC state of the art.

### 3.4. System Performance

There is a subtle distinction between system performance and EMC "goodness." A higher system performance score (neglecting EMC considerations) would usually be achieved by a communication system having higher power and a more sensitive receiver. Conversely, the equipment with lower power and a less sensitive receiver would generally be less likely to cause or experience harmful interference. EMC is one of many factors that contribute to system effectiveness. It is contended that, in the long run, better EMC characteristics will result in improved overall system performance when the complete operational environment is considered.

### 3.5. EMC Standards

The availability of the FOM scale will enable personnel who are devising standards to determine what to measure and to set limits that are meaningful in terms of the areas noted above. Selected numerical limits (e.g., decibels below or above some absolute level of power flux density or field strength per unit bandwidth) can be compared with the FOM, which, in turn, can be related to cost, system performance, and the state of the art. In this way, objective, meaningful standards can be established.

Now, let us address the process of developing the EMC FOM.

## 4. DEVELOPMENT OF AN EMC FOM

### 4.1. The Process

The process of developing an EMC FOM is illustrated in Figure 1. The first step is to define the requirements and specify the desirable features of the FOM. The second step is to define the criterion to be used to specify EMC merit. It is then necessary to choose a method of approach for deriving the FOM on the basis of the selected criterion. Identifying the significant EMC parameters is the next step. Then it is necessary to quantify the FOM by specifying how to measure (or calculate) values for the parameters and by developing scoring formulas for using the quantitative input data, taking into account the environment in which the equipment/system might be used--or some hypothetical environment(s). The scale on the FOM "yardstick" must be chosen and quantified, and its limitations must be explored. When these steps have been performed and the necessary input data have been obtained, it should be possible to compute EMC FOMs.

### 4.2. Requirements for the EMC FOM

#### 4.2.1. General Requirements

##### 4.2.1.1. Introductory Remarks

The FOM must be based on sound EMC concepts and must be expressed in user-relevant terms; therefore, one must specify the potential users, the uses that might be made, and the level of detail that might be relevant for each. The users of such an EMC FOM might include the hardware development team (equipment, EMC, and system engineers, and technical and administrative managers), the user who selects and uses the equipment or system to meet his operational requirements, and the spectrum manager who authorizes the use of the electromagnetic spectrum. Questions relative to all EMC FOM users are:

- What uses will they make of an FOM?
- Can one number satisfy them all?
- Does so much smoothing occur in boiling down the technical information to one number that the result obtained is meaningless?

In general, the managers will want less detail (i.e., they will want one number), and the engineers will want varying degrees of additional detail. Briefly, managers will probably want scores for receivers, transmitters, and systems in the context of cost versus benefit for their specific application (RACH, R. A. and SORKIN, I.J., 1974); whereas engineers are likely to want these scores as well as parameter scores and the detailed technical data on which they are based.

All the users of an EMC FOM will want the equipment or system to be able to perform its mission in a cost-beneficial manner without being subjected to unacceptable degradation (LUSTGARTEN, M. N., 1970)

164  
or causing harmful interference (ITU, 1968) to other spectrum-using systems. The system user and his developer have a primary interest in the probability of unacceptable performance degradation of the system being rated, as a function of both the system design variables and the environment(s) in which the system will be used. The spectrum manager, although interested in the problems of the user of the system being rated, is also interested in the probability of harmful interference to other spectrum-using systems that could be caused by the system being rated. Therefore, the FOM should provide an input for decisions among alternatives for system design, acquisition, and frequency selection and authorization. It can also provide guidance for EMC standards.

The remainder of this section discusses in greater detail possible requirements in each of the areas noted.

#### 4.2.1.2. Equipment Design

In general, the equipment designer considers EMC directly only if he is asked to comply with some EMC specification or standard. EMC standards are sometimes minimal and, consequently, sometimes inadequate for many co-site situations. The designer is primarily concerned with performance (in an interference-free environment) and cost. Reliability, maintainability, and a host of similar constraints must also be taken into account.

Better EMC is likely to involve higher cost, but design trade-offs are possible, and an EMC FOM should give guidance regarding them. For example, more linear receiver mixer characteristics are desirable, with avoidance of spurious responses and certain intermodulation (IM) interactions. One approach is to increase local oscillator (LO) levels, usually at added cost. This approach tends to increase LO radiation levels; allowable levels are specified by several existing standards. Although a trade-off exists, in general it appears that LO radiation effects are usually less significant than IM or spurious response effects in a co-site environment. The EMC FOM should quantify this trade-off.

#### 4.2.1.3. System Design

The system designer is usually not concerned with details of equipment design, per se, apart from performance characteristics and cost. He frequently selects "off-the-shelf" items that meet the required specifications. Given the equipment and system FOMs as a guide, he can select appropriate components after analyzing the various trade-offs. In some cases, he may be able to select equipment with relatively poor FOMs in conjunction with good couplers. It should be noted that the system designer rarely knows the frequencies that may be made available to the system when it becomes operational. If his system has a higher EMC FOM, it will be easier to accommodate.

#### 4.2.1.4. EMC Standards and Specifications

This is a highly complex area, partly because the work is performed by committees, the members of which have different motives, different backgrounds, and different degrees of competence. Numerous compromises are frequently made before a final product is obtained. As a result, many standards cannot be justified on a purely technical, objective basis. Two extreme cases are common: some standards essentially permit all equipment to pass, whereas others are virtually impossible to achieve within reasonable economic constraints. The result, in the latter case, is generally a waiver, after considerable expenditure of funds and time.

It should be emphasized that the standards-making task appears to be the key element of the EMC problem. Given appropriate standards, with appropriate enforcement, the cost impact of EMC requirements could be minimized. Also, spectrum management and operational problems could be greatly simplified. Without adequate standards, spectrum managers and users are faced with the increasingly difficult, if not impossible, task of "packing" the environment with pieces of equipment whose EMC characteristics are known to be well below the state of the art.

This committee did not address the numerous political and administrative problems involved in standards making; however, it noted that if the proposed EMC FOM concept is adopted, the nontechnical factors will become harder to justify.

#### 4.2.1.5. Spectrum Management

Spectrum management is another large and complex area involving national government and non-government groups, as well as international groups. The FOM is not a panacea for all the implied management problems. However, if adopted, it can help provide a more technical basis for several types of spectrum management decision making. Applicable areas are standard, frequency allocation, frequency assignment, interference minimization, and spectrum conservation. A detailed discussion of each of these areas is beyond the scope of this status report.

#### 4.2.1.6. Administration

This term refers to the various, numerous managers involved in research, development, production, and operations relating to components, equipment, and systems that involve various telecommunications

devices and systems. From their viewpoint, EMC is one relatively minor factor among many other pressing considerations. A quantitative FOM will make EMC and its role in telecommunications much more understandable to these people. They have, for example, accepted the reliability concept. Many of them might not understand the technical subtleties behind the term "95 percent reliable." But it is a number which, in some way, is appreciated for its importance and its cost implications.

Perhaps the requirement to focus the manager's attention on EMC is one of the best arguments for adopting the FOM concept. One cannot blame responsible people for ignoring something that appears (at least before a serious operational EMC problem confronts them) to be a rather vague need. If a number is supplied that is based on technical and cost considerations pertinent to his application, the manager is much more likely to give his support, since he can relate a quantitative value to benefits and the cost required to achieve them.

#### 4.2.2. Specific Requirements

A list of desirable EMC FOM characteristics includes:

- (1) The FOM should indicate how much better one equipment is, relative to another, in regard to EMC capability.
- (2) A capability for expressing the scores in general terms (i.e., categories meaningful to management) should be provided.
- (3) The FOM, for the equipment under consideration, should be based on the ability of the equipment to operate in a co-site environment.
- (4) The form(s) of the scoring formulas should be relatively simple. The input parameter values should be derivable from measurements performed in a standardized manner.
- (5) The formulas should be consistent with regard to analogous parameters and, insofar as possible, reflect the applicable physical phenomena.
- (6) A large sample of equipment should be used to develop the scoring formulas, to ensure that the total range of EMC capabilities (worst to best) will be considered adequately.
- (7) The results obtained by using the FOM formulas should be consistent, on a relative basis, with the subjective rank order that would be arrived at independently by qualified engineers who study the measured results for a given set of equipment.
- (8) The equipment that represents the EMC state of the art should be given the highest score. In other words, the equipment that can most readily be accommodated in a dense environment (from the standpoint of being less likely to cause or experience performance degradation due to interference) should be given the highest score.
- (9) Ideally, the range of FOM scores should be between 0 and 100, although, in some cases, scores greater than 100 and less than zero will occur. A score of 50 should represent the median equipment, that is, approximately half the equipment of the type under consideration will have scores above 50, while half will have scores below 50.

#### 4.3. Criteria for the EMC FOM

The committee considered several possible criteria for formulating an EMC FOM. Two of the most promising were:

- (1) The probability of achieving adequate EMC,  $p(\text{EMC})$ .
- (2) The number of channels,  $N_d$ , that would be denied by the system being rated to other systems that would subsequently be added to the same environment.

Computer programs exist for the computation of single-channel voice communication system performance both with and without interference [e.g., the co-site analysis model of LUSTGARTEN (1970), COSAM, can compute  $p(\text{EMC})$ ],\* but a detailed specification of the technical characteristics of all systems in the environment is required. For example, the exact frequencies of operation of these systems must be specified. Generally, the exact environment is not known before a system is deployed, and in some cases the system might have to operate in many environments. Therefore, it would be necessary to run COSAM many times (perhaps exhaustively, in a Monte Carlo mode) to obtain an EMC FOM based upon average  $p(\text{EMC})$  calculations. This could be rather time-consuming, and the interpretation of the results might be difficult. Furthermore, not all potential users of the FOM would have COSAM available.

A computer program, the denied-usage channel evaluator (DUCE) program, was developed for the computation of  $N_d$ . The program only requires specification of a simply defined environment; it does not

\* The probability of achieving adequate EMC can be considered as 1 minus the probability of unacceptable degradation.

166  
require the detailed input parameters COSAM requires. In effect, the program considers the frequency-spectrum dimension in detail and the space dimension in a simplified manner. The assumption is made that the input power levels from all emitters in the co-site environment are equal, and other simplifying assumptions are made for the test environment (see Sec. 1.7). A more complete channel definition--such as the one given by JTAC (1968) which encompasses frequency, space, and time--seems unduly complicated for a first attempt at an EMC FOM.

The denied-channel criterion was chosen by the committee because it met the requirements specified in Sec. 4.2 with the least-complicated assumed test environment that still incorporated the essential features.

#### 4.4. Methods of Approach

Two methods of approach were studied: (1) a direct approach that would involve obtaining a FOM for a system without first specifying the EMC goodness of the system components and (2) a building-block approach that would consist of specifying the EMC goodness of subsystems (e.g., equipment such as receivers and transmitters) and then somehow combining the equipment scores to give a system score. The direct approach would require the use of the DUCE program, and the basic score could be  $N_d$ , or an inverse relationship defined so that a higher score would mean a better system. The building-block approach was appealing because it would provide insight into the relative importance of each EMC parameter selected for each equipment, and such information might be useful in the EMC design trade-off and cost-benefit analyses. However, using the direct approach, one could still obtain the data needed for such analyses by keeping track of the causes of the channel denials as a function of the EMC parameters while running DUCE for the overall system.

The DUCE program might not always be available; also, it is desirable to have a simple FOM formula. It is possible to use DUCE on some diagnostic runs, to look for trends as a function of particular combinations of equipment and environments, and to use the results for guidance in determining the rules for combining parameter scores to yield equipment scores (i.e., for determining parameter weighting factors). The building-block approach was adopted and is discussed in the remainder of this paper.

The building-block approach is illustrated in Figure 2; it consists of:

- (1) Defining scores for transmitter and receiver EMC parameters on the basis of the amount of frequency spectrum they cause to be denied.
- (2) Combining the parameter scores with appropriate weighting factors on the basis of the relative number of channels denied, to give equipment scores.
- (3) Combining the equipment scores (properly weighted on the basis of denied channels), to obtain a system score.

#### 4.5. Parameter Identification

To develop equipment parameter scores, it is necessary to identify the important EMC-related parameters for each system component. One way to do this is to include many possible parameters, compute the number of channels that each denies, by using a DUCE-like program, and then make a value judgment to determine which parameters are sufficiently significant to include in an FOM formula. The committee chose a different method, the Delphi method (e.g., JOLSON, M. S., and ROSSOW, G. L., 1971), which consists of a panel of experts in the field stating which parameters they think are important, discussing these parameters, and then using their consensus to select specific parameters.

A set of measured data from UHF (225-400 MHz) AM transceivers was considered.\* The initial parameters were, for receivers: adjacent-signal interactions, two-signal third-order intermodulation (IM), and spurious responses; for transmitters: two-signal third-order IM and spurious emissions. Later, transmitter noise was considered. The committee members individually ranked several transceivers on a relative basis in terms of EMC "goodness" after reviewing measured data for each parameter. The results of the ranking exercise were quite enlightening. Essentially unanimous agreement was achieved for overall performance and for all parameters except receiver spurious responses (and, in some cases, the spurious emission interaction). The spurious cases represented a somewhat difficult interpretation problem. Electronic engineers normally consider spurious responses in terms of decibels relative to nominal sensitivity. In other words, spurious responses are stated as relative input power levels (e.g., 60 or 80 dB) greater than the sensitivity level, at frequencies other than the tuned frequency (outside some nominal bandwidth), that result in the same output as the "sensitivity" input power level at the tuned frequency. The levels of the responses are, of course, important, but the number of responses is also significant. No known receiver standard recognizes this situation. The relative importance of the levels and the number of responses depends upon the environment in which the receiver is used. After the committee recognized this situation it achieved a consensus on the relative ranking of the receivers' spurious response capabilities as germane to a moderately dense co-site environment.

\* Other bands and modulation types were subsequently considered.

Each parameter chosen had to be measurable with good confidence. It is desirable to be able to calculate values for the EMC parameters when measurements are not practical (or feasible, e.g., before the equipment has been built). The parameters for transmitters and receivers finally identified by using the Delphi method are summarized in Table 1. Transmitter noise has been discussed by SHEPHERD and SMITH (1958). The other parameters are relatively well known. The symmetrical, analogous relationships between transmitter and receiver parameters can be noted (e.g., the adjacent-signal interaction involves the effects of a single transmitter on a receiver at relatively small frequency separations, as does the transmitter noise interaction).

TABLE 1 PARAMETERS FOR EMC FOM

Transmitter Parameters	Receiver Parameters
Spurious Emissions (SE)	Spurious Responses (SR)
Transmitter Noise (TN)	Adjacent-Signal Interactions (AS)
Intermodulation (TIM)	Intermodulation (RIM)

#### 4.6. Parameter EMC FOM Scores

Standard procedures for measuring the necessary input data required to calculate parameter scores are given by IEEE/ECAC (1974). These procedures are consistent with MIL-STD 449D (U.S. DoD, 1973) to the extent that this standard provides the necessary information. Ideally, data for the scoring formulas could be obtained directly from the specification sheets of equipment manufacturers. However, the committee has found a lack of appropriate standard measurement procedures and data for some of the significant parameters (e.g., TN), and the manufacturers' specifications currently do not contain all the information required to compute the EMC FOM.

The formulas for computing the parameter scores,  $S_p$ , are given in Table 2 (see the Glossary at the end of this paper for a definition of the terms used in these formulas).

TABLE 2 FORMULAS FOR PARAMETER EMC FOM SCORES

Transmitter Parameters	Receiver Parameters
<p>Spurious Emissions (SE)</p> $S_{SE} = \frac{S_{SEI} + S_{SEO}}{2}$ $S_{SEI} = \frac{170}{N_{SEI}} - P_{SEI} - 80 ; S_{SEO} = \frac{170}{N_{SEO}} - P_{SEO} - 80$	<p>Spurious Responses (SR)</p> $S_{SR} = \frac{130}{N_{SR}} + 2.5 P_{SR} + 10$
<p>Transmitter Noise (TN)</p> $S_{TN} = \frac{S_{TN(94)} + S_{TN(64)}}{2}$ $S_{TN(94)} = \frac{7}{\Delta f_{TN(94)}} ; S_{TN(64)} = \frac{40}{\Delta f_{TN(64)}}$	<p>Adjacent Signal (AS)</p> $S_{AS} = \frac{S_{AS(10)} + S_{AS(20)}}{2}$ $S_{AS(10)} = \frac{10f_0^{1/4}}{\Delta f_{AS(10)}} ; S_{AS(20)} = \frac{5f_0^{1/4}}{\Delta f_{AS(20)}}$
<p>Intermodulation (TIM)</p> $S_{TIM} = -2.5 P_{TIM} - 50$	<p>Intermodulation (IM)</p> $S_{RIM} = \frac{-400 \Delta f_{RIM}}{f_0} + 105$

It was necessary to develop a method of scoring to reflect, on a relative basis and in a linear manner, the amount of spectrum denied due to each parameter. The formulas were refined by modifying the basic linear term or its equivalent with a scale factor and an additive constant (or equivalent) to relate the scale to the state of the art and to typical (median) equipment (IEEE/ECAC, 1973, 1974). These formulas were developed so that a typical (median) equipment from the sample used by the committee would have a parameter score of about 50, and a state of the art equipment would have a score of about 100. However, neither of the end points of the scale are fixed, and negative scores or scores greater than 100 are possible for any arbitrarily selected equipment. An absolute scale with fixed end points has been suggested by Schulz (1974b). If such a scale (i.e., zero to one) is adjusted to give a score of one for the state of the art system and zero for the poorest example system, then the scoring formulas will require modification as more equipment are considered and as the state of the art changes. Furthermore, the requirement to give the median equipment (at the time the formula is developed) a score close to 0.5 becomes difficult to implement because of the number of degrees of freedom required.

#### 4.7. Equipment EMC FOM Scores

Equipment EMC FOM scores can be computed from the parameter scores. This can be accomplished in a straightforward manner by summing the parameter scores ( $S_p$ ) obtained by using the formulas given in Table 2 with appropriate weighting factors ( $W_p$ ):

$$\text{Transmitter score} = S_T = W_{SE} \cdot S_{SE} + W_{TN} \cdot S_{TN} + W_{TIM} \cdot S_{TIM} \quad (1)$$

$$\text{Receiver score} = S_R = W_{SR} \cdot S_{SR} + W_{AS} \cdot S_{AS} + W_{RIM} \cdot S_{RIM} \quad (2)$$

The weighting factors depend on both the equipment characteristics and the environment. By definition the sum of the  $W_p$  factors is unity. It is possible to compute  $N_d$  as a function of the number of identical systems (transmitter-receiver pairs) by using DUCE and noting the number of channels denied by each EMC parameter. These data could be used to provide estimates of the weighting functions as a function of the environment to be used in Eqs. (1) and (2). This was done for poor, average, and good equipment involving the following parameters:

- Frequency band: 223-400 MHz
- Channel width: 100 kHz
- Modulation type: AM
- Transmitter power: +50 dBm
- Desired signal: 10 dB > receiver sensitivity
- Receiver sensitivity: Input power (dBm) to yield S/N = 10 dB (no interference)
- Coupling loss: 60 dB
- Channel denial criterion:  $\frac{(S + I + N)}{(I + N)} \leq 10 \text{ dB}$

When the number of identical systems ( $N_s$ ) exceeded about eight, the weights were relatively insensitive to the size of the environment (see Figures 3 and 4 for examples). Estimates for the parameter weights in a relatively dense co-site environment (12 systems) based on this type of analysis are:

$$W_{SE} = 0.25, \quad W_{TN} = 0.6, \quad W_{TIM} = 0.15$$

$$W_{SR} = 0.1, \quad W_{AS} = 0.3, \quad W_{RIM} = 0.6$$

#### 4.8. Systems EMC FOM Scores

The final step in the building-block approach is to combine the equipment scores into a system score. As indicated, we define a basic system consisting of a single transmitter-receiver pair. For simplicity we exclude the antennas, transmission lines, and any external couplers and filters, but the FOM methodology developed should be capable of extension to more complete and complex systems. The final report (IEEE/ECAC, 1974) includes a first attempt at including couplers. Again, a simple weighted sum represents a straightforward approach:

$$S_S = W_T \cdot S_T + W_R \cdot S_R$$

As before, it is possible to run DUCE, keep track of the relative number of channels denied by the transmitter and receiver, and deduce average values of  $W_T$  and  $W_R$  from the data on  $N_d$  obtained as a function of environment and the quality of the equipment. Preliminary analyses indicate that for  $W_R > W_T$ :

$$W_T = 0.3, \quad W_R = 0.7, \quad W_T + W_R = 1.0.$$

#### 5. EXAMPLE CALCULATIONS

As previously mentioned, the committee found that measured input data for all the EMC parameter scoring formulas are not currently available. Typically, when transmitter noise data were available, data for the other parameters were not. We were able to obtain data for selected HF, VHF, and UHF equipment. The results of example calculations are given in Table 3.

TABLE 3 EMC FOM SCORES OF SELECTED EQUIPMENT

Equipment	$S_{TN}$	$S_{SE}$	$S_{TIM}$	$S_{AS}$	$S_{SR}$	$S_{RIM}$	$S_T$	$S_R$	$S_S$
HF-1	45	-8	18	65	58	53	28	58	49
VHF-1	26	94	48	113	39	17	47	48	48
VHF-2	55	48	54	64	103	57	53	63	60
UHF-1	24	71	28	104	98	97	36	99	80

Note that for these examples the transmitter scores are lower than the receiver scores (e.g., UHF-1 has a very good receiver from an EMC standpoint, but the transmitter is below average).

## 6. INTERPRETATION OF THE EMC FOM SCORES

16-9

The scoring method described under the building-block approach produces system scores on an absolute scale, according to the formulas used. It should be recognized that, in spite of its quantitative nature, the FOM yardstick under development is not precise. Small differences are not significant (but what is small?). For example, VHF-2 (see Table 3) scored higher than VHF-1, but did it score significantly higher? Runs of the DUCE program indicate that two conditions away on a five-level scale (see Table 4) can be taken as significant, whereas equipment or systems in adjacent categories may not differ significantly--especially if each score is near the same category boundary. Figure 5 shows the results of a DUCE run for the poor (Category I) and the good (Category V) receivers discussed in Sec. 4.7. These receivers are significantly different, but VHF-1 and VHF-2 probably are not significantly different for most applications.

TABLE 4 SUGGESTED RELATIONSHIPS BETWEEN EMC FOM SCORES AND EMC CAPABILITY CATEGORIES

EMC FOM Scores	EMC Capability Category
≤ 20	I (poor)
> 20; ≤ 40	II (below average)
> 40; ≤ 60	III (average)
> 60; ≤ 80	IV (above average)
> 80	V (good)

Another question raised by Table 3 is: Should unlike equipment be rated on the same scale and with the same parameter values? It is apparent that one should not attempt to compare an HF-SSB communications system with a X-band tracking radar, other than noting, for example, that they are both "good" relative to the state of the art. The procedures adopted to score diverse equipments should be similar in principle but different in regard to scoring parameters. The key to the answer to this question lies in the use of the FOM to help make decisions between alternatives.

Confidence in the FOM and its proper interpretation can be obtained by additional use of the DUCE program and the Delphi approach, but the user will need to calibrate himself on the FOM scale for his specific application(s).

## 7. POSSIBLE EXTENSIONS OF THE EMC FOM

One natural extension of the work to date would involve further development of the FOM described in this paper so that it could be applied to a more complex single-channel voice communication system (e.g., to add antennas, transmission lines, and couplers or filters to the "basic system" consisting of a transmitter-receiver pair). Such an extension is relatively straightforward when using the direct approach (DUCE), although the treatment of the antenna could require some sophistication. However, there are problems with the building-block approach (e.g., the EMC worthiness of good equipment might be improved little by the addition of a filter, whereas that of poor equipment might be greatly improved). The EMC goodness of a filter or coupler in a system depends on both its inherent properties and the properties of the system in which it is used. Consequently, the weighting factors for filters or couplers may need to be a function of the EMC parameters of the transmitters and receivers to which they are attached.

The current formulation of the FOM is useful to define possible interference interactions. Time-domain information may be required to better define probable interactions. For example, the likelihood of three-signal IM is less than that of two-signal IM during push-to-talk operation. Therefore, a logical extension might be to use estimates of time on the air to refine the weighting factors. This would have the effect of decreasing the size of the IM weighting factors and increasing the other weighting factors.

Broadening the FOM to include directly the frequency, time, and space dimensions opens up many possibilities, and the p(EMC) criterion can be reconsidered. For example, the FOM could then be applied to the frequency re-use problem--a problem beyond the scope of the current FOM because space information is not explicitly included in the formulation--but much more input data would be required.

Another chain of possible extensions consists of beginning again and defining a FOM for other classes of equipment (e.g., multiple-channel voice communications or radar). Still another category of extension would be to use the existing FOM in a broader context such as that of SCHULZ (1973). One could determine the importance of EMC considerations relative to the other considerations involved in system effectiveness, mission effectiveness and so on.

All these extensions are worthy of consideration, but it should be recognized that the p(EMC) criterion, if properly implemented, involves a considerable increase in complexity over the channel denial criterion.

## 8. CONCLUSIONS AND RECOMMENDATIONS

### 8.1. Conclusions

The channel denial concept provides a sound basis for developing an EMC FOM. The building-block approach can be successfully implemented when the required weighting factors are derived by direct calculation

16-10  
of denied channels in an assumed, moderately dense co-site environment. The scoring formulas developed by the committee to illustrate the method demonstrate the feasibility of a relatively simple (but meaningful and practical) EMC FOM based on measured equipment parameters. More work is needed to better define the required minimum FOM scores for specific groups of equipment and categories of applications, and feedback from those who use the FOM on a trial basis will be an important input.

The committee's investigations unearthed a series of deficiencies (or inadequacies) in certain current EMC standards and associated measurement procedures. Briefly, existing standards do not contain pertinent criteria relative to several important EMC characteristics. Where measurements are specified, they are frequently not designed to describe transmitter and receiver EMC characteristics adequately. Some of these inadequacies are discussed below:

Spurious responses and emissions--Existing standards specify criteria in terms of relative levels (i.e., decibels relative to sensitivity or rated power, or, for emissions in some cases, a minimum acceptable spurious output power level). An acceptable absolute power level, above which a spurious response would not result, would be more meaningful than a relative measure. Of even more significance is the need to measure and record the number of significant spurious emissions and responses, particularly those within the tuning ranges of the equipment and adjacent bands.

Receiver intermodulation--Current practices call for measurements and criteria involving a small frequency separation, often only one channel. This is essentially a test of receiver mixer characteristics. The one-channel RIM test is of interest, but it was not selected for use in calculation of the FOM because of an attempt to reduce measurement requirements. The nonlinear characteristics of the first amplifier and the amount of rejection provided to the first stage of amplification are of more significance in co-site situations. Larger input power levels and larger frequency separations are required to test the receiver's relative EMC capabilities in this important area.

Transmitter intermodulation--As in the case of RIM, current TIM measurements usually involve small (generally unspecified) frequency separations. The test is of value if properly performed, but does not reflect the transmitter's output selectivity characteristics. The use of a 5-percent separation represents a simpler measurement problem, and its result will, if adequate precautions are taken, describe TIM characteristics satisfactorily.

Receiver adjacent-signal interactions--Existing tests evaluate the effects of relatively small frequency separations. This approach is probably adequate for narrowband FM receivers. It is not adequate for narrowband AM (DSB and SSB) receivers, since cross-modulation effects (due to relatively large input interfering levels) can be generated in the first amplifier, (e.g., RIM) and noted at the receiver output. Also, use of input power levels specified in absolute terms will provide more meaningful results for AM receivers and will also be applicable to FM receivers.

Transmitter noise--Most existing standards do not contain an adequate description of a measurement procedure for this important parameter. Where existing criteria are available, only one power threshold is specified. The noise spectrum should be sampled at more than one frequency since some transmitters exhibit relatively high noise levels in a band close to the tuned frequency and relatively low levels at larger separations, whereas others exhibit virtually flat characteristics over a wide band.

## 8.2. Recommendations

It is recommended that the denied channel concept be reviewed, the proposed scoring formulas be used on a trial basis by equipment manufacturers and users, and the resulting experience be reported to the committee.

It is further recommended that the current EMC FOM be extended, as applicable, to more complex systems and to other classes of equipment.

Finally, current EMC standards should be reexamined in the context of the denied usage concept.

## ACKNOWLEDGMENT

The authors want to emphasize that this paper summarizes the status of the work of the committee named in the text, and want to thank the other committee members for their comments on a draft of the paper. The authors are solely responsible, however, for any errors of omission or commission that appear. The committee wishes to acknowledge the many helpful comments received from the EMC community during the course of its work, and to express its appreciation for the continual encouragement and support of Mr. J. P. Georgi of ECAC.

## REFERENCES

BERRY, L. A., and EWING, D. R., 1972, "A Systems-Specific Unit of Measure of Spectrum Space Use," Policy Research Estimate, Office of Telecommunications, Department of Commerce, Boulder, Colo.



- DAVIE, M. C., 1959, RAND Corporation, Santa Monica, Calif. (private communication to Lustgarten).
- DUFF, W. G., 1969, "EMC Figure of Merit for Receivers," in 1969 IEEE EMC Symposium Record, pp. 257-262. 16-11
- DUFF, W. G., 1974, "Transmitter and Receiver FOM Scoring," presented at 1974 IEEE International Symposium on EMC, San Francisco, Calif., 18 July 1974.
- HAGN, G. H., 1974, "Problems in Obtaining a System Electromagnetic Compatibility (EMC) Figure of Merit (FOM)," Symposium Record, 1974 IEEE International Symposium on EMC, San Francisco, Calif., pp. 277-281.
- IEEE/ECAC EMC FIGURE OF MERIT COMMITTEE, 1973, "Interim Report of the Electromagnetic Compatibility Figure of Merit (EMC FOM) Committee," Electromagnetic Compatibility Analysis Center, Annapolis, Md.
- IEEE/ECAC EMC FIGURE OF MERIT COMMITTEE, 1974, "An EMC Figure of Merit for Single-Channel Voice Communication Equipment," Final Report, Electromagnetic Compatibility Analysis Center, Annapolis, Md. (in preparation).
- ITU, 1968, Radio Regulations, Article 1, No. 93, International Telecommunication Union, Geneva, Switz.
- JOLSON, M. S., and ROSSOW, G. L., 1971, "The Delphi Process in Market Decision Making," J. Marketing Research, Vol. 8, p. 443-448.
- JTAC, 1968, "Spectrum Engineering--The Key to Progress," Joint Technical Advisory Committee, IEEE, New York.
- LUSTGARTEN, M. N., 1970, "COSAM (Co-Site Analysis Model)," in Symposium Record, IEEE International Symposium on Electromagnetic Compatibility, Anaheim, Calif., pp. 394-406.
- LUSTGARTEN, M. N., 1974a, "A Status Report on the Electromagnetic Compatibility Figure of Merit (EMC FOM) Committee," in Conference Record, IEEE Communications Society International Conference on Communications, Minneapolis, Minnesota, 17-19 June 1974, Cat. 74CHO 859-9-CSCB, pp. 26A-1-5.
- LUSTGARTEN, M. N., 1974b, "A Status Report on the Electromagnetic Compatibility Figure of Merit Committee," in Symposium Record, 1974 IEEE International Symposium on EMC, San Francisco, Calif., pp. 267-271.
- MOHR, R. J., 1974, "Denied Usage as a Basis for an EMC-FOM," presented at 1974 IEEE International Symposium on EMC, San Francisco, Calif., 18 July 1974.
- RACH, R. A., and SORKIN, I. J., 1974, Lockheed Electronics, Tucson, Ariz. (private communication to Hagn).
- SCHULZ, R. B., 1973, "A Rational Basis for Determining the EMC Capability of a System," in 1973 IEEE EMC Symposium Record, pp. 315-322.
- SCHULZ, R. B., 1974a, "A Rational Basis for Determining the EMC Capability of a System," IEEE Trans. EMC, Vol. EMC-16, pp. 109-114.
- SCHULZ, R. B., 1974b, "Preliminary Thoughts on an EMC System FOM," in Symposium Record, 1974 IEEE International Symposium on EMC, San Francisco, Calif., pp. 273-276.
- SHEPHERD, N. H., and SMITH, J. S., 1958, "The Gaussian Curse--Transmitter Noise Limits Spectrum Utilization," IRE Trans. Vehicular Commun., Vol. PGV-10, pp. 27-32.
- U.S. DEPARTMENT OF DEFENSE (DoD), 1973, "Radio Frequency Spectrum Characteristics, Measurement of," Military Standard MIL-STD 449D.
- VERSAR, Inc., 1971, "An Investigation Concerning Concise Measures of Electromagnetic Compatibility and Their Application to a Decision Rule for Spectrum Management," Final Report, Contract No. OTP-SE-71-101, Falls Church, Va.

#### GLOSSARY

##### Score Designators

The symbol  $S_X$  is used to represent the FOM scores (e.g.,  $S_{TN}$ ), where X is:

TN: transmitter noise  
 SE: transmitter spurious emission  
 TIM: transmitter intermodulation  
 AS: receiver adjacent-signal interaction  
 SR: receiver spurious response  
 RIM: receiver intermodulation  
 R: receiver  
 T: transmitter  
 S: system (transmitter-receiver pair)

Other Pertinent Factors

S, I, N: signal, interference, noise, respectively; usually expressed in milliwatts and converted to ratios in dB; e.g., S/N, S/(I + N), etc.

$P_D$ : desired input power level, in dBm

$P_I$ : interfering input power level, in dBm

$\Delta f$ : frequency separation, in same units as  $f_0$ , generally in MHz

$f_0$ : tuned frequency, generally in MHz.

Transmitter Spurious Emission (SE) Terms

$P_{SEI}$  = the average in-band spurious emission level (dBm)

$P_{SEO}$  = the average out-of-band spurious emission level (dBm)

$N_{SEI}$  = the average number of significant in-band spurious emissions

$N_{SEO}$  = the average number of significant out-of-band spurious emissions

in-band:  $0.5 f_0 \leq f_0 \leq 2 f_0$

out-of-band:  $0.1 f_0 \leq f_0 < 0.5 f_0$ ;  $2 f_0 < f_0 \leq 10 f_0$

Transmitter Noise (TN) Terms

$\Delta f_{TN}(94)$  = the mean frequency separation (MHz) from  $f_0$  (the tuned frequency) at which the noise power spectral density ( $N_T$ ) is 94 dBkT<sub>0</sub>

$\Delta f_{TN}(64)$  = as above;  $N_T = 64$  dBkT<sub>0</sub>

dBkT<sub>0</sub> = decibels relative to kT<sub>0</sub>, where k is Boltzmann's constant; T<sub>0</sub> is 288°K. For example, 94 dBkT<sub>0</sub> = -50 dBm/kHz; 64 dBkT<sub>0</sub> = -80 dBm/kHz.

(Note: To determine these mean frequency separations,  $\Delta f$  values are averaged to calculate a mean value.)

Transmitter Intermodulation (TIM) Terms

$P_{TIM}$  = the average level (dBm) of the two-signal, third-order TIM product measured when  $\Delta f/f_0 = 0.05$  and  $P_I = -10$  dBm.

Receiver Spurious Response (SR) Terms

$P_{SR}$  = the average value of input power (dBm) required to produce a standard response at a frequency outside a specified frequency range close to  $f_0$

Standard response = an output ratio  $(S + I + N)/(I + N) = 10$  dB measured with a distortion analyzer

$N_{SR}$  = the average number of significant spurious responses in a specified band.

Receiver Adjacent Signal Interaction (AS) Terms

$\Delta f_{AS}(10)$  = the average frequency separation at which a standard response is achieved when  $P_I = -10$  dBm,  $P_D = R_S + 10$

$\Delta f_{AS}(20)$  = as above, except that  $P_D = R_S + 20$

$R_S$  = receiver sensitivity; the value of input power, suitably modulated, that results in a standard response.

Receiver Intermodulation (RIM) Terms

$\Delta f_{RIM}$  = the average frequency separation required, if  $P_I = -10$  dBm (for both interfering signal levels), to produce a two-signal, third-order product equal to the standard response.

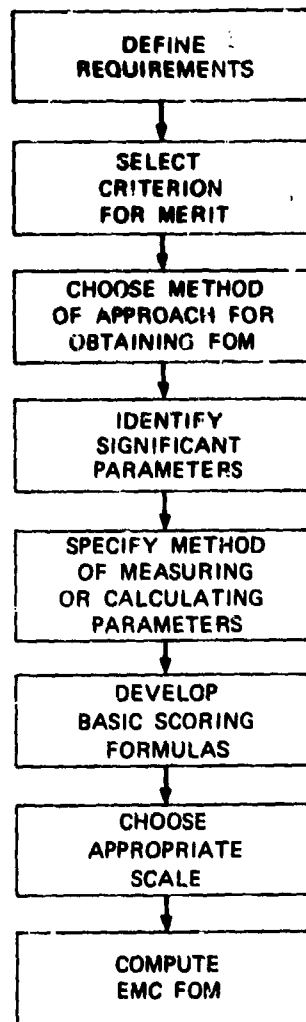


Fig. 1 Process of developing an EMC figure of merit

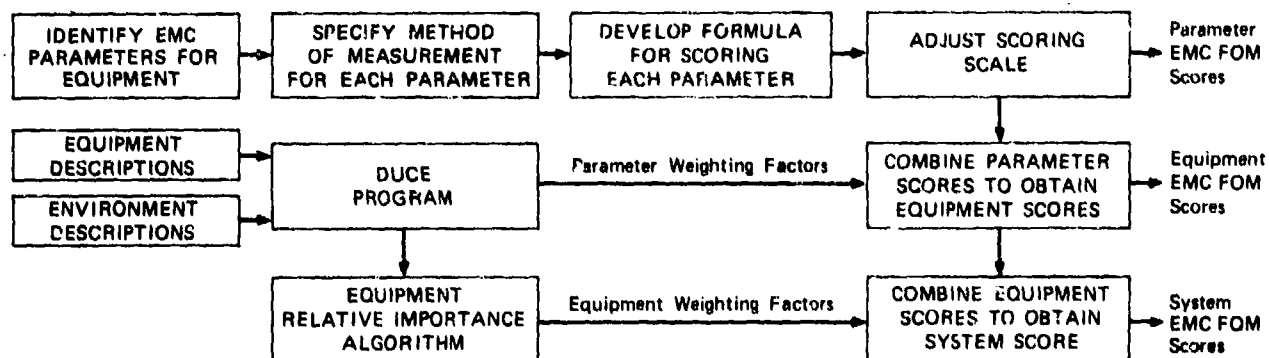


Fig. 2 Building-block approach for obtaining EMC FOM scores

16-14

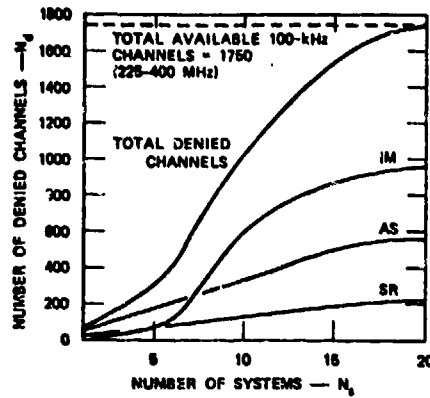


Fig. 5 Example comparison of poor and good-quality UHF receivers using Direct (DUCE) Approach

Fig. 3 Example of approximate relationship between  $N_d$  and  $N_s$  for a poor-EMC-quality UHF receiver

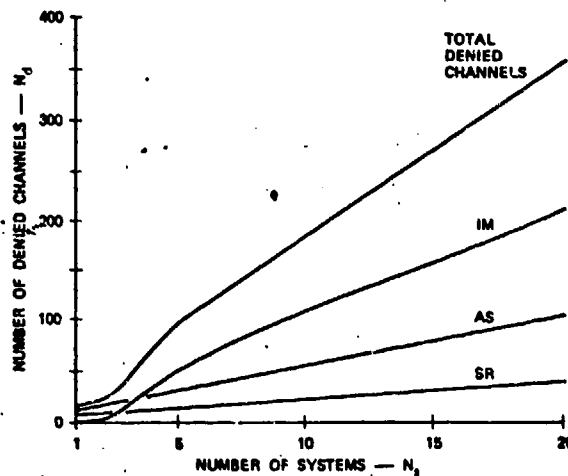
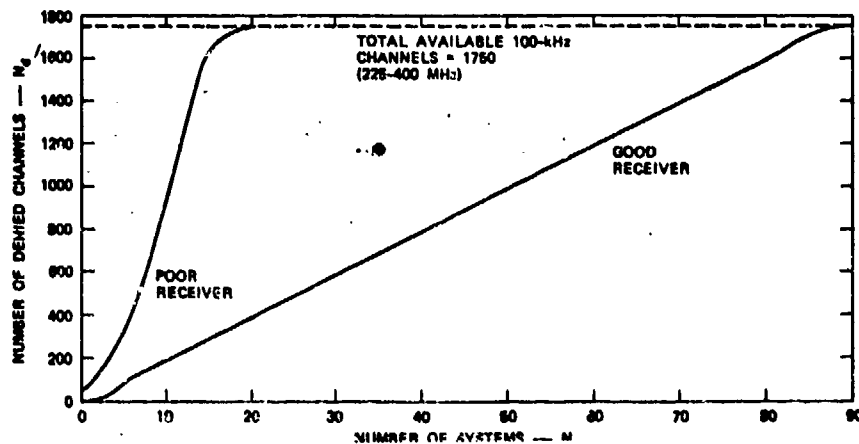


Fig. 4 Example of approximate relationship between  $N_d$  and  $N_s$  for a good-EMC-quality UHF receiver



## DISCUSSION

F. D. GREEN: Did your committee try this FOM in the real world?

G. HAGN: If one talks about computer models, yes--otherwise, no, although the members had some ideas of what systems were good or bad and these seemed to check out.

F. D. GREEN: I would assume, then, that another ad hoc committee would, during some forthcoming military exercise, test this FOM.

G. HAGN: Agree that this should be done, but it would require funds and effort to do so.

E. M. FROST: The way in which an equipment's performance changes with time is of great interest to maintainers. Has FOM been used to look at this problem?

G. HAGN: The FOM can be computed for new equipment or for equipment or systems in service which have been briefly taken out of operational use and sent to a laboratory for the required measurements. It would be interesting to check the change in FOM through the life cycle of an equipment from an FOM computed during the design stage to a measured FOM after some reasonable period in service.

R. J. MORROW: As you have stated, you still have to calibrate the EMC FOM method. Isn't this the same process as initially forming the method, with the exception that you have a given set of parameters? Would it have been more pertinent to have devised the method from realistic test scenarios using postulated parameters to produce a validated EMC FOM predictor?

G. HAGN: The committee discussed the possibility of computing the probability of some level of interference for specific scenarios using a simulation such as the Cosite Analysis Model (COSAM) and rejected this "self-calibrating" approach for several reasons: 1) A detailed specification of the environment is required to do the computation properly, and such information is generally not available. 2) It would be necessary to run the analysis model many times for different possible environments and average the results. 3) This approach would be time consuming and the results might be difficult to interpret.

For these reasons, the committee chose the simpler channel-denial approach to produce a scale of EMC quality which users of the FOM can relate to their own EMC requirements through feedback of information on operational EMC performance as it correlates to the FOM for a given equipment and through the use of their own simulations.

ELECTROMAGNETIC COMPATIBILITY IN MILITARY AIRCRAFT

D H Hight and W A Kelly

Procurement Executive, Ministry of Defence  
77 New Oxford Street  
London

COPYRIGHT ©  
CONTROLLER HMSO LONDON 1974

SUMMARY

This paper outlines common sources of electromagnetic compatibility problems and discusses the difficulties confronting engineers who are responsible for producing successful aircraft weapon systems. It starts with the definition of EMC and then considers EMC within the context of an aircraft weapon system. It argues that EMC problems can be minimised by (a) defining clearly the requirements of the weapon system (b) translating this requirement into an overall system specification (c) defining sub system and installation specifications (d) writing an EMC control plan and (e) producing a detailed test plan.

To achieve EMC a single responsible authority is desirable and this should extend to cover, as far as possible, all aspects of electronic installations in aircraft. Only then can information arising from measurement programmes and from curative action be collated in such a way as to produce an effective code of practice. Information can then be disseminated which will lead ultimately to a better general understanding of the problems and thence to better standards of specification, design, implementation and testing.

## 1. INTRODUCTION

The purpose of the paper is to present a broad introduction to the subject of electromagnetic compatibility in aircraft and a general appraisal of engineering techniques and organisational methods which can contribute to the reduction of EMC problems.

It is useful to commence with a practical definition of aircraft EMC. It may be stated that electromagnetic compatibility is the ability of each sub-system to function correctly in the presence and functioning of all other sub-systems within the confines and environment of the aircraft wherever such simultaneous functioning is necessary.

It is proposed for convenience to divide the total task into two aspects, namely, the aircraft avionics and weapon system per se, and the totality of the environment in which the aircraft must operate in order that its mission will be fulfilled. In the present paper only the former aspect will be treated on the grounds that many of the techniques of installation design, installation practice or task management efficacious for dealing with this aspect can be extended and modified to cover the environmental aspect as found necessary. There is little need to evolve new techniques.

Electronic systems fitted into military aircraft have continuously increased in number and complexity, in fact, it is probable that the only limitation to this increase is the volume and weight that can be made available within the aircraft. As the packing density of electronic components increases, systems become more numerous and complex. Problems and difficulties which we now face can only be expected to get worse; thus, it is not enough to remedy the present situation, means must be found to enable us to look into the future of aircraft electronic installation with greater confidence.

## 2. AIRCRAFT EMC PROBLEMS

The EMC problems encountered in military aircraft can vary from interference on the communications system as where a member of the crew of a large aircraft leans forward and brings his boom microphone into the magnetic field of the windscreen wipers, to the case where an HF transmitter would upset the aircraft autopilot and instruments to such an extent as to make the aircraft unsafe to fly.

Many of the major problems concern HF transmitters which can induce signals into aircraft wiring. This problem becomes more acute when the method of wet bonding aircraft panels is used to prevent corrosion, a technique which may introduce doubtful and variable electrical continuity across the skin of the aircraft. Similarly the increased use of fibre-glass particularly on helicopters removes the screening that once existed between the radiated signal and any aircraft wiring. The result is that the EM field inside the aircraft can be much greater than that quoted in EMC specifications against which electronic equipment is tested.

Situations have been detected where some of the radiated signal from an HF transmitter was picked up by the amplifiers of the control surface sensors of an autopilot system and could cause false operation. This indicates the seriousness of the problem.

Another common potential defect is where HF can get into the communications system and cause distortion or non-intelligibility of the speech.

Again HF can be picked up on control cables and cause the spurious operation of equipment such as ILS, the lighting of warning lights or the incorrect reading of flight instruments. Harmonics of the transmitter frequency get into VHF and UHF receivers so making a number of their channels unusable.

An associated problem is the siting of aeriels. Unless these are carefully chosen with relation to each other, as well as for optimum radiation at the operating frequency, there will be little isolation between aeriels. The significance of this is extremely difficult to determine in actual aircraft installations because the terminating impedances are rarely known at the interfering frequencies. To determine these values under all conditions would add considerably to the overall aircraft testing costs. Nevertheless, strong coupling can cause blocking or at least desensitisation of a receiver and may also have a dramatic effect on the polar diagram of the aerial so that communications range in a particular direction is reduced.

A further problem can arise in aircraft which use titanium for their construction. The material has a much lower conductivity than aluminium so where titanium has to be used in the vicinity of a notch aerial the losses will increase and the radiation efficiency of the aerial will deteriorate.

Some radar designs have introduced trouble by producing interference in the VHF band. It has been known for them to be the cause of an HF Aerial Tuning Unit (ATU), when it is in a strong radar beam, to retune to the wrong frequency without any indication on its control unit that this has happened.

Aircraft power supplies are derived from generators which besides producing power at the fundamental frequency inherently produce some at the harmonic frequencies and this is fed round the aircraft on supply lines. This problem is well known by generator and equipment manufacturers so providing the relevant specifications are met there is seldom any major difficulty encountered.

Pulses with fast edges carried on cables can cause embarrassment; for example, feeding a 2 MHz square wave between a radio and its controller. The sharpness of edge can result in interference at each even MHz throughout the HF, VHF and UHF bands, much in excess of specification levels. The use of double screened co-ax or balanced, twin co-ax cable may not be sufficient to eliminate the problem. It may take a considerable time to determine the solution.

One can find a system operating incorrectly in an aircraft although the equipment itself passed its EMC tests. In such a case a painstaking and costly process must follow in the course of which the equipment and installation are modified to enable the equipment to operate in its environment.

### 3. DIFFICULTIES CONFRONTING ENGINEERS

The difficulty in producing a good EMC installation will broadly depend upon the electronic complexity per unit volume of the aircraft although this is difficult to quantify. A list by general types of aircraft in order of increasing difficulty is shown below.

- (a) Transport aircraft
- (b) Other large aircraft
- (c) Helicopters
- (d) Strike aircraft

If the avionic equipment is developed in the same time frame as the aircraft the equipment cannot be checked in the airframe during the aircraft development. Development models of the equipment, if available, could help but are rarely fully representative of the production equipments, which is afterwards used as an excuse for any short fall in performance.

The checking of an installation for EMC is a time consuming negative process and so is competing with other testing that is required. Unless the system performance specification is well written there may be little to justify the aircraft contractor spending sufficient time on checking EMC. This can be very significant with a fixed price development if adequate consideration of EMC is not ensured in the tendering stage by a good clear specification. Thus in some cases it may not be until the aircraft clearance trials that the problems show up, and even then the incompleteness of the electronics fits may militate against the delivery of incompatibilities.

During the aircraft clearance trials the installation may not be complete because some development equipment will not be available. Then the equipment needs to have a separate evaluation trial, by which time the aircraft may be in production so that it will be much more difficult to introduce any necessary modifications to the installation. Further problems exist when a new equipment is required to operate in an in-service aircraft. In this case the installation has to be modified to fit the new equipment and this will be sent for trials. If the existing installation in the aircraft has not been tested to an EMC specification or at best to a lower standard this will increase the likelihood of difficulties.

#### 4. METHODS OF TECHNICAL IMPROVEMENT

There appears to be little point in tightening the equipment EMC specification in the hope of overcoming EMC problems because the changes in levels required would be so great as to prevent an equipment being produced at an acceptable cost, but equally, it is vital that all equipment does meet the requirements of a suitable EMC specification. Improvements must come from an integrated approach to aircraft weapon systems in which each installation is specified as a sub-system, tested and proved as much before being introduced into the aircraft, and by the application of good engineering practice during the design and manufacture of the aircraft and installation.

Electromagnetic interference (EMI) is caused mainly by

- (a) Radiation from aerial to wiring or equipment
- (b) Reception by aerial of interference from wiring or equipment
- (c) Coupling between aerials
- (d) Coupling between cables
- (e) Coupling due to common earth impedance
- (f) Coupling due to earth loops
- (g) Conduction along power supply lines.

The interference caused by these mechanisms can be reduced in general to an acceptable level by the following simple procedures.

(a) By ensuring electrical bonding of aircraft panels and earth leads is satisfactory. By checking that paint, anti corrosion duralac, anodising or corrosion do not prevent good electrical connection. The bonding of panels is particularly important in the vicinity of an HF aerial, where large circulating currents must flow in the aircraft skin to provide an effective communication media, otherwise high levels of harmonics and intermodulation frequencies will be produced by any non-linearities.

(b) By ensuring screening of cables is satisfactory at all irradiating frequencies and that plugs and socket are effective. Where there is fibreglass or open work construction of the airframe additional screening must be provided between an aerial and any cables or equipment, bearing in mind that significant amounts of power are diffracted over edges etc. The chief offender here of course is the HF radiator which may well be a sizeable portion of the airframe, but similar precautions may sometimes be necessary for higher frequency aerials especially at VHF and UHF.

(c) By making the distance between an HF aerial turning unit (ATU) and its radiator an absolute minimum and by screening the lead between the two. This screening will generally need to be in the form of a large diameter high conductivity tube because even small stray capacity to the feeder lead can prevent certain tuners from functioning correctly.

(d) By keeping signal and control circuits relatively low impedance to minimise the effect of capacitive coupling of interference from other circuits. Very low impedance circuits, however, would require relatively high signal currents and these could then couple inductively.

(e) By using screened balanced and matched twisted pair cable (duradio) to carry the the information along any exceptionally sensitive signal or control circuits.

(f) By separating susceptible signal lines from transmitter feeder cables, power lines and other possible sources of interference which may include other signal and control lines.

(g) By keeping the bandwidth of signal circuits to the minimum necessary to their function eg an audio amplifier should not respond to HF frequencies just because the transistors or integrated circuits have inherent gain at these frequencies. Pulse streams to and from digital equipment should have pulses shaped to minimise the harmonic power content and thus the radiation of high frequency interference.



(h) By avoiding ground loops to prevent inductive coupling. Where a screened cable cannot be run against an grounded metal structure it may be necessary to break the screen at some point so this does not form a loop with the grounded structure of the aircraft.

(i) By keeping ground leads as short and as straight as possible and also wide to minimise their inductance. By taking care to avoid resonant lengths.

(j) By providing a separate ground wherever possible especially for sensitive signal lines to avoid the coupling which arises from the common impedance introduced by common ground returns. By taking care to prevent these separate ground lines from coming into contact with other ground paths such as the airframe, due to wear and tear.

## 5 NEED FOR CONTROL

Good EMC will only be obtained with good technical control of the design and implementation of electronic installations and this can only be achieved if the requirements of the weapon system are clearly defined and interpreted. There are a number of well known and frequently-stated steps which are essential and include:

(a) A clear statement of what the aircraft weapon system is required to accomplish at all phases of the operation. The operational requirement must be quite clear about the operational performance required of each sub-system of the overall weapon system. It is little help to define equipments carried without clearly stating the performance required. It should be possible to deduce which sub-system will never have to operate at the same time as others as this may enable the cost of achieving EMC to be significantly reduced.

(b) This operational requirement has to be translated into an overall weapon system specification. At this stage the operational performance requirements are translated into electrical performance requirements. The siting of aeriels has to be arranged to ensure that the radiation characteristics are adequate with the minimum of mutual coupling between each in spite of the severe limitation imposed by mechanical and aerodynamic requirements.

(c) Detailed sub-system specifications are written which lead to detailed equipment, installation, and testing specifications to enable the equipment and its installation to be well designed and constructed. The specification for each sub-system and equipment is written so as to obtain the performance required of the weapon system. These specifications will call for EMC tests on each equipment. If equipments were defined in the operational requirement it will become clear whether the equipment quoted is capable of meeting the performance required.

(d) An EMC control plan is written to ensure that EMC requirements are considered throughout the development. It defines areas of responsibility, specifications and levels of test, and the engineering design procedures to achieve EMC. It may require the manufacture of a mock-up of the avionics installation to allow EMC tests to be made during the development and so help to give an early warning of any lack of EMC.

(e) A detailed plan is required to ensure that correct functioning of each sub-system is achieved in all circumstances. The EMC test plan will define tests to be performed with each sub-system, within the complete aircraft weapon system, to ensure that the sub-system works satisfactorily, does not interfere with any others and is not interfered with under any operational condition.

## 6 SINGLE AUTHORITY

EMI can be controlled individually for each aircraft development or be the responsibility of a specialist authority. This latter system has merits for the following reasons.

(a) It can provide a focal point to establish common approaches to the education of contractors and others in EMC, common approaches to research and provide stimulus to the specialist to reduce interference to other peoples equipment. If the only focal points are specific to aircraft there is a natural tendency to treat aircraft projects discretely so that a given project may not benefit from lessons learnt in seeking EMC in other projects.

(b) It has to be determined who should provide solutions to EMI problems: those responsible for the interfering equipment or those for the susceptible equipment? Where aircraft constructors have this responsibility, they may require expert assistance to deal with the wide range of problems which can arise so as to ensure the most cost effective solution is found.

(e) It allows documentation of information on EMC short-comings and troubles in service. Better documentation will make it easier to decide how much total effort is justified in tackling work programmes and what these should be.

A single authority concentrates available knowledge and experience so that proven advice can be given and so that a uniform and cost effective approach can be made to EMI for any weapon system.

## 7 CONCLUSION

Many EMC problems arise from the lack of clear specifications for electronic installation, which discourage the aircraft contractor from investigating the full implications of the design and implementation problems which will arise. This leads to an under estimate of the effort required to design, construct and test the installation so that an inadequate estimate of the cost involved in both time and money follows. Only by stating the requirement in the most precise terms will this be overcome. Where existing systems of EMC control are inadequate, this precision will result in an increase in the initial cost of new aircraft weapon systems. This increase should, however be more than offset by the reduction in number and cost of subsequent modifications, an earlier date into service and improved operational performance of the aircraft weapon system.

## REFERENCE

KELLY, W A and BURBERRY, R A, 1971, "A Review of Helicopter Aerial Problems", IEE Conference Publication Number 77 (Aerospace Antennas).

## DISCUSSION

G. H. HAGN: What impact on EMC in aircraft will the introduction of fiber optics cause, and is this being considered in the UK?

P. W. SMITH: Reference to fibre optic transmission is being worked on experimentally in the UK. Computer-to-computer links working up to 5M/bands over 75 metres have been constructed and work now proceeds to make operational fibre optic systems using multi-fibre, multimode systems. Perhaps later we shall be going towards using integrated optics and single fibre techniques.

## ELECTROMAGNETIC COMPATIBILITY CONTROL PLANS

P.D. Campbell, C.Eng. M.I.E.R.E.  
Lucas Aerospace Limited  
Maylands Avenue  
Hemel Hempstead  
Hertfordshire.

### SUMMARY

The spectrum and level of radio-interference have been measured for years and unwanted emissions reduced retrospectively. This remedial approach is now recognised as inefficient but the concept of electromagnetic compatibility as a design parameter still requires emphasising.

Electrical and mechanical system and equipment engineers are relatively inexperienced in E.M.C. measures and control plans advise and assist in this discipline.

The devices, circuits, components and constructional details which can contribute to the creation, conduction and emission of unwanted signals are indicated and means whereby their effects can be minimised are examined. The problems arising in creating and implementing a control plan for the development of a typical piece of electrical equipment are outlined and the difficulties experienced in balancing operational, theoretical, practical and contractual requirements are high-lighted.

### INTRODUCTION

The concepts on which systems and equipment design are based depend not only on the operational requirements including the electromagnetic environment but also on the susceptibility of other adjacent equipment. It is thus necessary to live and let live under operational conditions and the limits of each specification must be tailored to the individual conditions if this aim is to be achieved without undue size, weight and cost penalties.

The creation of an effective control plan thus involves early and close consultation between designer and E.M.C. engineer if optimum performance is to be achieved with a minimum of subsequent changes and this involves the following logical steps:-

- (1) Examination of the operational requirements of the equipment and decision on how they can best be met.
- (2) Breakdown into classes the functions which must be performed within the equipment and the circuits needed to carry them out.
- (3) Select the circuits either least likely to create conducted or radiated noise or those most simply suppressed.
- (4) Identify noisy components or leads and estimate the amplitude, waveform and frequencies involved.
- (5) Recommend protective measures to isolate emitting sources, to prevent the transmission of spurious conducted or radiated signals and to eliminate earthing problems. Protective measures must not affect operational performance.

### OPERATIONAL REQUIREMENTS

All equipment is required to perform a specific operational role which may be electrical, electromechanical, or mechanical and usually this role can be performed in a variety of ways. It is the function of the equipment design team and the E.M.C. engineers, to collaborate to achieve the desired end product in the simplest, most efficient and economical manner. Initial detailed design then proceeds on the agreed compromise between equipment performance and E.M.C. requirements and at the same time any justifiable deviations from the specification are negotiated with the procurement agency.

### CONTROL PLAN CONTENTS

The control plan will generally include the following aspects:-

- (1) Management Controls.
- (2) Frequency Selection.
- (3) Mechanical Design.
- (4) Electrical Design.
- (5) Wiring Layout.

## CONTROL PLAN CONTENTS (continued)

18-2 Management Controls is the subject of a separate paper and is not discussed here. Frequency Selection is of primary importance in communications, telemetry and data logging but in the low frequency electrical and electronic equipment field, it is less important since it is confined to oscillator frequencies, pulse rise times and harmonics.

### Mechanical Design

Mechanical design not only caters for the physical support of components and wiring but also provides inherent attenuation to electromagnetic radiation. Radiating fields must be contained or excluded from equipment boxes which must be of suitable materials of adequate thickness.

The fields maybe magnetic (low impedance), electric (high impedance), plane wave (characteristic impedance of 377 ohms) and to achieve high shielding effectiveness it may be necessary to use composite materials and nesting technique.

Internal field coupling can be reduced by providing individual screened compartments, e.g. at oscillators, transformers and chokes. To maintain shielding integrity, all lines entering or leaving equipment enclosures should be effectivity decoupled by suitable filters while signal and control lines may have to be twisted and/or screened. Methods of calculating shielding effectiveness and shielding theory are described in Reference 1 (SCHELKUNOFF S.A.).

Efficient bonding between equipments and enclosures is essential if shielding is to be effective and poor engineering techniques and practices can contribute to interference and degradation of performance. The bonding of units together prevents the development of electrical potentials between the individual cases so that they approximate electrically to a single homogenous structure. All control plans should recommend the following practices:-

- (1) Permanent bonds should be used wherever possible particularly where shielding integrity is at risk. Welded or brazed joints are preferred as soldered bonds need to be mechanically reinforced, while clamped joints depend entirely upon good assembly control techniques.
- (2) Bonds should be broad, thin, as short as possible and readily accessible. To ensure low impedance at radio frequencies a length to width ratio of 5 : 1 is commonly used. In addition the strap must be compatible with its environment, e.g. vibration, temperature variation, expansion and contraction.
- (3) Bonds must make good metal to metal contact over the surface of the joint which must be clean and free from low conductivity finishes. Where dissimilar metals have to be used select materials having an electro-chemical potential difference not exceeding 0.25 volts. In all cases the finished joint should have a protective coating of grease or polysulphate.
- (4) Spring fingered contacts, conducting gaskets, or bond straps as appropriate must be introduced to maintain shielding effectiveness of joints. These should be installed where there is a requirement for removable covers, hinged lids, anti-vibration mountings and other situations where movement can occur.
- (5) Ventilation of equipment enclosures is frequently required and it is essential that louvres, ducts, and holes are masked by metallic gauze or similar materials to prevent leakage of radiated fields. These must be bonded in accordance with the above recommended practices.
- (6) A good basic ground plane and ground point are essential to the interference free operation of equipment. The former should be as near to zero potential, zero impedance as can be achieved practically and the physical layout, size and length of ground connections must be selected to give minimum impedance. The plane may be used as a reference for signal circuits or a means of eliminating unwanted signals and ideally should absorb all signals and remain stable. If a ground connection is improperly made circuit operation may be impaired and more interference introduced than would have occurred by its omission.

Equipment manufacturers are seldom allowed to select ground points or ground planes and can only minimise the inductance and impedance of the bond straps taking account of local resonant circuits, skin effects and coupling factors.

### Electrical Design

Interference may be inadvertant, a consequential by-product of a specific circuit function or accessory operation. It may also be generated spuriously by poor circuit design, bad wiring techniques, low quality components or accessories used in the equipment design. The most prolific generators of interference are switches of either mechanical or semi-conductor types, while semi-conductors themselves can produce spurious interference in many circuit applications. Some of the more important sources are discussed and some methods of interference reduction are indicated.

## Electrical Design (continued)

Wherever possible interference is reduced to tolerable levels at source, but when this cannot be achieved shielding as previously described is used to contain the interference source and the input and output lines are filtered to attenuate the noise.

### Mechanical Switches

Any switch normally cannot make or interrupt the current flowing through its contacts without causing an electromagnetic disturbance, that is there cannot be a smooth transition between the "ON" state and the "OFF" state and vice-versa. Upon closing a pair of switch contacts the final mating at the contact surfaces is preceded by a series of premature closures, or bridging of the contacts. Similarly on opening the final parting of the contacts is preceded by transient premature openings. These changes in impedance generate interference whose characteristics are governed by local circuits. When separating contacts create an arc this may self-oscillate or cause associated circuits to oscillate. When a switch breaks a highly inductive circuit, high voltages are generated at the contacts which can cause a spark or glow discharge both of which generate interference.

The change of current between the ON and OFF conditions produces interference which is significant at low frequencies up to a 1.0 MHz. approximately thereafter it will decrease at a rate of 40 dB/decade. The bridging phenomena has a minimal effect at low frequencies but increases with relative significance to about a 1,000 MHz. where it can be as severe as the interference produced by sawteeth.

The interference produced by sawteeth extends over the frequency range 10 KHz. -1,000 MHz. and is more severe than that generated by the other sources having a broad peak over a frequency range of 100 KHz. to about 5.0 MHz. for the more usual circuit parameters.

The reduction of interference from switches and the associated loads may be achieved by resistance and capacitor combinations, diodes and/or Zener diodes. The disposition of the components either at the switch contacts or at the load is determined from the circuit application, space available, practical considerations and the economics of including the suppression components. In severe cases additional suppression is achieved by adding filter networks to the switch circuitry.

### Transistors

Interference generated by transistor circuits is either noise inherent in all transistors or spurious signals generated by the operation of the associated circuits. Transistor noise may be thermal or recombination agitation in the base region or diffusion fluctuation of minority carriers after crossing a junction. These effects only become important in very low signal applications which is a specialised field.

It is convenient to analyse transistor circuits in terms of either small or large signal operation. In small signal operation it is safe to assume linear operation and in general interference is tolerable in most electronic circuitry. Communication equipment is more susceptible and may respond to interference causing image, spurious and harmonic responses and can also affect I.F. stages, but these effects are not considered in this paper. Large signal operation can occur in communication equipment and can cause a transistor to be driven into the non-linear region producing spurious interference such as cross modulation, desensitization and blocking. Recognition of the possible consequences of these spurious responses should be noted early in the design stage and remedial action introduced into the equipment design.

In electrical and electronic equipment applications transistors are used in the large signal switching mode to obtain high efficiency and irrespective of whether they are used in single shot or repetitive circuits high levels of interference are generated. This may be narrowband, broadband, or a mixture of both over a defined frequency range. The essence of any control plan lies in reconciling reduction of interference without loss of efficiency.

### Silicon Controlled Rectifiers (S.C.R.)

The regenerative turning on action of a S.C.R. produces a very rapid switching which may excite associated devices or supply lines by shock action and the resulting fast rate of current change can cause induced voltages to appear. Power supply lines with their distributed inductance and capacitance resonate readily at frequencies dependant on their parameters typically between 250 KHz. and 5.0 MHz.

There are two basic interference reduction procedures one where an r.f. ground is not available, for example, power supplies in building installations, the second where there is an effective ground available. The power supplies in aircraft and military vehicles are invariably contained in a metal case which can be considered as an r.f. ground.

## Silicon Controlled Rectifiers (S.R.C.) (continued)

184 Where an r.f. ground is not available Figure 1a. is an example of an interference reduction circuit while Figure 1b. illustrates an example where a r.f. ground is readily available. The two examples assume that the device switching speed is non-critical and both methods contain and localise the initial high rate of current rise to the smallest practicable section of the device circuit. The capacitor, which should be non-inductive, provides a return path for the high frequency component of the interference circuit. The inductors are usually required to exhibit their full value only during the initial turn on and their physical size can thus be reduced by allowing them to saturate. The radiated interference must be contained by electrostatic screening which should be volumetrically small so that the high rate of change of current is confined to the immediate surroundings of the device.

## Semi-Conductor Diodes

Diodes can generate broadband interference over a considerable frequency range. Generally a diode cannot switch instantaneously from a conducting to a non-conducting state. When a diode passing forward current is forced into a non-conducting state by reverse biasing the current carriers in transit through the junction are trapped in the semi-conductor material and must suddenly attempt to reverse their direction of flow. The resulting surge of current through the diode and associated load results in the generation of broadband interference whose amplitude and frequency spectrum are functions of the diodes transient characteristics and the load parameters. Diodes must be carefully selected and the following rules assist in choosing a diode for a particular application.

- (a) The operating current density should be low in comparison with the manufacturers maximum current rating.
- (b) The diode should be selected such that the peak working and peak inverse voltage ratings are never exceeded.
- (c) The intensity of interference from diodes is a function of the device switching rate, the faster the rate, the higher the levels of interference, hence choose the slowest switching rate commensurate with the application.

When diodes have to be suppressed by the addition of filter networks these must be fitted as close to the diodes as is physically practicable to give maximum effectiveness.

## Transformers

Low power transformers at line frequencies can often be susceptible to interference voltages e.g. when induced by stray magnetic fields, common mode signals, or machine made disturbances. The effects of external magnetic fields can be reduced by screening with cans constructed from mumetal and when this gives insufficient attenuation two or more of these can be nested together with copper interleaving reducing signals by over 100 dB.

The levels of pick up which can be obtained will depend upon the physical orientation of the transformer with respect to the interfering magnetic field. The positioning of transformer and chokes relative to each other and other components in any assembly must thus be considered to obtain minimum interaction.

A Faraday Shield is used between transformer windings to give a high level of electrostatic isolation. It is a grounded area of metal placed between the field and the winding to be protected and positioned parallel with the magnetic field and must not form a short circuited turn. The impedance of the shield should be as low as possible so that it approaches a true equipotential surface.

## Suppression Filters

Suppression filter design and applications are very fully described in current technical literature but there are some aspects which merit discussion. The manufacturers of proprietary filters quote "INSERTION LOSS" in a 50 ohm matched system and not an attenuation value. The actual impedance is seldom 50 ohms or matched, consequently attenuation values may be significantly different from the expected figure, in addition they may not damp resonances which can occur between the suppressor and its load. Designs to overcome these difficulties are described in Reference 2 (JARVIS M.L., 1972). Consideration must be given to voltage, current and temperature ratings of the filter as well as the resistance presented to the circuit. The effect of filter capacitance to ground is also significant in some applications and can influence the choice of filter configuration.

## Oscillators

Radio frequency oscillators can generate harmonics in addition to the natural frequency both of which can cause interference. This type of oscillator can affect analog amplifiers but seldom affects digital equipment providing the interfering field is kept within 2.0 volts per metre. To reduce the interference effects of r.f. oscillators the following can be introduced into a design:-

### Oscillators (continued)

- (1) Avoid excessive voltage swings.
- (2) Keep the harmonic content low.
- (3) Screen all oscillator sections and keep the wiring within short so as to avoid coupling loops.
- (4) Filter the power supply to the oscillator using feedthrough or bulkhead suppressors which have been correctly installed into the screen.
- (5) Screen the output from the oscillator or judiciously route it within the unit container.

Oscillators of the switching variety particularly in the power sections of equipments are sources of interference, which may have an undesirable influence upon digital circuitry. The high rate of change of current associated with these oscillators produce fields which in general exceed the levels produced by r.f. oscillators.

The effects of switching oscillators can be minimised by all or some of the following actions:-

- (1) Keep rates of change of voltage and/or current to a minimum consistent with operational requirements.
- (2) Screen the oscillator section.
- (3) Incorporate filters into the oscillator screen assembly.
- (4) Avoid large coupling loops within the assembly.
- (5) Where possible filter oscillator output, where this is not possible twist and screen output leads.
- (6) The active devices contained in the oscillator should have switching times which are commensurate with each other.

### PREDICTING LEVELS OF INTERFERENCE AND SUSCEPTIBILITY THRESHOLDS

It is desirable to predict the levels of interference associated with pulses of differing shapes and the method of evaluating pulse interference described in Reference 3 (REHKOPF H. L., 1962) has been found to give dependable results. The method enables designers to determine the type and degree of suppression so that compliance with the application specification can be achieved, this results in rapid and simpler design because filtering and shielding can be kept to a minimum.

If the prediction forecasts non-compliance with the specification or indicates unacceptable penalties, tailoring of the specified limits must be requested from the procurement agency. The revised limits must ensure that the equipment will remain compatible with the E.M.C. environment, installation and operational requirements.

Additionally, procurement agencies often ask for the impossible for instance fully meeting the requirements of RE.01 of specification MIL-STD-461A which is intended for underwater vehicles and normally not for avionic requirements.

The following examples show the implications of fully meeting the requirements of RS.01 and RE.01 of MIL-STD-461A. They are modelled on a single loop turn and a frequency range restricted to the frequency range 30 Hz. - 1 KHz. The details are given in Figure 2.

The susceptibility loop model represents an electronic circuit operating at a current of 10 mAmpere typical of many circuits which may operate at frequencies above 0.5 MHz. but remain susceptible to low frequency signals. The levels are shown in Table 1(a) and the results indicate that a shielding enclosure must reduce the specified level by 46 dB.pT. at 30 Hz. for the circuit to be susceptibility free, the table gives the thickness and weight of materials for an enclosure of 14 cm side.

The radiating loop model represents a low power electric circuit operating at a current of 1.0 ampere and Table 1(b) shows the levels generated by the loop together with the thickness and weight of material needed to provide shielding. The weight penalty imposed by meeting specification fully are clearly indicated for an enclosure of 14 cm side.

It is usual practice to shield low frequency magnetic fields with ferrous materials or alloys, but as frequency increases the choice of materials is less restricted and non-ferrous materials can be used to advantage. Both examples underline the significance of attempting to comply with the requirements below 400 Hz. and how essential it is to define problem areas early in a design programme.

The broad principles which must be followed in preparing a control plan have been described above but the critical test of such procedures lies in their effectiveness during the design of the equipment. The problems arising in the design of a jet engine ignition unit and their solution is examined in detail. The electrical requirements are given in Table 2. This unit has been chosen since it combines the effects of electronic switching, magnetic couplings and heavy discharge current within one envelope whose physical dimensions and weight were based on previous unsuppressed designs, thus severely restricting both electrical and E.M.C. design. The circuit diagram is shown in Figure 3. The unit consists of two channels a 6 joule channel for engine starting energised from 28 volts d.c. and a 3 joule channel for continuous ignition supplied from 115 volts, 400 Hz. The d.c. channel consists of a blocking oscillator which charges the capacitor C6 and simultaneously C5 is permitted to charge through diodes D10 and D11, loss of energy into the a.c. charging circuit being prevented by the bridge connected diodes D6 to D9. Figure 10(a) of the input current shows clearly that the oscillator pulse rate increases progressively until the energy stored in C5 and C6 is discharged into the sparking plug via the barrier gap. The "ON" time of the pulse remains constant whereas the "OFF" time is progressively reduced. The expression for the d.c. peak current is:-

$$I = \frac{E}{L} \quad \text{where } E = \text{the supply voltage.}$$

$$I = \text{the input current ampere.}$$

$$L = \text{primary winding inductance.}$$

It should be observed that at discharge the short circuit presented to the oscillator inhibits the regenerative action. The output energy released to the igniter is unidirectional due to the output circuit L4 and the free wheeling diodes D12 and D13. The current output is shown on Figure 10(b) and indicates a peak current of 900 amperes. The a.c. energised section discharging circuit operates in exactly the same way as the d.c. energised section except that in this case the storage capacitor C5 is charged via bridge diodes D6 to D9. Loss of energy into the d.c. section charging circuit is prevented by the blocking action of the diodes D10 and D11. The control of energy into the step up transformer TR1 is achieved by the tapped inductors L1 and L2 which in conjunction with capacitor C2 keep the input current constant and sinusoidal except during the release of energy. The a.c. input current is 325 milliamperes peak to peak.

The control plan was sub-divided into three basic areas:-

- (1) d.c. charging circuit.
- (2) discharge circuit.
- (3) a.c. charging circuit.

#### 28 Volt d.c. Charging Circuit

The input current was analysed and levels of conducted interference were predicted to be above the specified limits particularly in the range 20 Hz. -20 KHz. A variety of filters were designed but it became apparent that the interference levels could only be attenuated down to 2 KHz. To meet the requirement below these frequencies demanded filters of prohibitive size and weight. Alternative charging circuits were examined by the Design and E.M.C. Engineers but the alternatives could not be accommodated in the space and weight limitations imposed and the original blocking oscillator was retained. The filter giving the best compromise and weight is shown in Figure 3, assembly (1). It was also recommended that the filter be contained in an aluminium case which was nickel plated to enable the case and lid to be soft soldered and a simple Faraday screen of 0.010 inch copper be incorporated between the primary and secondary of the transformer. The screen was considered necessary to reduce secondary circuit effects upon the primary.

An assessment of the diodes in the charging circuit chosen by the unit designer was also made and it was considered that these would contribute low levels of interference in comparison with the switching circuit.

#### Discharge Circuits

A jet engine surface discharge plug needs a voltage peak of 2 KV followed by a high energy pulse of current to ensure efficient ignition. These conditions naturally produce high levels of interference which cannot be attenuated without serious loss of energy therefore the only solution is to contain the energy within the ignition system. It was also realised that there was no adequate knowledge of the behaviour of igniter cable and its screening efficiency under pulse conditions, therefore, a separate study formed part of the control plan.

Spurious emissions from the discharge circuit are naturally created by the discharge gap, the free wheeling diodes and components subjected to the rapid rise of current in the igniter plug circuit.



### Discharge Circuits (continued)

Observations confirmed by calculation showed the necessity of additional screening of the discharge circuit because of the presence of high secondary voltage and peak discharge currents. It was proposed that the components causing emission be assembled in one of the two compartments created by a stainless steel wall which had already been incorporated for mechanical strength and each compartment should contain an additional 0.020 inch copper screen insulated from the main case but bonded to it at one point only. Other materials were considered, but copper offered the best compromise for cost, weight and screening effectiveness. The additional screen in the primary circuit compartment was recommended because it appeared impractical to mount the transformer in a drop through configuration to prevent intercoupling with the discharge circuit. 18-7

### Cable Assessment

The test configuration shown in Figure 4 was used to measure the interference radiated by different types of cable and provide data on which to base recommendations for suppression. A 6 joule ignition unit and power supply were installed in the double screened steel test vehicle while the discharge plug was surrounded by a  $\frac{1}{4}$  inch thick copper sheath. This sheath could be bonded directly to the test vehicle for measurement of the basic interference level or to the ground plane for results using a cable.

The selection of conducting, insulating and sheath materials for the cable is severely restricted by the engine environment in which it must operate and only four cables were available in addition to the copper tube reference. These were:-

- (1) Reference Cable (Sample 1) - solid copper tube 0.375 inch O.D. 0.314 inch I.D. containing conventional unplughitemp No. 10 cable.
- (2) Conventional Harness (Sample 2) - Unplughitemp No. 10 enclosed in top lock hose and covered by stainless steel braid.
- (3) Sample 3 - Unplughitemp No. 10 enclosed in sheath comprised of copper braid covered by Magnetoflex convoluted hose with a stainless steel braid outer.
- (4) Sample 4 - Identical to Sample (3) except the stainless steel braid was replaced by pure nickel braid.
- (5) Sample 5 - Unplughitemp No. 10 covered by copper braid wrapped with Kapton film insulation enclosed in two layers of tinned steel braid insulated externally by a further layer of Kapton film.

The test results obtained with a 1 metre length of each cable are given in Figures 5 and 6, and all samples exhibit amplitudes in excess of specification around a frequency of 100 MHz, including the basic set up of igniter at test vehicle only. Action to reduce the excessive levels is discussed later and the results indicate that only Sample 4 could fully meet requirements. The cable construction meets the flexibility and other engine environmental restrictions although the nickel braiding is relatively soft compared with conventional stainless steel and will require careful handling during installation on the engine. The cable will obviously be acceptable for use in 3 joule circuits as well as 6 joule.

### A.C. Charging Circuit

This channel is contained in the same double screened container as the D.C. input and the discharge energy is transmitted by a common circuit and cable to the igniter plug. The only remaining interference sources requiring to be considered are the input to the A.C. channel and the effect of stored energy release upon the A.C. input.

It is convenient to control the rate of charge of the storage capacitor C5 by the inclusion of chokes in the primary input to the channel and the input current amplitude variations can also be controlled by the addition of a capacitor C2. Inspection of the choke inductance values indicated that these would give considerable attenuation over most of the frequency range except for the effects of the discharge of energy into the igniter as shown in oscillogram Figure 10(c). A Faraday screen of 0.005 inch copper was inserted between the primary and secondary of transformer TR1 to minimise the effects of the secondary circuit discharge. To prevent radiation and intercoupling effects chokes L1 and L2 together with C2 were contained in an aluminium can assembly (2) on Figure 3. This is similar to assembly (1) previously described. It was proposed that an experimental channel be set up and tested to the conducted emission requirements before designs were frozen to enable the system interference levels to be verified. The results of these tests indicated that compliance could be obtained down to about 3 kHz, capacitor C2 being added to remove some excess amplitudes in the range 25-100 MHz.

The above work enabled the control plan to be finalised and to contain all the recommended interference reduction techniques, e.g. circuit and device analysis, choice of circuit configurations, materials and the use of experimental data. The control plan took cognisance of the anomalies recorded at the frequencies centered around 100 MHz, during the experimental tests and although remedial action would normally be proposed in the plan it was decided in this instance to postpone it. The decision was made because it was felt that a unit constructed to the proposed production standards might not exhibit similar results. Experience suggested that the out of limit levels could be attributed to output component

### A.C. Charging Circuit (continued)

earths carrying high circulating pulse currents during energy discharge and thus could only be proven on a production unit. Consequently a fully engineered unit to the recommended standards was manufactured and subjected to the tests called out in the design specification.

The results of tests for radiated emission levels as defined in test method RE.02 are shown on Figure 7, Curves (1) and (2) and indicate virtual compliance with the specified requirements except at 14 KHz. Curve (1) and at 90 MHz. on both curves the limits are exceeded in a pattern similar to the experimental results. The excess levels at 90 MHz. were removed by shortening the discharge circuit ground lead and by increasing the size of the grounding stud. The stud was brazed to a copper ring which in turn was brazed to the case, the ring circumscribing the outlet socket. Previously the ground was located in the base of the unit and required a longer grounding strap, which was incorporated for ease of manufacture rather than effective grounding. Test results with the modified configuration are shown by Curves (3) and (4) on Figure 7. The test results obtained after carrying out conducted emission test to the requirements of CE.01 are shown on Figure 8, Curves (1) and (2) indicate compliance with the limit over the frequency range 2 KHz. -20 KHz. They do not comply with the limits for the range 20 Hz. -2 KHz. and to obtain compliance with the limits would require filtering of astronomical proportions as indicated previously.

It is relevant to quote the method of measurement used in this range of frequencies. The measuring set bandwidth (Fairchild EMC.10E) was set to 50 Hz. and calibrated against an impulse generator set to approximately the repetition rate of the unit under test, i.e. 120 pulses per minute. The impulse generator output was fed into a 50 ohm load and the resulting current measured by the usual current probe. The results shown on Figure 9 indicate compliance with the requirements of test method CE.03 between 14 KHz. and 100 MHz. A unit designed to the standards laid down in the E.M.C. control plan which had been drawn up in association with the design engineers with the operational requirements in mind, has been shown to virtually meet E.M.I. specification requirements except where these are particularly arduous. It is of interest to note that test method CE.01 conducted broadband emission test which could not be met in practice in the range 20-2,000 Hz. has been deleted from the specification by the action of Notice 3.

### CONCLUSION

The above study shows that close collaboration between design and E.M.C. engineering enables control plans to be compiled which enable equipments to meet both operational and E.M.C. requirements. This does not imply that all equipments even with close control will meet the specification limits, since frequently there will be conflicting parameters and a compromise will be necessary. Conditions and limits can often be met technically but the penalties involved in size, weight and cost are totally unacceptable. It is noticeable that American military specifications in the E.M.C. field which are widely adopted elsewhere are non-mandatory documents and are, in fact, design aims which can be tailored to specific applications. The tailoring does not always make the requirements less severe. It is essential that detailed discussions between the engineering representatives of the procurement agencies and the equipment manufacturers are held to settle the specification constraints for the particular application as early as possible and before finalisation of contract. Control and Test plans must then be drawn up clearly defining the agreed aims.

European standards are mandatory documents demanding full compliance although in some instances some tailoring may be agreed. In the United Kingdom particularly relaxation of limits may be granted on the basis of results and their effect in a given installation. This has been essential as designs have usually been created without the use of control or test plans and compatibility is achieved subsequently by interference reduction techniques. This arbitrary approach is no longer acceptable due to the greatly increased interdependence of systems and equipment installed in aircraft. Control and test plans can and do eliminate unnecessary interference generators and pin point and evaluate areas of incompatibility which can then be eradicated with minimum delay and cost.

# REFERENCES

- (1) CHELKUNOFF S.A., "Electromagnetic Waves", Princeton N.J., VAN NOSTRAND 1943, p.p. 223-225; 303-306.
- (2) JARVIS M. L., "Improved Design and Measurement of Attenuation Characteristics of R.F. Suppressors", I.E.E.E. International Symposium, Chicago, July 18-20 1972.
- (3) REHKOPF H. L., "Prediction of Pulse Spectral Levels", I.R.E. Symposium on R.F.I., June 28-29 1962.

# GLOSSARY OF TERMS

- A = loop area in square metres.
- E = Volts.
- $E\phi$  = Electric field strength, volts/metre.
- $H_0$  and  $H_r$  = Magnetic field strength, amperes/metre.
- L = Inductance, henries.
- I = Current, amperes.
- N = Number of turns.
- r = Distance from loop to antenna in metres.
- $\lambda$  = wavelength in metres.
- $\beta$  =  $\frac{2\pi}{\lambda}$
- $\eta$  = 377 ohms impedance of free space.

TABLE 1Table 1(a)

Frequency Hz.	MIL-STD-461A Limit RS.01 dB. pT.	Loop Level dB. pT.	Shielding Attenuation dB.	Material Thickness (cms)		Material Weight (Kg)	
				Copper	Aluminium	Copper	Aluminium
30	140	94	46	6.35	8.2	66.4	26.7
100	119	94	25	1.9	2.44	20.0	7.9
400	95	94	1.0	0.38	0.48	0.398	0.151
800	82	94	-	0.38	0.48	0.398	0.151

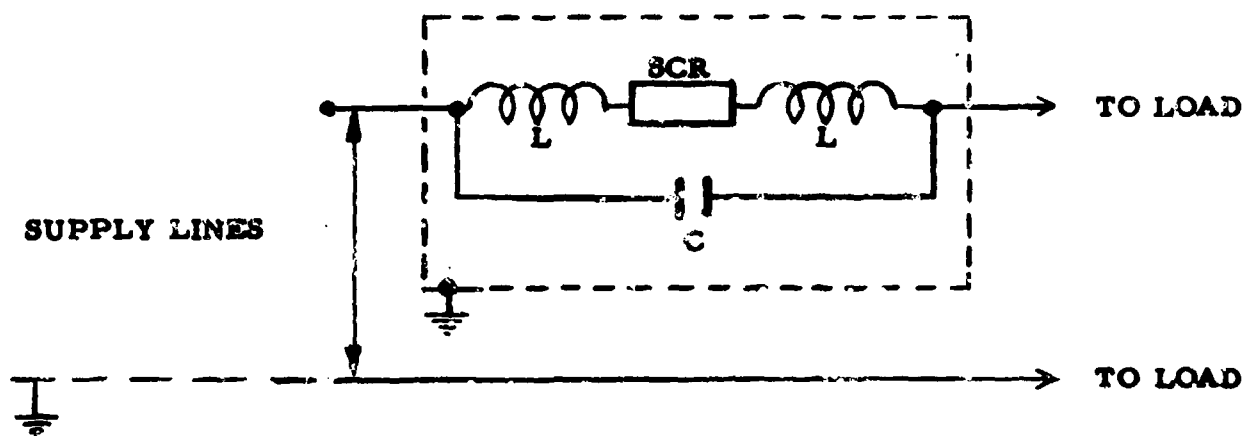
Table 1(b)

Frequency Hz.	MIL-STD-461A Limit RE.01 dB. pT.	Loop Level dB. pT.	Shielding Attenuation dB.	Material Thickness (mm)		Material Weight (Kg)	
				Aluminium	Mumetal	Aluminium	Mumetal
30	140	134	-	-	-	-	-
100	119	134	9	9.6	0.38	3.1	0.36
400	95	134	33	8.6	0.26	2.8	0.24
500	82	134	46	10.0	0.40	3.2	0.365

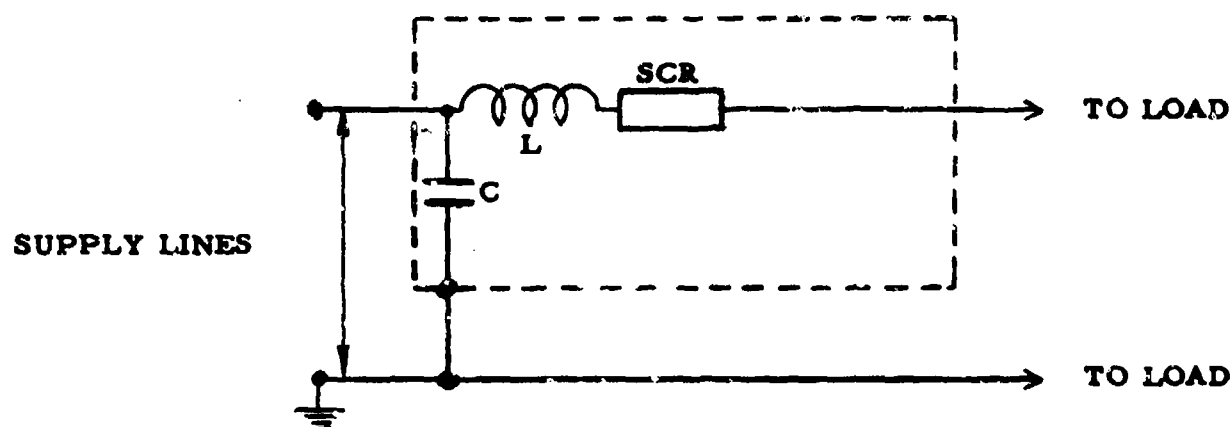
TABLE 2  
SPECIFICATION

UNIT: High Energy Ignition Unit  
CODE: NB.10902

	<u>Starting</u>	<u>Continuous</u>
(1) Stored Energy (Joules)	6	3
(2) Main Storage Capacitor ( $\mu$ F)	1.5 + 1.5	1.5
(3) Operating Supply	14.5 to 31 V.d.c.	98 V., 380 Hz. min. 124 V., 420 Hz. max.
(4) Operating Duty	5 cycles 30 secs. "ON", 30 secs. "OFF"	5 hours
(5) Max. Input Power	50 watts	75VA
(6) Discharge Voltage	2000 $\pm$ 100	
(7) Operating Temperature Range		
(a) Continuous	-40°C to +110°C	
(b) Cycling	-40°C to +155°C	
(8) Maximum Altitude	60,000 feet	
(9) Sparking Rate (spark/min.) at normal input voltage	60 minimum at minimum input voltage	
(a) at 20°C	120 minimum	
(b) at 155°C	90 minimum	
(10) Estimated Weight	Nominal Maximum	2.681 Kg. 2.820 Kg.
(11) Radio Interference	MIL-STD-461A, Notice 2, Tests CE01, CE03, RE01.	

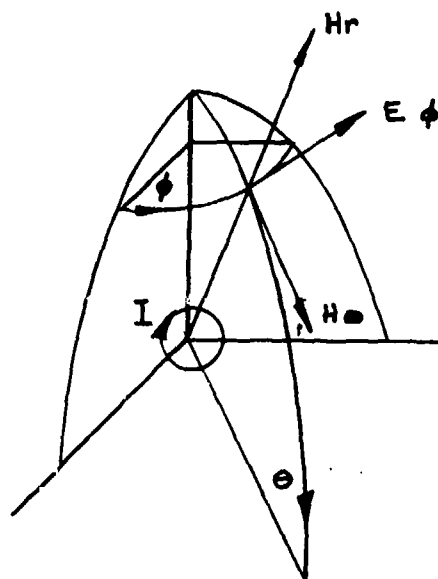


(a) CONDUCTED EMISSION SUPPRESSION WITH r.f. GROUND INACCESSIBLE



(b) CONDUCTED EMISSION SUPPRESSION WITH ACCESSIBLE r.f. GROUND

Figure 1



The fields resulting from a current flowing in a loop can be obtained from the following equations:

$$E_{\phi} = \frac{NIA\beta r}{4\pi r^3} (1 + j\beta r) e^{-j\beta r} \sin \phi \text{ Volt / metre} \dots\dots\dots (1)$$

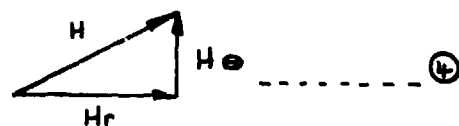
$$H_{\theta} = \frac{NIA}{4\pi r^3} [1 - j\beta r - (\beta r)^2] e^{-j\beta r} \sin \theta \text{ amperes/metre} \dots\dots\dots (2)$$

$$H_r = \frac{NIA}{2\pi r^3} [1 + j\beta r] e^{-j\beta r} \cos \theta \text{ amperes/metre} \dots\dots\dots (3)$$

The above figure depicts the fields described by these equations

The resultant magnetic field  $\bar{H} = \bar{H}_r + \bar{H}_{\theta}$

$$\text{or } H^2 = H_r^2 + H_{\theta}^2$$



Equation (3) assumes that  $\beta = \frac{2\pi}{\lambda} \rightarrow 0$  for frequencies between 30 Hz to 1 KHz. and that  $e^{-j\beta r}$  a retardance expression which is negligible in the frequency range 30 Hz - 1 KHz and over short distances

Additionally consider that  $\cos \theta$  and  $\sin \phi = 1$  for max. fields.

$$\text{Hence } H^2 = \left[ \frac{NIA}{2\pi r^3} \right]^2 \left[ 1^2 + \left( \frac{1}{2} \right)^2 \right] \dots\dots\dots (5)$$

$$H = \sqrt{5} \frac{NIA}{4\pi r^3} \dots\dots\dots (6)$$

Figure 2

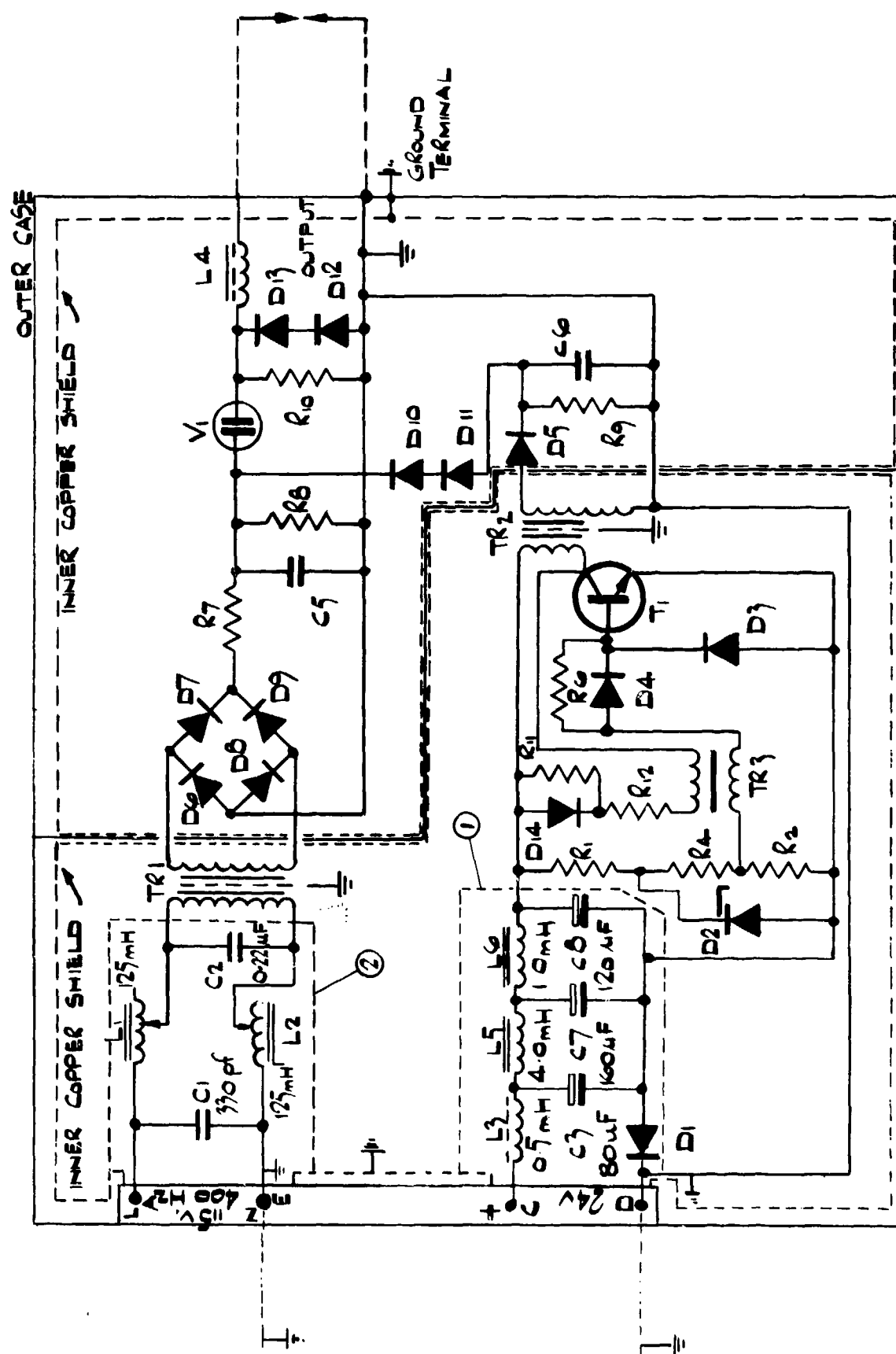


Fig. 3 Circuit diagram of high energy ignition unit

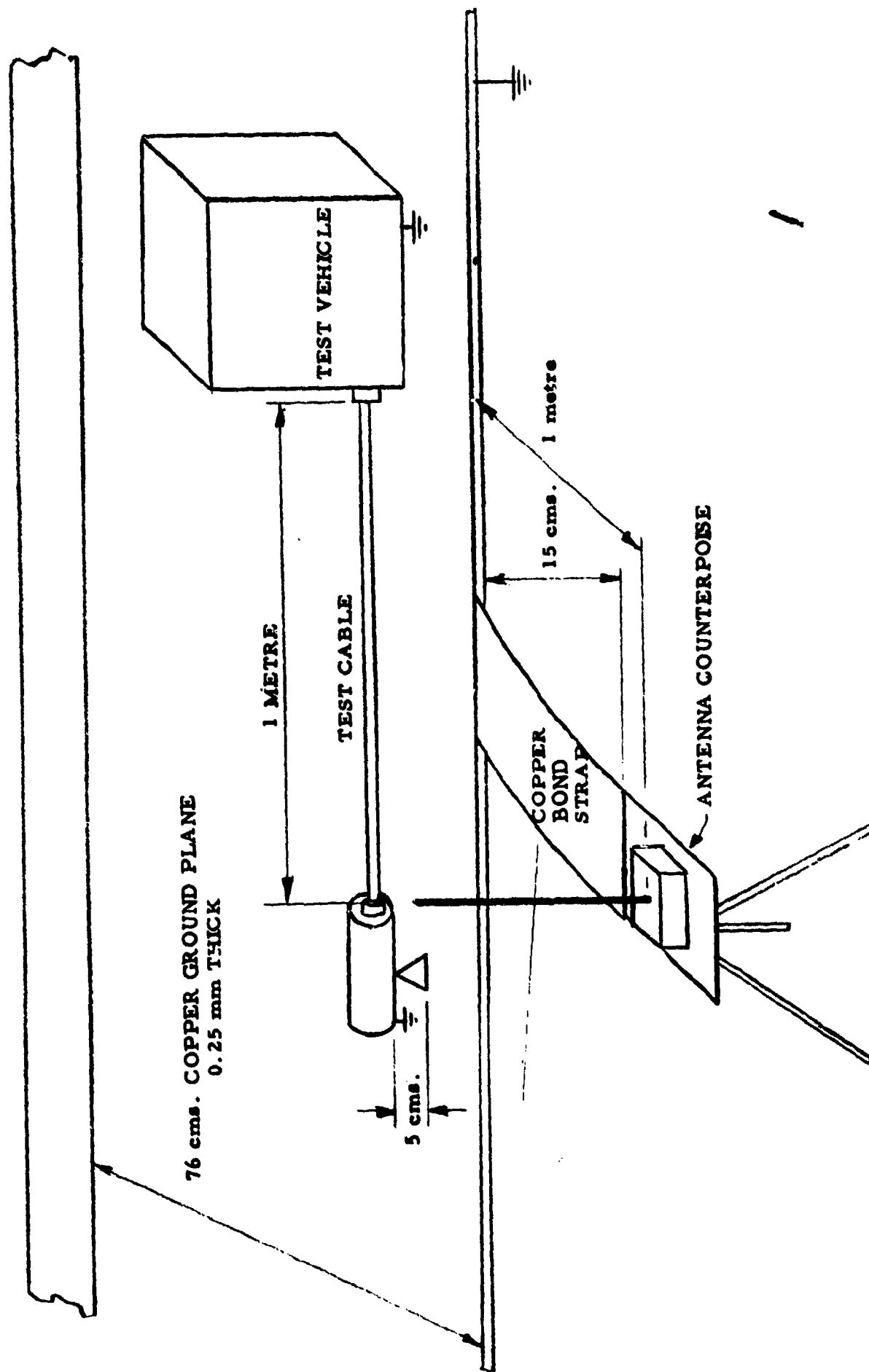


Figure 4



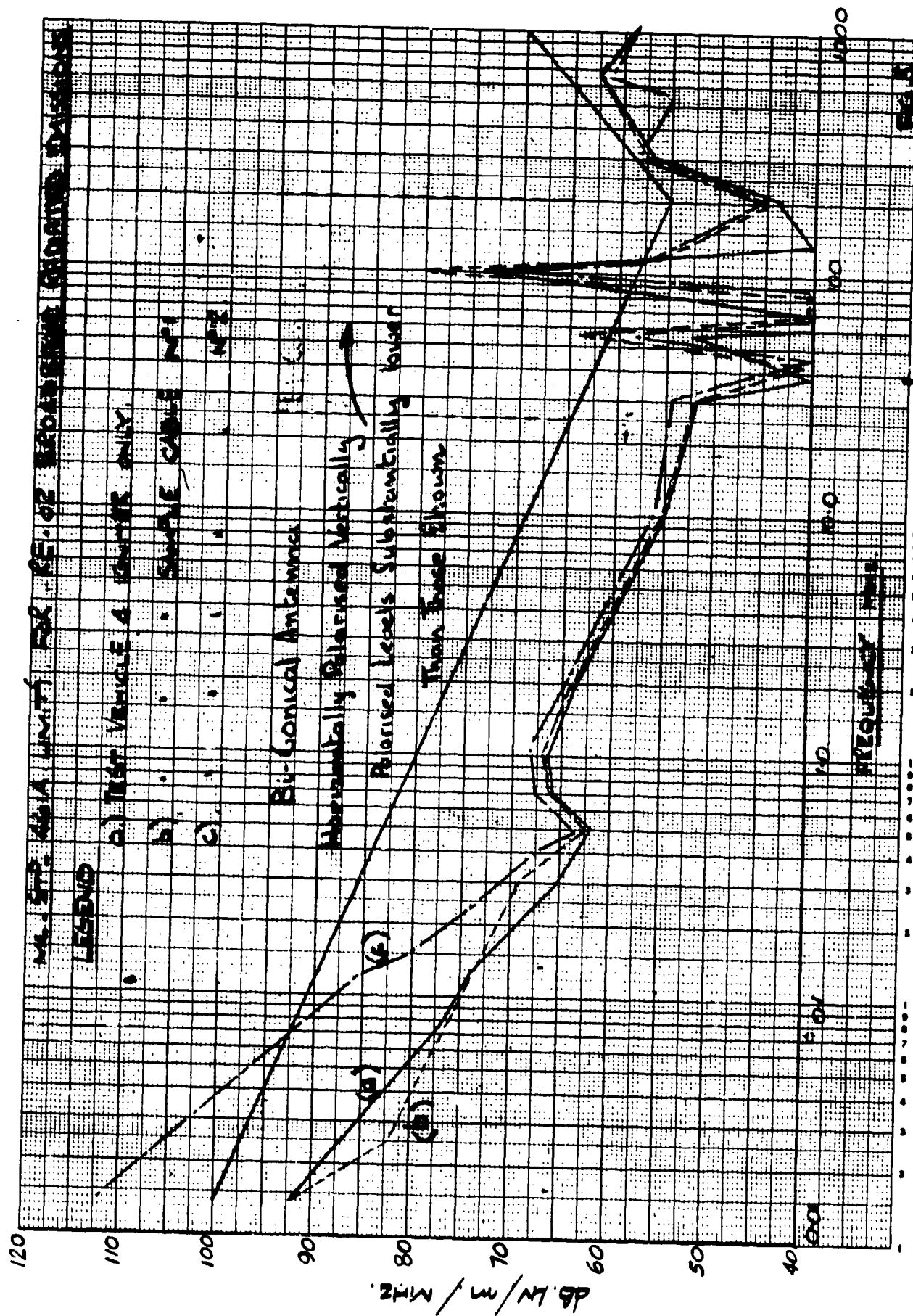


Figure 5

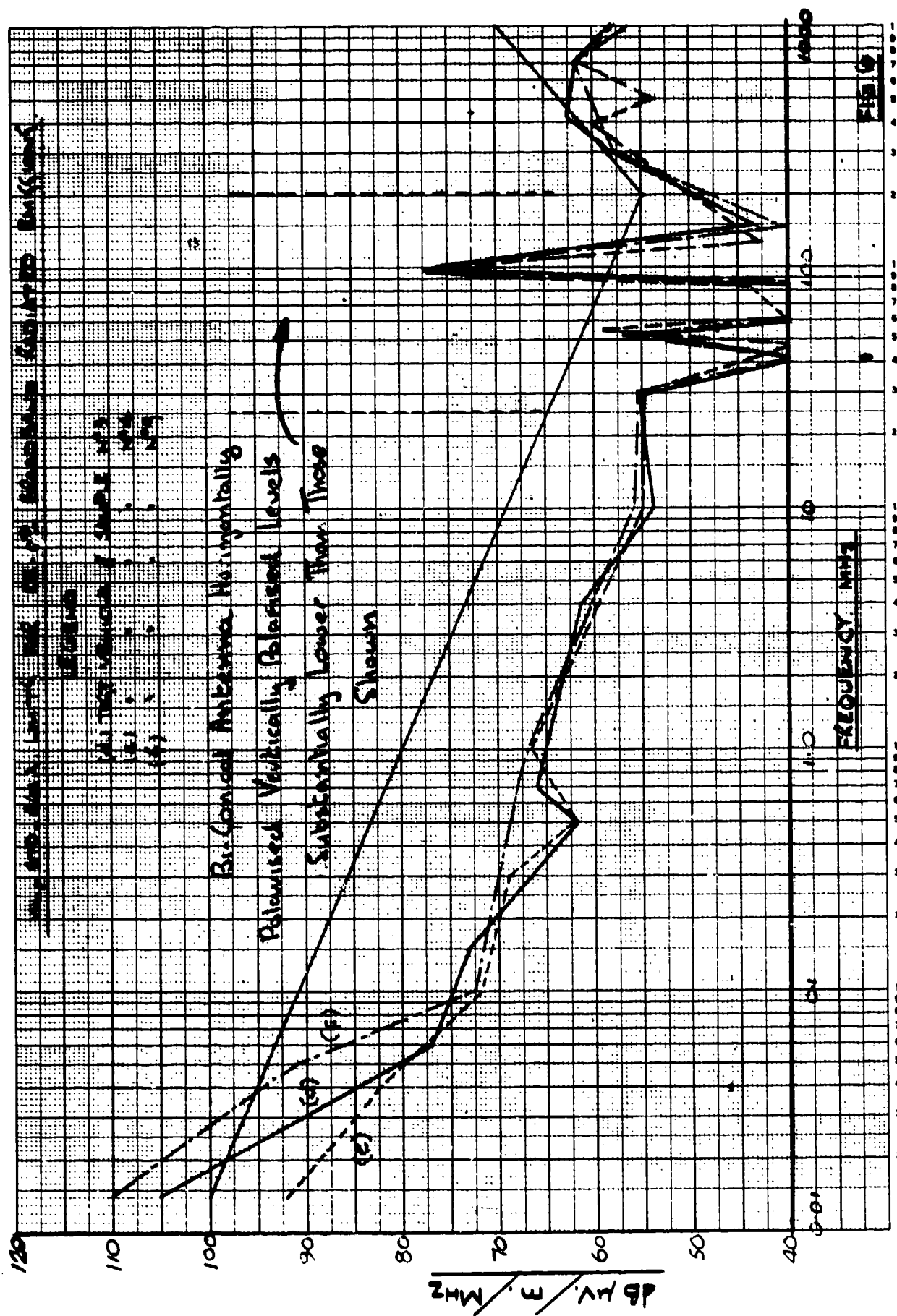


Figure 6

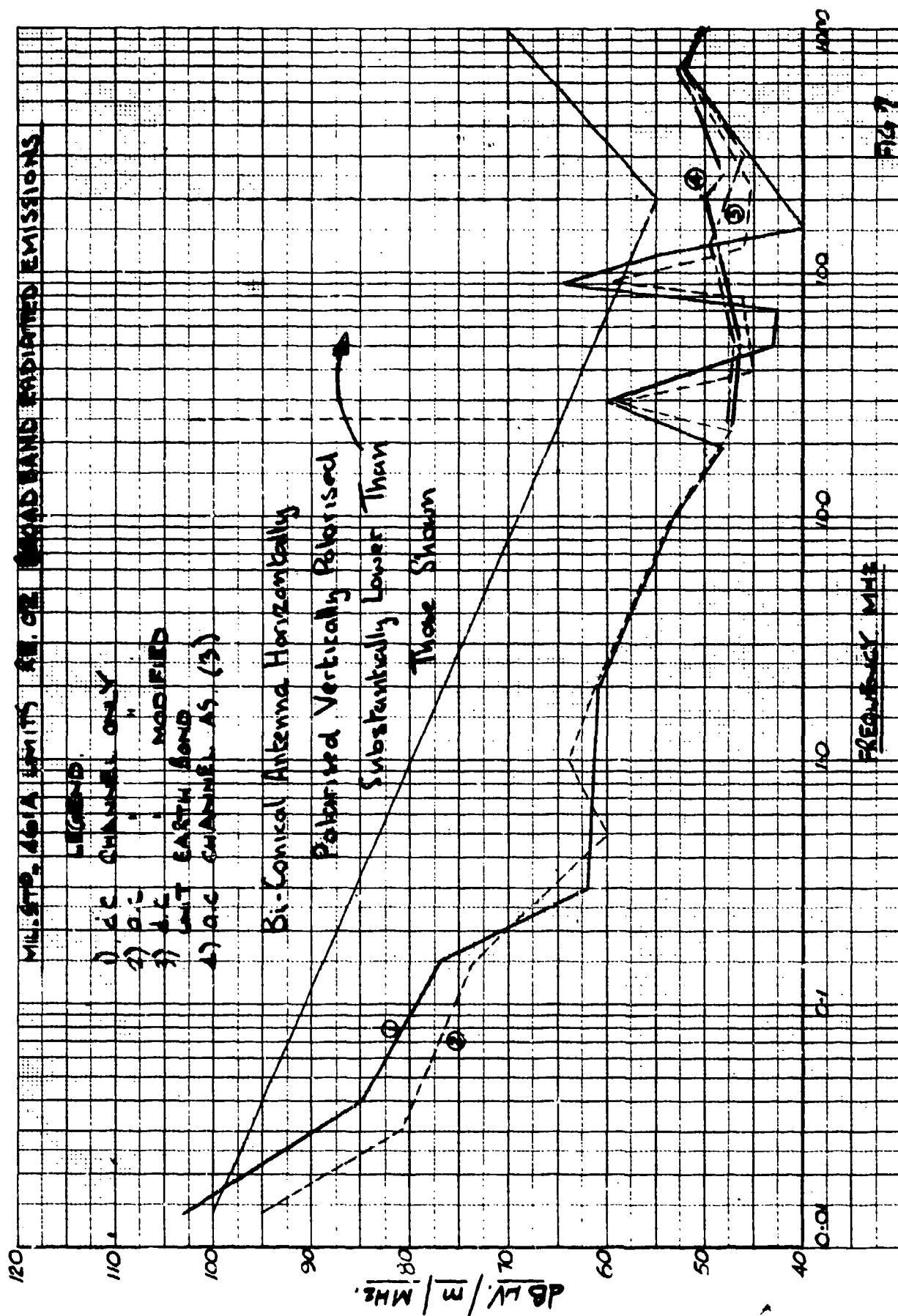


Figure 7

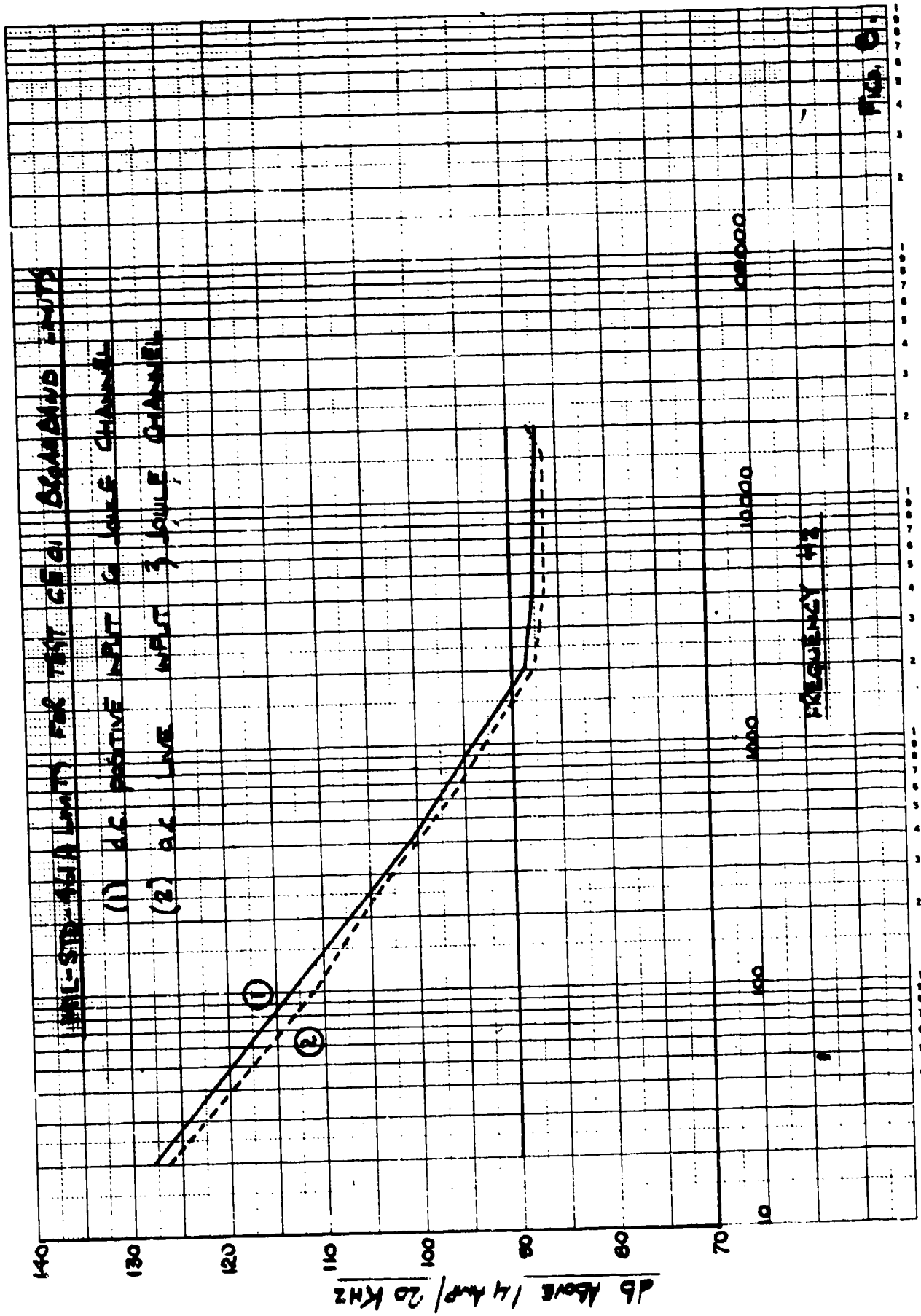


Figure 8

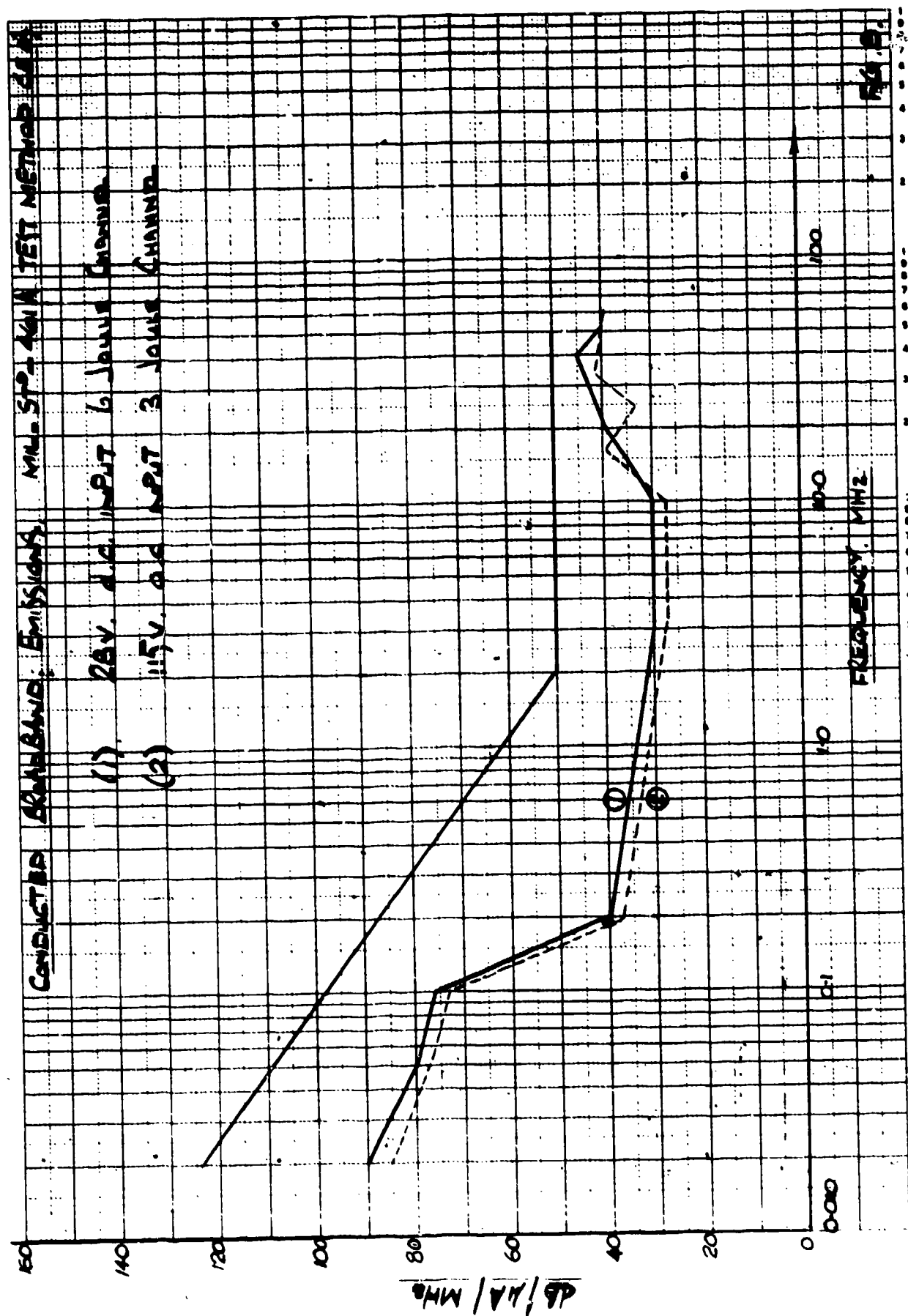


Figure 9

18-20

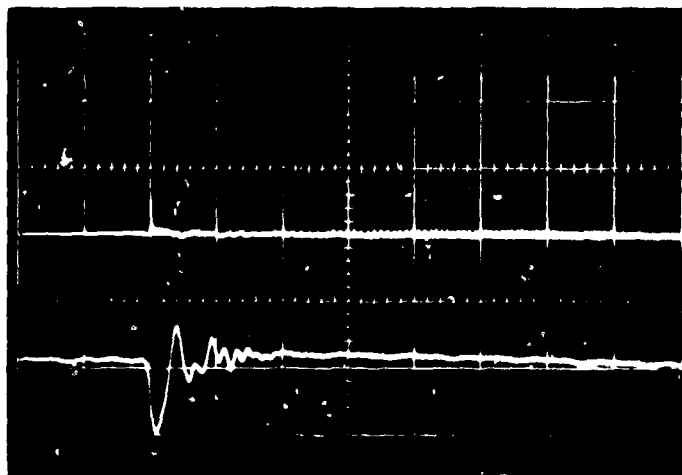


Fig. 10(a) D.C. channel input current, Upper trace — unsuppressed 1.3 amp/cm, Lower trace — suppressed 1.0 amp/cm, Horizontal scale — 10 mSec/cm

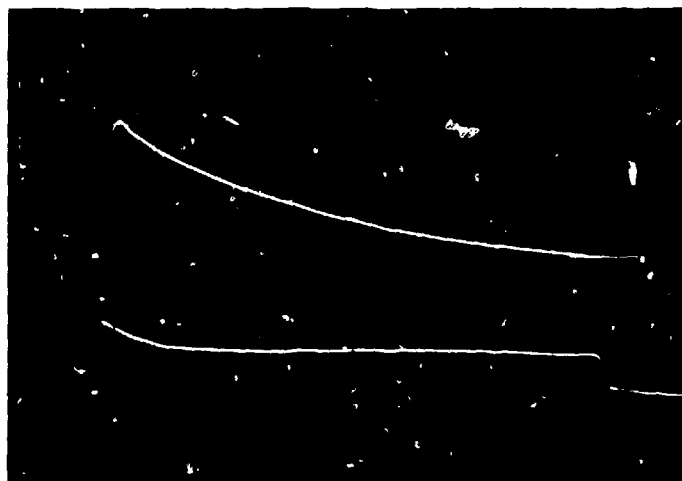


Fig. 10(b) Plug discharge characteristics, Upper trace — current 450 amp/cm, Lower trace — voltage 50 volts/cm, Horizontal scale — 20  $\mu$ Sec/cm

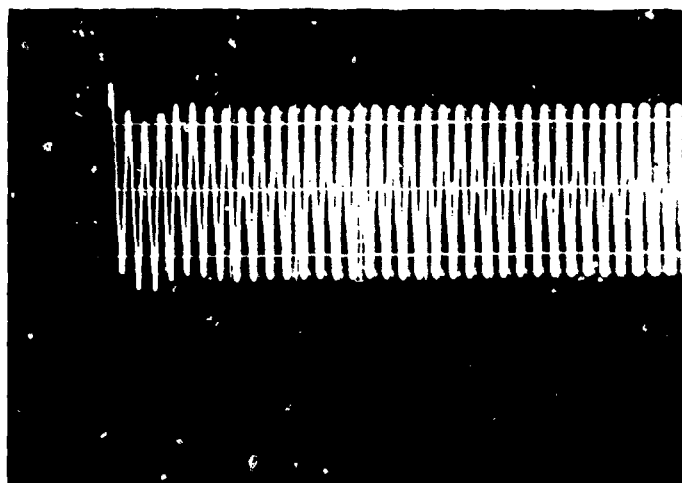


Fig. 10(c) A.C. channel input current (suppressed), Vertical scale — 0.15 amp/cm, Horizontal scale — 10 mSec/cm

## DISCUSSION

K. LANDT: How do you stop the RF getting out of the shielded boxes and getting from one box into the other at the penetration holes of the wiring without appropriate feed-through filters?

P. D. CAMPBELL: The electrostatic screen prevents high frequency coupling through the transformer. Any interference radiated from secondary to primary is adequately suppressed by the power input filters. It may have been possible to use a less efficient power line input filter if feed-through capacitors had been used on the transformer's primary and secondary box interfaces.

K. LANDT: What is the reason for the intentional ground connection between primary 24 DC ground and high-voltage ground?

P. D. CAMPBELL: The drawing is misleading in Figure 3. The secondary ground on Tr. 2 is connected locally to the box and not as shown at the 28-volt negative terminal.

K. LANDT: Don't you think that an adequate shielding of the external high-voltage ignition circuit will be a very helpful remedial measure against radiation at RF?

P. D. CAMPBELL: Yes. This has been done by extending the Faraday cage effect of the ignition box via a triple screened cable to the ignition plug as described in the text Page 18-7, Cable Assessment, Sample 4, which is a uniplug hi-temp inner enclosed in a copper braided sheath covered by a magneto flex hose with a pure nickel braid outer. This type of cable improves the low frequency performance.

F. J. CHESTERMAN: In Figure 5 there is a resonance effect at 100 MHz. Can you explain in more detail the reason for this resonance?

P. D. CAMPBELL: The answer to the question is described on Page 18-8, second paragraph. All the radiated emission results exhibited a resonance effect in the vicinity of 100 MHz. The resonance was removed by improving the discharge circuit, by shortening the ground lead and increasing the size of the ground stud. The grounding stud was brayed to an annular ring which was in turn brayed to the back shell of the igniter cable socket located within the unit. Previously, the ground was located in the base of the unit and required a longer grounding strap. This method had been introduced for ease of manufacture rather than effective grounding. The improved grounding effects achieved with the incorporation of the modification is shown by curves (3) and (4) on graph Figure 7, Page 18-17. The resonance occurs because of the discharge circuit parameters. The discharge tube V1, Figure 3, has a capacitance of approximately 2pf ringing with the localized circuit inductances.

# MANAGEMENT OF AN EMC ENGINEERING DESIGN PLAN

by

J.E.R.Fogg and M.T.Le Grys  
Marconi-Elliott Avionics Systems Ltd  
Airport Works  
Rochester, Kent

PAPER NOT AVAILABLE AT TIME OF PRINTING.

## DISCUSSION

O. HARTAL: A basic problem we have come across is the information flow from design engineers to the EMC authority. Changes in the design may not come to the EMC engineers' knowledge, though they may have a profound effect on the system's performance. How do you deal with this problem?

J. E. R. FOGG: The EMC authority must be part of the design team. Attendance at the Project Design Review Meetings, with EMC listed as a separate agenda item, will help to insure that the impact of design changes are given early EMC consideration.

J. C. DELPECH: Would it be possible to know more accurately what a control plan contains? How is it written? What are the different chapters? Is there a standardized model for all the equipments? Could a precise example be given, with comments?

J. E. R. FOGG: The content of the control plan will be influenced by the complexity of the system to which it applies and by the installation into which it is to be integrated. As a model as to which areas should be given consideration, the best reference is probably MIL-STD-461A at the present time.

R. B. ROWLEY: Regarding coordination between EMC and project teams (Slide Fig. 7, Page 19-4 of paper), we consider that the project engineer is involved in all stages including the test report, in that the report requires analysis in terms of cause of problems and proposed solutions, with impact on programme. Author please comment.

M. T. LE GRYS: Agreed. The EMC test house originating the test report can make a factual statement of the results of the tests performed, but the detailed engineering comments as to what causes certain recorded effects can only be made by the design engineer.

R. J. MORROW: With respect, I would like to add my view of EMC. On one hand, it involves frequency management. It is in this area that we have the profusion of technical literature. On the other hand, it is a statement of good design. To obtain a good design, there is a need for discipline, thus the generation of specifications. There is a need to discipline engineering design with respect to EMC the consequence of his design. As with all discipline, it is disliked.

J. E. R. FOGG: There is indeed resistance to most disciplines and the newer the discipline the greater is the resistance. That is why the sooner the communication of the subject is simplified the sooner the engineering design will heed the recommendation of the EMC authority.

G. H. HAGN: Do you think an EMC figure of merit would be of use in facilitating communications between the EMC authority and the program manager?

M. T. LE GRYS: Methods which simplify the communication of what is a specialist technical area need to be evolved. The FOM could satisfy this need, but for it to have greater credibility the FOM for the "black box" would need to be supported by like figures down to board and subassembly level.



# A CASE FOR AN EVALUATION AND ADVISORY SERVICE

E M Frost

Signals Research & Development Establishment  
Procurement Executive Ministry of Defence  
Christchurch  
England

## SUMMARY

Activities have grown up independently to deal with problems arising from unacceptable, unexpected, unwanted or unnecessary electromagnetic relationships. The requirement to exchange, interwork and co-site equipments and systems, coupled with the widening use of semi-conductor devices for new as well as traditional applications, has led to the concept of an overall Electro-magnetic Compatibility (EMC) activity.

However there is no generally accepted definition for EMC as separate interests are tending to retain their own limited interpretations. It is believed that this is causing interface difficulties that will prevent EMC adapting itself sufficiently rapidly to deal with this changing and expanding electronic situation. After considering EMC as a typical pollution situation a suggestion is made for an evaluation and advisory service (EASE) that would provide an interface between other EMC and allied activities and also act as a focus and creative development point for new ideas and techniques.

### 1. DEFINITION

What do we understand by Electromagnetic Compatibility?

All of us could immediately, or with a little reflection, define or explain quite simply what our respective roles are within what we consider to be the general pattern of EMC. If however we were asked to expand on what we consider this general pattern to be, most, if not all of us would find this a much more difficult task, and very few of our answers would be in agreement.

If in addition the request was for a definitive statement, that is, a self-sufficient one which could be used to resolve differences, evaluate policy, and guide future actions by all involved with EMC, we would be defeated in the attempt, let alone in providing a satisfactory answer.

Why should we have this difficulty?

The reason is that what is called Electromagnetic Compatibility is a collective name given to a number of separate parts or activities related in a general way to electromagnetic effects.

If this is so why cannot we rationalise these into a whole?

In the electromagnetic area we are involved with a number of changing, open-ended situations where the EMC consequences of decisions made and actions undertaken are often governed by laws of nature rather than by rules and intentions of man.

Also many of the parts have an as strong or even stronger relationship or connection with non-electromagnetic activities than they do with EMC in the general sense, so that even if natural electromagnetic problems have been identified there is still an arbitrary uncertainty where the authority to resolve them lies; is it an equipment design responsibility, a financial or contractual matter, or a clear EMC matter?

Furthermore even the separate parts within EMC have developed independently with different time scales, degrees of sophistication and purposes, often having their own firmly established procedures, authority and vested interests.

It would seem therefore that, because of the nature and state of the art of EMC a statement defining the bounds and having any real authority is not possible until time or circumstances allow the various parts or activities both within a nation's civil and military organisations and internationally to be harmonised to a far greater extent than they are at the present.

What is much more important than the definition, as desirable as this is, is that we should have something substantial, effective and worthwhile to define.

What additional steps can we take towards bringing this about?

Two suggestions are made in this paper, one is philosophical and the other practical. The former postulates that the EMC situation shows the characteristics of a typical pollution situation both in the way it has developed and also in the methods used to try and solve it. Consideration

of the situation from this viewpoint can give insight into the way it tends to behave and also provides clues as to how it can be influenced in a positive and constructive manner.

Leading from this pollution concept the second suggestion is made for an activity providing an interface or bridge between the other various EMC parts or activities and a focus and creative development point for new ideas and techniques.

## 2. POLLUTION

Before tackling the problem of pollution we are again confronted with the difficulty of definitions.

As pollution is concerned with the effects and results what effects are we to consider?

In a pollution situation there is an unintended and often unexpected relationship between a sender and a receiver where neither has any direct responsibility for or obligation to the other. Under these conditions, particularly where there is a penalty in reducing the cause of pollution, there is a strong tendency towards reducing areas of involvement by administrative decision. Therefore a broad coverage for the scope of EMC is a necessary, indeed essential as a starting point for achieving effective compatibility. It would then be appropriate to say that 'the discipline of Electromagnetic Compatibility should take account of all electromagnetic phenomena whether of natural origin or deliberately or incidentally generated or received'.

What do we mean by pollution?

The dictionary definition states that to 'pollute' is to 'destroy the purity and sanctity of'.

In this context purity and sanctity convey two separate and distinct ideas or processes both of which must be pursued with equal vigour to obtain effective EMC. The former is concerned with the state of the electromagnetic mechanism itself and the latter with its effect on the rights and well-being of others.

Consider the following examples which, although illustrating radio communication situations, can be extended to cover a wide range of other situations.

(A) Assume that we have a radio station which is being interfered with by another independent and well separated radio station. Here we have purity of signal but conflict of sanctity.

(B) Consider the same radio station independent from source of unintended radiation that is interfering with it. Here we have both conflict of purity and sanctity.

(C) If however an interfering source and the radio station are part of the same equipment both being the responsibility of a single designer then there is a conflict of purity but no conflict of sanctity.

(D) If the radio station is neither independent nor at a distance from an interfering source which may be unintended or required in its own right, such as in a system or installation, there is no clear out distinction between purity and sanctity, or if it is a pollution or design consideration.

Let us now consider the above examples from the EMC viewpoint.

In (A) there is no doubt that we have an EMC problem and that problem is as old as the art of radio communication itself. Over the years a considerable authoritative body, the activity of frequency management, has been built up within the armed services, nationally and internationally. This pollution situation is caused by overcrowding and in the EMC context is almost entirely a deliberately radiated radio problem which is very much part of the function of the primary system. It is therefore to be expected that technological innovation to improve EMC will be generated, widely understood, and supported from within the primary systems themselves. Modelling and analysis techniques are also applicable to this form of EMC.

In (B) we also have a clear EMC problem. Four elements are required to produce pollution. They are, a cause, a relationship, a recipient, and the destruction of the purity and or the sanctity of the recipient. A difficulty that arises is that the equipment producing the cause is introduced into use as an independent unit and the other three elements are not in general known. To overcome this difficulty the unit is tested by established procedures and to predetermined limits calculated to ensure that pollution will not occur with any practical relationship and recipient. For susceptibility performance the same reasoning is applied to the cause and the relationship.

When we have a potential pollution situation we can reduce or eliminate the cause and or the relationship. Pollution is caused by unnecessary, uninterested, unintended or unsuspected relationships. Where the cause is essential to the function of the equipment the relationship must be broken by say screening or filtering; in other cases the cause can be reduced or eliminated.

EMC solutions may be in direct conflict with other design considerations or the pollution mechanism may be outside the designers knowledge so that one of the favoured methods of dealing with a pollution situation is to introduce legislation which in the EMC context takes the form of Standards. Standards are essential for the purpose of contract, management, inspection and quality control but as they make generalised technical assumptions they must be used with care when trying to resolve a particular technical situation.

In (C) no formal EMC requirement exists as the satisfactory resolution of internal compatibility should be explicit in the equipment specification. While EMC requirements, techniques and expertise may be called on for help in design and development these are only obligatory to the equipment's relation with its environment.

In (D) we have an area where as yet no common or accepted philosophy, practice or procedures have evolved. Control Plans are one approach but these still need refining.

#### CONCLUSION

A situation has been reached where the different activities that make up the EMC discipline cannot be used and developed independently of one another to obtain optimum EMC effectiveness. Some form of integrating activity is therefore urgently required and the remainder of the paper describes such an activity.

#### 3. EVALUATION AND ADVISORY SERVICE (EASE)

3.1 Historically methods of obtaining electromagnetic compatibility resulted from the piecemeal creation of different activities usually directed towards solving some particular embarrassment of the moment and then their developing into organisations often having considerable authority and status in their own right.

3.2 Within their own terms of reference and assessment of the problem these organisations could be effective. However if the assessment was not valid, or the situation changed or the terms of reference widened, adaptation to the new circumstances was strongly influenced by the existence of a pollution type situation and the choice of a new optimum solution could be impeded or prevented.

3.3 In recent times the terms of reference have been widened in an attempt to cope with changing conditions, and various activities and organisations have been considered under the generic heading of Electromagnetic Compatibility.

3.4 Adaptation problems, both collective and individual, experienced in rationalising the several activities within EMC are much more involved than with a single organisation. Not the least difficulty is establishing and maintaining effective interfaces both inside and outside the several activities.

3.5 The author is strongly of the opinion that the general EMC situation and activity as it is now constituted will not be able to adapt itself sufficiently rapidly to cope with the difficulties of the changing conditions due to the expanding magnitude, application and complexity of electronics.

3.6 If this assessment of the situation is a valid one it is clear that some means must be found to influence the development and nature of existing activities in a co-ordinated way to an overall pattern.

3.7 The method suggested in this paper is the creation of an Evaluation and Advisory Service (EASE). It must be stressed that the proposals suggested here are purely hypothetical, are put forward to stimulate discussion, and do not in any way imply approval of policy or describe an actual existing organisation.

3.8 The individual properties making up EASE are those already in use or are considered desirable in normal EMC practice. It is their selection, emphasis and relationship that gives the required overall characteristics.

3.9 The main properties and functions of EASE are detailed and discussed below:-

(a) A very wide range of equipments and systems must be considered. Ideally all facts should be taken into account in making an EMC assessment. In practice there will of course be limits, but apart from genuine security reasons, it is essential that there should be the 'right to know' unrestricted by external or internal administratively imposed limits.

(b) Staff should be encouraged to make personal contacts, attend meetings and discussions, and make personal observations and gain practical experience 'on site'.

(c) Consultation and liaison should take place with other EMC activities such as frequency management, user trials, inspection, and with other organisations or bodies influenced by or which influence the EMC situation.

(d) EASE should act as a focus, forum, clearing house, propagandist, prophet and memory and as far as one can use such a term the conscience on general EMC matters and ideas.

(e) It has been pointed out that interfaces, that is, boundaries between activities, organisations and procedures over which information must flow or action take place, are potential sources of inefficiency. Because interface situations are not always self-righting or self-adjusting EASE has a particular interest in this problem. Study will be undertaken, general and particular recommendations made and active help given. In some cases a complete mismatch or discontinuity may exist; in such cases EASE would act as a bridge by providing not only guidance but actually providing an activity.

(f) One of the most, if not the, important requirement of the EASE concept is that it must have a laboratory and staff actively carrying out measurements. Among the reasons for this are:-

(i) As a discipline for both individuals and the total activity. The subject to be covered is so large and the methods of approach so numerous that some reference point is necessary to give stability to the whole structure. In EASE this is provided by knowledge based on measurement.

(ii) Many damaging EMC symptoms arise from second or higher order effects, from subtle or obscure mechanisms, or from casual relationships, which are not amenable to calculation but can only be satisfactorily identified and quantified by fine measurement.

(iii) An important aim is to make designers self-sufficient in EMC matters; a practical demonstration of the use of instruments and techniques particularly on their own equipments can have a great and permanent educational value.

(iv) EMC must not be merely a 'cleaning up after the event' activity; it should also be concerned with looking into the future, anticipating problems, evaluating them and finding acceptable methods of avoiding them. EASE is very much involved in this, and practical research must go hand in hand with theoretical study.

(v) It is important that Standard inspection testing of equipments and components should be comprehensive and widespread. A factor against this is the cost of testing and therefore any improvements to speed up and reduce the cost of these tests is worthwhile. This is one of the areas where EASE should be active.

3.10 The effective use of Standards is influenced by two mutually conflicting requirements, one to remain constant and stable and the other to match continually changing circumstances. A responsible and impartial source of advice and guidance is necessary to minimise the effects of this conflict. EASE would be well suited for this role in three ways by:-

(a) Recommending and assisting in drafting amendments to existing Standards or suggesting new Standards.

(b) Adding authority to concessions.

(c) Investigating and determining valid equivalents and comparisons between Standards under different jurisdictions.

The position of EASE in the Standards activity must be carefully controlled; it can offer advice, but it must not presume on the authority, or take on the duties, of the established Standardisation activity.

3.11 A valuable part of the service would be to advise and provide assistance to Project Managers and Officers, EMC Officers and Boards and both system and equipment designers in the following manner:-

(a) Clarification and familiarisation of EMC documents, procedures and testing methods.

(b) Assistance in the preparation and drafting of EMC documents peculiar to the project.

(c) Introduction to and setting up of liaison links with other EMC and associated activities.

(d) Technical advice on equipment, system and design methods. This could also include evaluation measurements and modifications to equipments in the presence, and with the co-operation, of designers.

(e) Advice and temporary involvement of specialized test equipment.

(f) Attendance in a consultative capacity at meetings and trials and as a technical referee.

(g) Site survey and specialized electromagnetic environment measurements.

(h) Training of Project EMC Officers.

3.12 Although it might seem as if the flow of information is one way, this is not so as all the time EASE will be receiving information which it would store and process for possible use in other fields. This is an extremely valuable method of updating and improving the EMC system.

3.13 The study of EMC and associated problems would be carried out by paper exercises and by practical research both intra-murally and extra-murally. Facilities for placing research and investigation work with outside bodies would be required.

3.14 It is important that EASE must preserve its autonomy as a functional unit so that it can discharge its technological responsibilities without being overridden by local administrative restraints or by other activities or groups of activities.

3.15 EASE can give advice and undertake limited defined and agreed tasks but must not presume on the authority or take on the duties of functions of an established activity. In this way a Project

EMC Officer would be responsible to the Project Manager and would not be a member of an EASE. The equipment and skill to test to Standard requirements would be available but formal inspection would not be undertaken.

3.16 The work load would be divided into three classes:-

(a) Work for 'customers'. This would be effort that could be already accounted for against a specific project.

(b) 'Housekeeping'. EASE has to have available a range of 'tools' kept in good condition and ready for use at short notice. In this category would fall a technical library and data recording and processing system; a test laboratory and its maintenance and calibration; training and education of staffs; attendance at meetings and administrative effort.

(c) 'Research'. This would include investigation both theoretical and practical, not directly attributable to a project or to 'housekeeping' and would involve the study, design and development of new measurement methods and procedures, EMC problems and the presentation of technical papers.

Over a long period it is estimated that working time would be shared in equal parts over the three classes. Increase in output of 'customer' work should come from increases in preparedness, facilities and quality of the other classes and not by increasing the proportion of time spent on projects.

3.17 Although the optimum size for an EASE would have to be determined for a particular set of circumstances, the following guidelines can be laid down.

(a) The various members will have primary responsibility for an area of work in the 'housekeeping' and some of the 'research' class but each area should be understudied by other members.

(b) To deal with a 'customer' project or other specific task a team would be set up, the constitution of the team being determined by the nature of the task and the work load at the time.

(c) The whole unit should be close enough to allow daily contact with each other and to use common facilities.

(d) Although for short periods the whole unit could work on a project there must be enough redundancy to allow the 'housekeeping' to be carried out.

3.18 Although contact with projects will be required at all stages, including post-production, it is at the inception of a project that the greatest and most beneficial influence can be exerted. It is at this stage that the implications of EMC can be established with appropriate provision of time, management procedures and cost.

#### 4. CONCLUSION

EASE is presented as a method of obtaining more effective EMC.

In setting up a practical organization or activity the principles given above should be adhered to.

These principles have been determined after consideration of imperfections in the present EMC situation many of which became apparent after considering EMC as a pollution situation.

#### 5. ACKNOWLEDGEMENTS

British Crown Copyright reproduced with the permission of the Controller Her Britannic Majesty's Stationery Office.

INTERFERENCES DANS LES SYSTEMES A MODULATION DE FREQUENCE N° 21.

G. Crocombette,  
THOMSON-CSF  
55, Rue Greffulhe

92 - LEVALLOIS-PERRET.

This article of essential character treats interference problems resulting from experiences taken on telephony radio links, to multiplexage repeated in frequency. (FDM - FM).

This comprises two parts. Firstly a very general characteristic is applied to frequency modulation links.

It treats successively :

- Type of link organization and equipments.
- Origin of disturbess.
- Effects of disturbess on the functioning of equipments (capture of AGC and limiters) and on all-over performances (noise after demodulation).
- Proceeduses utilized to reduce the effects of disturbess.
- Calculate the level of disturbess from the antenna diagrams. The application has two particular events.

The second part is related exclusively to telephony radio links FDM - FM of medium to large capacity.

It gives the quantity of disturbances produced between the different radio links of normal capacities.

Finally, for example, a diagram of antenna radiation utilized for the realization of a network system.

Cet article de caractère essentiellement pratique traite le problème des interférences à partir de résultats expérimentaux relevés sur des faisceaux hertziens de téléphonie, à multiplexage par répartition en fréquence. (FDM - FM).

Il comprend deux parties. La première, de caractère très général, est applicable à tous les faisceaux à modulation de fréquence. Elle traite successivement de :

- Organisation type des liaisons et équipements.
- Origine des perturbateurs.
- Action des perturbateurs sur le fonctionnement des équipements (capture du CAG et des limiteurs) et sur les performances globales (bruit après démodulation).
- Procédés utilisés pour minimiser l'action des perturbateurs.
- Calcul du niveau des perturbateurs à partir des diagrammes d'antenne et application à deux cas particuliers.

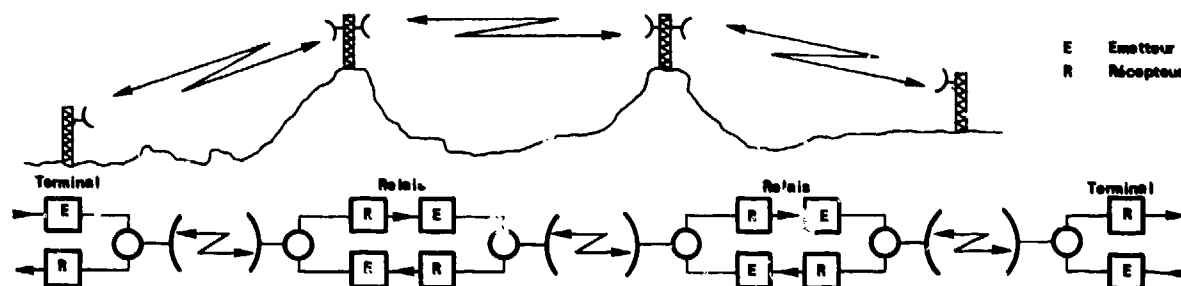
La deuxième partie se rapporte exclusivement aux faisceaux hertziens de téléphonie FDM - FM à moyenne et grande capacité. Elle donne les résultats de mesure de perturbations réciproques entre différents faisceaux de capacités normalisées. Enfin elle donne, à titre d'exemple, le diagramme de rayonnement d'une antenne utilisée pour la réalisation d'un réseau maillé.

## PARTIE I.

### 1. - ORGANISATION DES LIAISONS ET DES EQUIPEMENTS.

#### 1.1. - Organisation des liaisons.

Une des caractéristiques du Faisceau Hertzien est qu'il utilise, comme vecteur support d'information, des ondes à fréquence élevée se propageant, en première approximation, comme la lumière. De ce fait une liaison hertzienne, au sens habituel du terme, est constituée par une série de liaisons mises bout à bout, liaisons dont les extrémités sont en visibilité optique.



Ces liaisons sont en général équipées de plusieurs canaux bilatéraux et forment un réseau maillé comportant un nombre d'émetteurs récepteurs beaucoup plus grand que le nombre de fréquences disponibles. Ceci conduit à des risques d'interférences que l'on s'efforce de minimiser par l'emploi de plans de fréquence très stricts et par un choix judicieux de l'emplacement des stations.

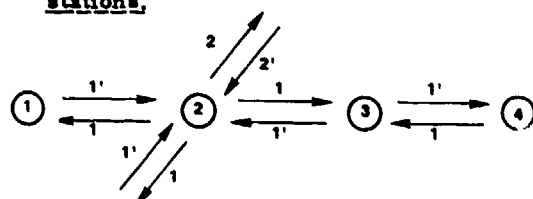
#### Plan de fréquence normalisé.



Demi bande basse  $f_n = f_0 - 208 + 29 n$

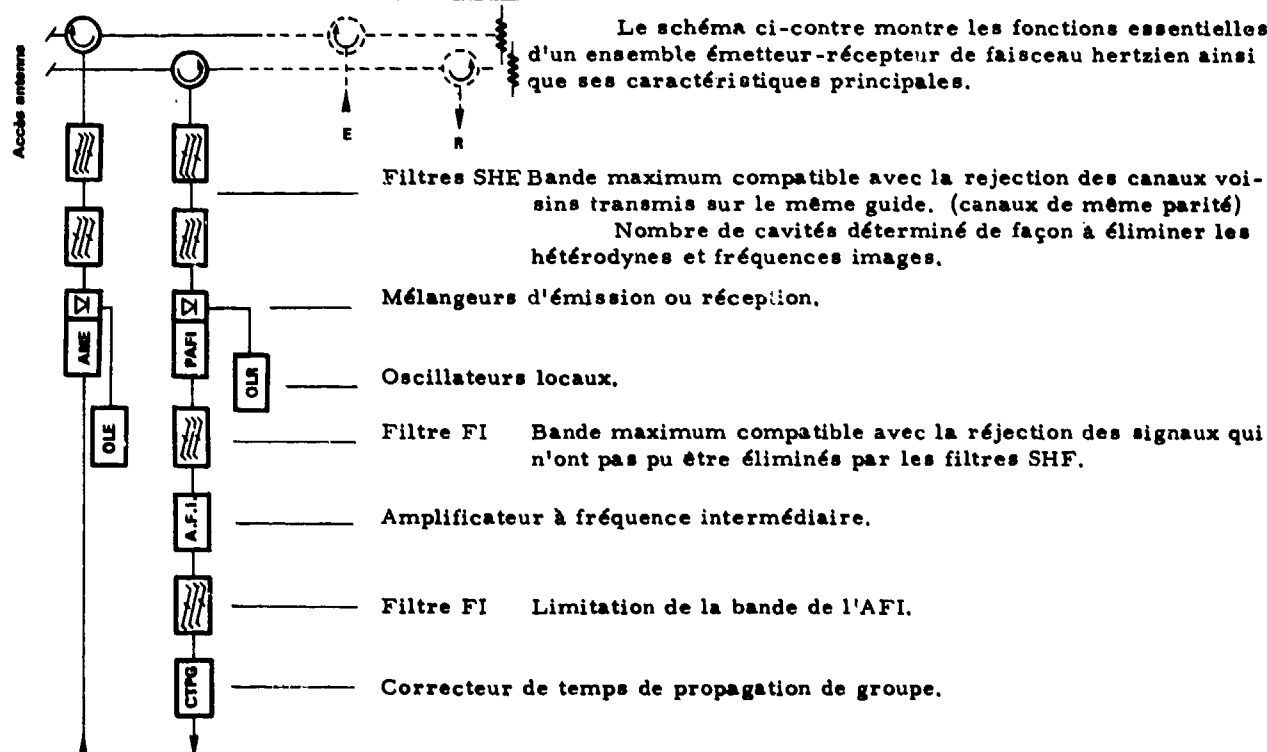
Demi bande haute  $f'_n = f_0 + 5 + 29 n$

#### Plan de fréquence d'un ensemble de stations.



Les figures ci-contre montrent à titre d'exemple le plan de fréquence normalisé dans une bande donnée (3,9 - 4,2 GHz) et l'arrangement des fréquences utilisé pour un ensemble de stations. On remarquera qu'une station émet toujours dans une demi bande et reçoit dans l'autre. (parité des stations) ce qui implique que toutes les mailles d'un réseau aient 2 p côtés. On remarquera également que la seule protection contre les perturbations issues d'une station adjacente est assurée par le découplage d'antenne, caractéristique qui, dans un réseau maillé, prend souvent le pas sur la caractéristique de gain.

#### 1.2. - Organisation type des équipements.



## 2. - ORIGINE DES PERTURBATEURS DANS UN SYSTEME HERTZIEN.

Les perturbations relevées sur une liaison réelle peuvent être classées en deux sortes.

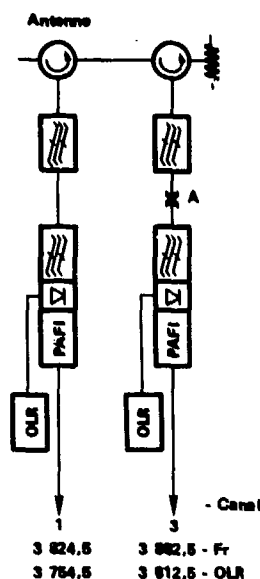
- a)- Perturbations du système par lui-même.
- b)- Perturbations dues à la présence de liaisons voisines.

La première famille de perturbations est éliminée lors de l'étude du matériel. C'est elle qui impose les caractéristiques des divers filtres, et à ce titre ressort de la conception du matériel.

La deuxième dépend des caractéristiques topographiques des liaisons et des antennes utilisées. A ce titre elle ressort de la conception de la liaison.

### 2.1. - Perturbations du système par lui-même.

Ce type de perturbations n'intéresse pas directement l'ingénieur d'étude de liaisons. Aussi seul le cas typique des perturbations par hétérodyne réception est-il donné à titre d'exemple.



L'examen du système ci-contre (faisceau à 4 GHz) montre que la fréquence OLR du canal 3 est à 12 MHz de la fréquence du canal 1 et, de ce fait, se situe dans la bande du récepteur du canal 1. Cette fréquence est normalement éliminée par les filtres et le circulateur de branchement du canal 3. Si leur atténuation était insuffisante, il conviendrait d'insérer un atténuateur unidirectionnel au point A.

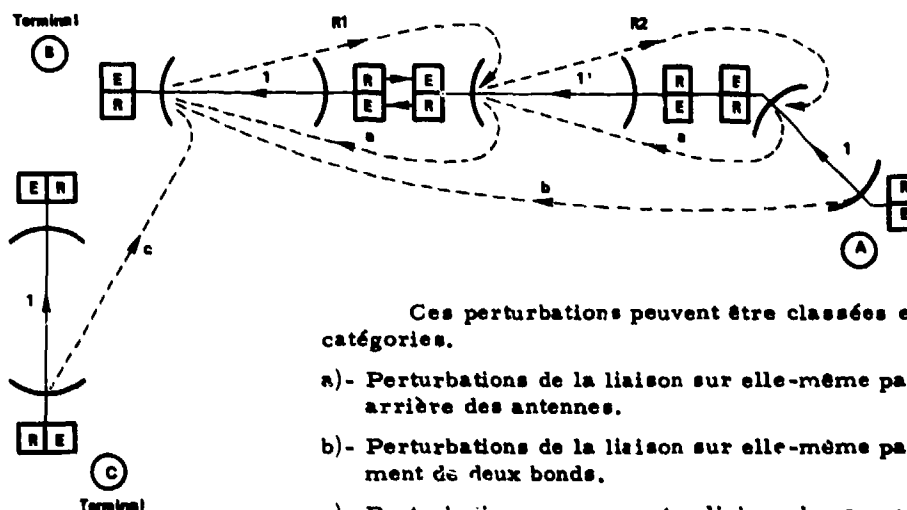
### 2.2. - Perturbations dues à la présence de liaisons voisines.

Ces perturbations proviennent presque toujours des signaux parasites captés par les antennes et tombant dans la bande passante des récepteurs.

Elles dépendent essentiellement des paramètres suivants :

- Caractéristiques de rayonnement des antennes.
- Tracé des liaisons.
- Plan de fréquence.

Le schéma ci-dessous représente un exemple de liaisons et les perturbations susceptibles de se produire sur la liaison A → B.

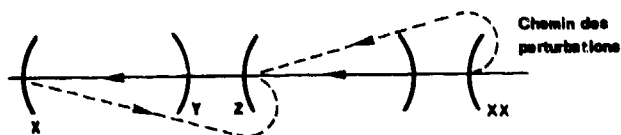


Ces perturbations peuvent être classées en trois catégories.

- a)- Perturbations de la liaison sur elle-même par rayonnement arrière des antennes.
- b)- Perturbations de la liaison sur elle-même par surpassement de deux bords.
- c)- Perturbations par une autre liaison due au rayonnement diffus des antennes.



### 2.2.1. - Perturbations par rayonnement arrière des antennes.



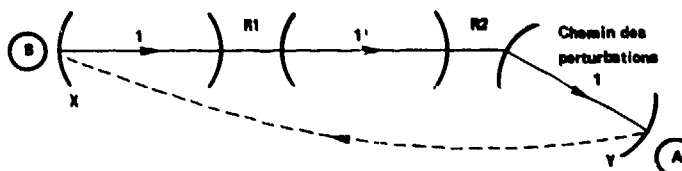
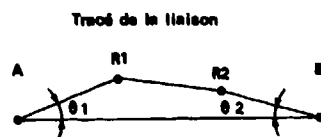
En général, dans une station relais les émetteurs travaillent à la même fréquence.

Dans ces conditions le rayonnement arrière de l'antenne z est captée par l'antenne x. De même l'antenne z reçoit une fraction de rayonnement émis par xx.

La parade à ce type de perturbation peut être obtenue de la manière suivante :

- Adoption d'un plan à 4 fréquences, mais dans ce cas le nombre de canaux radioélectriques est réduit de moitié.
- Adoption d'antenne à hautes performances.

### 2.2.2. - Perturbations par surpassement.



Cette perturbation résulte de la captation par l'antenne x d'une partie du rayonnement émis par l'antenne y située trois stations en amont.

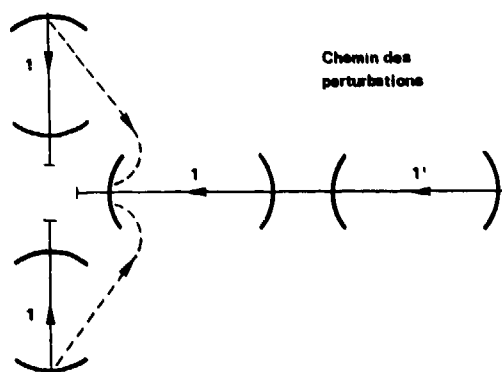
La parade à ce type de perturbation peut être obtenue de la manière suivante :

- Choix de l'emplacement des stations de façon à ce qu'elles ne soient jamais en visibilité radioélectrique. (Stations A et B séparées par une colline, et pylônes de hauteur minimum).
- Choix de l'emplacement des stations de façon à augmenter les angles  $\theta_1$  et  $\theta_2$  pour augmenter le découplage des antennes x et y.
- Adoption d'antennes à hautes performances.

#### Remarque sur la visibilité radioélectrique.

La zone de visibilité radioélectrique est d'autant plus étendue que le point choisi pour la station est un point haut. Lors de l'étude du tracé d'une liaison on peut être amené à abandonner un point très haut, tout à fait favorable à la propagation du faisceau principal, au profit d'un point moins dégagé mais dont la "zone de pollution" est moindre.

### 2.2.3. - Perturbations d'une liaison par d'autres liaisons.



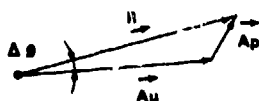
Ce type de perturbations se produit essentiellement sur les bonds ayant une extrémité commune. Il est de même nature que les perturbations par rayonnement arrière et a pour cause le rayonnement diffus des antennes.

Le rayonnement diffus étant d'autant plus élevé que l'angle entre deux liaisons est faible, il convient de porter une attention particulière à ce type de perturbations.

Dans certains cas, le seul remède réside dans l'emploi de plans de fréquence intercalaire. - cf. chapitre 4.

### 3. - ACTIONS DES PERTURBATEURS.

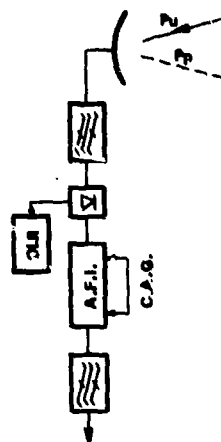
Avant limitation les signaux "utile" ( $\vec{Au}$ ) et "perturbateurs" ( $\vec{Ap}$ ) se combinent vectoriellement pour donner un signal modulé en amplitude et en phase ( $\vec{R}$ ).



La modulation d'amplitude peut agir sur le comportement du CAG et des limiteurs. La modulation de phase introduit un signal qui peut être réparti dans toute la bande - cas général - ou centré sur une seule fréquence - signal utile et signal perturbateur non modulé.

Outre la diaphonie qu'il introduit ce signal risque, dans certains cas de saturer les amplificateurs en bande de base.

### 3.1. - Capture du C.A.G.



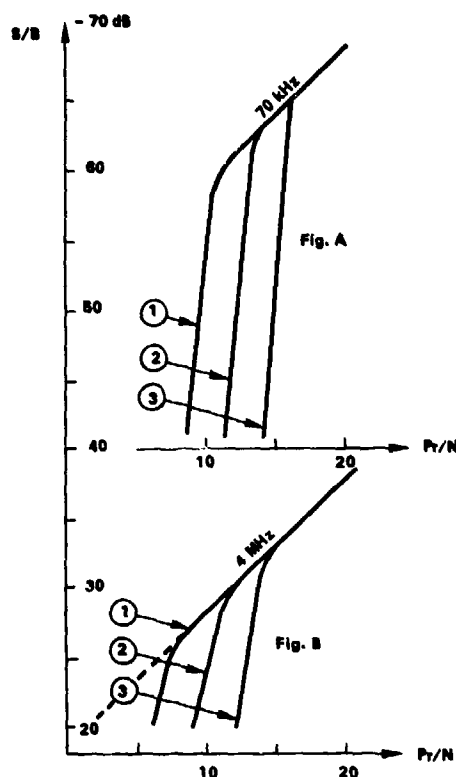
Dans un amplificateur à fréquence intermédiaire la commande de gain et la commande de régénération obéissent à l'amplitude globale du signal reçu.

Si le perturbateur est au-dessus du seuil de régénération et si son amplitude devient supérieure à celle du signal utile, le récepteur peut se caler sur le perturbateur sans que les équipements d'extrémités puissent déceler cette substitution.

En fait ce cas est un "cas d'école" car la capture du CAG a lieu pour un niveau beaucoup plus faible que le niveau de capture des limiteurs, lui-même inférieur au niveau de régénération. Il n'y a donc pas lieu d'en tenir compte dans l'étude d'une liaison.

21-5

### 3.2. - Capture des limiteurs.



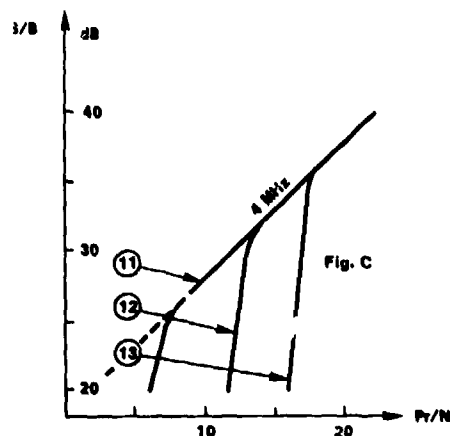
En présence de bruit blanc, les limiteurs fonctionnent correctement jusqu'à un rapport signal sur bruit de 10 dB environ. A ce rapport signal sur bruit correspond une puissance de réception qui est la puissance minimale admissible ou puissance de seuil en modulation de fréquence.

En présence des perturbateurs cette puissance minimale augmente et reste toujours supérieure à la puissance de seuil et à la puissance du ou des perturbateurs.

Les figures montrent l'évolution du rapport signal sur bruit dans une voie téléphonique dû à la détérioration du fonctionnement des limiteurs en présence de perturbateurs.

#### LEGENDE.

- Fenêtre de mesure 4 kHz centrée à 70 kHz ou 4 MHz.
- $\Delta f$  200 kHz eff.
- $P_r$  puissance de réception.
- $N = \mathcal{F} KTB$  (Bruit blanc avant limitation).
- Conditions de mesure fig. A et fig. B. Un seul perturbateur à 14 MHz environ aux niveaux suivants :
  - $P_1 = 0$  pour les courbes 1.
  - $P_1 = N$  pour les courbes 2.
  - $P_1 = 10 N$  pour les courbes 3.
- Conditions de mesure fig. C. Deux perturbateurs symétriques à 14 MHz environ aux niveaux suivants :
  - $P_1 = P_2 = 0$  pour la courbe 11.
  - $P_1 = P_2 = N$  pour la courbe 12.
  - $P_1 = P_2 = 10 N$  pour la courbe 13.



En première approximation, et pour un nombre limité de perturbateurs, on peut admettre que les limiteurs fonctionnent correctement lorsque la relation suivante est vérifiée,

$$U_r - \sum U_p > 10 U_b$$

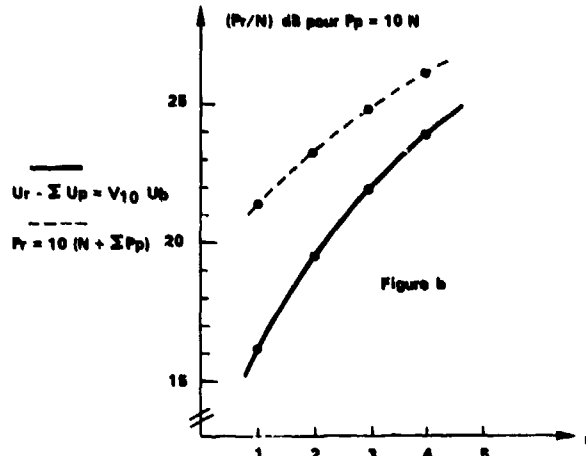
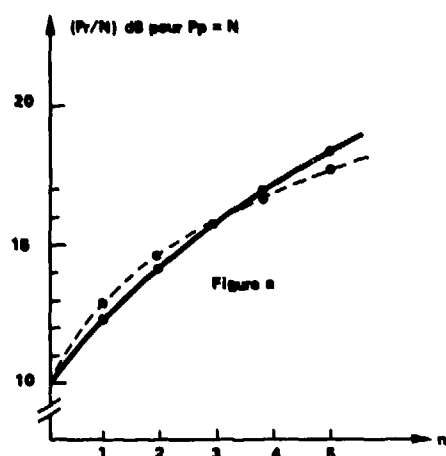
- $U_r$  Tension du signal utile.
- $U_p$  Tension du signal perturbateur.
- $U_b$  Tension efficace de bruit thermique.

En pratique on utilise plutôt la formule suivante un peu moins précise mais plus commode d'emploi.

$$P_r > 10 (N + \sum P_p).$$

Les figures ci-après montrent l'évolution de  $P_r/N$  en fonction du nombre de perturbateurs dans les deux cas particuliers suivants :

- a)- Puissance de chaque perturbateur égale au bruit thermique ( $P_p = N = \mathcal{F} KTB$  ;  $U_p = U_b$ ).
- b)- Puissance de chaque perturbateur égale à 10 N ( $P_p = 10 N$  ;  $U_p = \sqrt{10} U_b$ ).



### 3.3. - Perturbations après démodulation.

Après démodulation, les perturbations résultant de l'interférence d'un signal utile et d'un signal parasite peuvent être classées en deux grandes catégories.

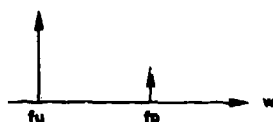
- Perturbation à fréquence pure due au battement de deux ondes non modulées.
- Perturbation répartie dans toute la bande due au battement de deux ondes dont l'une au moins est modulée.

#### Perturbation à fréquence pure (ou "sifflette").

- Spectre avant limitation

$$f_u = \frac{\omega_u}{2\pi} = \text{fréquence du signal utile}$$

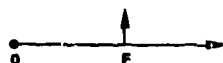
$$f_p = \frac{\omega_p}{2\pi} = \text{fréquence du signal parasite}$$



- Spectre après démodulation

$$F = f_u - f_p : \text{fréquence de la perturbation}$$

$$\Omega = \omega_u - \omega_p$$



- Diagramme de Fresnel des signaux avant limitation

- Hypothèse  $A_p \ll A_u$

- $\Delta \phi$  = modulation de phase perturbatrice

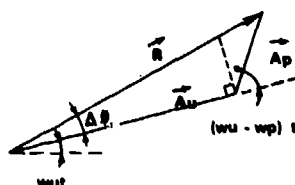
$$\Delta \phi = \frac{A_p}{A_u} \sin(\omega_u - \omega_p)t = \frac{A_p}{A_u} \sin \Omega t$$

- $df_p$  = modulation de fréquence résultante

$$df_p = \frac{1}{2\pi} \frac{d}{dt} (\Delta \phi) = \frac{A_p}{A_u} \frac{\Omega}{2\pi} \cos \Omega t = \frac{A_p}{A_u} F \cos \Omega t$$

- $f_p$  = excursion de fréquence résultante =  $\frac{A_p}{A_u} \times F$

- $f_c$  = excursion de fréquence produite par le signal de test à la fréquence F. (excursion de la voie considérée).



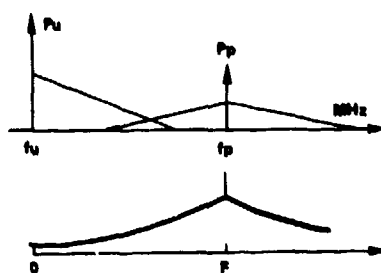
#### Rapport signal sur bruit correspondant :

$$\frac{S}{B} = \left( \frac{\Delta f_c}{\frac{A_p}{A_u} F} \right)^2 = \frac{P_u}{P_p} \times \left( \frac{\Delta f_c}{F} \right)^2$$

$$\text{soit en dB} \rightarrow \frac{S}{B} = P_u - P_p + 20 \log \left( \frac{\Delta f_c}{F} \right)$$

Les relations précédentes montrent que l'amplitude de la raie parasite est d'autant plus grande que  $(f_u - f_p)$  est élevé. Correspondant à un cas théorique, surtout depuis l'emploi de la dispersion d'énergie, elles servent essentiellement à vérifier que les amplificateurs en bande de base ne sont pas saturés.

### Perturbation répartie dans toute la bande.



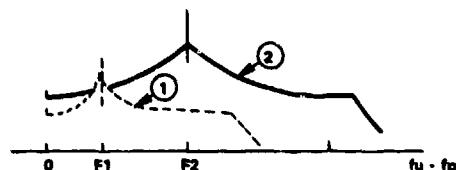
L'approche mathématique de ce type de perturbation étant assez difficile, et les résultats relevés en laboratoire étant exposés dans la phase II, le présent chapitre est limité à l'aspect qualitatif du phénomène.

- Spectre avant limitation (signaux utiles et perturbateurs modulés).

- Répartition du bruit dans la bande de base après démodulation

$$F = f_u - f_p$$

### - Bruit dans une voie téléphonique en fonction de l'écart $f_u - f_p$ .



• Signaux sans dispersion d'énergie.

(1) - Voie de mesure à la fréquence  $F_1$ .

(2) - Voie de mesure à la fréquence  $F_2$ .

### Résultats pratiques.

- Le bruit est maximum pour la voie de fréquence centrale ( $f_u - f_p$ ).
- La surcharge des amplis en bande de base est voisine de celle obtenue avec un perturbateur à fréquence pure.
- Le rapport signal sur bruit dans une voie téléphonique est donné par la formule :  $\frac{S}{B} \text{ dB} = P_u - P_p + \alpha$   
 $\alpha$  : Coefficient de protection de modulation dépendant de paramètres suivants  
 (Cf. partie II).

• Nature des signaux interférant

• Ecart de fréquence  $f_u - f_p$ .

• Fréquence de la voie téléphonique considérée

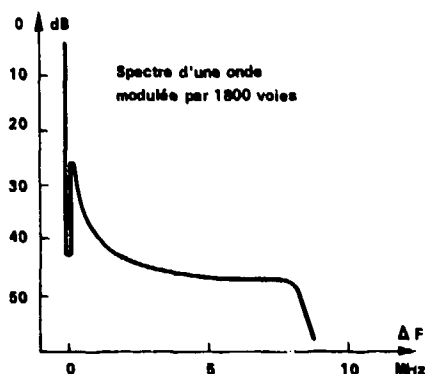
- Les bruits dus à plusieurs perturbateurs s'ajoutent "en puissance".
- La formule donnant le bruit de perturbation est de même nature que celle donnant le bruit thermique de propagation. Il peut s'en suivre une modification du seuil à  $10^6 \text{ pW}$  si celui-ci se produit avant le seuil de modulation de fréquence (960 - 1800 - 2700 voies).

### 4. - PROTECTION CONTRE LES EFFETS DES INTERFERENCES.

- Dispersion d'énergie.
- Plans de fréquence intercalaire.

#### 4.1. - Dispersion d'énergie.

Dans les faisceaux à grande capacité et dans les faisceaux à faible capacité peu chargés, une grande partie de l'énergie reste concentrée sur la porteuse.

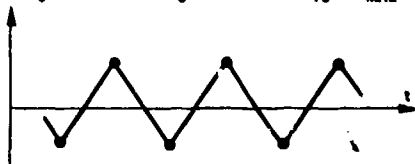


#### Spectre d'une onde modulée par 1800 voies.

L'interférence de deux signaux de ce type donne, après démodulation, les deux types de perturbations mentionnées dans le chapitre précédent.

• Perturbation à fréquence pure n'affectant qu'une seule voie mais dont le coefficient de protection de modulation  $\alpha$  peut devenir négatif si l'écart de fréquence entre les porteuses est suffisamment grand.

• Perturbation répartie dans la bande dont le coefficient  $\alpha$  est toujours positif dans les configurations habituelles.

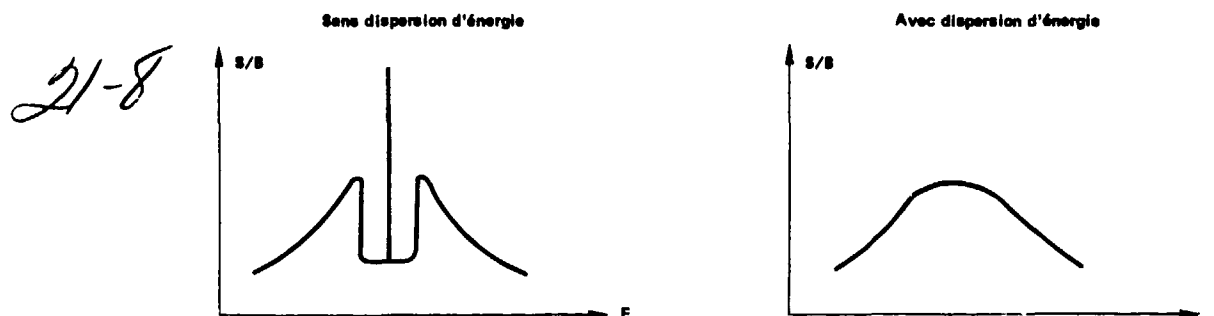


#### Signal de dispersion d'énergie.

L'emploi de la dispersion d'énergie "permet" d'étaler les perturbations du premier type sur un grand nombre de voies et de ramener, dans les configurations habituelles, le coefficient  $\alpha$  à une valeur positive.

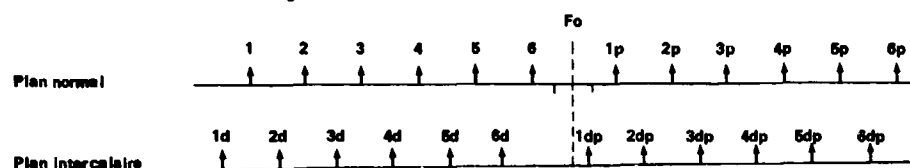
La dispersion d'énergie peut être obtenue en surimposant au signal multiplex un signal en dent de scie, d'une centaine de hertz, provoquant une excursion de fréquence de quelques centaines de kilohertz.

Les figures ci-dessous montrent l'influence de la dispersion d'énergie sur la répartition du bruit dans la bande de base.



#### 4.2. - Plans de fréquence intercalaire.

La figure ci-dessous montre l'emplacement relatif des canaux du plan normal et du plan intercalaire dans une bande de fréquence donnée.

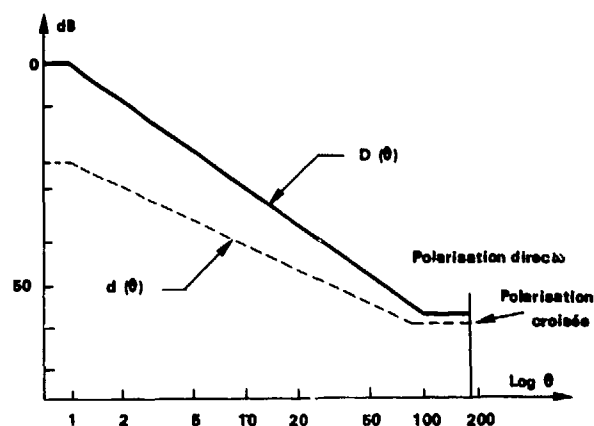


L'écart entre les porteuses du plan normal et du plan intercalaire est voisin de 14,5 MHz dans les bandes 4 et 6,2 GHz et est de 20 MHz dans la bande des 6,7 GHz.

La valeur de cet écart fait que les "perturbation à fréquence fixe" entre plan normal et plan intercalaire tombant au-delà de la bande de base et les "perturbations réparties" dans le haut de la même bande. De plus elle autorise pour les capacités inférieures ou égales à 960 voies un filtrage complémentaire éliminant une grande partie du spectre du signal perturbateur. L'adjonction de ce filtrage complémentaire ne doit se faire que dans les stations où il est indispensable car elle se traduit par une légère augmentation de la diaphonie due à la réduction de bande du récepteur.

Néanmoins, l'emploi des plans normaux et intercalaires avec filtrage complémentaire permet la réalisation de deux départs faisant entre eux un angle pouvant atteindre une dizaine de degrés.

#### 5. - CALCUL DES SIGNAUX PERTURBATEURS.



Le calcul des signaux perturbateurs fait intervenir les caractéristiques de rayonnement des antennes.

Celles-ci sont en général données sous forme d'un gain par rapport à l'antenne isotrope, d'un diagramme de rayonnement en polarisation directe et d'un diagramme de rayonnement en polarisation croisée.

La figure ci-contre donne un exemple de ces diagrammes.

L'examen des diagrammes ci-contre montre que le découplage en polarisation est en général supérieur au découplage en polarisation directe et que leur différence diminue jusqu'à pratiquement s'annuler lorsqu'on s'écarte de l'axe de l'antenne.

Du fait de deux diagrammes de rayonnement (polarisation directe ou croisée) à l'émission et à la réception il existe entre deux antennes quatre chemins de propagation correspondant aux configurations suivantes :

##### Emission en polarisation 1 :

- Réception en polarisation 1.
- Réception en polarisation 2.

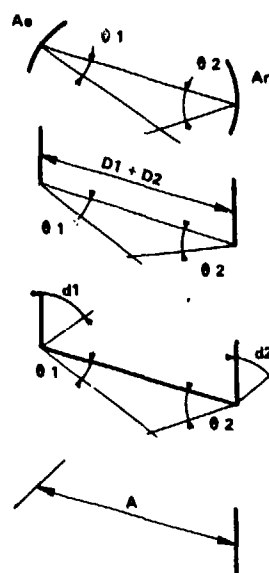
##### Emission en polarisation 2 :

- Réception en polarisation 1.
- Réception en polarisation 2.

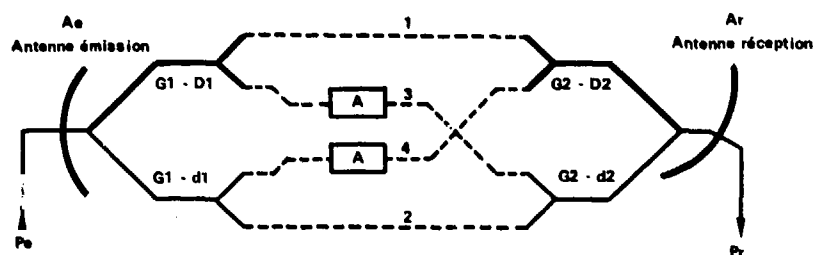
Les exemplaires donnés ci-après montrent le comportement de deux antennes fonctionnant sur la même polarisation et sur des polarisations croisées.

### Symboles utilisés.

$A_e$	Antenne d'émission
$A_r$	Antenne de réception
$\text{---}$	Signaux correspondant à la polarisation directe.
$\text{---}$	Signaux correspondant à la polarisation croisée.
$G_1 - G_2$	Gain des antennes.
$D_1 - D_2$	Découplage en polarisation directe.
$d_1 - d_2$	Découplage en polarisation croisée.
$A$	Atténuation de rotation de polarisation.



### Antennes fonctionnant sur la même polarisation.



### Evaluation relative des différents signaux reçus.

1 $\rightarrow$	$G_1 + G_2 - (D_1 + D_2)$	3 $\rightarrow$	$G_1 + G_2 - (A + D_1 + d_2)$
2 $\rightarrow$	$G_1 + G_2 - (d_1 + d_2)$	4 $\rightarrow$	$G_1 + G_2 - (A + d_1 + D_2)$

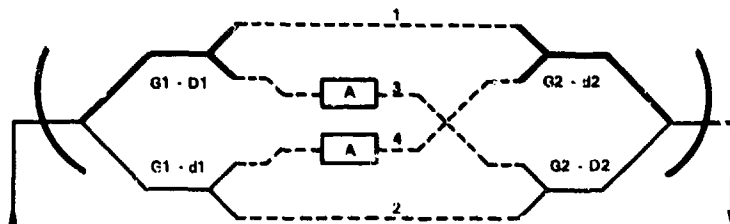
Par suite de la présence du terme  $A$  les signaux 3 et 4 sont beaucoup plus faibles que l'ensemble des signaux 1 et 2 et peuvent être négligés.

En posant  $d_1 = D_1 + \alpha_1$  et  $d_2 = D_2 + \alpha_2$ , l'expression des signaux reçus devient :

1 $\rightarrow$	$G_1 + G_2 - (D_1 + D_2)$
2 $\rightarrow$	$G_1 + G_2 - (D_1 + D_2) - (\alpha_1 + \alpha_2)$

Le signal prépondérant est le signal 1 et ce d'autant plus que l'on est proche des axes des antennes, c'est-à-dire que  $D_1$  et  $D_2$  tendent vers zéro.

### Antennes fonctionnant en polarisation croisée.



### Evaluation des différents signaux reçus.

1 $\rightarrow$	$G_1 + G_2 - (D_1 + d_2)$	3 $\rightarrow$	$G_1 + G_2 - (A + D_1 + D_2)$
2 $\rightarrow$	$G_1 + G_2 - (d_1 + D_2)$	4 $\rightarrow$	$G_1 + G_2 - (A + d_1 + d_2)$

Par suite de la présence du terme  $A$  les signaux 3 et 4 sont beaucoup plus faibles que l'ensemble des signaux 1 et 2 et peuvent être négligés.

En posant  $d1 = D1 + 1$  et  $d2 = D2 + 2$ , l'expression des signaux reçus devient :

- 1  $G1 + G2 - (D1 + D2) - \alpha 2$
- 2  $G1 + G2 - (D1 + D2) - \alpha 1$

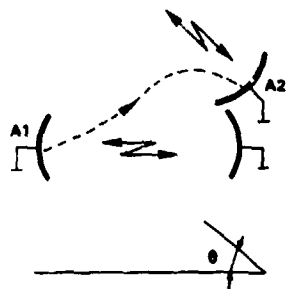
Le signal prépondérant est celui pour lequel le terme  $\alpha$  est plus faible. Dans le cas d'antennes identiques, il correspond au cas où l'on est le plus éloigné de l'axe, c'est-à-dire à la plus grande valeur de  $\theta$ .

#### Relation utilisées en pratique.

En pratique deux cas sont à considérer :

- Une des antennes est dans l'axe de l'autre.
- Aucune des antennes n'est dans l'axe de l'autre.

#### a) - Cas où une des antennes est dans l'axe de l'autre ( $D1 = 0$ ).

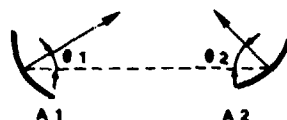


Ce cas est le plus courant car c'est le cas de stations adjacentes.

- Polarisation directe  $\frac{D2}{2}$
- Polarisation croisée  $d2 = D2 + \alpha 2$

En toute rigueur il convient de prendre la plus petite des valeurs ( $D2 + \alpha 2$ ) ou ( $D2 + \alpha 1$ ) ; mais compte tenu des caractéristiques d'antennes et de la valeur non nulle de l'angle  $\theta 2$ ,  $\alpha 2$  est presque toujours supérieur à  $\alpha 1$  même si les antennes ne sont pas identiques.

#### b) - Cas où aucune des antennes n'est dans l'axe de l'autre.



Ce cas correspond en général aux perturbations par surassement ou aux perturbations entre liaisons voisines.

$$\theta 2 > \theta 1.$$

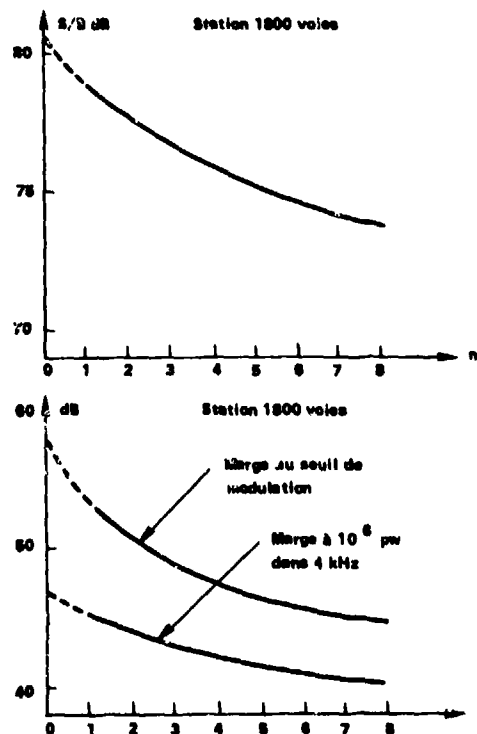
- Polarisation directe  $\frac{D1 + D2}{2}$
- Polarisation croisée
  - Antennes identiques  $D1 + D2 + \alpha 2 \rightarrow D1 + d2$
  - Antennes différentes

Dans ce cas il convient de prendre la plus petite des valeurs ( $D1 + d2 = D1 + D2 + \alpha 2$ ) ou ( $D2 + d1 = D1 + D2 + \alpha 1$ ), c'est-à-dire celle qui correspond à la valeur minimum de  $\theta$ .

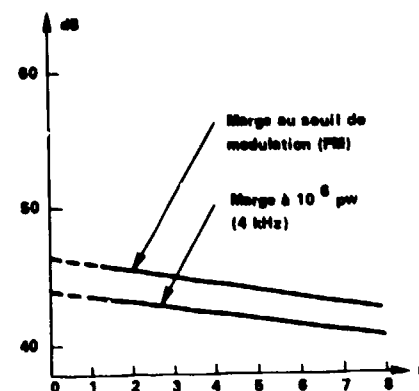
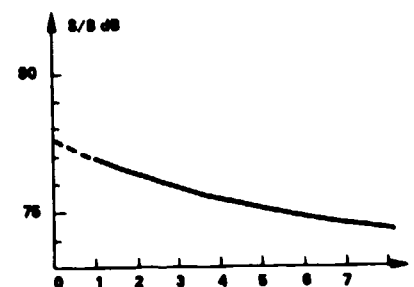
#### 6. - CALCUL DES PERTURBATIONS DANS QUELQUES CAS CARACTERISTIQUES.

Deux cas sont envisagés : le cas de la station où aboutissent uniquement des liaisons 1.800 voies et le cas de la station où aboutissent uniquement des liaisons 960 voies. Tous les bonds sont supposés avoir la même longueur (45 km) et utiliser des antennes identiques offrant un découplage de 64 dB aussi bien en polarisation directe qu'en polarisation croisée. Le calcul porte essentiellement sur l'évolution du bruit et du seuil en fonction du nombre de perturbateurs (n).

Systeme,		1 800 voies	960 voies
• Longueur du bond	km	45	45
• Longueur des feeders	m	50   50	50   50
• Puissance émission	dBm	42	30
• Atténuation de propagation à 6 GHz	dB	141,3	141,3
• Pertes de branchement	dB	5,4	5,4
• Pertes feeders	dB	5	5
• Gain des antennes	dB	44   44	44   44
• Atténuation entre E et R	dB	63,7	63,7
• Bruit de référence ( = 8 dB).	dBmop	- 102,2	- 111,2
• Puissance de seuil ( $10^6$ pW dans 4 kHz)	dBm	- 68,6	- 77,6
• Puissance de réception	dBm	- 21,7	- 33,7
• Puissance de seuil FM	dBm	- 80	- 80



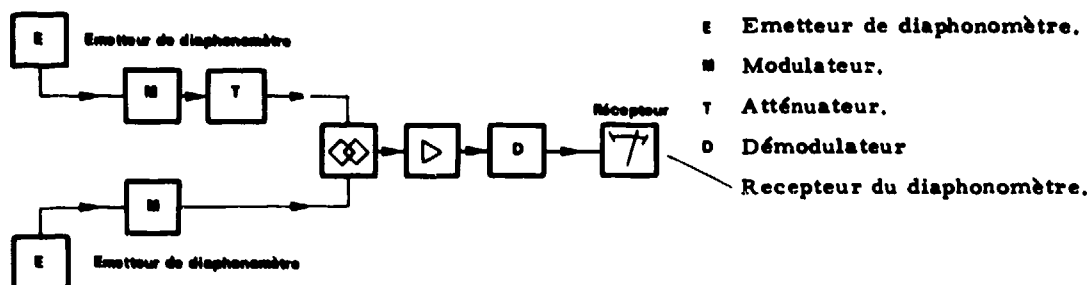
		<u>1 800 voies</u>	<u>960 voies</u>
● Rapport signal/bruit thermique	dB	80,5	77,5
● Bruit thermique de réception	pW	9	18
● Marge au seuil $10^6$ pW	dB	46,9	43,9
● Protection de modulation	dB	20	22
● Découplage d'antenne	dB	64	64
● Puissance d'un perturbateur	dBm	- 87,5	- 97,7
● Rapport signal sur perturbation	dB	84	86
● Bruit introduit par un perturbateur	pW	4	2,5
● Bruit total pour n perturbateur	pW	$9 + 4 n$	$18 + 2,5 n$





**PARTIE II.****PROTECTION DE MODULATION. - PERTURBATION REPARTIE DANS LA BANDE.**

Les résultats donnés ci-après sont des résultats expérimentaux se rapportant aux faisceaux de téléphonie FDM - FM à moyenne et grande capacité. (de 600 à 2 700 voies). Ils ont été obtenus à partir du montage suivant.



Conditions de mesure. Notations utilisées.

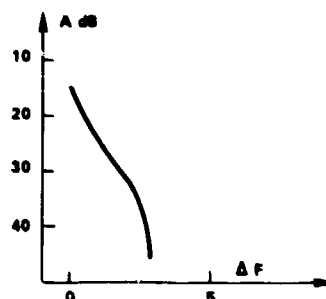
- Excursion de fréquence 400, 200, 140 kHz eff. suivant la capacité.
- Charge du multiplex :  $-15 + \log N$  ( $N$  = nombre de voies)
- Préaccentuation :  $\pm 4$  dB (selon avis du CCIR)
- $\Delta F$  écart de fréquence entre les signaux utiles et perturbateurs.
- A. Niveau par rapport à la porteuse non modulée (bande de mesure 25 kHz).
- $\mathcal{L}$  protection de modulation - valeur pondérée.
- Valeurs relevées sans dispersion d'énergie ce qui explique la présence d'une crête lorsque l'écart de fréquence  $\Delta F$  est égal à la fréquence de la fenêtre de mesure.

**1. - PERTURBATION D'UN SIGNAL A 600 VOIES PAR UN SIGNAL A 600 VOIES.****1.1. -  $\Delta f = 200$  kHz eff.**

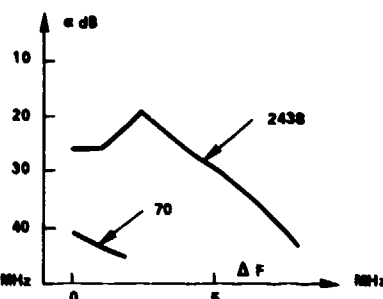
Voie 2.438 kHz

- $\Delta F = 0$   $\mathcal{L} \neq 27$  dB
- $\Delta f = 7$  MHz  $\neq 38$  dB
- $\Delta f = 14$  MHz  $> 45$  dB

Spectre de l'onde modulée



Bruit en présence d'une perturbateur modulé

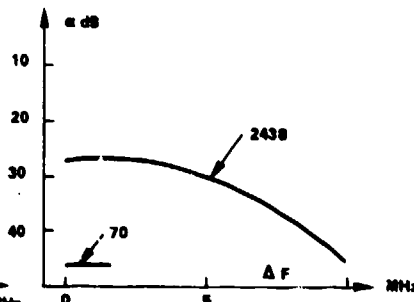
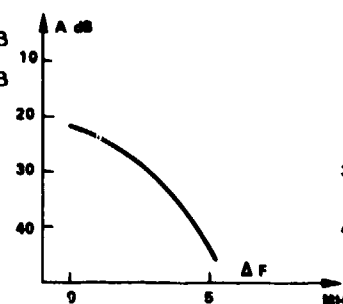


70 - Fréquence centrale de la fenêtre de mesure.

**1.2. -  $\Delta f = 400$  kHz eff.**

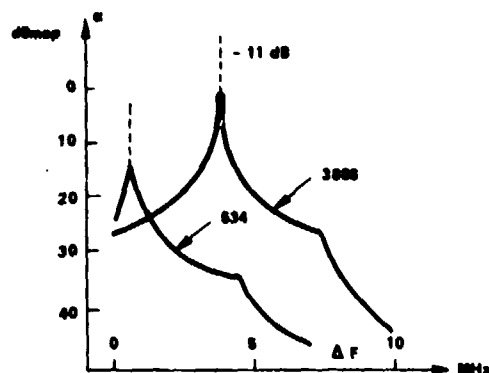
Voie 2.438 kHz

- $\Delta F = 0$   $\mathcal{L} \neq 27$  dB
- $\Delta F = 7$  MHz  $\mathcal{L} \neq 35$  dB
- $\Delta F = 14$  MHz  $\mathcal{L} > 45$  dB



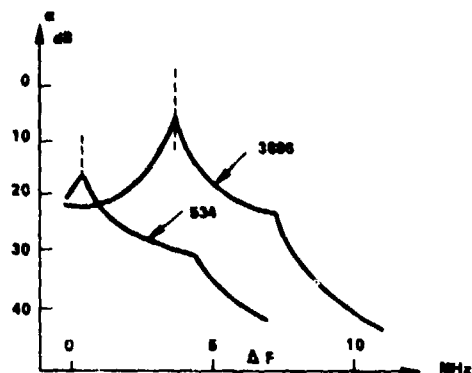
## 2. - PERTURBATION D'UN SIGNAL A 960 VOIES PAR UN SIGNAL A 960 VOIES.

Bruit en présence d'un perturbateur non modulé



$\Delta f = 0$	Voie 534 kHz	$\angle \neq$ 22 dB
	3886 kHz	$\angle \neq$ 26 dB
$\Delta f = 14,5$ MHz	534 kHz	$\angle \geq$ 50 dB
	3886 kHz	$\angle \geq$ 50 dB

Bruit en présence d'un perturbateur modulé

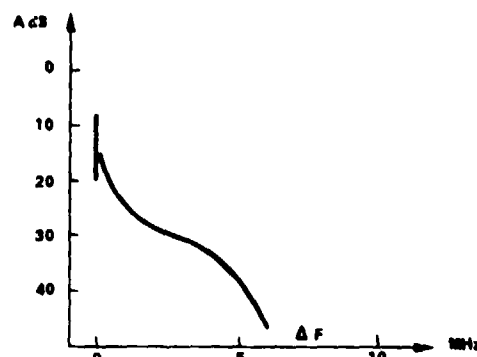
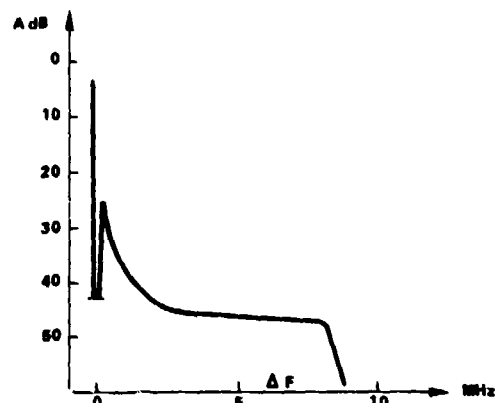


$\angle \neq$ 21 dB
$\angle \neq$ 22 dB
$\angle \geq$ 50 dB
$\angle \geq$ 50 dB

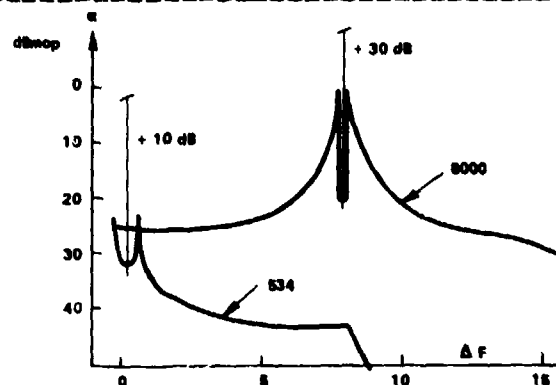
## 3. - PERTURBATION D'UN SIGNAL A 1800 VOIES PAR UN SIGNAL A 1800 VOIES.

Spectre de l'onde modulée

( $\Delta f = 140$  kHz eff)

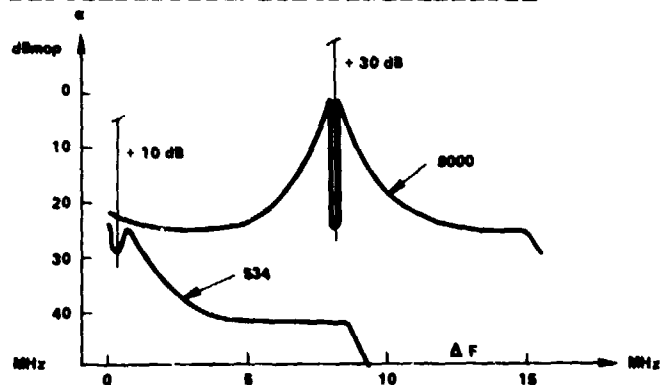


Bruit en présence d'un perturbateur non modulé



$\Delta f = 0$	Voie 534 kHz :	$\angle \neq$ 23 dB
	Voie 8 MHz :	$\angle \neq$ 23 dB

Bruit en présence d'un perturbateur modulé

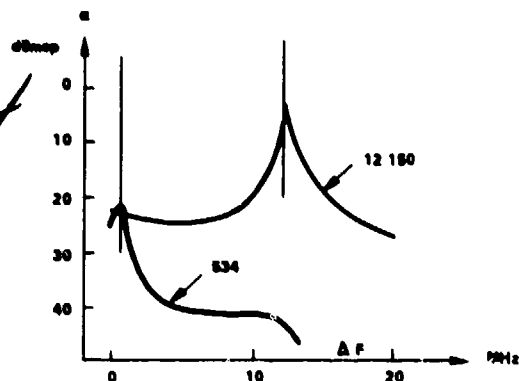


$\angle \neq$ 22 dB
$\angle \neq$ 20 dB

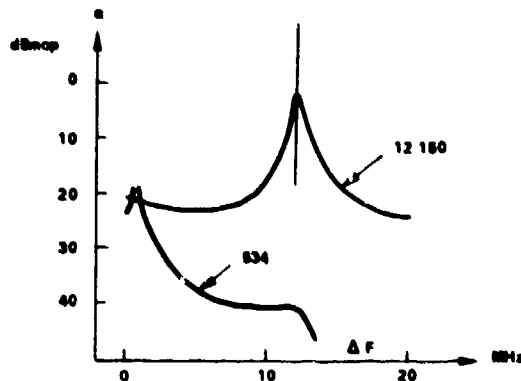
#### 4. - PERTURBATION D'UN SIGNAL A 2.700 VOIES PAR UN SIGNAL A 2.700 VOIES.

Bruit en présence d'un perturbateur non modulé

Bruit en présence d'un perturbateur modulé



$\Delta f = 0$  Voie 534 kHz  $\alpha \neq$  24 dB  
12.150 kHz  $\alpha \neq$  27 dB

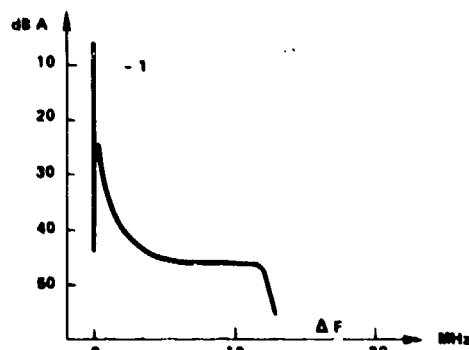


$\alpha \neq$  24 dB  
 $\alpha \neq$  20 dB

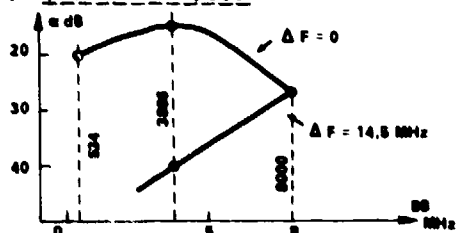
#### 5. - PERTURBATIONS RECIPROQUES ENTRE SIGNAUX DE NATURE DIFFERENTES

- 1 960 voies  $\rightarrow$  1.800 voies
- 2 1.800 voies  $\rightarrow$  960 voies
- 3 960 voies  $\rightarrow$  2.700 voies
- 4 2.700 voies  $\rightarrow$  960 voies

Les mesures suivantes ont été effectuées pour des écarts de fréquence ( $\Delta F$ ) fixes, caractéristiques des plans 5,9 - 6,4 GHz et 6,4 - 7,1 GHz.



##### 5.1. - 960 $\rightarrow$ 1.800



$\Delta F = 0$   $\Delta F = 14,5$  MHz

Voie 534  $\alpha \neq$  20 dB

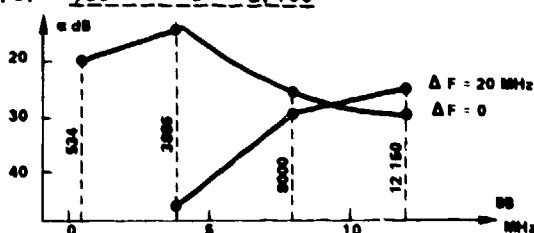
voie 3886  $\alpha \neq$  16 dB

Voie 8000  $\alpha \neq$  27 dB

3886  $\alpha \neq$  40 dB

8000  $\alpha \neq$  27 dB\*1

##### 5.3. - 960 $\rightarrow$ 2.700



$\Delta F = 0$   $\Delta F = 20$  MHz

Voie 534  $\alpha \neq$  20 dB

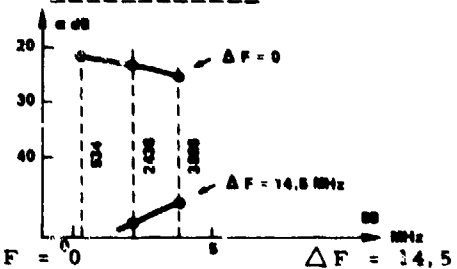
Voie 3886  $\alpha \neq$  15 dB

Voie 12150  $\alpha \neq$  30 dB

8000  $\alpha \neq$  29 dB

12520  $\alpha \neq$  25 dB

##### 5.2. - 1.800 $\rightarrow$ 960



$\Delta F = 0$   $\Delta F = 14,5$  MHz

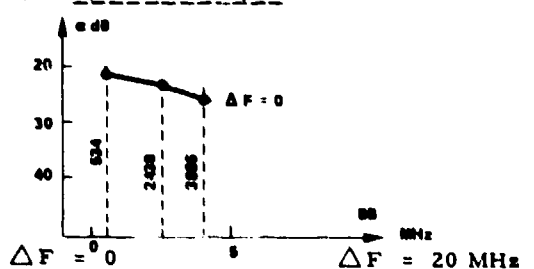
Voie 534  $\alpha \neq$  22 dB

Voie 3886  $\alpha \neq$  27 dB

$\alpha >$  50 dB

$\alpha \neq$  48 dB\*1

##### 5.4. - 2.700 $\rightarrow$ 960



$\Delta F = 0$   $\Delta F = 20$  MHz

Voie 534  $\alpha \neq$  22 dB

Voie 3886  $\alpha \neq$  26 dB

$\alpha >$  50 dB

$\alpha >$  50 dB

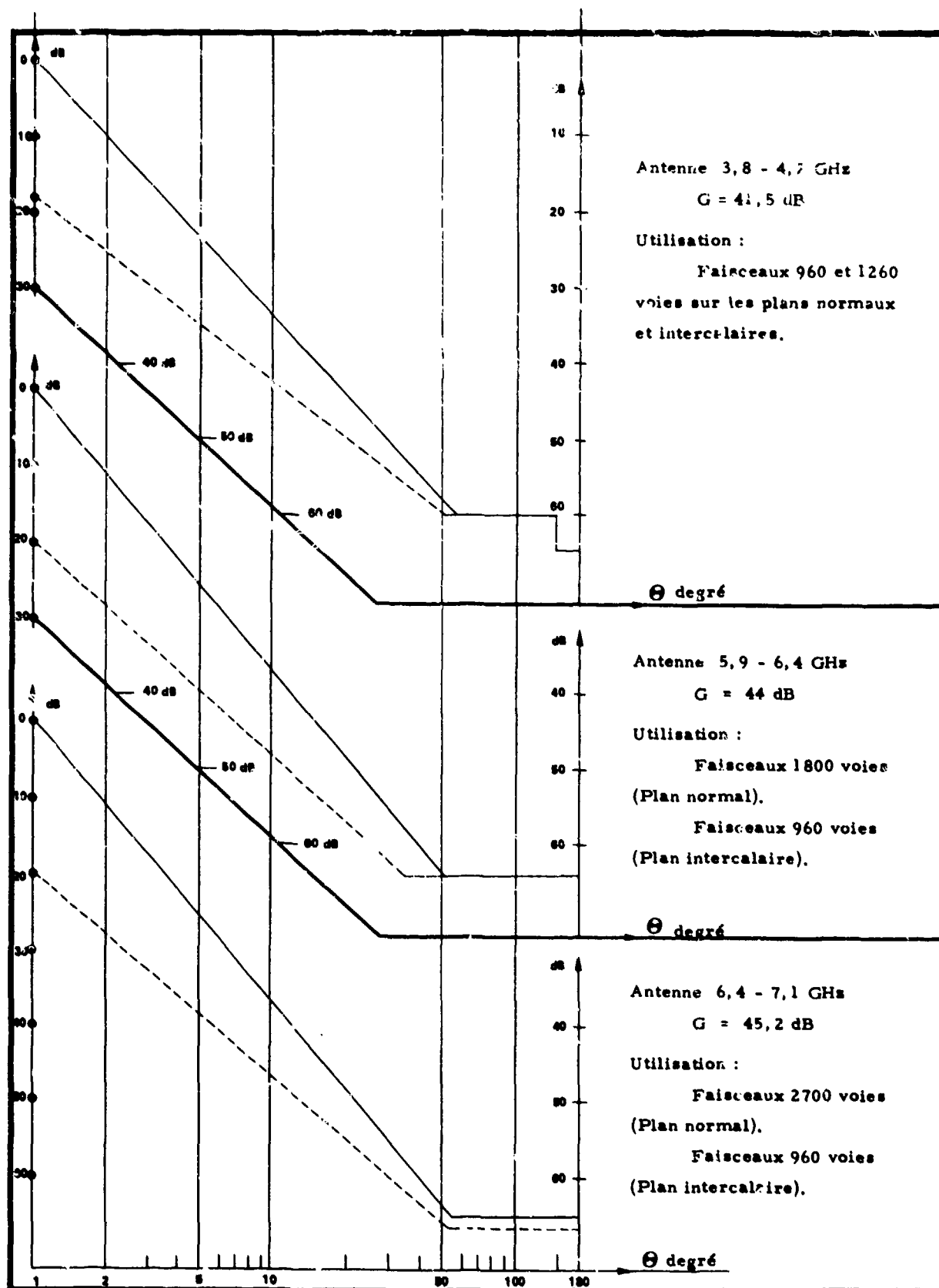
\*1. Dans le cas de perturbations 600  $\leftrightarrow$  1800 voies, ces chiffres sont plus élevés.

- Remerciements. - L'auteur tient à remercier M. Philippe Legendre Chef du service Technique des faisceaux hertziens à grande capacité de la Thomson-CSF qui lui a fourni la plupart des mesures servant de base à cet article.

# DIAGRAMMES D'ANTENNES.

Les figures ci-dessous donnent, à titre d'exemple, un diagramme type des antennes utilisées par l'Administration pour la réalisation du réseau national. Le découplage normal de 64 dB conduit, dans un réseau homogène à un rapport signal sur perturbation de 84 à 86 dB soit 40 à 25 pW.

21-15



## DISCUSSION

R. OLESCH: You mentioned that a white noise spectrum was assumed in your choice of the factor  $\sqrt{f}$  on the blackboard. Should the FM noise spectrum not be parabolic in frequency?

F. CROCOMBETTE: Prior to demodulation, the noise spectrum is a white spectrum, like in amplitude modulation. After demodulation, noise assumes a parabolic form (see equation and diagram on original text). In frequency modulation,  $\Delta f$  is constant, which accounts for this parabolic shape.

## RADAR INTERFERENCE REDUCTION TECHNIQUES

22-1

William Fishbein  
Reinhard Nlesch  
Otto Rittenbach  
US Army Electronics Command  
Fort Monmouth, N. J.  
USA

### SUMMARY

Techniques are described, applicable to radar, which enhance the compatibility of multiple systems in limited frequency space.

By appropriate combination of multiple frequencies, the spectral occupancy of a signal can be reduced through pulse shaping, without sacrifice in range resolution. This method is extended to continuous wave radar, resulting in sidelobe reduction without amplitude modulation. A function is defined relating mutual interference of two systems in terms of their waveforms, physical and spectral proximity, and is used as a measure of interference. Ordinary single sideband techniques are modified and applied to radar to reduce spectral width. Considerations for interlacing the discrete line spectra of several radars are given. They include single sideband processing of unidirectional doppler signals and a step scanning scheme which permits increasing the allowable pulse rate.

Experimental results and applications are given.

### 1. INTRODUCTION

The conservation of the electromagnetic spectrum is of vital importance, since available frequency bands are critically limited. This shortage is already so serious at the lower radar frequencies that allocations are virtually unavailable for high resolution radars. It is, therefore, imperative that spectral space be employed at the greatest possible efficiency.

Interference may be encountered by a radar due to direct reception of another radar's emission (via antenna mainlobes, sidelobes or combination of each). It may also occur as reflections from targets which were illuminated by the second radar.

Methods and their implementations are described herein which reduce interference in several ways. First, by shaping of the transmitted waveform (pulse or CW) which reduces interference from spectral sidelobes, hence allows greater spectral proximity between two radars; secondly, by decreasing the transmitted spectrum as much as 50% through single sideband techniques; thirdly, by providing techniques which allow several radars to share the same band.

### 2. SPECTRAL SIDELobe REDUCTION

#### a. Principles of Pulse Shaping

The usual method of decreasing the width of the radiated spectrum of a pulse radar is to shape the envelope of the transmitted pulse by filtering. This is difficult at radio frequencies (RF) for radars with tunable transmitters or when high power levels are involved. Further, this approach does not offer a solution for continuous wave (CW) radars. A CW radar with range resolution is basically similar to ordinary pulse radar. After all, the former waveform can be considered as a sum of multiple pulse waveforms. Both use time coded waveforms which produce echoes that are encoded according to the range where they originated. Both have wide frequency spectra, the width depending on the resolution achieved. The term "pulse" is, therefore, generalized here to include both waveforms. Considerations of the on-off waveform will be shown to provide insight for CW radars as well.

The pulse shaping approach considered here is based on the principle of reducing the first or nearby sidelobes of a spectrum from a rectangular pulse. By the addition of another spectrum, appropriately weighted and displaced in frequency, these sidelobes can be partially cancelled. Although other sidelobes may actually increase in this procedure, it will reduce rather than increase the spectral occupancy of the resultant signal. A more concentrated spectrum is, therefore, obtained. Thus, by combining ordinary rectangular pulse signals of different but related frequencies and phase, this method of bandwidth reduction effects a shaping of the spectrum, hence also of the corresponding time pulse. In the frequency domain, this process may be represented as the addition of si-shaped spectra ( $\text{si } x = (\sin x)/x$ ) in such a way that the resulting combined spectrum has sidelobes that fall off at a higher rate than those of the spectra of the component pulse signals.

In the time domain the pulse shape corresponding to such a composite spectrum will be in general of the form  $\cos^n$ , its shaping (smoothness) depending on  $n$  and thereby on the number of component signals.

#### b. The Rectangular Pulse

An ordinary rectangular pulse, contained within the switching function  $S(t)$ , is the simplest member of the family of pulse shapes given by  $\cos^n$ , i.e.,  $\cos^0$ . Assuming its amplitude to be unity, its width  $T$  and its center at time  $t = 0$  (Fig. 1a), its spectrum  $F_0(\omega)$  (subscript corresponding to the order

of smoothness) will be given by

$$22-2 \quad F_0(w) = \int_0^T S(t) \cos^0 wt \cos wt \, dt = \frac{2 \sin(wT/2)}{w} = T \operatorname{si}(wT/2)$$

Here  $w$  represents radian frequency. When this pulse modulates an RF carrier,  $w_c$ , the same spectrum will exist, centered at  $w = w_c$ . It is noted that for this spectrum the sidelobe peaks fall off as  $1/w$ .

The mutual interference between two radars depends on many factors, some of which are their given physical separation and siting, their antenna patterns, power levels, receiver sensitivities, antenna alignment, frequency separation, and occupied bandwidths. A mutual interference function  $I$  is defined in Appendix 1. It represents the output of a particular receiver to an input conditioned by these parameters. For the rectangular pulse  $I$ , as a function of the spectral separation,  $w_d$  between matched and received signals is

$$I = \frac{\sin(w_d T/2)}{w_d} = (T/2) \operatorname{si}(w_d T/2)$$

It is apparent that, given a fixed  $T$ , for some values of frequency separation (i.e., when  $w_d T/2 = kw$ ;  $k = 1, 2, \dots$ ) the interference approaches 0. However, various instabilities as well as neglected higher order terms and the geometrical relation between radars and targets make a realization of this choice difficult. Hence the "envelope" of this function,  $1/w_d$ , is considered the factor which determines the allowable spectral proximity of 2 rectangular pulse radars.

If, for example, it were required that the interference from an adjacent si-shaped spectrum be 48 dB down, Appendix 1 shows that a separation of  $r \approx 81.5$  phase revolutions is required, where  $r = w_d T/2w$ . Since the spectrum,  $F_0(w)$ , for both of the interfering signals has nulls at  $wT = 2k\pi$ ;  $k = 1, 2, \dots$ , this value of  $r$  requires that the two spectra be separated by approximately 81.5 sidelobes. In particular, for a 1  $\mu$ s rectangular pulse, 81.5 MHz separation is required to assure the interference to be below -48 dB.

### c. The Cosine Pulse

The first order of improvement of the rectangular pulse is the cosine pulse. By removing the discontinuities of the waveform a reduction in the sidelobe level, hence in the spectral occupancy of the signal, is achieved.

If pulse shaping by means of filters is to be avoided, the cosine pulse is produced by appropriate modulation, as shown in Fig. 1. The RF carrier, Fig. 1c, is balanced modulated by the shaping function of 1b and gated by  $S(t)$  to form a pulse train. The resulting pulse, Fig. 2d, has the desired cosine envelope.

In order to analyze this pulse it is noted that the modulation of the carrier by the shaping function results in two frequency components. Letting the carrier  $f_c(t) = \cos w_c t$  and the shaping function  $f_s(t) = \cos \pi t/T$ , the cosine pulse  $f_1(t)$  is given by:

$$f_1(t) = S(t) f_s(t) f_c(t) = S(t) \cos(\pi t/T) \cos(w_c t) = \frac{1}{2} (\cos(w_c + \pi/T)t + \cos(w_c - \pi/T)t) S(t)$$

The cosine shaped RF pulse is thus the sum of two separate signals, one below and one above the carrier frequency. They differ in frequency by  $w_a = 2\pi/T$  and are shown in Fig. 1e.

The phase relation of these two signals is of importance and must be as shown in Fig. 1e. If one signal is considered to be a new carrier, the second represents the same signal linearly phase shifted by  $2\pi$  radians during the pulse duration  $T$ . This relationship gives rise to a modulation technique applicable to CW radar, as will be discussed later.

The addition of two rectangular RF pulses corresponds to the sum of two si-shaped spectra in the frequency domain. Fig. 2 shows the spectra associated with the signals of Fig. 1e, namely  $\frac{1}{2} F_0(w - w_c + \frac{w_a}{2})$  and  $\frac{1}{2} F_0(w - w_c - \frac{w_a}{2})$  and their sum  $F_1(w - w_c)$ , the spectrum of the cosine pulse, Fig. 1d.

From the definitions of  $F_0(w)$  and  $w_a$ ,  $F_1(w)$  can be expressed as

$$F_1(w) = \frac{1}{2} \left[ \frac{1}{w + w_a/2} - \frac{1}{w - w_a/2} \right] \cos \frac{wT}{2}$$

which is the baseband spectrum of the cosine pulse.

Fig. 2 alludes to the general procedure of spectral sidelobe reduction through pulse shaping. In particular, the component spectra are placed symmetrically about  $w_c$  so that the center of one is aligned with the first null of the other. The result is a partial cancellation of the first sidelobe by the mainlobe skirt of the second spectrum. Also, the maxima of the other sidelobes are aligned with those of the second spectrum so as to oppose each other. The sum of the two spectra has, therefore, significantly reduced sidelobes as they are the difference between the sidelobes of the individual spectra. The sidelobe improvement of the cosine pulse spectrum  $F_1$  over that of  $F_0$  is apparent if the component spectra of  $F_1$  are centered about  $w = w_a/2$ , i.e., when  $F_1(w + w_a/2)$  is formed. The frequency shifted  $F_1$  is given by

$$F_1(w + w_a/2) = \frac{1}{2} [F_0(w) + F_0(w + w_a)] = \frac{w_a}{2(w + w_a)} F_0(w)$$

This form of  $F_1$  shows an  $F_0$  modified by an additional pole. As was apparent from  $F_1(w)$  the cosine pulse spectral sidelobes decay almost as  $1/w^2$ . Fig. 3 (solid lines) shows a technique for generating a cosine pulse train in accordance with Fig. 2. The modulating frequency  $w_a/2$  is mixed with the carrier  $w_c$  in a multiplier. The resulting product is then gated by  $S(t)$ , which is accomplished by the pulse train generator and the RF switch. The variable delay serves to adjust the gating time so as to insure the proper synchronism with the shaping function  $\cos(w_a t/2)$ . The pulse width must also be adjustable to allow a match between the nulls of the modulation result and the end of the gate.

To evaluate any advantage in spectral occupancy of the cosine shaped pulse, the interference criterion is employed again. Appendix 2 shows the interference between radars using cosine pulses as

$$I = \left[ \frac{2}{w_d} - \frac{1}{w_d + w_a} - \frac{1}{w_d - w_a} \right] \frac{\sin(w_d T/2)}{4}$$

22-3

which falls off approximately as the third power of frequency separation, rather than the first as was the case for the rectangular pulse.

Using the previous level of -48 dB maximum interference, it is found that the spectral proximity,  $r$ , for two such signals is only  $r \approx 4.4$  i.e., they may be as near as 4.4 sidelobes' width to each other. This is a significant improvement over the previous requirement of 81.5 sidelobes for the case of the si-shaped spectrum.

#### d. The $\cos^2$ Pulse

To form this pulse in an analogous manner, three si-shaped spectra, displaced from one another by the spectral distance  $w_a = 2\pi/T$  are summed. A choice of component signals  $\cos w_c$ ,  $\cos(w_c + w_a)$ , and  $\cos(w_c - w_a)$  appears logical. However, the latter two signals are now weighted by a factor of  $1/2$  relative to the center frequency. This weighting arises from the requirements of symmetry of the sum spectrum and the fact that higher order sidelobes require smaller signals for cancellation. The baseband spectrum  $F_2(w)$  is given by:

$$F_2(w) = (1/4)F_0(w - w_a) + (1/2)F_0(w) + (1/4)F_0(w + w_a) = \frac{1}{4}(\sin(wT/2)) \left[ \frac{2}{w} - \frac{1}{(w - w_a)} - \frac{1}{(w + w_a)} \right]$$

The addition of one more si-spectrum has added one pole in the expression for the spectrum. The sidelobes of  $F_2(w)$  thus fall off about as  $1/w^3$ , which is an even more desirable behavior from the standpoint of spectral occupancy. The center of  $F_2(w)$  is located at  $w = 0$  (at the carrier  $w = w_c$  for the modulated signal), or again at the mean of center frequencies of the component spectra.

In the time domain, this process is simply a summation of three carriers, modulated by rectangular pulses. The resultant pulse shape,  $f_2(t)$ , is:

$$f_2(t) = \frac{1}{4}S(t) \cos w_c t + (1/4)S(t) \cos(w + w_a)t + (1/4)S(t) \cos(w - w_a)t = S(t) \cos w_c t \cos^2 w_a t/2$$

a  $\cos^2$ -shaped envelope on a carrier of frequency  $w_c$ . Consistent with the improved sidelobe behavior of its spectrum, this signal has an envelope of one degree smoother than the cosine pulse.

The measure of spectral occupancy  $I$  is again applied and is (see Appendix 3):

$$I = \left[ \frac{1}{w_d - 2w_a} - \frac{4}{w_d - w_a} + \frac{6}{w_d} - \frac{4}{w_d + w_a} + \frac{1}{w_d + 2w_a} \right] \frac{\sin(w_d T/2)}{16}$$

which decays approximately as the fifth power of spectral separation. As defined previously,  $r \approx 3.5$  which indicates a further saving in spectral occupancy. The improvement over the cosine pulse shape is diminishing, however, since for small values of  $r$  the increasing mainlobe widths of the spectra are dominant. The advantage of higher order pulse shapes becomes apparent when greater interference attenuation is required.

A technique for generating the  $\cos^2$  pulse is given by Fig. 3 if the dashed portion is used. The modulation frequency generator now produces  $\cos w_c t$  and the multiplier output is  $\cos(w_c + w_a)t$  and  $\cos(w_c - w_a)t$ , as shown in Fig. 4b. This signal is combined with the carrier  $\cos w_c t$  (Fig. 4a) and noted as before. Fig. 4c shows the output. The previous requirements for phase relationship between component signals and weighting still hold and  $S(t)$  must be properly synchronized.

#### e. Generalization of Filterless Pulse Shaping

As the process of combining rectangular RF pulses, properly related in amplitude, phase and frequency, is expanded higher orders of smoothness of the time function accompanied by corresponding sidelobe reduction is obtained. General requirements and properties of the  $\cos^n$  shaped RF pulse are obtained by expanding the expression for the baseband pulse. From Appendix 4 this is:

$$f_n(t) = S(t) \cos^n(w_a T/2) = \frac{1}{2^n} \sum_{p=0}^n \binom{n}{p} \cos(p - n/2)w_a t$$

where  $\binom{n}{p}$  are the  $n + 1$  binomial coefficients. This expression shows that the  $\cos^n$  shaped RF pulse is composed of  $n + 1$  rectangular RF pulses, all in phase at  $t = 0$  and having frequencies that differ by  $w_a = 2\pi/T$ . Their relative weights are given by the binomial coefficients associated with  $n$  and the normalization factor is the sum of the coefficients or  $2^n$ .

In the frequency domain these  $n + 1$  components result in  $n + 1$  si-shaped spectra similarly weighted and spaced at intervals of  $w_a$  symmetrically located about the carrier. In terms of baseband spectra:

$$F_n(w) = \frac{1}{2^n} \sum_{p=0}^n \binom{n}{p} F_0[w - (p - n/2)w_a]$$

The center of the sum spectrum  $F_n(w - w_c)$  will lie at  $w_c$  or, in general, at the mean of the component frequencies. For even  $N$  an odd number of components exist at  $w_c$ ,  $w_c + w_a$ ,  $w_c + 2w_a$ , etc. The spectrum will be of the form  $\sin x/x^{n+1}$  for large  $w$ . For odd  $n$  the  $n + 1$  components lie at  $w_c + w_a/2$ ,  $w_c + 3w_a/2$ ,  $w_c + 5w_a/2$ , etc. and the spectrum  $F_n$  will be of the form  $\cos x/x^{n+1}$  for large  $w$ . It should be noted that for odd  $n$  the spectrum may be shifted by  $w_a/2$  so that  $F_n(w - w_a/2)$  will also be of the form  $\sin x/x^{n+1}$  for large  $w$ .

It is noted that each additional component spectrum adds one order of smoothness of the resultant pulse by adding one pole to the expression for the spectrum. At the same time one null is removed from the spectrum. However, while the sidelobes are cancelled more strongly, the main lobe widens by  $w_a/2$  with each additional component spectrum. Effectively, the power of the signal is concentrated nearer the spectral



center at the expense of sidelobe power. Thus, while the bandwidth, as measured by the nulls bracketing the main lobe, is actually widened, the effective width of the spectrum (rms bandwidth) is decreased in the limit as  $n \rightarrow \infty$  the sidelobes vanish completely and a gaussian spectrum remains.

22-4 From the examples of Appendices 1 to 3, it is seen that  $I$ , as calculated there (signal and receiver matched except for center frequency), is of a form similar to that of  $F_n(w)$ . It appears that for any one interference level assumed it is not efficient to increase  $n$  indefinitely since  $r$  diminishes only slightly after a certain  $n$  is reached. By the use of  $I$ , calculated for design signals and receiver (and other radar parameters) together with a specified maximum interference level, a trade-off of  $r$  versus pulse shaping  $n$  must be conducted for each specific design.

Extending the technique of Fig. 3, Fig. 5 shows the general method of generating  $\cos^n$ -shaped RF pulses. Here the mixer produces many harmonics between the RF carrier signal and the modulator signal. The RF bandpass filters select the desired harmonics,  $n$  being odd multiples if the modulation frequency is  $w/2$  and all multiples if it is  $w$  ( $n$  odd or even respectively). These components are then adjusted in amplitude (weighting) and phase (linearity) and summed. The gating pulse generator is again adjustable in respect to the pulse length and starting time so as to assure gating the appropriate segment of the modulation product.

Instead of summing  $n + 1$  weighted rectangular pulses (si-spectra) to form a  $\cos^n$  pulse, it should be noted that, alternately, two unity weighted but previously shaped waveforms may be combined to form a resultant shape of greater smoothness. This arises from the fact that any series of binomial coefficients,  $\binom{n}{p}$ , can be obtained by adding two of the preceding series  $\binom{n-1}{p}$  displaced by one element. The following example illustrates this (at baseband), showing how a signal may be "built" up from other shaped pulses.

Component center frequency:	$-2w_a$	$-w_a$	0	$w_a$	$2w_a$	$3w_a$
$\cos^4$ Components of weight:	1	4	6	4	1	
$\cos^4$ Components of weight:		1	4	6	4	1
$\cos^5$ Resultant Components:	1	5	10	10	5	1

Spectral sidelobe level is often used as a measure of interference or quality of spectral shape. For the  $\cos^n$  family of pulse shapes this is not necessary since sidelobes decrease monotonically with increasing frequency and  $n$ . The parameter  $n$  describes the signal completely. It is possible, however, to obtain various sidelobe behaviors by varying either weights or center frequencies (or both) of component spectra. By selection of other than binomial weights and spacing of  $w_a$  selected sidelobes may be cancelled to various degrees. In this case  $n$  does not describe the signal completely since this technique redistributes signal power to the outer sidelobes which generally increase. This method of pulse shaping may have merit in certain cases, especially when only the maximum sidelobe level is specified.

#### f. CW Radar Applications

The concept of pulse shaping also applies to CW radars with range resolution. Although less obvious, a "pulse" shape can usually be defined in the time domain. The basic similarity of radars with range resolution is best observed in their power spectrum and autocorrelation function of the modulating waveform which can be the same for both radar types.

An example of a CW radar, having a rectangular "pulse" shape employs phase reversal modulation and a binary pseudo-random code as modulating function.<sup>1</sup> A single carrier frequency is transmitted whose phase is switched by  $\pi$  radians (phase reversed) corresponding to a change in the state of the code. This process is equivalent to a direct multiplication of the carrier by the numerical value (+1 or -1) of the code at any instant in time, hence represents a modulation of the carrier by the rectangular pulses that constitute the code. The spectrum for this radar, using a 15-element code, is shown in Fig. 6. It has clearly the si envelope associated with a rectangular pulse.

Fig. 6 also shows the spectrum for another CW radar<sup>2</sup> which exhibits the shape and the sidelobe behavior of the spectrum for a cosine pulse. This effective pulse shape was achieved by the use of two RF frequencies in the modulation process of the CW radar and is thus consistent with the previously derived criteria for pulse shaping. A binary pseudo random code was again employed as modulating function. The transmitted signal consisted of the carrier frequency for all time during which the code takes on the first value. The carrier is linearly phase shifted when the code assumes the second value. For this particular radar, a 15-element code was used; the linear phase shift was  $\pi$  radians over the interval of one code element. A phase shift of  $\pi$  was chosen because of the structure of this particular modulating function for which a  $2\pi$  phase shift would result in a strong predominance of the carrier. A shift of  $\pi$  rather than  $2\pi$  results in a distribution of the power among the sidebands rather than in the carrier. As Fig. 6 indicates, the carrier is considerably lower than the envelope of the spectrum and would completely vanish if the binary values were evenly distributed among the code elements. It should also be noted that the spectrum is asymmetric with respect to the carrier. Most important, however, the  $1/w^2$  behavior of the sidelobes, typical of the cosine pulse is in evidence.

### 3. SINGLE SIDEBAND AND SKEWED SIDEBAND SCHEMES

#### a. General

Ordinary amplitude and frequency modulation produce symmetric pairs of sidebands which, by their symmetry can be considered redundant. Single sideband operation, which transmits all information by means of one sideband only, has long been of great value in communication to reduce spectral occupancy. It may also find application for this purpose in radar. However, here the techniques must be somewhat modified since radar requires that for each resolved target the phase of the carrier be available as well as the sidebands' phases in relation to it. If one sideband only (without carrier) were received and demodulated with a carrier of arbitrary phase, then the modulation function thus recovered would be shifted in phase by an arbitrary amount also. Assuming a carrier  $\cos w_c t$  with phase  $\phi_c$  and a modulation function  $\cos w_m t$ , the resulting sidebands would be:

$$\cos(\omega_c t + \phi_c) \cos \omega_m t = 1/2 \cos(\omega_c t + \omega_m t + \phi_c) + 1/2 \cos(\omega_c t - \omega_m t + \phi_c)$$

Demodulation of either sidebands alone by a carrier of arbitrary phase  $\theta$  yields:

$$\cos(\omega_c t \pm \omega_m t + \phi_c) \cos(\omega_c t + \theta) = 1/2 \cos(2\omega_c t \pm \omega_m t + \phi_c + \theta) + 1/2 \cos(\pm \omega_m t + \phi_c - \theta)$$

22-5

The first term of the result is usually filtered out. The second term contains the information which is sought. It can be seen that the phase  $\theta$  of the demodulation reference must be the same as that of the carrier if an undistorted modulation signal is to be recovered. Fig. 7 illustrates a rectangular pulse modulating function, distorted by a  $\pi/2$  radian phase shift, i.e., its Hilbert transform. For other phase shifts the zero crossing would generally be displaced from the center but the distortion can still be significant. It is apparent that phase distortion of the recovered modulation function would seriously degrade the resolution of the radar or exceed dynamic ranges. Ideally, then, transmitting the carrier for phase reference and one sideband, completely preserved, would meet the requirements of radar operation. Several schemes are presented which approach this ideal case to various extents.

#### b. Minimum Bandwidth Radar

For a continuous spectrum, the ideal case of deleting one entire sideband would require an infinitely sharp cut-off filter but would result in the saving of 50% of the spectral occupancy. For the case of a discrete radar spectrum, this maximum saving can be approached very closely by employing a filter, sharp enough to cut off below the first PRF line of the spectrum. Figs. 8a and b show this condition for a simplified spectrum. Fig. 9 shows a technique to generate such a signal. Combining the output of the RF and modulation frequency generators, the RF modulator produces an ordinary double-sideband modulated RF signal. Assuming that the modulation frequency is the ordinary pulse train, a line spectrum results. Bandpass 1, having the properties described above, removes one sideband and sends the single sideband signal and carrier (Fig. 8b) to the antenna via the circulator. On reception, the signal enters two channels in which the carrier and sideband are separated and then coherently demodulated by mixing with the RF carrier. The sideband channel, containing the target information, is then range-gated by the modulation frequency demodulator and correlated with the demodulated carrier which provides the phase reference for detection. Maximum efficiency is achieved if the power is divided evenly between carrier and sideband.

It must be noted that the single-sideband Bandpasses 1 and 2 perform most critical operations. Not only must the cut-off of the undesired sideband be very sharp, but the filters must accomplish the necessary phase compensation to produce constant delay for all frequencies of the received sideband. This phase compensation may be distributed between the transmitter and Bandpass 2 of the receiver. However, it is important that any phase shift produced peaks do not exceed the dynamic range of the various subsystems, especially the high power transmitter stages.

#### c. Nyquist Filtering

An alternate scheme is possible to generate a narrow spectrum similar to that of a single-sideband signal. It is similar to the above except that gradual cut-off filtering (Nyquist filtering) is employed during transmission and reception. Fig. 10 shows a simplified spectrum and the operations which are performed on it by this technique. The block diagram of Fig. 9 again illustrates the processes. The single-sideband Bandpass 1 is now a filter which removes one sideband, but doing so incompletely, as shown in Fig. 10b. The carrier and sideband filters in the receiver have similar gradual cut-off characteristics so that the signals entering the two channels of the receiver are as shown in Figs. 10c and 10d. The processing of the signals is otherwise the same as previously described. Also, the same requirements of phase linearity and phase relation between carrier and sideband signals are again imposed on this filter.

Nyquist filtering, although it results in less bandwidth saving than the previous scheme, is mentioned here because it is a feasible technique. It is commonly employed in television transmission and can be implemented for radars of similar frequency. A single-sideband radar differs only in the added carrier channel which is needed as a range reference during reception. In the example shown in Fig. 10, the distribution of power between carrier and sideband channels of the receiver is not equal, as required for best correlation. Practical constraints on filters will often cause such a condition. However, even a distribution such as shown would still result in acceptable correlation. The saving of spectral occupancy is always below the maximum 50% and depends on the roll-off of the sideband filter.

An alternate RF modulation and single sideband generation scheme may be employed. In principle it consists of two channels in which quadrature RF signals are mixed with quadrature modulation functions respectively. The sum of these two products will be a signal with one of the sidebands cancelled.

Fig. 11 illustrates this method, slightly modified for a more practical implementation. The modulating function can be rectangular pulse commonly used in radar. To derive the required quadrature signals two sets of phase shifting operations are performed, resulting in shift of  $+\pi/4$  and  $-\pi/4$  radians rather than one shift of  $\pi/2$ . RF carrier and modulation are thus processed in Phase Shifters 1 and 2. The upper and lower channels will, therefore, be in quadrature as required. For sinusoidal modulation the result is as follows:

$$\cos(\omega_c t + \pi/4) \cos(\omega_m t - \pi/4) = (1/2) \cos(\omega_c t + \omega_m t) + (1/2) \cos(\omega_c t - \omega_m t + \pi/2)$$

$$\cos(\omega_c t - \pi/4) \cos(\omega_m t + \pi/4) = (1/2) \cos(\omega_c t + \omega_m t) + (1/2) \cos(\omega_c t - \omega_m t - \pi/2)$$

The sum of these terms, i.e., the signal into the circulator, is  $\cos(\omega_c + \omega_m)t$ . Fig. 12 illustrates this process graphically.

The example of a pulse radar given here requires that a rectangular pulse be phase shifted by  $+\pi/4$  radians. This is not a simple matter, since the pulse contains a wide band of frequencies, all of which must be shifted the same constant amount. Also, waveforms as illustrated by Fig. 7 must be avoided. Further, during reception the Doppler shift of the echo requires again that a frequency band rather than a single frequency be phase shifted. A practical implementation of such a phase shifter applies phase shift functions  $\phi_1(\omega)$  and  $\phi_2(\omega)$  to the modulation signal rather than discrete shifts of  $-\pi/4$  and  $+\pi/4$ . Here  $\phi_2(\omega) - \phi_1(\omega) \approx \pi/2$  over the frequency range of interest. When this substitution is made in the above equations, the difference terms will cancel upon addition as before. The sum terms are again equal but will

226 add to  $\cos(w_c t + w_m t + \phi + \pi/4)$ . A delay equalizer is, therefore, shown in Fig. 11 to remove the distorting effect of this residual phase shift as well as any others that may have been incurred elsewhere. This is accomplished by adding a frequency dependent phase correction so that in the resulting signal the combined phase term is proportional to frequency, i.e., that all frequencies are delayed by an equal amount. The carrier, inserted for transmission, is not shown, although required for the radar case.

On reception, the converse of this operation takes place. Ordinary demodulation could be employed if the transmitted signal were the only one received. However, single sideband demodulation is used here to reject any signals in the unused sideband. The two demodulations produce (in Multipliers 1 and 2 of Fig. 11 respectively):

$$\cos(w_c + w_m)t \cos(w_c t + \pi/4) = 1/2 \cos(2w_c t + w_m t + \pi/4) + 1/2 \cos(w_m t + \pi/4)$$

$$\cos(w_c - w_m)t \cos(w_c t - \pi/4) = 1/2 \cos(2w_c t - w_m t - \pi/4) + 1/2 \cos(w_m t - \pi/4)$$

The upper and lower signs represent processing for upper and lower sideband respectively. Terms containing  $2w_c t$  are filtered out, leaving the modulation function, but shifted in phase.

If processing for the upper sideband is desired, the resultant signals will be phase shifted  $\pi/4$  and  $-\pi/4$  respectively and added. In that case it is seen that the demodulation result of the upper-sideband processing yields  $\cos w_m t$  while those of the lower sideband cancel. Processing for the lower sideband requires opposite phase shifts prior to summing. The single-sideband demodulation scheme for either of the sidebands is illustrated in Fig. 13.

#### d. Skewed Sideband Radar

From the Nyquist filter technique, which employs a narrow and relatively strong carrier "band" along with a wider sideband, an analogous scheme was derived in which two otherwise independent radar signals perform the functions of the carrier and sideband channels. The first such channel is high power but narrow-band, thus providing only coarse range resolution. The second, a lower power signal, contributes the required fine resolution at correspondingly greater bandwidth. Upon separate demodulation and processing of these two channels, they are again combined in a correlation process as for the previous single-sideband schemes. Analogously, the narrow band channel serves as a reference for the lower power high resolution signal.

Fig. 14 shows a simplified block diagram for such a radar.<sup>3</sup> It combines several of the previously discussed topics, namely the cosine pulse generation by means of two component signals and the single sideband principle for spectrum conservation.

The modulation waveform is an ordinary pulse train. The RF generator produces a CW signal which is frequency modulated by linearly shifting its phase through  $2\pi$  radians during the pulse period (see Figs. 15a and b). The resulting signal has two noteworthy properties: Its spectrum has the sideband behavior of that for the cosine pulse and it is located asymmetrically (skewed) with respect to the carrier.

The signal described by Fig. 15b may be thought of as being composed of the following three signals: The continuous carrier  $w_c$ ; the negative of the carrier multiplied by the gating function  $S(t)$ ; the modified carrier  $w_c + w_a$  during the pulse interval. The composite signal  $f(t)$  may therefore be written as:

$$f(t) = \cos w_c t - S(t) \cos w_c t - S(t) \cos(w_c + w_a)t$$

The sign of the last term is minus due to the fact that at  $t = 0$  this signal is exactly of opposite phase in relation to the unshifted carrier. When compared to Fig. 1e, this signal differs by the presence of the CW component and the phasing at  $t = 0$ . The resulting spectrum is composed of the cosine-pulse spectrum, skewed with respect to the carrier, centered at  $w = w_c + w_a/2$ , with a strong component at  $w = w_c$ . It has, therefore, some of the characteristics of a single sideband spectrum.

Upon reception the signal is demodulated by mixing with the carrier  $w_c$ . Figs. 15c and d show the phase relationship between transmitted and received signals. Figs. 15e and f illustrate two possible demodulation results depending on the Doppler phase shift  $\phi_0$  incurred by the echo signal. The combination of these signals results in an effective pulse train, as shown in Fig. 15g.

After demodulation (Fig. 14) the signal is separated into two channels, an all-range channel without range indication and a range resolution channel. In the all-range channel, target signals from all ranges are extracted by doppler bandpass filtering. In the range resolution channel the modulation waveform is extracted, the signal range gated (Modulation Frequency Demodulator) and bandpass filtered to obtain target doppler information from one discrete range cell. The correlator output combines the features of both channels providing range resolution and doppler information as well as sensitivity for weak targets.

### 4. SPECTRUM SHARING

#### a. General

Besides the reduction of the effective bandwidth through pulse shaping techniques, more efficient use of the given spectral space has been achieved in some applications through the sharing of a spectrum by two or more radars. The spectrum of a coherent pulse radar ideally consists of lines whose spacing is given by the pulse repetition frequency (PRF). Unused inter-line spacing may, therefore, be occupied by corresponding spectral lines of other radars, thereby allowing two or more users to share the same allocated spectrum. Fig. 16 illustrates this principle of interlacing the spectral lines of two signals.

The diagram also indicates that with each spectral line there must be associated a certain width within which no other signal may lie. This band about each spectral line may, therefore, be considered the effective width of the spectral lines. This constraint limits the number of lines of other spectra that may lie within one interline space, hence the number of radars that can share the same spectrum. The width of the spectral lines is due to several modulations which either the transmitted or received radar signal contains. Some of the contributing factors to this line width are transmitter instabilities, scan modulation, doppler modulation and filtering properties of the receiver.

Design factors and techniques are considered here which serve to both reduce the band around each line and widen the inter-line space. These, together with the physical geometry of cooperating radars,

define the necessary conditions under which successful spectral interlacing is feasible.

b. Maximizing the Usable Inter-line Space

22-7

An important contributor to the frequency band associated with each spectral line is the stability of the transmitted signal. Pulse-to-pulse frequency and phase jitter, as well as long-term frequency drift, should be reduced as much as practical. This may be achieved by deriving the frequencies of all cooperating radars from one source (cable connection or RF link) or by employing very stable sources in these radars and re-synchronizing when necessary.

The doppler band width is perhaps the most significant contributor to the band around each spectral line. It can ordinarily not be reduced except by the choice of a lower PRF. However, when targets are unidirectional, such as in the case of ground control radars for incoming aircraft, only half of the doppler band is occupied. In this case, the single sideband demodulation technique shown in Fig. 13 may again be employed to reject signals in the sideband not of interest. This provides a significant reduction in the effective width of the spectral lines by allowing half of the ordinary doppler band to be used by other radars.

The rejection of interfering signals by the receiver is another factor which may be improved to effect a smaller width of the spectral lines. This characteristic may be considered as the receiver's sensitivity to signals outside the doppler band of interest. It is determined by the sharpness of the MTI filters or other processing performed.

A final consideration in the process of maximizing the usable interline space is the increase in the line spacing itself. This can be achieved only by increasing the PRF of the radar. The maximum PRF is constrained by the required unambiguous range which is given by  $c/(2 \text{ PRF})$ , where  $c$  is the velocity of light.

There exists, however, a potential improvement which is due to the fact that the operating range of many radars is often significantly less than the unambiguous range given by the PRF. This choice is made when multiple-time-around echoes may be high enough to be confused with returns from within the operating range. After transmission of a pulse and "listening" for a time corresponding to the operating range, the receiver, therefore, remains "off" until the returning echoes fall below the level for valid targets, at which time the next pulse is transmitted. If, for example, an attenuation of 48 dB ( $2^{16}$ ) is again assumed for such interfering signals, then this requires that the unambiguous range is  $2^4 = 16$  times the operating range (due to the fourth-power-of-range decay of echoes). In this case the off-time of the system exceeds the on-time by a factor of 15.

For a step scanning radar, there exists a scheme which permits the increase of its PRF by a factor of 15 without adverse effects. This is accomplished by switching the beam after transmission of one pulse, to another, non-adjacent beam position. This step is selected sufficiently large to assure that multiple-time-around echoes, entering the sidelobes, are sufficiently small due to space and sidelobe attenuation.

Fig. 19 gives an example where 15 separate beam positions must be illuminated. The PRF of the transmitter is increased by a factor of 15 so as to set the unambiguous range equal to the operating range. The sequence of scanning is indicated by arrows. It can be seen that consecutively illuminated beam positions are not adjacent in space. In any beam position an interfering echo will, therefore, precede the valid pulse by one step in time and two beam positions in space. If this second-time-around echo is to be attenuated 48 dB at the receiver, since 12 dB will be obtained from space loss, then 36 dB attenuation must be obtained from the antenna pattern. While this may not ordinarily be available at two beamwidths from bore-sight, an antenna designed with a null at this particular angle may be employed to obtain the full potential 48 dB attenuation.

The diagram also shows that physically adjacent beam positions are illuminated by pulses separated in time by 7 interpulse periods. Here the attenuation of the 8th-time-around return accounts for 36 dB attenuation while the antenna pattern would have to contribute 12 dB.

Jump scanning permits a significant improvement, not only by widening of spectral lines, permitting sharing of spectral space, but also due to increase in average pulses per beamwidth.

A variety of such schemes is possible, depending on the number of positions that must be scanned, and the antenna pattern. If the latter causes excessive crosstalk between positions, a PRF less than maximum may have to be utilized. However, in general, the jump scanning technique provides a widening of the interline spacing, up to a factor equal to the ratio of unambiguous to operating range.

The necessity for spectrum sharing implies spatial proximity among radars. Interference may be encountered in such situations due to either direct radiation or via reflecting objects. Simple precautionary design features, such as pulse-to-pulse synchronization and scan synchronization, would serve effectively to avoid receiver overload or damage, and false target indication. Pulse-to-pulse synchronization, whereby the first radar transmits, then listens, then blanks its receiver while the second system transmits, can be considered temporal interlacing (multiplexing) and can be used for non-coherent pulse radars also.

5. APPLICATIONS AND CONCLUSIONS

Most of the techniques discussed herein were demonstrated to be feasible and practicable. Radars have been built, some in quantities, which utilize one or more of them.

To implement the shaped-spectrum scheme for CW radar, illustrated by Fig. 15, radars were built employing a signal linearly phase shifted through  $\pi$  radians in accordance with a pseudo-random code modulating function. The resulting spectrum exhibited the shape associated with the cosine pulse, similar to that given in Fig. 6. Fig. 18 shows spectrum analyzer displays of one using a 7 element code. Although these spectra are relatively coarse due to this very short code, the significant features are apparent. These are the sidelobe envelope shape of the spectrum and its skewed position with respect to the carrier. The latter characteristic was exemplified by reversing the polarity of the code, thereby reversing the asymmetry of the spectrum. The two signals displayed in Fig. 18 differ in this manner. Other radars were built employing the same principles but using code lengths of both 15 and more elements.

While these coded radars realized the spectral saving associated with pulse shaping only, a pulse frequency modulated radar was built which achieved the vestigial sideband approximation described. This radar was modulated in accordance with a rectangular pulse train (without code) whereby the frequency was shifted

228 during the pulse period so as to advance the phase by  $2\pi$  radians during that interval. The radar used the dual channel processing of carrier and sideband signals with correlation of both outputs. A more recent radar employs the same technique but uses a shift of  $\pi$  only. This results in a symmetric spectrum but achieves good sidelobe behavior with concentration of the signal power near the center of the spectrum.

A low frequency radar was built particularly suitable for spectral interlacing, due to its combination of PRF, doppler bandwidth and operating. Since about 93% of its interline frequency space is unused, 10 of such systems could potentially share the same frequency spectrum.

Although the techniques discussed have been treated from the radar standpoint, many apply to communications systems as well.

## 6. REFERENCES

1. Fishbein, W., Rittenbach, O., Correlation Radar using Pseudo-Random Modulation, IRE International Convention Record, 1961.
2. Craig, S., Fishbein, W., Rittenbach, O., Continuous-Wave Radar with High Range Resolution and Unambiguous Velocity Determination, IRE Transactions on Military Electronics, Vol MIL-6, No. 2, April 1962.
3. Fishbein, W., Rittenbach, O., Multifunction Radar Waveforms, EASCON Record, 1969.
4. Skolnik, M.I., Radar Handbook, McGraw Hill, 1970, p. 3-9.

## APPENDIX I

When a signal  $h_R(t)$  appears at the input to a receiver with impulse response  $h_R^*(-t)$ , receiver and signal are considered matched. This is generally not the case for an interference signal. Assuming such an interfering signal emitted from some source arrives at the receiver input, then the receiver output is defined as the Mutual Interference Function,  $I$ . It serves as a measure of the interfering effect of the source on the receiver.  $I$  is given by the convolution of the signal and receiver impulse response, namely

$$I = \int_{-\infty}^{\infty} h_R^*(-n) S_A(\tau + n) dn$$

where  $S_A(t)$  is the input.  $S_A(t)$  can be expressed in terms of the signal generated by the transmitter of the carrier  $w_T$  (radian frequency), modified by the travel time delay  $\tau_s$  between transmitter and receiver, amplitude factor is  $a$  and  $w_D$  represents the doppler shift it may have encountered if reflected from a moving object or due to the relative motion between transmitter and receiver. Therefore,

$$S_A(t) = a S(t - \tau_s) e^{j(w_C - w_D)(t - \tau_s)}$$

$h_R(t)$  may also be expressed in analytic form as

$$h_R(t) = h(t) e^{j w_R t}$$

where  $w_R$  is the frequency to which the receiver is matched.  $I$  therefore becomes

$$I = a \int_{-\infty}^{\infty} h^*(-n) e^{-j w_R n} S(\tau + n - \tau_s) e^{j(w_C - w_D)(\tau + n - \tau_s)} dn$$

where some constant delay and frequency terms of the impulse response are deleted.

Letting  $\tau' = \tau - \tau_s$  and  $w_C - w_R = w_d$ , the difference frequency between the carriers,  $w_s = w_d - w_D$

$$I = a e^{j(w_C - w_D)\tau'} \int_{-\infty}^{\infty} h^*(-n) S(n + \tau') e^{j w_s n} dn$$

which is in the form of a low frequency complex modulation (integral) on a carrier  $w_C - w_D$ . Analogous to the well known radar ambiguity function<sup>4</sup> which assumes receiver and signal matched, the integral is defined as the Mutual Ambiguity Function  $A$ , since it deals with arbitrary receiver and signal.

$$A(\tau; w_s) = \int_{-\infty}^{\infty} h^*(t) S(\tau' - t) e^{-j w_s t} dt$$

where  $w_s$  is the sum frequency of  $w_d$  and any doppler shift  $w_D$ ,  $h(t)$  a form of the receiver complex impulse response and  $s(t)$  the complex transmitter modulation waveform. When  $s(t)$  and  $h(t)$  are matched  $A$  becomes the radar ambiguity function.

For the simple case of the receiver matched to a rectangular pulse of its own frequency but receiving a similar pulse of different center frequency, the output  $I$  is the convolution of the two signals  $f_1(t)$  and  $f_2(t)$ . Thus,

$$I = \int_{-\infty}^{\infty} f_1(t) f_2(\tau - t) dt$$

If  $f_1(t)$  and  $f_2(t)$  are rectangular pulses having carriers  $\cos w_1 t$  and  $\cos w_2 t$  and duration  $T$  this expression will become:

$$I = \int_{-T/2+\tau}^{T/2} \cos w_1 t \cos w_2 (t - \tau) dt$$

Assuming a mean frequency  $w_m$  between  $w_1$  and  $w_2$  and a difference  $\Delta$  such that  $w_1 = w_m - \Delta$  and  $w_2 = w_m + \Delta$  the expression for  $I$  becomes:

$$I = 1/2 \int_{-T/2+\tau}^{T/2} \cos [2w_m t - (w_m + \Delta)\tau] dt + 1/2 \int_{-T/2+\tau}^{T/2} \cos [2\Delta t - (w_m - \Delta)\tau] dt$$

After integration this becomes:

$$I = \frac{\sin w_m(T - \tau) \cos \Delta \tau}{2 w_m} + \frac{\sin \Delta(T - \tau) \cos w_m \tau}{2 \Delta}$$

Since usually  $w_m \gg \Delta$  and letting  $2\Delta = w_d$ , so that  $w_2 - w_1 = w_d$ , I becomes

$$I = \frac{\sin[w_d(T - \tau)/2] \cos w_m \tau}{w_d}$$

This function will have its maximum at  $\tau = 0$ , hence

$$I = \frac{\sin(w_d T/2)}{w_d}$$

For I to be down 48 dB ( $2^8$  in voltage) requires that

$$\frac{I(\text{at } w_d = 0)}{I \text{ envelope}} = \frac{T/2}{1/w_d} = 2^8$$

Hence  $w_d T = 2^9$  radians. Normalizing this angular separation to  $\frac{w_d T}{2\pi} = r$  (r in phase revolutions), one obtains  $r \approx 81.5$ .

## APPENDIX 2

### SPECTRAL OCCUPANCY OF A COSINE PULSE SIGNAL

If the two pulse signals of Appendix 1 are cosine pulses (having the same carriers and duration), the expression for I will be:

$$I = \int_{-T/2+\tau}^{T/2} \cos(\pi t/T) \cos w_1 t \cos[\pi(t - \tau)/T] \cos[w_2(t - \tau)] dt$$

It can be shown that this convolution will also be maximum at  $\tau = 0$ : carrying out the integration and upon expansion, integration and substitution of limits, using  $w_m$  and  $\Delta$  as before, the terms having  $w_m$  in the denominator are neglected in favor of those containing only  $\Delta$ . The expression written in terms of  $w_d$  then becomes:

$$I = \left[ \frac{2}{w_d} - \frac{1}{w_d - w_a} - \frac{1}{w_d + w_a} \right] \frac{\sin(w_d T/2)}{4} = \frac{w_a^2}{w_d(w_a^2 - w_d^2)} \frac{\sin(w_d T/2)}{2} \text{ where } w_a = 2\pi/T.$$

To derive a frequency separation, at which I is down 48 dB, the same ratio is formed as in Appendix 1.

$$\frac{I(\text{at } w_d = 0)}{I \text{ envelope}} = \frac{(T/4) 2w_d(w_a^2 - w_d^2)}{w_a^2} = 2^8$$

Letting  $r = w_d T/2\pi$  as before, hence  $r = w_d/w_a$ , and the above equation becomes:  $r(1 - r^2) = 2^8/\pi$  so that  $r \approx 4.4$  (phase revolutions).

## APPENDIX 3

### SPECTRAL OCCUPANCY OF A $\cos^2$ PULSE SIGNAL

If the two pulse signals of Appendix 1 are  $\cos^2$  pulses with the same carriers, duration and peak amplitude, and letting  $\tau = 0$  in the expression for the convolution, the integral for I will be:

$$I = 2 \int_0^{T/2} \cos^4(\pi t/T) \cos w_1 t \cos w_2 t dt$$

Using the previous derivations and definitions, expanding, integrating and substituting the limits for this integral, the result consists of terms having  $w_m$  and  $\Delta$  only in their denominators. Neglecting again those containing  $w_m$  the expression becomes:

$$I = \left[ \frac{6}{w_d} - \frac{4}{w_d - w_a} - \frac{4}{w_d + w_a} + \frac{1}{w_d - 2w_a} + \frac{1}{w_d + 2w_a} \right] \frac{\sin(w_d T/2)}{16} = \frac{3w_a^4}{2w_d(w_d^2 - w_a^2)(w_d^2 - 4w_a^2)} \sin w_d T/2$$

To derive a separation r for a 48 dB interference attenuation, the same ratio is formed as before:

$$\frac{I(\text{at } w_d = 0)}{I \text{ envelope}} = \frac{(3T/16) 2w_d(w_d^2 - w_a^2)(w_d^2 - 4w_a^2)}{3w_a^4} = 2^8 \text{ or } r(r^2 - 1)(r^2 - 4) = 2^{10}/\pi; \text{ hence } r \approx 3.5.$$

## APPENDIX 4

THE  $\cos^n$  PULSE SIGNAL

The general form of the pulse signal treated herein is  $S(t) \cos^n(\omega_a t/2) \cos \omega_c t$  where  $S(t)$  is the rectangular gating function from  $-T/2$  to  $T/2$ ,  $\omega_c$  is some carrier frequency and  $\omega_a \leq 2\pi/T$ . The composition of this signal can be recognized by expanding it in a binomial series.

Neglecting the carrier term, since it merely produces a translation in the frequency domain and  $S(t)$ , since it is a constant multiplier and does not affect the expansion, the signal may be expressed as:

$$\begin{aligned} \cos^n(\omega_a t/2) &= (1/2)^n (e^{j\omega_a t/2} - e^{-j\omega_a t/2})^n = 1/2^n \sum_{p=0}^n \binom{n}{p} e^{j\omega_a t(n-p)/2} e^{-j\omega_a t p/2} \\ &= 1/2^n \sum_{p=0}^n \binom{n}{p} e^{-j\omega_a t(p - n/2)} = 1/2^n \sum_{p=0}^n \binom{n}{p} [\cos[(n - n/2)\omega_a t] - j \sin[(n - n/2)\omega_a t]] \end{aligned}$$

where  $\binom{n}{p}$  are the binomial coefficients given by

$$\binom{n}{p} = \frac{n!}{p!(n-p)!}$$

For odd  $n$  the summation will consist of an even number of complex terms spaced apart by multiples of  $\omega_a$ . Due to the symmetry of  $\binom{n}{p}$  and the fact that the sine function is odd, the sine terms will cancel in pairs. For even  $n$ , an odd number of coefficients  $\binom{n}{p}$  will result: the same cancellation will occur for all  $n$  except the center term  $p = n/2$ . However, for that case the sine is zero so that the quadrature term may be deleted for all cases. The expansion, therefore, becomes

$$\cos^n(\omega_a t/2) = 1/2^n \sum_{p=0}^n \binom{n}{p} \cos[(n - n/2)\omega_a t]$$

If this function is modulated by  $S(t)$  and the carrier  $\cos \omega_c t$ , it is apparent that the  $\cos^n$  shaped pulse is produced by means of  $n + 1$  frequency shifted components.

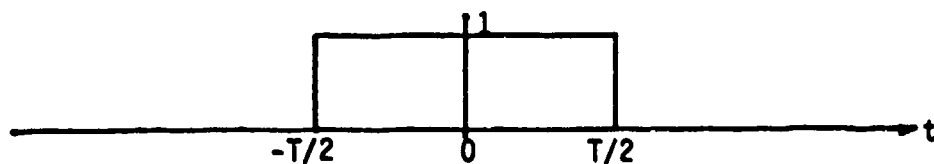
The baseband spectrum  $F_n(\omega)$  is therefore:

$$F_n(\omega) = 1/2^n \sum_{p=0}^n \binom{n}{p} F_0[\omega - (n - n/2)\omega_a]$$

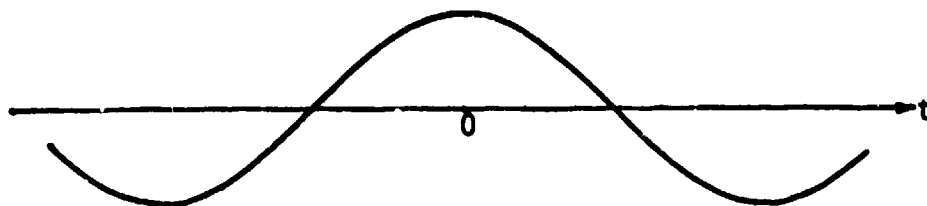
Using the definitions of Appendices 1 to 3, the mutual interference of two  $\cos^n$  shaped pulse signals can be shown to be:

$$I_n = 1/2^n \left\{ \frac{\sin(\omega_d T/2)}{\cos(\omega_d T/2)} \right\} \sum_{p=0}^n \binom{n}{p} \frac{1}{\omega_d + (n - n/2)\omega_a} \left\{ \frac{\cos(n - n/2)\pi}{\sin(n - n/2)\pi} \right\}$$

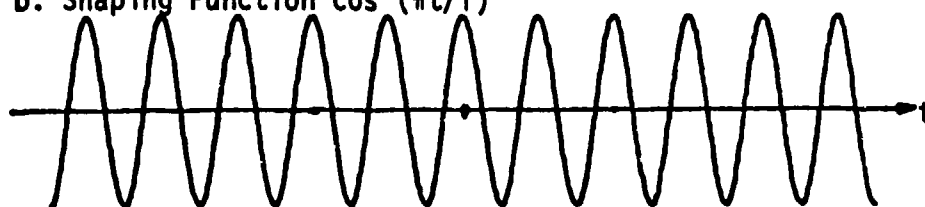
WHERE  $\begin{cases} n \text{ even} \\ n \text{ odd} \end{cases}$



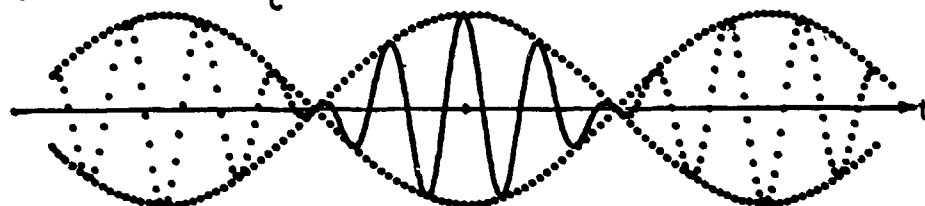
a. Rectangular Pulse (Switching Function  $S(t)$ )



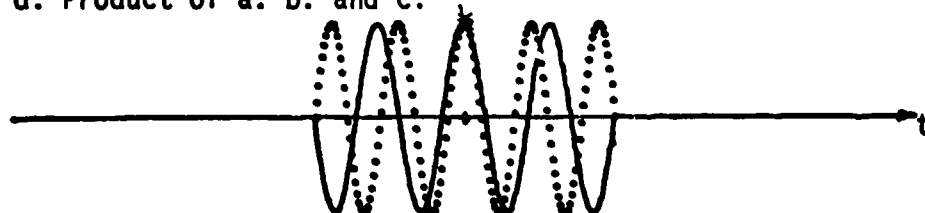
b. Shaping Function  $\cos(\pi t/T)$



c. Carrier  $\cos \omega_c t$



d. Product of a. b. and c.



e. Component Signals for Cosine Shaped Pulse

Fig.1 Generation of  $\cos^0$  and  $\cos^1$  pulses



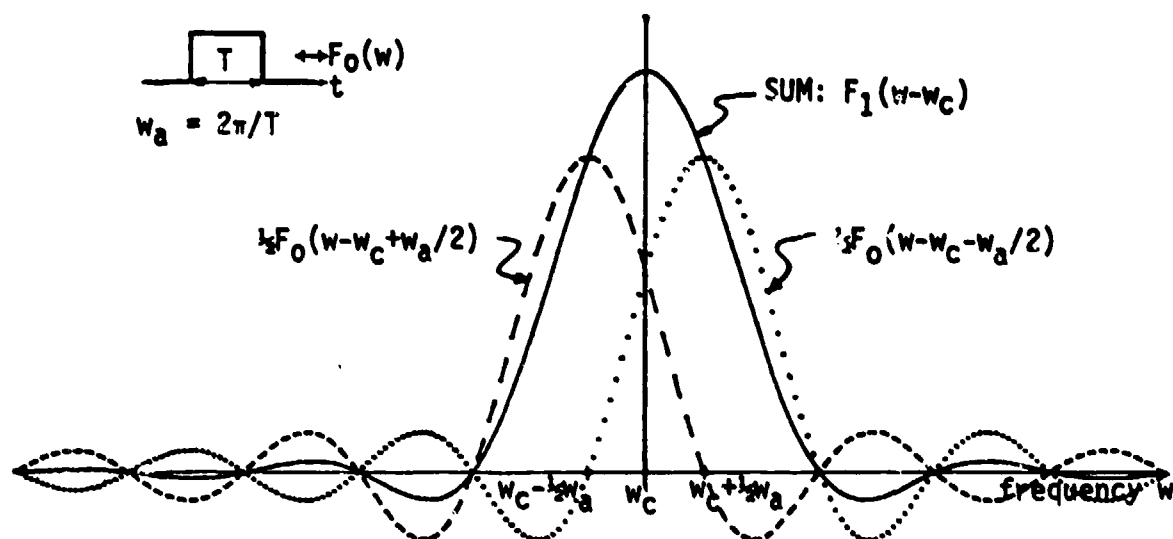


Fig.2 Cosine pulse spectrum and components

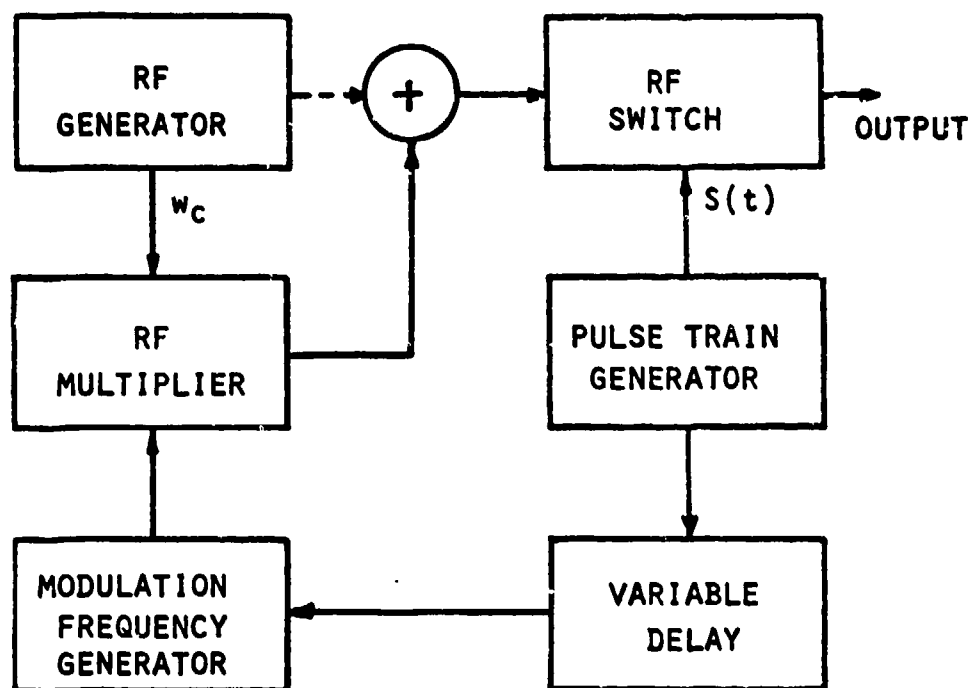
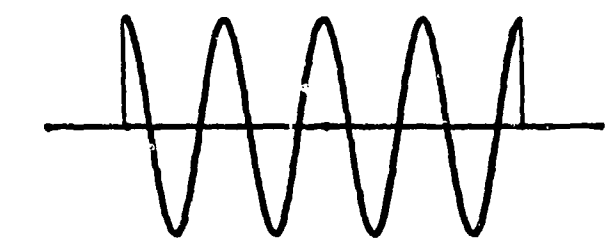
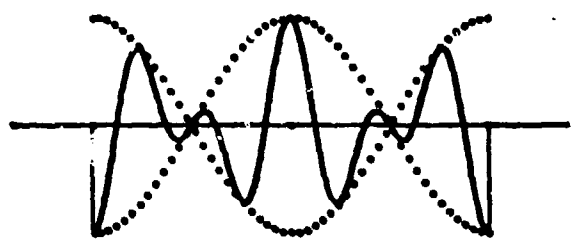


Fig.3 Cosine pulse train generator

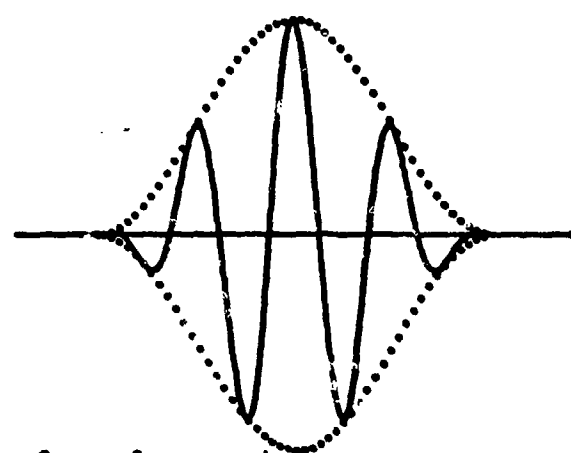
22-13



a. Carrier Pulse



b. Sum of Sideband Pulses



c. Sum of a. and b.

Fig.4 Waveforms for  $\cos^2$ -pulse generation

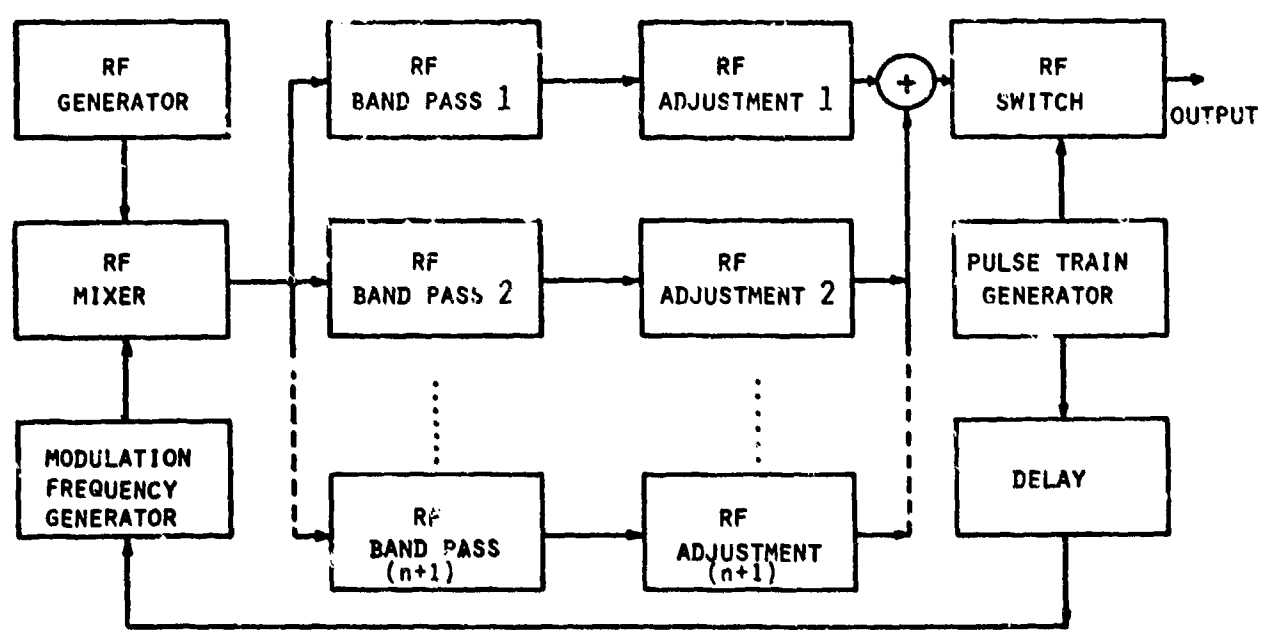


Fig.5 RF pulse generator for  $\cos^n$  pulses

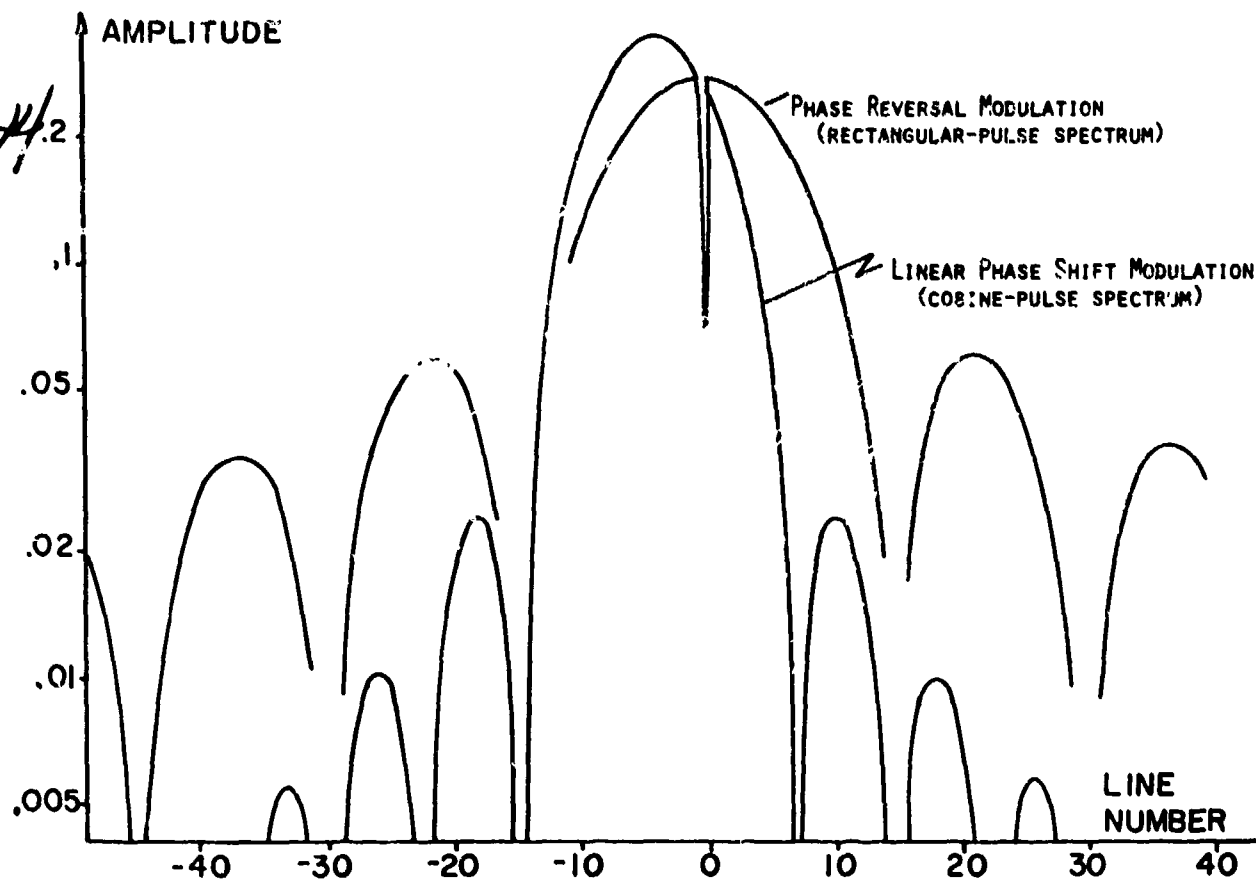
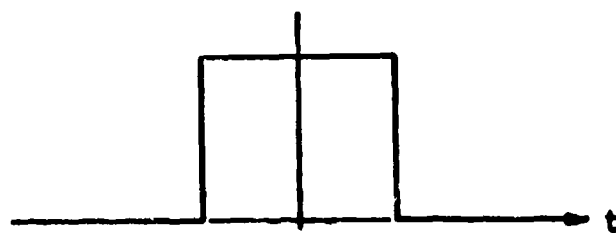
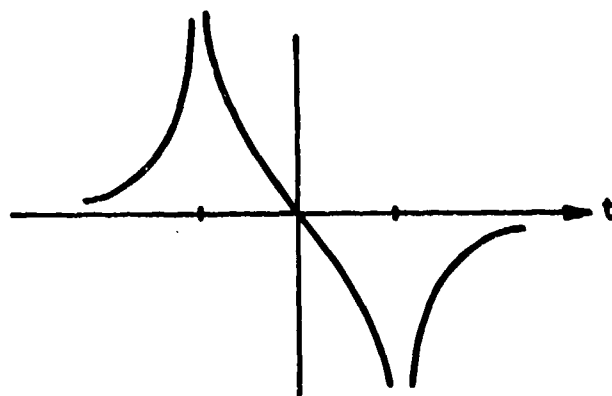


Fig.6 Continuous wave (CW) radar spectra (15 element code)



a. Pulse



b. Hilbert Transform of Pulse

Fig.7 Hilbert transform pair

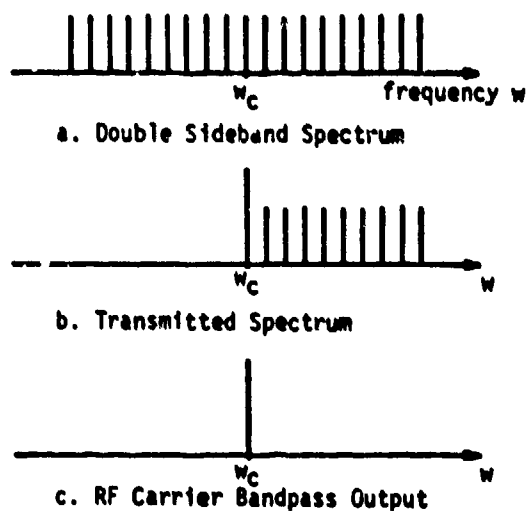


Fig. 8 Single sideband (minimum bandwidth) radar spectrum

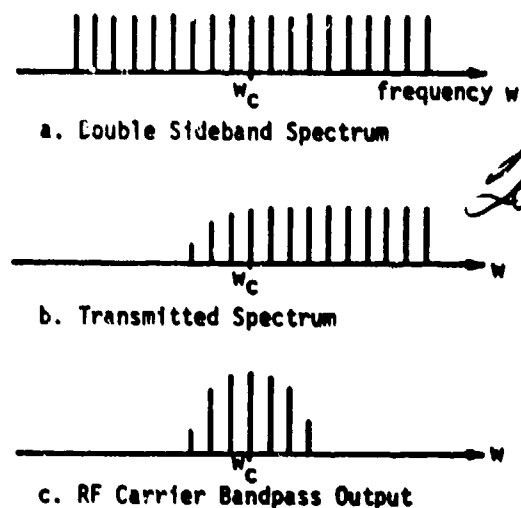


Fig. 10 Skewed (vestigial) sideband radar

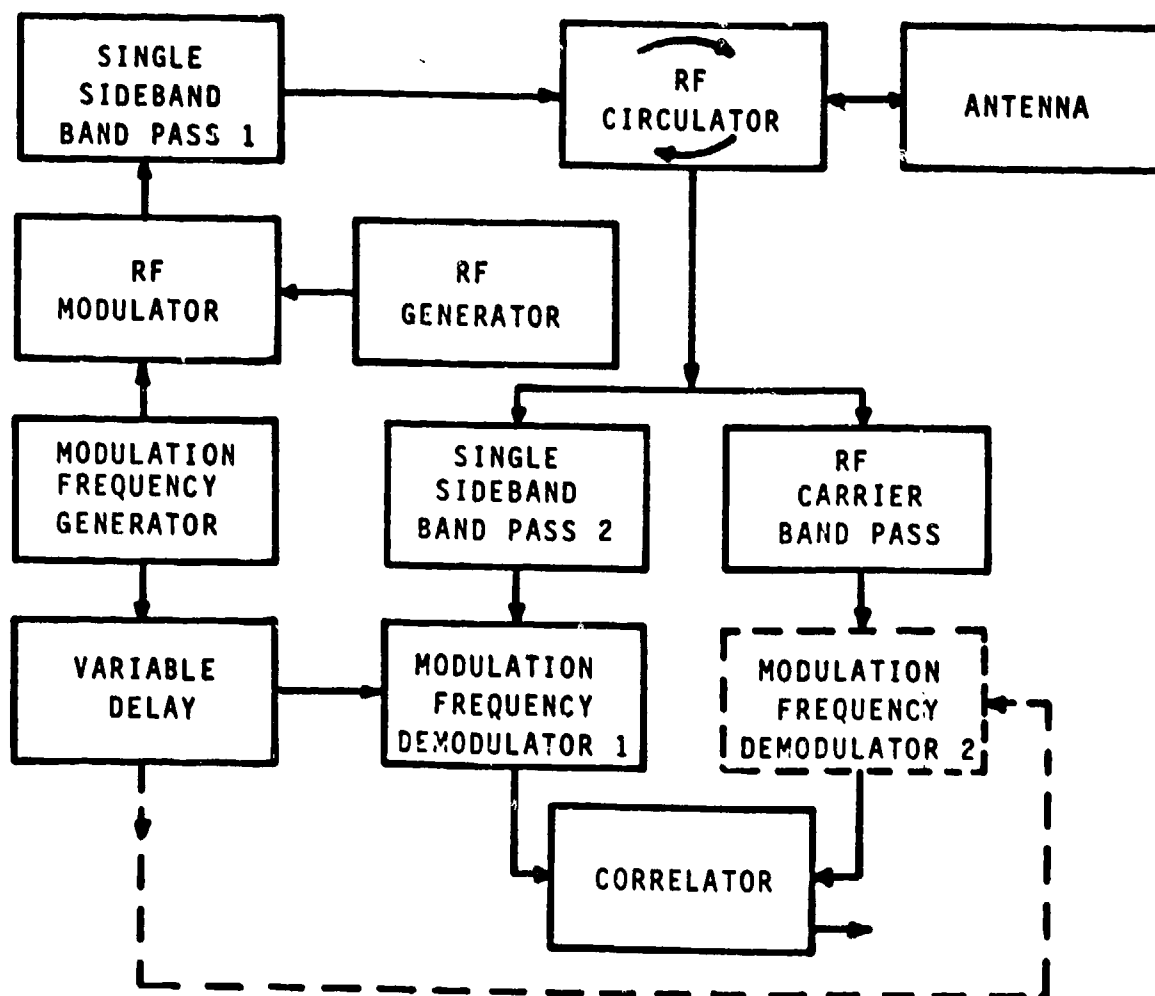


Fig. 9 Asymmetrical sideband radar

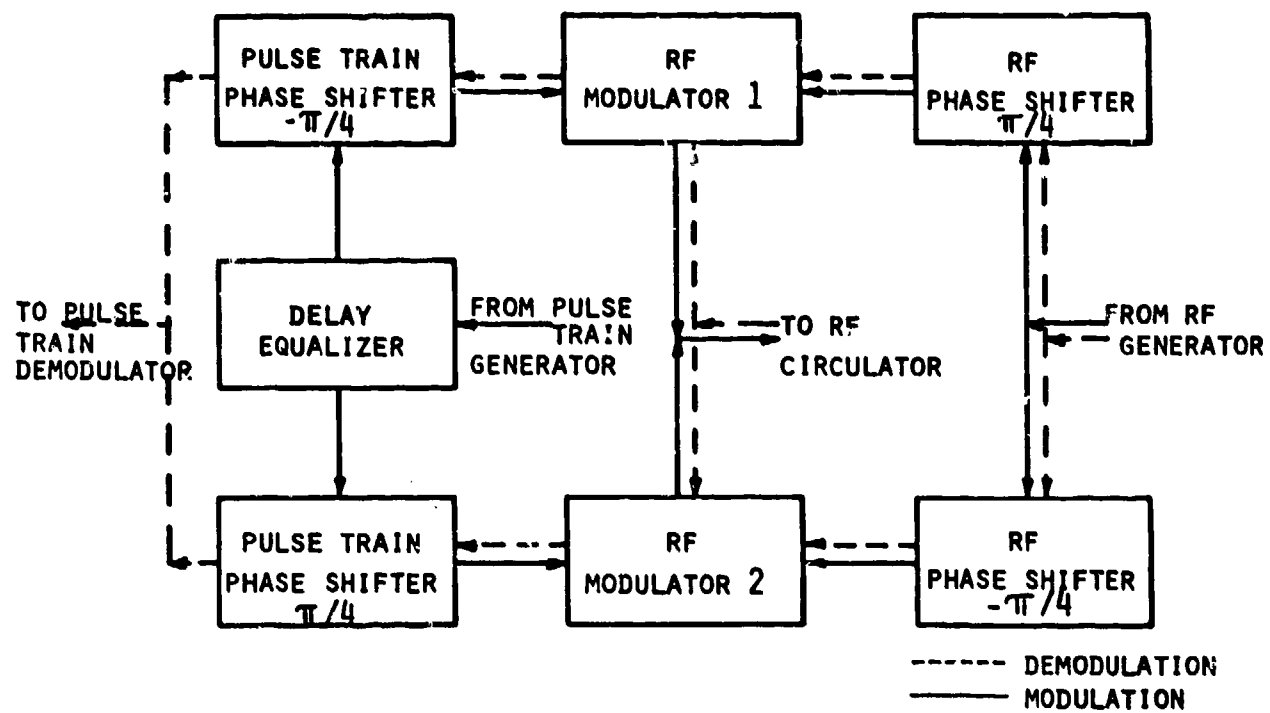


Fig.11 Single sideband radar modulator/demodulator

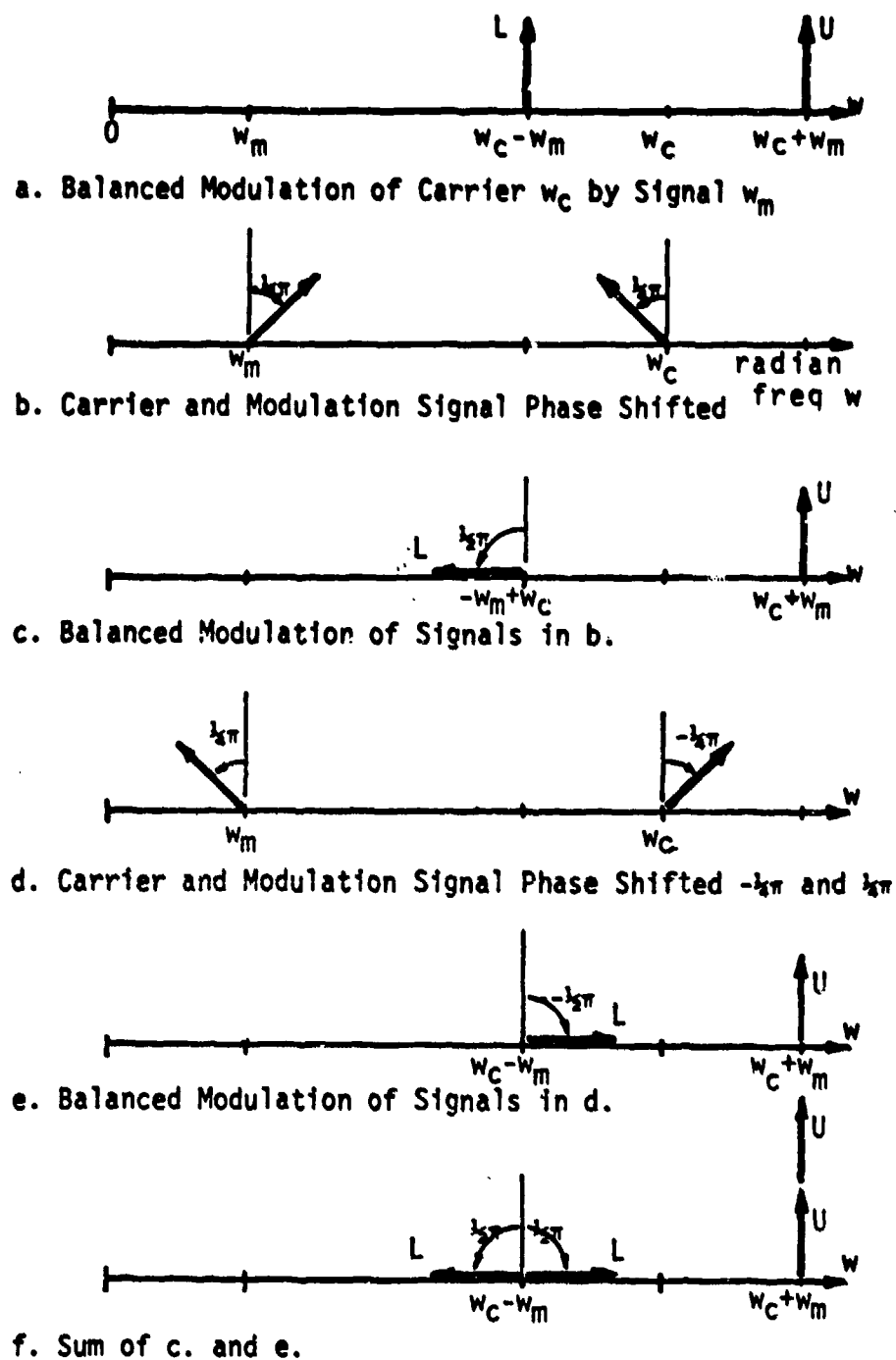


Fig.12 Single sideband generation through modulation

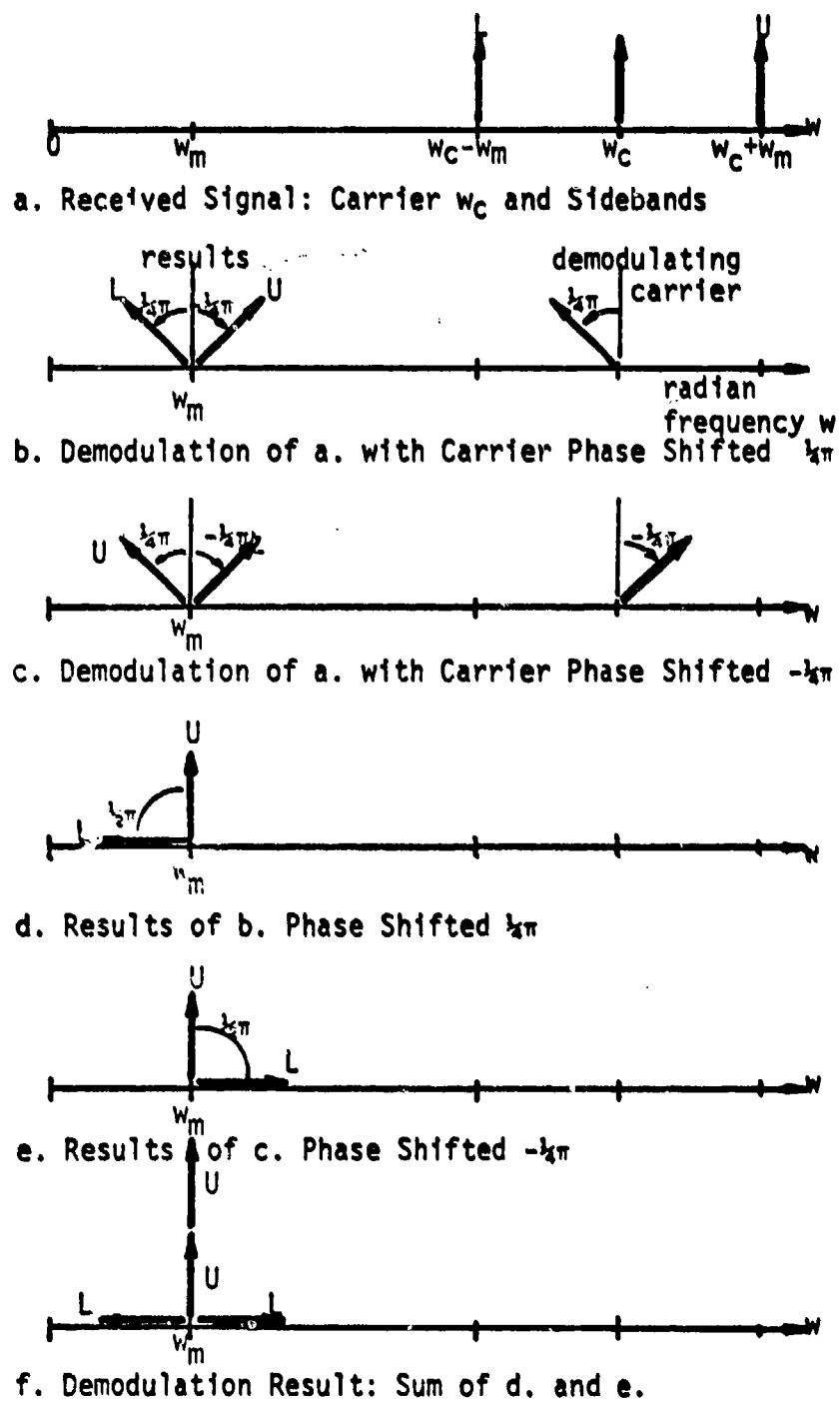


Fig. 1.3 Single sideband demodulation

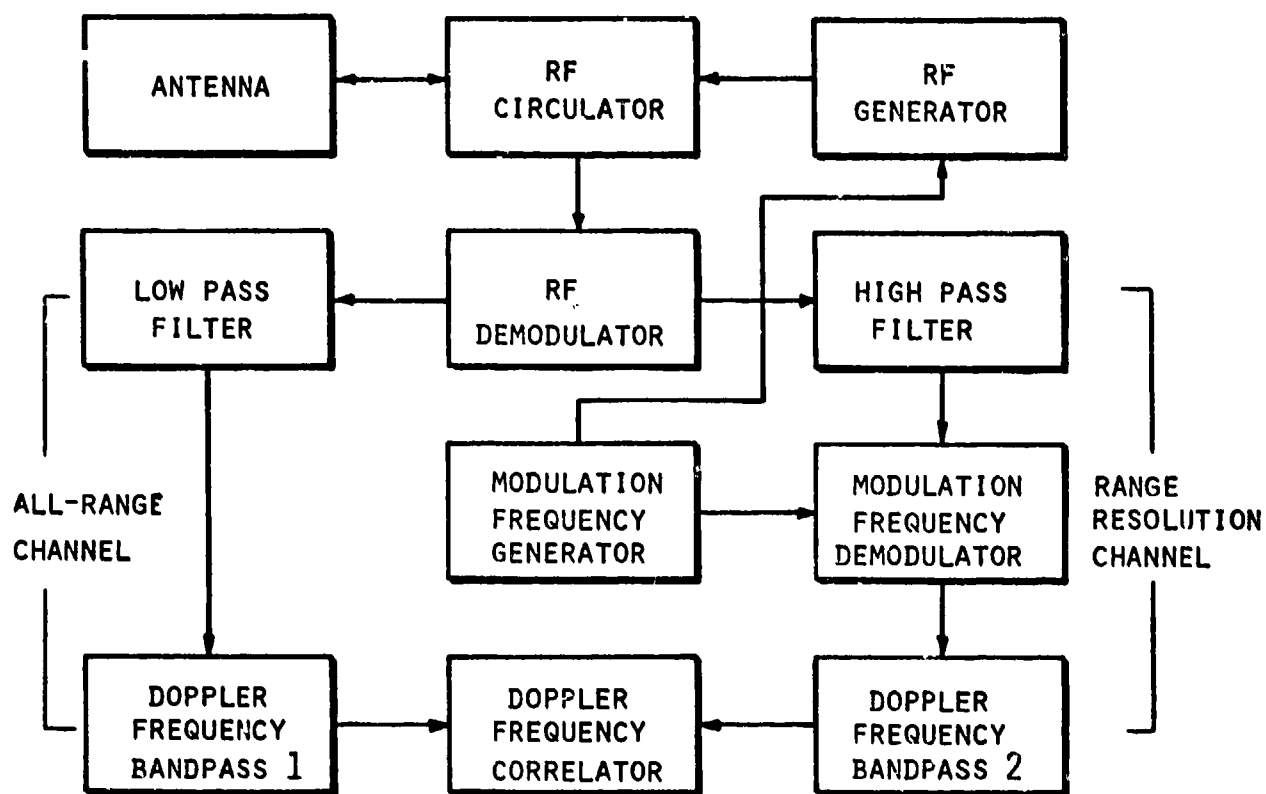


Fig.14 Skewed sideband radar



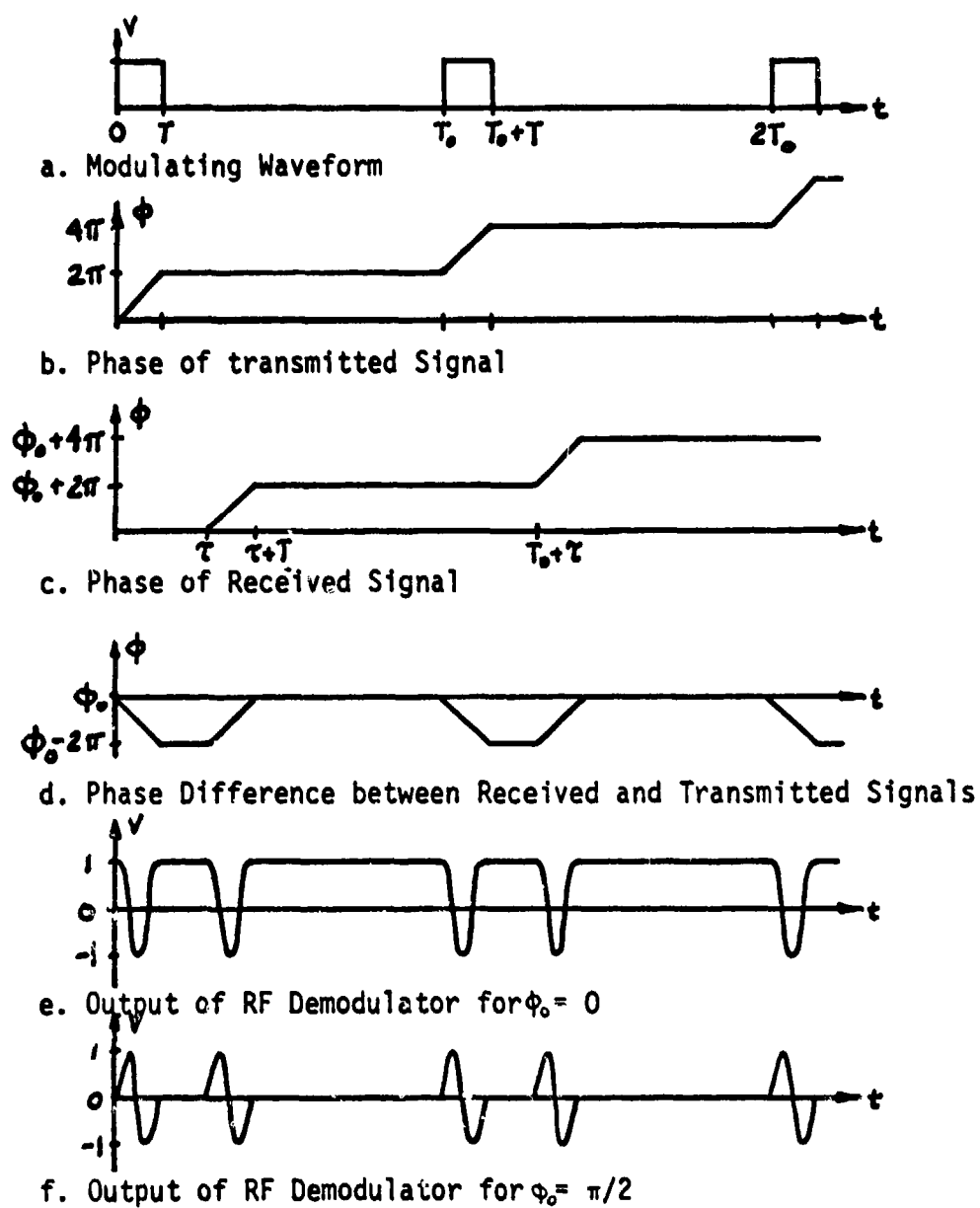


Fig.15 Waveforms for radar using pulse train frequency modulation ( $2\pi$  radians phase shift)

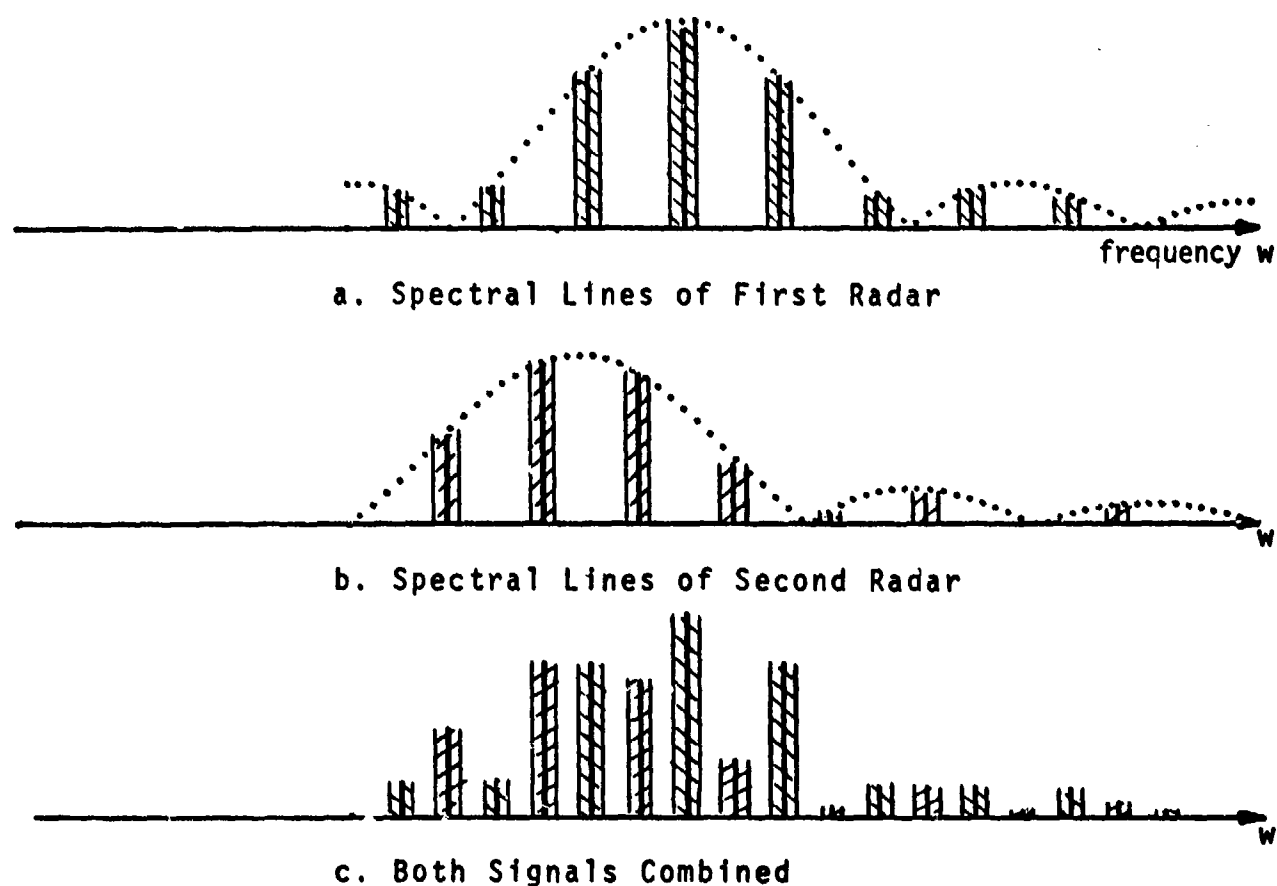


Fig.16 Spectral interlacing of radar signals

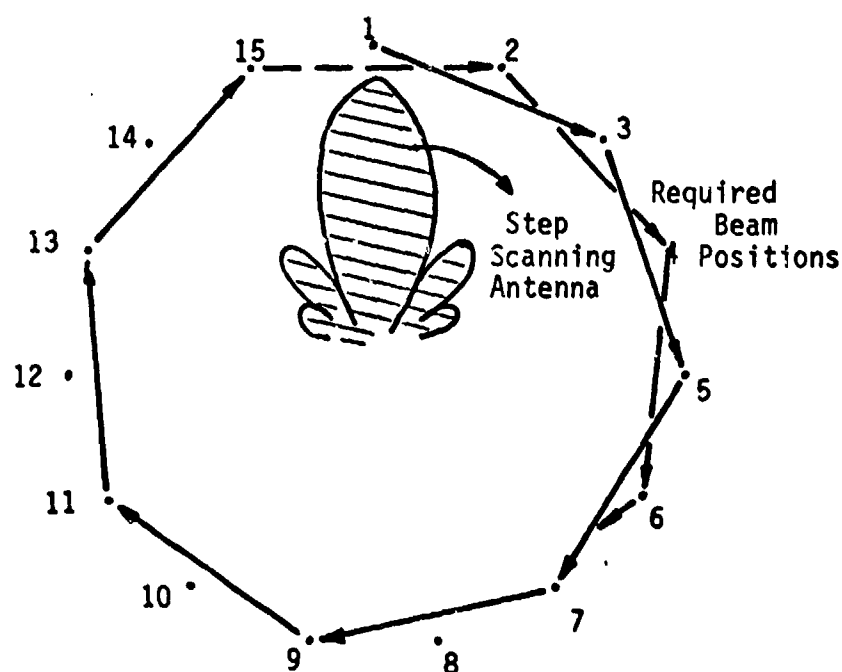


Fig.17 Jump scanning principle

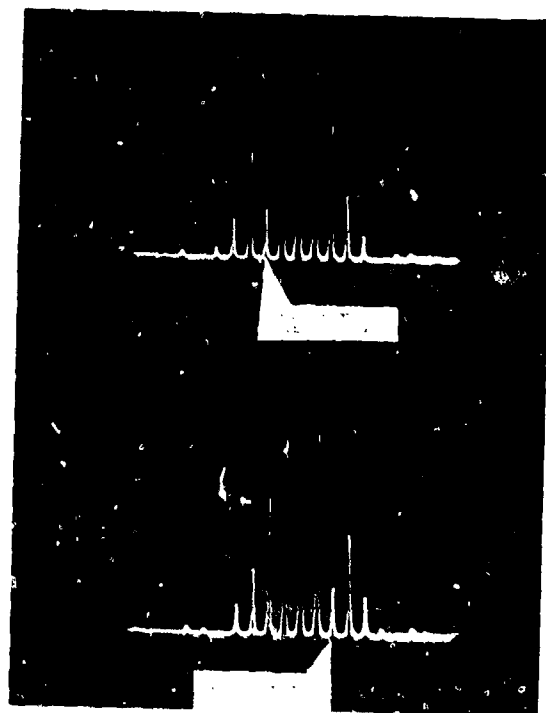


Fig.18 Spectrogram of pseudo random frequency modulated radar (7 element code)

## DISCUSSION

F. D. GREEN: You have described how the transmitted pulses can be sharpened without interference. The receiver still has to cope with these sharp pulses. Can this be done?

R. OLESCH: Yes. The receiver spectral response can and should be shaped according to the shaped pulse spectrum. Especially for a matched filter radar, the optimum receiver (power) spectral response is the same as the spectrum of the transmitted signal; therefore, for a better behaved transmit spectrum, the receiver spectrum will also be better behaved, resulting in less noise intake as well as lower interference from out-of-band emitters. This is expressed in the Interference Function  $I$  which shows that the interference (for correspondingly shaped receiver and waveform spectra) decays with double the exponent  $(2n + 1)$  which describes the shaped pulse,  $\cos^n$ .

F. J. CHESTERMAN: Can the  $\cos^2$  pulse shaping, which is suitable for long-range surveillance, be adapted easily for short-range, high-accuracy weapon systems demanding a sharp leading edge to the pulse?

R. OLESCH: Yes. The autocorrelation function of the smoothed pulse is not inferior to that of the rectangular pulse, or that waveform used in practical systems.

APPLICATION OF PROGRAMMABLE CALCULATORS  
TO EMC ANALYSIS

J. PAUL GEORGI  
DEPARTMENT OF DEFENSE

PAUL D. NEWHOUSE  
IIT RESEARCH INSTITUTE

ELECTROMAGNETIC COMPATIBILITY ANALYSIS CENTER  
Annapolis, Maryland  
United States of America

SUMMARY

The use of programmable calculators is suggested for making electromagnetic compatibility (EMC) calculations conveniently and economically. Programmable calculators are available at prices ranging from about \$800 to \$5000. Programs recorded on magnetic cards or tapes for use with the popular U.S. makes of calculators will be available from the Department of Defense, Electromagnetic Compatibility Analysis Center (ECAC) in 1975. Detailed explanations of several of the ECAC programs are given to illustrate the kinds of calculations that can be performed and to indicate the ease with which the programs can be used. Guidelines for the selection of calculators, and the pros and cons of using them are given. The calculator programs that ECAC will issue in 1975 are listed. The establishment of a central library of calculator programs developed by the EMC community is suggested as a means for facilitating the exchange of programs.

1. INTRODUCTION

Organizations engaged in frequency management or other EMC activities will soon have an economical and convenient set of analytical tools available for performing various kinds of EMC calculations. Appropriate mathematical models from ECAC's existing library of computer programs are being adapted to programmable pocket-size and desk-top calculators.

Semi-annually ECAC will issue to subscribing organizations a package of 5 to 10 mathematical models programmed for each subscriber's calculator, provided it is one of the popular U.S. makes. Each package will include a set of programs recorded on magnetic cards or tapes, operating instructions, and supporting technical information.

Examples of the kind of calculations that can be performed with such models are:

1. Propagation path loss for both over-the-horizon and line-of-sight situations.
2. Signal-to-noise ratios.
3. Interference-to-noise ratios.
4. Intermodulation frequencies.
5. Coupling between antennas.
6. Envelopes of emission spectra.
7. Conversion of map coordinates (UTM to and from Geographic).
8. Great circle distance between two locations.
9. Frequency assignment aids.

The programs will be convenient to use, even by individuals who have only an occasional need to perform EMC calculations. After the program card or tape has been inserted into the calculator, the user presses the GO button to begin the operation. The process proceeds step-by-step to allow the user to key in the input values. For most models, the entire process -- including inserting the magnetic card or tape, keying in the input values, and waiting for the answer to be displayed or printed -- takes less than one minute when a programmable desk-top calculator is used.

The cost of a programmable calculator ranges from about \$5000 for the desk-top size with an alphanumeric printer down to about \$800 for a hand-held size.

The cost to an organization to obtain the calculator programs from ECAC has not yet been determined. Factors which will be considered in determining the cost will include the cost associated with developing the basic computer analysis programs and the cost of adapting those programs for calculator use. After some experience has been gained in working with U.S. military organizations, a decision can be made concerning supplying the adapted programs to other organizations.

2. EXAMPLES OF EMC CALCULATIONS

The application of programmable calculators to EMC analysis will be illustrated by several examples which indicate the kinds of calculations that can be executed and the ease with which they can be performed. The equations used in the examples are explained briefly. Detailed explanations can be found in the references cited.

2.1. Interference-to-Noise Ratio

One of the criteria often used in EMC analyses is the interference-to-noise ratio (INR) at the victim receiver. The INR depends on the characteristics of both the interfering transmitter and the victim receiver, and on the propagation path, as indicated in Figure 1.

$$INR = PT + GT + GR - RS - LP + OFR$$

(1)

where:

PT = Transmitter peak power (dbm)  
 GT = Gain of transmitting antenna (dB)  
 GR = Gain of receiving antenna (dB)  
 RS = Sensitivity of receiver (dBm)  
 LP = Propagation path loss (dB)  
 OFR = Off-frequency rejection (dB) - This is the attenuation caused by: any mismatch between the interference-signal spectrum and the selectivity of the receiver; and the frequency displacement between the two equipments.

As indicated in the flow diagram in Figure 2 the values for PT, GT, GR, RS, are inputs to the process. The values of LP and OFR must be calculated using models that are appropriate for the situation to be analyzed. The models that will be used as subroutines in the calculator programs for calculating LP and OFR are listed in TABLE 1.

The propagation path loss (LP) depends on the relative locations of the two antennas, the nature of the propagation path, and the frequency. Two of the propagation path loss models listed in TABLE 1 will be illustrated here. The first pertains to ground-based systems and the second situation pertains to a pair of antennas installed on the fuselage of an airplane. In both cases the antennas are separated so that they are in the far field of one another.

TABLE 1

## MODELS USED AS SUBROUTINES IN INR PROGRAM

## PROPAGATION PATH LOSS MODEL (LP) - (all are for far field situations)

<u>TITLE</u>	<u>APPLICATION</u>
1. Smooth earth #1	20 to 100 MHz
2. *Smooth earth #2	100 to 10,000 MHz
3. Cosite #1	VHF
4. Cosite #2	UHF
5. *Aircraft #1	Cylindrical surface
6. Aircraft #2	Conical surface
(additional models to be developed)	

## OFF-FREQUENCY REJECTION MODELS (OFR)

\*Pulsed Interference Signals  
 . Analog Interference Signals

\* These are the two propagation models and the OFR model used in the examples presented in this paper.

## 2.1.1. Path Between Ground-based Antennas (Lustgarten, M.N., 1973)

The propagation model used for ground-based equipments includes 3 modes of propagation: line-of-sight, diffraction, and troposcatter. The inputs to the model are:

HT = Height of transmitter antenna (feet)  
 HR = Height of receiver antenna (feet)  
 D = Distance between antennas (statute miles)  
 FO = Frequency of the interfering signal (MHz)

A flow diagram for the model is shown in Figure 3. The model is used for frequencies in excess of 100 MHz and the design is optimized to be most accurate for the paths having losses of 200 dB or less, which is the range of interest in most EMC analyses. The model was developed by fitting curves to data reduced from hundreds of measurements made by the Institute for Telecommunication Sciences. An example of a printout obtained with this propagation model is shown in Figure 4.

The convenience of using a programmable calculator is apparent from an examination of this sample printout. After the operator inserts the magnetic card into the calculator and presses the GO button the process involves the following steps:

1. Title of program is printed.
2. First set of instructions is printed.
3. The operator follows the instructions and keys in the values for HT, HR, and D.
4. The second instruction is printed.
5. The operator keys in the value for FO.
6. The answer is printed.

When this program is used the entire process can be accomplished with a calculator in about 30 seconds. To do the calculations manually would take about 10 to 15 minutes if the person were well acquainted with the mathematical procedures involved or much longer if not.

For the example pertaining to antennas mounted on an airplane fuselage, the path loss is calculated using methods described in the reference (Khan, P.J., et al, 1964). The procedure entails calculating the path loss between the antennas assuming they are mounted on a flat conducting plane and then adding a correcting factor to account for the curvature of the actual surface. When the surface between the antennas is cylindrical, the path loss is calculated using the procedure shown in the flow diagram in Figure 5. The inputs to the model are: the radius of the cylinder (fuselage), the distance between the antennas along the axis of the cylinder, the angle between the antennas (projected on a plane perpendicular to the axis), and the transmitter frequency. An example of a printout produced with this model is shown in Figure 6.

## 2.1.3. Off-Frequency Rejection (Newhouse, P.D., 1969), (Mason, S., 1960)

The OFR which depends upon the spectral characteristics of the interfering signal and the victim receiver. For pulsed interference signals, the OFR is calculated using the model shown in the flow diagram in Figure 7. An example of a printout obtained with this model is shown in Figure 8. The input parameters, which are identified in the sample printout in Figure 8, are:

BW = Bandwidth of the victim receiver (MHz)  
 TAU = Pulse width (between half-voltage points) of the interfering pulse (micro-seconds)  
 DEL = Rise time of the interfering pulse (micro-seconds)  
 FO = Carrier frequency of the interfering signal (MHz)  
 FR = Tuned frequency of the victim receiver (MHz)

For analog interference signals, the OFR is the attenuation resulting from the selectivity of the receiver.

## 2.1.4. INR as a Function of Frequency Separation

The INR calculated with Equation (1) pertains to a particular value of  $\Delta f$ , the frequency separation between the carrier frequency of the interference signal and the tuned frequency of the victim receiver.

In some EMC analyses, the INR as a function of  $\Delta f$  is of interest. An example of a printout obtained with a program that calculates INR vs  $\Delta f$  is shown in Figure 9.

Families of INR vs  $\Delta f$  curves can be plotted as in Figure 10 to show the trade-offs between INR,  $\Delta f$  (frequency separation) and D (distance separation) for a particular pair of nomenclatures. A set of curves such as this can be useful to siting engineers and operational personnel who are concerned with deploying and selecting frequencies for radar and radio equipment.

## 2.2 INTERMODULATION

An important consideration in selecting frequencies, especially for communication equipments, is the possibility of intermodulation. The mathematical relationships that cause intermodulation of various orders is generally well known and can be found in the literature. (RADC., 1966). In the example, here, we are concerned with third order intermodulation which results when the following conditions are met

$$|2F_1 - F_2 - F_3| \leq G \quad (2)$$

where,  $F_1$ ,  $F_2$ , and  $F_3$  are three frequencies taken from a given list of available frequencies.  $G$  is the guard bandwidth or minimum separation between frequencies, including those frequencies produced by intermodulation. When the above condition is satisfied, one of the three frequencies should be eliminated from the list to prevent the possibility of third order intermodulation.

Each frequency and all the possible pairs of the other frequencies in the list are examined in this way to identify the combinations that are subject to third order intermodulation. For each combination so identified, one of the frequencies is eliminated to yield a list of frequencies that can be used without third order intermodulation.

The flow diagram of an algorithm for processing a list of frequencies is shown in Figure 11. As shown in an example printout in Figure 12, this algorithm gives three alternative list of frequencies free of third order intermodulation.

## 3. CALCULATOR FEATURES

ECAC will provide programs for both desk-top and pocket-size programmable calculators. Desk-top calculators are preferred because they can accommodate larger programs and have more data registers and time-saving features. Pocket-size calculators, however, are much less expensive and are expected to be used by organizations that cannot justify the cost of desk-top calculators.

## 3.1 Pocket-size Calculators

A pocket-size calculator is available that can accommodate a 100-step program from either the keyboard or from a magnetic card. There is also a slightly larger calculator that can accommodate two 80-step programs from the keyboard. These calculators impose a greater burden on the operator than the desk-top calculators, but they are attractive from a price standpoint — about \$800 each.

A program that exceeds the capacity of one of these small programmable calculators can be run in sections. For example, the program for calculating the interference-to-noise ratios (INR) includes subroutines for calculating the propagation path loss and the off-frequency rejection (OFR), and thus

entails several hundred program steps. This program can be recorded on several cards and executed by the pocket-size calculator in 3 runs. This kind of operation requires the operator to be especially alert so that the runs are executed in the proper sequence.

### 3.2 Desk-top Calculators

Programmable, desk-top calculators are available with a variety of features and options. The features that are important to the capabilities planned by ECAC are:

#### 3.2.1. Mathematical Function Keys

These are essential in the application of the ECAC models. The keys provided should include trigonometric, logarithmic, and exponential functions.

#### 3.2.2. Printer

Two basic capabilities are available: (1) Numeric, or (2) Alphanumeric. The alphanumeric printout capability is preferred because it can produce a printout that more clearly identifies input and output data. Even more important, the alphanumeric capability enables the calculator to communicate with the user in words, that is, it can printout step-by-step instructions for the user to follow, which almost eliminates the learning time that would otherwise be required to use any one of the ECAC models.

#### 3.2.3. Number of Data Registers

Basic desk-top calculators have from 51 to 128 data registers, depending on the make. The number of registers is expandable, either at the factory or in the field, to yield a total of from 111 to over 8000. At this time, it is estimated that 80% of the programs to be supplied by ECAC will require less than 51 data registers; and that 95% will require less than 111 data registers. The 5% of the programs that are expected to require more than 111 data registers are those involving the processing of a large number of frequencies. These programs have not yet been defined and will be the last to be developed.

#### 3.2.4. Number of Program Steps

A basic calculator can accommodate 500 to 1024 program steps, depending on the make. This number is also expandable, either at the factory or in the field, to a total from 2036 to over 8000. It is estimated that 50% of the programs will require less than 500 steps, 90% will require less than 1000 steps, and 100% will require less than 2000 steps.

#### 3.2.5. XY Plotter

Many makes of calculators are designed to operate with XY plotters. This capability is very convenient, but not essential in the application of the programs to be supplied by ECAC. However, several of the programs produce outputs that are most useful when plotted as curves. The programs will printout the coordinates so that the plotting can be done manually if an XY plotter is not available.

#### 3.2.6. Recommended Desk-top Configurations

Most makes of programmable desk-top calculators are designed so that they can be expanded; various options and peripherals can be added in the field. Thus an organization is not forever bound to the configuration of an original purchase.

ECAC's objective is to provide the EMC community with mathematical models that are convenient to use, even by individuals who have only an occasional need to perform EMC calculations. To take maximum advantage of this convenience, a participating organization should have a calculator with the following features:

1. Mathematical function keys.
2. Alphanumeric printer.
3. Data registers -- at least 100.
4. Program steps -- at least 2000.
5. Programmable from magnetic cards or tapes.

Several makes of calculators that have all of the above features are available for about \$5000.

Calculators having less capability will also be able to employ the ECAC programs, but not as conveniently. For example, a calculator with only 500 program steps would have to make more than one run to perform all of the calculations required by some models. A calculator that has a numeric rather than alphanumeric printout will require the user to rely more on the instruction manual to know how to use the model, thereby imposing a much longer learning time than a calculator equipped with an alphanumeric printer.

### 4. COST EFFECTIVENESS CONSIDERATIONS

The calculation and decision processes involved in the models to be supplied by ECAC could be performed either by hand or with a large computer, as an alternative to using a calculator. In comparing the cost effectiveness of these alternatives, an organization should consider the possible advantages and disadvantages of using a calculator.



#### 4.1. Advantages of Calculator Over Hand Calculations

1. Greatly reduces the computation time; most calculations can be accomplished in less than one minute, including the time to key in the input data.
2. Provides greater accuracy.
3. Assures the user of proven analytical procedures developed by EMC specialists.
4. Provides a printout that records all input data, output data, and the procedures used in making the calculations. (Applies only to desk-top calculations with printer.)
5. Almost eliminates the learning time to apply a particular mathematical model. This could save several hours on each occasion the model is used. (Applies only to desk-top calculators with alphanumeric printer.)

#### 4.2. Advantages of Calculator Over a Large Computer

1. The calculator programs supplied by ECAC will be ready to go; no redesign to tailor the programs to a particular computer will be required.
2. No program maintenance required.
3. Usually more accessible and faster turn-around time.
4. Minimal security risk, all the registers go to zero when the calculator is turned off.
5. Simple to use.

#### 4.3. Possible Disadvantages of the Calculator

1. If a large number of people in an office must share a calculator, accessibility could be more of a problem than it is with batch-processing in a large centrally operated computer.
2. Because of their limited storage capacity, calculators are not practical to use with mathematical models that require a large data base.

#### 5. PROGRAMS TO BE OFFERED BY ECAC

As explained in the introduction, ECAC is going to issue a package of calculator programs semi-annually. The titles of the programs that are scheduled to be issued during 1975 are listed in TABLE 2. This selection of programs is based on our judgement of the kinds of programs that will be most useful to subscribing organizations and also upon the ease with which our existing computer programs can be adapted to calculators. In 1975 the programs actually issued may differ from those in the table if the subscribers indicate a preference for a different selection or if we encounter any difficult problems in adapting any of our existing computer programs to calculators.

A detailed explanation of ECAC's offer and the steps that an organization can take to become a subscriber can be found in the reference (ECAC, 1974).

TABLE 2

#### TENTATIVE CALCULATOR PROGRAMS

##### To Be Issued by ECAC in January 1975

1. Propagation Path Loss (20 to 10,000 MHz)
2. Off-frequency Rejection (OFR)
3. Signal-to-Noise Ratio (SNR)
4. Interference-to-Noise Ratio (INR)
5. Basic Intermodulation Analysis System
6. Harmonic Intermodulation Analysis System
7. Coordinate Conversion Program
8. Bearing and Distance
9. LAT/LON From Bearing and Distance
10. Antenna Coupling Loss

##### To Be Issued by ECAC in July 1975

1. Airplane Antenna Coupling Loss
2. Conformance of Radar Emission Spectrum to OTP Standard
3. Fourier Transforms of Trapezoidal Pulses with FM (Magnetron Spectrum)
4. Cosite Analysis Subroutines
5. Frequency Analysis Evaluation

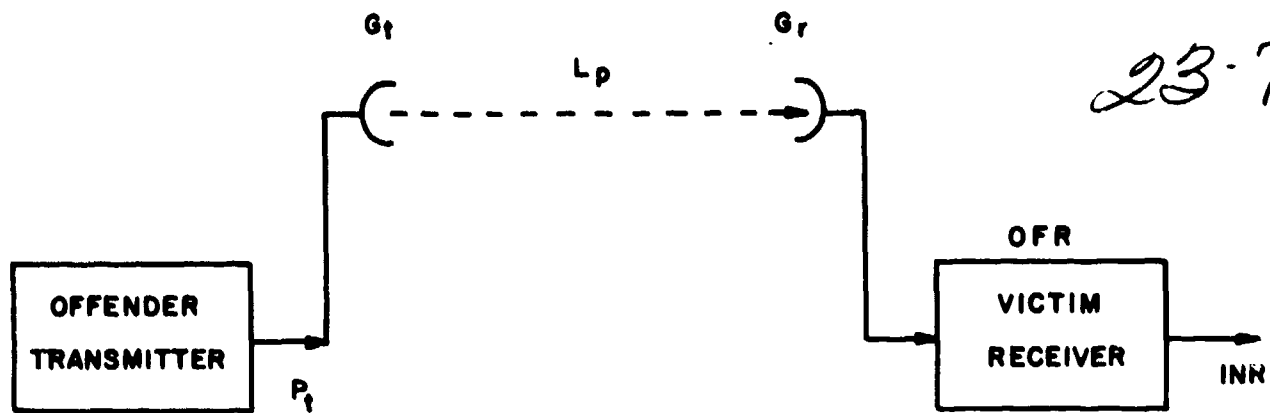
#### 6. PROGRAM EXCHANGE

Many of the military organizations involved in EMC activities either have or plan to obtain programmable calculators. These organizations will no doubt use programs that they develop themselves as well as the programs that will be supplied by ECAC. If the various programs were to be collected and kept in a central library, they could be used by all of the members of the EMC community. An arrangement for exchanging calculator programs for EMC analysis would be a great convenience and help to minimize the cost of performing EMC calculations.

Since ECAC will soon have an extensive library of calculator programs, ECAC could maintain a central library of programs developed by the members of the EMC community and provide the means for distributing the programs as requested by the members.

## REFERENCES

1. ECAC Newsletter, February 1974, "EMC Analytical Models for Programmable Calculators," Department of Defense, Electromagnetic Compatibility Analysis Center, Annapolis, MD 21402.
2. Khan, P.J., et al., April 1964, "Derivation of Aerospace Antennas Coupling-Factor Interference Prediction Techniques," 04957-8-F, Cooley Electronics Laboratory, University of Michigan.
3. Lustgarten, M.N. & Cohen, D., May 1973, "An Initial EMC Statistical Propagation Loss Model, (EPM-73)," ECAC-TN-73-12, Department of Defense, Electromagnetic Compatibility Analysis Center, Annapolis, MD 21402.
4. Mason, S., & Zimmerman, H., 1960, "Electronic Circuits, Signals, and Systems," John Wiley and Sons, Inc.
5. Morgan, G., 1970, "Avionics Interference Prediction Model," ESD-TR-70-268, Department of Defense, Electromagnetic Compatibility Analysis Center, Annapolis, MD 21402.
6. Newhouse, P., May 1969, "Peak Output Power in Victim Receivers," ECAC Radar Analysis Bulletin, No. 2, Department of Defense, Electromagnetic Compatibility Analysis Center, Annapolis, MD 21402.
7. RADC-TR-66-1, 1966, "Interference Handbook," Rome Air Development Center, Griffiss AFB, NY 134401



$$INR = P_t + G_t - L_p + G_r + OFR - R_s$$

Fig. 1 Interference-to-noise ratio parameters.

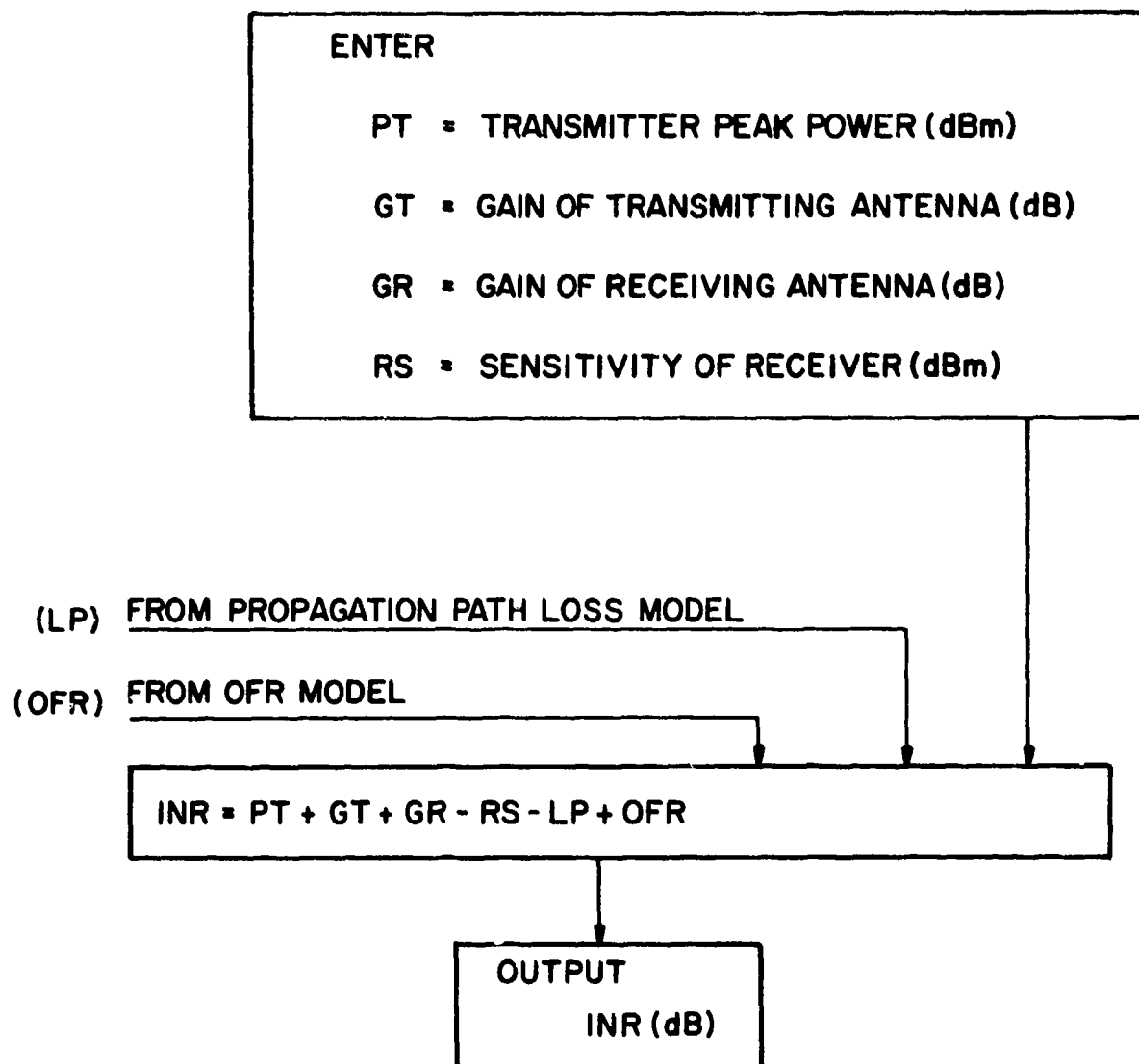


Fig. 2 Interference-to-noise ratio (INR) model flow diagram.

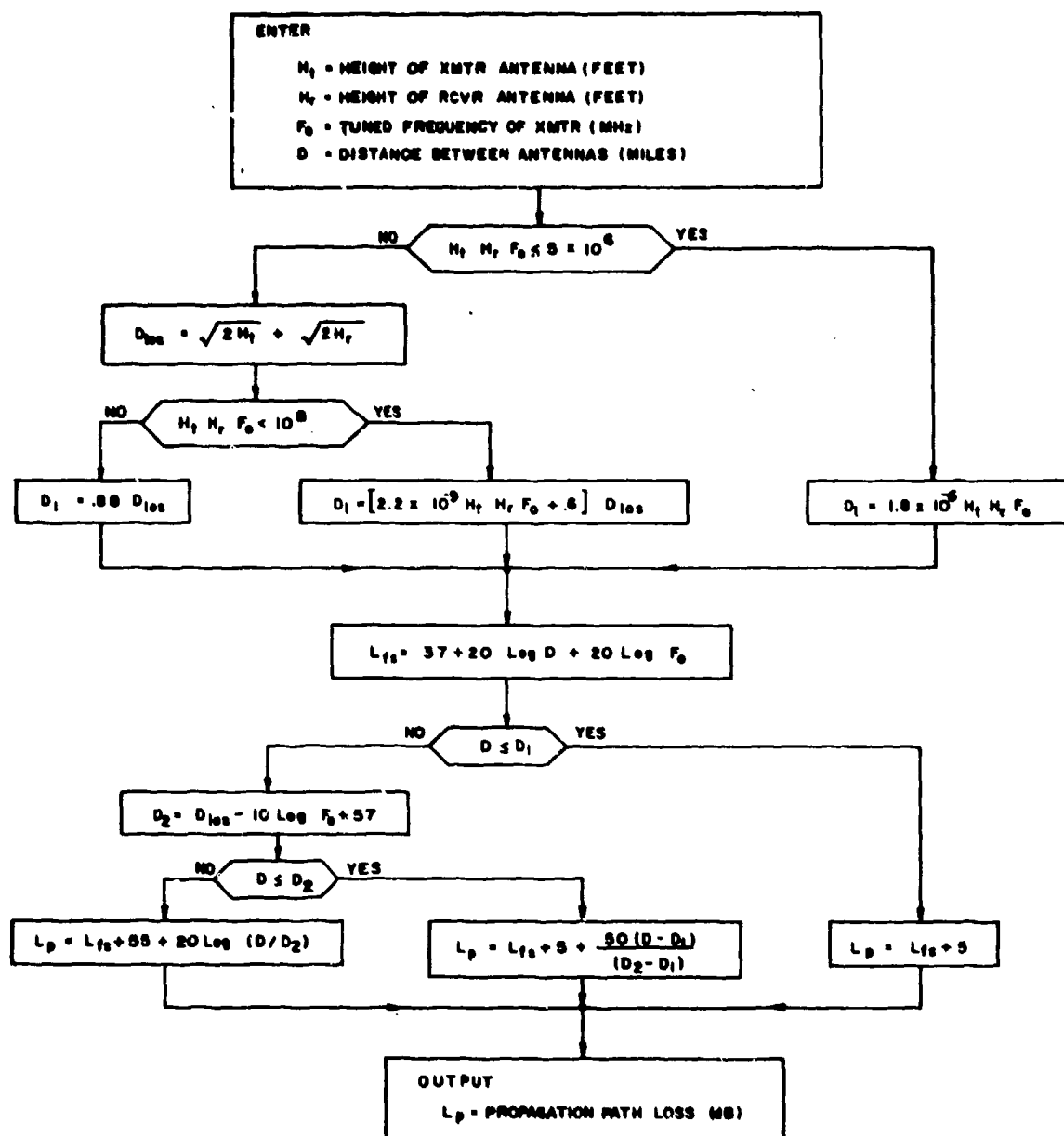


Fig. 3 Propagation path loss model flow diagram, ground-based antennas (identified as "smooth earth #2" in Table I)

PRINTOUT	EXPLANATION
<p>PROPAGATION PATH LOSS</p> <p>ENTER HT, HR, D XXXXXX</p> <p>100. 50. 40.</p> <p>ENTER FO XXXXXX</p> <p>4000.</p> <p>LP =</p> <p>187.</p> <p>XX DONE XX</p>	<p>TITLE</p> <p>FIRST INSTRUCTIONS</p> <p>INPUTS PRINTED AFTER THEY ARE KEYED IN BY THE OPERATOR</p> <p>NEXT INSTRUCTION</p> <p>INPUT PRINTED AFTER IT IS KEYED IN BY THE OPERATOR</p> <p>ANSWER</p> <p>END OF RUN INDICATED</p>

239

Fig. 4 Example of printout obtained with the propagation path loss model (ground-based antennas)

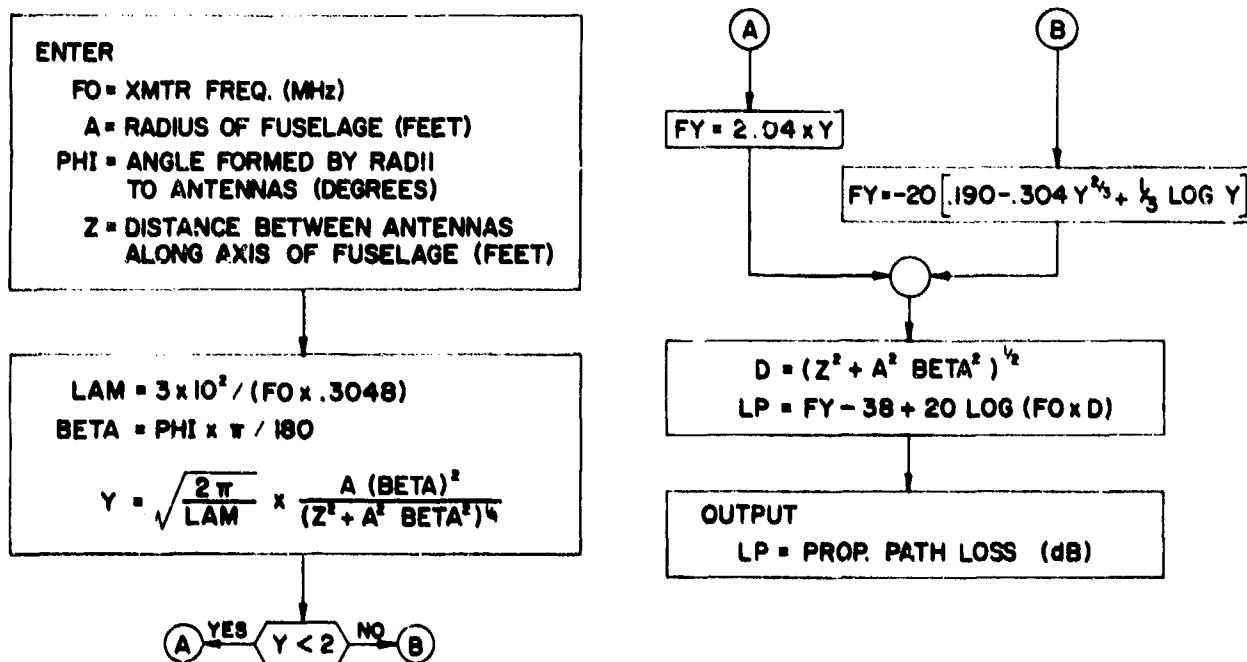


Fig. 5 Propagation path loss model flow diagram, aircraft antenna (identified as "aircraft #1" in Table 1)

# PROPAGATION PATH LOSS

ENTER FO, A

2750.00  
3.00

ENTER PHI, Z

30.00  
25.00

LP =

42.61

XX DONE XX

Fig. 6 Example of printout obtained with the propagation path loss model (aircraft antenna)

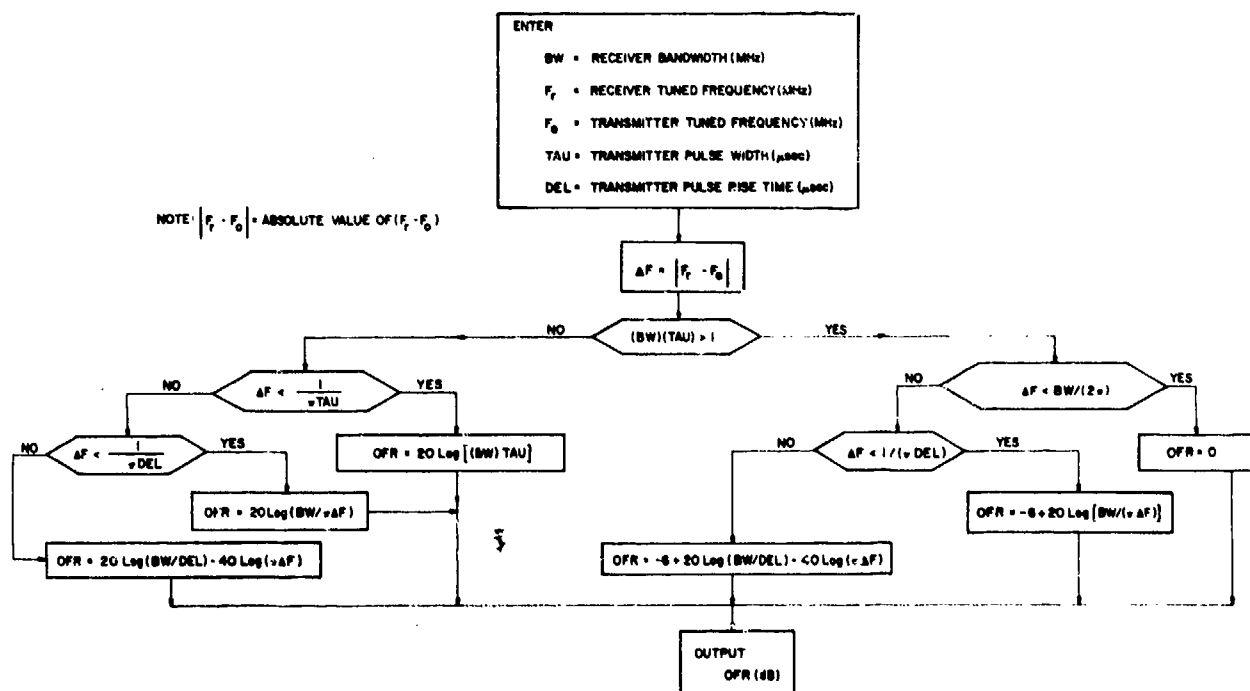


Fig. 7 Off-frequency rejection (OFR) model flow diagram

OFF-FREQUENCY  
REJECTION  
(OFR)

23-11

ENTER BW, TAU, DEL  
XXXXXX

2.00  
1.00  
0.05

ENTER FO, FR  
XXXXXX

1150.00  
1165.00

OFR =

-37.89

XX DONE XX

Fig. 8 Example of printout obtained with the OFR program

INR	2.00	OFR =	OFR =
CALCULATION	1.00	-13.59	-70.84
INR VS FREQUENCY	0.05		
ENTER HT, HR, D	ANY ERRORS?	INR =	INR =
XXXXXX	ENTER FR	11.31	-45.34
	XXXXXX	FD =	FD =
50.00		2.15	100.00
75.00	2800.00	XXXXXX	XXXXXX
85.00		OFR =	OFR =
	ANY ERRORS?	-20.26	-84.18
ANY ERRORS?	OFR =	INR =	INR =
ENTER FO	0.00	4.65	-59.28
XXXXXX	INR =	FD =	FD =
2800.00	24.90	4.64	215.44
LP =	FD =	XXXXXX	XXXXXX
205.10	0.00	OFR =	XXDNEXX
ENTER PT, GT, GR	XXXXXX	-44.18	
XXXXXX	OFR =	INR =	
90.00	-6.92	-19.28	
35.00	INR =	FD =	
15.00	17.98	21.54	
ANY ERRORS?	FD =	XXXXXX	
ENTER RS, LS	1.00	OFR =	
XXXXXX	XXXXXX	-57.51	
-90.00		INR =	
0.00		-32.61	
ANY ERRORS?		FD =	
ENTER BW		46.42	
TAU, DEL		XXXXXX	
XXXXXX			

Fig. 9 Example of printout obtained with the INR program when the frequency separation is varied, (FD =  $\Delta f$ ).

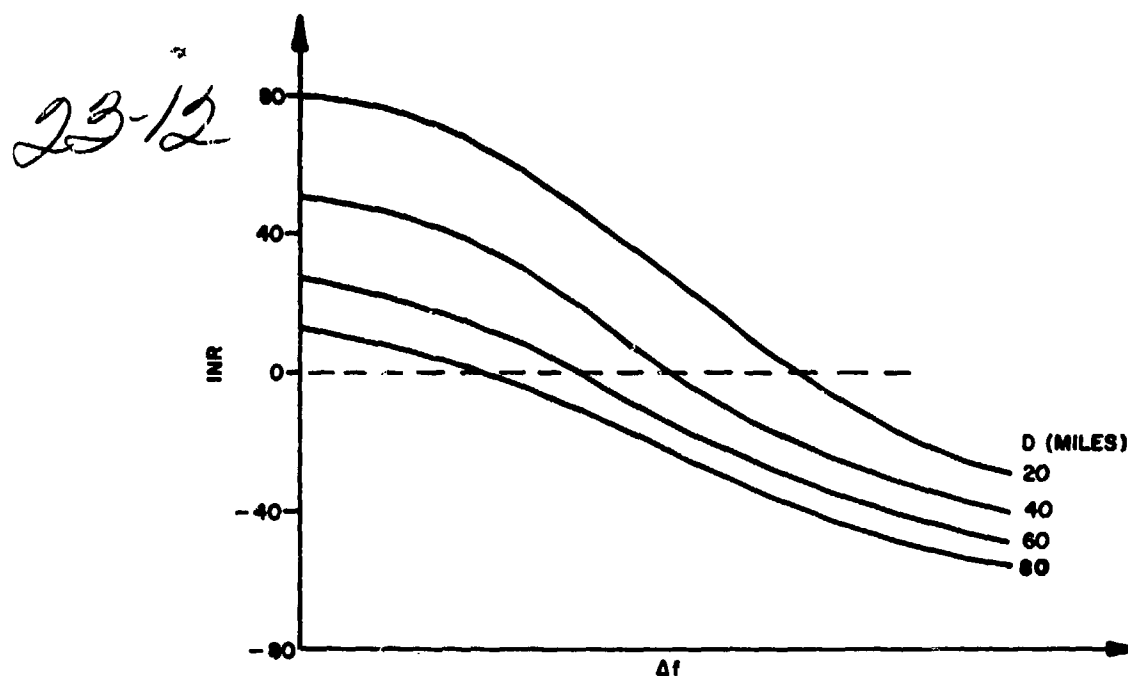
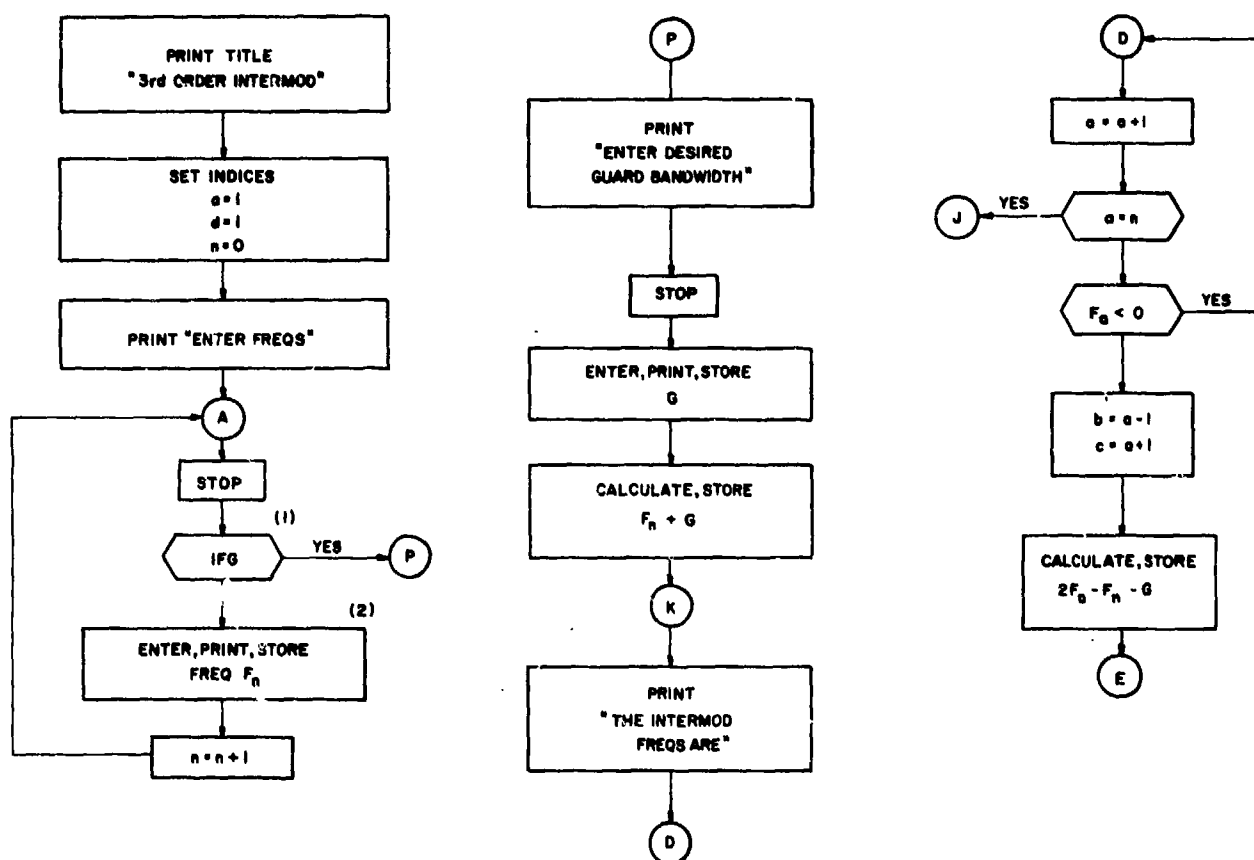


Fig. 10 Trade-off curves for  $INR/\Delta F/D$  relationship for a particular type of transmitter and receiver



NOTE:

- n = TOTAL NUMBER OF FREQS ENTERED
- a } INDICES FOR FREQS., USED FOR INDIRECT ADDRESSING
- b }
- c }
- d = INDEX FOR ALTERNATIVE RESULTS
- CONDITION FOR 3rd ORDER INTERMOD,  $2F_a - F_b - F_c \approx 0$
- G = GUARD BANDWIDTH

(1) FLAG SET BY OPERATOR WHEN ALL FREQS HAVE BEEN ENTERED

(2) FREQS MUST BE ENTERED IN ASCENDING ORDER

Fig. 11(a) 3rd order intermodulation model flow diagram



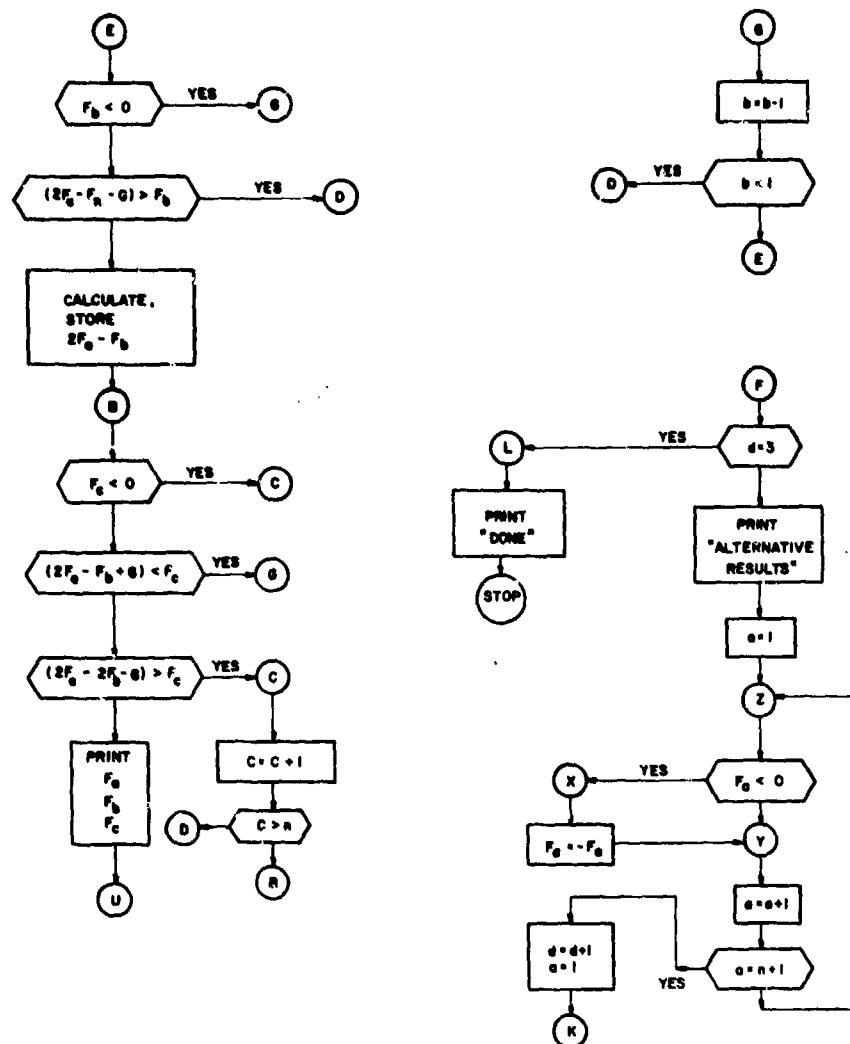


Fig. 11(b) 3rd order intermodulation model flow diagram

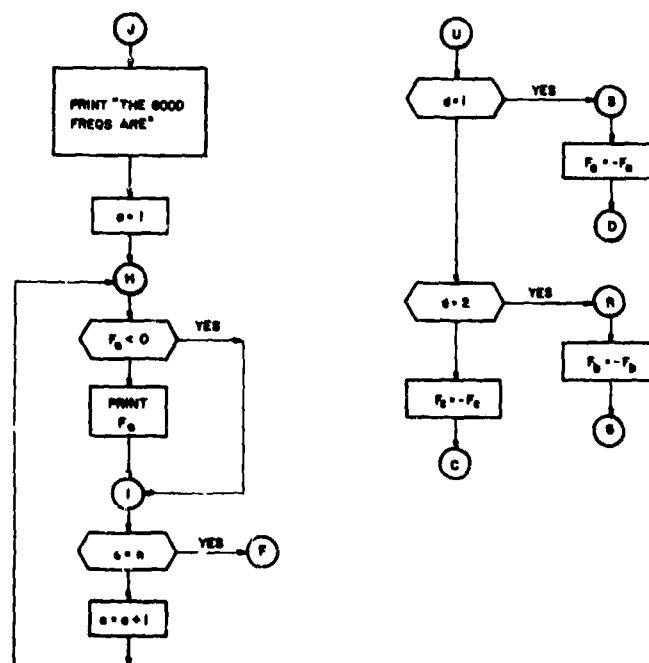


Fig. 11(c) 3rd order intermodulation model flow diagram

3rd ORDER INTERMOD	THE INTERMOD COMBINATIONS ARE	ALTERNATIVE RESULTS	THE GOOD FREQS ARE	THE GOOD FREQS ARE
ENTER FREQS		THE INTERMOD COMBINATIONS ARE		
1.00	3.00		3.00	1.00
3.00	1.00		15.00	3.00
5.00	5.00		20.00	10.00
10.00	10.00	3.00	23.00	15.00
15.00	5.00	1.00	30.00	16.00
16.00	15.00	5.00	33.00	23.00
20.00			35.00	33.00
23.00	20.00	10.00		35.00
30.00	5.00	5.00	XXXXX	
33.00	35.00	15.00	ALTERNATIVE RESULTS	XX DONE XX
35.00		15.00	THE INTERMOD COMBINATIONS ARE	
ENTER DESIRED GUARD BANDWIDTH	23.00	10.00		
0.10	16.00	20.00		
	30.00	23.00		
	THE GOOD FREQS ARE	16.00	3.00	
	1.00	30.00	1.00	
	5.00		5.00	
	15.00		15.00	
	16.00		10.00	
	30.00		20.00	
	33.00		23.00	
	35.00		16.00	
	XXXXXX		30.00	

Fig. 12 Example of printout obtained with the 3rd order intermodulation program.

24-1

APPLICATION OF MARKOV CHAIN THEORY  
TO THE MODELLING OF IFF/SSR SYSTEMS

Stephen J. Sutton  
C. Wayne Ehler  
IIT Research Institute  
at the  
Department of Defense  
Electromagnetic Compatibility Analysis Center  
Annapolis, Maryland

SUMMARY

Secondary surveillance Radar (SSR) is an important means of air traffic surveillance and identification for both military and civil air operations. The reliance on SSR generated the need for simulation and mathematical models to assist with the analysis of IFF/SSR performance. One such model was developed at the DoD Electromagnetic Compatibility Analysis Center in Annapolis, MD.

An efficient and versatile mathematical technique was sought to answer questions such as: Will a transponder reply, and how often will interrogations be garbled? Markov chain theory was selected as the best technique for this purpose. A Markov chain was created for each transponder type (military, air carrier, general aviation). The states of each chain represent the logic and timing within the transpondering equipment. The probabilities of transitioning between states are calculated as a function of the transmitter and signal environment detected by the transponder. Solving the steady-state equations derived from the transition probabilities, permits the calculation of probability of reply, probability of garble, interrogation rates, fruit rates and other transponder performance parameters.

The automated IFF/SSR prediction model was constructed around the Markov chain models. Inputs to the prediction model include the interrogator environment and an air traffic deployment for a specific geographic area. For each transponder in the deployment the model determines those interrogators whose signals are received; calculates the transition probabilities; selects the proper Markov chain; and calculates transponder performance parameters. These parameters are then used to calculate the performance of a selected interrogator system.

To gain confidence in the model predictions, results were compared with predictions from a previously validated simulation and with available measured interrogation and suppression arrival rates. The comparison showed that the IFF/SSR model predictions correlated well with both the other predicted data and the measured data.

The results of this paper show that the IFF/SSR prediction model with Markov chain transponder models provides a powerful, flexible, reliable, and accurate analysis capability.

1. INTRODUCTION

Secondary Surveillance Radar (SSR) is now an important means of air traffic surveillance as well as military identification (IFF) in Europe and the United States. Because of this dependency on SSR for air traffic control, studies of SSR equipments and performance have increased. Automated, mathematical and simulation models have been developed to assist in the analysis of IFF/SSR performance (FAA, 1974; CEAC, 1973; UK IFF/SSR Policy Board, 1970). This paper discusses an automated IFF/SSR performance prediction model (PPM) developed at the Department of Defense Electromagnetic Compatibility Analysis Center (DoD ECAC) in Annapolis, Maryland (Sutton and Ehler, 1973). The mathematical basis for this model is the application of Markov chain theory to the modelling of the IFF/SSR transponder. The probabilities of transitioning between states are calculated as a function of the transmitter and signal environment detected by the transponder. Solution of the steady-state equations for the Markov chain produces the IFF/SSR transponder performance.

The Markov chain transponder models are the core of the PPM, which uses deployments and characteristics of IFF/SSR interrogators and airborne transponders to predict both transponder performance and overall SSR system performance.

This paper is divided into four sections: 1) a brief description of the SSR system 2) a discussion on the Markov chain transponder model 3) a brief description of the IFF/SSR PPM; and 4) a discussion of how the PPM results compare with results from another model and measured data.

2. IFF/SSR DESCRIPTION

Figure 1 shows the general configuration of IFF/SSR equipments. The coder/decoder prepares the interrogations (i.e., target identity requests) and sends them to the interrogator. The interrogations are pulse amplitude modulated on a 1030 MHz carrier. Aircraft, properly equipped, will detect the interrogations, decode them, and transmit a reply at 1090 MHz. Replies received at the interrogator are decoded and displayed on a Plan Position Indicator (PPI).

Four interrogation modes (1, 2, 3/A, C) can provide position and identity information of properly equipped military and civilian aircraft. The interrogations may be transmitted at a rate which is a submultiple of the pulse repetition frequency (PRF) of the associated primary radar. When IFF/SSR equipments are not used with a primary radar, an internal trigger establishes the PRF. The modes are transmitted automatically in a given repetitive sequence (mode interlace) at the IFF/SSR PRF. Modes 1, 2, 3/A are normally used by the military for identification and air traffic control. The civil air traffic control systems use mode 3/A for identification and surveillance. Both military and civilian may use mode C for altitude determination.

### 2.1. The IFF/SSR Interrogation Modes.

These modes have the form shown in Figure 2. The  $P_1$  and  $P_3$  pulses represent the interrogation. The  $P_2$  pulse is the Interrogator Sidelobe Suppression (ISLS) pulse. The time spacing between  $P_1$  and  $P_3$  uniquely identifies the interrogation mode. The tables in Figure 2 give the pulse spacing and amplitude requirements for valid mode 1, 2, 3/A, and C interrogations and the specifications for the interrogation pulses (FAA, 1971).

The airborne transponder, depending on its function, may have the capability to decode all, some, or any one of the modes. When the transponder detects an interrogation, it prepares a proper reply. All replies have the same format (Figure 3). The code pulse content is determined by the four-digit octal code selected by the pilot (e.g., Figure 4). The pilot can indicate emergencies and communications failures by setting the transponder to reply with mode 3 codes 7700 and 7600 respectively.

The decoders interfacing with the interrogator identify the signal as a reply by the spacing of the framing pulses, the code pulse content, and the mode of interrogation. The pilot can further validate his identity by transmitting with his replies another pulse (Special Identification Pulse) spaced  $24.65 \pm 0.05$   $\mu$ s after  $P_1$  (Figure 3). This pulse causes the reply on the PPI to be different from any other aircraft with the same code.

Mode C requests altitude information from properly equipped transponders and altimeters. The altimeter encodes the aircraft altitude in binary coded decimal (BCD) format. When the transponder decodes a mode C interrogation the altitude is encoded in the basic IFF/SSR reply format. Mode C is always interlaced with at least one of the other IFF/SSR modes.

### 2.2. The IFF/SSR Transponder.

Figure 5 is a block diagram of a transponder employing all the IFF/SSR modes. When the transponder detects a valid interrogation, the transponder suppresses each mode decoder for a time period not to exceed 125  $\mu$ s (FAA, 1971). During this deadtime the transponder prepares and transmits a reply. The time required to transmit the reply is approximately 30  $\mu$ s. Additional deadtime is sometimes provided to prevent transponder replies to reflections of the original interrogation.

When a sidelobe suppression interrogation enters the transponder, all mode decoders are inhibited for  $35 \pm 10$   $\mu$ s.

The transponder receiver can be suppressed from external sources such as a Tactical Air Navigation (TACAN) interrogator or an SSR associated Collision Avoidance System. The TACAN suppression occurs for approximately 20  $\mu$ s at a rate of 30/s in track and 150/s in search. A collision avoidance system could cause the transponder not to reply to valid interrogations 4.5 percent of the time. (Special Committee 116-B, 1970.)

Transponder overload circuitry senses reply rate, sidelobe suppression rate, and pulse rate, and, if the preset limits for these parameters are exceeded, the transponder reduces sensitivity as a means of bringing the monitored rates below the preset limit.

This transponder feature not only protects the transmitter, but also helps maintain adequate SSR system performance. The reply rate is kept at a tolerable level and allows the interrogators interested in a particular aircraft to have their queries answered. The preset limits may be adjusted to optimize transponder and system performance.

### 2.3. Sidelobe Suppression.

The interrogator receives replies created in response to its own mainbeam interrogations. Unwanted replies or other random signals entering the receiver interfere with the detection of valid replies. This interference can be reduced by interrogator sidelobe suppression (ISLS). ISLS forces transponders to reply only to mainbeam interrogations. Interrogations emanating from the sidelobes of the interrogator antenna do not generate replies from the transponders. This reduces the number of unwanted replies which could (1) interfere with the detection of valid replies at the interrogator of interest or other interrogators and (2) overload the transponder transmitter.

The interrogator provides this capability by adding a third pulse to the basic interrogation (See Figure 2). This pulse is placed  $2 \pm 0.15$   $\mu$ s after the leading edge of the first pulse and is transmitted via an omni-directional antenna. The gain of this antenna is greater than the gain of the major sidelobes of the directional antenna, but at least 9 dB below the mainbeam gain. The U.S. National Standard FAA, 1971 for the IFF MARK X (SIF) Air Traffic Control Radar Beacon System and Attachment B to Part I, ICAO Annex 10, Aeronautical Telecommunications state the transponder will reply to a valid interrogation when  $P_2$  (ISLS pulse) is at least 9 dB below  $P_1$ . When  $P_2 \geq P_1$  the transponder suppresses for  $35 \pm 10$   $\mu$ s and transmits no reply.

In Figure 6 the reflected mainbeam interrogation is received at the transponder and the transponder replies. This creates a false target along the azimuth of the mainbeam. The  $P_1$  pulse from the sidelobe of the directional antenna and the  $P_2$  pulse from the omni did not cause a suppression before the arrival of the reflected interrogation because the received power of the  $P_1$  pulse was below the transponder sensitivity and not detected by the transponder. To alleviate this problem  $P_1$  and  $P_2$  are transmitted by the omni antenna. The  $P_2$  input power to the omni antenna is twice that of  $P_1$ .  $P_1$  and  $P_3$  continue to be transmitted directionally. Now the transponder will suppress prior to receiving the reflected mainbeam interrogation because  $P_1$  and  $P_2$  are both received. No false target occurs. This system is called Improved Interrogator Sidelobe Suppression, and is employed with SSR systems in the United States and Europe.

### 3. MARKOV CHAIN TRANSPONDER MODEL

In order to measure the performance characteristics of a transponder, the most efficient and best model was sought. A technique was needed which could provide answers to such questions as the following:

1. Will a transponder reply when it is challenged?
2. How long was the transponder in a state of suppression?
3. How many mainbeam and sidelobe interrogations were received by the transponder?
4. Was a certain mode interrogation changed to another mode by the presence of an undesired interrogation from another interrogator?
5. How many of these changes took place, and how did they degrade overall system performance?

Many other similar questions were considered. All required in depth analysis, but were interrelated so that an answer to one would be conditioned by the other. To obtain predictions about aircraft transponder performance characteristics, a modelling approach using a Markov chain was developed.

A Markov chain is a process which moves from one state or condition to another state or condition with a certain finite probability. If at any time the process is in state  $s_i$ , then it moves in the next step to state  $s_j$  with a probability  $p_{ij}$ . A matrix of inter-state transition probabilities can be produced to show how the process may move. Movement should only be conditioned upon the present state of the system. (Kemeny and Snell, 1960.)

Markov chains are classified according to whether it is possible to transition from a given state to another given state in the chain. Two states are said to communicate if in a finite number of steps, transition can be made from one to the other and back again. States, therefore, are classified into sets of either transient or non-transient (ergodic) states. If a process leaves a transient set of states, it can never return, while if it enters an ergodic set of states it may never leave.

The Markov chain developed to model the IFF/SSR transponder contains states which form an ergodic set. A 2 micro-second time step was used as the basic time unit for transitioning between states since this was the spacing between the  $P_1$  and  $P_2$  pulses in the IFF/SSR interrogation.

Figure 7 displays the Markov chain which models a transponder capable of replying only to mode 3 IFF interrogations. There are 25 states in this chain, so that at any given time the transponder is operating in one of these 25 states. State number 1 is the condition of the process in which the transponder is open, ready to receive an interrogation. State 2 is the condition that a sidelobe suppression has entered the transponder. States 4, 5, 6, and 7 are conditions where a valid mode 3 mainbeam interrogation is received. To be in state 3, an interfering interrogation must occur when the transponder was in state 5, then the mainbeam interrogation will be changed to a sidelobe suppression. States 8 through 25 imply a deadtime condition, when the transponder has been interrogated and is not open to further interrogations until state 25 has been reached. These states may be reached by the occurrence of a sidelobe interrogation, a garbled mainbeam interrogation or a mainbeam interrogation itself.

The 25 states shown in Figure 7 are connected with arrows to indicate how transition may take place when the transponder is in any given state. Within a finite number of time steps, it will be possible to transition from any beginning state to any other state and back again, therefore, all states communicate with one another and form an ergodic set.

Based upon the number of interrogators in a ground environment, probabilities of transition from one state to another are calculated for one time period. That is, if the process is in state 1, what is the probability that within the next time increment it will be in state 1, or state 2, etc? These one-step transition probabilities are displayed in Figure 8 as a matrix of transition probabilities. If a state cannot be reached from another state in one time step, then the probability assigned is zero. The value of  $p_{ij}$  is found by using an  $i$  in the left hand column and a  $j$  in the top row, then the row/column intersection is the probability of transitioning from state  $i$  to state  $j$  in one time step.

To obtain the probability that in two time steps a transition between two states occurs, the one step transition matrix is squared. To find the  $n$ -step transition matrix, the one-step transition matrix is raised to the  $n^{\text{th}}$  power. As  $n$  becomes large, the matrix multiplication produces a steady state matrix of probabilities, each row contains the same or nearly the same values. These values predict the probability that at any given time the transponder is in any given state.

An alternate method of generating these steady state probabilities is to develop a set of simultaneous equations using the one step transition matrix. If  $P_i$  represents the steady state probability of being in state  $i$ , then

$$P_i = \sum_j p_{ji} P_j \quad ; \quad \forall_j \text{ where } p_{ji} \geq 0$$

where  $p_{ji}$  is the probability of transitioning from state  $j$  to state  $i$  in one step. There will be  $i$  of these equations and these together with the constraint

$$\sum_{i=1}^{\text{\# of states}} P_i = 1$$

forms a set of simultaneous equations which can be solved for the values of  $P_i$   $i = 1, 2, \dots$  number of states.

Figure 9 shows a Markov chain for a transponder capable of replying to modes 1, 2, 3/A, and C. It contains 84 states.

Figure 10 is a mode 1, 2, and 3/A chain with 61 states. Other Markov chains were developed for other mode combinations.

### 3.1. Transition Probability Calculations.

The transition probabilities (TABLE 1) depend on the IFF/SSR interrogation received by the transponder. To explain how the probabilities are calculated using the environmental information, an example calculation is outlined below.

Consider a transponder receiving signals from a set  $S$  of  $N$  interrogators with each interrogator having one of three mode interlaces: 3, 33C, or 23C. The  $N$  interrogators are grouped according to mode interlace into three independent groups. Group (or set)  $S_1$  has  $N_1$  interrogators using mode 3 interlace. In group  $S_2$  there are  $N_2$  interrogators using the 33C interlace, and in group  $S_3$  there are  $N_3$  interrogators using the 23C mode interlace, so that  $N_1 + N_2 + N_3 = N$ .

Each of these three groups are further divided into three independent subgroups, so that in group  $N_1$ ,  $S_{m_1}$  is the subgroup of  $N_{m_1}$  interrogators whose mainbeam interrogations only are received by the transponder. A subgroup  $S_{s_1}$  has  $N_{s_1}$  interrogators whose mainbeam interrogations and sidelobe suppressions are received. Finally, subgroup  $S_{b_1}$  contains  $N_{b_1}$  interrogators whose mainbeam, sidelobe and backlobe signals are received ( $N_{m_1} + N_{s_1} + N_{b_1} = N_1$ ).

Interrogators in each group are assumed for modelling purposes to have identical PRF's. This PRF is the average of the PRF's of all of the interrogators in the group. It is assumed further that the interrogator antenna azimuth characteristics are identical for all of the interrogators in the group and are obtained from averaging the azimuth beamwidths of all of the interrogators in the group. (The interrogator antenna azimuth pattern is assumed to have a mainbeam, a sidelobe, a backlobe, and a null where, mainbeam width + sidelobe width + backlobe width + null width =  $360^\circ$ .)

Using these assumptions, probability calculations can be made using Bernoulli trials by taking one experiment which can occur  $N$  number of times.

The transition probability B3 (the probability that the first pulse of a mode 3, mainbeam interrogation arrives at the transponder) is used to demonstrate the calculation technique.

From group  $S_1$  with  $N_1$  interrogators the three independent subgroups are used. The first pulse of mode 3, mainbeam interrogation may be received from any interrogator in subgroup  $N_{m_1}$ . The probability of this occurring is the product of the probability that the interrogator is interrogating at that time, and that the mainbeam is pointed at the transponder.

$$\text{probability of receiving the first pulse of a mode 3, mainbeam interrogation} = p = (2 \cdot 10^{-6}) \cdot \text{Average PRF}_{S_1} \cdot \frac{\text{Average mainbeam width in } S_1}{360}$$

Then  $1-p$  is the probability that the pulse is not received from an interrogator in this subgroup. Therefore, the probability of obtaining exactly 1 occurrence of a mode 3, mainbeam first pulse from the subgroup is binomially distributed and can be calculated by

$$\binom{N_{m_1}}{1} p^1 (1-p)^{[N_{m_1}-1]}$$

Now the interrogators in subgroup  $S_{s_1}$  are considered. Mainbeam interrogations and sidelobe suppressions are received at the transponder from this subgroup. The 3 different events which can occur from this subgroup are receiving 1) the first pulse of a mode 3, mainbeam interrogation 2) the first pulse of a mode 3, sidelobe suppression or 3) neither a mainbeam or sidelobe signal. The probabilities are calculated as before:

$$\text{probability of receiving the first pulse of a mode 3, mainbeam interrogation} = P_{MB} = (2 \cdot 10^{-6}) \cdot \text{Average PRF}_{S_1} \cdot \frac{\text{Average mainbeam width in } S_1}{360}$$

$$\text{probability of receiving the first pulse of a mode 3, sidelobe suppression} = P_{SL} = (2 \cdot 10^{-6}) \cdot \text{Average PRF}_{S_1} \cdot \frac{\text{Average sidelobe width in } S_1}{360}$$

The probability of not receiving an interrogation from any member of this subgroup is  $1 - P_{MB} - P_{SL}$ . For this subgroup, the probability of obtaining exactly one mode 3, mainbeam interrogation is of the form,

$$\binom{N_{s1}}{1} [P_{MB}]^1 [P_{SL}]^0 \cdot [1 - P_{MB} - P_{SL}]^{[N_{s1} - 1]}$$

24-5

For the subgroup with  $N_{b1}$  interrogators, the probabilities are calculated in the same manner as above, except that the sidelobe and backlobe suppressions are classes together as one type to give, in effect, a wider sidelobe. The probability of exactly one mode 3, mainbeam, first pulse is given by,

$$\binom{N_{b1}}{1} \cdot [P_{MB}]^1 \cdot [P_{SLBL}]^0 \cdot [1 - P_{MB} - P_{SLBL}]^{[N_{b1} - 1]}$$

Then the probability of receiving the first pulse of a mode 3, mainbeam interrogation from the interrogators with a 3/A interlace is the sum of the three independent subgroup calculations.

For the second and third groups respectively, an average mode 3 PRF is calculated as a function of the number of mode 3 interrogations in the mode interlace. Similar equations are developed as for the first group, and the probability of receiving the first pulse of a mode 3 mainbeam interrogation from each subgroup is calculated. However, these subgroups may produce mode 2 and mode C interrogations, so that in calculating the probability of receiving a mode 3 interrogation and no other interrogations, the probability of receiving the first pulse of a mode 3 interrogation must be multiplied by the probability of not receiving mode 2 or mode C respectively for the second and third interrogator groups. Then to calculate B3, all probabilities of receiving the first pulse of a mode 3, mainbeam interrogation from all of the three groups are summed.

The other transition probabilities with the exception of TP may be calculated similarly to B3. The general equations used for transition probability calculations are given in TABLE 2. TABLES 3, 4, and 5 define the notation.

The calculation for the probability TP (the probability of receiving an interfering pulse) uses the assumption that all interfering signals have identical characteristics. Since the signals received by the transponder may consist of all modes of operation, the interfering interrogation has a length which is the expected value of the interrogation lengths actually in the environment.

By postulating that all interfering signals received at the transponder look the same, each interrogator can be considered an identical independent experiment. This set of  $N$  experiments (all interrogators whose signals are received by the transponder) can be sorted into three independent groups  $S_{mt}$ ,  $S_{st}$ , and  $S_{bt}$ . Each experiment in each subset has two or three mutually exclusive events as specified in TABLE 6.  $S_{mt}$  has  $N_{mt}$  interrogators (i.e., all the interrogators such that only the mainbeam signals are received by the transponder).  $S_{st}$  has  $N_{st}$  interrogators,  $S_{bt}$  has  $N_{bt}$  interrogators.

Receiving an interfering interrogation means that two interrogations have entered the transponder together, one the desired signal and the other the interfering signal. Therefore, TP is the probability of receiving two mainbeam interrogations or a mainbeam and a sidelobe interrogation or

$$\begin{aligned} TP &= P2MB + PMBSL \\ \text{where,} \\ P2MB &= P(2, N_{mt} - 2) P(0, 0, N_{st}) P(0, 0, N_{bt}) + P(1, N_{mt} - 1) \\ &\quad [P(1, 0, N_{st} - 1) P(0, 0, N_{bt}) + P(0, 0, N_{st}) P(1, 0, N_{bt} - 1)] + \\ &\quad P(0, N_{mt}) [P(2, 0, N_{st} - 2) P(0, 0, N_{bt}) + P(1, 0, N_{st} - 1) \\ &\quad P(1, 0, N_{bt} - 1) + P(0, 0, N_{st}) P(2, 0, N_{bt} - 2)] \\ PMBSL &= P(1, N_{mt} - 1) [P(0, 1, N_{st} - 1) P(0, 0, N_{bt}) + P(0, 0, N_{st}) \\ &\quad P(0, 1, N_{bt} - 1)] + P(0, N_{mt}) [P(1, 1, N_{st} - 2) P(0, 0, N_{bt}) + \\ &\quad P(1, 0, N_{st} - 1) P(0, 1, N_{bt} - 1) + P(0, 1, N_{st} - 1) \\ &\quad P(1, 0, N_{bt} - 1) + P(0, 0, N_{st}) P(1, 1, N_{bt} - 2)] \end{aligned}$$

### 3.2. Transponder Performance Calculation.

The steady state probabilities obtained from the Markov Process are used to determine the various factors which affect system performance. One most important factor is establishing whether or not any interrogator will elicit a reply from the transponder. For any transponder model, this is determined by predicting if the transponder is open ready to receive and, if so, whether the ensuing interrogation passes through the interrogation decoding phase of the transponder intact and unchanged.

For the transponder replying to mode 3 only, (Figure 7), the probability of being open is the steady state probability  $P_1$ . The probability of not changing a mainbeam mode 3 interrogation to a sidelobe suppression by inserting a pulse in the proper sidelobe position is the probability that the system is in state 7 divided by the probability that it enters the interrogation phase. The product, then, of  $P_1$  and  $P_7/P_4$  determines the probability of reply for the transponder. This is the primary measure of transponder effectiveness.

246 The steady state probabilities can be used to obtain the expected number of times per second that the system is in a particular state. As an example, state 7 represents the last step in a valid interrogation phase.  $P_7$ , the probability that the system is in state 7, is based on a 2 microsecond time interval. Therefore, for every 2 microseconds, the system would be expected to be in state 7,  $(P_7) \times (100)$  percent of the time. So that in one second, the expected number of completed valid interrogations or number of replies equal  $(P_7) \times (500,000)$ . Also the expected number of sidelobe suppressions per second is  $(P_2) \times (500,000)$ . Other calculations can be similarly made for each of the other states in the chain.

#### 4. AN IFF/SSR PERFORMANCE PREDICTION MODEL (PPM)

The Markov chain transponder models were developed as the basis of an automated, environmental IFF/SSR performance prediction model. The PPM (Figure 11) accepts as inputs 1) the deployment and characteristics of an interrogator environment and 2) the deployment and characteristics of airborne transponders. The model first calculates the performance of each transponder. Taking one transponder at a time the model determines, using free-space path loss, interrogator and transponder antenna gains, and transponder receiver sensitivity, those interrogators whose transmissions are received at the transponder. These interrogators are then grouped as discussed in paragraph 3.1, in preparation for the transition probability calculation.

After the probabilities are calculated, the PPM then selects a Markov chain transponder model. Because transponder characteristics are a function of the type (military, airline, general aviation), nineteen transponder models were developed to represent transponder types having different deadtime and mode characteristics. The model selection depends on the type, the interrogation modes receiveable, and the mode capability of the transponder.

After selecting the proper model, the PPM solves the simultaneous equations for the steady-state probabilities which are then used to calculate the transponder performance parameters (TABLE 7). With the transponder performance parameters calculated, the PPM determines the performance of a designated, subject interrogator. This performance is defined as 1) the non-synchronous reply rate (fruit/sec) received by the subject interrogator as its antenna points at each transponder, and 2) the probability of target detection for the interrogator automatic target detection equipment.

##### 4.1. Optional Capabilities.

The PPM was designed as a flexible analysis tool with a variety of capabilities. The model can accept any properly formatted interrogator environment and associated transponder deployment. The individual equipment characteristics are the choice of the analyst, which allows parametric analysis if required.

The analyst also has the option to use:

1. a two-path propagation prediction model which uses the vertical antenna patterns of the transmitter and receiver antennas.
2. transponders with single antenna (top or bottom), switching antennas, or diversity antennas (the spherical pattern of the antennas is used).
3. a terrain shielding model.
4. a model which calculates the standard deviation of transponder performance parameters.

#### 5. COMPARING PREDICTED RESULTS WITH RESULTS FROM ANOTHER MODEL AND WITH MEASURED DATA.

##### 5.1. Comparison with Another Model.

Results from the automated IFF/SSR PPM using Markov chain transponder models were compared with similar results from a previously developed and validated ATCRBS IFF MARK X (SIF) PPM (Freeman, E.F. 1969). The input information for both models consisted of the same interrogator environment and aircraft deployment. The comparison was made for the following outputs, common to both models: interrogation arrival rate at each transponder, sidelobe suppression arrival rate at each transponder, and the probability of transponder reply.

###### 5.1.1. Interrogation Arrival Rate.

Figure 12 shows how the IFF/SSR PPM predictions for interrogation rate deviated from the predictions made by the IFF MARK X (SIF) PPM. This graph shows that 82% of the predictions were within  $\pm 10\%$  of the IFF MARK X (SIF) PPM predictions. Some new IFF/SSR PPM interrogation rate predictions differ greatly from the IFF MARK X model predictions. However, these few dispersions are statistically insignificant. A least squares linear regression was applied to the predictions of both models. The coefficient of correlation calculated was greater than 90%.

###### 5.1.2. Sidelobe Suppression Arrival Rate.

Figure 13 shows the deviation of the new IFF/SSR PPM prediction of sidelobe suppression rate from the IFF MARK X model prediction. Sixty-seven percent of the IFF/SSR predictions fall within  $\pm 20\%$  of the IFF MARK X prediction. Eighty-three percent of the predictions fall within  $-20\%$  to  $+30\%$  of the IFF MARK X predictions.

###### 5.1.3. Probability of Reply (Round Reliability).

Figure 14 is the dispersion of probability of reply calculated by the new IFF/SSR PPM with respect to that calculated by the IFF MARK X model. This shows that 94.5% of the IFF/SSR PPM predictions fall within  $-2.2$  to  $1.1\%$  of the IFF MARK X predictions.



#### 5.1.4. Summary.

The new IFF/SSR predictions track closely with those from the IFF MARK X PPM for a majority of transponders in the deployment. These limited results provide a degree of confidence in the Markov chain modelling techniques used in the PPM.

#### 5.2. Comparison with Measured Data.

Measurements of interrogation arrival rates and sidelobe suppression arrival rates were made in the Northeastern United States in January 1973 (Harman, W.H., 1973) Figure 15 shows the flight paths of the instrumented aircraft. The aircraft flew at altitudes of 6500 feet and 7500 feet during the flights. The transponder sensitivity referred to the antenna was -73.5 dBm.

The new IFF/SSR PPM was employed to make interrogation and sidelobe suppression arrival rate predictions along the same flight path. The interrogator environment which was thought to operate full-time and transponders located at points along the flight path were inputs to the model. The characteristics of the transponders were the same as for the measuring equipment. The aircraft antenna pattern was assumed to be omni-directional with 0 dBi gain. The results of the simulation and the measured data are plotted in Figures 16 and 17.

The measured and predicted interrogation rates compare favorably with one another. The differences which do occur could be attributed to assuming an omni-directional aircraft antenna pattern and the uncertainty as to which interrogators were actually operating when the measurements were taken.

The measured and predicted sidelobe suppression rates differ considerably. This could be attributed again to assuming an omni-directional aircraft antenna pattern and the uncertainty in the actual environment and the radiated powers of interrogators. To see the effect of the aircraft antenna pattern the IFF/SSR PPM was again employed but an actual aircraft antenna pattern was used instead of the omni. Figure 18 shows the comparison again for this new condition. The predictions and measurements through not close tend to decrease and increase together. Based on this result, with a more accurate knowledge of the interrogator environment and the aircraft orientation, the predictions would more closely match the measured data. The differences are a function of the model inputs and not of the Markov chain modelling techniques.

Again, this limited validation provides confidence in the Markov chain modelling techniques.

#### 6. CONCLUSION

Employing Markov Chain Theory for the modelling of IFF/SSR transponders permits the calculation of many and varied performance parameters. The Markov chains form the basis of a powerful, flexible, reliable, and accurate automated, environmental IFF/SSR analysis capability.

#### REFERENCES

1. CEAC Secondary Radar Sub-Group, 1973, "Final Report by the CEAC Secondary Radar Sub-Group on Over-Interrogation," AC/92D/559, Committee for European Airspace Coordination.
2. Federal Aviation Administration (FAA), "Selection Order: U.S. National Aviation Standard for the MARK X (SIF) Air Traffic Control Radar Beacon System (ATCRBS) Characteristics," 1010.51A, Department of Transportation.
3. Federal Aviation Administration (FAA), 1974, "National Improvement Program for Air Traffic Control Radar Beacon System," Departments of Transportation and Defense.
4. Freeman, E.F., 1969, "The IFF MARK X (SIF) Air Traffic Control Radar Beacon System Performance Prediction Model," ESD-TR-69-274, DoD, Electromagnetic Compatibility Analysis Center.
5. Harman, W.H., 1973, "Measured IFF/ATCRBS Uplink Interference Rates," MIT Lincoln Laboratory.
6. Kemeny, J.G., and Snell, J.L., 1960, "Finite Markov Chains," D. Van Nostrand Company, Inc.
7. National Joint IFF/SSR Policy Board, 1970, "Operation of IFF/SSR Interrogators in the United Kingdom: Planning Principles," Department of Trade and Industry, Ministry of Defense, Ministry of Aviation Supply.
8. Special Committee 116-B, 1970, "Change 1 to Document No. DO-144: Minimum Operational Characteristics - Airborne ATC Transponder Systems," Radio Technical Commission for Aeronautics.
9. Sutton, S.J., and Ehler, C.W., 1973, "AIMS Performance Prediction Model System Report (U)," ESD-TR-72-286, DoD Electromagnetic Compatibility Analysis Center.

TABLE 1

TRANSITION PROBABILITY DEFINITIONS

24-8

ASIF	=	P (receiving a SIF sidelobe interrogation first pulse).
B1	=	P (receiving a mode 1 mainbeam interrogation first pulse).
B2	=	P (receiving a mode 2 mainbeam interrogation first pulse).
B3	=	P (receiving a mode 3 mainbeam interrogation first pulse).
BC	=	P (receiving a mode C mainbeam interrogation first pulse).
CC	=	P (transponder open to receive an interrogation).
	=	$1 - ASIF - B1 - B2 - B3 - BC$
TP	=	P (receiving an interfering pulse).
TP <sub>i</sub>	=	P (normal transition from one state to another).
	=	$1 - TP$

TABLE 2

TRANSITION PROBABILITY EQUATIONS

$$\begin{aligned}
 B1 &= \sum_i^M \left\{ (P1_{i,1} + P2_{i,1} + P3_{i,1}) \left( \prod_{j=1}^4 \prod_{k=1}^{M^*} P0_{k,j} \right) \right\} \\
 &\quad \text{when } k=i \\
 &\quad \quad j \neq 1 \\
 B2 &= \sum_i^M \left\{ (P1_{i,2} + P2_{i,2} + P3_{i,2}) \left( \prod_{j=1}^4 \prod_{k=1}^M P0_{k,j} \right) \right\} \\
 &\quad \text{when } k=i \\
 &\quad \quad j \neq 2 \\
 B3 &= \sum_i^M \left\{ (P1_{i,3} + P2_{i,3} + P3_{i,3}) \left( \prod_{j=1}^4 \prod_{k=1}^M P0_{k,j} \right) \right\} \\
 &\quad \text{when } k=i \\
 &\quad \quad j \neq 3 \\
 BC &= \sum_i^M \left\{ (P1_{i,c} + P2_{i,c} + P3_{i,c}) \left( \prod_{j=1}^4 \prod_{k=1}^M P0_{k,j} \right) \right\} \\
 &\quad \text{when } k=i \\
 &\quad \quad j \neq c \\
 ASIF &= \sum_j \left\{ \sum_i \left( P4_{i,j} + P5_{i,j} \right) \left( \prod_{\ell=1}^M \prod_{k=1}^M P0_{k,\ell} \right) \right\} \begin{cases} j=1, 2, 3, C \\ \ell=1, 2, 3, C. \end{cases} \\
 &\quad \text{when } k=i \\
 &\quad \quad \ell \neq j
 \end{aligned}$$

\*M = # groups or sets

$$CC = 1 - ASIF - B1 - B2 - B3 - BC$$

**TABLE 3**  
**DEFINITION OF PROBABILITIES**

Variable	Definition	Equation
$P0_{i,j}$	Probability of the transponder receiving no mode $j$ interrogation first pulses from the $i^{th}$ subset.	$\cdot (R1_{i,j}) (R2_{i,j}) (R3_{i,j})$
$P1_{i,j}$	Probability of the transponder receiving a mode $j$ mainbeam interrogation first pulse only from $S_{m_i}$ .	$\cdot (R4_{i,j}) (R2_{i,j}) (R3_{i,j})$
$P2_{i,j}$	Probability of the transponder receiving a mode $j$ mainbeam interrogation first pulse only from $S_{s_i}$ .	$\cdot (R1_{i,j}) (R5_{i,j}) (R3_{i,j})$
$P3_{i,j}$	Probability of the transponder receiving a mode $j$ mainbeam interrogation first pulse only from $S_{b_i}$ .	$\cdot (R1_{i,j}) (R2_{i,j}) (R6_{i,j})$
$P4_{i,j}$	Probability of the transponder receiving a mode $j$ sidelobe interrogation first pulse only from $S_{s_i}$ .	$\cdot (R1_{i,j}) (R7_{i,j}) (R3_{i,j})$
$P5_{i,j}$	Probability of the transponder receiving a mode $j$ sidelobe or backlobe interrogation first pulse only from $S_{b_i}$ .	$\cdot (R1_{i,j}) (R2_{i,j}) (R8_{i,j})$

**TABLE 4**  
**DEFINITION OF VARIABLES**

Variable	Definition
$R1_{i,j}$	$\cdot P(0, N_{m_i})_{i,j}$
$R2_{i,j}$	$\cdot P(0, 0, N_{s_i})_{i,j}$
$R3_{i,j}$	$\cdot P(0, 0, N_{b_i})_{i,j}$
$R4_{i,j}$	$\cdot P(1, N_{m_i} - 1)_{i,j}$
$R5_{i,j}$	$\cdot P(1, 0, N_{s_i} - 1)_{i,j}$
$R6_{i,j}$	$\cdot P(1, 0, N_{b_i} - 1)_{i,j}$
$R7_{i,j}$	$\cdot P(0, 1, N_{s_i} - 1)_{i,j}$
$R8_{i,j}$	$\cdot P(0, 1, N_{b_i} - 1)_{i,j}$

**TABLE 5**  
**NOTATION FOR BERNOULLI TRIALS**

Symbol	Definition	Equation
$P(M, N_{m_i} - M)_{i,j}$	Probability of the transponder receiving exactly M mode j mainbeam interrogation first pulses from minor subset $S_{m_i}$ of the $i^{\text{th}}$ subset.	$= \frac{(N_{m_i}!) (PM1_{i,j})^M (PM2_{i,j})^{N_{m_i} - M}}{M! (N_{m_i} - M)!}$
$P(M, S_{s_i} - M - S)_{i,j}$	Probability of the transponder receiving exactly M mode j mainbeam interrogation and S mode j sidelobe interrogation first pulses from minor subset $S_{s_i}$ of the $i^{\text{th}}$ subset.	$= \frac{N_{s_i}!}{M! S! (N_{s_i} - M - S)!} (PS1_{i,j})^M (PS2_{i,j})^S (PS3_{i,j})^{N_{s_i} - M - S}$
$P(M, B, N_{b_i} - M - B)_{i,j}$	Probability of the transponder receiving exactly M mode j mainbeam interrogation and B mode j sidelobe or backlobe interrogation first pulses from minor subset $S_{b_i}$ of the $i^{\text{th}}$ subset.	$= \frac{N_{b_i}!}{M! B! (N_{b_i} - M - B)!} (PB1_{i,j})^M (PB2_{i,j})^B (PB3_{i,j})^{N_{b_i} - M - B}$

TABLE 6

## MUTUALLY EXCLUSIVE EVENTS AND PROBABILITIES FOR TP CALCULATION

Subset	Event	Definition	Probability Assigned to Event
$S_{m_t}$	{MT1}	Interrogator transmits a mainbeam interrogation which is receivable at the transponder.	$PMT1 = (L_L)(\bar{f}_t) \left( \frac{\bar{W}_{m_t}}{360} \right)$
	{MT2}	Interrogator transmits an interrogation which is not receivable at the transponder.	$PMT2 = 1 - PMT1$
$S_{s_t}$	{ST1}	Interrogator transmits a mainbeam interrogation which is receivable at the transponder.	$PST1 = (L_L)(\bar{f}_t) \left( \frac{\bar{W}_{m_t}}{360} \right)$
	{ST2}	Interrogator transmits a sidelobe interrogation which is receivable at the transponder.	$PST2 = (L_L)(\bar{f}_t) \left( \frac{\bar{W}_{s_t}}{360} \right)$
	{ST3}	Interrogator transmits an interrogation which is not receivable at the transponder.	$PST3 = 1 - PST1 - PST2$
$S_{b_t}$	{BT1}	Interrogator transmits a mainbeam interrogation which is receivable at the transponder.	$PBT1 = (L_L)(\bar{f}_t) \left( \frac{\bar{W}_{m_t}}{360} \right)$
	{BT2}	Interrogator transmits a sidelobe or backlobe interrogation which is receivable at the transponder.	$PBT2 = (L_L)(\bar{f}_t) \left( \frac{\bar{W}_{s_t} + \bar{W}_{b_t}}{360} \right)$
	{BT3}	Interrogator transmits an interrogation which is not receivable at the transponder.	$PBT3 = 1 - PBT1 - PBT2$

## NOTES:

1.  $L_L$  = expected interfering interrogation length =  $(3 \times 10^{-6}) \frac{B1}{B} + (5 \times 10^{-6}) \frac{B2}{B} + (8 \times 10^{-6}) \frac{B3}{B} + (21 \times 10^{-6}) \frac{BC}{B}$   
 $B = B1 + B2 + B3 + BC$ .
2.  $\bar{f}_t$  = average interrogation rate obtained by averaging the PRF's from all N interrogators.
3.  $\bar{W}_{a_t}$  = average beamwidth, obtained by averaging individual beamwidths of all N interrogators, where  $a = m, s, b$ .

TABLE 7

## TRANSPONDER PERFORMANCE PREDICTIONS

Probability of reply to all modes  
 Probability of reply for mode 1  
 Probability of reply to mode 2  
 Probability of reply to mode 3  
 Probability of reply to mode C

Probability of a garble in any mode  
 Probability of an intermode garble (e.g., mode 3 interrogation elicits mode 1 reply)  
 Probability of an SLS garble (e.g., mode 3 interrogation elicits an SLS)  
 Probability of sidelobe suppression  
 Probability of transponder receiver open (not suppressed)  
 Probability of deadtime

Mode 1 reply rate  
 Mode 2 reply rate  
 Mode 3 reply rate  
 Mode C reply rate

Mode 1 interrogation rate (mainbeam interrogations per second entering the transponder)  
 Expected mode 1 environment rate (mainbeam interrogations per second capable of entering the transponder)  
 Mode 2 interrogation rate  
 Expected mode 2 environment rate  
 Mode 3 interrogation rate  
 Expected mode 3 environment rate  
 Mode C interrogation rate  
 Expected mode C environment rate

Sidelobe suppression rate  
 Expected sidelobe suppression environment rate  
 Expected pulse transmission rate

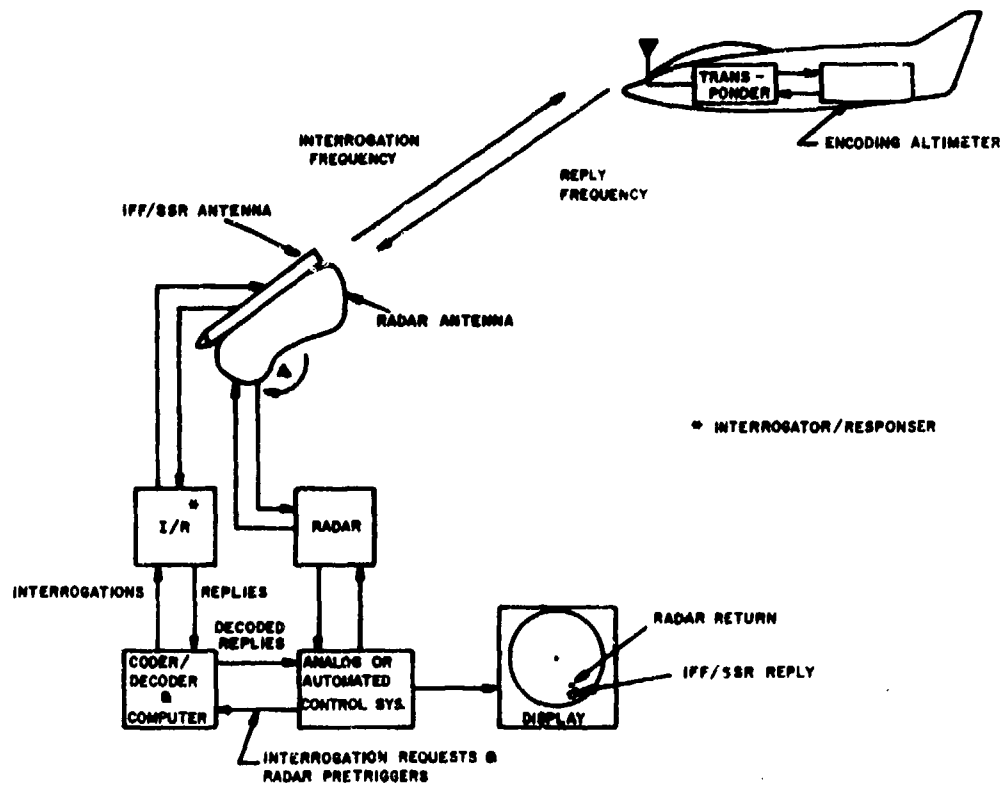


Fig. 1 General configuration of IFF/SSR equipments

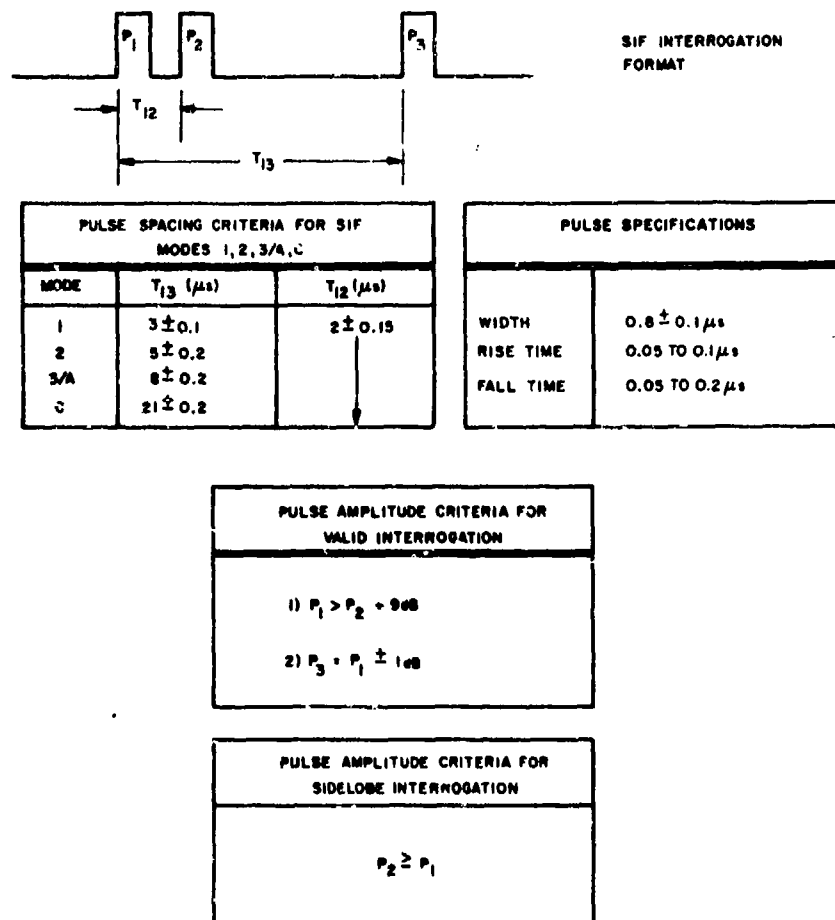
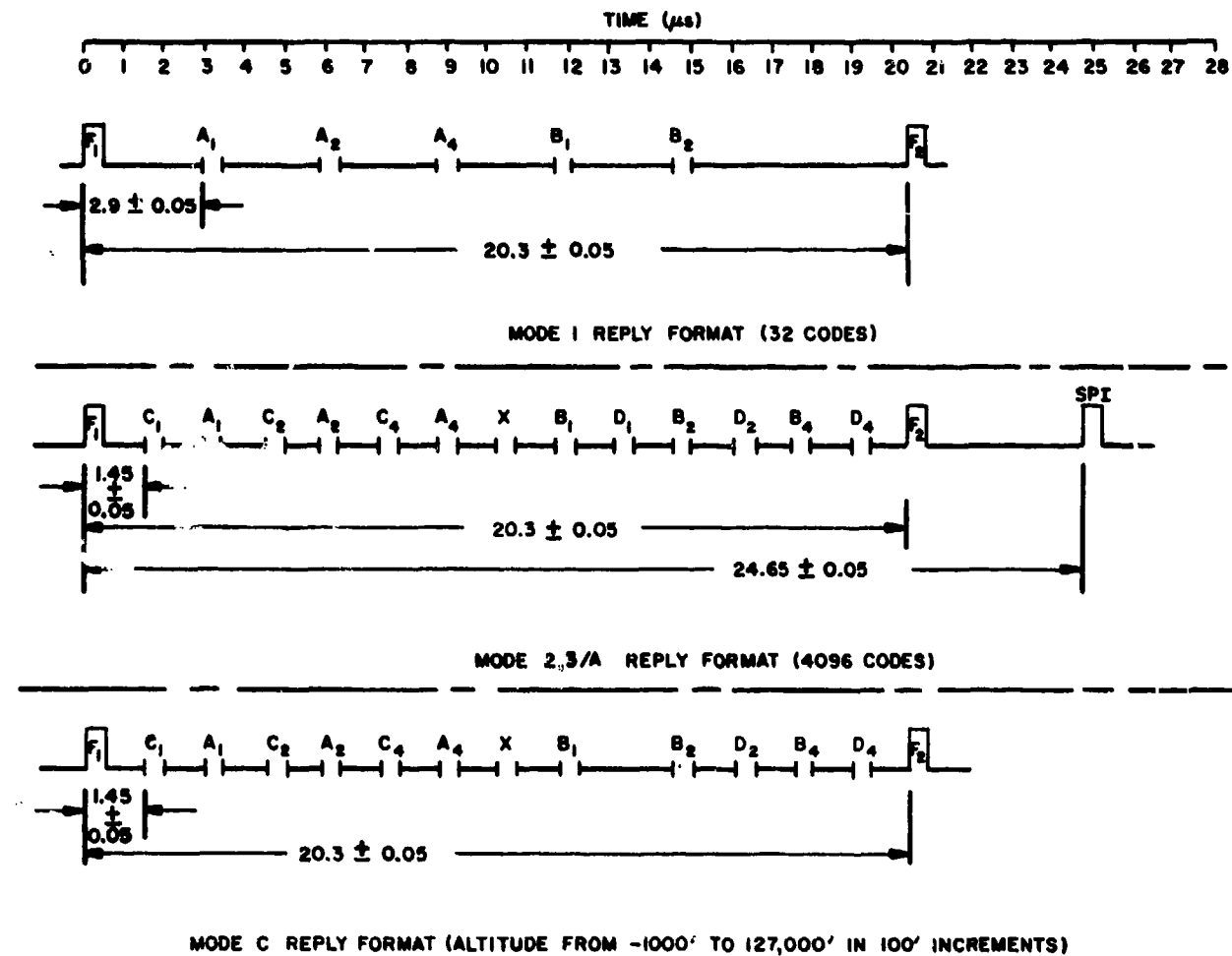


Fig. 2 IFF/SSR interrogation characteristics.



REPLY PULSE SPECIFICATIONS	
WIDTH	$0.45 \pm 0.10 \mu$ s
RISE TIME	0.05 TO $0.10 \mu$ s
FALL TIME	0.05 TO $0.20 \mu$ s

NOTE: "X" PULSE POSITION NOT NORMALLY FILLED.

Fig. 3 IFF/SSR reply characteristics

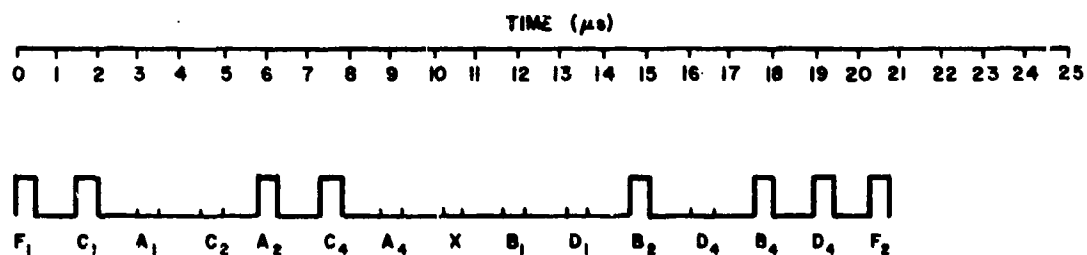


Fig. 4 Reply mode 2 or 3/A for code 2654



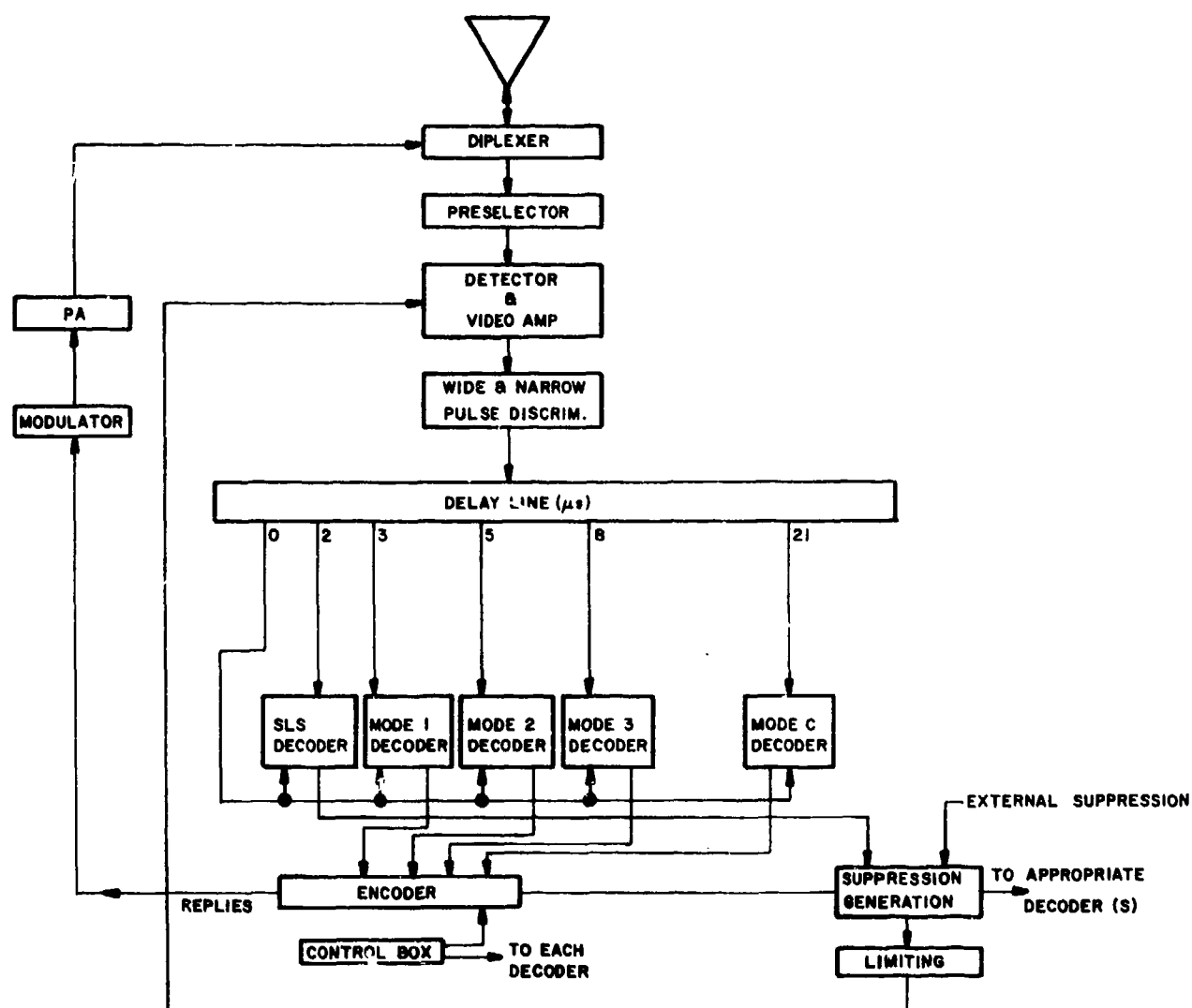


Fig. 5 Block diagram of IFF/SSR transponder

2416

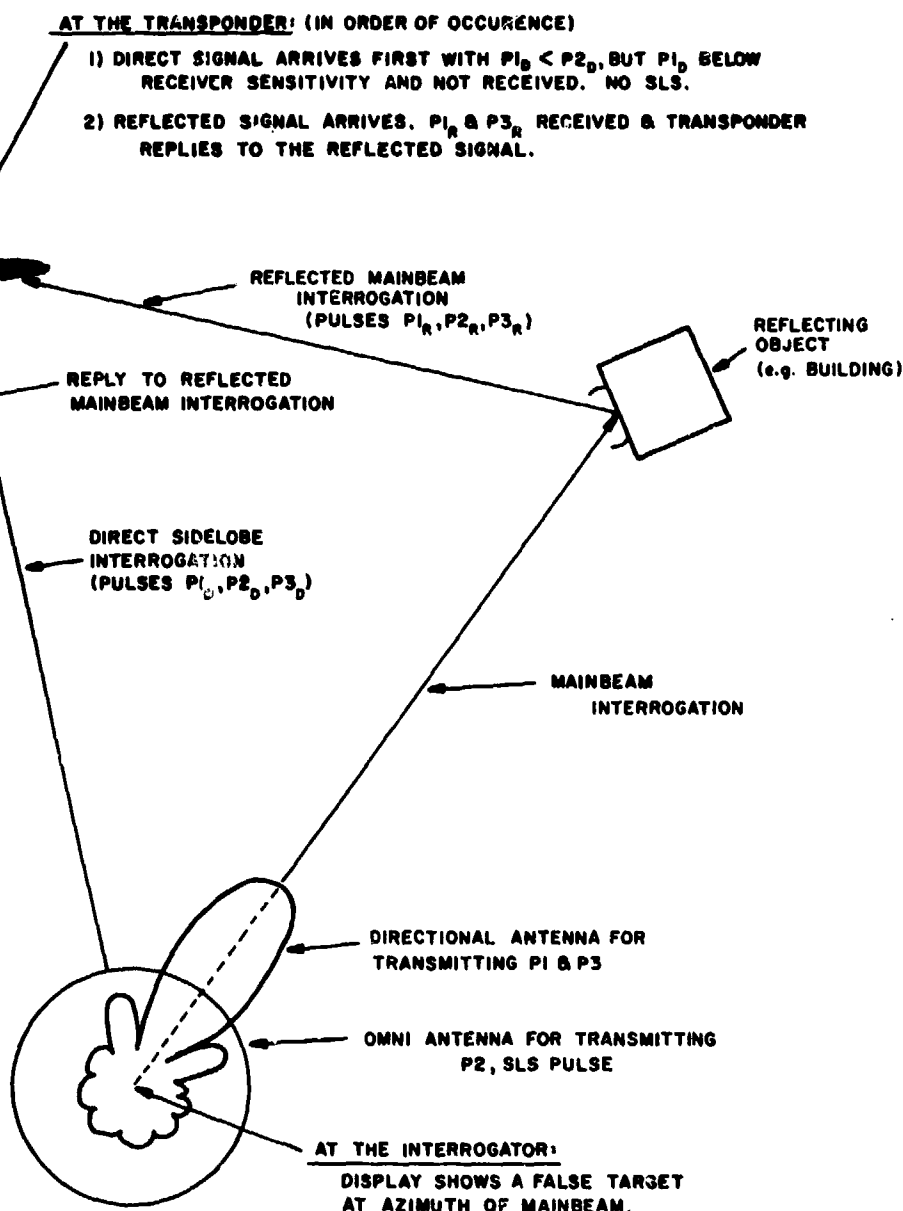


Fig. 6 Reflected interrogation causes false targets

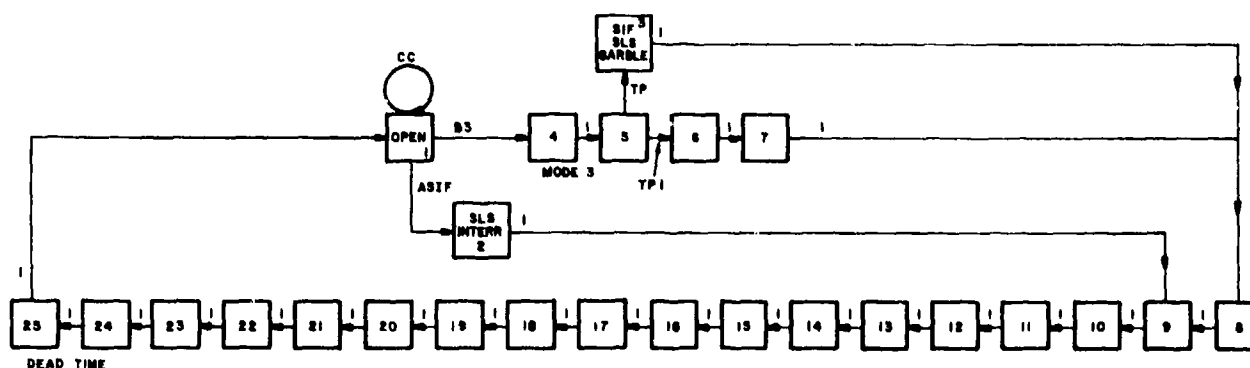


Fig. 7 Markov chain transponder model (mode 3 only)

STATE 1

STATE 1

STATE 1	1	2	3	4	5	6	7	8	9	10	11	12	13	14	15	16	17	18	19	20	21	22	23	24	25
1	CC	AS2P	0	BS	0	0	0	0	0	0	0	0	0	0	0	0	0	0	0	0	0	0	0	0	0
2	0	0	0	0	0	0	0	0	1	0	0	0	0	0	0	0	0	0	0	0	0	0	0	0	0
3	0	0	0	0	0	0	0	1	0	0	0	0	0	0	0	0	0	0	0	0	0	0	0	0	0
4	0	0	0	0	1	0	0	0	0	0	0	0	0	0	0	0	0	0	0	0	0	0	0	0	0
5	0	0	TP	0	0	TP	0	0	0	0	0	0	0	0	0	0	0	0	0	0	0	0	0	0	0
6	0	0	0	0	0	0	1	0	0	0	0	0	0	0	0	0	0	0	0	0	0	0	0	0	0
7	0	0	0	0	0	0	0	1	0	0	0	0	0	0	0	0	0	0	0	0	0	0	0	0	0
8	0	0	0	0	0	0	0	0	1	0	0	0	0	0	0	0	0	0	0	0	0	0	0	0	0
9	0	0	0	0	0	0	0	0	0	1	0	0	0	0	0	0	0	0	0	0	0	0	0	0	0
10	0	0	0	0	0	0	0	0	0	0	1	0	0	0	0	0	0	0	0	0	0	0	0	0	0
11	0	0	0	0	0	0	0	0	0	0	0	1	0	0	0	0	0	0	0	0	0	0	0	0	0
12	0	0	0	0	0	0	0	0	0	0	0	0	1	0	0	0	0	0	0	0	0	0	0	0	0
13	0	0	0	0	0	0	0	0	0	0	0	0	0	1	0	0	0	0	0	0	0	0	0	0	0
14	0	0	0	0	0	0	0	0	0	0	0	0	0	0	1	0	0	0	0	0	0	0	0	0	0
15	0	0	0	0	0	0	0	0	0	0	0	0	0	0	0	1	0	0	0	0	0	0	0	0	0
16	0	0	0	0	0	0	0	0	0	0	0	0	0	0	0	0	1	0	0	0	0	0	0	0	0
17	0	0	0	0	0	0	0	0	0	0	0	0	0	0	0	0	0	1	0	0	0	0	0	0	0
18	0	0	0	0	0	0	0	0	0	0	0	0	0	0	0	0	0	0	1	0	0	0	0	0	0
19	0	0	0	0	0	0	0	0	0	0	0	0	0	0	0	0	0	0	0	1	0	0	0	0	0
20	0	0	0	0	0	0	0	0	0	0	0	0	0	0	0	0	0	0	0	0	1	0	0	0	0
21	0	0	0	0	0	0	0	0	0	0	0	0	0	0	0	0	0	0	0	0	0	1	0	0	0
22	0	0	0	0	0	0	0	0	0	0	0	0	0	0	0	0	0	0	0	0	0	0	1	0	0
23	0	0	0	0	0	0	0	0	0	0	0	0	0	0	0	0	0	0	0	0	0	0	0	1	0
24	0	0	0	0	0	0	0	0	0	0	0	0	0	0	0	0	0	0	0	0	0	0	0	0	1
25	1	0	0	0	0	0	0	0	0	0	0	0	0	0	0	0	0	0	0	0	0	0	0	0	0

24-17

Fig. 8 One-step transition probability matrix

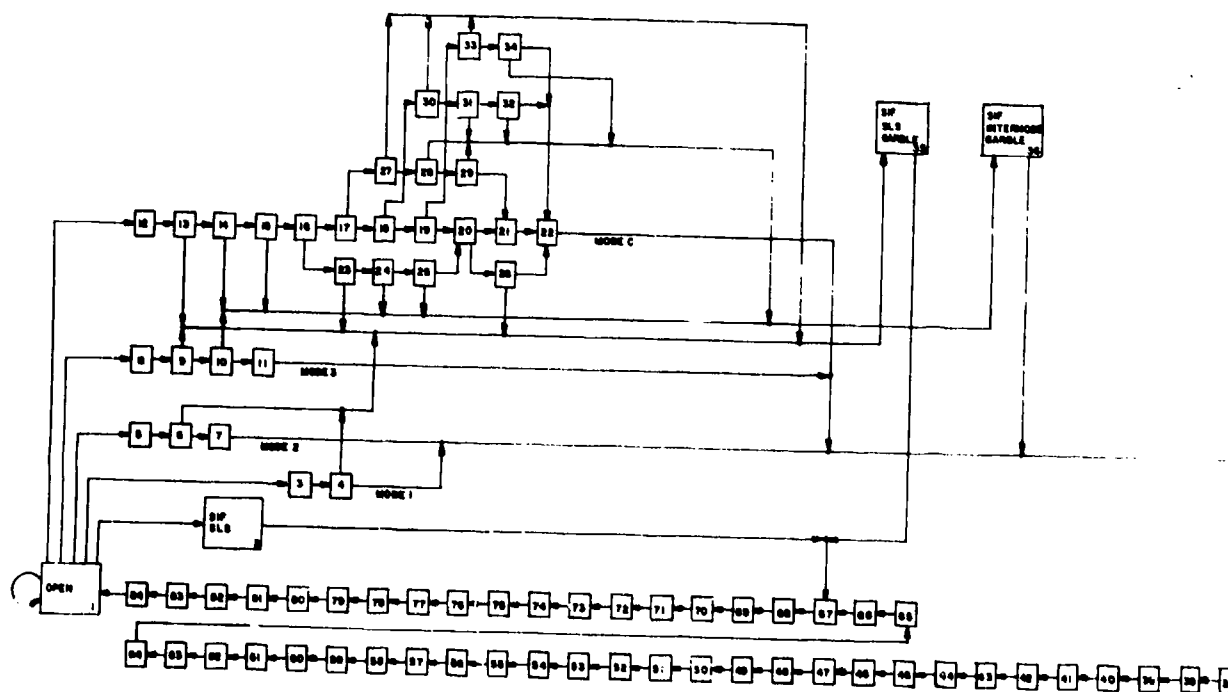


Fig. 9 Markov chain transponder model (modes 1, 2, 3/A, C)

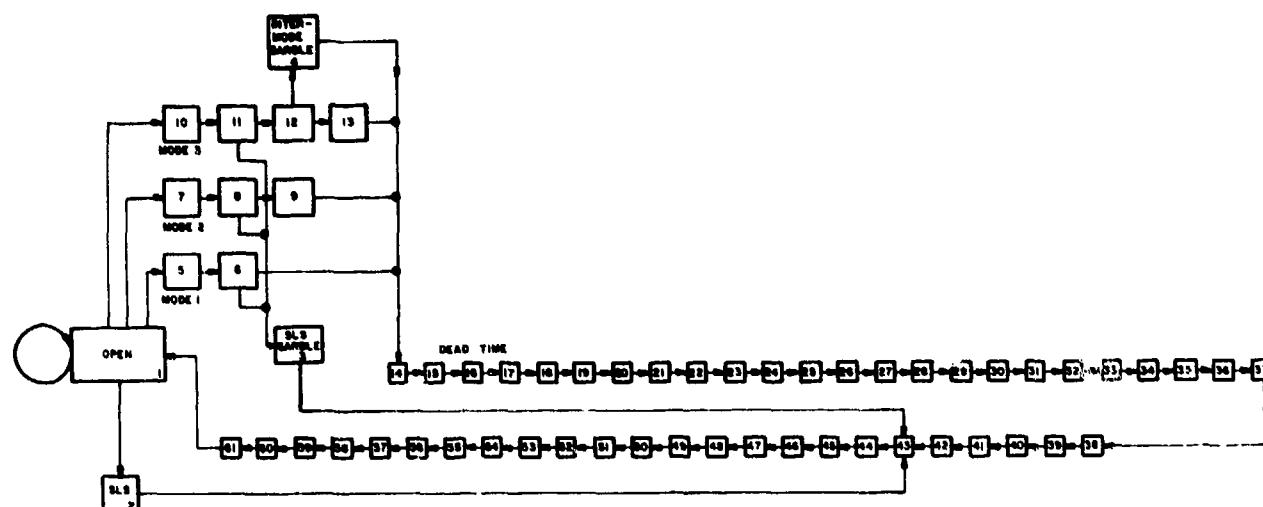


Fig. 10 Markov chain transponder model (modes 1, 2, 3/A).

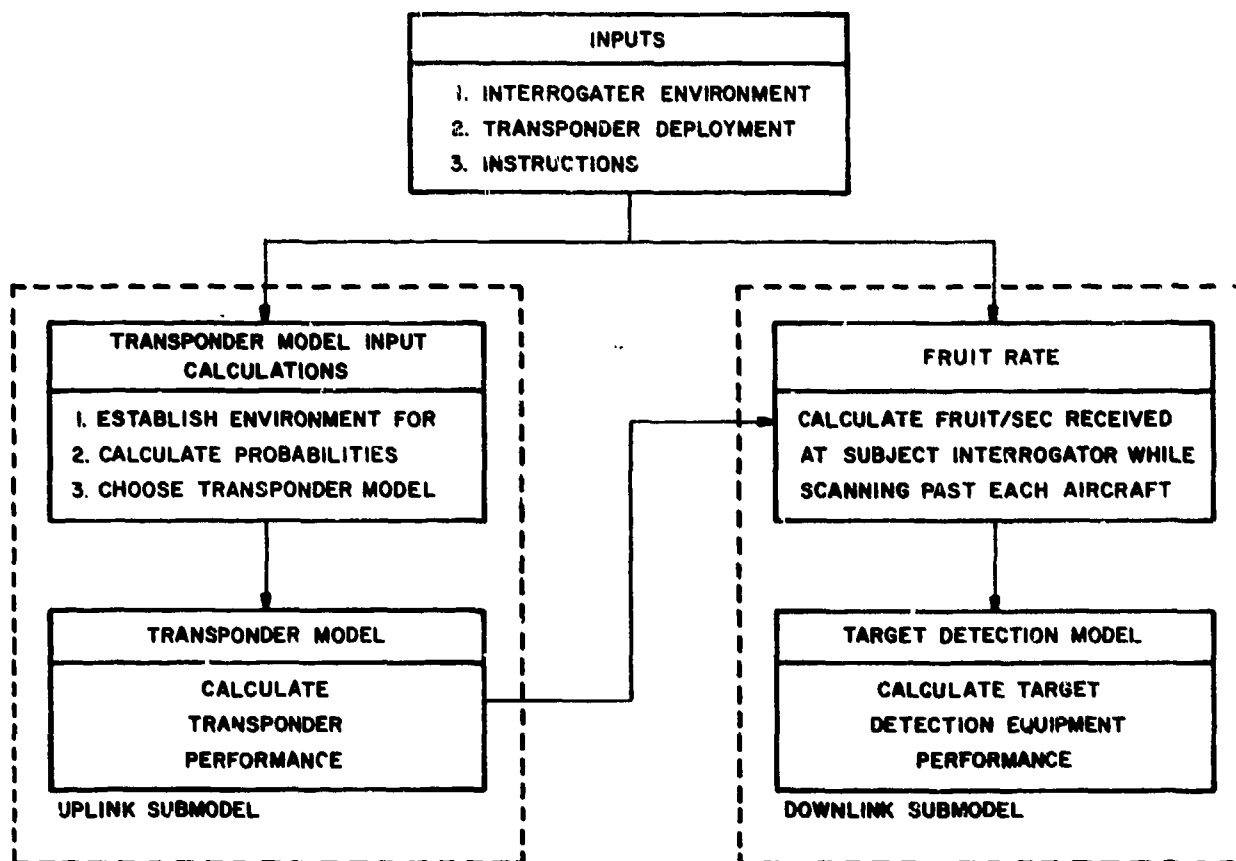


Fig. 11 Performance prediction model flow chart

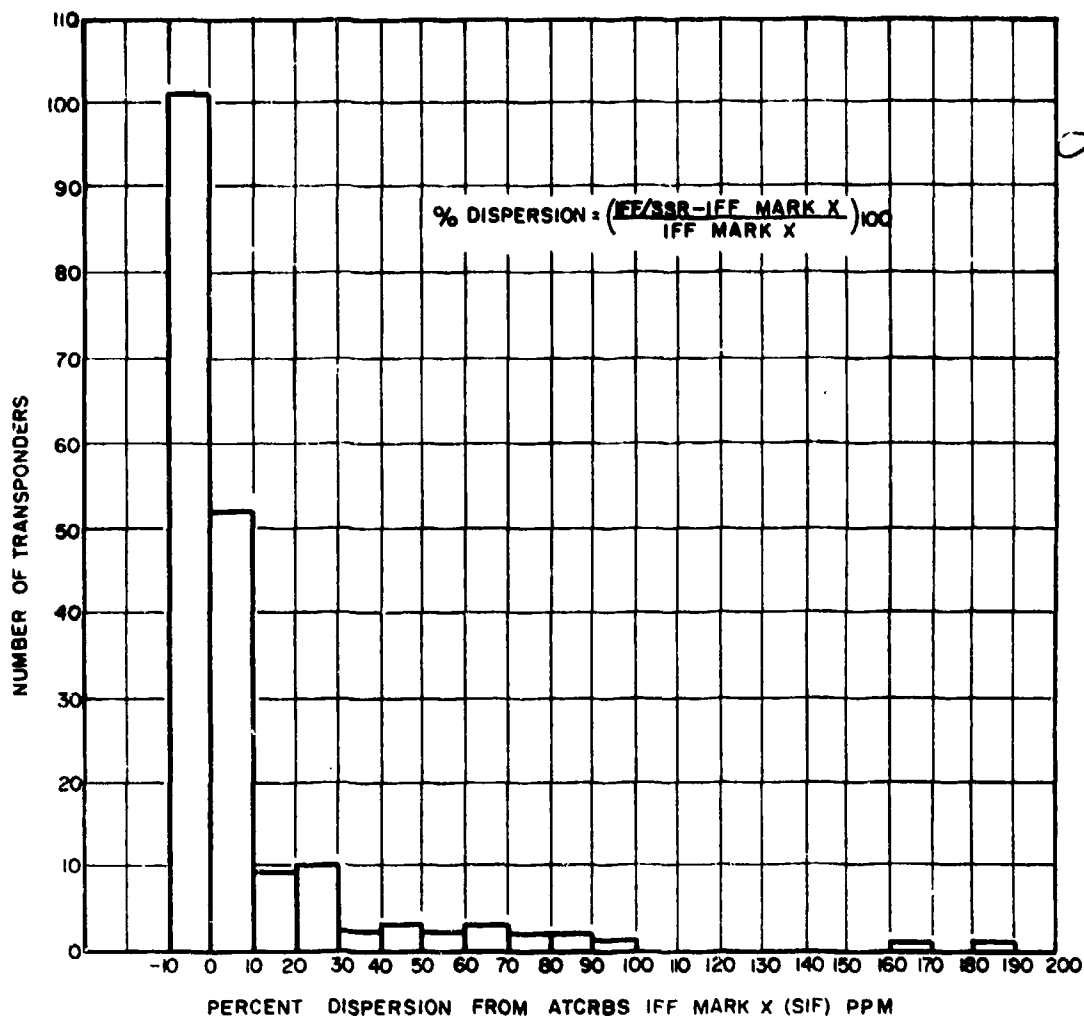


Fig. 12 Percent dispersion of total interrogation arrival rate calculated by IFF/SSR PPM with respect to total interrogation arrival rate calculated by ATRBS IFF mark X (SIF) PPM.

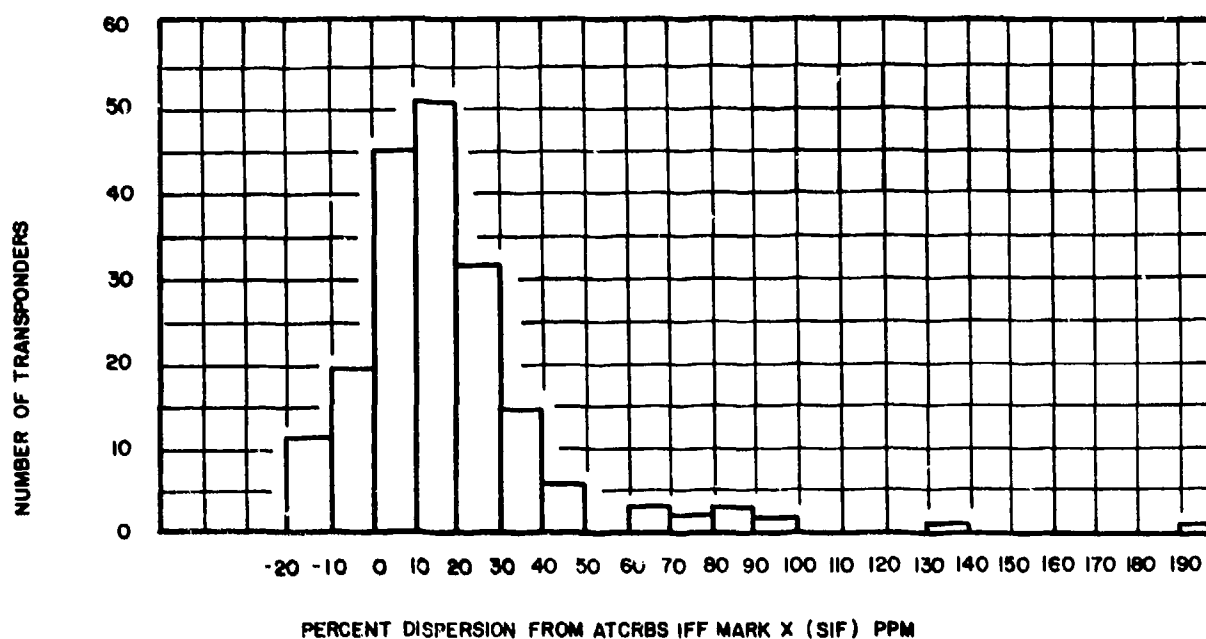


Fig. 13 Percent dispersion of sidelobe suppression arrival rate calculated by IFF/SSR PPM with respect to sidelobe suppression arrival rate calculated by ATRBS IFF mark X (SIF) PPM

24-20

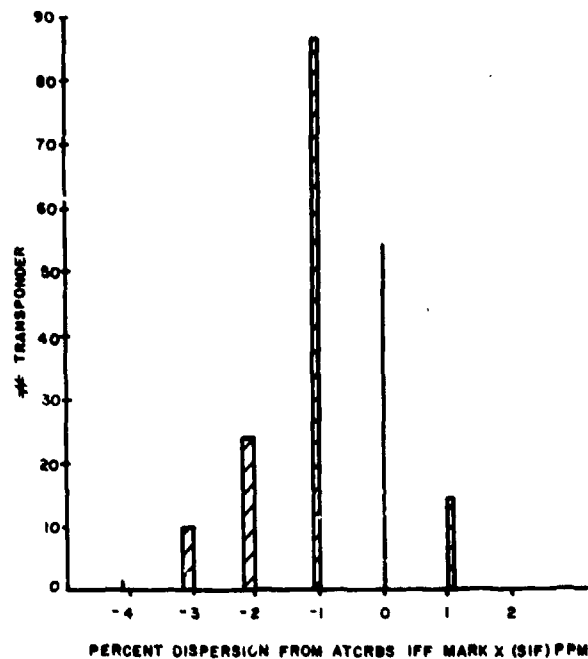


Fig. 14 Percent dispersion of probability of reply calculated by IFF/SSR PPM with respect to probability of reply calculated by ATCRBS IFF mark X (SIF) PPM

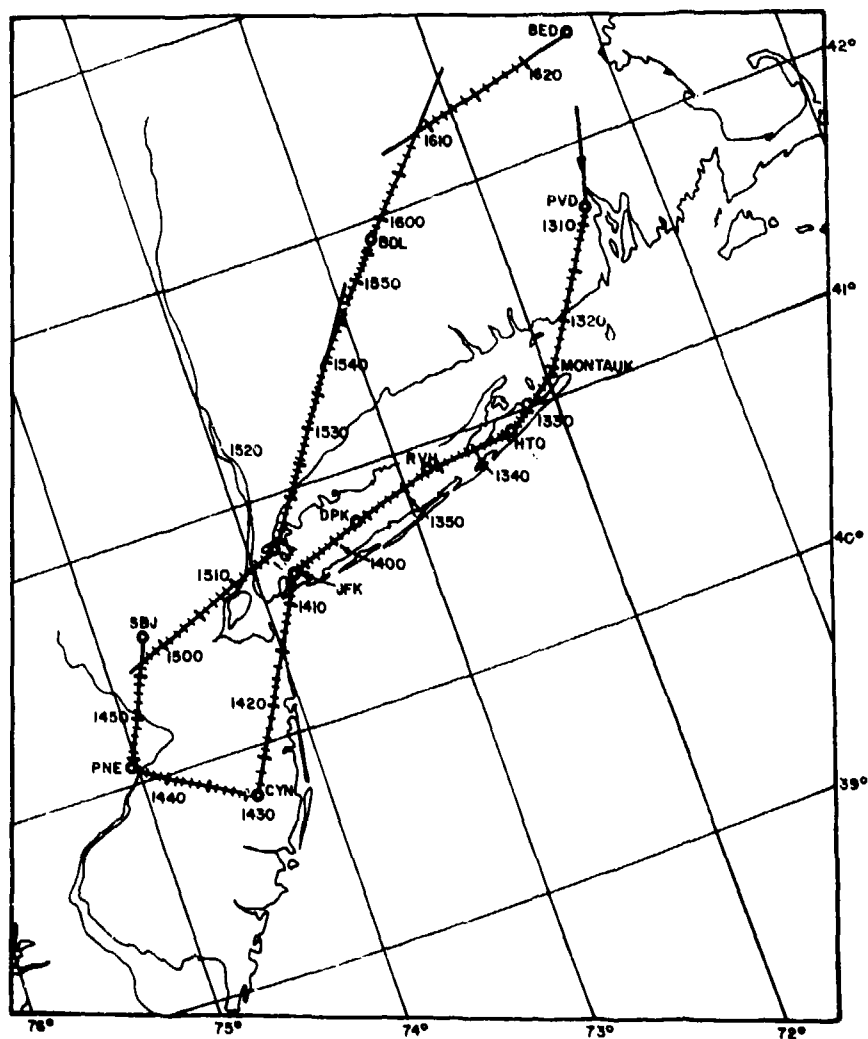


Fig. 15 Flight path

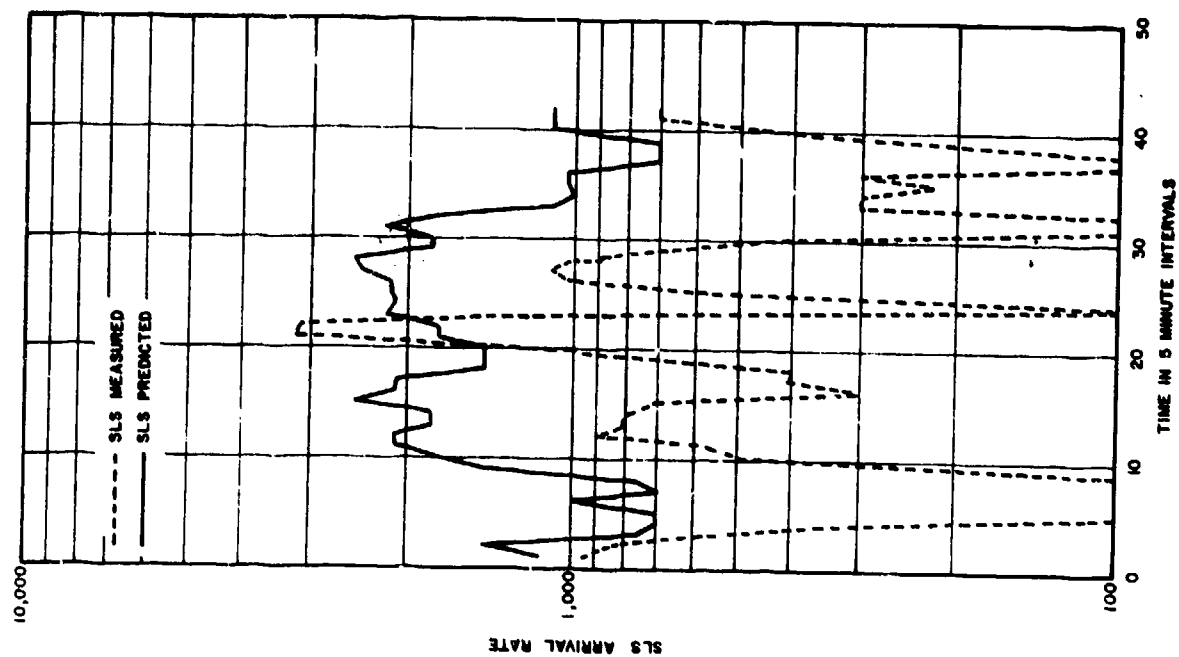


Fig. 16 Predicted and measured interrogation arrival rates

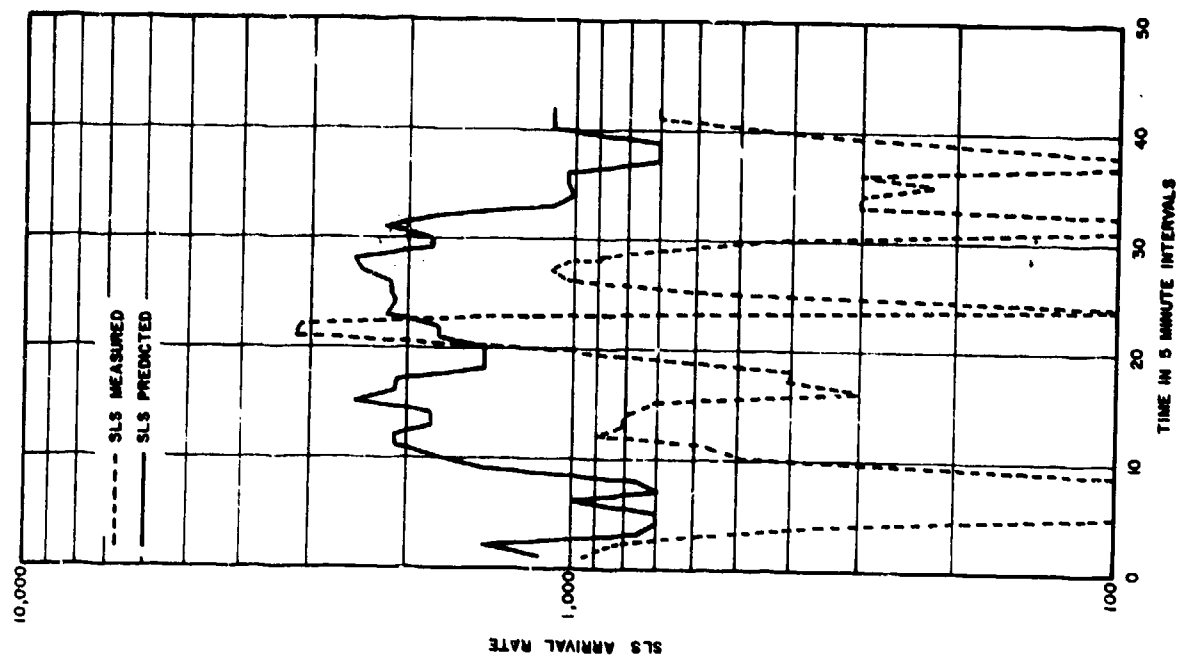


Fig. 17 Predicted and measured sidelobe suppression arrival rates (omni aircraft; antenna pattern)

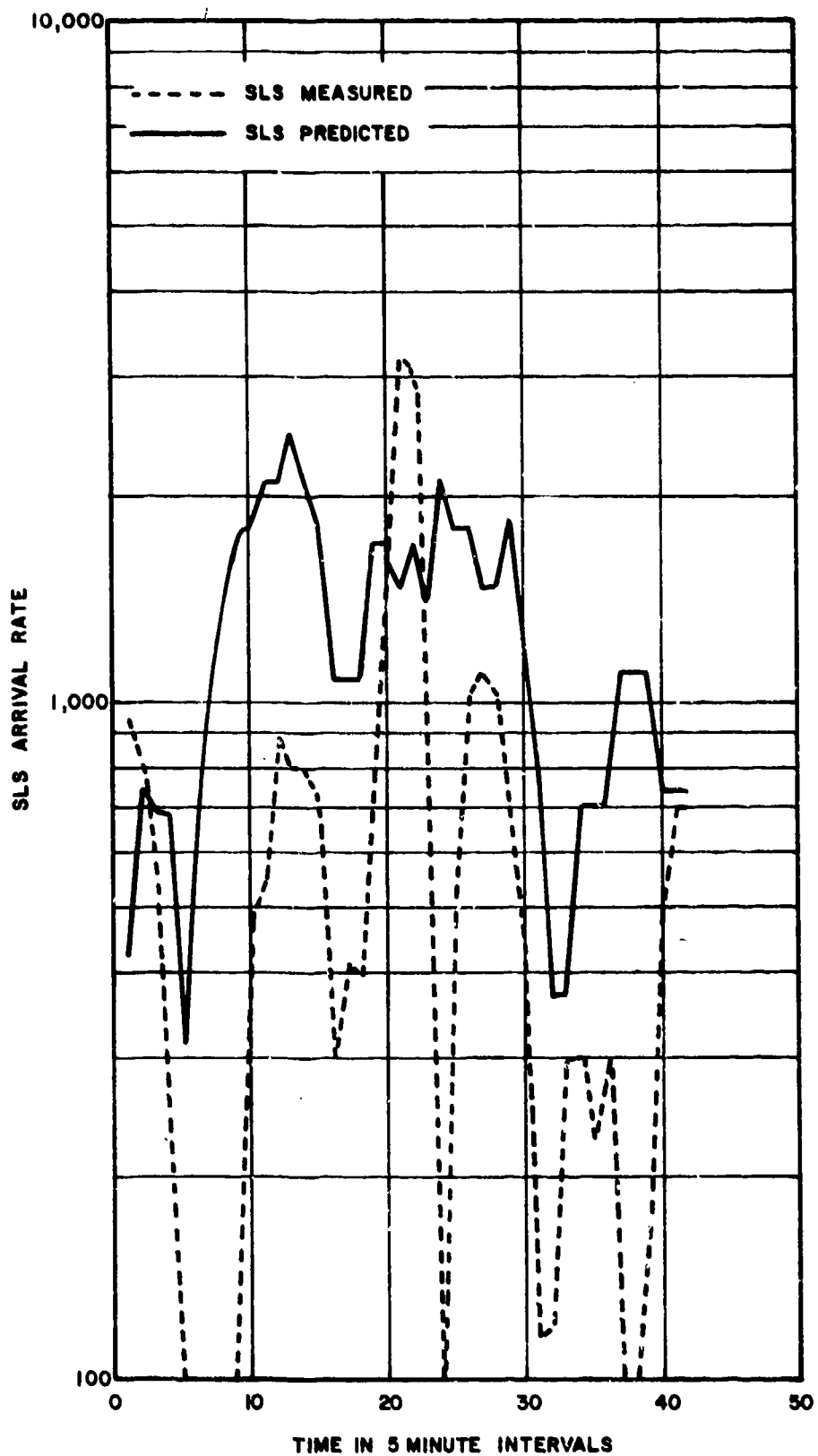


Fig. 18 Predicted and measured sidelobe suppression arrival rates (actual aircraft antenna pattern)



## DISCUSSION

F. D. GREEN: I understood you to say that the antenna on the a/c was changed to one which was "less omnidirectional". Surely, an omnidirectional antenna is necessary for IFF.

S. J. SUTTON: Yes, but very few, if any, antennas are omnidirectional on an a/c. Some of the later applications use an antenna both on top and under the a/c.

D. H. MEHRTENS: While modeling the SSR environment in the UK, it was found by Cossor that if the interrogations from separate interrogators were considered to be random, theory and practice did not agree. A model which took into account the possibility of near synchronism of the interrogator prfs produced much improved results. Does your model address itself to this area?

C. W. EHLER: Our model calculates expected values and assumes the random (actually Poisson) arrival of interrogations. It will not account for the actual occurrences of near synchronous prfs. A time-event stove simulation developed by the U. S. Department of Transportation Transportation Systems Center (TSC) does account for the time of arrival of each interrogation and can reproduce the near synchronous interference. A current ECAC project for the U. S. Federal Aviation Administration will use both the ECAC and TSC models to further analyze the effects of near synchronous on definers (interference blankers) and automatic processors.

H. J. ALBRECHT: Referring to the influence of propagation parameters, the effect of terrain shielding is essential. Which model has been found to be particularly suitable?

S. J. SUTTON: With this model we account for terrain shielding by using the ECAC Topographic Data File. This file contains elevation information at 0.5 nmi intervals for the U. S. and other parts of the world. For the terrain profile between each radar and aircraft, we determine whether terrain obstructs the line-of-sight path.

I am aware that at STC the effect of terrain is considered by specifying the lowest usable elevation angle for azimuth positions around each secondary radar site.

F. J. CHESTERMAN: Do you set a threshold for S/N ratio, and can you say how probability of response falls with S/N in the transponder system?

S. J. SUTTON: As long as the received signal is equal or greater than the receiver sensitivity, we assume it is received by the transponder. The ICAO and U. S. standards for secondary radar require the transponder to respond 90% of the time for signals received at a level of -71dBm referred to the antenna.

Thus, as long as the signal exceeds the receiver sensitivity, and this will be at least 3dB in most cases, it should be detected. Thus, it is more the competition among interrogations for transponder service which affects the probability of reply and not the S/N that affects transponder performance.

COMPUTER GENERATION OF AMBIGUITY SURFACES  
FOR RADAR WAVEFORM SYNTHESIS

R.J.Morrow and G.Wyman  
 British Aircraft Corporation  
 Electronic Systems Group  
 Filton, Bristol  
 England

## 1. INTRODUCTION

Recent advances in the field of surface acoustic devices<sup>1</sup> are likely to encourage the implementation of complex forms of matched filter radars. As a consequence, the system designer and EMC Analyst will require convenient methods establishing the likely system performance obtained from the various forms of signal processing.

One well established technique used to determine the theoretical performance of matched filter or correlation receivers is through the application of the ambiguity function. This function has wide application as it may be employed to evaluate the theoretical received signal response in both the time and doppler domains. As this function handles both matched and unmatched signals it provides a convenient method of assessing both the design and eventual electromagnetic compatibility of the system. With these considerations in mind a general computer method of solving the ambiguity function has been developed and is described in this paper.

## 2. AUTO AND CROSS-AMBIGUITY FUNCTIONS

The ambiguity function as a concept was first investigated by Ville<sup>2</sup> and its development with particular application to radar systems was initiated by Woodward<sup>3</sup>. The function can be directly applied to the matched filter/correlation receiver which maximises the signal to noise of the receiver. In practice this receiver is used as a compromise since, though the information is preserved, the waveform is altered in character. We thus follow Woodward's development with the assumption that the matched filter concept can be generally applied.

The information regarding the target is impressed on the transmitted waveform and is normally received where the primary waveform is available. Thus it is postulated that the received signature is known a priori. An intuitive measure of the difference between these two waveforms would be the mean square departure of the received waveform from that of the primary source.

$$\text{i.e. } \int_{-\infty}^{\infty} | \psi(t) - \psi(t + \tau, f + \phi) |^2 dt \quad \text{-----1}$$

Or by the frequency domain equivalent which may be derived by invoking Parseval's theorem

$$\text{i.e. } \int_{-\infty}^{\infty} | \beta(f) - \beta(f + \phi, t + \tau) |^2 df \quad \text{-----2}$$

where  $\psi(t)$  maps into  $\beta(f)$  by the Fourier transform.

From a consideration of the terms dependent on  $\tau$  and  $\phi$  we obtain

$$\text{Re } \int_{-\infty}^{\infty} \psi(t) \psi^*(t + \tau, f + \phi) dt \quad \text{-----3}$$

For theoretical analysis the most satisfactory waveform to consider is the analytic signal representation where the real waveform is,

$$S(t) = a(t) \cos [2\pi f_0 t + \theta(t)] \quad \text{-----4}$$

$$\text{i.e. } S(t) = \text{Re} [ \psi(t) ] \quad \text{-----5}$$

For narrowband signals we can specify

$$\begin{aligned} \psi(t) &= v(t) \exp [i 2\pi f_0 t] \\ &= a(t) \exp [i(2\pi f_0 t + \theta(t))] \end{aligned} \quad \text{-----6}$$

or for wideband signals the Gabor form must be used

$$\text{i.e. } \psi(t) = S(t) - \frac{i}{\pi} \int_{-\infty}^{\infty} \frac{S(\tau)}{t-\tau} d\tau \quad \text{-----7}$$

where the imaginary part is the Hilbert transform of  $S(t)$

Substituting the narrowband signal representation into expression (3) gives the following,

$$\int_{-\infty}^{\infty} u(t) u^*(t + \tau) \exp [-i 2\pi f_0 \tau] \exp [-i \pi \phi \tau] dt \quad \text{-----8}$$

The rapid time varying function is ignored and the envelope

25-2  $\int_{-\infty}^{\infty} u(t) v^*(t + \tau) \exp [-2j\pi\phi \tau] d\tau$   
is defined as the chi or uncertainty function  $\chi(\tau, \phi)$  and  $|\chi(\tau, \phi)|^2$  is taken as the ambiguity function.

The interpretation of this function is dependent on the conditions imposed on its use, however, the mathematical concept derived from the mean square departure of the transmitted waveform is of direct relevance to matched filters. Its frequency domain equivalent is given by

$$\begin{aligned} F(\tau, \phi) &= \exp [i2\pi f_0 \tau] \int_{-\infty}^{\infty} \beta^*(f) \beta(f + \phi) \exp (i2\pi f \tau) df & - - - -9 \\ \text{i.e. } F(\tau, \phi) &= \exp [i2\pi f_0 \tau] \chi(-\tau, \phi) & - - - -10 \end{aligned}$$

From this expression it is seen that the envelope of the carrier is the important part, as the carrier contains no information. This point is of practical significance when analogue simulation is contemplated.

The preceding discussion has been confined to matched signals and the ambiguity function for this case may be defined as the auto-ambiguity function. This may now be extended to include the case of a mis-matched or interfering signal, in fact, the general solution for any arbitrary pair of waveforms.

In this case a signal  $v(t)$  is received by a receiver matched to a signal  $u(t)$  and the  $\chi$  function may be shown to be

$$\chi_{uv}(\tau, \phi) = \int_{-\infty}^{\infty} u(t) v^*(t + \tau) \exp [-i2\pi\phi\tau] d\tau \quad - - - -11$$

where  $|\chi_{uv}(\tau, \phi)|^2$  is defined as the cross ambiguity function of signal  $v(t)$  to a receiver matched to  $u(t)$ .

The importance of the ambiguity function in the design and study of radar waveforms has resulted in extensive studies of its properties which are now well documented in the available literature<sup>4</sup>. It is worth noting three of these properties as they have relevance to later discussions.

$$\text{i) } |\chi(0, 0)|^2 = (2E)^2 \quad - - - -12$$

i.e. The maximum height of the auto-ambiguity function occurs at the origin and is a function of the energy of the matched waveform.

$$\text{ii) } \int_{-\infty}^{\infty} \int_{-\infty}^{\infty} |\chi(\tau, \phi)|^2 d\phi d\tau = (2E)^2 \quad - - - -13$$

i.e. The integral under the ambiguity surface is constant, which implies that improvements in one area of the  $\tau, \phi$  plane leads to degradation in other areas.

$$\text{iii) } \int_{-\infty}^{\infty} \int_{-\infty}^{\infty} |\chi_{uv}(\tau, \phi)|^2 d\phi d\tau = \int_{-\infty}^{\infty} |u(t)|^2 dt \int_{-\infty}^{\infty} |v(t)|^2 dt \quad - - - -14$$

i.e. The integral over all space of the cross-ambiguity function is the product of the energies in each waveform.

### 3. COMPUTER GENERATION

#### 3.1 Introduction

The solution of the ambiguity function of any pair of arbitrary waveforms is arrived at from two operations which essentially solve the function in two dimensions forming the complete surface. The first operation is the solution in the  $\chi(\tau, \phi_n)$  plane. Consider two waveforms  $u(t)$  and  $v(t)$  the solution of  $\chi(\tau, 0)$  becomes the correlation integral.

$$\int_{-\infty}^{\infty} u(t) v^*(t + \tau) dt \quad - - - -15$$

The second operation is to increment  $v(t)$  in frequency by  $\phi_j$  relative to  $u(t)$  and form the  $j$ th slice, the composite surface  $\sum_{j=0}^N \phi_j(t)$  is then expressed as

$$\int_{-\infty}^{\infty} u(t) v^*(t + \tau) \exp [-i2\pi\phi\tau] dt \quad - - - -16$$

The basis of the method developed and reported here is to generate  $u(t, f)$  and  $v(t, f)$  using a time and frequency scaled analogue computer simulation. These waveforms are generated for various values of  $\phi$ , which is defined as the value of the frequency translation of  $v(t)$  relative to  $u(t)$ . The analogue signals are transferred from the analogue computer via an associated digital computer to magnetic tape where they are stored. The individual files stored on magnetic tape provide a library of waveforms which can be further processed to form ambiguity function solutions. The final solution, in the form of a set of slices of constant doppler, is stored on magnetic tape either for immediate display on a storage scope or for subsequent use.

The technique has been implemented using an EAI 8945 hybrid computer which consists of an EAI 8800 analogue computer having patchable, parallel logic and analogue components; 32 channels of A to D and D to A conversion equipment; an EAI 640 digital computer and an associated magnetic tape unit.

### 3.2 Waveform Generation

The philosophy of waveform simulation using hybrid computer techniques has been treated in a previous paper<sup>5</sup>. For this reason only a limited discussion has been included.

Most radar waveforms require the simulation of pulse streams, oscillators and voltage controlled oscillators. From these basic blocks complex waveforms may be generated. The simplest case is that of a pulsed tone signal. This is obtained by deriving the pulse stream, suitably time scaled, using the parallel patchable logic of the analogue computer. This is fed to a multiplier whose other input comes from a simulated oscillator. Oscillators are represented by a transfer function of the form.

$$1/(s^2 + \omega^2) \text{ and thus have poles at } s = \pm i\omega$$

They are therefore, quasi-stable and it is usual to incorporate an amplitude correction circuit of the form  $A_1 \cos^2 \omega t + A_2 \sin^2 \omega t - A = \text{error}$ . This basic oscillator is simulated as two integrators in cascade with an appropriate feedback loop. Potentiometers are included between the integrators to set the desired frequency of oscillation. The potentiometers are servo controlled, hence the oscillation frequency may be set by the digital computer. The initial condition input of the two integrators may be used to set the phase conditions at the start of the pulse. From the application of suitable control waveforms various phase coded pulse sequences or other complex waveforms may be obtained.

This basic oscillator simulation may be modified by the inclusion of multipliers in series with each potentiometer. The application of a control voltage to the two multipliers gives a proportional change in the output frequency thus forming a voltage controlled oscillator. The use of a ramp control waveform allows the generation of linear f.m. signals whose time bandwidth product is a function of the ramp duration and slope. More complex waveforms may be simulated by applying suitable control waveforms to both integrator initial condition inputs and the multipliers. These techniques enable the generation of waveforms having variable parameters such as pulse sequence and linear or non linear frequency characteristics.

### 3.3 Solution Through Waveform Correlation

The general solution of the ambiguity function is obtained through the use of correlation techniques. Three solutions are possible using a hybrid computer, i.e. analogue correlation, direct time domain correlation and correlation through the use of transformation. The particular method implemented depends on the nature of the problem under analysis.

#### 3.3.1 Analogue Correlation

With this type of correlator the time delay is achieved using the digital computer while multiplication and integration are obtained using analogue computer components. Two signals  $u(t)$  and  $v(t)$  are generated using the analogue. One of these signals is passed to the digital computer where a digital delay line programme incrementally delays this signal and passes it back to the analogue computer. The two signals are multiplied using an analogue multiplier and integrated using a simple lag circuit to produce a single correlation value for incremental delay  $\tau_n$ . This process is repeated for increasing values of delay to build up the correlation integral. Correlation from  $+\tau$  to  $-\tau$  is obtained by switching the waveforms passed to the delay line programme. These individual correlation values are stored on magnetic tape. The full process is repeated for incremental frequency shifts of  $v(t)$  to build up the correlation values for the full two dimensional chi function. This chi function solution is formed from simulated signals and therefore contains the simulated carrier information. The ambiguity function, which only reflects the change in the envelope, is formed from the chi function values by passing them through a peak detection programme which acts as an envelope detector. It has been found that it is not economic to employ this method with large time bandwidth signals due to the upper frequency bound imposed by the analogue computer.

#### 3.3.2 Direct time domain correlation

With this method the full process after waveform generation is performed by the digital computer. The basic operation is to generate and store each waveform as a time series on magnetic tape. The correlation is performed by a digital computer programme which operates on selected time series. The time series are stored as sequential blocks of data defining a slice taken along the axis at a particular value of  $\phi$ . The correlation programme consists of a simple algorithm which integrates successive shifts in  $\tau$  of the sampled waveform. This method has particular value for signals with large time bandwidth products.

#### 3.3.3 Correlation through use of Transforms

For this method use is made of the fast Fourier transform,<sup>6</sup> f.f.t. by invoking the correlation theorem<sup>7</sup> (i.e. multiplication of  $u(t)$  with the complex conjugate of  $v(t)$  in the frequency domain), to form the solution of the correlation integral. As in the previous methods the waveforms are generated by the analogue computer. These are converted to time series and mapped into the frequency domain through the use of the f.f.t. The correlation integral is solved by multiplying the first transformed time series by the complex conjugate of the second transformed time series which is regarded as the received signal.

254  
This result is transformed back into the time domain to form a slice at  $\phi_n$  of the chi function. The process is repeated for the various time series defining slices of the chi function at different values of  $\phi$ . The ambiguity function solution is obtained by including an envelope detection routine. This method provides the most economic solution for most waveforms having practical values of time bandwidth product.

### 3.3.4 Display Techniques

In order to analyse the result of the computation it is convenient to use various forms of graphical display. The particular display chosen depends on the nature of the analysis to be performed.

#### Constant $\phi$ or $\tau$ Plots

These may be produced either as a line printer, storage scope or plotter output using the matrix of data stored on magnetic tape. Through the introduction of a suitable digital computer routine these plots may be produced with either arithmetic or logarithmic amplitude scales. This type of output is useful when a detailed analysis of specific portions of the ambiguity function is required.

#### Three Dimensional Surface Plots

The full matrix solution defining the function in both  $\tau$  and  $\phi$  may be used with a suitable three dimensional plotting program to produce a graphical display of the surface. The ambiguity function is even-symmetric\* with respect to the  $\tau, \phi$  origin, thus the half plane solution defines the whole and the mapping on to the other half plane is simple. It has been found useful to display only the half plane solution (FIG 1) as this highlights the nature of the  $|\chi(\tau, \phi)|^2$  slice and allows a simple visual interpretation of the range side lobes to be made. The full three dimensional surface plot is useful for the general radar receiver response analysis. It has been found convenient to display the surface using a storage scope immediately after computing the solution, prior to line plotting, as it provides a quick method of checking the validity of the computation.

#### Contour Plots

A third particularly useful type of plot may be produced by using the computed matrix of data with a contour plotting program to produce contours of the surface. This type of output Fig 2, provides a useful backup to the three dimensional plots as they accurately define the relative response levels of the major features of the surface.

## 4 APPLICATIONS

Use is made of the ambiguity function in the design and assessment of high resolution, pulse compression, radar systems. The suitability of a pulse compression radar for a given application is dependent upon the type of waveform selected. The prime factors influencing the selection of a particular modulated waveform are usually the radar requirements of a given range coverage, doppler coverage, range and doppler side lobe levels, interference rejection and the signal to noise ratio. These factors may be examined through the generation and evaluation of auto-and cross-ambiguity functions of the modulated waveform.

### 4.1 Theoretical Waveform Analysis

An infinite variety of waveforms may be produced which give a system advantage due to pulse compression. Of these waveforms the majority may be classified according to the basic modulation types, i.e. amplitude, frequency, phase and pulse modulation. Higher order modulated waveforms may be derived through the use of two or more of these types, i.e. phase coded pulse sequences, bilateral weighted linear frequency modulation etc.

The general method used in the analysis of waveforms is to derive an analogue computer simulation of the required modulated transmitted waveform using the techniques described in section 3.2. This waveform, having a scaled carrier frequency,  $f_1$ , is passed via an analogue to digital converter to a digital computer where it is stored on magnetic tape. This procedure is repeated for incremental frequency translation of the spectra. The resulting arrays stored on magnetic tape provide a library of waveforms. If it is required to produce an auto-ambiguity function of the stored waveform, the record pairs corresponding to  $f_1$  and  $f_n$  are correlated using either direct time domain correlation or correlation through the use of transform methods. The resulting slices through the ambiguity function at  $f_n - f_1$  may be displayed in a three dimensional form using a storage oscilloscope. In order to demonstrate the generality of the techniques the ambiguity functions of three widely different modulated waveforms obtained using this technique are shown in FIG's. 1, 3 and 6.

The ambiguity function of linear frequency modulation<sup>8</sup> having a time bandwidth product of 120 and second order cosine weighting is shown in FIG 1. The basic unweighted linear frequency modulated waveform was obtained using an analogue computer simulation of a voltage controlled oscillator. The amplitude weighting is obtained by modifying the values of the time domain waveform samples prior to correlation using an analytic expression of the desired window shape. If it is more convenient to express the weighting function in the frequency domain then the spectrum samples after transformation may be modified.

\* even-symmetric  $\chi(\tau, \phi) = \chi^*(-\tau, -\phi)$

The ambiguity function of a quaternary coded waveform<sup>9</sup> is shown in FIG 3. The four level code made up of positive and negative slope linear frequency modulated elements having zero or  $\pi$  phase changes at the beginning of each element. The time bandwidth product of each element is 34. The change from positive to negative slope and the phase changes describes a 13 element Barker<sup>10</sup> code. The waveform produced is shown diagrammatically in FIG 4.

As with the previous example the modulated waveform is obtained using basic analogue computer simulation of a voltage controlled oscillator. The required waveform is obtained using three control waveforms as shown in FIG 5. The first waveform, A, alters the sense of the slope of the frequency modulation, the second, B, the duration of each element of the code and the third, C, the phase condition at the start of each element. Waveforms A and B are applied to the multipliers and waveform, C is applied to the initial condition input of the integrators forming the simulated voltage controlled oscillator. This technique may be used to generate many forms of quaternary coding using both constant and variable slope frequency modulated elements.

The ambiguity function of a set of complementary coded pulse sequences<sup>11</sup> is shown in FIG 6. One set of Golay codes<sup>12</sup> 00011101 and 00010010 have been used to phase modulate a carrier. The two independent codes are formed using logic elements. Each code is passed to a multiplier whose other input is fed from a simulated voltage controlled oscillator acting as the carrier frequency. The output from each multiplier is passed via A to D converters to the digital computer where they are stored on magnetic tape. Individual records are made for various incremental increases of the simulated carrier frequency. Record pairs at frequencies  $f_1$  and  $f_n$  for the first code are taken by the digital computer and correlated. This is repeated for the identical frequency record pair of the other code. The two correlation functions are summed and envelope detected to form a slice of the ambiguity function at  $f_n - f_1$ . The full surface is formed by taking record pairs of each code at different frequencies and displaying the output as shown in the figure.

Degradation of the theoretical waveforms due to practical implementation may be studied using this technique. The analogue computer may be used to simulate AM to AM and AM to PM characteristics. These may be included in the simulation of the transmitted waveform and the resulting ambiguity function evaluated. The effect of limiting the received waveform may be analysed by including the limiter characteristics in the waveform generation through the use of diode function generators.

#### 4.2 Point and Distributed Target Analysis

The ambiguity surface formed by the return from a point target may be determined by mapping the ambiguity surface associated with the given return waveform into the plane of the radar by a change of its  $\tau, \phi$  origin. The position in the new plane is determined from a knowledge of the polar co-ordinates  $r, \theta$  and  $\dot{r}$ . The second derivative  $\ddot{r}$  relating to the target acceleration is not included in this analysis since the surface so formed would be four dimensional. In principle this effect could be carried through the calculation but a visual display would be difficult to achieve.

If it is postulated that the propagation medium is homogeneous and the receiver front end linear then superposition theory may be used. Now, in the case of multiple point targets, individual targets may be mapped to the  $\tau, \phi$  plane of the radar. The final response of the radar may be obtained from the summation, previously described by Mitchell et al<sup>13</sup>. If the ambiguity surface of a given required point target is  $x_j(\tau, \phi)$  then the responses of other targets relative to that required may be calculated by including a constant multiplying factor which accounts for the difference in range, target cross section and antenna gain. This factor  $K$ , say, can be computed using the radar range equation thus mapping the respective normalised ambiguity surfaces on to the  $\tau, \phi$  plane of the radar. This composite response  $x(\tau, \phi)$  is computed from:-

$$x(\tau, \phi) = \sum_{j=1}^n K_j x_j(\tau - \tau_j, \phi - \phi_j) \quad - - - - - 17$$

where  $\tau_j, \phi_j$  is the mapped origin of each target.

This approach to multiple point targets can be extended to distributed targets by considering the distributed targets as a series of point targets. In order to account for the statistical nature of either point or distributed target the factor  $K$  becomes a value selected from a defined statistical distribution. The various statistical distributions are selected according to the nature of the target. A complex spatial environment may be constructed by producing a matrix overlay of a given terrain where each element of the matrix defines the location and statistical characteristics of each point target. This approach had been used by Mitchell et al<sup>13</sup> and is described in detail in their paper.

An alternative approach, that has been proposed but not implemented by the authors, would be to characterise time varying radar return as an analogue. The waveform thus produced could be used to form multiple ambiguity surfaces of the composite signals for different  $\tau, \phi$  origins. In theory, the propagation path including the reflections could be modelled using a time varying filter characterisation<sup>14, 15</sup>. In practice this may be implemented using a tap delay line whose input is the simulated pulse compression waveform, FIG 7. A complex tap gain function  $g(t)$  is used to modify the output of each unit delay to account for the characteristics of the signal reflections. The composite signal received by the radar is obtained from the summation of all delayed signal components. An extension to this approach would be to form a hybrid solution where specific returns are handled by the summation of point targets and other returns are included using the analogue approach.

### 4.3 Electromagnetic Compatibility Analysis

In order to study the total radar electromagnetic environment consideration must be given to both matched returns, from desired targets and undesired clutter, and unmatched signals received from other emitting equipment in the same area. A first order EMC assessment may be made from an analysis of the radar response to the likely unmatched interference signals through the use of the cross-ambiguity function. The cross-ambiguity function describes the complete three-dimensional receiver response to interfering or unmatched signals as a function of time and frequency. The rejection offered by the radar receiver to interference may be determined through the use of both auto and cross-ambiguity functions. The method adopted is to form a library of cross-ambiguity surfaces for various interference waveform types requiring examination. Each surface represents the response of a mismatched signal of equivalent energy to that of the matched signal with all values normalised to the peak of the auto-ambiguity function  $\chi(0,0)$ . Thus if  $u(t)$  with associated energy  $E_u$  is the matched waveform and  $v(t)$  with associated energy  $E_v$  then the value  $\chi_{uv}(0,0)$  of the auto-ambiguity function may be computed and equated to  $E_u$ . The cross-ambiguity function is determined from the expression.

$$\chi_{uv}(\tau, \phi) = \int_{-\infty}^{\infty} u(t) v^*(t + \tau) \exp[-i2\pi \phi t] dt \quad - - - - - 18$$

Now if  $E_u$  is made equal to  $E_v$  then the cross-ambiguity surface may be normalised using the value computed for  $\chi_{uu}(0,0)$  since the integral of the surface over all space is equal to unity

$$\text{i.e.} \quad \int_{-\infty}^{\infty} \int_{-\infty}^{\infty} |\chi_{uv}(\tau, \phi)|^2 d\tau d\phi = 1 \quad - - - - - 19$$

These stored normalised cross-ambiguity functions may be used to determine the performance of the radar for various signal and interference powers through the use of a scaling factor. This scaling factor is the ratio of the matched to unmatched signal energies.

$$\text{i.e.} \quad \chi(\tau, \phi) = \chi_{uv}(\tau - \tau_v, \phi - \phi_v) \frac{E_v}{E_u} \quad - - - - - 20$$

Also the effect of several potential interferers may be analysed by mapping each on to the  $\tau, \phi$  plane of the receiver. Thus if  $\tau_j, \phi_j$  is the origin of the interference on the  $\tau, \phi$  plane of the unmatched signal  $v_j(t)$

$$\chi(\tau, \phi) = \sum_{j=1}^n \chi_j(\tau - \tau_j, \phi - \phi_j) \frac{E_j}{E_u} \quad - - - - - 21$$

This method for treating interference may be incorporated with those techniques previously described for point and distributed targets to obtain a comprehensive analysis of the radar performance.

## 5 CONCLUSION

A simple method of evaluating the ambiguity function for any pair of arbitrary waveforms has been given. The generality of the technique is obtained through the use of an analogue computer to generate the waveforms in a form suitable for digital computer evaluation of the ambiguity function. It has been demonstrated that a wide range of complex modulated waveforms can be evaluated and displayed as either a three dimensional or contour plot.

This technique for generating ambiguity function solutions may be employed as an integral part of any analysis of matched filter or correlation radars. In particular a knowledge of the auto and cross-ambiguity functions for various waveforms provides a basis for determining the expected radar performance from both the design and EMC aspects.

## 6 ACKNOWLEDGEMENTS

The authors wish to thank their colleagues at the British Aircraft Corporation EMC Analysis Facility who have helped to develop the techniques discussed in this paper. In particular the authors would like to thank Dr. G. Botting and Mr. E. Lord for their help in developing the analogue and digital computer techniques.

The work was carried out as part of a Ministry of Defence Contract. The authors thank the Ministry of Defence, Army EMC Agency and the Directors of the British Aircraft Corporation for permission to publish this paper.

7. REFERENCES

1. MAINES, J.D., "Application of Surface Wave Devices" Conference proceedings Microwave 70, Brighton, England. (JUNE 1973).
2. VILLE, J. "Theory and application of the notion of complex signals" Cahiers de transmission, No. 1, (1948), 61.
3. WOODWARD, P.M., "Probability and Information theory, with application to radar". Pergamon Press London. (1953).
4. COOK, C.E., and BERNFIELD, M., "Radar Signals - An introduction to Theory and Application". Academic Press Inc., New York, 1967.
5. MORROW, R.J., and WARREN, C.S. "Hybrid Computer Simulation applied to digital communication systems". The Radio and Electronic Engineer Vol. 43, No. 9 (Sept. 1973).
6. COOLEY, J.W. and TUKEY J.W., "An algorithm for machine calculation of complex Fourier series". Maths. Comput., Vol 19, 1965
7. BRACEWELL, R., "The Fourier transform and its applications" McGraw-Hill, New York., (1965), 115.
8. RIHACZEK, A.W., "Principles of High Resolution Radar". McGraw-Hill Book Co., Ch. 7 (1969)
9. WELTI, R.G., "Quaternary Codes for Pulsed Radar" I.R.P. Transaction on Information Theory, Vol. I.T. (June 1960), 400-408.
10. BARKER, R.H., "Group Synchronizing of Binary Digital Systems", in W. Jackson (ed) "Communication Theory", Academic Press Inc. New York (1953), 273-287.
11. T.SENG, G., "Signal Multiplexing in Surface-Wave Delay Lines using orthogonal pairs of Golay's complementing sequence". I.E.E.E. Transaction on Sonics and Ultrasonics, Vol-SU-18 No.2 (April 1971), 103-107.
12. GOLAY, M.J.E., "Complementary Series" I.R.E. transaction on Information Theory, Vol IT-7 (April 1961), 82-87.
13. MITCHELL, R.L., and WALKER, J.F. "Radar system simulation techniques" I.E.E. CONFERENCE No. 105, "Radar Present and Future", (October 1973), 251-256.
14. KAILASH, T., "Lectures on Communication System Theory". McGraw-Hill, Chapter 6, (1961), edited E.J. Baghdady.
15. BELLO, P.A., "Characterisation of Randomly Time - Variant linear channels". I.E.E. Trans. Comm. Syst. Vol.CS-11 (1963), 360-293.
16. COHEN, S.A., "Cross-Ambiguity Function for a Linear FM pulse compression radar". I.E.E.E Transaction on Electromagnetic Compatibility, Vol. EMC-14 No. 3 (August 1972) 85-91.



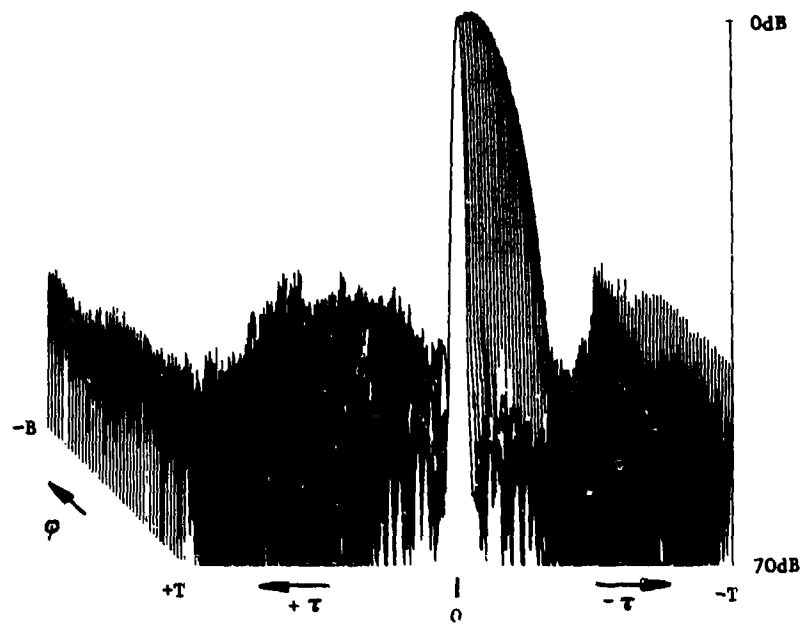


Fig. 1 Linear FM, TB 120 with second order cosine weighting

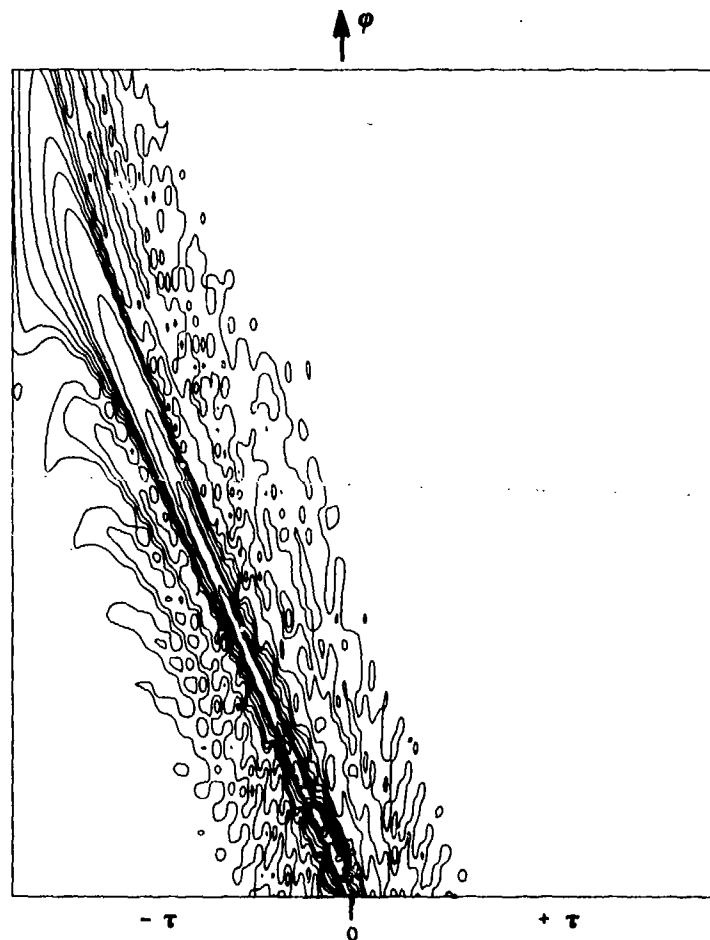


Fig. 2 Contour plot linear FM TB 34

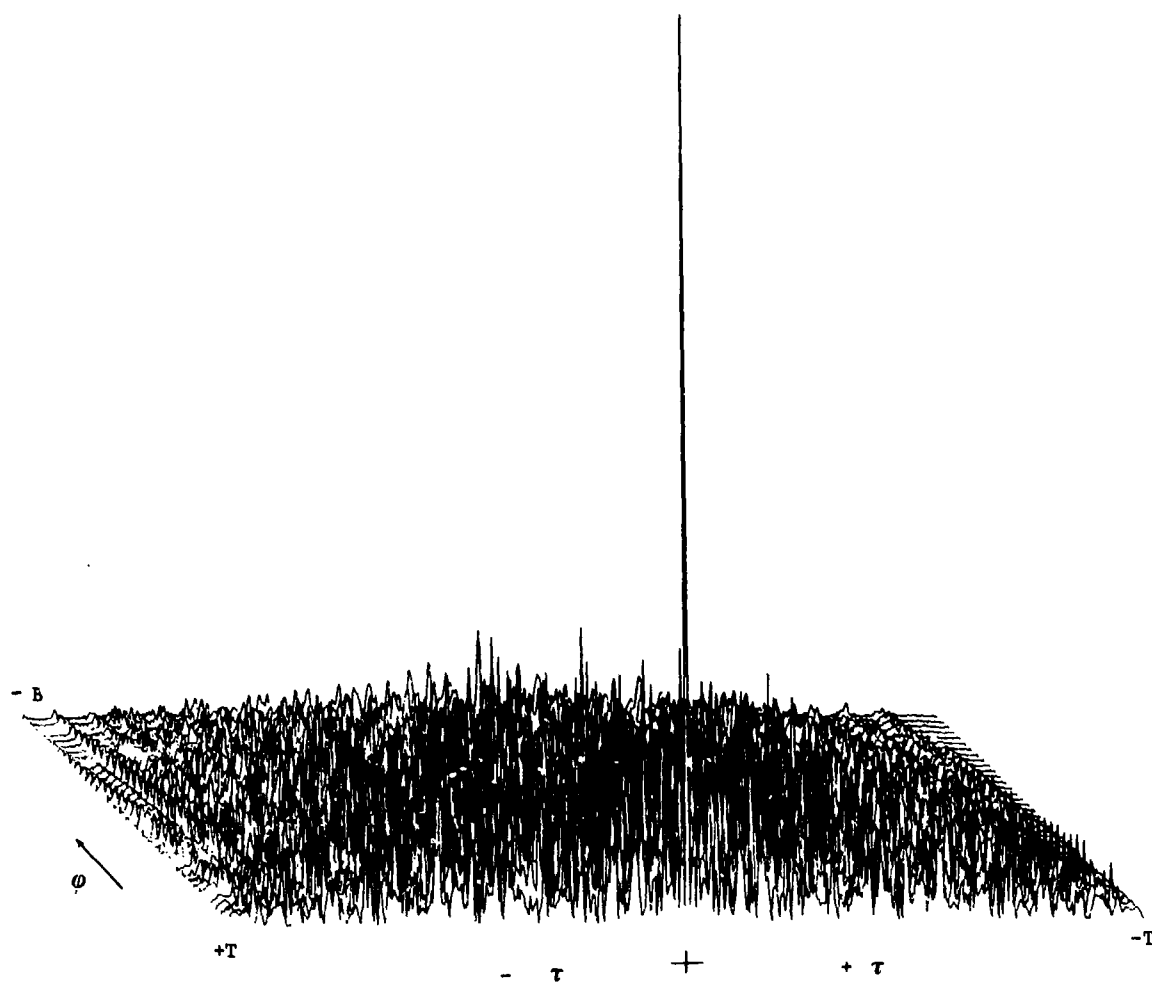


Fig. 3 Quaternary coded waveform

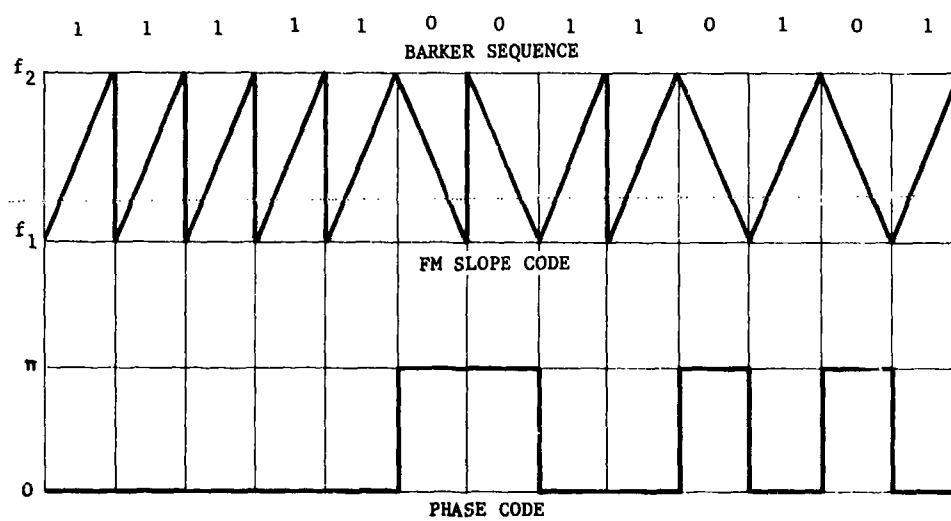


Fig. 4 Quaternary coding control waveforms

25-10

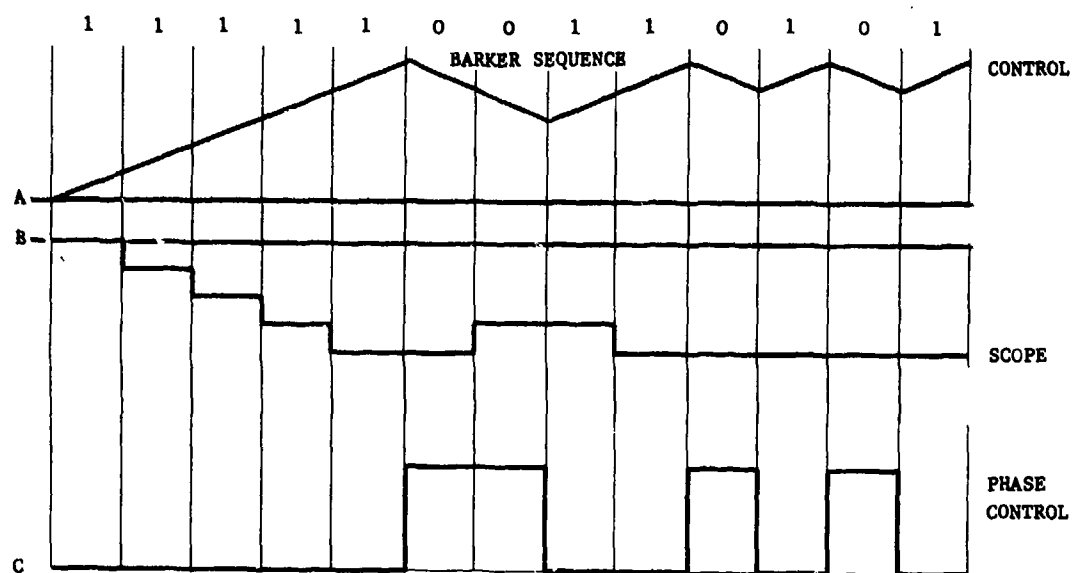


Fig. 5 Quaternary coding control waveforms

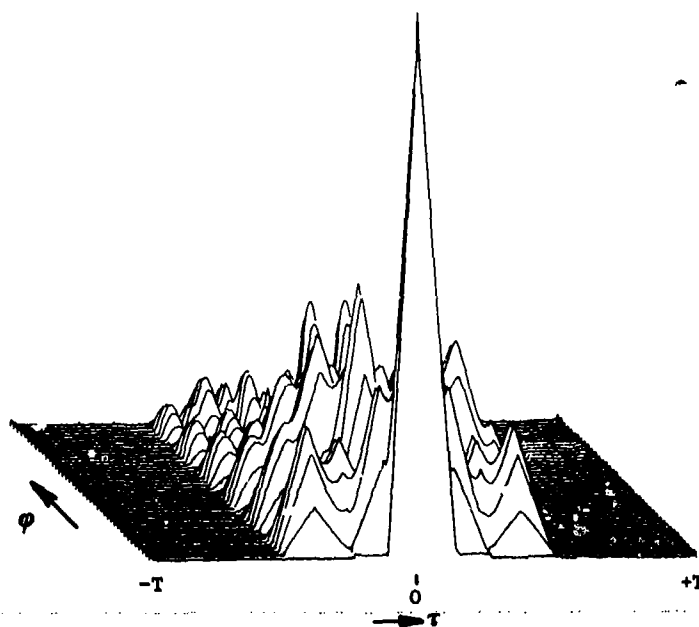


Fig. 6 Ambiguity surface complementary coded waveform

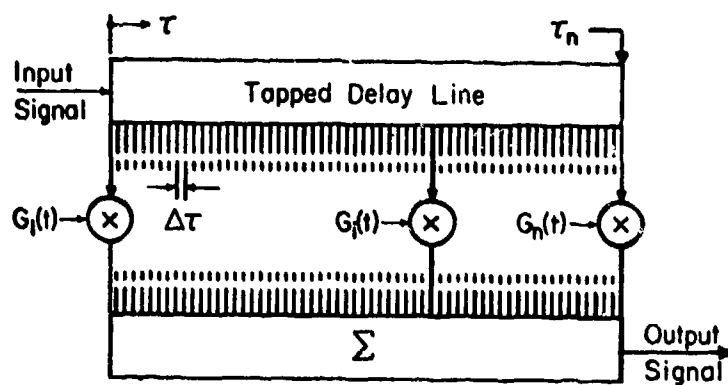


Fig. 7 Linear time varying filter model

## DISCUSSION

R. N. LORD: In my own work on Moving Target Indicator (MTI) systems, I simulate distributed targets (clutter) by pseudorandom number generators and spectral shaping. Have you considered using this technique?

R. J. MORROW: Presently, we are considering a distributed target as a summation of point targets in the radar space  $(r, \phi)$ . An amplitude term is incorporated when summing the elemental ambiguity function; this amplitude  $k$  (in text) is selected from a given probability distribution. The bivariate Gaussian distribution suggested by weighting two pseudorandom generators is an alternative approach which could well be implemented. A further function, which would take into account the characteristics of the antenna, could be included to modify the distribution in  $r$ .

E. J. FREMOUW: Could you describe briefly the model you used to account for back-scatter from distributed targets such as clouds?

R. J. MORROW: No, I couldn't, but there is extensive literature on the subject.

26-1

ANTENNA-TO-ANTENNA EMC ANALYSIS OF  
COMPLEX AIRBORNE COMMUNICATION SYSTEMS

William L. Dillion  
Electronic Communications, Inc.  
A Subsidiary of NCR  
St. Petersburg, Florida  
U. S. A.

SUMMARY

This paper presents the methodology and applied techniques for antenna-to-antenna electromagnetic compatibility (EMC) analysis of complex airborne communication systems. The alternative objectives of such an analysis are discussed to establish the proper starting point of the analysis. Methods are introduced to reduce the magnitude of a complex analysis to simple problems which expedite the analysis. Potential interference modes and system isolation factors are examined in conjunction with a typical equipment complement. A method of analysis is discussed which uses computer calibrated antenna space isolations with conventional analysis techniques. Some typical analysis results are presented in summary form. Antenna isolation is discussed as a limited factor for EMC optimization. The results of past analysis clearly show the need for frequency management to effect interference control as an integral part of the antenna-to-antenna EMC profile of complex airborne systems.

1. INTRODUCTION

Antenna-to-antenna electromagnetic compatibility (EMC) is concerned with radiated signals from one antenna propagating to other antennas within the same system to produce interference with the other equipment associated with these antennas. The antenna conducted signals may be either desired or undesired radiations such as harmonics, spurious emissions, or intermodulation products. Within a given pair of antennas several potential modes of interference may exist. In complex airborne systems the number of antennas is large and confined within the proximity of an airframe thus the EMC problem becomes very significant. The equipment on the aircraft includes a full complement of flight related avionics and a large complement of equipment for mission related communications. The resulting equipment complement contains a large quantity of many different types of equipment for both transmitting and receiving which must operate simultaneously at frequencies ranging from VLF to UHF.

In addition to radiations at desired frequencies each transmitting equipment radiates undesired signals at several spurious and harmonic frequencies and each receiving equipment has several inherent susceptibility frequencies and also may be overloaded by high level undesired signals radiated in the same proximity. A typical complex airborne system of this type may have as many as 40 separate antennas some of which radiate power up to 1 kilowatt levels and some that simultaneously receive signals of power levels ranging from -90 dBm to -100 dBm.

In order to ensure total system electromagnetic compatibility such that all electronic subsystems may collectively operate with the desired performance requires the use of all available EMC resources and techniques.

This paper is concerned with the methodology used to analyze the predominant interference modes encountered in complex systems and presents typical results which have been obtained from past analysis.

2. OBJECTIVES

The objective or end results desired must be considered before formulating the final approach to performing the analysis.

The purpose for which the analysis is performed may be one or more of the following:

- (a) Determine equipment performance characteristics required to ensure EMC of a system design and antenna locations. The equipment characteristic requirements may then be imposed on the equipment selected for use in the system.
- (b) To determine optimum antenna locations within constraints imposed by other system requirements.
- (c) To reveal incompatibility factors in electromagnetic radiators and/or receptors and to determine the magnitude of such incompatibilities.
- (d) Evaluate system configuration alternatives.
- (e) Establish frequency management and interference control requirements and criteria.

The specific objective of a particular analysis problem depends upon which parameters of the system design are fixed or flexible and which ones are known and unknown. It is common to find that the design for a complex communication system proceeds with very little coordination or communication between those responsible for the equipment design and those responsible for the system design.

202 Therefore, the specific objective of the analysis is determined by which particular parameters of the system design are dependent or independent variables. The method of analysis is similar regardless of the objective but the unknown parameters to be determined alter the approach to achieve the objectives.

An analysis will rarely be performed in which all parameters are variable. Such a case would only exist for a totally new system design where all electronic equipment is to be newly developed. A typical analysis problem involves a combination of mostly existing equipment with some new equipment to be developed and conventional subsystem designs to be changed only where necessary and with a cost-effective approach.

In many cases the purpose of the analysis is to reveal the potential incompatibilities in a system so that corrective measures may be implemented which effect a resulting compatible system. These corrective measures may include:

- (a) Imposing more severe equipment performance requirements for EMC related characteristics.
- (b) System redesign involving the addition of RF filters, multicouplers, antennas, etc.
- (c) Relocation of antennas to optimize space isolation.
- (d) Imposition of interference control via frequency management requirements.

The results of the typical analysis will usually indicate that a potential incompatibility may be eliminated by more than one of these corrective measures, thus the selection of the most appropriate measure must be a trade-off evaluated in terms of other factors such as complexity, cost, and operator convenience.

### 3. APPROACH

When considering the complexity of the total problem, with both desired and undesired signals simultaneously radiating over the same spectrum that many sensitive reception devices are operating, the quantity of the analysis to be performed appears to be extremely large. The analysis of a particular type of interference between any two pairs of equipment can be a major task by itself. When this type of analysis is magnified by the variety of equipment involved, the quantity, and the different types of interference which may occur, the analysis to be performed appears to be overwhelming. In addition, the variable parameters of the system design, equipment characteristics, system design alternatives, antenna location options, interference control techniques further complicate the total magnitude of the problem and make it difficult to determine a point of departure for the analysis. Therefore, the key to the expeditious performance of the analysis is to simplify. In order to do this, it must be recognized from the outset that a preliminary analysis must be performed to eliminate from further consideration those subsystems which will not create interference.

The initial approach to the analysis should be to reduce the complexity of the system and hence the magnitude of the analysis which must be performed. This simplification can be performed on a subsystem to subsystem basis by considering the worst case characteristics of the worst case equipment examples between subsystems. Each receiving subsystem must be evaluated in conjunction with each radiating subsystem to determine if a potential for interference exists. The parameters of such an evaluation are the equipment performance characteristics, system configuration and antenna locations. Since isolation between radiators and receptors is the parameter which ultimately determines whether interference will occur or not all factors that influence this parameter must be established for each subsystem. Factors which comprise the total isolation between subsystems are: antenna-to-antenna space isolation, antenna gain and directivity, filter rejection provided in the system, and characteristics of individual interference modes. A typical interference model is illustrated in Figure 1. Since all of these factors are frequency related, the essence of the analysis is to determine as a function of frequency and for each potential interference mode the:

- (a) Radiation levels
- (b) Susceptibility level of receivers
- (c) Isolation between the radiator and receptors

The preliminary analysis is performed to a simplified interference criteria and with worst case antenna isolation values. A detailed analysis concerning the intricacies of each interference mode to an explicit level of accuracy is not the objective but instead to screen the system with worst case conditions to categorize the equipment and subsystems into categories that may have potential interference problems and those that do not. This approach identifies those subsystems or equipments which may be eliminated from further analysis and can significantly reduce the magnitude of the remaining analysis. In addition, by using the worst case equipment example in each subsystem, the analysis is applicable for the entire quantity of identical equipments within that subsystem. In the event that a potential interference problem

is revealed in a subsystem, a subsequent resolution of this problem for the worst case equipment will effect a solution for the entire subsystem.

After the preliminary screening, efforts can be directed to more detailed analysis of potential problem areas and to find solutions to these interference problems.

Thus, the approach should be directed to rapidly reduce the magnitude of the analysis required thru the use of screening and the identification of incompatibilities requiring some form of action for resolution. The desired end achievement is a compatible system design rather than a rigorous detailed analysis of each equipment and interference mode in the system.

### 3.1 Equipment Complement - Typical

A typical equipment complement pertinent to the analysis is summarized in terms of the associated antenna locations in Figure 2. Antennas located on the top portion of the fuselage are identified by single letters and those on the bottom of the fuselage by double letters. The antenna locations in station units (inches) are also given for each antenna.

The equipment types in such a complement typically are:

Radar	HF Communications
TACAN	VHF Communications
Marker Beacon	UHF Communications
Radio Altimeter	Satellite Communication
Identification Transponder	Other Specialized Communications
Glide Slope	Automatic Direction Finders
VOR/ILS	

The communications equipment is provided for both flight and mission related functions and consists of several equipments of each type. The quantity of equipment typically requires the use of approximately forty antennas on the airframe.

### 3.2 Transmitter/Receiver Characteristics

Extensive data on each equipment type should be compiled for use in the analysis and all pertinent equipment in-band and out-of-band characteristics evaluated and applied to both the computer and manual analysis. Some of the salient characteristics are:

Operating Frequency Range	Receiver Sensitivity
Transmitter Power Output	Bandwidth RF & IF
Harmonic Output Levels	Image Rejection
Spurious Output Levels	Spurious Rejection

In most instances specification characteristics are available but where such a variety of equipment types exist it is inevitable that some assumptions must be made. Since receiver RF selectivity and transmitter output selectivity are not commonly specified engineering judgment is required to establish these characteristics. The selectivity can be approximated by evaluating the associated circuitry and other related specifications such as harmonic, spurious, and image rejection.

### 3.3 Potential Interference Modes

The modes of electromagnetic interference which present the most serious potential for interference include the following:

- (a) Generation of spurious signals by transmitters at receiver operating frequencies resulting in receiver desensitization.
- (b) Desensitization of receivers through saturation or cross-modulation by RF energy from transmitters.
- (c) Desensitization of receivers through appearance of transmitter outputs on receiver spurious response frequencies.
- (d) Interference with the operation of transmitters and/or generation of external intermodulation products through coupling of outputs from other transmitters.

Each mode is a potential source of interference in certain areas of the RF spectrum of interest. The first three modes are common mechanisms for interference. However, transmitter intermodulation interference is less common and is usually encountered only where collocated high power transmitters must share a limited range of the spectrum. Since the equipment complement typically uses several high power UHF transmitters this interference mode is a major concern.

#### 4.1 Interference Threshold

The equipment complement contains electronic equipment designed for specific operational purposes which vary widely, thus the characteristics of these equipments also vary widely. The power output of transmitters and the sensitivity level of receivers differ as do the modulation types used. Some equipments use pulse type modulation with various pulse durations and differing peak power outputs. Other equipments utilize continuous modulation of amplitude modulated signals, narrowband FM signals, wide-band FM signals, in addition to special purpose modulation types. Also, depending on the operating mode selected, different transmitted power spectrums may be radiated from a single equipment type. Rigorous analysis of each operating mode and modulation type encountered would require exacting detail to each modulation type and its potential interference mechanism, together with the potential interference mechanism of each modulation type on all other modulation types to be encountered. To conduct such an analysis would require many hours of careful attention to exacting detail. The results obtained would not provide a significant increase of useful information beyond that which would be obtained by establishing some safe, worst case criteria for interference. Thus, for the bulk of the analysis to be performed, a generalized criteria of interference should be established which does not consider the modulation type involved.

Interference can generally be defined as that disturbance occurring when the peak radiated signal from a generating source referred to the input of a receptor exceeds a threshold specified for that particular receptor. In applied analysis problems a good approach is to define the interference threshold of a receptor specified as 10 dB lower than the sensitivity level specified for that equipment. The threshold of interference may vary from this 10 dB criteria but the use of a generalized interference definition permits the analysis to proceed by treating all equipment types as equals. The analysis can then proceed to eliminate some enlarged segments of the equipment complement as potential interference problems based on worst case values. In those areas where equipment problems are indicated as marginal, further detailed analysis is applied to determine if the potential interference revealed is real or the result of utilizing worst case values in the analysis. In some cases, it may be necessary to re-evaluate the accuracy of the interference threshold if the potential for interference is marginal.

#### 4.2 Computer Analysis Techniques

The computer analysis techniques based upon existing programs (Bogdanor, Dr. J. L., 1971) can be used for computation of antenna isolations and the subsequent computation of EMI interference levels between equipments for frequency coincidence.

A three-dimensional mathematical model of the airframe is used in conjunction with antenna locations and characteristics to calculate antenna isolations between specified subsystems. The isolation is calculated in three components: free space, wing shading, and fuselage curvature. Frequency coincidence and signal level calculations can be performed according to equipment generator or receptor characteristics. The program readout identifies the interference margins (positive and negative levels) and antenna isolation components between generator and receptor subsystems.

The basic program can be adapted to perform computations for interference types other than direct and harmonic frequency coincidence interference. This can be achieved by prudent selection of equipment characteristics and multiple inputs to provide a series of interference calculations. The basic program input parameters for a transmitter include a power output level, lower band-upper band limits, and lower skirt-upper skirt limits. The transmitter can be made to appear as a spurious generator by lowering the power output to a spurious level and giving the transmitter an output selectivity of the transmitter-tuned output characteristics. Similarly, the spurious response characteristics of a receiver may be simulated by changing the receiver sensitivity to a receiver spurious susceptibility level, and broadening the receiver selectivity characteristics to include the RF front end selectivity.

Adjacent channel interference can be analyzed by providing a transmitter power at a discrete frequency and utilizing a receiver with identical characteristics but operating at specific frequency increments from the transmitter frequency. Thus the level obtained can be used to plot an interfering signal level versus frequency separation. Several computer runs can be performed to obtain antenna isolations for all preliminary antenna locations.

#### 4.3 Manual Analysis

Conventional analysis techniques can be applied using the antenna isolations calculated by computer techniques. A simple but extremely useful tool is a plot of transmitter power output and receiver sensitivity levels as illustrated in Figure 3. Transmitter harmonic levels as extracted from equipment specifications provides additional information. Visual examination of these simple plots result in the determination of the isolation requirements between specific transmitting and receiving equipments. An evaluation of the specific equipments involved must be made to consider the components of isolation present in any particular subsystem. Components which typically impact the isolation in addition to space isolation are antenna directivity, antenna efficiency, and equipment selectivity or filtering. After consideration of these factors a comparison of the isolation required and the space isolation can be performed to establish the potential for interference. This is obviously a simple summation but a visual presentation ensures that all subsystems are collectively reviewed.



## 5. ANTENNA ISOLATION CONSIDERATIONS 26-6

The potential for improvement of the antenna-to-antenna EMC profile of an aircraft by antenna relocation is limited to: a) Increase in antenna space isolation; b) Optimum placement of antenna to reduce interactions between interfering and susceptible equipments.

The increase in antenna isolation resulting from increased space isolation cannot have a major impact on the aircraft EMC profile because the magnitude of the increase is limited. An examination of isolation calculations reveals the extent of the limit. The isolation of top-to-top or bottom-to-bottom located antennas is essentially the same as free space propagation and may be calculated as follows.

The power received by a receptor antenna is defined as follows:

$$P_r = G_r G_t P_t \left( \frac{3 \times 10^2 \times 3.28}{4 f d} \right)^2$$

Where:  $P_r$  = Received power (watts)  
 $G_r$  = Receiver antenna gain  
 $G_t$  = Transmitter antenna gain  
 $P_t$  = Transmitter power (watts)  
 $d$  = Antenna separation (feet)  
 $f$  = Transmitter frequency (MHz)

When considering unity for antenna gain, for example  $G_t = 1$ ,  $G_r = 1$ , these terms are omitted with an isolation equation given as:

$$\frac{P_r}{P_t} = 1.635 \times 10^{-4} f^2 d^2$$

This expression gives a space isolation figure in a power ratio between antennas as a function of frequency. This ratio when expressed in dB of space isolation is plotted in Figure 4 for a number of typical frequencies and for antenna spacings of 1 to 100 feet.

### 5.1 Isolation Limitations

The effective free space antenna isolation is a function of the square of both the frequency and antenna space separation. Thus a two-fold increase in either the frequency or distance between antennas results in a 6 dB increase in antenna isolation. Thus at the worse case UHF of 225 MHz and a distance of 10 feet, the isolation would be 29 dB. Increasing the separation to 20 feet will increase the isolation to 35 dB. Figure 5 illustrates the effect of doubling the antenna separation. An eight-fold increase will result in an 18 dB increase in isolation.

The maximum isolation which could be obtained on an airframe for a top-to-top or bottom-to-bottom UHF antenna pair is 55 dB (225 MHz) assuming a usable fuselage length of approximately 200 feet.

Comparing the relative dimensions of some typical large airframes such as the Boeing 707 and 747 (129 and 225 feet respectively) and assuming that all antennas are located on the airframes in the same respective general locations, the antenna space isolation on the 747 will be  $225 \div 129$  or 1.75 times that on the 707. This is equivalent to 5 dB of antenna space isolation.

Such a hypothetical case is a very real situation because the same factors which influenced the selection of antenna locations on each aircraft and the equipment complement are nearly identical. Principal factors influencing the antenna locations are antenna pattern coverage requirements, proximity to equipment, EMC, and physical constraints. The most important of these factors is antenna pattern coverage and the same requirements are valid regardless of the aircraft size.

### 5.2 Antenna Location Considerations

In some instances an advantage can be obtained by degrading the isolation between antennas where the interference mode is predictable and can be controlled by frequency management in order to maximize the isolation between other antennas. An example of this is the UHF high power transmit and UHF receive antennas. Grouping the transmit antennas in one group on the forward top area of the airframe degrades the transmitter-to-transmitter intermodulation product interference mode but permits the UHF receive antenna to be located in areas to maintain maximum space isolation between transmit and receiver antennas which enhances performance in all other interference modes. Transmitter-to-transmitter intermodulation products can then be calculated and during the frequency allocation process these frequencies avoided for the UHF receive frequencies assigned.

Other obviously prudent measures should be taken in the assignment of antenna locations. Where directive antennas are employed in a fixed direction these should be located such that other antennas are not in the beam pattern. Wing shading can also be used to maximize the space isolation between antennas located on the top and bottom of the fuselage. The use of computer calculations that provide data on the

three isolation components due to space isolation, fuselage curvature, and wing shading can provide a good indication of the advantages which can be obtained due to these components.

## 6. ANALYSIS RESULTS - TYPICAL 26-7

This section presents some of the results of analyses which have been performed in the past. These examples are supplied to illustrate the type and magnitude of the data obtained from such an analysis.

### 6.1 Antenna Isolation

Antenna-to-antenna isolation values should be computed at several frequencies over the range of application. However, in a worst case evaluation the isolation value for the lowest frequency of application should be used. Table I contains some typical antenna isolations which have been selected from past analyses. Minimum and maximum isolations represent the range that can be expected for antennas that are spaced near and far respectively within the confines of an airframe.

### 6.2 Frequency Coincidence Interference

Frequency coincidence interference may occur when an operating transmitter is tuned so that either a fundamental, spurious, or harmonic output frequency falls on the operating frequency of a receiver at a signal level near the receiver threshold.

Interference by direct frequency coincidence will occur for virtually all equipments (transmitters and receivers) unless sufficient separation of operating frequencies is maintained.

The operating ranges of all pertinent equipments are illustrated in Figure 3. Both transmitter power output and receiver sensitivity levels are plotted versus frequency. This figure illustrates direct frequency coincidence between transmitters and receivers.

Transmitted power levels range between +40 dBm and +60 dBm and receiver sensitivities generally range between -93.0 dBm and -99 dBm. Thus, to avoid all interference isolations in the range of 126.5 to 159 dB must be achieved. This is illustrated in Figure 6. For direct frequency coincidence, the only significant factor contributing to isolation is antenna isolation. For the large quantity of antennas required, it is immediately obvious that isolations of the magnitude required to avoid interference cannot be achieved within the confines of an airframe. Therefore, the only alternative to provide satisfactory performance of multiple equipments within a limited frequency range is to maintain separation between the operating frequencies of individual equipments according to frequency allocation criteria which precludes interfering signals.

### 6.3 Harmonic Frequency Coincidence

The harmonic output of all transmitters must be analyzed to determine if the signal level of these harmonics at the receiver input is of sufficient level to cause interference. Of primary interest in the harmonic area is the HF equipments interfering with the VHF and UHF equipments, the VHF interfering with the UHF, and the UHF interfering with the TACAN receivers. VHF transmitter 2nd and 3rd harmonics are typically 60 dB down from the carrier level and fall within the UHF frequency band. The total isolation required to prevent interference is 83 dB. Examination of the worst case VHF-to-UHF antenna isolations makes it obvious that total isolation required cannot be achieved except in rare instances. Therefore, frequency management must be utilized to prevent UHF interference due to VHF transmitter harmonics. Such management requires the exclusion of tuning a VHF transmitter whose 2nd or 3rd harmonic falls upon a receive frequency in the UHF band.

A similar condition exists for the UHF 3rd harmonic which has coincidence with the identification transponder and TACAN receivers. Isolations required are 67 dB for the transponder and 93 dB for the TACAN receiver. Again the isolations required are quite high; however, the possibility of false indications will be inhibited by the modulation rejection characteristics of the receivers. Both equipments utilize a pulse-type modulation which may provide some rejection to the AM or FM type modulated signal which would be radiating from the UHF equipments.

The harmonic outputs of the HF transmitter are numerous since the operating range of the equipment covers several octaves of the frequency spectrum. Since space antenna isolations at HF are quite small (typically may be 6 dB) and the receiver sensitivity is -107 dBm, frequency management must be used to prevent interference with HF receivers.

For other HF operating frequencies the harmonics that fall in VHF and UHF bands were evaluated and the worst case values were plotted in Figure 7. Since isolations of 62 to 84.5 dB will be difficult to achieve, frequency management is required to avoid interference.

### 6.4 Transmitter Spurious Interference

The spurious outputs from high power UHF transmitters are a serious source of interference. These are typically required to be only 80 dB down from the desired carrier level. Thus, for a transmitted carrier level of +60 dB the spurious emissions may be radiating at a level as high as -20 dBm. An adjacent UHF receiver with a typical antenna isolation of 40 dB would receive this signal at -60 dBm.

which is much higher than the interference threshold (typically -107 dBm). The only feasible solution to this type of interference is to reduce the spurious level by the use of RF filters in the transmitter group. Filters are available which provide an additional 60 dB of isolation at  $\pm 5$  MHz of the carrier frequency but a compromise must be made in accepting the additional size, weight, and cost.

#### 6.5 Transmitter Intermodulation

UHF transmitter intermodulation interference is a major problem due to quantity of equipment involved. An example is illustrated in Figure 8 for transmitter Q radiating into transmitter P both of which are operating in close proximity to each other. An intermodulation product level will be shown to be a function of frequency separation and transmitter output filtering action. Line losses are neglected and no transmitter modulation is assumed (a worst case).

The orderly flow of interfering transmitter IM signal to result in a receiver compromise (worst case UHF system).

a.	XMTR output power	+60 dBm
b.	XMTR Q to XMTR P antenna isolation loss	-23.5 dB
c.	XMTR P IM conversion coefficient	-30 dB
d.	XMTR P rejection to Q (depends upon frequency separation)	To Be Determined
e.	Resulting IM signal power radiating from XMTR P (disregarding (d) )	+6.5 dBm
f.	XMTR rejection to IM (same as (d) )	To Be Determined
g.	XMTR P to RCVR K antenna isolation	38.5 dB
h.	Resulting IM signal level appearing at RCVR K input (assumes $f_{lm} = f_r = 2f_p - f_Q$ )	-32 dBm
i.	RCVR K sensitivity minus 10 dB	-109 dBm
j.	Required amount of IM suppression to result in no compromise	77 dB

The selectivity required at the transmitter output by either the normal output selectivity or by the combined transmitter output and an output filter selectivity may be one-half the suppression required above. This results from the interfering signal Q entering transmitter P off frequency and the resulting IM leaves the transmitter at the same frequency separation from P's center frequency but to the other side. The minimum frequency separation allowable to obtain the 77 dB with the normal rejection due to the output stage of the transmitter is 43 MHz. Such frequency separation is not feasible to maintain within a system using a high density of transmitting equipments operating in the same basic frequency range. Also, the isolation required is not achievable and therefore it must be concluded that frequency separation criteria is not a feasible solution for the transmitter-to-transmitter intermodulation problem encountered on this system. The alternative solution to this problem is to provide an analysis prior to assigning frequencies to ensure that transmitter intermodulation products do not fall on assigned receiver frequencies. The use of filters at the UHF transmitter output could be used to make frequency separation a feasible approach.

#### 6.6 Radar

Radar receivers use a waveguide transmission line for coupling the RF energy between the receiver/transmitter and the antenna. The radar receiver operates at a frequency of approximately 10 GHz. Typically waveguide transmission lines used for radar act as a waveguide below cutoff with an extremely high signal attenuation below the desired operating frequency. Since all potential sources of interference are well below the operating frequency of the radar receiver, the isolation is sufficiently great to preclude interference. The radar transmitter peak pulse output of +78 dBm at 10 GHz will be sufficiently isolated by a combination of antenna isolation and receptor antenna efficiencies to preclude out-of-band interference to other receptors of the aircraft. Antenna isolation at this higher frequency will account for approximately 70 dB attenuation to the nearest receive equipments. The directive nature of the radar antenna serves to enhance the electromagnetic isolation between equipments.

#### 6.7 TACAN

The TACAN receiver operates on a selected channel in the operating frequency range of 900 to 1213 MHz. The potential interference source for the TACAN receiver is the UHF transmitter 3rd harmonics. The potential for interference exists if the 3rd harmonic is a direct frequency coincidence with the receive TACAN frequency. TACAN has a sufficiently sharp selectivity characteristic to make feasible the use of frequency management to avoid this interference by not operating a UHF transmitter on a frequency that has a 3rd harmonic which coincides with the TACAN channel selected.

## 6.8 VHF Communications Equipment

The potential source of inband interference for the VHF equipment are the higher harmonics of the HF transmitters which are -73 dB and -83.7 dB below the fundamental frequency. For the worst case situation, the harmonic radiation from the HF transmitter would appear at a -13 dBm level and require 84.5 dB of additional isolation from the VHF equipment receiver sensitivity of 97.5 dBm. Typical antenna space isolation at these frequencies and approximately 100 feet distant from the HF probe antennas is 44 dB. The HF harmonics could therefore exceed the VHF receiver sensitivity by approximately 40 dB and be a serious source of interference. Frequency management techniques will be required to avoid tuning the HF transmitters such that harmonics fall on assigned VHF receiver frequencies.

## 6.9 Radio Altimeter

The radio altimeter uses transmit and receive antennas located on the bottom of the fuselage and operates in the frequency range of 4.25 to 4.35 GHz. This equipment is sufficiently isolated in frequency from the UHF and VHF communication equipments, such that any harmonics would be attenuated by equipment characteristics, antenna space isolation, and the downward directivity characteristic of the receive antenna to preclude the occurrence of interference.

## 6.10 ADF Equipments

Proper usage of ADF equipment always requires the employment of prudent operator judgment to insure that the desired signals are being obtained. Interference will occur if direct frequency coincidence of either fundamental or harmonic frequencies fall on the desired receiver operating frequency. Therefore, they must be treated as any other receiver operating in their frequency range. If it is desired, for instance, to use the ADF equipment in the UHF range, it would not be possible to accurately detect a distant signal which was on the same frequency as an operating UHF transmitter.

## 7. INTERFERENCE CONTROL

During the analysis many potential areas of interference which require frequency management to avoid will be identified. It must be concluded that collocation of a large quantity of RF transmitters and receivers within the confines of the airframe induces the requirement for interference control, via frequency management as a system design parameter.

### 7.1 General Frequency Management Criteria

Throughout the analysis specific frequency managements should be tabulated in detail. A summary of those areas requiring frequency management are illustrated in the matrix of Table II. The matrix identifies the receiving equipment in the first column and the source and type of interference in the second and third columns respectively. The last column contains the operating constraint required for effective control of the potential interferences.

Several types of operational constraints are required as follows:

- (a) Transmitter fundamental or harmonic frequencies must avoid fixed receiver frequencies.
- (b) Transmitter or receiver frequencies which are both variable must be selected to preclude mutual interference. Priority must be established for either transmit or receive operation.
- (c) Transmitter to receiver operating frequency separation must be maintained.
- (d) UHF Transmitter-to-transmitter 3rd and 5th intermodulation products must not fall on assigned receiver operating frequencies. Priority must be established for either transmit or receive operating frequencies.
- (e) Fixed transmit and receive frequencies such as guard channels, FAA traffic control, satellite, etc., must be considered to avoid frequency coincidence.

Transmitter and receiver operating frequency separations within the same operating ranges are required to achieve isolation via the equipment selectivity to preclude either receiver spurious responses or transmitter spurious output interference. Both types of interference occur at discrete frequencies which may or may not be predictable. However, even when predictable, the location of these interference types vary as a function of operating frequency and the large number of potential interference frequencies make it a difficult task to use interference control for each discrete interference frequency. Therefore, control is implemented over the frequency range in which discrete interference may occur by maintaining frequency separation between operating frequencies. It should be noted that interference free operation within this frequency range may be possible due to the discrete frequency nature of the interference.

### 7.2 Frequency Management Plan

The total frequency management plan to be used must be developed using inputs from the analysis and other sources. The information obtained from the analysis represents only one set of constraints for the total frequency management plan. The plan must consider all operational interfaces and the available

degrees of freedom for frequency allocations. The complexity of such a frequency plan makes it a laborious and difficult task to select compatible frequency assignments. The use of computer techniques for selected frequency assignments could be used to make this task relatively simple. An initial outlay would be required to develop the computer program, but new frequency assignments could be generated rapidly which could offset the cost of developing the program over the long term.

#### 8. REFERENCES

Bogdanor, Dr. J. L., Siegle M. D., and Weinstock, G. L., July 1971, "Intra-Vehicle Electromagnetic Compatibility Analysis Report" AFAL-TR-71-155, U.S. Air Force Avionics Laboratory, Wright Patterson Air Force Base, Ohio, U.S.A.

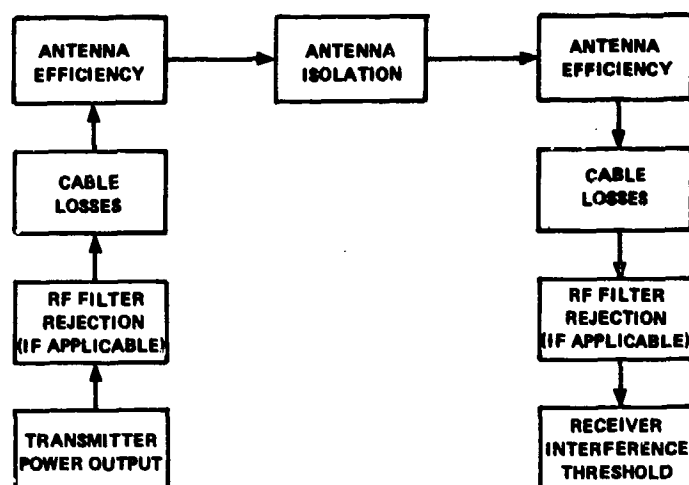


FIGURE 1. TYPICAL INTERFERENCE MODEL

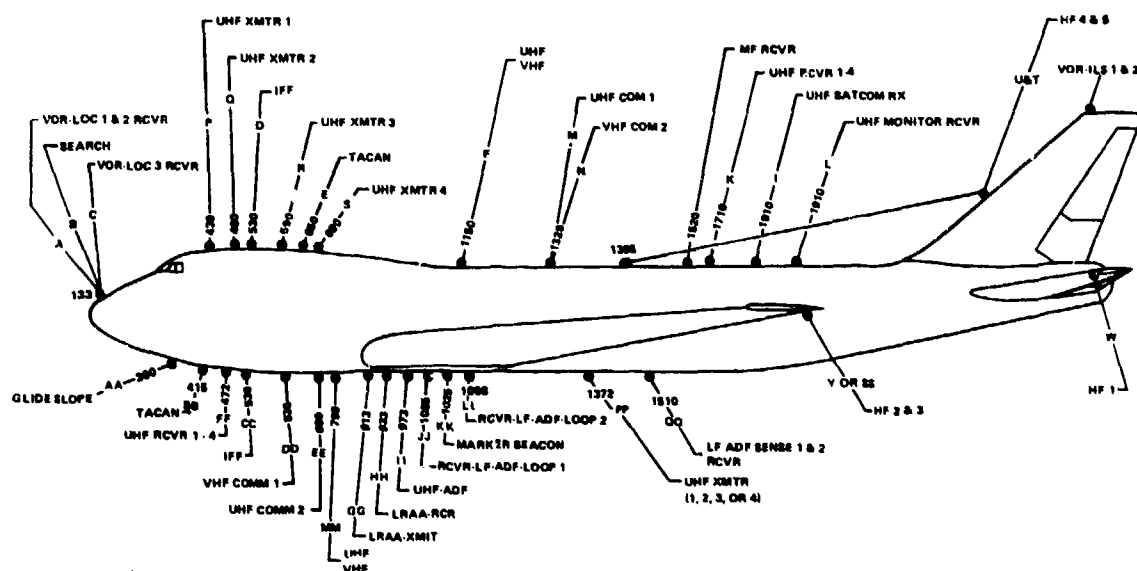


FIGURE 2. TYPICAL ANTENNA LOCATIONS

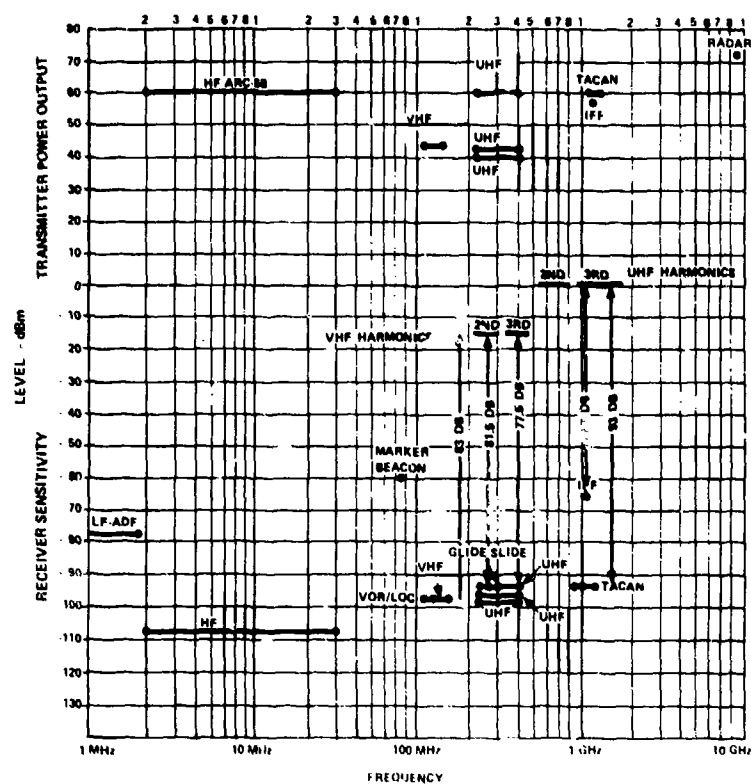


FIGURE 3. TRANSMITTER POWER OUTPUT AND RECEIVER SENSITIVITY VERSUS FREQUENCY

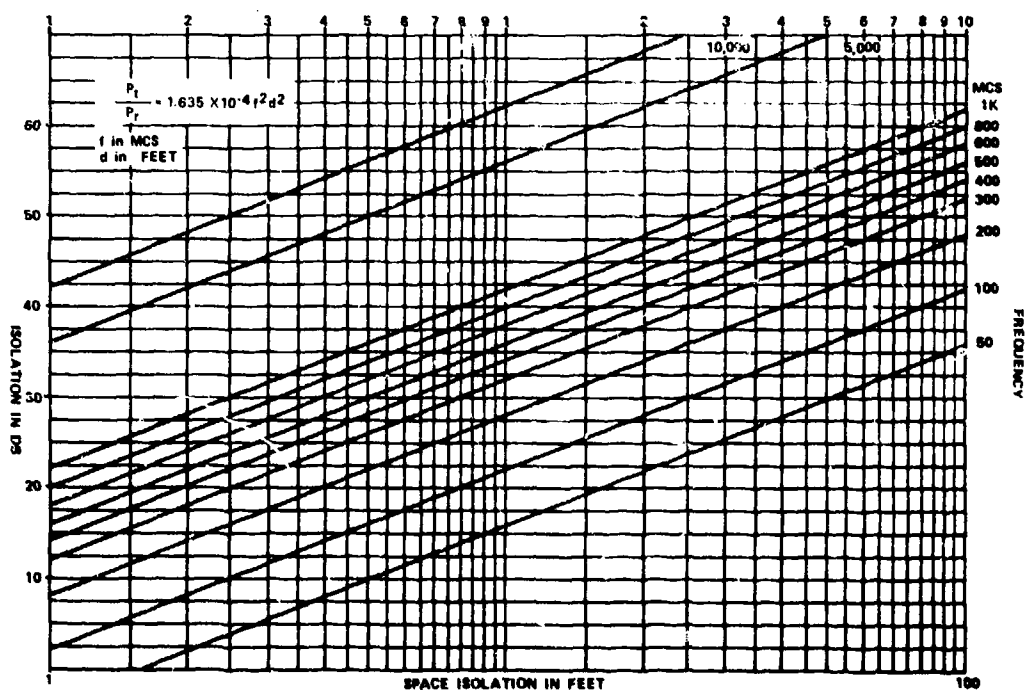


FIGURE 4. SPACE ISOLATION CHART FOR ISOTROPIC ANTENNA

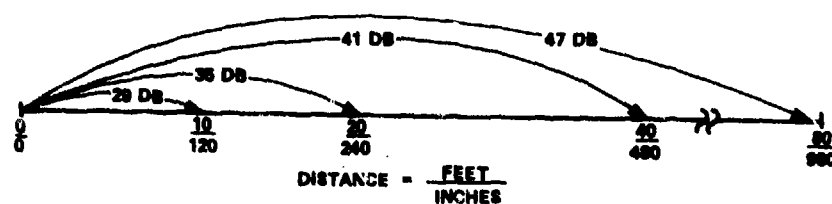


FIGURE 5. TYPICAL ANTENNA ISOLATION - 2.15 MHZ

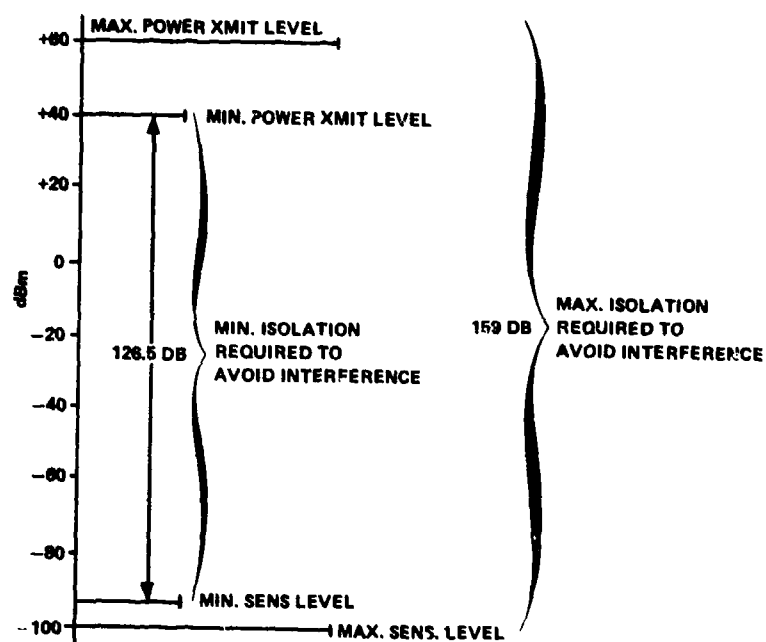


FIGURE 6. ISOLATION RANGE REQUIRED TO AVOID INTERFERENCE



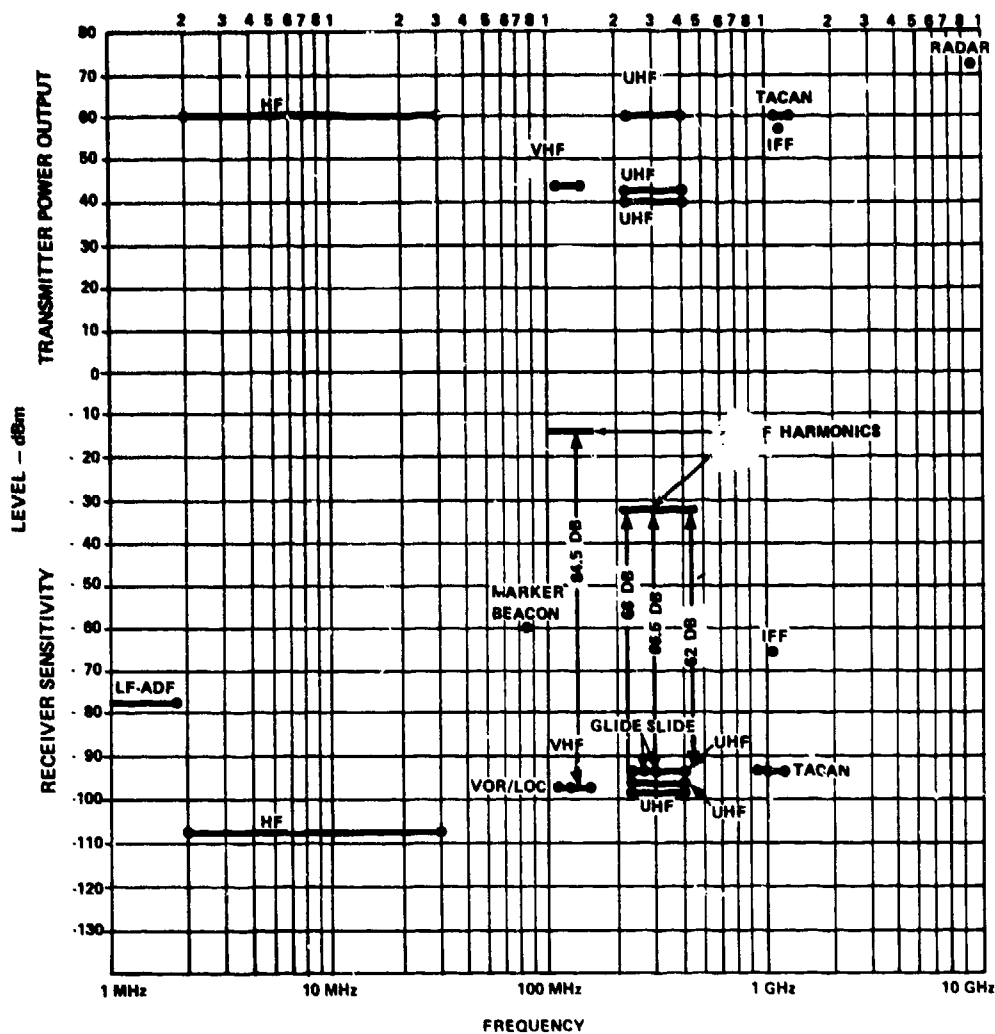


FIGURE 7. HF HARMONIC ISOLATION REQUIRED

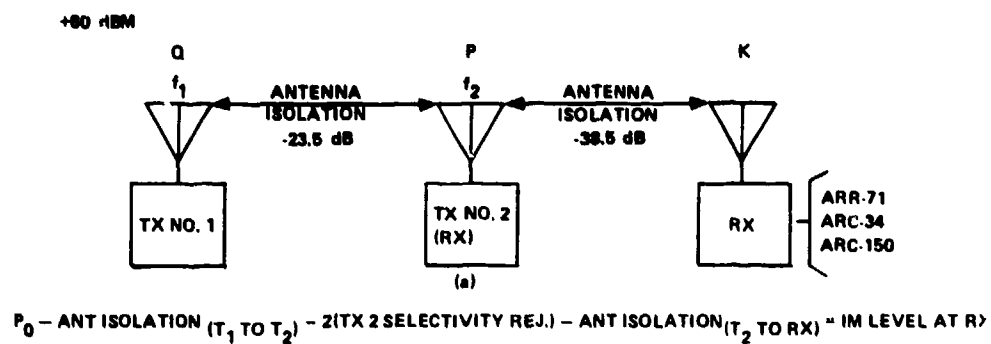


FIGURE 8.  
TRANSMITTER INTERMODULATION MODEL

**TABLE I**  
**TYPICAL ANTENNA ISOLATIONS**

ANTENNA PAIRS	ISOLATION AT LOWEST FREQUENCY RANGE - dB	
	MINIMUM	MAXIMUM
<b>UHF Transmit to UHF Receive</b>		
Top-to-Top	35	47
Top-to-Bottom	57	70
Wing Shading	0	24
Fuselage Curvature	1.4	3.6 (Typ)
Free Space	28	46
<b>UHF Transmit to UHF Transmit</b>		
Top-to-Top	19	33
Top-to-Bottom	48	61
<b>UHF Transmit 3rd Harmonic to TACAN</b>		
Top-to-Top	31	50
Top-to-Bottom	82	109
UHF to Glide Slope	48	75
VHF to VHF	22	51
VHF to VOR/LOC	33	55

**TABLE II. INTERFERENCE CONTROL SUMMARY**

RECEIVE EQUIPMENT	SOURCE OF INTERFERENCE				TYPE OF INTERFERENCE			SEVERITY OF INTERFERENCE	INTERFERENCE CONTROL REQUIRED
	HF	VHF	UHF	OTHER	HARMONICS OF LOWER FREQ. XMITR	RCVR DESENSITIZATION	XMITR IM		
HF	X					X		GREAT	SEPARATE RX & TX FREQ.
	X						X	GREAT	FREQ. MANAGEMENT
VHF-FM	X				X			SLIGHT	FREQ. MANAGEMENT
		X				X		GREAT	SEPARATE RX & TX FREQ. BY 8 MHz.
		X					X	SLIGHT	FREQ. MANAGEMENT
VHF-VOR/LOC	X				X			SLIGHT	FREQ. MANAGEMENT
		X				X		GREAT	VHF-FM DO NOT XMIT ON 108-118 MHz
		X						SLIGHT	FREQ. MANAGEMENT
MARKER BEACON	X				X			GREAT	HF DO NOT XMIT ON 25 MHz
UHF		X			X			GREAT	FREQ. MANAGEMENT
			X			X		GREAT	SEPARATE TX & RX FREQ. BY 16 MHz
			X				X	GREAT	FREQ. MANAGEMENT
UHF SATCOM			X			X		GREAT	DO NOT XMIT
			X				X	GREAT	FREQ. MANAGEMENT
		X			X			GREAT	FREQ. MANAGEMENT
UHF GLIDE SLOPE			X			X		GREAT	DO NOT XMIT ON 329-336 MHz
			X				X	GREAT	FREQ. MANAGEMENT
IFF					X			GREAT	FREQ. MANAGEMENT 3RD HARMONIC
				TACAN		X		GREAT	FREQ. MANAGEMENT
TACAN					X			GREAT	FREQ. MANAGEMENT 3RD HARMONIC
				IFF		X		GREAT	FREQ. MANAGEMENT

# ANALYSE DU BRUIT ET DE SON INFLUENCE SUR LES SYSTEMES DE COMMUNICATION

par Roger Gouillou

Office National d'Etudes et de Recherches Aéronautiques (ONERA)  
92320 Châtillon (France)

## RESUME

Cet article vise à fournir à l'ingénieur de télécommunications un guide pour réduire au minimum la perte d'information à travers la chaîne de réception d'un signal, en maintenant à un aussi faible niveau que possible l'introduction de bruit aux divers stades du traitement. Il résume, de ce point de vue, les nombreux travaux publiés sur ce sujet, et met en lumière les moyens pratiques conduisant au résultat.

Le bruit et le signal y sont considérés à travers leurs représentations spectrales respectives. Ceci permet, à l'aide de notions connues de chacun, de définir l'effet de masquage du signal par le bruit et de calculer l'évolution du niveau de bruit en fonction des traitements subis. Les formules ainsi établies sont aisément applicables dans les divers cas pratiques. Au passage, on examine les problèmes posés par la reconnaissance de la présence d'un signal dans le bruit.

Le présent article résume une Note Technique ONERA (n° 231) à paraître prochainement.

## ANALYSIS OF THE NOISE AND ITS INFLUENCE ON COMMUNICATION SYSTEMS

### SUMMARY

The paper aims at providing the communications engineer with guidelines in view to minimize the loss of information through signal reception and processing, by keeping to a minimum the introduction of noise at the different stages of data treatment. It summarizes, from this point of view, the many theoretical works found in the literature, and emphasizes the practical steps leading to the results.

Noise and signal are considered through their respective spectral representations. This permits, through well known concepts, a definition of the effect of signal masking by the noise, and the calculation of the noise level as a function of processing means. Formulas established this way are easily applicable to various practical cases. Problems raised by the discovery of the signal within the noise are also mentioned.

The present paper summarizes an ONERA Technical Note (n° 231) to be published shortly.

### I - INTRODUCTION

Dans tout système de communication radioélectrique, la limitation finale des performances résulte de la présence des bruits parasites qui se superposent au signal transmis. Il est indispensable d'en tenir compte pour déterminer le récepteur afin que le signal utile ne soit pas dégradé de façon excessive par le bruit, tout au long des traitements subis. Ceci fait l'objet de la théorie du signal ou de la théorie de la communication. Celles-ci ont été traitées entre autres par D. Gabor 1946, W.R. Bennet 1965, B. Picinbono 1964 et 1967, E. Roubine 1970 et J. Dupraz 1973. Il n'est cependant pas indispensable de connaître ces théories à fond pour comprendre les propriétés du bruit et suivre l'évolution du rapport entre le signal et le bruit tout au long du récepteur. Les données groupées dans le texte ci-après permettent de suivre cette évolution.

### II - LE BRUIT

Dans l'ensemble des signaux perturbateurs qui peuvent être captés par un récepteur, certains occupent une bande passante étroite. Ces brouilleurs sont relativement peu gênants car ils peuvent être aisément éliminés par un choix judicieux de la fréquence. Les autres ont une bande passante très large. Ils constituent le bruit de fond inévitable dans toute opération de traitement du signal. Remarquons tout d'abord que, si ces impulsions brèves de bruit ne se produisaient que de temps en temps, ou si leur cadence de répétition suivait une loi déterministe, il serait relativement aisé de réduire profondément leur influence sur le signal reçu. Aussi ne nous intéresserons-nous ci-après qu'aux bruits créés par des impulsions se succédant de façon erratique. Le spectre de ces bruits est continu dans une bande passante qui est en général large devant celle du récepteur. Il en résulte que la partie du spectre de bruit qui pénètre dans le récepteur est presque uniforme, d'où l'intérêt présenté par l'étude d'un « bruit blanc » hypothétique qui aurait une répartition spectrale constante d'un bout à l'autre de la bande de réception et dont le caractère erratique serait contenu dans le seul paramètre disponible du spectre ainsi décrit, c'est-à-dire porté par la phase des raies du spectre, laquelle varierait aléatoirement d'une raie à l'autre. Rappelons que la raie spectrale d'un bruit blanc est définie par sa largeur, laquelle est inséparable du temps total T, pendant lequel le signal est observé. Deux raies de bruit ont une existence individuelle quand l'observateur peut les séparer, c'est-à-dire quand elles sont écartées de  $1/T$ . Consulter par exemple P.M. Woodward 1953, P. Grivet 1958, A. Blanc-Lapierre 1953 et 1963.

La tension obtenue par l'addition de toutes ces raies spectrales a une valeur moyenne nulle et une puissance moyenne égale à la somme des puissances des raies du spectre. Quant à la valeur instantanée  $\vec{b}$  de cette tension, elle est caractérisée par la loi de répartition de son amplitude : c'est une courbe de Gauss, et par la loi de répartition des phases : toutes les valeurs angulaires sont équiprobables. Il est cependant bien commode de tenir compte de la puissance de bruit en introduisant une tension fictive  $\bar{b}$  qui aurait la même puissance que le bruit.

272

On peut déduire des propriétés ci-dessus, la probabilité  $P(|\vec{b}| > u)$  d'avoir le module  $|\vec{b}|$  du bruit supérieur à une valeur  $u$ . Elle est égale à la surface délimitée par la courbe de Gauss, au-delà des abscisses  $\pm u/\bar{b}$ .

Il vient

$$(1) \quad P(|\vec{b}| > u) = 1 - \sqrt{\frac{1}{2\pi}} \int_{-u/\bar{b}}^{+u/\bar{b}} e^{-(y/\bar{b})^2} dy$$

$P(|\vec{b}| > u)$  est tracé sur la figure 1.

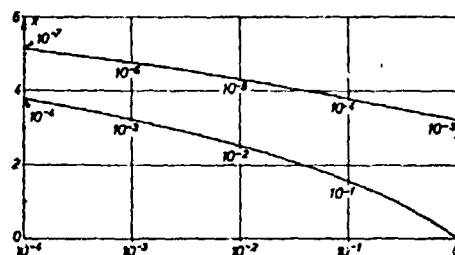


Fig. 1 - Probabilité de dépassement  $P(x)$  pour un bruit blanc  
 $P(|\vec{b}| > u) \quad x = u/\bar{b}$

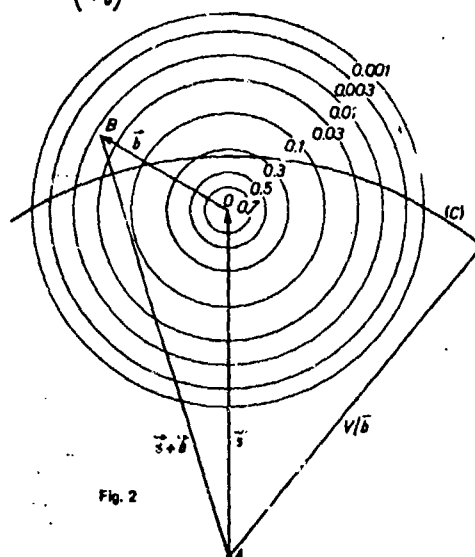


Fig. 2

Le fait que la phase du bruit a une répartition uniforme de probabilité permet de représenter l'addition d'un signal et du bruit par le diagramme vectoriel de la figure 2. Dans ce diagramme,  $\vec{OA}$  correspond au signal  $\vec{s}$ ,  $\vec{b}$  est représenté par un vecteur ayant une de ses extrémités au point O et l'autre extrémité dans le plan de la figure avec la probabilité  $P(|\vec{b}| > u)$  d'avoir un module  $|\vec{b}|$  supérieur à  $u$ . Les cercles ont pour rayon  $u/\bar{b}$  et portent le long de la circonférence le chiffre  $P(|\vec{b}| > u)$ .

La probabilité  $dP$  que le vecteur  $\vec{b}$  sorte d'un cercle de rayon  $u/\bar{b}$  par une zone angulaire déterminée de largeur  $d\Omega$  est

$$(2) \quad dP = P(|\vec{b}| > u) \cdot \frac{d\Omega}{2\pi}$$

La probabilité d'avoir le module de la somme du signal et du bruit supérieur à une certaine tension  $V$  est calculable par intégration des probabilités partielles constatées en chaque point du cercle  $c$  de rayon  $v/\bar{b}$  centré en A.

$$(3) \quad P(|\vec{s} + \vec{b}| > v) = \int_c P(\vec{b} > u) \frac{d\Omega}{2\pi}$$

La tension  $V_0$  pour laquelle on a

$$(4) \quad P(|\vec{s} + \vec{b}| > V_0) = 0,5$$

est donnée par

$$(5) \quad V_0^2 = s^2 + \bar{b}^2$$

La courbe  $P(|\vec{s} + \vec{b}| > v)$  est tracée sur la figure 3. Elle est valable tant que le rapport signal sur bruit est supérieur à 10 dB ( $s/\bar{b} > 10$  dB).

Sur la figure 3 a également été tracée la courbe symétrique donnant  $P(|\vec{s} + \vec{b}| < v)$  ainsi qu'une courbe parallèle à  $P(|\vec{b}| > u)$  passant par le point de probabilité 0,5 des courbes précédentes. On peut constater qu'il y a peu de différences entre  $P(|\vec{s} + \vec{b}| > v)$  et cette parallèle à  $P(|\vec{b}| > u)$ . En première approximation on peut donc écrire

$$(6) \quad P(|\vec{s} + \vec{b}| > v) \approx P(|\vec{b}| > v - s + 0,65 \bar{b}) \quad \text{pour } v > s$$

$$(7) \quad \text{et} \quad P(|\vec{s} + \vec{b}| < v) \approx P(|\vec{b}| < s - v + 0,65 \bar{b}) \quad \text{pour } v < s$$

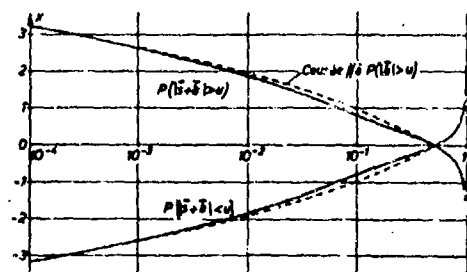


Fig. 3 - Probabilité d'avoir  $|\vec{s} + \vec{b}| > v$  ou  $< v$   $x = \frac{v - s}{\bar{b}}$

Ces expressions approchées peuvent faciliter certaines comparaisons.

Ces courbes de probabilité de dépassement doivent être utilisées à chaque fois que l'on doit rechercher la présence d'un signal dans le bruit. Appliquons-les à deux cas particuliers.

#### a) Recherche d'un signal à l'aide d'une batterie de filtres

Supposons qu'il puisse exister un signal occupant une bande de fréquence très étroite, quelque part à l'intérieur d'une bande passante large, et que l'on dispose d'un temps d'observation  $T$  pour déceler ce signal. Il est souhaitable de séparer la bande totale en un grand nombre de bandes élémentaires étroites, égales à  $1/T$ , vu que le bruit présent dans chacune d'elles sera plus faible que le bruit total tandis que dans l'une d'elles pourra apparaître le signal attendu. Des groupements de 500 filtres adjacents sont fréquemment utilisés dans ce but. Une transformée de Fourier à 500 points donnerait le même résultat. La figure 4 obtient expérimentalement représentée l'une quelconque des situations constatées à la sortie d'un ensemble de 500 filtres:

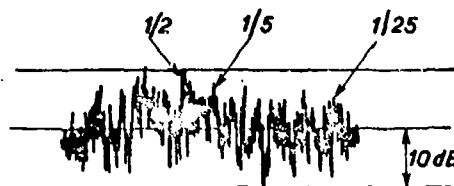


Fig. 4

La question principale que l'on se pose à l'examen d'une telle figure est de savoir s'il peut y avoir un signal superposé au bruit dans l'un ou l'autre des filtres. La réponse est obtenue à l'aide de la figure 3 qui permet de connaître la probabilité d'avoir la somme du bruit et du signal inférieure ou égale à ce que donne le bruit seul. Ainsi, dans l'hypothèse d'un signal qui serait 10 dB supérieur au niveau de bruit constaté dans chacun des filtres élémentaires, il y a une chance sur deux d'avoir le module de la somme du signal et du bruit plus faible que la plus forte tension de bruit constatée sur la figure 4. Ce module a une chance sur cinq d'être 2 dB plus bas et une chance sur vingt cinq d'être 5 dB plus bas que ce niveau de bruit maximum probable sur 500 filtres. Ce qui montre qu'un rapport signal sur bruit de 10 dB ne permet pas de prendre de décision en ce qui concerne la présence du signal, sauf si plusieurs spectres successifs sont examinés. Il faut  $s/b > 12$  dB pour avoir neuf chances sur dix que la tension du filtre contenant le signal soit plus forte que le bruit seul dans l'un quelconque des 500 filtres.

#### b) Utilisation d'un seuil pour déceler la présence d'un signal impulsionnel

Il est fréquent de vouloir déceler la présence d'un signal impulsionnel en vérifiant si la tension de sortie du récepteur dépasse un certain niveau. Il faut que ce seuil de tension soit assez élevé afin que le taux de fausses alarmes ne soit pas excessif. (Ce taux correspond au nombre de fois chaque seconde où le bruit excède le seuil). Mais il ne doit pas l'être de trop afin que les impulsions utiles soient effectivement détectées.

Soient  $U$  la tension de seuil et  $B$  la bande passante du récepteur, chiffrée en Hertz.

Le taux de fausses alarmes est donné par

$$(8) \quad \bar{\alpha} = B \times P(|\tilde{b}| > u)$$

La probabilité de non détection du signal est  $k = P(|\tilde{s} + \tilde{b}| < u)$

exemple : soient  $B = 1$  MHz ;  $\bar{\alpha} \leq 100$  ;  $k \leq 1/100$ , il vient :

$$(9) \quad P(|\tilde{b}| > u) \leq 10^{-4} \Rightarrow u \geq 3,7\bar{b}$$

$$(10) \quad P(|\tilde{s} + \tilde{b}| < u) \leq 10^{-2} \Rightarrow u - \sqrt{s^2 + \bar{b}^2} < -1,9\bar{b}$$

d'où

$$(11) \quad \text{ou} \quad \begin{aligned} s &> 5,6\bar{b} \\ s/\bar{b} &> 15 \text{ dB} \end{aligned}$$

### III - TRANSFORMATIONS SUBIES PAR LE SIGNAL ET LE BRUIT A L'INTERIEUR D'UN RECEPTEUR

#### 3.1. Rapport signal sur bruit à l'entrée du récepteur

Les opérations subies par le signal et le bruit à l'intérieur du récepteur sont des amplifications, des mélanges avec d'autres signaux, des filtrages et des détections. Sauf en ce qui concerne l'amplification, ces opérations dégradent l'information reçue en accroissant le niveau de bruit par rapport au niveau du signal. Pour chiffrer cette dégradation nous allons calculer le rapport signal/bruit obtenu à la sortie du récepteur et le comparer au rapport signal/bruit fictif qui aurait été obtenu sans aucune perte de qualité et qui existe potentiellement à l'entrée du récepteur.

Soit  $(s/b)_e$  ce rapport. Il est obtenu en divisant la tension  $s$  du signal par la tension que créerait le bruit entrant dans le récepteur s'il était limité à une bande de fréquence de largeur  $\beta$  égale à celle utilisée dans le filtre de sortie du récepteur. Désignons par  $W_b$  la puissance de bruit obtenue dans la bande passante effective  $B$  des circuits de filtrage moyenne fréquence du récepteur et par  $W_s$  la puissance du signal.

Il vient alors

$$(12) \quad (s/b)_e = \sqrt{\frac{W_b}{W_s \beta}}$$

### 3.2. Bruit obtenu à la sortie d'un mélangeur

27-4

Considérons le cas d'un mélangeur dans lequel les deux signaux  $S_1$  et  $S_2$  seraient brouillés par des bruits  $b_1$  et  $b_2$ . Le rôle du mélangeur est d'effectuer le produit des signaux présents sur ses deux bornes d'entrée, puis de filtrer le signal de sortie. Ceci correspond à l'opération

$$(13) \quad \frac{1}{2} (S_1 + b_1)(S_2^* + b_2^*) = \frac{1}{2} (S_1 S_2^* + b_1 S_2^* + S_1 b_2^* + b_1 b_2^*)$$

(l'astérisque désigne la quantité imaginaire conjuguée).

La seule partie utile du signal sortant du mélangeur provient du terme  $S_1 S_2^*$ . Chacun des trois autres termes correspond à un bruit parasite.

Afin de connaître le niveau de bruit à la sortie du mélangeur, il faut tout d'abord calculer la répartition spectrale obtenue par l'addition des trois termes de bruit. Pour cela on définit les signaux et les bruits par leurs spectres de fréquence

$$(14) \quad S_1 = \mathcal{R} \sum_k a_{1k} e^{j 2\pi (F_1 + f_k) t + \varphi_k}$$

$$(15) \quad S_2 = \mathcal{R} \sum_l a_{2l} e^{j 2\pi (F_2 + f_l) t + \varphi_l}$$

$$(16) \quad b_1 = \mathcal{R} \sum_k d_{1k} e^{j 2\pi (F_1 + g_k) t + \theta_k}$$

$$(17) \quad b_2 = \mathcal{R} \sum_l d_{2l} e^{j 2\pi (F_2 + g_l) t + \theta_l}$$

auxquels correspondent les puissances moyennes

$$(18) \quad W_1 = \frac{1}{2} \sum_k a_{1k}^2$$

$$(19) \quad W_2 = \frac{1}{2} \sum_l a_{2l}^2$$

$$(20) \quad W_{b1} = \frac{1}{2} \sum_k d_{1k}^2$$

$$(21) \quad W_{b2} = \frac{1}{2} \sum_l d_{2l}^2$$

Puis on recherche quels sont les produits élémentaires entre raies de bruits ou entre les raies spectrales des signaux et celles des bruits qui sont capables de faire apparaître une fréquence  $F_1 - F_2 + \nu$  donnée. Les phases étant aléatoires, la puissance de la raie correspondant  $\nu$  dans le spectre cherché est obtenue par addition des puissances des termes élémentaires.

A titre d'exemple, la figure 5 représente le spectre des signaux et des bruits  $S_1$ ,  $b_1$  centrés sur la fréquence  $F_1$  et  $S_2$ ,  $b_2$  centrés sur  $F_2$ , la répartition spectrale de puissance correspondant aux produits  $b_1 b_2^*$ ,  $s_1 b_2^*$  et  $s_2 b_1^*$  ainsi que le spectre global de bruit obtenu après mélange. Un filtre centré sur  $F_1 - F_2$ , ayant une bande passante étroite  $\beta$ , recueillirait une puissance de bruit donnée par l'expression

$$(22) \quad W_\beta = [W_{b1} \cdot W_{b2} + W_1 W_{b2} + W_2 W_{b1}] \frac{\beta}{2B}$$

### 3.3. Corrélation de deux signaux semblables

Considérons le cas d'une corrélation entre deux signaux  $S_1$  et  $S_2$  très voisins l'un de l'autre; superposés chacun à des bruits  $b_1$  et  $b_2$ . La corrélation consiste à mesurer le niveau de la composante de fréquence  $F_1 - F_2$  résultant du mélange, laquelle est séparée des autres signaux par un filtre de bande passante  $\beta$ .

Dans ce cas, ce niveau est donné par :

$$(23) \quad \begin{aligned} \rho &= S_1 S_2^* = \frac{1}{2} \mathcal{R} \sum_k a_{1k} e^{j 2\pi (F_1 + f_k) t + \varphi_k} \\ &\quad \sum_l a_{2l} e^{-j 2\pi (F_2 + f_l) t + \varphi_l} \end{aligned}$$

avec

$$k = l \quad \text{et} \quad a_{1k} = a_{2k} = a_k \quad W_1 = W_2$$

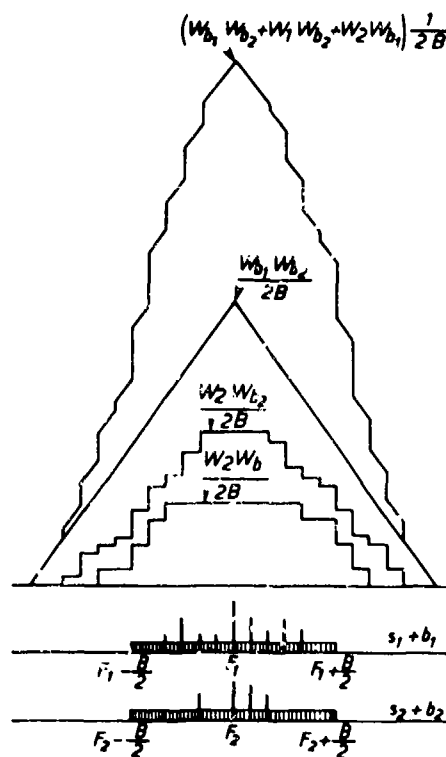


Fig. 5

$$(24) \quad s = \Re \sum \frac{1}{2} \alpha_i^2 e^{j 2\pi (f_i - f_c) t} = W \Re e^{j 2\pi (f_c - f_s) t}$$

27-5

Tandis que le niveau du bruit de sortie  $b_1$  est obtenu à partir de l'expression (22) pour  $W = W_1 = W_2$  et  $W_{b1} \approx W_{b2}$

$$(25) \quad W_{\beta s} = (W_b^2 + 2 W W_b) \frac{\beta}{2 B}$$

$$(26) \quad b_s = \sqrt{2 W_{\beta s}} = \sqrt{(W_b^2 + 2 W W_b) \frac{\beta}{B}}$$

$$(27) \quad b_s = \sqrt{2 W W_b \frac{\beta}{B}} \sqrt{1 + \frac{W_b}{2 W}}$$

d'où le rapport signal/bruit après corrélation

$$(28) \quad (s/b)_s = \frac{W}{\sqrt{2 W W_b \frac{\beta}{B}} \sqrt{2(1 + W_b/2W)}} = \sqrt{\frac{W B}{W_b \beta}} \frac{1}{\sqrt{2(1 + \frac{W_b}{2W})}}$$

ce qui, d'après (8) peut s'écrire

$$(29) \quad (s/b)_s = (s/b)_e \frac{1}{\sqrt{2 + (\frac{b}{s})^2 \frac{B}{\beta}}}$$

La dégradation de  $s/b$  dans le mélange peut être importante.

exemple : soit  $(s/b)_e = 17$  dB et  $B/\beta = 10^4$ , il vient

$$(30) \quad \sqrt{2 + (\frac{b}{s})^2 \frac{B}{\beta}} = \sqrt{2 + \frac{10^4}{50}} = \sqrt{202} = 14 \Rightarrow 23 \text{ dB}$$

Le rapport signal/bruit est dégradé de 23 dB.

### 3.4. Cas du récepteur adapté

Supposons que le signal  $S_2$  appliqué sur la 2<sup>e</sup> voie du mélangeur soit créé localement et ne contienne aucun bruit. C'est ce qui est réalisé dans les récepteurs dits adaptés au signal attendu où  $S_2$  est une réplique locale reproduisant aussi fidèlement que possible le signal que l'on escompte recevoir.

On a alors dans (22)  $W_{b2} = 0$  ce que donne

$$(31) \quad (s/b)_s = \frac{\sqrt{W_1 W_2}}{\sqrt{W_2 W_{b1} \frac{\beta}{B}}} = \sqrt{\frac{W_1}{W_{b1} \frac{\beta}{B}}}$$

d'où

$$(32) \quad (s/b)_s = (s/b)_e$$

Le traitement effectué dans le récepteur adapté ne dégrade pas le rapport signal/bruit.

### 3.5. Cas de la détection quadratique

La détection quadratique correspond à l'opération

$$(33) \quad \frac{1}{2} (s_1 + b_1)(s_1^* + b_1^*)$$

Le cas de la détection linéaire en est voisin. Il a été traité par K. Franz 1941, W.R. Bennet 1944, R.H. de Lano 1949.

Dans le calcul, il faut tenir compte de ce que les deux facteurs de (33) contiennent le même bruit. Effectuons-le dans le cas où  $S_1$  est modulé en amplitude par un seul signal basse fréquence.

On a alors :

$$(34) \quad S_1 = A (1 + m \cos \Omega t) \cos \omega t$$

ou encore :

$$(35) \quad S_1 = \Re \left\{ A e^{j\omega t} + \frac{mA}{2} e^{j(\omega+\Omega)t} + \frac{mA}{2} e^{j(\omega-\Omega)t} \right\}$$



La puissance de ce signal est

$$(36) \quad W = \frac{a^2}{2} \left( 1 + \frac{m^2}{2} \right)$$

27-6

Par ailleurs :

$$(37) \quad b_i = \Re \left\{ \sum_l d_l e^{j(\omega + 2\pi f_l)t + \theta_l} \right\}$$

La sommation est étendue à la bande  $B$  du récepteur d'où la puissance de bruit

$$(38) \quad W_b = B \frac{d^2}{2}$$

Calculons tout d'abord  $b_i b_i^*$

$$(39) \quad \frac{1}{2} b_i b_i^* = \frac{d_i^2}{2} \sum_l \sum_k e^{j2\pi(f_l - f_k)t + \theta_l - \theta_k}$$

Il diffère des calculs précédents par le fait que pour  $i = k$ , c'est-à-dire à la fréquence zéro, la phase de tous les termes élémentaires est nulle

$$(40) \quad \theta_i - \theta_k = 0 \text{ pour } i = k$$

Ceci donne naissance à une raie dont l'amplitude est

$$(41) \quad V = B \frac{d^2}{2} = W_b$$

alors que l'amplitude des raies de fréquence voisine dans une bande de fréquence étroite  $\beta$  est donnée par

$$(42) \quad U = \sqrt{\frac{2\beta}{B}} W_b$$

De même l'identité des bruits intervient dans le calcul de  $S_i b_i^*$  et de  $S_i^* b_i$

$$(43) \quad \frac{1}{2} S_i b_i = \Re \sum_l \frac{a d_l}{2} e^{-j(2\pi f_l t + \theta_l)} + \Re \sum_l \frac{m a d_l}{4} e^{j(\Omega - 2\pi f_l t - \theta_l)} + \Re \sum_l \frac{m a d_l}{4} e^{-j(\Omega + 2\pi f_l t + \theta_l)}$$

$$(44) \quad \frac{1}{2} S_i^* b_i = \Re \sum_l \frac{a d_l}{2} e^{j(2\pi f_l t + \theta_l)} + \Re \sum_l \frac{m a d_l}{4} e^{-j(\Omega - 2\pi f_l t - \theta_l)} + \Re \sum_l \frac{m a d_l}{4} e^{j(\Omega + 2\pi f_l t + \theta_l)}$$

La somme de ces deux produits peut s'écrire, en remarquant que le signe de la phase ne modifie pas les parties réelles

$$(45) \quad \frac{1}{2} S_i b_i + \frac{1}{2} S_i^* b_i = \Re \sum_l a d_l e^{j(2\pi f_l t + \theta_l)} + \Re \sum_l \frac{m a d_l}{2} e^{j(\Omega - 2\pi f_l t - \theta_l)} + \Re \sum_l \frac{m a d_l}{2} e^{j(\Omega + 2\pi f_l t + \theta_l)}$$

à partir de quoi la méthode précédemment décrite conduit aux répartitions spectrales de puissance de la figure 6.

Par ailleurs le produit  $S_i S_i^*$  donne

$$(46) \quad \frac{1}{2} S_i S_i^* = \Re \left\{ \frac{a^2}{2} \left( 1 + \frac{m^2}{2} \right) + m a^2 e^{j\Omega t} + \frac{m^2 a^2}{4} e^{j2\Omega t} \right\}$$

Un filtre de largeur de bande  $\beta$  centré sur  $\Omega/2\pi$  recueille alors le signal  $s$  et un bruit  $b$  avec

$$(47) \quad s = m a^2$$

ou d'après (32)

$$(48) \quad s = \frac{4mW}{2+m^2}$$

et  $b$ , dépendant légèrement de  $\Omega$ .

Si  $\Omega/2\pi \ll B/2$  il vient

$$(49) \quad b_s = 2 \sqrt{W W_b \frac{\beta}{B}} \sqrt{2 + \frac{W_b}{2W}}$$

d'où

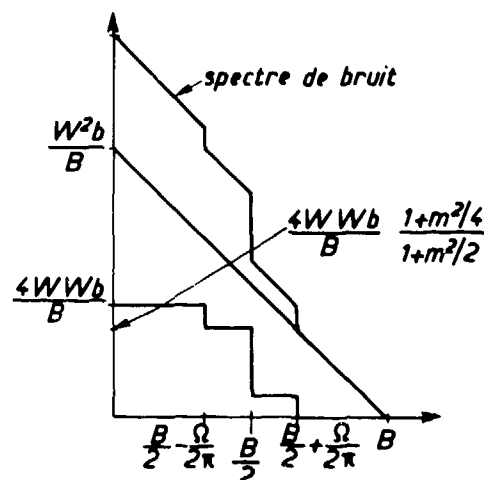


Fig. 6

$$(50) \quad \left(\frac{a}{b}\right)_a = \frac{m}{1+\frac{m^2}{2}} \sqrt{\frac{WB}{W_b \beta}} \frac{1}{\sqrt{2+\frac{W_b}{2W}}}$$

ou encore

$$(51) \quad \left(\frac{a}{b}\right)_a = \left(\frac{a}{b}\right)_e \frac{m}{1+\frac{m^2}{2}} \frac{1}{\sqrt{2+\frac{(b/a)^2}{2} \frac{B}{\beta}}}$$

Dans le cas où  $\Omega/2\pi \approx B/2$  on trouve

$$(52) \quad b_a = 2 \sqrt{W W_b \frac{\beta}{B}} \sqrt{\frac{4+m^2}{2+m^2} + \frac{W_b}{4W}}$$

et

$$(53) \quad \left(\frac{a}{b}\right)_a = \left(\frac{a}{b}\right)_e \frac{m}{1+\frac{m^2}{2}} \frac{1}{\sqrt{\frac{4+m^2}{2+m^2} + \left(\frac{b}{a}\right)_e^2 \frac{B}{4\beta}}}$$

application : soit  $\left(\frac{a}{b}\right)_e = 20$  dB

$m = 1$   $B = 100$  kHz  $\beta = 10$  Hz

dans le cas où  $\Omega/2\pi \ll B/2$  (47) donne  $\left(\frac{a}{b}\right)_a = 10 \frac{1}{1,5} \times \frac{1}{\sqrt{52}} = 0,93$

et si  $\Omega/2\pi \approx B/2$  (49) donne  $\left(\frac{a}{b}\right)_a = 10 \times \frac{1}{1,5} \frac{1}{\sqrt{\frac{5}{3} + 25}} = 1,3$

## CONCLUSION

Faisant suite à une analyse des perturbations provoquées par le bruit sur un signal, un examen des différents termes de bruit obtenus au cours du traitement effectué à l'intérieur du récepteur a permis de calculer le rapport signal sur bruit existant à la sortie du récepteur à l'aide d'une méthode simple ne nécessitant pas le recours aux théories précises habituelles. Les exemples donnés peuvent être généralisés aux diverses opérations effectuées au cours du traitement de l'information dans les systèmes de communication.

## BIBLIOGRAPHIE

- W.R. BENNET - Response of linear rectifier to signal and noise. Bell Syst. Tech. Jour., New York, Jan. 1944.
- W.R. BENNET - a) Theory of Noise (chap. 2)  
b) Response of devices to noise (chap. 3)  
c) Noise plus signal situations in radar (chap. 4)  
dans Modern Radar, part II, édité par R.S. Berkowitz - Wiley, New York, 1965.
- A. BLANC-LAPIERRE, R. FORTET - Théorie des fonctions aléatoires, Masson, Paris 1953.
- A. BLANC-LAPIERRE, and al. - Modèles statistiques pour l'étude des phénomènes de fluctuation, Masson, Paris, 1963.
- R.H. DE LANO - Signal to noise ratios of linear detectors. P.I.R.E., Oct. 1949.
- J. DUPRAZ - Théorie de la communication - Eyrolles, Paris 1973.
- K. FRANZ - Passage de bruit à travers un détecteur linéaire. H.F. Tech. El. Ak., juin 1941.
- D. GABOR - Theory of communication, Pt III vol. 93 (1946). J.I.E.E. (London).
- P. GRIVET, A. BLAQUIERE - Le bruit de fond, Masson, Paris (1958).
- B. PICINBONO - Problèmes liés à l'utilisation des corrélateurs (p. 53-62) et Généralités sur les problèmes de fluctuation en physique (p. 63-72) - Revue du CETHEDC n° 1, Paris 1964.
- B. PICINBONO - Eléments sur les théories du signal, de la détection et de l'information.  
1<sup>re</sup> partie - Théorie du signal (p. 3-33)  
2<sup>e</sup> partie - Théorie de la détection (p. 35-72)  
3<sup>e</sup> partie - Eléments sur la théorie de l'information (p. 73-98) } Revue du CETHEDC n° 11, Paris 1967.
- E. ROUBINE - Introduction à la théorie de la communication. Tome I, Signaux non aléatoires - Tome II, Signaux aléatoires, Tome III, Théorie de l'information. Masson, Paris 1970.
- P.M. WOODWARD - Probability and information theory. Pergamon Press, Oxford (1953) et Mac Graw Hill, New York (1953).

27-7

COMPUTER MODELING OF COMMUNICATIONS RECEIVERS  
FOR DISTORTION ANALYSIS

28-1

J.F. Spina  
Rome Air Development Center  
United States Air Force  
Griffiss Air Force Base, New York

D.D. Weiner  
Syracuse University  
Syracuse, New York

SUMMARY

The purpose of this paper is to present the details of an analysis technique and companion computer program having application in the area of design and analysis of electronic circuits. Particular emphasis is placed upon the application of the program to the modeling of nonlinear distortion effects in communication receivers. The paper will begin with a discussion of "moderately" nonlinear systems and the treatment of such systems using the nonlinear transfer function approach. Following this, the discussion will center upon application in circuit analysis as a potential tool in designing and evaluating circuits from an electromagnetic compatibility point of view. The final section will present an overview of the computer program in terms of some of its more salient features.

1. INTRODUCTION

Although the digital computer has played a key role in the Electromagnetic Compatibility (EMC) field for many years (DOD, March 1969), the recent thrust for incorporating in EMC in the early phases of the system acquisition cycle (Rand Report, R-1114-PR, May 1973, An Electromagnetic Compatibility Program for the 1970s) has put a new and clear focus upon the computer. The development of large system modeling programs that aid system planners and designers require computer code that is equipment-design oriented. A necessary ingredient in the large EMC system model is the ability to characterize the nonlinear behavior of the individual equipments that comprise the system. Consideration of all system aspects such as propagation paths, coupling to cables and wire bundles, antenna behavior, etc. is of course required, but will not be treated here. The emphasis, in this paper will be focused upon modeling and analysis of nonlinear effects in communications receivers. The ability to adequately account for the behavior of the receivers in a large system provides the system designers with the information needed to assign frequencies, guard band spacing, and determine filtering requirements among others. The large majority of interference problems that manifest themselves in receivers are caused by nonlinear behavior of the receivers. Such familiar interference effects such as intermodulation, desensitization, gain compression/expansion, cross-modulation, and spurious responses are all nonlinear effects. Intermodulation and cross-modulation, in particular, can be very significant problems in congested collocated equipment environments.

A thorough understanding of the distortion mechanism in nonlinear circuits is essential in order to determine optimal system design.

2. THE NONLINEAR TRANSFER FUNCTION APPROACH TO CIRCUIT ANALYSIS

The purpose of this section is to present the basic theory behind the approach for characterizing electronic systems that, due to nonlinear behavior, are susceptible to radio frequency interference. First, a brief introduction to the Volterra-Wiener analysis of nonlinear networks is presented. This material provides the framework for characterizing the nonlinear transfer functions of complex nonlinear networks. Next, the canonic model concept is presented whereby large circuits can be represented in terms of circuit independent building blocks of known form and circuit dependent parameters. This representation allows attention to be focused on the various nonlinear distortion products and their relationship to the circuit nonlinear transfer functions.

The basis of our approach to modeling equipments that exhibit nonlinear behavior is known as the Volterra, (Volterra, 1930) functional series. This series takes the form

$$w(t) = \int_{-\infty}^{\infty} h_1(\tau) x(t-\tau) d\tau + \iint_{-\infty}^{\infty} h_2(\tau_1, \tau_2) x(t-\tau_1) x(t-\tau_2) d\tau_1 d\tau_2 + \dots \quad (1)$$

This can be written as

$$w(t) = \sum_{k=1}^{\infty} \int \dots \int h_k(\tau_1, \tau_2, \dots, \tau_k) x(t-\tau_1) x(t-\tau_2) \dots x(t-\tau_k) d\tau_1 \dots d\tau_k \quad (2)$$

Nobert Wiener (Wiener, N., 1942) applied the Volterra series to the analysis of nonlinear systems. He recognized that the Volterra series could be used to relate the input of a nonlinear system,  $x(t)$ , to

the output,  $w(t)$ , via the Volterra series. Figure 1 illustrates conceptually a nonlinear system in terms of the Volterra series. In equation (2)  $h_k(\tau_1, \tau_2, \dots, \tau_k)$  is called the nonlinear impulse response of  $k^{\text{th}}$  order. The Fourier transform of the time domain kernel is called the  $k^{\text{th}}$  order nonlinear transfer function and is given by

$$28-2 \quad H_k(f_1, f_2, \dots, f_k) = \int_{-\infty}^{\infty} \dots \int_{-\infty}^{\infty} h_k(\tau_1, \tau_2, \dots, \tau_k) e^{-j2\pi(f_1\tau_1 + \dots + f_k\tau_k)} d\tau_1 \dots d\tau_k \quad (3)$$

The inverse Fourier transform produces

$$h_k(\tau_1, \tau_2, \dots, \tau_k) = \int_{-\infty}^{\infty} \dots \int_{-\infty}^{\infty} H_k(f_1, \dots, f_k) e^{j2\pi(f_1\tau_1 + \dots + f_k\tau_k)} df_1 \dots df_k \quad (4)$$

Substituting (4) into (1) yields

$$w(t) = \sum_{k=1}^{\infty} \int_{-\infty}^{\infty} \dots \int_{-\infty}^{\infty} H_k(f_1, \dots, f_k) \chi(f_q) e^{j2\pi f_q t} df_q \quad (5)$$

Here the output time function is expressed in terms of the input frequency function  $\chi(f)$ . This is illustrated in Figure 2.

Equations (1) and (2) imply that nonlinear systems, in general, can be characterized by the block diagrams in Figures 1 and 2. This approach assumes that the response of a nonlinear system can be represented as the sum of  $N$  components; the first due to the linear portion of the system, the second due to the quadratic portion of the system, and so on. Only  $N$  blocks are included in the model because it is assumed that higher order portions of the system contribute negligibly to the output.

It can be shown (Bussgang, J., 1974) that the nonlinear transfer functions,  $H_k(f_1, f_2, \dots, f_k)$ ;  $k=1, 2, 3, \dots, N$ , completely characterize a nonlinear system of highest significant order  $N$ . Given the nonlinear transfer functions, it is possible to determine the response to any input.

Although equations (1) and (2) are valid for arbitrary inputs, the case for which  $x(t)$  is a sum of complex exponentials is of particular interest. Let

$$x(t) = \sum_{i=1}^N e^{j2\pi f_i t} \quad (6)$$

Substitution of equation (6) into equation (2) and use of equation (3) results in

$$\begin{aligned} w(t) = & \sum_{i=1}^N H_1(f_i) e^{j2\pi f_i t} + \sum_{i_1=1}^n \sum_{i_2=1}^n H_2(f_{i_1}, f_{i_2}) e^{j2\pi(f_{i_1} + f_{i_2})t} \\ & + \sum_{i_1=1}^n \sum_{i_2=1}^n \sum_{i_3=1}^n H_3(f_{i_1}, f_{i_2}, f_{i_3}) e^{j2\pi(f_{i_1} + f_{i_2} + f_{i_3})t} \\ & + \dots \\ & + \sum_{i_1=1}^n \sum_{i_2=1}^n \dots \sum_{i_N=1}^n H_N(f_{i_1}, f_{i_2}, \dots, f_{i_N}) e^{j2\pi(f_{i_1} + f_{i_2} + \dots + f_{i_N})t} \end{aligned} \quad (7)$$

Note that  $H_p(f_{i_1}, f_{i_2}, \dots, f_{i_p})$  is the nonlinear transfer function associated with the complex exponential output at frequency  $(f_{i_1} + f_{i_2} + \dots + f_{i_p})$ . (For the case in which the input consists of a single complex exponential at frequency  $f_0$

$$x(t) = e^{j2\pi f_0 t} \quad (8)$$

and Eq. (7) reduces to

$$w(t) = \sum_{p=1}^N H_p(f_0, \dots, f_0) e^{j2\pi p f_0 t} \quad (9)$$

Eq. (7) demonstrates that, when a nonlinear system is excited by a sum of frequencies as in Eq. (6), the output contains new frequency components in addition to those at the input frequencies. The set of possible frequencies is given by  $m_1 f_1 + m_2 f_2 + \dots + m_n f_n$  where the  $(m_p)$  are integers such that  $0 \leq m_p \leq N$  and  $\sum_{p=1}^n m_p \leq N$ . Knowledge of the nonlinear transfer functions is sufficient to determine various frequency components of the response.

The nonlinear transfer functions can be derived using conventional circuit analysis techniques. Consider the transistor amplifier of Figure 3. Figure 4 illustrates the linear incremental equivalent circuit using the convention T model for the transistor. In actuality,  $r_e$ ,  $C_e$ ,  $C_c$ , and  $\alpha$  are not linear components. The base-emitter resistance  $r_e$  is a nonlinear function of the emitter current which is, in itself, a function of  $v_2$ . In Figure 5 this nonlinearity is represented by the current source  $K(v_2)$ . The capacitance  $C_e$  is the parallel combination of the diffusion capacitance  $C_D$  and the space charge layer capacitance  $C_{j_s}$ . Both capacitances are nonlinear functions of voltage  $v_2$  and their behavior is summarized in Figure 5 by the current source  $y_e(v_2)$ . The varactor capacitance  $C_c$  is a nonlinear function of the voltage  $(v_3 - v_2)$  and results in the current source  $y_c(v_3 - v_2)$ . Finally,  $\alpha$  is a nonlinear function that is characterized by the current generator  $g(v_2, v_3 - v_1)$ .

Each current generator represents an analytical expression relating the current in the generator to the appropriate node-to-datum voltages. The first step is to use Kirchoff's current law to write a set of nodal equations at nodes 1, 2, and 3. Placing the Taylor series linear terms on the left side of the equation results in the matrix equation.

$$\begin{bmatrix} P(p) \end{bmatrix} \begin{bmatrix} v_1(t) \\ v_2(t) \\ v_3(t) \end{bmatrix} = \begin{bmatrix} \frac{x(t)}{z_g(p)} \\ 0 \\ 0 \end{bmatrix} + \begin{bmatrix} \text{second and} \\ \text{higher order} \\ \text{terms from} \\ \text{each Taylor series} \end{bmatrix} \quad (10)$$

where  $p$  denotes the operator  $\frac{d}{dt}$  and  $P(p)$  is the admittance matrix of the linearized network in Figure 4. (Recall that the linear equivalent circuit of Figure 4 is simply a model which contains only the linear terms from the Taylor series of each of the transistor nonlinearities.) Note that the second and higher order terms from each Taylor series are functions of the nodal voltages  $v_1, v_2$ , and  $v_3$ . They appear on the right side of Eq. (10), as equivalent current sources.

The next step is to assume  $x(t)$  is a sum of complex exponentials as given by Eq. (6). The nodal voltages can then be expressed in the form of Eq. (7) where, for convenience, let  $A_p(f_1, f_{i2}, \dots, f_{ip})$ ,  $B_p(f_1, f_{i2}, \dots, f_{ip})$  and  $C_p(f_1, f_{i2}, \dots, f_{ip})$  be the nonlinear transfer functions

associated with the nodal voltages  $v_1, v_2$ , and  $v_3$ , respectively. The fourth step is to substitute the nonlinear transfer function series for each nodal voltage into Eq. (10) and equate terms of identical frequencies on both sides of the equation. Equating terms at frequency  $f_1$  results in the matrix equation

$$\begin{bmatrix} P(f_1) \end{bmatrix} \begin{bmatrix} A_1(f_1) \\ B_1(f_1) \\ C_1(f_1) \end{bmatrix} = \begin{bmatrix} \frac{1}{z_g(f_1)} e^{j2\pi f_1 t} \\ 0 \\ 0 \end{bmatrix} + \begin{bmatrix} \text{second and} \\ \text{higher order} \\ \text{terms from} \\ \text{each Taylor series} \end{bmatrix} \quad (11)$$

The first order transfer functions are, therefore, given by

$$\begin{bmatrix} A_1(f_1) \\ B_1(f_1) \\ C_1(f_1) \end{bmatrix} = \begin{bmatrix} \frac{1}{z_g(f_1)} \\ 0 \\ 0 \end{bmatrix} p^{-1}(f_1) \quad (12)$$

Similarly, equating terms at frequency  $(f_1 + f_g)$  results in the matrix equation

$$\begin{bmatrix} P(f_1 + f_g) \end{bmatrix} \begin{bmatrix} A_2(f_1, f_g) \\ B_2(f_1, f_g) \\ C_2(f_1, f_g) \end{bmatrix} = \begin{bmatrix} I_{2a} \\ I_{2b} \\ I_{2c} \end{bmatrix} e^{j2\pi(f_1 + f_g)t} \quad (13)$$

It can be shown that  $I_{2a}$ ,  $I_{2b}$ , and  $I_{2c}$  are quadratic functions of the linear transfer functions  $A_1(f_1)$ ,  $A_1(f_g)$ ,  $B_1(f_1)$ ,  $B_1(f_g)$ ,  $C_1(f_1)$ ,  $C_1(f_g)$  and the frequency  $(f_1 + f_g)$ . Since the linear transfer functions are known by virtue of Eq. (12), Eq. (13) is completely specified. Thus, the second order transfer functions are given by

28-4

$$\begin{bmatrix} A_2(f_1, f_g) \\ B_2(f_1, f_g) \\ C_2(f_1, f_g) \end{bmatrix} = \begin{bmatrix} p^{-1}(f_1 + f_g) \\ \\ \end{bmatrix} \begin{bmatrix} I_{2a} \\ I_{2b} \\ I_{2c} \end{bmatrix} \quad (14)$$

Similar solutions are obtained for the higher-order transfer functions. In particular,

$$\begin{bmatrix} A_p(f_{i_1}, f_{i_2}, \dots, f_{i_p}) \\ B_p(f_{i_1}, f_{i_2}, \dots, f_{i_p}) \\ C_p(f_{i_1}, f_{i_2}, \dots, f_{i_p}) \end{bmatrix} = \begin{bmatrix} p^{-1}(f_{i_1} + f_{i_2} + \dots + f_{i_p}) \\ \\ \end{bmatrix} \begin{bmatrix} I_{pa} \\ I_{pb} \\ I_{pc} \end{bmatrix} \quad (15)$$

where it can be shown that  $I_{pa}$ ,  $I_{pb}$ , and  $I_{pc}$  depend only on the transfer functions of orders 1 through  $(p-1)$ . Thus, by starting with the linear transfer functions and by successively determining higher order ones, it is possible to obtain transfer functions of any order. The important point to note is that, for any order, the solution always involves inverting only the admittance matrix of the linearized network. The second and higher order nonlinearities appear as equivalent current sources driving the linearized network. Although the above discussion has been in terms of the circuit of Figure 5, the procedure is quite general and can be applied to any network for which the nonlinearities can be expressed as a Taylor series of the nodal voltages.

## 2.1 Nonlinear Canonic Models

Having determined the nonlinear transfer functions, the output waveforms for arbitrary inputs can be obtained by means of Eq. (5). This is a difficult procedure because the  $p^{\text{th}}$  term of Eq. (5) involves a  $p$ -fold integration. The input-output representation can be simplified considerably by taking advantage of certain properties of the input signals and system characteristics. Models resulting from such simplifications are referred to as canonic models.

The simplest canonic model is termed the frequency power series model. It is applicable when the input consists of a narrow-band desired signal and narrow-band interfering signals all of which have bandwidths that are small compared to that of the pass band of the system. Such signals are conveniently characterized in terms of their complex envelopes. Thus, the amplitude and phase modulated signal

$$x(t) = r(t) \cos[2\pi f t + \theta(t)] \quad (16)$$

is denoted by

$$x(t) = \text{Re}\{z(t) e^{j2\pi f t}\} \quad (17)$$

where

$$z(t) = r(t) e^{j\theta(t)} \quad (18)$$

is the complex envelope and  $\text{re}\{\}$  means "real part of". The magnitude of  $z(t)$  is the amplitude modulation of  $x(t)$  while the angle of  $z(t)$  is the phase modulation of  $x(t)$ . The frequency power series model results by expanding the nonlinear transfer functions in a power series about the center frequencies of the input signals.

For example, assume the input is given by

$$x(t) = \text{Re}\{S_1(t) e^{j2\pi f_1 t} + I_2(t) e^{j2\pi f_2 t} + I_3(t) e^{j2\pi f_3 t}\} \quad (19)$$

$S_1(t)$  is the complex envelope of the desired signal at frequency  $f_1$  and  $I_2(t)$  and  $I_3(t)$  are, respectively, the complex envelopes of the two interfering signals at frequencies  $f_2$  and  $f_3$ . For simplicity assume that the only significant interference components occur at the frequencies  $f_1$ ,  $f_2$ ,  $f_3$ ,  $(2f_2 - f_3)$  and  $(2f_3 - f_2)$ . Using the leading terms of the frequency power series model, the output can be shown to be

$$\begin{aligned} w(t) = & \text{Re}\{H_1(f_1) S_1(t) [1 + \frac{3}{2} \frac{H_3(f_1, f_1, -f_1)}{H_1(f_1)} |S_1(t)|^2 \\ & + \frac{3}{2} \frac{H_3(f_1, f_2, -f_2)}{H_1(f_1)} |I_2(t)|^2 + \frac{3}{2} \frac{H_3(f_1, f_3, -f_3)}{H_1(f_1)} |I_3(t)|^2] e^{j2\pi f_1 t} \\ & + H_1(f_2) I_2(t) e^{j2\pi f_2 t} + H_1(f_3) I_3(t) e^{j2\pi f_3 t} \\ & + \frac{3}{4} H_3(f_2, f_2, -f_3) I_2^2(t) I_3^*(t) e^{j2\pi(2f_2 - f_3)t} \\ & + \frac{3}{4} H_3(-f_2, f_3, f_3) I_2^*(t) I_3^2(t) e^{j2\pi(2f_3 - f_2)t} \} \end{aligned} \quad (20)$$

The response is seen to combine the nonlinear transfer functions of the frequency domain with the complex envelopes of the individual signals in the time domain. Eq. (20) is valid for all signal modulations as long as the signal bandwidths are small compared to that of the pass band of the system. Focus attention on the response at  $f_1$ . The term involving  $|S_1(t)|^2$  is the signal compression term while the terms involving  $|I_2(t)|^2$  and  $|I_3(t)|^2$  are crossmodulation terms. Together they may combine to produce desensitization of the system. Depending upon the pass band of the system the responses at  $f_2$  and  $f_3$  may contribute to co-channel or adjacent channel interference. Finally, the responses at  $(2f_2 - f_3)$  and  $(2f_3 - f_2)$  represent third-order intermodulation distortion components. Note that the response in Eq. (20) is obtained without the need for integration. The feature is characteristic of each of the canonic models. 285

Additional canonic models that have been derived are called the input bandwidth constraint and finite memory models. The input bandwidth constraint model is applicable to the case of bandlimited input signals and involves the use of tapped delay lines with taps spaced at the reciprocal of the bandwidths of the input signals. Appropriate sets of tap outputs are multiplied together and added after appropriate weighting to form the output. The finite memory model has the same basic structure but now the tapped delay line is replaced by a bank of parallel band pass filters, with each filter replacing a single delay unit. This model is based upon the assumption of the system having finite memory. This implies that the  $p$ th order impulse responses are time limited.

The canonic models involve operations that are particularly well suited for the computer. Consequently, they are much easier to use than is the relation in equation (5).

In the next section we discuss how to determine the nonlinear transfer functions from the circuit diagram of a system and consider an example which emphasizes the potential of the nonlinear transfer function approach as a tool in circuit design.

### 3. DETERMINATION OF NONLINEAR TRANSFER FUNCTIONS FROM CIRCUIT DIAGRAMS

This paper considers nonlinear systems containing one or more soft nonlinearities. Soft nonlinearities have the property that their behavior is adequately described by the leading terms of a power series expansion. Let  $v(t)$  represent the voltage across a nonlinear element while  $i(t)$  represents the current flowing through it. It can be shown that the terminal relationships for nonlinear resistors, conductors, capacitors, and inductors are given by (Graham, 1973):

$$\text{Nonlinear Resistor: } v(t) = \sum_{n=1}^N r_n i^n(t)$$

$$\text{Nonlinear Conductor: } i(t) = \sum_{n=1}^N g_n v^n(t) \quad (21)$$

$$\text{Nonlinear capacitor: } i(t) = \sum_{n=1}^N C_n \frac{d}{dt} [v^n(t)]$$

$$\text{Nonlinear Inductor: } v(t) = \sum_{n=1}^N L_n \frac{d}{dt} [i^n(t)]$$

Note that the first term in each expression yields the familiar linear relationship. Since the expressions for nonlinear capacitors and inductors involve time derivatives, these elements contain memory. Nonlinear resistors and conductors, on the other hand, do not. Another group of nonlinear elements arising in the circuit diagrams consists of the various types of nonlinear controlled sources that may occur in the circuit models of active devices. As an example, a softly nonlinear voltage-controlled voltage source has a terminal relationship of the form

$$v(t) = \sum_{n=1}^N \mu_n v_c^n(t) \quad (22)$$

where  $v_c(t)$  represents the control voltage. Recall that the voltage across the source terminals depends only upon the control voltage and is independent of the current flowing through the source. Similar relationships to Eq. (22) exist for nonlinear voltage-controlled current sources, current-controlled voltage sources, and current-controlled current sources.

Given the circuit diagram of a moderately nonlinear system, the nonlinear transfer functions are obtained in a straightforward manner. Although the techniques are readily generalized, we choose to present the key elements of the procedure by working out the solutions to a relatively simple problem.

As an example, consider the single loop network of Fig. 6 consisting of a linear inductor and nonlinear resistor in series with an independent voltage source. The voltage-current relationship for the nonlinear resistor is assumed to be

$$e_R(t) = r_1 i(t) + r_2 i^2(t) \quad (23)$$

Our objective is to determine the loop current  $i(t)$ . Once this is known, the remaining voltages in the circuit can be easily calculated. Application of Kirchhoff's voltage law yields the differential

equation

$$286 \quad e_s(t) = e_L(t) + e_R(t) = L \frac{di(t)}{dt} + r_1 i(t) + r_2 i^2(t) \quad (24)$$

Rearrangement of Eq. (24) such that only terms linear in  $i(t)$  appear on one side of the equation results in

$$L \frac{di(t)}{dt} + r_1 i(t) = e_s(t) - r_2 i^2(t) \quad (25)$$

Eq. (25) can be interpreted in terms of the network shown in Fig. 7. Observe that the nonlinear resistor has been replaced by a linear resistor  $r_1$  in series with a current-controlled voltage source. The nonlinear portion of the resistor can now be viewed as a controlled source in series with the independent source driving the linearized network which is composed of the linear inductor  $L$  in series with the linear resistor  $r_1$ .

The nonlinear transfer functions are determined successively by selecting as the excitation a sequence of complex exponentials which are used to "probe" the circuit. Specifically, the excitation used to solve for the  $n^{\text{th}}$ -order transfer function is given by

$$e_s(t) = \sum_{q=1}^n e^{j2\pi f_q t} \quad (26)$$

where the input frequencies are chosen to be positive and incommensurable so as to insure that all output frequencies are distinct. Because negative frequencies are not allowed in Eq. (26), the terms cannot be grouped in conjugate pairs. As a result,  $e_s(t)$  does not correspond to a physically realizable signal. Nevertheless, it is a useful signal for analytically determining the nonlinear transfer functions. It follows from Eq. (7) that the  $n^{\text{th}}$ -order portion of the current can be expressed as

$$i_n(t) = \sum_{q_1=1}^n \dots \sum_{q_n=1}^n H_n(f_{q_1}, \dots, f_{q_n}) e^{j2\pi(f_{q_1} + \dots + f_{q_n})t} \quad (27)$$

the total current is given by

$$i(t) = i_1(t) + i_2(t) + \dots + i_N(t) \quad (28)$$

where  $N$  denotes the highest order portion of the response that contributes significantly to the total output. In general,  $N$  cannot be determined in a particular problem until the nonlinear transfer functions and actual input levels are known.

To evaluate the first-order transfer function, we begin with

$$e_s(t) = e^{j2\pi f_1 t} \quad (29)$$

From Eq. (27) and Eq. (28) the total current becomes

$$i(t) = H_1(f_1) e^{j2\pi f_1 t} + H_2(f_1, f_1) e^{j2\pi(2f_1)t} + \dots + \underbrace{H_N(f_1, \dots, f_1)}_{N \text{ times}} e^{j2\pi(Nf_1)t} \quad (30)$$

As expected, when the input to a nonlinear system consists of a single frequency, the output frequencies are given by the various harmonics of the input frequency. Substitution of Eq. (29) and (30) into (25) results in

$$\begin{aligned} & j2\pi f_1 L H_1(f_1) e^{j2\pi f_1 t} + j2\pi(2f_1) L H_2(f_1, f_1) e^{j2\pi(2f_1)t} + \\ & j2\pi(3f_1) L H_3(f_1, f_1, f_1) e^{j2\pi(3f_1)t} + \dots + r_1 H_1(f_1) e^{j2\pi f_1 t} + \\ & r_1 H_2(f_1, f_1) e^{j2\pi(2f_1)t} + r_1 H_3(f_1, f_1, f_1) e^{j2\pi(3f_1)t} + \dots \\ & = e^{j2\pi f_1 t} - r_2 [H_1(f_1)]^2 e^{j2\pi(2f_1)t} - 2r_2 H_1(f_1) H_2(f_1, f_1) e^{j2\pi(3f_1)t} - \dots \end{aligned} \quad (31)$$

where, for simplicity, only terms up to third order appear explicitly in Eq. (31). Exponentials have the property that they are linearly independent. Consequently, an exponential with a specified exponent cannot be obtained by adding together exponentials with differing exponents. Since Eq. (31) must be satisfied for all  $t$  and for all values of  $f_1$ , terms involving specific harmonics can be equated. For example, equating



terms involving the first harmonic at frequency  $f_1$ , dividing through by  $\exp(j2\pi f_1 t)$ , and solving for the first-order transfer function yields

$$H_1(f_1) = \frac{1}{r_1 + j2\pi f_1 L} = \frac{1}{Z(f_1)} = Y(f_1) \quad (32)$$

where  $Z(f)$  and  $Y(f)$  are the impedance and admittance, respectively, of the linearized network in Fig. 7. This is a reasonable result since we would expect the first-order portion of the current to be related to the voltage excitation by the admittance of the linearized network.

Eq. (31) can also be used to solve for the higher order transfer functions. Thus, equating terms involving the second harmonic at frequency  $2f_1$ , dividing through by  $\exp[j2\pi(2f_1)t]$ , and solving for the second-order transfer function yields

$$H_2(f_1, f_1) = -\frac{r_2 [H_1(f_1)]^2}{r_1 + j2\pi(2f_1)L} = -r_2 [Y(f_1)]^2 Y(2f_1) \quad (33)$$

similarly, the third-order transfer function is given by

$$H_3(f_1, f_1, f_1) = -\frac{2r_2 H_1(f_1) H_2(f_1, f_1)}{r_1 + j2\pi(3f_1)L} = -2r_2^2 [Y(f_1)]^3 Y(3f_1) \quad (34)$$

The expressions given in Eq. (33) and (34) are unnecessarily restrictive. Since all of the arguments in the second and third-order transfer functions are evaluated at the single frequency  $f_1$ , they are useful only for relating the second and third harmonics, respectively, to the input at  $f_1$ . Should the network be excited by an input containing tones at  $f_1$  and  $f_2$ , where  $f_1 \neq f_2$ , the transfer functions as given by Eq. (33) and (34) could not be used to evaluate responses at such frequencies as  $f_1 + f_2$  and  $2f_1 + f_2$ . This difficulty is removed when the  $n$ th-order transfer function is determined using the excitation specified by Eq. (26). We illustrate this point by now solving for  $H_2(f_1, f_2)$  and  $H_3(f_1, f_2, f_3)$ .

To obtain the second-order transfer function, we let the excitation be

$$e_s(t) = e^{j2\pi f_1 t} + e^{j2\pi f_2 t} \quad (35)$$

where  $f_1$  and  $f_2$  are assumed to be positive incommensurable frequencies. From Eq. (27) and (28) the total current is now given by

$$i(t) = \sum_{q_1=1}^2 H_1(f_{q_1}) e^{j2\pi f_{q_1} t} + \sum_{q_1=1}^2 \sum_{q_2=1}^2 H_2(f_{q_1}, f_{q_2}) e^{j2\pi(f_{q_1} + f_{q_2})t} + \dots + \sum_{q_1=1}^2 \dots \sum_{q_N=1}^2 H_N(f_{q_1}, \dots, f_{q_N}) e^{j2\pi(f_{q_1} + \dots + f_{q_N})t} \quad (36)$$

We see that the output frequencies are those obtained by taking all possible combinations of the two input frequencies from one at a time all the way up to  $N$  at a time. Substitution of Eq. (35) and (36) into the network differential equation given by Eq. (25) yields

$$\begin{aligned} & \sum_{q_1=1}^2 j2\pi f_{q_1} L H_1(f_{q_1}) e^{j2\pi f_{q_1} t} + \sum_{q_1=1}^2 \sum_{q_2=1}^2 j2\pi(f_{q_1} + f_{q_2}) L H_2(f_{q_1}, f_{q_2}) e^{j2\pi(f_{q_1} + f_{q_2})t} + \dots \\ & \dots + r_1 \sum_{q_1=1}^2 H_1(f_{q_1}) e^{j2\pi f_{q_1} t} + r_1 \sum_{q_1=1}^2 \sum_{q_2=1}^2 H_2(f_{q_1}, f_{q_2}) e^{j2\pi(f_{q_1} + f_{q_2})t} \\ & + \dots = e^{j2\pi f_1 t} + e^{j2\pi f_2 t} - r_2 \sum_{q_1=1}^2 \sum_{q_2=1}^2 H_1(f_{q_1}) H_1(f_{q_2}) e^{j2\pi(f_{q_1} + f_{q_2})t} - \dots \end{aligned} \quad (37)$$

where, for simplicity, only terms up to second-order are indicated in detail. To solve for  $H_2(f_1, f_2)$  it is merely necessary to focus attention on those terms involving the sum frequency  $(f_1 + f_2)$ . These are contained in the double summations of Eq. (37). Since  $H_2(f_1, f_2)$ ,  $H_1(f_1)H_1(f_2)$ , and  $(f_1 + f_2)$  are all symmetrical in their arguments, they are not altered by interchanging the frequencies  $f_1$  and  $f_2$ . Thus, each double summation contains 2 identical terms of sum frequency  $(f_1 + f_2)$ . Equating all of the terms involving this frequency on both side of the equation, we get

$$2 [r_1 + j2\pi(f_1 + f_2) L] H_2(f_1, f_2) e^{j2\pi(f_1 + f_2)t} = -2r_2 H_1(f_1) H_1(f_2) e^{j2\pi(f_1 + f_2)t} \quad (38)$$

Solution for  $H_2(f_1, f_2)$  results in

$$H_2(f_1, f_2) = -r_2 H_1(f_1) H_1(f_2) Y(f_1 + f_2) = -r_2 Y(f_1) Y(f_2) Y(f_1 + f_2) \quad (39)$$

where  $[H_1(f_1) H_2(f_2, f_3)]_p$  is defined to be

$$[H_1(f_1) H_2(f_2, f_3)]_p = \frac{1}{6} [H_1(f_1) H_2(f_2, f_3) + H_1(f_1) H_2(f_3, f_2) + H_1(f_2) H_2(f_1, f_3) + H_1(f_2) H_2(f_1, f_1) + H_1(f_3) H_2(f_1, f_2) + H_1(f_3) H_2(f_2, f_1)] \quad (45)$$

Note that  $[H_1(f_1) H_2(f_2, f_3)]_p$  corresponds to an average over all possible permutations of the arguments in  $H_1(f_1) H_2(f_2, f_3)$ . Finally, substitution for  $H_1(f_1)$  and  $H_2(f_2, f_3)$  from Eq. (32) and (39), respectively, yields

$$H_3(f_1, f_2, f_3) = 2r_2^2 [y(f_1)y(f_2)y(f_3)y(f_2+f_3)]_p y(f_1+f_2+f_3) \quad (46)$$

As with  $H_2(f_1, f_2)$ , the third-order nonlinear transfer function depends critically on the admittance of the linearized network. Also, even though we assumed the input frequencies to be positive and incommensurable, it can be shown that Eq. (46) is applicable for all frequencies both positive and negative. Note, for example, that Eq. (46) reduces to (34) when  $f_1 = f_2 = f_3$ .

The expression for the third-order transfer function gives insight into a possible design procedure for minimizing undesired intermodulation components. The most bothersome of these are usually produced by third-order mixes of the type  $(f_a + f_b - f_b)$ . To obtain an appreciation for this, consider a superheterodyne receiver excited by two sinusoidal adjacent channel interferers at frequencies  $f_a$  and  $f_b$  where  $f_a > f_b$ . Including positive and negative frequencies, the input spectrum consists of spectral lines at  $-f_a, -f_b, f_a, f_b$ . When the two interferers combine nonlinearly in the RF amplifier to produce a response at  $2f_a - f_b$  near the receiver's tuned frequency, severe interference may result because the original signals fall inside the RF passband while the intermodulation component falls inside the IF passband. Consequently, the third-order mix corresponding to  $(f_a + f_b - f_b)$  is likely to be extremely troublesome. In terms of transfer functions, the magnitude of the intermodulation component is proportional to  $|H_3(f_a, f_a, -f_b)|$ . Although the circuit in Fig. 6 is not one that would appear in a communications receiver, we now examine the expression in Eq. (44) to gain insight as to how the magnitude of the third-order transfer function might be effectively minimized.

From Eq. (44), (45), (32), and (39)

$$H_3(f_a, f_a, -f_b) = \frac{2}{3} r_2^2 [y(f_a)]^2 y(-f_b) [y(f_a + f_b) = 2y(f_a - f_b)] y(2f_a - f_b). \quad (47)$$

we see that  $|H_3(f_a, f_a, -f_b)|$  can be minimized by minimizing the magnitudes of any or all of the factors in Eq. (47). However, for the interference situation discussed in the previous paragraph, the frequencies  $f_a, -f_b$ , and  $2f_a - f_b$  are frequencies comparatively close to the desired frequency. As a result, it is difficult to modify  $y(f_a), y(-f_b)$ , and  $y(2f_a - f_b)$  without also modifying the desired passband. On the other hand,  $f_a + f_b$  corresponds to a frequency which is approximately twice the desired frequency while  $f_a - f_b$  corresponds to a relatively low frequency. Therefore, the linear admittance can be modified in the regions about  $f_a + f_b$  and  $f_a - f_b$  without altering the admittance in the vicinity of the desired frequency. We conclude that the most effective design procedure for minimizing  $|H_3(f_a, f_a, -f_b)|$  is to minimize  $|y(f_a + f_b) + 2y(f_a - f_b)|$ . This is really a remarkable result because it suggests that third-order responses occurring inside or near a desired frequency band can be controlled by proper design of the linear frequency response well outside of this band. Although the network studied in Fig. 6 does not represent a practical network, it can be shown that the design principle mentioned above can be extended to circuits typically appearing in electronic equipments.

Having derived the first three transfer functions, the general nature of the analysis procedure is now apparent. Higher order nonlinear transfer functions are derived in a similar manner. In general, determination of the  $(n+1)$ th-order nonlinear transfer function requires knowledge of the first through  $n$  order nonlinear transfer functions. Therefore, the procedure is a boot strap technique by which the lower order transfer functions are used to determine higher order transfer functions.

The method discussed in this section made use of a loop analysis. An example utilizing nodal analysis could just as well have been presented. Both analysis methods are easily generalized. In fact, a computer program implemented at the Rome Air Development Center uses the nodal analysis approach. This program is described in the next section.

#### 4. A COMPUTER PROGRAM FOR NONLINEAR CIRCUIT ANALYSIS

A computer program (Graham, 1973) which incorporates the circuit analysis techniques described in Section 3 has been developed for the United States Air Force Rome Air Development Center. The program solves for the nonlinear transfer functions of an arbitrary circuit containing resistors, inductors, capacitors, transistors, vacuum tubes, and diodes. The present software can analyze up to 50 nodes directly. The output of the program is the nonlinear transfer functions, up to the desired order, at all nodes in the network.

Structurally, the computer program solves the nonlinear network problem by forming both the nodal admittance matrix for the entire network, and the first order generator (current source) excitation vector, for all of the linear sources in the network. The generators can be located at any node in the network, and can have any desired frequency, amplitude, and phase. The usual procedure of premultiplying the generator vector by the inverse  $Y$  matrix results in the first order nodal voltage vector for the network, the elements of which are the first order transfer functions at all nodes in the network at the given excitation frequency. When there is more than one generator at a given frequency, the first order (linear) transfer function will be the total transfer function due to the superposition of the generators. The higher order transfer functions are solved iteratively as described in Section 2 and illustrated by example in Section 4.

The nonlinear transfer function analysis performed by the computer program requires the user to specify the circuit to be analyzed and the order of and frequencies at which the nonlinear analysis will be performed. The program recognizes the following circuit elements: resistors, capacitors, inductors, bipolar junction transistors, semiconductor diodes, vacuum diodes, vacuum triodes, vacuum pentodes, field effect transistors, and voltage sources. The program can analyze any circuit made up of interconnections of these elements. The computer program has been used to model a VHF solid state receiver and an HF vacuum tube receiver (Graham, Ehrman, 1973) with excellent results. It provides a systematic means of modeling the nonlinear behavior of electronic circuits and can be very useful in the area of design and evaluation of EMC effects.

#### REFERENCES

Busgang, J. J., Ehrman, L., Graham, J.W., August 1974, "Analysis of Nonlinear Systems with Multiple Inputs", Proceedings of the IEEE.

Department of Defense, Electromagnetic Compatibility Analysis Center, March 1969, "Analytical Services and Data Available from the ECAC", ECAC-DAC-1-69.

Graham, J.W., Ehrman, L., June 1973, "Nonlinear System Modeling and Analysis with Applications to Communications Receivers", RADC Technical Report, RADC-TR-73-178.

Hiebert, A.L., Scharff, S. A., May 1973, "An Electromagnetic Compatibility Program for the 1970's", Rand Report, R-1114-PR.

Volterra, V., 1930 "Theory of Functionals and of Integral and Integro-Differential Equations", Blackie & Sons Ltd., London.

Weiner, N., 1942, "Response of Nonlinear Devices to Noise", Report V-165, Radiation Laboratory, Massachusetts Institute of Technology.

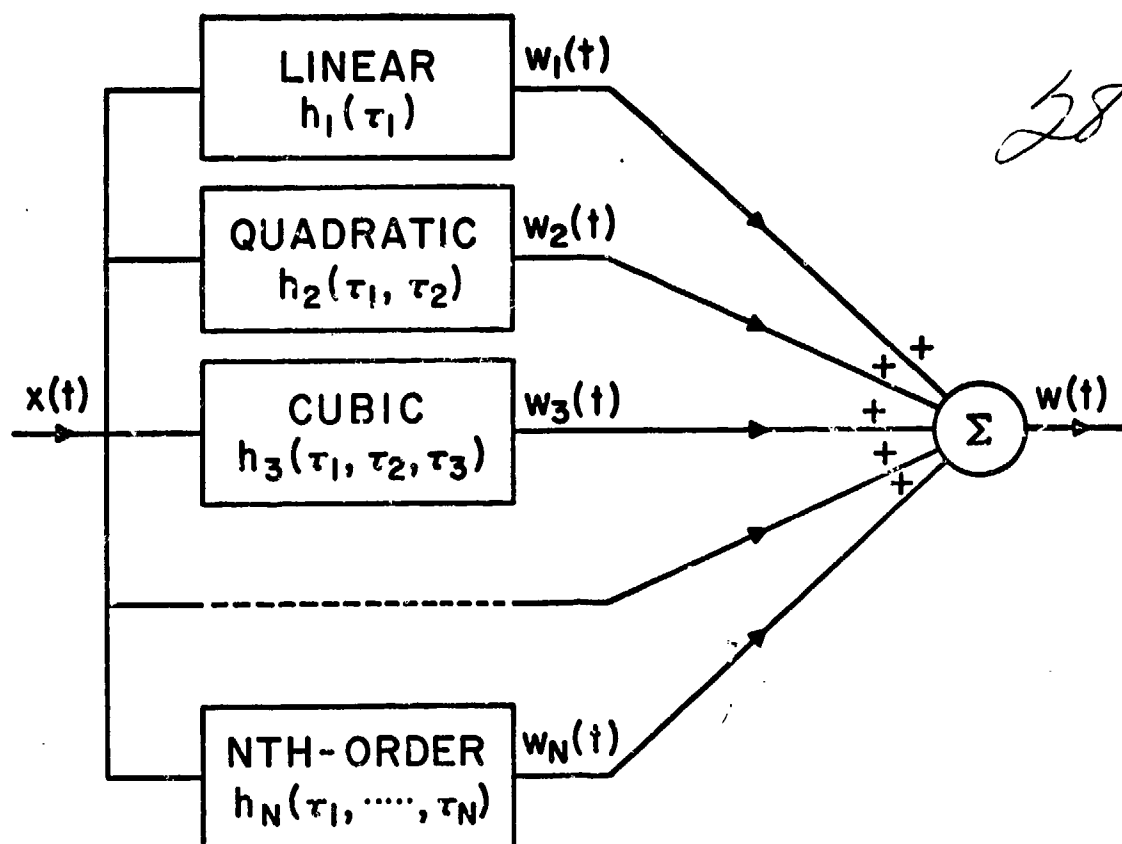


Fig. 1 Characterization of a nonlinear system in terms of its  $N$  impulse responses,  $h_p(\tau_1, \dots, \tau_p)$ ;  $p = 1, 2, \dots, N$

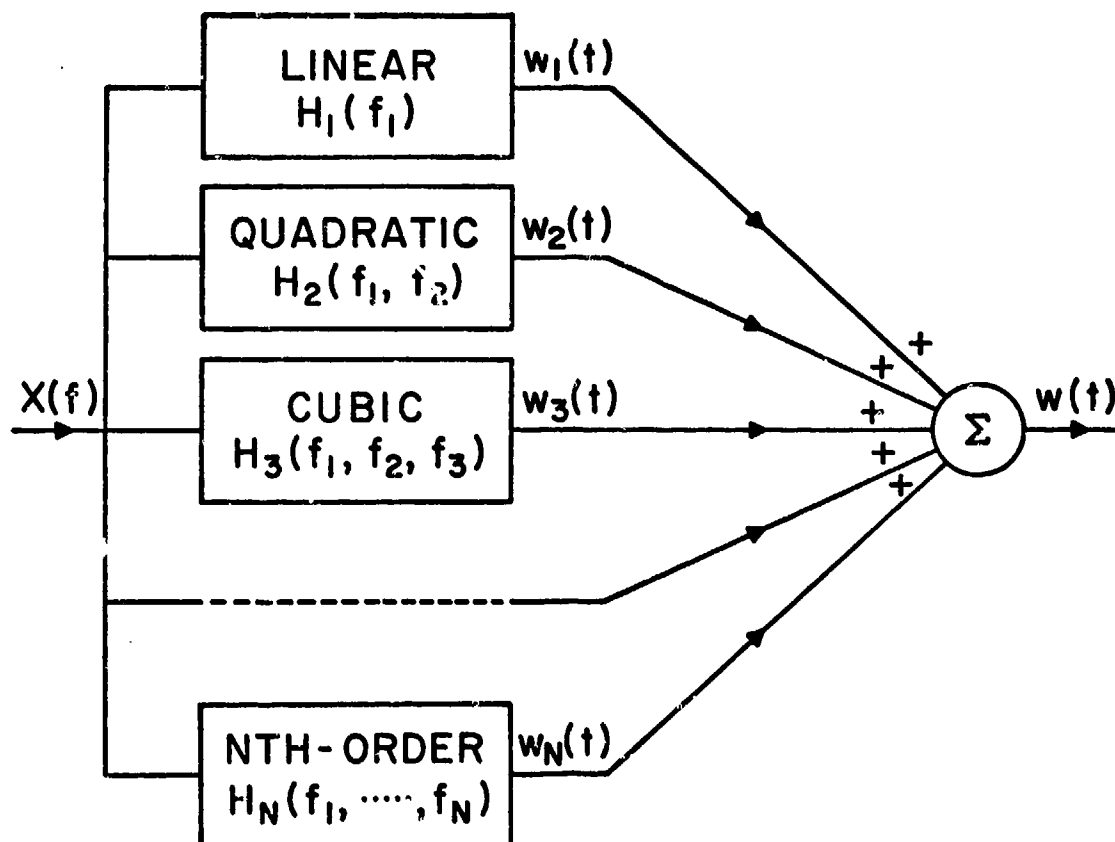


Fig. 2 Characterization of a nonlinear system with memory in terms of its  $N$  transfer functions,  $H_p(f_1, \dots, f_p)$ ;  $p = 1, 2, \dots, N$

28-12

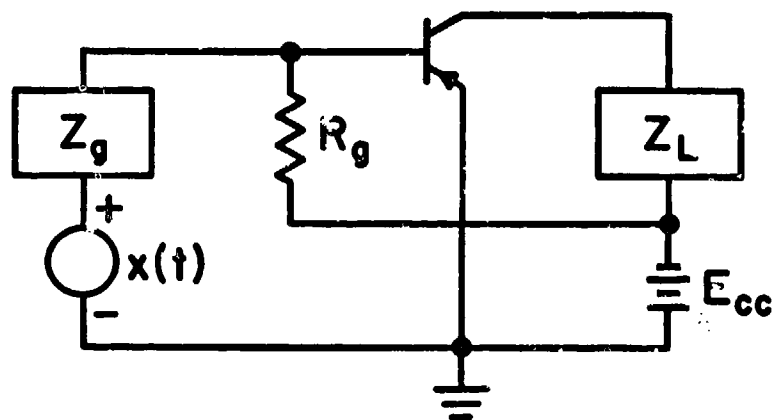


Fig. 3 Transistor amplifier in the common-emitter configuration

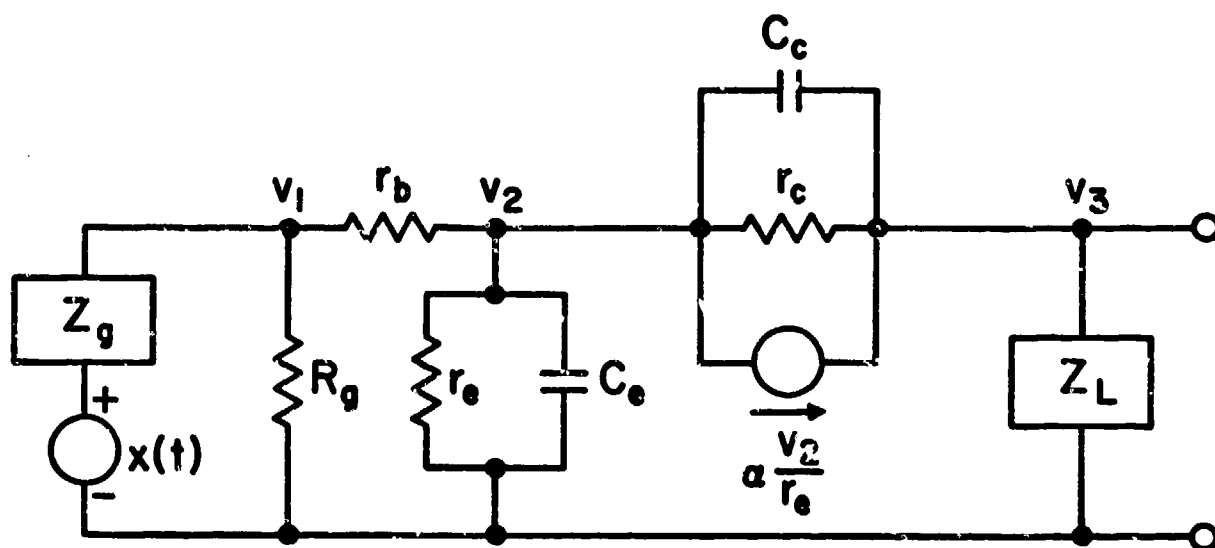


Fig. 4 Linear incremental equivalent circuit of the transistor amplifier shown in Figure 3

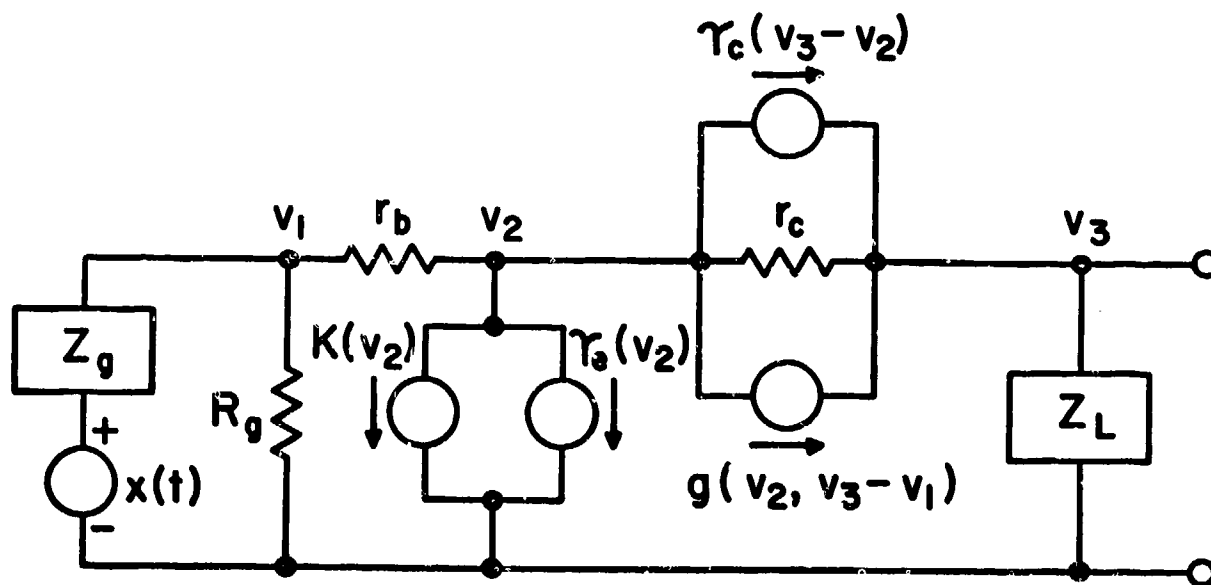


Fig. 5 Incremental equivalent circuit of the transistor amplifier shown in Figure 3

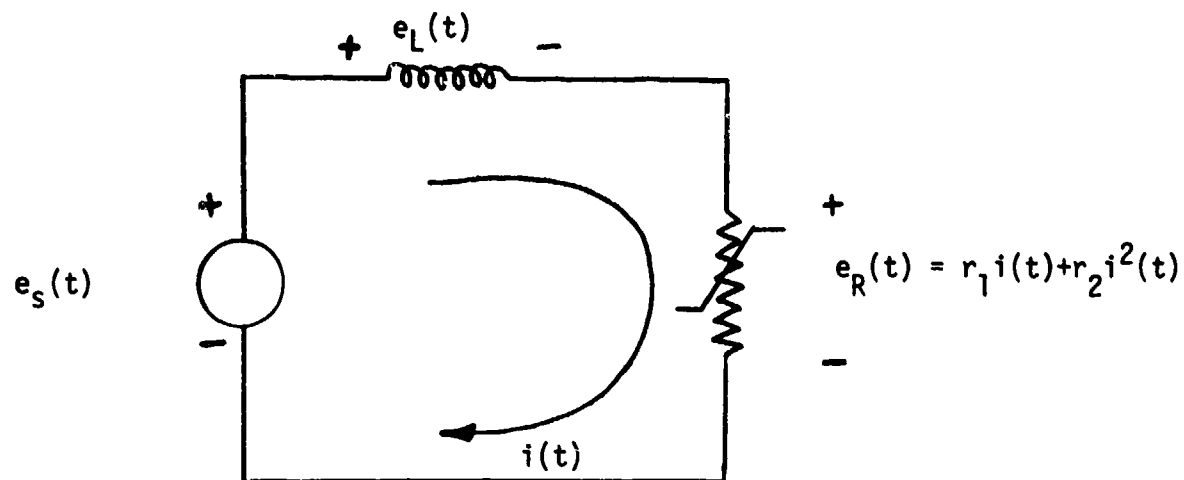


Fig. 6 Nonlinear circuit example involving a single nonlinear resistor

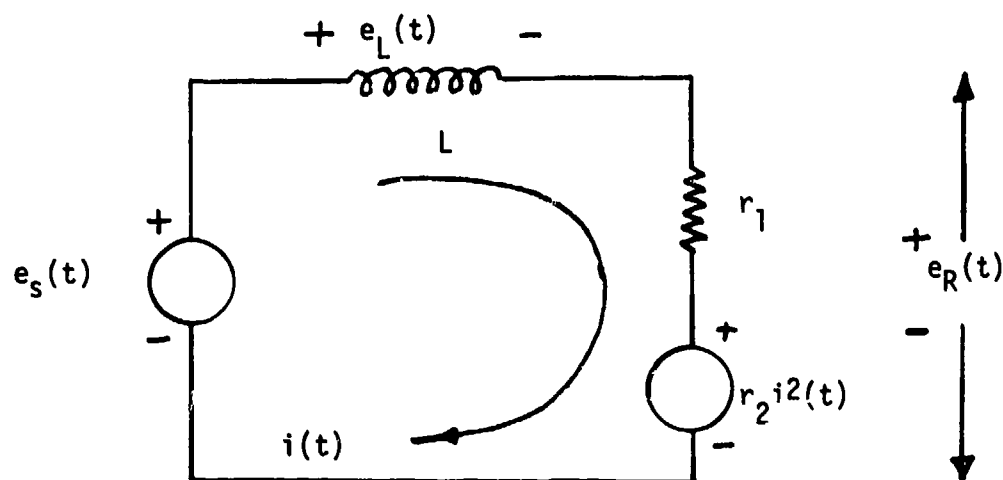


Fig. 7 Linearized circuit of circuit in Figure 6

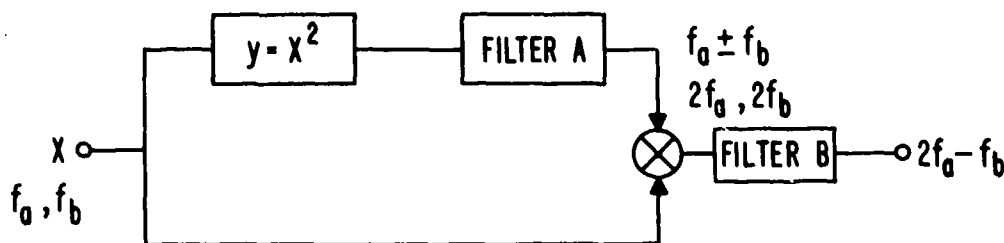
## DISCUSSION

R. OLESCH: What limits the nonlinear transfer function approach to "moderately" nonlinear systems?

J. F. SPINA: This approach formulates the response in terms of a series representation. The more severe the nonlinearity, the more terms that are needed to adequately approximate the response. We have found this method of analysis to be most useful in circuits that are designed to be linear but nevertheless suffer from nonlinear behavior. In such situations, the nonlinearities are moderate and the response is nicely approximated by a small number of terms. In theory, the approach could be applied to circuits containing "hard" nonlinearities such as a limiter; however, now a very large number of terms are needed making this approach impractical.

R. OLESCH: Can you give a more intuitive explanation as to how interference effects inside a frequency of interest can be reduced by controlling the network admittance far outside of this band?

J. F. SPINA: In general, it is difficult to give an intuitive explanation for this effect; however, specific examples do lend themselves to intuitive explanations. Consider, for example, the third-order system shown below:



The third-order nonlinearity arises from multiplication of the linear branch by the second-order branch. The input consists of two tones at frequencies  $f_a$  and  $f_b$ . Assume that filter B is sharply tuned at  $2f_a - f_b$  so that only the output at frequency  $2f_a - f_b$  is of interest. The second-order branch contains frequency components at  $f_a + f_b$ ,  $2f_a$ , and  $2f_b$ , all of which are far removed from the desired output at  $2f_a - f_b$ . Nevertheless, intuitively it is easy to see that the output at  $2f_a - f_b$  can be significantly reduced by designing filter A so as to suppress the signals in the second-order branch at  $2f_a$ ,  $2f_b$ , and  $f_a + f_b$ .

R. OLESCH: Are your analysis programs available?

J. F. SPINA: Although no formal mechanism exists at the present time for distribution of the analysis program, qualified organizations can request these programs from RADC and every attempt will be made to satisfy each such request.

F. J. CHESTERMAN: You mentioned that you had discussed selection of front-end transistors for receivers with receiver designers. Have you considered or looked at other nonlinear devices in systems, particularly in the high-power output portion of systems?

J. F. SPINA: Our work to date has concentrated only on devices such as transistors and vacuum tubes and their nonlinear characterization. For example, we have not examined the so-called "rusty-bolt" problem, i.e., nonlinear interaction due to oxidized metal in contact with unoxidized metal.

S. BURTON: It is clear that an experimental program would be very worthwhile to give physical insight into mathematical results. Do you have a fundamental experiment in mind?

J. F. SPINA: Not yet, but we hope to have within six months.

# COMPARATIVE ANALYSIS OF MICROWAVE LANDING SYSTEMS

## WITH REGARD TO THEIR SENSITIVITY TO COHERENT INTERFERENCE

Børje Forssell  
ELAB  
N-7034 Trondheim-NTH  
Norway

### SUMMARY

Several organizations are at present trying to select the post-1980 landing system. Different Operational Requirements (OR) have been established and the performances of candidate systems are compared with these OR.

An important part of the OR concerns accuracy. A very crucial factor in this respect is the influence of coherent interference (multipath). While the absolute accuracy of a system may be difficult to assess, a very informative comparison between systems can be made with regard to their sensitivity to coherent interference.

ELAB has carried out such comparisons in a study for NATO Industrial Advisory Group (NIAG). Proposed landing systems were computer simulated to examine their behaviour in a realistic multipath environment. Models of airfields were elaborated and the reflected and direct signal components were used as inputs to mathematical models of the receiving systems to compute the resulting position errors.

This study showed that it would be possible to use groups of synthetic interference components for the same purpose. By carefully choosing the distribution of the coherent interference, the significance of the comparison can be improved and the amount of work reduced.

### 1. INTRODUCTION

At present, NATO among other national and international organizations is occupied by the problem of selecting the future international landing system which is to be operative in the post-1980 period. There is a lot of confusion as to what criteria should be used in this selection. Not only are there doubts whether the Operational Requirements (OR) on which the system development is based are relevant in every detail, but there is also some discord and uncertainty with respect to the interpretation of the OR. This makes it difficult to reach agreements on the selection (or rejection) of systems in an international forum all the more as commercial and political realities must be considered.

The OR only contain criteria for the rejection of systems the performances of which do not meet the requirements. Even if the requirements and the way of performance testing can be agreed upon, the problem of selecting the "best" system remains unsolved.

One of the most important parts of the OR concerns accuracy. In this respect, the influence of coherent interference is very decisive. It may be difficult to determine the absolute accuracy of a microwave landing system in every case, but many people agree that the most pertinent technical comparison between systems can be made with regard to their sensitivity to coherent interference.

In 1971, a specially organized subgroup of NATO Industrial Advisory Group (NIAG) invited interested industries to submit proposals for a new landing system in accordance with the OR worked out by the group. For the assessment of the qualities of submitted



24-2  
proposals, NIAG turned to the Electronics Research Laboratory of Trondheim Norway, (ELAB) to get a technical evaluation. According to the aforementioned principles of comparison, the main part of the evaluation study was devoted to an examination of the sensitivities of the systems to coherent interference. The other parts of the study concerned the sensitivities to non-coherent interference (interference from other signal sources) and the utilization of the available frequency spectrum.\*

## 2. PRINCIPLES OF THE EVALUATION OF THE SENSITIVITIES TO COHERENT INTERFERENCE

### 2.1. General.

Three model airfields were specified to ELAB at which the performances of the proposed systems were to be studied. Computer models of the reflection properties of these airfields were developed with regard to the terrain, the positions of buildings and aircraft and the antenna sitings. The resulting signals in space were used as inputs to mathematical models of the receivers for computation of position errors on a number of flight paths.

### 2.2. Airfield modelling.

The three airfields utilized for evaluation of system performance were: a fictive main airport with two parallel concrete runways, a real small airfield with a gravel runway in mountainous surroundings and a fictive small military landing site surrounded by a thick forest. The same modelling technique was utilized for all these airfields.

The model was based on the fact that nearly all surfaces existing in nature must be considered rough at microwave frequencies. As in most theories treating reflection and scattering from rough surfaces, it was assumed that they were planar on the average and that the small-scale roughness could be described by a statistical model. In this model, the surface was characterized by its height distribution, assumed to be Gaussian and its correlation coefficient, the latter representing the correlation between two surface points with respect to the height.

The airfields and their surroundings were divided into triangles and parallelograms, and the electrical properties of the ground were assumed homogeneous over each such surface element and specified by its roughness and its complex dielectric constant. Buildings and trucks were treated by the same procedure.

It is usual to consider the electromagnetic field scattered from a rough surface as the sum of two components, the specular and the diffuse component. Specular reflection is of the same type as that caused by a smooth surface, it is directional (obeys the laws of optics), its phase is coherent and it comes from a relatively small area. Diffuse reflection has less directivity and takes place over a much larger area than the specular one. Its phase is incoherent and its amplitude is Rayleigh distributed. In the general case, both components are simultaneously present. When the roughness is small compared with the wavelength of radiation, the specular component is predominant, but in the opposite case, the specular component is negligible.

The scattering from aircraft was calculated on the basis of bistatic cross-section functions that as closely as possible showed the main features of experimentally recorded cross sections.

With the positions of the transmitting and receiving antennas given, the transmission coefficients between these antennas were computed according to what has been said above. The output of the interference computation contained the amplitudes of the specular and diffuse reflection components, normalized to that of the direct signal,

\*Prof. T. Schaug-Pettersen was project leader at ELAB. The study was supervised by a Study Control Group representing the NIAG subgroup. This Study Control Group which was chaired by Mr. S.A.W. Jolliffe of U.K. participated in the work in a very active and most fruitful way.

the time delays of the specular and diffuse components, relative to that of the direct signal as well as the time derivative of that delay for certain aircraft velocities and the coordinates of the reflection points (i.e. the incident directions of the reflected components).

### 2.3. Signal processing.

29-3

The computations of the position errors were made at certain given points in space. The aircraft antennas were assumed to be omnidirectional. Detailed mathematical models of the systems with regard to signal processing and detection characteristics were elaborated.

The systems were assumed to be ideal within their specification limits and no imperfections in the hardware solutions of the system proposals were considered. Realistic figures of antenna radiation patterns, pulse shapes, frequency drifts, etc. were used. Thermal noise as well as transients were neglected. The only error sources considered were coherent interference and quantization.

For each system, a computer program was developed to compute the apparent position of the aircraft antenna relative to the ground antennas. The input quantities of this program were:

1. Ground antenna positions.
2. Ground antenna radiation patterns (vertical and horizontal) and coverage volumes.
3. Mathematical model of the signal processing in the receiver.
4. Output quantities of the interference program: coordinates of the aircraft positions and of all reflection points, specular and diffuse reflection amplitudes relative to that of the direct signal, time delays of specular and diffuse components relative to that of the direct signal, time derivatives of all time delays.

In the coherent interference model all predetection filtering was combined in a single predetector bandwidth. The effect of filtering was simulated by individual modification of the different signal amplitudes before the addition according to the respective filter characteristics, similar to the effect of the antenna characteristics.

After the computation of the total signal received, the mathematical model of the detection system was used for computation of the coordinates of the aircraft antenna, giving the errors as the differences between the computed and the nominal coordinates.

The system were compared at a standard measuring rate of 5 Hz corresponding to a measuring interval of 0.2 s. For systems with 5 Hz updating rate, the midpoint of the interval was used. For systems with higher updating rates, additional points within the interval were taken into account by means of extrapolation. The errors within the interval were weighted by a filter function and the weighted errors were then treated by computational procedures to calculate the means and the standard deviations of the errors.

To summarize the simulation study, figure 1 shows a flow chart of the principal lines of information flow and the main structure of the process.

## 3. WAYS OF IMPROVING THE COMPARATIVE ANALYSIS

### 3.1. Experiences from the NIAG study.

It is clear from the description in chapter 2 above that the simulation of the proposed landing systems which ELAB carried out for NIAG was very comprehensive and required a lot of computer time. Such a study of landing systems had never been executed before, a fact which influenced the input given to ELAB as well as the work strategy.

#### 3.1.1. Antenna sitings.

As one might expect, the sitings of the ground antennas appeared to have great

influence on the system accuracy. The azimuth antennas are generally sited at the far end of the runway, and a small change of site does not influence the azimuth measurement very much, but the results of the elevation measurements are often crucially dependent on the siting of the elevation antenna. The reason for this is mainly that the reflections from the elevation antenna have the greatest influence when the elevation angle, as seen from the antenna, is small. During the last phase of the landing, this elevation angle is strongly dependent on the antenna siting.

When scattering aircraft are present, systems with differently sited antennas can be differently influenced by the shadowing effects of these aircraft.

Finally, differently sited antennas have different coverage volumes relative to a fixed point in space even if their coverage volumes relative to the respective antenna are identical.

### 3.1.2. Calculation of reflection components.

When a simulation is to be carried out at given airfields, the reflection coefficients have to be calculated as accurately as possible. Even though the available literature on theory and experimental data is utilized, the values of some constants used, e.g. permeability and conductivity, can always be questioned. There might be cases for example, where an increase in reflection coefficients influences one system more than the other so, in this way, the choice of such constants is not unimportant.

### 3.1.3. System specifications.

As the proposals consisted of detailed system specifications, it was inevitable that parts of these specifications differed between different proposals even if, for technical reasons, these parts could have been identical. Some examples: receiver bandwidths and pulse shapes of DME subsystems, and lengths of linear array antennas.

### 3.2. Some improvements of the methods.

On the basis of experiences from the work described above, it is possible to make some improvements of the methods of analysis.

It has been shown by several authors that there are analogies between different landing system concepts. (By system concepts, we mean for example scanning beam, Doppler scan and interferometer concepts). Because of these analogies, detailed solutions belonging to different concepts but with similar bandwidths, antenna sizes, transmitter powers, updating rates etc. should be able to reach about the same accuracies. For a fair comparison, it is then essential to prevent differences in detailed system specifications from concealing the real differences between concepts. Therefore, in order to find the best solution as far as coherent interference is concerned, the comparison should deal with concepts rather than systems. In that case, the parameters should be similar as far as possible in view of the analogies mentioned.

The objects of comparison should be exposed to the same interference if possible. This implies that the ground antennas should be identically sited (within realistic limits), thereby eliminating the differences in coverage shadowing, reflecting surfaces, etc.

For the sake of comparison, it is not at all necessary to simulate the behaviour on specified airfields. A comparative study may well be executed by use of synthetic interference, but, of course, such interference must be of a realistic type. The comprehensive interference computations during the NIAG study present a good basis for synthesizing an interference pattern which is representative of the situation at a somewhat complicated airport and which is also decisive for the comparison. The life-like modelling of a real airport should then be reserved for cases where the behaviour of a specific system at a specific airport is to be examined.

#### 4. SYNTHESIZED INTERFERENCE PATTERNS

As described in 3.3, the synthesization of interference patterns must be based on a thorough knowledge of airport coherent interference. Therefore, the considerable amount of interference data originating from the NIAG work has been analysed in detail and statistical distribution and density functions of interference parameters have been derived. These functions are dependent on the positions of the points of evaluation, i.e. on the positions of the aircraft. The functions are used for the composition of synthetic interference patterns in the following way.

At each point of evaluation, a group of one direct signal and 5 - 8 interfering (multipath) signals is utilized. The incident direction of one of the interference components is chosen to simulate a specular ground reflection of the direct signal. The amplitude of the specular ground reflection, and the phase, the amplitude and the direction of incidence of the other interfering components are selected according to the distributions derived.

A combination of a number of the aforementioned group forms a statistical basis for the investigation of the interference sensitivity of a landing system or a landing system concept. Those groups approximately correspond to a certain distribution of evaluation points within the coverage volume. It is sometimes suitable to simulate one or two specular reflections (one of which being a specular ground reflection) which vary quite slowly between the groups (corresponding to a slow variation along a flight path), a case which is fairly frequent in real life. This is implemented by keeping those two interfering components constant within a series of groups.

The synthesized interference is used as input to the mathematical model of the receiver as described in paragraph 2.3. It can be utilized not only for comparison of system concepts, but also for comparison of different signal processing methods in the receiver of one specific system. In both cases, there may be a need for detailed control of the synthesized interference in order to find out possible differences in the sensitivities to changes of different interference parameters. Then, the parameters the influences of which are to be examined are chosen manually without consideration of the statistical functions mentioned.

#### 5. EVALUATION OF PERFORMANCE

The distribution and density functions describing the relative amplitudes and time delays of the interference components are computed out of the interference at the model airports as described. These functions express the conditions partly at single evaluation points in the coverage volume, partly in the coverage volume as a whole. When the functions are utilized to find relevant interference data, the resulting system performance computed is not a point performance but a volume performance. As there is a difference between interference levels at large and at small distances from the runway, it may be appropriate some times to compute and use the statistical functions separately for those two cases in order to find possible differences of the comparison results. However, in many cases a total computation without dividing the coverage volume seems preferable.

At the evaluation of the computational results, the means and the variances for the total coverage volume should be compared at first. The next step is to find differences of the behaviour at certain evaluation points. The third step is to find the reasons of established differences of performance. Here, it may be helpful to vary the parameters of the interference components to find differences of influence.

## 6. CONCLUSION

When the best concept for the future landing system is to be selected, the accuracy in the presence of coherent interference should be examined as this seems to be the best way of technical comparison. To make the comparison as fair as possible, one should start with concepts with identical parameters (antenna lengths, bandwidths, etc.) as far as this is technically realistic. A further comparison can then deal with specific system solutions. To reduce costs and the necessary amount of work, synthesized interference patterns are useful as replacements of real world conditions. Such patterns can also be utilized for the examination of the sensitivities to specific interference parameters.

To be able to synthesize realistic and decisive interference patterns, it is necessary to have a comprehensive knowledge of multipath conditions at real airports. Such knowledge was acquired by ELAR during the study executed for NIAG.

29-7

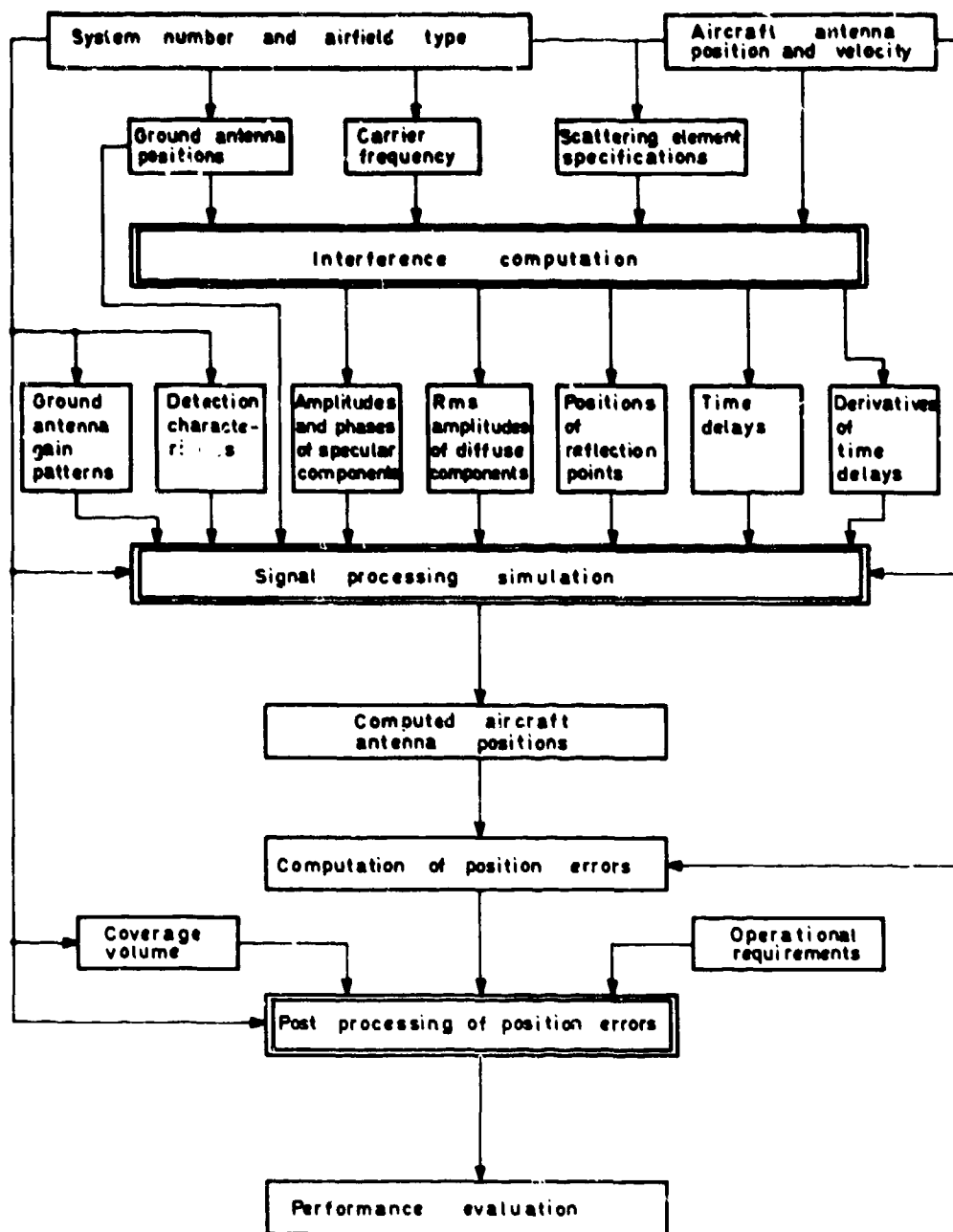


Figure 1. Information flow and main structure of the computer program utilized for evaluation of landing system proposals with regard to their sensitivity to coherent interference.

## DISCUSSION

H. J. ALBRECHT: Referring to the requirement of knowing multipath conditions at real airports, such conditions are not constant. They change due to variations of reflection characteristics on a seasonal basis, as, for instance, caused by vegetation, or even on a daily or hourly basis, after rainfall and appropriately higher water contents in the upper surface layer. How could such changes be taken into account?

B. FORSELL: In the NIAG simulation, "summer" conditions were assumed, i.e., a normal soil humidity and no snow. The ambient conditions used in the computations were assumed to represent a reasonably good mean of the real conditions.

As far as the comparative analysis is concerned, the synthetic interference should be chosen to represent a fairly difficult airport to be decisive. Here, the comparison between systems is emphasized and reflection parameters are allowed to vary only to find differences of influence on the respective system.

H. J. ALBRECHT: It may additionally be suggested to attempt a prediction of such variations and to use such information as supplementary input data. Within a certain degree, it may be possible to predict those changes of reflection characteristics.

B. FORSELL: Yes, this is of course possible.

R. OLESCH: You gave the distribution for returns having various time delays. Should not the corresponding signal amplitudes also be given simultaneously to indicate whether a particular signal is likely to produce an error?

B. FORSELL: There is a relationship between reflection amplitudes and time delays as, generally, a component having a long time delay also has a small amplitude. This is due to the distance of propagation and to the fact that a certain reflecting area close to the direct signal path receives more energy than a similar area far away from that path; however, there are cases when a strong reflection component also has a long time delay and a few such components should be used to get a realistic simulation.

R. GOUILLOU: I would like to know if you have compared the various microwave landing devices and published the results of these comparisons.

B. FORSELL: The simulation work carried out by N.I.A.G., together with its results, have been described in a long report; however, this report is the property of NATO and of the MODs of the various NATO countries, and it is confidential. Discussions regarding the publication of this report have taken place, but I believe it is still confidential. Therefore, if you wish to read it, I advise you get in touch with your own MOD.

R. OLESCH: This comment is in response to the previous question where the asking party proposed the Doppler Microwave Landing System to remove unwanted reflections from fixed targets. I would like to point out that the so-called Doppler system does not perform MTI action as generally associated with a Doppler radar.

30-1

THE CROSSED-DIPOLE STRUCTURE OF AIRCRAFT  
IN AN ELECTROMAGNETIC PULSE ENVIRONMENT

Robert W. Burton  
Department of Electrical Engineering  
Naval Postgraduate School  
Monterey, California  
United States

SUMMARY

The crossed-dipole receiving antenna has been used as a representative model to approximate electromagnetic pulse effects on aircraft. This paper presents significant experimental and theoretical advances which correctly describe the electromagnetic properties of the crossed-dipole receiving antenna illuminated by a monochromatic source. Results are presented for electrically moderately thin structures.

In practice, when a crossed-dipole receiving antenna is excited by a broad spectrum electromagnetic pulse, certain important electrical resonances occur; that is, at specific single frequencies of excitation some portions of the structure can support large amplitude standing waves of current and/or charge. Under such conditions a current maximum/charge minimum, current minimum/charge minimum, or current minimum/charge maximum may occur at the junction region. Examples of resonant and antiresonant situations for the parasitic monopole and the crossed dipole which highlight the possible interactions between the arms of the crossed dipole are presented which give insight into methods of analyzing aircraft in an electromagnetic pulse environment.

1. INTRODUCTION

For some time there has been considerable interest (Taylor, C. D., 1969; Taylor, C. D. et al., 1970; Butler, C. M., 1972; Chao, H. H. and Strait, B. J., 1972) in utilizing the high-speed digital computer in the theoretical study of electromagnetic scattering from arbitrary configurations of relatively thin cylindrical wires both from the point of view of determining the radar cross section of the scatterers as well as their coupling to the electromagnetic field through induced charges and currents. Inevitably, this process leads to assumptions of boundary conditions in the vicinity of the junction and the realization that thin wire theory (Mei, K. K., 1965) does not apply in this region. The essence of this nonapplicability lies in the fact that there is not rotational symmetry in the region closer than  $\lambda/10$  from the junction with the result that measured charge and current densities presented in this paper differ significantly from results predicted using thin wire theory both in the junction region as well as along the entire structure.

In order to gain insight into junction effects, experiments were performed to measure the induced surface charge and current distributions on both the simple receiving monopole mounted over a conducting ground plane and the crossed-dipole receiving antenna likewise mounted over a conducting ground plane (figure 1). In each case the receiving structure was illuminated by a vertically polarized, monochromatic incident plane wave. Using various arm lengths on the receiving crossed dipole, resonant coupling lengths between various cross members were examined. In particular, junction effects were investigated at current maximum/charge minimum, current minimum/charge minimum, and current minimum/charge maximum as well as one intermediate case. For polarizations other than vertical the results of this paper may be generalized through superposition and symmetry considerations.

2. MEASUREMENT OF DISTRIBUTIONS OF CURRENT AND CHARGE PER UNIT LENGTH

The apparatus for measuring current and charge per unit length was specifically designed to study the distributions near the junction of the crossed-dipole receiving antenna. Both the parasitic monopole and the crossed dipole consisted of brass tubes slotted for internally mounted probes terminated in flat end caps and mounted vertically over a large aluminum ground plane. They were illuminated by a vertically polarized electromagnetic field generated by a driven monopole with a corner reflector nearly ten wavelengths away so that the phase fronts of the incident waves at the receiving elements approximated a plane wave. Measurements were made at two frequencies for which the electrical radius of the antenna was  $ka = 0.033$  and  $ka = 0.044$  where  $k = 2\pi/\lambda$  and  $a$  is the outer radius of the brass tubing.

The instrumentation consisted of a flush-mounted monopole for a charge probe and a small shielded loop as a current probe. These could be moved along the slots in the vertical and horizontal arms of the receiving antenna by an internal mechanism controlled by a rack-and-pinion positioner mounted beneath the ground plane. In order to obtain various standing-wave patterns and resonant interactions, the lengths of both the vertical member and horizontal arms were varied over a wide range.

3. DESCRIPTION OF EXPERIMENTAL RESULTS FOR RECEIVING MONOPOLE

The principal reason for examining in detail the standing-wave patterns of the induced current and charge per unit length along a conductor with the electric field parallel to its axis is to establish a physical basis of understanding for the far more complicated distributions occurring on the crossed dipole. The first parasitic or receiving monopole investigated was  $3\lambda/4$  long, a length near resonance. The theoretical distributions of current and charge per unit length are shown in figure 2. Both amplitudes and phases resemble those along a resonant open-ended section of coaxial line in that the maxima of the current and the minima of the charge are virtually coincident near  $kz = 0$  and  $\pi$  or at  $\lambda/4$  and  $3\lambda/4$  from the open end. Correspondingly, the minima of the current and maxima of the charge occur close together at  $kz = \pi/2$  and at the open end  $kz = kh = 3\pi/2$ . Rapid changes in phase by  $180^\circ$  occur near the minima, indi-



302 eating a reversal in direction of the principal components of both current and charge. While the amplitude and phase of the charge behave very closely like those in a coaxial line with an open end, there are significant differences in the distribution of current. These include a minimum that is not as sharp and deep, two maxima that differ greatly from each other in amplitude - the one at  $kz = 0$  is much smaller, and a phase angle  $\theta_I$  that changes only gradually through the  $180^\circ$ . These differences are a consequence of the continuous uniform excitation along the entire length instead of by a single localized generator. Measured curves for the same electrical length but with a slightly smaller value of  $ka$  are shown in figure 3. All four curves are seen to agree well in all significant details with the corresponding theoretical ones.

When the length of the monopole is increased to  $3\lambda/2$  as shown in figure 4, the distribution of charge remains conventional in both amplitude and phase. Maxima occur at intervals of  $\lambda/2$ ; and these are displaced by  $\lambda/4$  from the minima. The phase angle  $\theta_q$  changes rapidly by  $180^\circ$  at the minima. The distribution of current is quite different. Its maxima occur at intervals of  $\lambda$ , as do its minima. The phase angle  $\theta_I$  is sensibly constant over the entire length of the antenna with only relatively small (compared with variations in  $\theta_q$ ) dips at the minima of current.

The measured curves for  $h = 3\lambda/2$  are shown in figure 5. As indicated previously, measurements were designed only to be made in the junction region of the crossed dipole and were made only out a distance  $kz = 3\pi/2$  from the ground plane. A comparison of figures 4 and 5 shows that the theoretical and measured magnitudes  $|q(z)|$  and phase angles  $\theta_q$  of the charge per unit length agree well as do the phase angles  $\theta_I$  of the currents. However, whereas the theoretical current amplitude has a minimum at  $kz = \pi$ , the measured curve shows a peculiar minor maximum. This is not an error but is readily explained with the help of a slight increase in the length of the antenna for the theoretical calculation. Figure 6 shows the same theoretical curves but for  $kh = 10.2$  instead of  $kh = 3\pi$ . The amplitude and phase angle of the charge and the phase angle of the current show little change. But, a minor maximum now occurs at  $kz = \pi$  in the graph for  $|I(z)|$  in close correspondence with the measured curve in figure 5. Actually, this minor maximum is considerably greater than the measured one, indicating that an even smaller increase in length would have sufficed. Thus, it is seen that the standing-wave pattern of current can be very sensitive to the length of the antenna.

The final example of the distributions of current and charge per unit length is for a near resonant length with  $h = 5\lambda/4$ , a half-wavelength longer in half-length than used in figure 2. In this case the charge distribution once again looks conventional with maxima at intervals of a half-wavelength and  $180^\circ$  changes in the phase angle as the amplitude goes through a minimum. A zero of charge per unit length is at the ground plane, a maximum at the open end. The current has maxima at the minima of charge, but whereas the maxima at  $kz = 0$  and  $kz = 2\pi$  are almost equal in magnitude and quite large, that at  $kz = \pi$  is much smaller. Furthermore, the phase angle  $\theta_I$  has equal values near  $kz = 0$  and  $kz = 2\pi$ , but quite a different range of values near  $kz = \pi$ . Measured curves for an antenna of length  $kh = 5\pi/2$  are shown in figure 7. The theoretical and measured distributions of both amplitudes and phase angles are very much alike.

A study of the several distribution curves in figures 2 through 7 shows that the charge per unit length behaves in a very simple and predictable manner. In a zero-order approximation it is given by

$$q(z) \sim \sin kz \quad (1)$$

At the base of a monopole or the center of a dipole the charge per unit length must vanish to satisfy the symmetry condition  $q(-z) = -q(z)$ . All of the graphs of  $q(z)$  are quite well approximated by the simple form (Eq. 1) except for the occurrence of deep minima instead of nulls which are accounted for by higher-order terms.

In order to understand the peculiarities in the standing-wave patterns of current, it is advantageous to examine the behavior of the components of the induced currents that are in phase and in phase quadrature with the incident field. A complete discussion of this aspect as well as a thorough analysis of the parasitic monopole is presented by King and this author (Burton, R. W. and King, R. W. P., to be published).

The principal reason for examining in detail the standing-wave patterns of the induced current and charge per unit length of the receiving monopole was to establish a physical basis of understanding for the much more complicated distributions which result from a second conductor being connected perpendicular to the first. The coupling of this horizontal element which would have otherwise been completely uncoupled from the vertically polarized incident field before the connection was made is determined in part by the currents and charges present at the proposed junction region of the receiving monopole and, as will be described later, by the various combinations of resonant lengths which result from the connection.

#### 4. DESCRIPTION OF EXPERIMENTAL RESULTS FOR RECEIVING CROSSED DIPOLE

With the use of Eq. 1 and the shifted cosine distribution for current (King, R. W. P., 1956), a number of special cases can readily be constructed which give insight into conditions in the junction region (figure 8). The horizontal mark on each of the cases in figure 8 locates the proposed junction location for the horizontal cross arm. It is clear that if a horizontal cross arm is located at  $h = \lambda/2$  above the ground plane, junction effects may be studied for perturbations in an area of current maximum and charge minimum on the vertical member as in Cases 1 and 2, and current minimum/charge minimum in Case 3. Similarly, if the cross arm is located at  $h = 3\lambda/4$ , junction effects may be investigated for a condition of current minimum and charge maximum as in Cases 4 and 5. Case 6 is an intermediate case and is included to examine the situation when there is both charge and current present in the junction region. In order to shift the junction from  $h = \lambda/2$  to  $h = 3\lambda/4$ , the frequency of the incident plane wave was merely changed by the appropriate amount, which of course causes a shift of  $ka$ . To summarize, for the cases where the cross arms are located at  $h = \lambda/2$ ,  $ka = 0.044$ ; when they are located at  $h = 3\lambda/4$ ,  $ka = 0.033$ .

A vertically polarized incident wave will clearly not excite longitudinal currents along the axis of a dipole located horizontally and parallel to the plane-wave front. However, when the horizontal and

vertical dipoles are joined together, significant charge and current densities are observed along the horizontal member at various combinations of resonant lengths. A resonant length for the crossed dipole is considered to be any length measured through the junction involving any two of the four arms which gives rise to resonant effects.

30-3

When the horizontal dipole is joined to the vertical dipole, it is useful for physical insight to consider the vertical receiving dipole (which is coupled to the incident vertically polarized wave) as driving the otherwise uncoupled horizontal member through the interaction of the charges and currents present in the junction region. The amount of coupling is essentially determined by the various possible resonant lengths as measured through the junction.

The addition to the vertical dipole of the horizontal cross member can best be regarded as loading the junction, whereas the cross member becomes an antisymmetrically driven antenna. The drive comes about from the source currents and charges existing in the junction region. When the horizontal member is added these source currents and charges spread out onto the cross arm, thereby causing an observable dip in the charge and current distributions as measured along the vertical member. The currents and charges on a driven antenna may be separated (King, R. W. P., 1956) into symmetrical and antisymmetrical components (figure 9). In the case of the horizontal cross member of the crossed dipole under investigation, the currents on the vertical dipole branch out in the junction region onto the cross arms and drive the horizontal member antisymmetrically. From another point of view the distribution patterns of currents and charges are the result of a superposition of resonant and forced distributions.

For the moderately thick dipole (Kao, C. C., 1969), Kao has shown that transverse currents exist only near the ends. It, therefore, follows that for the crossed dipole under study with symmetrical arms the only transverse currents present in the junction region will be symmetrical transverse currents branching out from the centerline to the horizontal arms, given that the junction is reasonably far (i.e.,  $\gg \lambda/4$ ) from the end caps. It should be noted that the use of a rotatable current probe verified this fact on a somewhat fatter model than the crossed dipole described here.

The perturbations of the charge and current density on a vertical receiving monopole which result from the addition of horizontal cross arms of various lengths were investigated for each of the six cases described in figure 8. Likewise, the charge and current densities along the horizontal arms which were associated with these perturbations were measured out to a distance  $\approx \lambda/4$  from the center of the junction. These results are summarized in figures 10 through 22.

The degree of interaction between the horizontal cross arms and the vertical member is determined by the magnitude of the current and charge in the junction region of the parasitic monopole and the new resonant conditions brought into being by the addition of the cross arms. Case 1, described in figures 10 and 11, clearly demonstrates this resonance between the vertical and horizontal cross arms with a condition of charge minimum/current maximum existing at the junction, whereas Case 2 (figures 12 and 13) portrays the marked difference occurring when the horizontal cross arm is antiresonant. A similar situation is observed in Case 3 for a condition of charge minimum/current minimum. When the horizontal cross arms are varied from a half-length of  $\lambda/4$  to  $\lambda/2$  (figures 14 and 15). For conditions of charge maximum/current minimum on the parasitic monopole (Cases 4 and 5), significant perturbations in both charge and current densities are observed which demonstrate the interaction of resonant lengths when the horizontal cross arms are added (figures 16 through 19). Case 6 presents an interesting observation of an intermediate case wherein situations of resonance and antiresonance between horizontal and vertical members are highlighted (figures 20 and 21).

It should be noted that the initial data point on the horizontal cross arms,  $x \approx 0$ , was taken on the front surface of the horizontal arm directly over the edge of the vertical cylinder projected through the junction region. Therefore, it should be observed that using the longitudinally oriented current probe, the measured current in this area does not show the transverse components of the currents in the immediate junction region until they blend into longitudinal components several radii out along the horizontal arm.

## 5. CONCLUSIONS

The existence of standing waves of both current and charge on the parasitic monopole gives rise to situations in which sizable currents and/or charges may be observed in the junction region of a crossed-dipole receiving antenna. When horizontal cross arms are added to the vertical parasitic monopole illuminated by a vertically polarized monochromatic plane wave, charges and currents are coupled to these horizontal members. The amount of coupling is a function of both the charge and current present at the location of the junction on the parasitic monopole and the new resonant lengths which occur from the addition of the cross arms. Experimental results have been presented which demonstrate these standing waves and resonant interactions.

Recently, in conjunction with this work, King and Wu have provided a complete analytic solution for the electrically thin crossed dipole which employs corrected boundary conditions and a new integral-differential equation developed in terms of trigonometric functions of the various arm lengths of the crossed dipole (King, R. W. P. and Wu, T. T., to be published). Preliminary comparisons of this theory with the experimental results presented in this paper show close agreement and will be the subject of a sequel to that paper (Burton, R. W. and King, R. W. P., work in progress). The expansion of the distributions in terms of trigonometric functions of arm lengths clearly demonstrates that some combinations of individual arm lengths bring certain sine and cosine terms into play especially at resonances and antiresonances, thus explaining the experimental interactions observed.

## 6. REFERENCES

BURTON, R. W. and KING, R. W. P., to be published, "Currents and Charges on Cylinders in an Electric Field."

- BURTON, R. W. and KING, R. W. P., work in progress, "The Crossed Dipole: Theory and Experiment."
- BUTLER, C. M., 1972, "Currents Induced on a Pair of Skew Crossed Wires," IEEE Trans. Antennas Propagat., vol. AP-20, pp. 731-736.
- CHAO, H. H. and STRAIT, B. J., 1972, "Radiation and Scattering by Configurations of Bent Wires with Junctions," IEEE Trans. Antennas Propagat., vol. AP-19, pp. 701-702.
- KAO, C. C., 1969, "Three-Dimensional Electromagnetic Scattering from a Circular Tube of Finite Length," J. Appl. Phys., vol. 40(12), pp. 4732-4740.
- KING, R. W. P., 1956, Theory of Linear Antennas. Cambridge, Mass.: Harvard University Press, Chapter IV; Chapter III.
- KING, R. W. P. and WU, T. T., to be published, "Analysis of Crossed Wires in a Plane-Wave Field."
- MEI, K. K., 1965, "On the Integral Equations of Thin Wire Antennas," IEEE Trans. Antennas Propagat., vol. AP-13, pp. 374-378.
- TAYLOR, C. D., 1969, "Electromagnetic Scattering from Arbitrary Configuration of Wires," IEEE Trans. Antennas Propagat., vol. AP-17, pp. 662-663.
- TAYLOR, C. D., LIN, S. M., and MC ADAMS, H. V., 1970, "Electromagnetic Scattering from Crossed Wires," IEEE Trans. Antennas Propagat., vol. AP-18, pp. 133-135.

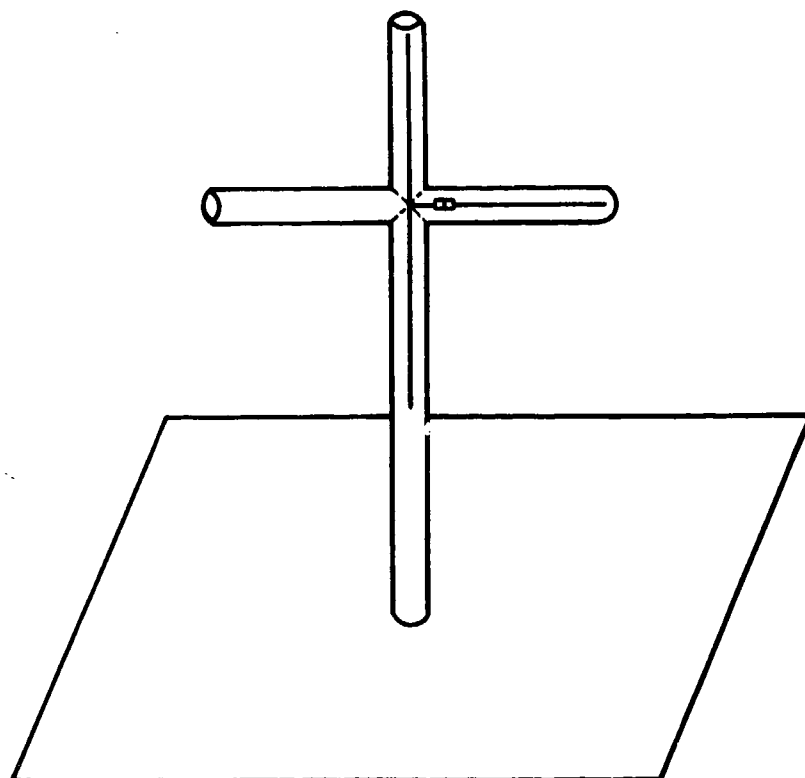


Fig. 1. Crossed-dipole antenna.

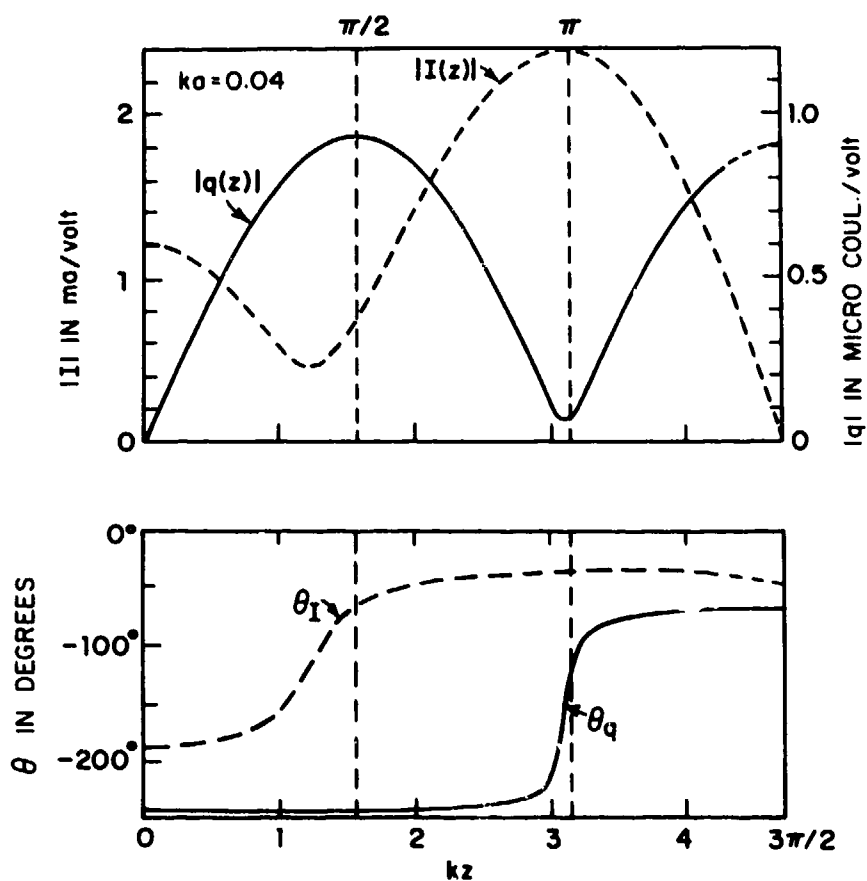


Fig. 2. Theoretical distributions of current and charge in parasitic monopole in normally incident field;  $h = 3\lambda/4$ .

30-6

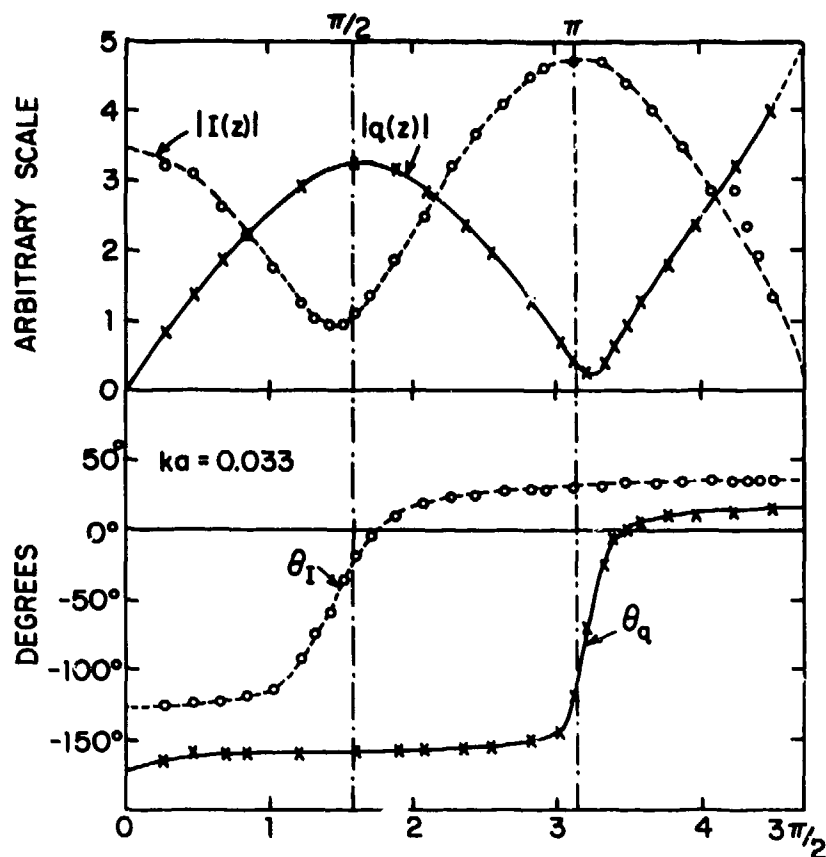


Fig. 3. Measured distributions of current and charge in parasitic monopole in normally incident field;  $h = 3\lambda/4$ .

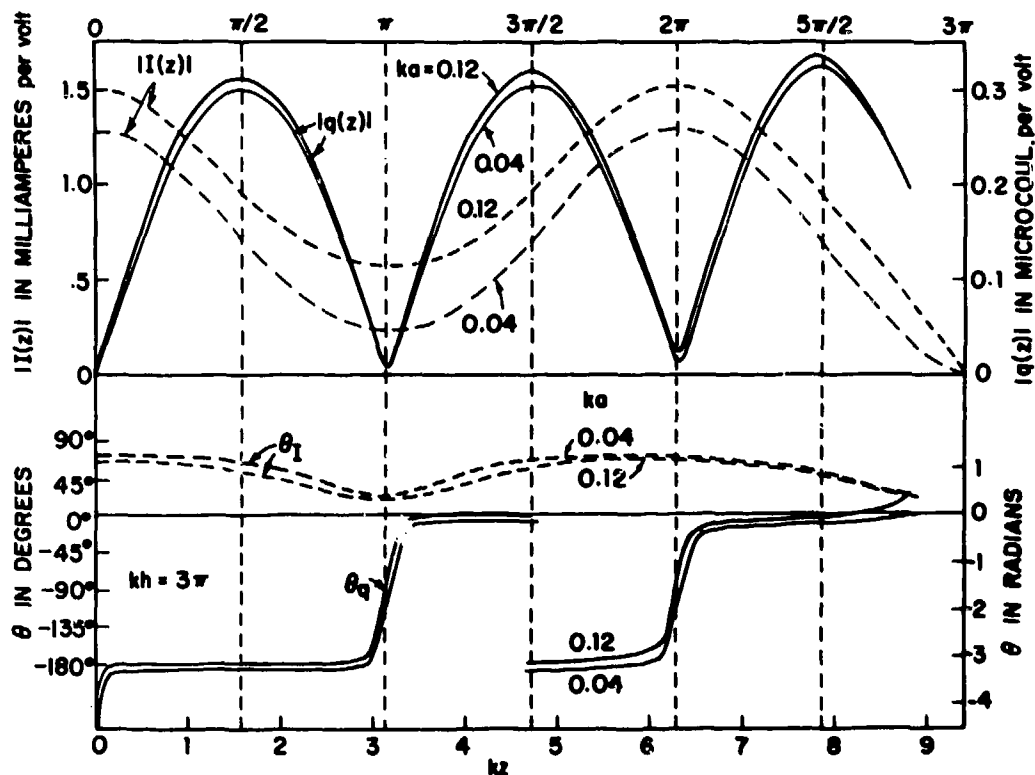


Fig. 4. Theoretical distributions of current and charge in parasitic antenna in normally incident field;  $h = 1.5\lambda$ .

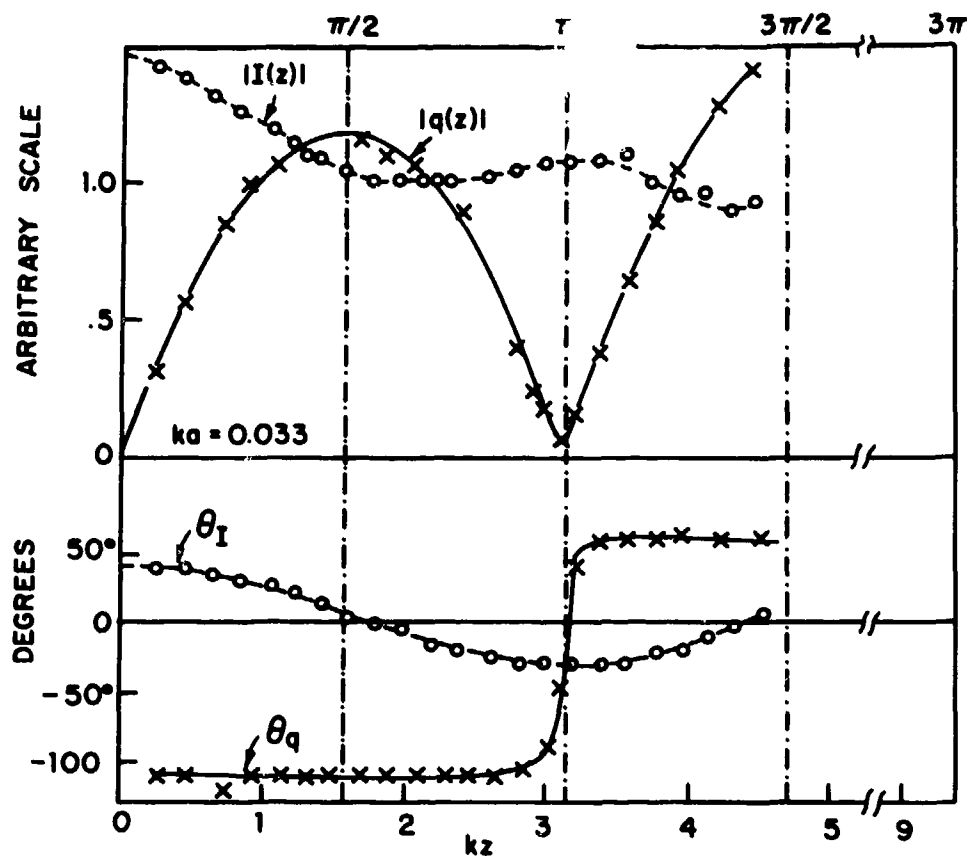


Fig. 5. Measured distributions of current and charge in parasitic monopole in normally incident field;  $h = 1.5\lambda$ .

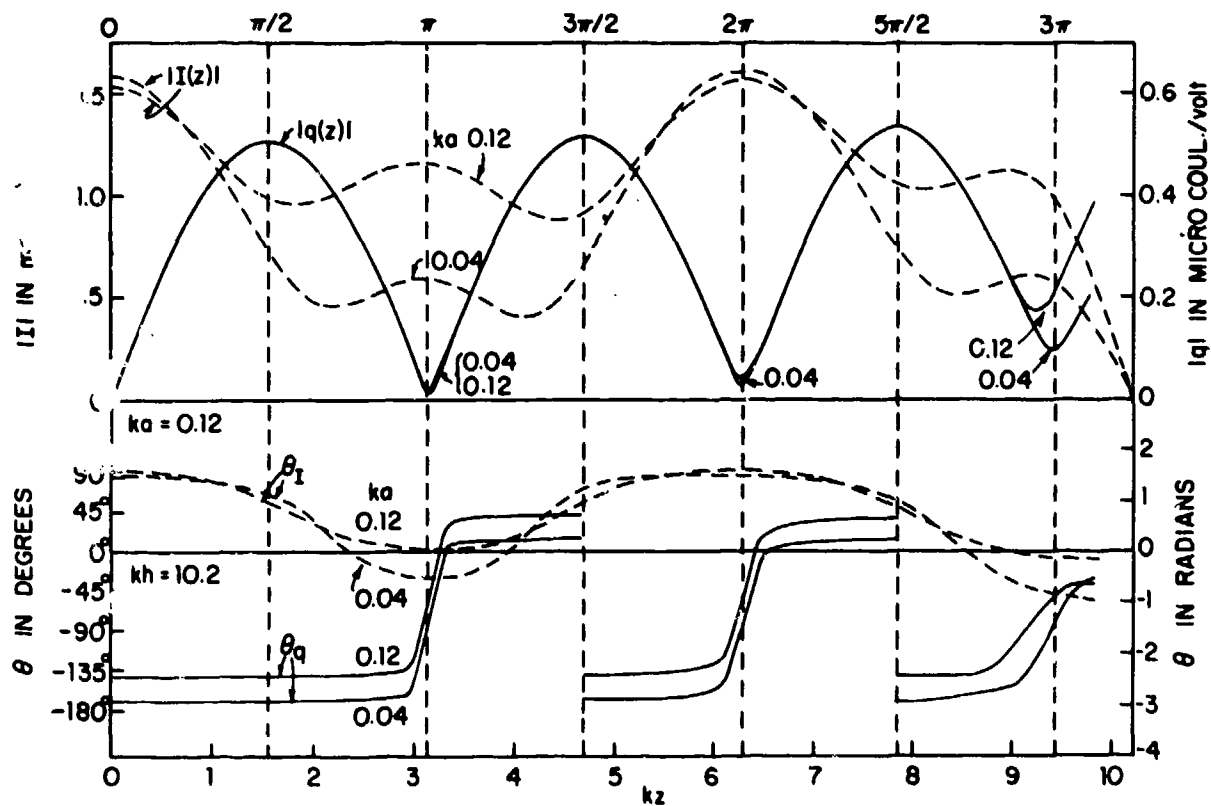


Fig. 6. Theoretical distributions of current and charge per unit length in parasitic antenna in normally incident field;  $h = 1.62\lambda$ .

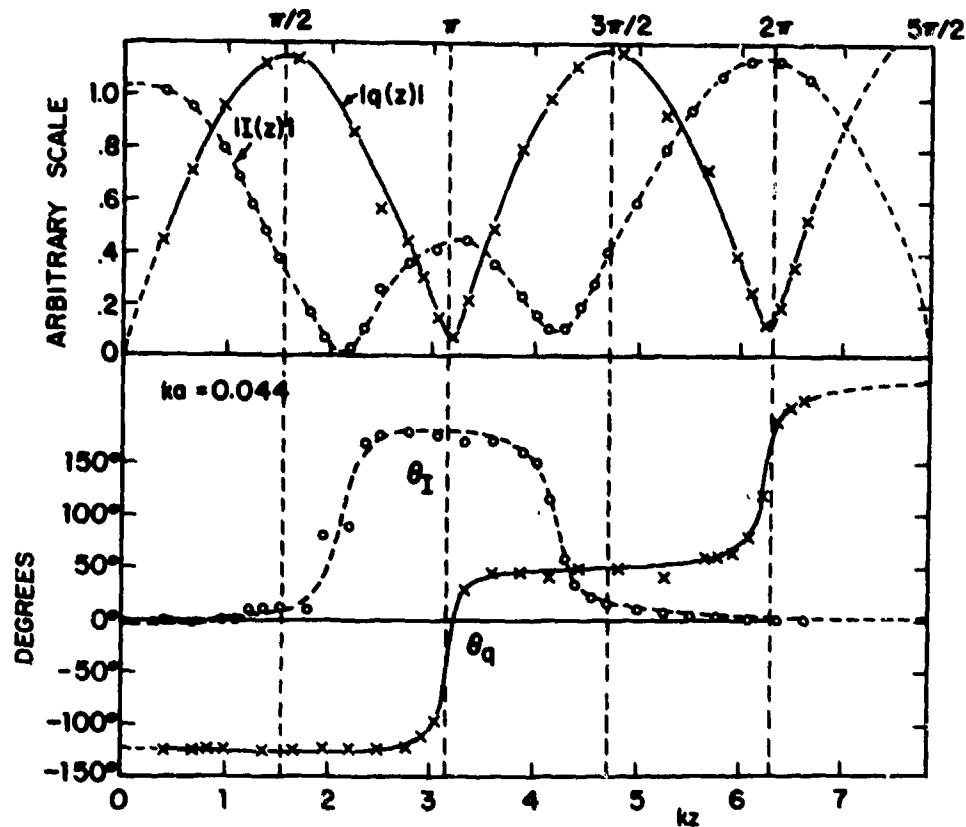


Fig. 7. Measured distributions of current and charge per unit length in parasitic monopoles;  $h = 5\lambda/4$ .

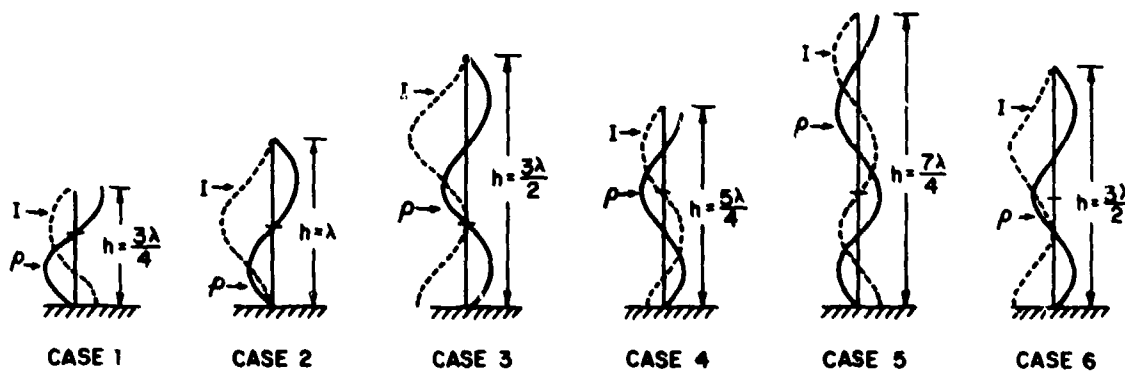


Fig. 8. Charge and current density on dipole receiving antenna mounted over conducting ground plane as a function of antenna length,  $h$ .

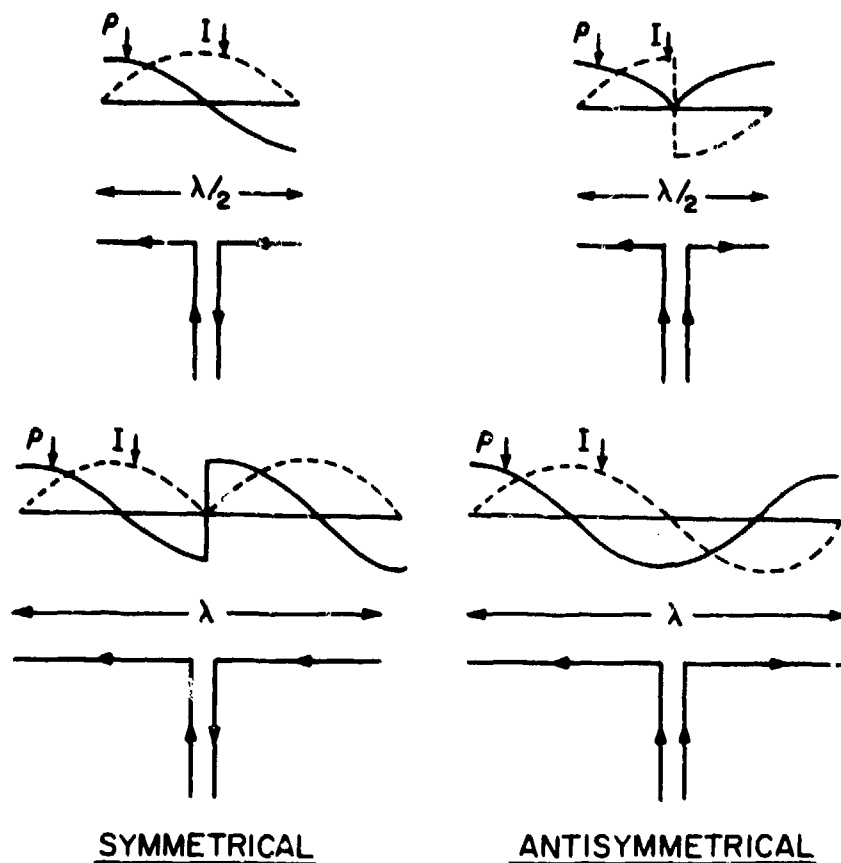


Fig. 9. Current and charge density on symmetrical and antisymmetrical driven antennas.

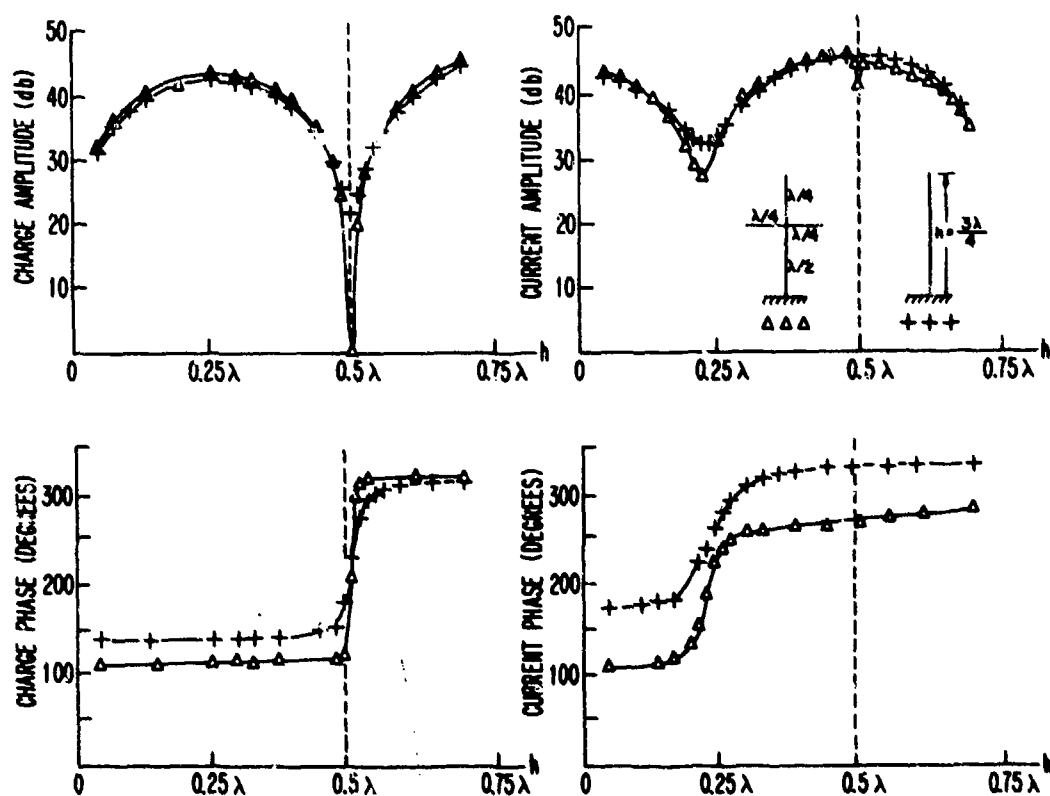


Fig. 10. Amplitude and phase distributions of charge and longitudinal current density on vertical dipole and cross dipole illuminated by a vertically polarized plane wave as a function of antenna height,  $h$ : Case 1.



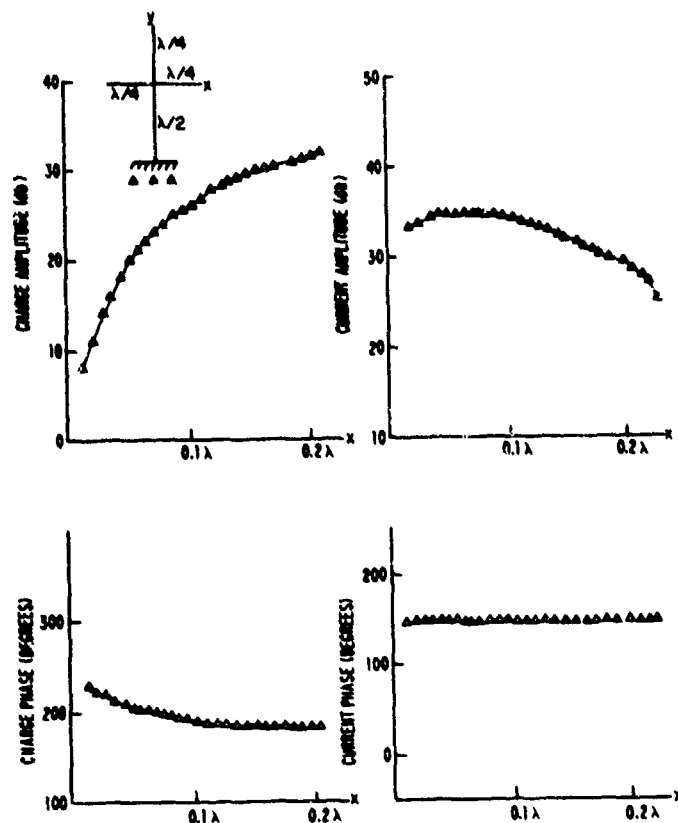


Fig. 11. Amplitude and phase distributions of charge and longitudinal current density on horizontal element of crossed-dipole receiving antenna illuminated by a vertically polarized plane wave as a function of distance (wavelengths) measured from junction: Case 1.

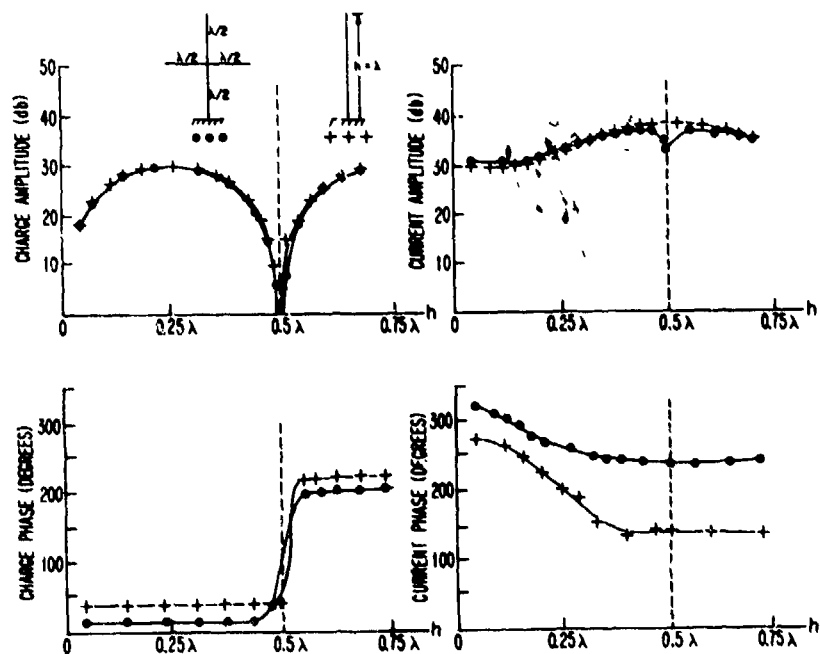


Fig. 12. Amplitude and phase distributions of charge and longitudinal current density on vertical dipoles and crossed dipole illuminated by a vertically polarized plane wave as a function of antenna height,  $h$ : Case 2.

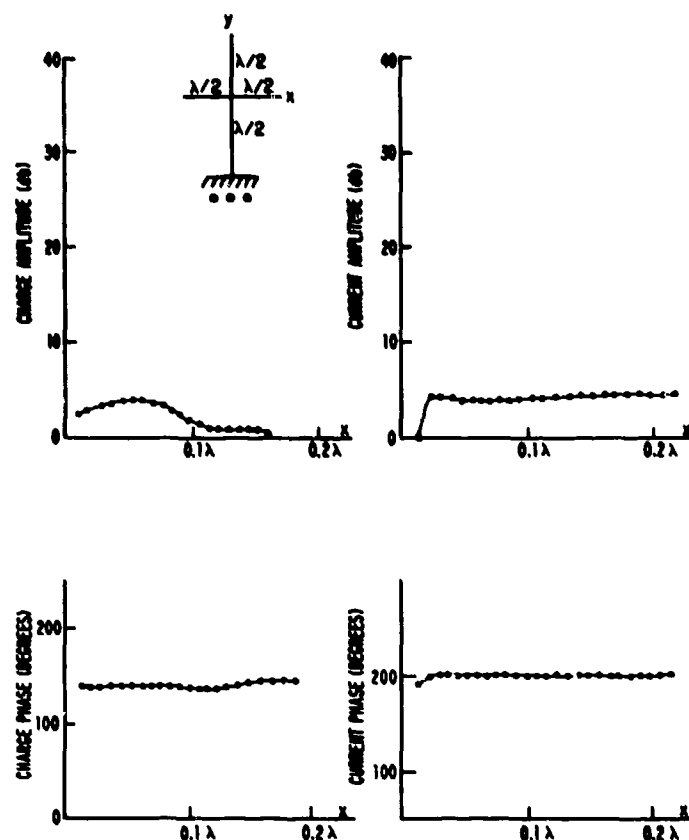


Fig. 13. Amplitude and phase distributions of charge and longitudinal current density on horizontal element of crossed-dipole receiving antenna illuminated by a vertically polarized plane wave as a function of distance (wavelengths) measured from junction: Case 2.

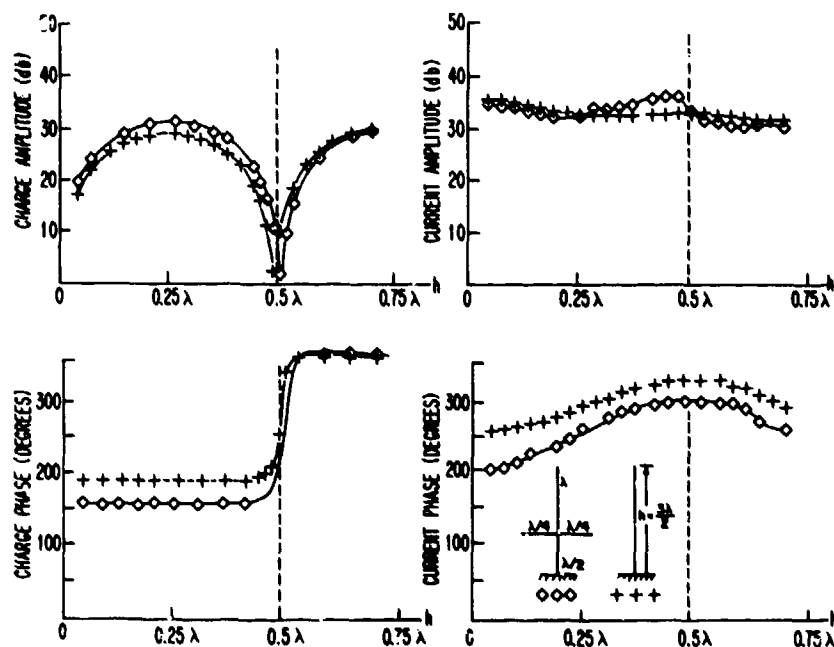


Fig. 14. Amplitude and phase distributions of charge and longitudinal current density on vertical dipole and crossed dipole illuminated by a vertically polarized plane wave as a function of antenna height,  $h$ : Case 3.

30-12

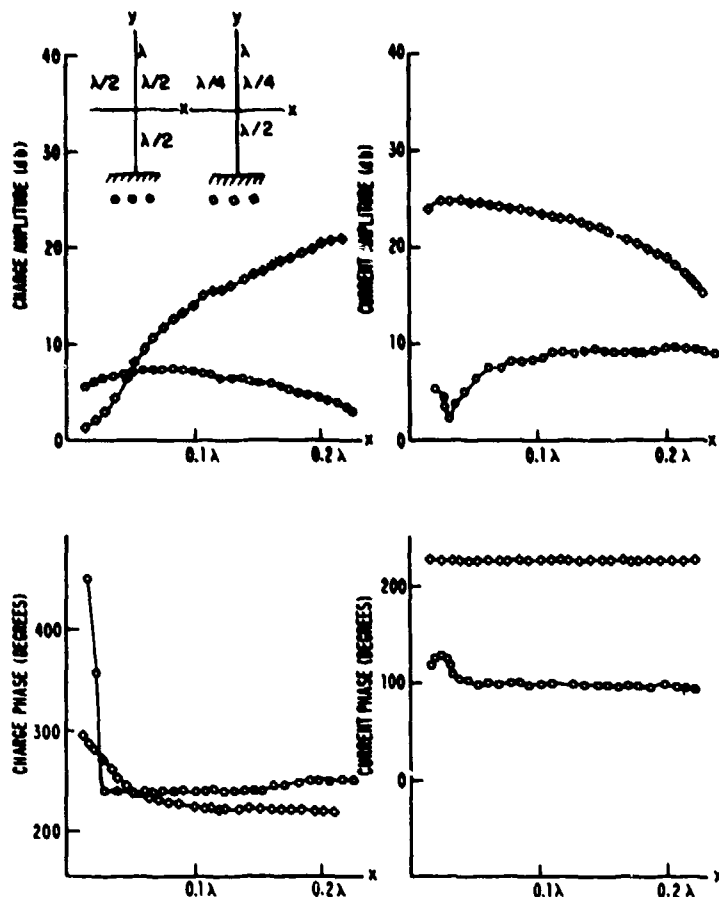


Fig. 15. Amplitude and phase distributions of charge and longitudinal current density on horizontal element of crossed-dipole receiving antenna illuminated by a vertically polarized plane wave as a function of distance (wavelengths) measured from junction: Case 3.

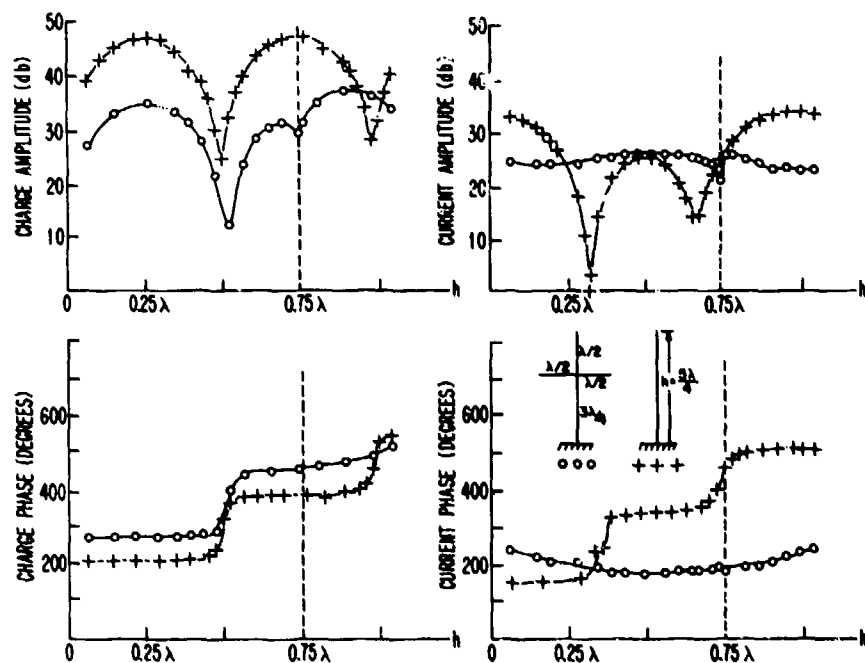
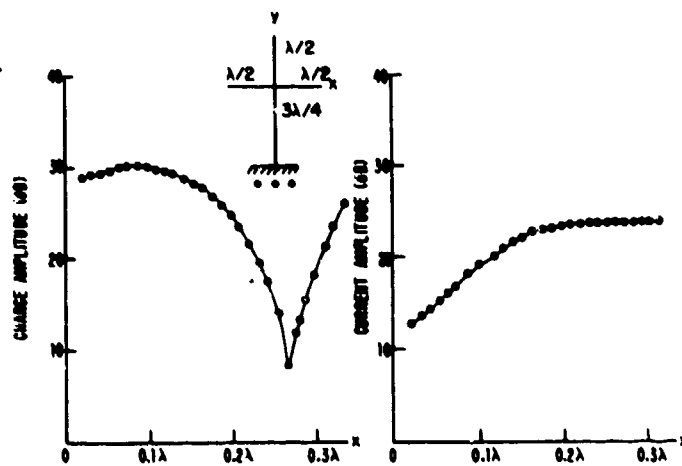


Fig. 16. Amplitude and phase distributions of charge and longitudinal current density on vertical dipole and crossed dipole illuminated by a vertically polarized plane wave as a function of antenna height,  $h$ : Case 4.



30-13

Fig. 17. Amplitude and phase distributions of charge and longitudinal current density on horizontal element of crossed-dipole receiving antenna illuminated by a vertically polarized plane wave as a function of distance (wavelengths) measured from junction: Case 4.

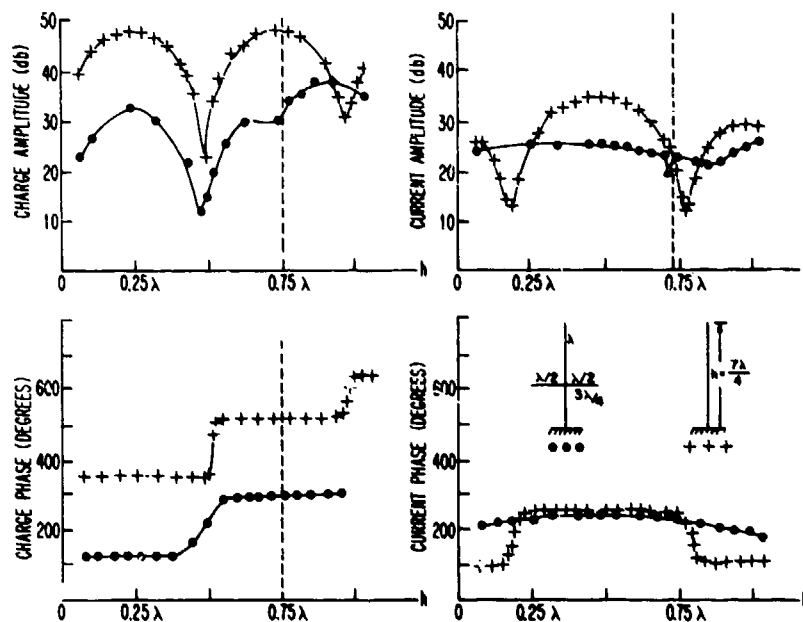


Fig. 18. Amplitude and phase distributions of charge and longitudinal current density on vertical dipole and crossed dipole illuminated by a vertically polarized plane wave as a function of antenna height,  $h$ : Case 5.

30-14

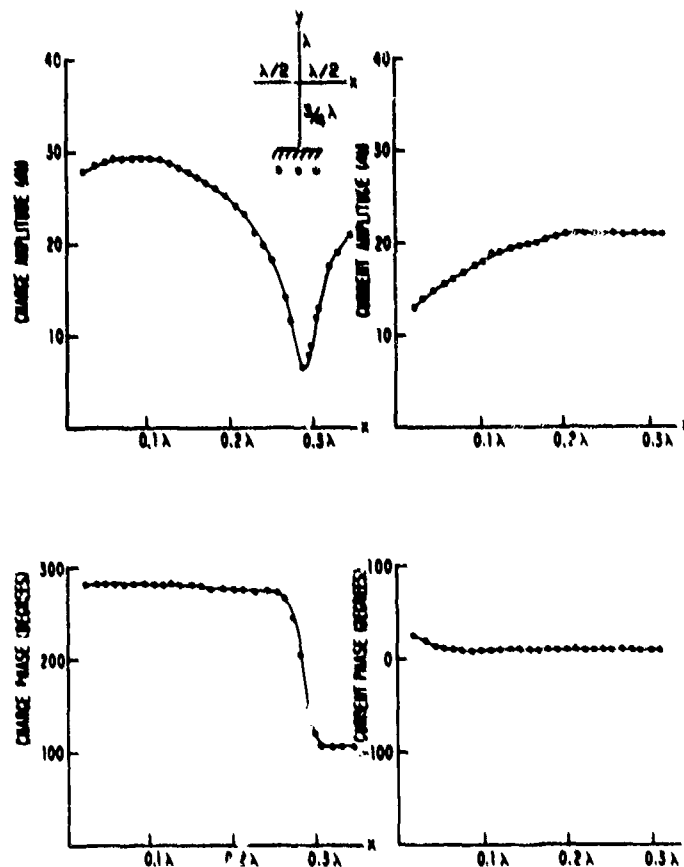


Fig. 19. Amplitude and phase distributions of charge and longitudinal current density on horizontal element of crossed-dipole receiving antenna illuminated by a vertically polarized plane wave as a function of distance (wavelengths) measured from junction; Case 5.

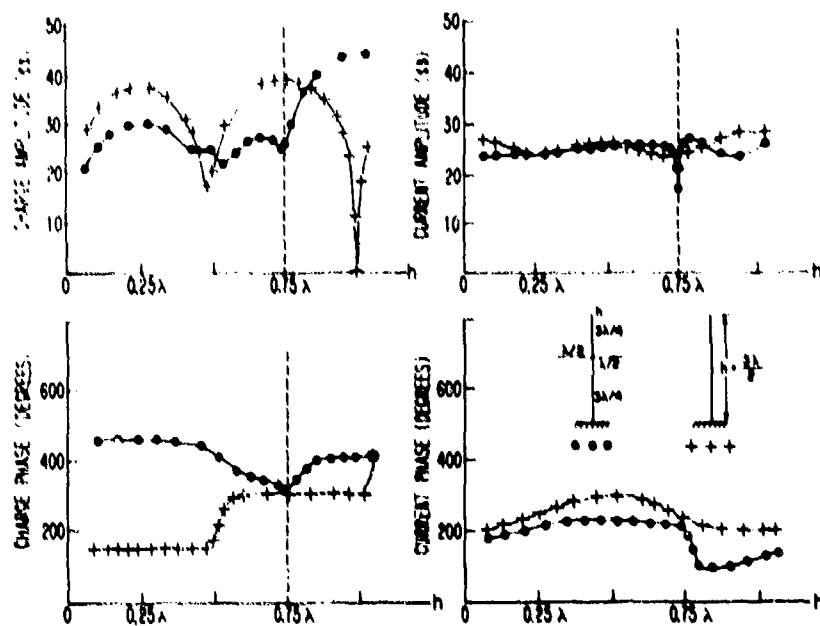


Fig. 20. Amplitude and phase distributions of charge and longitudinal current density on vertical dipole and crossed dipole illuminated by a vertically polarized plane wave as a function of antenna height,  $h$ ; Case 6.

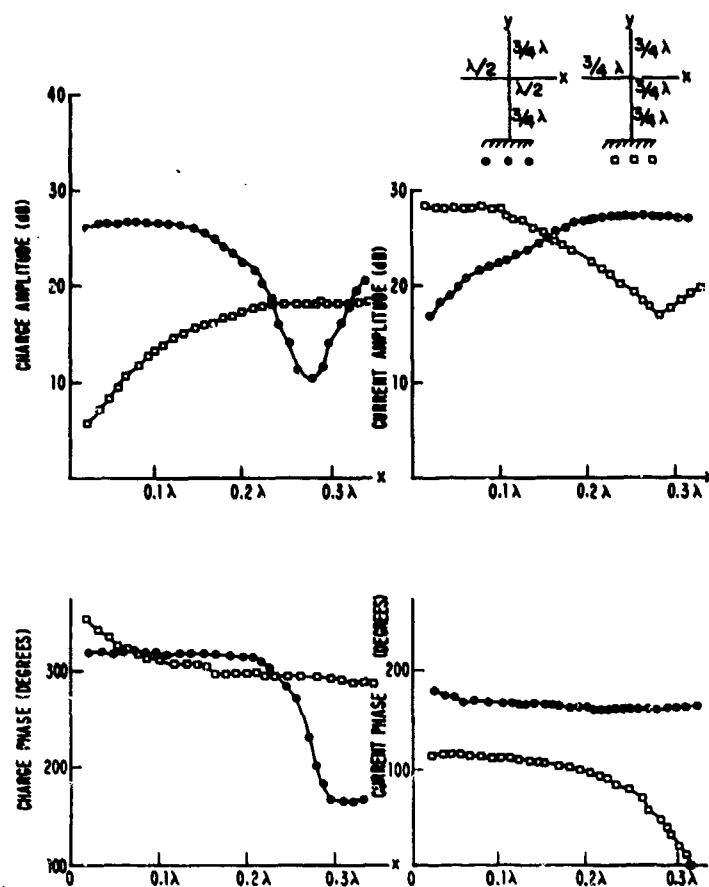


Fig. 21. Amplitude and phase distributions of charge and longitudinal current density on horizontal element of crossed-dipole receiving antenna illuminated by a vertically polarized plane wave as a function of distance (wavelengths) measured from junction: Case 6.

# PROBLEMES POSES PAR LA TRANSMISSION DANS UN SYSTEME INTEGRE AEROPORTE

par

MM. G. David et Vannetzel  
T.R.T.  
5, Avenue Réaumur - Le Plessis-Robinson  
France

31-1

## SOMMAIRE

Un système de transmission intégré doit posséder une redondance suffisante pour garantir un service complet à la première panne, il faut cependant limiter l'importance du matériel mis en oeuvre pour assurer les secours c'est pourquoi nous avons retenu une redondance d'ordre deux qui consiste à doubler le système de transmission.

Nous donnons des structures séries ou parallèles raisonnablement envisageables d'où l'on peut dégager les principes des échanges. Nous supposons qu'ils sont toujours pilotés à partir d'une unité de gestion.

Nous examinons succinctement quelques uns des problèmes qui apparaissent au niveau de la transmission et des échanges entre le système de transmission et les équipements.

Les échanges d'information entre la transmission et les équipements peuvent avoir lieu en bande de base avec un codage du type NRZ.

Au niveau de la transmission compte tenu des distances, un codage biphase est préférable car il élimine toute composante continue sur la ligne de transmission principale.

Enfin les échanges numériques facilitent le contrôle des informations et par la même diminuent les risques d'erreur.

## 1. GENERALITES

L'électronique déjà largement présente sur les avions par les équipements de communications voit son champ s'étendre dans les domaines de la navigation (Radio navigation) et les systèmes de vol où elle se substitue aux procédés électromécaniques.

Les interconnexions entre les équipements sont encore réalisées par l'ancien procédé qui consiste à utiliser un fil par information d'où une prolifération extraordinaire des cablages dans les avions actuels.

Il apparait un décalage important entre les possibilités de traitement, de génération, d'utilisation des informations et leur transport d'où l'idée de réduire les cablages en multiplexant dans le temps les informations sur un nombre restreint de fils.

Avec un marché du S.T.T.A., T.R.T. a étudié la faisabilité d'un système de multiplexage à l'aide d'une ligne omnibus exploitée en temps partagé à bord d'aéronefs. Cette étude a été menée avec la collaboration des Sociétés A.M.D. et S.E.S.A. Un tel système de multiplexage doit répondre aux objectifs suivants:

- Diminuer le volume et le poids des cablages,
- Améliorer l'implantation et l'interconnexion des équipements,
- Permettre les modifications et en particulier la pose ou la dépose d'un équipement du fait de l'évolution de l'équipement ou d'une nouvelle génération,
- Connecter facilement les équipements,
- Faciliter les opérations de maintenance et de dépannage.

Une des principales contraintes du système de transmission est d'acheminer des informations qui considérées à l'état brut ne sont pas à un format unique, sans cadence de prélèvement uniforme pour toutes les informations, avec en fonction des situations de vol la possibilité de voir apparaître des demandes évolutives ou des répétitions.

Une unité de gestion assure les échanges dans des situations stables mais peut recevoir des modifications de programme venant d'une organe plus élaboré capable de synthétiser la situation des besoins en échanges d'information.

Le système de transmission doit posséder une souplesse suffisante pour satisfaire les contraintes aéronautiques tout en ayant un haut degré de sécurité de fonctionnement.

Dans la mesure où le système de transmission est unique il faut que sa fiabilité soit bonne mais il doit être muni de dispositifs de contrôle pour garantir la validité des informations transmises et en cas de défaillance d'un élément de la chaîne de transmission, il faut détecter le défaut et éliminer l'élément ou partie d'équipement incriminé de façon à rétablir l'intégrité des échanges.

Bien entendu, il est impossible d'envisager un système capable de conserver l'intégrité des échanges quel que soit le nombre des pannes successives pouvant advenir, sa complexité et son volume iraient à l'encontre de la simplification recherchée.

## 2. REDONDANCE DU SYSTEME DE TRANSMISSION

La redondance améliore considérablement la disponibilité du système.

Trois types de redondance sont possibles:

- Redondance active où tous les dispositifs fonctionnent en même temps,
- Redondance passive où un seul dispositif fonctionne à la fois,
- Redondance majoritaire qui permet au système de se rallier à la majorité des dispositifs.

Le système d'échanges d'informations à bord d'avion doit être capable d'éviter ou de réduire l'interruption des échanges en cas de défaillance d'un élément de la chaîne de transmission, ce qui implique en cas de défaillance une reprise des échanges en un temps minimal.

Cette remarque implique que la redondance choisie s'apparente à la redondance active, ainsi la reprise des échanges a lieu immédiatement sans attendre le temps de démarrage d'un dispositif électronique.

En considérant un équipement sans autre considération quant à son doublement éventuel, le système d'échanges est relié à un équipement unique. Le système d'échanges étant redondant il est nécessaire qu'un système d'aiguillage permette à l'équipement d'avoir accès seulement à la partie du système d'échanges qui est active, pour éviter toute diaphonie au niveau de l'équipement entre la partie active et les redondances.

Par ailleurs une étude de circuits nous a montré qu'une redondance majoritaire d'ordre 3 (trois dispositifs de transmission) avec la logique de décision associée nécessite plus de circuits qu'un simple dispositif d'aiguillage propre à une redondance d'ordre 2.

Une redondance active d'ordre 2 apparaît comme un compromis bien adapté aux contraintes aéronautiques.

## 3. STRUCTURE DES SYSTEMES D'ECHANGES

### 3.1 Considérations Générales

La structure choisie pour le système influe sur la conception des procédures d'échanges, les interfaces et la fiabilité.

Les structures présentées ici tiennent compte des remarques du paragraphe précédent et sont limitées à une redondance d'ordre deux.

La géométrie d'un système d'échange est caractérisée par le mode de connexion des équipements. Celui-ci peut être:

- "Série". La ligne de transmission est interrompue de part et d'autre de l'équipement et se trouve découpée en tronçons élémentaires.
- "Parallèle" ou en dérivation. Les équipements sont couplés en dérivation sur la ligne de transmission.

Dans ces systèmes, l'unité de gestion est capable d'organiser les échanges selon un programme préétabli, ce qui évite d'avoir à pénaliser un calculateur pour assurer des échanges de routine.

La calculatrice peut intervenir dans le système pour modifier l'ordonnement des échanges à partir de critères compliqués que l'unité de gestion n'est pas capable d'interpréter.



### 3.2 Structure Série

#### 3.2.1 Structure Série Constituée de Deux Lignes Double Unidirectionnelles

31-3

Un tel système comporte deux unités de gestion l'une est en service et la seconde en secours. Chacune pilote l'une des deux lignes doubles unidirectionnelles. Les équipements sont raccordés à ces deux lignes (voir figure 1).

Les échanges sont susceptibles d'être assurés avec la procédure suivante:

- Dans le sens de transmission unité de gestion équipements, ou trajet aller, on effectue la collecte d'une ou plusieurs informations,
- Dans le sens opposé, au trajet retour on diffuse aux équipements récepteurs les informations précédemment collectées.

Le passage par l'unité de gestion facilite le contrôle des échanges.

La sauvegarde de la transmission est assurée par redondance des unités de gestion, des supports de transmission des circuits de raccordement des équipements.

#### 3.2.2 Structure Série Composée de Deux Lignes Bidirectionnelles Indépendantes

La structure représentée figure 2 a les mêmes propriétés que la précédente, elle divise simplement par deux le nombre des lignes de transmission.

#### 3.2.3 Structure Série Composée de Deux Lignes Unidirectionnelles Bouclées Indépendantes

Le système se compose de deux réseaux indépendants chacun d'entre eux étant piloté par une unité de gestion (voir figure 3). En fonctionnement normal, un seul réseau réalise les échanges, le second réseau n'intervient qu'en cas de panne du premier.

L'on peut concevoir que l'exploitation d'un tel réseau se fasse en deux temps:

- Collecte des informations,
- Diffusion des informations.

Bien que redondant d'ordre 2 ce système ne peut résister à plus d'une défaillance sur l'un et l'autre réseau.

#### 3.2.4 Structure Série Composée d'un Ligne Bidirectionnelle Bouclée

Le système possède deux unités de gestion comme il est indiqué figure 4, une seule est en service à un instant donné.

En fonctionnement normal, la ligne est exploitée en mode unidirectionnelle; le mode bidirectionnelle n'est utilisé qu'après une défaillance d'un élément.

Les unités de gestion ont un dialogue possible grâce à une ligne directe ce qui permet d'exploiter au mieux les redondances et de résoudre beaucoup de cas de pannes avec un support de transmission minimum.

### 3.3 Structure Parallèle

#### 3.3.1 Structure Parallèle Composée de Deux Lignes Indépendantes

Le système se compose de deux lignes pilotées chacune par un organe central comme le montre la figure 5.

Le branchement en parallèle de tous les équipements suppose qu'à un instant donné un seul équipement soit émetteur pour que le message puisse être décodé convenablement. Cette remarque oblige à compliquer le système pour éviter deux émissions simultanées, par ailleurs il importe de protéger la ligne contre un court circuit.

#### 3.3.2 Structure Parallèle Composée de Deux Lignes Bouclées Indépendantes

Les deux unités de gestion sont indépendantes et pilotent chacune une ligne de transmission (figure 6).

L'unité de gestion en veille reçoit en permanence les informations de la ligne active. Il lui est ainsi possible de détecter toute anomalie de transmission et de prendre le relais.

#### 3.3.3 Structure Parallèle Comportant Deux Lignes Doubles et non Bouclées

Chaque unité de gestion est indépendante et pilote une ligne double, une ligne sert à la transmission de l'unité de gestion vers les équipements alors que l'autre ligne est utilisée dans l'autre sens (voir figure 7).

Dans la mesure où les unités de gestion peuvent dialoguer entre elles l'on peut envisager toutes les combinaisons pour la sauvegarde du système.

### 3.4 Comparaison Entre les Structures Séries et Parallèles

Les exemples précédentes, pour une redondance d'ordre deux, font apparaître la diversité de structures possibles, sans préjuger des procédures d'échanges aussi les comparaisons ne porteront que sur les caractéristiques liées à la transmission sans évaluation complète des systèmes.

Les caractéristiques prises en compte concernent:

- le couplage électrique au support de transmission,
- les possibilités de transmission bidirectionnelle des informations,
- la sécurité de la transmission,
- les possibilités d'extension.
- les procédures d'échanges autorisées.

#### 3.4.1 Couplage Electrique des Equipements

Avec une structure série, chaque raccordement joue le rôle d'un répéteur et restitue un signal débarrassé des défauts de propagation. Les impédances vues depuis la ligne du côté de l'émetteur comme du côté du récepteur peuvent être rendues égales à l'impédance caractéristique du support.

Avec une structure parallèle, chaque coupleur prélève une fraction de l'énergie disponible sur la ligne au droit de la dérivation.

Il est nécessaire de faire un compromis entre la fraction d'énergie prélevée à chaque dérivation et le nombre de celles-ci.

Si chaque coupleur prélève une part trop importante d'énergie, la perte d'énergie au niveau de la ligne doit être compensée par un gain plus important du récepteur d'où une augmentation de la sensibilité aux parasites.

Le branchement en parallèle peut s'effectuer selon deux procédés:

- branchement à haute impédance. Les récepteurs d'impédance successives sont susceptibles de provoquer une déformation des signaux du fait des réflexions à chaque désadaptation. Ceci ajouté aux distorsions causées par les imperfections accroît la sensibilité aux parasites.
- branchement par dispositif adapté, ce type de couplage a des pertes et demande l'interruption du support de transmission.

#### 3.4.2 Possibilité de Transmission Bilatérale

Avec une structure parallèle, les signaux doivent être émis par un seul équipement. Le support n'est donc utilisable qu'à l'alternat. Par contre avec une structure série, il est possible de superposer des signaux se propageant dans les deux sens de transmission en utilisant des coupleurs spéciaux capables d'extraire le signal reçu, mais en un point on ne reçoit qu'un seul signal. La transmission bilatérale simultanée est intéressante car elle est susceptible de permettre une reconfiguration de la structure série en utilisant un unique support de transmission.

#### 3.4.3 Cadence Possible de Transmission

Avec une structure série du fait de l'adaptation de tous les tronçons de ligne, un débit de 10 M bit/S est envisageable sans poser de problème technologique insurmontable, à condition de choisir un support de transmission de bonne qualité comme par exemple un câble coaxial.

Une structure parallèle du fait des ruptures d'impédance du support de transmission permet des débits moindres, de l'ordre du Mégabit par seconde, dans ces conditions le support de transmission peut être une paire torsadée.

#### 3.4.4 Procédures d'Echanges

A partir d'une structure série toutes les procédures d'échanges sont possibles y compris celles gérées de manière décentralisée où une information venant d'un équipement est insérée en un point précis d'un multiplex temporel.

Par contre les structures parallèles doivent être gérées de manière centralisée et nécessitent des procédures d'échanges du type interrogation réponse, l'unité de gestion n'interrogeant qu'un seul équipement à la fois.

## 4. RACCORDEMENT DES EQUIPEMENTS AU SUPPORT DE TRANSMISSION

### 4.1 Définition des Frontières

31-5

Le raccordement ou coupleur est un dispositif nécessaire pour:

- Adapter le débit et le format des informations en provenance du support de transmission aux besoins de l'équipement numérisé.
- Extraire et présenter les informations au bon instant sur le support de transmission.

Il apparaît deux types de couplage:

- Un coupleur au niveau de la transmission ou coupleur de BUS,
- Un coupleur du côté équipement ou coupleur de sous-système.

C'est le coupleur sous-système qui est délicat à définir, en effet il faut laisser aux constructeurs d'équipements la possibilité d'utiliser leurs équipements dans plusieurs systèmes d'échanges différents, et à la limite, leur laisser la possibilité de raccorder les équipements sans système d'échanges.

L'interface au niveau du coupleur de BUS peut être définie sans contrainte particulière puis-qu'il s'agit en fait d'une partie intégrante du système d'échanges.

Un échange d'informations entre deux équipements est géré par une procédure d'échanges qui définit les différentes phases de l'échange ainsi que les commandes à engendrer pour en permettre la réalisation. Pour banaliser au mieux le coupleur il est intéressant qu'une même procédure de base puisse régir tous les échanges car cela risque d'influer sur la standardisation des interfaces et par là même des coupleurs.

Figure 8 nous rappelle comment se situent les jonctions pour raccorder un équipement au sous-système.

### 4.2 Schéma Fonctionnel d'un Raccordement Simple

Nous n'aborderons pas le problème des redondances au niveau des raccordements car il faudrait considérer la technologie, la structure du système d'échanges, procédures d'échanges. . .

Le couplage du sous système est différent suivant le mode de branchement choisi: série ou parallèle.

Mais l'on retrouve toujours sensiblement le même ensemble de circuits destiné à analyser les ordres venant de l'unité de gestion et dont le rôle est de commander les échanges.

De son côté l'équipement ou sous système est muni de registres d'entrée et de sortie destinés à stocker les informations, il s'agit de les utiliser au mieux pour éviter les duplications inutiles de matériel.

Les principaux circuits intervenant dans l'échange des informations entre le BUS et le sous système sont indiqués par la figure 9.

Il comprend deux parties, le coupleur de BUS pour réaliser la transmission et contrôler les échanges et le coupleur sous système qui dialogue directement avec les équipements.

### 4.3 Nature des Signaux Echangés

#### 4.3.1 Signaux Transmis sur les Lignes BUS

Quelle que soit la structure, il est intéressant de transmettre des signaux sans composante continue, de façon à avoir la possibilité de réaliser une isolation galvanique entre les éléments disposés sur la ligne de transmission. Les équipements peuvent être distants les uns des autres, alimentés à partir de sources différentes, il importe d'éviter les courants de circulation qui accentuent la sensibilité aux parasites de la transmission.

Pour ces raisons, le message de base est codé avant d'être transmis.

Aujourd'hui, deux codages paraissent faire l'unanimité des constructeurs:

- le code bi phase Manchester,
- le code bi phase avec retour à zéro.

Ces deux codes ont l'avantage de contenir l'horloge de la transmission donc d'éviter une ligne supplémentaire pour transmettre cette information. De plus, lorsque l'horloge est directement extraite des données il n'y a pas de décalage entre l'information et des transitions d'horloge d'où un risque moindre d'erreur.

#### 4.3.2 Signaux Echangés entre le Coupleur Sous Système et le Sous Système

La distance séparant le coupleur sous système et le sous système est faible, et dans de nombreux cas ils seront alimentés par la même source d'énergie.

Dans ces conditions rien ne s'oppose à ce que les données entre sous système et coupleur sous système soient échangées en codage N R Z.

Sous cette forme les signaux s'exploitent facilement.

Pour diminuer au maximum les redondances, il sera sans doute avantageux que la transmission exploite directement les registres des équipements qui stockent l'information. Une procédure d'exploitation mixte de ces registres est à envisager, surtout si l'on désire une extraction sous forme série du côté transmission pour réaliser le maximum d'économie de circuits.

### 5. CONCLUSIONS

Un système d'échanges numérisé semble attrayant par le fait même qu'il diminue considérablement les câblages entre les équipements mais il est important que la transmission soit sûre.

Pour cela deux supports sont actuellement retenus pour les lignes BUS:

- le cable coaxial,
- la paire torsadée blindée.

Ces deux supports résistent bien à l'induction de parasites extérieurs et évidemment les signaux qu'ils véhiculent rayonnent peu.

L'utilisation d'un codage sans composante continue pour la transmission sur des distances de quelques mètres ou dizaines de mètres améliore la sûreté de transmission.

Les messages eux-mêmes peuvent être contrôlés par l'adjonction de bits de parité et une procédure de demande de répétition. Il faut cependant éviter d'aller trop loin dans cette voie sous peine d'augmenter considérablement le volume de l'électronique à mettre en oeuvre, ce qui réagit sur la fiabilité.

Nous remarquons que les circuits logiques admettent un haut degré d'intégration et la réduction de volume qui s'en suit permet le blindage facile des circuits pour limiter leur rayonnement.

Enfin les circuits logiques eux mêmes sont difficilement brouillables dans la mesure où les longueurs des interconnexions restent faibles et les impédances pas trop élevées; nous retrouvons là le dilemme consommation - efficacité.

### REFERENCES

- |         |  |
|---------|--|
| CORE    | <i>Methodologie et Gestion de la Fiabilité des Systèmes Cours Polycopié.</i> ENSAE, 1972.                          |
| C N R S | <i>Journées d'Etudes sur les Calculateurs Numériques Embarqués et Leurs Applications.</i><br>Edition PRIVAT, 1974. |
| T R T   | Rapport final de l'étude S T T A. <i>Intégration, Communication, Navigation, Equipements,</i><br>1974.             |

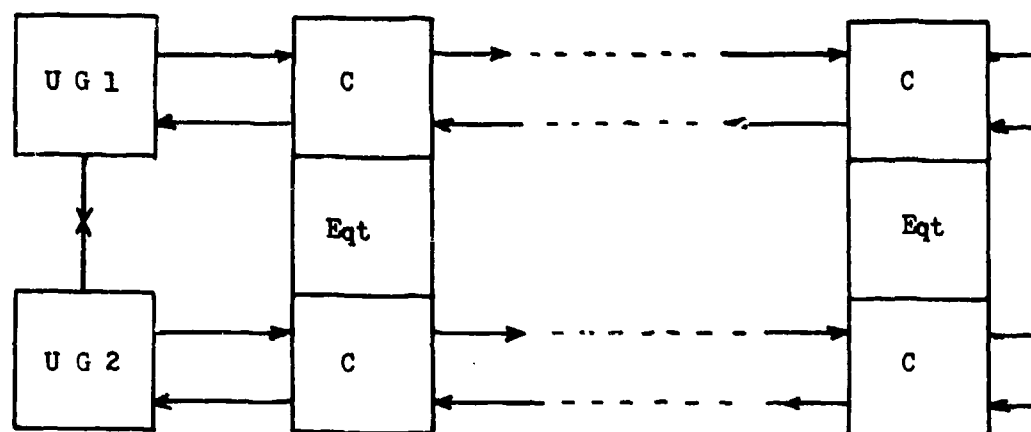


Fig.1 Structure série: deux lignes double unidirectionnelles

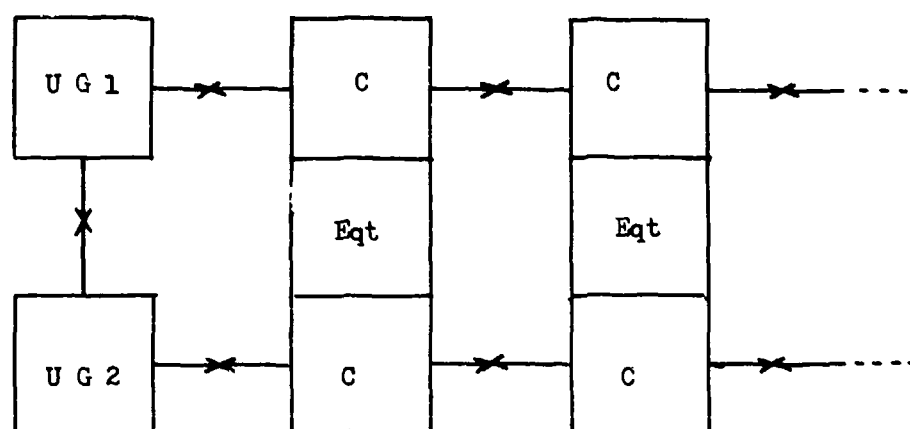


Fig.2 Structure série: deux lignes bidirectionnelles indépendantes

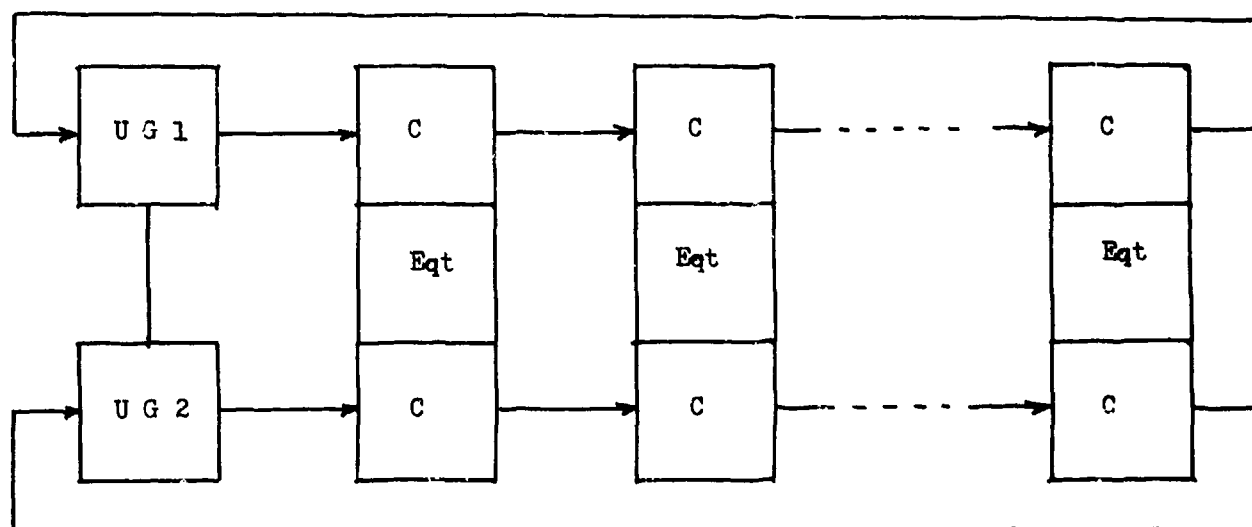


Fig.3 Structure série: deux lignes unidirectionnelles bouclées indépendantes

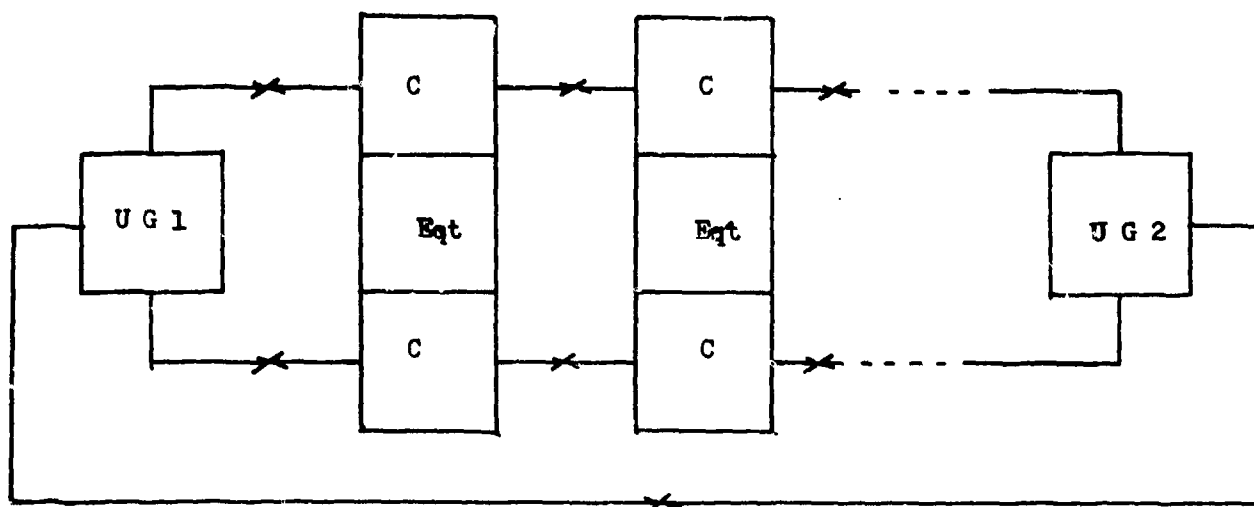


Fig.4 Structure série: ligne bidirectionnelle bouclée

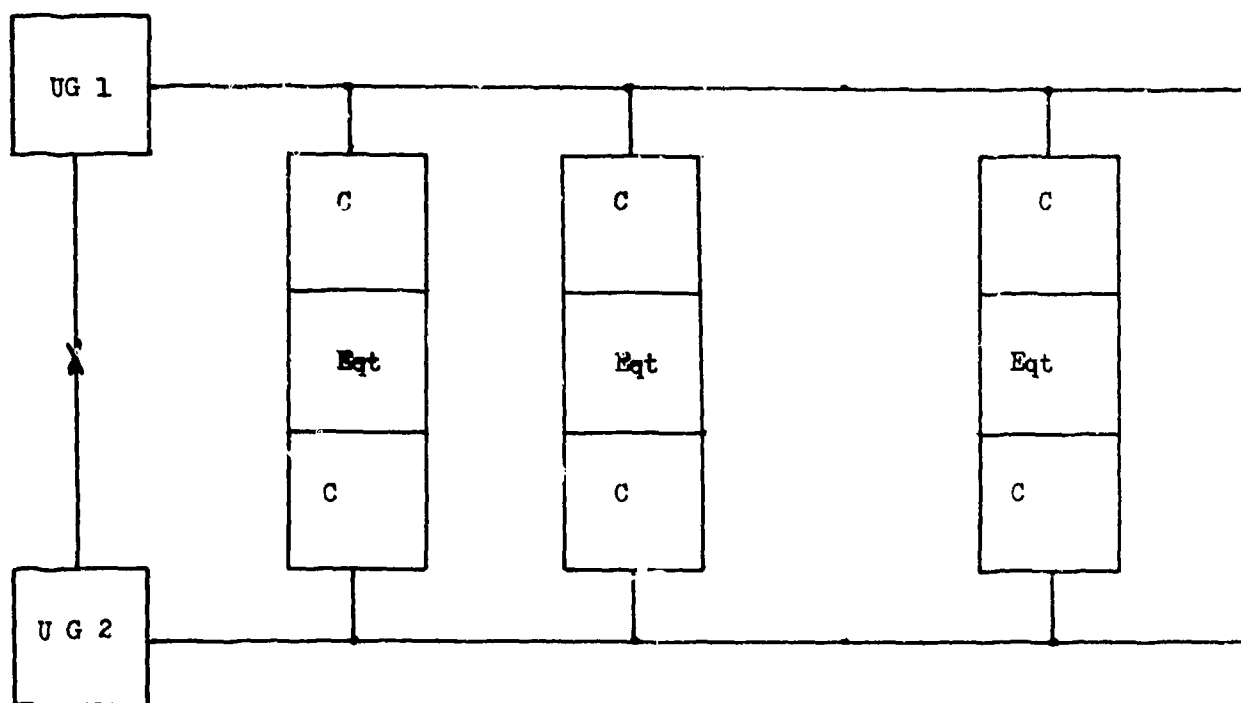


Fig.5 Structure parallèle: deux lignes indépendantes

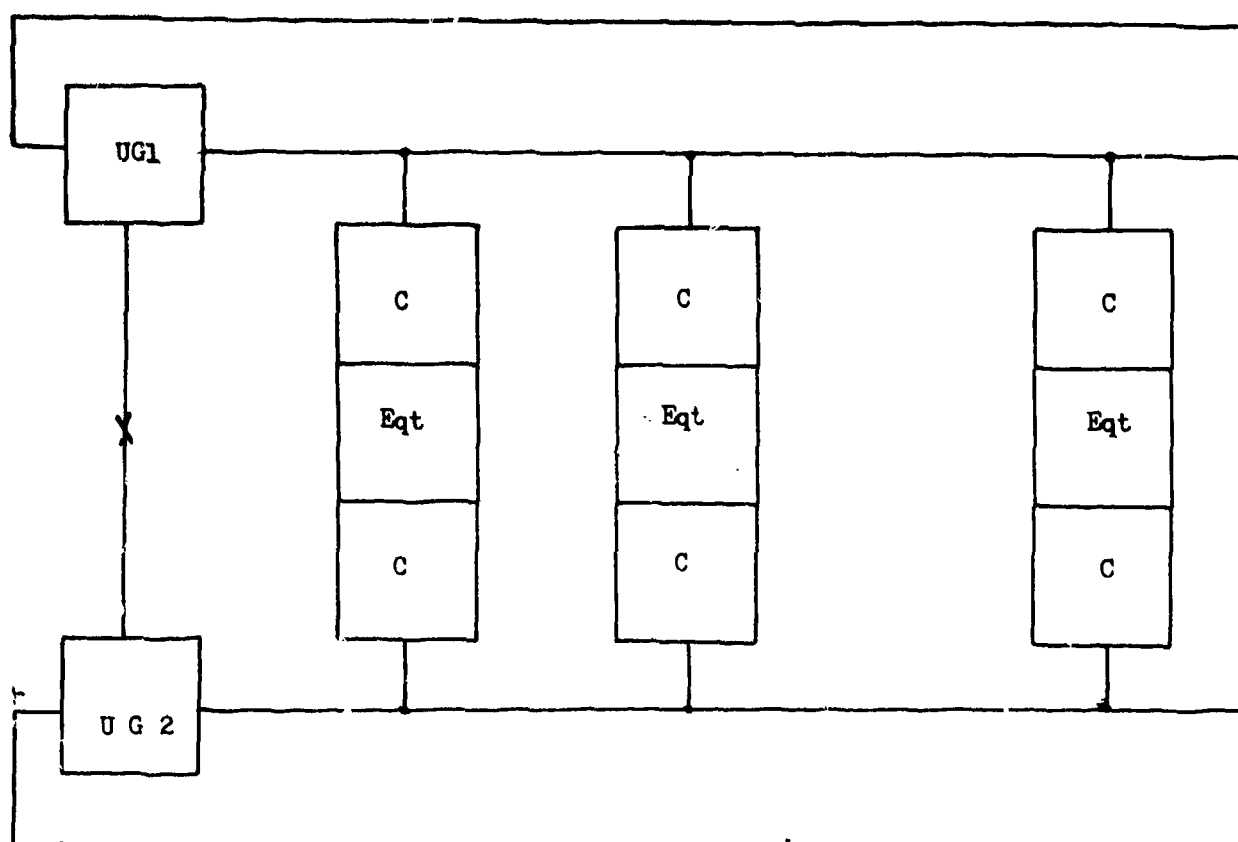


Fig.6 Structure parallèle: deux lignes bouclées indépendantes

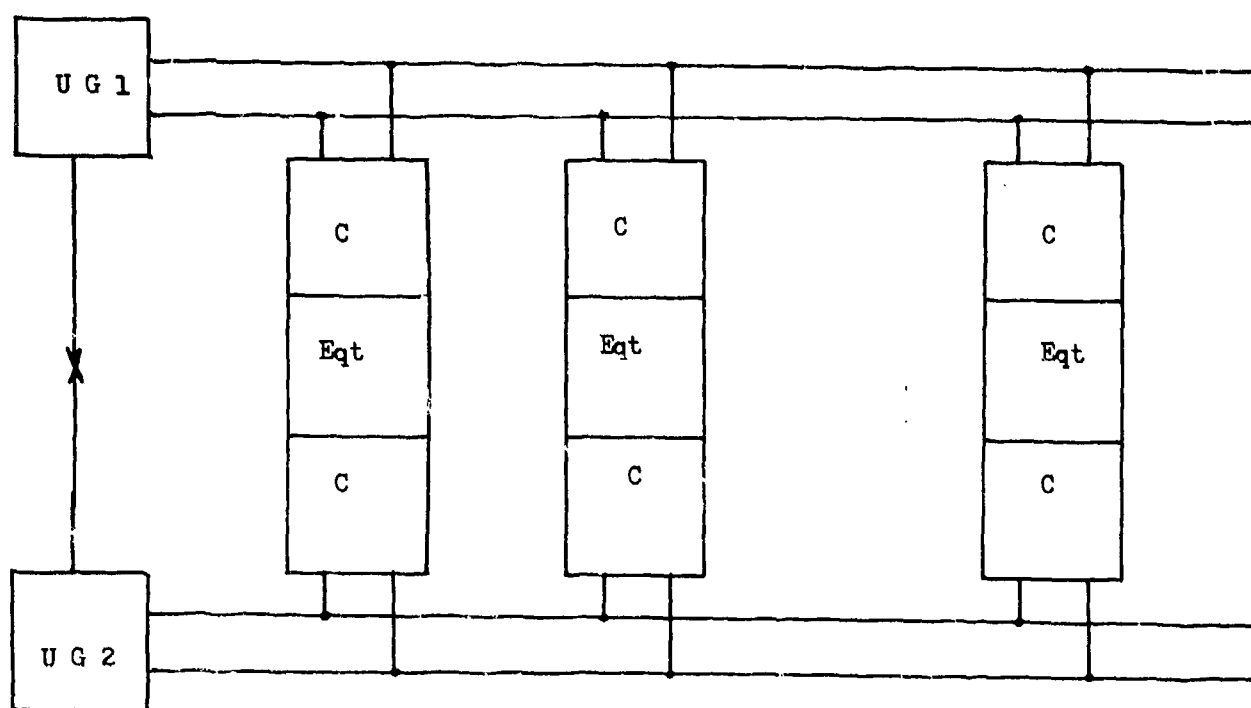


Fig.7 Structure parallèle: deux lignes doublées non bouclées

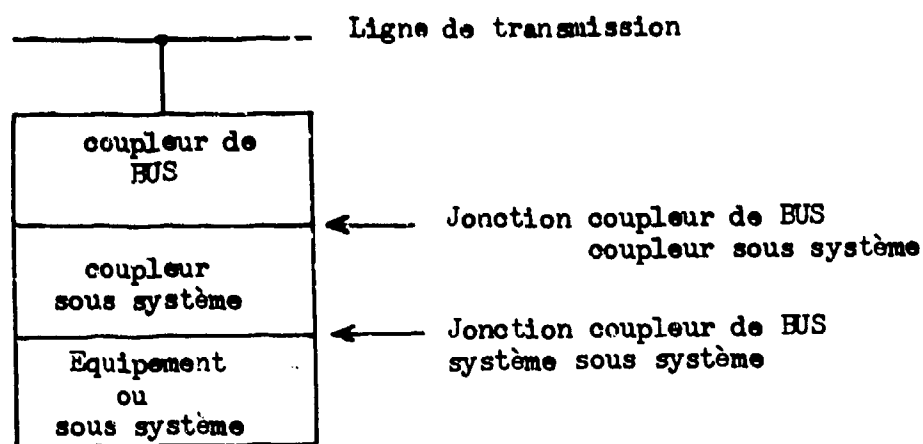


Fig.8 Raccordement d'un sous système

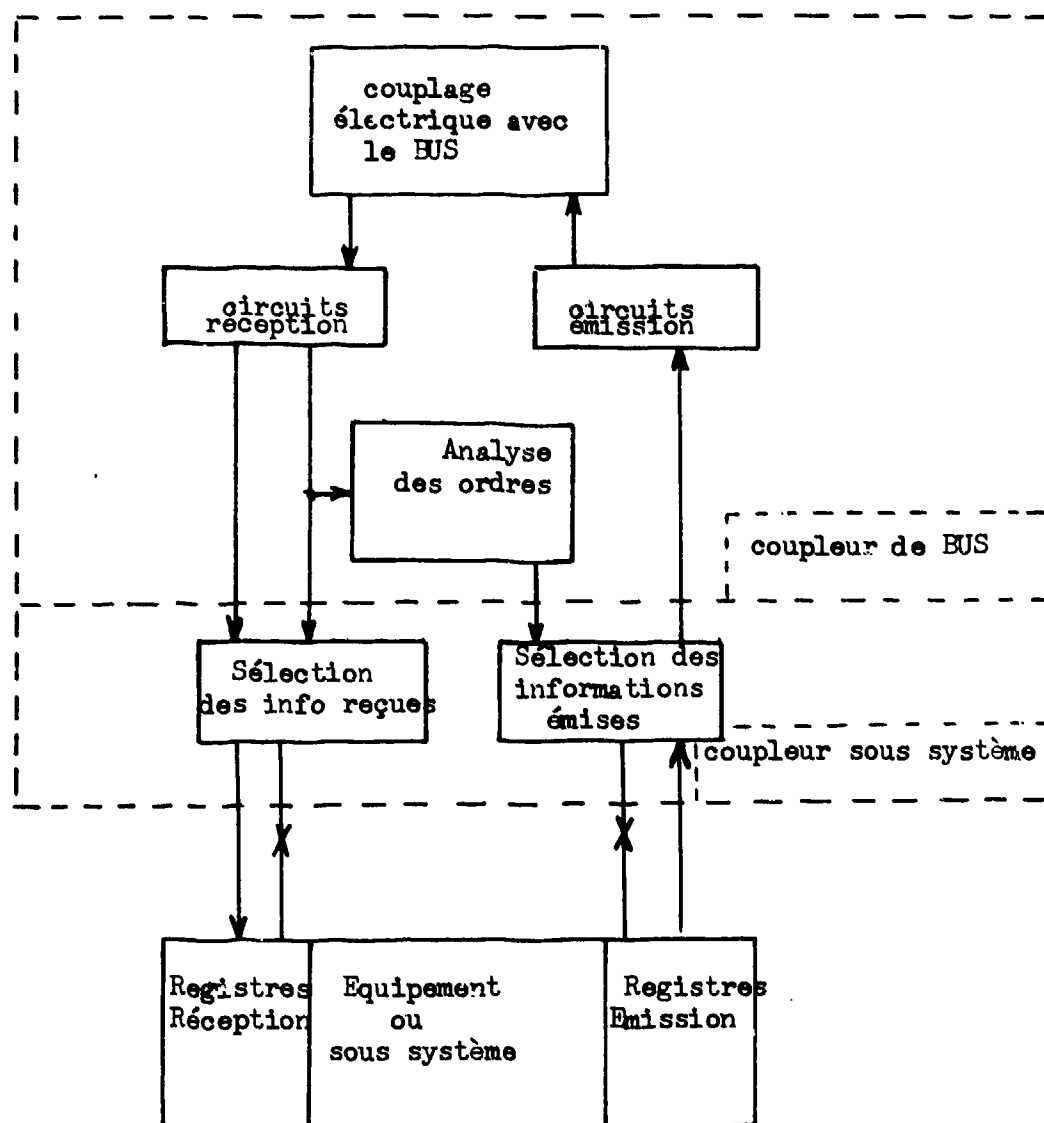


Fig.9 Schéma fonctionnel du raccordement d'un sous système



DIGITAL DATA TRANSMISSION IN AIRCRAFT  
EMC-PROBLEMS AND POSSIBLE SOLUTIONS

R. Rode  
 Messerschmitt-Bölkow-Blohm GmbH  
 Ottobrunn/Munich  
 Germany

SUMMARY

In the use of digital systems in aircraft, where a great deal of interference emission and very sensitive equipment are concentrated in a small space, new problems can arise due to the special type of emission and susceptibility of the digital systems. Great care must therefore be laid on the selection of the cabling (twisting rate, shielding), the line drivers and receivers, the rise and fall time, and the transmission rate. To prove in practice the meaning of theoretical evaluations of a choice of line drivers, line receivers and cables, special tests were performed on the EMC-test-facilities at MBB. These tests also covered the different shielding and earthing possibilities. The experience obtained from theory and practice found their implementation in European aircraft-program.

Special EMC-tests were established to prove the compatibility of the digital systems with the complete aircraft system.

1. INTRODUCTION

Modern aircraft require more and more sophisticated equipment operating on a digital basis. These systems can be the Primary Flight Control (fly by wire), the Auto-pilot, the Air Intake Control, the Air Data Computer, the Inertial Navigation or the stores management system. It can be seen that all these systems are important for flight safety and mission success. It is therefore necessary to design the digital data transmission with a high noise immunity. Great care has to be laid on the selection and calibration of the line drivers and line receivers in view of rise time, fall time and transmission rate; also the selection of the connecting wires is important in view of twisting rate and shielding effect. Practical tests have then to indicate the susceptibility limits and the level of conducted and radiated emission to be sure to achieve an overall compatible aircraft system.

2. LAYOUT OF THE TRANSMISSION SYSTEM

2.1. General Layout.

Several studies have been conducted to optimize a data transmission system from an EMC point of view, where the unwanted emission from the transmission cables is as important as the susceptibility to external interference sources. As a result, fig. 1 shows the proposed configuration where the data together with the data identification (TAG) are transmitted on one twisted pair, a second twisted pair carrying the clock pulses for bit synchronization. This system is proposed on the grounds of optimization of weight, connection number, mission safety, costs and development risk. The necessary clock frequency is limited to high frequencies by the rising cable radiation (short rise and fall times necessary) and the usable cable types (twisted pairs). The minimum possible clock frequency can be calculated from the necessary data flow per unit of time. Finally a clock frequency of  $64 \text{ kHz} \pm 5\%$  is proposed as a compromise. A pulse coded modulation shall be used as a modulation frequency because other modulation techniques as pulse position modulation or pulse width modulation need much higher bit frequencies which means a higher emission of interference. The data signal format shall be of the type "non-return-to-zero" because all "return-to-zero" formats have more edges to the waveform and the transmission therefore radiates more interference at higher frequencies. An important part of the general layout is to assure as much transmission safety as possible. Faults can occur due to equipment failures or interference from external sources (other equipment, lightning strikes, EMP).

The data signals shall be transmitted on the two lines in both "true" and "complement" form, each being the logic inverse of the other. The two lines are twisted together so that both lines experience the same electromagnetic environment on the route to the receiver. Thus any noise picked up would induce the same effect on both lines. Usual receivers are designed to detect the difference between the two lines and reject the noise which is the same on both lines (common-mode rejection). The symmetry of the true and complement waveforms must be maintained since well-balanced waveforms will tend to cancel the radiated field of the other.

Fig. 2 shows the serial data transfer which seems to be an optimal solution for transmission safety.

Bit No.	Name	Bit No.	Name
1	Control Bit	9	Least Significant Data Bit
2	Spare Bit 1	10 - 23	Data Bits
3	Least Significant Bit (TAG)	24	Most Significant Data Bit
4 - 6	Identification Bit (TAG)	25	Spare Bit 3
7	Most Significant Bit (TAG)	26	Parity Bit
8	Spare Bit 2	27 - 32	Word Synch Clock Bits

Correct and undisturbed transmission can be checked as follows:

- The control bit (1) shall be set to a logic "1" when the transmitting equipment is in order.
- The spare bits (2, 8, 25) shall always be set to digital "0" and to the correct position.
- The identification (3-7) and data word (9-24) shall always have the fixed word length.
- The parity bit (26) shall be set so that the total parity of the data word (26 bits) is odd.
- A missing synchronization indicates a transmission fault.

All these above mentioned checks are important for correct data transmission and are used later on as susceptibility criteria during the EMC-tests.

## 2.2. Line Drivers and Receivers.

Since most of the avionic equipment will be designed using standard logic operating from a 5 V power supply, this voltage shall also be used with the following definition: Digital "1" = +5 V; Digital "0" = 0 V.

A transmission system designed to operate in an aircraft should be able to operate with a 20 meter cable-length between line driver and receiver. The driver and receiver have to be chosen accordingly. Integrated circuits shall be used for reasons of space, cost, weight, and reliability. The most important part of the line driver and receiver layout from an EMC point of view is the definition of the transmitted waveform. Limiting the rise and fall time of the transmitted signal reduces the radiated emission. As a possible solution fig. 3 shows the proposed waveform, where the time between the 10% to the 90% value is about 1  $\mu$ s which means a much lower rise and fall time than usual (10 ns). The waveform shall not exhibit any sharp discontinuities between transition from one logic level to another. Every deviation from the ideal waveshape shall be limited as much as possible. Fig. 4 shows the proposed limits for permitted deviations from the ideal waveshape (overshoot, undershoot, pulse ringing, pulse droop and pulse jitter). Every sharp discontinuity increases the radiated interference and therefore the cross-coupling to other sensitive lines. Since the line receiver should only need to operate with signals having 64 kHz repetition frequency, it can be designed to have an input noise bandwidth of less than 2 MHz which means a rejection of all high frequency noise at the receiver input, therefore reducing the susceptibility of the transmission system.

## 2.3. Cable Selection.

As stated before, the proposed solution for the DDT system is to use two screened twisted-pair cables. On the grounds of space, weight and simplicity it is preferable to have only one cable per channel and it is therefore proposed to adopt a twisted-quad cable as shown in fig. 5. Tests with several types of cable indicates that the use of a quad cable does not reduce the compatibility of the system when good screening efficiency is assured (a woven copper screen with a coverage of more than 90% proved satisfactory). In order to achieve matched conditions for the transmission system the characteristic impedance of the cable at 64 kHz shall be about 100  $\Omega$ . During the EMC-tests several possibilities for connecting the screen with an earth-point were tested and will be discussed later. The signal lines themselves shall be ungrounded (balanced signals) which is also important to avoid earth loops and possible potential differences between line driver and receiver. Fig. 6 shows a collection of the proposed data for the selected transmission system which were adopted for testing and later on for aircraft use.

## 3. EMC-TEST

### 3.1. Test Set-Up.

A special EMC-test-program was established at MBB to prove the effectiveness of the envisaged measures. The test set-up is shown in fig. 7, and indicates that the attempt was made to simulate some typical aircraft conditions as closely as possible:

- Cable length: 20 m (twisted-quad).
- Ground plane (aluminum), simulating the aircraft structure, width 1 m, test cable mounted midway between its edges.
- Height of cable above ground plane: 5 cm (medium distance possible in an aircraft, also distance as required for MIL-STD 461 A, 462 testing).
- Test wire directly attached to the DDT cable, coupling length 4 m.
- Line drivers and receivers with the necessary circuits driven by batteries mounted in screened enclosures.

- (f) A bulkhead connector simulation was mounted in a vertical aluminum plate mounted transversely on the ground plane to test the different earthing possibilities of the screen at this point.

The test program consisted of different susceptibility and emission tests performed with several line drivers, receivers and cables with different earthing conditions of the screen. Not all of the tests performed shall be detailed in this lecture and only the main results can be given in compressed form.

### 3.2. Emission Tests.

Two basically different results were received during the emission tests, dependent on the rise and fall time of the transmitted signal (64 kHz). The cable used mainly was the proposed shielded twisted-quad. Different earthings of the screen conditions were checked with the following possibilities (fig. 8):

- (a) Screen connected to earth on transmitter or receiver end only.
- (b) Screen fed-through bulkhead connector via a separate pin
- (c) Screen connected to earth at the bulkhead connector at transmitter or receiver side or on both sides.

With these different conditions the inductive and capacitive coupling on a length of 4 m to a fixed wire was measured with narrowband detection in the frequency range 14 kHz to 100 MHz. Narrowband detection was used because the measured interference was mainly of the narrowband type (at least up to 10 MHz). No measurements are necessary for frequencies lower than 14 kHz because the lowest detectable frequency was 32 kHz. Some important results of the measurements are plotted in the following figures where the first tests were performed with the earthing configuration:

- Screen on Tx end connected to earth
- Screen on Rx end open
- Screen at bulkhead connector through a pin, not earthed at the bulkhead connector.

Fig. 9 shows a comparison of two different line driver/receiver-systems in view of inductive coupling. For this measurement the test wire was shortened and the interference current induced in this loop measured with a current probe. The upper curve is the result achieved with a line transmitting pulses with 20 ns rise and fall time. The lower curve was achieved with a line driver transmitting pulses of 1  $\mu$ s rise and fall time. The result indicates differences of up to 50 dB. The importance of this result can be seen in the comparison with the limit curve of MIL-STD 461 A, test CE 03, CE 04. It can easily be calculated that a second DDT cable in parallel would raise the induced current by 6 dB and then the result in the frequency range 1.5 to 50 MHz would already lie above the limit. This can be the case for a power supply cable running in parallel with the same DDT lines to the same equipment. During a bench test required by MIL-STD 461 A, 462 for military equipment this specific equipment would fail to meet the required limits. A solution which means a reduction of the detected interference on the power line could only be achieved by changing the signal characteristics of the DDT cables as proposed before. Fig. 10 shows the same comparison in view of capacitive coupling. This measurement was performed with a 1.1 k $\Omega$  resistor in series with the 50  $\Omega$  input of the measuring receiver. In comparison with the low impedance of the test wire this can be seen as the case "test wire open" and the measured voltage is a criterion of the capacitive coupling. The voltage across the "open" ends of the test wire can be calculated by adding 27 dB to the values indicated in the diagram. The upper curve is the result achieved with pulses of 20 ns rise and fall time, the lower curve with pulses of 1  $\mu$ s rise and fall time. Differences of up to 30 dB can be calculated from the diagram. The capacitive coupling is an important factor for sensitive signal lines running in parallel with the DDT cables. The maximum level coupled to the test wire was 70 mV (at 7 and 15 MHz). This level can already affect sensitive systems and will be increased, the more the digital lines are in the same cable bundle.

Fig. 11 shows a comparison of the different earthing conditions, as shown in fig. 8 previously in view of inductive coupling. The different earthing possibilities are:

- (a) Screen at Tx and Rx end connected to earth.  
Screen at bulkhead connector earthed on both sides.
- (b) Screen at Tx end connected to earth.  
Screen at Rx end open.  
Screen at bulkhead connector earthed on Rx side.
- (c) Screen at Tx end connected to earth.  
Screen at Rx end open.  
Screen at bulkhead connector through a pin, not earthed at the bulkhead connector.
- (d) Screen at Tx end open.  
Screen at Rx end connected to earth.  
Screen at bulkhead connector earthed on Tx side.

The best solution is obviously case (a) which means earthing the screen at both ends (Tx and Rx) and on both sides of the bulkhead connector. The next possibility is case (c) where the screen is earthed at the transmitter end only, at the bulkhead connector fed through via a separate pin. The distance between the best and worst solution (case (a) and (d)) can be calculated to be up to 50 dB (at 500 kHz).

22-3

Fig. 12 shows the same comparison in view of capacitive coupling. Again case (a) can be seen to be the best solution, followed by case (c). The distance between the best and the worst solution (case (a) and (d)) can be calculated to be again up to 50 dB (at 300 kHz) where it has to be mentioned that case (d) (earthing the screen at the receiver end) is not the worst case for frequencies above 600 kHz.

### 3.3. Susceptibility Tests.

For the susceptibility tests the transmitted bit rate was reduced from 64 kBit per second to 1 Bit per second to be able to monitor the Tx signal and the received signal by digital counters in the form of a direct check. Any deviation between the two digital readings was defined as a malfunction.

All susceptibility tests were performed with the two DDT systems:

- (a) Rise/fall time 20 ns
- (b) Rise/fall time 1  $\mu$ s

For these tests the screen was earthed at the transmitter end, fed through the bulkhead connector via a separate pin (case (d)). This configuration was used although the most favourable solution for emission reasons was to earth the screen at both ends and at the bulkhead connector (case (a)). In view of susceptibilities the earth loops created in case (a) act as antennas for magnetic fields and affect the data transmission. A second reason is the interference current flowing in the aircraft structure which would also flow in the screen via a closed earth loop and would be coupled to the data cables. No susceptibilities could be detected applying an electric field of more than 10 V/m to the DDT system in the frequency range 100 MHz to 3 GHz. This frequency range was chosen because a lot of equipment in an aircraft transmits in this range (V/UHF, TACAN, IFF or the RADAR). No susceptibilities could be detected on applying a CW current of 30 Amps at 400 Hz to the test wire. This case can certainly occur in an aircraft. Some susceptibilities were detected applying 10  $\mu$ s current spikes to the test wire. The susceptibility limits were found in the range 20 to 40 Amps but dependent on the common-mode rejection and matching conditions of the used receivers, mostly independent of the rise and fall time of the transmitted signal. Voltage tests were also performed. A CW-signal of 25 V in the frequency range 100 Hz to 500 kHz was applied to the test wire. No susceptibility could be detected. Some susceptibilities were found on applying voltage spikes (10  $\mu$ s) to the test wire at levels of about 200 V. Again these susceptibilities depend mainly on the common-mode rejection and good matching conditions of the receiver. For some types of receivers no susceptibilities were detected although current pulses of 70 Amps and voltage pulses of 700 V were applied.

## 4. CONCLUSIONS

The EMC-tests performed on the proposed DDT system indicated that for susceptibility reasons a good common-mode rejection and the matching of the line receiver is important. Under realistic environmental conditions, as expected in an aircraft, only susceptibilities against spikes could be detected. In an aircraft the produced spikes (switching operations) should therefore be suppressed to nondangerous levels (20 A current spikes, 200 V voltage spikes). Under this condition the proposed layout of the DDT system is satisfactory which was also proven with the results of the emission tests. The proposed transmission frequency of 64 kHz together with a rise/fall time of 1  $\mu$ s are satisfactory to reduce the emitted interference to an acceptable level. A good transmission safety can be achieved by means of the proposed Control Bits, a parity check and a synchronization check. A twisted-quad cable is proposed for the transmission and proved satisfactory. The complete proposed transmission system was installed in various aircraft equipment. The experience gained from practical use indicates good agreement with the theoretical evaluations and the results of the performed EMC-tests. Fig. 13 to 15 show some photographs taken during the measurements.

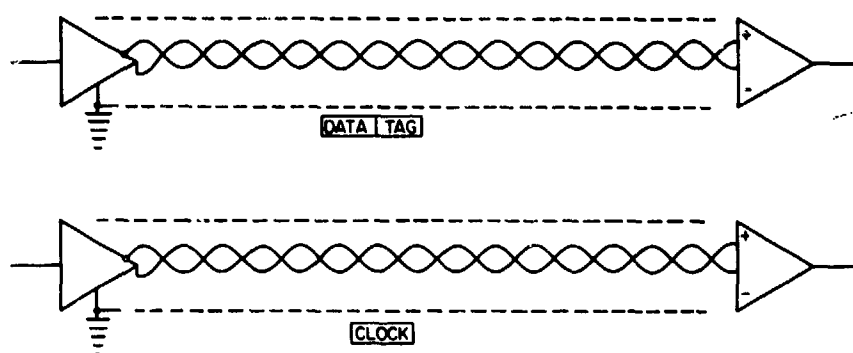


Fig. 1 Two twisted pair configuration of the digital data transmission

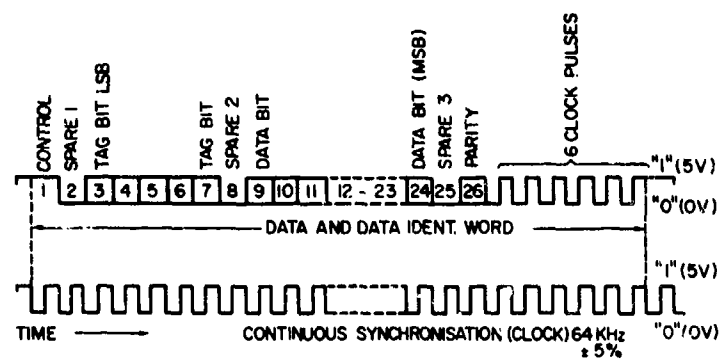


Fig. 2 Serial data transfer

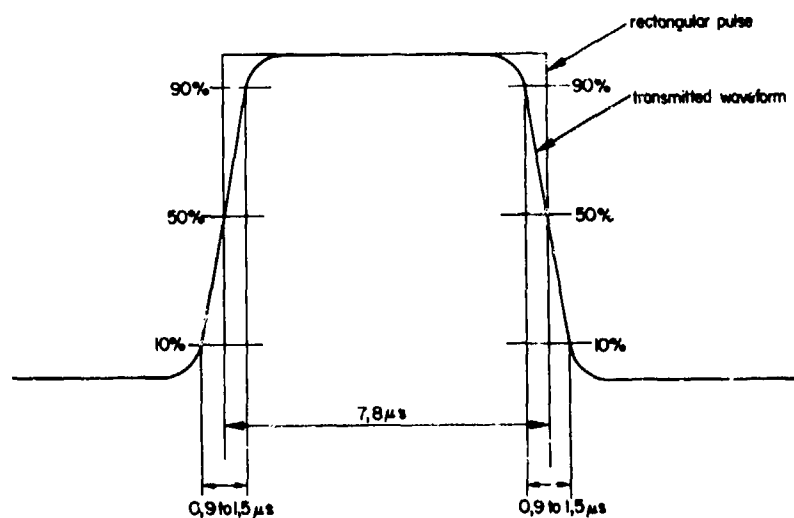


Fig. 3 Permitted tolerances on differential waveshape

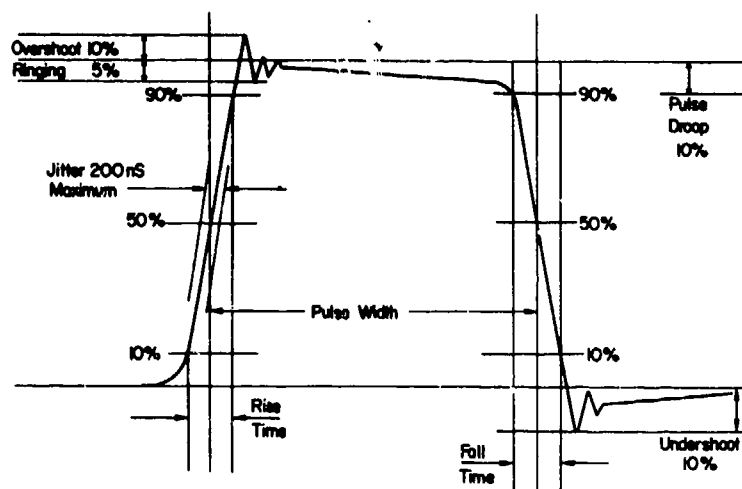


Fig. 4 Permitted distortion of waveshape.

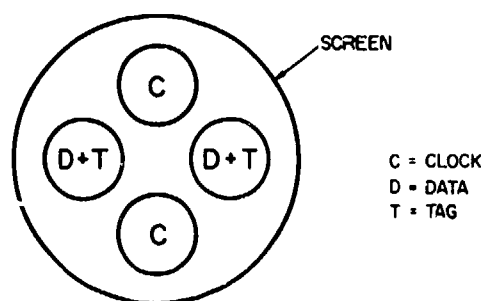


Fig. 5 Screened twisted quad cable

Number of lines	2 x twisted pairs
Clock frequency	64 KHz $\pm$ 5%
Modulation technique	Pulse coded modulation
Data signal format	"Non-return-to-zero"
Transmission	"True" and "Complement" form
Check for correct transmission by	a) Control bit at the beginning b) Spare bits at defined positions c) Word length check d) Parity check e) Synchronization check
Voltage	5 V (for digital '1')
Rise / Fall time	1 $\mu$ sec
Cable type	Screened twisted quad cable
Cable impedance	100 $\Omega$ at 64 KHz

Fig. 6 Characteristics of the selected and tested data transmission system

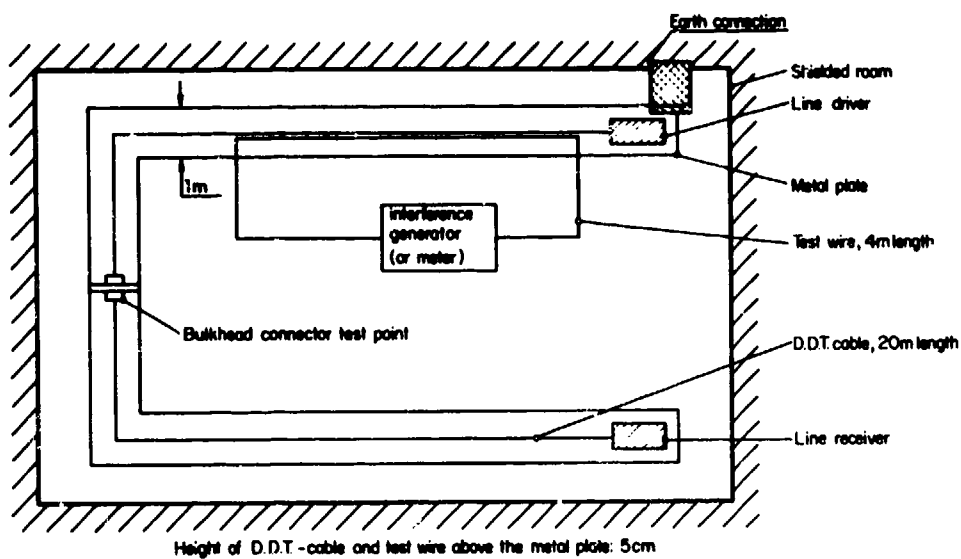


Fig. 7 General test set figuration

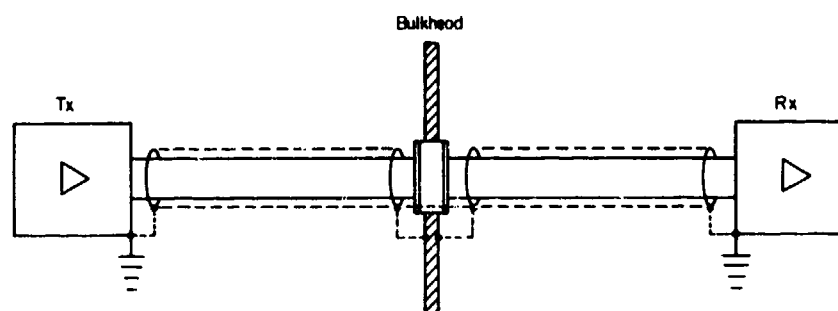


Fig. 8 Different screen earthing possibilities

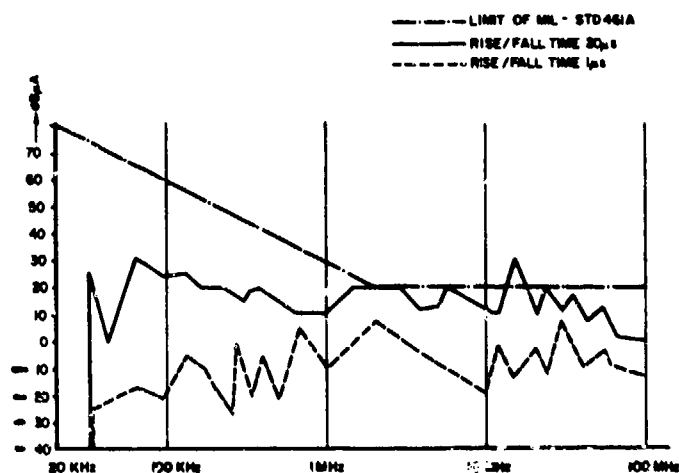


Fig. 9 Comparison of two different DDT systems (inductive coupling) envelope of measured values

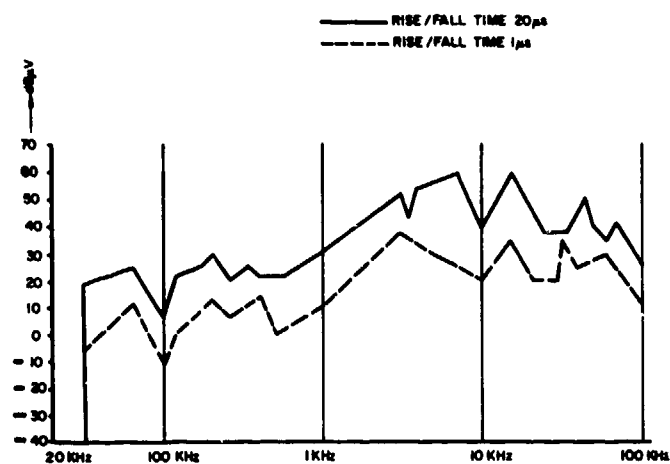


Fig. 10 Comparison of two different DDT systems (capacitive coupling) envelope of measured values.

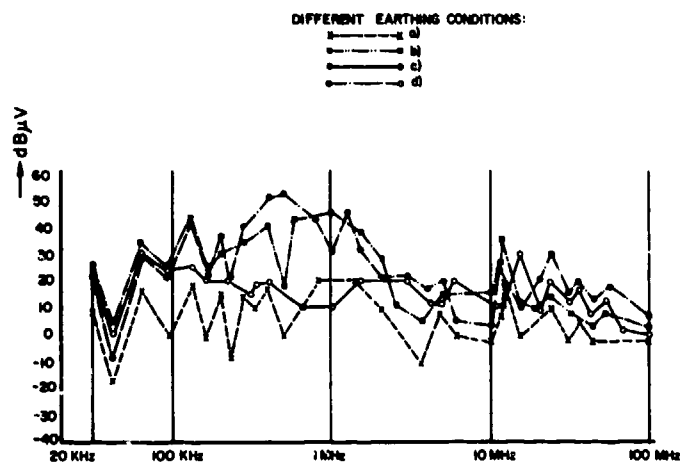


Fig. 11 Comparison of different earthing conditions (inductive coupling) envelope of measured values.

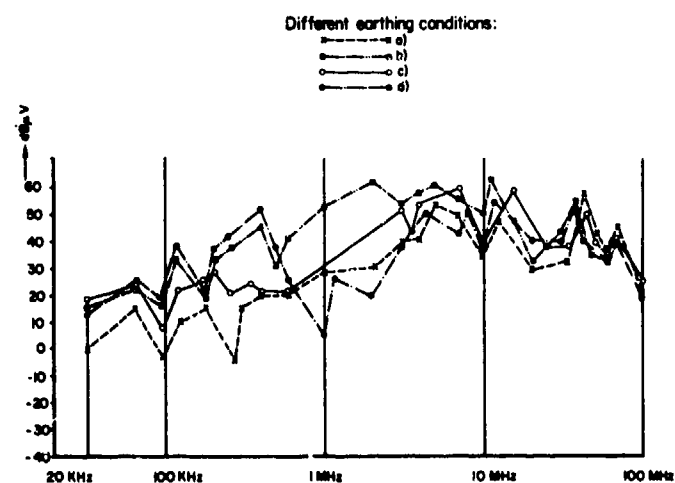
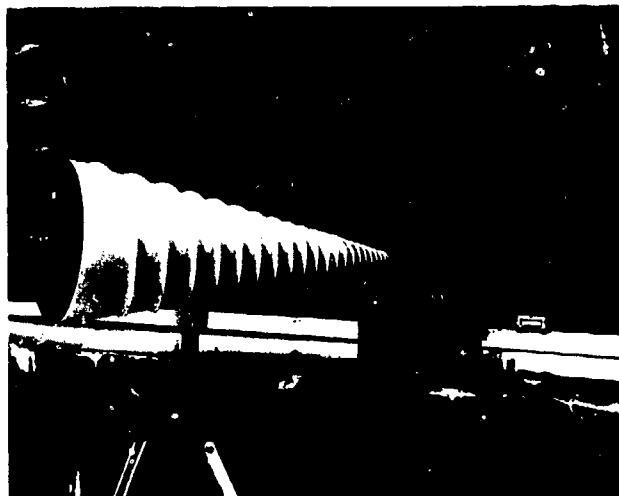


Fig. 12 Comparison of different earthing conditions (capacitive coupling) envelope of measured values





32-9

Fig. 13 Measurement of radiated susceptibility: the picture shows the logarithmic antenna (0,2 -- 1GHz) and the bulkhead connector with a field intensity probe



Fig. 14 DDT cable with test wire (4 m length)

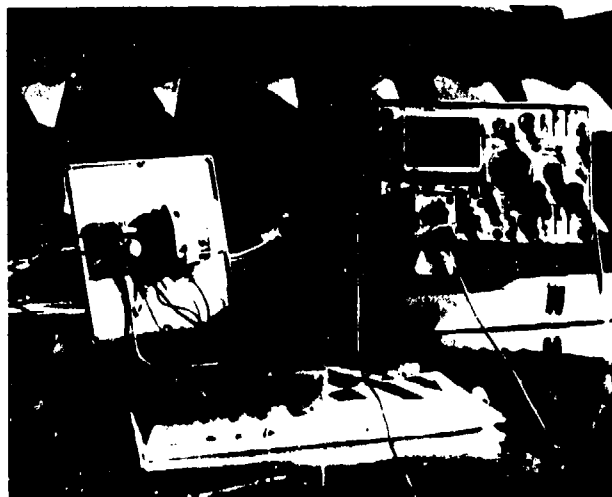


Fig. 15 Line receiver circuit in the shielded enclosure (opened)

## DISCUSSION

D. H. HIGHT: Would you please inform me of the accuracy to which the line was balanced and how this was obtained.

R. RODE: After connection of the line driver/receiver circuits with the connecting data line, the transmitted signal was monitored with an oscilloscope to check the correct signal characteristic. The optimal matching was then achieved by adding a capacitor and a resistor to the line driver circuit until the wanted signal characteristic regarding overshoot, undershoot, pulse droop, etc., was reached. No measurements were performed under unmatched conditions.

A. HOPWOOD: 1) What effect does the length of the cable have on the amount of RF energy being radiated from the cable? 2) The HF transmitter is usually the cause of most interference problems on aircraft. What susceptibility tests did you perform in this frequency band?

R. RODE: 1) The radiated RF energy is directly proportional to the cable length (up to the first cable resonance), but the measured field strength at a certain point is then depending on the loading of the cable. During our tests, a fixed length of 20m was used simulating a possible aircraft condition. 2) During other tests also, the range of HF transmitters (2 to 30MHz) was covered and no susceptibility could be detected on the DDT channels.

These tests were not performed with field strengths above 70V/m and therefore, it cannot be stated up to now whether a susceptibility in the actual aircraft with possible field strengths of up to 60V/m can occur or not. Special on-aircraft tests with the HF system have been established for this reason.

O. HARTAL: From my experience, DC power lines are a source of transient interference, and from aircraft I am familiar with, this current has its return in the aircraft skin. Were any of your susceptibility tests conducted in this manner?

R. RODE: No susceptibility tests have been performed injecting interference in the simulated aircraft skin. By our opinion, this problem area is covered by the tests where interferences were injected in the wire in parallel with the DDT cable. A direct injection in the screen of the DDT cables in the aircraft is not possible in our case for two reasons:

a) The screen is connected to earth on the transmitter end only (only a few connections were given).

b) The DC return current is flowing in wires to a limited number of raised earth points where a low impedance connection to the central earth area is guaranteed.

O. PIETERSEN: Can you tell me what modulation frequency you used during the susceptibility tests? (This in view of the transmitted bit rate of 1 bit per second.)

R. RODE: During the susceptibility tests, the same pulse coded modulation as for the emission tests was used, only reducing the transmitted bit rate from 64K bit per second to 1 bit per second to be able to monitor the received signal directly by a digital counter.

J. C. DELPECH: I would like to express two comments:

1) In the Example you give, you work at relatively low frequencies (64 KHz) with climb fronts whose duration is approximately 1µs. At "Aerospatiale", we have carried out measurements of interferences produced on a multiplexing line made up by a twisted shrouded pair, in TTL logic at 1M bits/s. In order that the electric field produced be below the limit prescribed by the document DO138 of RTCA, the shrouding of the data link line must be earthed every two meters, which raises problems on board an aircraft.

2) This line is also perturbed if there is an induction coupling through which runs the transient of a current resulting from the disconnection of the coil of a high-power aircraft switch, the length of the coupling being 3 meters.

# GENERATIONS ET EFFETS DES TENSIONS PARASITES DE CONDUCTION ET DE RAYONNEMENT ENTRE ENSEMBLES D'UN MEME SYSTEME

A. QUIDET

ELECTRONIQUE MARCEL DASSAULT  
92214 - SAINT-CLOUD - FRANCE

## 1. INTRODUCTION

Les systèmes aéroportés font intervenir un nombre toujours plus grand de matériels plus ou moins dispersés dans l'avion et entre lesquels doivent s'effectuer des échanges d'informations précises.

En outre, au cours de ces dernières années, l'introduction des techniques numériques, bien qu'apportant de nombreux avantages par ailleurs, a cependant rendu plus difficile la cohabitation d'équipements utilisant ces techniques nouvelles et ceux qui sont restés fidèles aux techniques traditionnelles analogiques.

Il en résulte une importance accrue du problème de la protection et, les méthodes mises en oeuvre pour le résoudre doivent déborder le cadre de l'équipement individuel travaillant de façon pratiquement autonome pour être désormais non seulement étendues aux câblages de l'avion qui assurent l'interconnexion des équipements complémentaires, mais, aussi, homogénéisés entre ces différents équipements pour répondre à une politique générale commune.

Sans cette homogénéisation, la protection a en effet toutes les chances d'être illusoire et son amélioration, en cas de défaut, est extrêmement difficile et lourde de conséquences pour ne pas dire impossible.

Il est alors hautement souhaitable d'analyser les principales sources d'interférences contre lesquelles il faut se prémunir et d'en déduire les lignes directrices d'une politique de protection.

Cette politique repose sur trois objectifs, peut-être évidents, mais souvent négligés. Ces objectifs sont les suivants :

- limiter dans la mesure du possible le nombre de générateurs de parasites,
- réduire les couplages indésirables,
- échapper aux effets perturbateurs en choisissant pour le traitement des informations des méthodes appropriées.

De plus les équipements aéronautiques, comme bien d'autres, sont assujettis en ce qui concerne les perturbations électromagnétiques à des normes telles que :

- AIR 510 C Edition n° 4 du 15/02/1963,
- MIL STD 461 A du 01/08/1968,
- MIL STD 462 du 31/07/1967.

A propos de ces normes, vieilles de cinq à dix ans, une question intéressante est de savoir si elles sont bien adaptées aux techniques numériques nouvelles et si les mêmes causes ont les mêmes effets en analogique et en numérique. Mais ceci est un autre débat.

## 2. COUPLAGES INDESIRABLES

D'une manière générale, les couplages entre deux circuits peuvent exister sous trois formes qui peuvent d'ailleurs être simultanées :

Couplage résistif ,                      Couplage inductif ,                      Couplage capacitif.

Mais avant toute chose, comment sont générés les parasites ?

## 2.1. Génération des parasites

Les générateurs de parasites peuvent être classés en deux catégories :

Les  $di/dt$ ,                      les  $dv/dt$ .

Les uns créent des champs parasites qui perturbent les circuits qu'ils atteignent ; les autres, par le jeu des capacités parasites, créent des courants pouvant être nuisibles et dont la répartition est difficile à prévoir.

Il faut donc, dans la mesure du possible, éviter ces variations, ou tout au moins fixer leurs valeurs au minimum compatibles avec le bon fonctionnement du système car l'amplitude des parasites engendrés est inversement proportionnelle à la durée des fronts.

L'action doit donc porter sur la réduction de la rapidité des variations des grandeurs électriques suivantes :

Impédance,                      courant,                      tension.

Il faut également noter qu'entre les  $di/dt$  et les  $dv/dt$ , interviennent les circuits magnétiques qui se présentent comme des générateurs d'harmoniques.

## 2.2. Couplage résistif

Dans cette première catégorie entrent tous les couplages qui ont pour origine un courant circulant dans une branche commune à deux circuits.

Soit à titre d'exemple, un équipement A devant exploiter sous forme électrique quatre informations élaborées dans un autre équipement B sous forme mécanique et comportant par suite quatre potentiomètres de un  $k\Omega$  (figure 1).

Ces potentiomètres sont alimentés en tension de référence 25 V par l'équipement A à travers des câblages de 0,4 mm<sup>2</sup> et d'environ 10 mètres de longueur.

Si le fil de masse qui sert de référence est l'un des fils d'alimentation il présente une résistance de l'ordre de 500 m $\Omega$  et est traversé par un courant de 100 mA de sorte qu'il existe entre les deux points "a" et "b", qui sont les masses de référence respectives des deux équipements, une tension de 50 mV c'est-à-dire de 2/1000 de la référence.

Si donc les potentiomètres sont destinés à transmettre une information précise au 1/1000 un tel montage est à rejeter.

A fortiori, il ne saurait être question d'utiliser des voies communes aux circuits de puissance :

- Excitation de synchro transmetteurs.
- Phase fixe de moteurs diphasés.

Dans ce cas, l'information serait non seulement faussée en amplitude mais se verrait également affectée d'une quadrature ou d'harmoniques risquant de nuire à son exploitation ultérieure.

A plus forte raison encore, il serait absurde d'utiliser, comme circuit de retour, la masse avion dans laquelle peuvent circuler toutes sortes de courants à tous niveaux et toutes fréquences.

La véritable solution consiste à séparer effectivement tous les circuits qui peuvent avoir entre eux des influences parasites. On est ainsi certain de ne laisser subsister aucune portion de circuit commune (figure 2).

En particulier, il est indispensable de conserver un caractère équipotentiel aux circuits de masse devant servir de référence de mesure et par conséquent de ne les faire parcourir par aucun courant.

Cette séparation peut en général être obtenue assez facilement à condition d'être envisagée suffisamment tôt au cours de l'étude en ayant éventuellement recours à des transformateurs d'isolement (figure 3).

Toutefois, lorsque l'on se heurte à des impossibilités ou des difficultés de réalisation il y a lieu d'envisager des solutions particulières parmi lesquelles l'équilibrage des circuits mérite d'être noté comme apportant une solution très satisfaisante. (Figure 4).

Cet équilibrage fait intervenir nécessairement deux tensions d'alimentation en opposition de phase et exploitées de telle sorte qu'il y ait compensation des courants dans les circuits de retour.

Il est à noter que cette chasse au trajet commun ne doit pas se limiter aux schémas, mais elle doit être poursuivie jusque dans la réalisation même du câblage ; en particulier l'équilibrage d'un circuit doit se faire le plus près possible de la portion de circuit qu'il s'agit d'équilibrer (Figure 5).

### 2.3. Couplage inductif

Ces couplages sont dus à l'action sur une boucle d'un champ variable, généralement créé par un courant.

Ils sont proportionnels à la fréquence, à l'amplitude du champ et à la surface de la boucle.

Ils sont d'autant plus à craindre que la fréquence du champ parasite est élevée mais c'est là une donnée du problème sur laquelle il est pratiquement impossible d'agir.

Les deux autres facteurs dictent immédiatement les protections à envisager :

- Réduction des champs parasites.
- Suppression des boucles ou tout au moins de la surface offerte aux champs inducteurs.

#### 2.3.1. Réduction des champs parasites

Lorsque les champs parasites sont dus à des courants il est souvent possible de les réduire à l'origine même en véhiculant conjointement par des fils torsadés, ou aussi voisins que possible, des courants dont la somme vectorielle est nulle à chaque instant :

- Courants aller-retour en monophasé.
- Courants triphasés équilibrés.

On peut espérer une réduction des champs au voisinage des circuits de puissance en exploitant des blindages tressés couramment utilisés bien que moins efficaces vis-à-vis des champs électromagnétiques que les blindages continus. Cela constitue une excellente précaution qui doit être adoptée en l'absence d'impératifs contraires.

Pour réduire encore, au niveau des circuits de mesure, les champs parasites créés par les circuits de puissance, le trajet de ces réseaux sera étudié de façon à les éloigner le plus possible, surtout dans les portions parallèles.

Comme au niveau des circuits de puissance, le blindage des circuits de mesure permet d'escompter une réduction des champs susceptibles d'atteindre les conducteurs.

Si un couplage inductif est inévitable on peut étudier la possibilité d'annuler son effet en induisant volontairement des courants supplémentaires déphasés. Ceci peut être réalisé à l'aide de petits transformateurs réglables (figure 6).

Pour réduire encore le couplage inductif à un niveau acceptable, il peut être nécessaire d'installer des blindages magnétiques qui constitueront de véritables courts-circuits même aux basses fréquences.

#### 2.3.2. Suppression des boucles

Finalement les champs électromagnétiques n'auraient aucune action parasite s'il n'existait pas de boucles dans les circuits de mesure.

Le grand principe consiste donc à éviter toute boucle et à réduire au maximum la surface de celles qui ne peuvent être évitées.

Le premier point s'applique en particulier aux circuits de masse servant de référence de mesure.

Ils doivent nécessairement présenter une structure en arbre ou en arête de poisson et ne jamais se boucler sur eux-mêmes.

En ce qui concerne les blindages, il ne semble pas que dans les applications analogiques actuelles, l'existence de boucles de masse par mise en parallèle de plusieurs blindages et connexion à la masse aux deux extrémités soit pratiquement lourde de conséquences.

Il n'en reste pas moins vrai que la présence de boucles est peu souhaitable. Objets de couplages inductifs et résistifs ces bouclages non nécessaires a priori, interdisent en outre la connaissance précise des distributions des courants capacitifs que les blindages en tant que protection électrostatique sont précisément chargés de dériver à la masse et par suite nuisent à leur utilisation convenable ainsi qu'à une mise au point facile en cas de difficultés.

Ce sont là des raisons suffisantes pour considérer que les blindages ne doivent pas, en général, être interconnectés suivant une structure maillée, mais au contraire être isolés entre eux sur toute leur longueur et reliés à la masse suivant une structure en arbre.

Pour réduire la surface des boucles inévitables, et en particulier toutes les fois qu'une information sera disponible en "flottant", on aura recours soit au conducteur coaxial soit aux fils torsadés.

Le fil coaxial, ou à la rigueur le fil blindé isolé (lorsque sa capacité n'est pas gênante), dans lequel le conducteur central sert de circuit aller, le retour étant assuré par la gaine extérieure, présente une boucle de surface pratiquement nulle et constitue la meilleure solution en tant que protection.

Il a l'inconvénient de nécessiter pour chaque liaison deux broches par prise et parfois de nécessiter des prises spéciales.

Par ailleurs, la capacité du blindage par rapport à la masse peut, dans certains cas, fermer la boucle et donner lieu à un courant de circulation créant un couplage résistif (figure 7).

Pratiquement, une protection presque aussi efficace est obtenue par l'utilisation de deux fils torsadés sous blindage qui par ailleurs ne nécessitent pas de prises spéciales.

Les fils torsadés présentent en outre l'avantage par rapport au coaxial de permettre les liaisons par plus de deux conducteurs.

#### 2.4. Couplage capacitif

Il y a couplage capacitif toutes les fois qu'existe aux bornes d'une capacité, une différence de potentiel variable.

Cette capacité, en refermant le circuit, donne lieu à des courants qui peuvent créer un couplage résistif indésirable.

L'importance de ces couplages est évidemment proportionnelle à :

- l'amplitude et la fréquence de la différence de potentiel variable,
- la valeur de la capacité de couplage,
- le niveau d'impédance du circuit suivi par le courant de défaut.

La protection vis-à-vis de ces couplages capacitifs résulte directement de ces considérations.

Sous une forme ou sous une autre, cette protection consiste :

- à réduire l'amplitude des différences de potentiel aux bornes des capacités parasites en fixant de façon convenable les potentiels électrostatiques des circuits non reliés par résistance,
- à réduire la valeur des capacités parasites entre les circuits nécessairement à des potentiels différents et variables, soit en les éloignant, soit en ajoutant en série avec la capacité parasite une capacité plus faible (utilisation de coaxial par exemple),
- à canaliser les courants de défaut pour éliminer les couplages résistifs indésirables.

Sans avoir la prétention d'envisager tous les cas possibles extrêmement variés, quelques exemples vont permettre d'illustrer ces considérations (figure 8).

Soit un transformateur bobiné "deux fils en main" (primaire et secondaire bobinés simultanément) et présentant de ce fait une capacité parasite importante entre enroulement primaire et secondaire, le secondaire étant supposé relié à la masse en A, divers cas peuvent être envisagés :

- le primaire peut être laissé entièrement flottant ; son potentiel électrostatique, fixé alors uniquement par des capacités parasites peut être quelconque ce qui est très gênant s'il se trouve à proximité de circuits à haute tension et fréquence élevée,

- en l'absence d'impératifs contraires, il y a donc généralement intérêt à fixer ce potentiel en réunissant l'un des points primaires à un potentiel voisin du potentiel secondaire et en particulier à la masse ; toutefois, le choix du point à mettre à la masse n'est pas indifférent :
  - dans un cas la différence de potentiel aux bornes des capacités parasites est maximale tout au long des enroulements et il en résulte un courant de défaut important qui, en retournant à la masse à travers l'enroulement donne lieu à des couplages résistifs qui peuvent être extrêmement gênants,
  - au contraire dans l'autre cas, les capacités parasites sont soumises à des différences de potentiel minimales et le défaut précédent est réduit,
- toujours en l'absence d'impératif contraire, (minimisation de la self de fuite par exemple), une meilleure solution consiste à réduire la capacité parasite entre enroulements en bobinant séparément primaire et secondaire,
- enfin, une dernière amélioration consiste à introduire entre les deux bobinages un écran relié à la masse par un circuit à très faible impédance. Cet écran tout en remplaçant les capacités parasites par d'autres, peut-être même plus grandes, a l'avantage de dériver à la masse les courants de défauts par un circuit distinct du circuit de mesure, parfaitement connu et qui, n'étant pas soumis aux mêmes exigences que le circuit de mesure peut être éventuellement plus facilement étudié pour remplir au mieux la fonction qui lui est dévolue.

Cet exemple du transformateur a permis de grossir les phénomènes et de les rendre par suite plus facilement accessibles.

### 3. LIAISONS POUR TRANSMISSION D'INFORMATIONS NUMERIQUES

Les nouveaux systèmes qui sont mis en place sur les avions modernes utilisent de plus en plus pour les échanges d'informations entre les équipements composant ces systèmes, la technique numérique de liaison multiplexée ou liaison omnibus.

Par définition, une liaison omnibus est une liaison physique à 2 conducteurs, ou davantage, alimentée à l'une de ses extrémités par un générateur, et chargée de transmettre une information de nature quelconque à plusieurs récepteurs disposés sur le cheminement de la liaison.

Sans entrer dans le détail de ce type de liaison, il est cependant très utile de noter l'importance de cette liaison, éventuellement redondante, qui est l'unique support d'échanges entre les équipements composant le système.

D'où les nombreuses précautions qui doivent être prises, en particulier vis-à-vis des perturbations électromagnétiques, pour assurer une sécurité de fonctionnement élevée.

Parmi ces précautions, les liaisons de masses entre équipements sont particulièrement intéressantes à examiner.

Pour ce faire, il est utile d'analyser les conséquences de l'apparition de tensions parasites et les effets de ceux qui sont induits par rayonnement.

De telle sorte que les effets des blindages peuvent être étudiés et un mode de connexion préconisé.

#### 3.1. Liaisons de masse entre équipements

Chaque équipement, ensemble ou sous-ensemble, partie d'un système possède une masse mécanique qui doit toujours être distincte et isolée de sa masse électrique.

La masse mécanique doit être réunie localement à la structure par l'intermédiaire soit de tresses métalliques, soit des fixations mécaniques dans l'aéronef.

Lorsqu'un ensemble, entrant dans un système, est composé de plusieurs sous-ensembles, tous de même conception, et formant un tout dans leur fonction, il est fréquent d'organiser les masses électriques de la manière suivante.

Au niveau de chaque sous-ensemble, la masse électrique est la réunion de plusieurs autres masses (par exemple : masse logique, masse analogique, reprise blindage, etc...) (Figure 9). Toutes les masses électriques (ME) émanant de ces sous-ensembles sont réunies en un noeud commun au niveau du sous-ensemble principal, ou désigné comme tel (en général, celui qui reçoit l'énergie primaire qu'il distribue ensuite).

La connexion de la masse électrique principale (MEp) est alors réunie en un seul point de la structure. Ce point, servant de référence de masse aux génératrices de bord, est dénommé cœur électrique.

Lorsque plusieurs ensembles ou équipements, composites ou non, sont rassemblés pour conduire à un système, chacun d'eux doit donc être réuni par une connexion unique (MEp) à ce point de référence.

Il résulte de cette structure en "arbre" que tous les équipements devraient être équipotentiels, si, comme cela doit être, aucune circulation de courant ne s'effectue dans les connexions MEp (Figure 10).

Ainsi, il apparaît que si les équipements sont correctement réalisés et si le cœur électrique est bien un point de référence à peu près ponctuel, aucune différence de potentiel ne devrait exister entre 2 équipements. Comme toutes les conditions ci-dessus ne peuvent ou ne sont pas entièrement respectées, des tensions parasites apparaissent entre les divers ensembles d'un système. Les tensions sont en général composites dans leur nature (continu, alternatif, fréquence...) mais leur amplitude reste cependant assez faible (quelques centaines de mV à quelques volts au plus).

Il en est de même en ce qui concerne les différences de potentiel parasites entre masses mécaniques. Ces prises de masses multiples sur une structure qui sert de retour à des courants parfois intenses (génération de bord) ne sont pas davantage équipotentielles. Cependant, leur effet est bien moindre car, ainsi que nous l'avons vu précédemment, les masses mécaniques sont isolées des circuits électriques et n'ont donc pas une influence directe sur ceux-ci.

Lorsqu'une liaison par ligne bus est établie entre plusieurs ensembles, ces tensions parasites entre masses électriques se manifestent et peuvent se présenter schématiquement par une source VME connectée entre les 2 ensembles (Figure 11).

### 3.2. Conséquences de l'apparition de tensions parasites

Du fait de la présence de la source VME, les circuits d'interface Emission/Réception voient la tension parasite VME superposée au signal utile. Autrement dit, un récepteur voit sur ses 2 entrées cette tension VME en mode commun, celle-ci s'additionnant au signal à recevoir lorsque celui-ci est présent.

Il apparaît donc la nécessité :

- a) d'assurer une admission suffisante en tension de mode commun des récepteurs,
- b) de réaliser un isolement minimal entre les circuits d'émission-réception et la ligne bus, ceci afin de limiter le courant de circulation qui se trouve créé dans la boucle (figure 11).

Cet isolement peut être élevé en continu et jusqu'aux fréquences hautes si l'on emploie au niveau de chaque interface, des organes de couplage du genre transformateurs ou dispositifs opto-électroniques. En réalité, un isolement aussi élevé n'est pas indispensable : on peut admettre que, tant que le courant parasite ainsi créé reste inférieur à quelques % du courant de circulation normal, l'effet reste négligeable. Ceci montre que, quelques centaines d'ohms à quelques k $\Omega$  peuvent suffire pour assurer un découplage satisfaisant. A noter que ce raisonnement n'est valable que parce qu'il s'agit de liaisons sur lesquelles circulent des informations numériques. Il en irait tout autrement s'il s'agissait de liaisons analogiques pour lesquelles on s'attache essentiellement à la qualité du signal.

Vis-à-vis des tensions parasites apparaissant en mode commun sur les entrées du récepteur, ces tensions ne donneront pas lieu à signal de sortie, tant que leur amplitude sera dans les limites acceptées par le récepteur et tant que celui-ci aura une réjection suffisante pour ces tensions en mode commun. Les caractéristiques du récepteur seront donc à étudier et optimiser à ce point de vue. De plus, la symétrie de la ligne devra être réalisée avec soin, sinon, toute dissymétrie, soit sur la ligne, soit au niveau des éléments émetteurs et récepteurs qui lui sont associés, transformera les tensions en mode commun en tensions différentielles. Celles-ci seront alors interprétées comme un signal utile.

Pour la part de tensions parasites apparaissant ainsi en différentiel la protection doit être recherchée au niveau du récepteur par une caractéristique de transfert à hystérésis et la mise en place d'un réseau de filtrage approprié.

### 3.3. Effet des parasites induits par rayonnement

Les liaisons par lignes bus bifilaires peuvent voisiner des lignes parcourues par des courants commutés.



Les caractéristiques à surveiller au point de vue de la susceptibilité des liaisons bus sont : le couplage avec les câbles véhiculant ces courants, l'amplitude de ces courants et leur fréquence de commutation. Des courants parasites impulsifs peuvent être induits dans la ligne, donnant naissance à des tensions en mode commun, d'un niveau très supérieur à celui mentionné précédemment. On peut en chiffrer l'ordre de grandeur de la dizaine au millier de volts, selon les conditions. Fort heureusement, leur durée est brève et ces tensions ne compromettent pas en général le fonctionnement des constituants électroniques de la ligne. Ceux-ci supportent en fonctionnement impulsif à faible facteur de forme, des caractéristiques dynamiques très supérieures à leurs caractéristiques en régime statique.

La protection des liaisons bus vis-à-vis de ces parasites utilise cette propriété et l'on s'efforce ainsi d'obtenir, en statique, une bonne immunité aux parasites de mode commun (50 à 100 volts par exemple) garantissant par là, une bonne tenue vis-à-vis de parasites à niveau élevé. C'est ainsi que des expérimentations de parasitage sur ligne bus ont eu lieu à l'ELECTRONIQUE MARCEL DASSAULT.

#### 3.3.1. Générateur de parasites

Pour effectuer les essais de susceptibilité électrique des lignes bus, un générateur de parasites a été développé à l'ELECTRONIQUE MARCEL DASSAULT.

Un autotransformateur, alimenté par le réseau 400 Hz permet la charge d'un condensateur de 1  $\mu$ F sous une tension de 1000 à 8000 volts (figure 12). Un voltmètre contrôle la tension de charge.

La décharge brutale du condensateur est provoquée par la fermeture d'un contact de relais. Ce relais est commandé par un interrupteur externe alimenté sous 28 volts. Il est possible de provoquer cette décharge, soit directement dans le fil de parasitage avec un éclateur interne au générateur, soit avec un éclateur externe au générateur.

Pour le premier type de fonctionnement, le fil de parasitage est couplé à la ligne de transmission par cheminement parallèle. Selon la tension de charge du condensateur, le courant crête parcourant le fil de parasitage varie de 250 à 2000 ampères avec une pseudo-période de 1,5  $\mu$ s à 20  $\mu$ s. Le couplage entre le blindage du bus et le fil de parasitage, selon le type de bus, varie entre 1/2 et 1. Ainsi, le courant induit dans le blindage du bus varie entre 125 et 1000 ampères.

Le deuxième type de fonctionnement permet d'induire dans le blindage un courant analogue au précédent en approchant de l'éclateur externe une prise de raccordement du bus.

Bien que les résultats obtenus soient plus qualitatifs que quantitatifs, à cause des difficultés de mesures, les conclusions suivantes peuvent être données. Les résultats relatifs à une longueur de 100 mètres semblent montrer que, quelle que soit la configuration, le bus est parasité pour une tension de 4000 à 5000 volts, ce qui correspond à un courant crête de parasitage de 400 ampères, soit une puissance crête de parasitage de l'ordre de 1,5 mégawatts.

#### 3.4. Effet des blindages et mode de connexion

Le blindage enveloppant la ligne bifilaire remplit tout d'abord un rôle d'écran électrostatique. Ensuite, pour une liaison différentielle, il est important de savoir comment connecter le blindage de la ligne bifilaire.

Pour une transmission de grandeurs analogiques pour laquelle la précision est primordiale, un courant permanent de circulation dans le blindage risque d'induire sur la ligne un courant trop important pour maintenir la précision voulue. Pour cette raison, le blindage n'est mis à la masse qu'à une seule extrémité.

Pour une liaison numérique différentielle, la précision des tensions en ligne est secondaire et les courants permanents de circulation dans le blindage induisent en mode commun sur la ligne des tensions de quelques millivolts qui ne perturbent pas la liaison. Lorsque le blindage est relié à la masse aux 2 extrémités, il se comporte vis-à-vis des parasites de la même façon que la ligne d'information en mode commun, mais avec une impédance beaucoup plus faible (figure 13).

En effet, la boucle de masse (blindage + liaison de masse) et la liaison (ligne + liaison de masse) sont couplées de la même façon à une source de parasites quelconque. Ce système est équivalent à un transformateur à 2 secondaires identiques et alimenté au primaire par un générateur à puissance constante P, P étant la puissance crête de parasites disponible. Lorsque le blindage n'est relié qu'à une extrémité, le circuit (1) équivalent est ouvert (figure 14) et toute la puissance délivrée par le générateur est dissipée dans la liaison (circuit (2)) et induit aux bornes de 2 liaison, une tension :

$$V_0 = \sqrt{P \cdot Z_{\text{liaison}}}$$

Lorsque le blindage est relié aux 2 extrémités, le circuit (1) équivalent est fermé sur 2 boucles de masse (figure 15).

La puissance  $P$  se répartit entre les impédances de la boucle de masse et de la liaison et induit aux bornes de  $Z$  liaison une tension :

$$V'_0 = \sqrt{P \cdot \frac{Z \text{ liaison} \times Z \text{ boucle masse}}{Z \text{ liaison} + Z \text{ boucle masse}}}$$

Si  $Z$  boucle de masse = 0,  $V'_0$  est nulle. En pratique, cette impédance n'est pas nulle, mais reste faible et le gain obtenu est alors :

$$\frac{V_0}{V'_0} = \sqrt{1 + \frac{Z \text{ liaison}}{Z \text{ boucle masse}}}$$

Ce gain peut être notable et peut varier de 2 à 10 selon les cas.

#### 4. CONCLUSION

En faisant la relation entre les développements qui précèdent, il apparaît que les techniques de raccordement des blindages pour la transmission d'informations analogiques ou pour celle d'informations numériques sont différentes. En effet, le fait de réunir le blindage aux 2 extrémités, c'est-à-dire, à la masse des 2 ensembles, se révèle bénéfique lorsqu'il s'agit de la transmission d'informations numériques car la qualité du signal transmis n'a pas la même importance que dans le cas d'une transmission d'informations analogiques. L'application de cette technique a pu être vérifiée par expérimentation en constatant en particulier que l'effet du courant dû à la source parasite  $V_{ME}$  est d'autant moins sensible sur la liaison lorsqu'il parcourt le blindage, ce qui peut sembler a priori paradoxal.

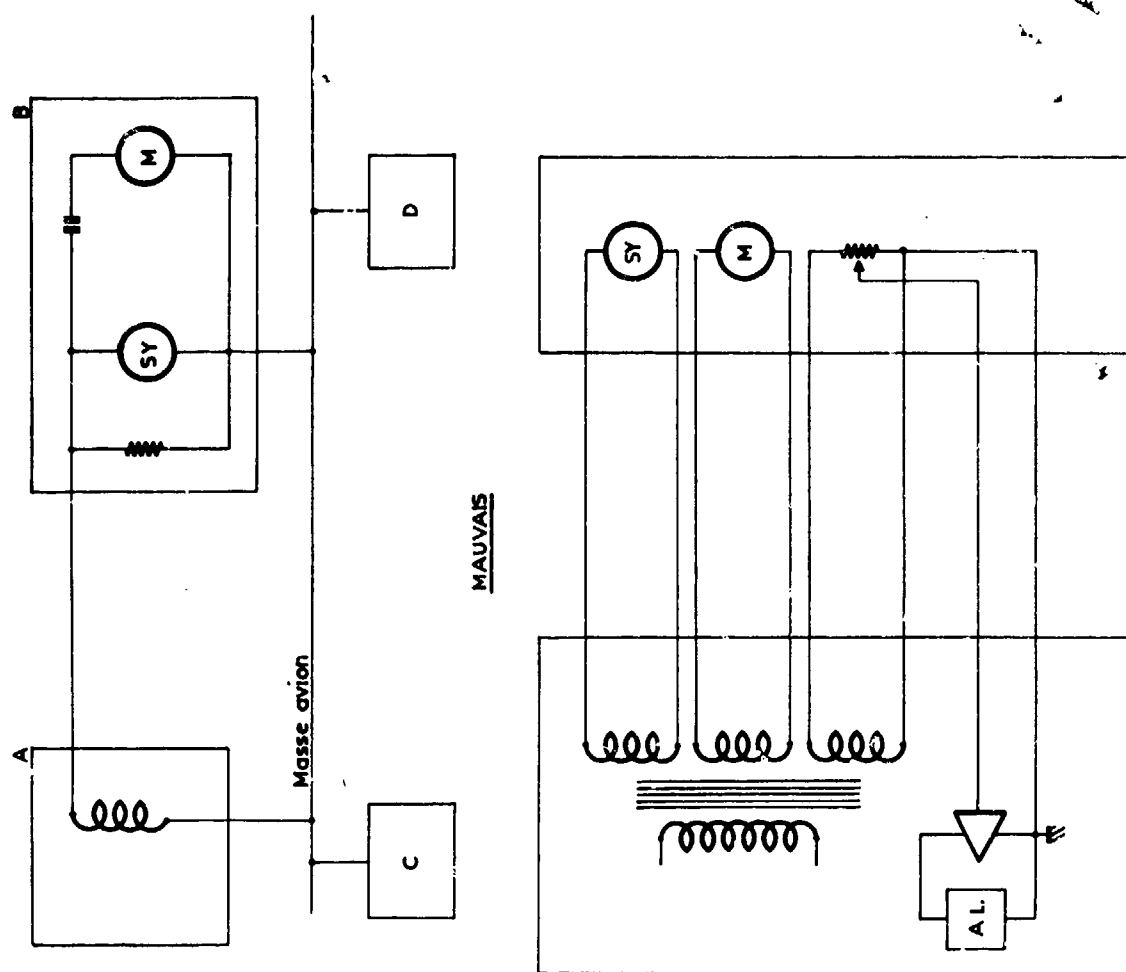


Fig. 2 Couplage et découplage de circuits de puissance

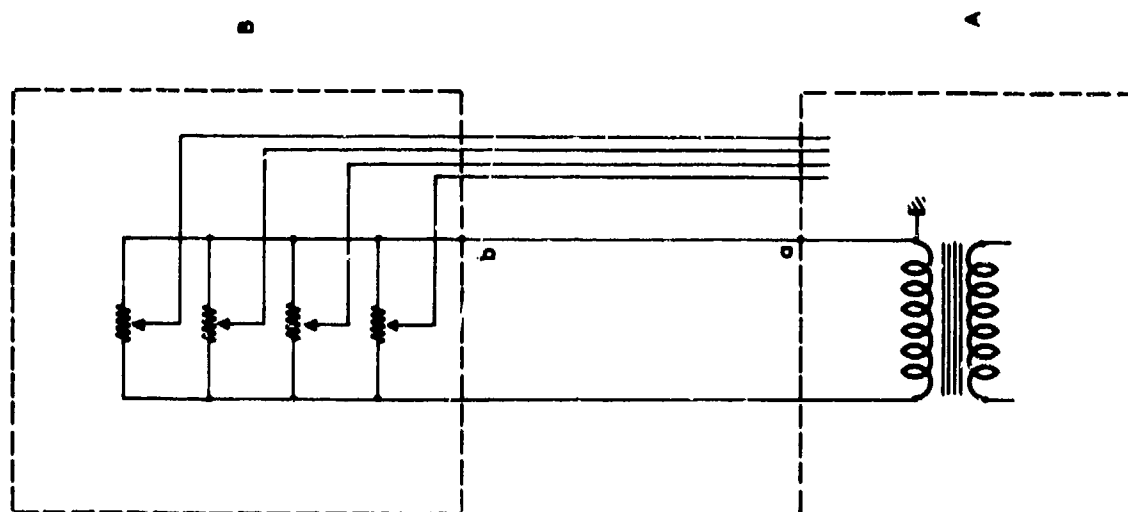


Fig. 1 Couplage résistif d'une tension de référence

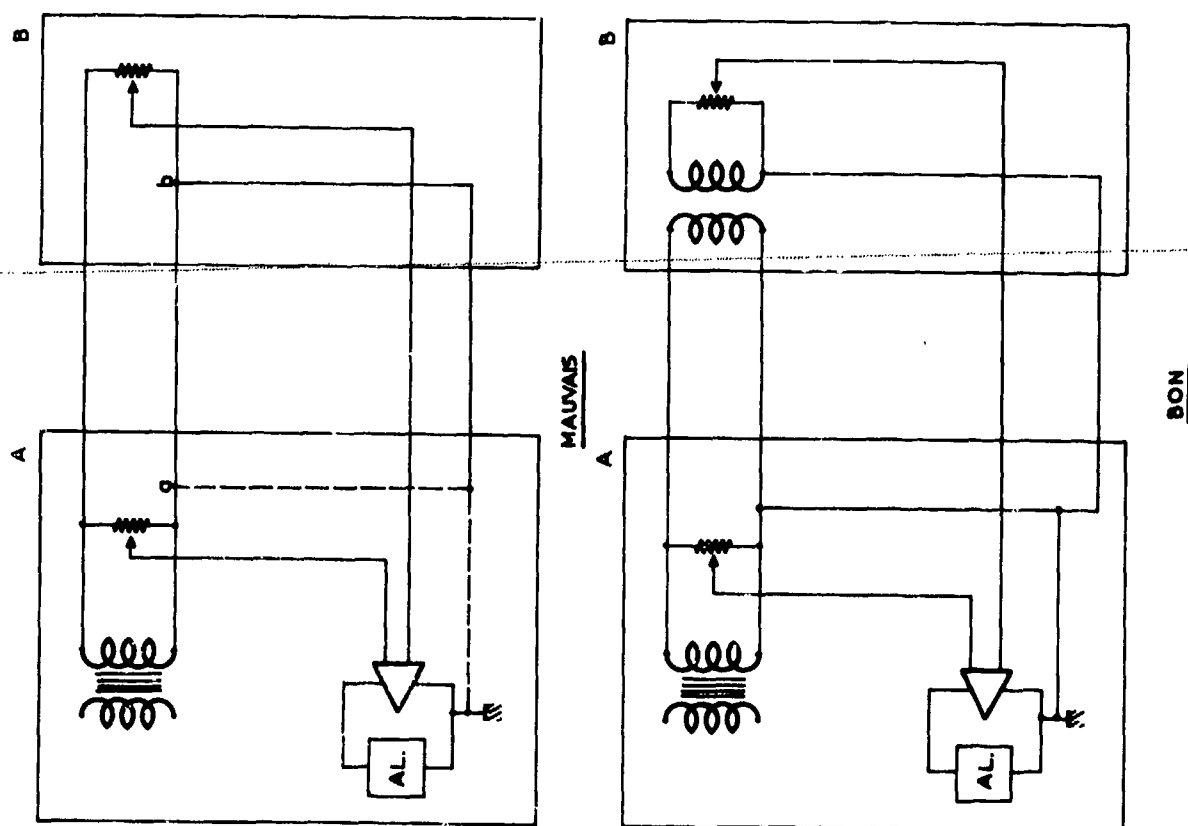


Fig. 3 Découplage par transformateur d'isolement

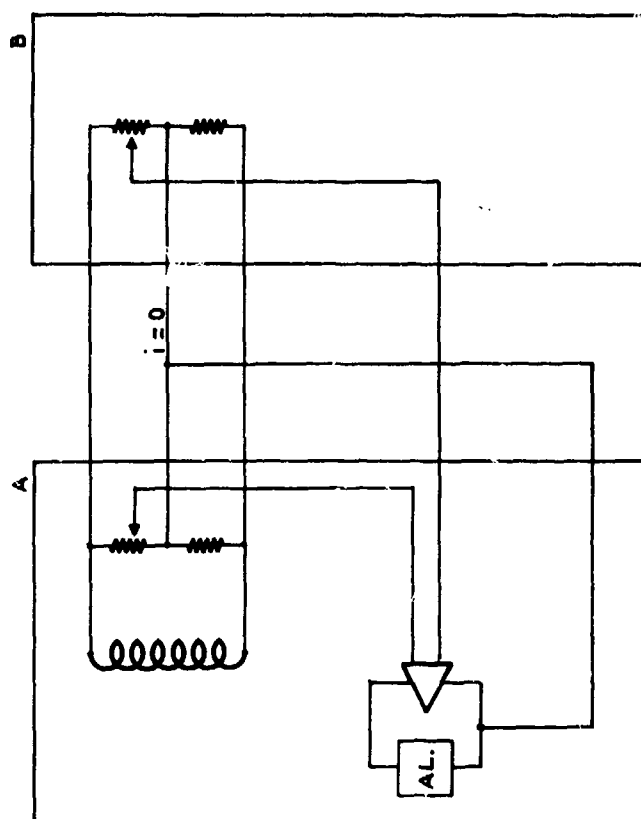
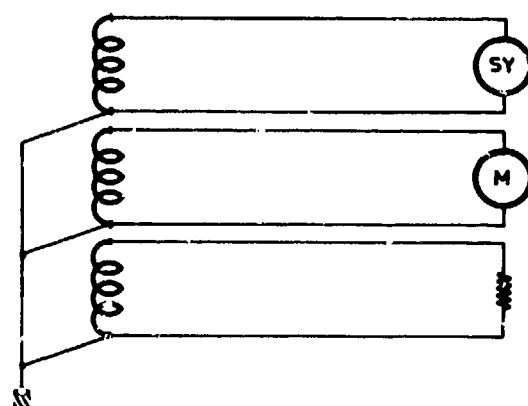
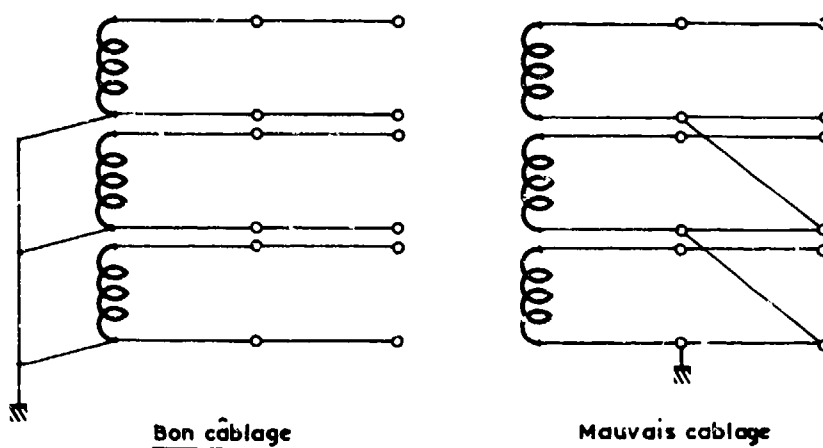


Fig. 4 Découplage par équilibrage



SCHEMA DE PRINCIPE



Bon câblage

Mauvais câblage

Fig. 5 Distribution d'une référence de masse

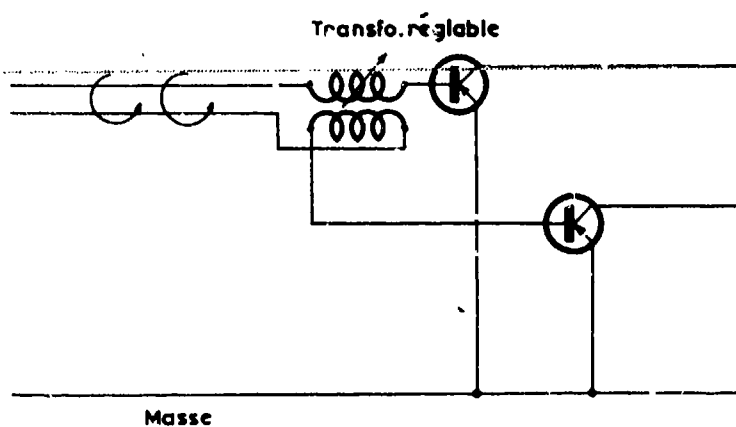


Fig. 6 Réduction de couplage inductif par transformateur réglable

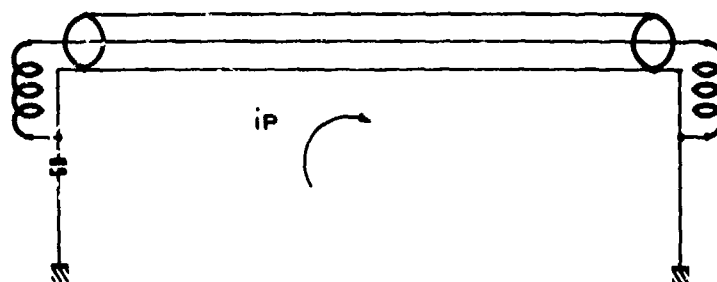


Fig. 7 Courant de circulation dû à la capacité d'un blindage

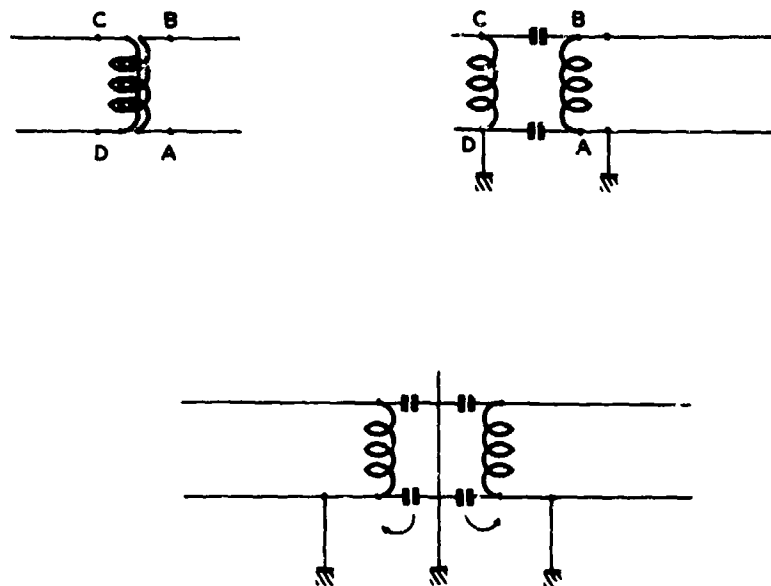


Fig. 8 Couplage capacitif d'un transformateur bobiné "2 fils en main"

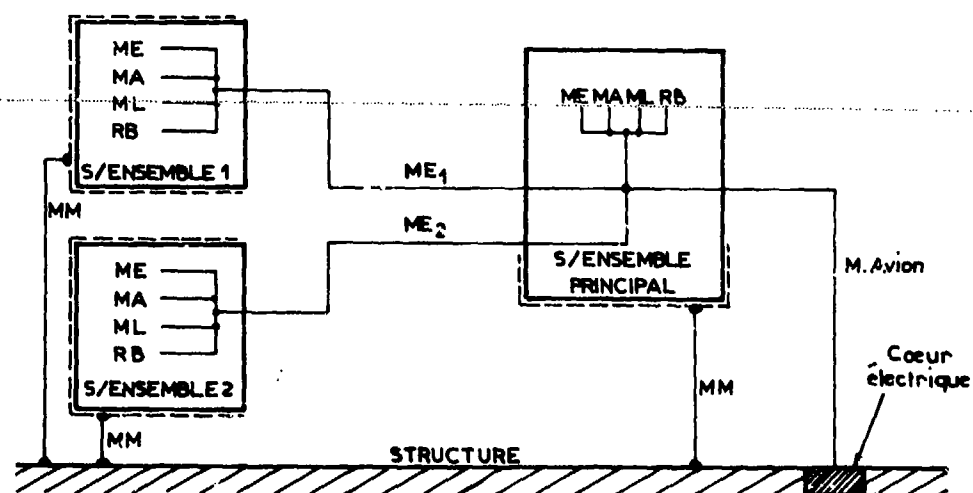


Fig. 9 Organisation des masses entre sous-ensembles. MM = Masse mécanique, ME = Masse électrique, MA = Masse analogique, ML = Masse logique, RB = Reprise blindages

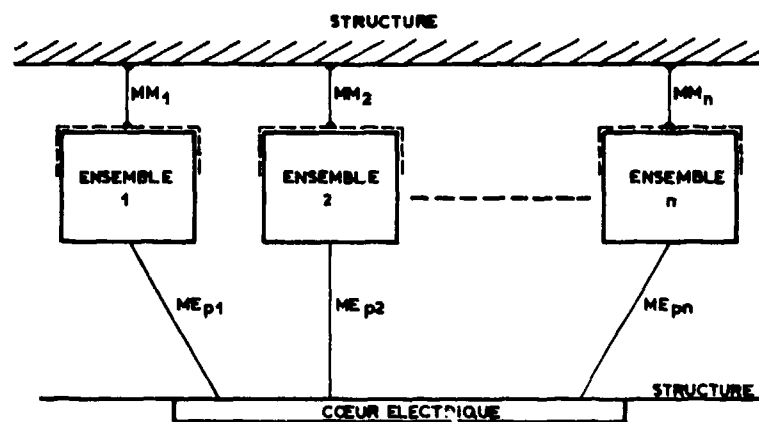


Fig. 10 Distribution des masses

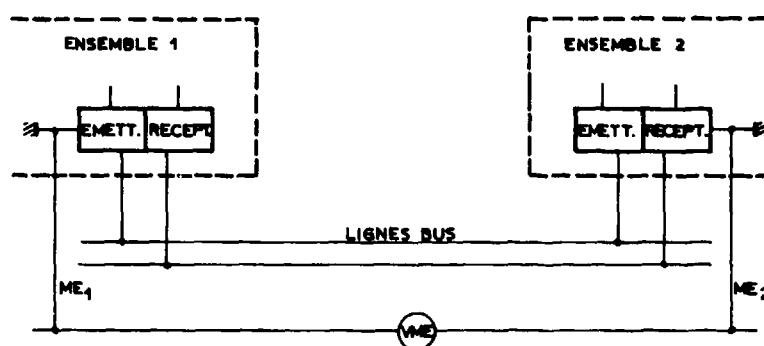


Fig. 11 Représentation schématique des sources parasites

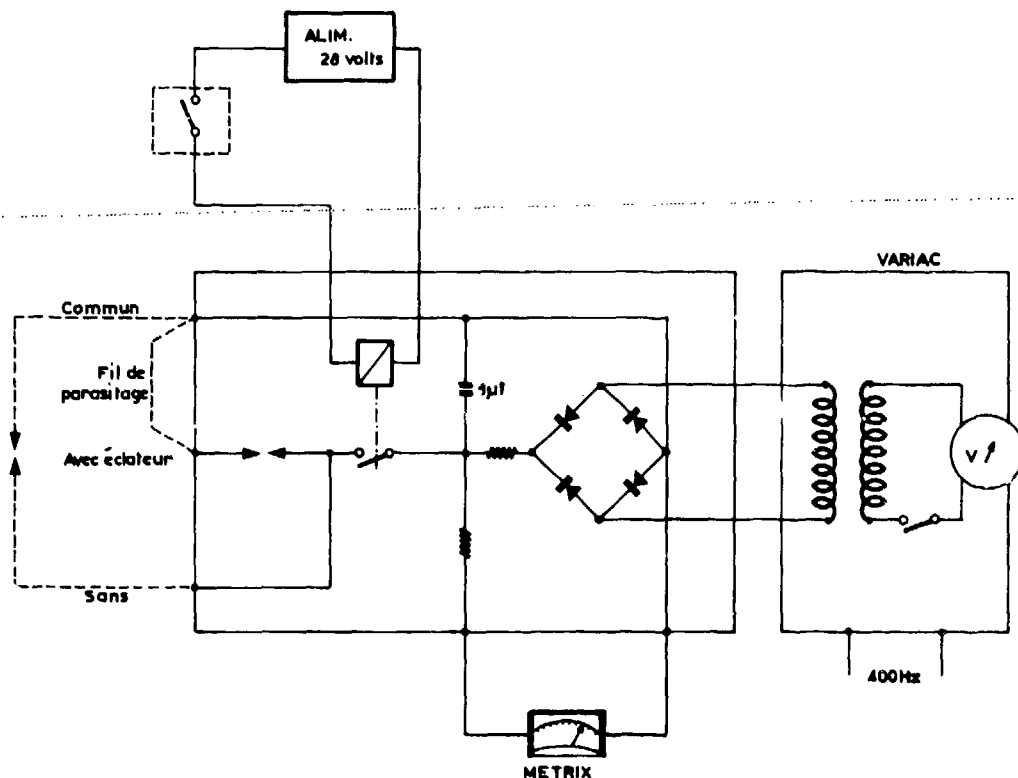


Fig. 12 Schéma du générateur de parasites

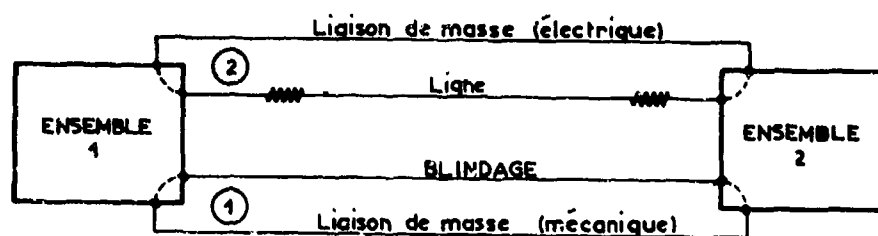


Fig. 13 Boucle de masse créée par le blindage. ( $Z_{\text{Liaison}} = Z_{\text{Ligne}} + Z_{\text{Liaison de masse}}$   
 $Z_{\text{Boucle de masse}} = Z_{\text{Blindage}} + Z_{\text{Liaison de masse}}$ )

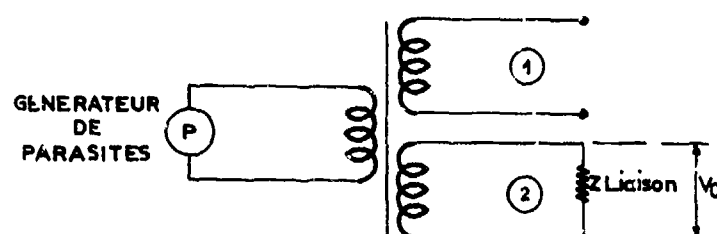


Fig. 14 Schéma équivalent avec blindage en circuit ouvert

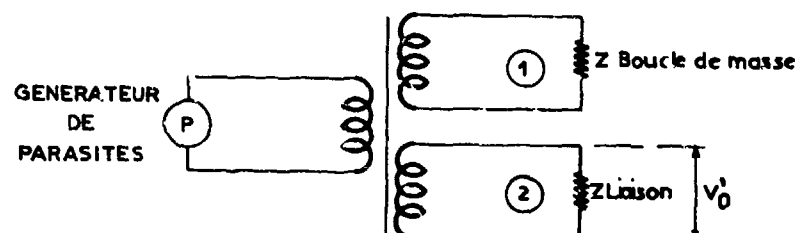


Fig. 15 Schéma équivalent avec blindage en circuit fermé

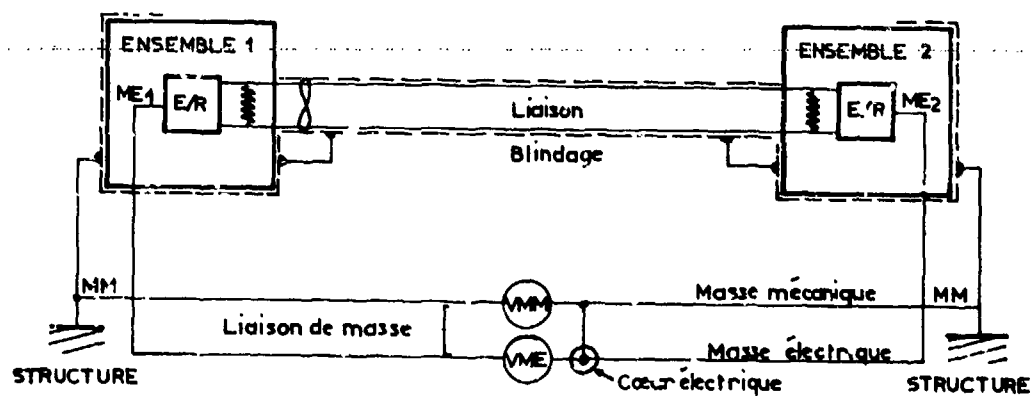


Fig. 16 Configuration schématique d'une liaison



THE REDUCTION OF ELECTROMAGNETIC COMPATIBILITY DUE TO  
NON-LINEAR ELEMENTS AND UNINTENDED RANDOM CONTACTING IN THE  
PROXIMITY OF THE ANTENNAS OF HIGH-POWER RF-TRANSMITTERS

K.Landt  
Siemens AG  
8000 Munich 70  
Hofmannstraße 51  
Germany

SUMMARY

With the aid of selective filters it is possible to almost completely eliminate harmonics, spurious emissions and wideband interfering signals on the output of RF-transmitters, even those operating at very high output powers. These interfering signals are again generated, if non-linear junctions or unintended random contacting creates secondary radiation sources in the proximity of the transmitting antennas.

The problems indicated will be discussed with reference to an example for the co-site-installation of a UHF-unit and an Avionic-device in an aircraft, as well as on the example of an installation on board a ship.

Possible means of overcoming these problems are outlined in the paper. So far, satisfactory solutions have not been achieved in all cases. Therefore it is important to know that sometimes unavoidable spectrum pollution, due to the effects previously described, might occur in the proximity of the antennas of high-power RF-transmitters. This has to be taken into account by the frequency-management.

The paper deals with a considerable problem in the electromagnetic environment of avionics and communications-electronics systems.

## 1. INTRODUCTION

Nowadays it can generally be taken for granted that the significance of electromagnetic compatibility (EMC) for tactical defense systems is understood. A high degree of EMC is required for these systems to fulfill their missions. In such complex electronic systems sensitive receivers and high-power transmitters must very often be operated simultaneously in adjacent frequency ranges.

The possible interaction between transmitters and receivers in the same system (aircraft, ship or tactical vehicle) via cabling - the power and the interconnecting lines - can easily be controlled.

If, however, the transmitters and receivers influence each other in the radiation field of the antennas the remedial measures can sometimes be very complex and expensive. The simplest measure - increasing the isolation by increasing the distances between the interference sources and between susceptible receivers - is not feasible in view of the lack of space in typical air-, naval- and ground-weapon-systems.

Two possible causes for the reduction of EMC for radio transmission of information will be dealt with below. A quantitative assessment should provide a guide to the conditions under which the effects described are likely to occur. Possible remedies will be discussed.

## 2. EMC CHARACTERISTICS AT THE ANTENNA TERMINALS OF TRANSMITTERS AND RECEIVERS

### 2.1. Transmitters

A transmitter primarily produces RF energy at a specified frequency in order to radiate information. The radiated signal requires a certain bandwidth, depending on the type of modulation used.

In addition to this desired radiation every transmitter also produces a number of undesired spurious emissions, which can be classified as follows:

- 1) the emission of harmonics of the operating frequency and of the master oscillator frequency
- 2) non-harmonic emissions - all the remaining unwanted discrete frequencies generated which are not harmonically related to the frequencies produced in the transmitter
- 3) Broadband noise.

Fig. 1 shows these signal components.

34-2 The typical appearance of such a transmitted signal containing all these components over a wide frequency range is shown in Fig. 2.

The substantial reduction in spurious emissions apparent in Fig. 2 indicates that this transmitter is already provided with an effective output filter, as is customary, to suppress the spurious emissions (White, D.R., 1973). With a more complex filter arrangement a further reduction for the frequency range.

$$f/f_{OT} \leq 0.5 \text{ and } f/f_{OT} \geq 2$$

can easily be achieved.

Normally these spurious emissions are additionally attenuated along the propagation path from the transmitting antenna to the antenna of the sensitive receiver to such a degree that interference-free reception is guaranteed. This is also true if the transmitter and receiver are located side by side in the same system, id est in the air-craft, on the ship or in the tactical-vehicle.

This only applies, of course, if the transmission path has an exactly linear transfer-function response in the antenna-assembly and in the radiation field.

## 2.2. Receivers

Fig. 3 shows the typical sensitivity characteristics of a receiver as a function of the frequency at its antenna terminal. The receivers normally employ adequate means of selectivity in front of the first mixer so that undesired spurious responses are reduced by about 60 to 80 dB. For our further considerations the receiver characteristics are only for interest with respect to the actual operating frequency of the receiver.

## 3. EMC PROPERTIES OF THE TRANSMITTING AND RECEIVING ANTENNAS

The use of directional antennas also increases the isolation between transmitters and receivers in the radiation field. For tactical reasons only omni-directional antennas are used in the case of mobile systems below 1 GHz. These antennas must of necessity be vertically polarized so that an isolation gain cannot be achieved by using cross-polarization.

Furthermore, the gain of the antennas outside their operating frequency range is of decisive importance for further considerations.

The gain of typical antennas associated with non-linear junctions remains nearly constant for the UHF-range from 200 to 1000 MHz. Halfdipoles are generally used. For the 3rd, 5th etc. harmonics, the radiation resistance comes back very closely to the matching point at the fundamental. At the 2nd, 4th, 6th etc. harmonics the radiation resistance will be approximately three to four times higher, and therefore a loss in the antenna efficiency of about 6 dB maximum can be assumed for those harmonics. Thus the gain will be sufficient for significant radiations of regenerated harmonics of the illumination frequency.

## 4. EMC CHARACTERISTICS OF ANTENNA CABLES WITH CABLE CONNECTORS AND OF WAVEGUIDES

Antenna leads, antenna cables and their plugs as well as waveguides have a broadband character and are specified fairly adequately by:

- attenuation response
- reflection properties and
- RF-shielding properties.

Coaxial cables intended to satisfy the requirement for higher flexibility, such as cable RG-214 U, have a stranded (twisted) inner conductor.

If the cable moves slightly or if its position is altered, the current transfer points will be shifted somewhat between the individual strands of the inner conductor.

It should be noted that with an exactly concentric arrangement in such a cable, the cross points in the outer, screening conductor are free from RF currents. Thus changes in the transfer impedance at these points in the screening should not initially affect the cable characteristics.

The company of Rohde and Schwarz (Neubauer, H., 1970) has examined cables of this type and ascertained variations in the harmonic behavior. The test equipment used was able to measure a harmonic suppression of up to 150 dB at a frequency of 300 MHz with a 20 W transmitter and a sensitivity of 0.5  $\mu$ V at the receiver. Measurements on a cable with plugs revealed variations of harmonic suppression of between 110 and 145 dB when the cable was moved.

The cable plugs alone proved to be more stable and manifested harmonic suppression of more than 150 dB. Only after they had been greatly corroded - by artificial means - did the harmonic suppression value of the plugs come down to about 110 dB.

Prompted by the subject of intermodulation distortion in 4 GHz broadband telecommunication systems, the Siemens AG (Löw, W., 1962) investigated the generation of combination frequencies when waveguides and coaxial components operate with several frequencies. In the case of broadband telecommunication systems several transmitters and receivers are connected to the same antenna system by the waveguide as the common antenna line. Since with harmonic phenomena it is primarily cubic order combination frequency which occurs as a result of the difference between  $2f_2$  and  $f_1$  in the operating frequency band. A harmonic suppression of 130 to 140 dB is required for the interference-free operation of such telecommunication systems.

Löw carried out investigations on the harmonic behavior of contact points as they occur in waveguides and coaxial components with reference to the following parameters:

- signal level
- contact material
- contact shape (spherical or pointed junction)
- contact pressure.

The power of the cubic distortion products increases as the cubic order of the exciting signal power, as can easily be demonstrated, in accordance with the relationship:

$$P_D = c \cdot p^3$$

where "p" is the excitation-power and "c" a typical constant factor of the setup.

Silver proved to be the most advantageous material. Aluminium is by far the most unfavorable, but most widely used for aircraft and ship construction.

A flattish contacting surface proved more favorable than a pointed contact. A certain specific contact pressure must be exerted.

The important results of these investigations are reproduced in Fig. 4.

The measured values show a worst-case harmonic suppression of  $a_D \geq 70$  dB for an excitation power of approximately 4 W.

The following points must be borne in mind:

- the harmonic suppression may be less than 70 dB when poor contact is made in the case of aluminium.
- with transmitting powers above 1 W we must reckon with harmonic distortion as a result of non-linear junctions.
- the contact strength must be as great as possible for aluminium contacts.
- cracks in soft solder points are possible sources of harmonic distortion.
- non-linear junctions, similar to those of waveguides, may occur in transmitting antennas.

## 5. EMISSION OF HARMONICS TO THE TRANSMITTER FUNDAMENTAL DUE TO UNINTENDED NON-LINEAR JUNCTIONS IN THE TRANSMITTING ANTENNA

- Prediction and comparison with a practical example.

### 5.1. Prediction of the possible influence on a receiver

In the preceding section we dealt with the influencing effects of combination frequencies which can occur at non-linear junctions excited by two or more transmitting signals.

However, even sufficiently high excitation of non-linear junctions by one transmitter alone may generate the second, third, fourth and higher-order harmonics and produce excessive intra-system interference to receivers in frequency ranges above the transmitting frequency.

It is generally a simple matter to suppress the harmonics with low-pass filters at the transmitter output to prevent them reaching the antenna. A harmonic suppression value of 80 dB is normal, and values of 120 dB can easily be obtained. It goes without saying that the harmonics, suppressed by expensive filtering, must not be allowed to occur again in the antenna system.

It should be assumed for the purpose of predicting the possible influence on the receiver that the non-linear junction will be excited by a UHF-communication-transmitter (220 to 400 MHz) with a transmitting power of approximately 16 W.

Since the harmonic power increases with cubic order of the excitation power, the harmonic suppression would decrease by 18 dB to a value of approximately  $\geq 52$  dB according to the rise in transmitting power from 4 to 16 W.

Assuming this transmitter is connected to a broadband omnidirectional antenna which can still radiate the third and higher harmonics at sufficient power and which, due to poor design, contains non-linear junctions, harmonic levels approximately of -50 to -60 dB relative to the transmitter-fundamental can be expected in the radiation field.

It is immediately apparent that harmonic filters which normally have a stop-band attenuation of 60 to 80 dB will have little or no effect under these conditions. The typical setup for EMI-prediction is given in Fig. 5.

The following example, discussed with reference to Fig. 5, shows how unfavorable the situation may be for the disturbed receiver.

The front-end of the IFF-receiver will be susceptible to spurious signals at 1030+4 MHz if the interference level is above -3 to -10 dB relative to the level of the intended input signal. Standard input level of the receiver will be at PRN = -72 dBm, the receiver threshold at PRT = -76 dBm.

The table in Fig. 5 shows how the low-pass-filter, matched to a 50  $\Omega$ -load, provides sufficient harmonic suppression for the 3rd and 5th harmonics of the UHF-transmitter-fundamental.

Non-linear elements in the antenna assembly regenerate the harmonics to a level of PD3 = -10 dBm and PD4 = -16 dBm respectively. The values can be brought down by the path-loss between the two antennas only to a level of PRD3 = -70 dBm or PRD4 = -76 dBm at the input of the receiver. The receiver will be susceptible to this as can be seen easily in the last column of the table in Fig. 5.

If non-linear elements in the transmitting antenna did not occur, the interference levels at the receiver front-end would be down to PRD3 = -118 dBm and PRD4 = -133 dBm and would not be harmful to the receiver.

## 5.2. Results obtained in practice with an aircraft

The interference experienced with this model in practice has led to investigations of the described effect.

Fig. 6 shows a schematic diagram of the aircraft with the antenna locations. The isolation values measured for the frequency of 1030 MHz have been entered in the diagram. The prediction made in section 5.1 above is valid for the two antennas UHF<sub>Top</sub> and IFF<sub>1</sub>.

All the observations of interest are compiled below:

- (a) The interference factors were ascertained during the flight test and examined more closely afterwards in the aircraft hangar.
- (b) When the UHF unit was operated at 257.5 MHz, about 20 equally spaced channels in the bandwidth of  $4 \times \pm 0.5$  MHz =  $\pm 2$  MHz at 1030 MHz caused interference to the IFF-receiver.
- (c) When the UHF unit was operated at 343.3 MHz, about 40 equally spaced channels in the bandwidth of  $3 \times \pm 2$  MHz =  $\pm 6$  MHz at 1030 MHz caused interference to the IFF-receiver.
- (d) The harmonic level measured at the IFF antenna output was approximately -76 dBm at  $4 \times 257.5$  MHz and approximately -70 dBm at  $3 \times 343.3$  MHz.
- (e) The presence of these interference signals at the transponder input resulted, in the absence of an interrogation signal, in "random triggering" when the interfering transmitter was switched on and off.
- (f) Measurements in the radiation field revealed that the insertion of a 20-dB attenuator preceding the transmitting antenna of the UHF unit reduced the field strength at the fundamental frequency of the transmitter by 20 dB, as anticipated. The attenuation at the frequency of the harmonics, however, was more than 40 dB.
- (g) The observations made so far all refer to the initially unmodulated interference carrier. If the UHF transmitter is modulated by voice or a ringing tone (1000 Hz) the "random-trigger-rate" rises appreciably. The same applies to the sensitivity-reduction of the transponder.

- (i) The tendency of the non-linear junctions to be modulated by vibrations transmitted through the aircraft-structure was observed. Measurements made in the radiation field near the aircraft demonstrated that only the new harmonics of the transmitter fundamental frequency generated at the non-linear junctions were affected by this modulation. As a result of this behavior we were able to detect interference levels which were about 20 dB higher still on the brake-test-site during the jet-engine test-runs.
- (k) It was a simple matter to reproduce the effect observed with the aircraft under laboratory conditions with a completely different antenna pair (UHF-IFF antenna). In this case, too, the harmonic level in the radiation field could only be reduced to a certain level by inserting low-pass filters before the antenna. Furthermore, the insertion of the low-pass filters had no effect, even though it was possible to show that the harmonic level at the output of the low-pass filters matched to a 50  $\Omega$ -load was reduced in accordance with the stop-band attenuation of the filters.

#### 6. INTERFERENCE IN THE RADIATION FIELD OF HIGH-POWER TRANSMITTERS BY RANDOM SWITCHING OF UNINTENTIONAL CONTACTS

A further effect which can greatly reduce EMC is the broadband interference which is produced by the random, undesired switching of undefined RF-contacts.

This interference often occurs in the nearfield of antennas of high-power shortwave transmitters - 400 W to 1 kW power - in the 1.5 MHz to 30 MHz frequency range.

On ships, in particular, cables and lines and other similar conductors in the proximity of the transmitting antennas can pick up RF-energy. The vibrations when the ship moves may cause such elements to come into contact with each other sporadically. Since their isolation from the antennas is often very low, powers of up to several Watts may be switched.

The switching of mechanical contacts creates spikes with rise times of a few nanoseconds. Thus, substantially high-level interference occurs in the entire frequency range up to about 1 GHz and above.

In one - albeit very unfavorable - case which we have observed, interference voltages of up to 60 dB  $\mu$ V/10 kHz have occurred at adjacent receiver antennas.

Generally, interference levels of up to 20 dB  $\mu$ V/10 kHz have been observed. Often, it was very difficult to locate these so-called "secondary interference sources" because of the interaction of a number of individual interference sources involved.

#### 7. MEASURES TO EFFECTIVELY REMEDY THE EFFECTS DESCRIBED ABOVE

Improvements in mechanical design provide a simple remedy to the effect described above, the random contacting in the nearfield of the antennas. Such measures result in the "electrical uniformity" of the surface, the reference ground of a system or of a device. Every junction which might be instable is bypassed by means of defined "bonding straps". Exact instructions on this matter are laid down in MIL-STD-1310A/1310C, "Shipboard Bonding, Grounding, and other Techniques for Electromagnetic Compatibility and Safety". These instructions in their present form only apply to ships, but the meaningful application of their contents to cover aircraft and tactical vehicles, too, seems appropriate.

The simplest way of dealing with the case quoted initially in the example - namely, interference produced on the IFF receiver, the receiver of the IFF-transponder, by the harmonics from the UHF-transmitter - would be to block the corresponding channels close to the critical frequencies in the UHF band. It would then be necessary to block about 20 channels in the case of  $F_{OT} = 257.5$  MHz and about 40 channels in the case of  $F_{OT} = 343.3$  MHz. 60 out of a total of 2500 channels would therefore be blocked. This solution is not acceptable for tactical reasons.

The problem was solved by a certain time-sharing. The IFF-transponder was able to decode and reply for correct aircraft-identification between the excitation periods of the UHF-transmitter with voice-modulation.

Furthermore, it would undoubtedly be a difficult matter to realize the remedial design measures to offset the effect of non-linear elements in the case of junctions in the proximity of transmitting antennas. Suitable shaping and high contact pressure will initially be advantageous in the case of aluminium contacts. As a safety precaution a more better contact material such as tin- and silvercoated brass, copper and beryllium-bronze or stainless steel.

Recent measurements were made on a ships' installation satisfying the requirements of MIL-STD-1310A/1310C and demonstrated that this installation is a very successful solution to the problems of reducing the described effects. The suppression for cubic and higher order harmonics in the radiated field was above 70 dB in the HF-frequency range and more than 130 dB in the UHF-frequency range.

In the HF-frequency range no spurious amplitude modulation on the harmonics and combination frequencies, which is typical for the presence of non-linear junctions in connection with the vibrations of a ship, could be detected.

In the UHF-frequency range the use of dipole antennas provided sufficiently low harmonic levels, even if the UHF-transmitting-power was 1 kW. In contrast, the use of monopole antennas, like the UHF-antenna in the aircraft, seems to reinforce the regeneration of harmonics to a high degree, because the aircrafts' structure acts as a counterpoise to the monopole antenna.

Strangely enough, we have not yet found any reference to the problem of non-linear junctions as discussed above in the EMC literature known to us, apart from MIL-STD-1310A/1310C and an advertisement in "The Microwave Journal" in which the Company of Microlab/FXR is offering an intermodulation detector for non-linear junctions (Microlab, 1973).

## 8. CONCLUSION

We hope that we have sufficiently emphasized the importance of these EMC problems, which we have encountered in practice, particularly the importance of the non-linear junction effect.

Our experience would indicate that a satisfactory solution for ships' installations has been found for the future.

Unfortunately, our limited investigations can only act as a general guide. Comprehensive experience should be gathered or gained to find an answer to the following question:

"Is it generally possible, with economically justifiable means, to reduce the described effects in the systems to a tolerable level, or do we have to make any concessions in EMC-predictions for a certain inevitable "frequency spectrum pollution" due to the non-linear junctions?"

## 9. REFERENCES

- Loew, W., 1963, "Investigations into the non-linear behavior of current-carrying contact points on waveguide and coaxial components", Frequenz, 1963, Part 3, pp 94-102
- Microlab/FXR, 1973, "Intermodulation Detector, Model C4", Technical Bulletin and Manual, Sept. 1973, Ten Microlab Road, Livingston, N.J. 07039
- Neubauer, H., 1970, "Connector Intermodulation Phenomena", NTZ, 1970, Part 5, pp 266-267
- White, D.R., 1973, "Electromagnetic Interference and Compatibility", Volume 3, 1973, Germantown

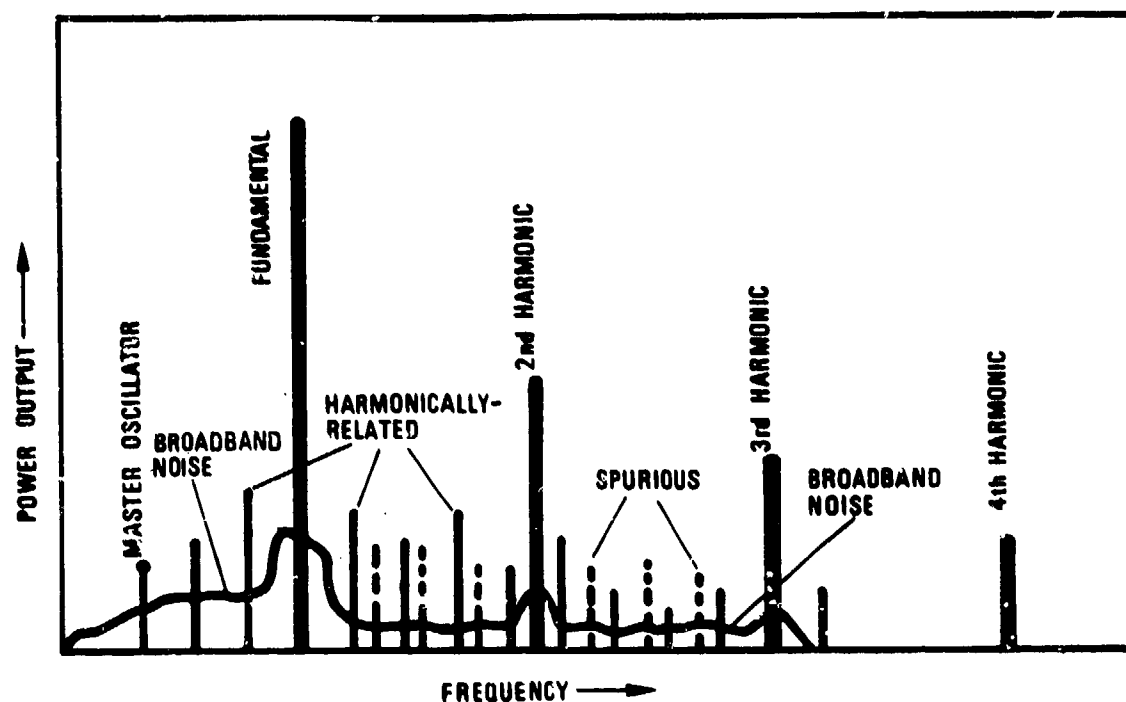


Fig.1 Typical transmitter emission spectra

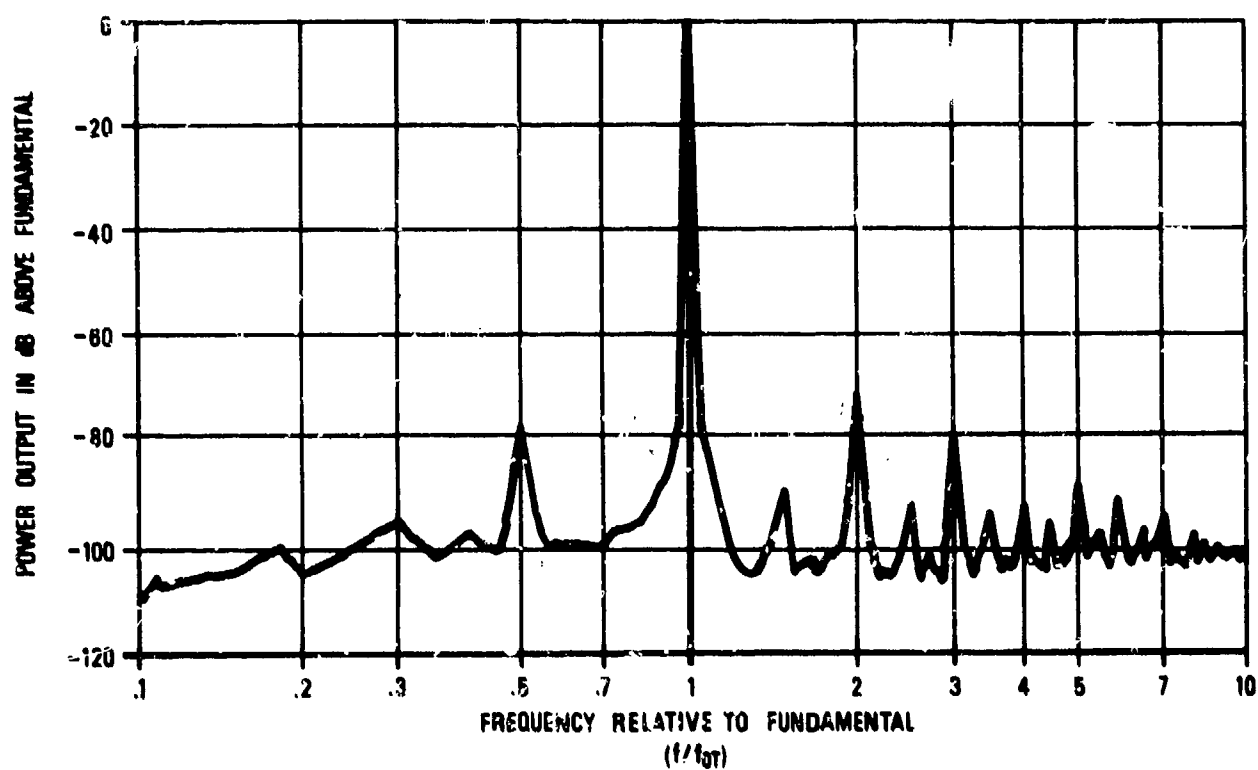


Fig.2 Transmitter output spectrum, composed of broadband noise and discrete emissions

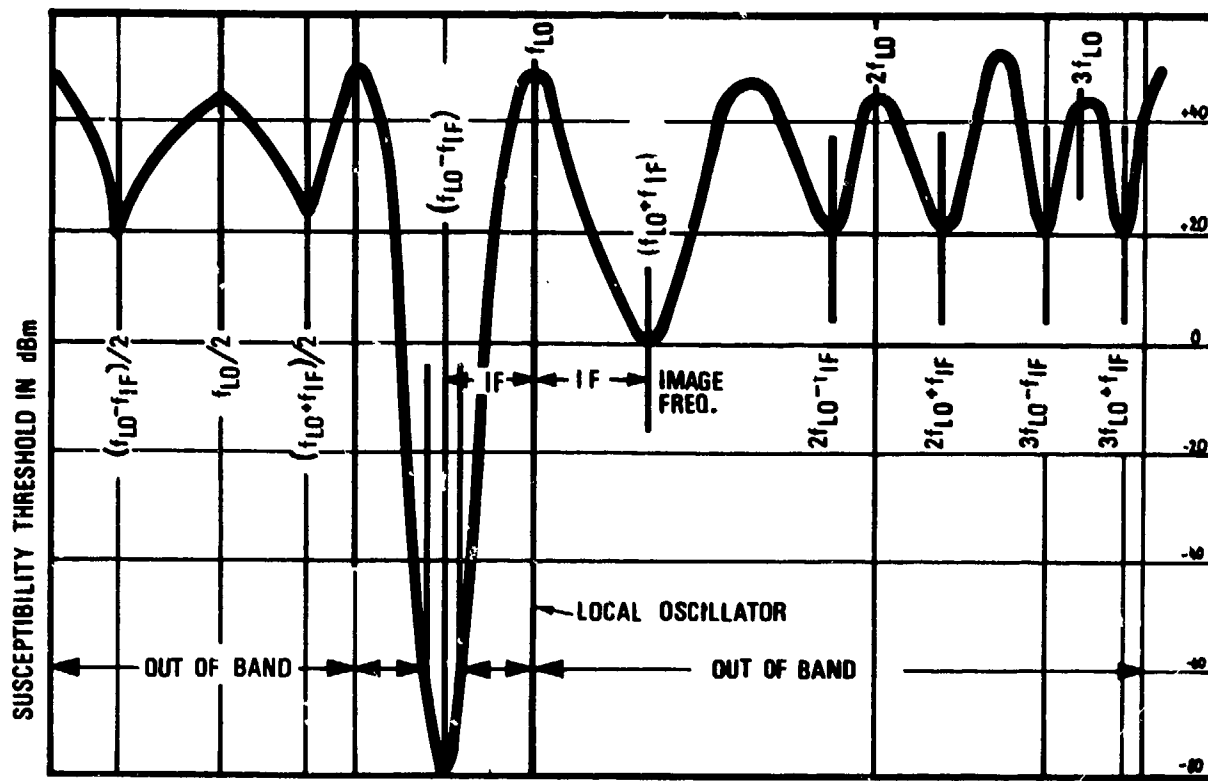


Fig.3 Typical receiver susceptibility characteristics

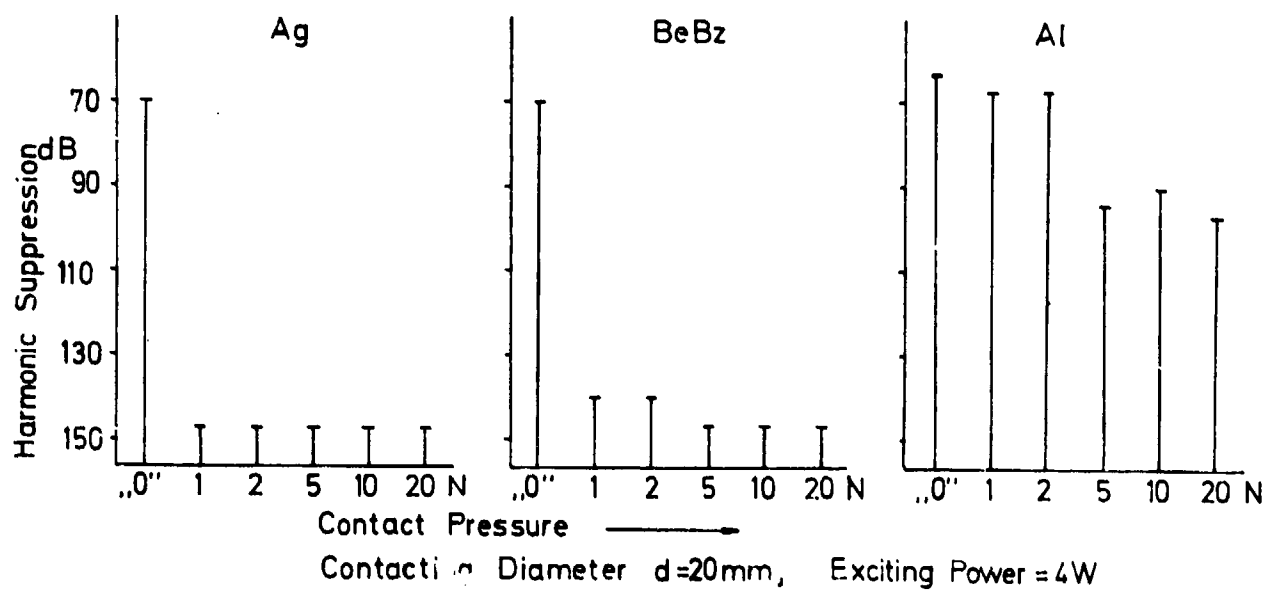


Fig.4 Harmonic suppression due to the contact-pressure



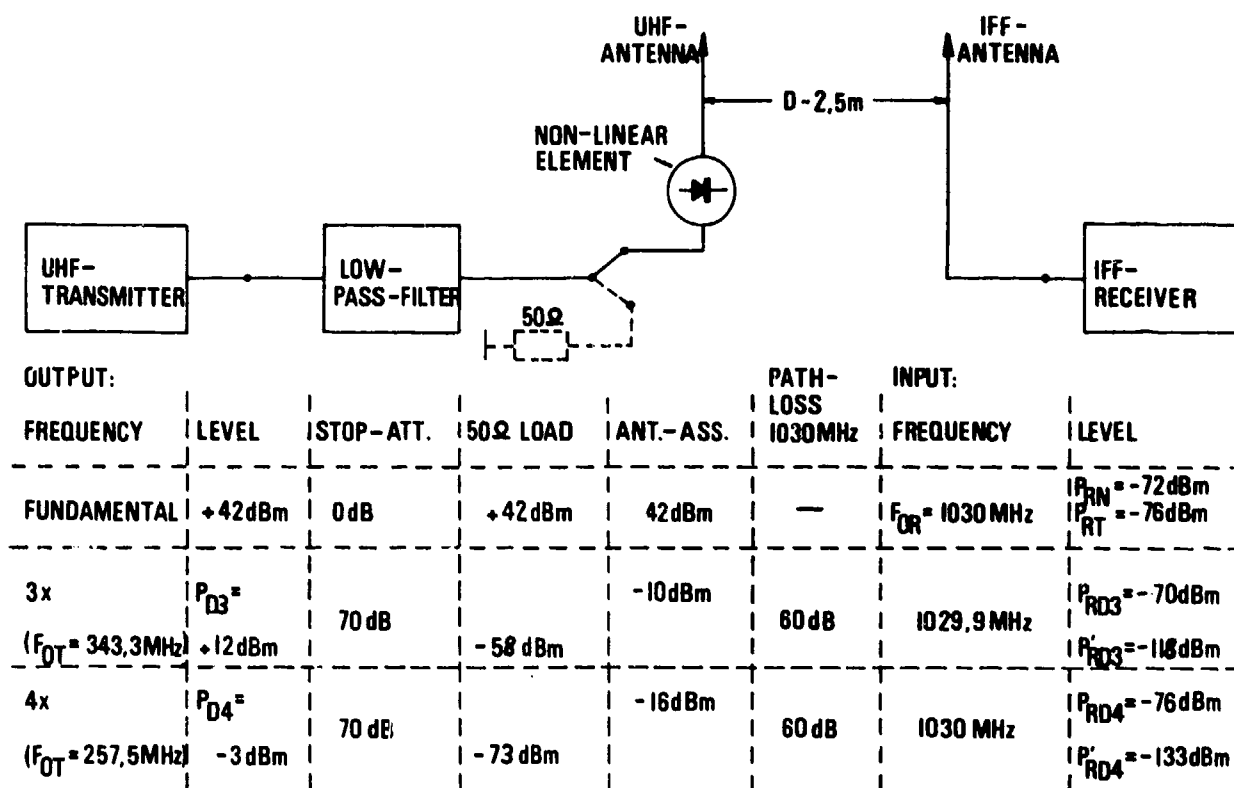


Fig.5 Typical setup for EMI-prediction

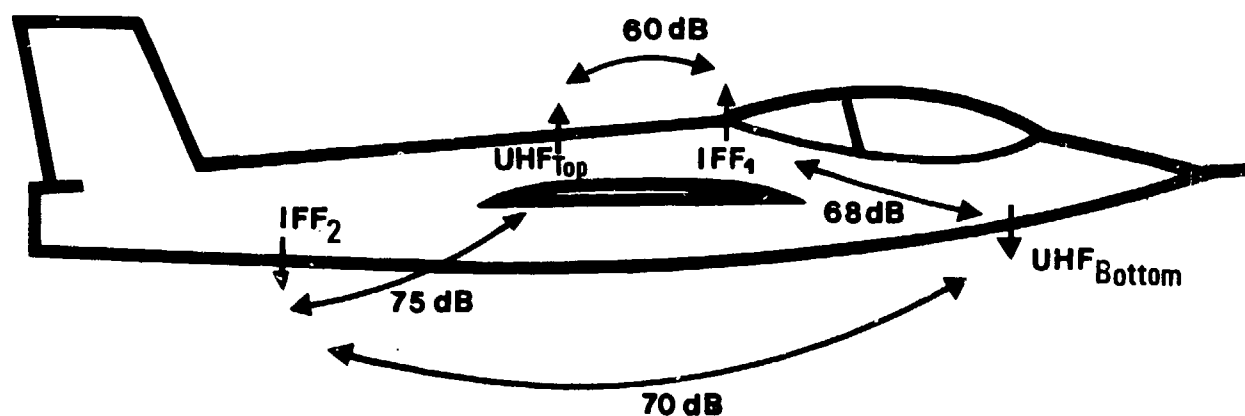


Fig.6 Isolation (dB) at 1030 MHz between the UHF- and IFF-antennas in the aircraft

## DISCUSSION

P. SEVAT: 1) What is the material of the other part of the contacts in your Fig. 4? 2) I think in this respect, the place of the material in the potential series can be important, especially in the long run.

K. LANDT: 1) Investigations had been performed when contacting was between silver to silver, beryllium bronze to beryllium bronze and aluminum to aluminum. 2) If the contact pressure will be so high that the junction becomes cold welded, the junction will be stable for a long time. There will be no effect due to potential series. We measured the resistance of a riveted ream (steel-aluminum) on a German ship about ten years after construction. The resistance was below  $1\text{m}\Omega$  up to 30MHz.

E. M. FROST: The ranking order for the harmonic/pressure characteristics for the metals given in Fig. 4 is the same as those for their "dc" contact resistance/pressure values; however, stainless steel was mentioned as a "good" material which does not agree with its "dc" performance. Can the author give a possible explanation?

K. LANDT: I would say yes, because silver oxide is conductive and aluminum oxide has insulating character.

In the frequency range where the skin effect is valid and the penetration depth of the HF is much less than the thickness of the material, the "dc" performance is not more important.

S. C. KLEINE: 1) What do you mean with the variation of harmonic suppression of a cable being moved? 2) What are your conclusions from this variation in the harmonic behavior of a cable being moved for the design of transmitters/receivers?

K. LANDT: 1) The cable is no harmonic suppressor, but it has a certain harmonic suppression according to its transmission properties. If the cable is moved, this typical value may vary. 2) The harmonic suppression at the transmitter output/cable input should not be higher than the harmonic suppression of the cable itself. On the receive end there will be no effect because the excitation power from the transmitter fundamental is respectively too low.

# IMPROVED DESIGN OF INTERFERENCE SUPPRESSORS AND MEASUREMENT OF ATTENUATION CHARACTERISTICS

by

M. L. Jarvis

J. D. Hawkett

Engineering Physics Department,

Royal Aircraft Establishment, Farnborough, Hants, England

35-1

## SUMMARY

This Paper describes briefly the mathematic approach and results obtained in the development of a new design of interference suppressor which eliminates the resonances normally occurring between a suppressor and its load.

The Paper also describes the shortcomings of conventional 50 ohm insertion loss measurements, and proposes a characteristic based on critical load conditions.

## INTRODUCTION

As part of a research programme seeking a cure for the increasing number of EMC problems on aircraft, a programme of work was initiated into suppressor design and performance based on the characteristics of the individual components of passive suppressor networks.

Further, since it was realised that suppressors always work into an unknown complex load which varies with frequency, the present method of determining the attenuation characteristic from an insertion loss measurement in a 50 ohm resistive system was considered to have little value, and a more realistic performance characteristic was sought.

This Paper gives a brief description of a mathematic approach to suppressor design and of the results obtained. A more realistic attenuation characteristic is proposed based on the attenuation achieved at each frequency when a suppressor is loaded with its critical load. The introduction of a resistor in the output component of a suppressor is shown to damp out the resonances which can occur between suppressors and their loads.

## MATHEMATIC APPROACH

A simple approach was adopted using matrix algebra. A suppressor was considered to be a four terminal network, which can be completely described by its 'A' matrix, and comprising any number of inductive, capacitive or resistive components.

If the voltage and current sent and the voltage and current received under open and short circuit conditions are measured it is possible to calculate the complex impedances of the components in the network. Conversely, knowing the component values in complex terms it is possible to calculate the poles of the 'A' matrix.

The matrix equations of a four terminal network are shown in Fig.1.

## DEFINITION OF T AND $\pi$ NETWORKS

In order to clarify the confusion which can sometimes arise when defining the values of components in T and  $\pi$  sections for the calculation of cut off frequency and iterative impedance, it was decided to consider each type as part of a long series, as shown in Fig.2. The component values are  $\frac{L}{2}$ , C and  $\frac{L}{2}$  for the T suppressor and  $\frac{C}{2}$ , L and  $\frac{C}{2}$  for the  $\pi$  suppressor; for both types the cut off frequency is  $\frac{1}{\pi\sqrt{LC}}$ , and the iterative impedance is  $\frac{L}{C}$ .

By writing the 'A' matrix for each component in the suppressor,  $\begin{bmatrix} 1 & Z \\ 0 & 1 \end{bmatrix}$  for the series element and  $\begin{bmatrix} 1 & 0 \\ Y & 1 \end{bmatrix}$  for the shunt element, where Y and Z are the admittance and impedance values of the components in complex terms, and multiplying these matrices together it is possible to complete the 'A' matrices for single T and  $\pi$  suppressors. Fig.2 also shows the suppressor elements and their matrices.

## PRACTICAL WORK

Equivalent T and  $\pi$  suppressors were constructed having components chosen to have values whose complex impedances could be measured using available equipment over a reasonable frequency range.

These values were, the inductive series element  $\frac{L}{2} = 1.31$  millihenry and the shunt capacitive element  $\frac{C}{2} = 0.005$  microfarad, and the frequency range considered was 0 to 300 kHz.

These component values gave for both types of suppressor a cut off frequency of 62.3 kHz, and an iterative impedance of 512 ohms.

Measurements on the suppressors were used to check the computer programmes and the theoretical concept of minimum attenuation.

## 352 THEORETICAL WORK

A computer programme was prepared to determine the 'A' matrix, the open circuit voltage ratio and the insertion loss characteristic over the frequency range 0 to 300 kHz for both T and  $\pi$  suppressors.

In addition the computer was programmed to determine the ratio of voltage sent to voltage received across a large number of complex loads at one particular frequency, 100 kHz.

The results of the attenuation found at 100 kHz, under complex load conditions, were plotted in the impedance plane, and points representing loads giving the same attenuation through the suppressor were joined together to give contours of constant voltage attenuation. Fig.3 shows the results obtained for a double T suppressor.

These contours proved to be a family of coaxial circles, from which it is possible to deduce the attenuation through the suppressor when connected to any complex load. In the case shown in Fig.3 the attenuation when connected to a load of  $(800 + j600)$  or  $(600 + j0)$  or  $(200 - j180)$  ohms will be 34 dB.

However, it is difficult to extrapolate this family of coaxial circles, as the position of the circle centre and the scale of each circle changes for each value of attenuation.

If, however, the same information is plotted in the admittance plane as shown in Fig.4, another family of circles representing contours of constant voltage attenuation is obtained. In this case the family is much easier to extrapolate since the circles are concentric and the ratio of the circle diameters is directly proportional to the attenuation, for example the 100:1 circle (40 dB) is 10 times the diameter of the 10:1 circle (20 dB). The admittances of the loads above also lie on the 34dB circle, e.g.

$$\frac{1}{(600 + j0)} = 1.66 \text{ mmhos}.$$

A generalised figure of this family of circles of constant voltage attenuation can be constructed as shown in Fig.5. The circle centre is given mathematically as minus the reciprocal of the Thévenin impedance

$\left[ -\frac{a_{11}}{a_{12}} \right]$  of the 'A' matrix, and the radius of each circle is equal to  $M$  (the voltage ratio) divided by the modulus of the transfer impedance  $(|a_{12}| \text{ of the 'A' matrix})$ .

It is thus possible to predict the performance of a suppressor with any complex load condition from two measurements at each frequency; the complex Thévenin impedance, which can be measured with a bridge, and the transfer impedance modulus which can be determined with a measuring set and a current probe.

### MINIMUM ATTENUATION

For the passive suppressors being considered the resistive term of the complex Thévenin impedance will be positive so that the common circle centre, which is defined as minus the reciprocal of the Thévenin impedance will lie to the left of the susceptance axis in the admittance plane as shown in Fig.5. For all practical passive loads, that is loads with a positive conductance, there is a minimum realisable attenuation represented by the dotted circle.

This minimum attenuation is achieved when the load on the suppressor is purely reactive and has a susceptance equal to the conjugate of the susceptance of the Thévenin impedance.

### EXPLANATION OF THE SUPPRESSOR AND LOAD RESONANCE

The typical low pass suppressor shown in Fig.6 can be represented by Thévenin's Theorem as a voltage with zero source impedance in series with an impedance equal to the impedance of the suppressor in the reverse direction with the input short circuited. The voltage source has an EMF equal to the open circuit voltage through the suppressor  $V_{oc}$ .

In the example shown, above cut off, the T suppressor has an inductive impedance, so that a purely capacitive load with a reactance equal to the conjugate of the reactance of the Thévenin impedance will cause the circuit to resonate, and the voltage across the load will be  $Q$  times the applied voltage  $V_{oc}$ . In many instances, when the  $Q$  of the suppressor is high, the voltage across the critical load may even exceed the input voltage to the suppressor  $V_{in}$ .

### VARIATION OF ATTENUATION WITH FREQUENCY

The previous discussion has covered the characteristics of a suppressor at one particular frequency and has shown that a pattern of concentric circles exists in the admittance plane which enables the performance of the suppressor to be predicted under any load condition by knowing the transfer impedance and the Thévenin impedance.

Both of these impedances, however, change with frequency and it is necessary to know how they change in order to predict the performance over the entire frequency range.

Fig.7 is derived from the Thévenin impedance and shows how the position of the common circle centre changes with frequency for the experimental double T suppressor.

The locus describes two circular paths and has 4 resonant frequencies at which the Thévenin impedance is purely resistive, which could be expected for a network with 5 components. As frequency is increased the critical load therefore alternates between capacitive and inductive values until finally above cut off it remains capacitive.

For the experimental double  $\pi$  suppressor the locus of the common circle centre with varying frequency, shown in Fig.8, has only one circular path and has only 3 resonant frequencies, contrary to what is expected for a network with 5 components. This is explained by the short circuiting of the input capacitor when making the Thevenin impedance measurement required to calculate the position of the circle centre.

The cut off frequency for both the T and  $\pi$  suppressors is the highest finite resonant frequency, all other resonances occurring in the pass band. 35-3

The critical load for both T and  $\pi$  suppressors changes sign each time the suppressor passes through a resonant frequency. Above cut off it remains capacitive for the T suppressor and inductive for the  $\pi$  suppressor.

#### VARIATION OF CRITICAL LOAD WITH FREQUENCY

Figs.9 and 10 show how the critical load for T and  $\pi$  suppressors vary with frequency.

For the T suppressor the critical capacitive load tends to a constant value of about 1000 pf for the network under consideration, so that the capacitance of the cables connected to the output of the suppressor could easily adversely terminate the suppressor over a wide frequency range.

For the  $\pi$  suppressor the critical load above cut off tends to a value of 50 microhenries.

#### MINIMUM ATTENUATION CHARACTERISTIC

All the previous work has shown that for every frequency there is a critical load at which the attenuation through the suppressor is a minimum, and conversely for every load there is a frequency which causes resonance between the suppressor and that load.

This theory has led to the proposal that the characteristics of a suppressor would be better defined as a minimum attenuation characteristic, that is the attenuation achieved at each frequency when the suppressor is critically loaded.

In practice the attenuation would be much greater than this value over the majority of the frequency range, and only at discrete frequencies would resonance occur and the minimum attenuation value be approached.

#### COMPARISON OF MINIMUM ATTENUATION, OPEN CIRCUIT AND INSERTION LOSS CHARACTERISTICS

Figs.11 and 12 compare the proposed minimum attenuation characteristic with the conventional insertion loss and open circuit characteristics for the experimental T and  $\pi$  suppressors.

For the T suppressor (Fig.11) the insertion loss characteristic gives an optimistic attenuation compared with the open circuit attenuation because of the high iterative impedance (512 ohms) of the network compared with the input impedance of the measuring set (50 ohms). The proposed minimum attenuation characteristic indicates what could result in practice under the worst loading conditions and shows a gain to be possible between dc and twice the conventional cut off frequency.

For the  $\pi$  suppressor (Fig.12), the open circuit characteristic is the same as that for the equivalent T suppressor, as is expected, but the insertion loss characteristic is less than that of the equivalent T suppressor. The proposed minimum attenuation characteristic shows the  $\pi$  suppressor to be in gain from dc to four times the conventional cut off frequency.

Comparison of Figs.11 and 12 shows a significant difference between T and  $\pi$  suppressors. With conventional insertion loss and open circuit measurements, a voltage attenuation through either type is obtained above cut off frequency: the proposed minimum attenuation characteristic, however, shows that under critical load conditions the frequency at which an attenuation is achieved is no longer related to the cut off frequency, but is a function of the overall Q of the suppressor and the number of components used in the network.

#### IMPROVEMENT OF MINIMUM ATTENUATION CHARACTERISTIC

It is possible to improve the minimum attenuation characteristic by loading the suppressor with a resistance equal to the iterative impedance of the network as is that practice in filter design. This resistive load has the effect of shifting the locus of the centres of circles of constant voltage attenuation (Fig.4) to the left by an amount equal to the conductance of the load and the minimum attenuation circle is then larger in diameter.

For power line suppressors, however, this external loading is not practical since such a resistive load would shunt the power supply with consequent waste of power and heat dissipation problems.

A more practical alternative has been found to have a similar effect above cut off frequency. If a resistance equal to the iterative impedance of the suppressor is connected, either in parallel with the output inductor of a T network, or in series with the output capacitor of a  $\pi$  network, the overall Q of the suppressor is reduced. This damping resistor has the desired effect of holding the Thévenin impedance R term constant as the frequency is increased above cut off.

Fig.13 shows the locus of the centre of circles of constant voltage attenuation for the modified experimental T suppressor, and it shows that at low frequencies the damping resistance has little effect but that above cut off the diameter of each circle is much larger than that of the unmodified suppressor (Fig.4).

35-4

This damping resistor is not required to carry current at power frequencies and is therefore of minimum size and weight.

#### MINIMUM ATTENUATION CHARACTERISTICS OF MODIFIED T SUPPRESSORS

The minimum attenuation and open circuit characteristics of modified T and  $\pi$  suppressors incorporating a damping resistor are shown in Figs. 14 and 15 respectively.

The curves show that above cut off the two characteristics are almost identical and that both suppressors are now independent of load. The minimum attenuation for the T and  $\pi$  suppressor are not the same, the T suppressor having a greater voltage attenuation than that of the equivalent  $\pi$  suppressor.

#### MEASUREMENTS ON AN AIRCRAFT

Fig. 16 shows the results of practical measurements made on an aircraft electrical system. The upper curve is a record of the interference measured on the field of an engine driven generator when the voltage was controlled by a variable mark space regulator.

The levels recorded show the interference to be well above the British Standard Requirements the limits of which are shown dotted.

After a conventional suppressor was designed and fitted, with components as shown, the levels of interference were again measured and by careful operation of the measuring equipment, resonances were found, thus demonstrating practically the theoretical work described above.

When a damping resistor was added the resonances were eliminated and the interference levels fell to 0 dB/ $\mu$ V above 3 MHz.

#### CURRENT ATTENUATION

All of the theoretical work described in this Paper has covered the voltage attenuation through the suppressor when connected to a complex load.

This theory can be adapted to describe current attenuation by simple duality, when the circles of constant current attenuation, with a common circle centre, are obtained in the impedance plane.

The circle centre is defined as minus the Norton impedance compared with minus the reciprocal of the Thévenin impedance, and the scale is inversely proportional to the transfer admittance, compared with the transfer impedance.

#### MEASUREMENTS TO DETERMINE THE MINIMUM ATTENUATION

From the circles of constant voltage attenuation in the admittance plane it can be shown mathematically that the minimum attenuation at a particular frequency is defined by:

$$\text{Voltage minimum attenuation} = 20 \log_{10} (Z_T) RP \left\{ \frac{1}{Z_{\text{Thév}}} \right\}$$

where  $Z_T$  is the modulus of the transfer impedance and  $RP \left\{ \frac{1}{Z_{\text{Thév}}} \right\}$  is the real part of the Thévenin admittance. The minimum attenuation can therefore be calculated from measurements of these two impedances at the particular frequency.

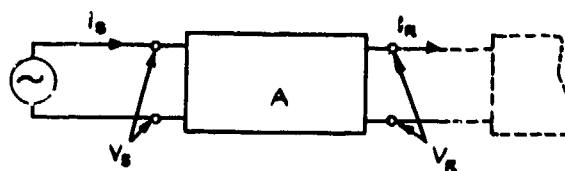
Similarly the current minimum attenuation at a particular frequency is given by:

$$\text{Current minimum attenuation} = 20 \log_{10} (Y_T) RP \left\{ Z_{\text{Norton}} \right\}$$

where  $Y_T$  is the transfer admittance, and  $RP \left\{ Z_{\text{Norton}} \right\}$  is the real part of the Norton impedance.

#### CONCLUSIONS

1. This work confirms that the present method of defining the characteristics of suppressors as an insertion loss of a 50 ohm, resistive, system is not representative of actual conditions since suppressors are always loaded by an unknown, varying complex load.
2. The proposed characteristic of minimum attenuation is based on worst case loading conditions at each frequency and in practice attenuations greater than this minimum would be expected over the majority of the frequency range and only occasionally rising to the minimum attenuation as the load and suppressor resonate.
3. The introduction of a damping resistance in the output components of a conventional low pass suppressor network improves the minimum attenuation characteristic and eliminates the resonances which occur between the network and the load. This characteristic then approaches that achieved under open circuit conditions.



$$V_S = a_{11} V_R + a_{12} I_R$$

$$I_S = a_{21} V_R + a_{22} I_R$$

$$\begin{bmatrix} V_S \\ I_S \end{bmatrix} = \begin{bmatrix} a_{11} & a_{12} \\ a_{21} & a_{22} \end{bmatrix} \times \begin{bmatrix} V_R \\ I_R \end{bmatrix}$$

$$a_{11} = \frac{V_S}{V_R} \text{ on } \%$$

$$a_{21} = \frac{I_S}{V_R} \text{ on } \%$$

$$a_{12} = \frac{V_S}{I_R} \text{ on } \%$$

$$a_{22} = \frac{I_S}{I_R} \text{ on } \%$$

Fig. 1 'A' matrix of a four terminal network

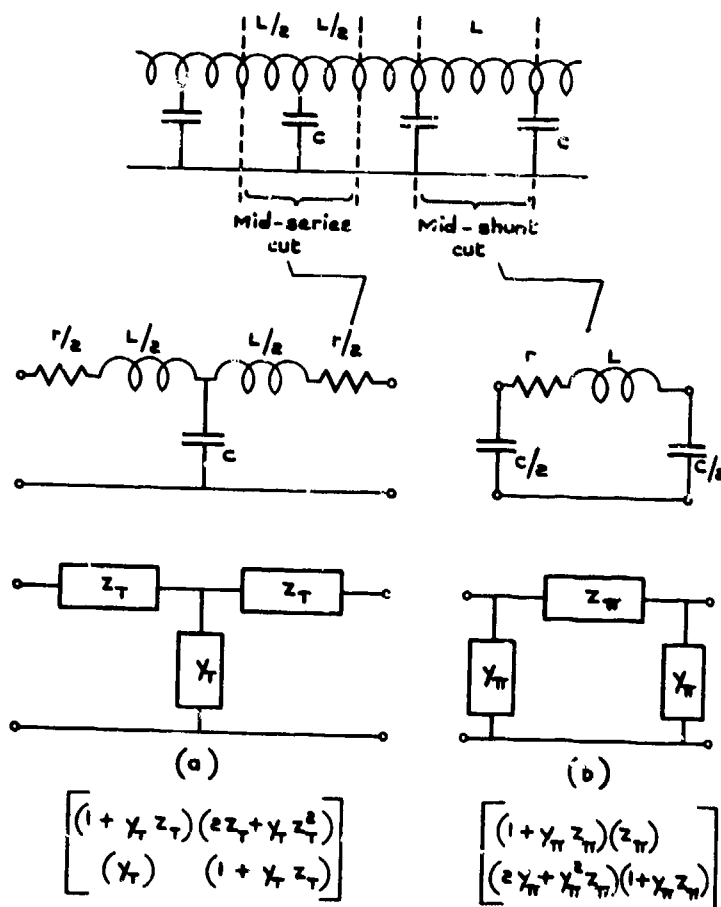


Fig. 2 'T' and 'pi' filter elements and their 'A' matrices

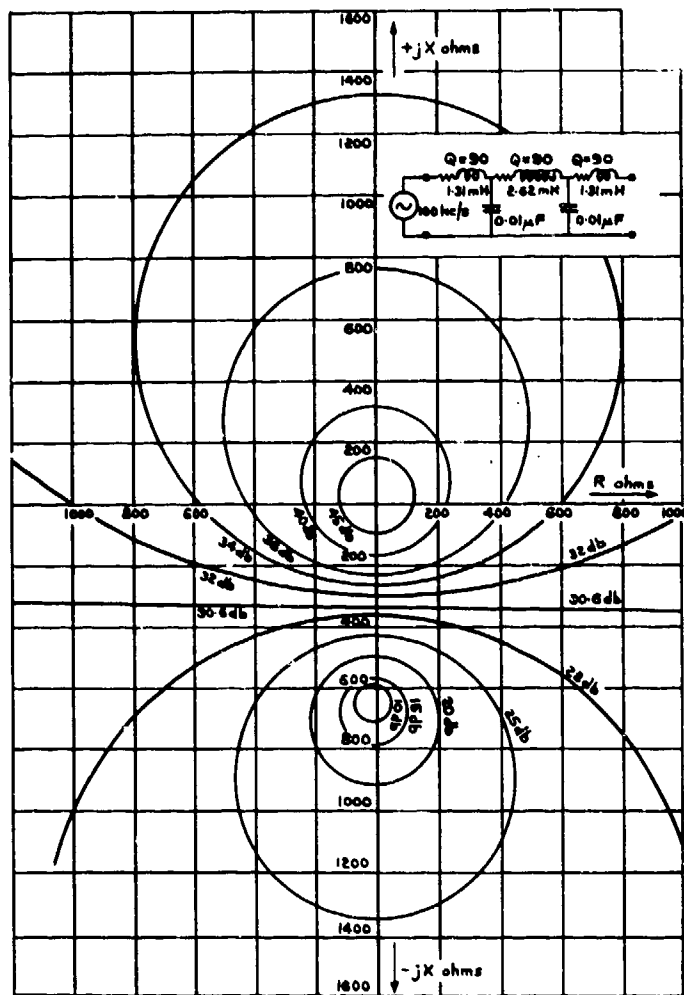


Fig.3 Contours of constant voltage attenuation in load impedance plane

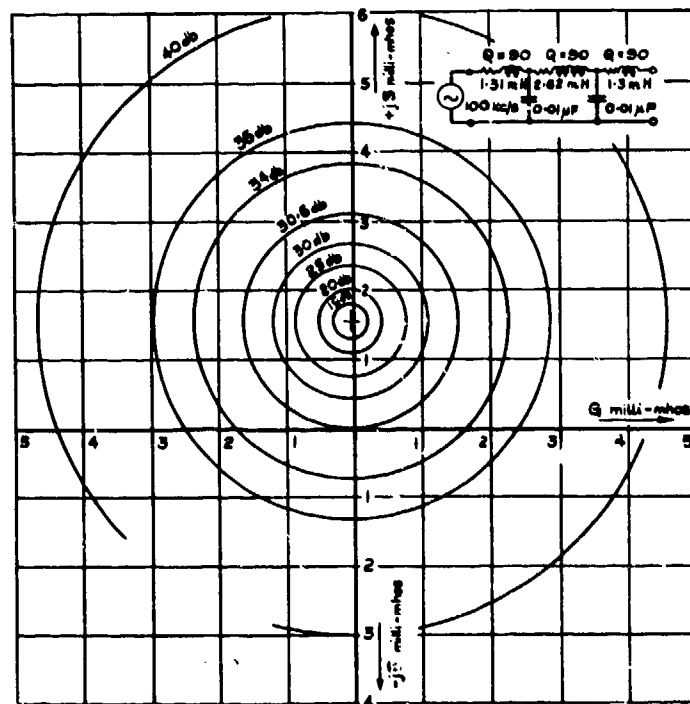


Fig.4 Contours of constant voltage attenuation in load admittance plane



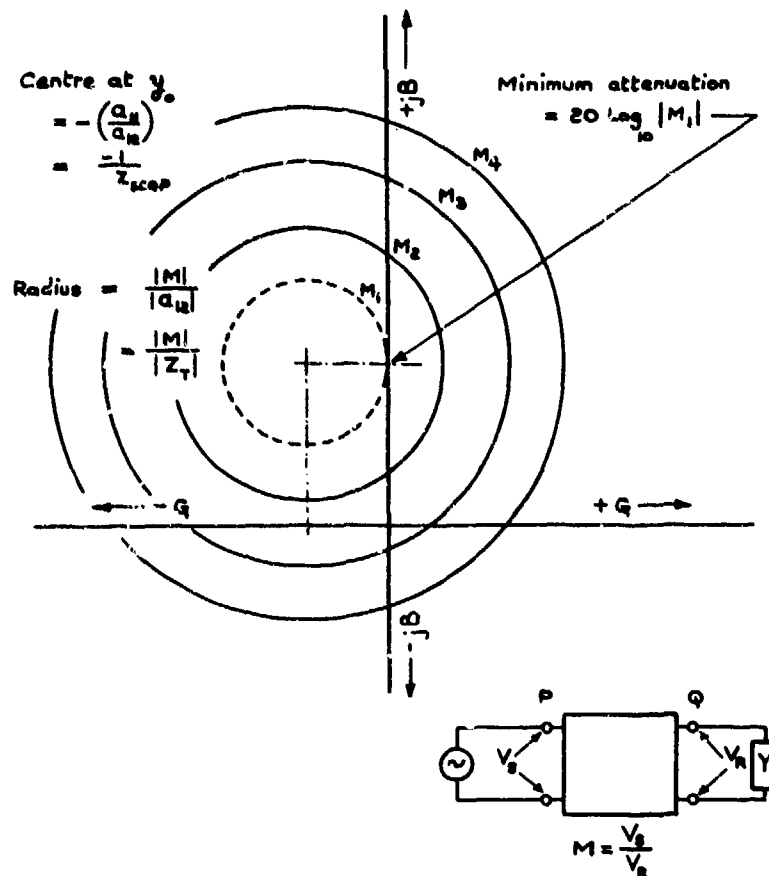


Fig.5 Circles of constant voltage attenuation in the admittance plane

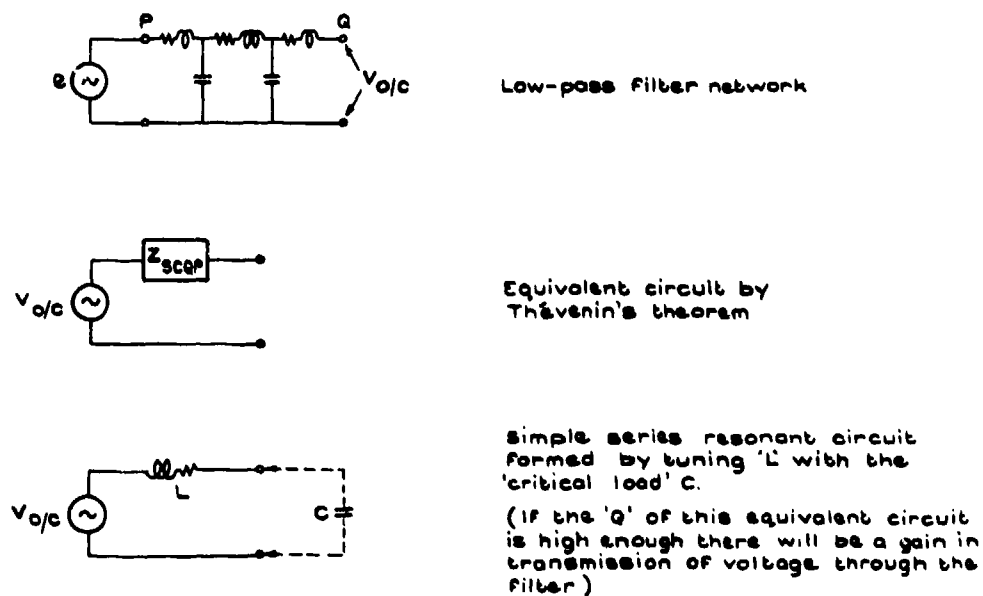


Fig.6 Explanation of filter cancellation using Thévenin's theorem

35-8

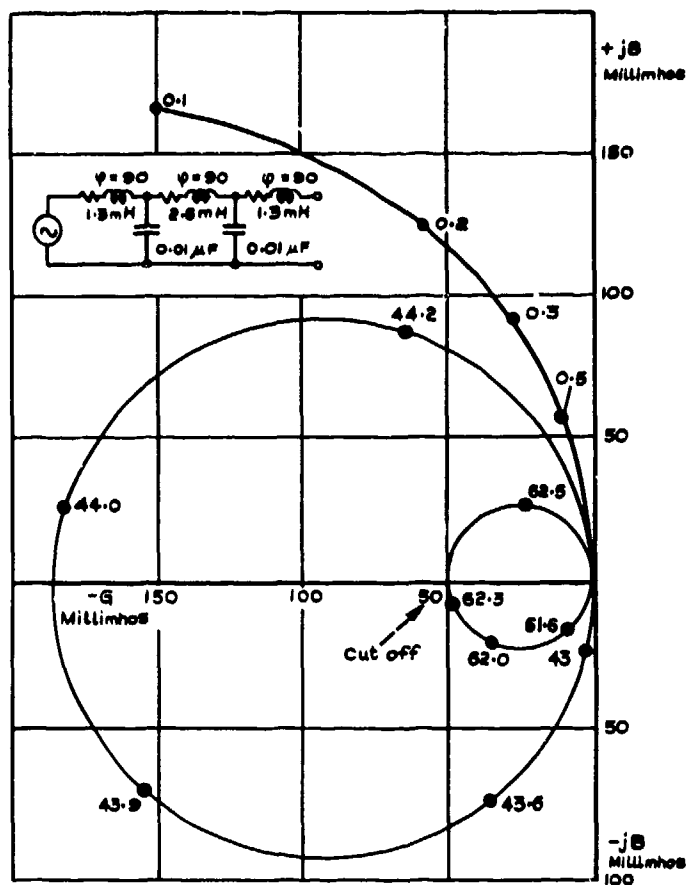


Fig. 7. Locus of circle centres with frequency

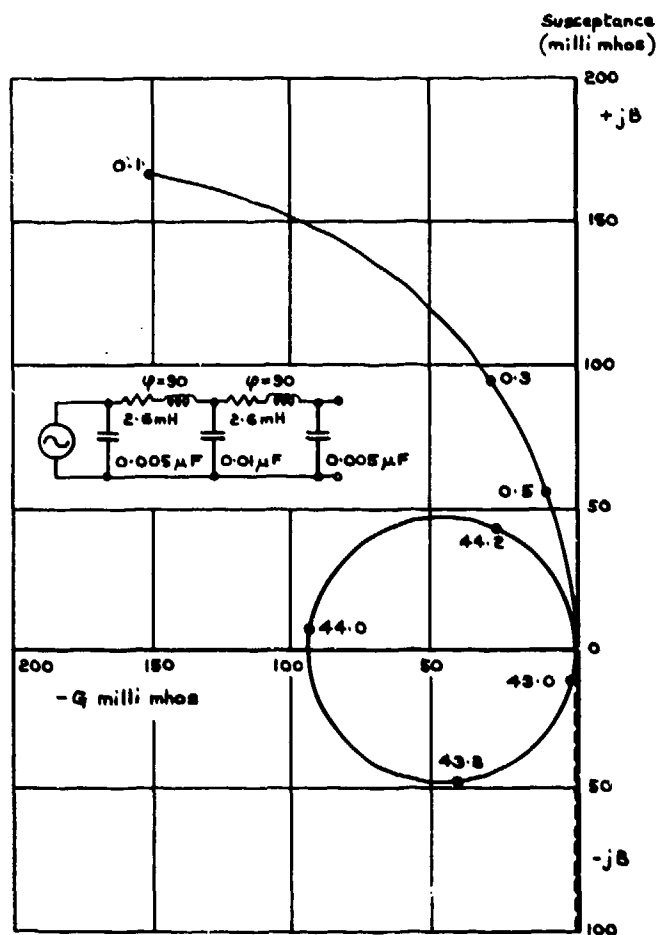


Fig. 8 Locus of circle centres with frequency

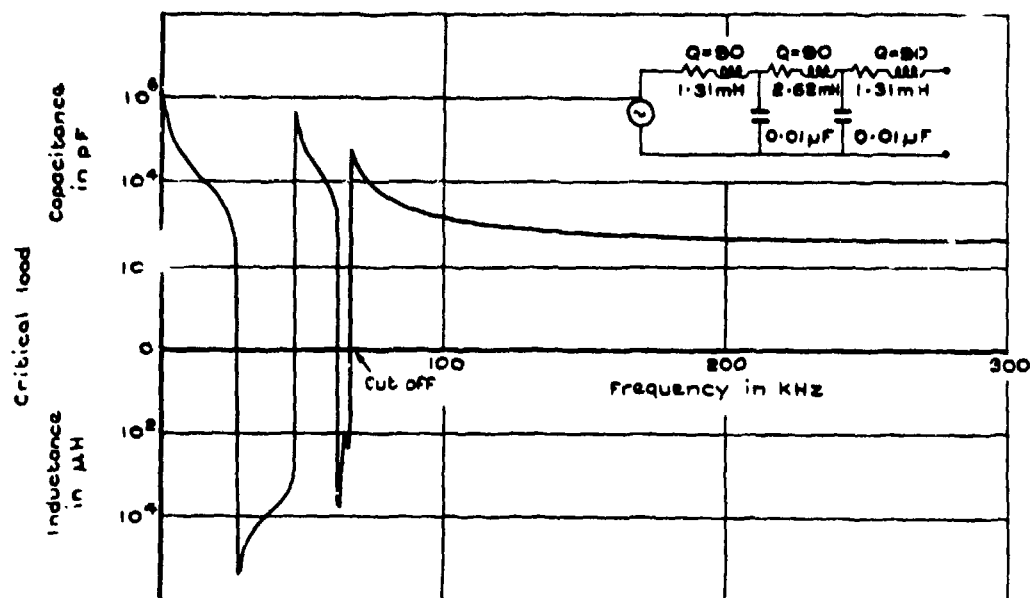
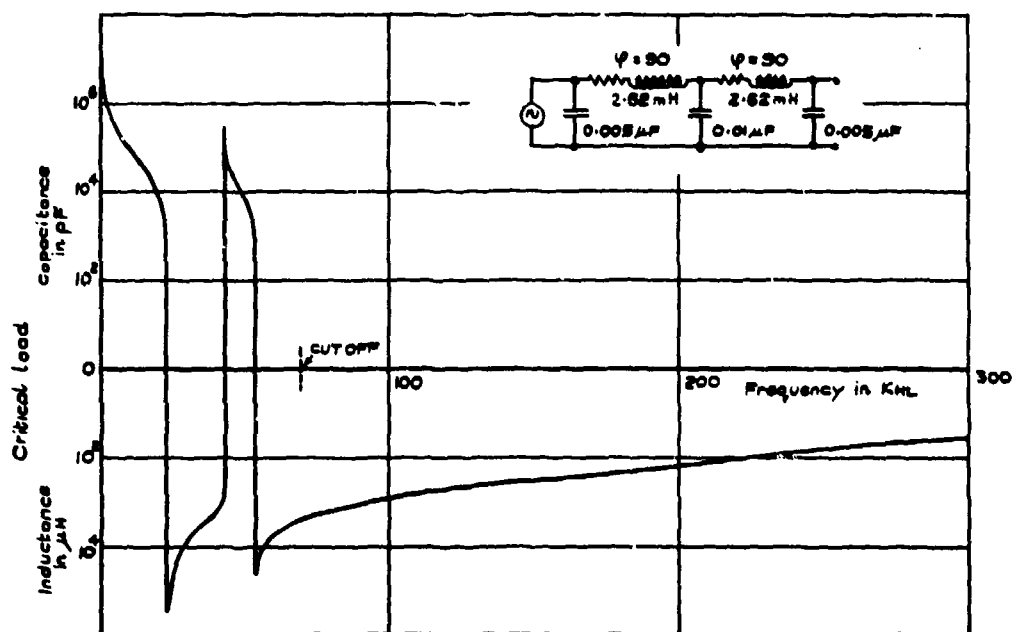


Fig.9 Critical load v frequency for T suppressor

Fig.10 Critical load v frequency for  $\pi$  suppressor

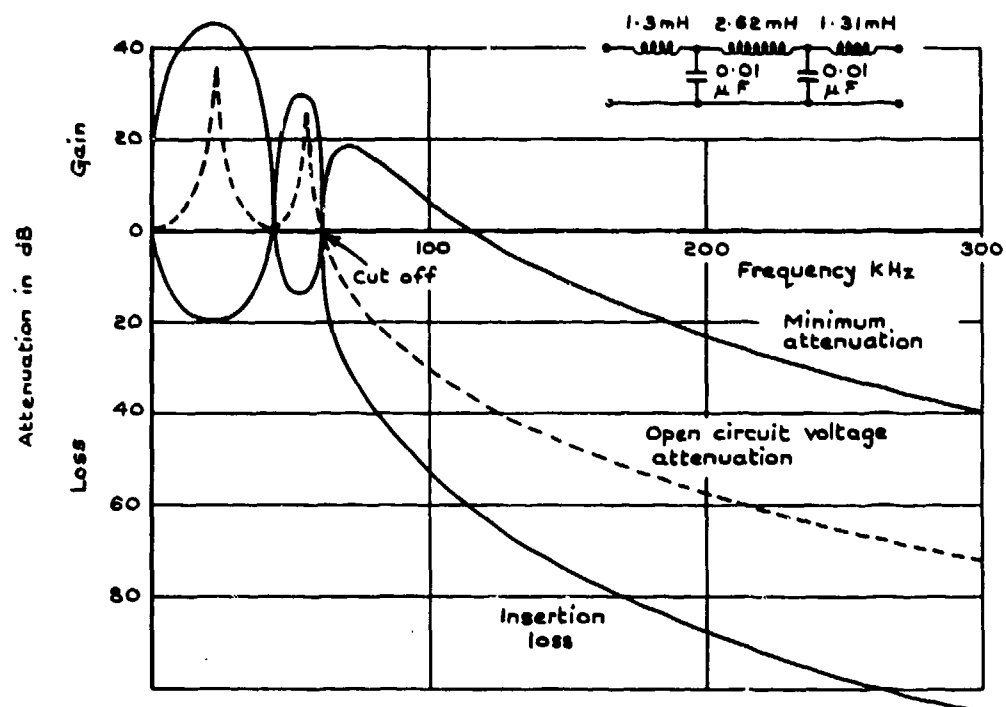


Fig.11 Attenuation v frequency characteristics

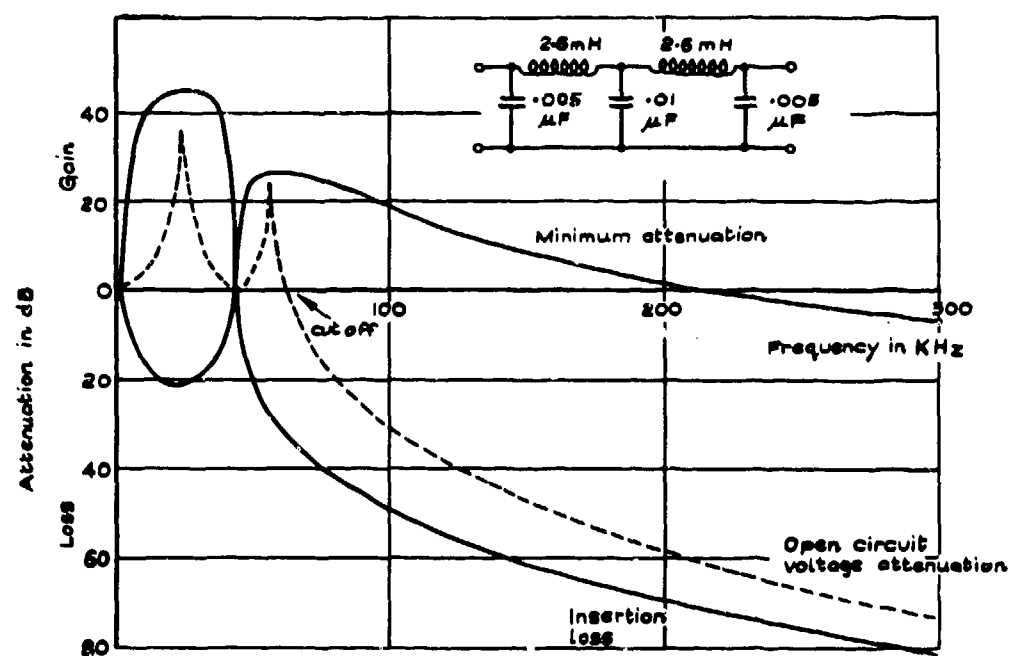


Fig.12 Attenuation v frequency characteristics

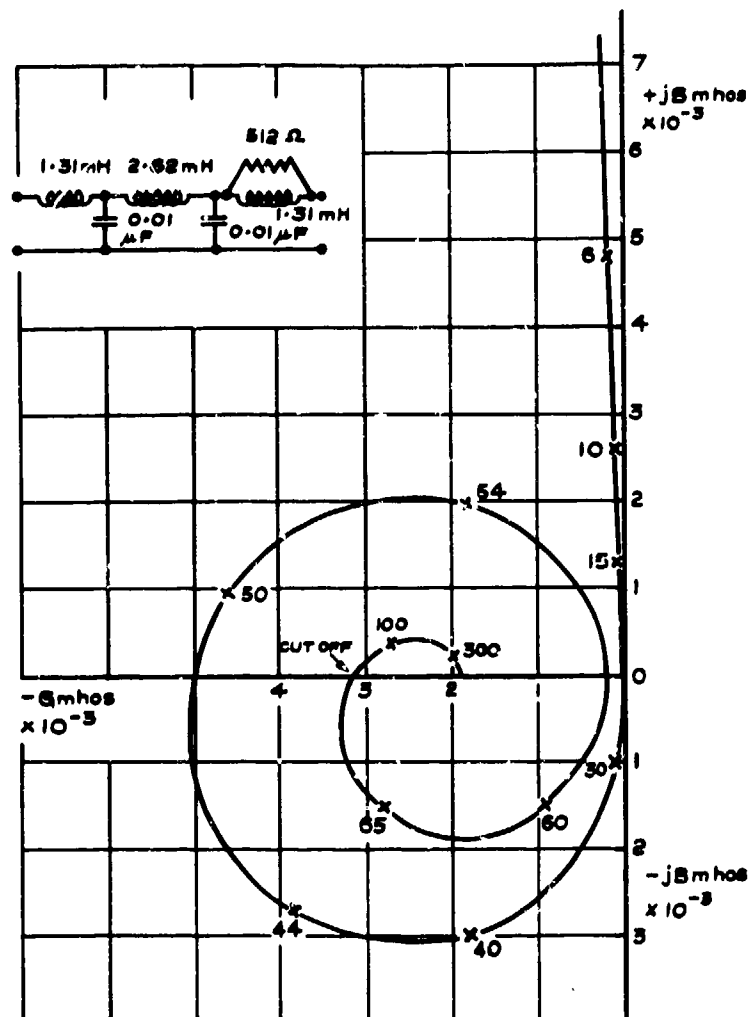


Fig.13 Locus of circle centre against frequency with damping resistor

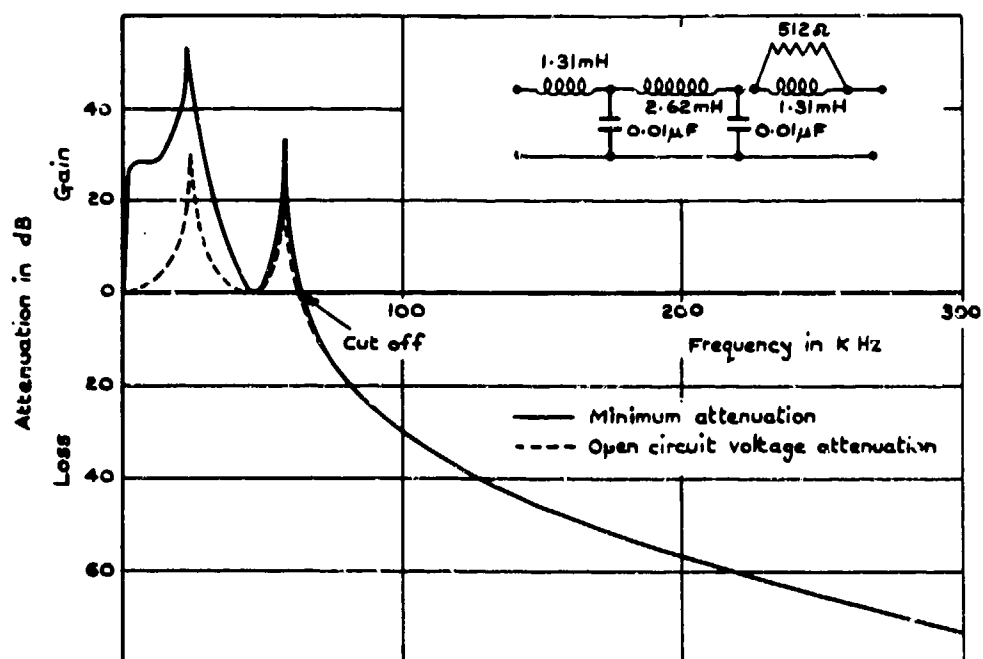


Fig.14 Attenuation v frequency characteristics

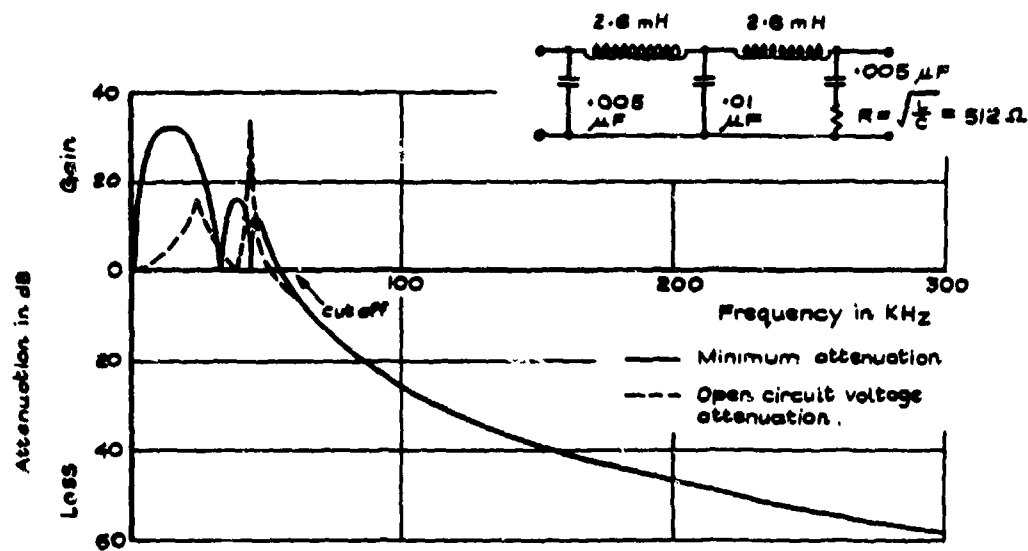


Fig. 15 Attenuation v frequency characteristics

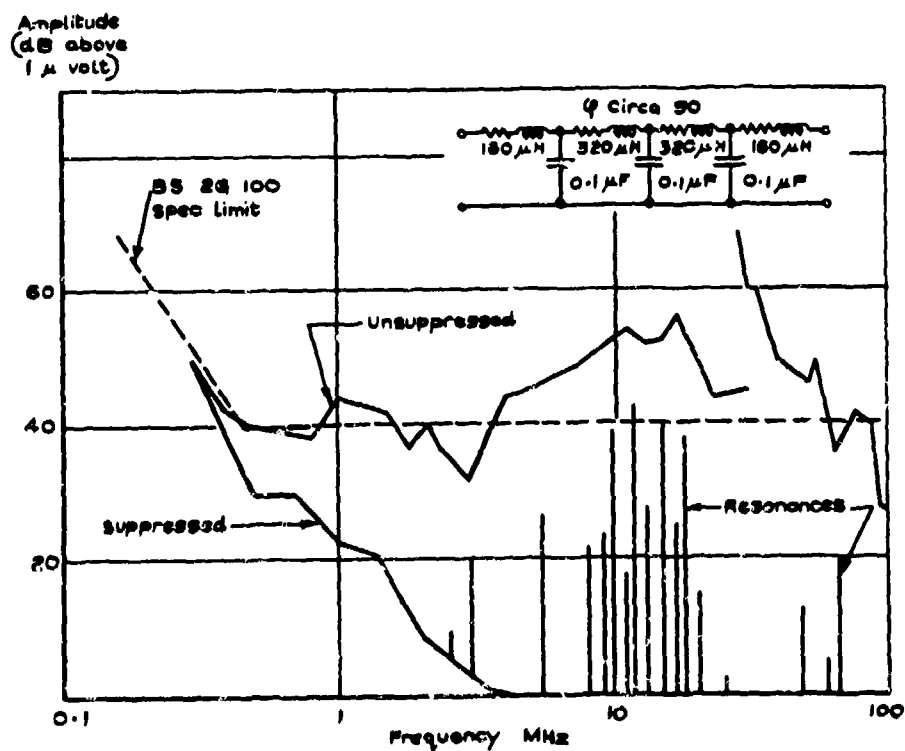


Fig. 16 Cancellation of conventional filter by adverse load.

## DISCUSSION

P. SEVAT: You have measured the insertion loss of your filters as a function of frequency (discrete frequencies). Do you have any experience with impulsive interference? Your contribution can be of great value for CISPR which is struggling with the same problem.

M. L. JARVIS: The attenuation characteristics of the suppressor are valid for broad-band, narrow-band and impulsive interference. If the amplitude/frequency characteristics of impulsive interference such as EMP effects, lightning and load switching transients are known, then the suppression effects through the suppressor can be calculated. Experience has shown that the damage effects of these impulses are reduced, but that audio and visual displays still exhibit a "click" type of disturbance.

## MISSILE INTERSYSTEM EMC TESTING

Charles D. Ponds  
Army Missile Command - AMSMI-RTF  
Redstone Arsenal  
Alabama 35809

36-1

### SUMMARY

The intersystem EMC testing of missiles is described. Systems compatibility to a world wide electromagnetic (EM) environment is demonstrated by the Army Missile Command by using a mini-computer controlled, broad band emitters, a unique data acquisition system, an infrared (IR) data link and a mini-computer data reduction system. Also, redesign information is acquired which will provide EM hardened missiles.

The simulation facility used to provide an EM environment from 100 KHz to 15 GHz is described giving the emitter power output, modulations, sweep capabilities, log periodic and horn antenna, transmission line transverse electromagnetic mode (TEM) test chamber and a mini-computer for close loop control of emitters, power and frequency controller, data acquisition and reduction.

The data acquisition system described is an in-house designed infrared system used to collect signals and transmitted by IR light to the data processor and analyzer. Signals from the monitored circuits are linked to a signal processor, via an IR emitting diode, a 45 meter fiber optic, and signal processing equipment.

#### 1. INTRODUCTION

Our complex communication networks, both military and civilian, can establish some very high energy electromagnetic (EM) fields in which our missile systems must survive in their stock-pile to target sequence. These high level EM fields can: cause systems to falsely program flight information on the launcher; cause premature ignition of propulsion systems during shipping, in storage, on launcher or in flight; and can result in guidance system malfunctioning. (See illustration #1).

The testing described here is geared to research and development requirements to provide adequate design hardening so the missile system will operate reliably and be safe to handle and store in the predicted world wide environment and to meet requirements of Army Regulation (AR) 11-13. The worse case environments for premature ignition (hazards) and system operation (reliability) are different, since shipment of systems is unrestricted, while the operation or actual set-up and firing of systems does have some restrictions. The design criteria for Army missile system EMC testing includes fields designated in volts per meter assuming to be in the far field of the antenna and with an impedance of 377 ohms. The frequency range of interest is 100 KHz to 15 GHz.

Missile intersystem EMC testing is actually identified by two type tests - electromagnetic hazards and electromagnetic effects. In the electromagnetic hazard tests the electro explosive devices (EED's) or squibs are instrumented with miniature thermocouples to sense a heat rise in the bridge wire and voltage detected with a diode from bridge wire pin to the EED case. In the electromagnetic effects tests the control functions of the system are monitored to determine degradation or system reliability.

#### 2. TESTING TECHNIQUES

The most important thing about this type testing, intersystem EMC testing, is that the test item must be configured as much as possible to the actual fielded missile system. All the data collection instrumentation has to be inclosed within the air frame of the missile. This is usually accomplished by using the propellant space since all propellant and warhead material are not used for the test. The signal processing part of data collection instrumentation has to be completely shielded from the environment. This is usually accomplished by packaging in a cylinder with threaded end caps sized to fit the propulsion or warhead section. (See photograph #1 for such a package). Signals from this package are brought out through a fiber optic link to the data processor. No cables are used to link the missile with off board instrumentation or test equipment. (Riley, L.H., 1971).

The test item is positioned with respect to the antenna to give as high field strength as possible and remain in the far field if possible. (See illustration #2). In some cases the design criteria cannot be reached using our broad band generating equipment, thus the test data is extrapolated. The fields are measured prior to setting up the test item. It is also desirable to have the men that fire and/or operate the system in the test loop. The design criteria used on missile system is:

For Electromagnetic Hazards (EMH)

##### A. Average Fields

###### 1. Vertical Polarization

- a. 100 volts per meter (v/m) in frequency range of 100 KHz to 100 MHz.
- b. 200 v/m in frequency range of 100 MHz to 15 GHz.



## 2. Horizontal Polarization

- a. 10 v/m in frequency range of 100 KHz to 10 MHz.
- b. 100 v/m in frequency range of 10 MHz to 100 MHz.
- c. 200 v/m in frequency range of 100 MHz to 15 GHz.

## B. Peak Fields

### 1. Vertical Polarization

- a. 200 v/m in frequency range of 100 KHz to 100 MHz.
- b. 40,000 v/m in frequency range of 100 MHz to 15 GHz.

### 2. Horizontal Polarization

- a. 20 v/m in frequency range of 100 KHz to 100 MHz.
- b. 40,000 v/m in frequency range of 100 MHz to 15 GHz.

## For Electromagnetic Effects (EME)

### A. Prelaunch and Flight

Communication equipment with continuous wave (CW) and amplitude modulation (AM), for both horizontal and vertical polarizations:

- 1. 25 v/m average or CW and 50 v/m peak envelop field strength in frequency range of 100 KHz to 2 MHz.
- 2. 50 v/m average or CW and 100 v/m peak envelop field strength in frequency range of 2 MHz to 100 MHz.
- 3. 25 v/m average or CW and 50 v/m peak envelop field strength in frequency range of 100 MHz to 500 MHz.
- 4. 50 v/m average or CW and 100 v/m peak envelop field strength in frequency range of 500 MHz to 1000 MHz.

Modulations applicable to the above are:

- a. Frequency Modulation (FM) in the frequency range of 20 MHz to 100 MHz to include:
  - (1) 400 Hz
  - (2) 1000 Hz
  - (3) All system operational frequencies.
- b. AM in the frequency range of 100 KHz to 1000 MHz to include:
  - (1) 400 Hz
  - (2) 1000 Hz
  - (3) All system operational frequencies.

### B. Prelaunch

Radar emitters using pulse modulation, for both horizontal and vertical polarizations:

- 1. 50 v/m average and 10,000 v/m peak in the frequency range of 400 MHz to 1200 MHz.
- 2. 200 v/m average and 40,000 v/m peak in the frequency range of 1200 MHz to 15 GHz.

### C. Flight only - Radar emitters using pulse modulation

- 1. 50 v/m average and 10,000 v/m peak in the frequency range of 400 MHz to 1200 MHz.
- 2. 300 v/m average and 60,000 v/m peak in the frequency range of 1200 MHz to 15 GHz.

Test planning is a very important part of the test program. Theoretical analysis of the system is required for the selection of the circuits and the configuration to be tested since it is virtually impossible to monitor all circuits and test to every sequence that missiles go through. Also, frequency modulations affecting fail and safe circuit criteria have to be determined for the pre-test analysis and planning. Typically antenna analysis is used to take a quick look, or if a thorough analysis is required we use a digital computer program, transmission-line analysis. (GTE Sylvania, 1971).

In order to conserve testing time and to prevent problems in obtaining frequency clearances at high power levels the missile system is setup for test and then the frequency spectrum for the generating equipment for the test area is swept through at low level fields, one to two volts per meter, to determine resonance or peak responses of the monitored circuits and then at these resonances, thresholds are determined. If possible, thresholds are determined in far field or where (electric field/magnetic field) E/H is 377 ohms. Where thresholds can not be obtained due to limitations of the facility, extrapolations are made based on the minimum sensitivity of the instrumentation. During the low level sweep probing tests the worse case or critical responses to modulation frequencies, missile orientation and field orientation and field polarizations are selected.

A typical R&D EMC test planning and testing of a missile takes the following sequence of events:

1. A missile system project office prepares a scope of work and furnishes funds to our laboratory for the EMC tests.
2. A test planning meeting held with representatives from the project office, system contractor, warhead and fuze agency, and Test and Evaluation Command. This meeting makes sure that everyone's test requirements are included in the test plan. Also, that support in conducting the tests are supplied by the applicable groups.
3. A test plan is written. During this period a theoretical analysis is performed for inputs to the test plan and instrumentation.
4. An instrumentation package is designed and fabricated.
5. Test plan is coordinated with applicable groups.
6. System assembled and checked out with instrumentation. This step requires that the system is operational without the environment, also, that the instrumentation is not a source of EM pickup.
7. Exploratory tests - These tests are required to determine critical frequency bands and modulations for indepth testing.
8. Indepth testing to determine thresholds.
9. Data analysis to determine system problem.
10. Design review to determine fixes required.
11. Implement design fixes.
12. Retest to determine effectiveness of design fixes.
13. Prepare test report.

### 3. TESTING EQUIPMENT

Electromagnetic compatibility testing is accomplished using a broad band, high power sweep generating system employing a unique arrangement of antennas and a fully automated electronic control and data acquisition unit. The frequency range covered is 100 KHz to 15 GHz at output powers up to 5 KW average power.

The lower frequencies, 100 KHz to 500 MHz, are generated by a variable inductance cavity tuned signal amplifying system. This system is capable of sweeping bands of frequencies when transmitting in the continuous wave mode and some modulations. The transmitter is capable of keyed CW, amplitude modulation, frequency modulation MHz and 2.5 KW from 350 MHz to 500 MHz. (See photograph #2).

Test frequencies from 500 MHz to 15 GHz are produced by amplifier driven broad band high power traveling wave tube transmitter. This unit is capable of sweeping in bands at an output power of 1.5 KW. (See photograph #2).

Power is radiated through a series of antennas starting at the low frequencies, 100 KHz to 30 MHz, with a broad band high field intensity array of elemental horns, sometimes referred to as a Transverse Electric Mode (TEM) wave guide chamber. (See photograph #3). This unique array is capable of launching a plane wave from one end of a 10 X 10 X 10 meter chamber, radiating a test object and collecting the energy at the other end of the chamber to be dissipated as heat thru resistors.

A log periodic antenna is used in the 30 MHz to 350 MHz region (see photograph #4) and standard gain horn antennas up to 15 GHz.

The IBM System/7 computing system is used and designed to acquire physical data such as voltages, current, temperature, pressure and other measurements directly from transducers. (See photograph #5).

The System/7, because of its modular design, can handle the far ranging variety of instrumentation signals generated by modern missile systems.

Each module is multifunctional in that it can provide input of 128 discrete binary data channels as well as 64 channels of digital output. Two channels of analog output are provided with 32 channels of analog input data, which can be read at a rate of 20,000 samples per second.

The System/7 has up to 64,000 words of monolithic storage and a processor that is faster than either the IBM 360 or the IBM 370. Additional storage is provided by a one fixed and one removable disk cartridge which can store 2,576,000 words.

The System/7 serves EMC testing in four capacities: (1) control of RF transmitters, (2) power and frequency controller for Federal Communication Commission (FCC) limitations (3) data acquisition and (4) data reduction.

The EM power transmitters used are capable of sweeping frequency as well as power as previously mentioned. It is very desirable to maintain a constant and known E-field at the test item location as the frequency of the transmitter is being swept. The System/7 has in memory for all transmittable frequencies, a three dimension E-field map. The E-field map is used by the computer to control the EM power of the transmitter to produce a constant E-field strength at the location of the test item.

Once the transmitter has been made operative and the desired frequency band selected the System/7 will take over all operator functions. The System/7 has two other type of transmitter controls: (1) fixed frequency and fixed E-field and (2) fixed frequency and swept E-field. No other known test facility has this capability of sweeping frequency while maintaining a constant E-field.

The EM transmitters have the power and frequency range to cause local and regional EM interference. FCC requires that some frequencies not to be transmitted on and others at reduced power. The System/7 detects these frequencies and reduces the transmitter power to meet the FCC requirements.

The System/7 has three levels of programming: (1) assembly language (2) MSP/7 (3) Fortran IV, all of which can be assembled or compiled on the System/7 as a stand-a-lone system. The three methods of programming can be prepared on the IBM 1130, 1800, 360 or 370 computers if desired.

This flexibility gives the programmer ease in creating new or modifying existing computer programs to meet the need of new and complex missile systems electromagnetic compatibility testing.

#### 4. DATA COLLECTION, REDUCTION AND ANALYSIS

In missile intersystem EMC testing it is highly desirable to monitor test results continuously during testing. The System/7 controlled data collection system allows this. The EM environment can then be adjusted to provide optimum test data. This is a closed loop test in that test results can control the primary test variable which is the EM field intensity.

One major problem in this type testing is the transfer of data from the missile during testing without causing unrealistic condition or system degradation. An infrared data link system was developed in-house in the 1964-66 era. It was first used on Army missile systems tests in 1966 and this was the first known such used for EMC testing. (See illustration #3 for a typical EED monitoring system.) (Riley, L.H., 1971) (Muro, R.B., 1973).

Most of the missile system measurement points are not accessible for calibration after assembly of the system. It is necessary that instrumentation be temperature and age stable. Analog data is converted to time base modulation data or frequency modulated (FM) for transmission so that variations in data path length do not affect the data. This stable FM data acquisition system is calibrated in the laboratory for field use.

The data acquisition system provides sensitive instrumentation to measure low field intensity effects so the data can be extrapolated into qualification levels.

The temperature monitoring system is designed for use with thermocouples rise times as low as 250 microseconds. The system used to monitor control function is designed to monitor rise times as low as 5 microseconds.

The test item is not changed by the instrumentation. The instrumentation package is designed small enough to fit inside the missile system without affecting the missile electronics.

A low level voltage controlled oscillator system used in conjunction with a Gallium Arsenide light transmitter is used to handle the data inside the missile. The data is conveyed 45 meters to light reception, discrimination and data processing equipment by fiber optics.

The data can be processed with System/7 recorded simultaneously with a direct write strip chart and tape recorder.

Less than 10% time capacity of System/7 is needed for the control functions of the transmitter. The remaining computer time is used for data acquisition from the test item. Each channel of data, analog or digital, is read into the computer then stored on disk for data reduction at a later date.

At the end of a test run the data for each channel can be displayed on a x, y graph giving a frequency verse channel data plot. Multiple plots can be made on one graph giving a clear relationship between channels of data. Additional graphics cathode-ray tube (CRT) display terminal with hard copies can produce report quality graphs in less than 30 sec. which is 1000 times faster than previous methods.

Data taken from these electromagnetic compatibility tests are analyzed to determine coupling and leakage points, and circuit component degradation in the system. From this test analysis, design is reviewed and a determination is made on the type fixes to be incorporated into the system.

## 5. COST IMPACT

Test cost varies with missile size and complexity. A land combat antitank missile with approximately 10 data channels can be tested thru the target to stock pile sequence for \$150K actual testing cost plus a system of hardware. The time required is approximately 4 months. A complex air defense system with a radar guidance system and approximately 50 channels of instrumentation can be tested thru the target to stock pile sequence for \$350K plus a complete system of hardware. The time required for the test would be approximately 10 months.

Tests described would be for a missile system in the research and development cycle. To develop fixes and retrofit systems it would cost 2 to 5 million dollars depending upon the complexity of the fixes and the systems deployed. If conducted in research and development cycle and incorporated in the design the total cost of EMC hardening of the system would be .5 to 1 million dollars.

## 6. GENERAL INFORMATION

### 6.1 References

a. Riley, L.H., 1971, "Infrared Data Link For Electromagnetic Effects Testing", Institute of Electrical and Electronic Engineers (IEEE), Groups on Aerospace Electronic Systems and Communications Technology, Boston, Mass.

b. GTE Sylvania Incorporated, Communication Systems Division, 1971, Final Report, "Digital Computer Program For EMR Effects on Electronic Systems", GTE Sylvania.

c. Rubin, R.B., 1973, "Electromagnetic Radiation-Electronic Circuit Interactions", University of Texas at El Paso, Texas.

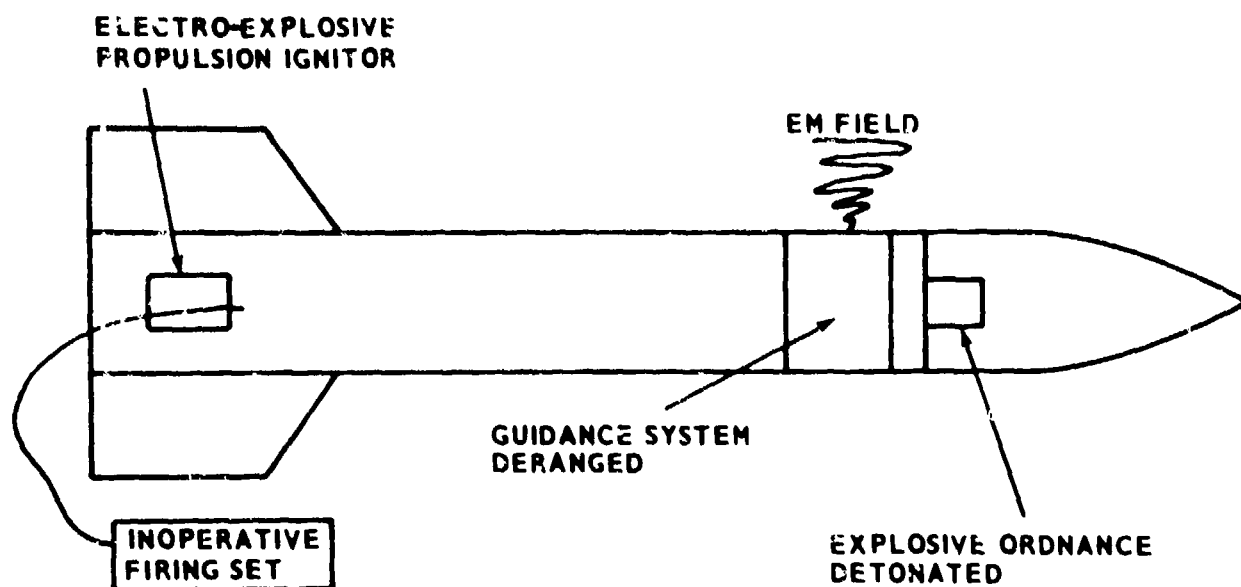


Illustration #1 - Problems of EMC



Photograph #1 - Typical Instrumentation Package

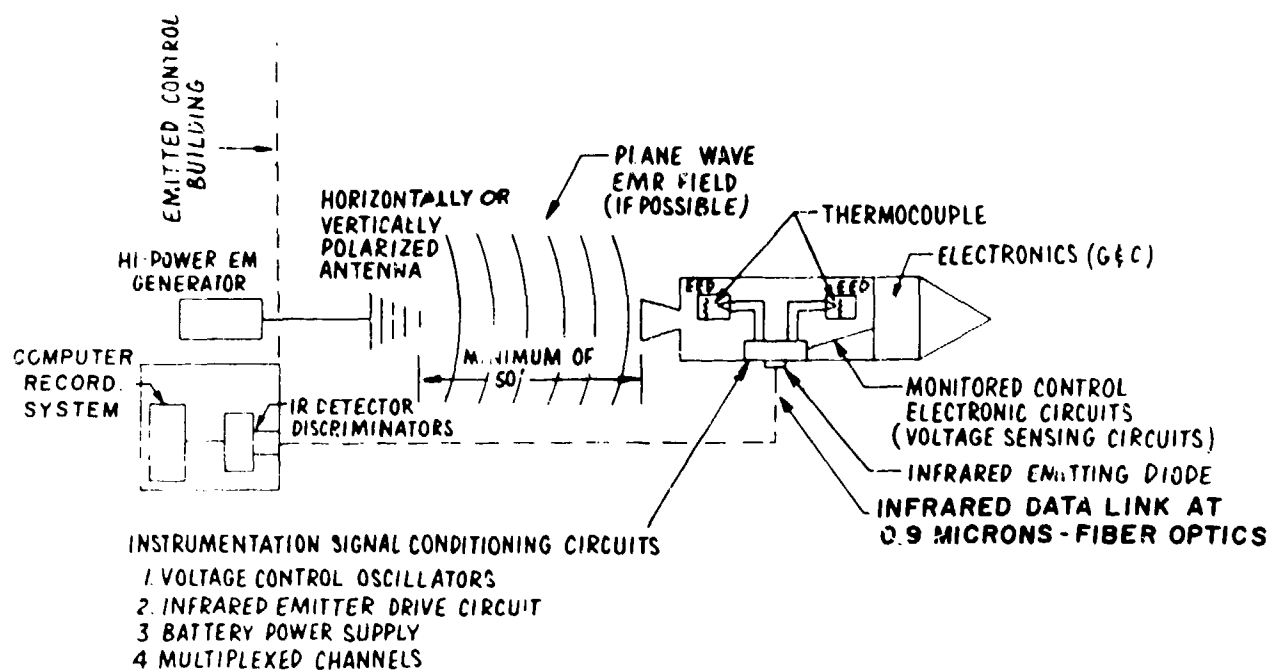
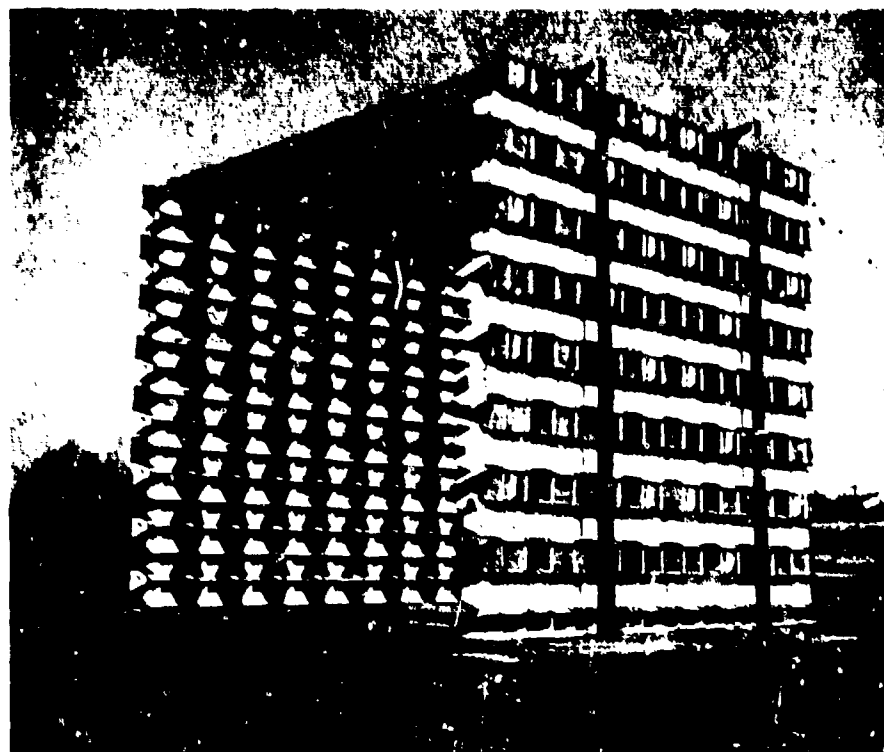


Illustration #2 - Typical Intersystem EMC Test Set-Up

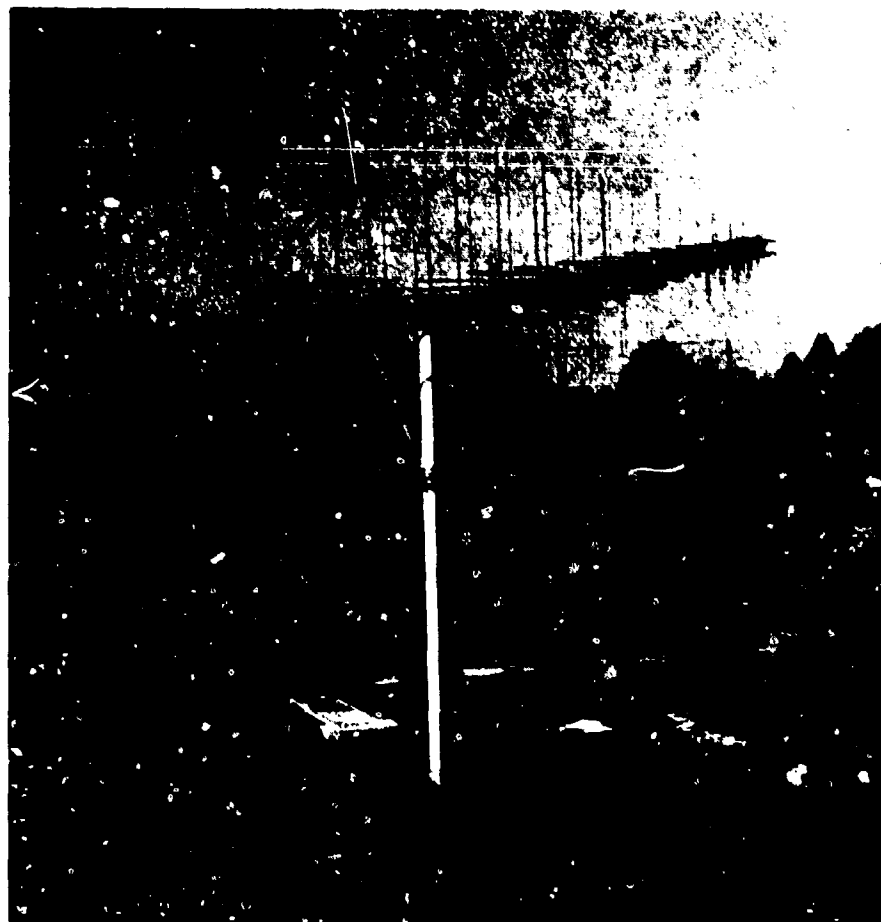


Photograph #2 - Signal Generating Equipment (Transmitters)

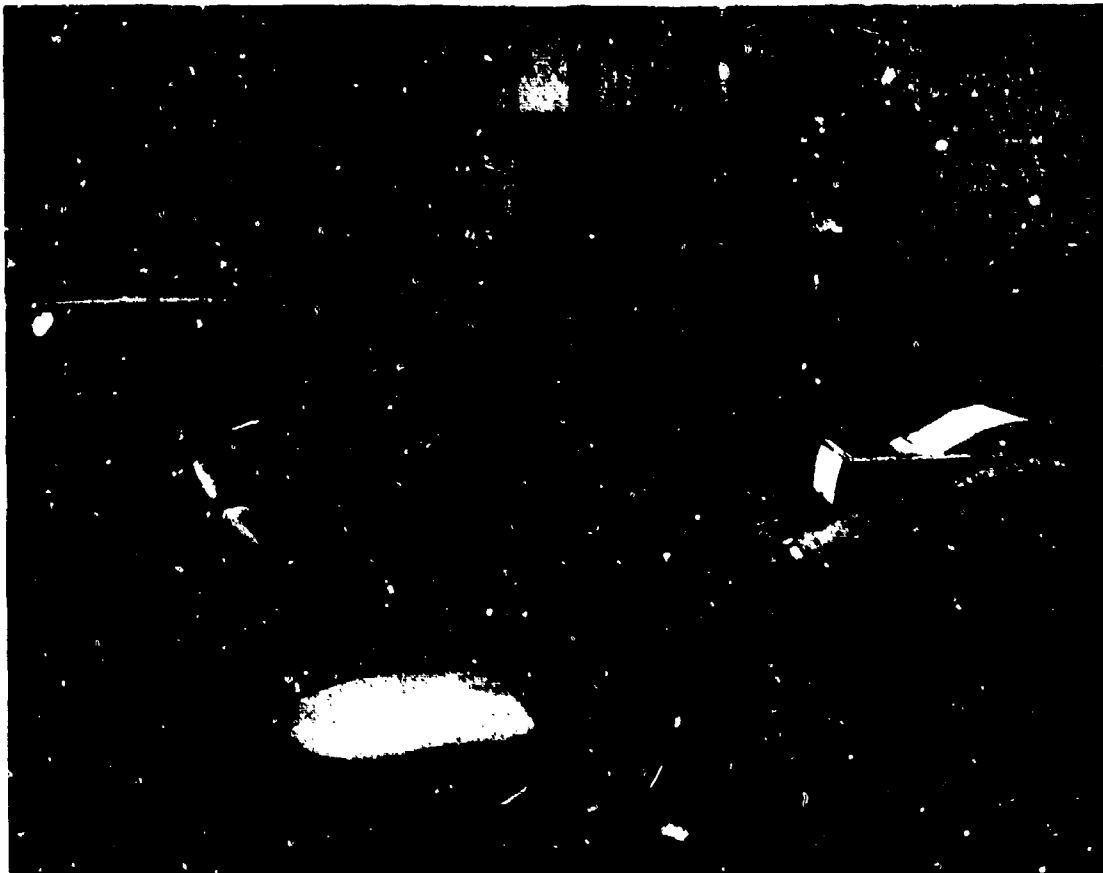
36-8



Photograph #3 - Transverse Electric Mode Wave Guide Chamber (100 KHz to 30 MHz)



Photograph #4 - Log-Periodic Antenna (30 MHz to 350 MHz)



Photograph #5 - IBM System/7 Computer/Controller

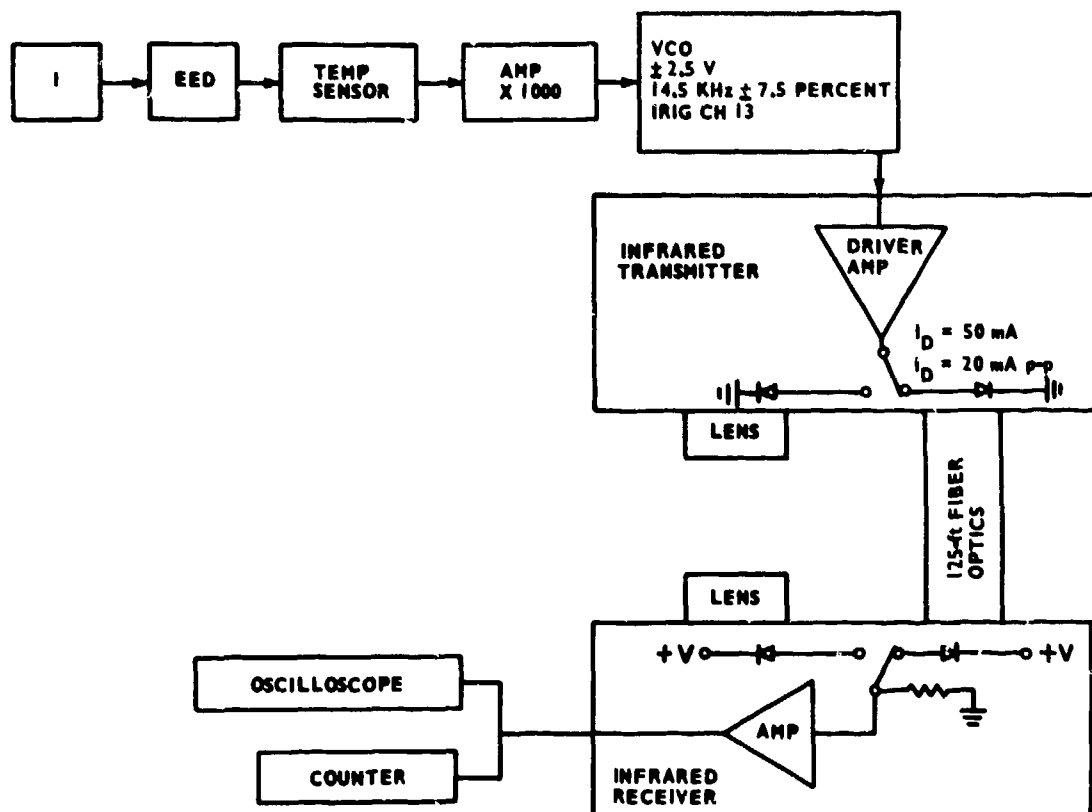


Illustration #3 - Infrared Data Link



## DISCUSSION

E. M. FROST: To what extent do you involve the designers of the tested equipment in the actual tests?

C. D. PONDS: The system contractor's design and EMC engineers are a part of the test plan and conduction by the requirements of the contract.

G. TREVASKIS: With respect to the generation of the very high power levels at frequencies within the GHz range, using "traveling wave tubes", are there any problems with the harmonics generated and is any filtering used on the output to remove this type of distortion?

C. D. PONDS: Yes, if we drive the TWT above saturation. The 1.5kw cw is the operation below saturation. At present, we have no filter in the system to operate in the saturation area.

P. SEVAT: You are testing your systems at very high frequencies with peak voltages as high as 40,000v/m. How do you transmit your system responses from your system to the computer record system by an infrared data link with a bandwidth you mentioned?

C. D. PONDS: With our present system, we cannot reach 40,000v/m peak field. We either extrapolate from lower fields, or do further work on the bench. We use the infrared data link as described. The 40,000v/m peak fields are only a carrier for the modulations we do, not the very high frequency responses.

O. HARTAL: 1) How do you ascertain that the measurement wires inside the system do not pick up more energy than the system wires? 2) When testing EEDs, you measure temperature. A bridge wire is covered by primary explosive with temperature characteristics different from those of air. If removed, the wire will achieve a lower temperature due to conduction and radiation to the environment. Do you take account of this factor, and how? 3) How do you measure the 20db EMC margin required in 6051 for EEDs? 4) How do you make sure the EED does not pick up and radiate EM energy into the thermocouple and this is picked up as a legitimate signal?

C. D. PONDS: 1) By using a no-operational system in the environment to check for energy pickup of the instrumentation wiring. 2) We do remove the primary explosive and it does affect the temperature pickup of the thermocouple. We really do not account for this, except we do RF Brusten test to determine RF current differences. 3) We account for the 20db safety factor by extrapolations of the threshold results by 20db to see if it still comes within the test criteria. 4) We measure on the bench using RF sensitive instrumentation. Also, the system can be tested by starting at very low field levels and then go to higher levels in steps. The results should be a straight-line response. If not, there is an instrumentation coupling problem.

## MEASUREMENT OF INTERWIRING

Coupled Noise

B. Audone and L. Bolla  
AERITALIA GRUPPO S.A.S.  
Torino - Italy -

SUMMARY

One of the major problems arising in the electromagnetic compatibility analysis of a complex system such as an airplane is the wiring interconnecting the equipments. A large amount of interference is picked-up among cables in the same loom when, due to limited available space, emitting and sensitive wires are not sufficiently separated.

The prediction of wiring coupled effects is not an easy task because of the many parameters involved related both to the geometrical configuration of the cable loom and to the electrical loads of the inter-connected circuits. On the other hand the measurement of wiring emission and susceptibility is not covered sufficiently in the present EMC specifications. While conducted emission and susceptibility problems are considered rather deeply, wiring radiated emission and susceptibility effects are scarcely evaluated.

A test method to measure the coupling interference and susceptibility in different load configurations (open or short circuit) is proposed with the advantage of having a realistic simulation of the wiring coupling mechanism and valid guidelines for a better cable separation philosophy.

## 1. INTRODUCTION

In MIL-STD-461/462 the radiated emission from cables is measured by means of test method RE01 (Magnetic field 30 Hz to 30 KHz) and test method RE02 (Electric field 14 KHz to 10 GHz). In RE01 test it is stated that a loop antenna shall be positioned at a distance of 7 cm between the center of the loop and the cable. The plane of the loop and the cable shall coincide. In this case one is measuring the magnetic field emitted by the current instead of the cable radiated emission which should mainly take into account the cable length. The actual purpose of this test seems to consist in the control of the interaction between the cable under test and a unit situated close to it. In RE02 test the situation is even worse because the measuring antenna is positioned at a distance of 1 metre from the test sample. No clear indications about the actual wiring layout are given in the test description. When this test is carried out, it is never clear which is the source of the radiated interference: the test sample or the wiring. In general, most of emitted noise is produced by the wiring and only a minimum part is generated by the test sample. The problem of defining the source of radiated interference is quite important because, in some cases, it may have influence in establishing whose responsibility it is to reduce the level of emitted noise within EMC specification limits. If, in fact, it depends on the unit under test the responsibility lies with the supplier, if it depends on the wiring the responsibility lies with who defined the equipment interfaces. In conclusion it appears that RE01 and RE02 tests are not adequate to measure the interwiring coupled noise mainly because they are based on the unrealistic assumption that the coupling happens between the wiring and the measuring antenna.

The same criticism is applicable to radiated susceptibility tests. In MIL-STD-461/462 RS01 test (Radiated Susceptibility 30 Hz to 30 KHz Magnetic Field) and RS03 test (Radiated Susceptibility 14 KHz to 10 GHz Electric Field) are again an unrealistic representation of the wiring coupling mechanism while RS02 test (Radiated Susceptibility magnetic induction field) even if more realistic only examines the particular case of the magnetic induction fields of power frequency and spike signals.

## 2. MATHEMATICAL ANALYSIS OF THE TEST METHOD

The equivalent circuit of coupled lines for a length  $\Delta x$  is shown in Fig. 1. Applying the network equations and the matrix theory it follows

$$\begin{aligned} \frac{d\bar{V}}{dx} &= -\bar{Z}\bar{I} \\ \frac{d\bar{I}}{dx} &= -\bar{Y}\bar{V} \end{aligned} \quad (1)$$

where

$$\bar{Z} = \begin{bmatrix} L_{11} & L_{12} \\ L_{21} & L_{22} \end{bmatrix}$$

$$L_{11} = L_1$$

$$L_{22} = L_2$$

$$L_{12} = L_c = L_{21}$$

$$\bar{Y} = \begin{bmatrix} C_{11} & C_{12} \\ C_{21} & C_{22} \end{bmatrix}$$

(2)

$$C_{11} = C_1 + C_c$$

$$C_{22} = C_2 + C_c$$

$$C_{12} = -C_c = C_{21}$$

Equations (1) can be written as

$$\frac{d\bar{P}}{dx} = -\bar{A}\bar{P} \quad (3)$$

where

$$\bar{P} = \begin{bmatrix} V_1 \\ V_2 \\ I_1 \\ I_2 \end{bmatrix} = \begin{bmatrix} \bar{V} \\ \bar{I} \end{bmatrix}$$

$$\bar{A} = \begin{bmatrix} \bar{O} & \bar{Z} \\ \bar{Y} & \bar{O} \end{bmatrix}$$

From the relationship

$$\bar{A}\bar{R} = \bar{R}\bar{\Lambda} \quad (4)$$

where

$$\bar{R} = \begin{bmatrix} \bar{R}_1 & \bar{R}_2 \\ \bar{R}_3 & \bar{R}_4 \end{bmatrix}$$

$$\bar{\Lambda} = \begin{bmatrix} \bar{\Lambda}_1 & \bar{O} \\ \bar{O} & \bar{\Lambda}_2 \end{bmatrix}$$

by some calculations it follows

$$\bar{Z}\bar{Y}\bar{R}_1 = \bar{R}_1\bar{\Lambda}_1^{-1}$$

$$\bar{R}_1 = \bar{R}_2$$

$$\bar{Y}\bar{Z}\bar{R}_3 = \bar{R}_3\bar{\Lambda}_2$$

$$\bar{R}_3 = -\bar{R}_4$$

$$\bar{R}_3 = \bar{Y}\bar{R}_1\bar{\Lambda}_1^{-1}$$

$$\bar{\Lambda}_1 = -\bar{\Lambda}_2$$

It will be useful to use the following notations

$$K_1 = \sqrt{\frac{L_{11}}{C_{11}}}$$

$$K_2 = \sqrt{\frac{L_{22}}{C_{22}}}$$

$$\gamma_1 = \sqrt{L_{11}C_{11}}$$

$$\gamma_2 = \sqrt{L_{22}C_{22}}$$

$$0 < M_L = \frac{L_{12}}{\sqrt{L_{11}L_{22}}} < 1$$

$$0 < M_C = \frac{-C_{12}}{\sqrt{C_{11}C_{22}}} < 1$$

(6)

Substituting (6) into (2)

$$\bar{Z} = \begin{bmatrix} \gamma_1 K_1 & M_L \sqrt{\gamma_1 \gamma_2 K_1 K_2} \\ M_L \sqrt{\gamma_1 \gamma_2 K_1 K_2} & \gamma_2 K_2 \end{bmatrix}$$

$$\bar{Y} = \begin{bmatrix} \frac{\gamma_2}{K_2} & -M_C \sqrt{\frac{\gamma_1 \gamma_2}{K_1 K_2}} \\ -M_C \sqrt{\frac{\gamma_1 \gamma_2}{K_1 K_2}} & \frac{\gamma_1}{K_1} \end{bmatrix}$$

Only the case  $\gamma_1 = \gamma_2$  will be examined

$$\bar{Z} \bar{Y} = \gamma^2 \begin{bmatrix} \gamma^2 (1 - M_c M_L) & \gamma^2 \sqrt{\frac{K_1}{K_2}} (M_L - M_c) \\ \gamma^2 \sqrt{\frac{K_2}{K_1}} (M_L - M_c) & \gamma^2 (1 - M_c M_L) \end{bmatrix} \quad (7)$$

Denoting

$$\begin{aligned} m_1^2 &= \gamma^2 \lambda_1^2 \\ m_2^2 &= \gamma^2 \lambda_2^2 \end{aligned} \quad (8)$$

the eigenvalues of  $\bar{Z} \bar{Y}$  it follows from (7)

$$m_1 = \gamma - \gamma \beta$$

$$m_2 = \gamma + \gamma \beta$$

where  $\beta = \frac{M_c - M_L}{2}$

Because  $\bar{\lambda}_1 = -\bar{\lambda}_2$  the eigenvalues of A are completely known.

Now the eigenvectors shall be calculated from the equation

$$[\bar{Z} \bar{Y} - m^2 \bar{I}] \begin{bmatrix} l_1 \\ l_2 \end{bmatrix} = 0 \quad (9)$$

where  $\begin{bmatrix} l_1 \\ l_2 \end{bmatrix}$  is the eigenvector of  $\bar{Z} \bar{Y}$

Remembering that

$$(\bar{Z} \bar{Y})' = \bar{Y} \bar{Z} \quad (10)$$

after long and tedious calculations the matrix R is completely determined as

$$\bar{R} = \begin{bmatrix} \sqrt{Z_{e1}} & \sqrt{\frac{K_1}{K_2}} \sqrt{Z_{o2}} & \sqrt{Z_{e2}} & \sqrt{\frac{K_1}{K_2}} \sqrt{Z_{o2}} \\ \sqrt{\frac{K_2}{K_1}} \sqrt{Z_{e1}} & -\sqrt{Z_{o2}} & \sqrt{\frac{K_2}{K_1}} \sqrt{Z_{e1}} & -\sqrt{Z_{o2}} \\ \frac{1}{\sqrt{Z_{e1}}} & \frac{1}{\sqrt{Z_{o2}}} \sqrt{\frac{K_2}{K_1}} & -\frac{1}{\sqrt{Z_{e1}}} & -\frac{1}{\sqrt{Z_{o2}}} \sqrt{\frac{K_2}{K_1}} \\ \frac{1}{\sqrt{Z_{e1}}} \sqrt{\frac{K_1}{K_2}} & -\frac{1}{\sqrt{Z_{o2}}} & -\frac{1}{\sqrt{Z_{e1}}} \sqrt{\frac{K_1}{K_2}} & \frac{1}{\sqrt{Z_{o2}}} \end{bmatrix} \quad (11)$$

where

$$Z_{e1} = K_1 \sqrt{\frac{1 + M_L}{1 - M_c}} \quad Z_{o1} = K_1 \sqrt{\frac{1 - M_L}{1 + M_c}} \quad (12)$$

$$Z_{o1} = K_1 \sqrt{\frac{1 - M_c}{1 + M_c}}$$

$$Z_{o2} = K_2 \sqrt{\frac{1 + M_c}{1 - M_c}}$$

If

$$Z_{e1} \cong Z_{o1} \cong K_1$$

$$Z_{e2} \cong Z_{o2} \cong K_2$$

$$\bar{R} = \begin{bmatrix} \sqrt{Z_{e1}} & \sqrt{Z_{e1}} & \sqrt{Z_{e1}} & \sqrt{Z_{e1}} \\ \sqrt{Z_{e2}} & -\sqrt{Z_{e2}} & \sqrt{Z_{e2}} & -\sqrt{Z_{e2}} \\ \frac{1}{\sqrt{Z_{e1}}} & \frac{1}{\sqrt{Z_{e1}}} & -\frac{1}{\sqrt{Z_{e1}}} & -\frac{1}{\sqrt{Z_{e1}}} \\ \frac{1}{\sqrt{Z_{e2}}} & -\frac{1}{\sqrt{Z_{e2}}} & -\frac{1}{\sqrt{Z_{e2}}} & \frac{1}{\sqrt{Z_{e2}}} \end{bmatrix} \quad (13)$$

From (3) substituting  $\bar{P} = \bar{R}\bar{S}$  it follows

$$\frac{d\bar{S}}{dx} = -\bar{R}^{-1}\bar{A}\bar{R}\bar{S}$$

$$\frac{d\bar{S}}{dx} = -\bar{\Lambda}\bar{S} = -\begin{bmatrix} \lambda_1 & & & \\ & \lambda_2 & & \\ & & -\lambda_1 & \\ & & & -\lambda_2 \end{bmatrix} \bar{S} \quad (14)$$

From (14)

$$\bar{S} = \begin{bmatrix} s_1 \\ s_2 \\ s_3 \\ s_4 \end{bmatrix} = \begin{bmatrix} B e^{-\lambda_1 x} \\ H e^{-\lambda_2 x} \\ D e^{\lambda_1 x} \\ C e^{\lambda_2 x} \end{bmatrix}$$

the matrix  $\bar{P}$  is completely known. Therefore the following equations are obtained:

$$\begin{aligned} V_1 &= \sqrt{Z_{e1}} \left[ e^{\gamma \beta x} (B e^{-\gamma x} + C e^{\gamma x}) + e^{-\gamma \beta x} (A e^{-\gamma x} + D e^{\gamma x}) \right] \\ V_2 &= \sqrt{Z_{e2}} \left[ e^{\gamma \beta x} (B e^{-\gamma x} - C e^{\gamma x}) - e^{-\gamma \beta x} (A e^{-\gamma x} - D e^{\gamma x}) \right] \\ I_1 &= \frac{1}{\sqrt{Z_{e1}}} \left[ e^{\gamma \beta x} (B e^{-\gamma x} - C e^{\gamma x}) + e^{-\gamma \beta x} (A e^{-\gamma x} - D e^{\gamma x}) \right] \\ I_2 &= \frac{1}{\sqrt{Z_{e2}}} \left[ e^{\gamma \beta x} (B e^{-\gamma x} + C e^{\gamma x}) - e^{-\gamma \beta x} (A e^{-\gamma x} + D e^{\gamma x}) \right] \end{aligned} \quad (15)$$

In Fig. 2 the diagram showing the geometrical and electrical configuration of two coupled lines is given. By substituting the boundary conditions in (15) after some calculations

$$V_{2ca/4ca} = 4JE\sqrt{\frac{Z_{e2}}{Z_{e1}}} \frac{\frac{Z_{L2}}{Z_{e2}} \sin \omega \gamma \beta (l-x_1) \cos \omega \gamma (l-x_1)}{\left(1 + \frac{Z_{g1}}{Z_{e1}}\right) e^{j\omega \gamma l} \left[ \left(1 + \frac{Z_{L2}}{Z_{e2}}\right) e^{j\omega \gamma (l-x_1)} + \left(1 - \frac{Z_{L2}}{Z_{e2}} \cos 2\omega \gamma \beta (l-x_1)\right) e^{-j\omega \gamma (l-x_1)} \right] + \left(1 - \frac{Z_{g1}}{Z_{e1}}\right) e^{-j\omega \gamma l} \left[ \left(1 + \frac{Z_{L2}}{Z_{e2}} \cos 2\omega \gamma \beta (l-x_1)\right) e^{j\omega \gamma (l-x_1)} + \left(1 - \frac{Z_{L2}}{Z_{e2}}\right) e^{-j\omega \gamma (l-x_1)} \right]} \quad (16)$$

$$V_{2cc/4ca} = 4JE\sqrt{\frac{Z_{e2}}{Z_{e1}}} \frac{\frac{Z_{L2}}{Z_{e2}} \sin \omega \gamma \beta (l-x_1) \sin \omega \gamma (l-x_1)}{\left(1 + \frac{Z_{g1}}{Z_{e1}}\right) e^{j\omega \gamma l} \left[ \left(1 + \frac{Z_{L2}}{Z_{e2}}\right) e^{j\omega \gamma (l-x_1)} - \left(1 - \frac{Z_{L2}}{Z_{e2}} \cos 2\omega \gamma \beta (l-x_1)\right) e^{-j\omega \gamma (l-x_1)} \right] + \left(1 - \frac{Z_{g1}}{Z_{e1}}\right) e^{-j\omega \gamma l} \left[ \left(1 + \frac{Z_{L2}}{Z_{e2}} \cos 2\omega \gamma \beta (l-x_1)\right) e^{j\omega \gamma (l-x_1)} - \left(1 - \frac{Z_{L2}}{Z_{e2}}\right) e^{-j\omega \gamma (l-x_1)} \right]} \quad (17)$$

where  $V_{2ca/4ca}$  represents  $V_2$  when  $Z_{g2} \rightarrow \infty$  and  $Z_{L1} \rightarrow \infty$   
 and  $V_{2cc/4ca}$  represents  $V_2$  when  $Z_{g2} = 0$  and  $Z_{L1} \rightarrow \infty$

the equations (16) and (17) are rather complex. However, some interesting conclusions can be achieved from their examination:

- at low frequency  $V_2$  is proportional to the frequency and to the coupling coefficient  $\beta$
- at high frequency  $V_2$  depends on the coupled length of the lines and is affected by cable resonances
- in both the numerators of (16) and (17) the term  $\sin \omega \gamma \beta (l-x_1)$  indicates that  $V_2$  is affected by an oscillatory component determined by mutual capacitance and inductance of the coupled lines.

It would be possible to calculate the exact values of  $V_2$  in a certain frequency range, but this is rather time consuming. Therefore the experimental approach has been used.

### 3. EXPERIMENTAL MEASUREMENT OF THE CABLE COUPLING TRANSFER FUNCTION

During the evaluation of the EMC performances of a digital data transmission system a simple test tool was used to simulate the wiring coupling mechanism. It consists of a copper tube (1 cm diameter) in parallel with the wire under test for a fixed length (100 cm) (Fig. 3). The A termination is left open (capacitive coupling) or short circuited (inductive coupling). The B termination is connected to the measuring device. The wire under test connecting the test sample to its load runs parallel to the test wire at a distance of 2 cm.

By means of the HP Spectrum Analyzer/Tracking Generator 8555A/8443 the cable coupling transfer function was measured in the frequency range 0 to 100 MHz in accordance with the test set up of Fig. 4 c.

In Fig. 5 and Fig. 6 three different curves are shown

- the curve N1 represents the cable test probe insertion loss when the A termination is open circuited (Fig. 5) or short circuited (Fig. 6) measured in accordance with the test set up of Fig. 4 (a)
- the curve N2 represents the cable under test insertion loss measured in accordance with the test set up of Fig. 4 (b)

- the curve N3 represents the cable coupling transfer function when the A termination is open circuited (Fig. 5) or when the A termination is short circuited (Fig. 6) measured in accordance with the test set up of Fig. 4 (c).

The curves N1, 2, 3 of Fig. 3 and Fig. 4 have been grouped in the same figure because some interesting conclusions can be obtained. It appears that the peaks of the cable coupling transfer function correspond to the resonance frequencies of the cable test probe and of the cable under test; the deep attenuation peaks, viceversa, correspond to the resonance between the two cables and are mainly determined by mutual capacitance and inductance of the cable coupled length.

In addition the following general conclusions are easily achieved:

- the emitted noise is proportional to the cable length only in the low frequency range (below the first cable resonance)
- in the high frequency range (above the first cable resonance) the emitted noise is no longer proportional to the cable length but it depends only on the resonance frequencies corresponding to  $n\lambda_c/4$  ( $\lambda_c$  is the cable wavelength;  $n$ : integer).

#### 4. MEASUREMENT OF INTERWIRING COUPLED NOISE

The test tool which has been previously described can be used to measure the wiring emitted noise in two load configurations (open circuit and short circuit). Fig. 7 (Fig. 8) shows the diagram of the interference generated by a digital data transmission unshielded twisted line when the A termination of the cable test probe is short circuited (open circuited). From these figures it appears that the peaks at 30 MHz and 80 MHz are due to the twisted cable resonance (this also appears from the comparison with the diagrams of Fig. 5 and Fig. 6). Knowledge of the existence of these frequency resonance peaks may be very useful in establishing valid criteria for cable separation.

Another considerable advantage of this test method consists in the possibility of evaluating the amount of radiated interference due to the wiring only, avoiding the difficulties of test RE02 of MIL-STD 461/462 where the total radiated emission from the equipment under test is measured.

The radiated emission generated by an impulse generator connected to its load by a cable two metres long has been measured in accordance with the test method RE02. The radiated interference is above the specification limit in the frequency range 30 MHz to 90 MHz (Fig. 9). As far as test RE02 is concerned, the equipment under test would not seem acceptable. The same test has been repeated disconnecting the equipment from the cable and connecting the load directly to its input terminals: no radiated interference was measured (Fig. 10). The conclusion is that the radiated interference measured in test RE02 only depends on the wiring.

The wiring coupled noise measured in accordance with the technique described here is shown in Fig. 11 and represents the measurement of the expected noise coupled into the cables running in proximity of the wiring under test.

The two curves show the open circuit and short circuit diagrams; it appears that below 5 MHz the emitted noise level is well below 70 dB $\mu$ V / MHz. The situation may become critical in the frequency range 10 to 100 MHz where the wire emitted noise is above 80 dB $\mu$ V / MHz; therefore some precautions shall be taken in order to prevent possible interference problems.

Wiring susceptibility tests can be performed using the same technique and the same cable test probe.

#### 5. CONCLUSIONS

The advantages of performing the proposed tests during a program of electromagnetic compatibility can be summarized as follows:

- Realistic simulation of the wiring coupling mechanism
- Possibility of determining the level of wiring radiated interference
- Possibility of classifying the cables in accordance with their emission levels for a better philosophy of cable separation
- Evaluation of radiated interference due to the wiring in comparison with the total radiated emission piece of equipment.

The measurement techniques described here has already been proved valid during the electromagnetic compatibility study of an aircraft.

- Acknowledgment -

The authors wish to express their thanks to the Managing Director of Centro Elettronico Avio for his encouragement in this work.

A special thank is due to Mr. Francheo for his help during the measurements and to Mr. L. Sartore for the preparation of the final format.

- References -

- (1) V. Rizzoli April 1972 Three wire lines and their use as directional couplers Alta Frequenza
- (2) J. McKenna and J.A. Morrison July August 1972 Exact Solutions to some deterministic and random transmission line Problems The Bell System Technical Journal
- (3) MIL-STD-461 Electromagnetic Interference Characteristic Requirements for Equipment
- (4) MIL-STD-462 Electromagnetic Interference Characteristics, Measurement of.



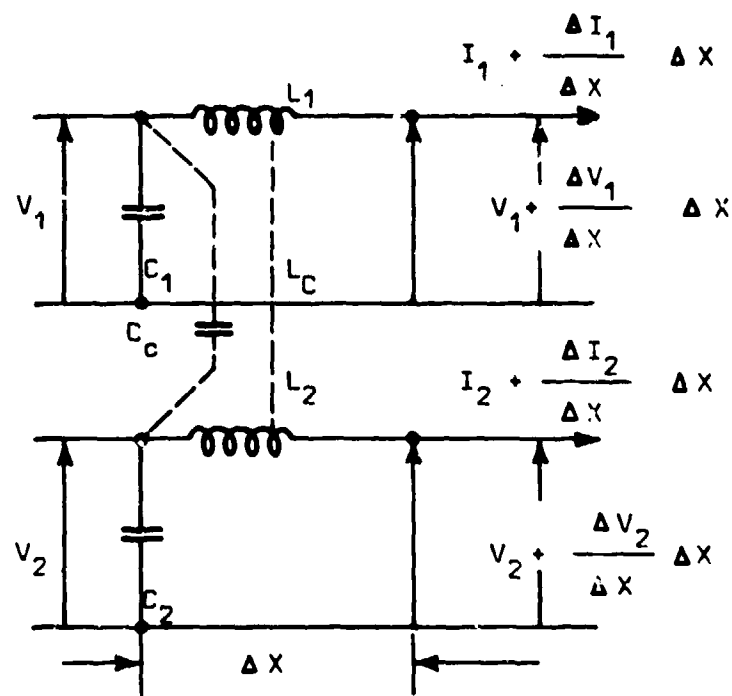


Fig. 1 Diagram of coupled lines

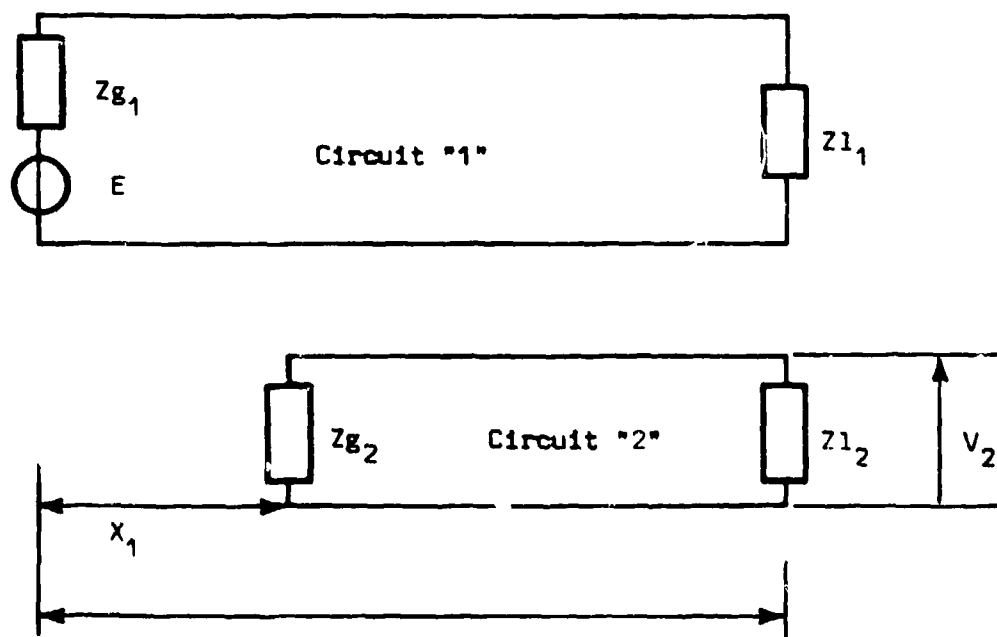


Fig. 2 Diagram showing the geometry of two coupled lines

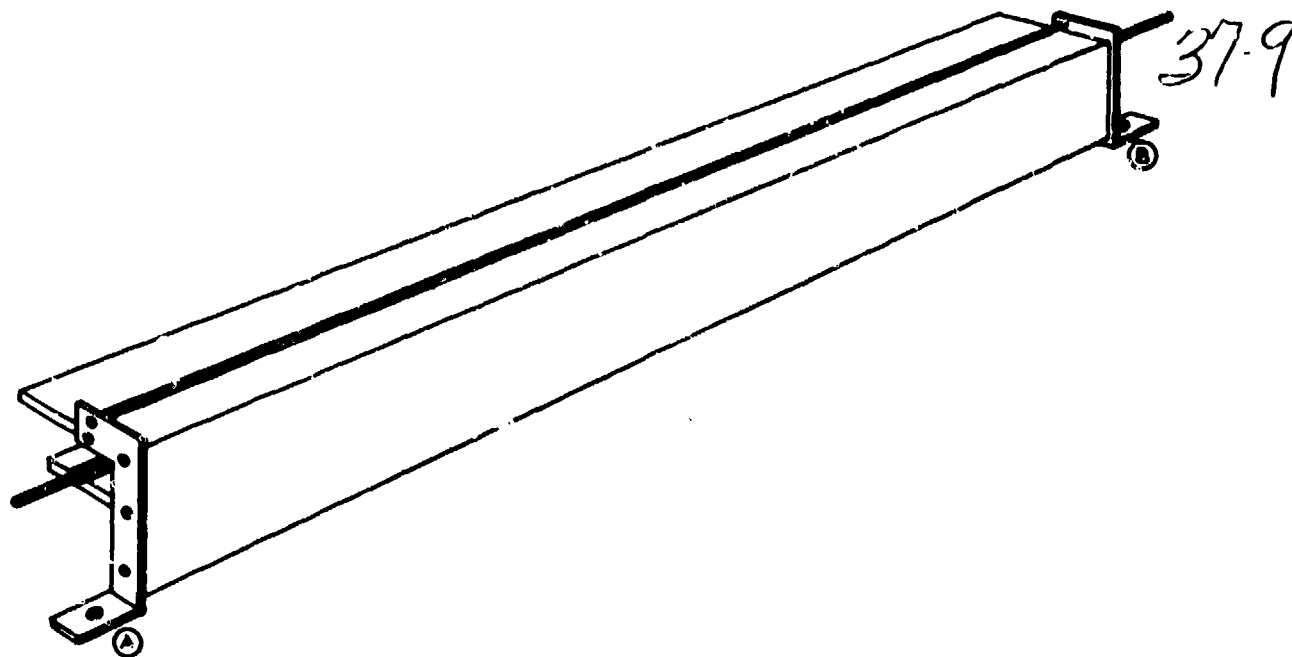
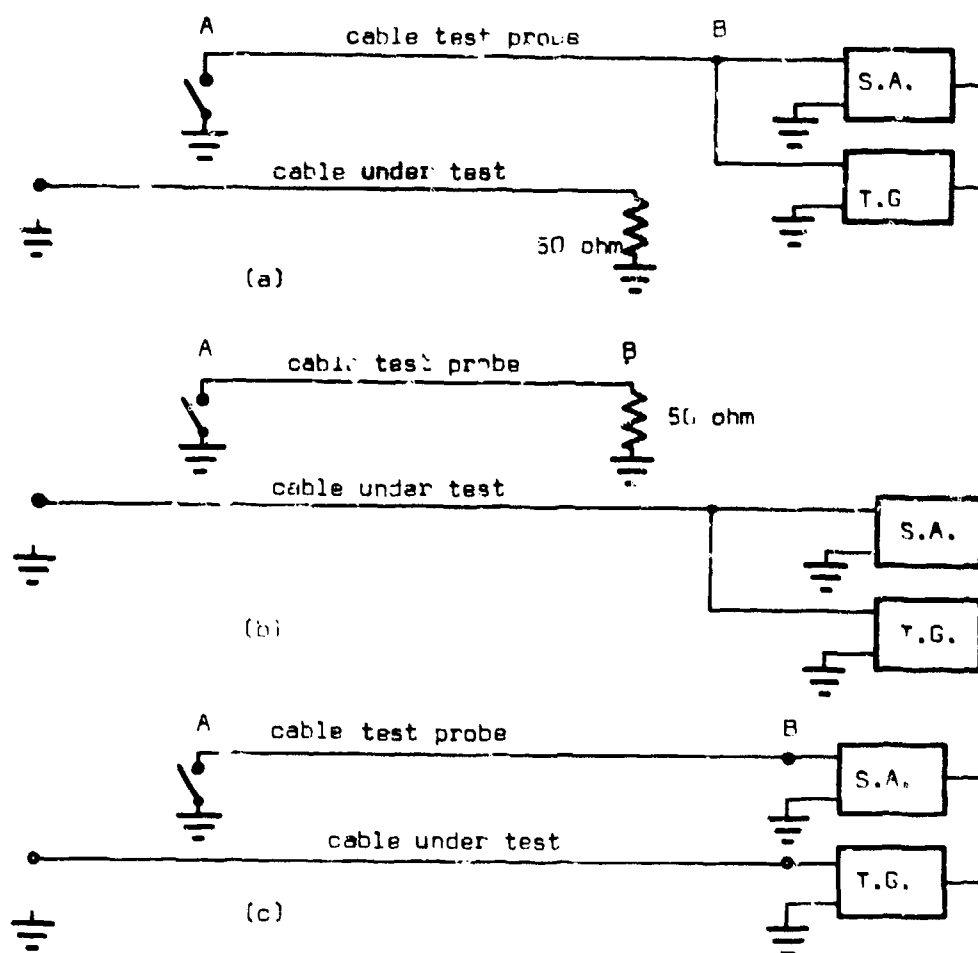


Fig. 3 Cable test probe



S.A. = Spectrum Analyzer  
T.G. = Tracking Generator

Fig. 4 Test set ups to determine the cable coupling transfer function

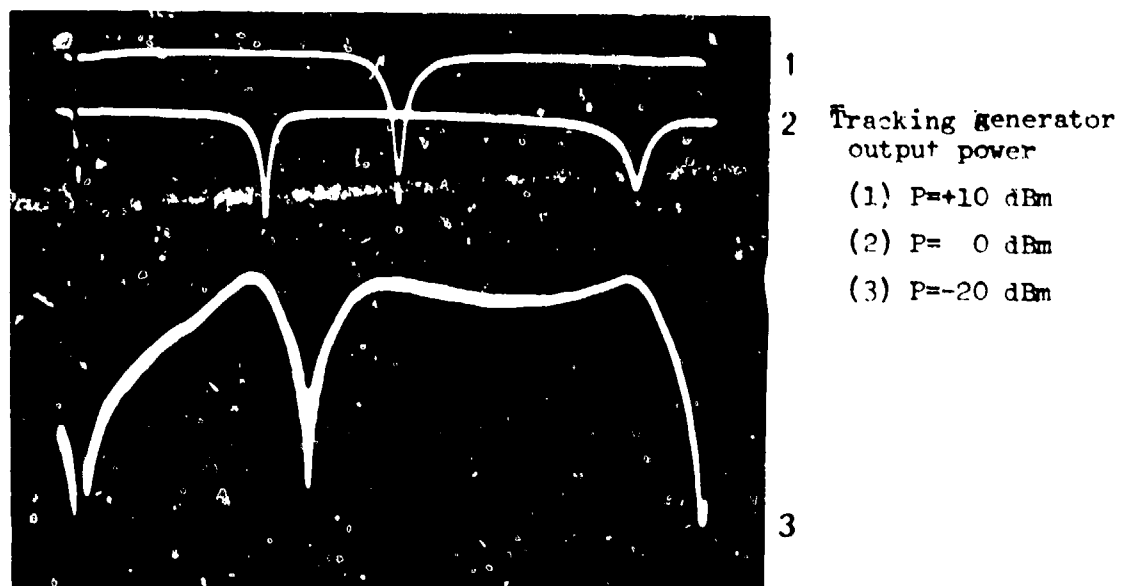


Fig. 5 Cable coupling transfer function (the A termination is open circuited) Ref. level + 10 dBm frequency range 0 to 100 MHz

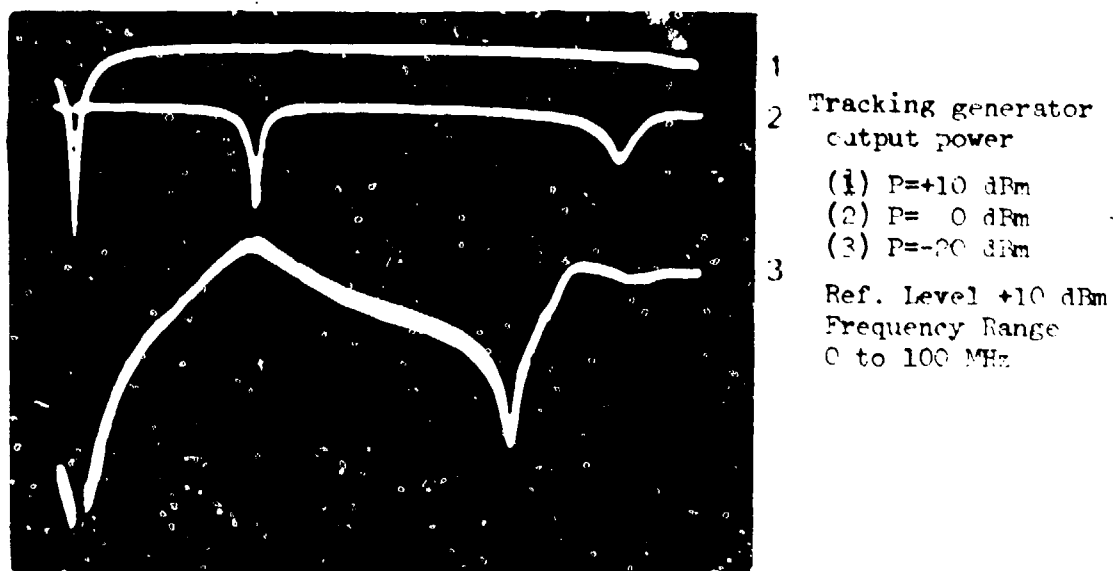


Fig. 6 Cable coupling transfer function (the A termination is short circuited) Ref. level + 10 dBm frequency range 0 to 100 MHz

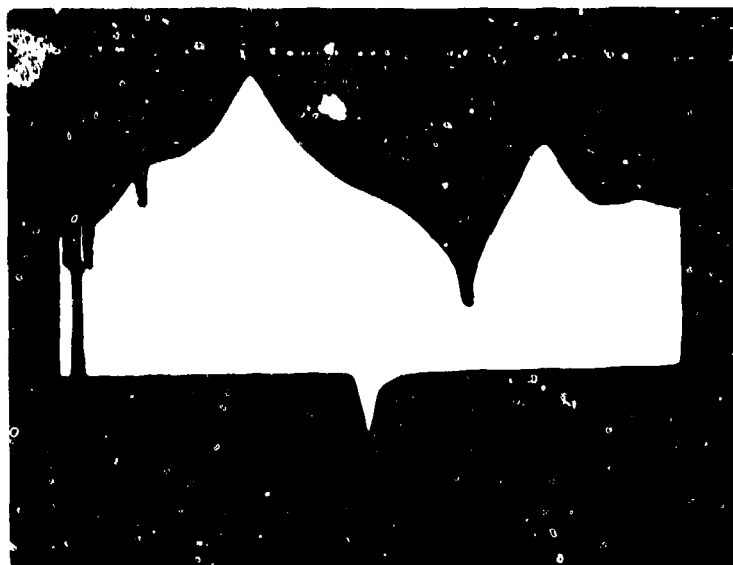


Fig. 7 Emitted noise generated by a DDT line (the A termination of the cable test probe is open circuited)  
Log Ref. level 30 dBm frequency range 0 to 100 MHz



Fig. 8 Emitted noise generated by a DDT line (the A termination of the cable test probe is open circuited)  
Log Ref. level 30 dBm frequency range 0 to 100 MHz

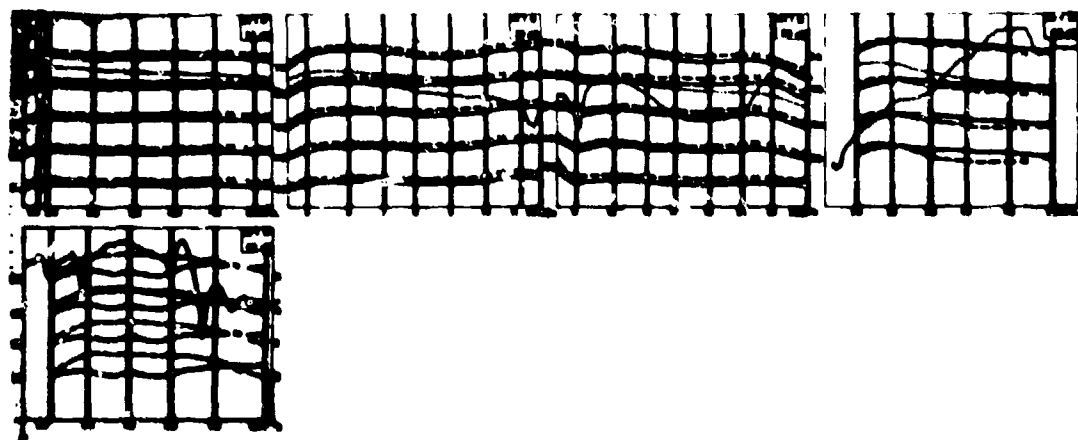


Fig. 9 Radiated interference test (test method RE02) (cable connected), —dB/uV/MHz, —dB/uV/m/MHz  
....Specification limit

....Specification limit

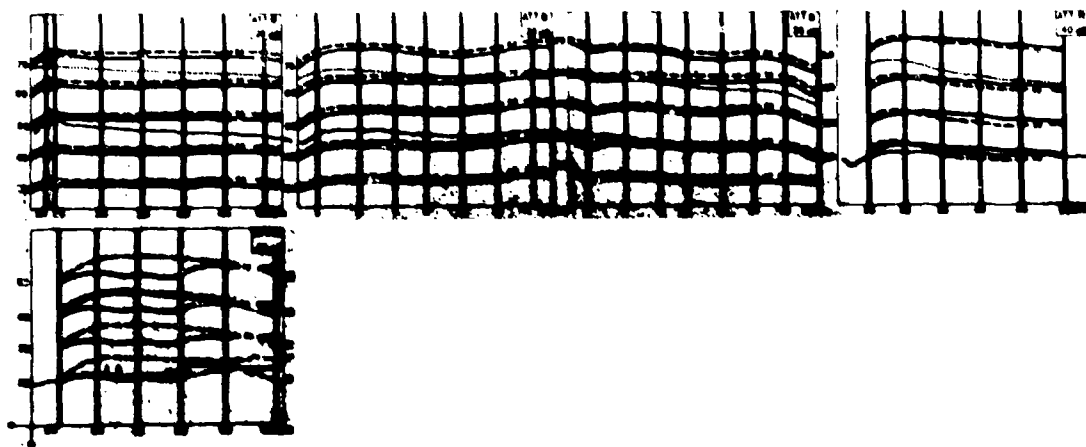


Fig. 10 Radiated interference test (test method RE02) (cable disconnected), —dB/uV/MHz, —dB/uV/m/MHz,  
....Specification limit

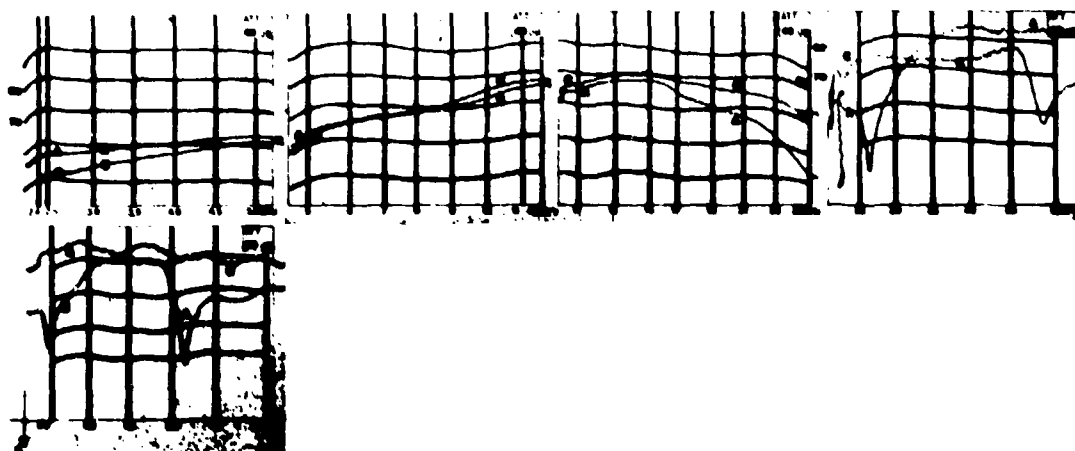


Fig. 11 Wiring radiated interference test, —dB/uV/MHz, A) open circuit, C) short circuit

## DISCUSSION

R. OLESCH: What is the db scale in Figure 7?

B. AUDONE: ~40db peak to minimum.

E. M. FROST: Your measurements are made up to 100 MHz. Within the last year or so, even the cheapest semiconductor devices will work up to at least 200MHz; therefore, EMC difficulties can be expected up to these frequencies from normally low frequency analogue circuits.

B. AUDONE: The measurement has been performed in the frequency range 0 to 100 MHz only as an example because of the particular table length chosen. The purpose of the test was to highlight the resonance cable problems only.

ON THE EVALUATION OF MAN-MADE ELECTROMAGNETIC NOISE  
INTERFERRING WITH COMMUNICATIONS IN THE E.L.F. RANGE

by

Giorgio Tacconi  
Istituto di Elettrotecnica  
Facoltà di Ingegneria  
Università di Genova & C.N.R. - Italy

SUMMARY

The electromagnetic waves in the Extremely low Frequency range have, even in a dispersive medium like sea water, a high penetration power. Their suitability for communications also with submerged receivers is therefore evident. Because of their negligible transmission losses it is possible to communicate informations also at circumterrestrial distances, even with a very small irradiated power. The propagation takes place in the earth-ionosphere cavity, which from the point of view of the noise is not properly an ideal transmission line. To obtain the best performance it is necessary as in any other type of telecommunications, to know the behaviour of the natural background noise with its spectral structure and statistical characteristics. Moreover there are also in such a "line" additional interferences introduced by man-made noise. The E.L.F. propagation in dispersive natural layered media such as the sea, the sea bed, and generally the earth's crust, can be used as a tool for investigating the internal structure of the geological layers and, as a consequence to localize underground resources. Some complex phenomena produced in the magnetosphere can be studied by means of this tool. Besides also a passive detection of a natural phenomena and its interpretation or measurement can be considered as an unidirectional transmission channel. This paper is intended to examine the "mechanics" of some aspects of the man-made electromagnetic noise at the E.L.F. that are the most favorable for propagation in dissipative media. In particular the e.m. noise is considered as generated by a moving ship in the vicinity of an electromagnetic sensor immersed in the sea. Mathematical and experimental approaches for an estimation of such noise are proposed. Some experimental results obtained in the Tyrrhenian sea are shown in accordance with theories and experiments developed by many authors (IEEE Transaction on COMMUNICATIONS, April 1974). Local natural background noise as well as nearby and far-off man-made noise will be considered in the context of a general transmission channel.

## 1. GENERAL

Communications in dispersive, layered, media such as, in the sense above mentioned can be performed by means not only of acoustic waves but also by using Electromagnetic waves in the ELF range. It is well known from the electromagnetic propagation theory in dissipative medium (Refs. 1, 2, 3, 4, 15, 18) that the dependence from the frequency of the field intensity is established in a given point of the space where the perturbation takes place, by means of the "characteristic frequency" of the medium which is a function of the electric conductivity ( $\sigma$ ) and of the dielectric constant ( $\epsilon$ ) of the medium and is expressed by the following expression

$$f_c = \frac{1}{2\pi} \frac{\sigma}{\epsilon}$$

The case considered here is that of an electromagnetic sensor (receiver) immersed in sea water. The signal (or noise) detected (and/or produced) in the sea by such a sensor is the resultant effect of the combination of many different noises, natural and man-made, which, furthermore, are affected by the different propagation conditions due to the broadband spectral structure of the signal, and by the intrinsic noise of the sensor (Fig. 1).

## 2. NATURAL NOISE

Noise of natural origin consists mainly of signals coming from far off thunderstorms or nearby lightnings in the earth-ionosphere cavity, or from other complex phenomena produced in the Magnetosphere (Ref. 5). These phenomena have been studied and are still being continuously surveyed by many scientists; any how some sort of classification of such noises has already been done (Refs. 6, 7, 17). The knowledge of this classification enables one within certain limits to reduce the disturbing effects of these phenomena on transmissions in the same frequency range, either with appropriate codification and signal processing, either with particular design and set up of the receiving antennas. The general aspect of the noise requires a statistically based evaluation for establishing its typical characteristics.

## 3. MAN-MADE NOISE

Man-made noise, in this particular case, is generally produced, by strong current transients or variations happening in the vicinity of the sensor:

- a) A.C. power lines on land (50, 60 Hz), railways, industries, Electric power generators, close to the coast line (but not necessarily as will be seen later), switchings in general.
- b) Underwater cables (i.e. telex, power lines) placed in the vicinity of the sensors.
- c) Ships of any type passing near the receiving sensors.

The noises related to a) and b) can be relatively well studied and classified, mainly because their geometrical position with respect to the receiver is fixed. Such geometry must be taken into account in every particular case.



The disturbance related to ship traffic (c), presents a vast casistic and variability which is due mainly to the following reasons:

- 1st: The intrinsic noise of the ship, which is essentially produced by electric machinery and electronic apparatus on board and by hull corrotion currents, presents always a complex spectral structure.
- 2nd: The geometry of the system, that is the relative motion of the ship with respect to the sensor, implies the knowledge of the velocity, direction (course), the boundary conditions of the propagation field and all the parameters of the medium involved in the propagation expressions.

The "Geometry Influence" which in principle could be calculated, even with some difficulty, on the base of the propagation theory in dissipative media, introduces an additional time dependence to the already complicated structure of the noise. Figure 2 shows some implications which must be considered when evaluating the noise received by a submerged sensor.

The interaction between the two above mentioned aspects (1st and 2nd) produce at the receiver a sort of quasi-deterministic process. A tentative model of approaching the problem is given below.

#### 4. SIMPLIFIED MATHEMATICAL MODEL

What we consider here is an elementary Rice-Transmitting system, consisting of the transmitting ship, the location of which is the origin of a cartesian reference plane X,Y, and a dipole receiving antenna moving along an arbitrary line ( $L_{arb}$ ) on the same plane. The coordinate system lies on the sea surface and the position of  $L_{arb}$  is defined by  $r_0$  and  $\varphi_0$  as shown in Fig. 3.

The electrical field vectors are given in this case by the relations: Refs. 8 & 9.

$$\vec{E}_\rho = \frac{I\ell}{2\pi\sigma} \cdot \frac{1}{r^3} [1 + (1 + \gamma_1 \cdot r) e^{-\gamma_1 \cdot r} \cos \varphi \cdot \hat{r}] \quad (1)$$

$$\vec{E}_\varphi = \frac{I\ell}{2\pi\sigma} \cdot \frac{1}{r^3} [2 - (1 + \gamma_1 \cdot r) e^{-\gamma_1 \cdot r} \sin \varphi \cdot \hat{\varphi}] \quad (2)$$

where

- I = current through the transmitting dipole
- $\ell$  = length of the transmitting dipole
- $\gamma = \sqrt{i\omega\mu\sigma}$  (propagation constant)
- $\omega = 2\pi f$  rad/s (frequency generated by the ship)
- $\mu = 4\pi \times 10^{-7}$  H/m
- $\sigma = 4$  mho/m (sea water conductivity)
- $r_0$  = closest distance  $L_{arb}$  - Origin
- r = instantaneous distance

These formulae are valid for all of the plane X,Y, and allow the value of the Electric field component in any point of the arbitrary line ( $L_{arb}$ ) to be computed:

$$E_{arb} = E_r \cos \alpha - E_\varphi \sin \alpha \quad (3)$$

where

$$\alpha = \frac{\pi}{2} + (\varphi - \varphi_0)$$

Setting  $A = (1 + \gamma_n r) e^{-\gamma_n r}$  we have

$$\begin{aligned} E_{arb} &= \frac{I\ell}{2\pi\sigma} \cdot \frac{1}{r^3} [(1+A) \cos \varphi \cos \alpha - (2-A) \sin \varphi \sin \alpha] \\ &= \frac{I\ell}{2\pi\sigma} \cdot \frac{1}{r^3} [\cos(\varphi + \alpha) - \sin \varphi \sin \alpha + A \cos(\varphi - \alpha)] \end{aligned} \quad (4)$$

From Fig. 3 we seen that

$$r = \sqrt{r_0^2 + X_{arb}^2}$$

and

$$\varphi = \varphi_0 - \text{Arctan} \frac{X_{arb}}{r_0}$$

where  $X_{arb}$  is computed from the point (of the line) most close to the origin 0 of the axis ( $X_0$ ).

In Fig. 4(b) the computed value is shown of  $\frac{E_{arb}}{I\ell}$  in function of  $r$  for  $r_0 = 30$  m,  $\theta = 90^\circ$ ,  $\varphi = 180^\circ$ , and in Fig. 4(a) for  $\theta = 0^\circ$ ,  $\varphi = 90^\circ$ .

Figure 5(b) shows an experimental result of a parallel passage of an artificial dipole source on the Receiving dipole, and Fig. 5(a) a perpendicular passage of the same source on the same Receiving dipole (Refs. 9, 16).

## 5. PRACTICAL MODEL

The moving ship is regarded as a transmitting dipole antenna (NT) with a known associated dipole moment ( $M = I\ell$ ), moving with a constant velocity  $v$  in a direction parallel to a fixed receiving dipole of the same size ( $R$ ) placed in the sea water (Fig. 6).

The general formula of the electric field component detected by  $R$  is

$$E = \frac{M}{2\pi\sigma} \cdot \frac{1}{r^3} \cos \{[\alpha + \beta - \sin \alpha \sin \beta + k \cos(\alpha - \beta)]\} \quad (5)$$

where

- $E$  = electric field component
- $\sigma$  = sea water conductivity
- $K_n$  = transmission coefficient =  $(1 + \gamma_n r) e^{-\gamma_n r}$
- $M = I\ell$  = dipole moment
- $\gamma_n = \sqrt{j\omega\mu\sigma} = \frac{1+j}{\delta_n}$  propagation constant
- $r$  = horizontal distance (NT - R)
- $r_0$  = shortest distance (NT - R)
- $\alpha \& \beta$  = relative angles
- $\delta_n$  = skin depth =  $\left(\frac{\lambda_n}{\pi\sigma\mu c}\right)^{\frac{1}{2}}$

With some simplifications due to the particular geometrical symmetry we obtain

$$E_i = \frac{M}{2\pi\sigma} \cdot \frac{1}{r^3} \left[ 1 - 3 \frac{r_0^2}{r} + K_i \right] \quad (6)$$

In which  $E_i$  clearly depends on the frequency, through  $K_i$ , a function of the frequency.

This frequency dependence is very important when the radiated noise is broadband. In such a case the broadband signal must be processed to establish its frequency components and to compute for each of them the relative partial electric field intensity  $E_i$  or the associated dipole moment of the source. The general formula (6) will be then applied to each frequency component in order to evaluate the total electric field intensity (or the total associated dipole moment), as follows:

$$\begin{aligned} E_1 &= \frac{M_1}{2\pi\sigma} \cdot \frac{1}{r^3} \left[ 1 - 3 \frac{r_0^2}{r} + K_1 \right] \\ E_2 &= \frac{M_2}{2\pi\sigma} \cdot \frac{1}{r^3} \left[ 1 - 3 \frac{r_0^2}{r} + K_2 \right] \\ &\dots\dots\dots \\ E_n &= \frac{M_n}{2\pi\sigma} \cdot \frac{1}{r^3} \left[ 1 - 3 \frac{r_0^2}{r} + K_n \right] \end{aligned} \quad (7)$$

where

$n = 1, 2, \dots i, \dots$  represents the order of the frequency component.

Simple mathematics gives also the associated total dipole moment  $M_{\text{eff}}$ .

$$M_{\text{eff}} = 2\pi\sigma \cdot r^3 \cdot \left\{ \sum_{i=1}^n \left| \frac{E_i^2}{\left[ 1 - 3 \frac{r_0^2}{r} + (1 + \gamma_i r) e^{-\gamma_i r} \right]^2} \right| \right\}^{-2} \quad (8)$$

The value of each single  $E_i^2$  can be determined by means of spectral analysis by comparison with a known calibrated signal (Fig. 7).

In the experimental model the intrinsic noise of the moving ship was simulated assuming it to have a rectangular shape with a basic frequency of 30 Hz; Figure 5(b) shows the signal detected by the parallel sensors. In Fig. 7 the power spectrum is shown of a constant 30 Hz square wave signal, the area of each spike component is proportional to the corresponding electric field intensity ( $E_i^2$ ). For reference a calibration signal is also shown in Fig. 7.

## 6. VELOCITY DEPENDENCE

In order to evaluate the influence of the velocity on the received noise we perform, now, another simplification of the model, viz., the intrinsic noise of the ship is assumed to be a pure sinusoid. In this case behaviour of the signal detected at the receiver will be similar to that shown in Fig. 5 but the harmonic content will be limited only to the fundamental. Figures 5(a) and 5(b) show clearly that the received signal is not stationary at all.

If the signal were a constant-level sinusoid, the relative power spectrum (for an infinite time sample) would be a very narrow spike; instead, when the constant level condition is not verified, a broadening of the narrow spectral spike is to be expected, corresponding to a frequency smear. In principle, it should then be to associate somehow the level variation with the corresponding frequency spreading  $\Delta f$ .

Assuming the condition verified that the propagating signal in the sea vanishes with the inverse cube law of the distance (Ref. 7) and keeping the ship's velocity  $v$  constant, one can express the intensity of the signal detected by the fixed sensor as follows:

$$I(t) = \frac{\sin \omega t}{(r - vt)^3} = \frac{\sin \omega t}{r^3 (1 - \frac{vt}{r})^3} \quad (9)$$

if we set  $vt \ll r$  with  $r > \delta$  (skin depth)

$$I(t) = e^{-\frac{3vt}{r}} \cdot \sin \omega t \quad (10)$$

The maximum values of function  $I(t)$  are found for:

$$t_1 = \frac{\pi}{2\omega}; \quad t_2 = \frac{5\pi}{2\omega}; \quad t_3 = \frac{9\pi}{2\omega}; \quad \dots \text{etc.} \quad (11)$$

then

$$I_1 = I(t_1) = e^{-3v\pi/2\omega r} \quad (12_1)$$

$$I_2 = I(t_2) = e^{-15v\pi/2\omega r} \quad (12_2)$$

and the ratio  $I_1/I_2$  will be

$$\frac{I_1}{I_2} = e^{-3v\pi/2\omega r(1-5)} = e^{-6v\pi/\omega r} \quad (13)$$

Consequently the logarithmic decrement is obtained:

$$\theta = \frac{6v\pi}{\omega r} \quad (14)$$

Similarly, for a harmonic motion with logarithmic damping we have:

$$\theta = \frac{\pi}{Q} = \frac{\pi \Delta f}{f} \quad (15)$$

then

$$\Delta f = \frac{\theta f}{\pi} = \frac{3v}{\pi r} \quad (16)$$

In Fig. 8 the computed values is shown of  $\Delta f$  in function of the distance for different values of ship's velocity  $v$ .

## 7. ANALYSIS OF THE NOISE

The bandwidth of the ship signal (man-made noise) is function of the source speed. This signal is detected by the submerged sensor together with the natural background noise:

$$N_R = N_S + N_N$$

where

$$N_R = \text{Total received noise}$$

$$N_S = \text{Ship noise (assumed to be sinusoidal)}$$

$$N_N = \text{Natural background noise}$$

To be analyzed,  $N_R$  is generally introduced into a filter, the response of which will be the resultant of two components

$$S_{NS} = \text{Response to } N_S \text{ (sinusoid)}$$

$$S_{NN} = \text{Response to } N_N \text{ (always present)}$$

To evaluate  $S_{NS}$  the processing is simple. In order to evaluate  $S_{NN}$ , it is necessary to investigate whether  $N_N$  is normally distributed. In such a case (Ref. 10) the r.m.s. value of the filter output is

$$\psi = \sqrt{B G_n}$$

where

$$G_n = \text{Power spectral distribution function}$$

$$B = \text{Noise bandwidth}$$

The level fluctuation of the noise in the filter will be characterized by the product

$$B \times T = 1$$

In fact the normalized standard error of the output amplitude is: (Ref. 10)

$$\epsilon = \frac{\text{s.d. } [\psi_n]}{\psi_n} \frac{1}{2\sqrt{BT}}$$

In other words, this expression represents the noise fluctuation in the filter, which then has a number of degrees of freedom:  $n = 2BT = 2$ . On this base it is possible to define the recognition threshold between  $N_S$  and  $N_N$ .

The background noise (in absence of ship) cannot be considered stationary because of the presence of "strange" spikes. A selection was then made of "quiet samples" and "spiky samples" of the received noise, Fig. 9. By means of a procedure suggested by Bendat and Piersol (Ref. 10) the following analysis conditions were established

T	B	n
16 s	0,6 Hz	20
160 s	0,6 Hz	200

The fluctuation of the power spectral density related to each single B can be expressed in terms of normalized standard error

$$\epsilon_t = \frac{\sigma_t}{M} \frac{1}{\sqrt{BT}}$$

where, in the present case:

$\sigma_t$  = Standard deviation of each of the independent measurements (in this case 100)

M = Mean value of all  $\sigma_t$

In the present analysis the following quantities were computed:

$\bar{M}_{10}$  = Mean value of 10 mean values ( $M_1, M_2, \dots, M_{10}$ ) of 10 independent measurements

$\sigma_{M_{10}}$  = Standard deviation of  $M_1, M_2, \dots, M_{10}$

Assuming  $R = 1/\epsilon_t$  it is possible to define the apparent value of R:

$$[R] = \frac{\bar{M}_{10}}{\sigma_{M_{10}}} \sqrt{BT} = \sqrt{10} = 3.3$$

In the analysis one generally finds, (Ref. 7)

$$[R] < \sqrt{10}$$

## 8. SOME RESULTS AND CONCLUSIONS

Figure 10 shows the power spectral analysis of a "quiet sample"; one can see that  $R \approx 2 < \sqrt{10}$ , and that the distribution is almost gaussian. The presence of the Schumann modes is evident (Refs. 7, 12, 14).

In Fig. 11 the same analysis was carried out for a "spiky sample", and it was observed that  $R < 2 < \sqrt{10}$ . This means that for samples of long duration the distribution of the background noise is not gaussian, as was demonstrated also by Bernstein et al. March 1974 (Ref. 11).

In Fig. 12 the power spectral analysis is shown of natural background noise detected by means of two parallel dipole antennas placed on the sea bottom (Tyrrhenian sea).

The remarkable fact is that the spike around 17 Hz disappears in the analysis of the difference of the two signals, as it does with Schumann modes this means that the signal reaches the two sensors, (spaced about 1 km apart) with the same phase and the same amplitude. This leads to the conclusion that the source is

quite far away from the sensor's zone. The spike in question can be produced by A.C railway power lines, with a frequency of  $16 \frac{2}{3}$  Hz used in some places in Europe.

Some approaches to the background noise evaluation problem in the ELF range, have been outlined above. This evaluation is essential for optimizing the performance of a transmission channel in such a frequency range (Ref. 13). For modelling some restrictive assumptions were made, but with a more complex and sophisticated signal processing, the results could be more detailed.

#### ACKNOWLEDGMENTS

The present work was carried out with the support of Italian National Research Council C.N.R.

## REFERENCES

1. AGARD Conf. No. 77.  
Electromagnetics at the sea, Paris, June 1970.
2. Baños, A.  
Dipole radiation in the presence of a conducting half space.  
Pergamon Press 1966.
3. Wait, J.  
Theory of the terrestrial propagation of a VLF electromagnetic waves.  
Lecture notes prepared for NATO Advanced Study Inst., Norway, April 1974.
4. Llanwyn Jones, D.  
ELF Propagation theory.  
Preprint for NATO Advanced Study Inst., Spatind, Norway, April 1974.
5. Egeland, A.  
Cosmical geophysics.  
Universitetsforlaget, Oslo, 1973.
6. Bleil, D.F.  
Natural electromagnetic phenomena below 30 Kc/s.  
Proceedings of a NATO Advanced Study Inst., July-August 1963.
7. Tacconi, G.  
The measurement of the ELF horizontal electrif field component of the  
background noise in the sea.  
Lecture notes for NATO Advanced Study Inst., Spatind, Norway, April 1974.
8. Tacconi, G.  
Sulle possibilità di comunicazione attraverso il mare mediante onde  
elettromagnetiche nella gamma delle basse frequenze.  
XX Conv. Internaz. delle Comunicazioni, Genova, Ottobre 1972.
9. Baños & Wensley  
The horizontal dipole in a conducting half space.  
Scripps Institute of Oceanography, 1953.
10. Bendat & Piersol  
Measurements and analysis of Random data, J. Wiley, 1966.
11. Bernstein, ecc.  
Long range communications at extremely low frequencies.  
Proceedings of the IEEE, Vol. 62, March 74.
12. Schumann, W.O.  
On the propagation along the earth surface of very long electric waves and  
the lightning discharge.  
Phys. Abs. 6155/1953, Z. angew. Phys. 1952.



13. IEEE. Transaction on Communications, April 1974.
14. Larsen, T.R.  
ELF Noise measurements.  
NATO ASI "ELF, VLF Radio Wave Propagation", Norway, April 1974.
15. Wait, J.R.  
Electromagnetic waves in stratified media.  
Pergamon Press, 1970.
16. Franceschetti, G., Bucci, M., Latmirel, G.  
Metallic and dielectric antennas in a conducting environment.  
Radio Science, Vol. 5, n. 12, Dicembre 1970.
17. Balser, M., Wagner, C.  
Diurnal power variation of the Earth Ionosphere cavity modes and their  
relationship to worldwide thunderstorm activity.  
J. Geophys. Res., February 1962.
18. Galejs, J.  
Terrestrial ELF propagation.  
NATO ASI, Bad Homburg, 1963.

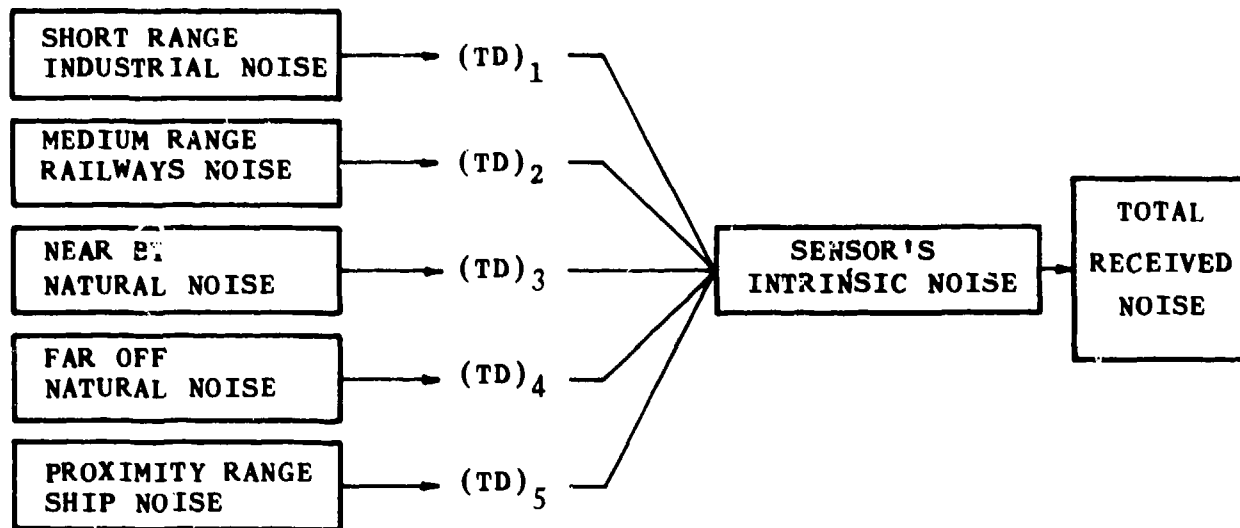


Fig.1 CLASSIFICATION OF VARIOUS ELECTROMAGNETIC NOISE COMPONENTS FOR A SUBMERGED RECEIVER

$(TD)_i$  = Time dependence for each single process

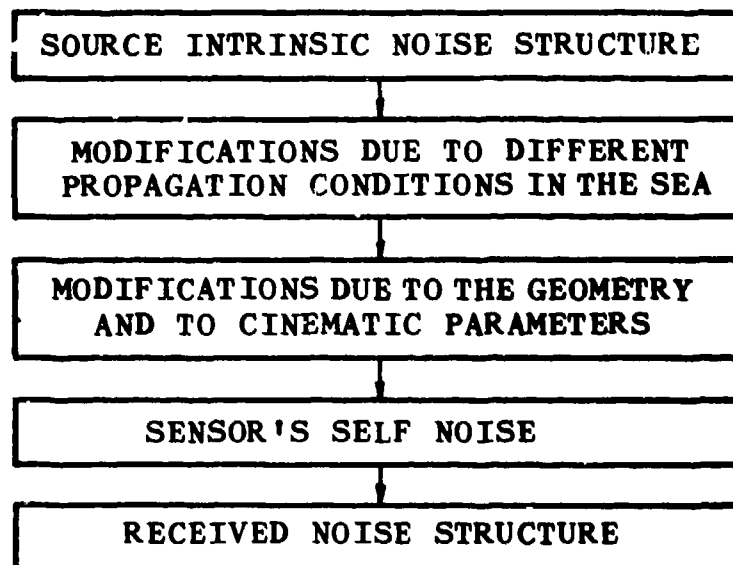


Fig.2 IMPLICATIONS FOR EVALUATING THE PROXIMITY-RANGE SHIP NOISE

Diagram illustrating the geometry of a transmitting dipole and a receiving dipole in a coordinate system.

- The **Transmitting Dipole** is oriented vertically along the  $\hat{y}$ -axis.
- The **Receiving Dipole** is oriented at an angle  $\alpha$  relative to the  $\hat{x}$ -axis.
- The distance between the dipoles is  $r$ .
- The position vector of the receiving dipole is  $\hat{r}$ .
- The unit vector along the receiving dipole is  $\hat{l}_{arb}$ .
- The electric field vector at the receiving dipole is  $E_{arb}$ .
- The angle  $\theta$  is defined as  $\theta = \theta_0 - \frac{\pi}{2}$ .
- Other labeled points and vectors include  $x_0$ ,  $x_{arb}$ ,  $r_0$ , and  $\theta_0$ .

Figure 1 is a graph showing the ratio of the arbitrary scale to the magnetic field,  $\frac{E_{arb}}{M}$ , versus the distance from the source,  $r$ , in meters. The y-axis is logarithmic, ranging from  $10^{-3}$  to 5. The x-axis is linear, ranging from 0 to 150 m. Two curves are plotted: (a) PERPENDICULAR COURSE ( $\theta = 90^\circ$ ,  $\phi = 180^\circ$ ) and (b) PARALLEL COURSE ( $\theta = 0^\circ$ ,  $\phi = 90^\circ$ ). Curve (a) is dashed and curve (b) is solid. Both curves show a peak near  $r=0$  and then decay. Curve (a) has a higher peak and decays faster than curve (b).

Fig.4 NORMALIZED FIELD STRENGTH VERSUS DISTANCE ALONG THE  
ARBITRARY LINE,  $L_{arb} \cdot (r_0 = 30 \text{ m})$

38-14

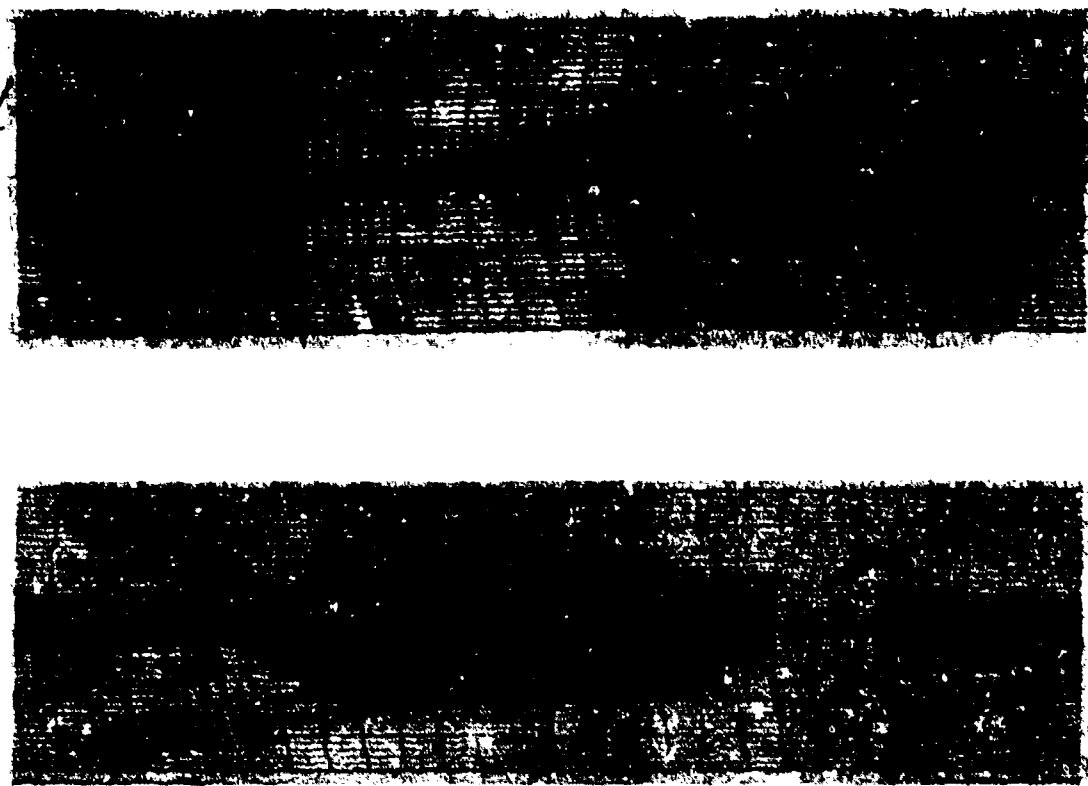


Fig.5 ARTIFICIAL SHIP NOISE RECEIVED BY A SUBMERGED SENSOR  
 5(a) PERPENDICULAR COURSE  
 5(b) PARALLEL COURSE

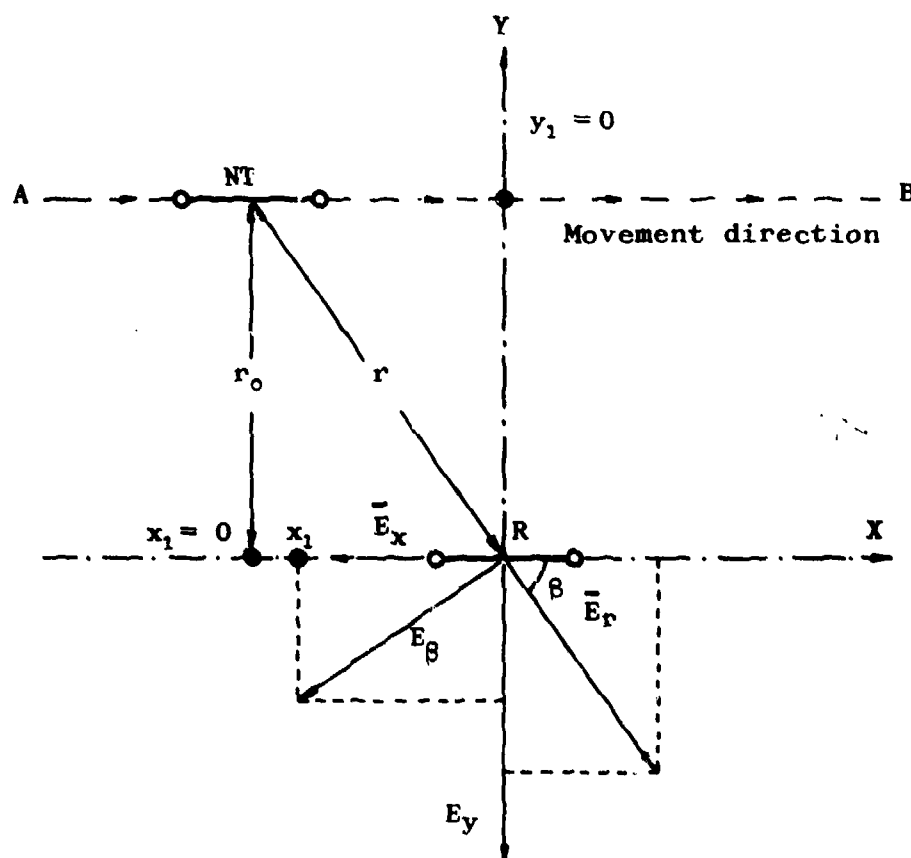


Fig.6 PRACTICAL MODEL (Parallel course)

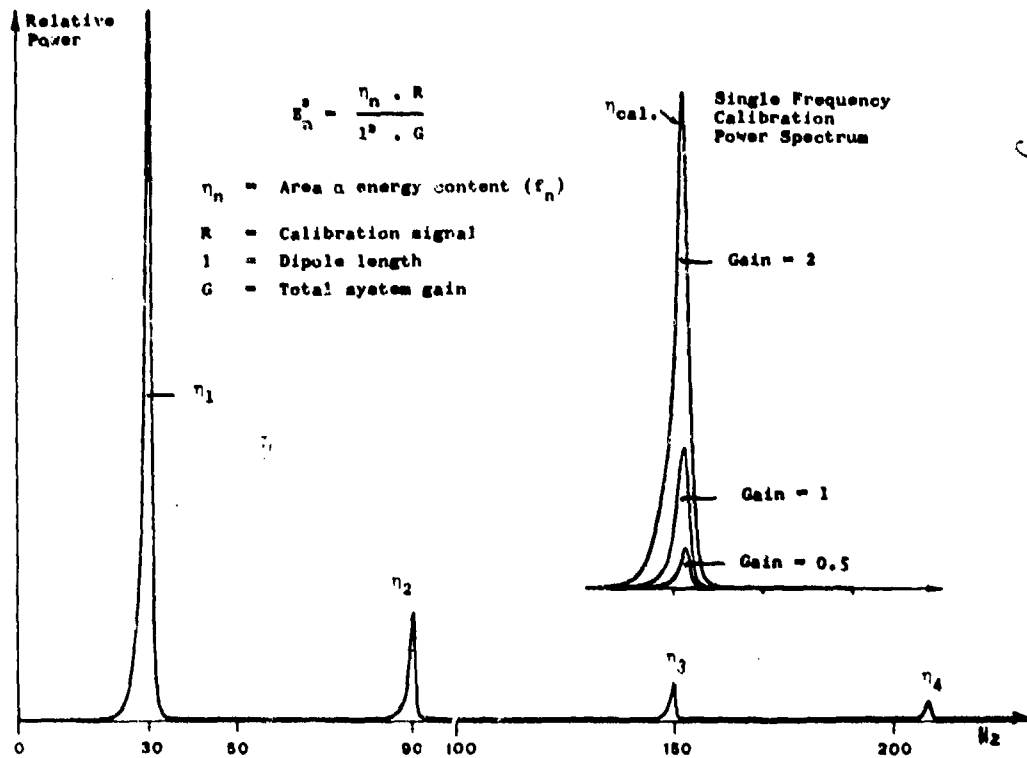


Fig.7 POWER SPECTRUM FOR A 30 HZ RECTANGULAR SIGNAL & CALIBRATION

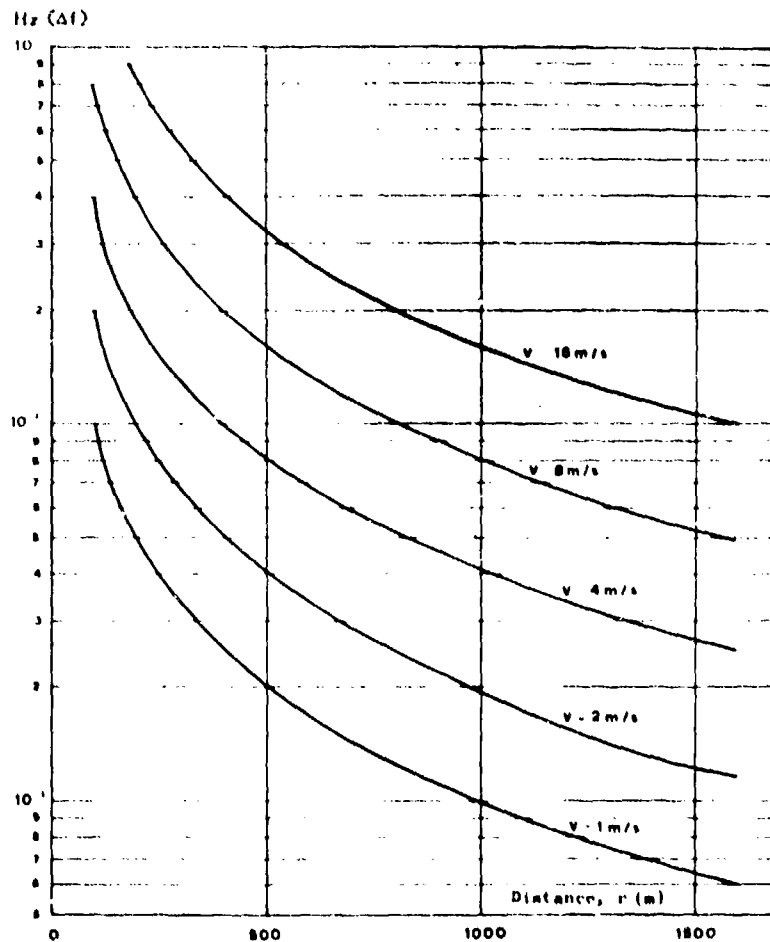


Fig.8 FREQUENCY SPREADING IN FUNCTION OF DISTANCE (r)

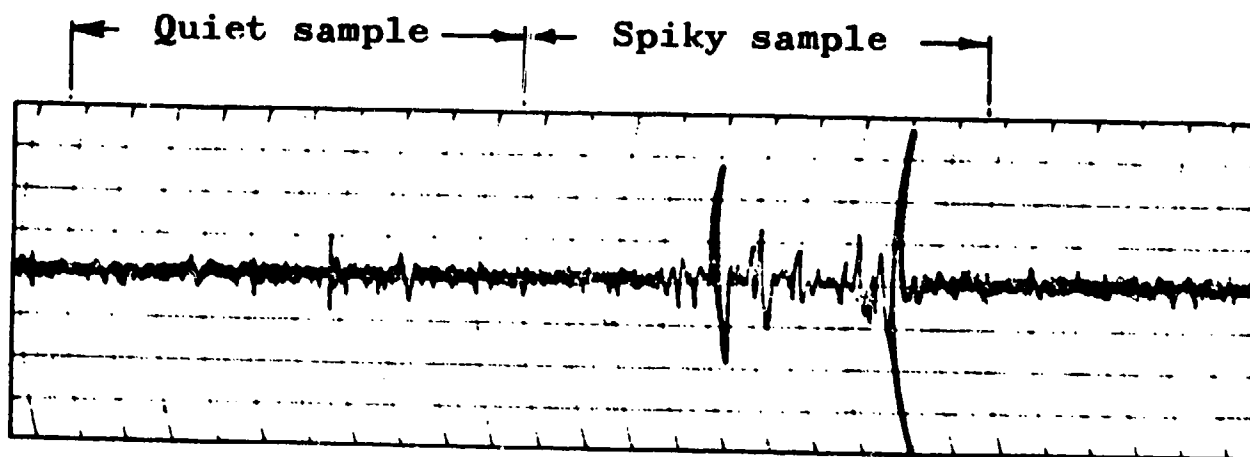


Fig.9 EXAMPLE OF BACKGROUND NOISE

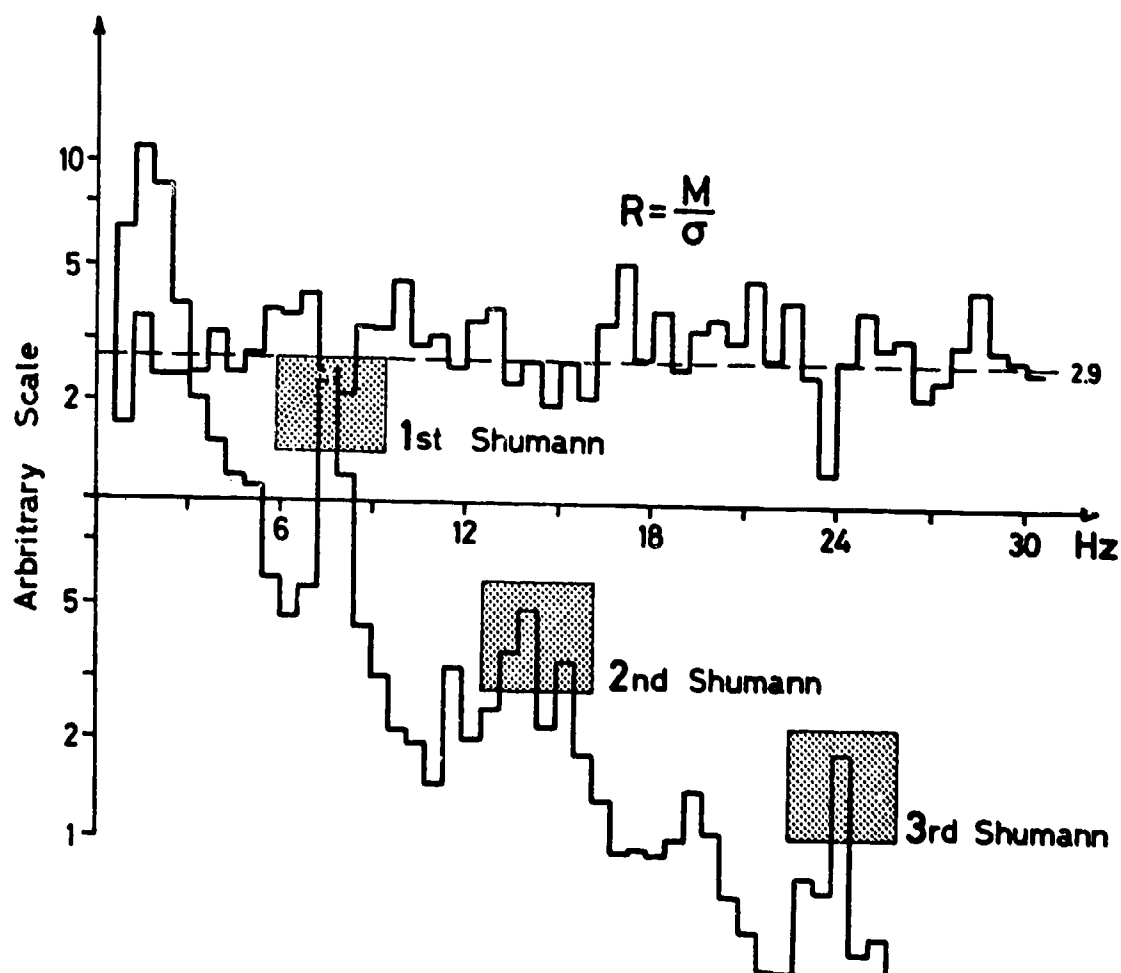


Fig.10 ANALYSIS OF A QUIET SAMPLE  
(G. Tacconi, NATO ASI, Spatind 74)

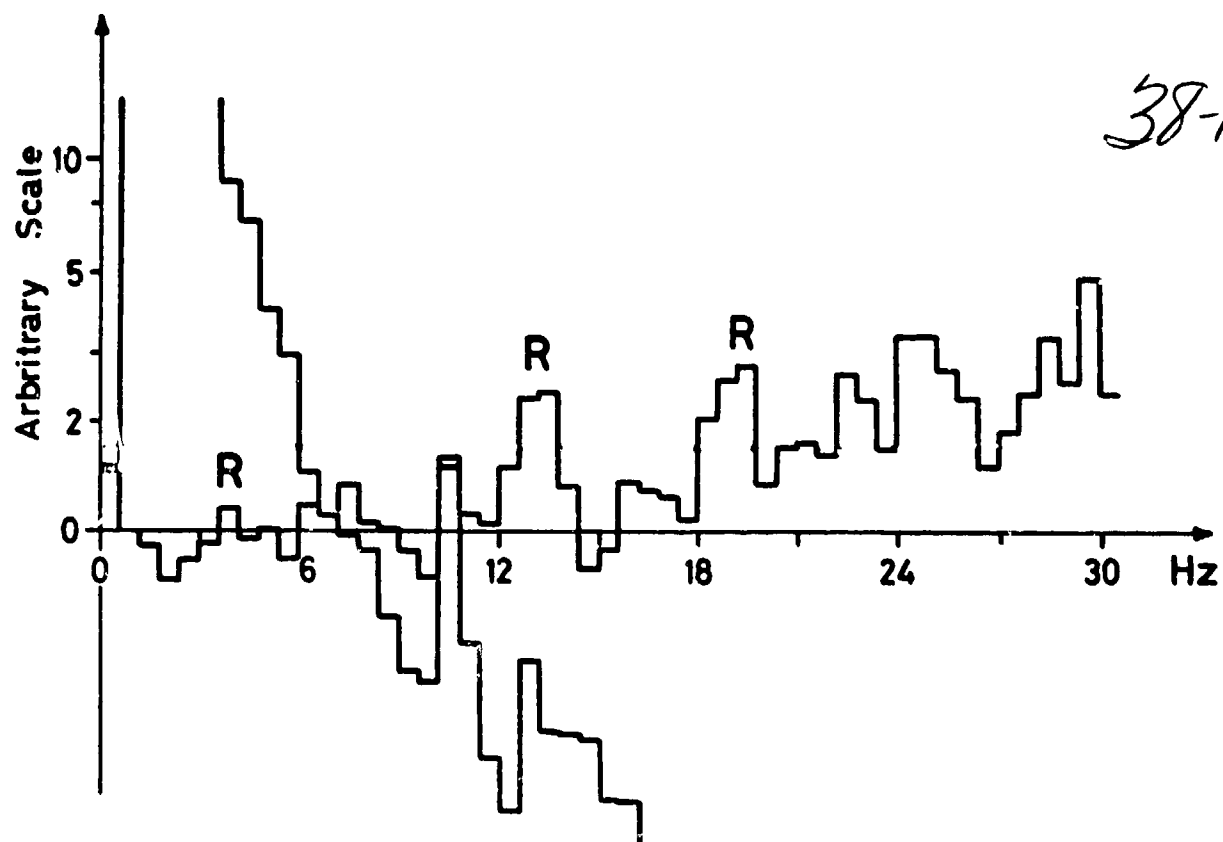


Fig.11 ANALYSIS OF A SPIKY SAMPLE  
(G. Tacconi, NATO ASI, Spatind 74)

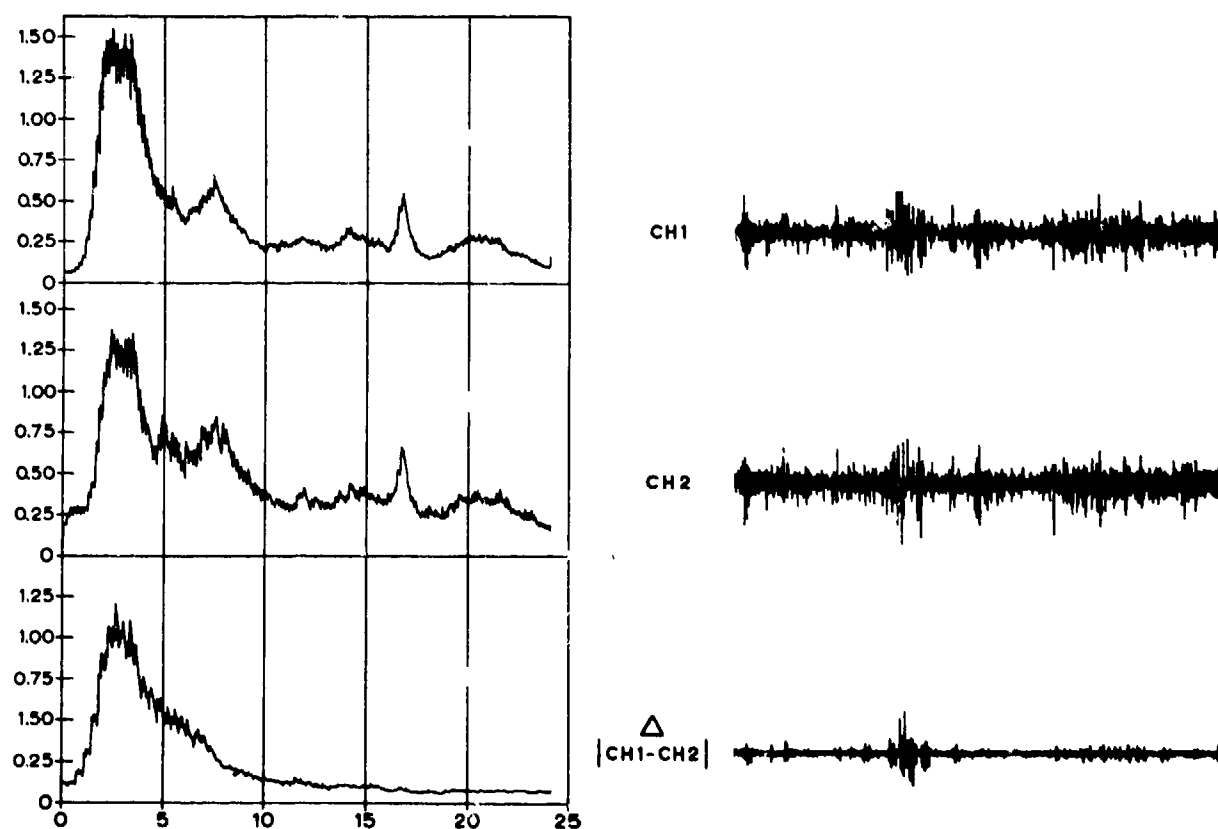


Fig.12 POWER SPECTRA OF FAR-OFF BACKGROUND NOISE:  
TWO SIGNALS AND THEIR DIFFERENCES

# DISCUSSION

G. H. HAGN: You attribute the energy at  $16 \frac{2}{3}$  Hz to train power lines in Norway. The railroads of Central Europe (e.g., Germany) operate on  $16 \frac{2}{3}$  Hz, and perhaps the energy observed in shallow water in the Tyrrhenian Sea comes partly from them as well as from those in Scandanavia.

G. TACCONI: I have not investigated completely the railway power supply distribution in Europe, but further investigation seems worthwhile. Thank you.



# AUTOMATIC TESTING OF AVIONICS SYSTEMS FOR ELECTROMAGNETIC COMPATIBILITY

Edmund T. Tognola  
Jack Rubin  
US Army Electronics Command  
Avionics Laboratory  
Fort Monmouth, NJ, USA

39-1

## SUMMARY

This paper describes a technique of semi-automatic electromagnetic compatibility (EMC) testing that has been developed at the US Army Avionics Laboratory, Fort Monmouth, NJ, USA. The technique was developed to reduce EMC testing effort and to provide a more comprehensive test program. The method used to accomplish the task involves the use of a data acquisition unit integrated into the aircraft avionics and electrical subsystems. This enables the test engineer to gather EMC performance data on the system in its natural environment. The on-board recorded data is subsequently reduced by computer using specially developed programs to determine areas of non-compatibility. The results of the investigation indicate that the technique of using a data acquisition system for EMC testing is feasible and requires less test effort and provides more complete and accurate results than conventional EMC testing.

### 1. INTRODUCTION

The problem of electromagnetic interference or EMI in aircraft systems has increased significantly in recent years due to the rapid growth in the development of complex electrical and electronic equipment now installed in operational aircraft. EMI has become a serious detriment to the operation of aircraft for the military because it degrades reliability and operational efficiency.

EMI can cause a problem in an aircraft due to an interaction between an avionics system or power system and other avionics systems installed in an aircraft. This interaction can produce undesirable effects which degrade the performance of such systems. This degradation results in loss of accuracy of interpretation whether presented orally, visually or mechanically. For example, EMI can cause excessive noise on audio channels, excessive bearing error in direction finding and compass systems, and cross modulation in transmitting and transponder systems.

As we look into the future, it can be assumed that the rapid growth in complexity of the electronic systems on board an aircraft will continue and we will need improved methods for detecting EMI problems in order to achieve electromagnetic compatibility (EMC).

At present, EMC testing of military aircraft generally requires considerable aircraft down time and man hours to accomplish. In addition, the EMC data obtained is often based on the subjective judgment of the person performing the test. The test procedures at present are to operate one equipment while monitoring all other equipments for evidence of malfunction, and to repeat this test so that all modes of operation of the equipments are checked. The testing must consider all combinations of equipments in the source/victim rolls. Because of the large number of different combinations of equipment, considerable time would be required to completely check an aircraft for EMC and the test plan must be compromised in order to select which of the many possible tests will be done in the time available.

In looking for ways to reduce this time and effort, the Army Electronics Command has explored the concept of developing an automated EMC test capability using a data acquisition system. The idea of such a system is to make EMC testing a simple procedure which can be done on the ground or in flight.

### 2. TECHNIQUE

Monitoring of EMC and system performance required provisions for incorporating an onboard EMC performance test system. Properly shielded cabling was run from all test points to an onboard data acquisition unit (DAU). Recording of data was accomplished on a sampling basis using an appropriate tape recording system. Recorded data was analyzed by computer to determine system performance.

The type of data measured automatically by this technique was the electrical bonding of the electronics equipments to the airframe and the measurements of electromagnetic interference data between aircraft subsystems. All tests were performed by the standard manual techniques in addition to using the automated data acquisition system. The data obtained by the two methods was compared.

### 3. DESCRIPTION OF ACHIEVEMENTS

#### 3.1 Bonding Measurements

The automated bonding measurements were made using a Wheatstone bridge circuit with the resistance of the bond as the unknown arm. (ANDERSON, C.F.W., 1974) The data acquisition system compared the unknown to a reference resistance. The manual bonding measurements were made using a Shallcross milliohmmeter. When the data obtained by the two methods was compared, it was found that there was poor agreement between the data acquisition system and Shallcross milliohmmeter bonding measurement values. It was determined that the physical pressure used by pressing the Shallcross probe to the bond actually changes the bonding resistance. It was concluded that the bonding measurements using the automated data acquisition system and the bridge circuit are more truly representative of the actual resistance of a

particular bonding path than measurements made using the Shallcross milliohmometer.

### 3.2 Electromagnetic Compatibility Test Results

39-2 Figure 1 shows a graphical comparison of the automated EMC data and manual voltmeter EMC data taken across the pilot's headset. The graph is a plot of millivolts versus run number where each run is a different combination of equipments keyed, different modes of operation, different tuned frequencies, etc. Each point on the automated data curve represents the absolute average of one thousand samples taken by the data acquisition system. Each point on the conventional curve was taken manually using a vacuum tube voltmeter. A comparison of the two curves shows general agreement to a fraction of a millivolt. The largest variation between the curves is during run numbers 27, 28, and 29 where the separation is about 1.4 millivolts. During these runs the landing light was turned on. The landing light draws more power than any other equipment during the test and it was found that there was magnetic coupling between the landing light cables and the signal leads to the DAU. This caused a slight increase in the recorded signal levels. In future installation, care must be taken to prevent such coupling by keeping signal leads separated from high current cables.

The high peak on run 17 shows interference data when the victim receiver is tuned to the second harmonic of a transmitter.

Figure 2 shows graphical comparisons of automated and manual ambient noise data. This data was obtained with all equipments turned off except the victim. The higher points on the curve (runs 3, 15 and 16) represented tests of the automatic direction finding equipment. This equipment has an untuned crystal detector front end and therefore the ambient noise is higher. This graphical comparison shows good agreement between the data obtained manually and with the data acquisition system.

### 3.3 Transient Testing

Automatic transient testing was accomplished by electronically integrating the short duration transients. This had the effect of stretching the input signal so that the data acquisition system could sample and process it. The automatic system was demonstrated to be capable of measuring EMC transients, and of providing a means of recording such disturbances which is superior to that of the conventional methods.

## 4. DATA COLLECTION SYSTEM DESCRIPTION

For the study in automated electromagnetic compatibility testing a R&D data acquisition system was used. The system, because of its broad capabilities, does not represent the prototype system that is anticipated as the final test system. The R&D system provides the opportunity to gather large quantities of data which completely describes the system performance of the units under test. It is designed to accept a wide variety of input signals, thereby making the system extremely versatile. Because of the capability of withstanding flight conditions, the data acquisition system is able to gather systems data as the test vehicle is flown in its natural environment.

The airborne system consists of the equipments shown in Figure 3. It includes:

- Data Acquisition Unit (DAU)
- DAU Control Unit
- Instrumentation Recorder
- Recorder Control Unit
- High Density Digital Encoder

The functional block diagram of the DAU is shown in Figure 4.

The DAU can accommodate 63 analog inputs, 55 of which can be signal conditioned, 3 synchro inputs, and 22 discrete or bilevel inputs. (VECTOR, 1972)

The signal conditioner is programable to accept analog inputs in several ranges either as a single-ended or differential input and has an independent programable bandwidth.

The conditioned inputs are then multiplexed together with the eight unconditioned inputs by the analog multiplexer. The information is then converted to a digital data word consisting of 10 bits, sign and parity by the analog-to-digital (A to D) converter.

The synchro converters accept a three wire synchro input plus a reference and outputs to the digital multiplexer, a 12 bit digital representation of the sampled angle.

The digital data stream from the A to D converter is multiplexed with the digital inputs from the control unit (elapsed time, event markers and run numbers), the synchro to digital converters, and the 22 discrete inputs. The multiplexed data is then applied to a parallel to serial converter where it is converted into a serial bit stream. The format converter arranges the data words into a predetermined format that is available for recording or transmission to a ground station via a telemetry transmitter.

The basic rate of the sampling system is 720,000 bits per second. This is equivalent to 60,000 twelve bit words per second or 500 frames of 120 twelve bit words. The basic rate can be reduced by a factor of five by an internal switch. A typical data frame as constructed by the format converter is shown in Figure 5. The data as it is recorded is a serial bit stream but for ease of presentation a 120 word data frame is constructed. The serial sequence of data can be visualized by scanning the frame in the same fashion as the written page is read. Several of the inputs are sampled 10 times per frame which is equivalent to 5000 samples per second.

Several sampling formats can be obtained by simply changing a prewired connector on the DAU.

The DAU control unit provides the following functions, controls and displays:

39-3

A deck of 3 thumbwheel switches, entitled WORD SELECT, provides the capability of displaying the sign and magnitude, in bits, of the selected data word. This can be used in airborne operations to monitor the parameters or in troubleshooting procedures to determine if the sampling, digitizing, and formatting is being performed properly. The display is provided by a LED readout entitled WORD DISPLAY.

A deck of 4 thumbwheel switches provides the capability of encoding with the data an identification number that can be used during decommutation and analysis to identify test operations. The switches, entitled RUN SELECT, can be used to identify the pilot, type of test, instrument being tested or any other information that simplifies the identification of the data.

Four separate event marker push button switches are available for noting special events. The buttons can be pushed in combination giving a total of 15 events that can be marked.

An elapsed time generator can be activated to provide timing information in minutes, seconds and tenths of a second. The information is recorded in the data frame. The elapsed time can be stopped and restarted without loss of time or it can be reset to zero at any time.

The magnetic tape recorder is specially configured for the system and has the following features:

- 14 track, record and reproduce heads designed specially for high density applications.
- 2 MHz bandwidth record and reproduce capability
- 24,000 bits/inch tape packing density.
- 1 hour record time per track at the 720,000 bits per second sampling rate.

The recorder control unit provides the operator with speed selection, tape breakage, end-of-tape and tape remaining indication and also provides the normal control functions such as forward, reverse, etc.

The high density digital encoder provides the capability of recording for 1 hour on a single track at the high data rate of 720 kilobits/second. The specially developed encoder permits data to be recorded at a packing density of 24,000 bits/inch on the magnetic tape which can be reproduced with a 1 bit in  $10^6$  error rate.

## 5. DATA REDUCTION

The data reduction system, used to transcribe data from the airborne recorded tape to the computer tape and used to verify the data and perform a limited analysis, consists of the following equipments shown in Figure 6:

- Instrumentation Recorder
- Reproduce/Monitor Unit
- High Density Digital Decoder
- PCM Signal Conditioner
- PCM Frame Synchronizer
- PDP-11 Minicomputer

The instrumentation recorder used for the data reduction system was of the same type as used in the airborne system.

The Reproduce/Monitor Unit and High Density Digital Decoder contain the necessary amplifiers and decoding electronics for reproducing the recorded data.

The PCM Signal Conditioner accepts the incoming serial data stream, rejects accompanying noise and sends the filtered data along with a clock signal extracted from the data to the PCM Frame Synchronizer. The Frame Synchronizer communicates with the PDP-11 Processor through specially designed interface which allows the computer to remotely program the Frame Synchronizer and then provides real time control and data handling. The Frame Synchronizer inspects the data stream for the occurrence of the 12-bit synchronization words. Once these have been found the Frame Synchronizer assembles the incoming data bits into 12-bit words and passes the words in bit-parallel fashion through the interface's direct memory input channel.

The processor in the Data Formatting System determines which of the incoming data frames are desired by monitoring the run code and event markers contained in the data and then blocks the data into logical records, transfers the records to the minicomputer magnetic tape unit, which produces the final  $\frac{1}{2}$  inch IBM compatible 9-track magnetic tape.

## 6. DATA ANALYSIS

Data analysis for the program was performed in two steps. Preliminary review of small samples of data was accomplished during the first step using the PDP-11 minicomputer. With specially developed software, written in PAL-11A assembly language, it was possible to direct the computer to perform such operations as "frame printout", conversion to engineering unit, data listing or calculation of basic information such as averages or root-mean squares (RMS). Having the programs in modular form allowed rapid modification to meet the existing requirements. The programs use less than 6K of the 16K memory.

The specific purpose for the analysis of smaller sections of data was to determine if the data acquisition system, from the input to the instrumentation recorder, was working properly and to determine if the results obtained using the sampling technique compared favorably with manually made readings.

The second step in the analysis of the data involved a complex program written for a high speed digital computer.

A general block diagram of the program is shown in Figure 7. The program reads in and stores large quantities of data used to determine the ambient conditions. Additional data is then checked against the ambient readings for an "out-of-spec" condition. If such an "out-of-spec" condition exists, the computer searches the data to determine what radios in the avionics system are on. Upon this determination a correlation is performed between the active radios to determine where the interference is emanating. The program could be expanded to include an interference analysis between all avionics and power system equipments.

## 7. CONCLUSIONS

Based upon the results obtained during the test program, it has been determined that the use of an automated system for electromagnetic compatibility testing is feasible if sufficient testing is anticipated to warrant the initial investment in the equipments required. The full impact of costs and a determination of the point at which a system would be cost effective to purchase should be undertaken prior to making a decision to automate all EMC testing.

The test program showed the data could be taken in three main areas: bonding, non-transient EMC measurements and transient EMC measurements.

It was demonstrated that the bridge circuit used in conjunction with the DAS would measure the bonding easier, quicker and more accurately. The readings were repeatable because there was not a varying mechanical load placed on the bond interface by any type of probe. Based on the above information, it was concluded that the technique was superior to the techniques using the conventional method.

It was also demonstrated during the tests that non-transient and transient EMC measurements could be made using the DAS. The transient measuring system required additional circuitry to integrate the transients in order that the data acquisition system could properly monitor and record the data.

All EMC measurements could be accurately recorded during a flight test program which allowed all equipments to be tested in their natural environment.

A more complete test was performed in less time because all equipments were monitored simultaneously. The elapsed time in each test mode was significantly shorter than with conventional test methods because no reading of a meter and recording of data on data sheets was required. The limiting factor in "quickness" of test was the operator's ability to manually select each mode of test. The required data was recorded in less than 5 seconds/mode.

## 8. RECOMMENDATIONS

In order to reduce test time and personnel still further without increasing the complexity of the data acquisition system significantly, the DAU control unit should include a sequencing switch that would operate the run mode and automatically enter event marks to isolate approximately 5 seconds of data. Following the sampling period a ready light could flash on the control unit to indicate the completion of the test mode. The co-pilot could then make the necessary changes in test mode and initiate a ready command via the control unit to start the process again. This added feature to the data acquisition system could eliminate the requirement for the test engineer to fly with the system and would reduce unnecessary test time caused by the required communications between the co-pilot and the test engineer in setting up the test modes.

Although the R&D data acquisition system used in this program was designed to be readily integrated into any of the existing Army aircraft from the OH-6 thru CH-47, it is desirable that the system designed for EMC testing be smaller and lighter so that it could be handcarried to various installations via commercial aircraft for EMC tests. Environmental specifications should be in accordance with existing specifications except for those stated for electromagnetic interference in MIL-STD-461. Because the equipments will be used in testing other equipments for EMC, the requirement for conducted and radiated limits should exceed those stated in MIL-STD-461 by at least 10 db.

Now that it has been determined that it is feasible to use a data acquisition system for electromagnetic compatibility testing, further investigations are planned to determine the characteristics of the prototype unit such as sampling rate and channel capacities. This will include a review of the requirements for existing helicopters and those in the planning stages. New techniques of acquiring data such as an integrator with a sample and hold circuit will be studied to determine the lower limits of data sampling. And as stated previously, a study of the cost effectiveness should be initiated to determine the point at which it is cost effective to automate the tests.

## REFERENCES

1. ANDERSON, C. F. W., Honeywell, Inc., June 1974, Technical Report for Avionics System EMC Test Program, Phases III & IV (ECOM 500 - 37/11).
2. VECTOR an AYDIN COMPANY, October 1972, Data Acquisition System DAS-401 Instruction Manual Volumes I & II.

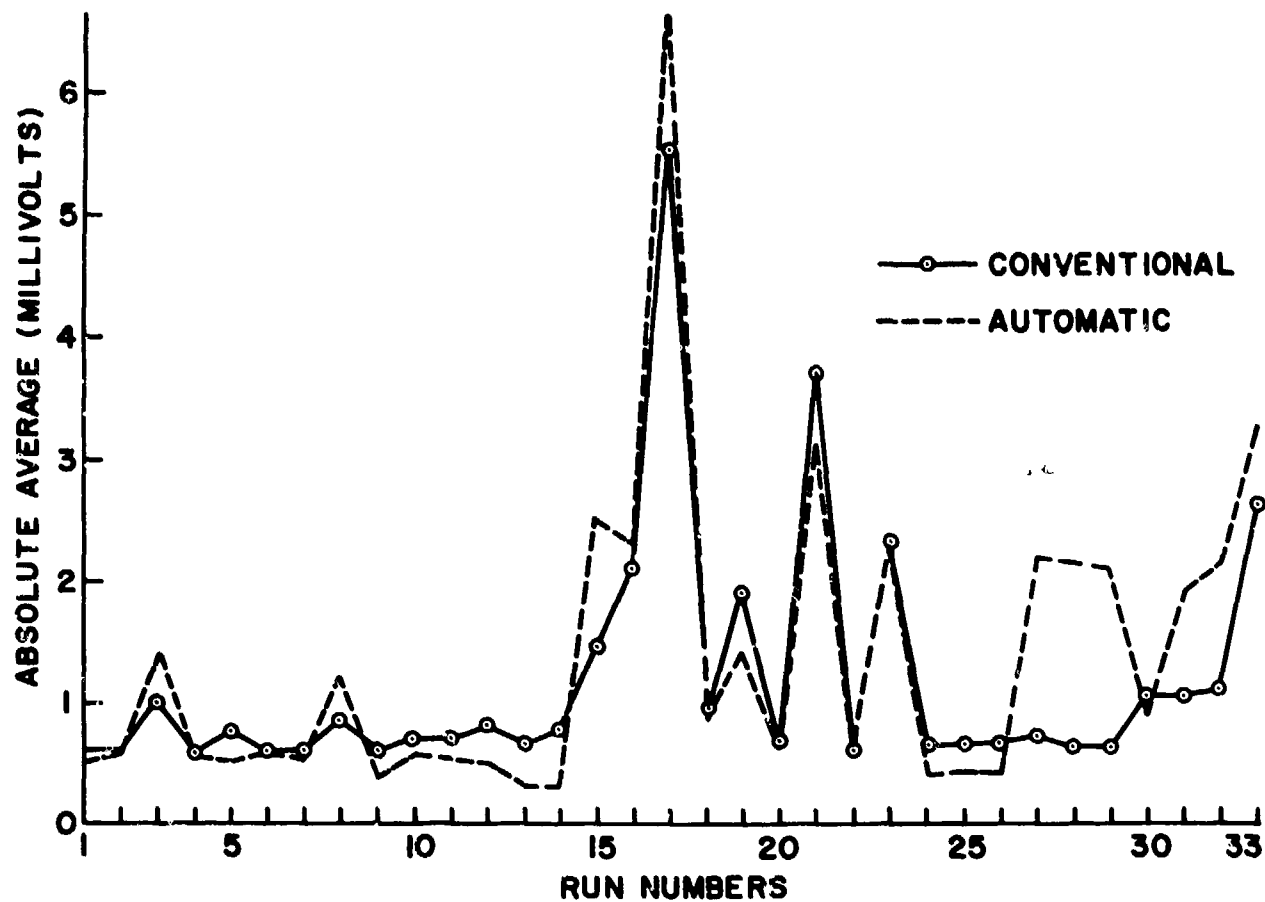


Fig. 1 Comparison of automated and manual EMC data on OH-58 aircraft

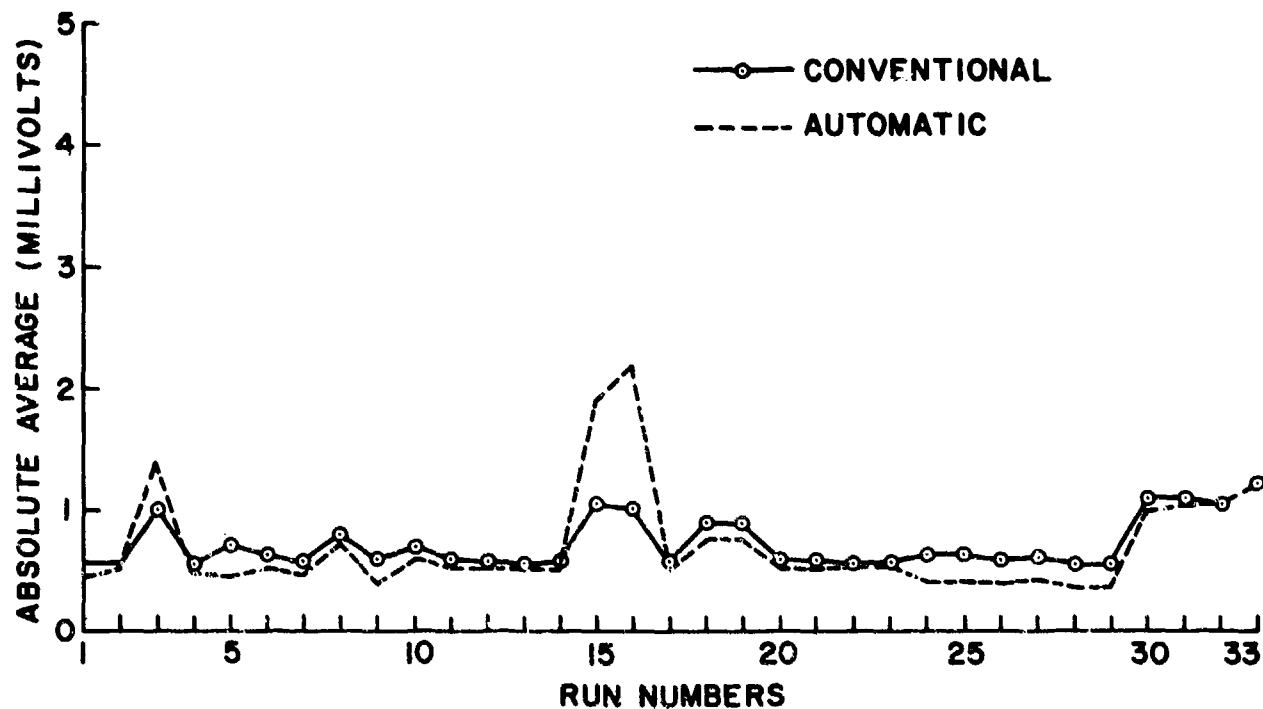


Fig. 2 Comparison of automated and manual ambient noise on OH-58 aircraft

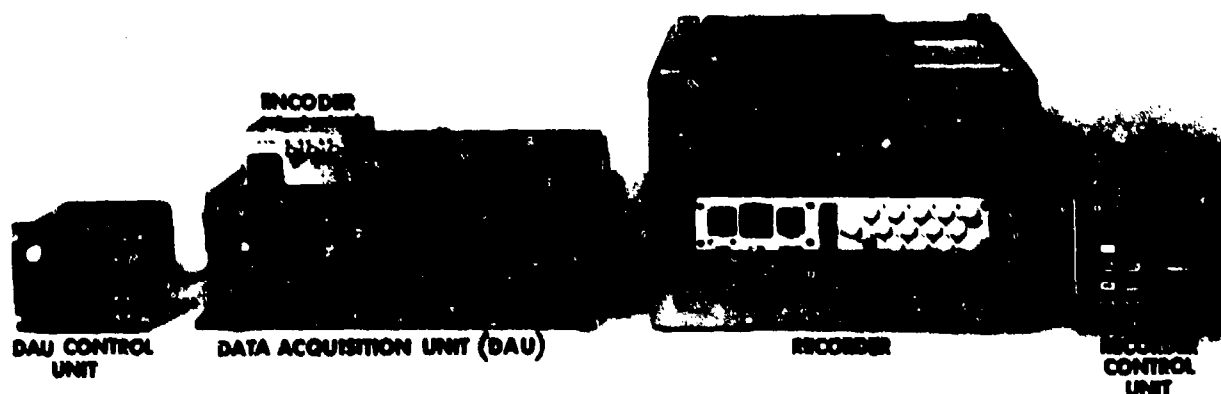


Fig. 3 Data acquisition system

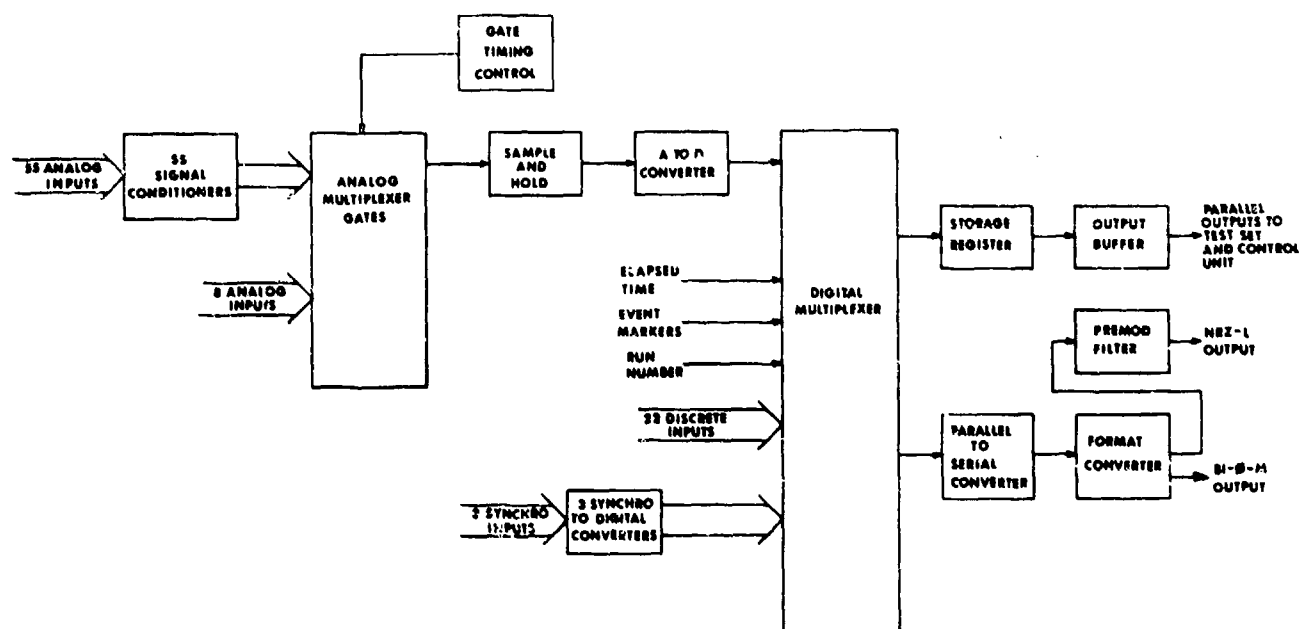


Fig. 4 Data acquisition unit (DAU) functional block diagram

39-8

D1	D2	D3	D4	D5	D6	D7	E9	E10	E11	E1	E2
D1	D2	D3	D4	D5	D6	D7	E12	E13	E14	E3	E4
D1	D2	D3	D4	D5	D6	D7	E15	E16	E17	E5	E6
D1	D2	D3	D4	D5	D6	D7	E18	E19	E20	E7	E8
D1	D2	D3	D4	D5	D6	D7	E21	E22	E23	C	SC1
D1	D2	D3	D4	D5	D6	D7	E24	E25	E26	SC2	SC3
D1	D2	D3	D4	D5	D6	D7	E27	E28	E29	DC1	DC2
D1	D2	D3	D4	D5	D6	D7	E30	E31	E32	DC3	EM
D1	D2	D3	D4	D5	D6	D7	E33	E34	E35	T1	T2
D1	D2	D3	D4	D5	D6	D7	E36	E37	E38	FS1	FS2

#### DAU INPUT CHANNELS

WORD	INPUT
D1-D7	HIGH RATE ANALOG
E1-E38	LOW RATE ANALOG
SC1-SC3	SYNCHRO
DC1, DC2	DISCRETE
DC3	RUN CODE
EM	EVENT MARKERS

#### DAU GENERATED INFORMATION

WORD	FUNCTION
C	CALIBRATION WORD
T1-T2	ELAPSED TIME
FS1-FS2	FRAME SYNCHRONIZATION

Fig. 5 DAU data frame



Fig. 6 Data reduction system



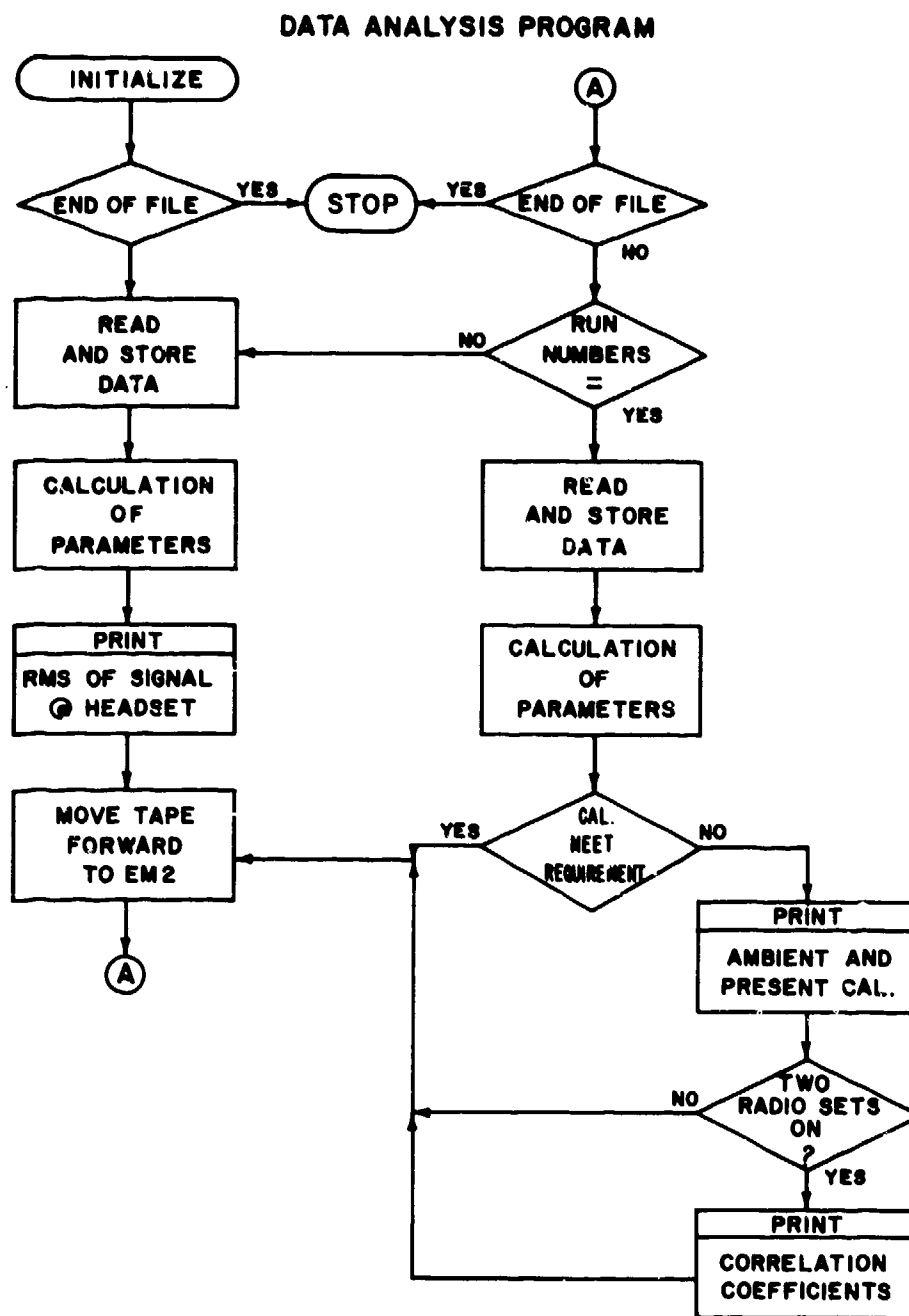


Fig. 7 Block diagram of data analysis program

## DISCUSSION

F. D. GREEN: You used the PDP II minicomputer for initial analysis and a large high-speed computer for final analysis. Did you use a high-speed printer for your initial printout?

E. TOGNOLA: Originally, we had only the teletype input/output. Soon we found that we needed a greater capability, so we added a medium-speed printer (100 characters per second). This has been adequate for the limited analysis performed prior to final data reduction on the IBM-360.

E. M. FROST: We have found it a useful facility to have a time marker or signal available to synchronize and identify separate voice signals on, say, intercom or separate tape recorder. Have you considered providing such a facility on your equipment?

E. TOGNOLA: Yes, but we have rejected the idea totally. The discrete words provide 33 pieces of information as to what is "on" or "off". Also available is the run number and event marker to aid in identifying data or special events. Special comments can also be made by noting the elapsed time and writing a comment on the test plan.

S. C. KLEINE: Do you have any plausible explanation why the deviation between conventional and automatic test results in Fig. 1 at run no. 27-29 and 15-16 in Fig. 2 suddenly increases to -10 db?

E. TOGNOLA: During the test modes for runs 27-29, the landing lights were "on". The input leads from several equipments were routed to the DAUs in close proximity to the cabling for the lights. There was a coupling effect between those cables which gave the higher reading for the automatic method. The manual method did not have any cabling in close proximity to the landing light cable and therefore did not indicate a high level. No investigation was made into the difference in level for runs 15 and 16 in Fig. 2. The difference in the reading was only 1 millivolt and still well within the specification.

H. MAIDMENT: 1) What procedures were adopted to prove the EMC of the instrumentation wiring to the system's test points, both from the point of view of pickup on the lines affecting the recording accuracy and the pickup degrading the system under test?  
2) What effort was involved (in man-hours) in proving the integrity of the monitoring system along the lines of (1) above?

E. TOGNOLA: 1) The system (DAS) was designed to meet the necessary EMC specifications. In addition, the DAU was also housed in a shielded box which was well grounded. The installation was done carefully, making sure the bonding was adequate. All grounds of one type were grounded at a common point and then the common points tied together at a single bus. Any problem that still existed was solved on an individual basis.  
2) Approximately 400 man-hours.

DESIGN OF A COMMUNICATIONS TEST (TEMPEST) RECEIVER  
FOR MAXIMUM BROADBAND DYNAMIC RANGE

J. B. Hager, Project Engineer  
J. C. Jones, Design Engineer  
J. R. Van Cleave, Lab. Manager

Communications Laboratory  
American Electronic Laboratories, Inc.  
Lansdale, Pa. 19426

40-1

SUMMARY

In any receiving system, but especially in communications test receiving systems, dynamic range is a key parameter. A particularly difficult receiving frequency range is 1 kHz to 1 MHz, where unshielded ambient noise intensity is very high, and adequate shielding is impractical. In a high noise ambient, the receiving system sensitivity becomes equal to the ambient level minus the receiving system dynamic range, which is invariably higher than KTB (thermal) noise.

The design of a receiver for maximum performance in detection of broadband signals is significantly more stringent than that of narrow band signals, and requires the techniques described in this paper. Importance is placed on 1) application of successive filtering of the receiver channel and 2) maximizing signal handling capability. The related considerations concerning local oscillator rejection for maximization of tuning range and equipment shielding are also presented.

1. INTRODUCTION

Receivers specifically designed to maximize broadband sensitivity and dynamic range are quite uncommon today, and have recently become important because of the need for measurements out of a screen room in ambients of atmospheric and man-made noise which is essentially broadband.

Broadband signals are altogether different from narrow band signals, and are unrelated to receiver bandwidth. Typical narrow band signals are CW, AM, SSB, FM, etc., and are in general modulations of a carrier. Narrow band signals have a center frequency, that can be tuned through with a conventional superheterodyne and have peak to average power ratios of perhaps up to 10:1.

Broadband signals however are generated by impulse like sources and are emitted only during rapid transitions in the time domain. They do not have a sharp peak frequency in general; their generated spectrum is  $\sin x/x$  in nature, and if generated by fast rise time pulses, can have relatively flat spectra out to several gigahertz. The peak to average power ratios are typically very high because of the duty cycle factor, and may be 10,000:1.

2. GENERAL INFORMATION

2.1 Handling of Broadband Signals

Since the broadband signals have relatively low energy but high instantaneous voltages, they do not always grossly degrade the CW signal to noise ratio providing that the receiver remains linear and does not saturate during peaks.

A key parameter in specifying the performance of a broadband signal receiver is the instantaneous dynamic range as opposed to the CW dynamic range. The instantaneous dynamic range is the ratio of maximum broadband signal that can be handled linearly to the minimum discernible signal, while CW dynamic range is properly defined as the ratio of maximum CW signal level that can be handled without saturation to CW MDS (minimum discernible signal) level. CW dynamic range should be properly measured with both the saturation and MDS test signals in the IF passband. Often, an intermodulation or spurious response level is quoted instead of the saturation level, which is quite proper for multi-channel communication or surveillance receivers, and in fact may result in a lower dynamic range if the test signals are within the RF bandpass. For CW dynamic range measurements, AGC is usually activated, but for instantaneous dynamic range measurements the AGC must be disabled.

For instantaneous dynamic range, it is not possible to arbitrarily specify the saturation signal out the IF or RF passband because the test signal is broadband and covers the entire RF band. Hence, the broadband instantaneous dynamic range test is a true indication of receiver signal handling capability. The test is conducted by connecting an impulse generator, with known flat noise output over the entire RF band to the receiver and recording the saturation to MDS level ratio.

As an example using the AEL LFR-100, the true CW dynamic range is about 70 db. The receiver will handle an out-of-IF band signal of 150 millivolts (or -4 dbm) RMS without saturation in the 20 Hz bandwidth with MDS of about -155 dbm, hence the receiver dynamic range could be specified as 151 db.

For time domain oriented test measurements, the importance of a large dynamic range is made apparent in Figure 1. Here the relative time of impulse arrival is the major element to be detected; yet, the important impulse

(This paper was presented at the AGARD Meeting in Paris, October 1974.)

40-2  
 is much smaller in amplitude than the ambient noise pulse. This is acceptable provided that the receiver does not saturate on the ambient impulse. If the signal of interest were a CW signal, the same philosophy would hold. Hence, a good broadband dynamic range is necessary for reception of any type of signal, broadband or narrow band, in the presence of a high ambient noise level.

## 2.2 Dynamic Range Design Charts

A typical CW dynamic range chart is shown in Figure 2. The CW MDS sensitivity vs IF bandwidth is a KTB relationship and is plotted as a straight line in semi-log graphics. The CW saturation level desired is 60 db above MDS and is also plotted. It can be seen that the receiver must handle a +48 db  $\mu$ V input at 100 kHz bandwidth in order to achieve this 60 db dynamic range without AGC. Since the lowest MDS is -49 db  $\mu$ V, the receiver must be able to handle a 97 db signal range over bandwidth variations. Note that an out-of-doors .25 meter effective height antenna will deliver an ambient peak impulsive output just within the saturation level at the 20 Hz bandwidth operation at a 40 Hz center frequency.

Figure 3 shows a typical impulsive dynamic range chart. Note the MDS level is lowest at the highest bandwidths due to the receiver voltage being directly proportional to the IF bandwidth. To require saturation 60 db above MDS in the 20 Hz bandwidth, requires an input signal of 106 db  $\mu$ V/MHz or about 200 millivolts/MHz peak at the receiver input. If the RF bandwidth is 1 MHz, then 0.20 volts peak must be applied to the receiver input in order to produce an output 60 db above MDS. Linear handling of such an input requires a careful receiver design.

## 2.3 Broadband Dynamic Range Design

The placement of gain and filtering is much more critical in the design of a broadband signal receiver than in the design of a narrow band signal unit if maximum signal handling capability is to be realized. It will be shown in fact that the MDS and saturation level criteria which form the upper and lower bounds on the dynamic range are not in sympathy with each other and present conflicting requirements.

An example will illustrate the proper design technique and the possible results if it is not applied. Suppose it is required to design a receiver with a 20 Hz IF bandwidth which must provide a 60 db instantaneous dynamic range, with a minimum noise level at the IF output of 5 mv RMS, and a receiver noise figure of 6 db maximum. Specification of the bandwidth, noise figure, and minimum IF output level determine the total required receiver gain. Utilizing the equation for thermal, band limited noise, and assuming a 50 ohm source and receiver input impedance it can be determined that the equivalent noise voltage at the receiver input, including the 6 db receiver noise figure, is 4.07 nV. Thus, the receiver gain needed is 122 db. Figure 4 illustrates a block diagram of a typical narrow band receiver. The gain is divided between the RF and the two IF stages and includes any loss or gain for the preselector, mixer or bandpass filter. It is assumed that the filter noise and impulse bandwidths are identical. The minimum detectable broadband signal for our receiver based on bandwidth and noise figure specifications is approximately +46 db  $\mu$ V/MHz. If a preselector bandwidth of 1 MHz is assumed, this input represents an MDS peak voltage of 199  $\mu$ V. The minimum saturation level is 60 db above MDS or an input level of 199 mV peak. The voltage levels at key points are shown in Table A for both the MDS and saturation RF input levels. Note that the peak output of the RF amplifier is 6.28 V. The RF output mixer input level is approximately 20 db above the compression point of conventional double-balanced mixers and the first IF stage output level is perhaps 40 db above the maximum level supplied by conventional semiconductor IF stages. Thus, our receiver is well into saturation and in fact has only 20 db of instantaneous broadband dynamic range.

This example shows the problems encountered when trying to receive broadband signals. The peak amplitude of an impulse is reduced by the ratio of the reduction of the bandwidth in which its energy is confined, 1 MHz/20 Hz or 50,000/1 in our example, thus, if the narrow band IF filtering is not placed early in the receiver and if the RF gain and bandwidth is not minimized, RF, mixer, and IF saturation will occur early. These techniques to maximize signal handling capability that is saturation level, may, however, result in poor sensitivity.

Receiver sensitivity for a given bandwidth is directly related to the overall noise figure. This parameter is a function of the noise figure and gain of every stage per the well-known relation

$$F_T = F_1 + \frac{F_2 - 1}{G_1} + \frac{F_3 - 1}{G_1 G_2} + \dots + \frac{F_n - 1}{G_1 G_2 \dots G_{n-1}}$$

This equation applied to the example receiver is shown in Figure 5. Losses are now assumed for the preselector, mixer, and bandpass filter. Attempting to increase signal handling and capability by minimizing RF and early IF gain ( $G_2$  and  $G_4$ ) will result in an increase in the third, and later terms, while attempting to place the lossy IF filter early in the system will cause an increase in the last term since the gain ahead of the filter will be reduced. Use of a very high Q preselector could be used to improve signal handling capability but may have a high loss and degrade the noise figure severely, and may cause tuning problems particularly if the receiver is to be used at very low frequencies. The requirements for maximum saturation level contradict those for lowest MDS.

A block diagram of a receiver to meet the example specification is shown in Figure 6 with the resulting signal levels shown in Table B. Note that although the gain preceding the 20 Hz IF bandpass filter is the same as in the previous example that the maximum RF output level is 1.1 V and the maximum IF level is 6.3 V. This RF level is easily handled by a high dynamic range double-balanced mixer while the IF level can be supplied by a semiconductor stage. It has been possible to achieve the performance without reducing RF or prefiltering IF gain to unacceptable levels and without resorting to tunable high Q preselection, by utilizing gradual bandwidth reduction. The preselector

limits the broadband energy to 1 MHz, then after 30 db gain the bandwidth is collapsed to 20 kHz and finally after an additional 33 db of gain the bandwidth is established at 20 Hz, the final value. Since all earlier filtering is much wider than the final IF bandwidth, the IF selectivity and time domain characteristics are dependent only upon the final filter. The fundamental idea in understanding the operation of this type of receiver is that the energy and thus peak amplitude of a broadband signal is reduced as the bandwidth through which it passes is reduced. Thus, by alternately filtering and amplifying, it is possible to keep the signal amplitudes within bounds while still achieving acceptable sensitivity and required overall gain. It should be recognized however that signal levels still become larger than normally found in conventional receivers and certain system blocks must in themselves possess large dynamic ranges; for example, the RF amplifier and mixer.

However, increasing mixer dynamic range requires higher LO power, hence more LO signal in the IF stages, which tends to saturate the IF's, etc., unless special techniques are used.

#### 2.4 Extended Low End Tuning Range

One of the inherent limitations of the superheterodyne receiving technique is the inability to receive signals at frequencies less than several IF bandwidths; i.e., less than 300 to 400 kHz for a receiver with a 100 kHz IF bandwidth due to feedthru of the local oscillator. Entry of the local oscillator frequency into the IF section of a receiver through the mixer will generally create one of the following problems: 1) saturation of the IF amplifiers; 2) saturation, desensitization or capture of the detectors.

Saturation of the IF amplifiers as a result of local oscillator feedthru is generally alleviated by a bandpass filter early in the IF. However, as the low frequency tuning range is extended (i.e., the LO frequency approaches the IF center frequency), the oscillator feedthru is attenuated less and less by the bandpass filter skirt and IF saturation ultimately occurs. There are two approaches to limiting this type of IF saturation: 1) steepen the IF filter skirts for improved LO rejection and 2) increase the LO to IF rejection of the mixer.

The choice of IF filter type and shape factor is in general based on the channel spacing and type of signal being received. In the case of broadband signal reception, the time domain response of the filter must be examined closely and most often the Gaussian filter or other combinational types are required for low overshoot. Unfortunately, filter types designed for low overshoot in the time domain do not exhibit low ratio shape factors. The typical shape factor of a Gaussian type filter will be in the area of 3:1 (6 to 60 db) or greater. If the use of a filter type with a high ratio shape factor is required by other system constraints, then the designer must look elsewhere for possible LO rejection.

Another area for increasing the rejection of the oscillator into the IF amplifiers is the mixer itself. Standard double-balanced mixers provide LO to IF rejection in the range of 25 to 50 db. If a high dynamic range mixer is being used with a 1 db compression point of +15 dbm, then an oscillator power of about +20 dbm is required. For a typical 25 db LO to IF rejection, the resultant entry of a -5 dbm signal into the IF places severe requirements on the bandpass filter to prevent saturation. A recent AEL development has resulted in a high dynamic range mixer circuit with 95 db LO to IF port rejection. This rejection allows lowering of the tuning range without impossible restraints on the filter shape factor.

Receiver shielding and grounding are as important as the filter shape factor. A brick wall filter will be of no value if the LO is allowed to radiate into a following stage or if circulating ground currents are present, thus bypassing the filter rejection. With high dynamic range mixers requiring high LO power, the importance of eliminating circulating ground currents cannot be emphasized enough. Isolated signal and DC ground returns should be provided wherever the possibility of ground currents mixing is present.

For VLF receivers the use of high permeability magnetic shielding with copper-nickel or copper chrome plating should be recognized as an effective method of containing the LO and other undesirable signals.

The low frequency tuning range may be extended to 1:1 tuned frequency to bandwidth ratio by use of these techniques.

### 3. CONCLUSION

We have presented the reasons why receiver broadband dynamic range is of such importance when considering the ambient signal "pollution." After emphasizing the importance, then the design considerations to achieve this broadband dynamic range were described. The concept treatment of broadband signals is becoming widely applied, yet, receiver techniques for maximizing performance are relatively unknown and quite rare. Little mathematics is useful; explanation and example provide the necessary insight.

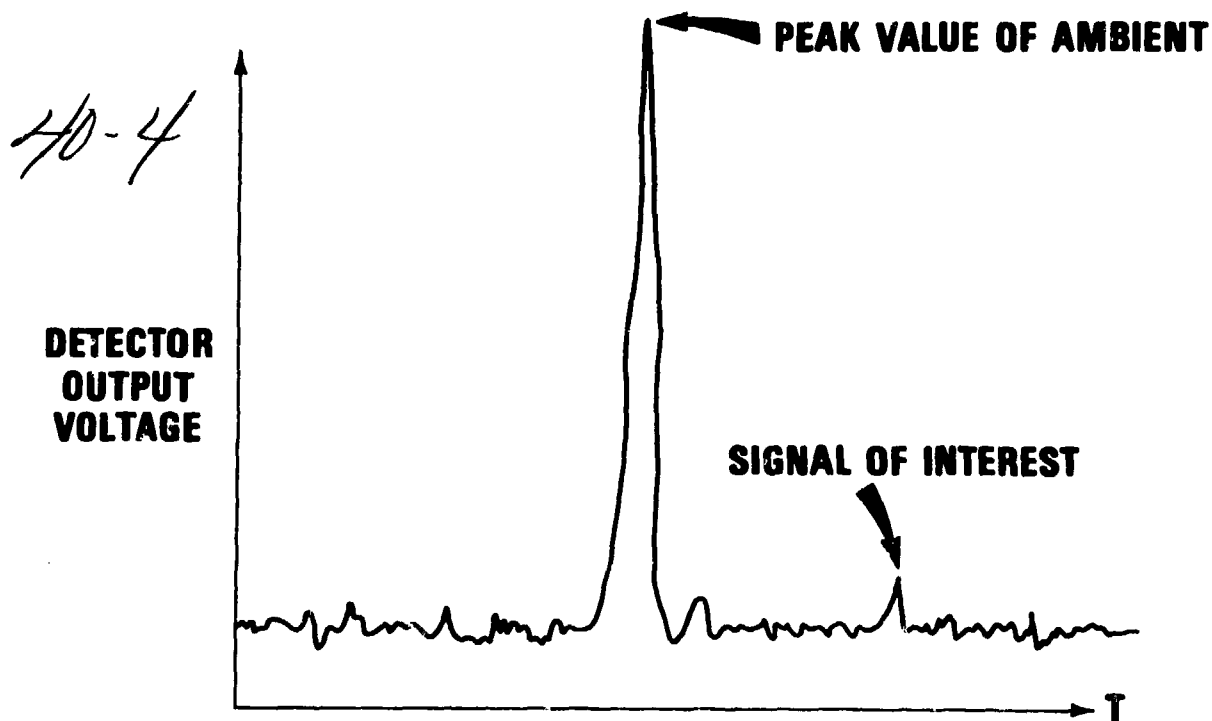


Figure 1. AM Detector Output in Time Domain

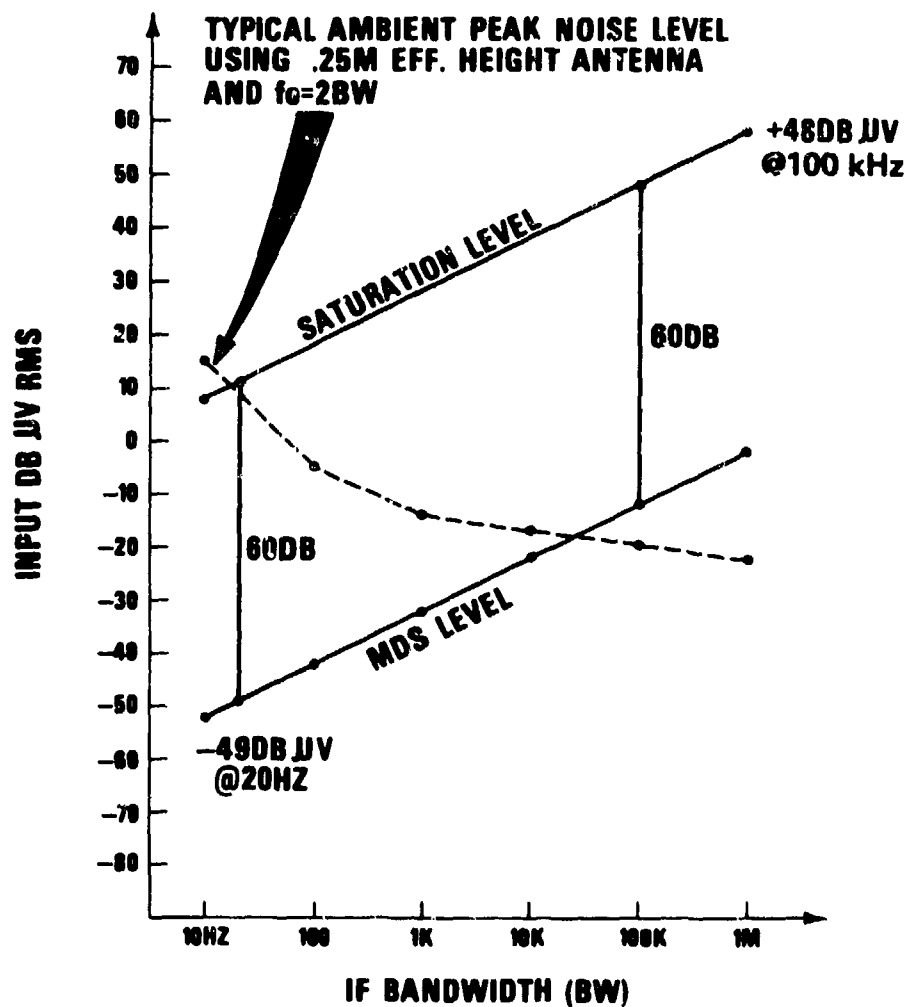


Figure 2. Dynamic Range Requirement 60 db CW

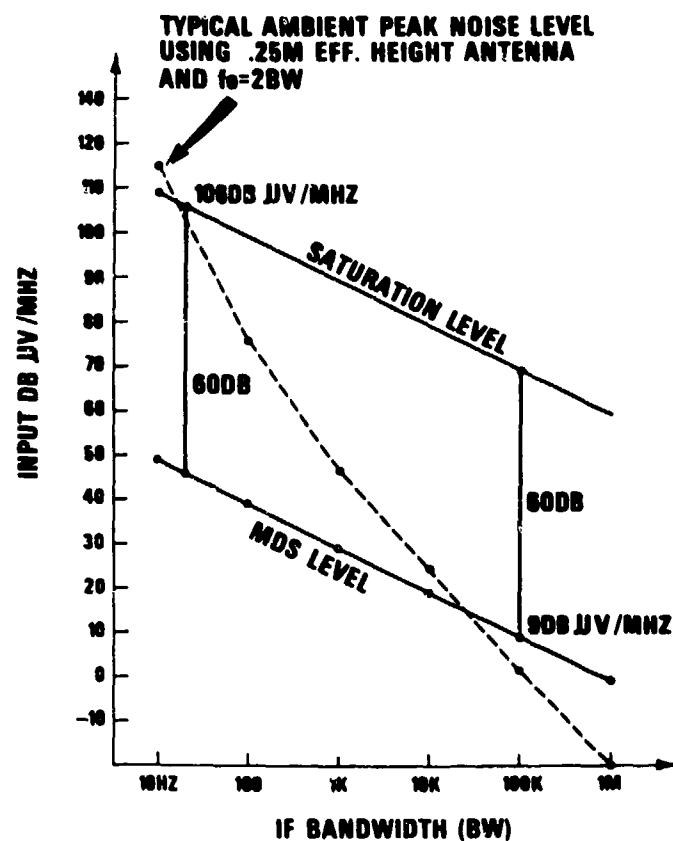
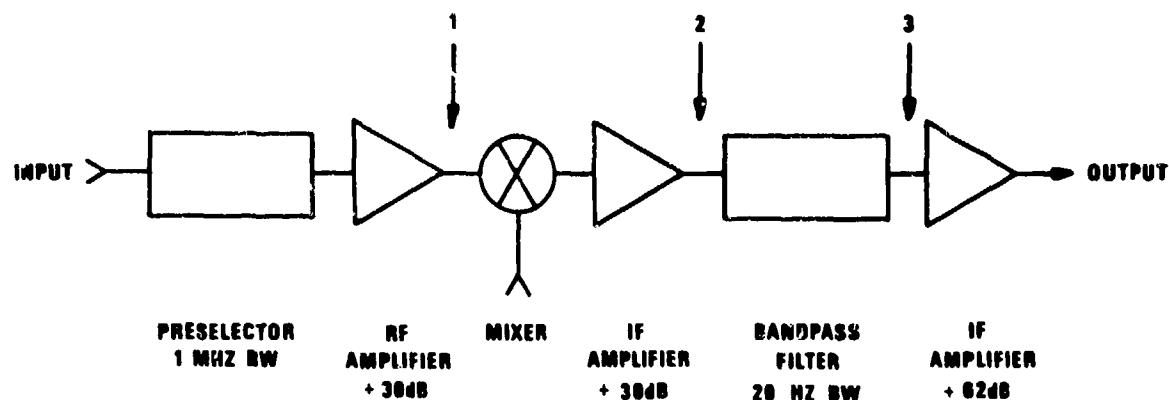


Figure 3. Dynamic Range Requirement 60 db Impulsive

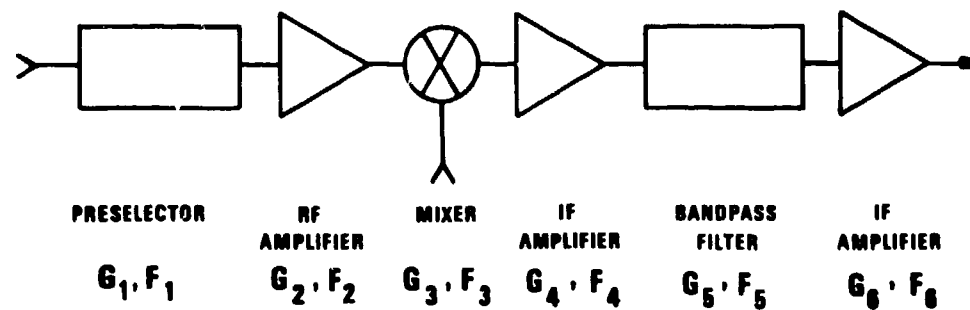


INPUT	1	2	3	OUTPUT
199UV	6.28MV	199MV	3.97UV	5.8MV
199MV	6.28V	199V	3.97MV	5V

TABLE A.

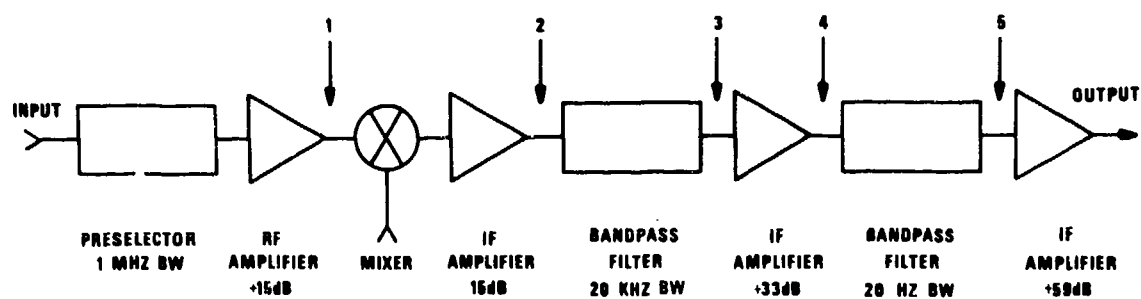
Figure 4. Typical Narrow Band Receiver

Table A. Receiver Signal Levels



$$F = F_1 + \frac{F_2 - 1}{G_1} + \frac{F_3 - 1}{G_1 G_2} + \frac{F_4 - 1}{G_1 G_2 G_3} + \frac{F_5 - 1}{G_1 G_2 G_3 G_4}$$

Figure 5. Noise Figure of a Superheterodyne Receiver



INPUT	1	2	3	4	5	OUTPUT
100UV	1.12MV	6.29MV	126UV	5.62MV	5.62UV	5MV
100MV	1.12V	6.29V	126MV	5.62V	5.62MV	5V

TABLE B.

Figure 6. Broadband Receiver

Table B. Receiver Signal Levels



# A STRAIGHT FORWARD COMPUTER ROUTINE FOR SYSTEM CABLE EMI ANALYSIS

by

M. Russo and O. Hartal  
Armament Development Authority,  
Ministry of Defense, Israel

41-1

## SUMMARY

In this article we have endeavoured to present the method we adopted to provide harness compatibility in a complex system, the design of which was time limited, and EMC requirements had to be generated in a hurry. The method outlined provides a way whereby engineering effort and a computational backup check are combined to generate the EMC requirements in as short a time as possible.

The data reduction phase is simple, time and effort saving and may be performed, after the primary effort phase, by non-EMC-skilled workers. The method as such is system oriented, and not general, and so meets the requirements of a specific design problem. On the basis of this concept, other programs can be developed to meet various other harness EMC problems.

It is hoped that the method outlined in this article will be of aid to EMC engineers confronted with the same type of problem.

In complex systems utilizing electronic hardware with interconnecting cables, interference to system operation may arise due to inter-wire coupling in the harness. An early estimate of the intercable EMI is essential to the successful completion of the system design.

Computerized methods for the achievement of this goal have been developed previously by various companies. References:

- (1) Intrasytem EMC in large aerospace systems - J.A. Spagon TRW systems.
- (2) Intra-vehicle EMC analysis - Dr J. Bogdanor et al. McDonnell Aircraft Co.

The advantage of the method described in this paper is in enabling the designer to obtain an estimate of the EMI in his system harness with a minimum knowledge of system and wire parameters. Data reduction on the CDC 6600 computer points out cases of expected interference in as many as 1000 wires in a harness. The analysis uses single number coupling parameter for typical wire and signal cases in the system to be analyzed.

Such a method is essential in the development phase when time is a factor and not all data is available.

The method may be extended to include more accurate wire coupling models and system susceptibility and interference parameters.

## FOREWORD

In complex airborne systems utilizing electronic hardware with interconnecting cables, and where space is limited, dense harness configurations are conducive to intra-wire coupling with resultant degradation of system performance.

The design of such an airborne system should bring this factor into consideration and provide EMC requirements on wire types and routes.

To this end an analysis of intercable EMI should be performed. An accurate analysis requires knowledge of all parameters, electrical and mechanical, governing the coupling between wires. It also requires a good knowledge of the system's electrical parameters.

Gathering all this information and processing it is a time consuming effort of skilled EMC personnel.

The problem has been dealt with in two major works, by TRW systems and the McDonnell Aircraft Co. The method used in these programs, which are general in type, require the data base of wire and system parameters

mentioned before; we estimated that the time and effort required to perform an analysis according to these references would be prohibitive and so we decided to relax on the accuracy and generality of the analytical method, and concentrate our efforts on a simple worst case EMI analysis which would provide the required results with a minimum effort of skilled personnel.

41-2 In striving to meet the EMC requirements of the system, a work procedure was set, with the following major steps; listed in Figure 1.

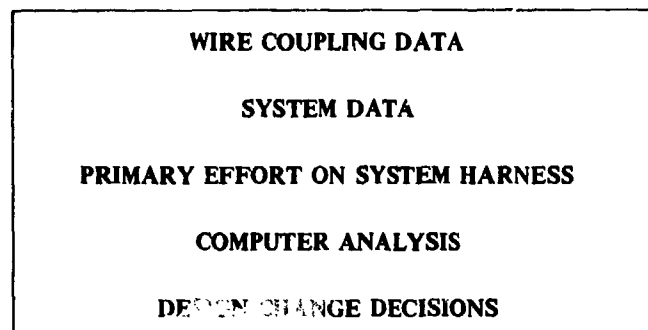


Figure 1

First, the existing data on cable to cable coupling from various references was reviewed, and was adapted to the system requirements, when specific data was unavailable, laboratory measurements were performed to provide it.

Next, all pertinent EMC data on the system, such as susceptibility levels, out-put voltages and currents load and generator impedances, harness layouts ETC, were gathered and depicted on the wiring drawings of the system.

The following step was to use the coupling data from the first step and good engineering practice, and assign wire types to each wire in the system. This is the primary effort on system harness.

All these steps required no computer involvement.

To check upon the engineering work performed in the primary effort step, the computer program was developed in view of providing a rough estimate of the EMI existing in a specific harness.

Upon receipt of the output of the computational step, the design engineer is able to scan through the results and pick up both cases of over design and those of probable interference and generate the required fixes.

We will now proceed and describe these work program steps in some detail.

Upon analysing a given system, typical cases where cable coupling may be a problem can be found. These cases cover about 90% of all wires included in the system. As an example, power lines, ac and dc, relay and solenoid lines are sources of interference to analog, digital and audio signal lines. These typical cases generally have typical parameters, geometrical and electrical.

For instance, power line impedances, being in the  $10\Omega$  range, digital and audio, in the  $K\Omega$  range, wire types can be unshielded in the power, shielded in the audio and twisted, or twisted-shielded in the digital line case.

A worst-case estimation of cable coupling can be provided, based upon analytical and experimental data from sources listed in the bibliography, or obtained from laboratory measurements.

#### WIRE COUPLING DATA

To provide the worst-case estimation of wire to wire coupling use was made of analytical and empirical expressions of the electro-magnetic energy transfer between adjacent wires over a conducting ground plane. From the models developed in references we find that the parameters governing the coupling may be divided into two categories, geometrical and electrical.

The geometrical category consists of cable properties such as wire and shield dimensions, twists per unit length, spacing between wires, common run length, height above ground plane, ground points etc.

Electrical properties dependent on geometrical ones are wire and cable impedances, mutual inductance and capacitance. Independent electrical properties are interference and susceptibility spectra and termination impedances. Determination of the degree of coupling existing in a harness should take account of all these parameters.

The dependence of coupling on geometrical and electrical properties of cables and circuits involved, will lead us to choose as fixed, a number of these properties which give the worst case condition, while other properties are chosen to fit the typical coupling case under consideration.

As an illustration of this approach let us examine the dependence of geometrical properties on the coupling.

In Figure 2 we notice that almost no change in coupling is evident above a height of 2". Also, the wire type combination involved in the coupling has a profound effect, as we see, on the degree of coupling. This is a variable factor and must be determined for each wire type combination.

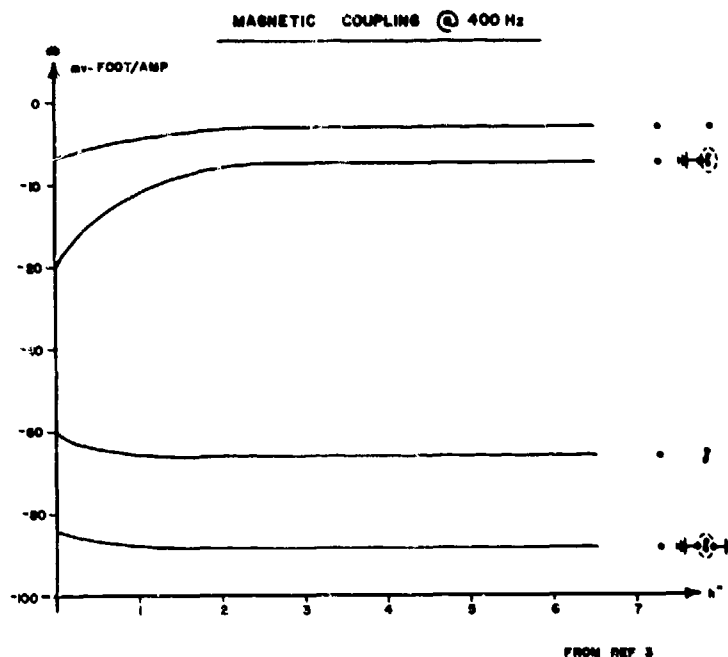


Figure 2

As the figures describing the degree of coupling existing between wires and the effect of geometrical and electrical properties vary to some extent among the referenced documents, caution was used when choosing a coupling parameter for a specific case, and when data was insufficient, laboratory measurements were performed to provide the required information.

#### THE METHOD USED IN THE ANALYSIS

All wires in the system were divided into four categories:

- AC power,
- DC power,
- Pulse circuits,
- Sensitive circuits.

These categories were assigned the following fixed properties:

- (1) Mechanical — Height above ground plane is 2".  
Spacing — Adjacent.
- (2) Wire type and electrical — as in Figure 3.
- (3) Coupling parameters — as in Figure 4.

414

CAT PROPERTY	AC POWER	DC POWER	PULSE	SENSITIVE
IMPEDANCE	100Ω	100Ω	2KΩ	4KΩ
WIRE TYPE	•	•	•	• 8 (•) (•)
	115V 400Hz AND 25V 0.5ms TRANSIENT	400Hz 2V AND 400V SPIKE AND 30V 0.5ms TRANSIENT	5V TTL PULSE	0.5V PEAK (DIGITAL) OR 5mV PEAK (OTHER) 30 AMP-METER TRANSIENT

Figure 3

The coupling parameters assigned to the various cases in the system:

SOURCE OF INTERFERENCE			VICTIM		COUPLING PARAMETER db/METER
CIRCUIT TYPE	WIRE TYPE	SIGNAL	CIRCUIT TYPE	WIRE	
AC POWER	•	400Hz 115V	SENSITIVE - AUDIO, ANALOG DIGITAL, EED	•	50
					70
				(•)	60
				(•)	
LOGIC	•	5V TTL PULSE	-H-	(•)	80
				•	30
					50
				(•)	40
AC, DC POWER	•	MIL-STD-704 TRANSIENT	-H-	ALL	30 AMP-METER MIL-STD-401 R502
					MAX ALLOWED INTERFERING CURRENT
DC POWER INTO RELAY		400V SPIKE (TYPICAL)			

Figure 4

In all cases, the interfering wire was chosen to be a single unshielded wire which is generally the case for AC, DC and relay circuits.

After these parameters have been set machine computation is performed on the following:

- (1) Common run length between sensitive and interfering wires.
- (2) Interference pickup from each AC carrying wire.
- (3) Comparison of pickup to susceptibility level.
- (4)\* Summation of all AC pickup, and comparison to susceptibility level.
- (5) Transient interference current in interfering wire.
- (6)† Interference pickup from each transient carrying wire.
- (7) Comparison of transient pickup to susceptibility level.
- (8) Print-out.

41-5

In order to perform these computations a first over view of the proposed wiring in the system to be designed must be performed. This is done in the primary EMC effort in the harnesses, which will be detailed in the following chapter.

Upon completion of computer run on the data, the EMC engineer will have to decide on remedial measures when cases of interference are spotted. These measures include sensitive and interfering wire type changes and common run length shortening. These can be performed either manually or automatically.

#### PRIMARY EMC EFFORT IN HARNESSES

Given a project in the design stage, all wiring diagrams were reviewed and each wire was categorized as mentioned above and when not limited by equipment or manufacture constraints, was assigned a wire type according to good engineering practices. As an example, audio lines were twisted shielded pairs, power lines were twisted whenever possible etc. Upon completion of this task, all data required for the analysis such as wire category and type, harness layout with dimensions, were punched on computer data cards (see Figure 5 overleaf).

#### THE COMPUTER PROGRAM

The aim of the computer analysis was to point out possible cases of interference after the primary effort had been completed, and to enable the designer to estimate if the case was really a problem and to choose a fix when necessary.

The program is constructed of three major blocks:

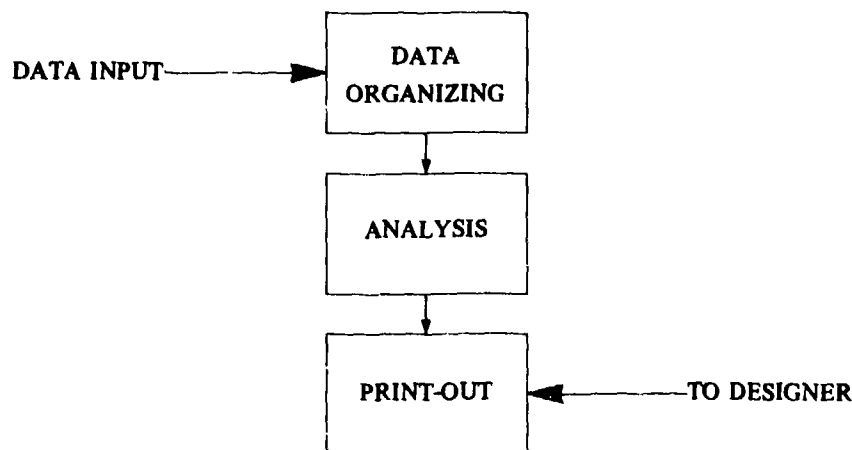


Figure 6

\* We have assumed here that all AC interfering currents are in phase, which may not be the case, but is in agreement with the worst-case trend.

† In this analysis we have assumed that transients do not occur simultaneously and that one transient pickup above the susceptibility level is not allowed.

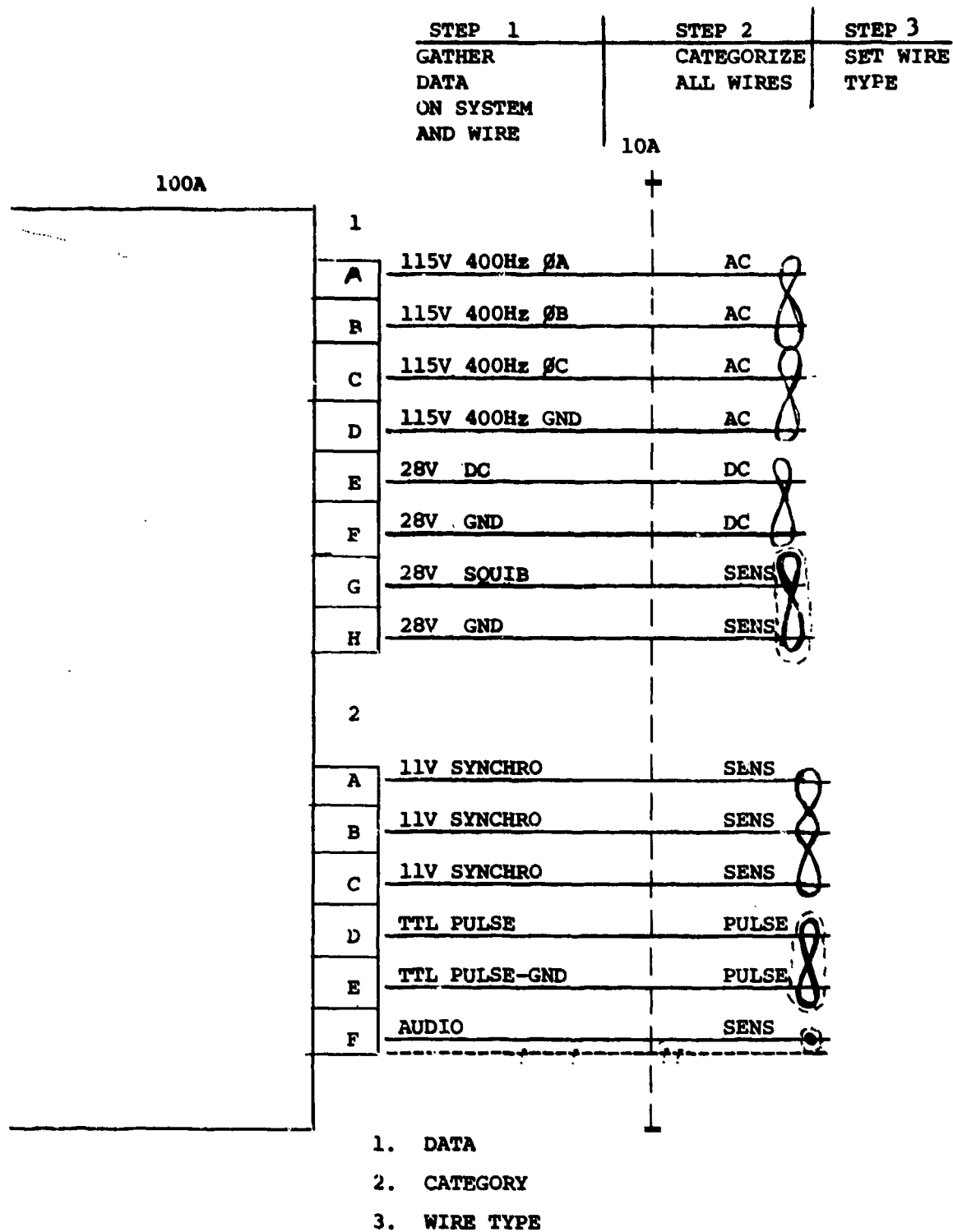


Fig.5 Primary EMC effort

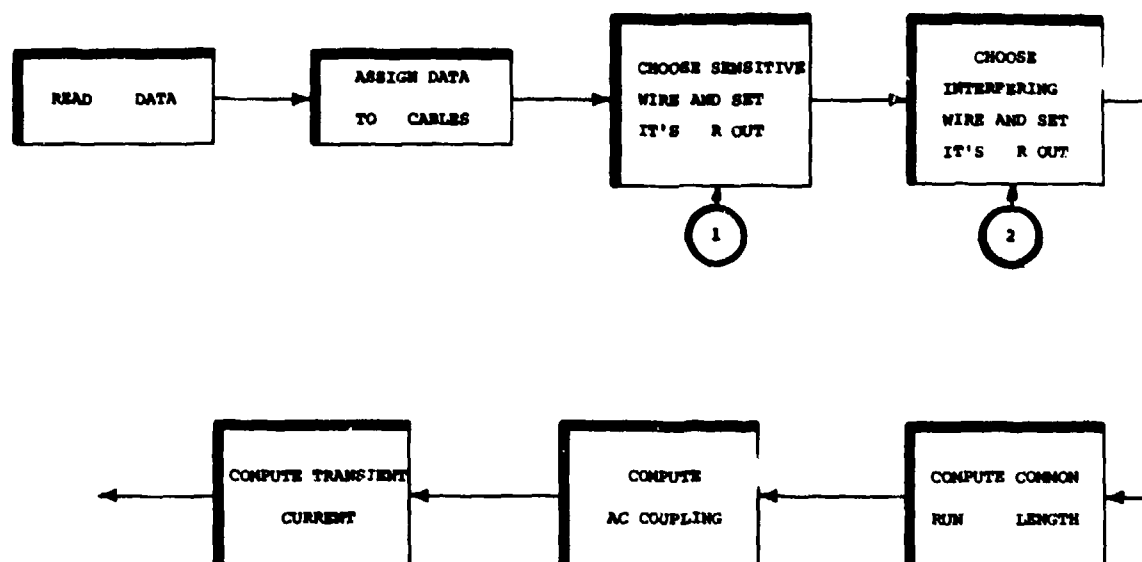


Figure 7

The first step is the reading of wire data from the punched cards. This data includes end point designators, wire type, and category. These cards also include the topography of the harnesses, with branch lengths and designations.

Next, each wire data is stored in the computer memory according to the cable to which it belongs.

The computational phase starts with a run through the first cable wires and stopping at the first sensitive wire encountered and setting its route according to the wire and harness data.

The first interfering wire is selected and its route is determined according to the wire and harness data.

The common run length is then computed. This is the only coupling dependent factor that is computed in this analysis, all other factors have been set according to category.

Following this step, the 400 Hz AC coupling is determined and stored.

The transient current, based upon the relay operation spikes, MIL-STD-704 transients, and the load resistance of the interfering wire is then computed.

If the common run length exceeds 1.5 m the transient current times length is then computed and stored, if common run length is less than 1.5 m the program continues to the next step.

If the interfering coupled AC voltage is above 6 db below the susceptibility level of the sensitive wire, it is then compared to the susceptibility level and if it is below this level, the interfering coupled voltage from this wire is printed with an addition o.k on the same line.

If the AC voltage transfer is below 6 db margin, the next phase is the summation of all contributions to this type of interference.

When the interference from a single wire exceeds the susceptibility level, a print out of this voltage is followed by the word "check" to alert the EMC engineer to a possible case of interference.

A summation of all AC coupled voltages to the sensitive wire is compared to the susceptibility level and a print out with o.k or "check" is generated, dependent on the resultant coupled interfering voltage.

A similar procedure is applied to the transient interference case. The basic difference being the assumption that transients do not occur simultaneously and may be dealt with as separate sources.

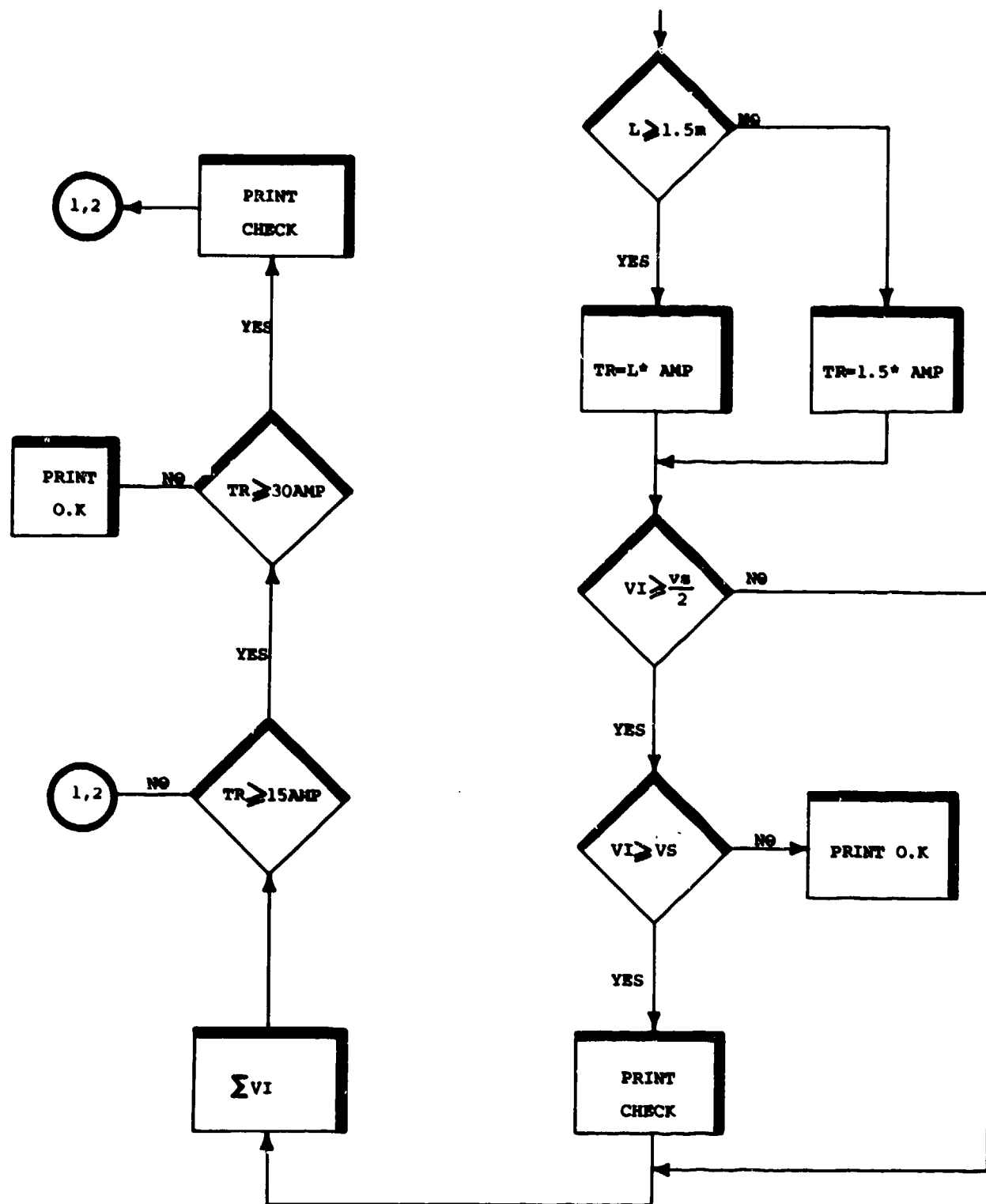


Figure 8



The transient current computed in an earlier phase of the computer program is now compared to a maximum allowed interference level of 30 amp-meter, as per the MIL-STD-461 limit of RS02. A 6 db margin is inserted and the comparison is first performed on a level of 15 amp-meter. If the interfering current times common run length is below this value, the next interfering wire is selected. If it is above 15 amp-meter then the comparison is performed on the 30 amp-meter level. If it is below this level, a print of the current times length is generated with the letters o.k if not, then the current times length will be followed by the word "check".

2119

## OUT-PUT DATA

This output format enables the EMC design engineer to review the EMI status of his system with ease, and decide on the best way to deal with the problem:

If there exists one wire or a number of wires in the AC category which are the prime contributors to the cable EMI, do they interfere with one or a number of sensitive wires? the same questions are valid for the transient case.

The decisions to be made are a result of the review of the results and the answers to the questions, for example, if the interference is caused by a single wire and picked up by a number sensitive wires, when it is best to deal with the single noisy wire, if possible.

### THE SEN. WIRE IS:

NO	BCP-IN	BCP-OUT	CAT	VOLT	TYPE	SEN(V)
70	X(2)C	Y(1)R	5	0.050	SH1	0.005

### THE CW INT. WIRES ARE:

NO	BCP-IN	BCP-OUT	CAT	VOLT	TYPE	COP(V)	DB
12	S(1)2	L(2)S	2	200	C	0.007-2.7	CHECK
27	M(7)X	N(3)L	3	35	C	0.002 5.8	O.K
55	P(4)R	G( )R	2	200	TW	0.003 3.2	O.K
56	P(4)S	G( )S	2	200	TW	0.003 3.2	O.K
57	P(4)T	G( )T	2	200	TW	0.003 3.2	O.K

### THE TR. INT. WIRES ARE:

NO	BCP-IN	BCP-OUT	CAT	VOLT	TYPE	TR(A.M)
44	X(2)D	Y(1)S	6	35	C	17.9 O.K
82	B(8)P	N(3)A	6	35	C	29.4 O.K
93	T(1)S	L(2)J	6	35	C	40.0 CHECK

Fig.9 Out-put format

When an interference problem is spotted after the analysis has been performed, and either the sensitive circuit wire type cannot be changed, or the victims are many and the number of interfering wires is small, the designer may choose to change interfering wire type. The following data will aid him to choose the new wire type; as depicted in Figure 10.

When used in practice, the program picked up and pointed to 10% of all wires in the system as possible cases of EMI. Many of those were discarded by the engineering decision phase as being too much on the worst-case side, and so very few wires were left to be dealt with and fixed.

An EMC test performed on the system after the method was implemented resulted in only minor cases of interference due to transient coupling, and causing nuisance type of interference only.

A few figures connected with the program are: a 60 second run is required for a 250 wire cable, and a capability of 1500 wire harness analysis, on the CDC 6600 computer.







INTERFERING SIGNAL	ORIGINAL WIRE TYPE			CHANGE TO WIRE TYPE			ADD - db
	Tx	GND	Rx	Tx	GND	Rx	
400Hz AC		•					25
							25
TRANSIENT AND TTL PULSE		•					15
							

Fig.10 Decoupling effect of interfering wire type change

#### REFERENCES

1. Spagon, A.J. *Intrasystem EMC in Large Aerospace Systems*. TRW Systems Group. 1 Space Park Redondo Calif. 90278.
2. Kaplit, M. *Electromagnetic Coupling Between Coaxial, Single-Wire, Two-Wire, and Shielded Twisted Pair Cables*. 9th TRI Service Conference on EMC, October 1963.
3. - *Designers Guide, Electrical Interference Reduction*. Boeing document No.DL-4156.
4. -- Study to establish electromagnetic compatibility specifications, contract NAS8-11426. General Dynamics Convair EMC group Report No.22K-65-027, 30 July 1965.
5. Nohr, R.J. *Coupling Between Open and Shielded Wire Lines Over a Ground Plane*. IEEE transactions on EMC Vol.9, No.2, September 1967.
6. Bogdanor, J.L.  
Siegel, M.O.  
Weinstock, G.L. *Intra Vehicle EMC Analysis*. McDonnell Aircraft Co. Technical Report AFAL-TR-71-155, December 1971.

**DISCUSSION**

**R.Oiesch:** Does the computer program consider the actual position of the wire in consideration and the interfering wire?

**O.Hartal:** The computer program actually determines coupling, based upon the coupling parameter for the specific wire-type combination involved, and the common run length. The coupling parameter includes the positions of interfering wire and the susceptible wire and this is 2" above ground plane and tight coupling, that is, spacing - adjacent.

A UNIVERSAL ELECTROMAGNETIC COMPATIBILITY (EMC) ANALYZER  
UTILIZING  
BASIC CIRCUIT MODULES

Karl E. Wieler  
American Electronic Laboratories, Inc.  
Lansdale, Pennsylvania  
U.S.A.

Warren A. Kesselman  
U.S. Army Electronics Command  
Fort Monmouth, New Jersey  
U.S.A.

SUMMARY

The multiplicity of test data required by EMI specifications is a well recognized problem. Interference measurements are complex and testing procedures are specialized. The problem is further complicated when one considers whether the tester is interested in making a site-survey or in analyzing equipment/system performance measurements. The measurement system developed utilizes plug-in modules; the modular concept permits the assembly into one package of only those modules required for a specific measurement task.

Controversy is continuing today in the areas of data correlation and measurement units. A measurement instrument was developed to give EMI-RFI testers more reliable information on received signals of an unknown nature. The amplitude distribution measurement can be applied to any situation where the distribution of a signal is desired.

An evaluation of various detector modules defined usable measurement techniques for various signal types. New measurement concepts are introduced to the EMI/RFI field to give increased data on a detected unknown signal and certainly more reliable data than that taken with present measurement techniques and systems.

1. INTRODUCTION

The Basic Circuit Modules program entailed the design of a modular electromagnetic interference (EMI) measurement receiving system to cover the frequency range from 30 Hz to 40 GHz. This receiving system is designed to provide a universal measuring device for all known present and future anticipated EMI requirements.

To provide a useful EMI measurement instrument, present uses must be considered as well as future requirements. Presently, most EMI measurements are performed according to numerous federal and military standards. These standards have been devised to evaluate the electromagnetic compatibility of the equipment under test with either existing equipment or with other parts of the same system.

Another use of EMI measurement receivers is to make site surveys. In this application an area, which is to be used for an installation where RF interference is critical, is checked to measure the intensity of RF signals which are normally present.

These two applications cause conflicting requirements to be considered in the design of any EMI measurement receiver. In testing to design standards, the test environment is usually a laboratory or test site where no serious restrictions of test equipment volume or weight need be considered. The amount of variation in the measurement equipment and the data recording equipment is almost unlimited. The site survey application is a completely different situation. In this case, portability is of prime importance which means that size, weight and power are all ultra-critical problems. This is especially true when the site survey is to be made in a remote location where the test equipment must be hand-carried. In this type of environment, the minimum amount of equipment to perform the required tests must be used.

From these two typical applications one set of problems is obvious. For laboratory testing, a sophisticated receiving system, supplemented by automatic or semi-automatic data recording and control equipment can be used. The time required to perform these measurements can be minimized by using fully automatic control and data recording. For site survey, a simple, less complicated system is required. Hardware size reduction is a necessity while measurement accuracy, consistent with present day receiver capability, must be maintained.

These conflicting requirements can be solved by utilizing modular techniques. The Basic Circuit Modules receiver is constructed so that only the modules needed for the pertinent application are used. For site survey work, only the modules necessary to perform the required task need be assembled to form the receiving system. The number and type of modules to be used must be determined for each measurement task. The receiving system can therefore vary from a fully automatic, computer-controlled system to a small portable, ruggedized unit suitable for field use.

The second problem, which must also be considered, in addition to the receiver design, is the measurement problem. Present day receiving systems provide meter indications which are essentially meaningless unless the type of input signal carrier and modulation are known. The problem in this area was to develop measurement techniques which are meaningful without adding significantly to the complexity of operation and hardware.

Typical practices call for recording meter data in field operations and then later converting this to absolute signal levels by signal substitution. This type of measurement technique can yield large errors in signal level if the proper type of signal and modulation characteristics are unknown. In addition, the data is often not reproducible.

Units of signal measurement are another point of confusion in EMI measurement instruments. The optimum set of measurement units must be established so that significant data can be evaluated. The best situation that could be achieved would be to develop the receiving system as a voltmeter whose output circuitry provides an RMS measurement of the input signal, regardless of the characteristics of the input signal. This problem of measurement was combined with the receiver configuration problem to develop an optimum EMI measurement instrument.

## 2. PROGRAM RESULTS

AEL has developed a universal electromagnetic compatibility (EMC) analyzer that will satisfy the numerous measurement requirements of the electromagnetic compatibility community. The measurement system utilizes plug-in modules for the convenience of the EMC testing facility. The modular concept permits the assembly into one package of only those modules required for a specific measurement task. The resulting design flexibility will permit any combination, from a simple four-module instrument, as shown in Figure 1, to a fully automated assemblage of all analyzer modules.

Utilization of plug-in receiver modules for a universal EMC analyzer provides a cost-effective instrument for all types of EMC test facilities. The purchase of an EMC analyzer, utilizing just the required basic receiver modules is more expeditious and economical than modifying existing equipment and purchasing additional auxiliary equipment. Additional receiver modules may always be added to the analyzer as new standards and measurement techniques are formulated.

The selection of analyzer modules, from an inventory listing, for a specific measurement results in an optimum instrument (required frequency range, sensitivity, dynamic range, measurement function, etc.) which leads to a high level of confidence that the data recorded is true data. One measurement system for all tests results in the standardization of parameters so that the problems of correlating data, taken by instruments of various characteristics, are eliminated.

## 3. RECEIVER DESCRIPTION

Figure 2 shows the generalized block diagram of the basic circuit modules receiver. This diagram shows the major modular division which was formulated during the design phase. Nine module types are required to implement the entire measurement system. These modules form a functional division of the measurement system.

Future development may allow combining some of these functions, as well as the introduction of new modules.

Three tuners were fabricated to demonstrate the modular concept, covering the frequency ranges of 1 to 2 MHz, 20 to 40 MHz and 500 to 1000 MHz. The block diagram of these three tuner modules is shown in Figure 3. The tuner configuration shown for all three frequency bands is a double-conversion superheterodyne receiver whose output is converted to a common IF frequency of 60 MHz. This allows the use of a single IF module for all tuner bands. An up-conversion is performed in the first mixer to raise the first IF frequency above the RF input frequency. This helps to minimize image problems and, in most cases, eases IF filtering problems. The RF environment is filtered with a tunable RF preselector at the tuner input. The first conversion in each tuner module utilizes the output of the wide range local oscillator, while the second conversion is performed using a fixed-frequency temperature-compensated crystal oscillator.

A block diagram of the local oscillator is given in Figure 4. This diagram shows that the LO section provides tuning signals for the entire 1 MHz to 1 GHz frequency range. A single VCO is used as the signal source for all frequency ranges. This oscillator is stepped under the control of a D/A converter in the automatic sweep mode and is controlled through the use of a phase-locked loop in the manual mode of operation. The output frequencies for each frequency band are indicated in the block diagram shown in Figure 4. The lowest frequency (1 to 10 MHz) is obtained, using a digital divider and filter network. The next frequency range (10 to 125 MHz) uses the oscillator output directly. The 125 to 1000 MHz range uses the multiplied output.

A block diagram of the IF module is shown in Figure 5. The input to this module is the tuner module output which has been converted to the 60 MHz IF frequency. The IF signal is passed through a series of amplifiers and filters which form the IF bandpass and provides compensating gains to maintain a constant noise level at the output of the video detector. This chain of filters and amplifiers is followed by a power splitter. One arm of the splitter is used as a sample output which is brought out to the front panel. The second output of the splitter is the main signal path which passes through an IF attenuator and onto the final high gain linear IF amplifier. The IF attenuator is remotely programmable and is controlled by two thumbwheels on the front panel of the IF module. A 59-dB range of attenuation is offered to maintain the signal amplitude within the post-amplifier dynamic range.

#### 4. AMPLITUDE DISTRIBUTION MEASUREMENT INSTRUMENT

The Amplitude Distribution Measurement Instrument, shown in Figure 6, was developed to give EMI-RFI users more reliable information on received signals of an unknown nature. The amplitude distribution measurement can also be applied in any situation where the distribution of a signal is desired. The Amplitude Distribution Measurement Instrument is designed to measure the percentage of the measurement time that the input voltage has spent in each of the instruments' fixed preset voltage levels. The output information, therefore, reflects amplitude and time duration information of the incoming waveforms. One of the most important undertakings of this program was to evaluate various detector modules. This study defined usable measurement techniques for various signal types. The goal was to introduce new measurement concepts to the EMI-RFI field to give increased data on a received unknown signal and certainly more reliable data than that taken with present measurement techniques and systems.

There are two general groups of signals that are desirable to evaluate; the deterministic and non-deterministic (random) signals. Deterministic signals are relatively simple to evaluate since they have a predictable pattern, however, random signals are very difficult to evaluate due to their unpredictable nature.

Random signals can be further divided into two types; stationary and non-stationary. Stationary random signals have statistical regularity in that certain averages formed over many samples do not depend on the particular time of measurement. Non-stationary random signals are most difficult to evaluate since averages formed are dependent on the time when the sample was taken.

Present measurement systems do not have the ability to obtain useful information on many types of signals. Average and RMS readings can be misleading and cannot provide useful measurement for all types of signals. For signals formed other than CW, the average type of measurement bears no relationship to the incoming RF signal or to the modulation signal.

Peak voltage measurements can be useful in defining a signal if the receiver bandwidth is wide enough to ensure that the measured peak is the true signal peak.

The mean-square voltage measurement was evaluated and it was shown that for only certain classes of signals can the video voltage output of an envelope detector be related to the average power of the RF signal. In particular, only for periodic CW and wide sense random stationary signals is this type of measurement meaningful.

The amplitude distribution-type system was also considered. The results indicated that the amplitude distribution of signals from various modulation systems could be expected to give repeatable data. Certain types of noise; such as, atmospheric, ignition, lightning, and corona, will tend to have statistical regularity, enabling some probability statement to be made. Periodic signals will produce repeatable data with the amplitude distribution measurement instrument.

Figure 7 summarizes the findings of the study program measurement system evaluation. The important conclusions drawn from this table are that three types of measurement systems are useful for all types of modulation:

- 1) The Amplitude Distribution System
- 2) The RMS Measurement
- 3) The Oscilloscope

It is felt that the oscilloscope is necessary to interpret both RMS meter readings and amplitude distribution information, and any measurement system should be used along with an oscilloscope to allow real time viewing of the video voltage.

#### 4.1 Amplitude Distribution Instrument Applications

##### 4.1.1 Applications as a Field Intensity Detector Module

With the large number of field intensity measurement systems and detectors that exist, one question that arises is; where can the amplitude distribution measurement technique be used most effectively? Considering some of the preceding information will supply some answers to this question, especially when a comparison with some existing measurement techniques are made. One example of an effective use of the AD is to monitor the occurrence of a transient condition that occurs very infrequently. This type of application may be encountered when testing a system for spurious emissions. As an example, using a waveform of a 20-microsecond pulse occurring once every fifty-seconds, it can be deduced that the amplitude and duration of the transient can be characterized without complex storage media and without utilizing a large amount of test equipment. True, the exact transient waveform is not specifically defined (especially if a complex signal were to be encountered), in this case, mainly due to the gross quantization intervals that have been selected to demonstrate the instrument capabilities. Finer quantizing intervals would produce a more accurate representation of the waveform. The occurrence of the transient is easily determined, however, which is certainly not easily done using average, RMS or even some peak reading meters.

A second application is to determine the characteristics of an unknown complex waveform. One example of this may be where a single frequency is being used for different applications, such as pulsed radar transmission and voice or coded data transmission. A simple meter reading will not be sufficient to detect the difference in signal characteristics if the RMS or average values are equal. The signature of the signal is required to distinguish the different types of transmission. This will be true, if real time observation of the signal is not possible due to the random nature of the demodulated signal, or due to alternating types of signal transmission.

In order to analyze the various types of signal waveforms that can occur, a library of signal signatures must be assembled, similar to that gathered in AEL Technical Report 1020-2, to provide some basis for comparison between the received (unknown) data and established (known) signal records. It is recommended that further investigation of the amplitude distribution characteristics of various types of signals be made such that full use of the measurement system can be realized in the field intensity detection application.

#### 4.1.2 Application in Other Fields

The use of the Amplitude Distribution Measurement technique has applications in any type of process where a large number of samples with varying parameters must be monitored and the variations of these parameters must be measured and, in some cases, controlled. Some examples of these types of processes are rolling, drawing and extruding of all types of metals; in this case, a tolerance distribution over a time period must be known in order to control the process or to inspect the final product to determine the quality of the resultant product.

Other types of monitoring, where the AD can be applied are pressure, temperature, air flow and environmental transducers of almost any kind. The measurement of the distribution of the variation in the transducer output is sometimes more important than absolute limit monitoring, especially where separation of product output into various categories is required, dependent on overall lot tolerance distribution.

Communication channel monitoring is another area where the AD can be applied. The quality of both the transmitted information, as well as the noise distribution in the channel can be monitored in order to determine the quality of the channel under varying conditions so that the operation of error detecting and correcting equipment can be put into use, depending on the channel quality.

In general, the Amplitude Distribution Measurement technique can be used in any application where the process can be monitored in discrete voltage levels and where time dependent interrogation can be performed, based on the measurement of the distribution of critical process parameters.

#### 4.2 Amplitude Distribution Instrument Development Considerations

The results of the measurement system study concluded that the AD measurement is applicable to all modulation forms; although it has not been fully evaluated for random signals and little is known concerning the implementation required to obtain the most meaningful results.

Of the three measurement systems that provide meaningful information, the oscilloscope is considered a necessity, the RMS measurement is fairly easy to implement and therefore the AD system remains to be given further attention.

Technical considerations constraining the AD instrument implementation were:

- 1) Information bandwidth (receiver bandwidth)
- 2) Output storage of data and interpretation of data output.

Since the processing is done at video, the information bandwidth is the widest receiver bandwidth used in present receivers. The widest receiver bandwidth implemented in the Basic Circuit Modules Receiver is 10 MHz, or a 5 MHz video bandwidth, therefore, a sampling clock rate of 20 MHz was chosen.

The block diagram shown in Figure 8 indicates the approach taken in implementing the AD measurement. The output of the linear detector is used as the instrument input. DC coupling was used in order to eliminate duty cycle problems which can occur with unknown signal forms.

The buffered detector output is applied to the four comparator inputs. Any number of comparators can be used but for discussion purposes we will use four. The comparator threshold voltages are applied to the other comparator inputs and are selected to uniformly cover the video detector dynamic range.



The comparators provide a level shift at their output when the threshold level is exceeded. This level shift is sent to an AND gate which has the 20 MHz clock pulses as the other input. As long as the threshold level of the comparator is exceeded, the gate will provide the 20 MHz clock to the counter. The number of counts which occur is a measure of the time the signal is above the set threshold. The counter output is then stored at the end of a measurement period.

The measurement time used will be such that the total sum of counts for a measurement interval is  $1 \times 10^x$  where  $x$  is some integer so that the counter output can be directly related to a percentage of time. The longer the measurement time the more accurate the measurement will be, however, the longer the time, the larger the counters must be to prevent overflow. If the measurement time is too long, the data may not be accurate, due to the input signal changing its form over a long time interval.

In implementing the AD measurement concept, a few more points of interest are raised;

- 1) What is the optimum number of threshold levels?
- 2) What is the optimum measurement time interval?
- 3) How should instruments be implemented to be compatible with present day receivers and how can its use be simplified?

Hardware limitations are the major restrictions to Items 1 and 2. Several refinements were made to the AD instrument block diagram, during its development, in order to make it more useful as a measurement instrument.

#### 4.3 Amplitude Distribution Instrument Expectations

In most EMI/RFI survey work, the majority of signals will appear to be random. By using the AD measurement, a conclusion can be made, stating the average waveform will be expected to spend some percentage of its time in a defined amplitude window. In other words, the goal is to be able to predict that, if the same measurement were made at different times on a random waveform, the data would be somewhat predictable. For this to be true, the signal must exhibit some statistical regularity. If this is so, then one can state that for an observation time, the probability that the RF voltage assumed a value within a voltage window is not dependent upon the time the measurement is made.

For the majority of types of random modulations, the most reasonable approach was to record the amplitude distribution of a signal for as many samples as possible. From a given sample it would most likely not be possible to determine a probability statement for the signal; but if several tests are made and the data analyzed, some trends or averages might appear.

The block diagram for the AD instrument is shown in more detail in Figure 9. Thumbwheel switches on the front panel are used in the threshold circuit to generate threshold levels for five comparators. An error light, mounted on the front panel, indicates that an error has been made in setting the threshold thumbwheel switches. The threshold levels, along with the detected video, are sent to the comparators. The comparators produce six output gates that indicate which window the signal is in at that time. The comparator window outputs are each sent to one of the six channels, along with the measurement clock signals. The six data channels use these signals to count the number of clock pulses that occur while the input signal is within that channel's voltage window.

A typical waveform and the corresponding comparator output and exclusive enabling output are shown in Figure 10. The exclusive enabling gate outputs drive a series of two input AND gates; the other input to these gates is the channel clock signal which is used to determine the time within each window. There are six outputs from the AND gates which form the input to the six measurement channels; four of these outputs are used to determine the time within the four windows generated by the five threshold levels, while the

remaining two outputs will determine time above the highest and below the lowest levels. These two have been added to aid in determining the gain change required to obtain the optimum measurement. The actual threshold levels are generated using two manually operated sets of thumbwheel switches. One set of thumbwheel switches generates the highest threshold while the other controls the lowest level. The remaining three levels are equally spaced by the four resistors placed between these two levels. 72-7

The system clock controls the timing and sequence of operation throughout the AD measurement instrument. The basic timing source is a 20-MHz crystal clock. This clock is used to generate the channel clock for the input AND gates. This clock source is counted down to form the measurement signals which determine how long the AD measurement is active. Two measurement times are available; 50 seconds and 5 seconds (long/short). The long (50-seconds) and short (5-seconds) measurement times are selectable by a switch on the front panel.

The channel outputs are sent to the printer output and the analog display outputs. The printer output provides the necessary signals to interface a digital printer while the analog display provides the necessary outputs to generate a display on an oscilloscope.

The system timer receives the front panel switch information for measurement time-type of measurement and start/stop data. The system timer also controls the operation of the six data channels and output circuitry.

The main output from the AD measurement system is an analog circuit which can be observed on an oscilloscope. This output is generated by taking the two most significant decades from the output storage in each channel and converting these to analog form and displaying this output on an oscilloscope. The data is gated through to the input of a D/A converter. The output voltage from the converter is proportional to the number of counts accumulated in each of the channel counters. A synchronization trigger is supplied for the oscilloscope. A typical display, which is generated, is shown in Figure 11. The oscilloscope is set for 2 volts/centimeter on the vertical axis and the sweep speed is set for 0.5 milliseconds/centimeter. The oscilloscope is triggered on the negative edge of the trigger output. With these conditions, the vertical deflection of each of the six horizontal divisions represent the output of each of the six channels; that is, the amplitude is proportional to the time in each of the six windows. The seventh division represents magnitude information. The display shown in Figure 11 shows that the received signal fell within the second and sixth windows more than in any of the others. The signal fell within the fifth window the least amount of times.

An evaluation of typical signals, along with data received from the amplitude distribution instrument, is contained in AEL Technical Report 1020-2, which shows the correlation between the two and verifies that the output data is correct for the incoming RF signal. Many types of signals were evaluated, such as; sine wave, triangular wave, pulses of various pulse widths, noise, and finally broadcast AM and FM station signals. Two other types of signals were also evaluated; audio FSK and TV video.

#### 4.4 Amplitude Distribution Instrument Conclusions

The data, describing the amplitude distribution tests, taken on standard waveforms (sine wave, square wave, pulse signals) shows close correlation with theoretical limits. This is shown in every case with no exception by comparing the predicted display with the actual photograph taken for each waveform. This series of tests was performed mainly to validate the operation of the overall system. After probing the system capabilities in this manner, tests on gaussian noise were made, since the amplitude distribution of this type of signal is well defined. Here again, the results tabulated showed good correlation with the predicted values.

The final set of data taken measured the distribution for AM-FM radio and TV stations. The conditions, under which the distributions were measured, were recorded to see if a change in the distribution could be detected when the type of information was changed; that is, when a music transmission was changed to a station announcement or news transmission. The results showed no noticeable change in distribution as the type of transmission was changed. These tests on radio and TV signals showed a need for finer threshold resolution in order to produce more definitive data on signals of this nature.

#### 4.5 Present A/D Instrument Limitations

Measurement instruments, that are in existence today, are designed to perform sophisticated correlation and probability analysis. These instruments present fine grain level sensing (hundreds of quantizing levels). However, some tradeoff in speed is made to obtain better accuracy. The AD instrument, just described, provides a simplified higher speed instrument at a significantly lower cost that can be used in applications where the fine grain accuracy is not required and wider bandwidth signals must be monitored.

The major limitations of the present AD instrument are:

- 1) the maximum input bandwidth
- 2) the number of channels utilized, and
- 3) the length of measurement time.

The input signal bandwidth is limited to 5 MHz in the present AD instrument, due to the 20 MHz sample rate. In future versions, the input bandwidth will be extended to 50 MHz with a clock rate of 200 MHz which is available utilizing present day hardware.

The number of channels was limited to six, in order to limit the physical size of the AD instrument and to minimize complexity.

The measurement time was selected to limit the channel circuitry. It is anticipated that in future AD instruments the channels will be extended with a reasonable increase in hardware. The AD instrument is planned to be hybridized and the present size would be drastically reduced. With this plan for a future instrument, channels would be added and channel capacity would be increased.

#### 5. RMS MEASUREMENT MODULE

Figure 12 shows a block diagram of the RMS meter module. The video input signal is obtained from the detector output. A compensating amplifier is used in the video path to eliminate the roll-off in the RMS module bandwidth, which is 3 dB down at 1 MHz. Additional gain is supplied with this amplifier at frequencies of 500 KHz and higher to compensate for its roll-off. The compensating amplifier provides 0 dB gain at lower frequencies. This amplifier is of a common-emitter configuration, using emitter-peaking to achieve the increased gain at higher frequencies. This allows the function module to provide useful information across the widest video bandwidth utilized which is 5 MHz.

The RMS module provides a DC voltage at its output which is equal to the RMS value of the input signal; that is, if the input signal is a 10-volt peak sine wave, then the output will be a DC voltage of 7.07 volts.

This module will handle signals up to 10 volts, peak-to-peak. This allows a large crest factor for all input signals, since the video output will limit at a value of 5 volts peak. The RMS module output will be used to drive an operational amplifier used as a voltage-follower which contains a series-resistor at its input and a 0 to 1 mA meter in the feedback loop. This produces meter scales of 0.1, 0.5, 1, 5 and 10 volts RMS.

The RMS module performs the following functions in sequence;

- 1) The input signal is squared
- 2) The squared output is integrated over a time period which is determined by external capacitors
- 3) The square-root of the integrator output is determined.

Please note that the RMS module is DC-coupled throughout. Compensation is added to minimize drift problems through a temperature range.

42-10

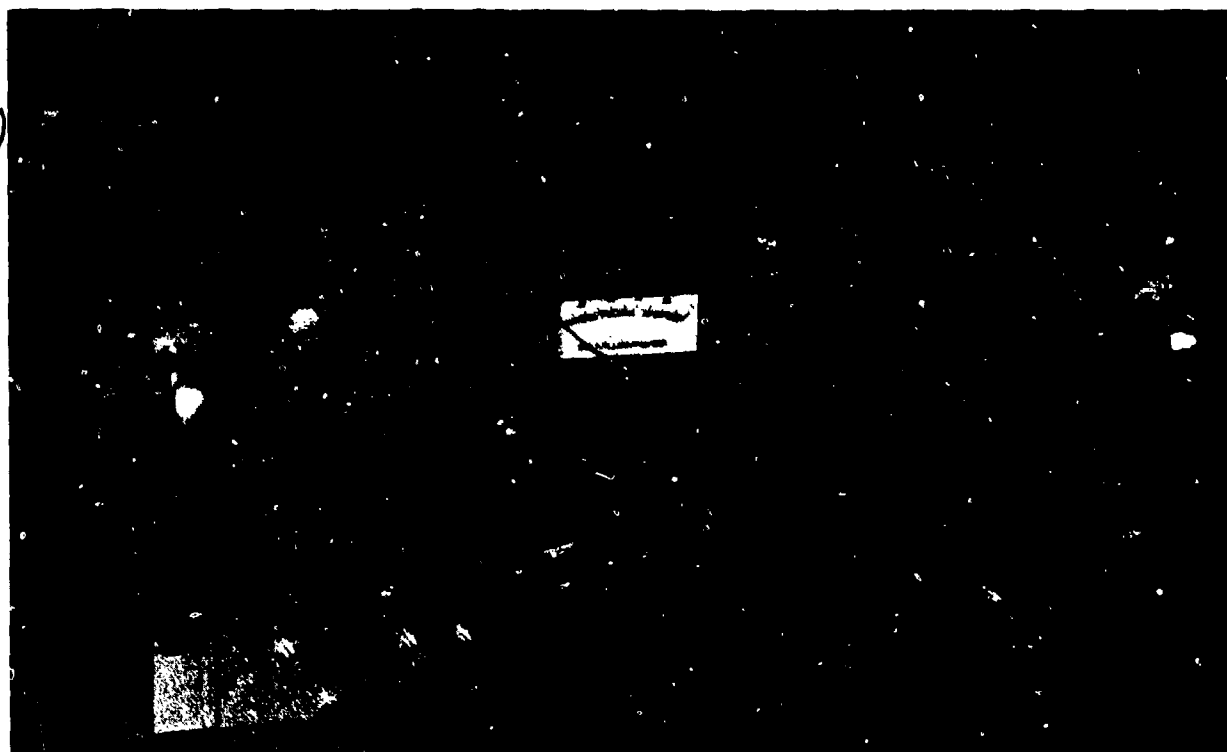


Fig. 1 Basic circuit modules mainframe

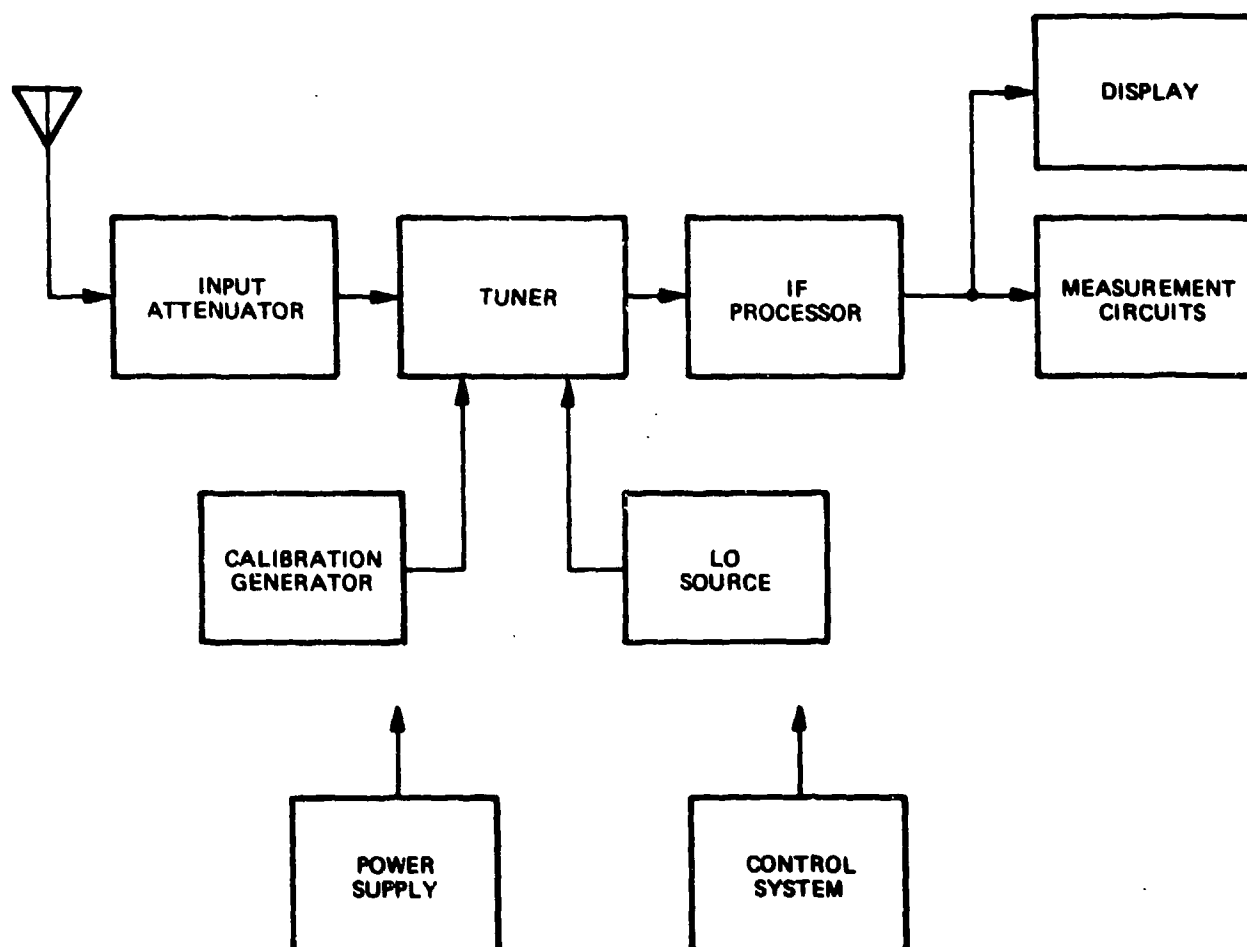


Fig. 2 Modular receiver block diagram

## 6. SYSTEM CONTROL

The block diagram shown in Figure 13 indicates the control system which is used with the Basic Circuit Modules Receiver and Measurement System. The block diagram shows a clock control logic block which produces the prime sweep signal input to the system. The clock control logic is activated by either the manual shaft encoder or the divided-down crystal-controlled clock, depending on whether the system is in the manual or automatic sweep mode. The output of the clock control is a signal at the desired sweep rate. This signal steps the true frequency counter. The true frequency outputs are used to provide an RF read-out when in the manually-tuned mode and to drive the VCO, RF preselectors and form the display sweep in both the manual and automatic modes. The true frequency counter is also the interface point between the control system and the programmable counter which is part of the phase-lock loop. The phase-lock loop will only be used in the manual tune mode when it is desired to stabilize the VCO at a signal frequency or tuned at a very slow rate. The true frequency counter outputs are converted to a control voltage in the D/A converter. The D/A converter output is then modified in the offset network to provide the control for the RF preselectors, VCO and the display.

## 7. CONCLUSION

An EMC analyzer has been demonstrated, solving the conflicting requirements between laboratory and site-survey testing by utilizing modular techniques. The number and type of modules used in the EMC analyzer is determined by each measurement task. The EMC analyzer can vary from a complete system covering the entire frequency range of 30 Hz to 40GHz for laboratory testing to a small, portable unit of limited frequency range for field use.

The Amplitude Distribution Measurement technique has been demonstrated to be applicable to all modulation forms by direct comparison between known input waveforms and the AD instruments output display. The comparison was validated by the use of many types of signals and with no exception, the AD instrument display correlated with the actual input waveform.

## ACKNOWLEDGEMENT

This work was sponsored by the U.S. Army Electronic Command, AMSEL-NL-C, Fort Monmouth, N.J., under Contract Number DAAB07-71-C-0339.

The author wishes to acknowledge the engineering efforts of L. Resinski, D. Legower and D. Mayse for their work on the subject program.

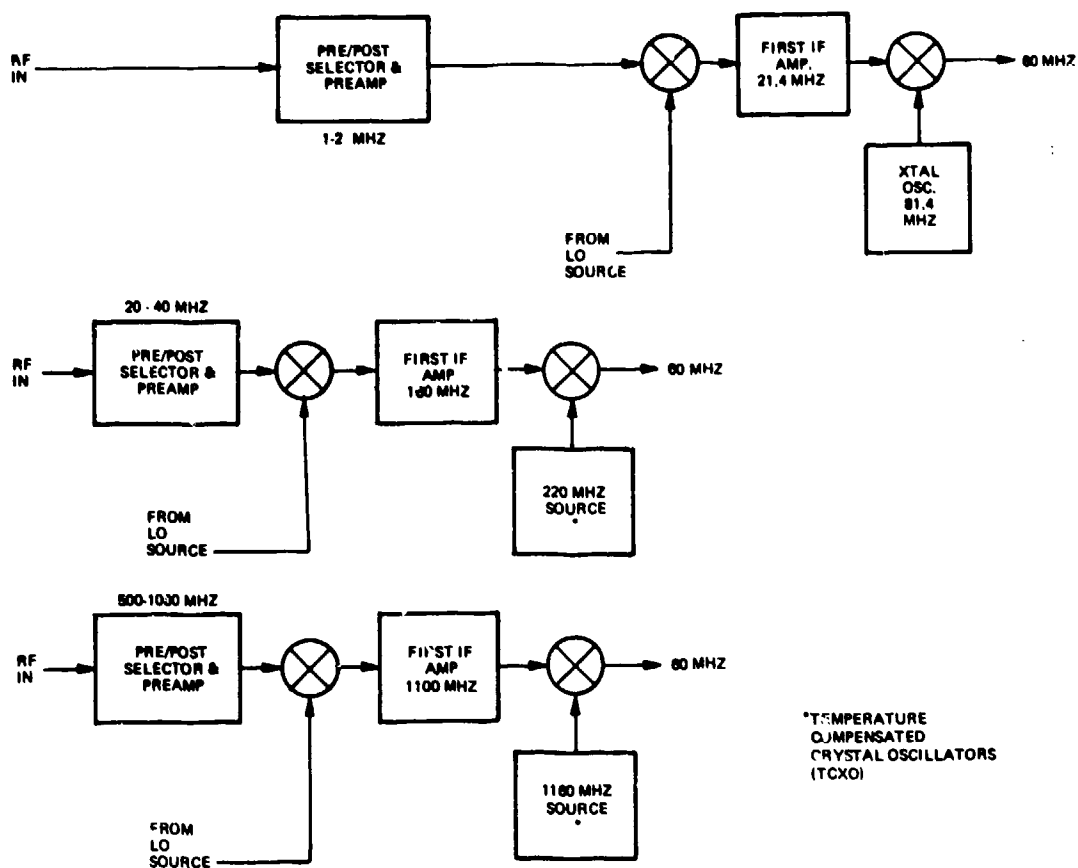


Fig. 3 RF tuner block diagrams

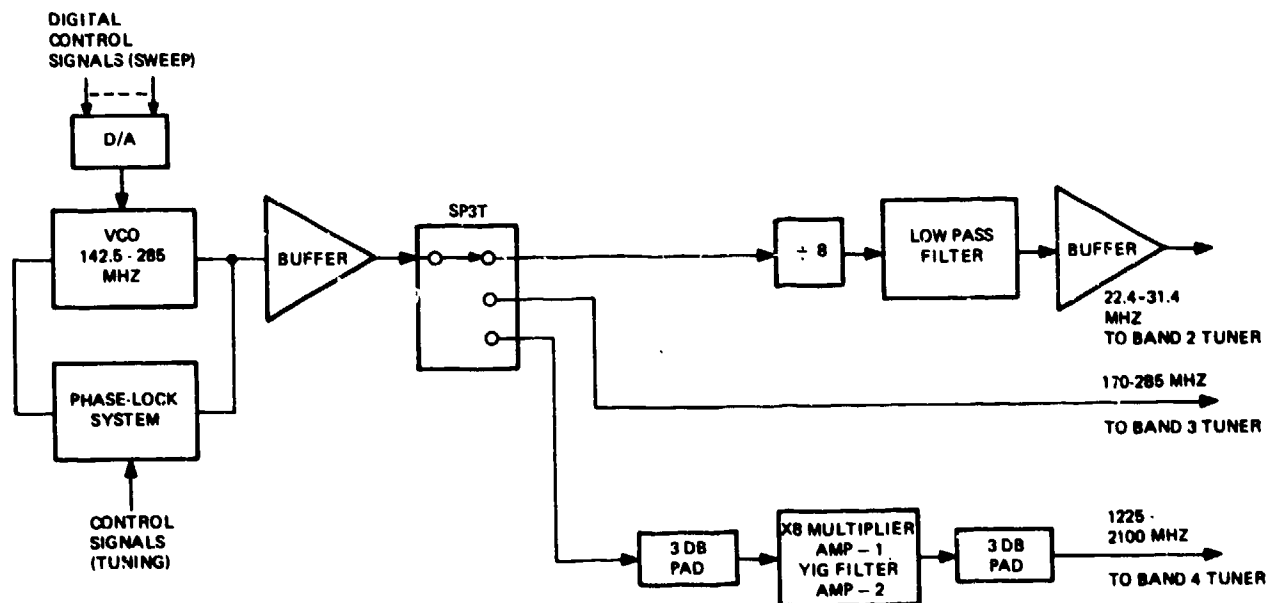


Fig. 4 LO module for basic circuit

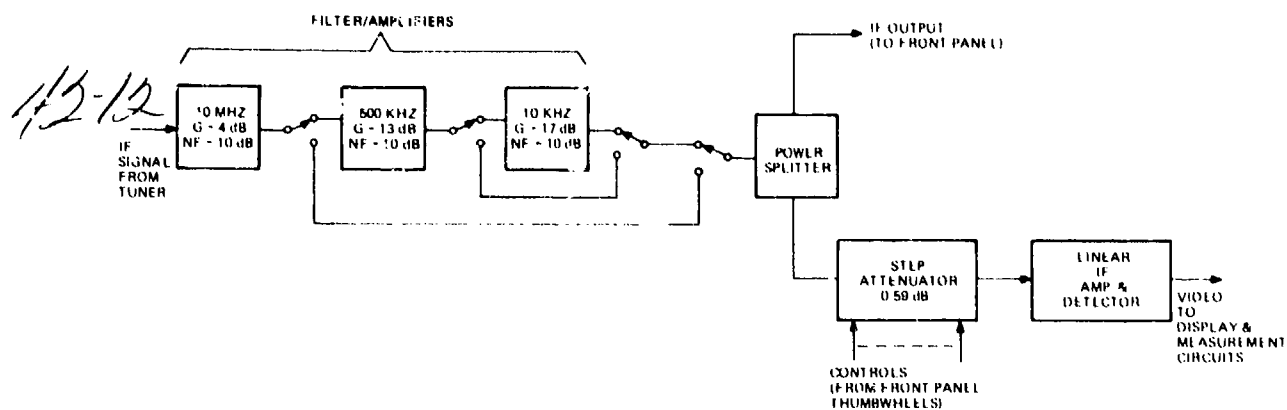


Fig. 5 IF module, block diagram

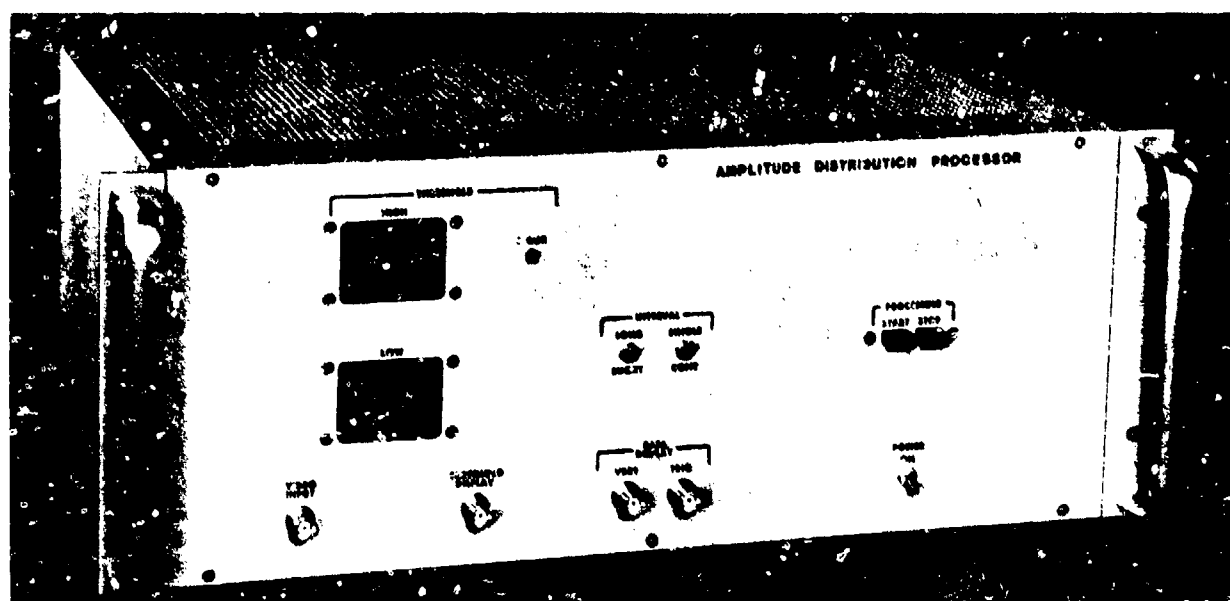


Fig. 6 Amplitude distribution measurement system

Modulation Type	Peak	Average or CW	Slide Back Peak	Mean Square	Amplitude Distribution	RMS Bolometer	FM Deviation	Oscilloscope	FM Discriminator
AM	X		X		X	X		X	
FM					X	X	X	X	X
PULSE	X		X		X	X		X	
FM/FM					X	X	X	X	X
FM/AM					X	X	X	X	X
PSF	X				X	X		X	X
FSK	X				X	X		X	X
SSB	X				X	X		X	
SPIKES/ NOISE	X		X		X	X		X	

Fig. 7 Types of modulation and useful methods of detection

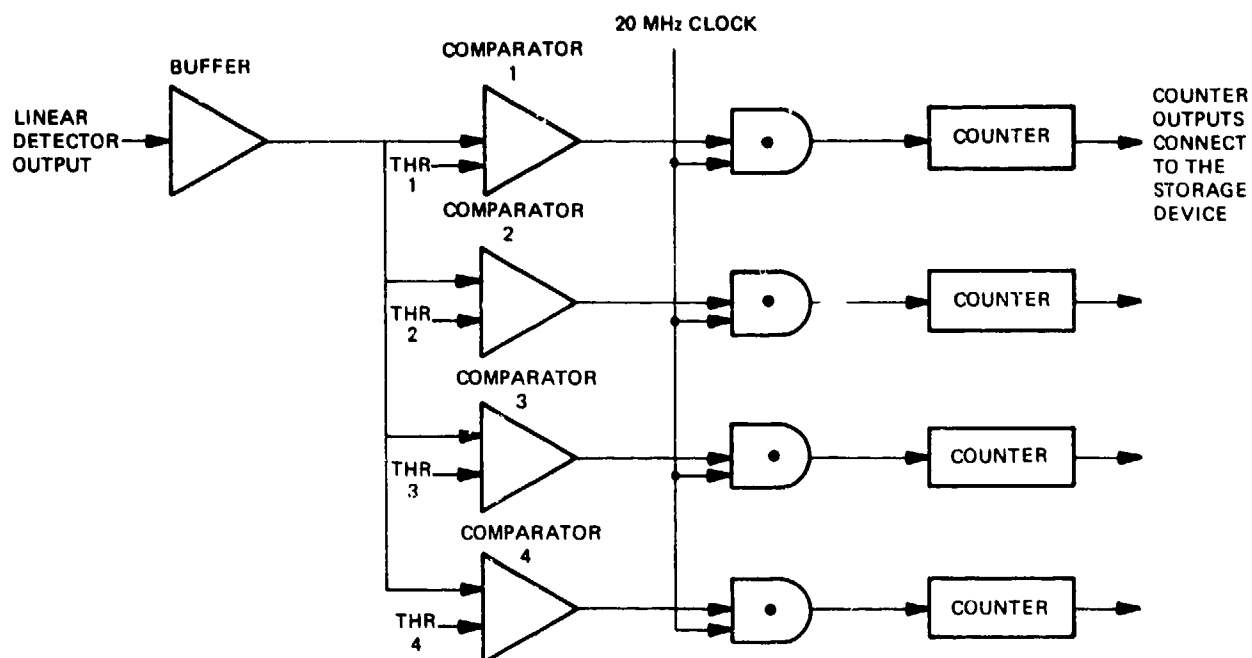


Fig. 8 AD simplified block diagram

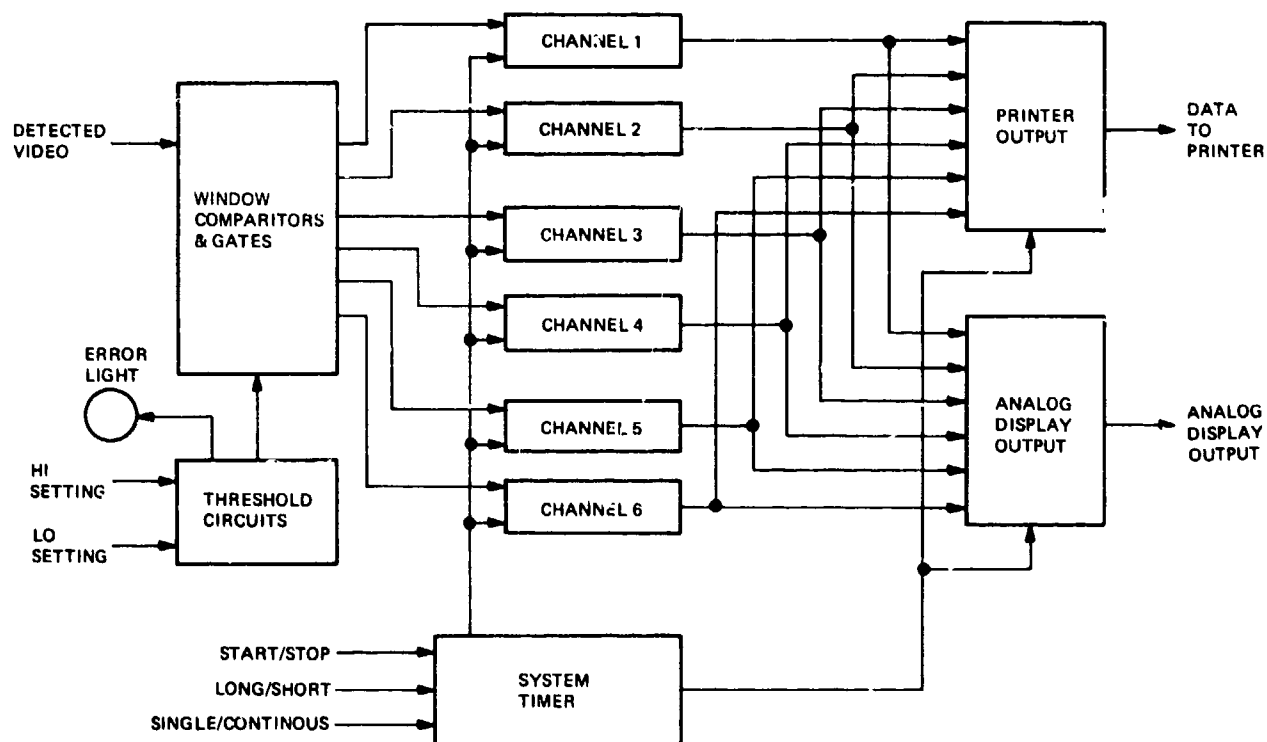


Fig. 9 AD instrument block diagram



42-14

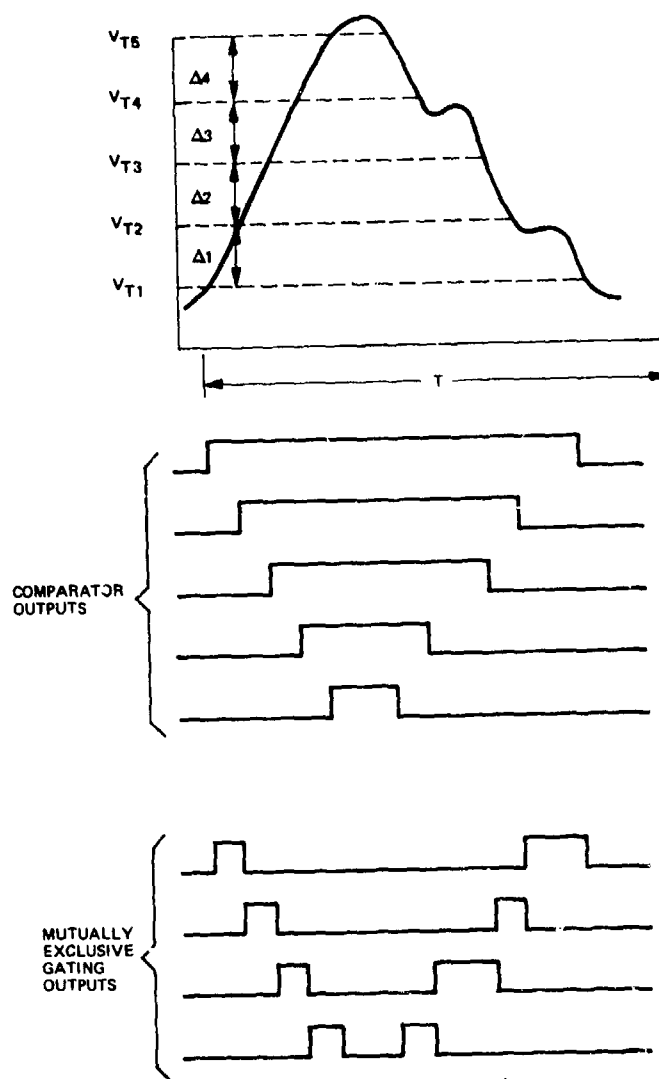


Fig. 10 Amplitude distribution level sensing

CRT SCREEN									
0	1	2	3	4	5	6	7	8	9
CH 1	CH 2	CH 3	CH 4	CH 5	CH 6	M A G	BLANK		

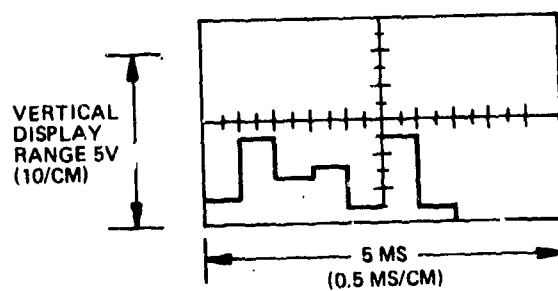


Fig. 11 AD typical display

The diagram illustrates a frequency synthesizer system. Key components and their interconnections include:

- COMPUTER INPUT:** Provides a signal to the **PRESET** block and the **CLOCK CONTROL LOGIC** block.
- SHAFT ENCODER:** Outputs to the **CLOCK CONTROL LOGIC** block.
- SWEEP & MODE SWITCH:** Outputs to the **CLOCK CONTROL LOGIC** block.
- BAND INFO.:** Provides input to the **CLOCK CONTROL LOGIC** block.
- CLOCK CONTROL LOGIC:** Receives inputs from the computer, shaft encoder, sweep switch, and band info. It outputs a **20 KHZ** signal to the **TRUE FREQUENCY COUNTER** and an **EOB** (End of Band) signal to the **END OF BAND** block.
- TRUE FREQUENCY COUNTER:** Receives the 20 KHZ signal and outputs to the **RF READOUT** block and the **END OF BAND** block.
- 1 MHZ XTAL OSC:** Provides a reference frequency that is divided by 50 ( $\div 50$ ) to provide a **20 KHZ** signal to the **CLOCK CONTROL LOGIC** and a **200 KHZ** signal to the **PRESCALER** block.
- PRESCALER:** Divides the 200 KHZ signal by  $M$  ( $\div M$ ) to provide a **20 KHZ** signal to the **CLOCK CONTROL LOGIC** and a **200 KHZ** signal to the  **$\div N$  PROGRAMMABLE COUNTER**.
- $\div N$  PROGRAMMABLE COUNTER:** Receives the 200 KHZ signal and outputs  $f_{OUT}$  to the **PHASE DET.** block.
- $\div X$  COUNTER:** Receives the 200 KHZ signal and outputs  $f_{REF.}$  to the **PHASE DET.** block.
- PHASE DET.:** Receives  $f_{OUT}$  and  $f_{REF.}$  and outputs to the **FILTER** block.
- FILTER:** Outputs to the **PLL IN** of the **LINEARIZED VCO** block.
- LINEARIZED VCO:** Receives the PLL IN signal and outputs  $f_{OSC}$ .
- MSD & LSD CONVERTER:** Receives the **TRUE FREQUENCY COUNTER** output and outputs to the **D/A 12 BITS** block.
- D/A 12 BITS:** Outputs to the **VCO PRESELECTION OFFSET AND GAIN AMPLIFIERS** block.
- VCO PRESELECTION OFFSET AND GAIN AMPLIFIERS:** Receives the D/A output and outputs **2A**, **3B**, **4C**, and **HORIZ SWEEP** signals.
- END OF BAND:** Receives the **EOB** signal and outputs to the **END OF BAND** block.

**Fig. 13 Control system block diagram**

## DISCUSSION

G. H. HAGN: I realize that the authors of the paper are not present, so I will make a comment rather than ask a question. I believe that Fig. 7 contains some apparent inconsistencies. For example, it is fundamental that noise be considered as a random process. As I pointed out in paper 1, one of the four basic measures of random data is the mean square value; therefore, I am puzzled to find the mean square column labeled "for periodic signals only". I suggest that the other columns of Fig. 7 should be reviewed rather carefully.

F. D. GREEN: I would like to know if the rms measurements can be reduced to power per unit bandwidth. If so, this type of measurement can be very useful universally, since it permits the use of various measurement equipments.

(J. B. Hager thought this could be done.)